Report

Rager Mountain Well #2244 Casing Failure Root Cause Analysis

Prepared for:
Equitrans, L.P.

Purpose:
RCA report on well #2244 7 in. casing failure root cause analysis.

2600 Network Boulevard, Suite 550
Frisco, Texas 75034

1-800-849-1545 (toll free)
+1 972-712-8407 (phone)
+1 972-712-8408 (fax)

16285 Park Ten Place, Suite 600
Houston, Texas 77084

1-800-319-2940 (toll free)
+1 281-206-2000 (phone)
+1 281-206-2005 (fax)

ISO 9001:2015 Certified
www.blade-energy.com

Date:
August 24, 2023

Version:
0

Project Number:
EQS-22-001

Blade Energy Partners, Ltd. and its affiliates (Blade) provide our services subject to our General Terms and Conditions (GTC) in effect at time of service, unless a GTC provision is expressly superseded in a separate agreement made with Blade. Blade's work product is based on information sources which we believe to be reliable, including information that was publicly available and that was provided by our client; but Blade does not guarantee the accuracy or completeness of the information provided. All statements are the opinions of Blade based on generally-accepted and reasonable practices in the industry. Our clients remain fully responsible for all clients' decisions, actions and omissions, whether based upon Blade's work product or not; and Blade's liability solely extends to the cost of its work product. This report is sensitive and confidential and contains confidential information that is intended only for the one or more individual(s) or entity(ies) for whom Blade prepared this report.

Version Record

Version	Issue Date	Issued As/ Type of Version	Authors	Checked By	Project Leader
0	August 24, 2023	Final	NA, RLR, NC, GA, PS, RM, KG, SK, MG, PC, RMK	RMK, DBL, PB	RMK

Table of Contents

1 Executive Summary 13
2 Introduction 17
3 Root Cause Analysis Approach 20
3.1 Phase 1: Data Collation and Analysis 20
3.2 Phase 2: Casing Extraction and Metallurgical Assessment 22
3.3 Phase 3: Root Cause Analysis 28
4 Rager Mountain Gas Storage Wells 30
4.1 Field Operations 32
4.2 Wells Summary 33
4.3 Well #2244 37
4.4 Prior Major Incidents 43
5 Equitrans Internal Procedures 45
5.1 Storage Integrity Management Program (SIMP) 45
5.2 Risk Assessments 51
5.3 Summary 52
6 Logging Data and Analysis 53
6.1 Summary of Rager Mountain Logs 53
6.2 Overall Summary of Integrity 65
7 Failure Analysis 68
7.1 #2244 7 in. Casing Failure Events and Sequence 68
7.2 Corrosion Analysis 115
7.3 Conclusions 151
8 Connection Testing 152
8.1 Background 152
8.2 Connection Testing 154
8.3 Results 158
8.4 Conclusions 168
9 Top Joint Corrosion Mechanism 169
9.1 Annulus Valve Height Survey 169
9.2 Well Surface Drainage Analysis 170
9.3 Integration and Interpretation 175

10 Magnetic Integrity Logging Limitations 177
10.1 Laser Scan Data vs. HR Vertilog (#2251 and #2248) 177
10.2 Corrosion Profiles in Well #2244 180
11 Internal Corrosion Threat 182
11.1 Logging Results 182
11.2 Corrosion Modeling 187
11.3 Implications 191
12 Well #2244 Flow Rate Analysis 193
12.1 Flow Path Models 196
12.2 Flow Path Calculations 199
13 Well #2244 Well Kill Discussion 202
13.1 Kill Operations Summary 202
13.2 Kill Modeling 203
13.3 Kill Analysis Conclusions 213
14 Gas Migration 217
14.1 Noise Logs 217
14.2 Gas Migration Discussion 218
14.3 Implications 220
15 Root Cause Analysis 222
15.1 Root Cause Analysis Process Background 222
15.2 Root Cause Analysis Results 224
15.3 Root Causes 242
15.4 Solutions 243
16 Mitigation 245
17 Nomenclature 248
17.1 Abbreviations and Acronyms 248
18 References 250
19 Appendices 254
Appendix A Detailed Information 255

List of Figures

Figure 1: Well #2244 (George L. Reade #1) Gas Leaking Through the Annulus Valve 17
Figure 2: Well #2244 Wellbore Schematic 19
Figure 3: Well #2248 Wellbore Schematic Post Top Joint Replacement 26
Figure 4: Well #2251 Wellbore Schematic Post Top Joint Replacement 27
Figure 5: Rager Mountain Field Map 31
Figure 6: Rager Mountain Gas Storage Inventory 32
Figure 7: Rager Mountain Daily Injection/Withdrawal Rates 33
Figure 8: Timeline for each Well, Workover (WO), and Major Events 34
Figure 9: Location of the Surface Casing (SC), Production Casing Size, Locations and Year of Casing Replacement (R-YYYY) by Well 35
Figure 10: Maximo Inspect Well Work Order for #2244, October 26, 2022, No Anomalies 38
Figure 11: Well #2244 DEP Inspection Remarks on October 26, 2022 [Reference DEP] 40
Figure 12: Well #2244 Venting Gas Out the Annulus Valve 41
Figure 13: Well #2244 Wellbore Schematic 42
Figure 14: Rational for Open Annulus (Vent) Valves (Yellow Highlight), Corrosion Mechanism (Blue Highlight), Mitigation (Green Highlight), SIMP 2005 47
Figure 15: Rager Mountain Logs by Type 53
Figure 16: Number of Joints, Class 2, Class 3, and Class 4, 2016 (Reprocessed) and 2022 HRVRT Logs 55
Figure 17: Count of HRVRT (>20%) Internal and External Metal Loss Defects, 2016 and 2022 56
Figure 18: Signal Analysis of Well #2244's HRVRT Log—2016 Original Processing (above) and 2016 Reprocessed (below) 57
Figure 19: Comparison of HRVRT Logs, Top Joints, #2244 (2016-reprocessed, top), #2248 (2022, middle), and #2251 (2022, bottom) 58
Figure 20: Location and Severity of Metal Loss, 9 5/8 in. Casing, #2244, March 13, 2023 62
Figure 21: #2244 Metal Loss from HRVRT Logs, 9 5/8 in. (2023, Left), 7 in. (2016, Right) 64
Figure 22: Timeline of Logging Activity 67
Figure 23: C001A Extraction 68
Figure 24: C001B Extraction 69
Figure 25: As-Received Condition of C001A and C001B Specimens 69
Figure 26: Photo of Axial Rupture and Parting of Joint C001 Rotated Approximately 180° 70
Figure 27: Paper Reconstruction of C001A (Downward Facing: a, b, c) and C001B (Upward Facing: d, e) 71
Figure 28: Completed Paper Reconstruction of Joint C001 Showing the Missing Failure Piece (white area) Rotated Views ~90° 71
Figure 29: (a) C001B and C001A Fracture Fragments Showing Location of Axial Rupture in C001A, (b) Crack Direction in Axial Rupture, and (c) Measurement of Axial Rupture Length 72
Figure 30: Axial Rupture Fracture Surfaces (a) C001A-1, (b) C001A-2, and (c) Upper Turning Point. 72
Figure 31: C001A-1 Axial Fracture Surface (a) Dashed Line Showing Cutting Location, (b) Protected Fracture Surface, and (c) After Cutting of Axial Fracture Surface C001A-1 73
Figure 32: Thickness Measurements Along the Axial Rupture in (a) C001A, (b) C001A-1, and (c) C001A-2 74
Figure 33: Plot of Thickness Measurements in C001A-1 Relative to the Upper Turning Point Location (Bottom of Figure 32b) 74
Figure 34: (a) Location of Thinnest Regions in C001A-1 and C001A-2 and (b) Matching Axial Fracture Surfaces 75

Figure 35: Stitched Stereoscope Image of C001A-1 Fracture Surface 75
Figure 36: Stitched Stereoscope Image of C001A-2 Fracture Surface 75
Figure 37: Features Observed on C001A-2 OD and ID Surfaces 76
Figure 38: Crack in the Upper Turning Point of C001A-2, Seen in both OD and ID Surfaces 76
Figure 39: Specimens Cut from C001A-2 77
Figure 40: Cut Specimens from C001A-1 77
Figure 41: Stitched Stereoscope Images of (a) C001A-1A and (b) C001A-2A Axial Rupture Fracture Surfaces 78
Figure 42: Stereoscope Image of C001A-1A Fracture Surface 78
Figure 43: Stitched SEM Image of C001A-1A Fracture Surface Region 1 79
Figure 44: SEM Images of Area 1 in C001A-1A Fracture Surface Taken at (a) 100x, (b) 500x, (c) 1,000x, and (d) 2,500x 79
Figure 45: SEM Images of Area 2 in C001A-1A Fracture Surface Taken at (a) 100x, (b) 500x, (c) 1,000x, and (d) 2,500x 80
Figure 46: Stitched SEM Image of C001A-1A Fracture Surface Region 2 80
Figure 47: SEM Images of Area 3 in C001A-1A Fracture Surface Taken at (a) 100x, (b) 500x, (c) 1,000x, and (d) 2,500x 81
Figure 48: Stitched SEM Image of C001A-1A Fracture Surface Region 3 82
Figure 49: SEM Images of Area 4 in C001A-1A Fracture Surface Taken at (a) 100x, (b) 500x, (c) 1,000x, and (d) 2,500x 82
Figure 50: Comparison of Fracture Surface Features in C001A-1A (a, b, c) and N80 Base Metal Tensile Specimen Fracture Surface Micro-Void Coalescence Features (d, e, f) Imaged at 500x, 1,000x, and 2,500x 83
Figure 51: Features in the OD of C001A-1A Imaged at (a) 500x, (b) 1,000x, and (c) 2,500x 83
Figure 52: Specimens for Metallography 84
Figure 53: Metallographic Images of C001A-1A2 Near the Fracture Surface, Etched in 2% Nital 84
Figure 54: Metallographic Images of C001A-1A2 Away from the Fracture Surface, Etched in 2% Nital 85
Figure 55: Location of Hardness Indentations 85
Figure 56: (a) Cut Specimens from C001A-1B, (b) Stereoscope Image of the Fracture Surface in C001A-1B1 and C001A-1B2 86
Figure 57: Representative SEM Images of C001A-1B Fracture Surface Taken at (a) 100x, (b) 500x, (c) 1,000x, and (d) 2,500x 87
Figure 58: Different C001A-2A Regions Examined in the SEM 87
Figure 59: SEM Image of C001A-2A Fracture Surface (Regions 1 to 4, from Top to Bottom) 88
Figure 60: Representative SEM Images in C001-1A (a) Region 1, (b) Region 2, (c) Region 3, and (d) Region 4 89
Figure 61: Region Used in Mating C001A-1A and C001A-2A Fracture Surfaces 90
Figure 62: Mating of C001A-1A and C001A-2A Fracture Surfaces 90
Figure 63: Opened Crack in Sample C001A-2B 91
Figure 64: C001A-2B1 and C001A-2B2 Fracture Surfaces 91
Figure 65: Attempted Mating Features in C001A-2B1 and C001A-2B2 92
Figure 66: High Magnification SEM Images of Area 2 in C001A-2B1 After Cleaning Taken at (a) 500x and (b) 1,000x 92
Figure 67: SEM images of 2244-C001A-2B1 Crack Face. SEI image (a) and SEI with EDS sulfur overlay (b) at 35x 93
Figure 68: 2244-C001A-2B1 Crack Face Raman and EDS Sulfur Map 93
Figure 69: Specimens Containing Circumferential Fracture Surfaces 95

Figure 70: Thickness Measurements along the Circumferential Fracture Surface of C001B-1 and C001A 95
Figure 71: Circumferential Fracture Surfaces from C001A and C001B-1 96
Figure 72: Circumferential Fracture Surface (a, b) 45° Shear and (c) Shear Lip 96
Figure 73: Stitched Stereoscope Image of C001A-1 Circumferential Fracture Surface 97
Figure 74: Stitched Stereoscope Image of the Step in Circumferential Fracture Surface in C001A 97
Figure 75: Stitched Stereoscope Image of Circumferential Fracture Surface in C001B-1 98
Figure 76: Circumferential Fracture Surface in C001A-1A Specimen 99
Figure 77: Cracks Observed in C001A-1A ID Surface and OD Surface 99
Figure 78: Circumferential Fracture Surface Excised from C001A 100
Figure 79: Areas of Examination in the C001A-4A Specimen 101
Figure 80: Stitched SEM Images of C001A-4A (OD Surface at the Top of the SEM Image) 102
Figure 81: SEM Images Taken from Areas 1 to 5 in C001A-4A at 100x and 500x Magnification 102
Figure 82: a. C001A-3B Cut Specimens, b. C001A-3B1 Fracture Surface, and c. C001A-3B3 Fracture Surface 103
Figure 83: SEM Image of the Fracture Surface in C001A-3B1 103
Figure 84: Stitched SEM Images of C001A-3B3 104
Figure 85: SEM Images Taken from Areas 1 to 5 in C001A-3B3 at 100x and 500x Magnification 104
Figure 86: Specimens from C001A-3A and C001A-3C 105
Figure 87: Representative SEM Images taken from C001A-3A1 (a, b), C001A-3C2 (c, d), and C001A-3C3 (e, f) at 100x and 500x Magnification 105
Figure 88: Orientation of Thickness Profile Used for Burst Pressure Estimation 107
Figure 89: Wall Thickness Profile along the Axial Rupture 107
Figure 90: Schematic of Wall Thinning Observed in Well #2244 Joint C001 108
Figure 91: Results of Failure Pressure Calculation 109
Figure 92: API 579 Level 3 – Material Specific FAD and Tearing Instability Analysis 110
Figure 93: Two-Dimensional Sequence Map 114
Figure 94: Three-Dimensional Sequence Map 115
Figure 95: Creaform HandySCAN 700 Scanner, Positioning Dots, and Laser Lines 116
Figure 96: C001B Areas Protected During Abrasive Blasting 117
Figure 97: 3D Color Map of Corrosion Analysis Results for C001B-2. Arrow Indicates Downhole Flow Direction 118
Figure 98: 360° Views Around C001B-2A 119
Figure 99: 360° Views Around C001B-2C 119
Figure 100: Maximum Wall Loss in C001B-2A, Dashed Line Indicates Masked Region 120
Figure 101: Corrosion Features in C001B-2A 121
Figure 102: Corrosion Features in C001B-2C 121
Figure 103: Corrosion Features in C001B-2E-1 121
Figure 104: Laser Scan Rendering of C002B 122
Figure 105: Shallow Corrosion Observed on C002B 122
Figure 106: Laser Scan Rendering of C005B 123
Figure 107: Deepest Corrosion in C005B 123
Figure 108: External Corrosion Distribution for Well #2244 124
Figure 109: C001 Joint from Well #2248 Before and After Cutting 125
Figure 110: Laser Scan Rendering of Well #2248 Joint C001-A and C001-C 126
Figure 111: External Corrosion Distribution for Well #2248 C001 126
Figure 112: Corrosion Features Observed in Well #2248 C001-A and C001-C 127
Figure 113: C001 Joint from Well #2251 Before and After Cutting 128

Figure 114: Laser Scan Rendering of Well #2251 Joint C001-A and C001-C 128
Figure 115: External Corrosion Distribution for Well #2251 C001 129
Figure 116: Corrosion Features Observed in #2251 C001-A 129
Figure 117: Corrosion Features Observed in #2251 C001-C 130
Figure 118: Example of OD Surface Scale and Deposit Collection and Bagging 130
Figure 119: Bulk XRD Mineralogy of Surface Scale Collected from (a) #2244, (b) #2248 and #2251 131
Figure 120: OD Casing Material Samples for EDS and Raman Spectroscopy 132
Figure 121: SEM Image of OD Casing Material Samples 134
Figure 122: Casing Sample #2244-C001B-2B1, Loc 1 &2 Raman and Average EDS, High Contaminant 135
Figure 123: Casing Sample #2248-C001B-1, Loc 1, Two Lasers, Raman and Average EDS, High S 135
Figure 124: Casing Sample #2251-C001B-1A, Loc 1, Raman and Average EDS, High Contaminant, High Cl 136
Figure 125: Corrosion Features Observed in the Top Joint of Well #2244 139
Figure 126: Common Morphologies Associated with MIC 140
Figure 127: General Corrosion Observed in the Oil and Gas Industry 140
Figure 128: Polarization Curves for N80 and J55 in Synthetic Groundwater 142
Figure 129: Corrosion at the Top Joint Adjacent to the Casing Slip 143
Figure 130: Corrosion Rate of Carbon Steel in Various Oxygen Levels 145
Figure 131: pH of Groundwater with Varying Amounts of Dissolved Oxygen 145
Figure 132: Corrosion Rate of Carbon Steel in Groundwater with CO_2 at Various Temperatures 147
Figure 133: Corrosion Rate of Carbon Steel in Groundwater with CO_2 and Dissolved Oxygen 148
Figure 134: #2244 Joint C001B a. Top Portion Covered with Thick Scale, b. Bottom of C001B Cut End 149
Figure 135: Top Joint from Wells #2248 (a, b), #2251 (c, d), and #2254 (e, f) 150
Figure 136: Casing Cutter on C002 152
Figure 137: API 8 Round (a) Thread Elements and (b) the Effects of Tension [56] 153
Figure 138: Leakage Capacity Estimation Process [55] 153
Figure 139: Single Gas Boot Example 154
Figure 140: Connection C002A and C007A 155
Figure 141: C007A Flow Rate Versus Time for Low and High Flow Rate Tests 156
Figure 142: C007A Cumulative Volume Versus Time for Low and High Flow Rate Tests 156
Figure 143: Interior Views of the Leak Test Structure 157
Figure 144: Connection C008A Leak Test 159
Figure 145: Connection C019A Leak Test 159
Figure 146: Connection C007A Single Boot 160
Figure 147: Double Boot for C007A 161
Figure 148: Connection C007A Mill Makeup Side 161
Figure 149: Connection C007A Field Makeup Side 162
Figure 150: Hoop Stress Versus Internal Pressure 163
Figure 151: Longitudinal Stress Versus Internal Pressure 163
Figure 152: Torque Turn Unit 164
Figure 153: C002A Torque Turn Plot 165
Figure 154: C007A Torque Turn Plot 165
Figure 155: C008 Torque Turn Plot 166
Figure 156: C019A Torque Turn Plot 166
Figure 157: Connection C007A Pin Threads 167

Figure 158: Galling on C008A Pin Threads 167
Figure 159: Well #2254, Annulus Valve Height Measurements, March 25, 2023, Open Side (Left) and Pressure Fitting Side (Right) 169
Figure 160: Well #2244 Wellhead, Tree, Annulus Valve at Various Dates [DEP] 171
Figure 161: Well #2248 December 10, 2020, Left; October 26, 2023, Middle and Right [DEP] 171
Figure 162: Well #2251 Dates Clockwise from Top Left, 2/13/2020, 12/10/2020, 9/22/2021, 10/26/2022 [DEP] 172
Figure 163: Well #2254 Laser Level Survey 172
Figure 164: 10 ft x 10 ft Drainage Surveys for Nine Rager Mountain Wells, High Spot (Yellow), Low Spot (Blue) 174
Figure 165: Material Found in the Annulus 175
Figure 166: Laser Scan (A) and HRVRT (B) Data for the Top Joint of Well #2248 178
Figure 167: HRVRT Versus Laser Scan Data for Wells #2248 (Top) and #2251 (Bottom) 179
Figure 168: Corrosion Profiles for Well #2244 180
Figure 169: Laser Scan Depiction of the Corrosion on #2244, #2248, and #2251 as a Function of Depth 181
Figure 170: Internal Corrosion, Well #2245 183
Figure 171: Internal Corrosion, Well #2246 184
Figure 172: Shut-in Pressures for all Wells, Including the Observation Wells. 185
Figure 173: Internal Corrosion, Well #2253 186
Figure 174: Internal Corrosion—HRVRT Log Compared with Caliper for #2253-July 2023 Logs 187
Figure 175. OLI Model – Brine without Bicarbonate – for Corrosion Rate Calculation 189
Figure 176. Corrosion Rate and pH as a Function of Temperature—Brine without Bicarbonate 190
Figure 177. OLI Model – Brine with Bicarbonate – for Corrosion Rate Calculation 190
Figure 178. Corrosion Rate and pH as a Function of Temperature – Brine with Bicarbonate. 191
Figure 179: Well #2244, Raw Signal with Grey Scale and Flux Lines Showing the Internal Defect at around 7,618 ft. 192
Figure 180: Annulus Valve 193
Figure 181: Flow Rate Estimate Paths 194
Figure 182: Well Test Report—PLT Injection Gas Distribution 196
Figure 183: #2244 Well Test Report—Falloff Summary 197
Figure 184: #2244 Well Test – Falloff Match 197
Figure 185: #2244 Well Test – Gradient Traverse 198
Figure 186: Rager Well #2244 Flow Rate Estimates during Blowout 201
Figure 187: Well #2244 Kill Model and Summary of Assumptions 206
Figure 188: Kill Attempt #1 Simulation Result – FWHP in psi vs. Cumulative Pumped Volume 209
Figure 189: Kill Attempt #2 Simulation Results – Normalized FWHP vs. Cumulative Pumped Volume 210
Figure 190: Kill Attempt #3 Simulation Results – Normalized FWHP vs. Cumulative Pumped Volume 211
Figure 191: Field Data Provides Better Input for Simulated Pump Ramp Up During Kill 212
Figure 192: Kill Attempt #4 Simulation Results – FWHP vs. Cumulative Pumped Volume 213
Figure 193: Noise Log Comparison for Well #2244, #2251, and #2248 217
Figure 194: Noise Log Comparison for Well #2248 218
Figure 195: Exponent Rager Conceptual Site Model 219
Figure 196: Rager Mountain Well and Sampling Locations 220
Figure 197: Causal Set 223
Figure 198: Casual Flowchart Development 223

Figure 199: Causes of the Primary Effect 225
Figure 200: RealityCharting Root Cause Analysis Flowchart 226
Figure 201: Ruptured 7 in. Casing Causes 227
Figure 202: 7 in. Casing in Contact with Hydrocarbon Gas with CO_2 and Water 228
Figure 203: Presence of Organic and Inorganic Matter in the Annulus 229
Figure 204: Gel Not Added to the Annulus 230
Figure 205: Wells Not Identified for Gelling 231
Figure 206: Gelling Decision Delayed 232
Figure 207: Open Annulus Valve 233
Figure 208: 7 in. Casing in Contact with Oxygen from Air and Water 233
Figure 209: 7 in. Casing in Wet–Dry Water Cycles 234
Figure 210: No Mitigation of Top Joint Corrosion 235
Figure 211: Lack of Insight into Top Joint Corrosion Rate 236
Figure 212: Lack of Insight into Top Joint Corrosion Rate 237
Figure 213: 7 in. Casing is a Single Barrier 238
Figure 214: Well #2244 was Killed in 14 Days 239
Figure 215: Well #2244 Kill Attempt November 17, 2022 239
Figure 216: Well #2244 Kill Attempt November 14, 2022 240
Figure 217: Well #2244 Kill Attempt November 11, 2022 241
Figure 218: November 19, 2022, Success Kill, Other Causes 242
Figure 219: Baker Hughes 2001 Logging Summary for Well #2244 277
Figure 220: Baker Hughes 2016 Logging Summary for Well #2244 278
Figure 221: #2244, #2245, #2246, #2247 286
Figure 222: #2248, #2249, #2250, #2251 287
Figure 223: #2252, #2253, #2254, #2255 288
Figure 224: #2245 HR Vertilog 2016 (Above) and 2022 (Below) 289
Figure 225: #2246 HR Vertilog 2016 (Above) and 2022 (Below) 289
Figure 226: #2247 HR Vertilog 2016 (Above) and 2022 (Below) 290
Figure 227: #2248 HR Vertilog 2016 (Above) and 2022 (Below) 290
Figure 228: #2249 HR Vertilog 2016 (Above) and 2022 (Below) 291
Figure 229: #2250 HR Vertilog 2016 (Above) and 2022 (Below) 291
Figure 230: #2251 HR Vertilog 2016 (Above) and 2022 (Below) 292
Figure 231: #2252 HR Vertilog 2016 (Above) and 2022 (Below) 292
Figure 232: #2253 HR Vertilog 2016 (Above) and 2022 (Below) 293
Figure 233: #2254 HR Vertilog 2016 (Above) and 2022 (Below) 293
Figure 234: #2255 HR Vertilog 2016 (Above) and 2022 (Below) 294
Figure 235: Laser Scan Data and HRVRT Data, Well #2248 295
Figure 236: Laser Scan Data and HRVRT Data, Well #2251 296
Figure 237: Top Joint of #2251, Laser Scan Data (A), HRVRT Insight Viewer (B) 297
Figure 238: Microstructure Along the Longitudinal Orientation (a, b) and Transverse Orientation (c, d) Taken at 200x (a, c) and 400x (b, d) 306
Figure 239: Higher-Magnification SEM Image of N80 Specimen Taken at 15 KV (a, b, c) and 2 KV (d) Accelerating Voltage 307
Figure 240: N80 Etched in Super Picral Showing Microstructure Along a. Longitudinal Orientation and b. Transverse Orientation 308
Figure 241: ASTM E23 CVN Specimen Dimensions 311
Figure 242: (a) ASTM E1823 Crack Plane Orientation [64] and (b) API 5CT CVN Orientations [65] . 312

Figure 243: Ductile Brittle Transition Temperature Curve Using Fracture Energy Values of Half-Size a. Longitudinal and b. Transverse Specimens..... 312
Figure 244: Ductile Brittle Transition Temperature Curve Using Percent Shear Values of Half-Size a. Longitudinal and b. Transverse Specimens..... 313
Figure 245: Dimensions of the SENB Specimens Used in the Fracture Toughness Test..... 315
Figure 246: J-R Curves for the Tests Performed at 70°F and 40°F..... 315

List of Tables

Table 1: #2244 Workover Summary to Recover and Replace Casing..... 22
Table 2: Casing Joints Recovered from #2244..... 24
Table 3: Casing Joints Recovered from #2248 and #2251..... 25
Table 4: Casing and Joint Replacement Wells..... 36
Table 5: Well Name Cross Reference..... 36
Table 6: Summary of Equitrans' Maximo Records for #2244..... 37
Table 7: Well #2244 Shut-in Pressures from Maximo Records..... 39
Table 8: #2244 Pre- and Post-Leak Event Timeline Summary..... 43
Table 9: Sequence of Events During Well #2245 Fire Incident in 1972..... 44
Table 10: Sequence of Events During Well #2246 Blowout in 1990..... 44
Table 11:Storage Integrity Management Program Logging, Threshold for Action, and Gelling..... 48
Table 12: Pre-incident Logs by Well and Type..... 54
Table 13: HRVRT Comparision of Deepest Top Joint Defects, 2016 Reprocessed and 2022..... 59
Table 14: Neutron Temperature Log Observations from 2016 and 2022/2023 and Annulus Pressure..... 60
Table 15: HRVT Joint Summary for 9 5/8 in. Casing, March 13, 2023..... 62
Table 16: Microhardness Measurements in C001A-1A2 and C001A-1A3..... 85
Table 17: List of Pipe Attributes and Material Properties Used in the Critical Length Calculation..... 110
Table 18: Ductile Tearing Instability Analysis of Assumed Circumferential Lengths and Depth..... 111
Table 19: Manual Verification of Wall Thickness..... 118
Table 20: Average EDS Surface Chemistry of OD Casing Material Samples..... 132
Table 21: Casing Slips Composition..... 142
Table 22: Groundwater Concentration [41]..... 143
Table 23: Average Gas Composition in Rager Mountain [46]..... 146
Table 24: Carbon Steel Corrosion Rate in Groundwater Mixed with Gas..... 146
Table 25: Carbon Steel Corrosion Rate of Groundwater with Dissolved Oxygen and Mixed with Gas..... 148
Table 26: Test Sequence..... 158
Table 27: Recommended Torque Values..... 164
Table 28: Torque Turn Results..... 165
Table 29: Height of Annulus Valves Above Ground Level..... 170
Table 30. Gas Samples Collected from Rager Mountain Wells [59]..... 188
Table 31. Concentration of the Chemical Constituents in Equitrans Rager Mtn. Pond [60]..... 188
Table 32. Reconciled Gas Composition..... 189
Table 33. Reconciled Brine Composition..... 189
Table 34. Reconciled Brine Composition..... 190
Table 35: Remaining Wall Thickness by Year Based on Bicarbonate Corrosion Model Predictions. 191
Table 36: Rager Well #2244 Storage Gas Composition During Blowout..... 195
Table 37: Rager Well #2244 Annulus Pressure vs. Time..... 195

Table 38: Rager Well #2244 Drainage Area Average Pressure During Blowout 195
Table 39: Rager Well #2244 Flow Path 1 Calculations 199
Table 40: Rager Well #2244 Flow Path 2 Calculations 199
Table 41: Rager Well #2244 Flow Path Differences 200
Table 42: #2244 Cudd Daily Reports Summary 202
Table 43: Coiled Tubing Dimensions (from the free end to the core end) 204
Table 44: Kill Fluid Viscosities at Kill Rate 205
Table 45: List of Identified Kill Attempts and Respective Driving Parameters 207
Table 46: Calibration of Blowout Model Preceding Kill Simulations 208
Table 47: Sensitivity Analysis Results Showing Failed and Successful Kill Scenarios as Well as Estimated Pump Pressures Necessary to Achieve a Kill on November 11, 2022. 215
Table 48: Sensitivity Analysis Showing the Minimum Kill Rate Necessary to Stop Different Rates of Influx from the Reservoir. 216
Table 49: Rager Mountain Field Pre-injection Mitigation Recommendations 246
Table 50:Rager Mountain Field Long Term Corrosion Management 247
Table 51: Pre-Incident Well Operations Records for Well #2244 (Chronological Order) 257
Table 52: Pre-Incident Maintenance Records (Maximo) for Well #2244 (Chronological Order) 263
Table 53: Rager Mountain Logs (Chronological Order) 268
Table 54: Summary of Baker Hughes Assessments, 1996 – 2016 279
Table 55: A.8 DEP Office of Oil and Gas Management Inspection Document Review -Equitrans 299
Table 56: A.8 DEP Office of Oil and Gas Management Inspection Document Review -Peoples Natural Gas 304
Table 57: Composition of N80 Material from Well #2244 and API Specification Limits in Wt% 305
Table 58: Hardness Measurements Using Vickers 10 kgf Load 308
Table 59: Hardness Measurements Using Vickers 0.5 kgf Load 309
Table 60: Results of Flattening Tensile Test 309
Table 61: Results of Round Bar Tensile Test 310
Table 62: Results of Critical Strain Determination Using Round Bar Specimen 310
Table 63: Toughness Values at Various Impact Temperatures 312
Table 64: Percent Shear at Various Impact Temperatures 313
Table 65: Fracture Toughness Results Summary 315

1 Executive Summary

The Rager Mountain Gas Storage field in Cambria County, Pennsylvania, is currently operated by Equitrans, L.P. (Equitrans). The storage field has 12 wells, including two monitoring wells. The discovery well (#2244) was drilled in 1965. Four more wells were drilled between 1965 to 1968. These wells were completed in the Huntersville Chert and Oriskany formations. In 1971, the field was converted from a conventional gas production field to a gas storage field. Peoples Natural Gas Company (PNG) operated the field from 1965 to 2013, and Equitrans has operated Rager Mountain since 2013.

On November 6, 2022, at approximately 3:30 pm, well #2244 experienced an uncontrolled hydrocarbon release through the annulus valve on the surface casing. Equitrans initiated their Storage Well Emergency Response Plan (SWERP) after immediately recognizing the incident and mobilized the well control company personnel, who arrived before midnight on November 6, 2022.

Early in the well control operation, the team estimated the gas blowout rates, conducted kill modeling, and prepared for operations with the available equipment. Initial analysis showed that 2 in. OD coil tubing (CT) might be sufficient to kill the well and was immediately available. A parallel effort to procure a 2 3/8 in. CT was also undertaken.

The first kill attempt on November 11, 2022, tagged a shallow obstruction, and the second kill was attempted on November 14, 2022. The CT was run to bottom, but the kill pump rate was inadequate. These two 2 in. CT runs provided valuable information on the location of the casing failure and allowed the team to ensure access to the bottom of the well. On November 14, 2022, the 2 3/8 in. CT was procured.

The third kill attempt on November 17, 2022, with 2 3/8 in. CT was successful. However, the fluid loss rate accelerated beyond the fluid that was available, and the well restarted flowing. The Equitrans and well control team identified the possibility that #2244 would consume significant amounts of brine and was ready with at least six brine tanks. However, that proved to be insufficient, and having additional brine available would have been logistically impractical. Consequently, during the fourth kill attempt on November 19, 2022, isolation plugs were set, bringing the well under control.

Following the successful control of well #2244, Equitrans retained Blade Energy Partners (Blade) to conduct a root cause analysis (RCA) of the uncontrolled hydrocarbon flow from well #2244. The Blade RCA team consisted of subject matter experts (SMEs) in several disciplines including metallurgy, failure analysis, well construction, well logging, reservoir, chemistry, and microbiology.

Blade undertook a systematic evidence-based approach to the RCA by dividing the process into three broad phases.

The first phase was focused on data collation and analysis. This included extensive discussions with various Equitrans teams that included personnel from senior management, Integrity, Operations, and Gas Systems. Equitrans provided extensive historical records of drilling, completion, workovers, logging, maintenance, and inspection records for all Rager Mountain wells. Equitrans exhibited transparency across the organization during the root cause process as Blade endeavored to collect relevant data from senior management, engineering, operations, and field personnel. Blade had access to key team members and records.

At Blade's request, Equitrans' contractors conducted diagnostic logging for some of the Rager Mountain wells for noise, temperature, cement condition, and casing condition. Equitrans also provided a broad range of procedural and process documents, including the Equitrans standard operating and emergency procedures, field and well guidelines, storage integrity management documents, and risk assessments.

The second phase focused on collecting and analyzing physical evidence. Blade, in conjunction with Equitrans and its contractors, extracted relevant casing joints and samples from wells #2244, #2248, and #2251. Blade had full access to all the Rager Mountain wells for site visits and casing examination.

Careful planning, safety studies, detailed procedures, extreme care, and custom storage and transportation solutions were employed to avoid damaging the evidence. Additional data was collected during site surveys of all wells. Blade performed a detailed holistic failure analysis incorporating metallurgical assessment, quantitative scale, and microbiological samples evaluation.

The third and final phase was the RCA. Blade utilized the Apollo RCA methodology [1] that integrated logging, drilling/completion/workover analysis, well deliverability and kill attempts, failure analysis, metallurgical observations, microbiological assessment, internal and external standards and procedures, regulatory guidelines, Equitrans discussions, etc.

The uncontrolled hydrocarbon release occurred because of the 7 in. casing failure in well #2244 resulted from direct and root causes. Direct causes, including contributing ones, are those that, if identified and prevented, would eliminate the occurrence of #2244 type events. Root causes are those that, if identified and prevented, would eliminate a #2244 type incident and other well integrity incidents with procedures, best practices, design, and management systems.

The direct cause for the 7 in. top joint casing rupture and parting failure was external corrosion due to ingress of water, air (oxygen), and organic/inorganic matter through the open annulus valve, which was further exacerbated by a leaking connection into the uncemented annulus.

The root causes for the #2244 uncontrolled release of hydrocarbon gas were:

- The 7 in. casing was a single barrier to the hydrocarbon gas.
- The open annulus valve allowed the ingress of fluids (water, air, organic and inorganic matter) and evaporation. This situation resulted in the rise and fall of the annulus liquid level in a wet-dry cycle, exacerbating corrosion.
- The top joint corrosion mechanism was not mitigated by gelling the annulus. The internal Storage Integrity documents discussed gelling but lacked specificity and triggers to mitigate production casing external corrosion.
- The surveillance logging (a trailing indicator) was considered adequate for top joint corrosion monitoring and follow-up mitigation. Despite replacing the top joints in multiple Rager Mountain wells, no evidence was provided that the corrosion *mechanism* was investigated or examined by the previous operator, PNG.
- The 2016 #2244 HRVRT log underestimated the corrosion wall loss. Magnetic logging tool technology, the best available for gas wells, has limitations with its ability to assess uniform corrosion and associated pitting or localized corrosion.

During the 14 days of uncontrolled release, the cumulative gas volume lost from the formation was estimated to be 1.164 billion cubic ft (BCF). However, due to the ID restriction of the annulus valve, the cumulative gas egress to the atmosphere was estimated to be 1.037 BCF. The remaining gas volume of 0.127 BCF was diverted to one or two permeable zones at approximately 1,794 ft and/or 3,000 ft. This was established using PROSPER modeling based on historical well test and pressure data.

Blade analyzed and modeled the kill attempts, reviewed documentation from Equitrans and the well control company, interviewed all parties, and concluded that the kill operation was effective and well executed, and the well was successfully controlled within 14 days.

Equitrans, PNG, and the Pennsylvania Department of Environment Protection (DEP) inspected each well site monthly and reported no annulus gas over the past 30 years. However, a month after well #2244 was successfully under control, the presence of annulus gas was recorded and measured. Two wells, #2248 and #2251, exhibited annulus gas post blow out. The annulus gas was measured, monitored, and analyzed. The source of the annulus gas was identified to be the blowout gas sequestered into a permeable zone and/or from other shallow hydrocarbon zones.

Future well integrity is not compromised by the presence of annulus gas; assuming the annulus is isolated from the aqueous environment and is gelled. Well #2248 requires a tubing-packer completion because the production casing did not pass a mechanical integrity test. Well #2251 passed the pressure test but data suggests communication between the casing and annulus. Options to mitigate the casing leak need to be evaluated to return the well to gas storage service; and if the mitigation is not effective, then a tubing-packer completion remains an option.

Wells #2244, #2248, and #2251 are in a safe condition with deep plug barriers and can be suspended in the current state while plans for these wells are finalized. Field injection can be safely restarted in other wells when certain pre-injection mitigation steps are completed. These include annulus valve modification, annulus gelling, and certain wells batch treated for internal corrosion.

Based on a detailed review of documents and data, it is apparent that Equitrans has a strong focus on safety, environment, and well integrity. The risk assessment process and the Storage Integrity Management Plan (SIMP) procedures are consistent and exceed API 1171, PHMSA, and DEP requirements.

However, based on the well #2244 rupture and subsequent hydrocarbon release, actions and solutions exist that would mitigate the identified root causes and prevent a reoccurrence of well integrity incidents at Rager Mountain.

The following solutions will prevent a reoccurrence of an incident similar to #2244 and prevent other well integrity incidents:

- Gelling should be a routine maintenance action that is intended to manage annuli corrosion independent of the surveillance logging results. Surveillance logging should be used to confirm that the gelling is effective. There should be clear accountability for well integrity decisions. The current organizational structure provides for this.
- Identify all possible threats to the wells and the field and develop an individual threat management plan for each well.
- Modify the annulus valve arrangement to install a relief valve, gel the annulus, monitor annulus pressure, and consequently mitigate the top joint *corrosion mechanism* at the Rager Mountain facility.
- Perform corrosion (internal/external) analysis, establish corrosion rates, and mitigate where possible; then use corrosion rates to establish a logging frequency based on the corrosion mechanism and rates, and the casing strength and loads.
- Evaluate tubing and packer completions as a solution for wells where the production casing has integrity challenges that cannot be otherwise mitigated.

The following solutions may not directly eliminate root causes but will further strengthen the well integrity program, and in some cases ensure appropriate implementation of some of the solutions listed above.

- To deal with external surface casing corrosion at Rager Mountain, evaluate and implement external cathodic protection when appropriate for surface casing to protect it from aquifer or groundwater corrosion.

- To further improve the response to blowout events, establish a well control plan that has individual well deliverability for all Rager Mountain wells and identifies ranges of kill fluid densities, pump rates and a logistics plan for equipment and other resources.
- To provide effective decision making for well integrity, establish a cross-functional team consisting of Operations, Well Integrity, and Gas Systems.
- To address downhole integrity challenges effectively, obtain additional well integrity resources to analyze all logging data beyond the logging vendor assessment for trends and changes over time and identify additional corrosion mechanisms and other threats for mitigation.
- To maintain information on the wells, develop up-to-date wellbore schematics with details of the casing size, weight, grade, and connection, etc., and the completion depth by well. Make available a directional survey for each well for relief well planning.
- To ensure integrity of new wells, designs should include cementing to the surface for all casing strings and metal-to-metal connections for tubing and casing exposed to gas. Blade has reviewed the Equitrans Design and Construction Standard that already calls for cementing casing strings to surface.

Once all the Rager Mountain wells have the modified annulus valve arrangement and the annuli have been gelled, the field will be ready for reinjection. Internal corrosion should be mitigated, especially for #2245, #2246, and #2253 through batch treatment, and will require a HRVRT log by the end of 2025. Equitrans is planning to drill out the plugs in #2244 and inspect the internal casing defects to ensure integrity.

2 Introduction

Equitrans operates the Rager Mountain gas storage field in Cambria County, Pennsylvania. The field is developed with ten injection-withdrawal wells and two observation wells. The field was converted from a gas field to a gas storage field in 1971. The average well depth is approximately 8,000 ft. Wells were completed with 7 in. and 5 1/2 in. casing.

Well #2244 had a leak on November 6, 2022, and natural gas was vented at surface through the 2 in. annulus ball valve. This valve accessed the 7 in. × 9 5/8 in. annulus. Figure 1 shows a picture of well #2244's wellhead and leaking gas. The well was killed on November 19, 2022.

Two flow-through plugs were run; the first plug failed to set and the second plug was set and stopped the flow. A cast iron bridge plug (CIBP) was set at 5,830 ft. A cement plug was set above the CIBP. The downhole plugs isolated the reservoir from the parted casing at the top of the well, stopping the leaking gas to the surface. Figure 2 shows the wellbore schematic post leak with the parted casing just below the wellhead that was found when the well was deconstructed as part of the RCA to recover the failed casing.

Figure 1: Well #2244 (George L. Reade #1) Gas Leaking Through the Annulus Valve

Blade was retained in early December 2022 to conduct a root cause analysis (RCA) for the #2244 well failure. The objective of the RCA was to mitigate and prevent all well integrity incidents at the Rager Mountain facility. As part of the RCA, the direct and contributory causes for the failure were identified first, followed by integrating all the data to identify the root causes.

This RCA report documents the work and analysis to determine the root causes of the casing failure. The document sections and titles are:

Section 1 Executive Summary

Section 2 Introduction

Section 3 Root Cause Analysis Approach

Section 4 Rager Mountain Gas Storage Wells

Section 5 Equitrans Internal Procedures

Section 6 Logging Data and Analysis

Section 7 Failure Analysis

Section 8 Connection Testing

Section 9 Top Joint Corrosion Mechanism

Section 10 Magnetic Integrity Logging Limitations

Section 11 Internal Corrosion Threat

Section 12 Well #2244 Flow Rate Analysis

Section 13 Well #2244 Well Kill Discussion

Section 14 Gas Migration

Section 15 Root Cause Analysis

Section 16 Mitigation

Section 17 Nomenclature

Section 18 References

Section 19 Appendices

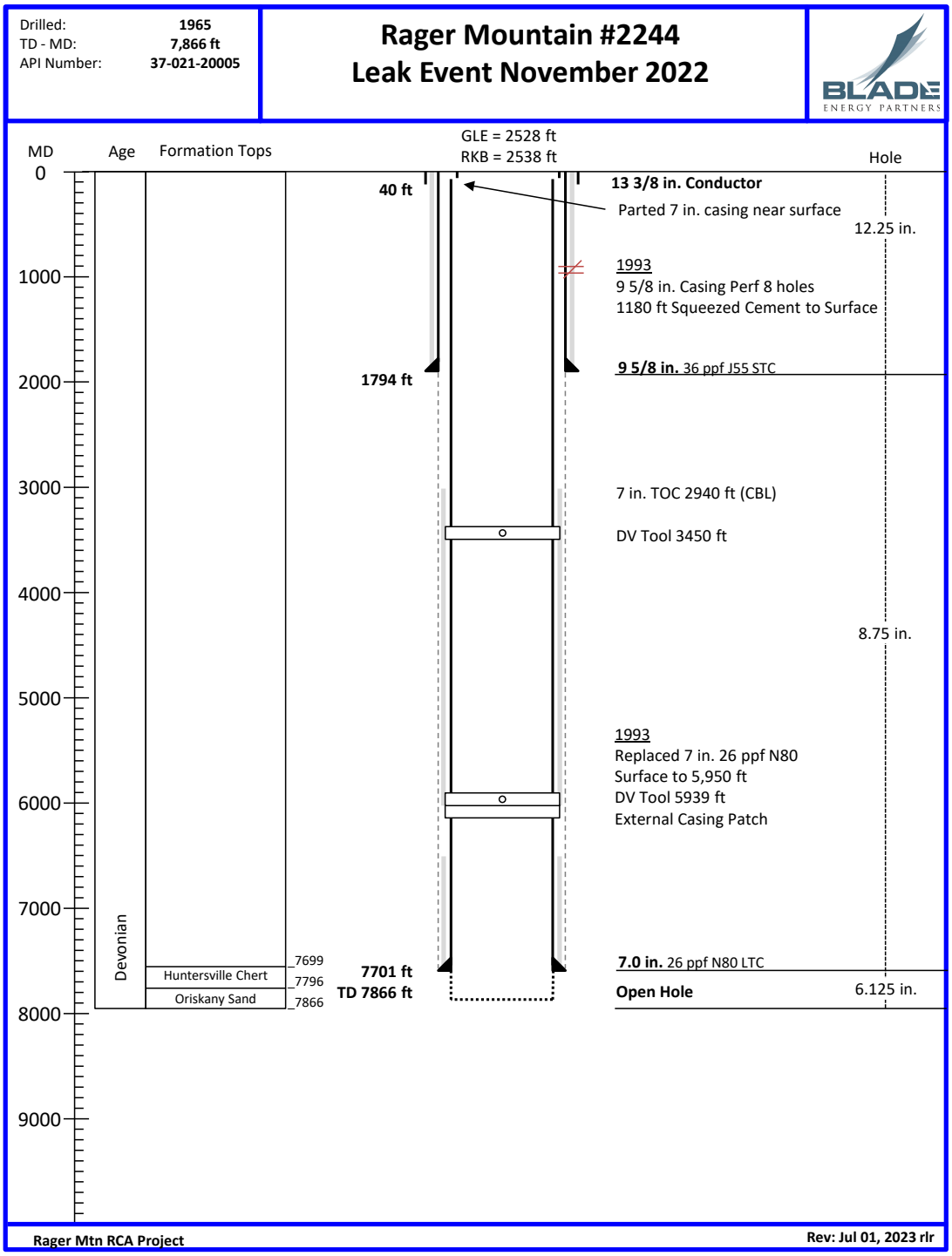

Figure 2: Well #2244 Wellbore Schematic

3 Root Cause Analysis Approach

The RCA approach was executed in three main phases:

- Phase 1: Data collection, collation (historical well and field, logging, fluid sampling, etc.), and analysis
- Phase 2: Failed casing extraction and metallurgical assessment
- Phase 3: Root cause analysis, documentation, and final report

The objective of this RCA project was twofold:

- To identify the direct and contributory causes for the storage well failure and thereby prevent such incidents in the future.
- To identify the root causes that, if identified and mitigated, will prevent all future well integrity incidents, including the leak incident, using updated procedures, best practices, design, and management systems.

3.1 Phase 1: Data Collation and Analysis

This phase focused on collecting relevant historical data and records, conducting interviews, followed by analyzing and assessing the data and information, as appropriate.

3.1.1 Data Collation

Equitrans provided a large amount of data that was useful for understanding the Rager Mountain Field operations and wells. The approximate volume of data provided was:

- More than 2,100 files
- More than 10 GB of data

Examples of the type of data files received and reviewed include:

- Drilling, completion, workover, and well servicing records, including the conversion to a gas storage well.
- Open hole and cased hole logs, casing inspection surveys, etc.
- Historical well and field pressure and surface temperature vs. time.
- Well integrity and well test data for the various wells in the Rager Mountain Field.
- Leak event well kill reports and data.
- Produced gas and water chemistry data.
- Standards and operational procedures for the field.

Blade conducted and attended numerous interviews and meetings with Equitrans staff, suppliers, field operators, and contract personnel in Pennsylvania regarding events related to the leak in #2244, and to clarify and follow up on the data provided.

When the Blade team returned to their home offices, numerous weekly and daily video conference calls were held in addition to weekly update meetings.

Examples include:

- The in-person project kickoff meeting in Canonsburg, PA.
- In-person HAZID and workover planning meetings in Canonsburg for wells #2244, #2248, and #2251.
- In-person meetings held in the Rager Mountain Field during casing extraction operations.
- Numerous calls to verify and collect facts and data related to the event timeline.
- Calls to understand how the wells and field were operated: the nature of the reservoir, injection/withdrawal history, pressure and temperature vs. time, historical corrosion issues, etc.
- Calls to review management of change, procedures, historical approach to integrity, etc.
- Calls to understand the field operations, technical, and operations support.
- Calls to understand the Equitrans and well control company response to the leak through their kill attempts, kill modeling efforts, kill logistics, etc.

Blade made recommendations for specific log runs in wells #2244, #2248, and #2251 and other wells in the field that were important to the RCA. The logging was carried out as requested by Blade. Examples of log and wireline work include:

- SLB isolation scanner.
- TGT Diagnostics Chorus high resolution noise and temperature.
- Reservoir fluid samples.
- Casing caliper.
- Downhole camera.

3.1.2 Analysis

Various subject matter experts performed analysis of the data:

- Corrosion logs were evaluated to estimate changes in casing wall thickness and condition between log runs in the same well.
- Noise and temperature logs were analyzed for several wells to determine if a correlation existed showing flow from the blowout well to other wells in the field.
- Corrosion modeling was conducted to estimate corrosion rates for various combinations of contaminants and water.
- Samples of casing material were tested for yield strength and for ductile-brittle behavior vs. temperature.
- Scale samples were collected and tested for corrosion compounds and bacteria to determine possible causes for casing corrosion.
- Made-up casing connections were cut from each joint of recovered casing and pressure tested to determine the leak resistance.
- Data from kill attempts were independently modeled to compare field data to model results.
- Modeling to assess the #2244 well deliverability and quantity of gas through the 2 in. valve.

3.2 Phase 2: Casing Extraction and Metallurgical Assessment

This phase focused on extracting the physical evidence and then conducting a detailed metallurgical/failure analysis.

3.2.1 Extraction

The crucial objective of extracting the 7 in. casing was to ensure that the condition was maintained as it was during the failure. The #2244 failure occurred shallow in the wellbore. The logging post failure provided data on the location and the type of failure. Blade made recommendations for logging that enhanced the available data. Logging tools included a casing caliper, ultrasonic inspection, and a downhole wellbore camera to develop a plan for extraction. The nature of the failure was characterized before extraction, and additional logging tools were considered during these examinations. The objective was to collect as much data as possible with the well intact and avoid the risk of damage to failed components caused by the extraction process.

Consequently, Blade made recommendations on how to recover the failed well components without any further damage by:

- Assisting in preparing procedures and protocols for well de-completion.
- Providing on-site assistance for the well de-completion process and recovery of failed components.
- Assisting in the preservation of failed equipment for on-site examination, additional inspection, and laboratory examination and shipment.

Extraction was a crucial step in the process and necessary to ensure the physical evidence provided the best insight into the events that led to the leak in the 7 in. casing.

Casing Recovery from #2244

A workover to recover the failed casing was conducted in March 2023. Blade assisted in the work plan to recover the casing and was onsite to assist. When the failed pieces of casing were recovered, Blade visually inspected and photo documented the pieces. Scale samples from the outside of the recovered casing were collected by Blade for laboratory analysis. The casing joints were carefully handled during the laydown process to avoid creating any marks or defects post recovery.

The failed casing and recovered casing joints were transported to a secure and dry location for further inspection, documentation, and packaging for shipment. The casing was cut at 1,488 ft and the joints were recovered, which included the parted top joint. Table 1 shows a summary of each day's operation to recover and replace the 7 in. casing in #2244.

Table 1: #2244 Workover Summary to Recover and Replace Casing

Report	Date	Operations Summary
1	Feb 24, 2023	Unbolted and removed the flow cross, wing valves, and crown valves. Moved the assembly in one piece to the compressor station. Unbolted the individual valves and components to inspect and photograph the inside of the components. Blade representatives witnessed the tree removal at the wellsite and disassembly at the auxiliary building.
2	Mar 2, 2023	Moved in Key Energy workover rig. Spotted rig over well. Rig up.
3	Mar 3, 2023	Rigged up. Removed the master valve. Transport the master valve to the auxiliary building for Blade.

Report	Date	Operations Summary
4	Mar 4, 2023	Loosen nuts on double studded packoff adapter (DSPA). Attempted to remove DSPA.
5	Mar 5, 2023	Cut the double studded packoff adapter (DSPA) studs. Removed the DSPA. Pulled the casing slips and packoff. Recovered the upper casing failed piece. Cut the 7 in. casing at 20.5 ft.
6	Mar 6, 2023	Recovered the lower part of the failed casing. Blade collected samples from the casing. Ran Schlumberger isolation scanner log. Made up spear for free pointing the casing.
7	Mar 7, 2023	Ran free point tool in the 7 in. casing. Casing is free below the 9 5/8 in. shoe at 1,794 ft based on stretch measurements. Rigged down Baker Hughes. Pick up cutter to cut the casing.
8	Mar 8, 2023	Ran casing cutter and cut the 7 in. casing at 1,475 ft. Pulled cutter. Circulated annulus fluid samples for Blade. Pulled casing to surface. Cut casing above the coupling. Laid down the casing.
9	Mar 9, 2023	Recovered and cut 21 joints of 7 in. casing. Visual inspection of the casing joints. Took samples from the casing OD. Total of 22 joints recovered.
10	Mar 10, 2023	The rig was shut down for poor weather conditions.
11	Mar 11, 2023	Pulled 11 joints + cutoff 7 in. casing joint. Shipped casing joints to the warehouse.
12	Mar 12, 2023	Ran EV Camera on Baker Hughes eline. Ran Baker Hughes 56-arm caliper log. Ran and pulled a 9 5/8 in. casing scraper to 200 ft and collected solids samples.
13	Mar 13, 2023	Ran casing scraper to 1,475 ft, circulated the well, and pulled out. Blade took solids samples from the scraper. Ran Baker Hughes HRVRT log, gamma ray-neutron-temperature log, and multi-finger caliper log.
14	Mar 14, 2023	Ran a Schlumberger isolation scanner log in the 9 5/8 in. casing from 1,470 ft to surface. Ran a dressing mill to dress the top of the 7 in. casing stub for tying back the casing using a casing patch.
15	Mar 15, 2023	Ran 7 in. 26 ppf N80 LTC casing and a casing patch. Circulated treated fresh water in the annulus. Picked up the last joint of casing and latched on to the casing stub with the casing patch.
16	Mar 16, 2023	Pressure tested 7 in. casing patch to 1,500 psi. Good test. Lifted BOP, installed slips. Cut off 7 in. casing. Installed seals. Installed double studded packoff adapter and master valve. Tested seals. Installed BOP and pressure tested.
17	Mar 17, 2023	Tripped in with a 7 in. casing scraper. Circulated and conditioned fluid. Pulled scraper.
18	Mar 18, 2023	RIH with Baker Hughes caliper log and HRVRT log. Logged from 4,655 ft to surface. Set RBP at 1,514 ft on wireline.
19	Mar 19, 2023	Swabbed approximately 55 bls of fluid from 7 in. casing.
20	Mar 20, 2023	Pressure tested the 7 in. casing with nitrogen to 3,600 psi.
21	Mar 21, 2023	Retrieved RBP. Rigged down. Final report.

Table 2 shows the joints of 7 in. 26 ppf N80 LTC casing recovered from #2244. The first joint was parted and recovered in two pieces. The casing was recovered from March 5 – 11, 2023. The lengths shown in the table are overall lengths. The joints were saw cut as the casing was pulled. Refer to document *Rager Mtn Well 2244 Handling Protocol Feb 23 2023.pdf* [2] for details of the casing handling, joint numbering, etc.

Table 2: Casing Joints Recovered from #2244

Joint ID	Length (ft)	Comments
C001A	2.63	Upper-parted casing joint
C001B	15.50	Lower-parted casing joint
C002	37.90	
C003	47.40	
C004	46.04	
C005	45.96	
C006	46.19	
C007	45.58	
C008	46.50	
C009	46.56	
C010	42.63	
C011	37.85	
C012	45.96	
C013	44.19	
C014	35.76	
C015	43.52	
C016	46.60	
C017	46.05	
C018	45.32	

Joint ID	Length (ft)	Comments
C019	47.24	
C020	47.25	
C021	47.17	
C022	47.27	
C023	45.60	
C024	46.52	
C025	37.25	
C026	45.90	
C027	35.58	
C028	34.63	
C029	46.33	
C030	45.71	
C031	45.08	
C032	46.17	
C033	46.54	
C034	35.77	
	1,468.15	Total footage

Casing Recovery from #2248 and #2251

Casing was recovered from #2248 and #2251 as part of the RCA. The top of cement in these two wells was near the surface. After cutting and removing sections of the top joint, a wash shoe and wash pipe was used to clean out the annulus cement to allow running a casing patch to connect the cut casing back to the wellhead at surface.

Table 3 shows the joints of 7 in. casing recovered from #2248 and #2251. The #2248 casing was recovered on March 26, 2023, and the #2251 casing on April 3, 2023.

Table 3: Casing Joints Recovered from #2248 and #2251

#2248 Joint ID	Length (ft)	Comments
C001	11.74	Cut and pulled section of casing
C002	17.05	Washed over section of casing

#2251 Joint ID	Length (ft)	Comments
C001	13.13	Cut and pulled section of casing

Figure 3 and Figure 4 show the respective wellbore schematics for wells #2248 and #2251.

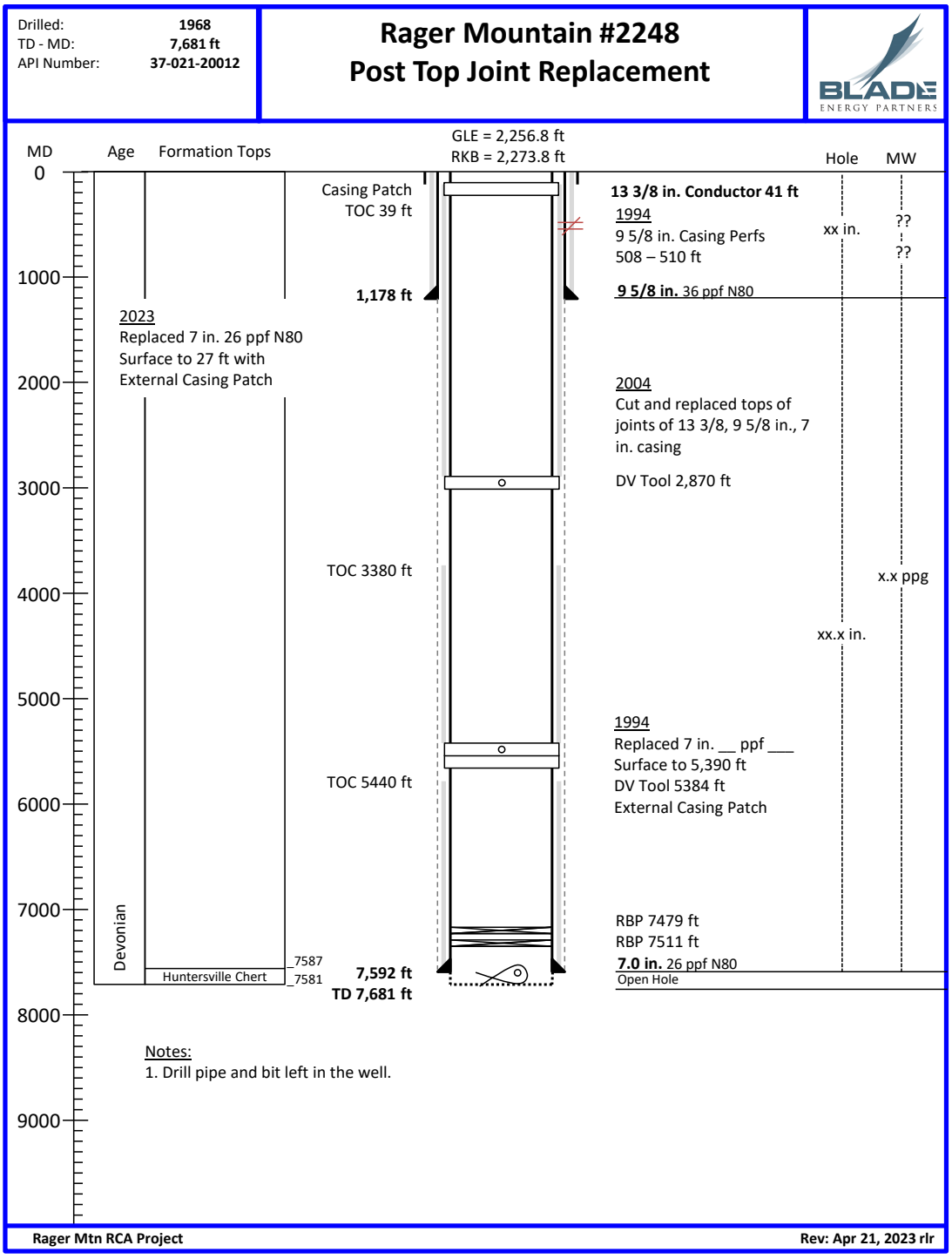

Figure 3: Well #2248 Wellbore Schematic Post Top Joint Replacement

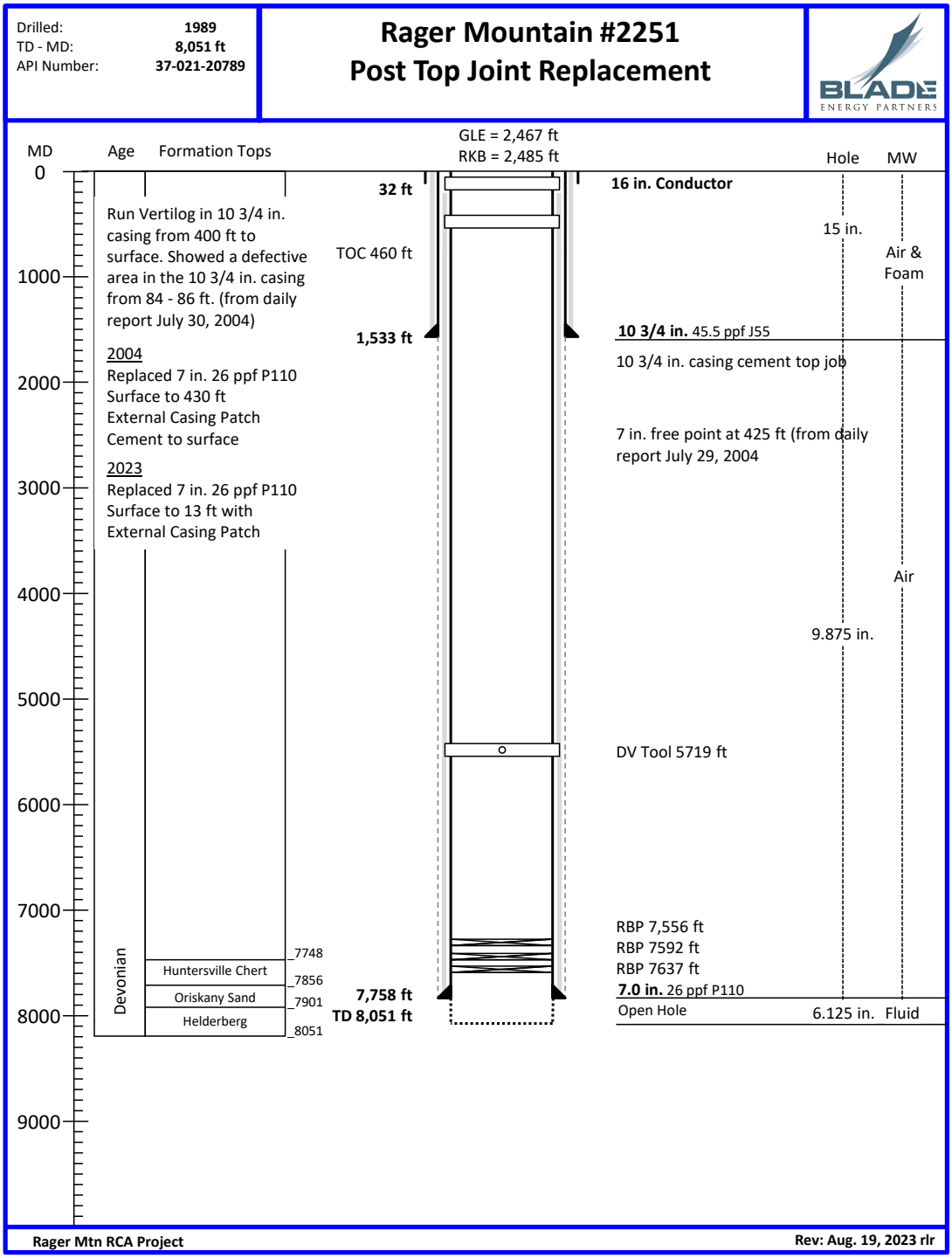

Figure 4: Well #2251 Wellbore Schematic Post Top Joint Replacement

3.2.2 Metallurgical/Failure Analysis

Blade was present during the extraction of the #2244 7 in. casing from the wellbore and provided guidance on operations to ensure minimal extraneous damage. After extraction, the samples were prepared for storage before evaluating the failed sample. Extraction and preservation procedures were defined before field operations started.

When the sample was available at the laboratory, the following metallurgical examination methodology was followed:

- Overall examination of the sample and conduct non-destructive examination (NDE) methods such as magnetic particle inspection (MPI) and ultrasonic testing (UT) shear wave to characterize all anomalies.
- Examination of local scale and other corrosion products using X-ray diffraction or Raman spectroscopy. Before cleaning in a laboratory region, localized regions were assessed for clues to the corrosion causes at the leak location. For example, the presence of CO_2 will indicate iron carbonate presence.
- Stereo-microscopic examination of smaller regions excised from the leak region. The specimens were examined in detail using optical microscopes. Sections of the failed areas were analyzed and sectioned as needed to conduct a more detailed study. Initiation and growth of the failure defect was carefully evaluated.
- Scanning electron microscopy to examine the fracture surface or the corrosion surface to understand the morphology of the damage. Such an examination was crucial to identifying the mechanism of corrosion, cracking, or other forms of damage.
- Characterization of the base material for chemistry, mechanical properties, fracture mechanics properties, and other parameters as a function of temperature (producing and shut-in). In addition, any local variation in properties was characterized.
- Examination of metallurgy and fractures to characterize them quantitatively through corrosion or fracture mechanics models to ensure they were consistent with interpretations and conclusions.
- Microbiological assessment of solids and fluids collected from well #2244 and other wells (#2248, #2251, and #2254).

3.3 Phase 3: Root Cause Analysis

Root cause analysis is a systematic process for identifying the root causes of problems or events and defining methods for responding to and preventing them. A major incident or failure rarely derives from a single cause; therefore, a systematic process that is supported by data, evidence, and technical analysis is necessary to identify the true underlying problems that contributed to the event, rather than just the symptoms.

The RCA process includes:

- Analysis of historical data, records, and data obtained from interviews.
- Analysis of company internal standards and procedures versus industry, federal and state regulatory, and commonly adopted guidelines.
- Failure analysis of #2244—an assessment of the nature of corrosion on casing from #2248 and #2251. This includes evaluation of the annulus water chemistry, microbiological evaluation, gas composition, etc.
- Sequence and timeline of the failure.
- Analysis of all new logs from all wells and correlations to existence of corrosion, movement, if any, of gas/liquid.
- Analysis and review of well gas flow rates during the leak event and kill attempts.

The goal of an RCA is to analyze situations or events to identify:

- What happened.
- How it happened.
- Why it happened.
- What actions are needed to prevent reoccurrence.

Many different methods and philosophies exist for conducting an RCA, such as 5-Whys, Fish-Bone Diagram, Fault Tree, Management Oversight, and Risk Tree Analysis, depending on the industry and type of problems investigated. However, most use preconceived or pre-defined categories of causes. Blade used the Apollo Root Cause Analysis (ARCA) approach because it is a structured, evidenced-based process that makes no assumptions about possible causes [1].

Blade used the ARCA companion RealityCharting software to develop a cause-and-effect chart, identify the root causes, and develop solutions. This methodology has been used in the energy, chemical, and aerospace industries. For example, Blade used this methodology during the Aliso Canyon root cause analysis process. Blade conducted an RCA for the Aliso Canyon storage well casing failure that occurred in October 2015.

Blade integrated the results of Phases 1 and 2, then applied the RCA process to identify solutions that will lead to the root cause analysis and ensure the prevention of well-integrity incidents in the future.

4 Rager Mountain Gas Storage Wells

The Rager Mountain natural gas storage field is in Jackson Township, Cambria County, Pennsylvania. The field is south of Highway 22 and west of Dishong Mountain Road. Refer to Figure 5.

The field was converted from a producing gas field to gas storage in 1971. The annual injection season is approximately May – October and withdrawal from November – April. Gas is purchased and transported via pipeline to the Rager Mountain compressor station, where the gas is injected in the ten injection/withdrawal (I–W/D) wells. The Rager Mountain Field is completed with ten I–W/D wells and two observation wells.

The field discovery well (well #2244) was drilled in 1965, and the field was developed by adding four additional wells. Additionally, two wells were drilled around the time of conversion in 1971 to gas storage, and five wells were drilled between 1989 and 2011. The Peoples Natural Gas Company (PNG) drilled and operated all of the wells. Field ownership and operatorship was transferred to Equitrans in 2013.

The well depths range from 7,681–8,100 ft with casing set near the top of the gas storage reservoir. The wells were completed with 7 in. and 5 1/2 in. outside diameter (OD) casing. The wells have open hole completions in the Huntersville Chert and Oriskany formations below the casing shoe.

Figure 5 shows a map of the wells and compressor station. The field reservoir structure lies in a generally southwest to northeast orientation. Well #2244, the casing failure well marked with a red circle, is southwest of the compressor station. The #2244 well was the discovery well drilled in 1965. The original well name was G.L. Reade et al. #1. Wells #2247 (most northeast well) and #2246 (most southwest well) are pressure observation wells. The approximate distance between the two observation wells is 4.2 miles.

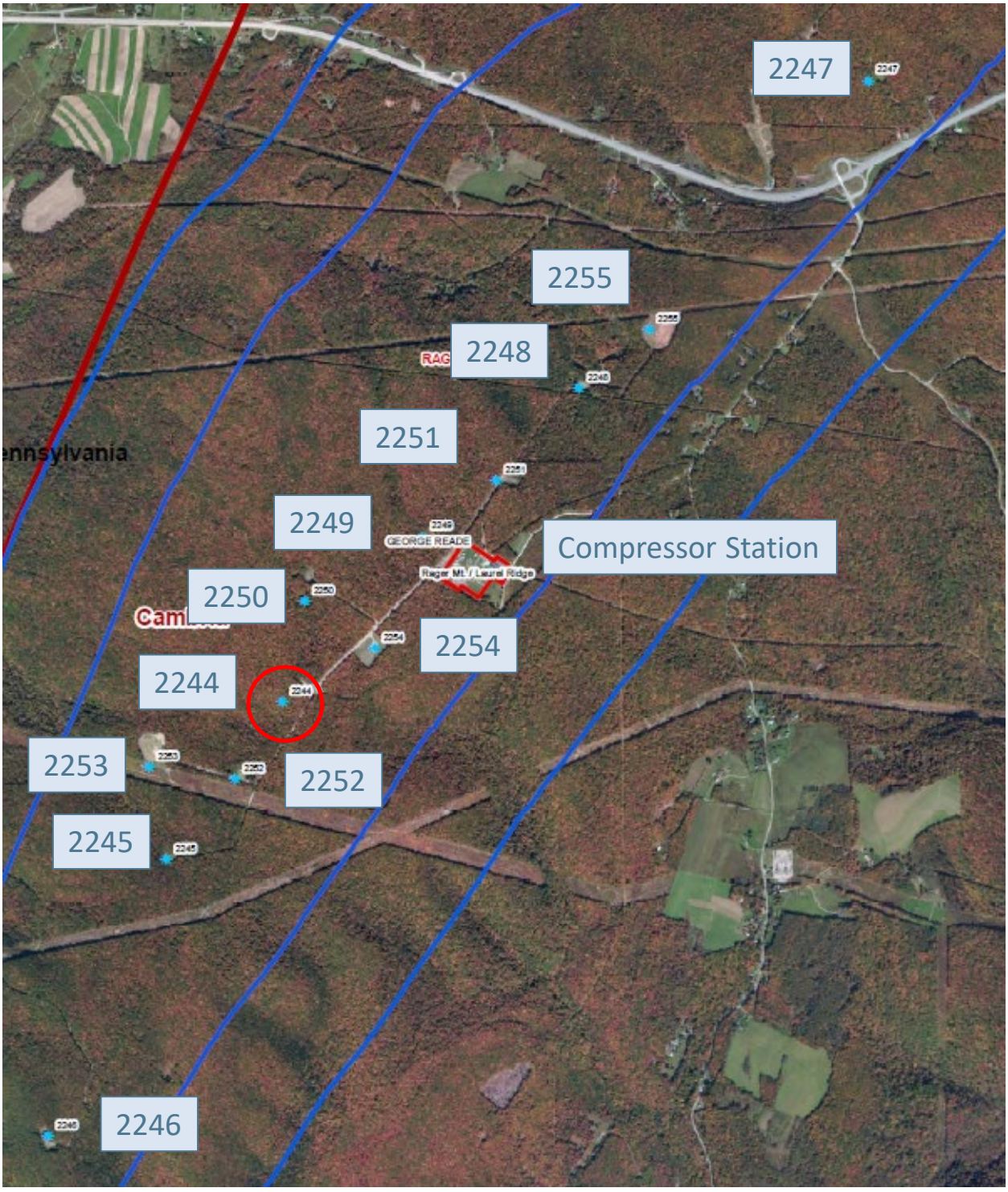

Figure 5: Rager Mountain Field Map

4.1 Field Operations

The field is operated by injecting gas annually from approximately May through October, the months of low demand, and withdrawing gas during the months of November through April to meet market demand. The typical cyclic field storage inventory for Rager Mountain is between 11.5 BCF and 5.5 BCF as shown in Figure 6.

The wells produce some water when the gas is being withdrawn. Water production has been a problem in the past. Water production was studied in 2017 and resulted in recommendations to bring the wells on-line in stages to reduce water production. Water production by well is not measured. Water removal occurs at the compressor station using a separator and dehydration units. The produced water is dumped into a catch pond and disposed offsite.

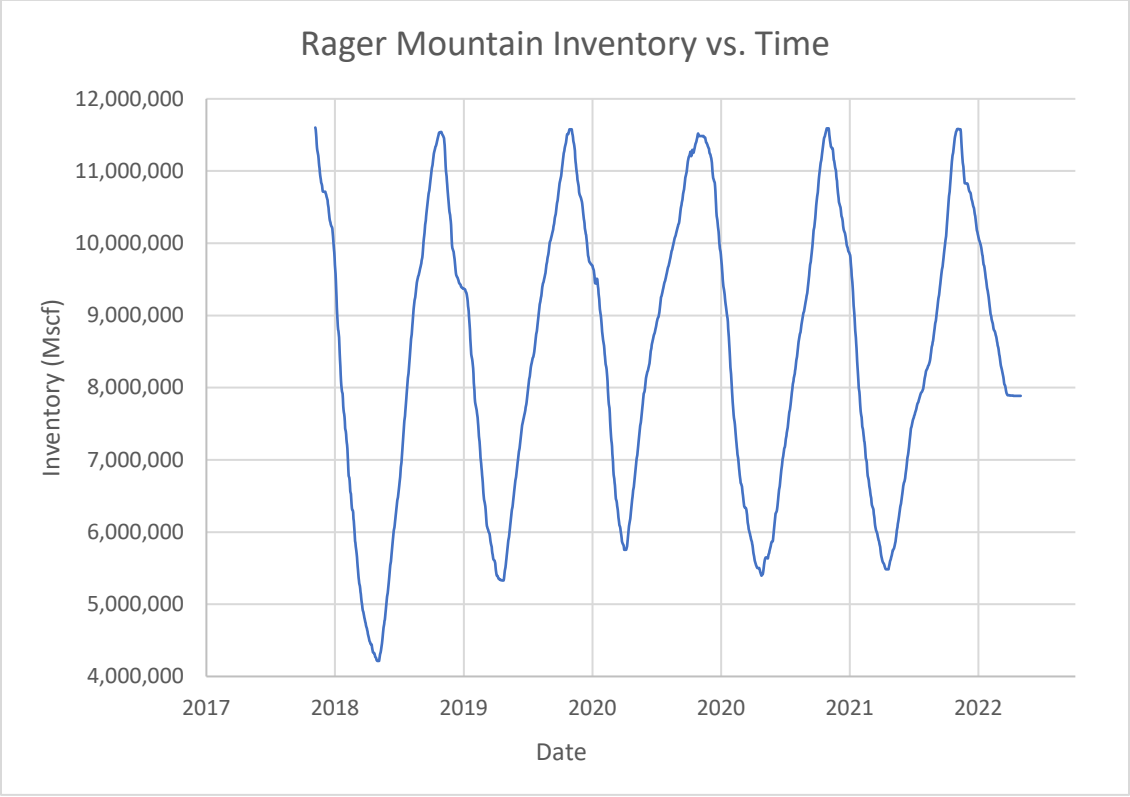

Figure 6: Rager Mountain Gas Storage Inventory

Figure 7 shows the historical daily rate of injection and withdrawal. Values above zero rate are injection rates, and negative rates indicate gas withdrawal. Maximum withdrawal rates approach 100 MMscf/D (million standard cubic feet per day) with a few rate excursions greater than 120 MMscf/D. Maximum daily injection rates are approximately 60 MMscf/D.

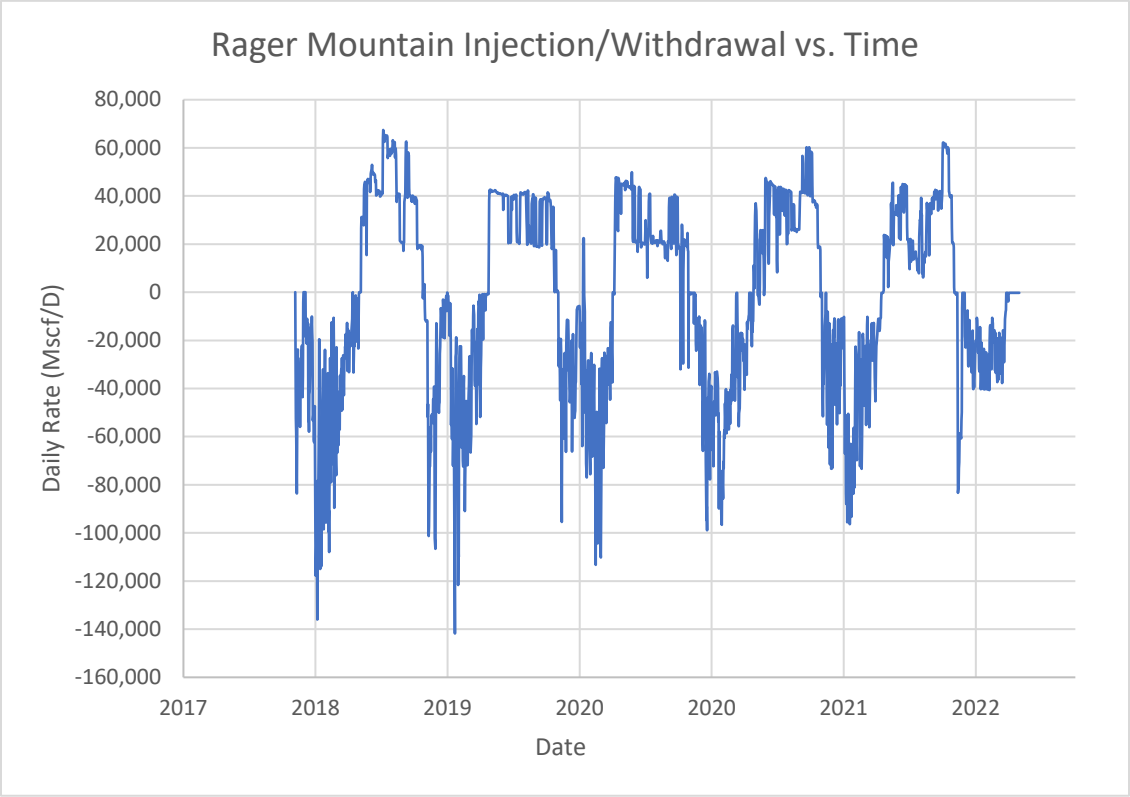

Figure 7: Rager Mountain Daily Injection/Withdrawal Rates

4.2 Wells Summary

Figure 8 shows the timeline of Rager Mountain well drilling and workover. The left edge of the blue bars corresponds to the spud date, which is the date drilling commenced. Workovers are denoted by "WO". The well names are listed on the y-axis, and the date in two-digit year is on the x-axis. All wells were drilled, and all the workovers were performed prior to Equitrans ownership in 2013. Of the 12 wells, 5 wells were drilled as gas producers prior to the conversion to gas storage in 1971, and 7 wells were drilled for gas storage operations. Appendix A.1 shows the casing size, weight, grade, and depths, as well as drilling fluid and DV (diverter valve cement stage) tool information.

The wells have no significant design differences. A minor difference is that two wells have 5.5 in. production casing, while the rest of the wells have 7 in. production casing. Eleven workovers were performed on seven wells. Five wells did not have workovers. Major events are denoted by red letters. Fire is denoted by "F", and blowout is denoted by "B". Well #2245 experienced a surface fire in 1972. More details are included in Section 4.4.1. The #2246 blowout is discussed later in Section 4.2.1.

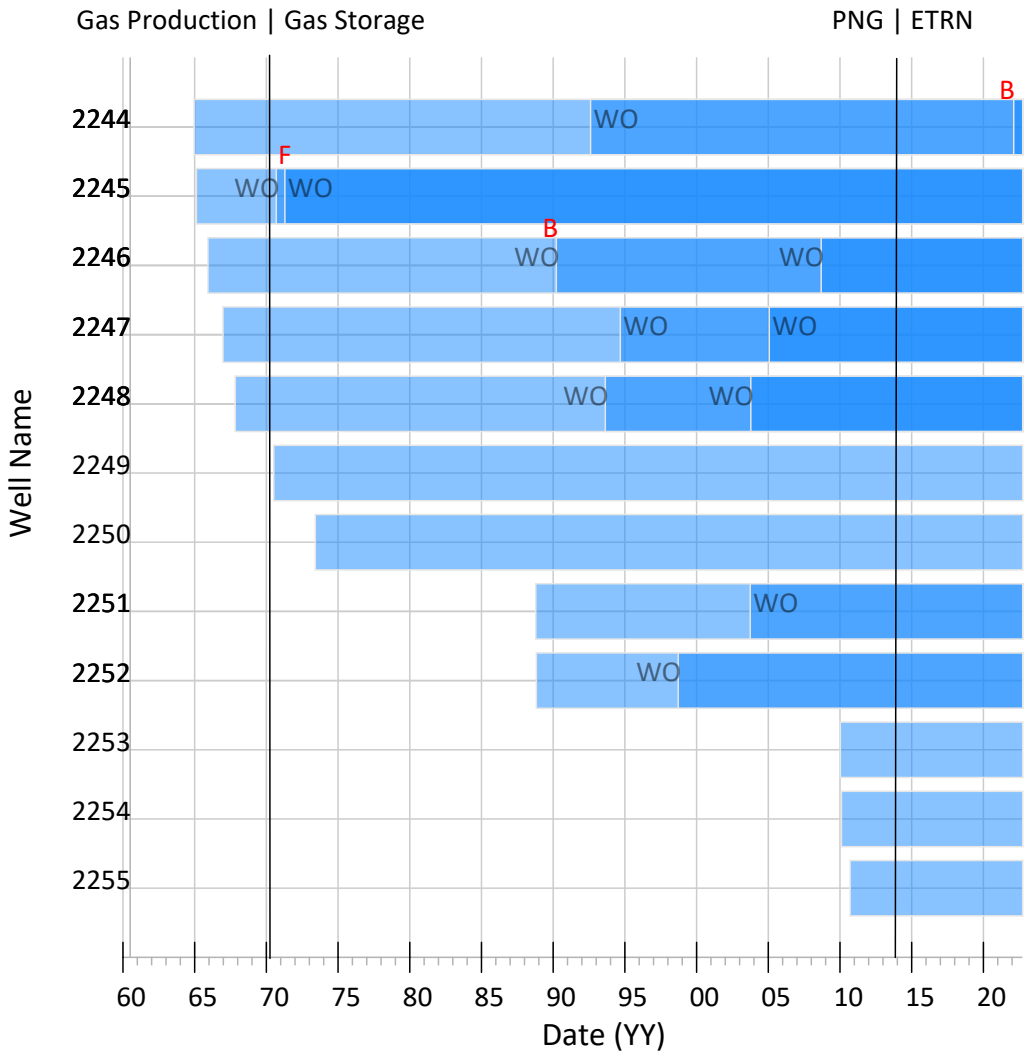

Figure 8: Timeline for each Well, Workover (WO), and Major Events

Figure 9 shows the location of the replaced casing related to these workovers. The y-axis shows the depth in feet. The x-axis shows the well name. Surface casing depth is denoted by "SC". The depth and type of production casing is denoted by 7 in. or 5.5 in. The letter "R" represents the location where the casing was replaced and is followed by the year of replacement. Two wells, #2245 and #2246 have 5.5 in. production casing. The rest of the wells have 7 in. production casing.

In five wells, the casing was replaced down to approximately 4,000 – 6,000 ft. These workovers occurred primarily in the 1990's. The reason for these workovers was due to internal corrosion deep in the well, and in some cases, top joint corrosion. A casing failure at 5,117 ft in well #2246 was attributed to internal corrosion (Section 4.2.1); this resulted in a blowout and is denoted by the letter "B". The upper joint(s) of casing have been replaced in five wells during 1999 – 2009 and are primarily related to external corrosion.

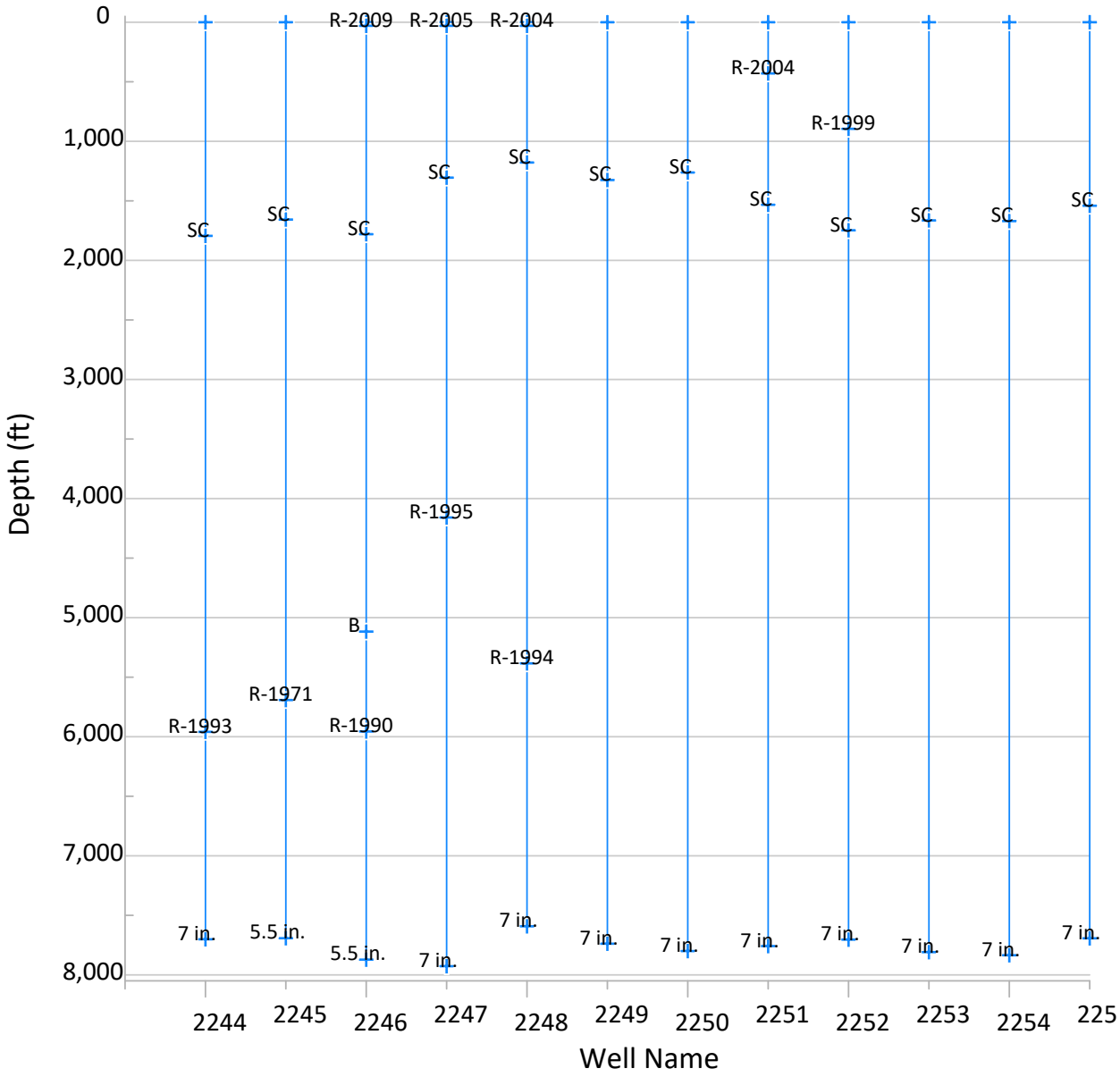

Figure 9: Location of the Surface Casing (SC), Production Casing Size, Locations and Year of Casing Replacement (R-YYYY) by Well

Several casing and joint replacements and workovers in the Rager Mountain Field were reported prior to November 2022. Table 4 shows a summary of workovers where casing and top joints were replaced. Daily report records were available for some of the work, while some work was inferred from less formal sources. Records showing the condition of the casing that was pulled were not available. It is unclear whether the top joint corrosion was ever examined, nor whether any corrosion analysis was performed.

Table 4: Casing and Joint Replacement Wells

Well	Year	Casing OD	Workover Summary
2245	1971	5.5 in.	Cut and pulled 5 1/2 in. casing at 5,692 ft. Ran a casing patch and DV tool and cemented to surface.
2246	1990	5.5 in.	Blowout up the annulus. Killed well. Milled outside the 5 1/2 in. casing at 5,117 ft. Pulled the casing and fished. Cut casing at 5,956 ft. Ran a casing patch and 2 stage tools. Cemented to surface.
2244	1993	7 in.	Cut and pulled 7 in. casing at 5,959 ft. Ran a casing patch and two DV tools. Cemented the first stage. Had problems with the second stage. Top of cement at 2,940 ft.
2248	1994	7 in.	Cut and pulled 7 in. casing at 5,384 ft. Ran a casing patch and two DV tools. Cemented to surface.
2247	1995	7 in.	Cut and pulled 7 in. casing at 4,159 ft. Ran a casing patch and DV tool. Cemented to surface.
2246	2001	5.5 in.	Log summary one page document with a handwritten note stating a top joint replacement in 2001.
2246	2009	5.5 in.	Replace the upper 13 3/8 in. and 8 5/8 in. casing by excavating, cutting, and welding. Cut and threaded the 5 1/2 in. casing and made up a new piece of casing. Daily reports not found. Invoices and tickets indicated the work was done.
2252	1996	7 in.	Hole in the 7 in. casing at 660 ft. Cut the 7 in. casing at 819 ft with a chemical cutter. Laid down the casing. Attempted to back off the casing at a connection below the cut, unsuccessful. Cut the casing at 894 ft and recovered the 7 in. casing. Ran a casing patch.
2248	2004	7 in.	Excavated around the wellhead. Replaced 9 ft of 13 3/8 in., 13 ft of 9 5/8 in., and 10 ft of 7 in. casing.
2247	2005	7 in.	Excavated and replaced the upper sections of the 13 3/8 in. and the 9 5/8 in. casing by welding. Bad spot in the 7 in. casing at 6 ft. Cut the 7 in. casing and threaded the stub. Made up new casing.

4.2.1 Well Names

The well names have changed throughout the years. Original well names were the lease name and well number. These evolved to a PNG well name and finally to an Equitrans well name. Table 5 shows the current Equitrans name and the historical well names that are used in the well records.

Table 5: Well Name Cross Reference

Equitrans Name	Spud Year	Original Name	PNG Name	DEP Name
2244	1965	Reade #1	4469	GEORGE L READE 1
2245	1965	Maude Emma Bole #1	4639-S	MAUDE EMMA BOLE ET AL 1
2246 (1)	1966	Charles Miller #1	4500	CHARLES MILLER 4500
2247 (1)	1967	Griffith #1	4538	GEORGE W GRIFFITH 1

Equitrans Name	Spud Year	Original Name	PNG Name	DEP Name
2248	1968	Johnstown Rod and Gun Club #1	4554-S	JOHNSTOWN ROD GUN CLUB 1
2249	1971	Reade #2	4676	GEORGE L READE 4676S
2250	1974	Reade #3	4845-S	GEORGE L READE 4845
2251	1989	PNG #1	5661	PEOPLES NATURAL GAS 1
2252	1989	Reade #4	5662	GEORGE L. READE 4
2253	2010	Reade #6	5674	READE 6
2254	2010	Reade #7	5673	READE 7
2255	2011	Johnstown Rod and Gun Club #2	5675	JOHNSTOWN ROD GUN CLUB 2
Notes:	[1] Observation well			

4.3 Well #2244

Section 4.2 shows an overall description of the wells. Section 4.3 contains additional information on the #2244 well. Appendix A.2, Table 51 shows a detailed recount of the historical daily well operations for the #2244 well. The dates in the table start from the spud date of September 12, 1965, to the wellhead replacement operation ending August 20, 2004.

4.3.1 Maximo Records

Equitrans uses a commercially available asset management software called IBM Maximo. Blade was provided with all maintenance records for the Rager Mountain wells—approximately 1,900 records. Appendix A.2, Table 52 shows the dates and work order descriptions for the #2244 well. Table 6 shows the overall summary of the #2244 work orders.

Blade reviewed the 163 work orders for well #2244. The first #2244 well inspection record was on December 18, 2013. The quantity of work orders for #2244 was similar to the other wells. The primary type of work order was “Inspect Well.” The specific activities for the well inspection were outlined in Equitrans’ Integrity Plans (discussed in Section 5) and Equitrans’ standard operating procedures.

Blade found a completed well inspection form for each month with no gaps. The details of the “AdHoc,” “General Operations,” “Echo Metering,” and other work orders were not included, but no anomalies were reported in the summary table. Equitrans has a Standard Operating Procedure (SOP) for gelling and information on gelling in their Storage Integrity Management documents, which are discussed in Section 5. No Maximo work order records were found for gelling in #2244 or any Rager Mountain wells. Equitrans confirmed that gelling was not performed at Rager Mountain. This is discussed in Section 6.1.5.

Table 6: Summary of Equitrans’ Maximo Records for #2244

Work Order Description	Number of Occurrences
Inspect Well – Rager Mtn – RAG2244 – (PNG4469)	107
GForms AdHoc – General WO	19
Shut-In Testing – Rager Mtn – RAG2244 – (PNG4469)	18

Work Order Description	Number of Occurrences
General Operations	5
Echo Metering – Rager Mtn – RAG2244 – (PNG4469)	4
GForms AdHoc – Field Investigation	4
GForms AdHoc – Surface Upkeep	1
General Operations Rager wells	1
Well Valve RAG2244, Isolation Test, I/W	1

Figure 10 shows details of the last #2244 pre-incident well inspection on October 26, 2022.

The well was said to be "in-line" (on injection), and the recorded pressure was 3,077 psi. This pressure matches other pressure readings from the same time. No leakage, vandalism, damage, observable (surface equipment) corrosion, or any other anomalies were reported on the October 26, 2022, inspection.

The annulus vent valves were open, and no gas was observed. This is consistent with the DEP inspector's report on the same day (as discussed in the section 4.3.2 and shown in Figure 11). The well was later visited on November 1, 2022, to shut-in the well. The plan was to end the shut-in period on November 7, 2022 [3].

WO Number Asset # Location	Description	Job Plan	Lead	Targ Start Date	Targ Comp Date	Act Finish	Site
3003439	Inspect Well - Rager Mtn - RAG2244 - (PNG4469)	JP1059	STRITTMATTERP	Oct 1, 2022	Oct 31, 2022	October 26, 2022	PA
137887	RAG2244						
000017	OPS-NORTH EAST						

Task	Description	Status
T2694496	Inspect well per SOP STR_OPS_Monthly_Inspection_of_Storage_Wells	COMP-P

Description	ALN Value	NUM Value	WO Spec ID	Asset Attribute	UM	Data Type
Record wellhead pressure		3077	18364331	A1522	PSIG	NUMERIC
Does well have a RTU?	NO		18364332	A747902		ALN
Record RTU Pressure. (Enter 0 if no RTU)		0	18364333	A747903	PSIG	NUMERIC
Is RTU within 10 PSI of well head pressure?	N/A		18364334	A747904		ALN
Record well status	In-Line		18364335	A1525		ALN
Was leakage detected on above-grade piping or fittings?	NO		18364336	A747905		ALN
If the well has an access road, is it functional?	Yes		18364337	A747906		ALN
Is well sign visible, with correct emergency number, and attached to well?	YES		18364338	A747907		ALN
Are valves on site secure?	YES		18364339	A747908		ALN
Are there any signs of damage/vandalism?	NO		18364340	A747909		ALN
Are there any new encroachments within 200 ft of the well?	NO		18364341	A1526		ALN
Is there evidence of progressive corrosion rusting or other signs of equipment deterioration?	NO		18364342	A1524		ALN

T2694497	If follow up work needed or any part of this inspection fails, please FAIL and create a follow up	COMP-P
T2694498	Pass if all annular vents open? Fail and create follow up for any closed vents to record pressure .	COMP-P
T2694499	Pass if no gas on annular vents? Fail and create follow up to record meter reading for gas detected.	COMP-P

Figure 10: Maximo Inspect Well Work Order for #2244, October 26, 2022, No Anomalies

Equitrans has an SOP for performing shut-in tests, which includes recording the initial shut-in pressure and ending shut-in pressure. Table 7 shows the starting and ending shut-in pressures for the #2244 well for 2014 – 2021. Typically, the pressure reduces by 4 – 47 psi from the initial shut-in to the ending shut-in readings. However only in one instance on November 3, 2021, the ending pressure was 57 psi higher than the starting pressure.

Table 7: Well #2244 Shut-in Pressures from Maximo Records

Date	Shut-In Starting Pressure (psi)	Date	Ending Shut-in Pressure	Difference (psi)
2014-11-06 11:00 AM	3,130	2014-11-11 1:16 PM	3,123	–7
2015-10-28 8:55 AM	3,127	2015-11-02 2:18 PM	3,123	–4
2016-10-27 8:15 AM	3,168	2016-11-01 8:25 AM	3,160	–8
2017-11-02 8:39 AM	3,140	2017-11-07 8:18 AM	3,118	–22
2018-10-25 8:21 AM	3,170	2018-10-30 8:34 AM	3,135	–35
2019-10-29 3:47 PM	3,144	2019-11-04 8:35 AM	3,097	–47
2020-10-30 8:15 AM	2,990	2020-11-04 8:15 AM	2,986	–4
2021-10-28 12:00 AM	3,000	2021-11-03 8:15 AM	3,057	57

4.3.2 DEP Table of Site Visits

Appendix A.9, DEP Office of Oil and Gas Management Inspection Document Review shows a pre-incident listing of the DEP inspection reports for Rager Mountain. There are 110 records spanning from September 30, 2014, to October 26, 2022 [4]. *No violations were noted pre-incident*. The DEP inspection reports were available online from October 19, 2017.

Blade downloaded and reviewed 73 online reports. Figure 11 shows an extract of the last inspection report for the #2244 well. The details listed in the report's remarks section are summarized, as follows:

- Well is in-line and current operation is gas injection.
- Wellhead pressure was 3,077 psi.
- Annulus was open and no gas was detected.
- Site is secure behind a locked fence.
- No spills or leaks observed.

The remarks of the DEP inspection are consistent with the Maximo work order report (Figure 10). No indication was given of any issues at #2244 or at any other well in the field on October 26, 2022. Blade did not find any reports, in the DEP or Equitrans records that it examined, of annulus gas flow in any of the wells.

Remarks:

On 10/26/2022 at 10:41, I arrived on location accompanied by [redacted] Operations Technician, to conduct a routine inspection of the storage well. At the time of this inspection the reservoir was being injected into. The wellhead pressure was 3077psi. At the time of this inspection the well was inline and open. The annulus was open and no gas was detected. The wellhead is secured behind a locked fence. No leaks or spills were observed. The GPS coordinates were updated as part of this inspection.

On Site Representative	DEP Representative
(signature)	[redacted]
(print name)	[redacted]

Date: 10/26/2022	Time Arrived: 10:41 AM	Time Departed: 10:46 AM

Figure 11: Well #2244 DEP Inspection Remarks on October 26, 2022 [Reference DEP]

Blade also reviewed the DEP inspection listing for when Peoples Natural Gas was the Rager Mountain operator. Approximately 265 inspections were performed from June 29, 1990, to October 18, 2013. Nine violations were found at Rager Mountain during this approximately 23-year time frame. Appendix A.9, Table 56 displays a list showing the violation dates. Three violations are shown for the #2244 well between September 12, 1990, and December 27, 1990. Blade believes these violations are related to bubbling observed in the cellar that was resolved in 1993. Five violations are shown in the date range of April 19, 2011, to September 1, 2011, for the #2251 and #2252 wells. The data are unclear as to the source of these violations.

4.3.3 Well #2244 Casing Failure

The Rager Mountain Field was at the end of the injection cycle in late October 2022. The wells and the field were shut in on Tuesday, November 1, 2022, for the semiannual inventory verification test. On Sunday, November 6, 2022, at 3:28 pm, Equitrans was notified of a possible event at the Rager Mountain storage field. Equitrans personnel investigated at 4:15 pm and found well #2244 was venting to the atmosphere through the open annulus valve. The annulus valve was in communication with the 7 in. × 9 5/8 in. casing annulus. Figure 12 shows the gas venting through the annulus valve. Wells in the Rager Mountain Field were normally operated with the annulus valve open.

Figure 12: Well #2244 Venting Gas Out the Annulus Valve

Figure 13 shows the wellbore schematic for #2244 with the parted 7 in. casing approximately 2 ft below the wellhead. The upper part of the casing from 5,950 ft to surface was replaced in 1993. During the casing replacement, the first stage cement job was pumped through the cement stage tool at 5,939 ft, and the tool was closed. A delay occurred in opening the stage tool at 3,450 ft, allowing the first stage cement job to set. The upper stage cement job was not pumped, leaving the top of cement in the 7 in. casing annulus at 2,940 ft. The original drilling fluid was left in the annulus and the top of cement was below the surface casing shoe at 1,794 ft.

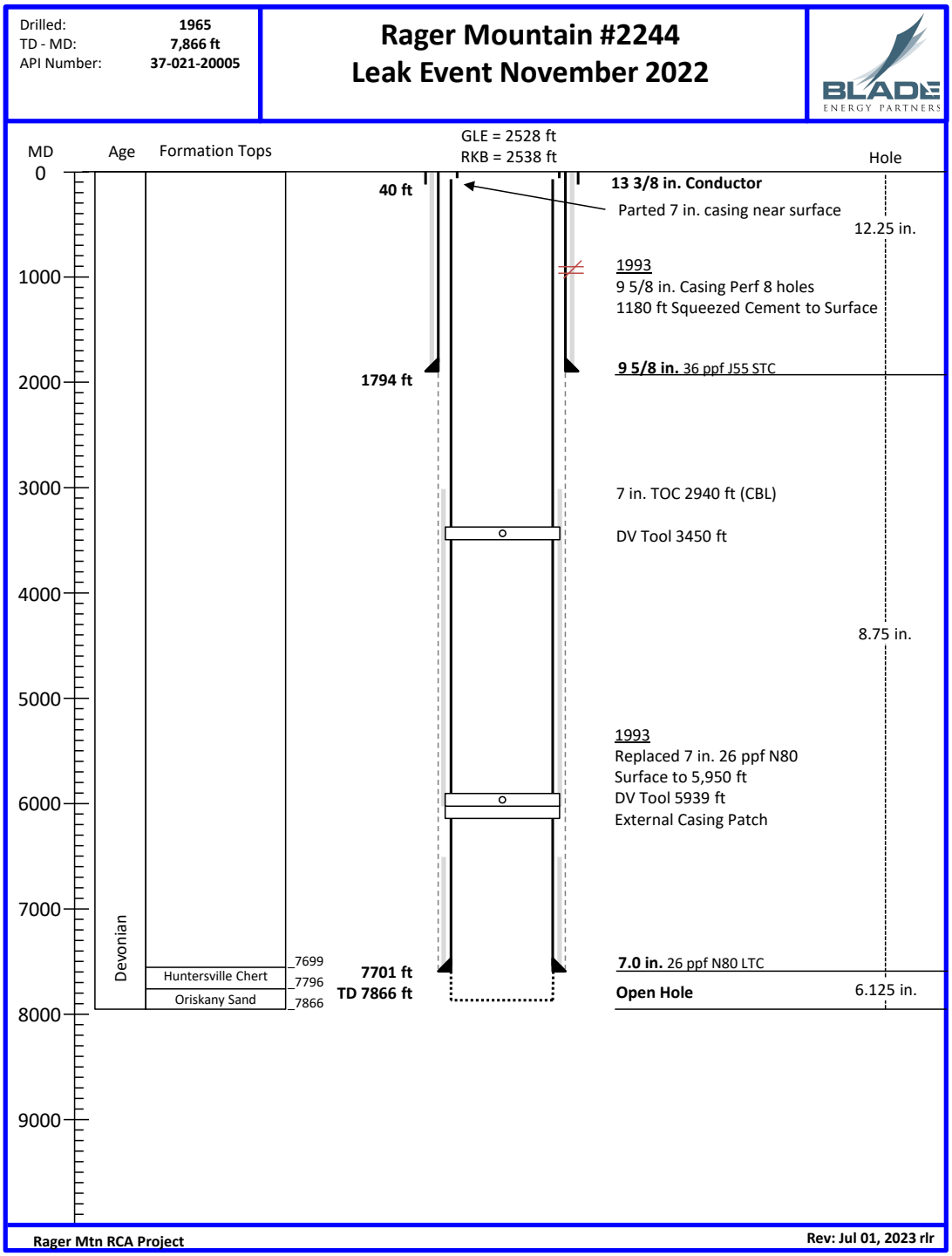

Figure 13: Well #2244 Wellbore Schematic

Table 8 contains a summary of the first few days of the event and efforts to regain control of the well. The timeline events details related to the emergency response can be found in the document *Item 1: Timeline of Events and Meeting Pertaining to Emergency Response and Remediation of the Incident* [5]. A summary of the kill operations by Cudd Well Control (Cudd) to regain control of the well is included in Table 42.

Table 8: #2244 Pre- and Post-Leak Event Timeline Summary

Date and Time	Event
November 1, 2022	Rager Mountain Field shut in for inventory verification
November 6, 2022, 3:28 pm	Peoples Natural Gas notified Equitrans that a loud noise near Rager Mountain had been reported to 911
November 6, 2022, 4:15 pm	Equitrans personnel arrived on site and observed gas venting from the well #2244 annulus valve
November 6, 2022, 4:15 pm	Equitrans emergency responders were notified
November 6, 2022, 4:30 pm	Equitrans Crisis Coordinator consults with the Storage Integrity Group and Incident Commander
November 6, 2022, 5:00 pm	Equitrans Crisis Team convened
November 6, 2022, 5:00 – 5:30 pm	Equitrans Land Department began notifying stake holders Equitrans notified the National Response Center Equitrans notified PHMSA
November 6, 2022, 5:30 – 6:50 pm	Equitrans contacted three approved well control specialists
November 6, 2022, 5:43 pm	Equitrans contacted the Pennsylvania Public Utilities Commission
November 6, 2022, 7:00 pm	Cudd Well Control dispatched a response team from Muncy, PA
November 6, 2022, 8:10 pm	Equitrans provided information to Cudd Well Control
November 6, 2022, 11:30 pm	Cudd Well Control response team arrived on site from Muncy
November 6, 2022, 11:45 pm	Additional Cudd resources requested from Houston
November 7, 2022, 5:30 am	Cudd response team from Houston arrives from Houston
November 7, 2022, 6:30 am	Additional equipment for well control requested

4.4 Prior Major Incidents

4.4.1 #2245 Fire

On January 6, 1972, an alcohol bottle was tied into the 4 in. production/injection lines leading to and from the 4 in. side gate valves on the tubing spool. The connection lines were 3/8 in. OD stainless steel rated for 14,000 psi, and the bottle had been pressure tested to 4,000 psi. The alcohol bottle was used to remove hydrates from the lines on January 7, and the well was subsequently placed on withdrawal.

On January 6, 1972, and January 7, 1972, several personnel were on location and no leakage was detected. On January 9, 1972, the main gate at the facility station was closed and the storage pool was shut-in for testing purposes. The wellhead valves remained open.

On the evening of January 9, 1972, numerous residents of the area reported hearing an explosion after 11:00 PM. The fire at the wellhead of #2245 was discovered the next day. No definite conclusion was reached regarding the initial source of the leak or cause of ignition.

There were multiple theories, one of which was the stainless steel lines (mentioned in the previous paragraph) failed and subsequently flailed against other nearby equipment, created a spark, which ignited the alcohol. Table 9 summarizes the sequence of events from the discovery of the fire until it was extinguished and the well killed.

Table 9: Sequence of Events During Well #2245 Fire Incident in 1972.

Date	Event
Jan. 10, 1972	The fire was discovered at 8:15 am. Flanges on lower wellhead separated, allowing a large volume of gas to escape. Red Adair was called.
Jan. 11, 1972	Fire allowed to burn while preparing to kill the well.
Jan. 12, 1972	Pumped water to extinguish the fire. Flanges were tightened. Killed well by pumping 9 ppg mud and followed by water. Ran out of fluid. Fire re-ignited due to safety concerns.
Jan. 13, 1972	Killed well at 4:30 PM with 400 bbl of 15 ppg mud. Tightened flanges. Replaced tubing and wellhead assembly.
Jan. 14, 1972	Top joint of tubing and entire wellhead above the 10 in. landing flange replaced.

4.4.2 #2246 Blowout

Well #2246 was being used as an observation well to monitor the deliverability of gas in the entire storage field. On September 11, 1990, the 5 1/2 in. production casing ruptured at approximately 5,117 ft, which led to the blowout. This rupture was attributed to extensive internal corrosion (discussed in Section 11). The gas traveled through the annulus of the 5.5 in. casing and vented from the annulus valve at surface. Table 10 shows the well kill operations. From September 14, 1990, to January 28, 1991 (136 days), many operations were performed that included milling, fishing, camera logging, running casing, cementing, logging, and flowback and cleanup. These events are not shown.

Table 10: Sequence of Events During Well #2246 Blowout in 1990.

Date	Event
Sep. 11, 1990	Blowout started at 10:15 PM.
Sep. 12, 1990	Mobilized tanks and equipment. 10 ppg brine kill fluid. Laid 2 3/8 in. kill lines.
Sep. 13, 1990	Pumped down 2 3/8 in. tubing and 5 1/2 in. casing. Pumped 220 bbl fluid. Almost dead. Piped annulus to flow to a tank. Well kicked 4 times. Pumped 1,500 bbl to circulate well. Well taking 15 bph.

5 Equitrans Internal Procedures

5.1 Storage Integrity Management Program (SIMP)

Equitrans provided Blade with approximately twenty historical and current integrity management documents for gas storage wells. The document titles varied over time, which included Storage Integrity Plan, Storage Integrity Guideline, and Integrity Management Program for Underground Gas Storage. Table 11 shows the titles of these documents along with the logging frequency and corrosion mitigation criteria. The titles and contents have changed over the years. Blade will refer to these documents collectively as SIMP.

From October 2016 onwards the document started reflecting API RP 1171 recommendations.

The chapters of the SIMP document in place prior to the #2244 incident were as follows:

1. Introduction
2. Identification and Characterization
3. Operating Parameters
4. Risk Assessment and Risk Mitigation
5. Field Inspections
6. Field Operations
7. Reservoir and Well Integrity
8. Safety
9. Emergency Response
10. Reporting and Record Keeping

Blade's assessment of the October 2022 SIMP version and the versions dating back to 2016 complied or exceeded the tenants of API RP 1171. Table 11 summarizes logging frequency, threshold anomaly size for action, and gelling and any annulus corrosion comments over time in the various versions of the SIMP document or equivalent. Table 11 also identifies the responsible organization team for gelling.

Since Equitrans' 2013 Rager Mountain acquisition from PNG until 2017, the Storage Engineering group consisted of individuals responsible for Well Integrity/Compliance, Reservoir, and Well Operations. From 2017 to 2020, organizational changes were initiated to realign functions. Well Integrity responsibilities were shared by the groups called Gas Systems and Compliance. Well Operations was housed within the overall Operations group, and Reservoir Performance was within the Gas Systems group. In 2020, the groups were changed to functional teams, Operations (including Well Operations), Gas Systems (including Reservoir), and Integrity/Compliance (including Well Integrity). The gelling guidelines and SIMP development have always been managed by the Well Integrity/Compliance team.

Following the acquisition of the Rager Mountain storage asset in 2013, Equitrans reviewed PNG's records. Equitrans recognized the presence of corrosion in these wells and conducted a logging program across all Rager Mountain wells in 2016. Equitrans informed Blade, had the #2244 incident not occurred, that the next logging campaign for Rager Mountain wells would have been 2027, which is 11 years after the 2016 campaign. SIMP in 2016 had a maximum logging frequency of 15 years. The logging frequency varied over time and was modified from 7, 10, 12, and 15 years. The current scheduled re-inspection frequency is 7 years, not to exceed 10 years.

Prior to 2015, the threshold for action based on logging data was to evaluate “severe anomalies.” From 2017 and onwards, severe anomalies were quantified as follows: to conduct a prompt evaluation of the potential risk and identification of mitigative steps at a level of 61% penetration and greater. At 80%, an immediate assessment of well safety and setting a plug was required.

The right-most column in Table 11 identifies annulus corrosion information in the various SIMP documents. The annulus corrosion mechanism was well described in a few paragraphs up to and including the 2015 versions. Figure 14 shows a section titled Casing Corrosion Inhibitors from the 2005 document that explains the corrosion problem and the recommended solution. Blade’s understanding is that the annulus (vent) valves are to remain open from when Equitrans acquired the Rager Mountain field in 2013 from PNG. PNG communicated via email (November 20, 2013) that PADEP wants the annulus valves left open [6]. The annulus valve position was reported on the DEP inspection forms.

Prior communication regarding the open annulus valves for #2244 occurred on June 30, 1993, in a letter from PNG to the Department of Environmental Resources Bureau of Oil and Gas. The letter explained the problems with cementing the upper stage of the casing replacement in 1993 where the stage tool failed to open preventing circulating cement to surface. The conclusion communicated to the Department of Environmental Resources was that “The annulus above the cement is filled with mud gel and the 2” annular valves are to remain open.” [7].

The intent of the open annulus valve was to prevent annulus gas pressure buildup on the shallow aquifers. The possibility of corrosion due to interaction of air with water on the cement top was identified in the older 2005 SIMP documents (Figure 14). The mitigation for this corrosion was proposed, which is to gravity feed in the annulus a viscous fluid containing corrosion inhibitor additives in a process known as gelling. These explanatory paragraphs were removed in 2016 as the entire document was overhauled to reflect the new API RP 1171 (1st Ed.) recommendations.

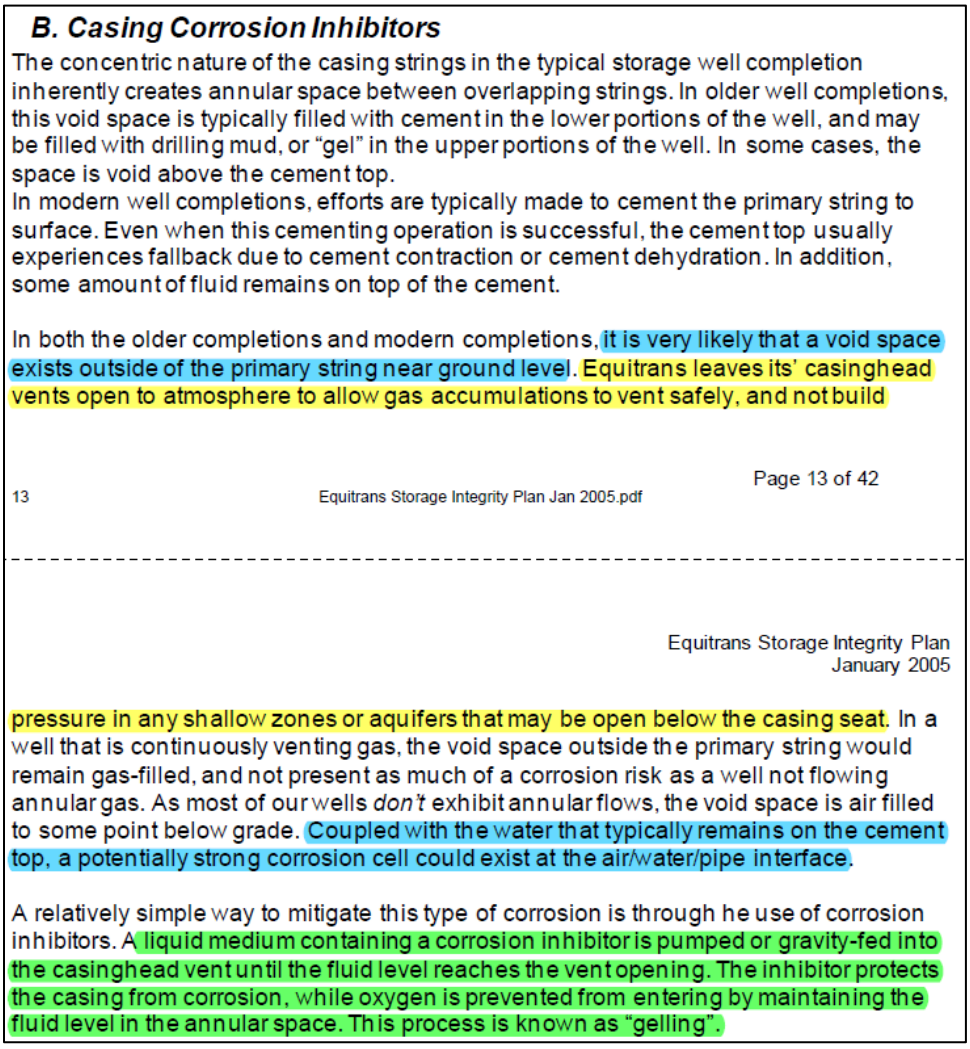

B. Casing Corrosion Inhibitors

The concentric nature of the casing strings in the typical storage well completion inherently creates annular space between overlapping strings. In older well completions, this void space is typically filled with cement in the lower portions of the well, and may be filled with drilling mud, or "gel" in the upper portions of the well. In some cases, the space is void above the cement top.
In modern well completions, efforts are typically made to cement the primary string to surface. Even when this cementing operation is successful, the cement top usually experiences fallback due to cement contraction or cement dehydration. In addition, some amount of fluid remains on top of the cement.

In both the older completions and modern completions, it is very likely that a void space exists outside of the primary string near ground level. Equitrans leaves its' casinghead vents open to atmosphere to allow gas accumulations to vent safely, and not build

13 Equitrans Storage Integrity Plan Jan 2005.pdf Page 13 of 42

Equitrans Storage Integrity Plan
January 2005

pressure in any shallow zones or aquifers that may be open below the casing seat. In a well that is continuously venting gas, the void space outside the primary string would remain gas-filled, and not present as much of a corrosion risk as a well not flowing annular gas. As most of our wells *don't* exhibit annular flows, the void space is air filled to some point below grade. Coupled with the water that typically remains on the cement top, a potentially strong corrosion cell could exist at the air/water/pipe interface.

A relatively simple way to mitigate this type of corrosion is through he use of corrosion inhibitors. A liquid medium containing a corrosion inhibitor is pumped or gravity-fed into the casinghead vent until the fluid level reaches the vent opening. The inhibitor protects the casing from corrosion, while oxygen is prevented from entering by maintaining the fluid level in the annular space. This process is known as "gelling".

Figure 14: Rational for Open Annulus (Vent) Valves (Yellow Highlight), Corrosion Mechanism (Blue Highlight), Mitigation (Green Highlight), SIMP 2005

Table 11:Storage Integrity Management Program Logging, Threshold for Action, and Gelling

Date	Document Title	Normal or Maximum Logging Interval (year)	Threshold for Action Based on Logging Data on Anomalies	Gelling and Corrosion Comments
Jan. 2005	Equitrans Storage Integrity Plan	10		• The corrosion mechanism is described. • Storage Optimization Department to ensure wells are treated each year. • Well selection guidance for gelling. • 4 year maximum interval for gelling
Nov. 2010	EQT Midstream Storage Integrity Plan	12	Severe anomalies	• The corrosion mechanism is described. • Storage Engineering Department responsible for gelling. • Well selection guidance for gelling. • 4 year maximum interval for gelling
Jan. 2012	EQT Midstream Gas Storage Guidelines	12	Severe anomalies	• The corrosion mechanism is described. • Storage Well Operations Manager responsible for gelling.
Sep. 2012	Storage Guidelines EQT Midstream September 2012	12	Severe anomalies	• The corrosion mechanism is described. • Operations and Storage will cooperatively select the wells to be gelled each year.

Date	Document Title	Normal or Maximum Logging Interval (year)	Threshold for Action Based on Logging Data on Anomalies	Gelling and Corrosion Comments
Mar. 2015	Storage Guidelines EQT Midstream March 2015	15	Severe anomalies	• The corrosion mechanism is described. • Operations and Storage will cooperatively select the wells to be gelled each year.
Oct. 2016	EQT Midstream Storage Integrity Plan	15	Storage will determine if wells identified with >80% metal loss need to be taken out of service and remediated	• Storage will select the wells to be gelled, as needed.
Dec. 2017	Storage Integrity Plan EQT Midstream 2017	15 20	Class 4 features (60% metal loss or greater) prompt evaluation. 80% - set plug	• Storage will select the wells to be gelled, as needed
Dec. 2018	Storage Integrity Plan Equitrans Midstream 2018	15 20	Class 4 features (60% metal loss or greater) prompt evaluation. 80% - set plug	• Storage will select the wells to be gelled, as needed
Apr. 2019	Storage Integrity Plan Equitrans Midstream 2019	15 20	Class 4 features (60% metal loss or greater) prompt evaluation. 80% - set plug	• Storage will select the wells to be gelled, as needed
Dec. 2019	Equitrans Midstream Corporation Integrity Management Program for Underground Gas Storage	15 20 (transitioning to 10)	Class 4 (61%) features require a prompt evaluation. 80% metal loss, an immediate assessment/plug	• Storage will select the wells to be gelled, as needed
Dec. 2019	Equitrans Midstream Corporation Integrity Management Program for Underground Gas Storage	15 20 (transitioning to 10)	Class 4 (61%) features require a prompt evaluation. 80% metal loss, an immediate assessment/plug	• Storage will select the wells to be gelled, as needed

Date	Document Title	Normal or Maximum Logging Interval (year)	Threshold for Action Based on Logging Data on Anomalies	Gelling and Corrosion Comments
2012	Equitrans Midstream Corporation Integrity Management Program for Underground Gas Storage	7 10	Class 4 (61%) features require a prompt evaluation. 80% metal loss, an immediate assessment/plug	• Storage Integrity will select the wells to be gelled, based on surveillance logging results.
Jun. 2012	Equitrans Midstream Corporation Integrity Management Program for Underground Gas Storage	7 10	Class 4 (61%) features require a prompt evaluation. 80% metal loss, an immediate assessment/plug	• Storage Integrity will select the wells to be gelled, based on surveillance logging results.
Oct. 2021	Equitrans Midstream Corporation Integrity Management Program for Underground Gas Storage	7 10	Class 4 (61%) features require a prompt evaluation. 80% metal loss, an immediate assessment/plug	• Storage Integrity will select the wells to be gelled, based on surveillance logging results.
Nov. 2021	Equitrans Midstream Corporation Integrity Management Program for Underground Gas Storage	7 10	Class 4 (61%) features require a prompt evaluation. 80% metal loss, an immediate assessment/plug	• Storage Integrity will select the wells to be gelled, based on surveillance logging results.
Jan. 2022	Equitrans Midstream Corporation Integrity Management Program for Underground Gas Storage	7 10	Class 4 (61%) features require a prompt evaluation. 80% metal loss, an immediate assessment/plug	• Storage Integrity will select the wells to be gelled, based on surveillance logging results.
May 2022	Equitrans Midstream Corporation Integrity Management Program for Underground Gas Storage	7 10	Class 4 (61%) features require a prompt evaluation. 80% metal loss, an immediate assessment/plug	• Storage Integrity will select the wells to be gelled, based on surveillance logging results.
Oct. 2022	Equitrans Midstream Corporation Integrity Management Program for Underground Gas Storage	7 10	Class 4 (61%) features require a prompt evaluation. 80% metal loss, an immediate assessment/plug	• Storage Integrity will select the wells to be gelled, based on surveillance logging results.

Date	Document Title	Normal or Maximum Logging Interval (year)	Threshold for Action Based on Logging Data on Anomalies	Gelling and Corrosion Comments
Jan. 2023	Equitrans Midstream Corporation Integrity Management Program for Underground Gas Storage	7 10	Class 4 (61%) features require a prompt evaluation. 80% metal loss, an immediate assessment/plug	• Storage Integrity will select the wells to be gelled, based on surveillance logging results.
May 2023	Equitrans Midstream Corporation Integrity Management Program for Underground Gas Storage	7 10	Class 4 (61%) features require a prompt evaluation. 80% metal loss, an immediate assessment/plug	• Storage Integrity will select the wells to be gelled, based on surveillance logging results.

5.2 Risk Assessments

Blade reviewed the Equitrans Risk Assessment [8] dated October 2022. This spreadsheet was based on Joint Industry Task Force guidance formulas [9] [10]. Equitrans had performed risk assessments of all wells since 2018. Meetings were held monthly to discuss and identify additional threats, mitigation, plugging, wellhead replacements, and logging results. The risk assessment changed throughout the year.

Annually, an Equitrans multidisciplinary team reviews the risk assessment and publishes a version for distribution. In 2022, the rank for #2244 was 20th overall, but it was number 1 within Rager Mountain wells. The consequence of failure calculation was affected by low population density (i.e., isolated region), insurance rates, 30-day flow in metric tons, and the cost of emergency response that was dramatically underestimated at that time.

The Rager Mountain Field was ranked second, primarily because of the volume and pressure of the field. The probability of failure calculation was affected by the number of Class 1 – 4 joints, number of workovers, single-barrier completion style, and cement height. Other Equitrans wells had a higher rank due to the proximity to inhabited areas.

In the Equitrans 2022 Risk Assessment presentation to PHMSA [11], the following actions were completed:

- Plugging of their highest risk well
- Installing pressure monitoring in two fields (not Rager Mountain)
- Logging of 46 wells using HRVRT

The planned work in 2022 was as follows:

- Logging of two fields
- Replacing a wellhead
- Plugging their 2nd highest risk well
- Verifying wellhead components

- Reviewing burst radius calculations
- Adding remote terminal unit (RTU) monitoring to Rager Mountain and another field
- Using monthly annular pressure, valve inspections, and atmospheric corrosion inspections to determine risk assessment values
- Revising probability factors for annulus gas and wellhead inspections

Blade's opinion of the 2022 risk assessment is that it was reasonable, and the mitigation activity completed and proposed was consistent with the SIMP. However, the consequence of failure was underestimated for #2244. The #2244 well was the highest ranked well in the field, in terms of deliverability (i.e., gas flow) and would likely be the most difficult and challenging to kill.

The individual well deliverability was not factored into the risk assessment. This could be considered as a parameter to add to the risk assessment. Increased flow rate results in higher temperatures and that could increase the corrosion rate. The probability of failure was also underestimated because the top joint corrosion was undersized by the logging tool, and the corrosion growth rate was an unknown. Because of the higher deliverability of the #2244 well, the temperature at the top joint was higher than the other Rager Mountain wells. Corrosion rates increase with increasing temperatures; this is discussed later in the report.

Blade's interpretation is that the risk assessment process itself is adequate, and the underlying threat and hazard identification and analysis are robust.

5.3 Summary

Actionable conditions were detailed in the Equitrans Storage Integrity Management documents. In 2016, the normal logging frequency was 15 years but was later revised to seven years in 2021. A detailed risk-assessment procedure had been in place for a few years, and intervention was performed on high-risk wells. Blade's overall review of Equitrans' integrity plans, SOPs, maintenance records, and logs was that they were adequate except for a few gaps. These specific gaps and proposed solutions are discussed in Section 15.

6 Logging Data and Analysis

6.1 Summary of Rager Mountain Logs

This section contains historical information and analysis of the Rager Mountain logging runs.

A total of 216 logs were run prior to the #2244 incident in 2022. Appendix A.3 summarizes the logs run in the Rager Mountain Field. Blade classified the log types by different categories based on log header and the information gathered. The log was classified as Leak Detection (Gamma Ray, Neutron, Temperature), Cement Evaluation, Casing Inspection, Formation Evaluation, and Other.

Figure 15 shows the breakdown of the 216 logs. Most were leak detection and casing inspection logs. The total number of years of service for all Rager Mountain wells is approximately 479 years. Dividing 479 years by 55 casing inspection logs results in each well's casing being inspected every 8.7 years, on average.

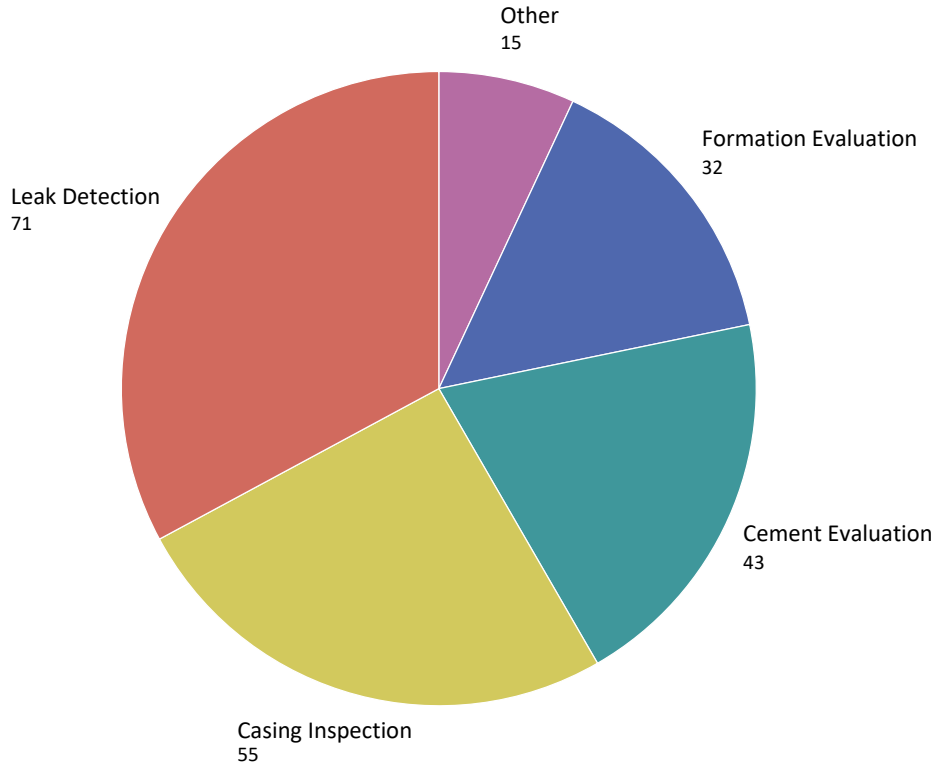

Figure 15: Rager Mountain Logs by Type

Table 12 shows the breakdown of the logs by type for each well. The well names are listed vertically, and the type of logs are presented horizontally. The #2244 well was one of the most logged wells, reflective of it being the discovery well, consequently the oldest. A total of five casing inspection logs were run in #2244. The well with the greatest number of casing inspection logs is #2247 with ten logs. This is because there were five casing inspection logs between May 31, 1995, and June 15, 1995, that were associated with a workover. Three wells have one casing integrity log each, namely #2249, #2253, and #2254; and two wells, #2253 and #2254 (the newest wells), have no cement evaluation logs. The most recent wells, #2253, #2254, and #2255, have the least amount of information from a logging perspective. Figure 22 displays the timeline of the logging activity.

Table 12: Pre-incident Logs by Well and Type

Well	Formation Evaluation (F)	Casing Inspection (I)	Leak Detection (L)	Cement Evaluation (C)	Other (O)	Total
#2244	5	5	6	7	6	29
#2245	4	6	12	4	2	28
#2246	2	9	6	0	1	18
#2247	1	10	9	5	1	26
#2248	4	3	8	7	3	25
#2249	4	1	6	6	0	17
#2250	5	4	7	3	0	19
#2251	3	6	8	6	1	24
#2252	1	8	6	4	0	19
#2253	1	1	1	0	0	3
#2254	1	1	1	0	0	3
#2255	1	1	1	1	1	5

6.1.1 Corrosion Overview

Two types of corrosion were found on the production casing amongst the Rager Mountain wells: top joint external corrosion and bottom of the well internal corrosion. Baker Hughes used their magnetic flux leakage logging technology to conduct all the casing wall thickness logging at Rager Mountain. After Equitrans acquired the asset, the first logging was conducted in 2016. The 2016 log interpretation that was provided to Equitrans in 2016 was re-interpreted in 2022 using an updated 2022 sizing algorithm from Baker Hughes. All the analysis and interpretation discussed here are based on the reprocessed 2016 log data.

Figure 16 shows a general overview of the location and prevalence of all metal loss defects in casing joints by well based on high-resolution Vertilog (HRVRT) logging in 2016 and 2022. This figure uses data from the reprocessed 2016 logs (2022 algorithm) to allow for a growth comparison to the 2022 logs.

Class 2 joints are joints that contain defects with 20–40% penetration in terms of percentage of wall thickness. Class 3 joints contain 40 – 60% metal loss defects, and Class 4 joints contain 60 – 80% defects. The well name is listed in the y-axis, and the number of joints is listed in the x-axis in three tracks. The number of Class 2 joints is shown on the left.

The number of Class 3 joints is shown in the middle, and the number of Class 3 joints is shown on the right. The number of Class 0 (0 – 20%) joints is not shown. The blue bars represent 2016, and red bars represent 2022.

Wells #2245 and #2246 have the highest number of joints that contain Class 2, 3, and 4 defects. Some wells, #2244, #2247, #2248, #2249, #2250, #2251, #2252, #2253, #2254, and #2255, have fewer than 10 Class 2, 3, and 4 joints. It is important to note that #2246 is the only well with Class 4 defects. Well #2244 was not inspected in 2022 with an HRVRT log, due to the November 6, 2022, incident.

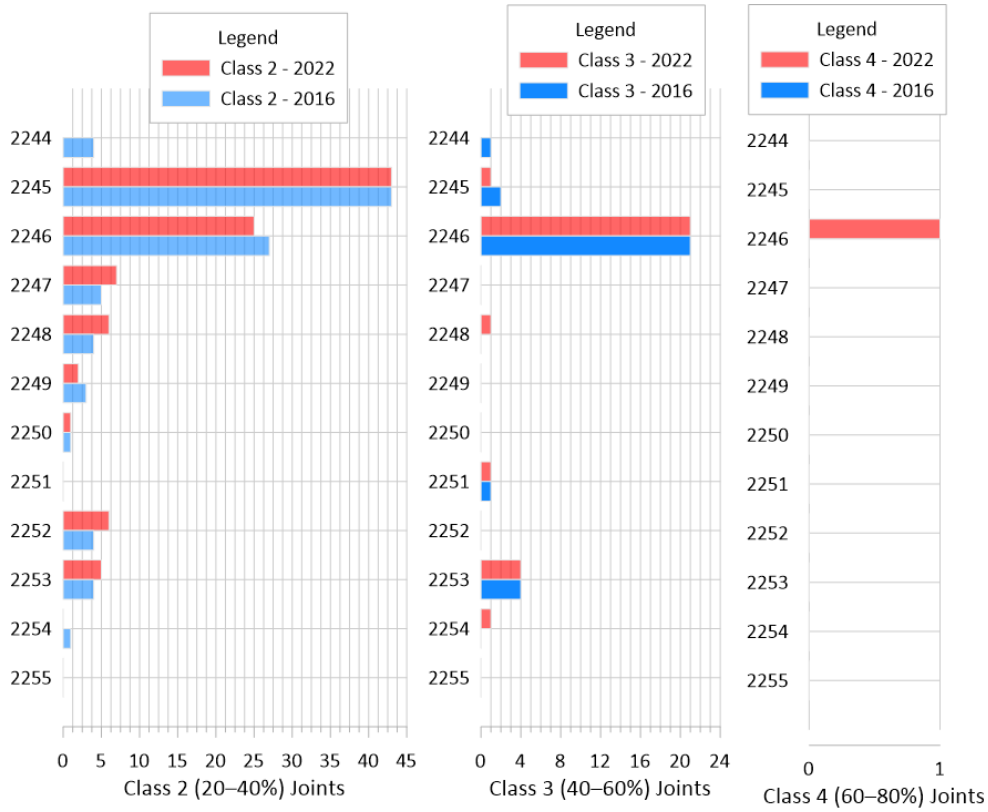

Figure 16: Number of Joints, Class 2, Class 3, and Class 4, 2016 (Reprocessed) and 2022 HRVRT Logs

Figure 17 shows the count of internal and external defects by well using the 2016 reprocessed and the 2022 HRVRT logs. The y-axis shows the well name. The left axis is the quantity of external defects from 0-90. The right axis is the quantity of internal defects from 0 to 2,400.

At a high-level joint/class (Figure 16) and defect count (Figure 17) perspective, well #2244 did not appear to be significant in terms of corrosion compared to other wells in the field.

The quantity of internal defects for wells #2246 and #2253 was much higher than the rest of the wells. The quantity of external defects is much lower than the internal defects. Wells #2253 and #2254 have a much larger number of external defects in 2022 as compared to 2016.

Another important perspective is that the number of internal defects increased in #2246 in 2022, whereas in #2253 the number went down in the 2023 log run. The 2022 HRVRT logging run in Well #2253 did not capture data from the bottom two joints because of scale and debris. After a debris cleanout, the HRVRT was re-run in 2023 and those are the results (on the legend referenced as 2022) are shown in Figure 16 and Figure 17. The number of internal defects appear to have decreased in the 2023 run when compared to 2016. This is either reflective of possible debris and scale, or the clustering in 2023 reduced the number of defects. The 2023 log as shown in the figures is a more accurate representation of the current internal defects in #2253.

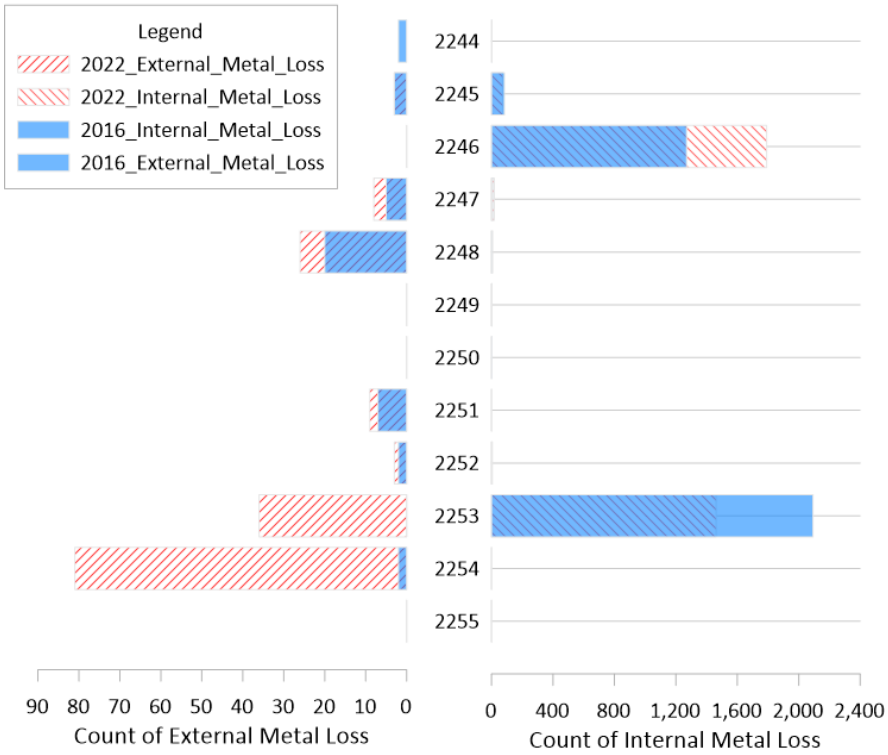

Figure 17: Count of HRVRT (>20%) Internal and External Metal Loss Defects, 2016 and 2022

6.1.2 External Corrosion (Top Joint)

The existence of corrosion was well known at Rager Mountain, but it is unclear whether the presence of top joint corrosion was specifically recognized as an issue. The previous operator, Peoples Natural Gas, managed the corrosion issues through logging and mitigation by replacement of casing, including the top joints. Equitrans also recognized that corrosion was an issue, not necessarily top joint corrosion, and continued with the approach of using logging to manage and mitigate. Such a strategy is dependent on the logging being reasonably accurate. Some of the inherent logging challenges are discussed in this section.

Well #2244

The 2016 HRVRT log results for the 7 in. casing are shown in Figure 18. Baker Hughes performed a 2-year calibration study that resulted in a new sizing algorithm for this tool. This new algorithm was released in September 2022; this was just before the incident in November 2022. The top half of the figure shows the 2016 originally processed magnetic flux leakage (MFL) signals. A single green box at approximately 10.3 ft is labeled 25%.

These values of percentage represent the amount of metal loss detected as a percentage of the nominal wall thickness, which in this casing is 0.362 in. The lower half of the figure shows the same log data using the 2022 sizing algorithm. Many features are sized using this new algorithm, specifically 9 metal loss clusters and 69 individual metal loss call boxes. The defect located at 10.3 ft was 25% in the original processing and is calculated at 40% using the September 2022 algorithm.

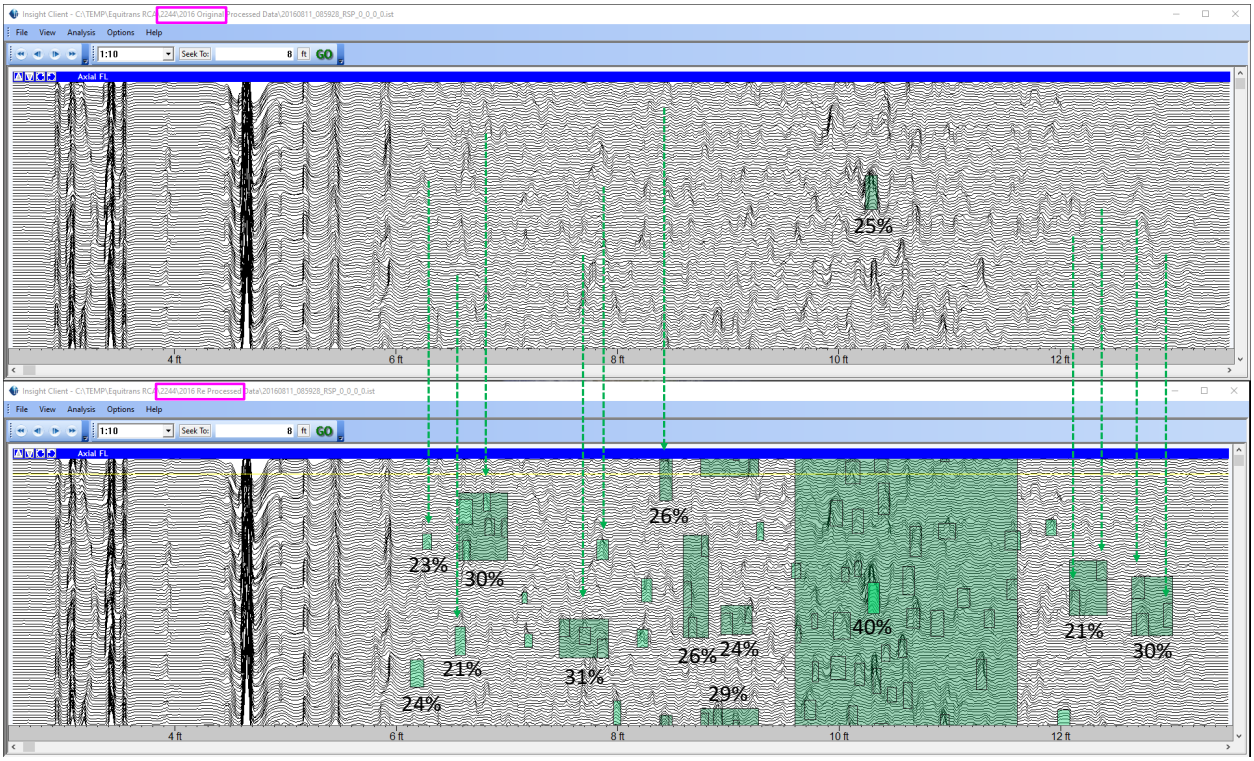

Figure 18: Signal Analysis of Well #2244's HRVRT Log—2016 Original Processing (above) and 2016 Reprocessed (below)

Figure 19 shows a comparison of the top joints of wells #2244 (2016), #2248 (2022), and #2251 (2022). Each green box represents individual metal loss defects or a defect cluster. The patterns of corrosion are not identical in terms of location and density. The #2244 well has a greater extent of corrosion than the #2248 and #2251 wells. During extraction, cement was observed a few feet below ground level in the #2248 and #2251 wells. Cement was not observed in the #2244 well.

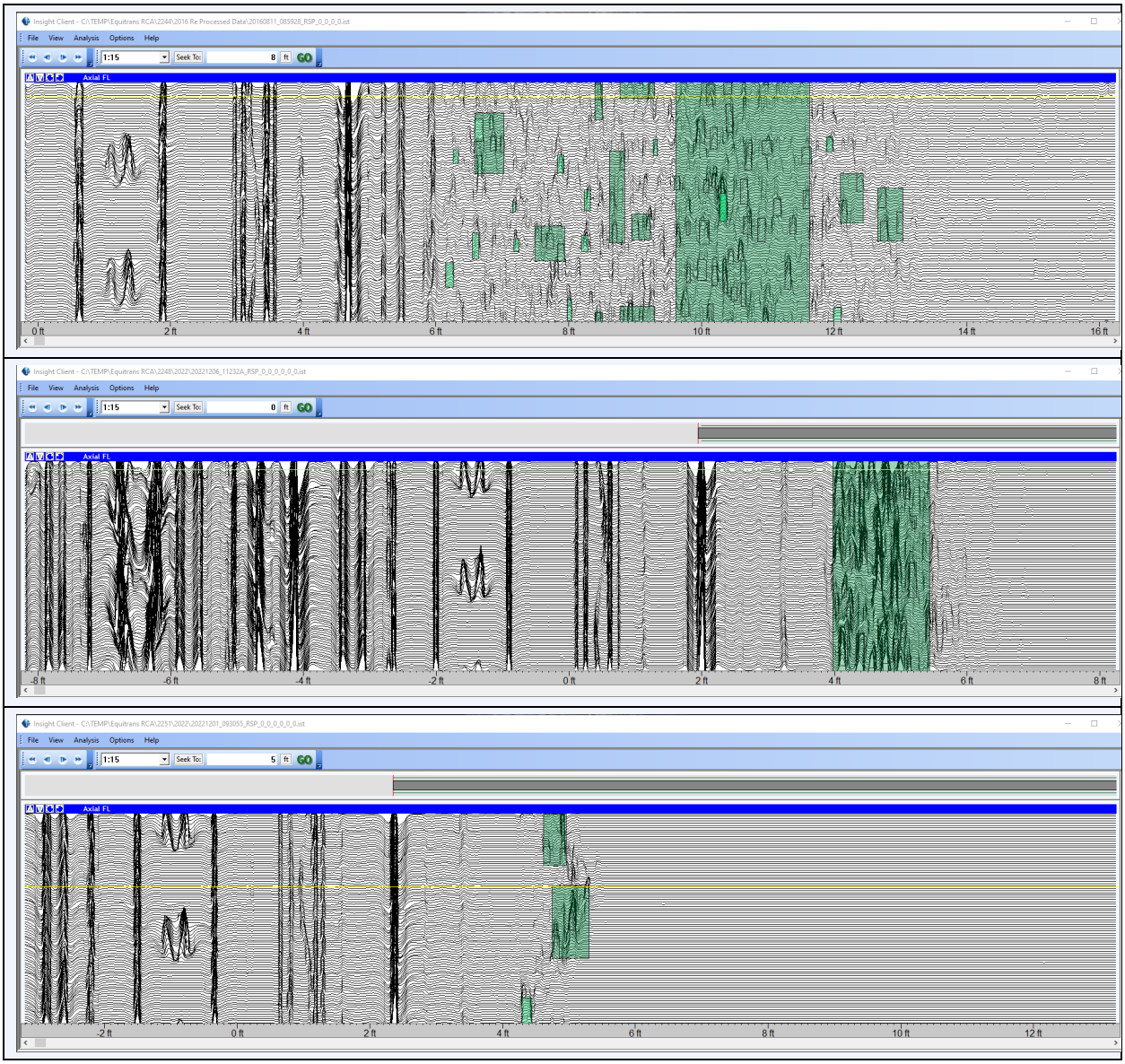

Figure 19: Comparison of HRVRT Logs, Top Joints, #2244 (2016-reprocessed, top), #2248 (2022, middle), and #2251 (2022, bottom)

Rager Mountain Wells (other than #2244)

Table 13 shows a summary of how the deepest defects in the top joints have changed from 2016 to 2022, using reported feature tables in the HRVRT logs. Five wells, namely #2246, #2249, #2249, #2250, and #2252, do not show defects based on the 20% reporting threshold. Six wells show some amount of top joint corrosion growth. The #2244, #2248, #2251, #2253 and #2254 wells had their top joints replaced in 2023.

Appendix A.6, Figure 224 to Figure 234 show a visual comparison of top joint corrosion using the 2016 reprocessed data compared to the 2022 HRVRT logs, as visualized using Baker Hughes Insight software. Additional data can be discerned from these visual comparisons.

The column titled "Visual Observations" contains a brief comment on the presence, location, or extent of corrosion in the top joint. In some wells, no defects were reported (numerically over the 20% threshold); however, a visual examination of the magnetic flux leakage signals shows some low level of corrosion present. All top joints in wells (#2244, #2248, #2251, #2254, #2253) where the corrosion rate appeared to be increasing or corrosion wall loss appeared significant were replaced in 2023.

Table 13: HRVRT Comparision of Deepest Top Joint Defects, 2016 Reprocessed and 2022

Well	HRVRT 2016 Reproc. (% WT)	HRVRT 2022 (% WT)	Change in 6 years	Figure in Appendix A.6	Visual Observations
2244	40	N/A	N/A	—	Casing failure
2245	0	23	23	Figure 224	Corrosion is barely visible but present.
2246	0	0	0	Figure 225	No corrosion is visible.
2247	21	32	11	Figure 226	Corrosion is visible.
2248	37	42	5	Figure 227	Corrosion is visible and over greater area in successive logs.
2249	0	0	0	Figure 228	Corrosion is barely visible but present.
2250	0	0	0	Figure 229	Corrosion is barely visible but present.
2251	43	49	6	Figure 230	Corrosion is visible. Location (i.e., extent) not changing.
2252	0	0	0	Figure 231	Corrosion is barely visible. May not be present.
2253	0	37	37	Figure 232	Corrosion is visible and significantly changing in extent.
2254	24	45	21	Figure 233	Corrosion is visible and significantly changing in extent.
2255	0	0	0	Figure 234	Corrosion is barely visible but present.

6.1.3 Gamma Ray, Neutron, and Temperature Log Observations

Blade reviewed the gamma ray, neutron, and temperature logs (GRNT) from 2016 and 2022. A standalone appendix (A.13.2) shows a large format composite log of the Rager Mountain wells from southwest to northeast. Table 14 shows a summary of Blade's observations. Blade's interpretations are as follows:

- There were no casing leaks. Casing leaks are identifiable by localized cooling, and no cooling was found.
- Each well had different maximum temperatures. The cooler temperatures are reflective of active gas storage wells. The observation (#2246 and #2247) and shut-in wells are the warmest.
- Two wells had indications of a liquid level within the casing at the bottom of the well.

  - Well #2246 had a liquid level of 7,727 ft in 2022. No liquid was observed in 2016. Blade's interpretation is that the rise and fall of reservoir water is related to internal corrosion. Well #2246 has internal corrosion, as discussed in Section 11.
  - Well #2254 may have a static liquid level at 7,984 ft (2022). This is in the open hole. One reason for this could be related to the well kill operations in #2244. Equitrans reported on November 18, 2022, that, "Some water came up through that well [#2254]." The GRNT log for #2254 was run on December 14, 2022.

- The annulus fluid level could not be determined (ND) for some wells, but it could be identified in others. The annulus liquid level did not change over long periods of time for five wells. The deepest annulus liquid level was approximately 633 ft in the #2252 well. Some wells, #2244, #2245, #2248, #2250, and #2251, had an annulus fluid level adjacent to the top joint depths.
- No differences were displayed in the neutron log at the bottom production casing joints. Blade's interpretation is that no gas was migrating out of the storage zone.
- No significant neutron log differences were observed between 2016 and 2022. Blade's interpretation is that the blowout gas from #2244 was not detected in the December 2022 logging GRNT campaign, however, recognizing the fact that a neutron log is a snapshot in time. The comparisons between neutron logs over time elicited some insight as summarized:
  - For the wells that had noise logs, #2248 and #2251 that exhibited noise, no observed differences were displayed in the neutron log. If there was appreciable annulus gas the neutron log should have detected it. The noise logs are discussed in Section 14.
  - For well #2245, Baker reported shallow annulus gas above the shoe at various intervals through the years and it does not appear to be changing (Table 54). The fluid level was identified to be at 20 ft. in 2002, 33 ft. in 2016, and 7 ft in 2022.
  - For the #2249 and #2250 wells, a common interval existed where neutron log differences were observed at approximately 5,200 to 5,300 ft. Baker interpreted this as possible annulus gas. This was observed in the 2009, 2016, and 2022 logs (Table 54).
  - For the #2252 well, an abrupt change in the neutron log from 1,591 to 1,598 ft was observed in 2016 that Baker Hughes identified as possible annulus gas (Table 54). However, this indication of annulus gas was absent in the 2022 neutron log.
- The wells that showed annulus pressure above 2 psi did not show any observable neutron log difference above the casing shoe. Neutron logging is a snapshot in time and was conducted in early December 2022. Significant annulus gas and pressure in some wells was recorded in late December 2022.

Table 14: Neutron Temperature Log Observations from 2016 and 2022/2023 and Annulus Pressure

Well	Year	Temp Anomaly Observed	Max. Temp	Liquid at Bottom ?	Annulus Liquid Level	Neutron Comparison at Bottom Joints	Depths of Neutron Difference	Annulus Pressure Average > 2 psi
2244	2016	No	128	No	11	n/a	n/a	No
	2023	No	104	n/a	n/a			
2245	2016	No	132	No	33	No change	280 – 290	No
	2022	No	132	No	7			

Well	Year	Temp Anomaly Observed	Max. Temp	Liquid at Bottom ?	Annulus Liquid Level	Neutron Comparison at Bottom Joints	Depths of Neutron Difference	Annulus Pressure Average > 2 psi
2246	2016	No	162	No	447	No change	—	Yes
	2022	No	168	Yes 7,727 ft	452			
2247	2016	No	159	No	58	No change	—	Yes
	2022	No	172	No	58			
2248	2016	No	135	No	15	No change	—	Yes
	2022	No	149	No	7			
2249	2016	No	142	No	ND (1)	No change	5,282 – 5,304	Yes
	2022	No	148	No	ND			
2250	2016	No	137	No	18	No change	5,200 – 5,218	No
	2022	No	158	No	13			
2251	2016	No	154	No	40	No change	—	Yes
	2022	No	163	No	40			
2252	2016	No	118	No	634	No change	1,591 – 1,598	No
	2022	No	131	No	632			
2253	2016	No	140	No	ND	No change	318 — 325	No
	2022	No	154	No	ND			
2254	2016	No	139	No	ND	No change	394 – 414, 7,674 – 7,690	No
	2022	No	155	Possible 7,984 ft	ND			
2255	2016	No	117	No	ND	No change	—	Yes
	2022	Possible 500, 850 ft	135	No	ND			
Notes: (1) Not determined.								

6.1.4 Surface Casing Corrosion (Well #2244)

In March 2023, during the #2244 workover, the 7 in. casing had been recovered to approximately 1,500 ft and exposed the surface casing. Baker Hughes logged the 9 5/8 in. surface casing of well #2244 on March 13, 2023, using HRVRT. Table 15 and Figure 20 summarize the results of the log. Table 15 shows four occurrences of Class 4 defects.

In Figure 20, the y-axis is well depth, and the x-axis is metal loss as a percentage of wall thickness. The two right-most plots show the deepest internal and external metal loss features for each joint. Forty-five joints were logged. A total of 1,658 metal loss features were reported (20% reporting threshold); 880 were identified as internal features, and 778 were identified as external features. The location of the metal loss was from surface down to approximately 550 ft. Blade's assessment is that there was a significant amount of deep corrosion.

Table 15: HRVT Joint Summary for 9 5/8 in. Casing, March 13, 2023

Occurrences	Description
27	Class 1 (0% – 20%)
9	Class 2 (20% – 40%)
5	Class 3 (40% – 60%)
4	Class 4 (60% – 100%)

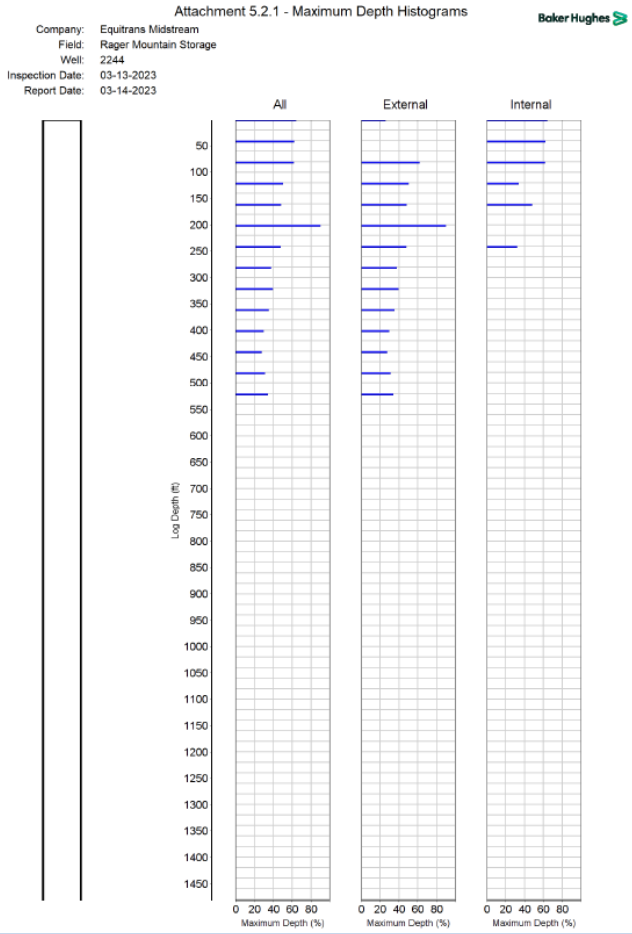

Metal Loss Features			Metal Loss Depth	Number of Joints
Internal	External	Total		
N/A	N/A	N/A	**0% ≤ d < 20%**	27
228	526	754	**20% ≤ d < 30%**	5
461	214	675	**30% ≤ d < 40%**	4
166	35	201	**40% ≤ d < 50%**	3
20	1	21	**50% ≤ d < 60%**	2
5	1	6	**60% ≤ d < 70%**	3
0	0	0	**70% ≤ d < 80%**	0
0	1	1	**80% ≤ d**	1
880	**778**	**1658**	**Total**	**45**

Figure 20: Location and Severity of Metal Loss, 9 5/8 in. Casing, #2244, March 13, 2023

Schlumberger (SLB) ran an Isolation Scanner log in the #2244 9 5/8 in. surface casing to 1,465 ft on March 14, 2023. The Isolation Scanner log showed good agreement with the HRVRT log in terms of location of internal corrosion and external corrosion from 0 – 300 ft. However, these logs did not agree well with the location and severity of external corrosion for depths of 300 – 550 ft. The HRVRT log has been consistent on external corrosion and is considered representative of the casing condition.

The Isolation Scanner did not find significant external corrosion in this region, whereas the HRVRT did. The Isolation Scanner log showed regions of liquid, gas, and solids in the region where severe corrosion was found by HRVRT. Blade's interpretation is that the shallow aerated groundwater in the vadose zone (i.e., soil and rock layer that is intermittently filled with air and/or water) is the cause of the surface casing *external* corrosion.

The comparison of the location of the corrosion predicted by the HRVRT on the 9 5/8 in. surface casing vis-à-vis the 7 in. production casing is summarized in Figure 21. The 9 5/8 in. is shown on the left, and the 7 in. is shown on the right in Figure 21. The blue circles are the internal defects, and the purple circles are the external defects.

Label '1' in a yellow box shows where external corrosion was found on the 7 in. casing, and internal corrosion was found at the same depth on the ID of the 9 5/8 in. casing. The same corrosion mechanism affected the OD of the 7 in. and the ID of the 9 5/8 in. It is important to note that the temperature of the 9 5/8 in. will often be lower than the 7 in., and that would result in a lower corrosion rate of the surface casing.

Label '2' shows a region of internal corrosion (denoted by blue dots) on the 9 5/8 in. casing. This region is from 35 – 80 ft. Blade's interpretation is that this internal corrosion at 35 – 80 ft on the 9 5/8 in. casing occurred before 1993. This is because the 7 in. at the same location exhibited wall loss, but lower than 20% nominal wall thickness (NWT). The lower extent of corrosion on the 7 in. casing is reflective of the fact that it was replaced in 1993, whereas the 9 5/8 in. was installed in 1965.

Label '3' identifies a region of external corrosion on the surface casing. This is believed to be the region of aquifers that would have resulted in the external corrosion. The corrosion changes from internal above this depth to mostly external corrosion below this depth.

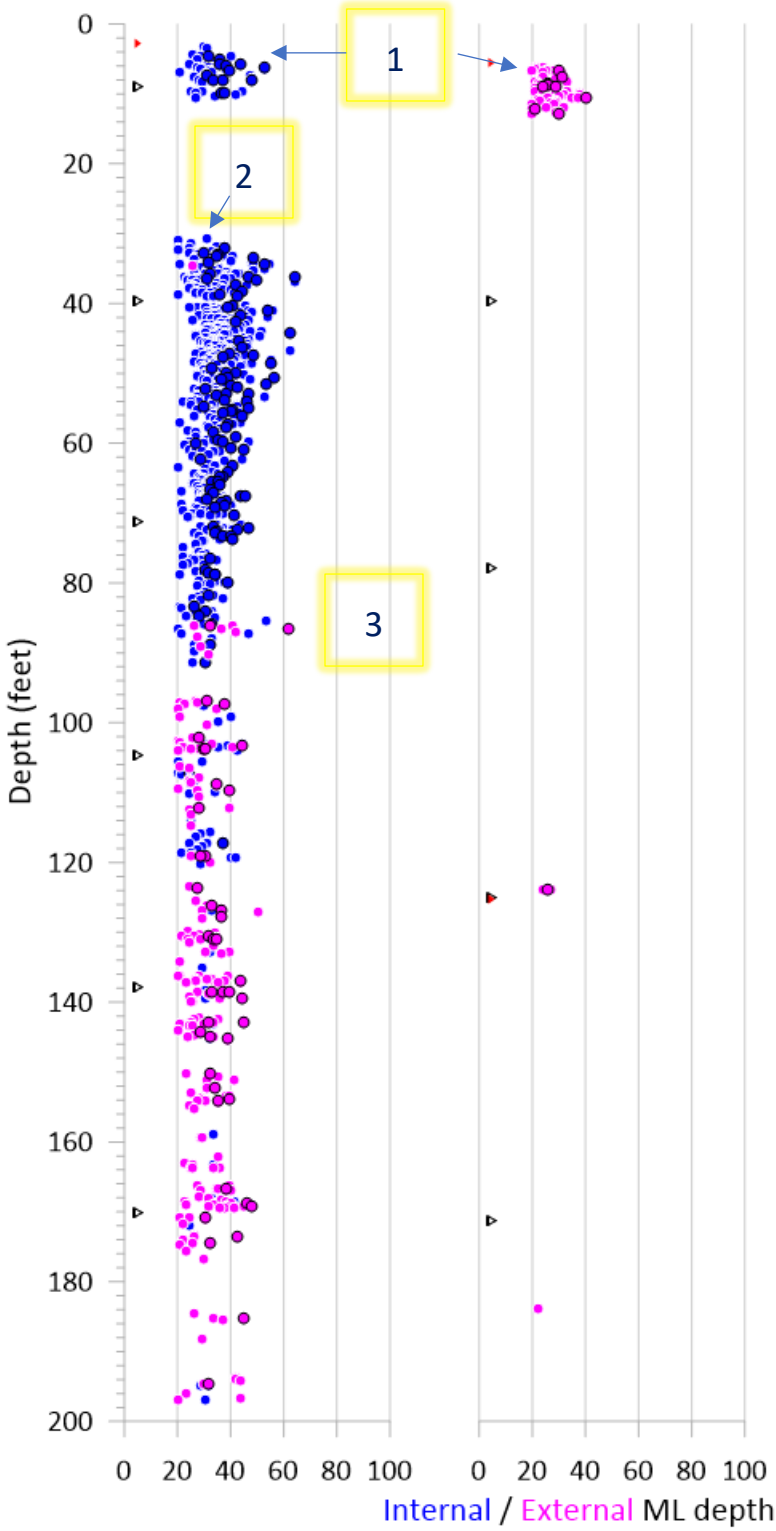

Figure 21: #2244 Metal Loss from HRVRT Logs, 9 5/8 in. (2023, Left), 7 in. (2016, Right)

6.1.5 Annulus Evaluation Logs

During the RCA, logging was performed in five wells, namely #2244, #2248, #2251, #2253, and #2254, to determine the condition of the annulus. The #2253 and #2254 wells were logged during the writing of this report. The logging tools used were the SLB Isolation Scanner and Baker Hughes INTex (Integrity Explorer) cement evaluation tools. Four of these wells show the absence of good cement from the surface to approximately 3,000 ft.

One well, namely #2251, shows good cement in this region. The #2248 Isolation Scanner summary is as follows:

- Across the interval approximately 7 ft – 2,568 ft, mostly gas-filled annulus or dry micro-annulus of large size.
- Across the intervals 4,580 – 4,597 ft, 4,643 – 4,773 ft, 4,983 – 5,013 ft, 5,303 – 5,311 ft, 5,460 – 5,500 ft, 6,592 – 6,657 ft, 6,689 – 6,829 ft, and 7,205 – 7,462 ft, high azimuthal coverage of cement with isolated liquid pockets is observed on the solids—liquid—gas (SLG) map.

6.2 Overall Summary of Integrity

Figure 22 shows a timeline of when three types of logs were run by well. The time frame is from January 1965 to April 2023. The types of logs displayed, casing inspection, leak detection, and cement evaluation are denoted by I, L, and C, respectively. This discussion will collectively refer to these types of logs as integrity logs. The formation evaluation and other types of logs are not displayed but listed in Appendix A.3.

The time interval between logging during 1990 and 2001 was 5 – 6 years. From 2002 – 2013, only four wells were integrity logged by PNG. Equitrans logged all wells in August 2016, approximately three years after acquiring the Rager Mountain field. The last instance when all wells were logged was in 2001, a 15-year interval. This logging interval was consistent with the Equitrans Storage Integrity Management document in 2015.

Workovers were performed and denoted by “WO.” Several workovers were performed in the same year as integrity logging. Blade did not have access to the Peoples Natural Gas Integrity Management Plan. Blade infers from the timeline that Peoples Natural Gas started in the 1990s with a 5-year interval, and by the 2010s moved to a new interval of approximately 12 or more years.

Approximately seven workovers were performed in the same year as integrity logging; each logging campaign resulted in one or more workovers. Blade’s interpretation was that Peoples Natural Gas’ integrity management approach was to log for corrosion and then replace casing joints wherever they deemed necessary.

Baker Hughes provided Equitrans and Peoples Natural Gas logging summaries for each Rager Mountain well in the time frame of 1996 – 2016. Unlike the prior years, Baker Hughes did not recommend to Equitrans any mitigation action such as gelling in any of the 2016 logging summary reports. Baker Hughes’ specific recommendations for nine of the wells logged was, “Return well to service and place on normal re-log schedule.” Only two wells, namely #2246 and #2251, had slightly different recommendations of, “Return well to service and place on accelerated re-log schedule”. This starkly contrasts with the 1996 – 2009 logging summaries, where there was specific guidance, as follows, “This well should be repaired soon. It appears that the corrosion is associated with the annular fluid level. Inhibitor may slow corrosion until repaired.” The log summaries by well and date are tabulated in Appendix A.4.

Equitrans used GRNT, HRVRT logging, and Baker Hughes logging summary reports to inform them of casing integrity issues. The deepest corrosion feature in #2246 2016 log (original algorithm) was 88% at 6,158 ft. In April 2017, Baker Hughes had stated that, “This feature appears to be the result of drilling induced metal loss; possibly overstated” and recommended to “Return the well to service and place on accelerated re-log schedule.” However, Equitrans ran a casing patch from 6,030 to 6,190 ft to isolate the top five deepest internal defects in #2246 in 2017. Equitrans executed mitigative action to #2246’s deepest defects as prescribed by their integrity plan even though it wasn’t specifically recommended by Baker Hughes.

Blade interviewed Equitrans integrity personnel on July 20, 2023, regarding the 2016 logging campaign. Equitrans had studied the inspection and workover records of the Rager Mountain wells at the time of the ownership change. Equitrans expected actionable corrosion levels to be present in the 2016 logging data like in previous Peoples Natural Gas logging campaigns. Other than the one actionable corrosion defect in #2246 there was no other significant anomaly per the 2016 SIMP.

There are records that indicate Equitrans had informally considered gelling all Rager Mountain wells based on the 2016 Baker Hughes HRVRT logs. However, there are no Maximo records of gelling; gelling was never executed.

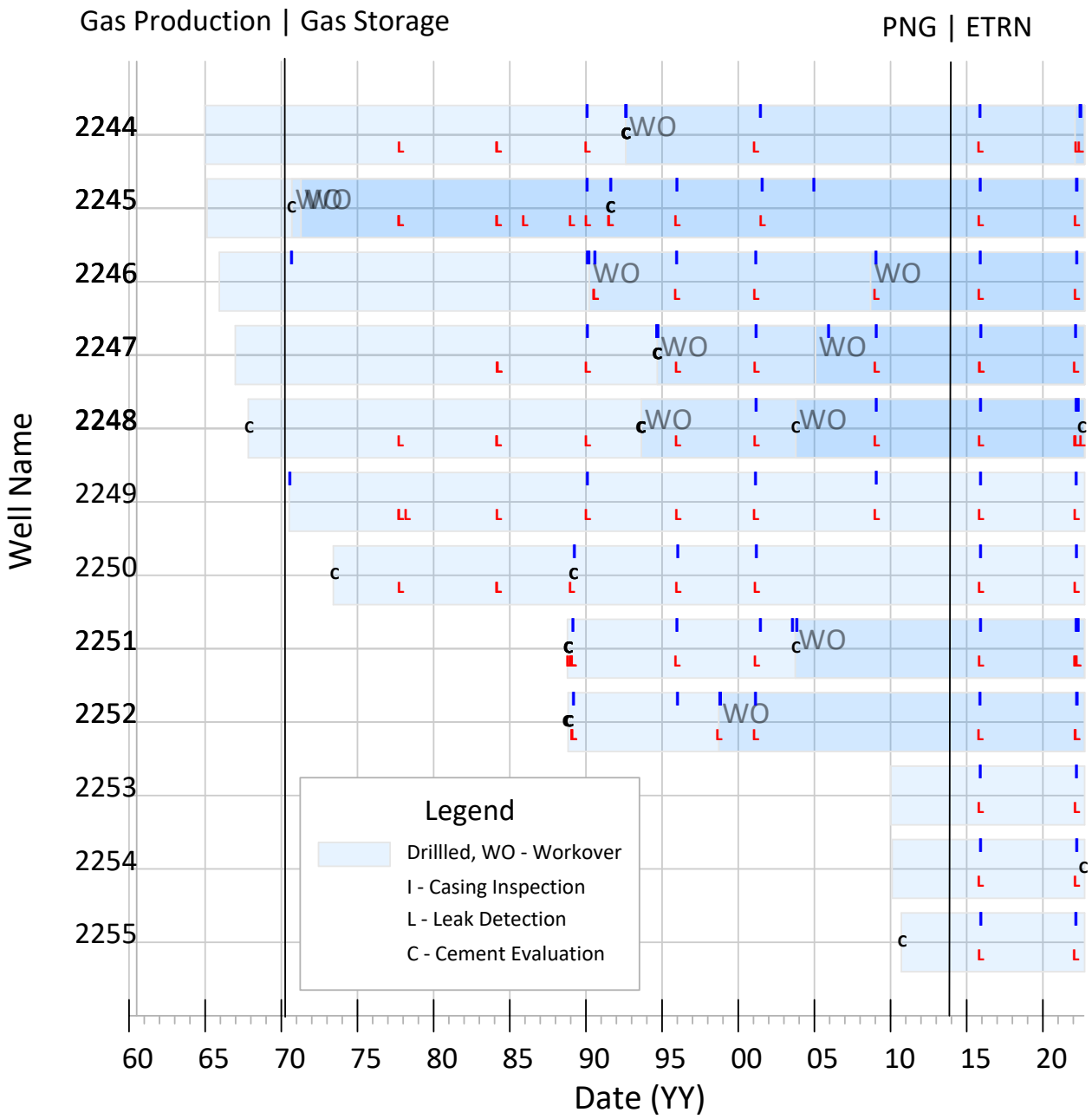

Figure 22: Timeline of Logging Activity

7 Failure Analysis

The overall objective of the failure analysis is to assess the direct cause of the rupture and parting of the 7 in. casing string. The approach was to first assess the sequence of the failure itself. This was then followed by the detailed evaluation of the extensive corrosion.

7.1 #2244 7 in. Casing Failure Events and Sequence

The intent here is to identify any missing fracture pieces through failure reconstruction. To interpret the nature of fracture and consequently establish the sequence, the available fracture surfaces were carefully examined. The failure pressure and the critical crack size for circumferential parting were estimated. This section provides details of these analyses.

7.1.1 Overview

A key step in the root cause analysis is the failure analysis of the parted 7 in. casing in well #2244. The casing parted in the first joint near the surface, allowing gas to escape through a 2 in. annulus valve.

The upper portion of the failed casing was extracted on March 5, 2023. The casing was then cut at a depth of 20.5 ft, and the lower portion of the failed joint was extracted. The upper and lower sections of the failed joint were designated C001A and C001B. Figure 23 and Figure 24 show the extraction of C001A and C001B, respectively. The fishing tool used to pull the upper section of casing is also shown in Figure 23.

Figure 23: C001A Extraction

Figure 24: C001B Extraction

Section 3.2.1. discusses the workover summary to recover well #2244 casing. Thirty-four joints were recovered from the well, totaling 1,468 ft of 7 in. casing. The results from the post-event logging and rig inspection of the extracted casing found the corrosion was isolated to the top joints. The top six joints (including the failure joint) were selected for further examination in Houston. Casing joint C030 was also selected as a representative sample for the remaining joints extracted from the well and was also shipped to Houston. Figure 25 shows the as-received condition of the crates with the C001A and C001B specimens.

Figure 25: As-Received Condition of C001A and C001B Specimens

Figure 26 shows the top (C001A) and bottom (C001B) fracture surfaces of the parted casing (C001) retrieved from well #2244. The downward-facing fracture surface from the top-parted casing (C001A) was 0.9 ft below the slips. C001A contained the axial rupture that has an upper turning point and a lower turning point. Visual examination of C001A showed that the axial rupture extends to circumferential parting at the lower turning point and a small circumferential crack at the upper turning point.

C001B contained the circumferential fracture surface that was facing upward in the well. Figure 26 also shows that a small portion of joint C001 is missing (i.e., not retrieved from the well). The fracture surfaces were examined in detail at the Blade Laboratory in Houston, TX. The results of the evaluation are provided in the following sections.

Figure 26: Photo of Axial Rupture and Parting of Joint C001 Rotated Approximately 180°

7.1.2 Failure Reconstruction

Fracture segments are sometimes lost during a failure. Fracture fragments can break off and remain downhole. Reconstruction of the fracture fragments was performed to establish whether all fracture surface fragments had been recovered from the well.

Fracture reconstruction was performed using a paper tracing technique [12]. The C001A and C001B fracture fragments were traced on butcher paper, cut out, and wrapped around a 7 in. pipe for visualization. The paper replicas of the failed pieces were rotated to align the mating fracture fragments. Figure 27 shows the paper replicas of the C001A and C001B failure pieces wrapped around each sample. Care was taken during the tracing process to prevent damage to the fracture surfaces.

Figure 28 shows the completed paper reconstruction. Visual examination of the reconstructed failure found that a piece of the failure was missing. The missing failure piece is indicated in Figure 28 by the white space between the C001A and B paper replicas. A deviation in the fracture path was noticed on one of the fracture surfaces associated with the missing failure piece.

A comparison of the trace with the actual failure piece found that the deviation was caused by damage to the upward-facing fracture surface (C001B). The damage is indicated in Figure 28 by the white arrow.

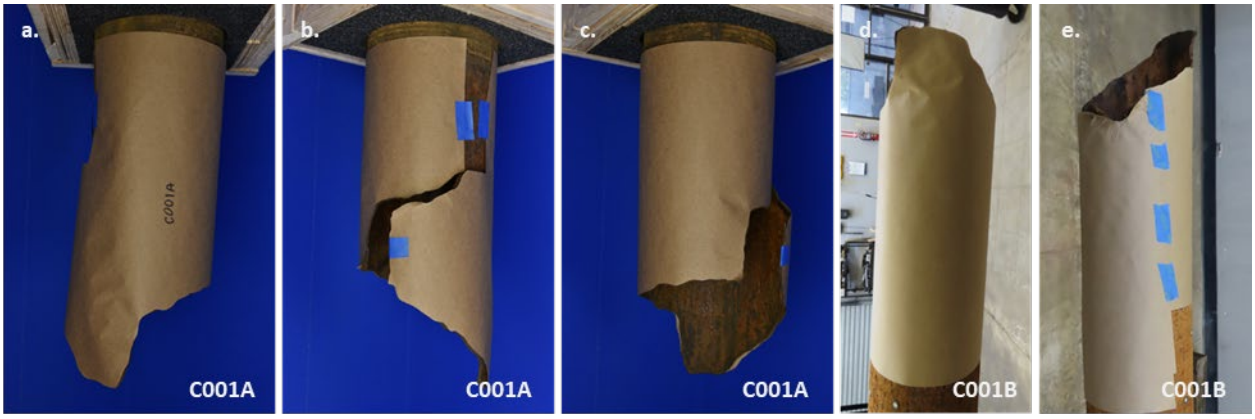

Figure 27: Paper Reconstruction of C001A (Downward Facing: a, b, c) and C001B (Upward Facing: d, e)

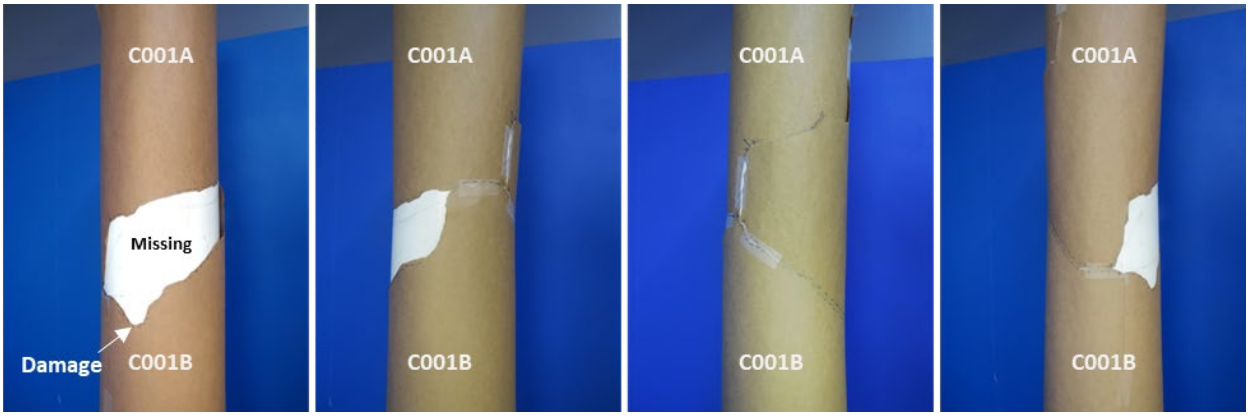

Figure 28: Completed Paper Reconstruction of Joint C001 Showing the Missing Failure Piece (white area) Rotated Views ~90°

7.1.3 Axial Rupture Analysis

Visual and Stereoscopic Examination

The objective of the visual and stereoscopic examination is to identify the key features of the axial rupture, such as the length of the axial rupture, the thickness along the axial rupture, and the location of the turning points. The axial rupture produced two mating surfaces: fracture surfaces 1 (C001A-1) and 2 (C001A-2). The length of the axial rupture is approximately 3.36 in.

Figure 29 shows C001A (bottom-facing fracture surface) and C001B (upward-facing fracture surface) rotated to align the mating fracture fragments. The axial rupture is only present on C001A. The figure also shows the upper and lower turning points in C001A. C001A-1 and C001A-2 experienced plastic deformation, as evidenced by the bulge in Figure 29 a and b. Figure 30 shows the fracture surfaces of the axial rupture (C001A-1 in Figure 30a and C001A-2 in Figure 30b) and the upper turning point (Figure 30c). Chevron marks were not identified during the visual examination of C001A-1 and C001A-2 fracture surfaces.

Figure 29: (a) C001B and C001A Fracture Fragments Showing Location of Axial Rupture in C001A, (b) Crack Direction in Axial Rupture, and (c) Measurement of Axial Rupture Length

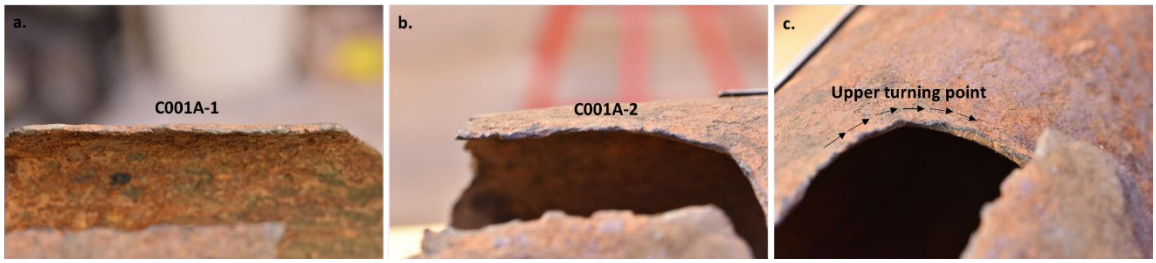

Figure 30: Axial Rupture Fracture Surfaces (a) C001A-1, (b) C001A-2, and (c) Upper Turning Point

The geometry of the failure piece made fracture surface extraction in the lab challenging. The objective was to remove the fracture surfaces without damaging any of the remaining surfaces. A portable band saw was selected to extract C001A-1. The surfaces were protected by securing the sample using wood or protective padding to prevent damage. Figure 31a shows the C001A-1 cut location, and Figure 31b and c show the protective padding used during the cut. Coolant was not used during the cut to avoid contamination of the fracture surface and scale products.

Figure 31: C001A-1 Axial Fracture Surface (a) Dashed Line Showing Cutting Location, (b) Protected Fracture Surface, and (c) After Cutting of Axial Fracture Surface C001A-1

The wall thickness along the axial rupture was measured using a point micrometer. Figure 32 shows the wall thickness measurements before and after excising the rupture split fracture surfaces (C001A-1 and C001A-2). Slight variations in the wall thickness measurements before and after cutting the specimens are due to pits in the sample. Additionally, variations in the wall thickness measurements may be caused by variations in the measurement location before and after cutting.

Figure 32 shows the thinnest region in both C001A-1 and C001A-2. The smallest wall thickness reading in C001A-1 and C001A-2 is 0.0473 and 0.0576 in., respectively. The thinnest wall in the C001A-1 specimen does not align with the thinnest wall region in C001A-2. Figure 33 shows the graph of measured wall thickness in C001A-1; distances are relative to the upper turning point location. The dashed red line is nominal wall thickness.

As discussed, the misalignment of the thinnest regions may be caused by the distribution of pits along the axial rupture. When C001A-1 and C001A-2 were placed side by side, some portions of C001A-1 matched with C001A-2, but others did not. Figure 34 (b) shows that a small region between C001A-1A and C001A-2A is missing.

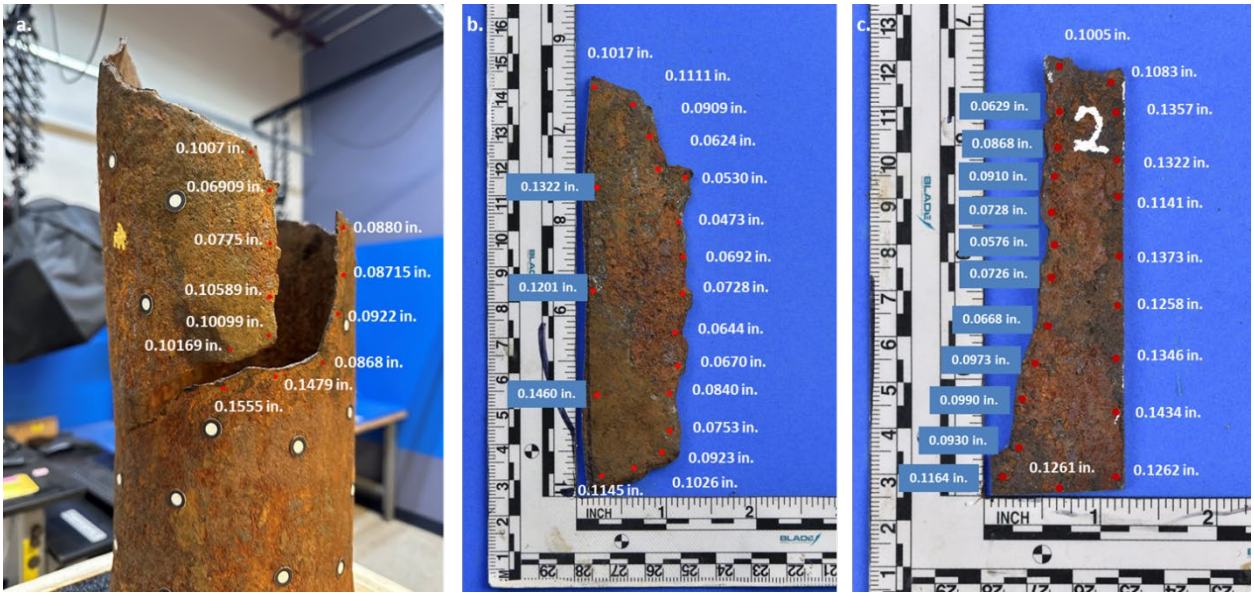

Figure 32: Thickness Measurements Along the Axial Rupture in (a) C001A, (b) C001A-1, and (c) C001A-2

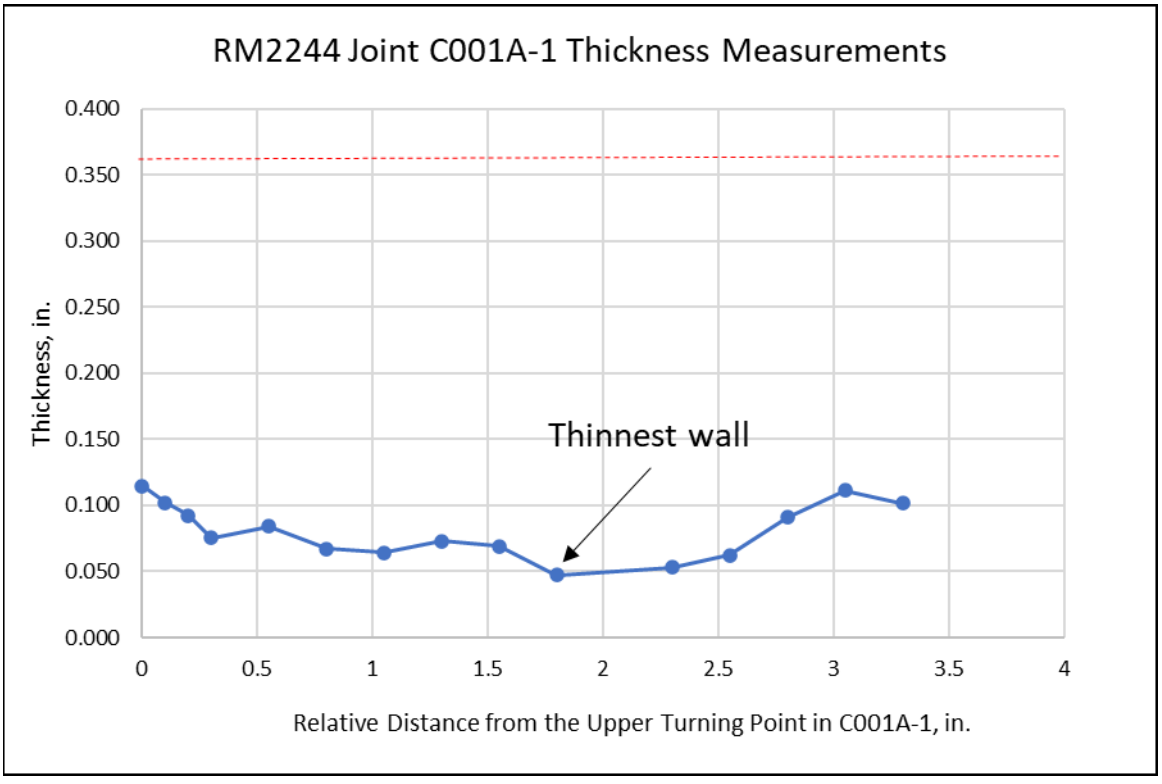

Figure 33: Plot of Thickness Measurements in C001A-1 Relative to the Upper Turning Point Location (Bottom of Figure 32b)

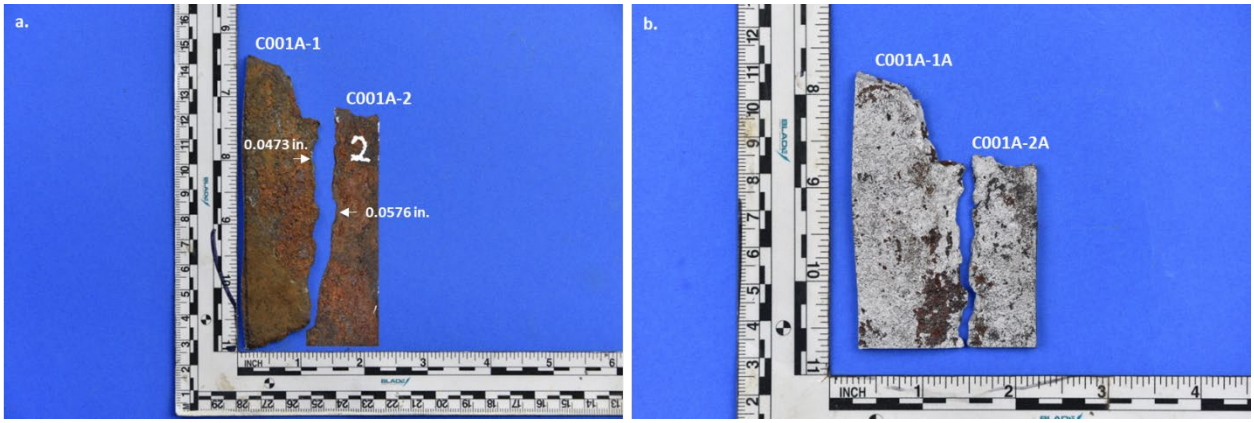

Figure 34: (a) Location of Thinnest Regions in C001A-1 and C001A-2 and (b) Matching Axial Fracture Surfaces

Figure 35 and Figure 36 show the stitched stereoscope image of the fracture surface of C001A-1 and C001A-2 before any cleaning was performed. A small crack was observed at the step in C001A-1. The C001A-1 crack is indicated in Figure 35 by the white arrow. More details are presented about this crack in the circumferential parting section of the report.

A similar small crack was observed in C001A-2 at the upper turning point. The location of the crack at the upper turning point is indicated by the white arrow in Figure 36. Features were not observed on the fracture surfaces during the stereoscope examination. Chevron marks were not observed, consistent with visual examination.

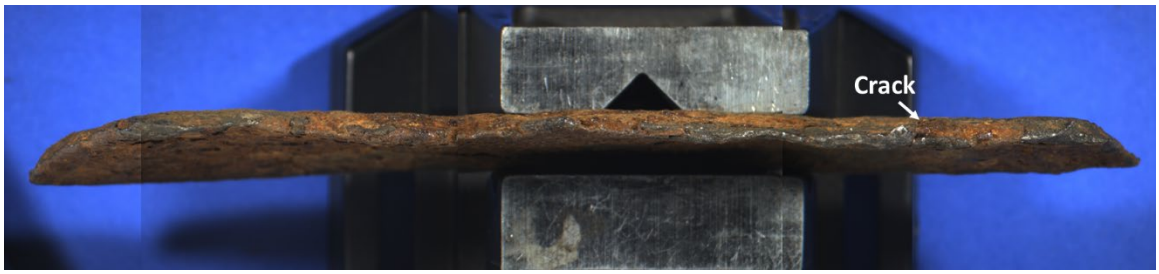

Figure 35: Stitched Stereoscope Image of C001A-1 Fracture Surface

Figure 36: Stitched Stereoscope Image of C001A-2 Fracture Surface

Figure 37 shows the features observed in the OD and ID surfaces of the C001A-2 specimen. Corrosion attack is visible on both the OD and ID surfaces of C001A-2. However, the corrosion pits on the OD surface are more prominent. Figure 38 shows the crack at the upper turning point region of C001A-2.

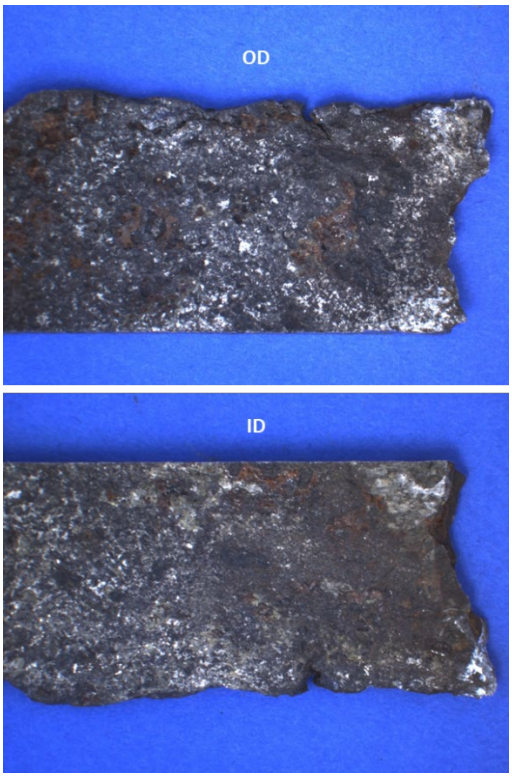

Figure 37: Features Observed on C001A-2 OD and ID Surfaces

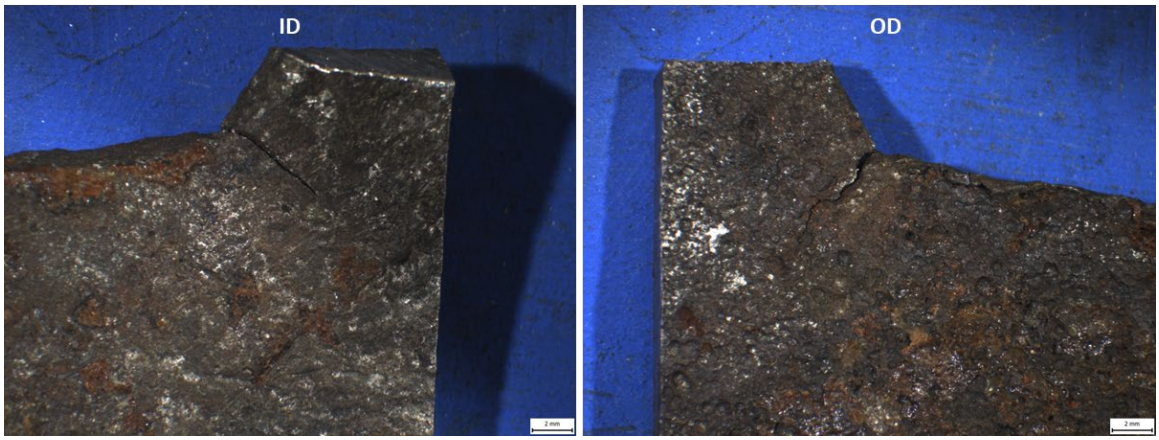

Figure 38: Crack in the Upper Turning Point of C001A-2, Seen in both OD and ID Surfaces

Sample C001A-2 was cut to excise the crack at the upper turning region. The crack was subsequently broken open in liquid nitrogen temperature for fracture surface examination. Figure 39 shows the specimens obtained by cutting C001A-2.

Sample C001A-1 was also cut into smaller pieces to enable scanning electron microscope (SEM) examination of the fracture surface. Figure 40 shows the specimens C001A-1A and C001A-1B after cutting. C001A-1B was used for establishing the cleaning procedure before SEM examination.

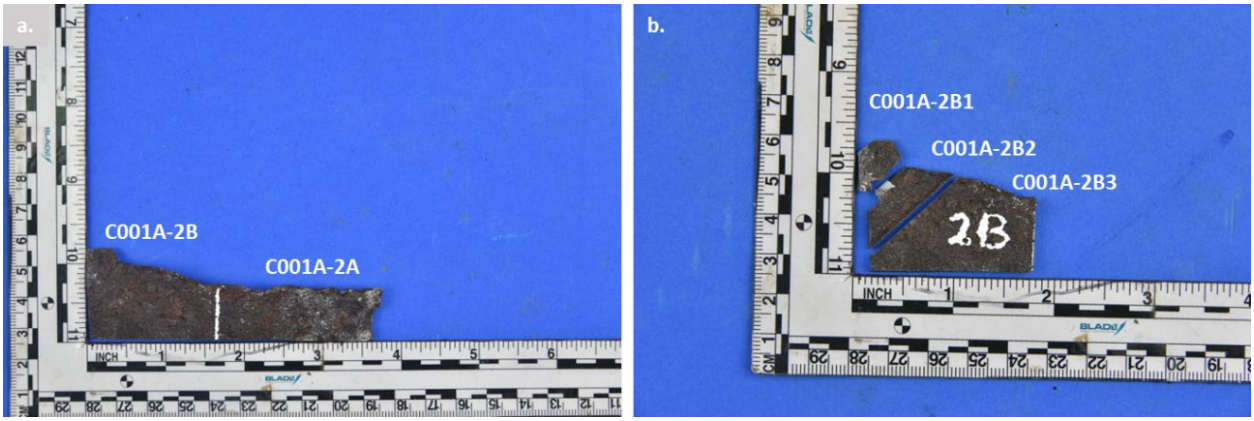

Figure 39: Specimens Cut from C001A-2

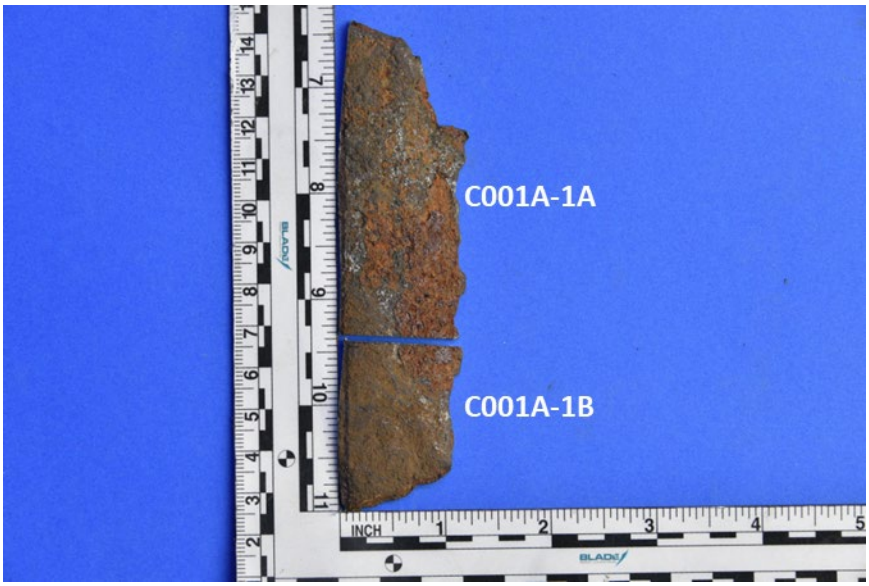

Figure 40: Cut Specimens from C001A-1

Subsequent sample cleaning was performed by sonicating in acetone for 10 minutes, followed by sonicating with 1% Alconox for 5 minutes, sonicating with acetone for another 10 minutes, and then rinsing with methanol.

This cleaning method was established by examining the fracture surface specimen in the SEM before and after each cleaning step. Examination with the SEM after each step ensured that the cleaning procedure did not attack the fracture surface by creating new pits.

If the first cleaning attempt did not remove the heavy scale or corrosion product, additional cleaning was performed by sonicating in 1% Alconox or 0.5% Citranox for 3 to 5 minutes at room temperature, followed by sonicating in acetone and rinsing with methanol.

Figure 41 shows the stitched stereoscope images of the C001A-1A and C001A-2A fracture surfaces. The scale and corrosion products were not completely removed. The stereoscope examination of the fracture surface after cleaning confirmed the lack of chevron marks on the fracture surfaces of the axial rupture. However, uneven thinning along the axial fracture surface is visible from the macro images.

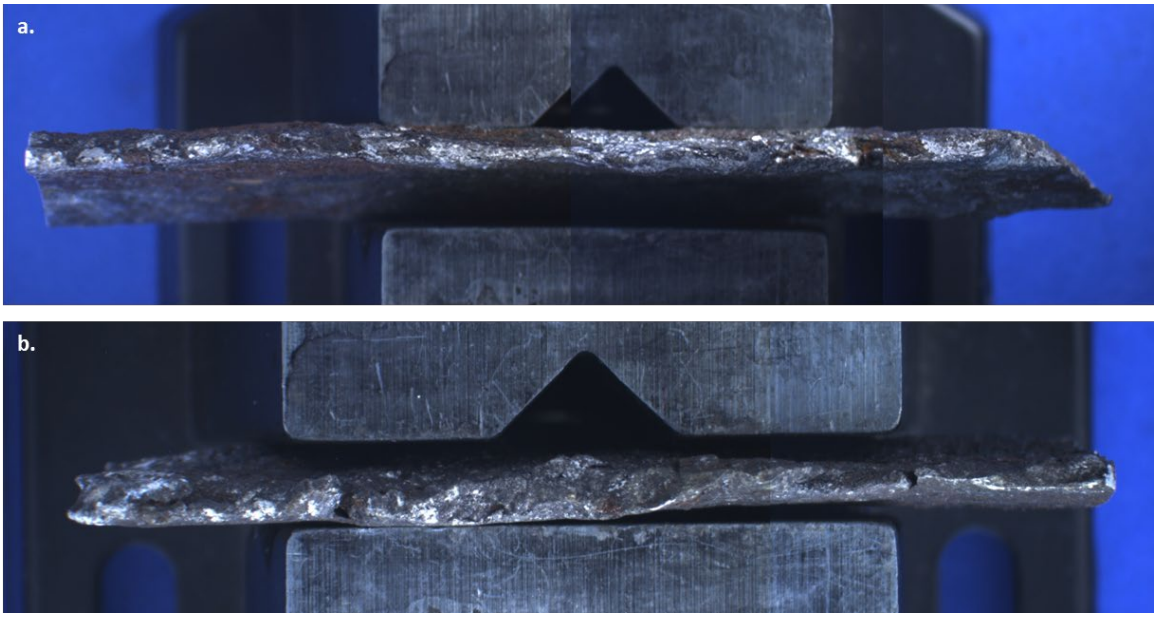

Figure 41: Stitched Stereoscope Images of (a) C001A-1A and (b) C001A-2A Axial Rupture Fracture Surfaces

Micro-Fractographic Characterization

The objectives of the micro-fractographic characterization are as follows:

- Characterize the fracture surface of the axial rupture.
- Identify the fracture mode of the axial rupture.
- Characterize the features on the OD and ID surfaces.

The fracture surface samples were cleaned using the protocol established in Section 7.1.3. The fracture surface examination was performed using the SEM. A general examination was performed at 30–50x magnification. Detailed examination were performed at various magnifications such as 100x, 250x, 500x, 1,000x, and 2,500x. The results of the micro-fractographic characterization are presented and discussed below.

C001A-1A

Figure 42 shows the stereoscope image of the fracture surface in C001A-1A and the three regions of the SEM examination. Region 1 includes the thinnest section in C001A-1A, and region 2 includes the rest of the fracture surface.

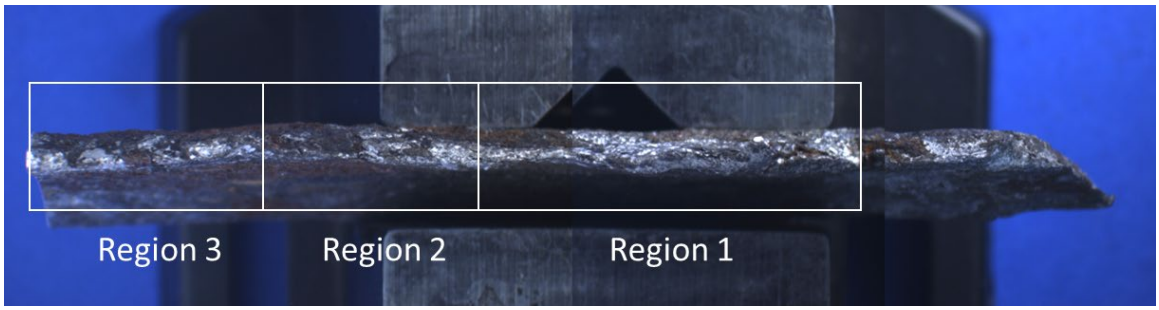

Figure 42: Stereoscope Image of C001A-1A Fracture Surface

Figure 43 shows the stitched SEM images taken at 35x magnification. The areas examined at higher magnification are identified in Figure 43 (A1 and A2). The features observed on the fracture surface are mostly rounded pits (dimple-like features), which are evidence that the fracture surface is corroded. No clear evidence of cleavage or facets was found in this region.

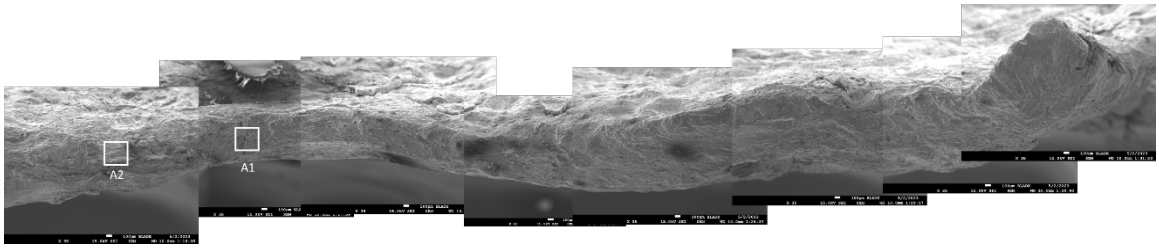

Figure 43: Stitched SEM Image of C001A-1A Fracture Surface Region 1

Area 1 is the thinnest region in C001A-1A specimen. Figure 44 shows the high magnification SEM images of Area 1. These images show the rounded pits observed on the fracture surface. Small, circular rounded pits are side by side and inside the bigger pits. Aside from the rounded pits, tiny (less than 10 µm) pits due to corrosion are also visible at 1000x and 2500x.

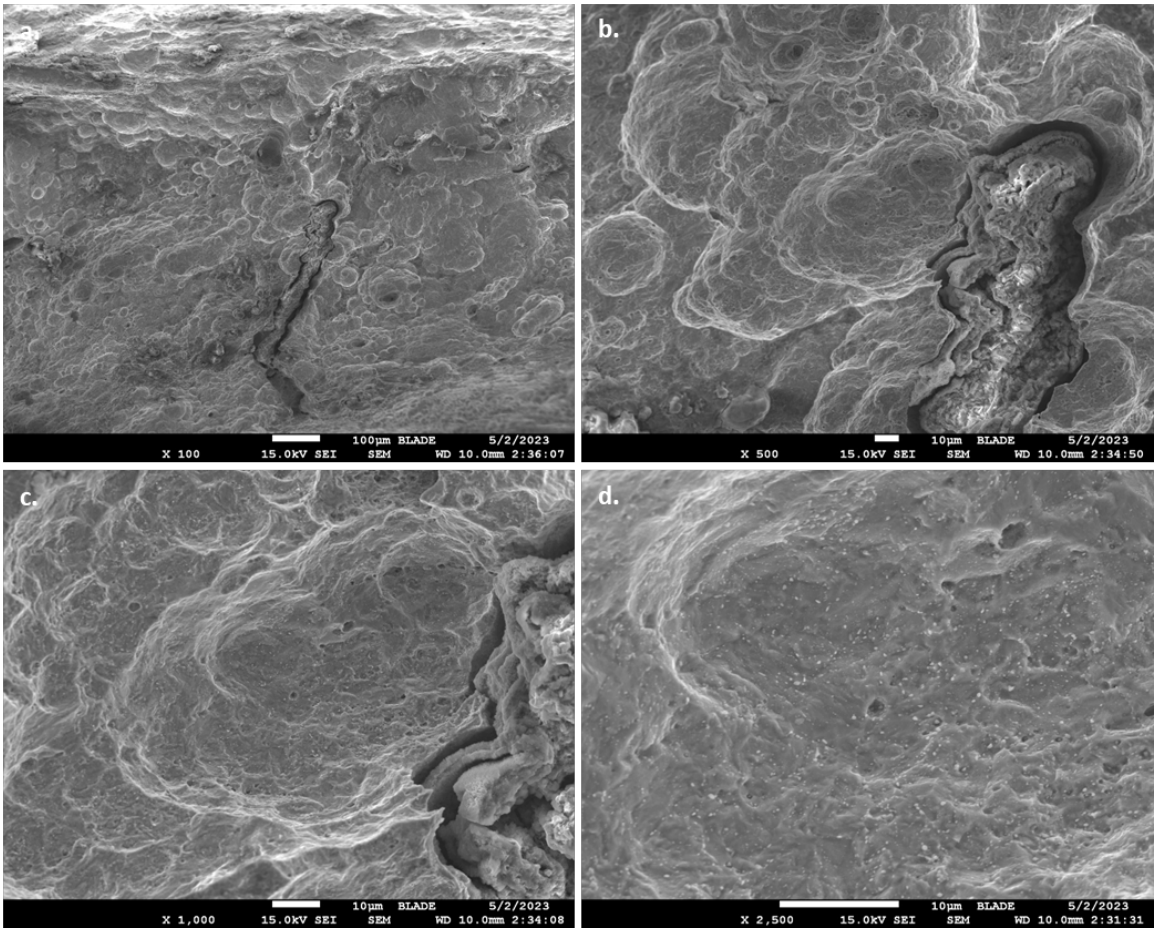

Figure 44: SEM Images of Area 1 in C001A-1A Fracture Surface Taken at (a) 100x, (b) 500x, (c) 1,000x, and (d) 2,500x

Figure 45 shows the higher magnification SEM images of Area 2 in the C001A-1A fracture surface. The images show the corrosion damage on the fracture surface, evidenced by the rounded pits and tiny pits observed on the fracture surface.

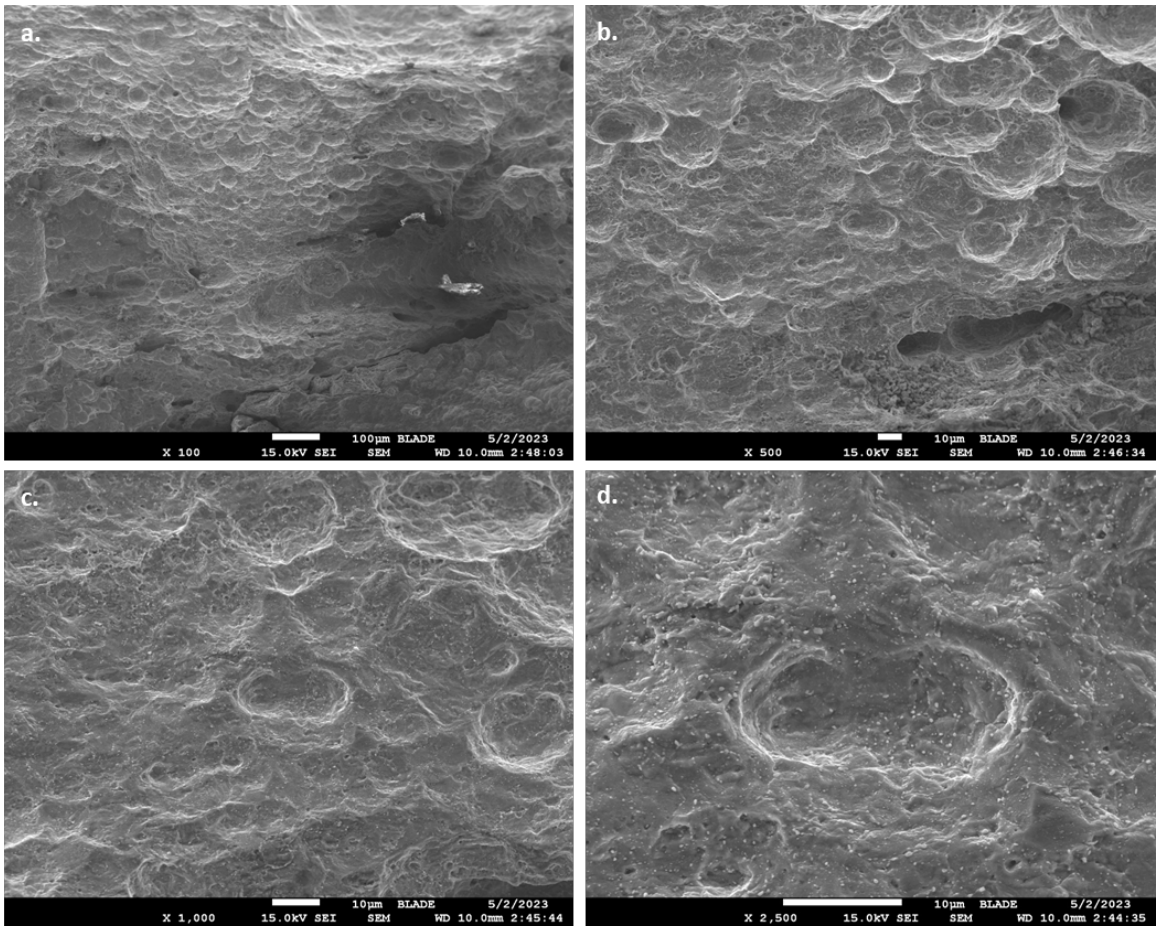

Figure 45: SEM Images of Area 2 in C001A-1A Fracture Surface Taken at (a) 100x, (b) 500x, (c) 1,000x, and (d) 2,500x

Figure 46 shows the stitched SEM image of the C001A-1A fracture surface region 2. Even after sonicating in Alconox and then in acetone, the scale or corrosion products were not completely removed. The fracture surface in this region is also corroded.

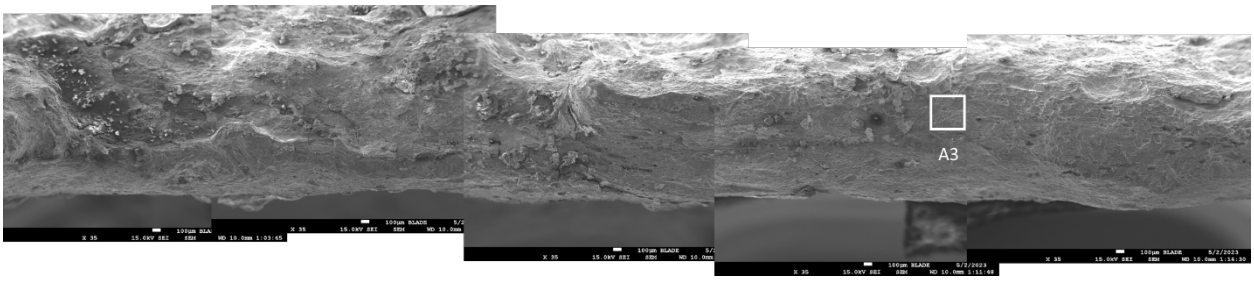

Figure 46: Stitched SEM Image of C001A-1A Fracture Surface Region 2

Figure 47 shows the SEM images of the corroded fracture surface in region 2. The circular pits are visible on the fracture surface. No clear evidence of cleavage nor facets exists in this region. The shape of the corroded region in Figure 47d takes the form of the underlying base metal microstructure (Figure 53 and Figure 238).

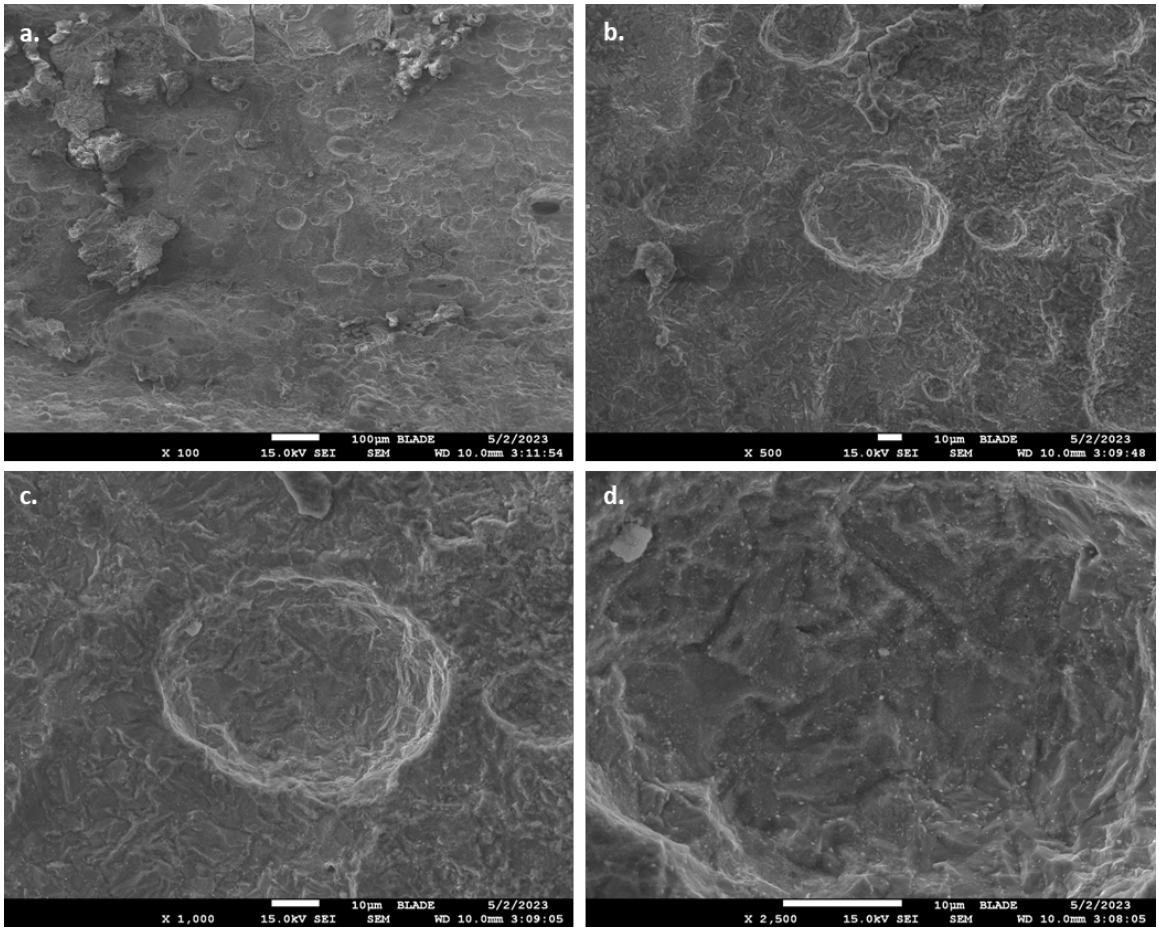

Figure 47: SEM Images of Area 3 in C001A-1A Fracture Surface Taken at (a) 100x, (b) 500x, (c) 1,000x, and (d) 2,500x

Figure 48 shows the stitched SEM image of the C001A-1A fracture surface region 3. Figure 49 shows the higher magnification images in area 4, located in region 3. The SEM images show corrosion damage with irregular shapes—some are oblong and some are circular on the fracture surface. No distinct cleavage or facet features are observed on the fracture surface.

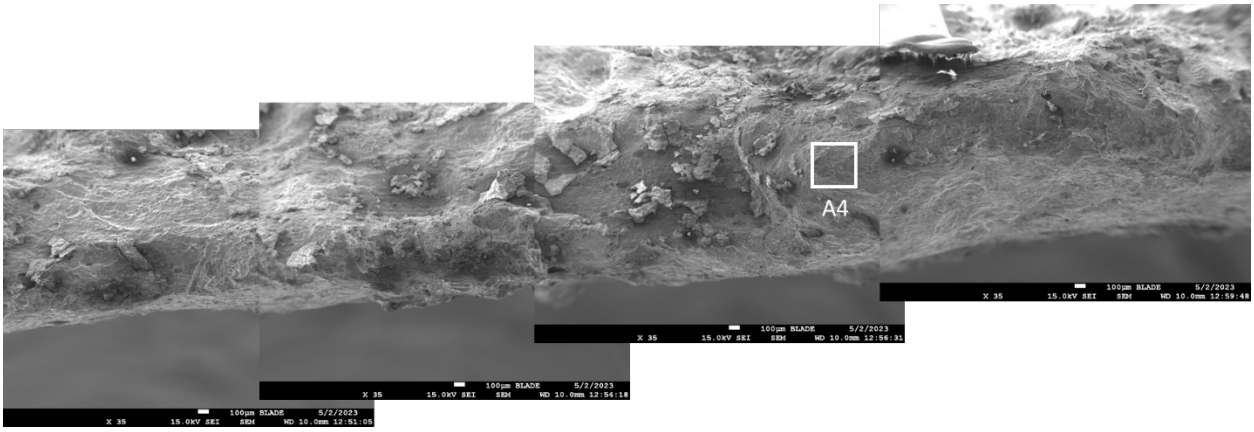

Figure 48: Stitched SEM Image of C001A-1A Fracture Surface Region 3

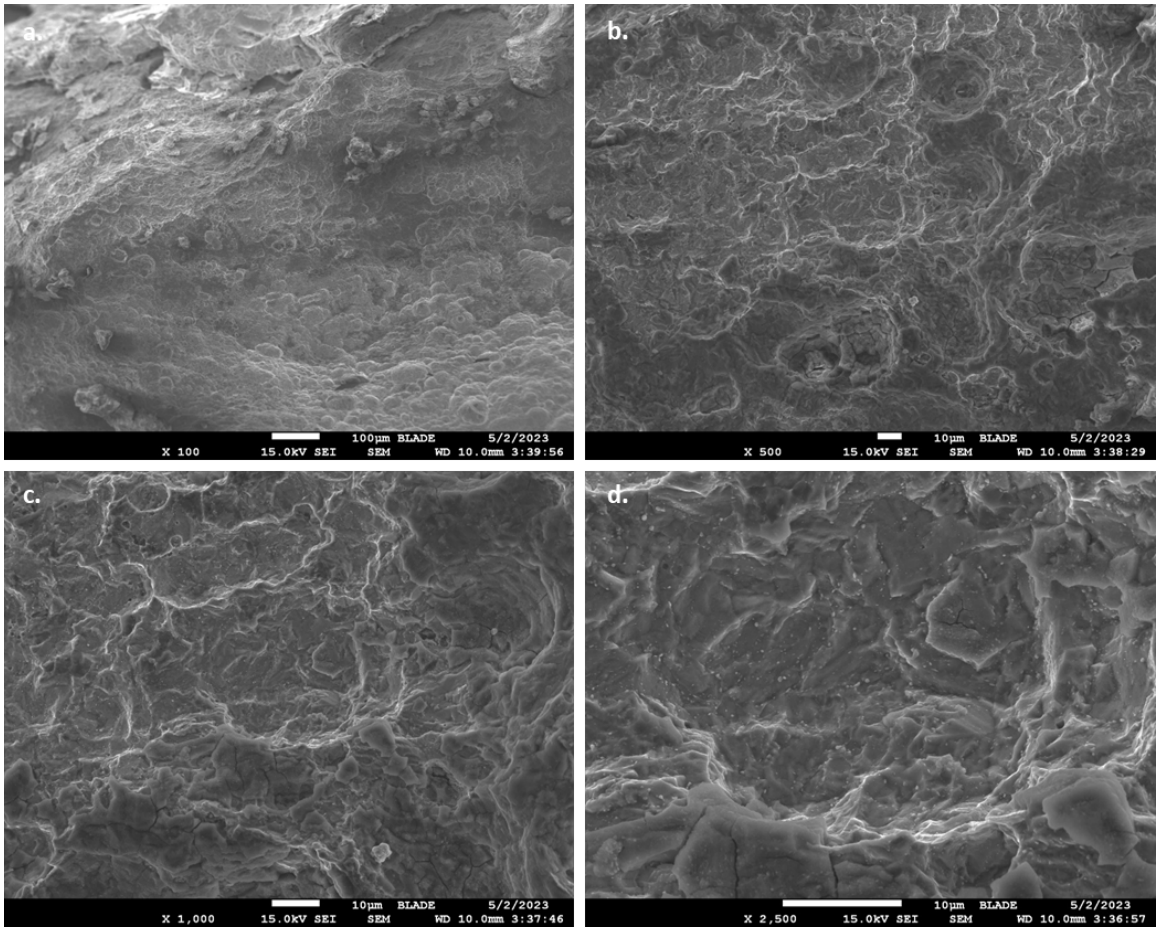

Figure 49: SEM Images of Area 4 in C001A-1A Fracture Surface Taken at (a) 100x, (b) 500x, (c) 1,000x, and (d) 2,500x

The SEM examination of the fracture surface mainly identified rounded pits. Distinct indications of cleavage features, flat facets, or any other indications of brittle or low energy failure were not observed. The rounded features are compared to the micro-void coalescence feature on the fracture surface of a tensile test specimen. Figure 50 a, b, and c show the features on the fracture surface of C001A-1A, while Figure 50 d, e, and f show the micro-void coalescence on a ductile tensile specimen.

The size of the features (rounded pits) in the C001A-1A fracture surface is generally larger than the micro-void coalescence feature on the ductile tensile specimen. The general shape of the C001A-1A fracture surface features (rounded pit) is hemispherical, which has some similarity to the general shape of the micro-void coalescence in the ductile tensile specimen.

Figure 51 shows the features observed on the OD surface of specimen C001A-1A. The images were taken at the same magnification as Figure 50. The images show similarities between the fracture surface features of C001A-1A and the features on the OD surface of C001A-1A, indicating that the fracture surface features of C001A-1A are due to corrosion and not ductile micro-void coalescence. The dimples in the tensile specimen are much finer than corrosion dimple-like features.

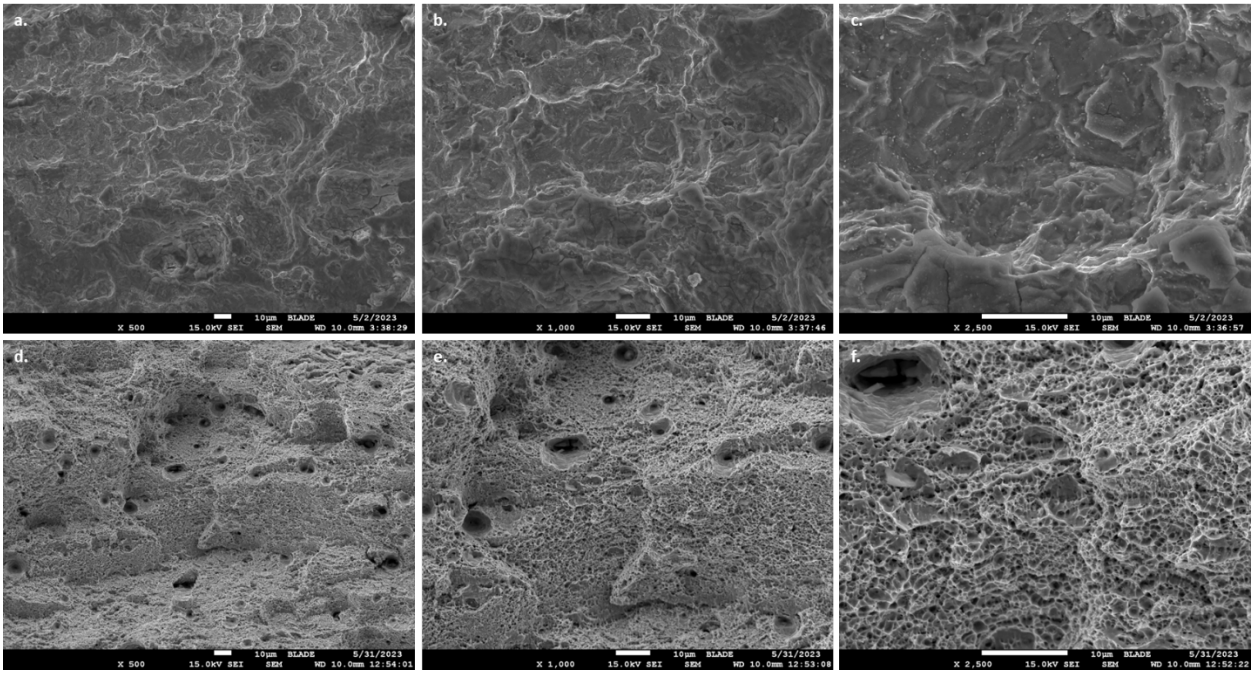

Figure 50: Comparison of Fracture Surface Features in C001A-1A (a, b, c) and N80 Base Metal Tensile Specimen Fracture Surface Micro-Void Coalescence Features (d, e, f) Imaged at 500x, 1,000x, and 2,500x

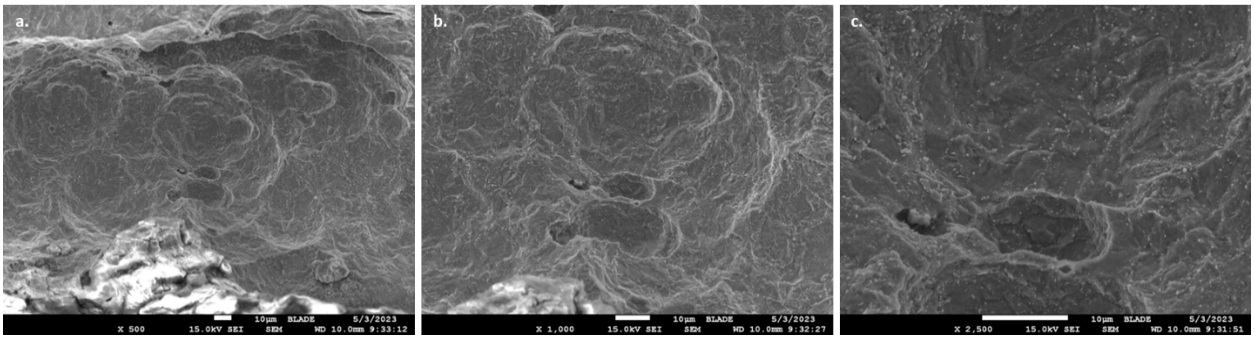

Figure 51: Features in the OD of C001A-1A Imaged at (a) 500x, (b) 1,000x, and (c) 2,500x

In addition to the SEM examination of the fracture surface, the thinnest region in sample C001A-1A was excised and polished for metallographic analysis. Figure 52 shows the cutting locations to excise the specimens for metallography. Figure 52 also shows the plane of polish. The C001A-1A2 specimen contains the fracture surface, and C001A-1A3 is the base metal used as a reference for microhardness.

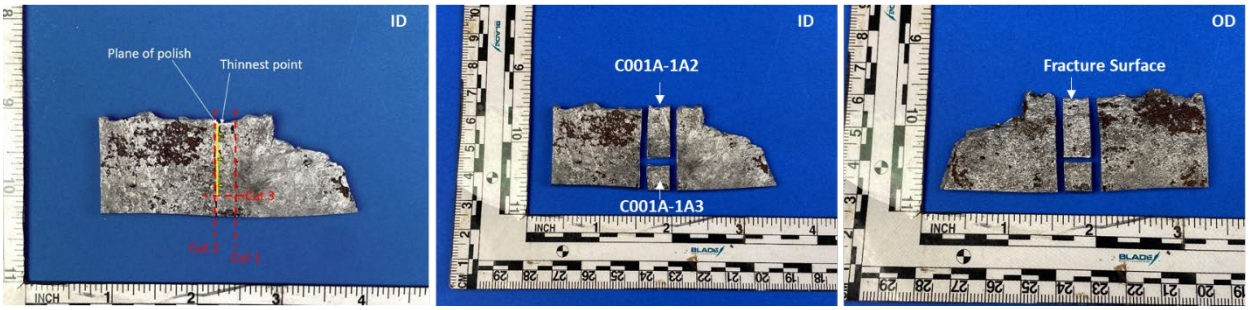

Figure 52: Specimens for Metallography

C001A-1A2 and C001A-1A3 were mounted using a hot mounting press. The samples were then prepared for metallographic examination by successive grinding in 120, 75, and 35 µm grinding pads. The samples were then polished using 3 and 0.25 µm diamond suspension. C001A-1A2 was etched with 2% Nital. An inverted metallurgical microscope was used to obtain the micrographs.

Figure 53 shows the stereoscopic image of C001A-1A2 and the micrographs near the fracture surface taken at 50x and 200x magnifications. The image shows the wall thickness profile of C001A-1A2. The wall thickness is the smallest near the fracture surface and increases away from the fracture surface (to the left side of the image).

The image also shows the pits on the OD surface near the fracture surface. The ID surface has minimal-to-negligible corrosion pits. Figure 53 shows that the grains near the fracture surface are more deformed compared to the grains in Figure 54, which shows the microstructure away from the fracture surface. The microstructure is similar to the base metal microstructure reported in Section A.10.2.

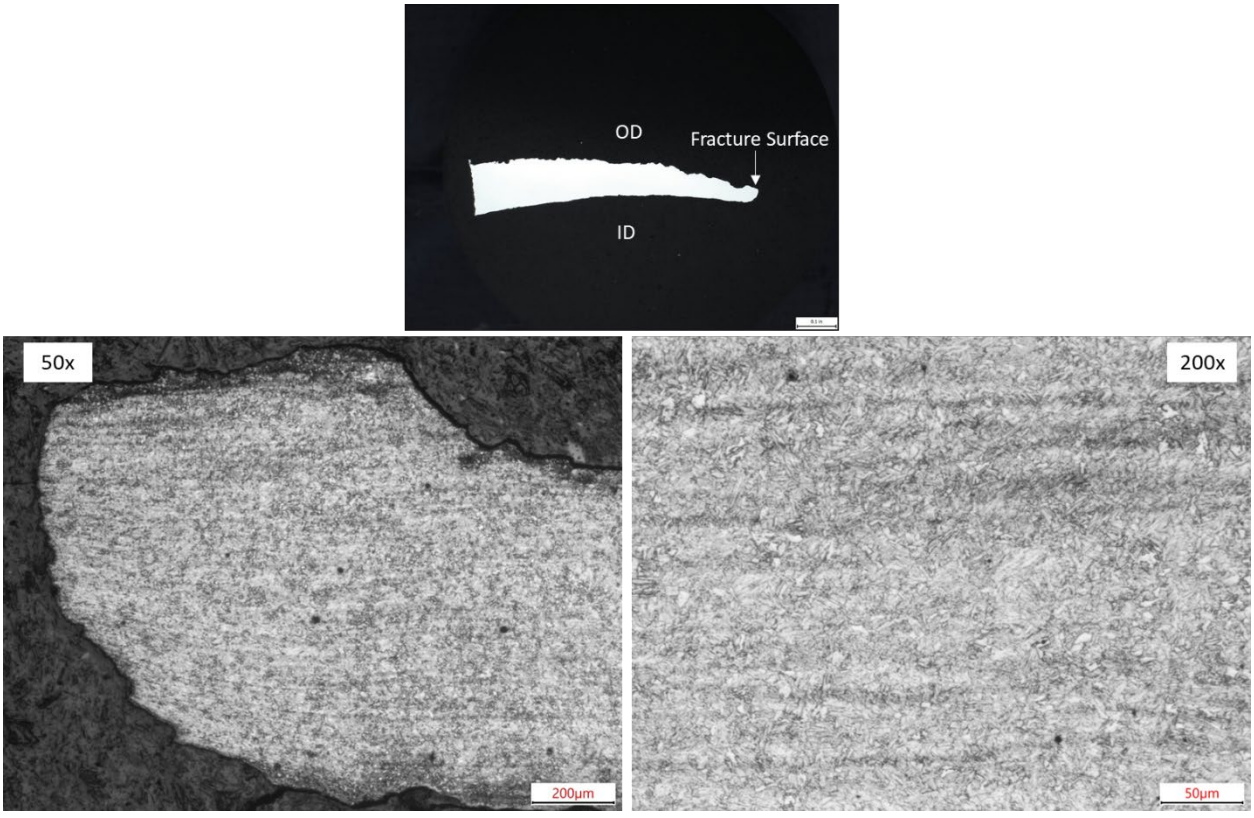

Figure 53: Metallographic Images of C001A-1A2 Near the Fracture Surface, Etched in 2% Nital

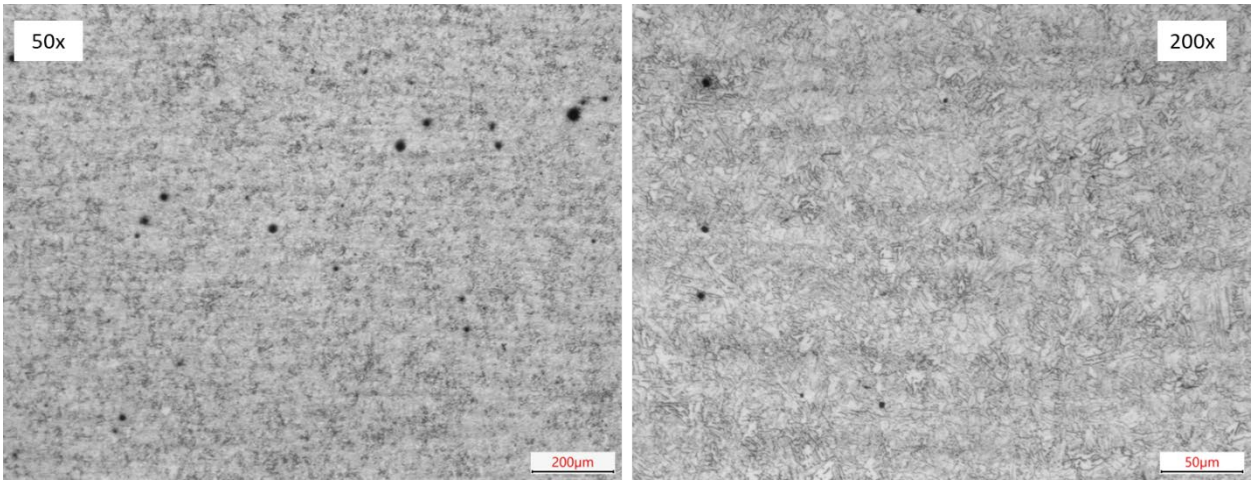

Figure 54: Metallographic Images of C001A-1A2 Away from the Fracture Surface, Etched in 2% Nital

Microhardness measurements were taken across the sample using a Vickers microhardness indenter with a 500 g load. Figure 55 shows the location of the Vickers microhardness indents. Table 16 shows the corresponding hardness values obtained from C001A-1A2 and C001A-1A3. The highest hardness measurement was obtained near the fracture surface. The values decrease from location 1 (near the fracture surface) to location 6 (away from the fracture surface). The higher hardness value near the fracture surface was expected due to ductile tearing during the axial rupture. Hardness values taken at locations 7 to 10 match the hardness values taken in the base metal sample in Section A.10.4.

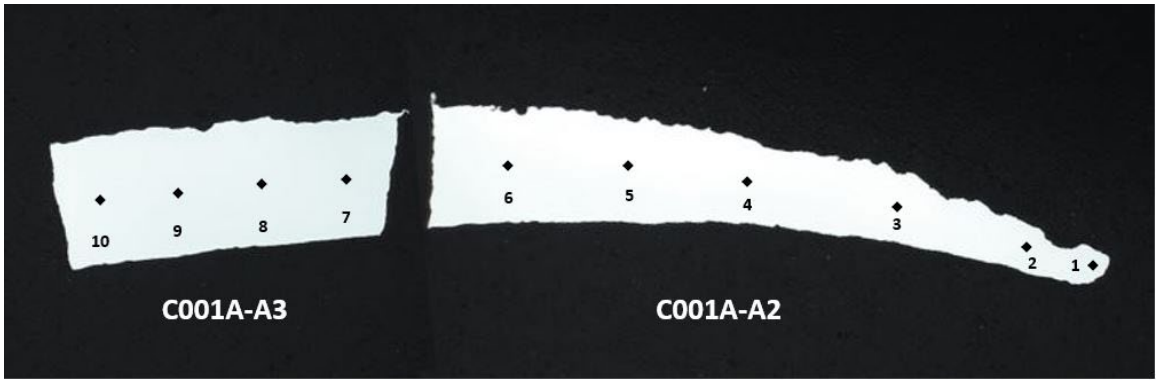

Figure 55: Location of Hardness Indentations

Table 16: Microhardness Measurements in C001A-1A2 and C001A-1A3

Location		$HV_{0.5\ kg}$	Conversions	
			HRB	HRC
C001A-1A2	1	256.3	—	23.4
	2	249.4	—	22.2
	3	237.1	99.5	—
	4	232.9	98.8	—
	5	230.2	98.4	—
	6	226.3	97.7	—

Location		$HV_{0.5\ kg}$	Conversions	
			HRB	HRC
C001A-1A3	7	223.7	97.3	—
	8	228.9	98.2	—
	9	221.8	97.0	—
	10	227.6	97.9	—

C001A-1B

The axial rupture fracture surface of C001A-1B was examined in the SEM to obtain a complete examination of the entire C001A-1 sample. The C001A-1B specimen was cut into two specimens to facilitate the examination of the fracture surfaces in the SEM. Figure 56 shows the cut location and the stereoscope image of the fracture surface in C001A-1B1 and C001A-1B2.

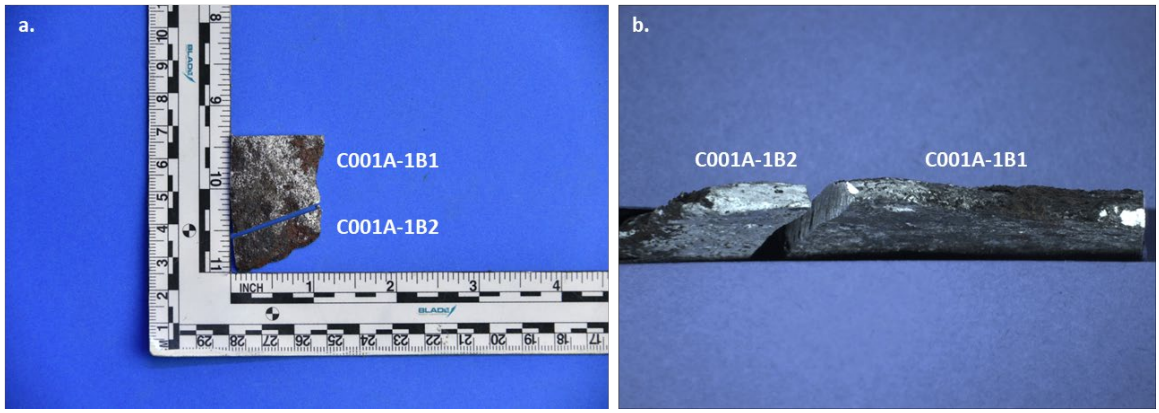

Figure 56: (a) Cut Specimens from C001A-1B, (b) Stereoscope Image of the Fracture Surface in C001A-1B1 and C001A-1B2

Figure 57 shows the higher–magnification images of the C001A-1B fracture surface. The fracture surface is corroded. No distinct cleavage or facet features are observed on the fracture surface.

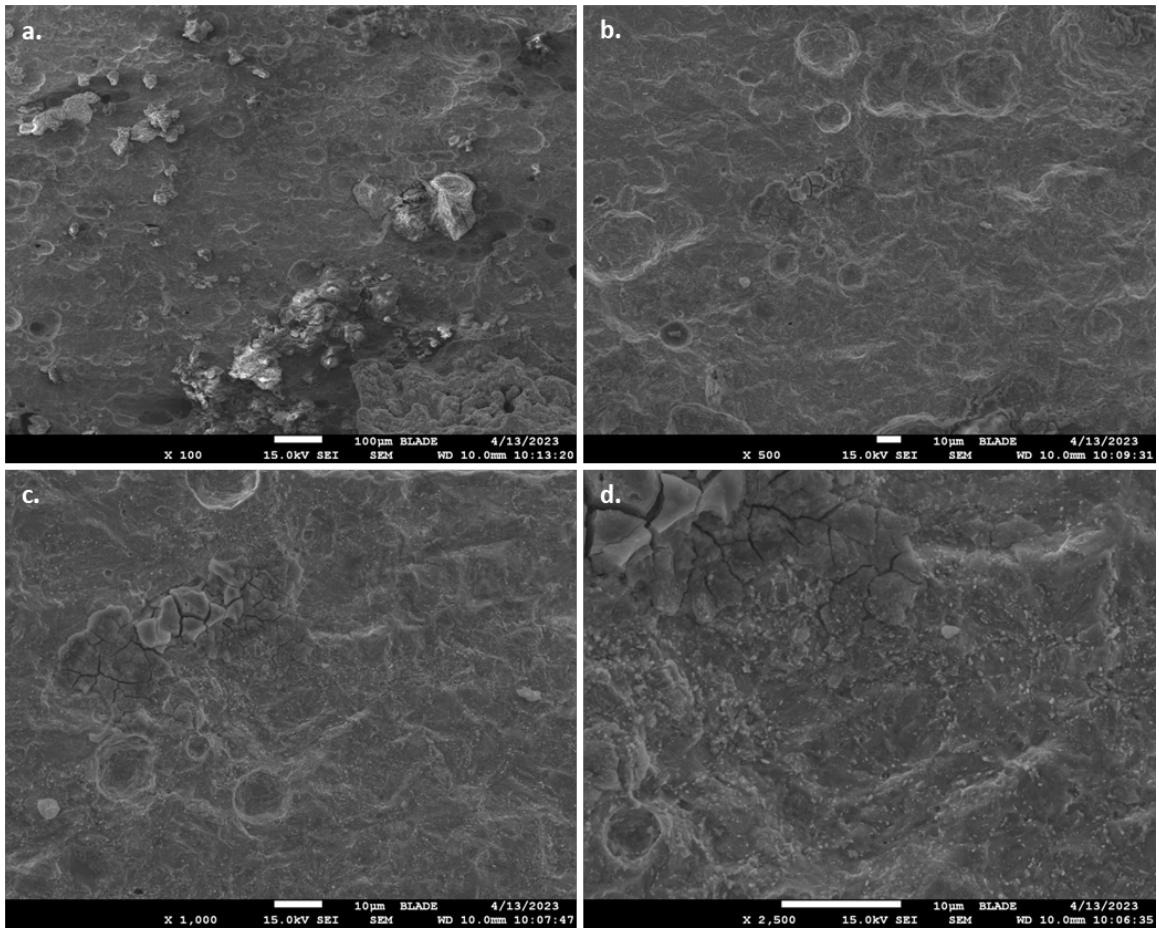

Figure 57: Representative SEM Images of C001A-1B Fracture Surface Taken at (a) 100x, (b) 500x, (c) 1,000x, and (d) 2,500x

C001A-2A

Figure 58 shows the four regions examined in the SEM in the C001A-2A specimen. Two small cracks are perpendicular to the axial fracture surface, one in region 1 and another in region 3. Figure 59 shows the stitched SEM photos of the four different regions. Based on the SEM examination, the features present in fracture surface of C001A-2A are similar to the ones observed in C001A-1A. The fracture surface contains rounded pits that signify corrosion damage. There are no distinct cleavage or facet features on the fracture surface. Figure 60 shows representative SEM images taken in each region.

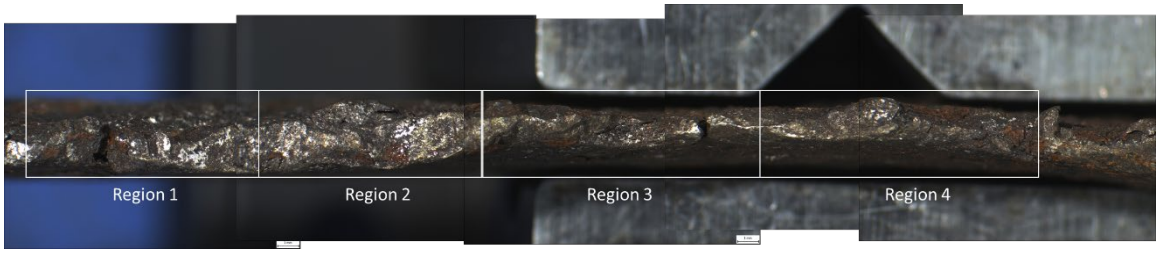

Figure 58: Different C001A-2A Regions Examined in the SEM

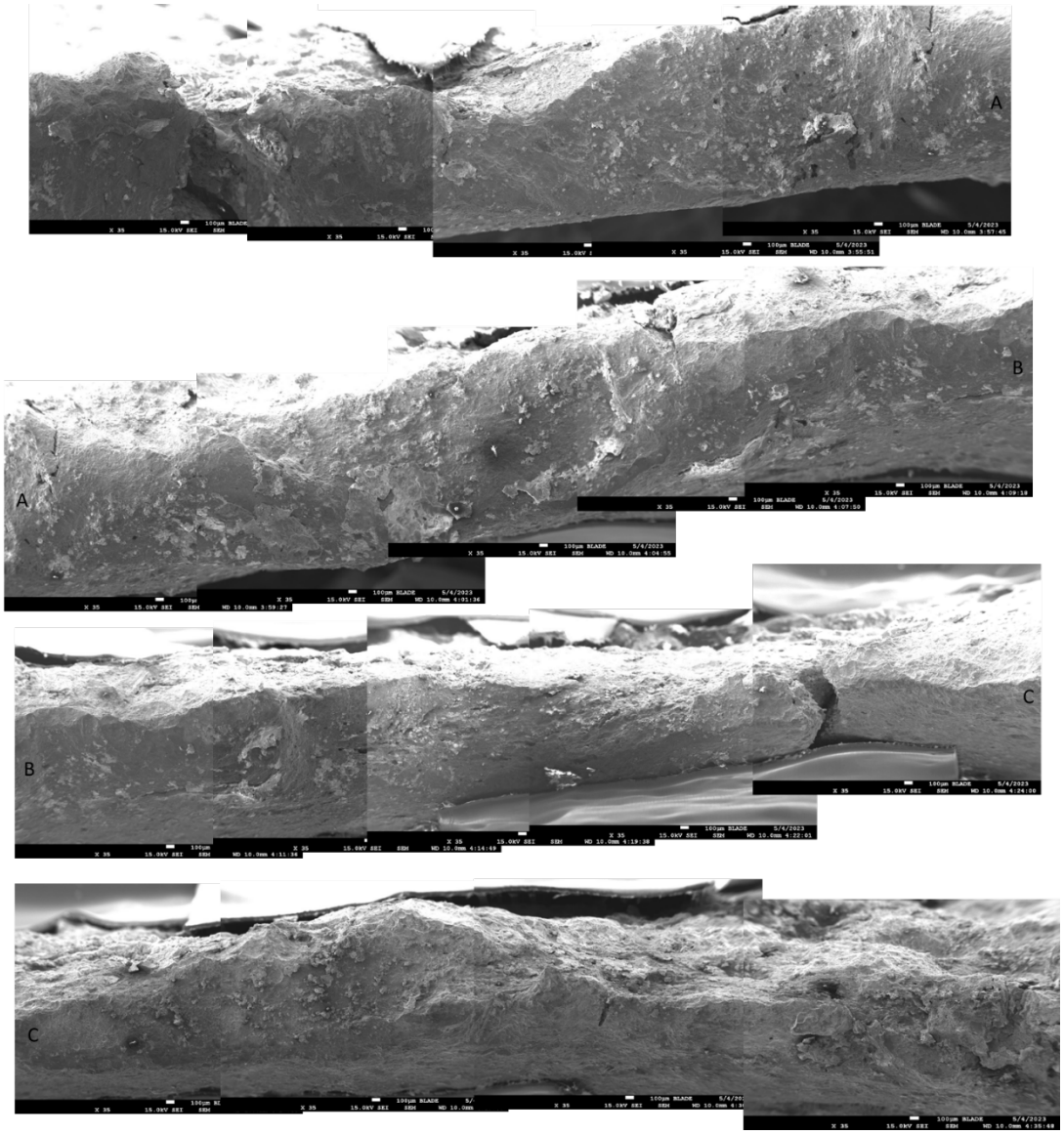

Figure 59: SEM Image of C001A-2A Fracture Surface (Regions 1 to 4, from Top to Bottom)

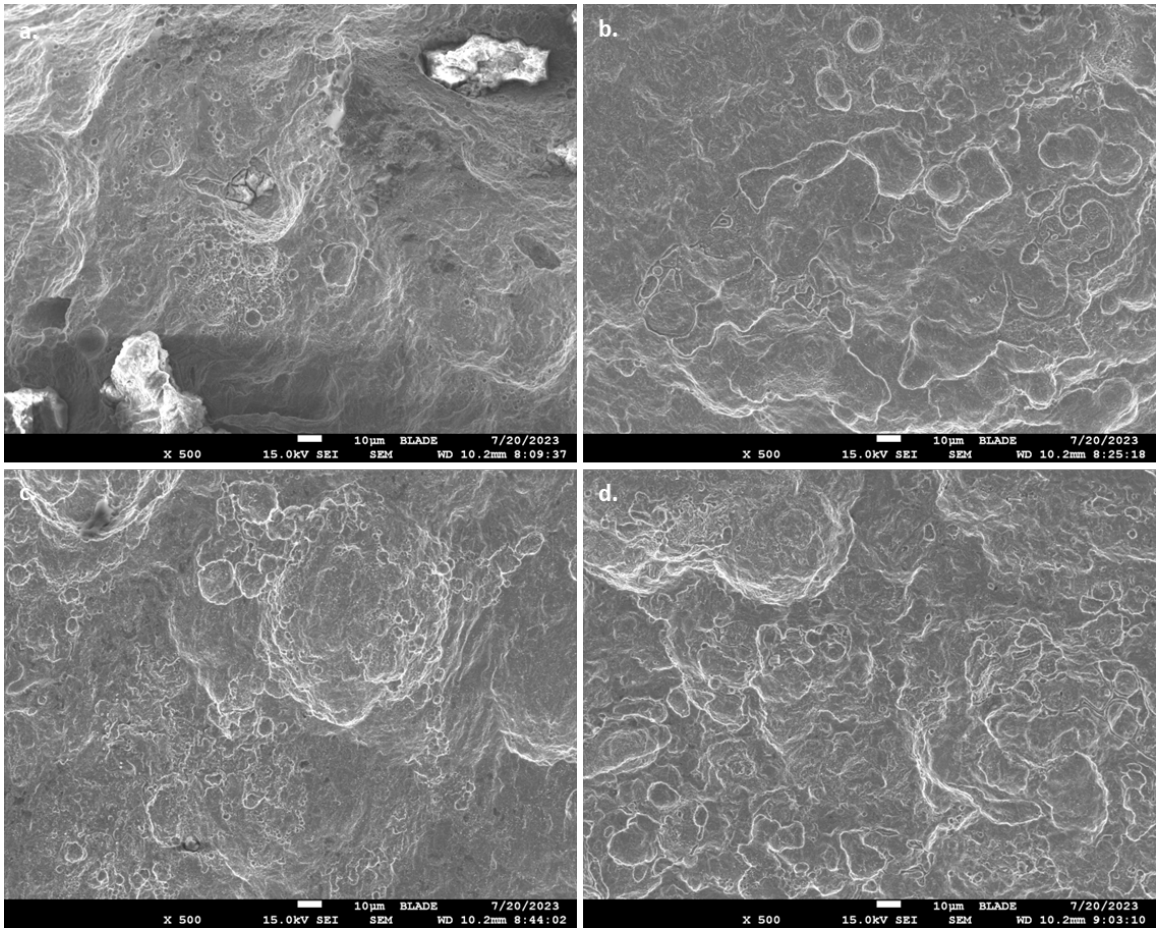

Figure 60: Representative SEM Images in C001-1A (a) Region 1, (b) Region 2, (c) Region 3, and (d) Region 4

Figure 61 shows an attempt to mate the fracture surface of C001A-2A with C001A-1A. Figure 62 shows the fracture surfaces of C001A-1A and C001A-2A. The general shape on some of the regions of the fracture surface is mated, but no specific feature at higher magnification image is mated. The observation supports the previous finding that the fracture surface has been severely damaged by corrosion or by high-velocity gas flow during the leak event, causing removal of metal.

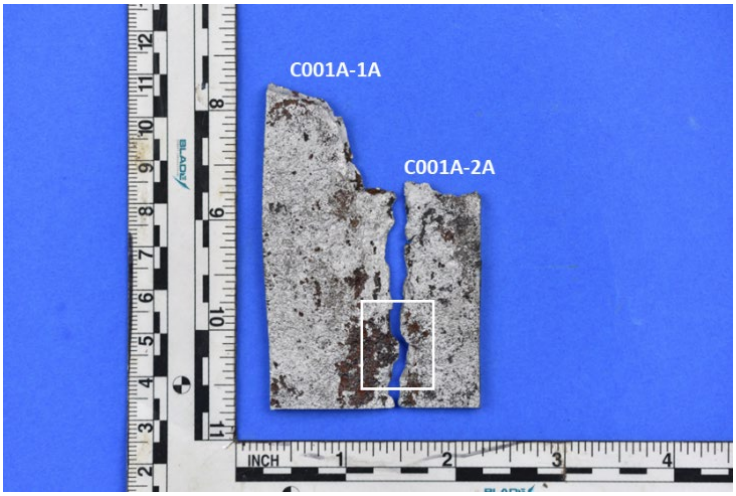

Figure 61: Region Used in Mating C001A-1A and C001A-2A Fracture Surfaces

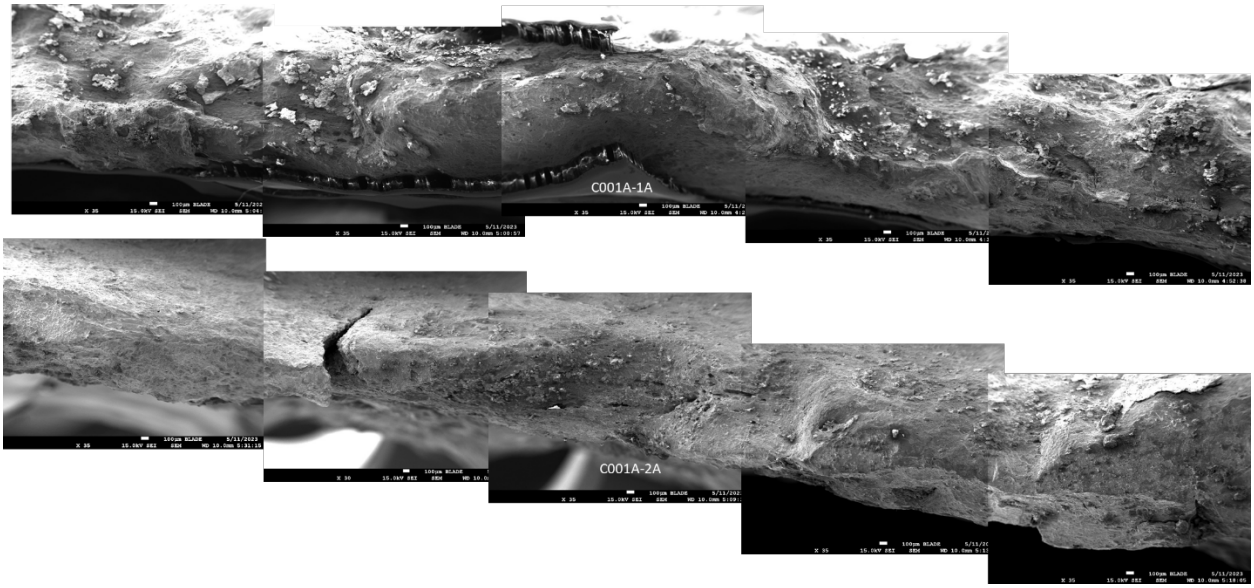

Figure 62: Mating of C001A-1A and C001A-2A Fracture Surfaces

C001A-2B

A small crack at the upper turning point in the C001A-2B specimen was identified during visual and stereoscopic examinations. Figure 63 shows the location of the small crack. The small crack was excised from C001A-2B and opened at liquid nitrogen temperature. The fracture surface was examined using the SEM.

Figure 64 shows the SEM images of the fracture surfaces of C001A-2B1 and C001A-2B2. The small crack was opened to identify the feature in the fracture surface that was least exposed to a corrosive environment. The examination was focused on the crack front where corrosion is least expected. The crack front was marked by the transition from the features (cleavage) produced by opening the crack at liquid nitrogen temperature. The figure also shows the location of SEM high-magnification imaging.

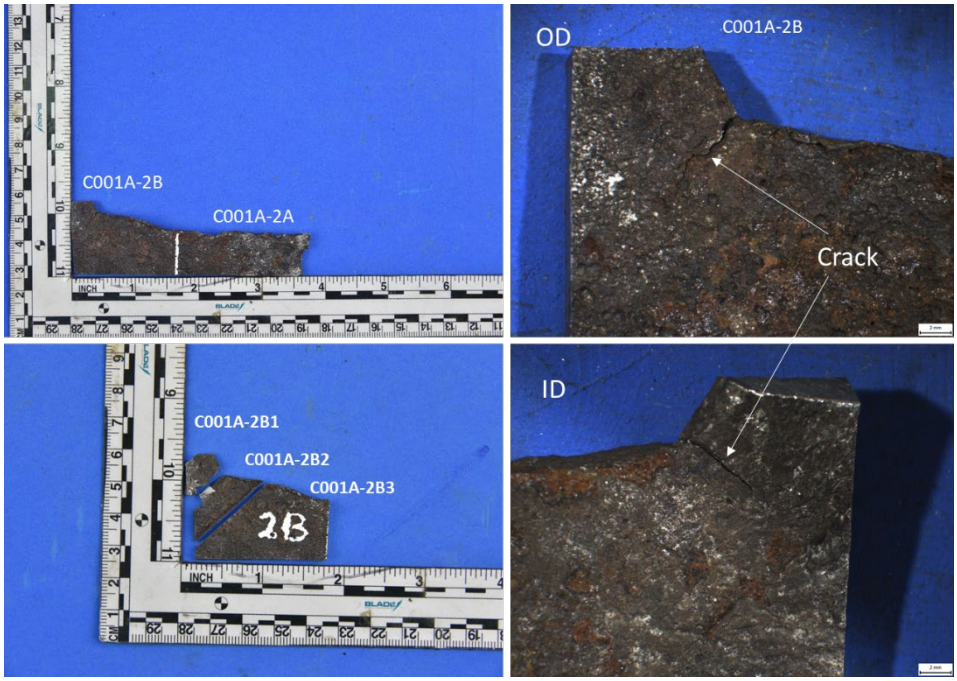

Figure 63: Opened Crack in Sample C001A-2B

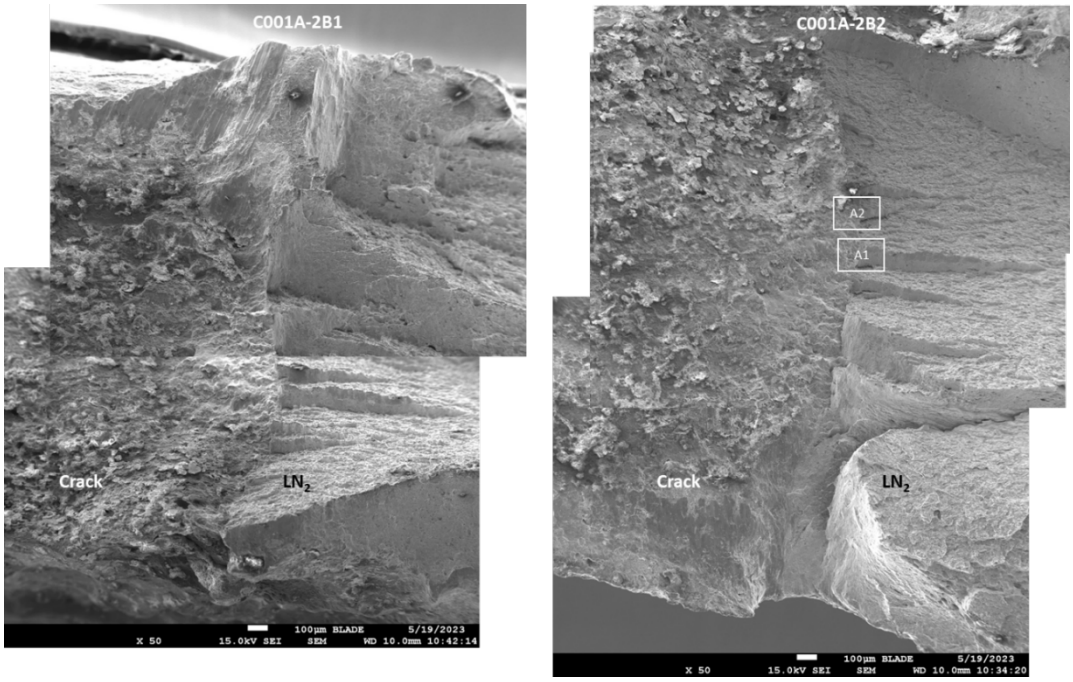

Figure 64: C001A-2B1 and C001A-2B2 Fracture Surfaces

Figure 65 shows the areas examined in C001A-2B1 and C001A-2B2. Mating of the fracture surfaces at the crack front was attempted. The results from the examination show that the crack front is still covered with oxide. The transition to the liquid nitrogen fracture feature is marked by tearing.

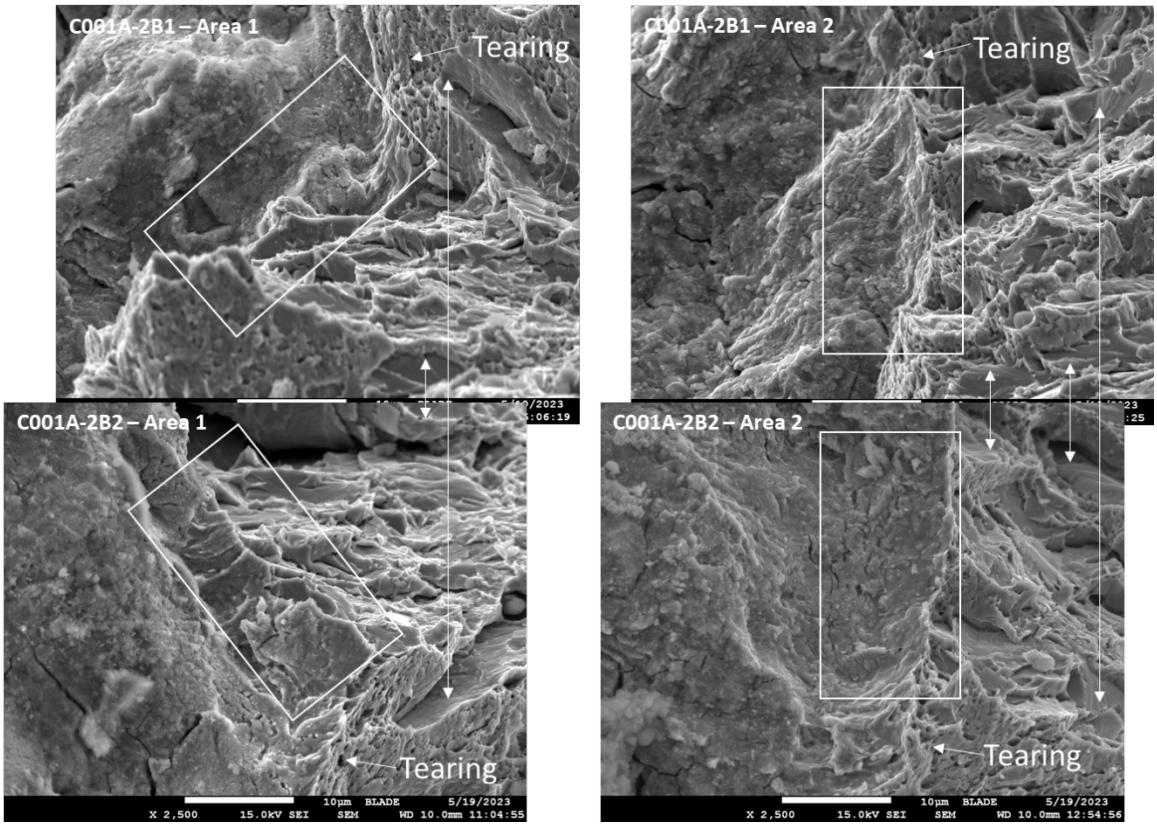

Figure 65: Attempted Mating Features in C001A-2B1 and C001A-2B2

Figure 66 shows the images of the C001A-2B1 fracture surface taken at the crack front after cleaning with Alconox and Citranox. The images show that the crack near the crack front did not produce distinct cleavage or facet features. The fracture surface also shows that the region behind the crack front (dashed line in Figure 66) is also damaged by corrosion.

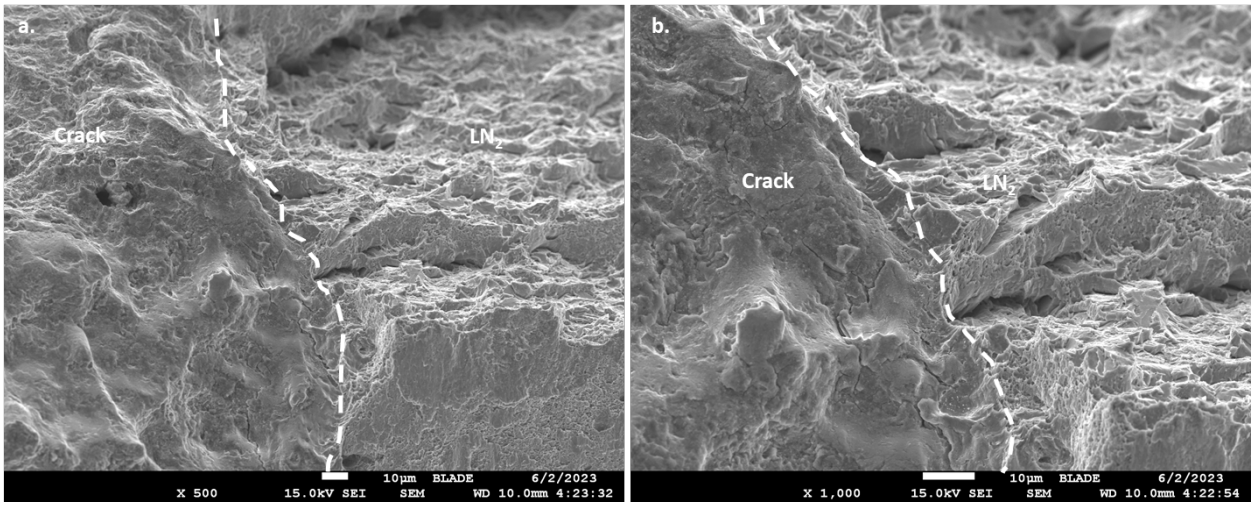

Figure 66: High Magnification SEM Images of Area 2 in C001A-2B1 After Cleaning Taken at (a) 500x and (b) 1,000x

Figure 67 is crack sample ID: C001A-2B1. This fracture surface was evaluated using EDS and Raman SEM at 35x. EDS was used to map the elements present on the surface semi-quantitatively. A slightly elevated sulfur EDS peak was observed, so the fracture surface was evaluated for $Fe_{1-x}S_y$ compounds. Figure 67a is the secondary electron image (SEI) SEM image of the crack face, and Figure 67b includes an EDS overlay indicating areas of concentrated sulfur in red. The average elemental wt% sulfur was less than 1wt% over the entire area. The highest sulfur region on the crack was 2.1wt% at Location (Loc) 2.

Raman analyses were performed on the crack face and in the base metal to identify the compounds on the surface in comparison with the base metal. Raman analyses indicated the base metal has a hematite layer that is probably formed by ambient humidity. Loc 2 had the highest elemental indication with EDS.

Raman analyses indicated crystalline mackinawite only at that location by the sharp peak at 212 cm^{-1} and the slightly broadened peak at 276 cm^{-1}. These peaks appear to be crystalline mackinawite, which forms early in the corrosion process [13] [14]. Crystalline mackinawite structure and is more likely to have formed on the fresh fracture surface after the failure. No evidence was found to link sulfur to the failure mechanism.

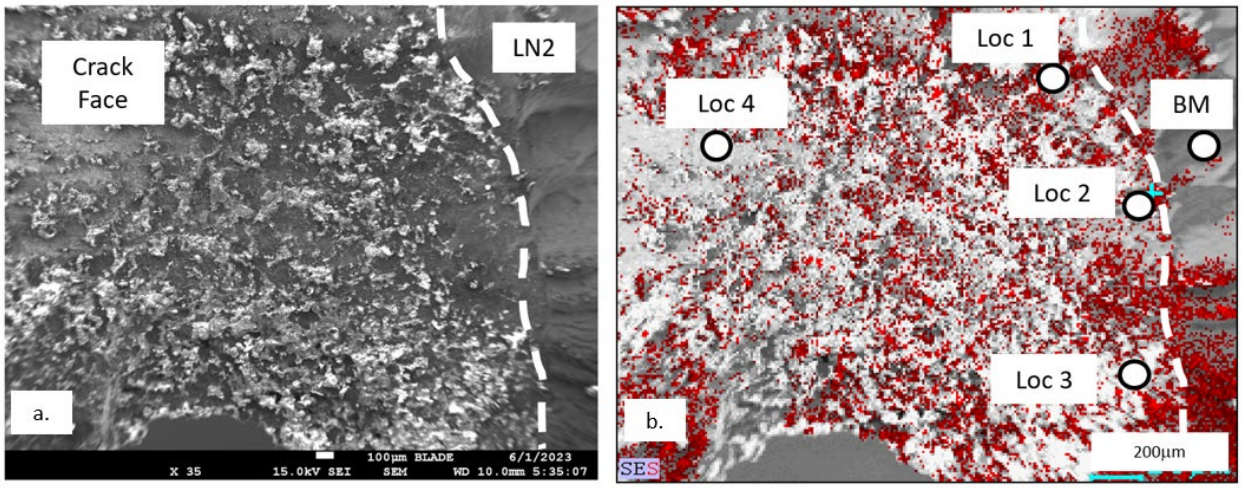

Figure 67: SEM images of 2244-C001A-2B1 Crack Face. SEI image (a) and SEI with EDS sulfur overlay (b) at 35x

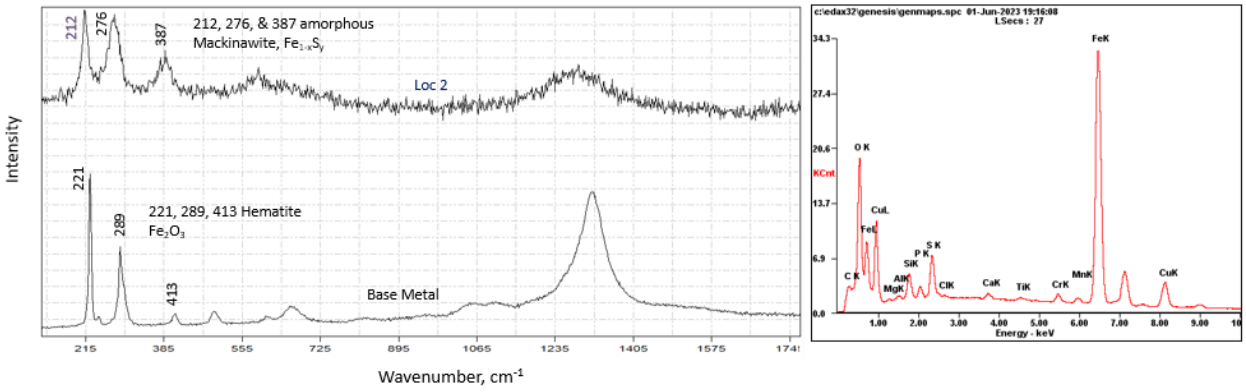

Figure 68: 2244-C001A-2B1 Crack Face Raman and EDS Sulfur Map

Summary of Findings

The key findings on the examination of the axial rupture specimens are as follows:

- The thinnest wall thickness was located off the center of the 3.36 in. axial rupture where the initiation site of the rupture was most likely located. The off-center initiation site may be understood by the casing slip constraint that is about 6 in. away from the rupture.
- Corrosion pits were observed on the OD surface of the axial rupture specimens. From SEM comparison, the morphology of corrosion pits on the OD surface appeared to be similar to those observed on the fracture surface of the axial rupture specimens. However, in mating the fracture surface analysis, no mated dimple-like features were found because of the corrosion event that occurred independently on each fracture surface. Therefore, the dimple-like features observed on the fracture surface of the axial rupture specimens are indeed due to corrosion. The original ductile tearing has been destroyed by corrosion.
- Minimal-to-negligible corrosion pitting was observed on the ID surface of the axial rupture specimens.
- Observations of the fracture features on the small crack at the upper turning point indicate that even the fracture surface behind the crack front is corroded. At the crack's very tip region, ductile tearing features are observed at the transition from ductile tearing to brittle separation due to opening at liquid nitrogen temperature.
- Microhardness measurement (Hv) shows decreasing values with increasing distance away from the fracture surface of axial rupture. This confirms plastic deformation hardening due to ductile tearing at/near the fracture surface compared to the undeformed based metal.

7.1.4 Circumferential Parting

Visual and Stereoscopic Examination

The objective of the visual and stereoscopic examination of the circumferential fracture is to identify key features related to the circumferential parting.

The circumferential downward-facing fracture surface is in C001A. The circumferential upward-facing fracture surface was cut from C001B and designated C001B-1. Figure 69 shows the specimens that contain the circumferential fracture surfaces. The circumferential fracture surface from C001A was chosen for the detailed fracture surface analysis, and the circumferential fracture surface from C001B-1 was preserved.

Figure 69: Specimens Containing Circumferential Fracture Surfaces

Thickness measurements were obtained along the circumferential fracture surface using a point micrometer. Figure 70 shows the individual values taken along the circumferential fracture surface in C001B-1 and C001A. The average wall thickness along the circumferential fracture surface in C001B is 0.133 in. The average wall thickness along the circumferential crack in C001A is 0.140 in.

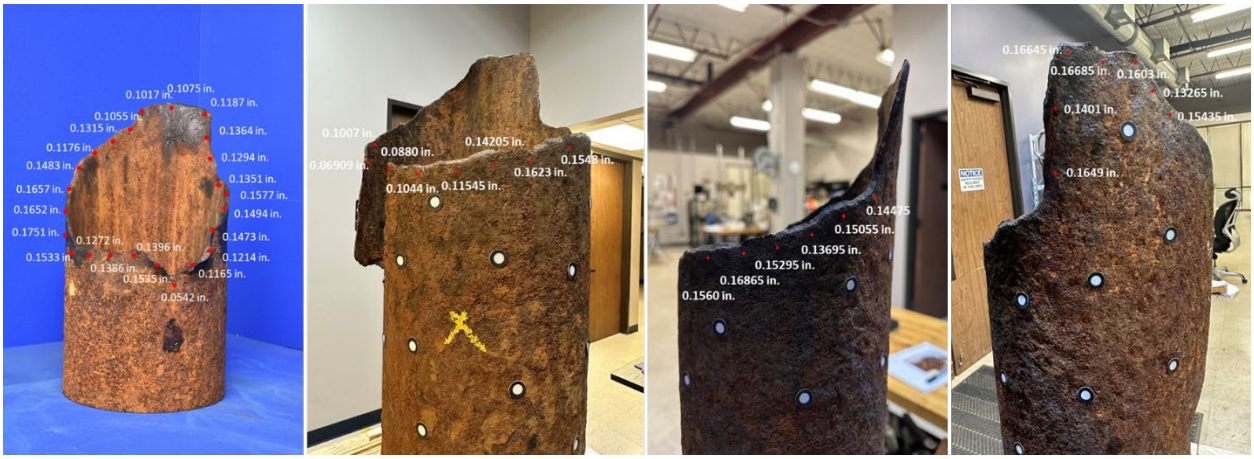

Figure 70: Thickness Measurements along the Circumferential Fracture Surface of C001B-1 and C001A

The circumferential fracture surface was examined and documented using a digital camera and a stereoscope. Figure 71 shows the circumferential fracture surface from C001A and C001B-1. Examination of C001A indicates that most of the circumferential fracture surface is 45° shear and contains a shear lip.

Figure 72a and b show the 45° shear with respect to the OD and ID surfaces, and Figure 72c shows the shear lip in the circumferential fracture surface. Figure 73 shows where the shear lip, mechanical damage, and the flat region were observed. Figure 74 shows the stereoscope image of the step in the circumferential crack in C001A. The C001B-1 circumferential fracture surface has mechanical damage.

Figure 75 shows the features observed on the circumferential fracture surface of C001B-1. Most likely, the mechanical damage was due to the inspection tool that was used before the retrieval of the joint from well #2244.

The region in which shear lip was observed in C001B-1 matched the region where the missing fracture piece is located. From visual examination, no chevron marks are observed on the circumferential fracture surface of both C001A and C001B-1.

Figure 71: Circumferential Fracture Surfaces from C001A and C001B-1

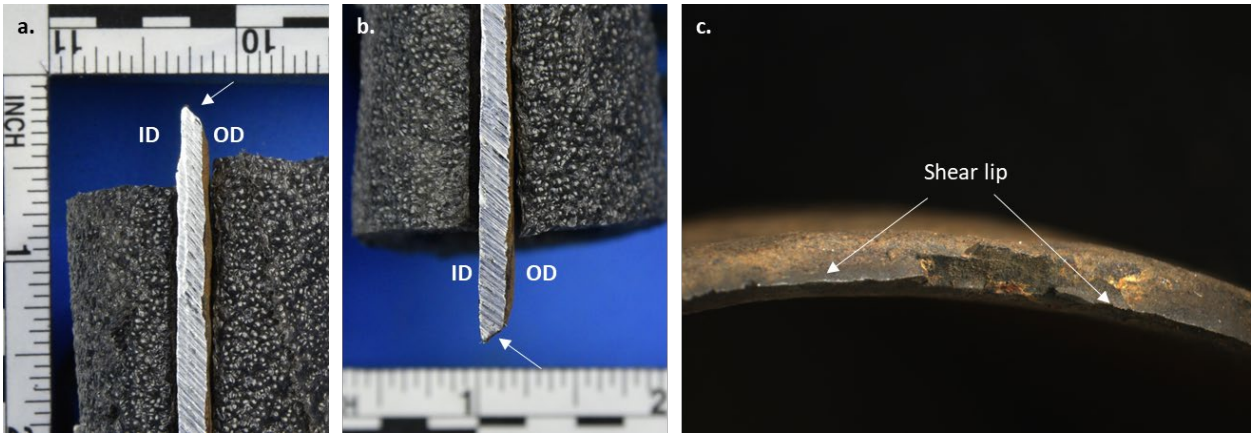

Figure 72: Circumferential Fracture Surface (a, b) 45° Shear and (c) Shear Lip

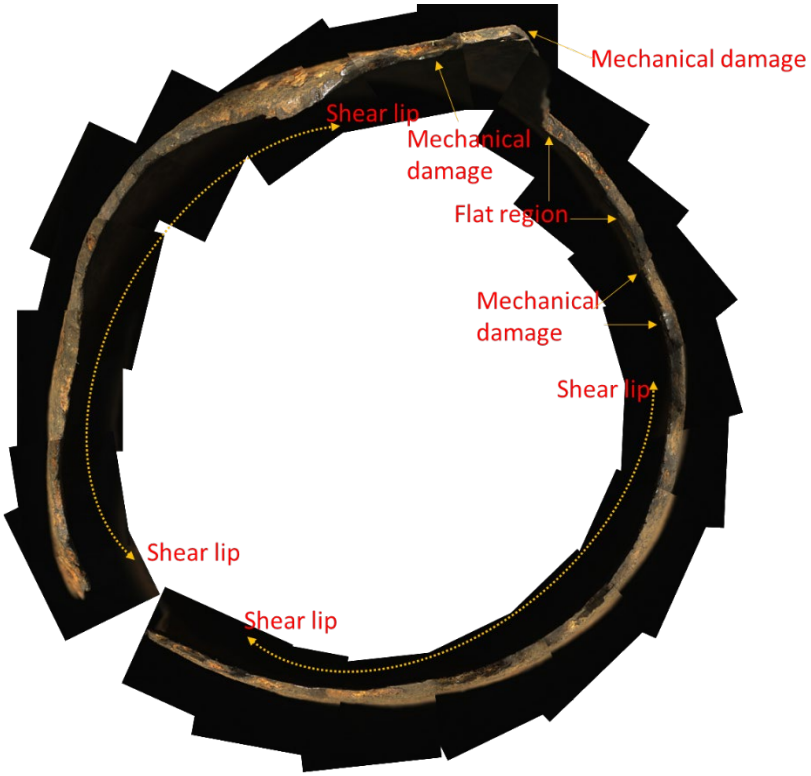

Figure 73: Stitched Stereoscope Image of C001A-1 Circumferential Fracture Surface

Figure 74: Stitched Stereoscope Image of the Step in Circumferential Fracture Surface in C001A

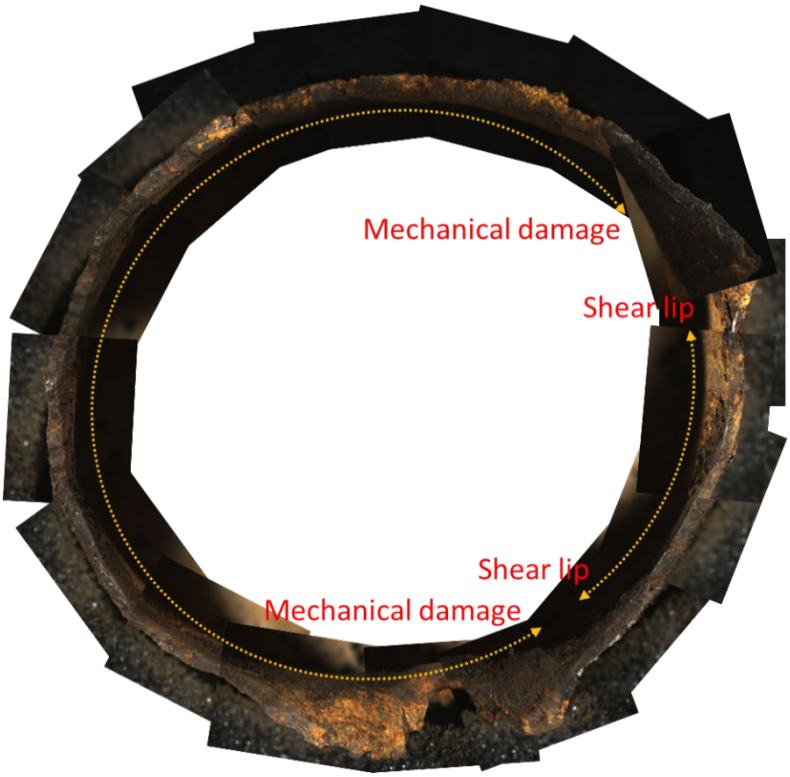

Figure 75: Stitched Stereoscope Image of Circumferential Fracture Surface in C001B-1

The arrows in Figure 76 show the circumferential fracture surface in C001A-1. The fracture surface is not perpendicular to the OD and ID surfaces, but about 45° oriented with respect to the OD and ID. The presence of a shear lip is prevalent in the circumferential fracture surface, indicating that the circumferential crack propagated in a shear-slip mode that is commonly considered as ductile.

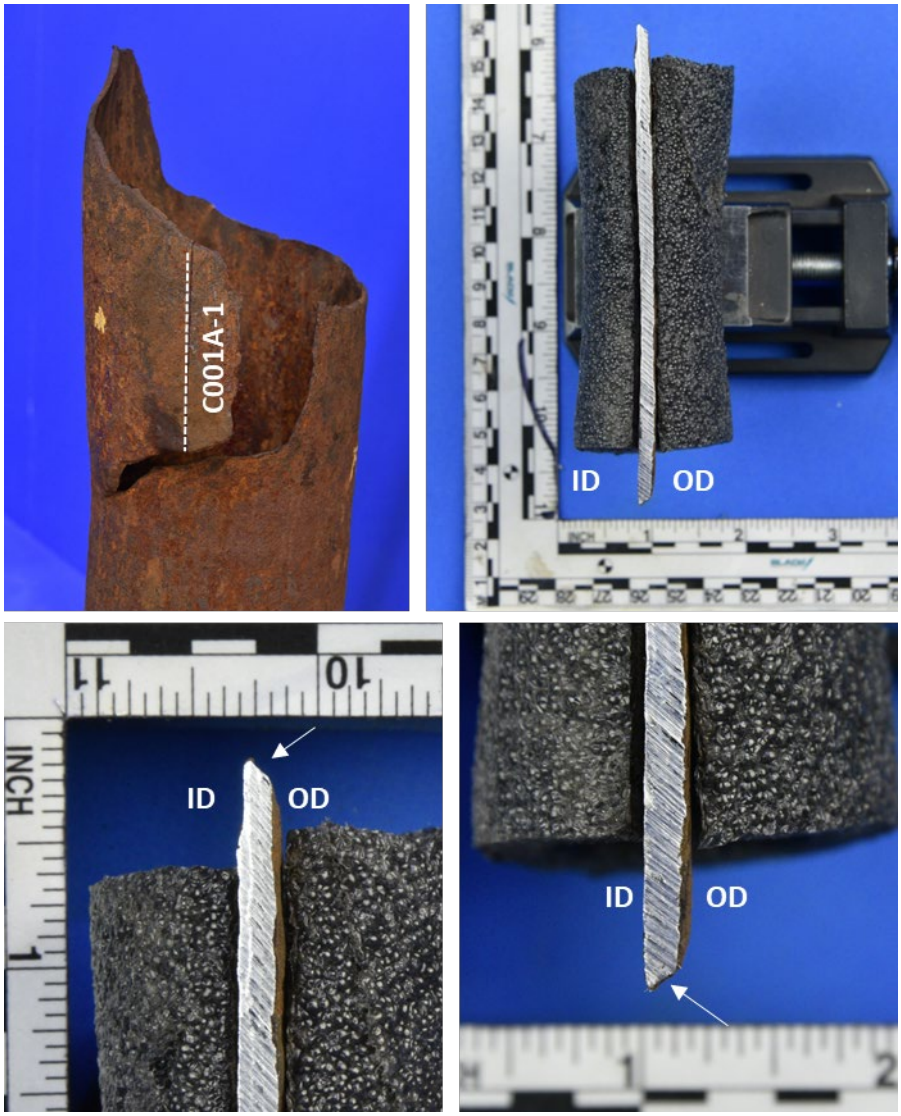

Figure 76: Circumferential Fracture Surface in C001A-1A Specimen

Some cracks were observed in C001A-1. Figure 77 shows the cracks observed on the ID and OD surfaces of C001A-1. These two cracks are connected through the thickness. However, the crack changed orientation as it propagated from one surface to the other. No further examination was performed on these cracks.

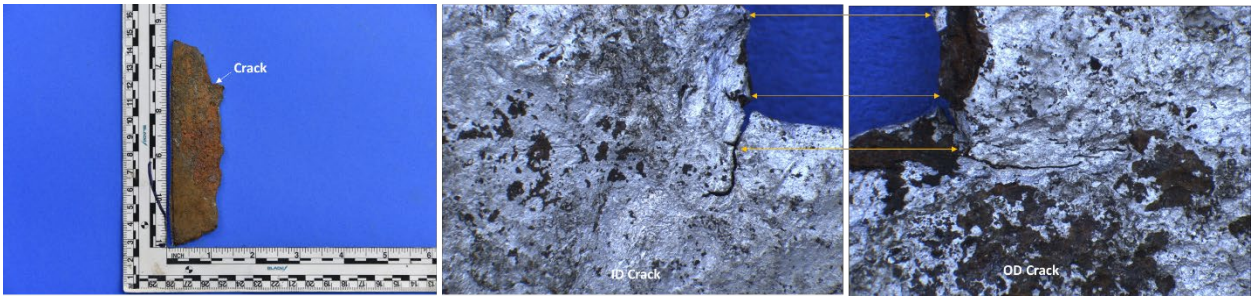

Figure 77: Cracks Observed in C001A-1A ID Surface and OD Surface

Micro-Fractographic Characterization

The objectives of the micro-fractographic characterization of the circumferential parting are to:

- Characterize the fracture surface of the circumferential parting.
- Identify the fracture mode of the circumferential parting.

The detailed micro-fractographic characterization of the circumferential parting was performed using the fracture surface in C001A. The circumferential fracture surface was excised from C001A by dry cutting using a portable band saw. The fracture surface was carefully protected to prevent mechanical damage during cutting. Protective padding or cushions were used during dry cutting.

Figure 78 shows the specimens containing the circumferential fracture surface from C001A. Some of the specimens shown in Figure 78 were further cut to facilitate examination in the SEM.

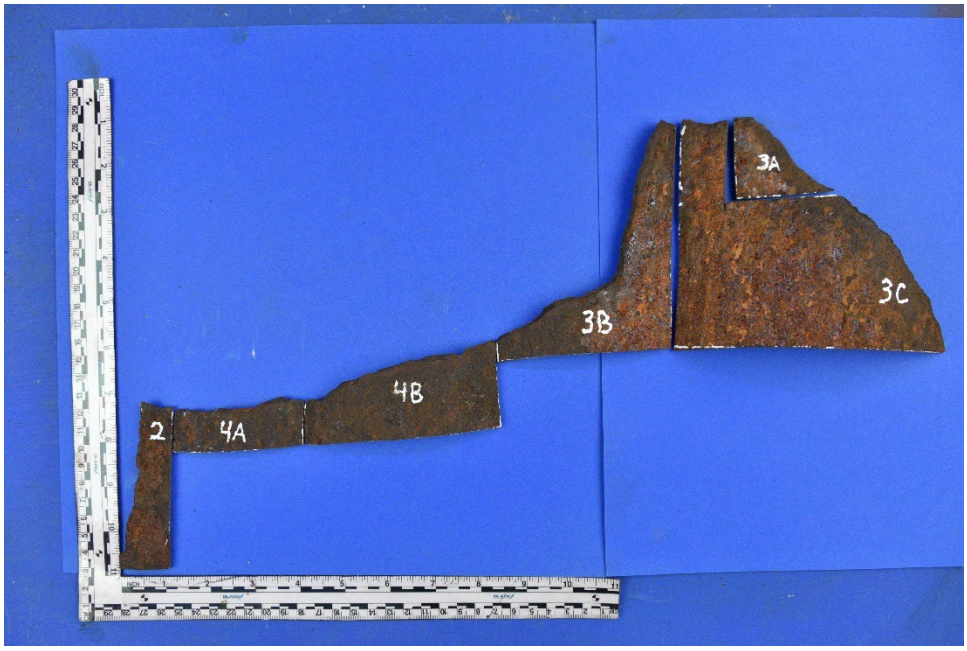

Figure 78: Circumferential Fracture Surface Excised from C001A

The majority of the circumferential fracture surface was examined in the SEM. Only the representative areas are included in this report. Figure 79 shows the stereoscope image of specimen C001A-4A and locations where high-magnification SEM images were taken. C001A-4A has a shear lip adjacent to the ID surface. C001A-4A was cleaned using the protocol described previously. The sample was successively sonicated in acetone, Alconox, and acetone at ambient room temperature.

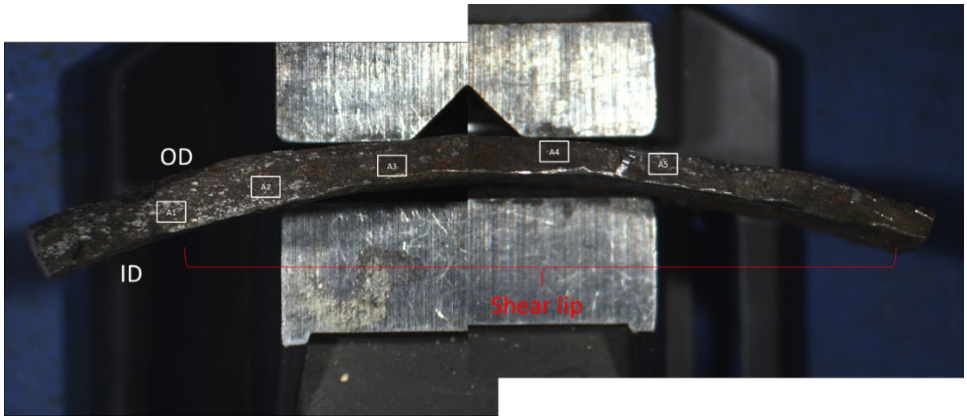

Figure 79: Areas of Examination in the C001A-4A Specimen

Figure 80 shows the span of the circumferential fracture surface in the C001A-4A specimen. The sample was oriented such that the OD surface was at the top of the SEM image, and the ID surface was at the bottom. The sample contains numerous rounded pits. Figure 81 shows higher-magnification SEM images taken from areas 1 to 5 in C001A-4A. Some rounded pits are on top of each other (i.e., small-rounded pits are within bigger rounded pits). Some of the rounded pits still have corrosion products on the surface, even after cleaning.

No distinct cleavage or flat features are observed on the fracture surface of C001A-4A. The circumferential fracture surface in C001A-4A is corroded. Although not presented here, the circumferential fracture surface in C001A-4B has the same features as C001A-4A. It has a shear lip and contains rounded pits. No distinct cleavage or flat features are observed on the fracture surface of C001A-4B.

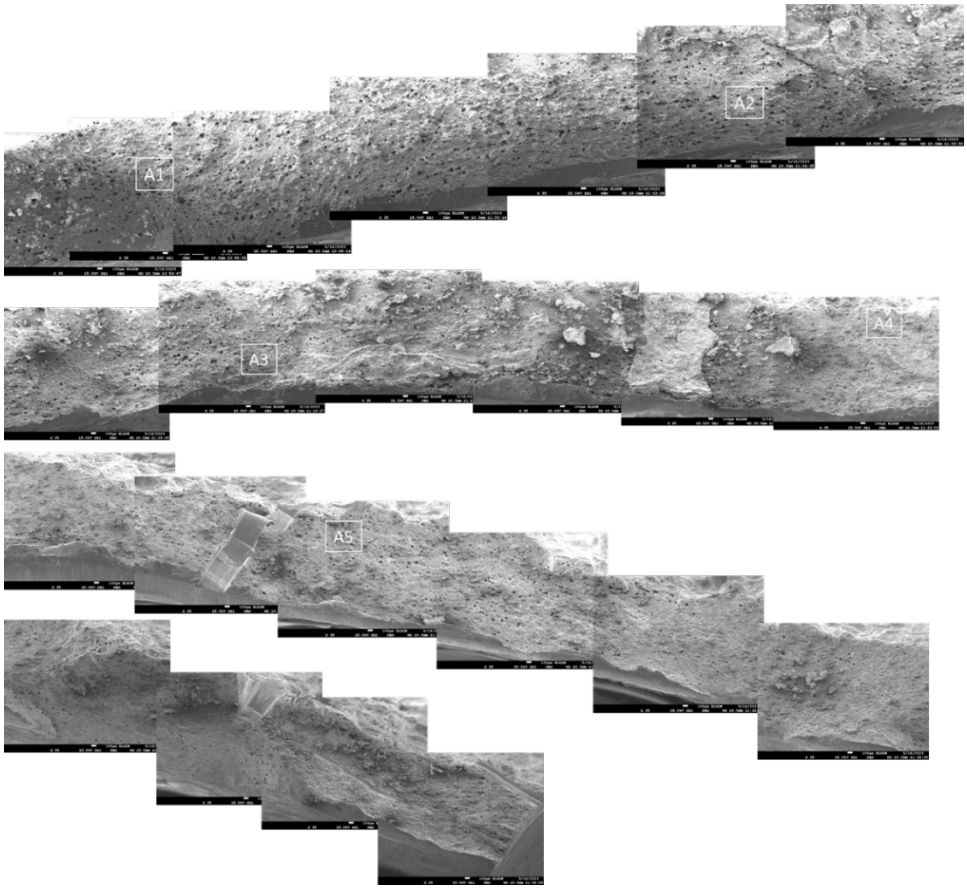

Figure 80: Stitched SEM Images of C001A-4A (OD Surface at the Top of the SEM Image)

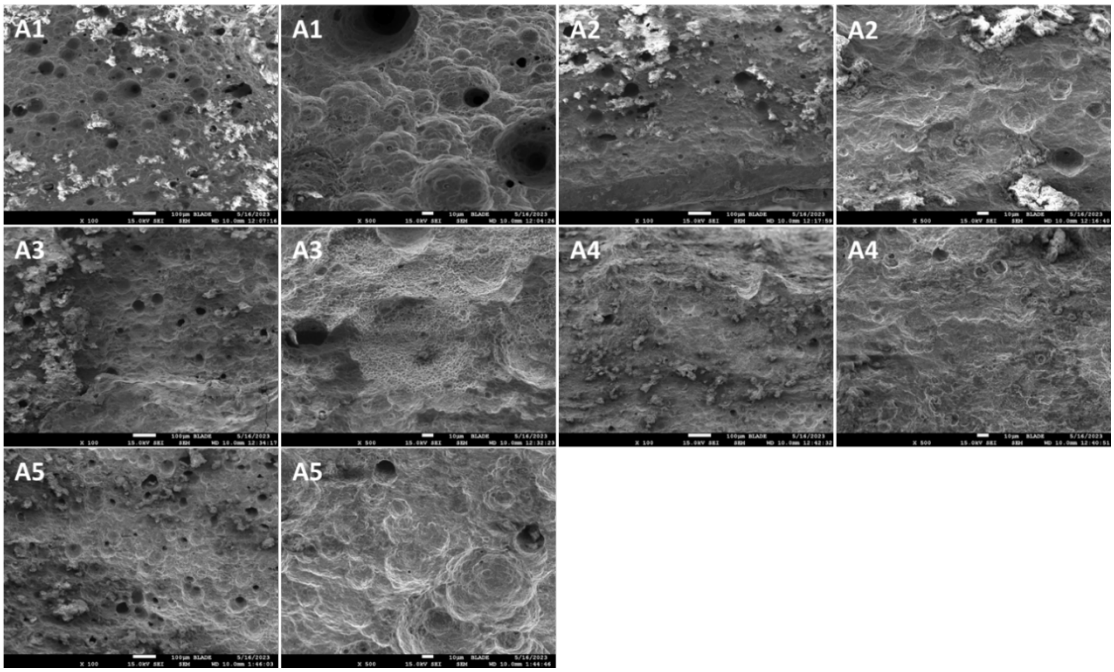

Figure 81: SEM Images Taken from Areas 1 to 5 in C001A-4A at 100x and 500x Magnification

C001A-3B from Figure 78 was further cut into smaller pieces to facilitate examination in the SEM. Figure 82 shows the specimens cut from C001A-3B. Figure 82 also shows the stereoscope images of the C001A-3B1 and C001A-3B3 fracture surfaces. Both specimens contain a shear lip on the ID side of the fracture surface.

The features observed on C001A-3B1 are similar to C001A-4A fracture features. The fracture surface contains rounded pits indicative of corrosion damage. Figure 83 shows a representative SEM image taken from the C001A-3B1 specimen.

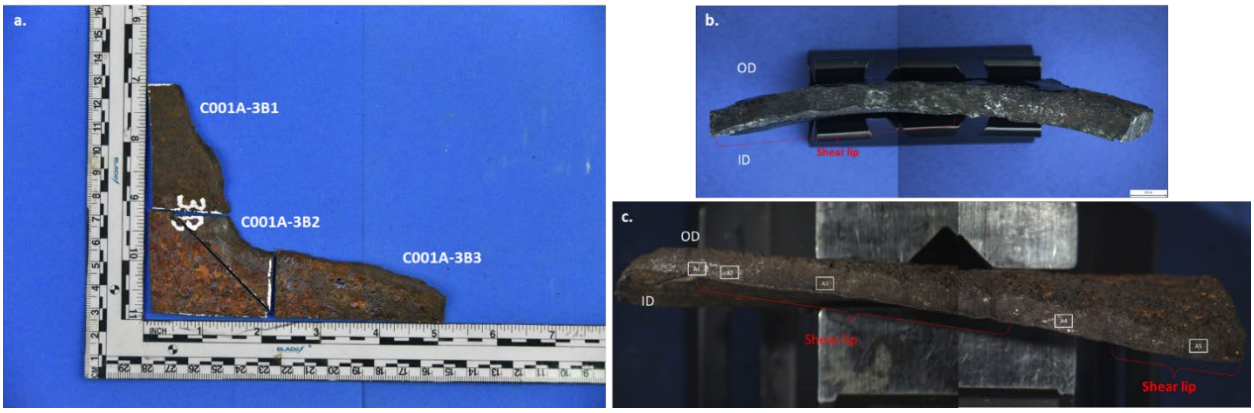

Figure 82: a. C001A-3B Cut Specimens, b. C001A-3B1 Fracture Surface, and c. C001A-3B3 Fracture Surface

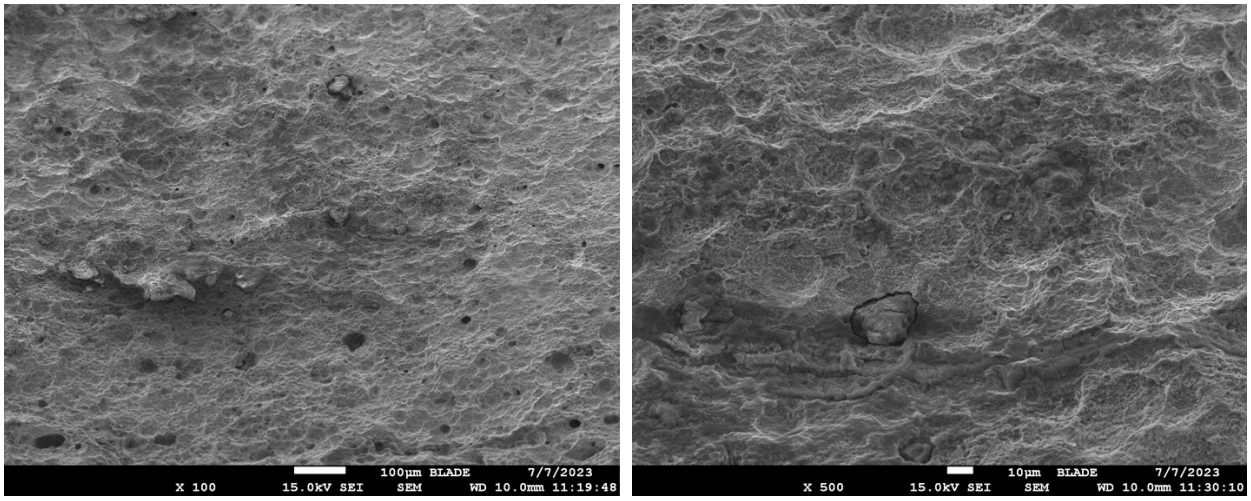

Figure 83: SEM Image of the Fracture Surface in C001A-3B1

Figure 84 shows the stitched SEM images taken from C001A-3B3. The locations of the representative images on the fracture surface in C001A-3B3 are indicated in Figure 84. Figure 85 shows SEM images taken at 100x and 500x at areas 1 to 5 in the fracture surface of C001A-3B3.

Rounded pits are also observed in the fracture surface of C001A-3B3. A3 in Figure 84 shows a relatively flat surface. This relatively flat region does not contain cleavage or flat facets. Instead, it is a smooth region, as shown in Figure 85 A3. The fracture surface in C001A-3B3 is corroded. Small corrosion pits are also observed on the fracture's surface.

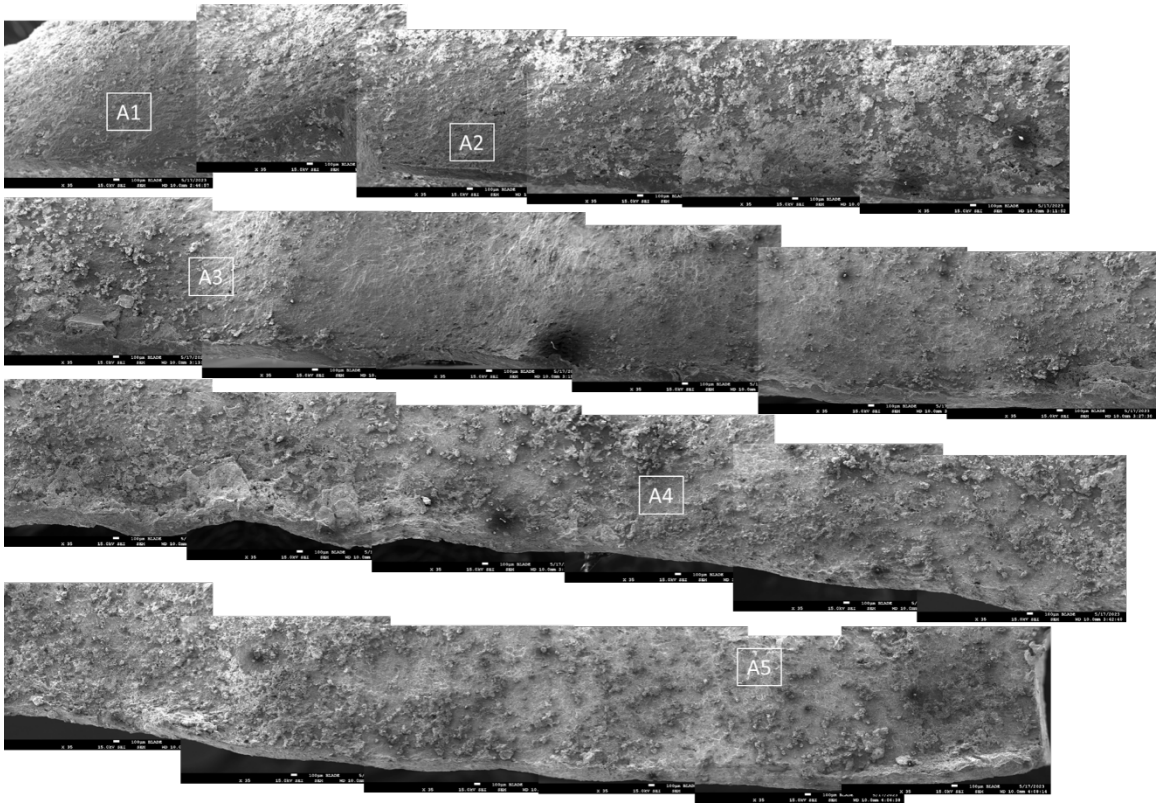

Figure 84: Stitched SEM Images of C001A-3B3

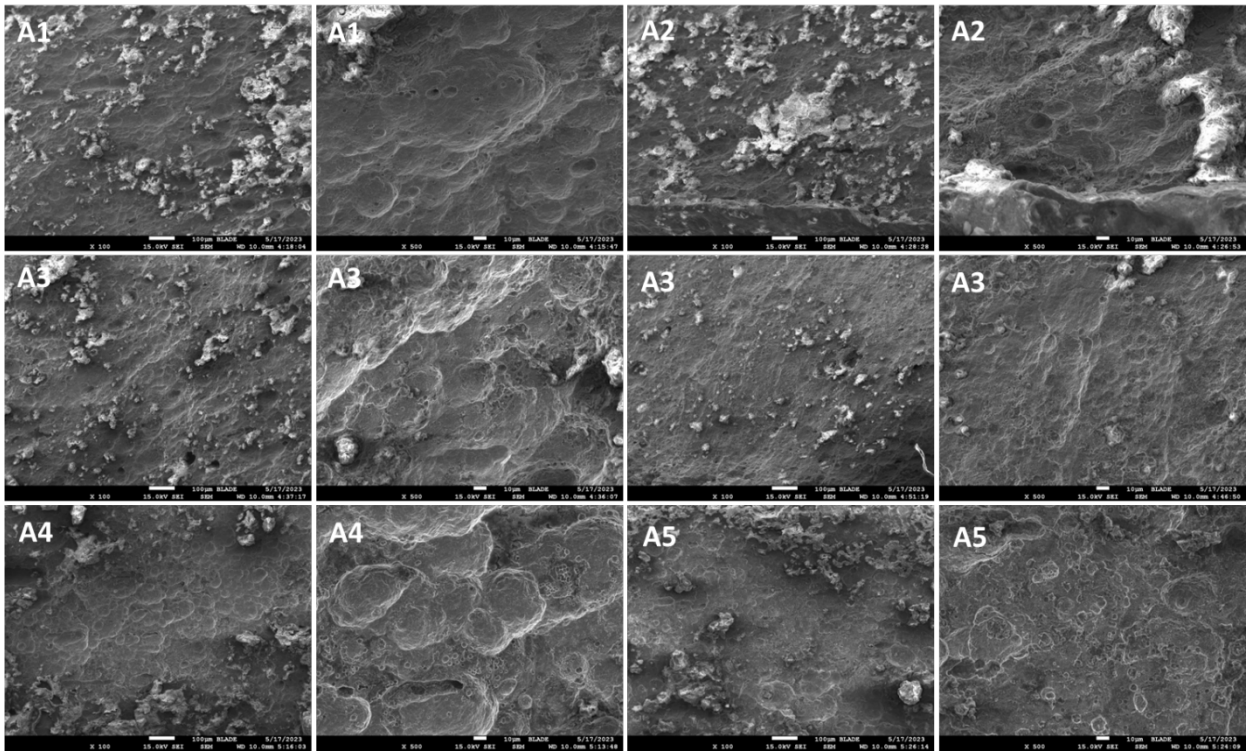

Figure 85: SEM Images Taken from Areas 1 to 5 in C001A-3B3 at 100x and 500x Magnification

Additional SEM images are taken from the C001A-3A1, C001A-3C2, and C001A-3C3 fracture surfaces. The images show that the fracture surface contains rounded pits. Some areas still contain corrosion products even after cleaning by sonicating successively in acetone, Alconox, and acetone. Some areas are smooth. However, no distinct cleavage or flat facets are observed from the fracture surface of these samples.

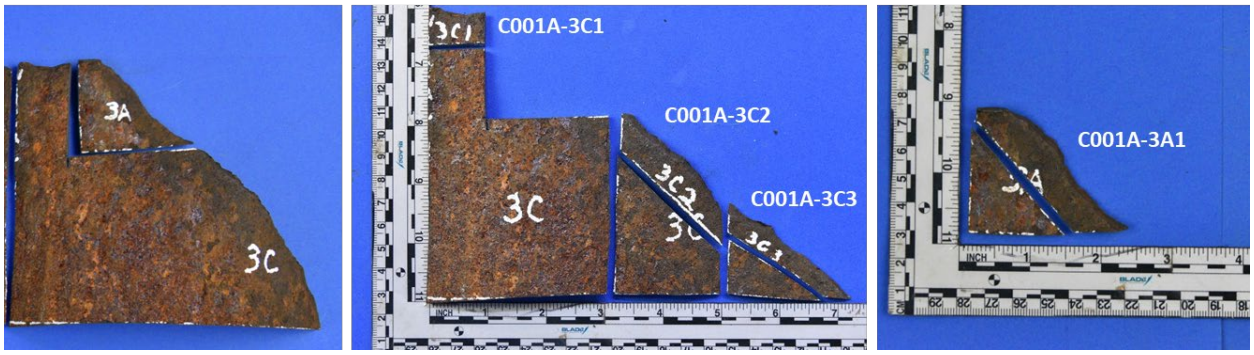

Figure 86: Specimens from C001A-3A and C001A-3C

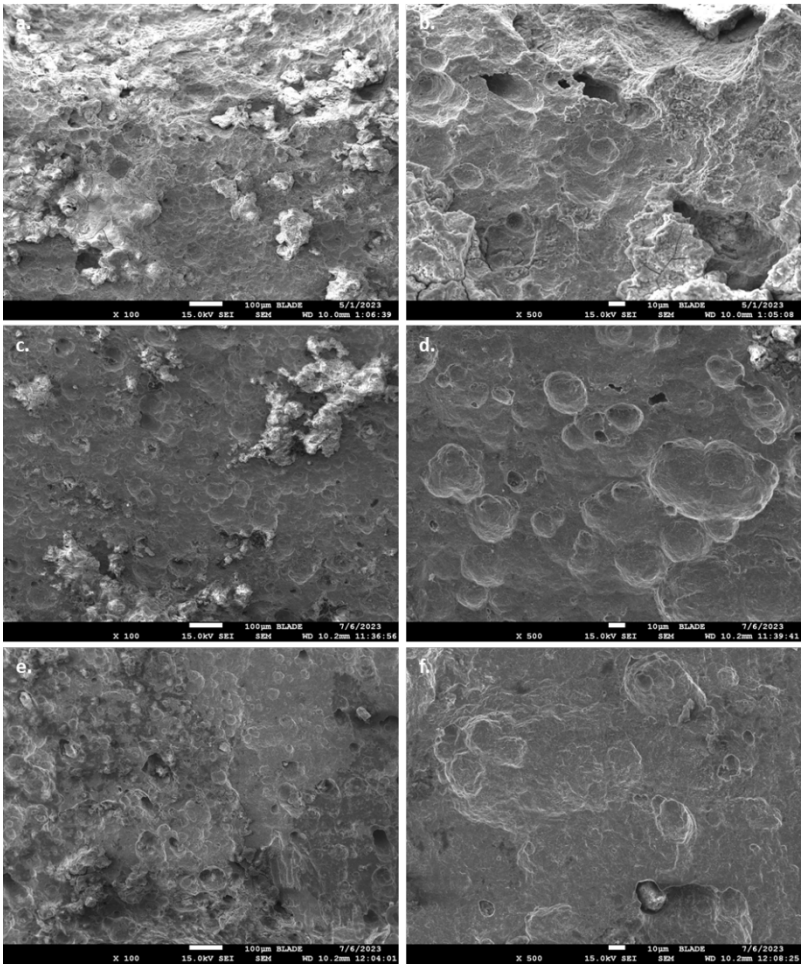

Figure 87: Representative SEM Images taken from C001A-3A1 (a, b), C001A-3C2 (c, d), and C001A-3C3 (e, f) at 100x and 500x Magnification

Summary of Findings

The key findings on the examination of the circumferential parting specimens are:

- The circumferential fracture surface is mainly shear-lips.
- The circumferential fracture surface is not perpendicular to the ID surface or OD surface. This indicates that the circumferential cracking is most likely ductile.
- The circumferential fracture has dense, rounded pits produced by corrosion damage.
- The circumferential fracture surface has some smooth regions. However, adjacent to the smooth regions are rounded corrosion pits, indicating that the fracture surface has been damaged by corrosion attack.
- The circumferential fracture surface displays no observable cleavage facet features.

7.1.5 Failure Pressure of Axial Rupture and Circumferential Parting Instability Analysis

Failure Pressure Estimation of Axial Rupture

The failure pressure was estimated in accordance with the ASME B31.6 guidelines based on the thickness of the top joint C001 in well #2244. The wall thickness profile along the rupture line was determined using a point micrometer. Figure 88 shows the rupture line along which the thickness profile was measured and used for failure pressure calculations. The wall thickness along the entire length of the C001-A and C001-B was measured using a combination of an ultrasonic thickness gauge and a point micrometer. The corrosion profile corresponding with the axial rupture was then estimated. Figure 89 shows the wall thickness profile along the axial rupture line. Figure 90 shows the schematic of the entire length of wall thinning observed in C001-A and C001-B.

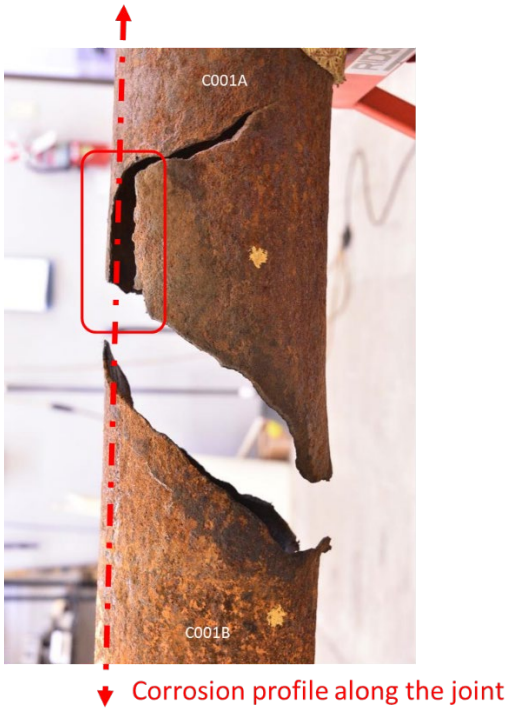

Figure 88: Orientation of Thickness Profile Used for Burst Pressure Estimation

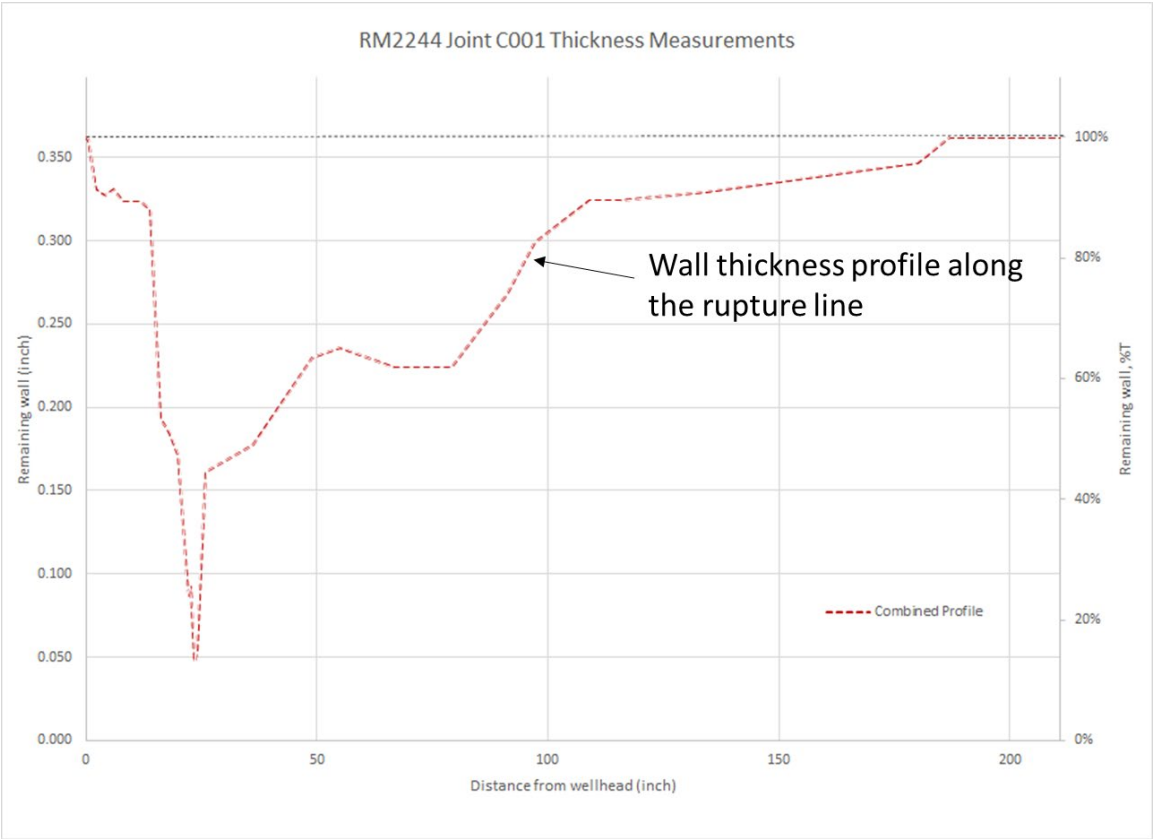

Figure 89: Wall Thickness Profile along the Axial Rupture

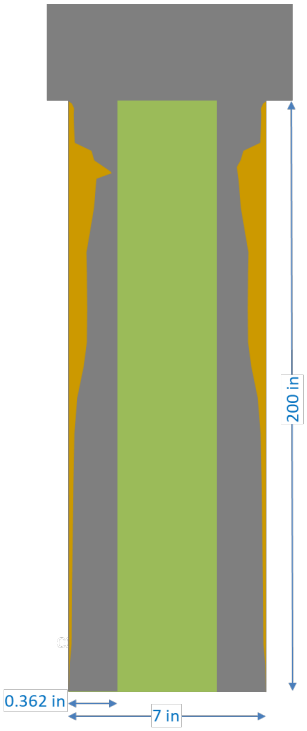

Figure 90: Schematic of Wall Thinning Observed in Well #2244 Joint C001

The failure pressure was estimated using the approach described in ASME B31.6, which provides a guideline for determining the remaining strength of corroded piping system. The failure pressure was estimated based on an effective area method.

A software called KAPA, developed by Kiefner and Associates, was used to determine the burst pressure. The inputs for the calculations are the pipe's external diameter, nominal pipe wall thickness, steel grade and yield strength, and axial corroded wall profile. The software performs iterative calculations to determine the effective corroded length and the failure pressure of the effective area. The effective length was calculated as 4.25 in., based on the estimated effective area. The result of the effective area estimation is presented in Figure 91.

Using the average transverse yield strength of 91,580 psi (see Table 62), the estimated failure pressure, based on the effective area method, is 2,852 psi. No actual failure pressure is available for comparison. However, comparing the estimated failure pressure with the highest pressure recorded (3,078 psi) prior to the failure of well #2244, the difference is approximately 7%.

The analysis results show that the top joint's failure is due to excessive wall thinning. The remaining wall thickness of the 7 in. casing could not withstand the internal pressure in well #2244.

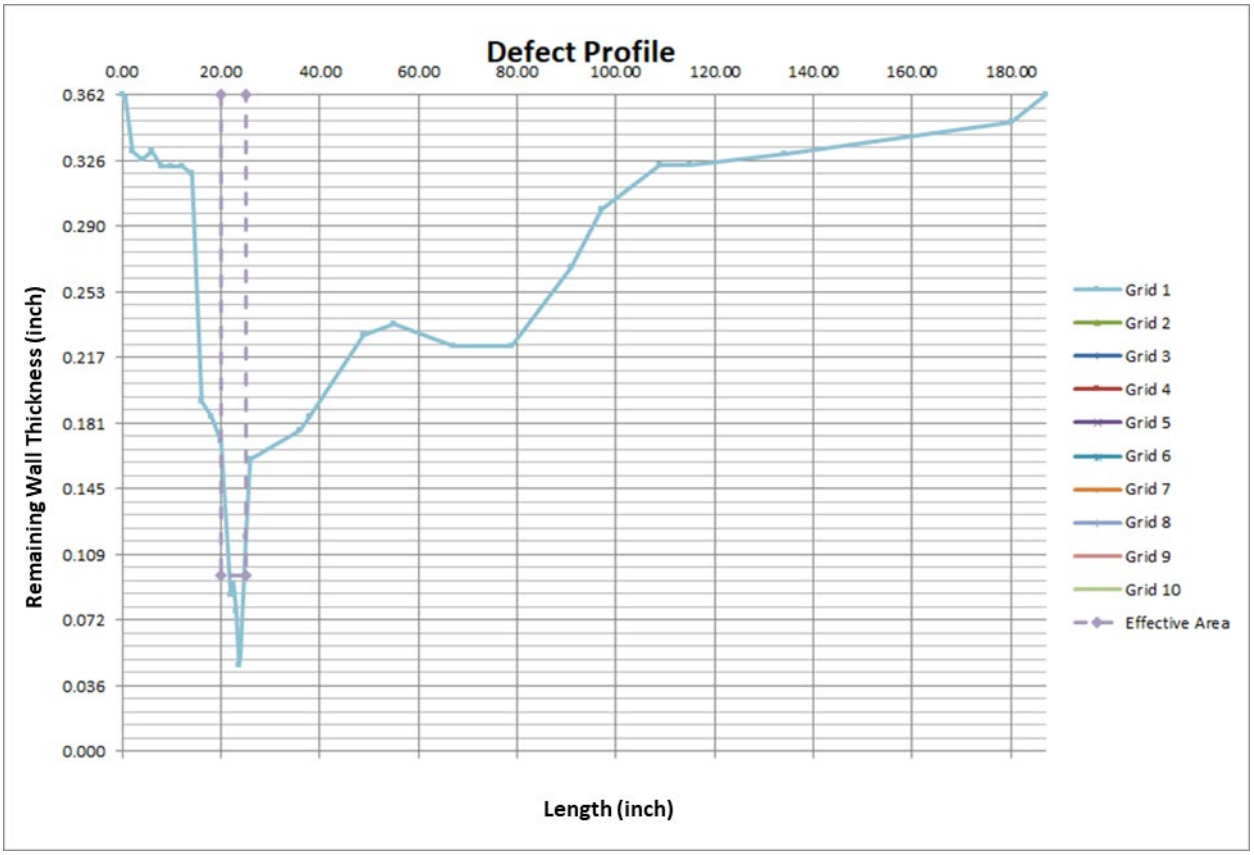

Figure 91: Results of Failure Pressure Calculation

Circumferential Parting Instability Analysis

This analysis aims to identify the critical circumferential crack size that would be unstable and lead to tearing instability with the applied pressure and axial load (i.e., casing weight). The assessment used the API 579 FAD Level 3 Assessment Method—Material-Specific FAD and Tearing Instability Analysis.

For materials that exhibit stable crack growth by ductile tearing, conditions for rupture can be assessed using API 579 Level 3 with material-specific FAD and ductile tearing instability analysis. The analysis requires the measured J-R curve, which is obtained from the material's fracture mechanical testing where J denotes J-integral, and R denotes crack propagation resistance. The J-R curve is plotted with a series of assessment points on the material-specific FAD.

Figure 92 illustrates (a) the construction of the assessment point from the J-R resistance curve and (b) conditions from the ductile tearing instability. If assessment points are tangent to the FAD curve, it means the crack is in a critical condition. Critical crack dimensions can be established at which ductile instability (rupture) would occur for a given pressure and axial load conditions.

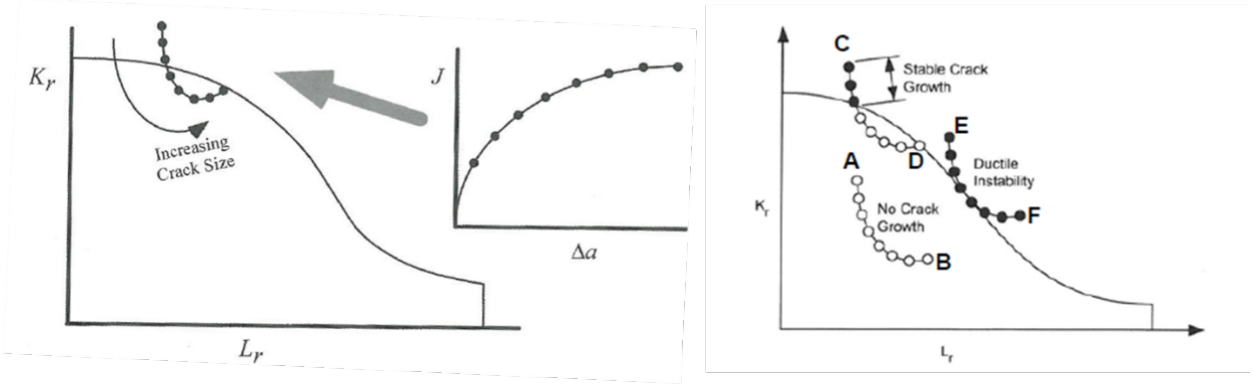

(a) Ductile tearing analysis with FAD using J-R curve

(b) Instability occurs when the assessment points is tangent to FAD

Figure 92: API 579 Level 3 – Material Specific FAD and Tearing Instability Analysis

API 579 Level 3 assessment of surface cracks is limited to 80% deep cracks. The limit exists because most stress-intensity solutions are inaccurate for very deep cracks due to high strain/plasticity effects. For example, KI solutions for a semi-elliptical surface crack are only accurate for a/t ≤80%, where a is the crack length and t represents wall thickness. Therefore, as a common practice, API 579 requires re-categorizing the deep surface crack to a through-thickness crack to achieve an accurate solution. API 579 provides the procedure and an equation below to use for re-categorization. Material-specific FAD is constructed using equations 9.19 and 9.20 from API 579 [15]. The stress intensity factor ratio, Kr, and load ratio, Lr, are determined using the flaw dimensions and are discussed in detail for cracks on a cylindrical body in API 579 [15].

Table 17: List of Pipe Attributes and Material Properties Used in the Critical Length Calculation

Property	Value
Wall Thickness (Measured Avg.)	0.1332 in
YS (Longitudinal Avg.) From Table 62	92.23 ksi
UTS (Longitudinal Avg.) From Table 62	106.05 ksi
Modulus of Elasticity	30,000 ksi
Poisson's ratio	0.3
Fracture Toughness, KJQ (From Table 65)	271 ksi-in.$^{0.5}$
Axial Load	131,500 lbf
Internal Pressure	3,078 psi

The true stress-strain curves obtained from Table 62 were used for the analysis. As illustrated in Figure 64, the FAD boundary is constructed using the measured material-specific true stress-strain curves at 70°F. Yield strength (YS) and ultimate tensile strength (UTS) are obtained as averages from the longitudinal tensile test data. The material properties used for the ductile tearing analysis are the actual-measured YS, UTS, and work-hardening exponent "n" from the ruptured joint. The material properties and the pipe attributes are listed in Table 17.

Next, the ductile tearing analysis is conducted to obtain the stability of the assumed crack length using the J-R curve. The J-R curve for the actual material is obtained and illustrated in Figure 246. J-Δa data corresponding to SENB-2 and SENB-3 were validated as per ASTM E1820 [16] and used for the analysis. The material fracture toughness used for each crack assessment point (i.e., crack depth and length) is determined from the J-R curve. Note that the fracture toughness will increase with the crack depth for a rising J-R curve. Various crack lengths ranging from 0.25 to 2 in. and crack depths ranging from 20 to 90% were analyzed.

Table 18 illustrates the results of the ductile tearing instability analysis of the assumed circumferential crack depths and lengths, where "2c" is the crack length, "a" is crack depth, and "t" is wall thickness. The circumferential crack length was increased, starting from 0.25 in. and going to 2 in. Note that a 2 in. circumferential crack is approximately 9% of the circumference.

Table 18: Ductile Tearing Instability Analysis of Assumed Circumferential Lengths and Depth

#	Crack Length 2c (in.)	a (in.)	a/t	Operating Pressure(psi)	Stability
1	0.25	0.02664	20%	3078	Stable
2	0.25	0.05328	40%	3078	Stable
3	0.25	0.07992	60%	3078	Stable
4	0.25	0.09324	70%	3078	Stable
5	0.25	0.098568	74%	3078	Stable
6	0.25	0.0999	75%	3078	Stable
7	0.25	0.10656	80%	3078	Unstable
8	0.25	0.11988	90%	3078	Unstable
9	0.50	0.02664	20%	3078	Stable
10	0.50	0.05328	40%	3078	Stable
11	0.50	0.07992	60%	3078	Stable
12	0.50	0.09324	70%	3078	Stable
13	0.50	0.098568	74%	3078	Stable
14	0.50	0.0999	75%	3078	Stable
15	0.50	0.10656	80%	3078	Unstable
16	0.50	0.11988	90%	3078	Unstable
17	0.75	0.02664	20%	3078	Stable
18	0.75	0.05328	40%	3078	Stable
19	0.75	0.07992	60%	3078	Stable
20	0.75	0.09324	70%	3078	Stable
21	0.75	0.098568	74%	3078	Stable
22	0.75	0.0999	75%	3078	Stable
23	0.75	0.10656	80%	3078	Unstable
24	0.75	0.11988	90%	3078	Unstable
25	1.00	0.02664	20%	3078	Stable
26	1.00	0.05328	40%	3078	Stable
27	1.00	0.07992	60%	3078	Stable

#	Crack Length 2c (in.)	a (in.)	a/t	Operating Pressure(psi)	Stability
28	1.00	0.09324	70%	3078	Stable
29	1.00	0.098568	74%	3078	Stable
30	1.00	0.0999	75%	3078	Stable
31	1.00	0.10656	80%	3078	Unstable
32	1.00	0.11988	90%	3078	Unstable
33	1.50	0.02664	20%	3078	Stable
34	1.50	0.05328	40%	3078	Stable
35	1.50	0.07992	60%	3078	Stable
36	1.50	0.09324	70%	3078	Stable
37	1.50	0.098568	74%	3078	Stable
38	1.50	0.0999	75%	3078	Stable
39	1.50	0.10656	80%	3078	Unstable
40	1.50	0.11988	90%	3078	Unstable
41	2.00	0.02664	20%	3078	Stable
42	2.00	0.05328	40%	3078	Stable
43	2.00	0.07992	60%	3078	Stable
44	2.00	0.09324	70%	3078	Stable
45	2.00	0.098568	74%	3078	Stable
46	2.00	0.0999	75%	3078	Unstable
47	2.00	0.10656	80%	3078	Unstable
48	2.00	0.11988	90%	3078	Unstable

The Level-3 assessment using several crack lengths and varying crack depth (20 – 90%) is summarized in Table 18. Ductile instability is predicted when the assessment point is tangent to FAD. Because the load is fixed, the locus of the assessment typically exhibits a “fish-hook” shape where the Kr reaches a minimum and then increases. The point of instability occurs when the locus of the assessment point is tangent to the FAD. For the 80% and above depth cases, the assessment points fall outside the FAD, and the crack is unstable.

Ductile tearing instability analysis showed that even a small circumferential crack with a length of 0.25 in. (i.e., approximately 1.1% of the circumference) becomes unstable with 80% crack depth. The applied axial load of 131,500 lb_f from the casing weight is significantly high, making any tiny through-wall crack unstable.

7.1.6 Event Sequence and Integration of Results

The evidence collected during the failure investigation has shown that the 7 in. casing failed in a ductile manner. First, bulging was observed at the axial rupture, indicating plastic deformation. Next, PROSPER modeling discussed in Section 12 has shown that the lowest temperature in well #2244 at the time of the failure was approximately 40°F. Blade conducted Charpy v-notch testing at various temperatures to determine the ductile-to-brittle transition temperature (DBTT). Details of the testing are discussed in the section A.10.6 The measured impact energy at 32°F of half-size specimens in the longitudinal and circumferential orientations was 50 and 30.3 ft-lb, respectively.

The testing showed that the casing behaved in a ductile manner despite the temperature drop during the failure event.

The fractographic analysis of the fracture surfaces also showed that the crack propagated in a ductile manner. Chevron marks were not identified on the circumferential fracture surface. The absence of chevron marks in combination with the Charpy v-notch impact testing at 32°F implies that the circumferential crack propagated in a ductile manner. Based on fracture mechanics analysis, a small crack (approximately 0.25 in.) in the circumferential direction would cause the 7 in. casing to part.

Figure 58 and Figure 59 show two small cracks, one in region 1 and another in region 2, perpendicular to the axial rupture fracture surface. Conversely, these small cracks did not continue to propagate in the circumferential direction. Only the top and bottom of the axial rupture turned and propagated circumferentially.

The observations described above indicate that the well #2244 failure was a single event. The axial rupture occurred first and propagated into circumferential cracking. The failure sequence was as follows:

- Corrosion of the 7 in. casing caused severe wall-thinning, eventually resulting in the axial rupture.
  - The physical wall measurements, visual observations, and pressure calculations support the conclusion that wall thinning caused the 7 in. failure.
- A crack initiated as an axial rupture and propagated in the axial direction to a length of 3.36 in.
- The upper crack front turned and continued propagating in the circumferential orientation until it eventually terminated.
- The lower crack front also turned and propagated in the circumferential orientation. However, unlike the upper crack front, the lower propagated circumferentially in two directions, causing the casing to part.
  - Because the circumferential parting was caused by two cracks traveling in opposite directions, a piece of the casing separated from the top and bottom failure sections.

Figure 93 shows a two-dimensional sequence map of the failure. The map is drawn to scale and was created by digitizing the paper replicas of failure pieces C001A and C001B. Arrows indicate crack paths and are assigned different colors to indicate various stages of crack propagation. The red arrows and the 3.36 in. dimension callout indicate the axial rupture. The black arrows above the axial rupture represent the upper circumferential crack path, which begins at the upper turning point and ends at the upper termination point.

The lower turning point is where the bottom of the axial rupture splits into two different circumferential crack paths. The lower circumferential cracks 1 and 2 are marked by blue and magenta arrows, respectively. Crack 1 (blue) initially propagates perpendicular to the axial rupture for approximately 3 in. Then, crack 1 changes direction from 90° (fully circumferential) to 75° (mostly circumferential) from the axial rupture and propagates for approximately 8.5 in. Finally, crack 1 changes direction from 75° (mostly circumferential) to 15° (mostly axial) from the axial rupture and terminates in the crack path of crack 2.

Crack 2 (magenta) initially propagates 50° from the axial in the opposite direction of crack 1 (blue). Crack 2 continues for approximately 9 in. and changes direction from 50° to 90° (fully circumferential) from the axial rupture. As crack 1 continues to propagate circumferentially, the crack path angle steadily becomes more shallow (more axial) until crack 2 (magenta) terminates in the crack path of crack 1 (blue).

Figure 93 shows the casing's missing piece (red region) separated by the propagation of the lower two circumferential cracks. The image shows how cracks 1 and 2 propagate past each other on different axial planes but eventually reconnect, separating the missing piece from the casing. The missing piece of the casing was never recovered and, therefore, was not included as part of the failure analysis.

Mechanical damage was observed on a portion of the C001B (upward-facing) fracture surface. The damage caused an anomaly in the paper replica of C001B. The yellow region identifies the anomaly in Figure 93. The damage most likely occurred after the missing piece separated from the casing, exposing the upward-facing fracture surface. The damaged section was neglected when plotting the crack path of crack 2 in Figure 93.

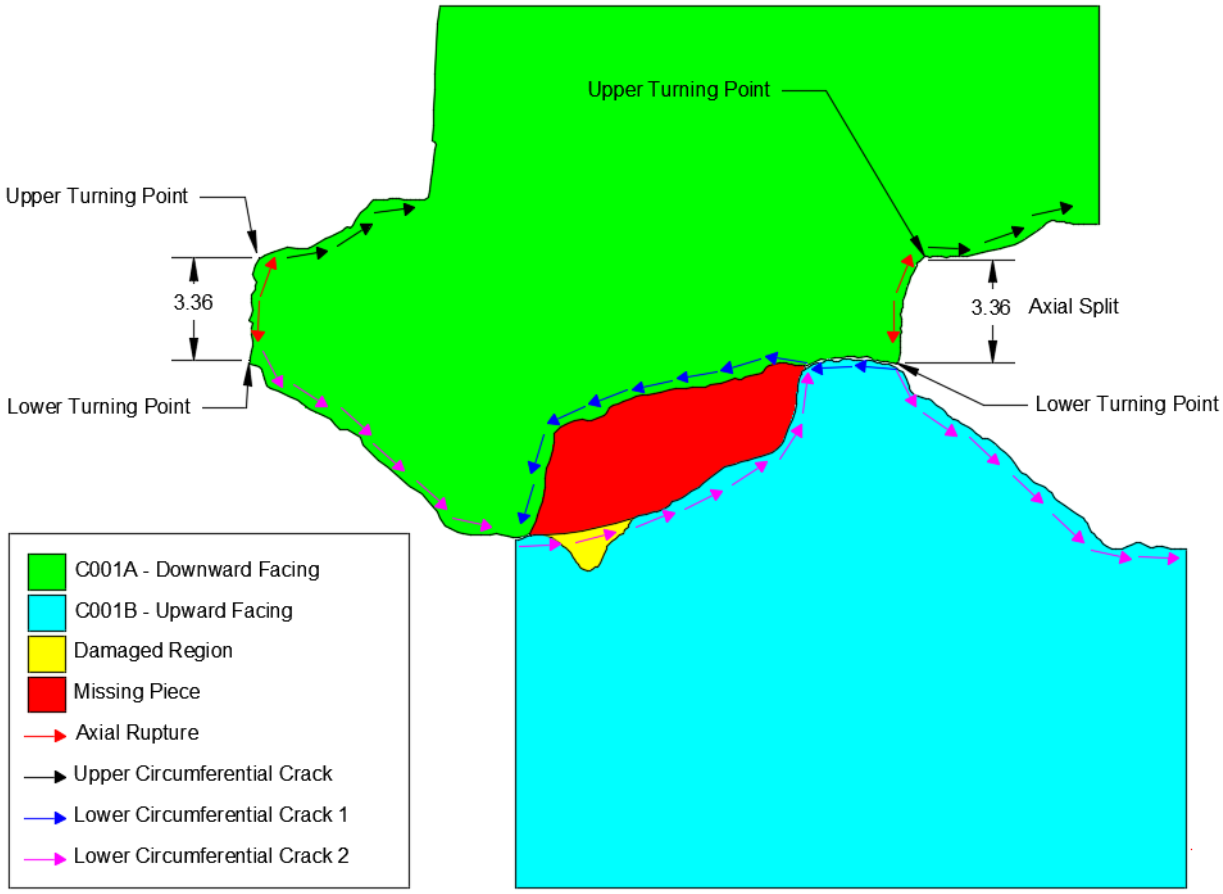

Figure 93: Two-Dimensional Sequence Map

Figure 94 shows a three-dimensional sequence map of the failure. The figure was created using the laser scan mesh from C001A and C001B. The meshes were imported into a single file and aligned to match the two-dimensional map. The three-dimensional sequence map contains the same information as the two-dimensional map; however, the laser scan mesh provides additional insight and perspective into the propagation of the cracks. A key difference between Figure 93 and Figure 94 is that the three-dimensional views include the plastic deformation and damage that occurred during the failure, causing misalignment of the fracture surfaces.

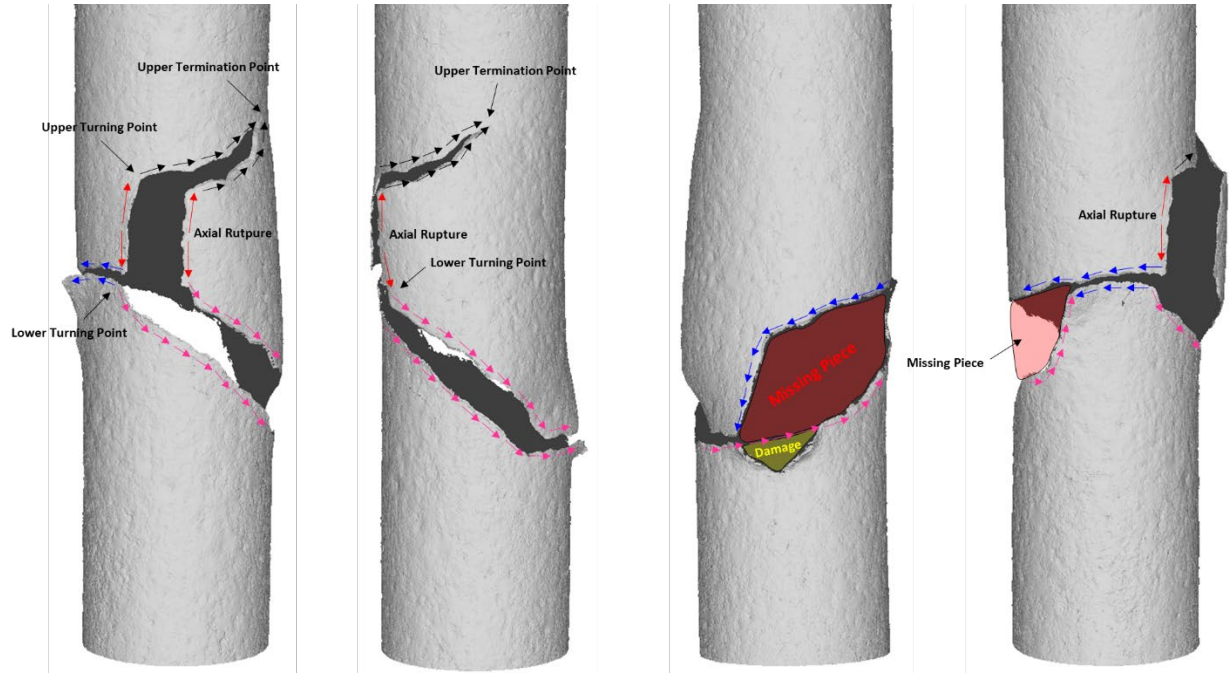

Figure 94: Three-Dimensional Sequence Map

7.2 Corrosion Analysis

The overall cause of the rupture itself is the wall thinning due to 7 in. casing external corrosion. Consequently, interpretation of the corrosion mechanism is crucial to mitigation.

The objectives of the corrosion analysis are to:

- Characterize the morphology of corrosion.
- Determine the distribution of corrosion along the available joints for examination.
- Characterize the scale samples collected from the field.
- Identify the possible corrosion mechanism.

7.2.1 Individual Well Analysis

Approach

Examination of casing wall metal loss due to corrosion was performed for some joints retrieved from wells #2244, #2248, and #2251. Based on field observations, wall loss occurred on some of the joints retrieved from the three wells. Some apparent pitting corrosion was also observed during field inspection.

Non-destructive evaluation (NDE) was carried out on the entire external surface of some of the joints retrieved from the three wells, using measurement methods such as laser scanning, pit gauge, caliper, and point micrometer. A full circumference (360°) graphical representation of the extent of wall loss was obtained, along with the depth, length, and width of the corrosion features. The depth profile and distribution of the corrosion along the casings were used to assess the failure pressure and to help identify patterns of the corrosion distribution.

Prior to NDE, the joints were abrasive blasted to remove any contaminants such as oil, dust, or scale from the OD surface of the casing joints. This is routinely used to clean surfaces of casing and pipelines to remove corrosion products and other debris.

Laser scan is a non-contact device that works on a line-of-sight basis; therefore, the surface of the pipe must be cleaned to prevent any material on the casing surface from obscuring corrosion features. Black Beauty extra fine was used as the blast media. Blade monitored the transportation and blasting of the joints.

Following blast cleaning, the OD surfaces were laser scanned with 1mm resolution using the Creaform HandySCAN 700 laser scanner. The technology uses auto-position stereo vision and positioning dots (targets) to create real-time rendering of objects. The rendered object is a 3D mesh of the OD surface. Figure 95 shows an image of the HandySCAN 700, the positioning dots, and the laser lines on the OD surface of a pipe.

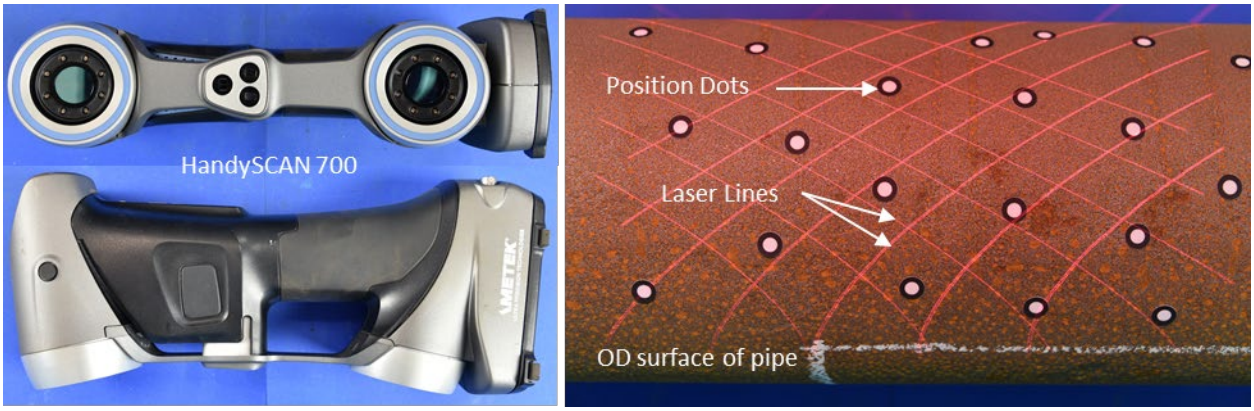

Figure 95: Creaform HandySCAN 700 Scanner, Positioning Dots, and Laser Lines

The axial direction and distances of the scan were aligned with the downhole direction and adjusted to the actual depth of each casing in the wells, using known references (e.g., slip and connection locations) and data logs.

All the data collected from the scans were analyzed using the Pipecheck Corrosion Module, except for the C001B-2 joint, which was analyzed with the Mechanical Damage Module due to the extensive wall thinning of the entire joint. The Corrosion Module requires that at least a small area of the scanned surface be free of corrosion (reference surface) to measure the depth of corrosion against this reference surface in the same way that the depth of a corrosion peak is measured with a pit gauge.

The Mechanical Damage Module gave a better result than the Corrosion Module in this case. The Corrosion Module gives better results for the analysis of discrete pitting or discrete corrosion features, but does not provide good results for the analysis of general wall thinning, and especially for pipes longer than 9 ft.

Different renderings of the casing OD surfaces were obtained for corrosion analysis. The nominal dimensions used for all the scans were 7 in. for the OD and 0.362 in. for the wall thickness. A threshold of 10% NWT was used for the analysis. Manual NDE was also used for verification of deep pitting corrosion measurements. The following sections provide a summary of the corrosion observations in some joints retrieved from wells #2244, #2248, and #2251.

Well #2244

Laser scans were obtained for the following joints retrieved from well #2244:

- C001B-2
- C001C
- C002B
- C003B
- C004B
- C005B
- C006B
- C030B

The upward-facing fracture surface was removed from C001B prior to abrasive blasting. The fracture surface was named C001B-1, and the remaining joint was named C001B-2. Some regions of C001B-2 with corrosion features were protected from abrasive blasting media using Saran wrap and duct tape. Figure 96 shows two regions that were masked. The protected regions of C001B-2 were subsequently used for Raman spectroscopy and EDS analyses.

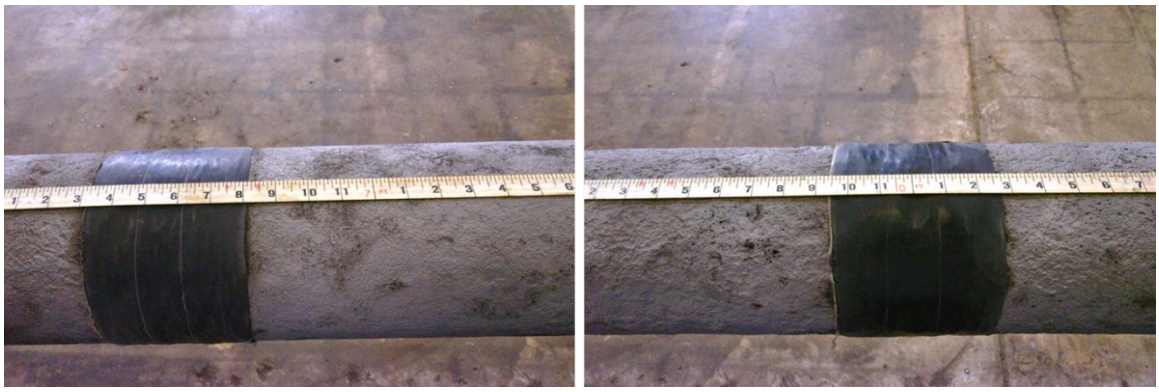

Figure 96: C001B Areas Protected During Abrasive Blasting

Figure 97 shows the 3D map of the corrosion on C001B-2. All indications greater than 10% NWT are identified in the images by different colors that range from yellow (for shallow corrosion) to red (for deep corrosion). Corroded areas with depths ≤ 10% NWT are shown in green color.

The 3D images in gray and in the corrosion color map of the C001B-2 joint are shown on the top and center of Figure 97. The length of the section and the downhole direction are also indicated in the graph.

The bottom of the figure shows the full circumference (360°) distribution of the corrosion and the locations of the areas protected from the blasting media (delimited with dashed lines), as well as the identification of the three subsections of joint C001B-2.

The wall thickness tapers down from the bottom side of C001B-2E-1 to the top side of C001B-2A. Excessive wall thinning was observed in C001B-2A and is reflected by the red color in the laser scan-rendered image.

Medium wall loss was observed in the C001B-2C region and is reflected by the yellow/orange color. Minimal-to-negligible wall loss observed in the C001B-2E-1 region is reflected by the green color. The

green color reflects the 10% NWT threshold used in the analysis. This indicates that C001B-2E-1 is within the 10% NWT wall loss.

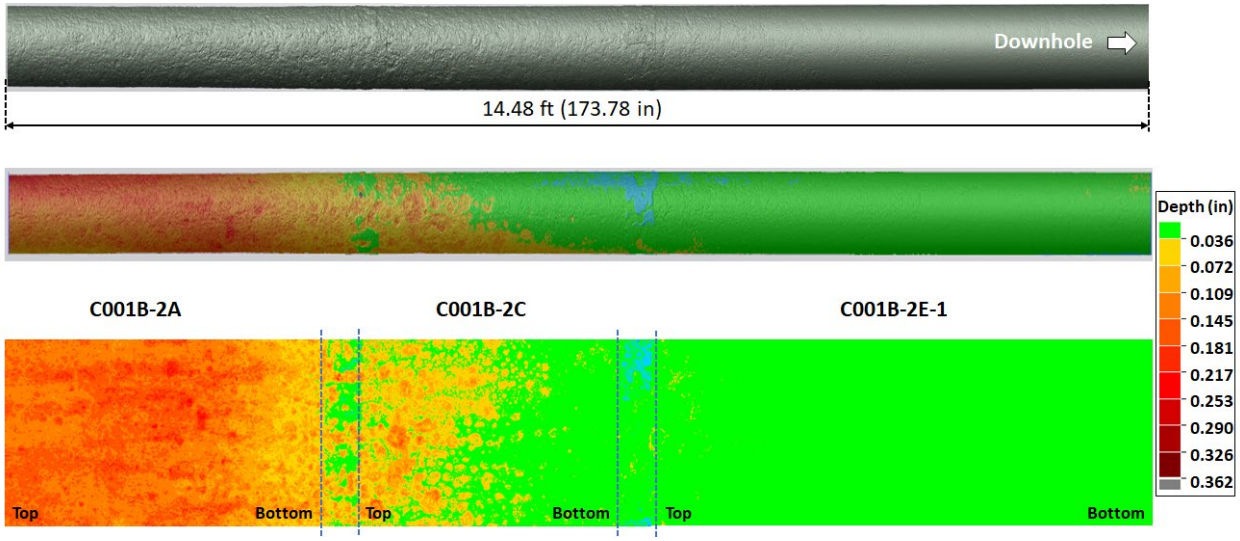

Figure 97: 3D Color Map of Corrosion Analysis Results for C001B-2. Arrow Indicates Downhole Flow Direction

The wall thickness from the cut ends of the C001B-2 subsections were measured using a point micrometer to validate the results of laser scan data analysis. Thickness measurements were obtained in arbitrarily assigned four quadrants of the casing. The four quadrants were based on the assigned reference orientation for 12:00 (0°) of the laser scan. Actual thickness measurements in the subsections of C001B-2 show that the remaining wall is between 51% to 96% NWT (NWT = 0.362 in.).

The laser scan data aligns with the manual wall thickness measurements. The red orange color corresponds to the remaining wall thickness at the top of C001B-2A, which is approximately 50% NWT; the green color in C001B-2E-1 corresponds to remaining wall thickness of C001B-2E-1, which is less than 10% NWT.

Table 19: Manual Verification of Wall Thickness

Circumferential Position hh:mm (Degree)	C001B-2A Top	C001B-2A Bottom	C001B-2C Top	C001B-2C Bottom	C001B-2E-1 Top	C001B-2E-1 Bottom
3:00 (90°)	0.220	0.259	0.292	0.320	0.330	0.355
6:00 (180°)	0.175	0.240	0.263	0.306	0.322	0.354
9:00 (270°)	0.176	0.261	0.256	0.339	0.333	0.342
12:00 (0°)	0.168	0.268	0.292	0.328	0.333	0.336
Average	0.185	0.257	0.276	0.323	0.329	0.347
Remaining Wall Thickness (% NWT)	51	71	76	89	91	96

Figure 98 and Figure 99 show, in detail, the 3D laser scan image of C001B-2A and C001B-2C around the entire circumference of the casing. These images indicate that wall thinning occurred in the entire circumference of the casing and was not concentrated on just one side. The areas that were masked from abrasive blasting are indicated by the dashed lines.

Figure 98: 360° Views Around C001B-2A

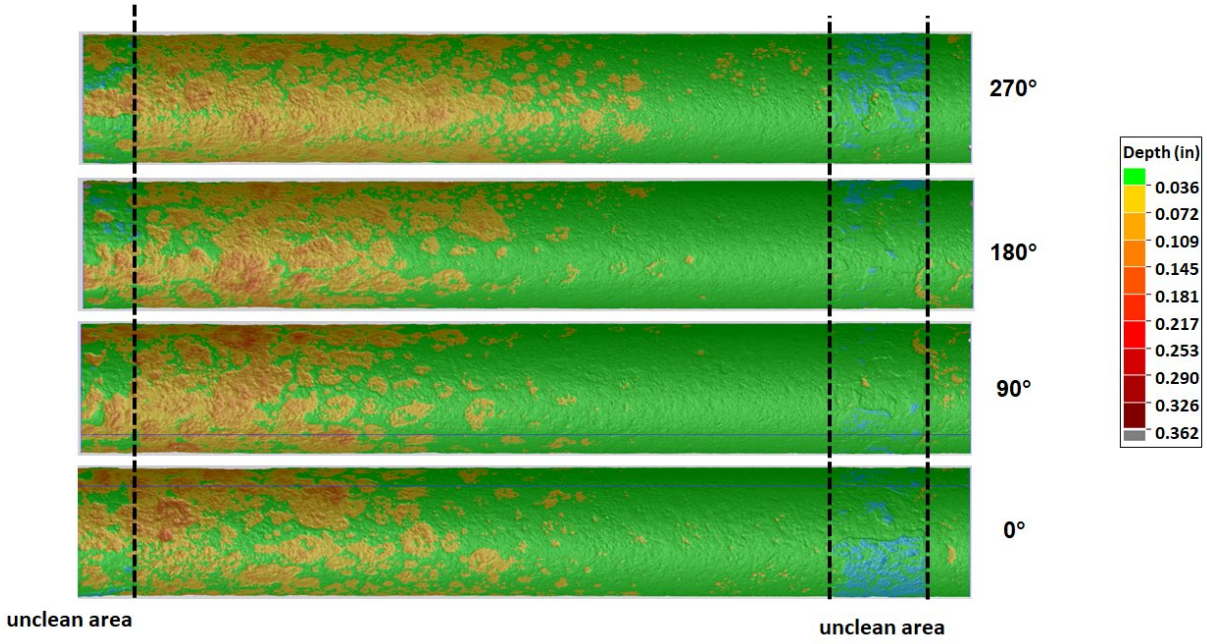

Figure 99: 360° Views Around C001B-2C

Figure 100 shows the axial and circumferential profiles for the highest wall loss in C001B-2A. Based on laser scan data, the maximum wall loss in this section is approximately 70% NWT. The percentage wall loss was calculated based on the nominal thickness of the pipe, 0.362 in.

Figure 100 also shows that some deeper corrosion pits can be found on areas along the length of the pipe and around the circumference of the pipe. The areas surrounding the location with the deepest corrosion have an average wall thinning of approximately 50% NWT.

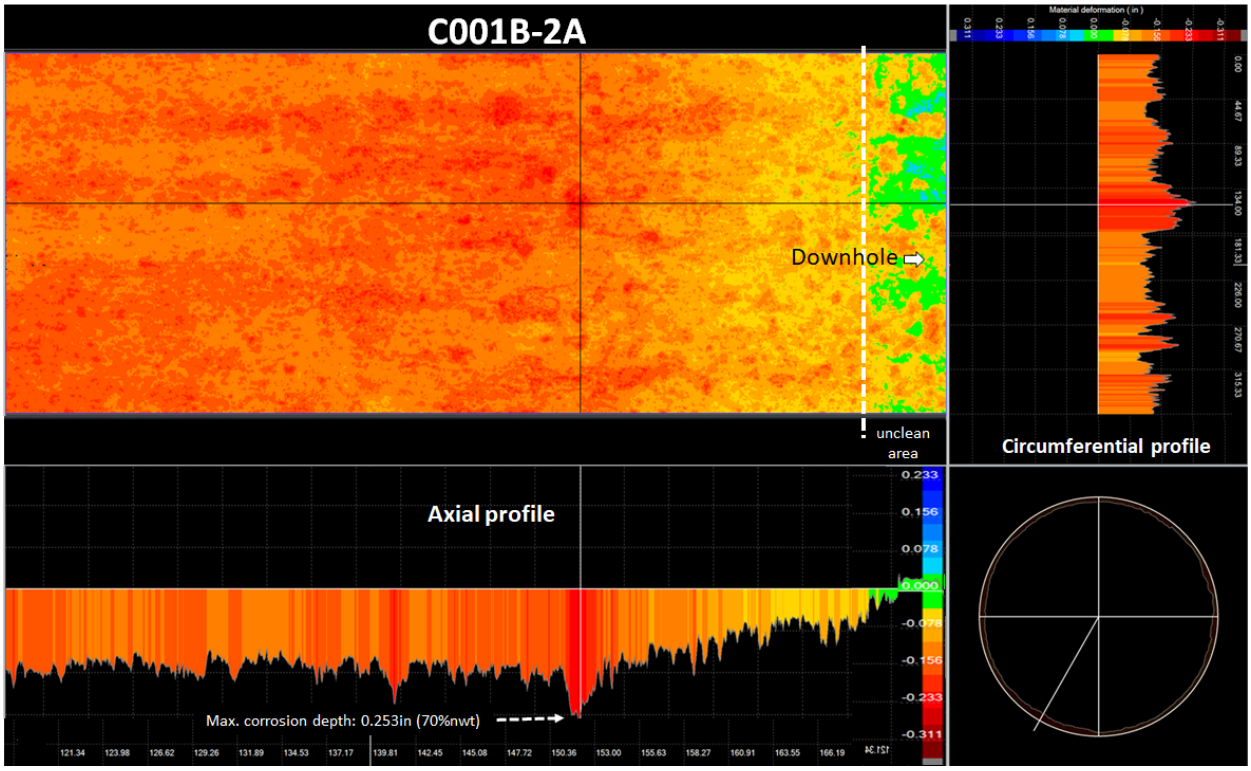

Figure 100: Maximum Wall Loss in C001B-2A, Dashed Line Indicates Masked Region

Figure 101 shows the common corrosion features observed in C001B-2A. This section has general corrosion with high-density corrosion pits. Pit diameters are roughly between 0.1 in. to 0.5 in. The average pit depth in this section is approximately 64 mil (0.064 in.). Note that the average pit depth is much smaller compared to the wall loss determined from laser scan. This is because the pit depths were measured using a pit gauge with a bridge span of 3 inches.

The pit gauge reference point is based on the general peak height on the OD surface of the pipe. It does not consider the material that was lost due to general wall thinning. Figure 102 shows the corrosion features observed in section C001B-2C. This section also contains high-density corrosion pits, with pit diameters ranging from 0.1 in. to 0.5 in. The average pit depth in this section is approximately 0.62 mil (0.00062 in.). The pit depth in this section is similar to the pit depth in C001B-2A. Figure 103 shows the small pits (pit diameter <0.1 in.) observed in C001B-2E-1. The average pit depth in this section is approximately 8 mil (0.008 in.).

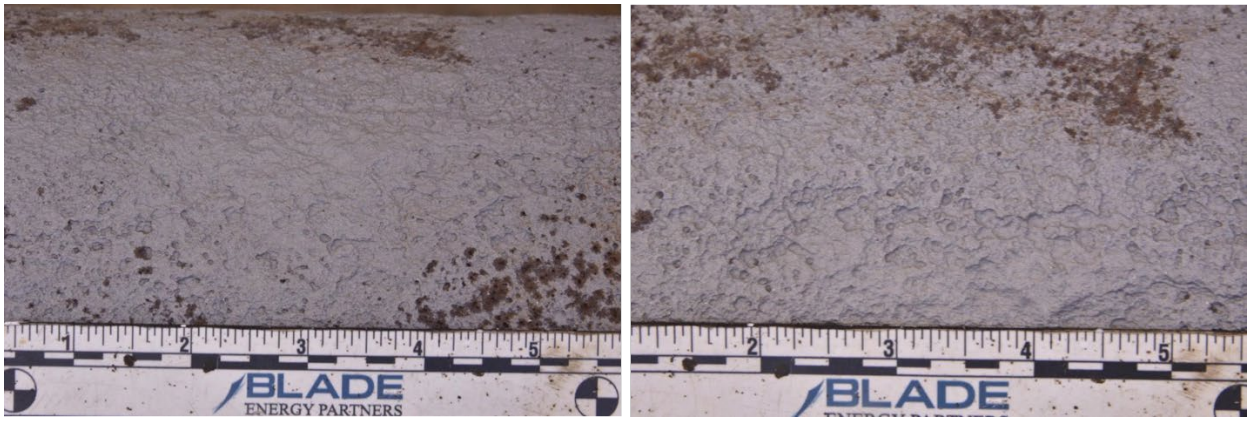

Figure 101: Corrosion Features in C001B-2A

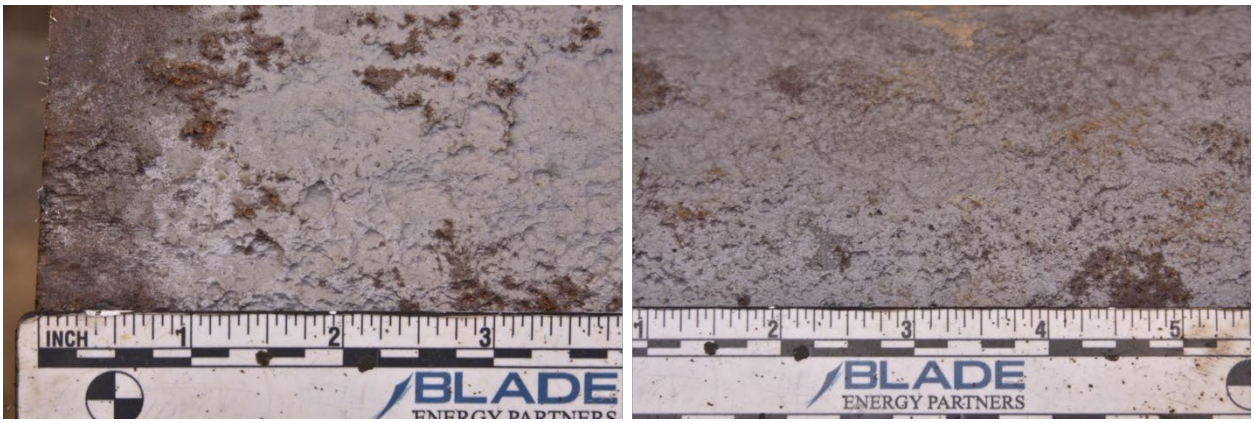

Figure 102: Corrosion Features in C001B-2C

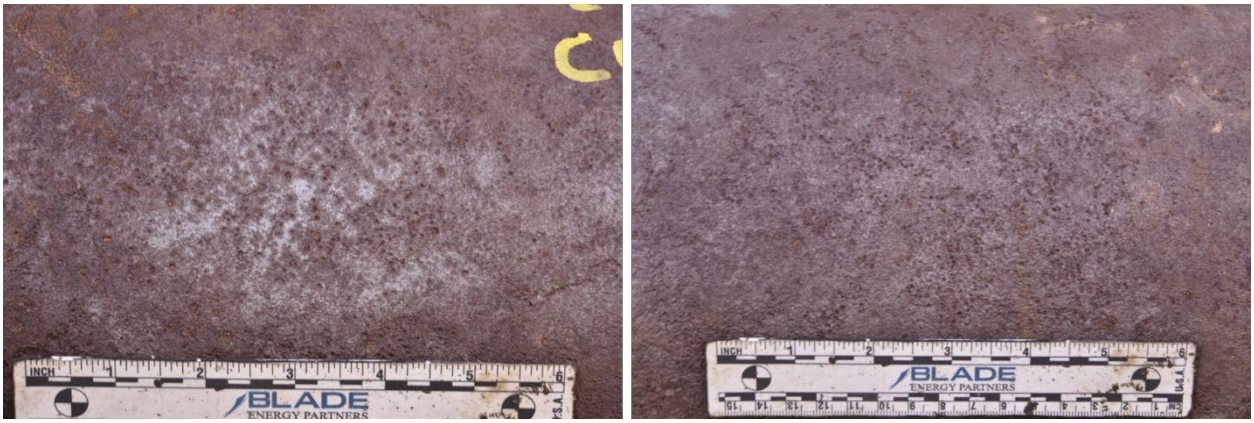

Figure 103: Corrosion Features in C001B-2E-1

The other joints from well #2244, C002B, C003B, C004B, C005B, C006B, and C030B, were also laser scanned. Only two of these joints contain corrosion features with depths greater than 20% NWT. Figure 104 shows the laser scan results of joint C002B. The arrow points to the downhole direction. Some corrosion features are present towards the bottom edge of the joint.

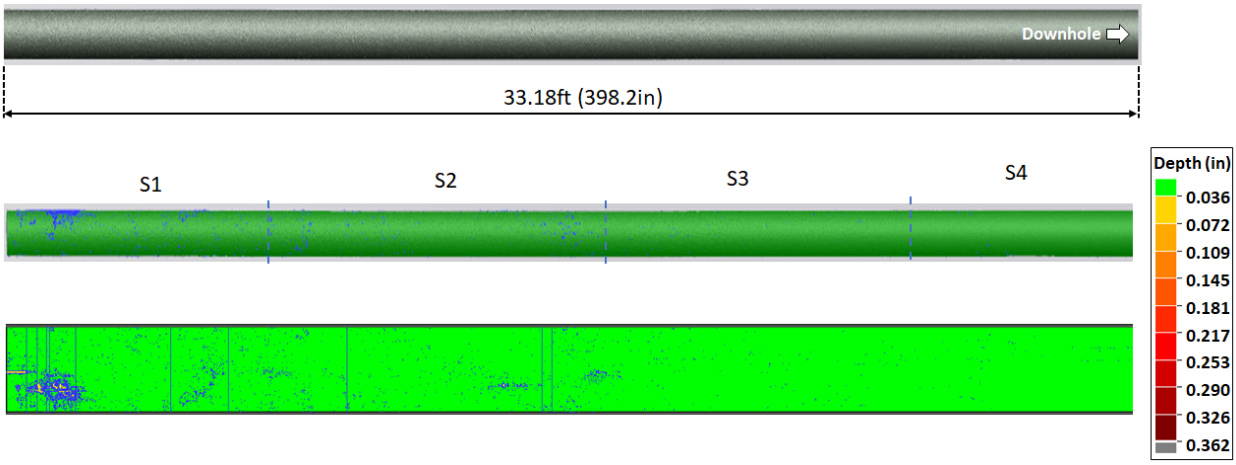

Figure 104: Laser Scan Rendering of C002B

Figure 105 shows the corrosion (blue areas) observed from the top edge of C002B. The corrosion is located between 3.58 in. to 28.66 in. from the top cut. The corrosion depth is about 0.089 in., which corresponds to 25% NWT wall loss. Other corrosion features in the middle of the joint have depths that are less than 20% NWT.

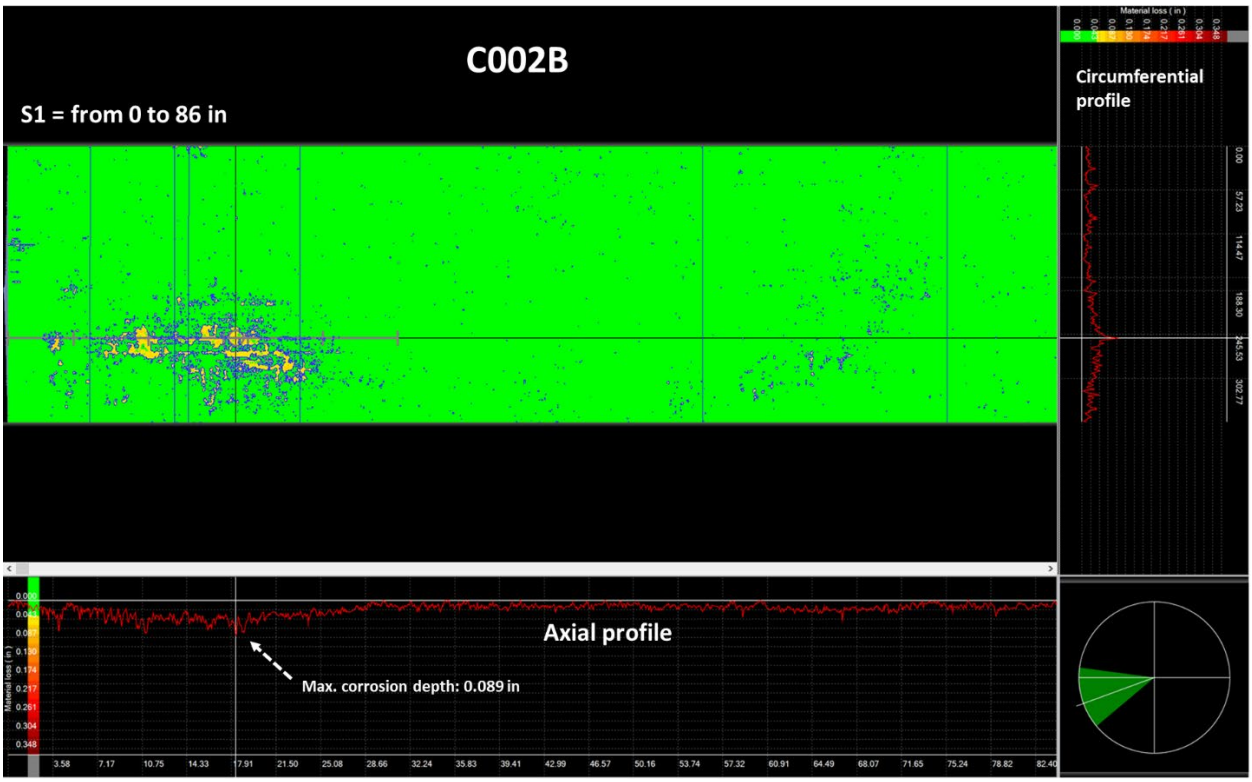

Figure 105: Shallow Corrosion Observed on C002B

Figure 106 shows the results of the laser scan analysis of C005B. The arrow points to the downhole direction. Corrosion features are present in the mid-section of the joint.

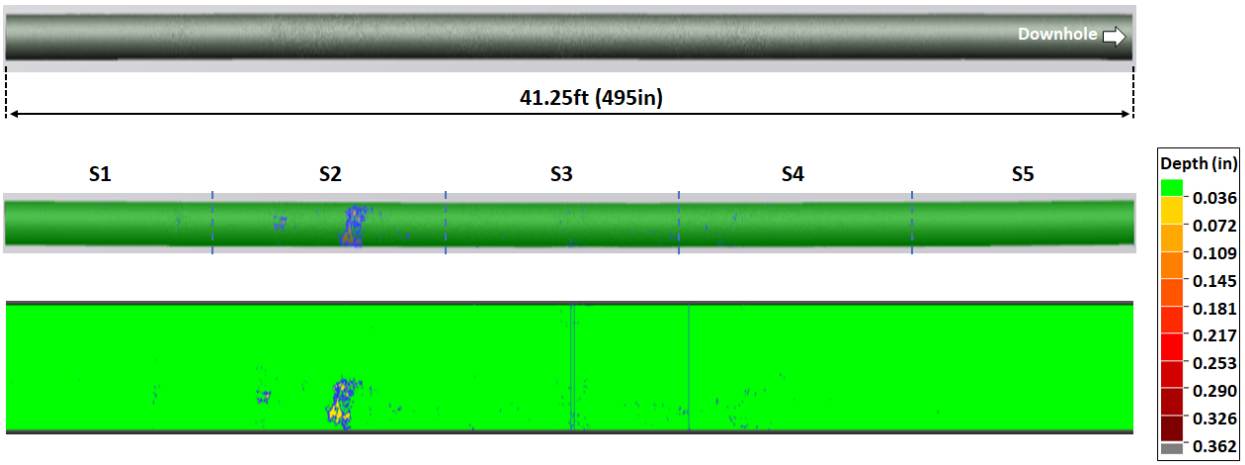

Figure 106: Laser Scan Rendering of C005B

Figure 107 shows the corrosion features in the mid-section of joint C005B. The deepest corrosion in this joint is located between 112 in. and 216 in. from the top edge. The corrosion depth is approximately 20% NWT.

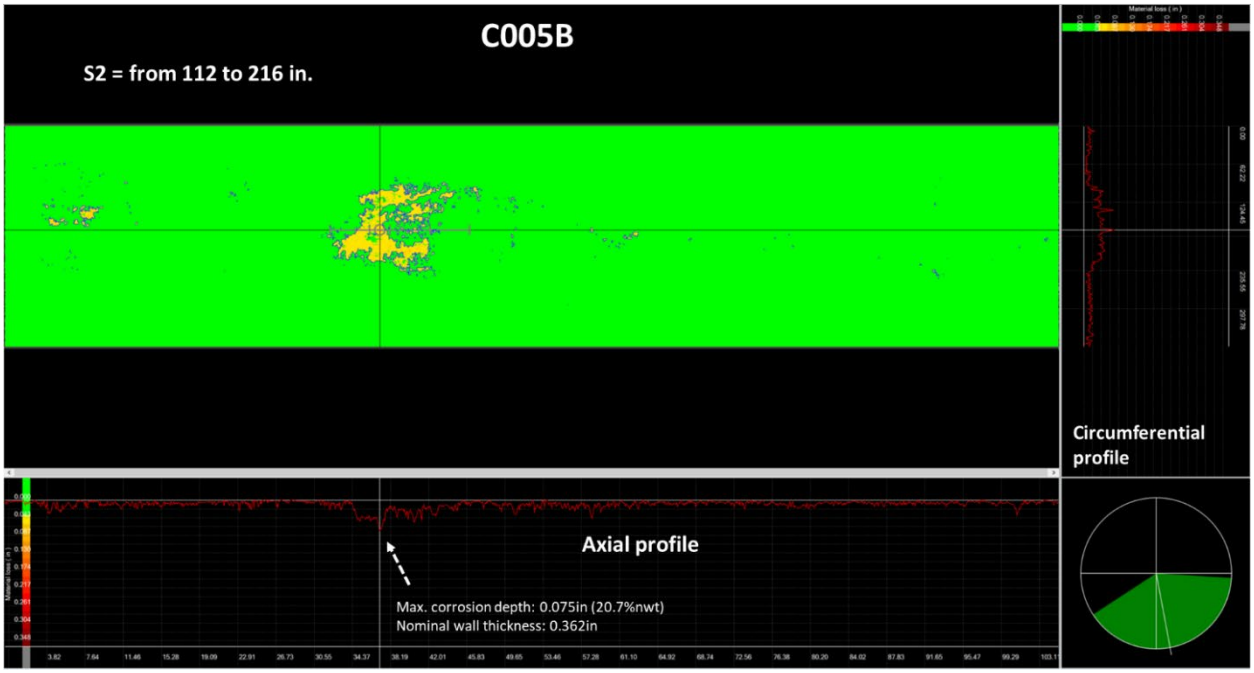

Figure 107: Deepest Corrosion in C005B

All scan data from joints of well #2244 (C001B-2, C002B, C003B, C004B, C005B, C006B, and C030B), as well as the NDE performed on sections C001A and C001B-1 were collected, aligned, and summarized in Figure 108. The figure shows the 360-degree corrosion map, the corrosion depth for all indications, and the maximum corrosion depth for each joint, demonstrating the corrosion distribution for the first six 7 in. production casings extracted, without including connections and cutoff ends from casings (approximately 4 ft between scanned joints).

The corrosion distribution in Figure 108 does not include C030B because all indications throughout C030 are within the 10% NWT threshold.

In terms of maximum corrosion depth, the failure joint C001 had a corrosion depth at the failure location that was 87% wall loss. All the corrosion features deeper than 25% NWT are located within the first 20 ft of the C001 joint. The C002 joint also has a high concentration of corrosion features but less than 25% NWT in depth. Below this joint, shallow corrosion was observed in scattered, small areas along C003 through C006. The C030 joint did not show any corrosion indication greater than 10% NWT.

The key observations for all the joints with corrosion is that the distribution is oriented around the circumference of the production casing. No preferential orientation was noted for the OD corrosion in the 7 in. production casing. The corrosion begins below the bottom slip mark, increasing uniformly around the circumference until maximum wall thinning is reached at the failure location, and then begins to decrease toward joint C002.

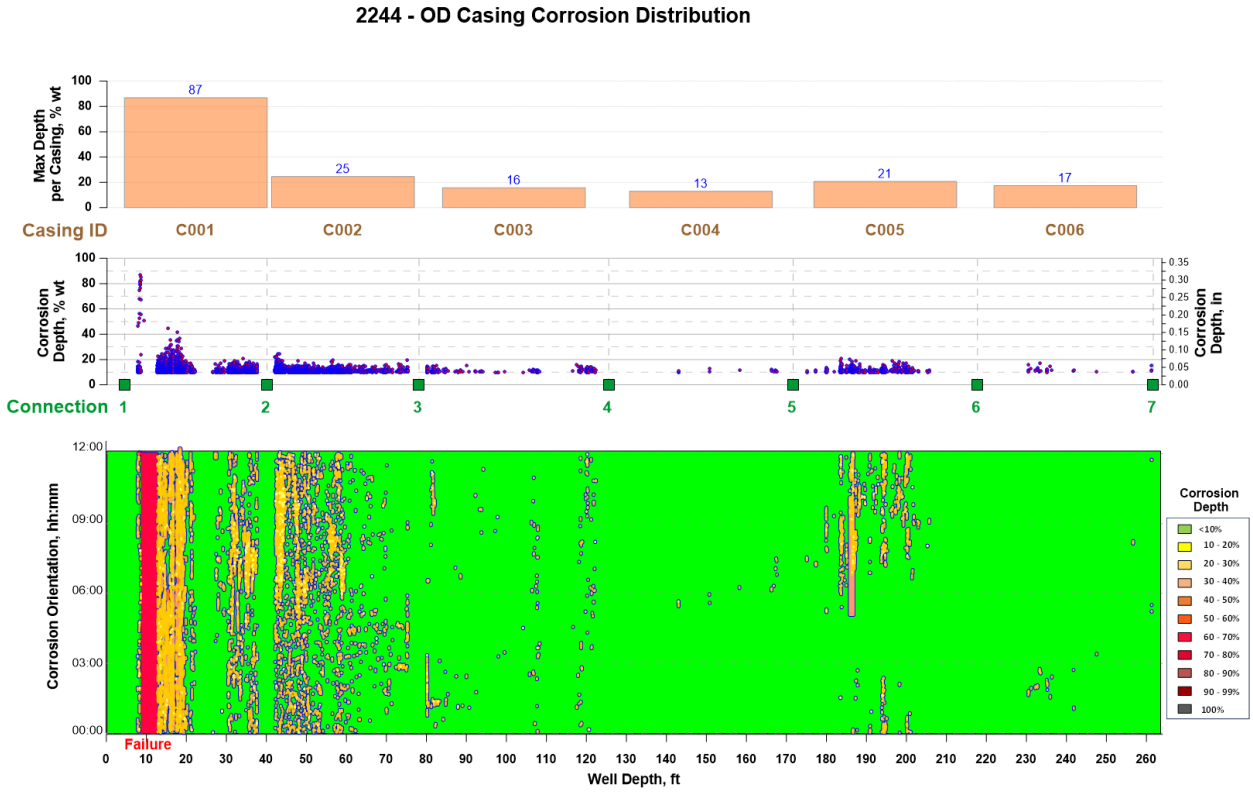

Figure 108: External Corrosion Distribution for Well #2244

Well #2248

Only the top joint was retrieved from well #2248. Joint C001 was cut into smaller sections. A 3 in. section for further corrosion scale and morphology analyses was excised from the joint prior to abrasive blasting. Figure 109 shows the subsections of joint C001 before and after cutting. After removing small samples for analysis, the remaining 3 in. section was brushed clean and scanned. The maximum corrosion depths were included in the corrosion distribution analysis.

Figure 110 shows the results of laser scan rendering of joint subsections C001-A and C001-C at different clock orientations. The arrow points to the downhole direction. The deepest corrosion at the 6:00 position of C001-C has a depth of 0.201 in. (55.5% NWT).

There is evident excessive wall thinning 1.9 ft. from the top cut end of C001-A, which is approximately 0.7 ft from the bottom slip mark (see Figure 109 and Figure 110). Figure 110 shows that the region between the slip mark and the region with evident wall loss (orange color) have a wall thickness greater than 90% NWT (green color), i.e., wall loss is less than the set threshold (10% NWT) for laser scan analysis.

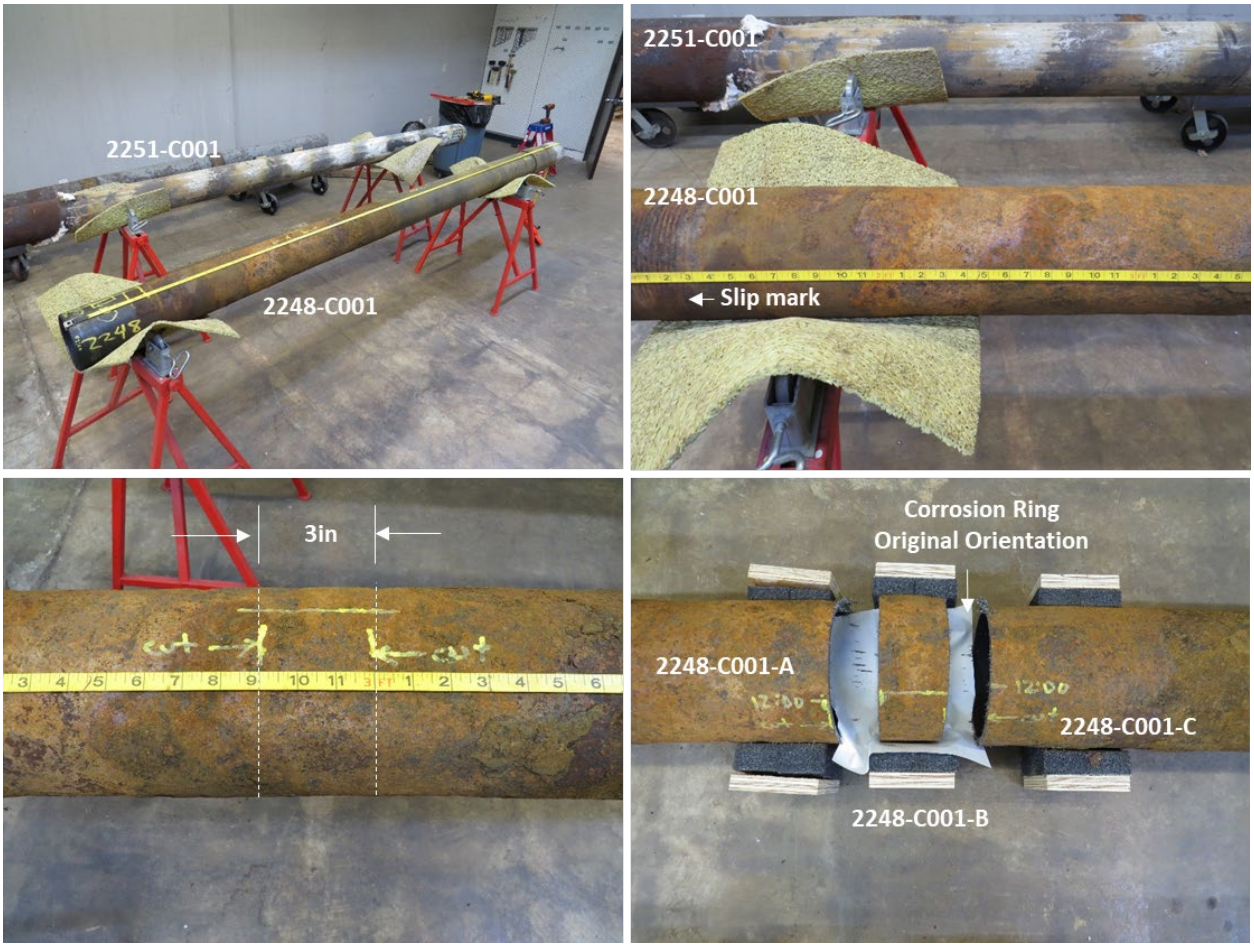

Figure 109: C001 Joint from Well #2248 Before and After Cutting

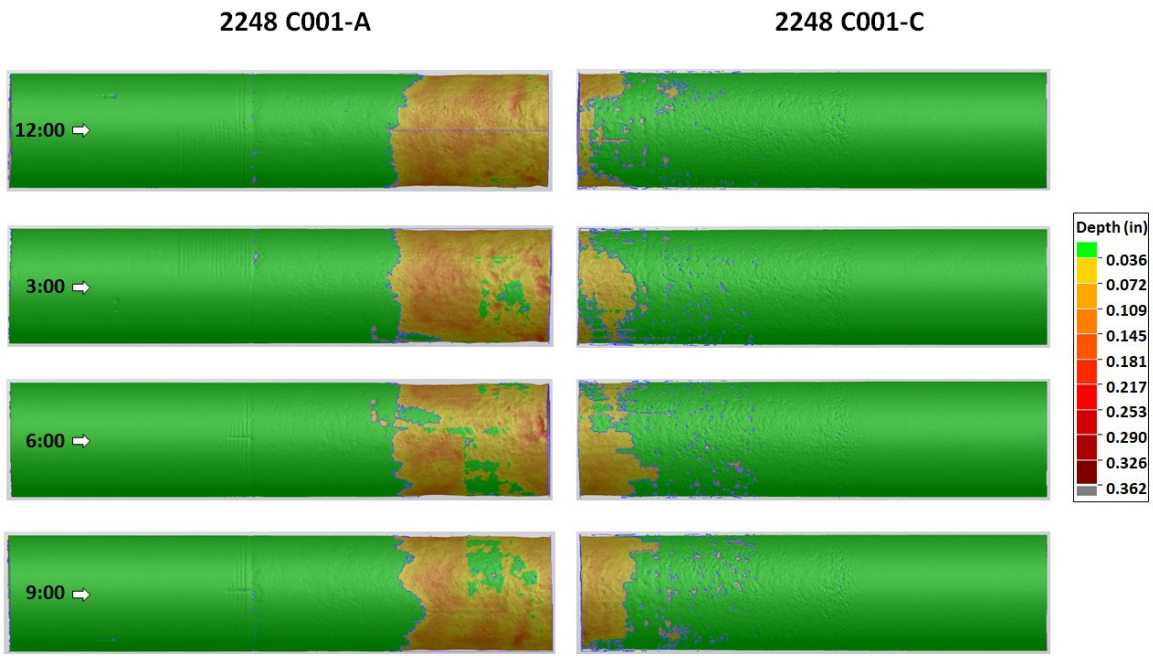

Figure 110: Laser Scan Rendering of Well #2248 Joint C001-A and C001-C

All scan data from well #2248 C001, as well as the NDE performed on the 3 in. section were collected, aligned, and summarized in Figure 111. From bottom to top, the Figure shows the 360° corrosion map, the corrosion depth for all indications, and the maximum corrosion depth per foot of casing, demonstrating all the distribution of corrosion for the C001 joint, without including the connection.

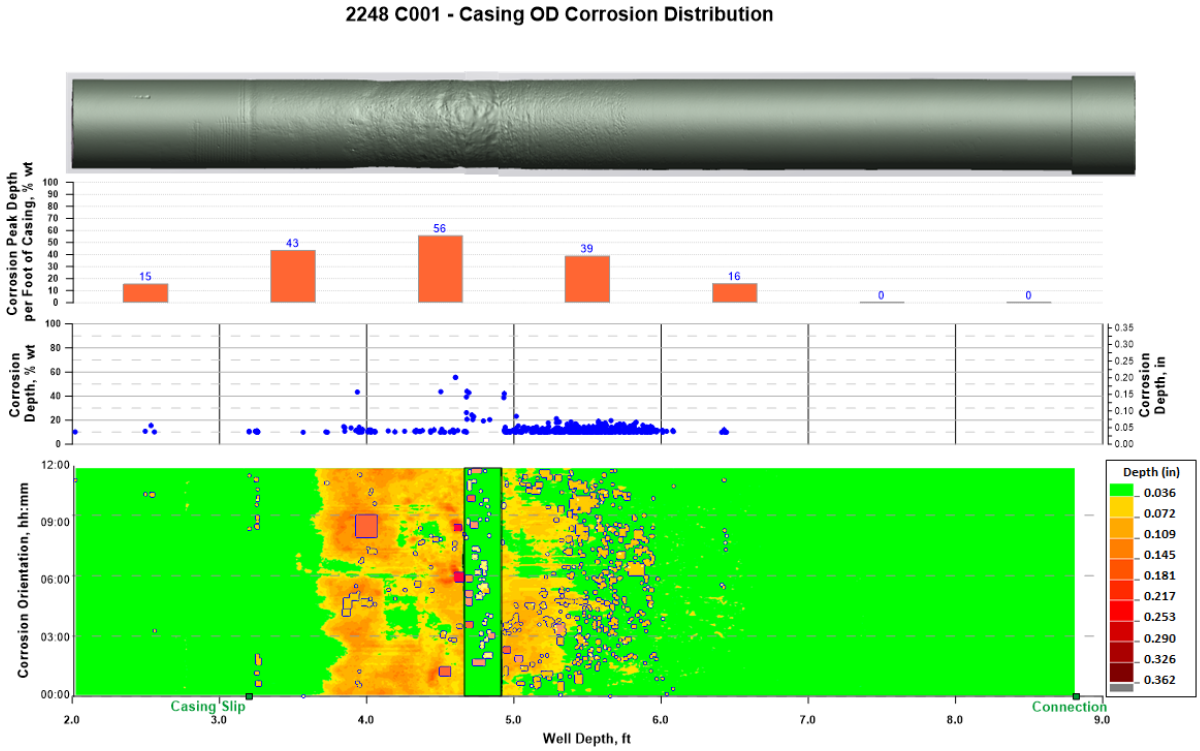

Figure 111: External Corrosion Distribution for Well #2248 C001

Figure 112 shows the common corrosion features observed in well #2248 joint sections C001-A and C001-C. The joint sections contain high-density corrosion pits. These features are similar to the features observed in well #2244. However, the EDS analysis of the surfaces suggests a slightly different aqueous environment and corrosion products.

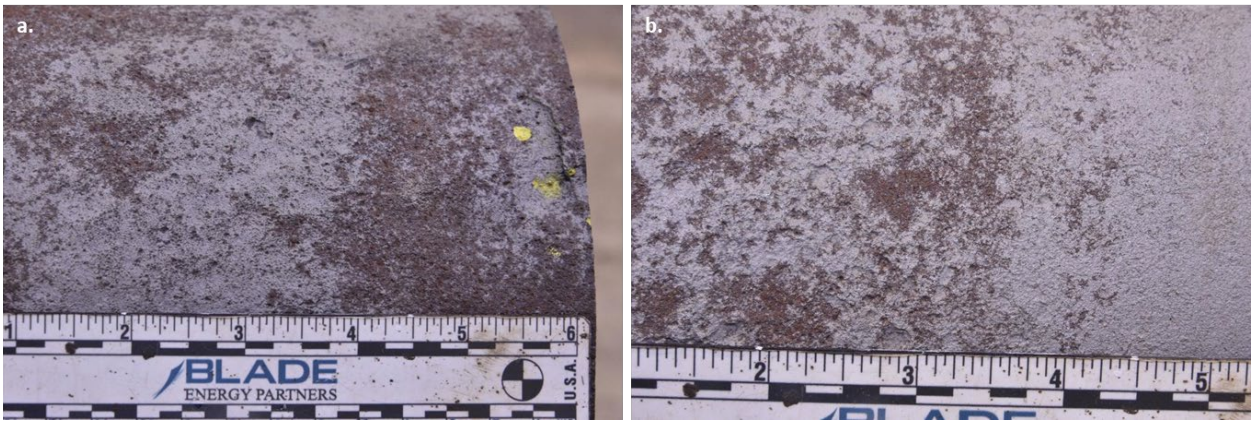

Figure 112: Corrosion Features Observed in Well #2248 C001-A and C001-C

Well #2251

Similar to #2248, only the top joint was retrieved from well #2251. Figure 113 shows joint C001 prior to cutting and abrasive blasting. A small portion of the joint was still covered with cement (approximately 2 ft away from the top of the joint cut end). Joint C001 was cut into smaller sections. A 4 in. section for further corrosion scale and morphology analyses was excised from the joint prior to abrasive blasting.

After removing small samples for analysis, the remaining 4 in. section was brushed clean and the deepest corrosion depths were measured with a micrometer, to be included in the corrosion distribution analysis. Figure 113 shows the location where the sample was extracted.

Figure 114 shows the laser scan rendering of #2251 joint subsections C001-A and C001-C. Based on laser scan data, the maximum depth of corrosion in C001-A is 0.156 in. (43% NWT), and the maximum depth of corrosion in C001-C is 0.237 in. (65% NWT).

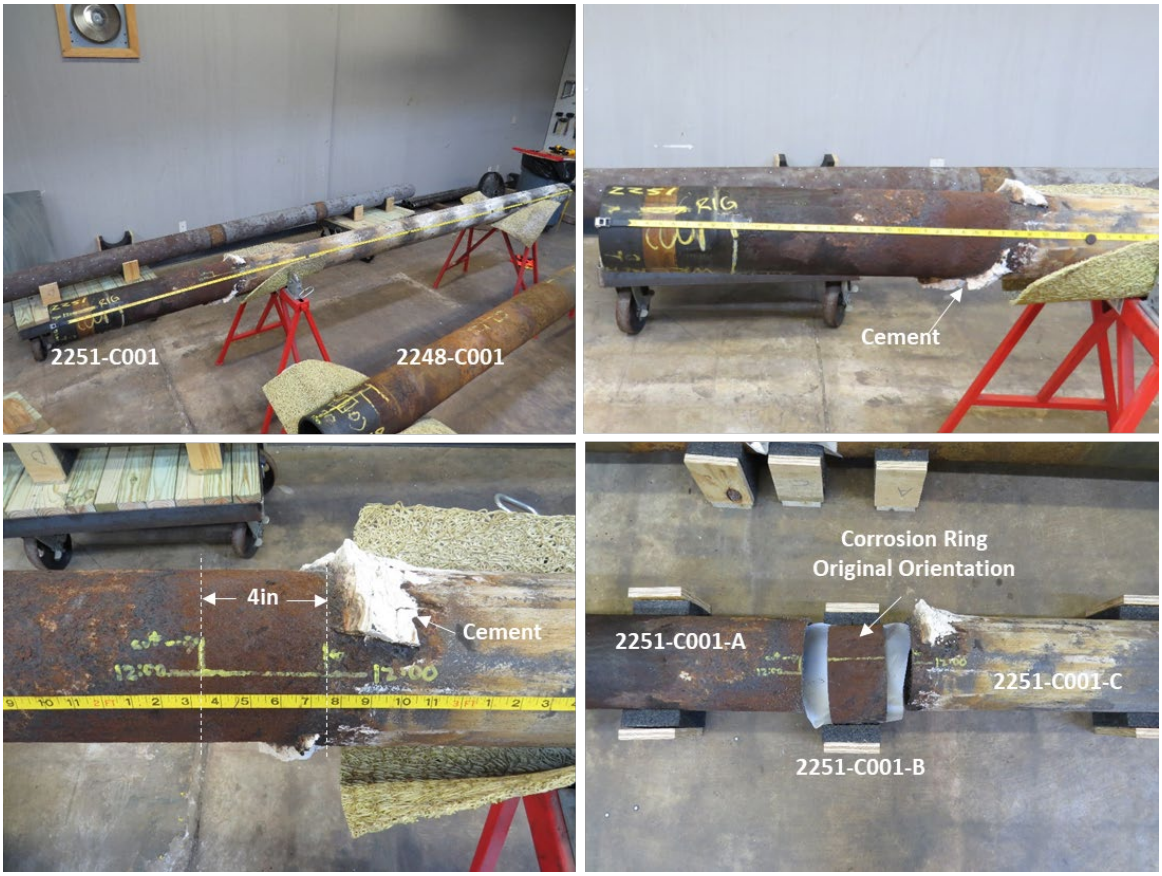

Figure 113: C001 Joint from Well #2251 Before and After Cutting

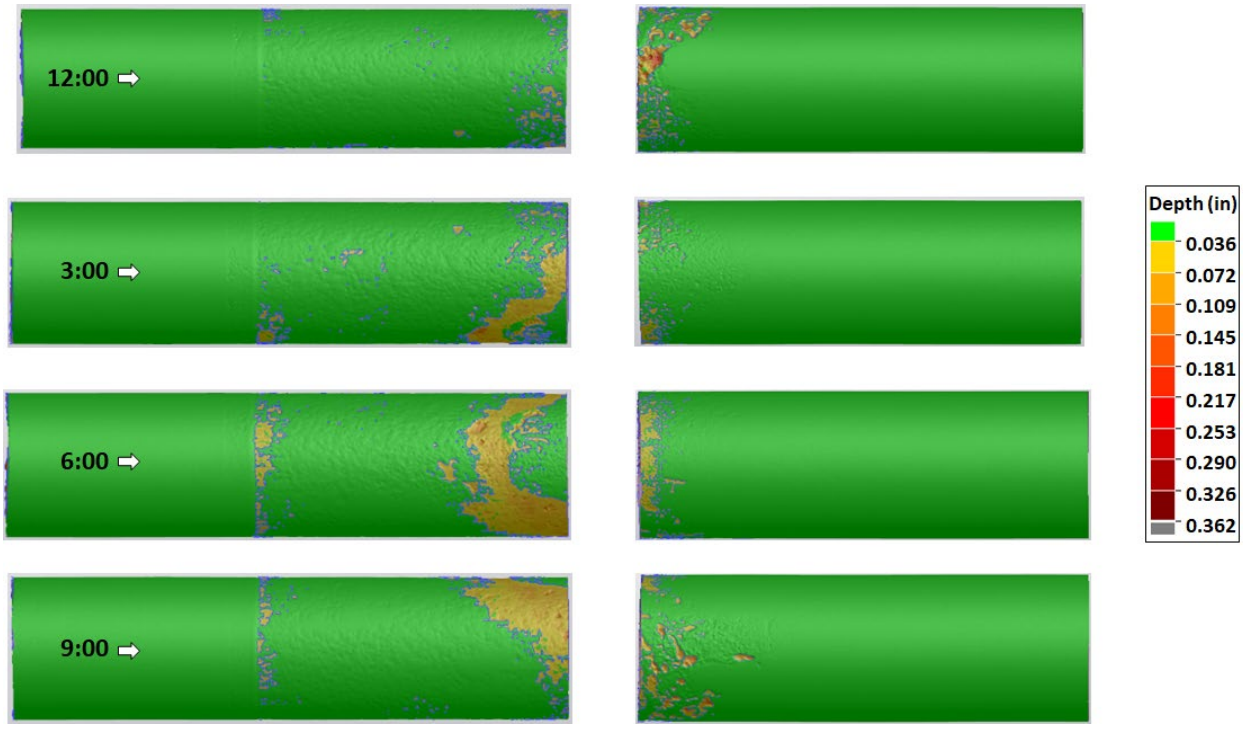

Figure 114: Laser Scan Rendering of Well #2251 Joint C001-A and C001-C

All scan data from well #2251 C001, as well as the NDE performed on the 4 in. section were collected, aligned, and summarized in Figure 115. From bottom to top, the Figure shows the 360° corrosion map, the corrosion depth for all indications, and the maximum corrosion depth per foot of casing, illustrating all the distribution of corrosion for this joint.

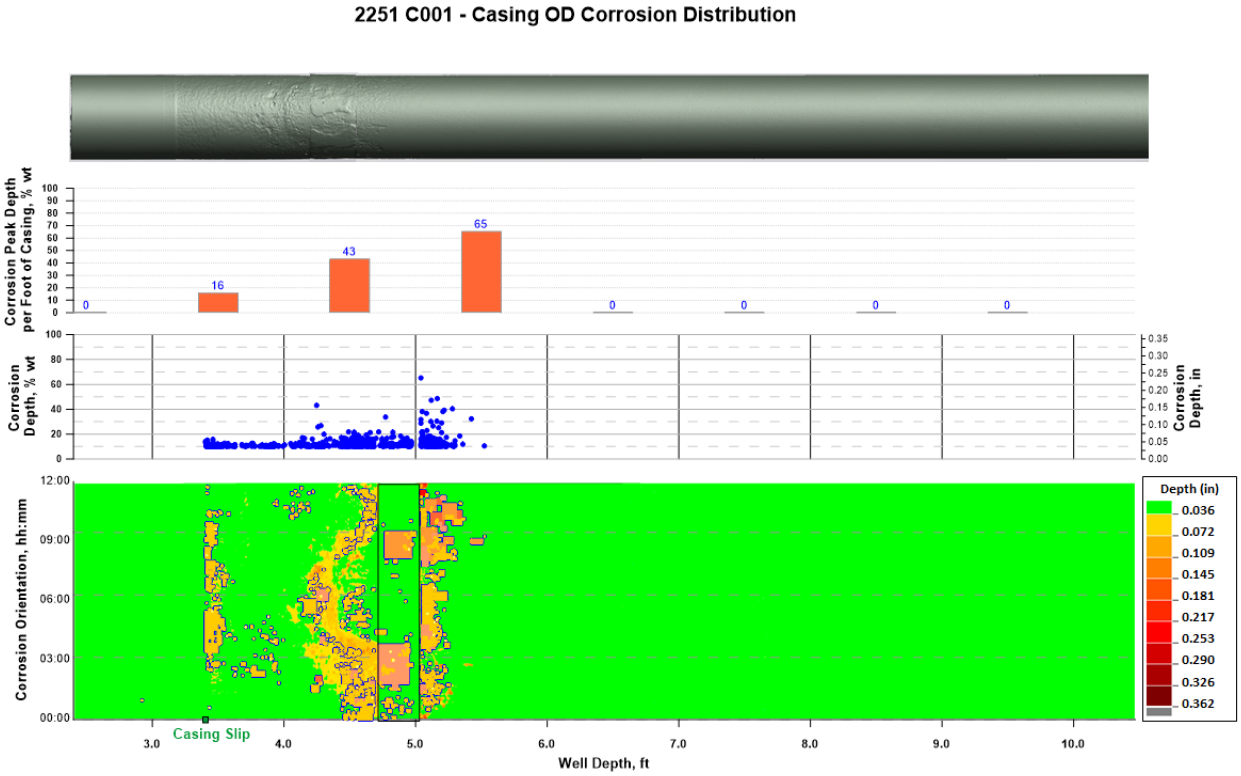

Figure 115: External Corrosion Distribution for Well #2251 C001

Figure 116 shows the corrosion features observed in C001-A. This section has high-density shallow pits. The diameter of the corrosion pits is less than 0.5 in. These features are similar to the features observed in well #2244.

Figure 117 shows the corrosion features observed in C001-C. The corrosion damage in this region has greater depth compared to the corrosion features observed from C001-A. The corrosion features in this section are most likely due to crevice corrosion, because the location where these corrosion features are observed coincides with the cemented location (see Figure 113).

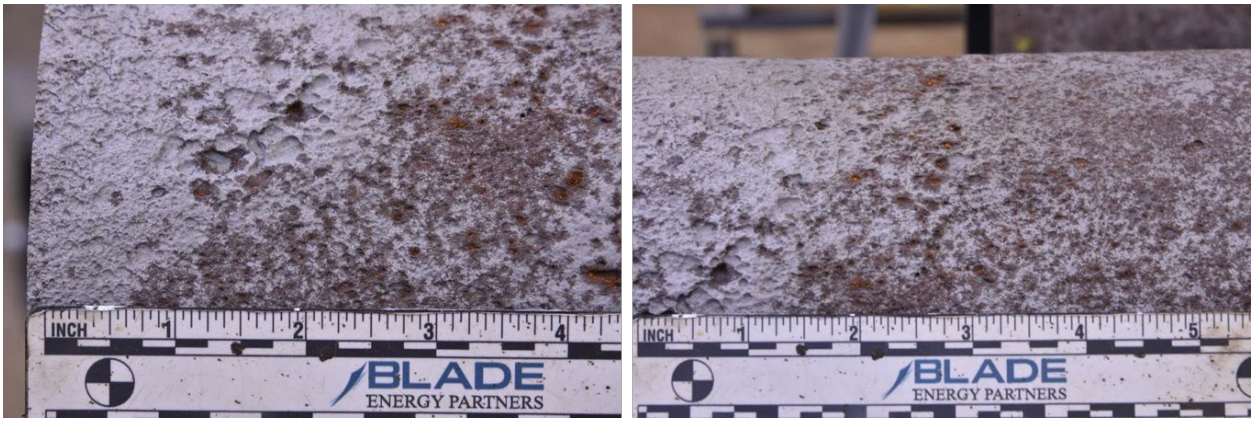

Figure 116: Corrosion Features Observed in #2251 C001-A

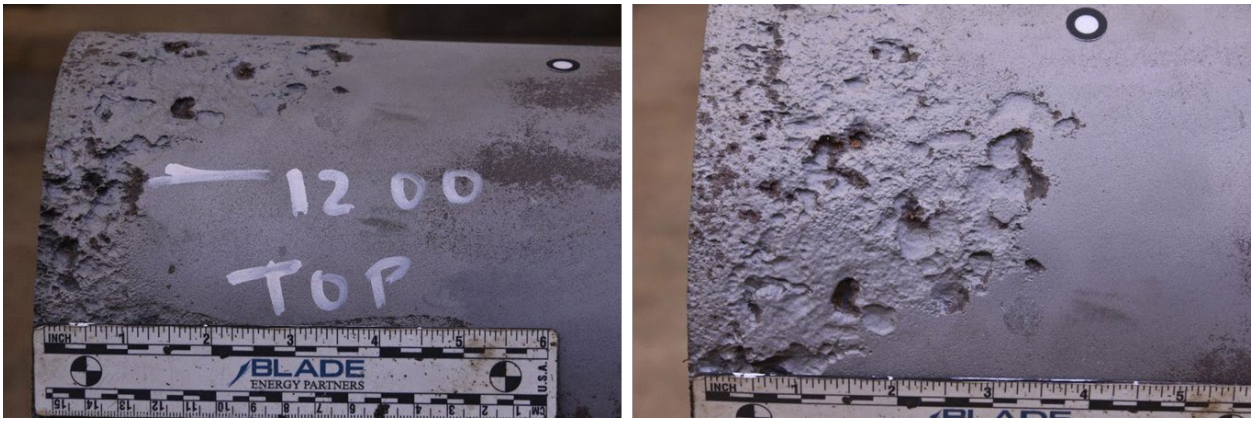

Figure 117: Corrosion Features Observed in #2251 C001-C

7.2.2 Scale Analysis

XRD Scale Analyses

When the top joints were extracted from wells #2244, #2248, and #2251, OD surface scale samples (corrosion compounds and other deposits) were collected, bagged, and stored for analysis. For well #2244, additional scale samples were collected from several other casing joints located farther downhole. An example of corrosion scale and surface deposit collection on #2248-C001 with sample identification is shown in Figure 118.

In Figure 118a, the surface of #2248-C001 was photographed immediately after extraction from the well bore. The bright orange color indicates the spontaneous formation of hematite (flash rust) as the joint dries in the sunlight. The darker-colored scale consists of older, more stable corrosion products, clays, and deposits. Figure 118b and Figure 118c show the same region of the pipe under fluorescent lighting a few hours later. The location as a function of depth from the top of the joint was recorded for each scale sample.

Samples were sealed in plastic bags and shipped immediately for analysis. The BLRM prefix indicates a biological sample. Additional samples were collected separately for XRD/EDS/Raman mineralogical/elemental/compound analyses. Nineteen scale samples were collected from well #2244 for XRD/EDS/Raman analyses, six from well #2248, and four from well #2251. Biological sampling is discussed in a later section of this report.

Figure 118: Example of OD Surface Scale and Deposit Collection and Bagging

Bulk mineralogy results of the scale samples are shown in bar chart format in Figure 119. Comparing the XRD results for the top or casing joint among the three wells shows similar corrosion compounds (goethite, lepidocrocite, magnetite, and siderite).

The graphs in Figure 119 indicate a greater ratio of lepidocrocite to goethite and a greater overall percentage of magnetite in well #2244 in comparison to wells #2248 and #2251. Several authors report lepidocrocite, γ-FeO(OH), forms initially in the corrosion process and is an unstable compound that transforms to the more stable goethite, α-FeO(OH), compound over time [17], [18]. Continuous wetting has been reported to be a requirement for the formation of magnetite, Fe_3O_4 [19]. A higher ratio of goethite to lepidocrocite at the top of wells #2248 and #2251 may suggest lower corrosion activity compared to #2244. Higher magnetite in #2244 may suggest the region where the compounds were collected held more local moisture in comparison to wells #2248 and #2251.

One mineral, siderite, that was observed in well #2244 was not observed in the other two wells. Siderite would require CO_2, and in well #2244 one of the connections was noted to have a very small leak, based on laboratory testing. Further, well #2244 was generally uncemented when compared to #2251 and #2248. The small leak in #2244 would have resulted in the siderite on the OD surface.

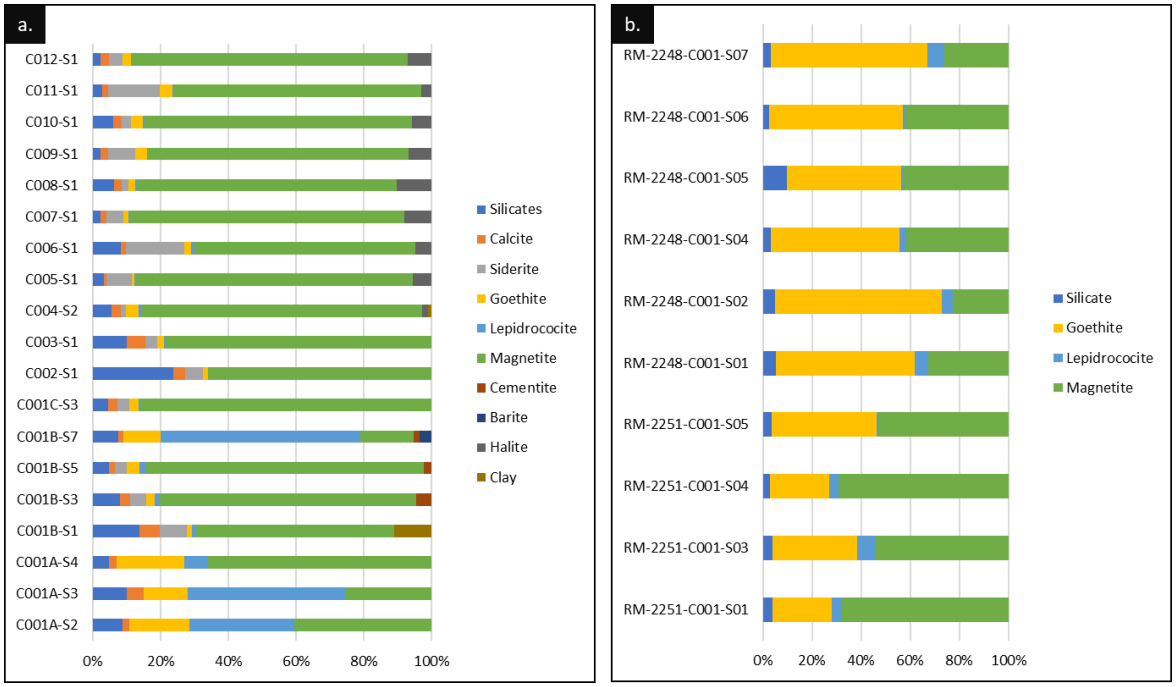

Figure 119: Bulk XRD Mineralogy of Surface Scale Collected from (a) #2244, (b) #2248 and #2251

EDS and Raman OD Corrosion Surfaces Comparison

A small OD surface sample from the top joint of each well was excised for EDS and Raman spectroscopic analysis to identify the corrosion products on the surface. These products would be indicative of the under-scale corrosion process taking place at the scale/metal interface at the time just prior to sample collection and may or may not reflect the cumulative history of local environmental conditions that created the bulk scale. EDS provides the semi-quantitative elemental composition of the surface, while Raman provides a complementary analysis by linking the spectra compound databases based on the elements present. EDS/Raman results were compared qualitatively to the bulk XRD results.

The EDS/Raman samples were taken approximately 4 ft from the top of the first joint for sample #2244-C001B-2B1, 2 ft 10 in. for sample #2248-C001B-1, and 2 ft 5 in. for sample #2251-C001B-1. These samples were retained in the as-received condition (not cleaned or altered) and are shown in Figure 120. The copper arrows indicate areas of interest for EDS and Raman analyses. The focal locations of analyses for EDS and Raman were within 100 μm.

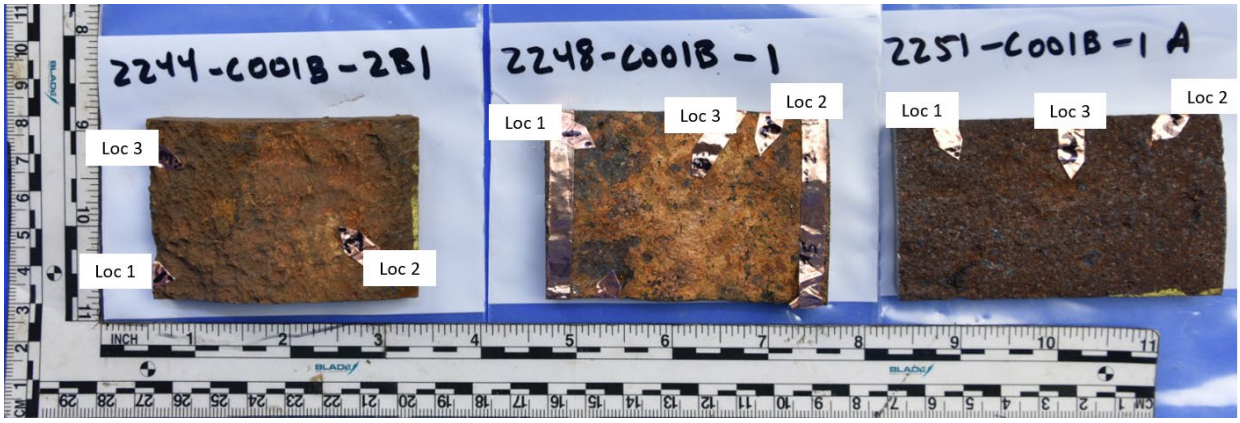

Figure 120: OD Casing Material Samples for EDS and Raman Spectroscopy

Scanning electron microscopy was used to image each EDS/Raman location area of interest at low magnification and at 5,000x to 10,000x to document the local corrosion compound morphology. Secondary electron imaging (SEI) and backscatter electron imaging (BEI) at various acceleration voltages captured the images because charging of the surface was an issue. EDS elemental analyses were taken consistently at 15 kV, avoiding highly charged areas. EDS data collection was obtained over broad areas to average the surface chemistry. Raman spectra were taken from the same areas analyzed by EDS to correlate chemistry, compound morphology, and Raman spectra. Not all locations produced viable data for all three techniques.

The averaged EDS results of two broad area locations on OD casing in each sample is shown in Table 20: Average EDS Surface Chemistry of OD Casing Material Samples. Chlorine is indicated on the surface of casing joints #2244-C001 and #2251-C001. Low levels of sulfur are indicated on samples #2244-C001 and #2248-C001.

SEM images taken at 5,000x and 10,000x of regions in three surface samples are shown in Figure 121 (a) through (f). Along the top row, (a) is likely magnetite, and (b) is likely a lepidocrocite/goethite. Along the middle row, image (c) could not be matched to images in the literature with reasonable certainty but was identified as a complex structure of hematite, mackinawite, and magnetite using multiple Raman laser wavelengths. The finding of mackinawite at this location correlates to the slightly elevated sulfur indicated by EDS. Image (d) is similar to (b) but finer in structure.

In the last row, the surface was difficult to image due to charging. The images shown are of one location at 5,000x and 10,000x. This structure was highly crystalline and consistent over the entire sample. Literature searching suggests this surface corrosion compound is likely akageneite, β-FeO(OH), or siderite, $FeCO_3$. Akageneite and siderite are corrosion products that form on steel in aqueous environments in the presence of CO_2 and Cl [20] [21], which correlates with the EDS results obtained on this sample showing elevated Cl on OD surface sample #2251-C001B-1A in comparison to samples #2244-C001B-2B1 and #2248-C001B-1A.

Table 20: Average EDS Surface Chemistry of OD Casing Material Samples

	Well #2244			Well #2248			Well #2251		
Element (K-band)	Loc 1 Atomic%	Loc 2 Atomic%	Avg.	Loc 1 Atomic%	Loc 3 Atomic%	Avg.	Loc 1 Atomic%	Loc 2 Atomic%	Avg.
CK	2.1	2.3	2.2	2.6	15.3	8.9	3.2	2.5	2.83

	Well #2244			Well #2248			Well #2251		
Element (K-band)	Loc 1 Atomic%	Loc 2 Atomic%	Avg.	Loc 1 Atomic%	Loc 3 Atomic%	Avg.	Loc 1 Atomic%	Loc 2 Atomic%	Avg.
OK	43.0	29.4	36.2	37.1	31.1	34.1	49.3	37.6	43.44
NaK	0.1	0.4	0.3	0.4	–	–	–	–	–
MgK	5.5	2.0	3.7	–	–	–	–	–	–
AlK	0.3	0.0	0.2	–	–	–	–	–	–
SiK	4.4	3.2	3.8	0.3	0.7	0.5	–	–	–
SK	0.4	0.8	0.6	3.1	2.2	2.7	–	0.3	0.31
KK	–	–	–	0.2	–	–	–	–	–
ClK	2.7	1.2	2.0	–	–	–	5.4	6.1	5.7
CaK	14.5	0.4	7.4	–	–	–	–	–	–
TiK	0.3	0.5	0.4	–	–	–	–	–	–
CrK	0.3	2.9	1.6	–	–	–	–	–	–
MnK	0.8	2.1	1.5	0.6	0.6	0.6	–	–	–
FeK	25.8	54.9	40.3	55.7	50.1	52.9	42.2	53.5	47.8

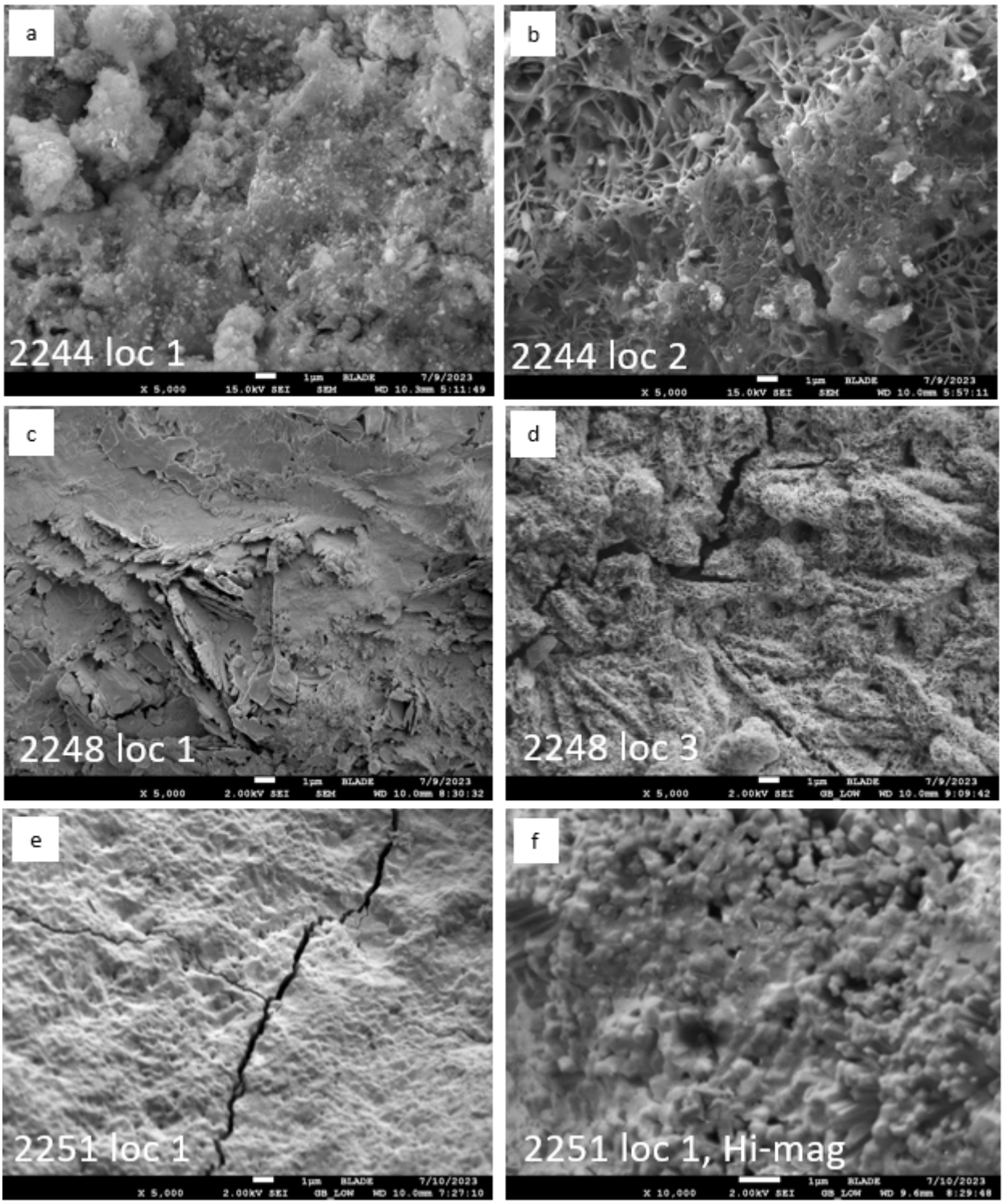

Figure 121: SEM Image of OD Casing Material Samples

The Raman Spectrographs of OD casing surface samples with annotated interpretation and corresponding EDS spectra are shown in Figure 122. Raman spectra of sample #2244-C001B-2B1 at locations 1 and 2 (referenced in Figure 120) were obtained using a 633 nm laser at 1 to 5% power. EDS results of the region gave indications of low levels of S and Cl along with several contaminant elements. There is a strong magnetite peak at Raman wavenumber 660cm^{-1}. There is an indication of lepidocrocite at 250 cm^{-1}.

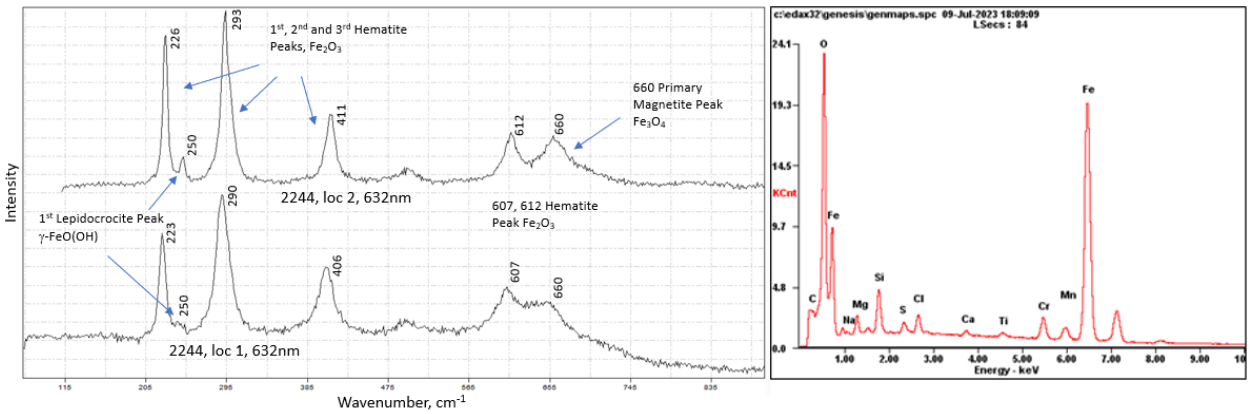

Figure 122: Casing Sample #2244-C001B-2B1, Loc 1 &2 Raman and Average EDS, High Contaminant

Figure 123 shows the Raman results for sample #2244-C001B-2B1 using a 532 nm and 633 nm laser at the same location as EDS. The 532 nm laser is less penetrating and gives better surface layer representation. The 532 nm analysis shows the characteristic mackinawite peak group [13] along with lepidocrocite/goethite peaks. The spectral data at the same point using the 633 nm laser at 1% power (deeper penetration) reveals hematite, lepidocrocite/goethite, and magnetite.

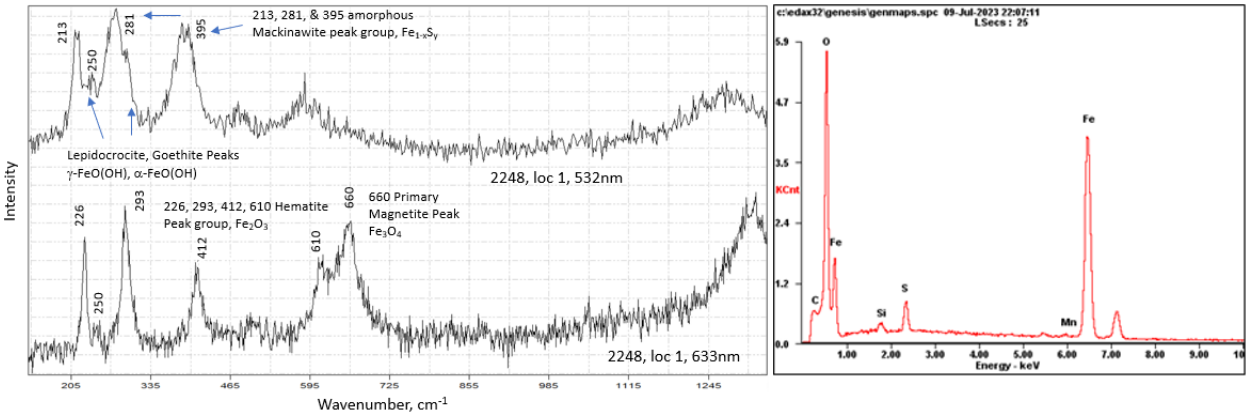

Figure 123: Casing Sample #2248-C001B-1, Loc 1, Two Lasers, Raman and Average EDS, High S

Figure 124 from #2251 has a characteristically different compound than shown in pervious Raman analyses. The EDS analysis shows elevated Cl. This spectrum was found to match akageneite most closely per Cambier [21]. Cambier reports the primary peaks for akageneite (Aka) to be 147, 310, 389, 495, and 531 cm^{-1}. Of equal probability, the iron carbonate/siderite/$FeCO_3$ may be exhibited at peaks 188, 290, and 732cm^{-1} [13], [22]. The peaks are broad and can accommodate multiple peaks. Additional techniques would be necessary to deconvolute analytical refinement. However, based on the Bulk XRD results, the interpretation of akageneite is more appropriate here.

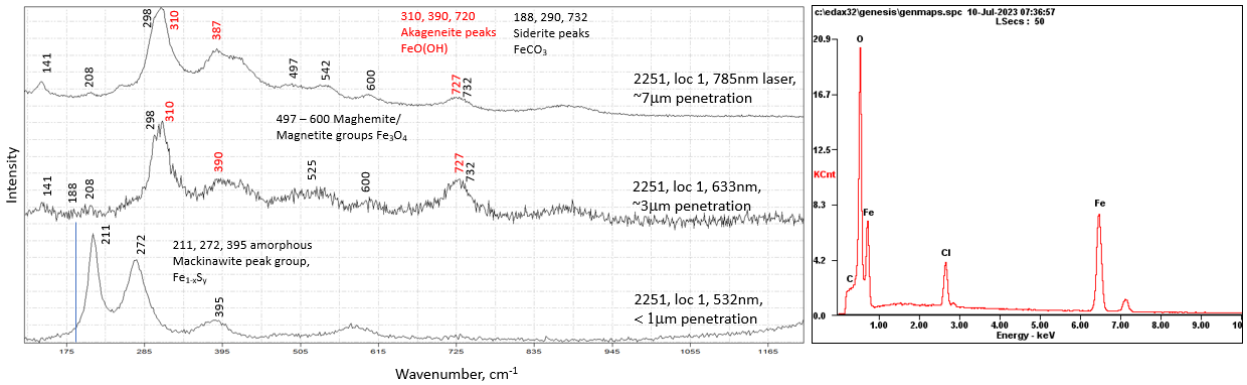

Figure 124: Casing Sample #2251-C001B-1A, Loc 1, Raman and Average EDS, High Contaminant, High Cl

7.2.3 Microbiological Analysis

Microbial contamination, especially by sulfidogenic (hydrogen sulfide) producing and acid-producing organisms, is known to contribute, or even cause, corrosion of subsurface infrastructure. The microbial populations of wells #2244, #2248, and #2251 were determined as part of a larger root cause analysis investigation into the leak of well #2244. Samples analyzed included casing scale solids, annulus fluids, and liquids from the separator station, as well as control samples such as surrounding area soils. Samples were collected in February and March 2023. Because the failure was in the C001 casing joint, it is possible that the microbial population of this joint experienced seasonal fluctuations, impacted by the time of year the samples were collected (cold winter as compared to warmer summer).

Microbial populations were determined using a combination of traditional culture-based approach (MPN "bug bottles") and two molecular methods based on DNA analysis. MPN is the traditional method that follows NACE standard guidelines, including TM0194-21224 [23], TM0212-21260 [24], and TM0106-21248 [25]. The NACE standards also allow for newer molecular techniques, with appropriate caveats. Each method results in a different type of data. MPN provides a quantitative analysis (cells per g or ml sample) of different phenotypes such as acid-producing bacteria (APB), sulfate-reducing bacteria (SRB), iron-reducing bacteria (IRB), and general heterotrophic bacteria/generalists (GHB).

Populations with elevated APB and SRB are potentially corrosive. The molecular methods used were qPCR and 16S amplicon metagenomics. qPCR provides an overall quantitative analysis (cells per g) of a sample, but no information on the types of organisms. Usually, quantification by MPN and qPCR does not yield the same values. This is expected because of limitations inherent to both methods. MPN requires live bacteria that can be cultured. qPCR requires that the sample does not contain inhibitors of the sensitive DNA isolation process. Usually, but not always, MPN values are several log orders lower than qPCR values. When this is not the case, it suggests the sample contains inhibitors of DNA isolation or that the cells are very resistant to lysis. The 16S amplicon metagenomics yields a "laundry list" or the organisms in the sample, and their relative abundance (% of the population). The list of organisms in the sample is screened for known corrosion-causing types of bacteria (for example, known SRB and APB).

Ultimately, interpretation of results is based on the types and concentrations of organisms in the sample. Corrosion-associated populations are expected to be dominated by corrosion-associated bacteria (e.g., they make up a significant percentage of the population), and for MIC to occur, there needs to be more than a negligible level of bacteria. However, as per NACE TM0194-94 1.1.8, "The simple presence of bacteria in a system does not necessarily indicate that they are causing a problem. In addition, bacterial populations causing problems in one situation, or system, may be harmless in another. Therefore, 'action'

concentrations for bacterial contamination cannot be given. Rather, bacterial population determination is one more diagnostic tool useful in assessing oilfield problems." [23]

Well #2244 Casing Joint C001: Failure Region Key Conclusions

Failure region key conclusions: Dry scale from well #2244 casing joint C001, above and below the failure point, was extensively analyzed. Triplicate MPN indicated that sulfidogens and acid-producing bacteria were present in the scale, at concentrations up to 9E+05 per g scale for APB and 6E+04 per g for SRB. There were multiple scale samples with significant microbial population, as determined by MPN but did not yield any DNA for analysis. From the results of metagenomic population analysis of the scales that yielded DNA sequence, the key organisms identified in the scale samples above the failure zone were general heterotrophic bacteria, Ralstonia, as well as Bacillus and unclassified members of Class Clostridia. Sulfidogens and APB were also identified using metagenomic population analysis, but they are present at a much lower abundance in the samples—less than 1%.

Ralstonia and Bacillus are not typically corrosion-associated organisms. It is formally possible that the organisms identified only to Class Clostridia are corrosion-associated organisms, but Class Clostridia includes many more species that are not corrosion associated. Sulfidogens, identified in the enrichment cultures, were present at less than 1% of the population. Because corrosion-associated bacteria were present but not the predominant organisms in the sample, these results did not clearly point to a role of MIC in the failure event, nor did they conclusively exclude MIC.

Well #2244 Casing Joints C002 to C034: Below Failure Region Key Conclusions

Failure region key conclusions: Dry scale from well #2244 casing joints C002 to C034, all below the failure point, were analyzed. Triplicate MPN indicated that sulfidogens and acid-producing bacteria were present in the scale, at concentrations of up to 5E+04 for APB and 9E+03 cells per g for sulfidogens. In the deepest portions of the well, the casing surface was dominated by the corrosion-associated organism, Halanaerobium, at 24% of the population. Halanaerobium was also abundant in the annulus fluids. Halanaerobium is an organism of particular concern because it has been found in oil wells experiencing rapid MIC corrosion. However, in the case of well #2244, Halanaerobium was present as only a minor component of the region experiencing the most corrosion.

Well #2248 Casing Joint C001 and #2251 Casing Joint C001 and Annulus Fluids Microbial Population

The 7 in. casing joint C001 from well #2248 was found to have APB levels as high as 5.6E+05 and SRB levels as high as 2.4E+04 cells per g solids. SRB and APB concentrations in the annulus valve solids were even higher, up to 3.5E+09 and 1.1E+05, respectively. However, general heterotrophic bacteria GHB were log orders higher in concentration. This profile was verified in the population analysis, which indicated the casing surface was dominated by GHB. The predominant organisms in well #2248 casing surface samples were not corrosion-associated organisms.

Well #2251 casing joint C001 was found to contain essentially negligible microbial levels, less than 250 cells per g solids for GHB and APB, and no sulfidogens were detected.

Compressor Station Fluids

Fluids from the pond and separator at the compressor station were also analyzed. Growth-based MPN analysis of the separator fluids indicated microbial level of less than 200 cells per ml, and no SRB. However, qPCR data indicated microbial load closer to 6.4E+04, indicating the bacteria in the sample did not grow in the culture media. The separator fluid population profile indicated the sample was dominated by a

single species, Thermoanaerobacterium saccharolyticum, which is both a sulfidogen and an acid-producing bacteria associated with spoilage but not corrosion. Samples from the pond contained normal levels of GHB (2.0E+05 and 4.5E+07), but APB and sulfidogen concentrations were 4 or more log orders lower, with the culture data being essentially mirrored by the molecular data, which found primarily GHB in the sample. This suggests that compressor station fluids are not a source of corrosion-associated bacteria.

7.2.4 OD Corrosion of the 7 in. Casing

This section presents different hypotheses on the corrosion mechanism and their possible contribution to the failure in well #2244. The following section provides some reasons whether each of the corrosion mechanisms may have contributed to the thinning of the top joint in well #2244.

Microbiologically-induced Corrosion

Microbiologically-induced corrosion (MIC) is a mechanism where corrosion is due to the presence and activities of microorganisms. Little, et al., indicated that microorganisms can accelerate rates of partial reactions in corrosion processes or shift the mechanism for corrosion [26]. The corrosion is directly related to the oxidation (anode) and reduction (cathode) reactions, and microbial processes require one- and two-electron transfers (either oxidation or reduction reactions). Microorganisms can involve a conversion of a protective metal oxide to a less-protective layer or removal of the oxide layer by metal oxide reduction or acid production [27].

Microorganisms do not produce unique types of corrosion; instead, they produce localized attack including pitting, dealloying, enhanced erosion corrosion, enhanced galvanic corrosion, stress corrosion cracking, and hydrogen embrittlement [26]. Microorganisms do not produce a unique corrosion morphology that distinguishes MIC from abiotically-produced corrosion [27]. Literature agrees that there is no specific fingerprint to indicate if the corrosion is MIC [26] [27] [28] [29] [30] [6]. A systematic analysis of available evidence is necessary.

Diagnosing MIC after it has occurred requires a combination of microbiological, metallurgical, and chemical analysis. The investigation of MIC involves (1) identifying causative microorganisms in the bulk medium or associated with corrosion products, (2) identifying a pit morphology consistent with MIC mechanisms, and (3) identifying a corrosion product chemistry that is consistent with the causative organisms [26]. Therefore, microbiological, chemical, and metallurgical evidence should be considered altogether to properly identify if MIC is a contributor to the corrosion of 7 in. casing.

Microbiological analysis shows that acid-producing bacteria (APB), iron-reducing bacteria (IRB), and sulfur-reducing bacteria (SRB) are present in scales collected from the OD surface of the 7 in. casing. Some of the identified bacteria in the 7 in. casing are known to cause MIC, but additional data would be needed to link these bacteria to the corrosion event in #2244. For example, halanaerobium, which is known to cause corrosion in shale wells [31], was detected at slightly elevated levels from the scale collected at the bottom of the 7 in. casing. In addition, halanaerobium was detected at a very low level from the scale collected from the top joint where fracture occurred. The reports related to microbiological analysis are included in the appendix A.12.

Chemical analysis of the scale shows that the compounds present on the OD surface of the 7 in. casing are mainly iron oxy-hydroxide products, iron oxides, and some iron carbonates. Literature indicates that mackinawite (FeS_{1-x}) and pyrite (FeS) are common products found in MIC due to the presence of SRB [32]. In addition, hematite, magnetite, goethite, and lepidocrocite are identified as common corrosion products in systems with MIC due to IRB, SRB, and methanogens [33] [34] [35].

Metallurgical evaluation of the corrosion morphology shows that the corrosion on the top joint was due to general wall thinning. Results of the laser scan analysis clearly indicate no indications of localized attack that have a morphology that could be attributed to MIC. Figure 125 shows the stereoscope images of corrosion features observed in the top joint (C001B) of well #2244.

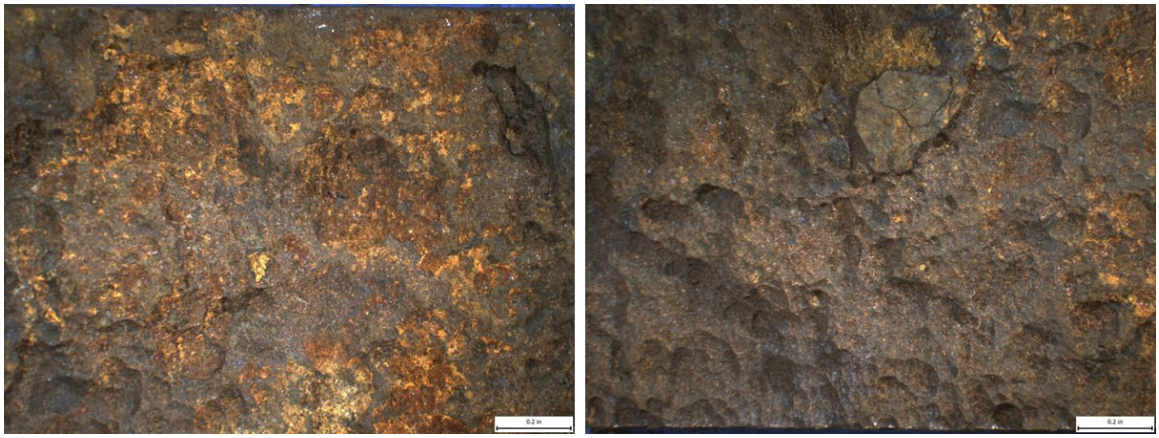

Figure 125: Corrosion Features Observed in the Top Joint of Well #2244

Based on literature, the following metallurgical features were observed on carbon steel with large numbers of APB and organic acids [36]:

- Large craters from 5–8 cm in diameter surrounded by uncorroded metal [36]
- Cup-type hemispherical pits on the pipe surface or in craters [36]
- Striations or contour lines in the pits or craters running parallel to the longitudinal axis [36]
- Tunnels at the ends of the craters running parallel to the longitudinal axis of the pipe [36].

Figure 126 shows common corrosion morphologies observed in MIC. Figure 126 a, b, and c were taken from the case history of MIC (SRB and APB) in Lost Hills Oilfield published by Strickland et. al. [37]. Figure 126 d was taken from a failure analysis involving methanogens [38]. These morphological features were not observed on the top 7 in. casing joint that contained the failure in well #2244. The corrosion features observed on C001A and C001B show high-density shallow pits. This type of corrosion feature is common to general corrosion. Figure 127 shows images of general corrosion observed in the field where large areas of the pipe are attacked and there is no localized metal attack or penetration.

Evaluation of the three sets of evidence (microbiological, metallurgical and chemical) indicates that MIC is not a primary nor a contributing mechanism for the OD corrosion of the #2244 7 in. casing.

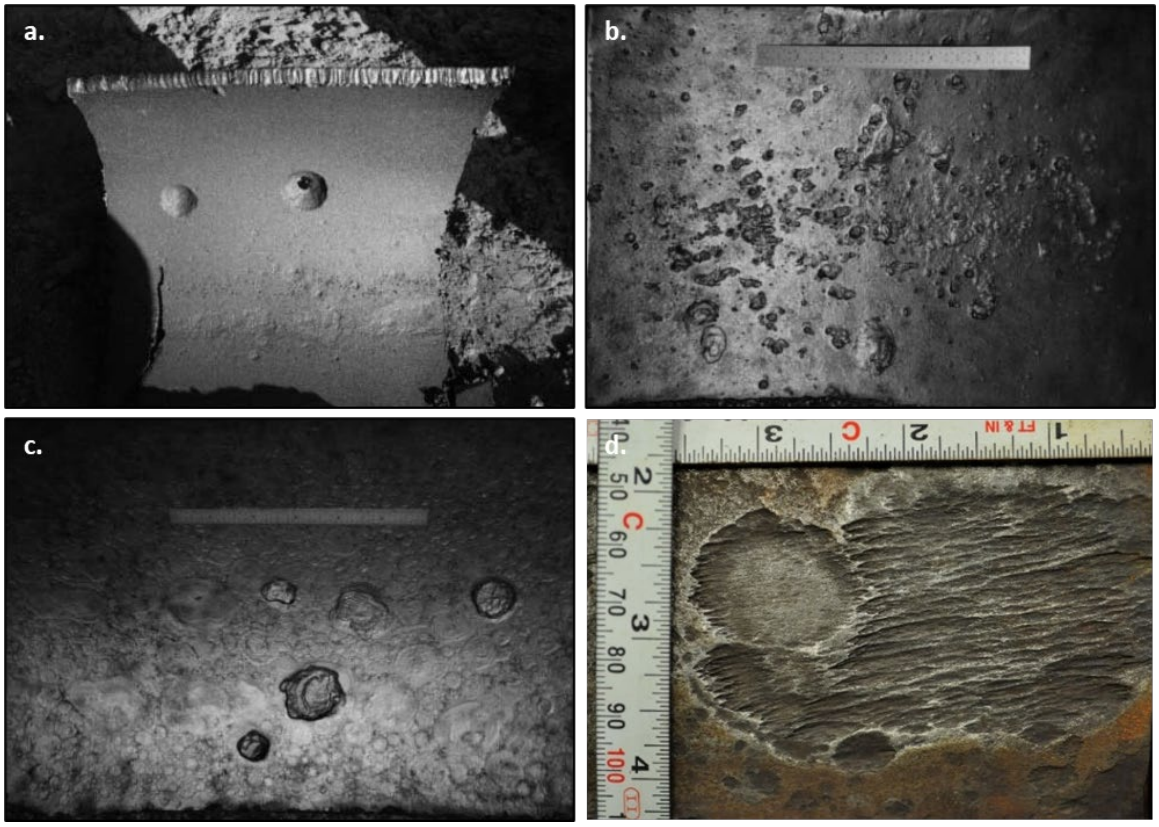

Figure 126: Common Morphologies Associated with MIC

Figure 127: General Corrosion Observed in the Oil and Gas Industry

Galvanic Corrosion

Galvanic corrosion can occur when dissimilar metals with electrical contact are exposed to the same electrolyte. When dissimilar metals are electrically coupled (i.e., galvanic coupling), corrosion of the less corrosion-resistant metal increases, and the surface becomes anodic, while the corrosion of the more corrosion-resistant metal decreases, and the surface becomes cathodic. The driving force for corrosion or galvanic current flow is the potential developed between the dissimilar metals. The difference in potential between dissimilar metals causes electron flow between them when they are electrically coupled in a conductive solution [39].

Whether corrosion will occur or not depends on the relative activity of the metals involved. The actual corrosion of an anodic metal in a galvanic pair is based on the electrical current flow [40].

In well #2244, the 7 in. casing is electrically connected to the 9 5/8 in. casing through the conductor. Both the 7 in. casing and the 9 5/8 in. casing are connected to the conductor completing the electrical path. The OD surface of the 7 in. casing shares the same electrolyte as the ID of the 9 5/8 in. casing, which is the annulus fluid. The 7 in. casing is made up of N80 carbon steel, while the 9 5/8 in. casing is made up of J55 carbon steel.

To assess if galvanic corrosion contributes to the corrosion of the top joint, a zero-resistance ammeter test was conducted using N80 carbon steel and J55 carbon steel. One of the factors that affects the extent of galvanic coupling is the anode-to-cathode area ratio. Larger areas of the cathodic metal in comparison to the anodic metal cause increased corrosion of the anodic metal [39]. The OD surface area of the 7 in. casing was determined, as well as the ID surface area of the 9 5/8 casing. The surface area ratio of the two casings was calculated. The exposed areas of the sample used in the ZRA test were based on the calculated surface area ratio—the N80 material being 1 cm^2, and the J55 material being 1.29 cm^2. The ZRA test was conducted using a Gamry 1010E potentiostat and an Ag/AgCl reference electrode. Synthetic groundwater was used as the electrolyte for the experiment.

Based on literature, surface water in the Pittsburgh area (Allegheny River basin) consists of approximately 5–268 mg/L Cl^- with a pH of approximately 2.5 to 8.3 [41]. From the values reported in the literature, the Allegheny River at Natrona surface water chemical analysis was used as a reference because the pH is slightly acidic (approximately 4.5). A solution with 38 mg/L NaCl was used in all the electrochemical experiments. The pH of the solution was adjusted to 4.5 using HCl. For the experiments, the exposed area of N80 was 1 cm^2, and the exposed area of J55 was 1.29 cm^2. In addition, the distance between the two electrodes was kept to 0.96 in.

Literature indicates that the distance between the anode and cathode in a galvanic couple affects the extent of galvanic corrosion. Metals in a galvanic couple that are in close physical proximity usually experience greater galvanic effects than those that are further apart [39]. Results of the experiment show a very small electrical current (94 pA) passing between the two metals when the distance is kept at 0.96 in. and the ratio of N80 to J55 is 1.29. The measured galvanic current translates into 73 pA/cm^2, which is equivalent to ~3x10E–5 mpy. The small galvanic current measured between the two metals was due to the experimental conditions and techniques used. Actual current passing through the 7 in. casing and 9 5/8 in. casing will be different because the actual fluid in the annulus is different. However, the magnitude of the galvanic current would still be negligible. Consequently, the corrosion rate due to galvanic coupling would also be negligible.

In addition, if galvanic corrosion is a contributor to the corrosion of the top joint, it is expected that J55 would tend to corrode more than the N80 material. Figure 128 shows the polarization curves of N80 and J55. Based on Tafel experiments performed on J55 and N80 material, J55 has lower potential in synthetic groundwater electrolyte compared to N80 material. This indicates that J55 is more anodic than N80. For well #2244, it is uncertain if the ID of the 9 5/8 casing has more severe corrosion damage than the N80 material. Corrosion due to galvanic coupling of N80 and J55 is less likely to be a contributing factor for the OD corrosion of the N80 7 in. casing in well #2244.

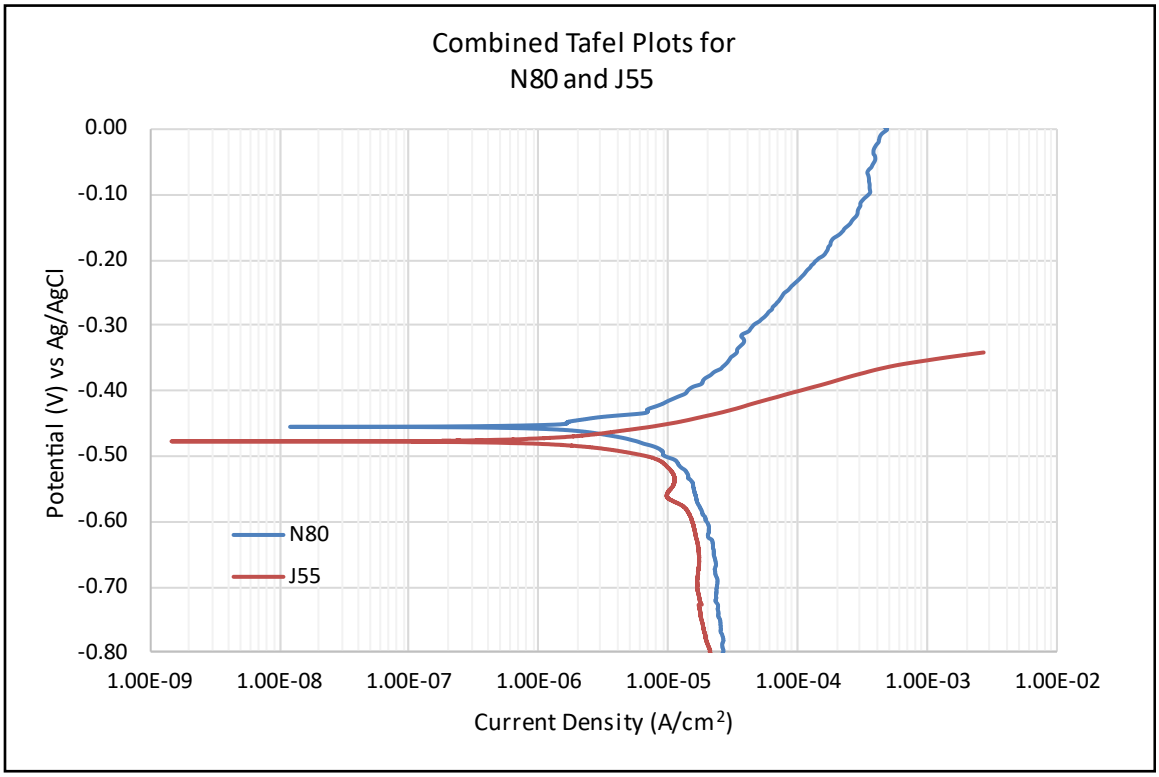

Figure 128: Polarization Curves for N80 and J55 in Synthetic Groundwater

Figure 129 shows the corroded region of the top joint from well #2244 below the casing slips. Another galvanic coupling effect that was considered in the analysis is the galvanic coupling of the N80 7 in. casing with the casing slips. The casing slips composition was analyzed in the field using Thermo Scientific XRF. The results are listed in Table 21. Thermodynamic modeling was not performed because the alloy was not available in the OLI databank. Actual measurement of galvanic current between N80 and the slips was not performed because the metal sample from the slips was also not available. The composition difference between the N80 7 in. casing and the casing slip is minimal. The casing slips have higher Cr, Co, Cu, and Ni content as compared to the N80 material as shown in Table 21. There would be insignificant galvanic current between the casing slips and N80, as evidenced by the experiments between N80 and J55.

The casing slip may not always be submerged to the annulus fluid. This condition would prevent any galvanic current to pass between the N80 7 in. casing and the casing slips. The corrosion profile just below the casing slips indicates that the highest wall loss is at the location of the axial rupture, which is approximately 6 in. away from the bottom of the casing slips. This also supports the hypothesis that galvanic coupling of the N80 7 in. casing, and the casing slips were not a contributing factor to the corrosion of the 7 in. casing.

Table 21: Casing Slips Composition

	Fe	Mn	Ni	Cr	Mo	Cu	Light Elements
Slips	97.01 ±0.29	0.784 ±0.90	0.431 ±0.098	0.524 ±0.049	0.200 ±0.040	0.304 ±0.066	0.675 ±0.011

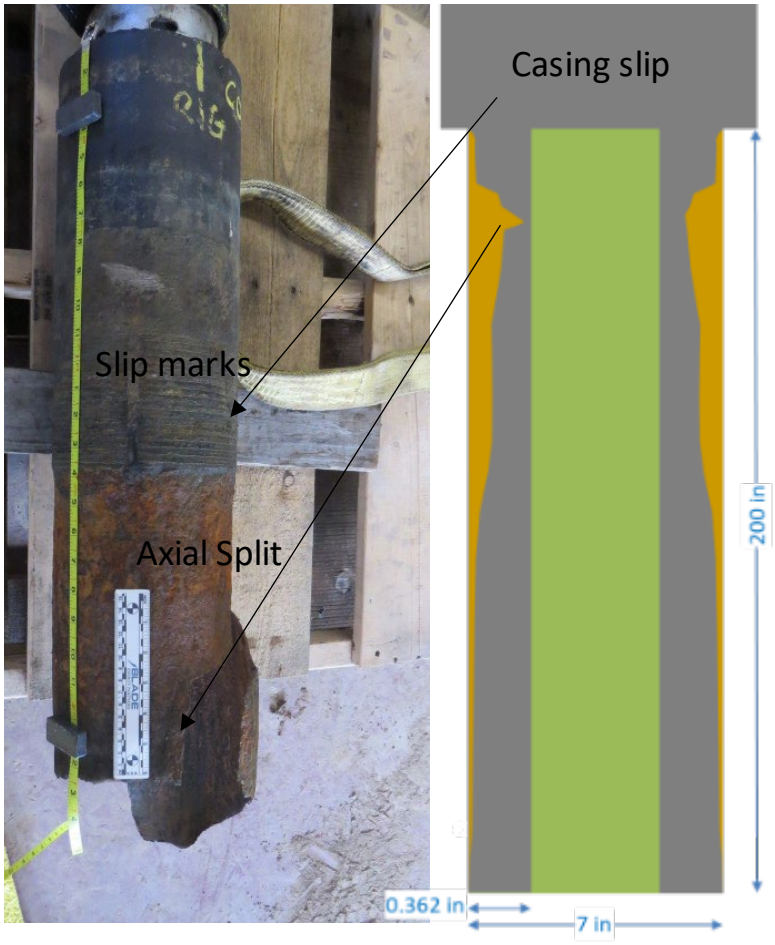

Figure 129: Corrosion at the Top Joint Adjacent to the Casing Slip

Oxygen Corrosion

The annulus between the 7 in. casing and the 9 5/8 in. casing had an open 2 in. annular valve. This allowed oxygen access to the annulus fluid. Literature indicates that oxygen affects the corrosion rate of carbon steel. In nearly neutral solutions (pH=7) with dissolved oxygen, the potential is lifted into the passive region where a protective surface film is formed. However, below a pH of 7 the film is not stable, and dissolved oxygen increases the corrosion rate [42].

The assessment of the effects of oxygen on the corrosion of the N80 7 in. casing was performed using thermodynamic modeling. The corrosion rate of carbon steel was estimated using a thermodynamic software called OLI v. 11.5. Average groundwater composition reported in the literature was used as the electrolyte for the corrosion model [41]. Table 22 shows the groundwater composition used in the model. Literature also reports the pH of the groundwater to be between 2.5 to 8.3. The estimated pH of the groundwater with concentration listed in Table 22 is 4.6.

Table 22: Groundwater Concentration [41]

Component	Concentration, mg/L
Na^{+1}	10.58
K^{+1}	10.58

Component	Concentration, mg/L
Ca^{+2}	36.00
Mg^{+2}	9.70
Fe^{+2}	0.035
Al^{+3}	4.30
Mn^{+2}	1.20
Cl^{-}	23.0
SO_4^{-2}	148.50
HCO_3^{-1}	2.50
SiO_2	5.65

The maximum solubility of dissolved oxygen in water is approximately 8 ppm at ambient temperature [42]. The corrosion rate of carbon steel in groundwater was estimated at various oxygen concentrations and at various temperature levels. The level of oxygen inside the annulus can vary. The highest amount of dissolved oxygen is expected at the top fluid level, and the amount of dissolved oxygen decreases going down the well. Figure 130 shows the estimated corrosion rates of carbon steel in groundwater for various dissolved oxygen concentrations.

The temperatures considered in the model ranged from 50°F to 125° and extend to 150°F. The temperature range was selected based on the recorded temperature in Rager Mountain. The neutron log of well #2244 on August 10, 2016, indicated that the casing temperature ranged from 93 to 97°F at the top 100 ft of the casing [43]. The average gas temperature recorded in the Rager Mountain compressor station from June 2020 to June 2023 was 79.2°F, with a standard deviation of 19.7°F. Table 14 shows that the maximum temperature in #2244 annulus is between 104 to 128°F.

The annulus temperature in well #2244 can vary during injection and withdrawal season. It is also affected by the ambient temperature in Rager Mountain. During injection the temperature of the gas in #2244 was between 80 to 100°F, and during withdrawal the temperature of the gas was between 60 to 80°F. From the results of the model, an increase in temperature can increase the corrosion rate of carbon steel in groundwater. The corrosion rates of carbon steel without dissolved oxygen are 1.2 mpy, 2.3 mpy, 3.9 mpy, and 6.6 mpy at 60°F, 80°F, 100°F, and 125°F, respectively.

The amount of oxygen would be highest at the water surface level, and oxygen is depleted at the bottom of the annulus. The amount of dissolved oxygen in the water is also dependent on temperature. Another model was made to determine the effects of dissolved oxygen and temperature on the corrosion rate of carbon steel in a stagnant condition. A survey was made by varying the amounts of oxygen input from 0 to 8 ppm. The results of the corrosion modeling show that at the lower end of the temperature spectrum, 60°F, the corrosion of carbon steel ranges from 1.3 mpy to 4.8 mpy when the oxygen input is between 0 to 8 ppm.

On the other hand, at an average temperature of 80°F, the corrosion of carbon steel in groundwater with 0 to 8 ppm oxygen input ranges from 2.3 to 7.3 mpy. At the higher end of the temperature range, 100°F, the corrosion rate of carbon steel is between 3.9 to 10.1 mpy for the oxygen input of 0 to 8 ppm. At 125°F, the corrosion rate of carbon steel is between 6.6 to 15.1 mpy for the oxygen input of 0 to 8 ppm. Results of the thermodynamic modeling show that dissolved oxygen increases the corrosion rate of carbon steel in groundwater. The results of the corrosion modeling of carbon steel in groundwater with dissolved oxygen agrees with literature, indicating a corrosion rate of approximately 10 mpy at approximately 30°C (95°F) [44].

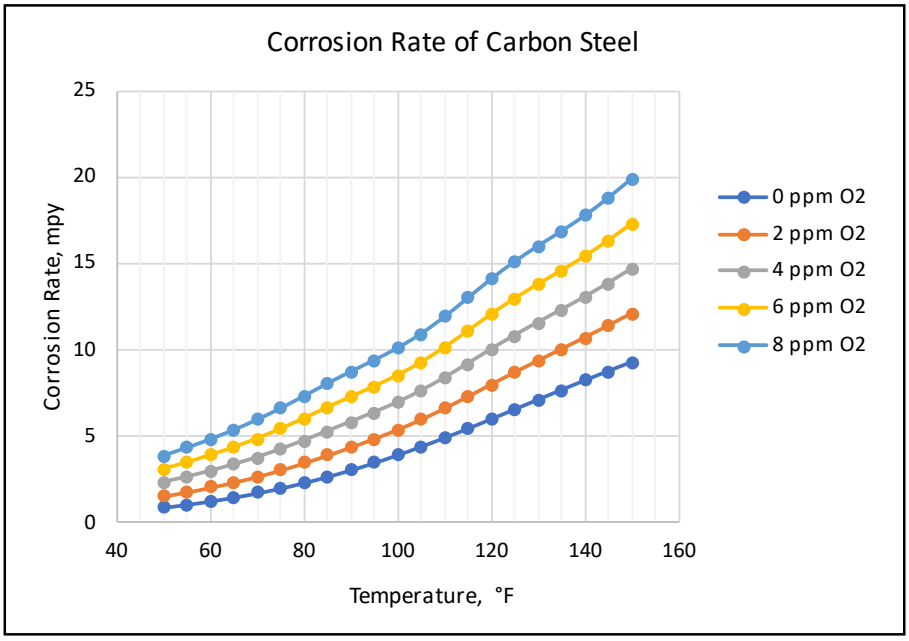

Figure 130: Corrosion Rate of Carbon Steel in Various Oxygen Levels

Figure 131 shows the pH of groundwater when the oxygen varies from 0 to 8 ppm. The pH of groundwater without dissolved oxygen ranges from 4.0 to 3.6 when the temperature is from 60°F to 125°F.

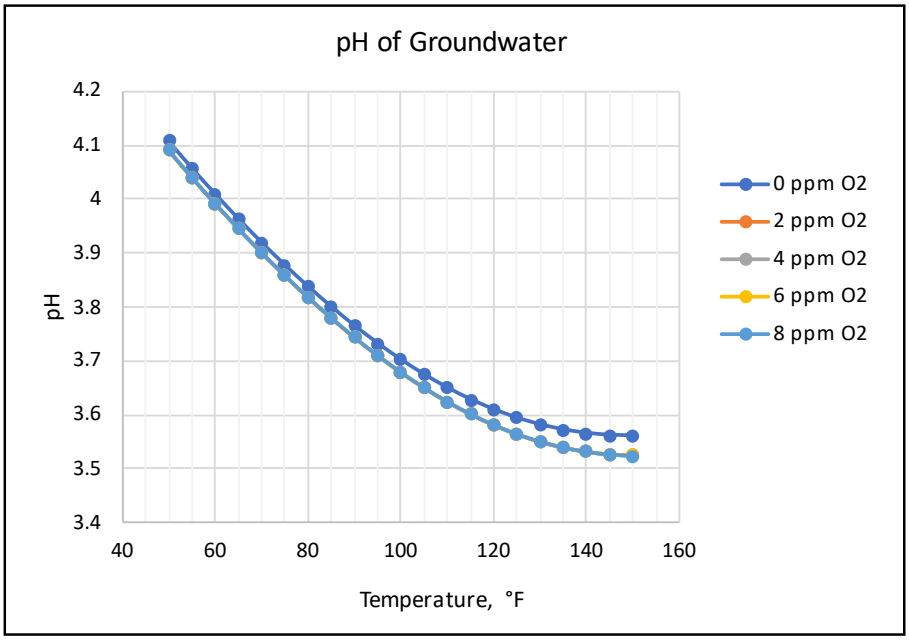

Figure 131: pH of Groundwater with Varying Amounts of Dissolved Oxygen

In addition to the effects of oxygen in corrosion of carbon steel in groundwater, the changes in the level of fluid similar to a wet–dry cycle inside the annulus can increase the corrosion rate. Seasons can affect the levels of the fluid inside the annulus. During a dry summer, the annulus fluid level can be low. The fluid level can rise when rain or snow enters the 2 in. annulus valve. It is reported in the literature that changes in the fluid level similar to a wet–dry cycle can cause an increase in the corrosion rate [45]. However, the water level on the average is most likely coincident to the location of the axial rupture because wall loss is highest at that region.

CO_2 Corrosion

The annulus fluid is not corrosive by itself. The results of corrosion modeling indicate a corrosion rate of 3.5 mpy without dissolved oxygen. Connection testing showed that at least one connection leaked gas into the annulus. Based on the results of connection testing, connection C007 has a leak rate of 70 cm^3/min. The corrosion rate of carbon steel in groundwater with CO_2 was also investigated using thermodynamic modeling. The composition of the gas used in the model is based on the analyses of gas obtained from #2248 and #2251. The average composition is listed in Table 23. It was assumed that the gas flow rate was 70 cm^3/min. It was also assumed that this gas mixes with 50 bbl of groundwater.

Table 23: Average Gas Composition in Rager Mountain [46]

Component	Concentration, mol%
CO_2	0.20
N_2	0.43
H_2	0.3162
He	0.0353
O_2	0.0360
C1	96.2033
C2	2.5325
C3	0.1878
iC4	0.0203
nC4	0.0279
iC5	0.0096
nC5	0.0067
C6	0.0223

Table 24 lists the summary of corrosion model results for 60, 80, 100, and 125°F. The corrosion rate of carbon steel in groundwater containing 1.8 mg/L CO_2 (approximately 0.02 psi CO_2 fugacity) is 0.76 mpy at 60°F, and the corrosion rate at 125°F is 5.3 mpy. The corrosion rate of carbon steel in groundwater with 1.8 mg/L CO_2 at 60°F (0.76 mpy) is slightly lower than the corrosion rate of carbon steel in groundwater not mixed with gas (1.2 mpy). This can be due to the slight increase in the pH when groundwater is mixed with the Rager Mountain gas.

The pH of the groundwater alone is 4.0 at 60°F, and the pH of groundwater mixed with Rager Mountain gas is 4.3. Figure 132 shows the plot of the carbon steel corrosion rate when the groundwater is mixed with Rager Mountain gas containing CO_2. The maximum temperatures detected using neutron logs in #2244 was 128 and 104°F in 2016 and 2023, respectively. The estimated carbon steel corrosion rates in groundwater mixed with gas at 100 and 125°F are 2.7 mpy and 5.3 mpy, respectively.

Table 24: Carbon Steel Corrosion Rate in Groundwater Mixed with Gas

Temperature (°F)	Dissolved Oxygen (mg/L)	Dissolved CO_2 (mg/L)	Corrosion Rate (mpy)	pH
60	–	1.8	0.76	4.3
80	–	1.8	1.5	4.0
100	–	1.8	2.7	3.9

Temperature (°F)	Dissolved Oxygen (mg/L)	Dissolved CO_2 (mg/L)	Corrosion Rate (mpy)	pH
125	–	1.8	5.3	3.7

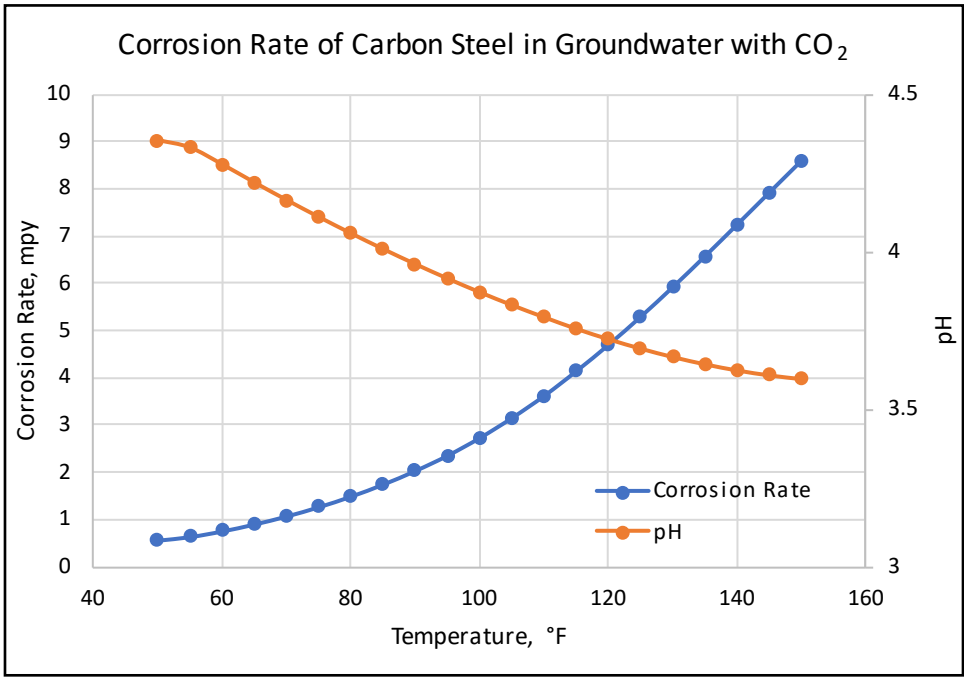

Figure 132: Corrosion Rate of Carbon Steel in Groundwater with CO_2 at Various Temperatures

Corrosion Due to Dissolved Oxygen and CO_2

An open 2 in. annulus valve in well #2244 allowed the access of oxygen to the annulus fluid. The amount of oxygen that dissolved in the annulus fluid can be up to a maximum of 8 ppm, which corresponds to the solubility of oxygen in water at ambient conditions. In addition to oxygen, CO_2 can also be present in the annulus fluid. Results of the connection testing show that at least one connection was leaking. The corrosion rate of carbon steel in groundwater with 8 ppm dissolved oxygen mixed with Rager Mountain gas flowing at a rate of 70 cm^3/min was estimated using thermodynamic modeling.

Table 25 shows the amount of dissolved oxygen and dissolved CO_2 in groundwater and their corresponding corrosion rates. The estimated corrosion rates of carbon steel in groundwater with dissolved oxygen and CO_2 at 60°F, 80°F, 100°F, 125°F are 4.3 mpy, 6.5 mpy, 8.8 mpy, and 13.7 mpy, respectively.

The corrosion rate of carbon steel in groundwater with dissolved oxygen and CO_2 at 60°F is higher than the corrosion rate of carbon steel in groundwater with dissolved oxygen alone, and the corrosion rate of carbon steel in groundwater mixed with CO_2.

However, the corrosion rate of carbon steel in groundwater with 6.6 ppm dissolved oxygen at 100°F is higher than the corrosion rate of carbon steel in groundwater with both dissolved oxygen and CO_2. This slight variation may be due to the higher pH (3.9) that develops when groundwater with dissolved oxygen mixes with Rager Mountain gas with 0.2 mol% CO_2, compared to the pH of the groundwater with 8 ppm oxygen input (3.7).

Figure 133 shows the plot of the carbon steel corrosion rate in groundwater with dissolved oxygen and mixed with gas containing CO_2. The corrosion rates at the temperatures measured in #2244, which were 100 to 125°F were between 8.8 to 13.7 mpy.

Table 25: Carbon Steel Corrosion Rate of Groundwater with Dissolved Oxygen and Mixed with Gas

Temperature (°F)	Dissolved Oxygen (mg/L)	Dissolved CO_2 (mg/L)	Corrosion Rate (mpy)	pH
60	9.8	3.6x10E-3	4.3	4.2
80	7.9	2.7x10E-3	6.5	4.0
100	6.5	1.9x10E-3	8.8	3.8
125	5.3	1.4x10E-3	13.7	3.7

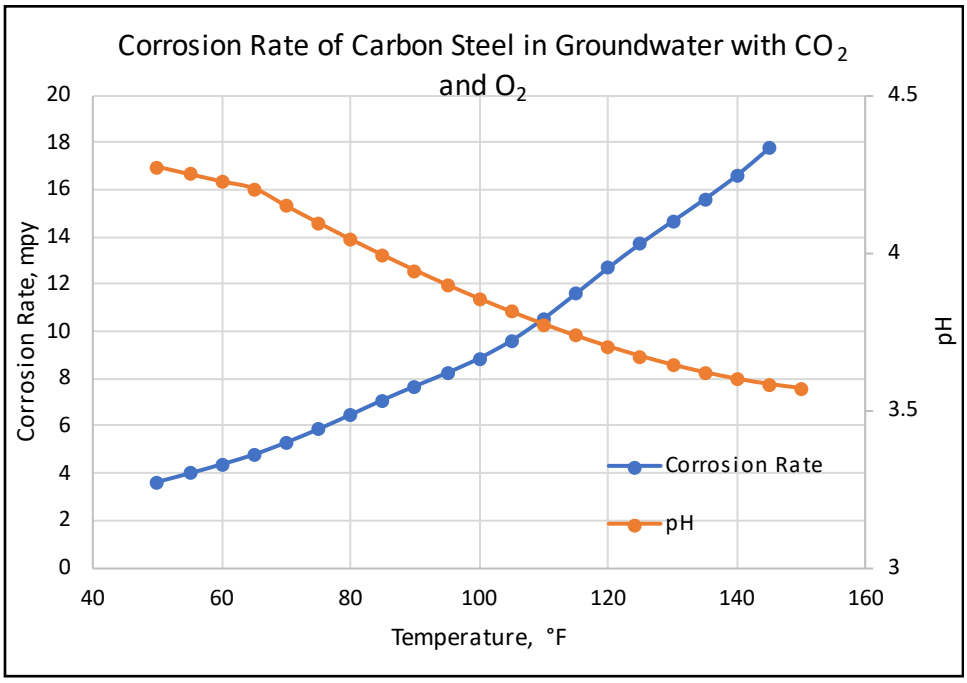

Figure 133: Corrosion Rate of Carbon Steel in Groundwater with CO_2 and Dissolved Oxygen

Under-Deposit Corrosion

Under-deposit corrosion refers to localized corrosion that develops beneath or around deposits present on a metal surface. Several mechanisms can lead to under-deposit corrosion. Vera et. al., presented a few scenarios where under-deposit corrosion can occur [47]. These are the following:

- Dominant internal anode (beneath the deposit) coupled to a dominant external anode (uncovered metal). The mechanism is similar to crevice corrosion where the galvanic driving force originates from different chemistry inside and outside the deposit, and this requires an ionic path. This typically occurs in high-water systems [47].
- Separation of anodes and cathodes beneath the deposit (no external cathode). The deposit mainly acts as a means of producing a chemistry suitable for pitting corrosion to occur. The anode/cathode separation may develop from small differences in local chemistry arising from irregular deposits [47].

- No local separation of anode and cathode, which would induce uniform corrosion beneath deposits [47].

Literature indicates that high corrosion rates are reported in systems with under-deposit corrosion problems [47] [48].

Some references indicate that under-deposit corrosion generally occurs with MIC [49] [50] [51]. For the case of Rager Mountain well #2244, the results of analyses indicate that MIC is not a contributing factor. Wang et al., indicated that when a metal is fully covered by microscopically homogenous deposits, there would be no local cathodes and anodes on the metal surface's under-deposit. If the deposits are porous and with poor protective capability, the under-deposit corrosion tends to occur uniformly [48] [52].

Some authors observed this uniform corrosion under-deposit and attributed it to the porous homogeneous features of the deposits of sands, corrosion products [52], and $CaCO_3$ [48]. In addition, Pang et. al., reported that dissolved O_2 can increase the general corrosion rate by promoting the oxygen reduction reaction [53].

For the case of Rager Mountain wells, it was observed that high rates of general wall loss were mainly occurring at the top joint. It was also observed from several wells where the top joint was pulled out, that a thick external deposit adhered to the top portion of the top joint. Inorganic and organic matter accessed the annular space due to the open valve. The debris mixed with the annular fluid and attached to the OD surface of the 7 in. casing.

Figure 134 shows the top portion joint C001B covered with scale or deposit after the joint was pulled out from the well. The amount of scale or deposit in the top portion of the joint is different from the portion near the cut end. Figure 135 shows the condition of the top joint from the other wells: #2248, #2251, and #2254 that is extensively covered with scale and debris.

Figure 134: #2244 Joint C001B a. Top Portion Covered with Thick Scale, b. Bottom of C001B Cut End

Under-deposit corrosion is a possible corrosion mechanism in Rager Mountain wells. Under-deposit corrosion may be related to the deposited debris on the top joint of the well. The area under the debris has depleted oxygen compared to the region without deposits. The area under the deposit acts as an anode, and the uncovered region acts as a cathode. General corrosion occurred in the region under the deposit.

Figure 135: Top Joint from Wells #2248 (a, b), #2251 (c, d), and #2254 (e, f)

7.2.5 Summary and Interpretation

Several possible corrosion mechanisms that could cause severe wall loss at the top joint of well #2244 were analyzed and discussed here. Each was carefully studied, and reasons were provided whether each corrosion mechanism was contributing to the failure. Results of the investigation suggest that the water level in the annulus varies. Based on the corrosion profile, the water level on average was most likely at the location of the axial rupture where wall loss was maximum.

The factors that significantly contributed to corrosion of the top joint are oxygen and the extensive debris and scale. Oxygen can enter the well through the opened 2 in. annulus valve. At the same time, debris can also enter the opened 2 in. annulus valve. The debris that floated in the annulus fluid stuck to the top portion of the top joint and caused a differential oxygen concentration cell between the covered and uncovered regions of the 7 in. casing. The uncovered OD surface of the 7 in. casing acted as a cathode. The region covered with deposits acted as an anode.

Because the deposits are porous, general corrosion occurred. Scale analysis also showed that the corrosion products are mostly iron oxides and iron oxy-hydroxides.

Based on 80% wall loss in the axial region and a field life of 30 years, the estimated corrosion rate of #2244 C001 is approximately 10 mpy. The predictions from the thermodynamic modeling for the corrosion rate of carbon steel in groundwater with oxygen is in the range from 6 to 15 mpy depending on the extent of oxygen. Consequently, oxygen and the debris were significant contributors to the 7 in. production casing wall loss.

CO_2 played a role in the OD corrosion of the top joint. The results of the scale analysis showed the presence of $FeCO_3$ (Siderite) at the OD surface of the joint. Corrosion modeling showed that there is an increase in carbon steel corrosion in groundwater when CO_2 mixes with oxygen when compared to just CO_2. The extent of role of CO_2 is unclear, however it did play a role as evidenced by the Siderite. Connection testing revealed that one out of nineteen connections tested exhibited a small leak, the source for CO_2 in the annulus.

The extensive testing and metallurgical evaluation lead one to conclude that MIC did not play a role in the corrosion of #2244, #2248 and #2251. Galvanic corrosion did not play a role in the wall loss at #2244 as evidenced by the testing and analysis conducted here.

7.3 Conclusions

The key conclusions of the failure analysis are:

- Wall thinning caused the failure of well #2244's 7 in. casing. The thinnest wall thickness was located off the center of the 3.36 in. axial rupture. The initiation site of the axial rupture is most likely in this region. The remaining wall thickness of the 7 in. casing was not able to sustain the pressure inside well #2244, causing ductile axial rupture.
- Mechanical, impact, and fracture toughness testing, including hardness measurements near the fracture surface, indicate that the failure is ductile. The dimple-like features observed on the fracture surface of the axial rupture specimens are due to corrosion. The original ductile tearing has been destroyed by corrosion.
- The circumferential fracture surface is mainly shear-lips. The circumferential fracture surface is not perpendicular to the ID or OD surface. Circumferential cracking is most likely ductile.
- The failure of well #2244 was a single event. Corrosion of the 7 in. casing caused severe wall thinning that resulted in the axial rupture. The crack initiated in the axial rupture and propagated in the axial direction to a length of 3.36 in. The upper crack front turned and propagated in the circumferential orientation until it terminated. The lower crack front turned and propagated in the circumferential orientation in two directions, causing the casing to part.
- The corrosion mechanisms that contributed to the failure of well #2244 were primarily oxygen corrosion and under-deposit corrosion. CO_2 and CO_2 plus oxygen did possibly play a secondary role as evidenced by the presence of Siderite. Variation in oxygen concentration along the depth inside the annulus was reflected by the corrosion profile in well #2244's 7 in. casing OD surface. In addition to oxygen, organic and inorganic debris accessed the annulus. Debris floating in the annulus fluid adhered to the OD surface and caused differential oxygen concentration cells.

8 Connection Testing

Thirty-three 7 in. 26 ppf N80 connections from well #2244 were sent to Blade Energy Laboratories in Houston, TX, for connection testing. The objective of the testing was to determine if the connections leaked and, if so, at what rate. The connections were removed from the string during field operations by cutting each joint approximately 2 ft above the connection using a casing cutter (Figure 136). The extracted joints were shipped to a storage facility in Johnstown, PA, where the connections were removed from the joint by making an additional cut approximately 2 ft below each connection. The resulting connection samples were approximately 5 ft long and were shipped to Houston, TX, in wood crates.

Figure 136: Casing Cutter on C002

8.1 Background

Well #2244 was constructed using API 8-round long threaded connections (LTC). LTC thread is widely used in the oil and gas industry; it has good connection strength, simple maintenance, and a low price. LTC connections are commonly used when extreme temperatures and pressures are not encountered.

Figure 137 shows elements of the API 8 round threads, including the crest, root, and flank seals. The crest and root of the thread profile have clearances that form a helical leak path that must be blocked with thread compound (dope). Contact pressure is generated during make up when the flanks make contact, resulting in interference between the pin and box. Although these connections are often used in gas well applications, they generally are not recommended because they rely on thread lubricant for a seal [54].

Pressure leak resistance in API LTC connections is achieved by two means. First, dope must be able to seal the thread clearances. Metal particles contained in the API Bul 5A2 lubricants provide sealability by plugging the clearances and creating a pressure drop over some length, resulting in no leakage. This required length is believed to be between 3 and 5 threads, which for a 7 in. casing is approximately 85 in. in circumference. The second means concerns the mating thread flanks. The flanks must have a contact pressure greater than the fluid pressure to maintain a seal. [55]

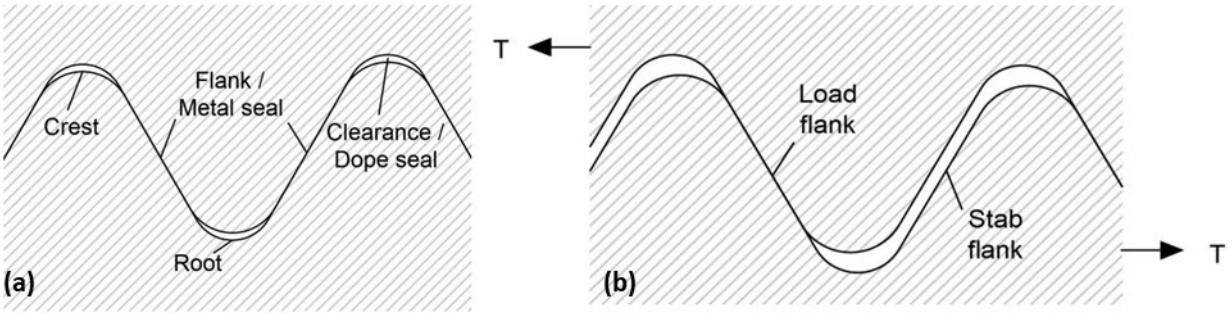

Figure 137: API 8 Round (a) Thread Elements and (b) the Effects of Tension [56]

Two parameters are often used to establish leak resistance: stab flank engaged length (SFEL) and stab flank contact pressure (SFCP). The SFEL is the sum of stab flank thread length for which SFCP is greater than zero. When the SFEL reaches zero, all the stab flanks separate, forming a helical leak path. Leakage resistance envelopes are limited by the axial load that causes loss of SFEL. In other words, if the connections experience a high enough tensile load to separate the stab flanks, it will create a leak path.

For SFEL greater than zero, leakage resistance is controlled by SFCP. The chosen value of SFCP can vary depending on the analyst. In one study [55], a discrete average of SFCP was selected for threads near the end of the pin, excluding the first thread. Other studies may define the SFCP using different criteria. The parameters are combined to form leakage envelopes for connections. Figure 138 shows an example of the average SFCP value used to calculate SFCP and a typical leak resistance envelope.

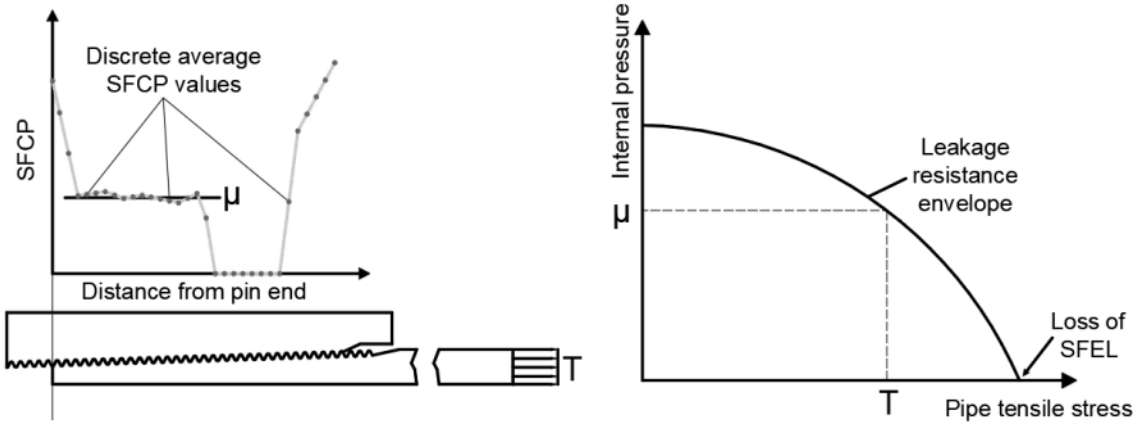

Figure 138: Leakage Capacity Estimation Process [55]

Several studies [55] [56] [57] have been conducted to evaluate the leak resistance of API 8 round connections that reviewed variables such as make-up torque, connection taper, applied tension, internal pressure, and thread compound type. Many studies relied on FEA to vary the parameters and determine their effect on leak resistance. Investigating API 8 round connections is beyond the scope of this work. The main conclusion from the studies is that API LTC connections are not considered gas-tight due to their dependency on dope to form a seal. The objective of the connection testing was to determine how many connections in well #2244 may have been leaking and at what rate.

8.2 Connection Testing

The connection testing uses nitrogen to pressurize the connection samples while monitoring for leaks. Blade uses mass flow meters to detect and measure leaking nitrogen. The approach is more accurate and sensitive than other techniques, such as the bubble method. Boots installed around the connection trap leaking nitrogen and force it through the flow meter. Blade uses several flow meters to cover a range of leak rates. The first flow meter used during connection testing is highly sensitive, ranging from 0 – 4 standard cubic centimeters per minute (SCC/minute). The high sensitivity of the meter ensures detection of any connection that leaks. When a leak is detected, the flow meters are exchanged for different ranges until the leak rate can be measured.

Boot Installation

The boot refers to the device installed around the connection to trap gas escaping. Nineteen connections were tested to estimate the leak rate within the well. A single boot was constructed to measure leaks from the connection's mill and field make-up side. The mill side refers to the side of the connection made up when the pipes were manufactured. The field side refers to the side of the connection made up on the rig in the field. The connection box is face up when constructing the string, which means the mill side was located below the field side when the string was in the slips. Knowing the difference between the field and mill side is essential if a leak is detected.

If a connection leaked, the leak rate was recorded, and the test was stopped. The single boot was then replaced with a double boot design, and the connection was retested. The double boot design isolates the mill and field sides and enables the operator to determine which side of the connection leaks.

Figure 139 shows an example of an installed single boot. A neoprene strip is adhered to the casing surface on each side of the connection. Plastic tubing is inserted through each neoprene strip to allow trapped gas to move from the boot to the flow meter. The tubing also enables the technician to pressure test the boot after installation is complete. A section of plastic tubing is also secured along the length of the connection to form a gas channel between the rig and field sides of the connection. The plastic tubing channel is only required for the single-boot design. The double-boot design is intended to isolate the rig and mill sides of the connection.

A neoprene sheet is stretched around the connection and adhered to the neoprene strips. Acrylic tape is then wrapped around the entire boot to reinforce the neoprene and minimize the gas volume. After installation, the boot is pressure and flow tested to ensure a good flow meter response.

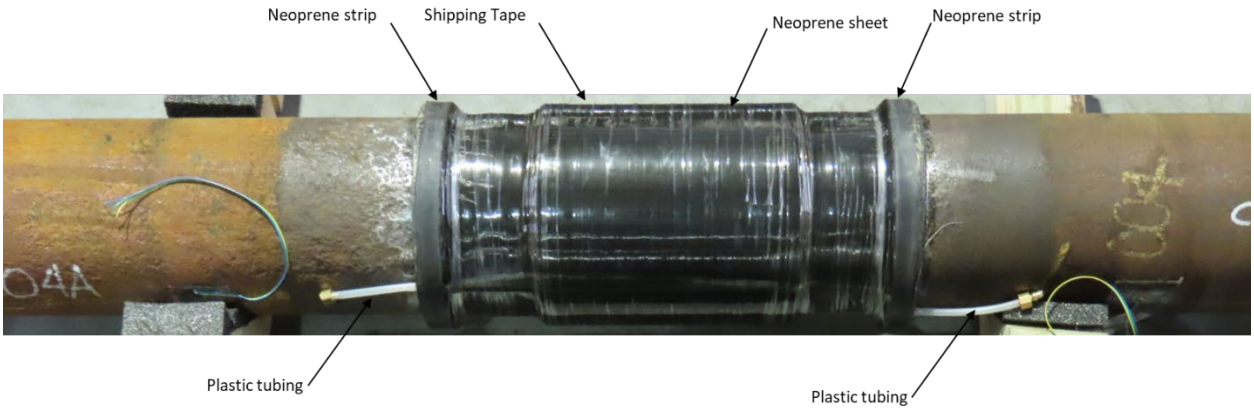

Figure 139: Single Gas Boot Example

The top joints (C002A, C003A, C004A, and C005A) had corrosion on the connection and the surrounding casing, consistent with the casing observations. The corroded casing surface required additional work to ensure a gas-tight seal between the neoprene and pipe surface, including extra cleaning in pitted areas and using epoxy to fill in corroded pits to ensure good adhesion.

Figure 140 shows the as-received conditions for C002A and C007A. The images show a clear difference between the surface conditions on the connection and pipe surfaces. C002A shows general corrosion and pitting, whereas C007A has a relatively clean surface free of corrosion and pitting.

Figure 140: Connection C002A and C007A

The pressure testing procedures for the boot were as follows:

1. Connect brass compression fittings to both plastic tubes extending from the boot.
2. Install a pressure gauge and valve on one of the plastic tubes (inlet) and a valve on the other (outlet).
3. Open the inlet valve and close the outlet valve and fill with air.
4. Read the pressure gauge after a 15-minute wait. If the pressure has not changed, then the boot is not leaking. If the pressure has dropped, the boot is leaking and mitigation must occur.

Mitigation techniques include tightening the pipe clamps to seal any possible leak points or sealing the leak after using soapy water to locate the leak path. The pressure test is repeated until the boot passes.

After the pressure test, a flow-through test is conducted to ensure the flow meter responds quickly and accurately to a leak. The flow-through test was performed using a syringe pump to simulate a leak through the boot. The syringe pump forced air through the boot at a predefined rate. A flow meter was installed on the outlet to read the leak rate.

The flow-through test procedure is as follows:

1. Connect a syringe pump to the boot inlet.
2. Connect the flow meter to the boot outlet.
3. Connect the syringe pump and flow meter to a computer and run Blade's custom software.
4. Run and monitor the test results in the software. Ensure that the flow meter reaches the correct rate and the total volume is within ±15% of the actual volume.

Figure 141 and Figure 142 show the flow-through test results for C007A. The plots are extracted from individual reports generated for each tested connection. Figure 141 (a) shows that the flow meter read the target flow rate (0.010 SCC/s) after approximately 500 s, and Figure 141 (b) shows that the flow meter read the high flow rate (0.067 SCC/s) at approximately 550 s.

The plots show that there is a delay in the flow meter reading as the boot fills with air. However, the plots also show that the flow meter responds almost instantly to the induced leak (syringe pump).

Figure 142 shows the cumulative volume versus time for the low and high flow rate tests. The plots show how the cumulative value has a delayed effect due to the boot filling with gas. However, the cumulative volume reaches the target value after the syringe pump has stopped and the boot empties. The flow-through tests show that the small range flow meter (0 – 4 SCC/minute) is both sensitive and accurate for measuring the flow rate of leaking gas.

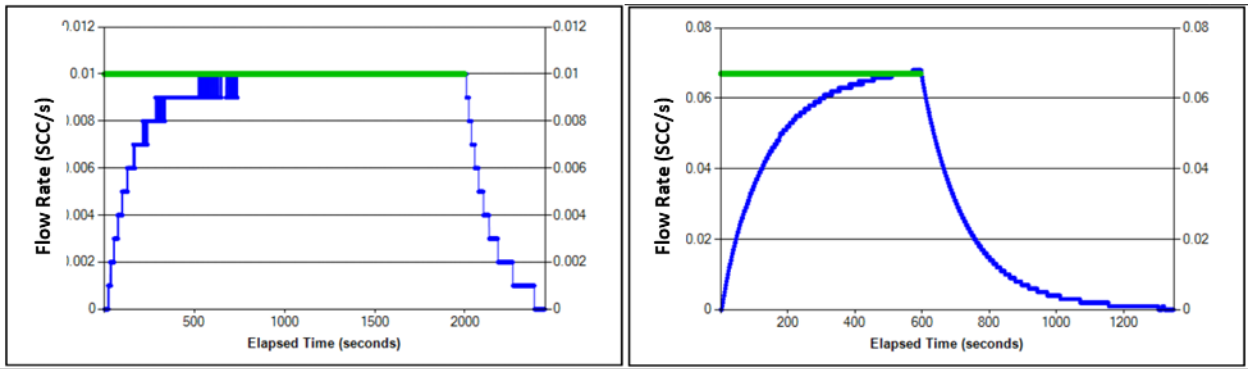

(a) C007A Low Flow Rate Test (0.010 SCC/s) (b) C007A High Flow Rate Test (0.067 SCC/s)

Figure 141: C007A Flow Rate Versus Time for Low and High Flow Rate Tests

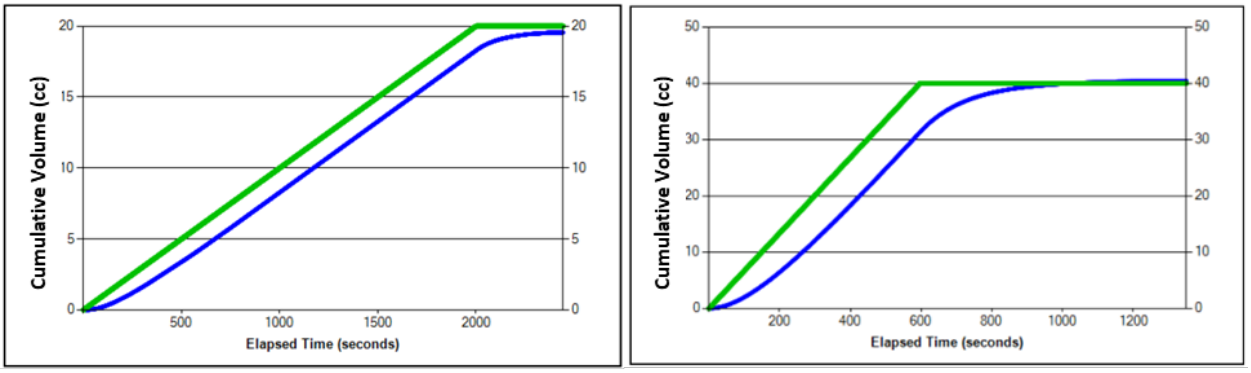

(a) C007A Low Flow Rate Test (0.010 SCC/s) (b) C007A High Flow Rate Test (0.067 SCC/s)

Figure 142: C007A Cumulative Volume Versus Time for Low and High Flow Rate Tests

Leak Testing

Blade conducted connection leak tests on 19 of the 33 connections sent to Houston for testing. The testing was conducted at Blade's warehouse inside a Conex (sea container) for safety. Figure 143 shows the interior views of the test structure. The image of the interior shows a table with wooden tie points to secure the connection during testing. The grey cabinets on the floor and mounted on the wall of the Conex are the pressure and Data Acquisition (DAQ) cabinets, which are labeled in Figure 143.

The pressure cabinet houses two pressure transducers and valves. The valves allow the operator to fill and evacuate the test specimen on command, and the pressure transducers communicate the state of the cabinet to the operator. The DAQ cabinet houses the acquisition system and has ports to attach the various sensors. The sensors used during testing included pressure transducers, thermocouples, strain gauges, and flow meters.

The pressure transducers were used to monitor the status of the pressure cabinet and the test specimen. The test specimen transducer was also used to control the automated test sequence. The thermocouples monitored the inlet (in-line with the gas flow), room, and pipe temperature. Temperature measurements are not required for the leak test but were applied as standard practice for testing.

The flow meters were used to detect and measure gas leaking from the connections. The strain gauges were used to monitor the status of the pipe during testing and act as a safety precaution and stress check for connection testing. The Houston-based company Aldinger verified all sensors before testing. Strain gauges were zeroed and shunt calibrated before each test.

Pressurized gas contains a significant amount of energy that is hazardous if a catastrophic failure occurs during testing. Aluminum filler bars were used to minimize the volume of gas needed to pressurize the pipe, thus reducing the stored energy within the test specimen. The pipe ends were sealed using test plugs designed for a maximum pressure of 8,000 psi. The plugs seal against the ID of the casing using a wedge mechanism to engage a seal. The wedge was activated by tightening four hex nuts with a torque wrench.

Figure 143: Interior Views of the Leak Test Structure

The system is automated and follows a test sequence supplied by the operator. Table 26 shows the test sequence used for the connection tests. A 5-minute hold was executed every 500 psi for load steps 0 – 6. Load step 7 only increased by 200 psi because the maximum pressure experienced by the connections was approximately 3,200 psi. Five minutes was considered sufficient for the hold due to the results from the flow-through boot tests.

The tests showed that the flow meters respond instantaneously to a leak; therefore, five minutes was sufficient to determine if a leak had occurred. The table also shows the calculated end cap force, hoop stress, and longitudinal stress based on the load step pressure and casing ID area. The maximum end cap force occurred at 3,200 psi, generating 98,993 lb of axial tension. The maximum hoop and longitudinal stresses caused by the internal pressure and resulting tension was 30,939 and 13,113 psi, respectively.

Table 26: Test Sequence

Load Step	Internal Pressure (psi)	Hold (min)	End Cap Force (lb)	Hoop Stress (psi)	Longitudinal Stress (psi)
0	0	0	0	0	0
1	500	5	15,468	4,834	2,049
2	1,000	5	30,935	9,669	4,098
3	1,500	5	46,403	14,503	6,147
4	2,000	5	61,871	19,337	8,196
5	2,510	5	77,648	24,268	10,286
6	3,000	5	92,806	29,006	12,294
7	3,200	5	98,993	30,939	13,113

8.3 Results

C007A was the only connection that leaked out of the 19 tested connections. Figure 144 and Figure 145 show the leak tests for C008A and C019A, respectively. C008A and C019A are examples of connections that did not leak. The y-axis on the left is pressure in psi, and the y-axis on the right is the flow meter output in SCC/minute. The blue line represents the pressure versus time, and the red line represents the flow rate. The slopes in the pressure data represent the pressure increases by the automated system.

The flat portions are the 5-minute holds. The plot shows that the system sufficiently pressurizes the connection and holds at the target loads.

The flow meter data shows small increases (< 0.25 SCC/minute) in flow rate during the pressure increases at the early load steps. The detected flow rate is caused by the tightening of the boot. As the connection expands due to internal pressure, the boot tightens, and gas inside the boot flows through the flow meter. This phenomenon is not a leak and was observed for every test. The key observation is that the detected flow is minimal and goes back to zero during the holds.

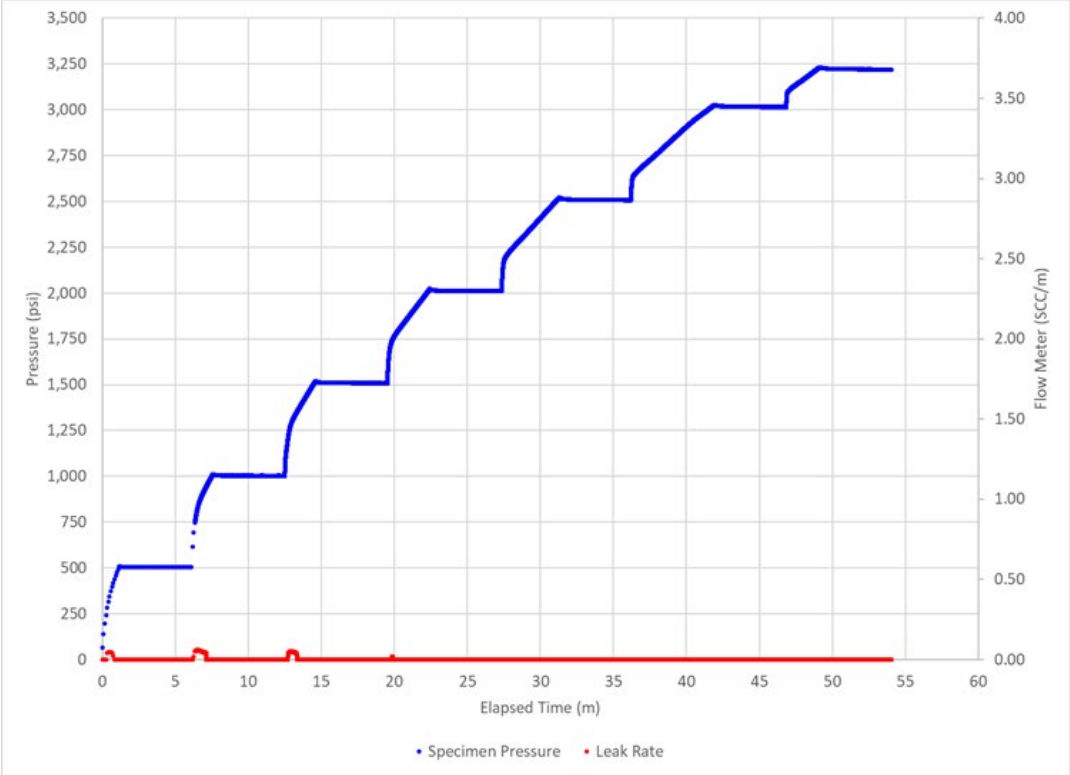

Figure 144: Connection C008A Leak Test

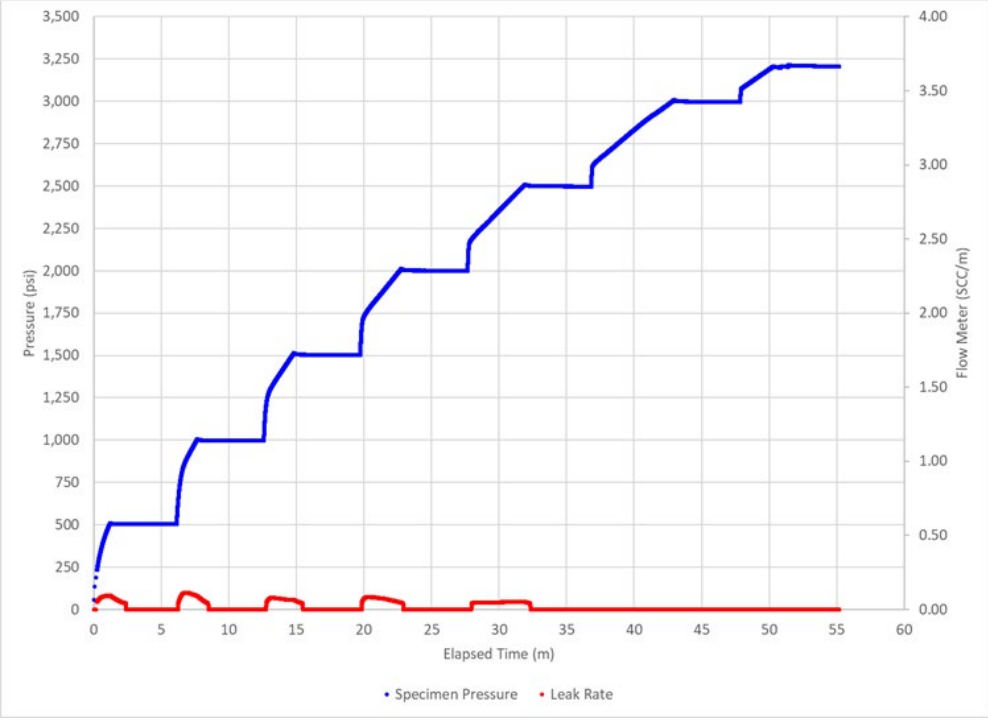

Figure 145: Connection C019A Leak Test

Figure 146 shows the results from leaked connection C007A. The connection was tested several times due to the high rate. The first test was conducted using the 0 – 4 SCC/minute flow meter. The 4 SCC/minute limit was reached while ramping up to 1,000 psi. The test was stopped, and the meter was replaced with a 0 – 50 SCC/minute flow meter.

The test was repeated, during which the 50 SCC/minute limit was reached while ramping up to 1,500 psi. The test was stopped again, and the meter was replaced with a 0 – 500 SCC/minute flow meter, which is shown in the data in Figure 146.

The flow meter data (red line) shows that the connection begins to leak almost instantly. The leak rate increases with each pressure increase until the connection reaches approximately 2,250 psi, at which point the leak rate reaches a peak of 325 SCC/minute and then begins to decrease.

At approximately 120 minutes into the test, the operator purges the boot by opening a valve connected to the boot (flow rate drops to less than 25 SCC/minute). After the purge valve is closed, the leak rate returns to the same decline observed prior to the purge, confirming the leak and the declining rate.

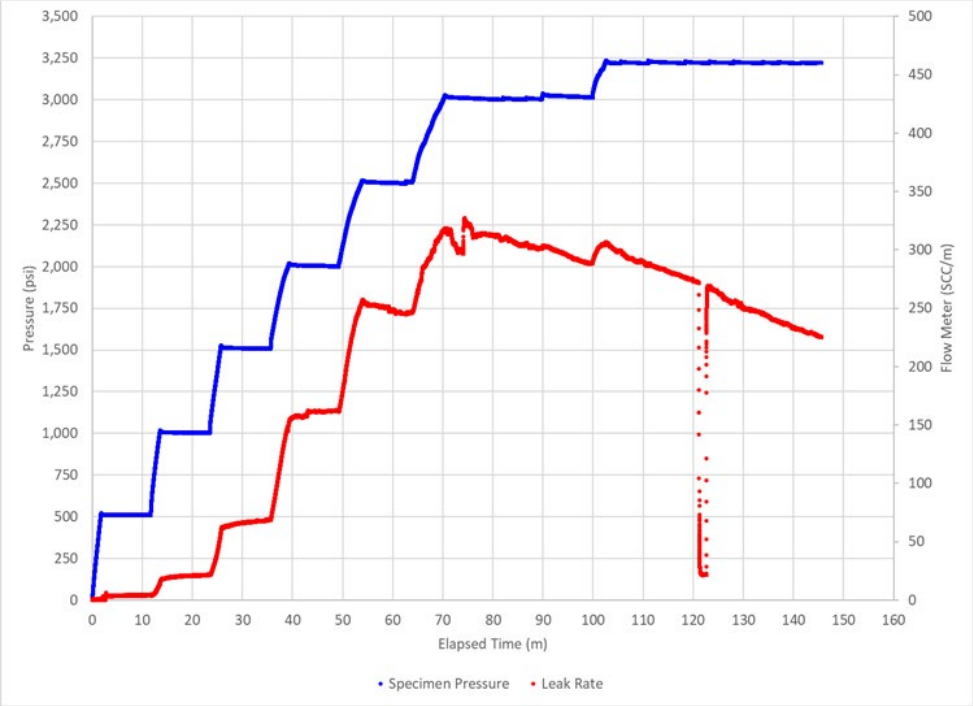

Figure 146: Connection C007A Single Boot

The single boot was removed and replaced with a double boot. The double boot isolated the mill and field side of the connection, allowing the engineer to determine which side of the connection was the source of the leak. Figure 147 shows the double boot after installation. Each boot was leak and flow-through tested, as done with the single boots. The mill side was tested first using the 0 – 4 SCC/minute flow meter. Figure 148 shows the results. The mill side of the connection did not leak.

Based on the single boot test results, the field side was tested using the 0 – 500 SCC/minute flow meter. Figure 149 shows the results of the test. The maximum leak rate was 69.4 SCC/minute and was reached at 3,200 psi.

The measured rate was significantly lower than the peak value (325 SCC/minute) reached using the single boot. The observation is consistent with the fact that the leak rate was declining during the single boot test. The leak rate appeared stable during the double boot test.

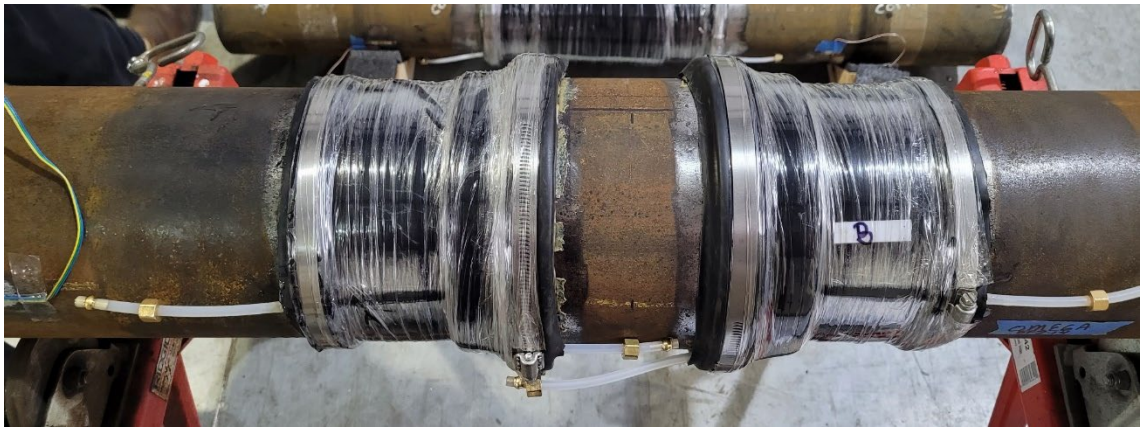

Figure 147: Double Boot for C007A

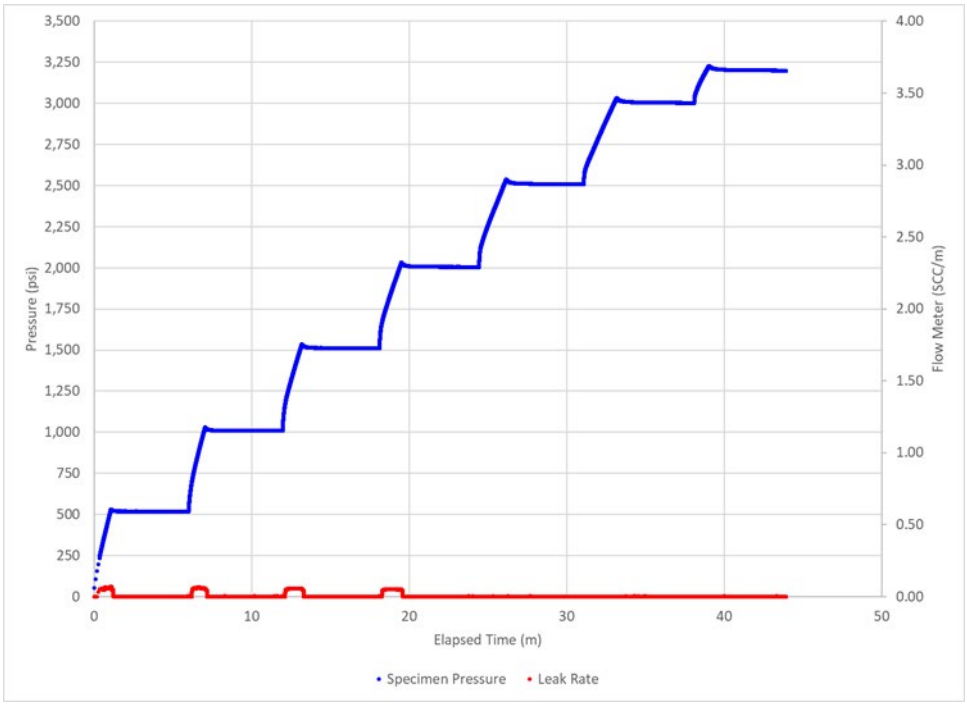

Figure 148: Connection C007A Mill Makeup Side

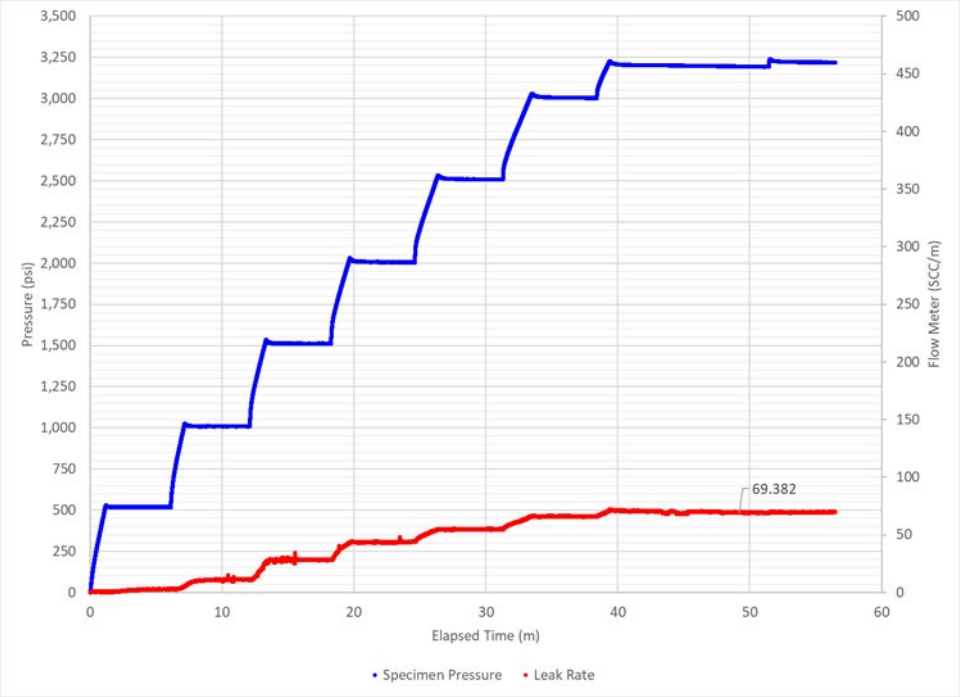

Figure 149: Connection C007A Field Makeup Side

Strain gauges were used to monitor the longitudinal and hoop stresses during the testing. The stress values varied slightly between tests, but most were relatively consistent. Figure 150 shows the hoop stress versus internal pressure for connections C002A, C007A, C008A, and C019A. The dotted black line represents the calculated hoop stress values based on Barlow's equation.

The plot shows that C002A is consistent with the theoretical values. Connections C007A, C008A, and C019A were consistent; however, they were lower than connection C002A and the calculated value.

Figure 151 shows the longitudinal stress versus internal pressure. The dotted black line is the longitudinal stress based on Barlow's equation. The strain gauge values are much lower than the theoretical values. The discrepancy between the calculated and measured values could be caused by:

- The proximity of the strain gauge to the wood tie downs, which restrain the pipe circumferentially and longitudinally.
- The variations in wall thickness at the strain gauge location.
- The proximity of the strain gauge to the end plug and connection. Both ends are constrained, causing changes in the local stress state.

The strain gauges were used for the purpose of safety and as a data check. The strain gauge data shows that the stress values and trends are consistent between the tested connections.

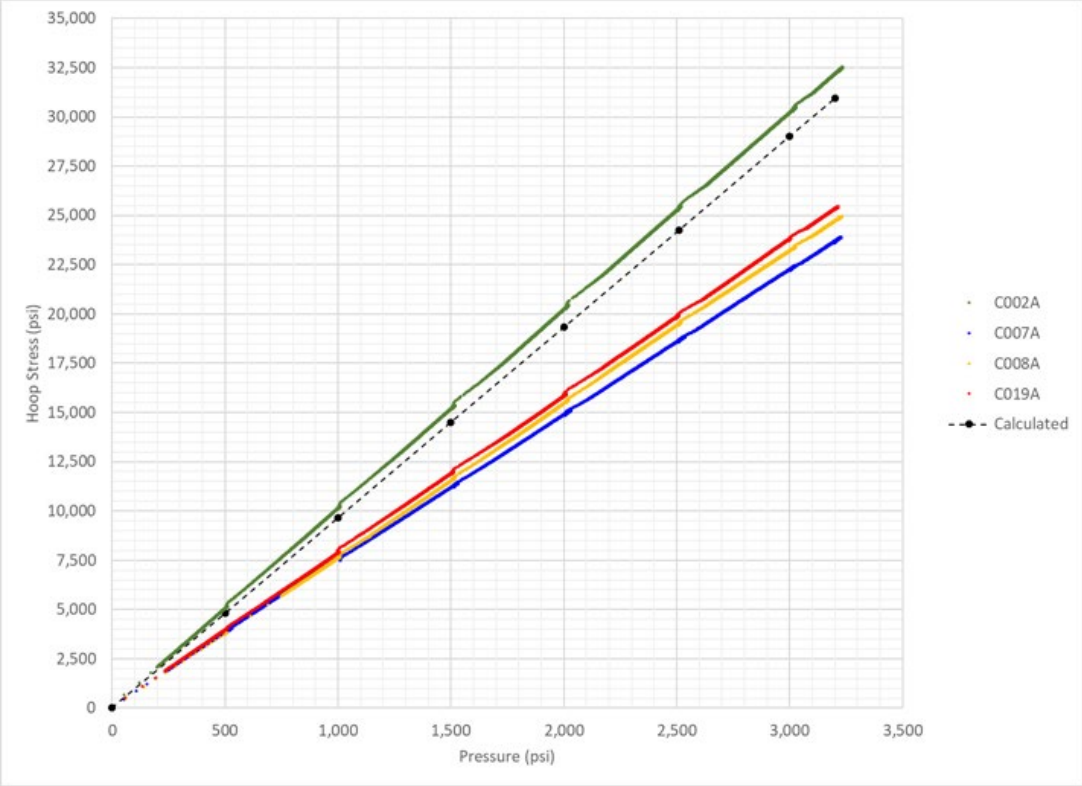

Figure 150: Hoop Stress Versus Internal Pressure

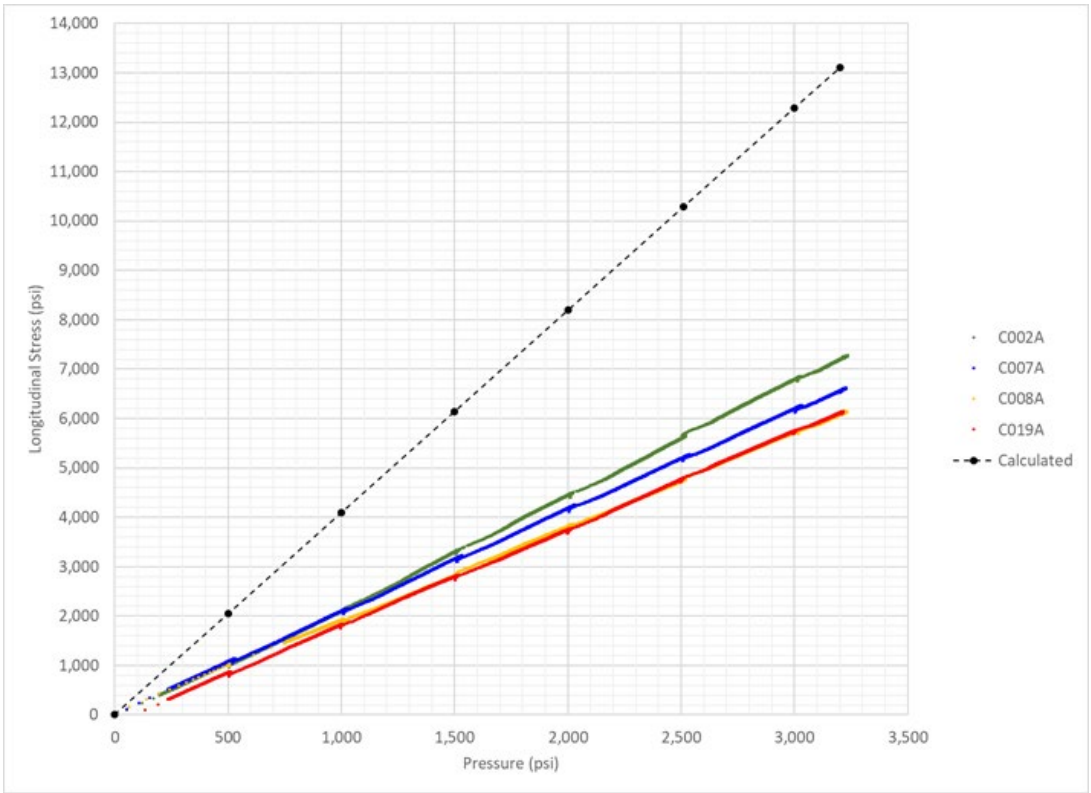

Figure 151: Longitudinal Stress Versus Internal Pressure

Connection Break Out

Four connections were chosen for breakout: C002A, C007A, C008A, and C019A. The connections were backed out using Blade's torque-turn unit. Figure 152 shows the torque-turn unit with a loaded specimen. The unit is made up of a tailstock and headstock.

The tailstock has six actuated grips that centralize and hold the specimen at the connection. The headstock also has six actuated grips that centralize and hold the casing on the rig side. The headstock rotates based on the input parameters supplied to the software. A hydraulic pressure of 900 psi was supplied to both grips based on the estimated breakout torque (Table 27).

Table 27: Recommended Torque Values

Minimum Torque	3,890 ft-lb
Optimum Torque	5,190 ft-lb
Maximum Torque	6,490 ft-lb

Figure 152: Torque Turn Unit

C002A, C008A, and C019A were selected to represent the non-leaking connections. C002A was selected to represent the upper corroded connections, C008A was selected based on its proximity to C007A (leaking connection), and C019A was selected to represent the lower non-leaking connections. The torque and number of turns were recorded for each connection as it was broken out. When the measured torque reached zero, the unit was stopped and the connection was removed by hand.

Table 28 shows the summary of the breakout data. C002A had the lowest breakout torque at 11,060 ft-lb. The highest breakout torque was 19,776 ft-lb and occurred while breaking out connection C008A. The leaking connection (C007A) had a breakout torque of 15,147 ft-lb, consistent with C019A (15,155 ft-lb). The table shows that all values are above the maximum torque of 6,490 ft-lb. The age of the connections and condition of the dope can explain the increase in torque during breakout. The values reported here may not reflect the torque values during the original make up.

Figure 153 through Figure 156 show the torque turn plots for connections C002A, C007A, C008A, and C019A. All plots show a spike in torque at the beginning of the breakout, followed by a smooth decline in torque as the number of turns increases. C008A had an anomaly at approximately 1.65 turns, where the torque increased momentarily and then resumed the downward trend. The other connections did not experience a similar anomaly.

Table 28: Torque Turn Results

Load Step	Leaked?	Achieved Torque (ft-lb)	Achieved Turns
C002A	No	11,063	3.325
C007A	Yes	15,147	3.409
C008A	No	19,776	4.725
C019A	No	15,155	3.995

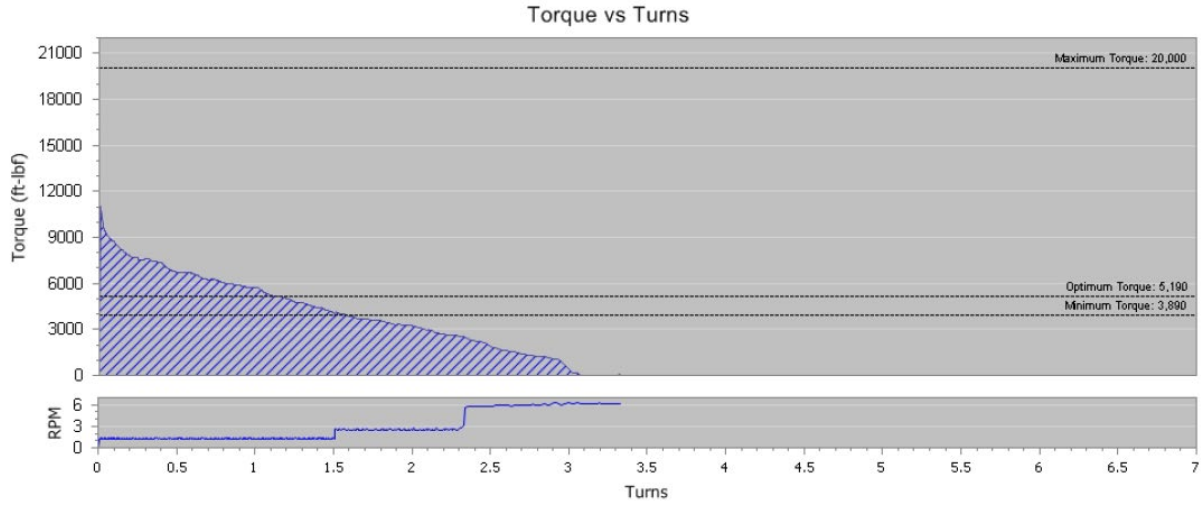

Figure 153: C002A Torque Turn Plot

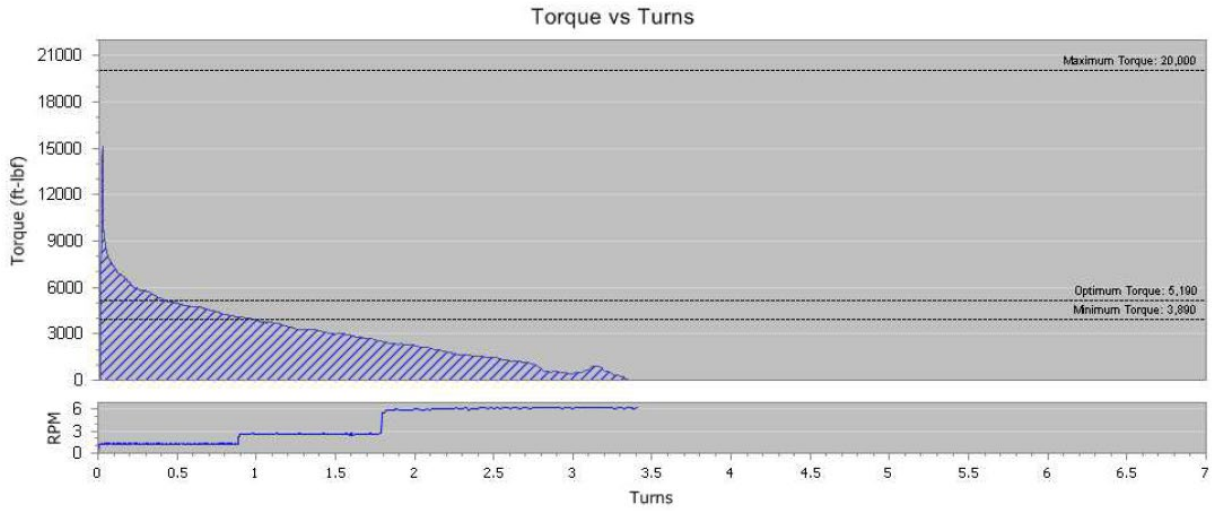

Figure 154: C007A Torque Turn Plot

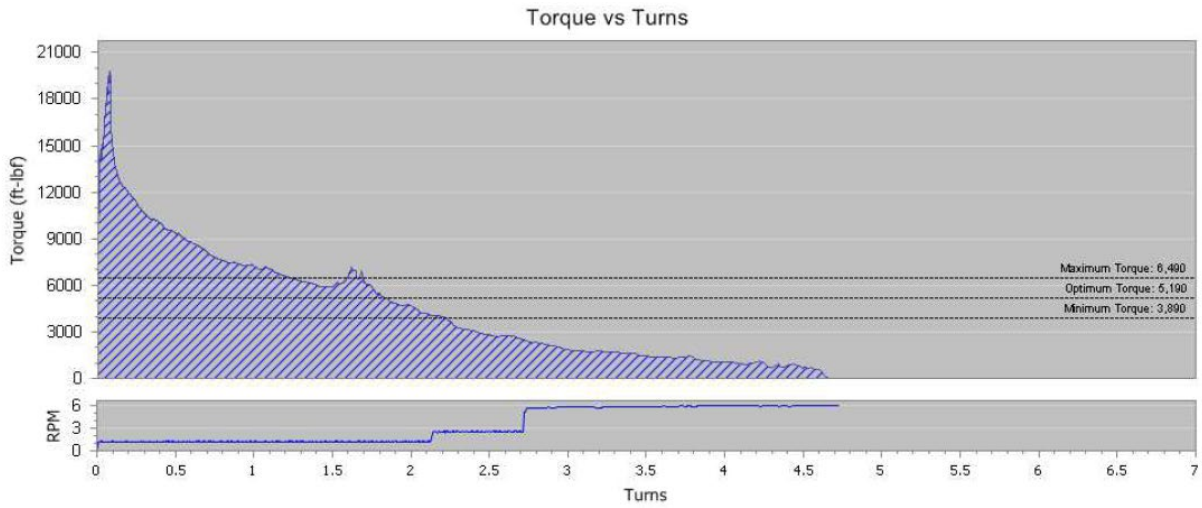

Figure 155: C008 Torque Turn Plot

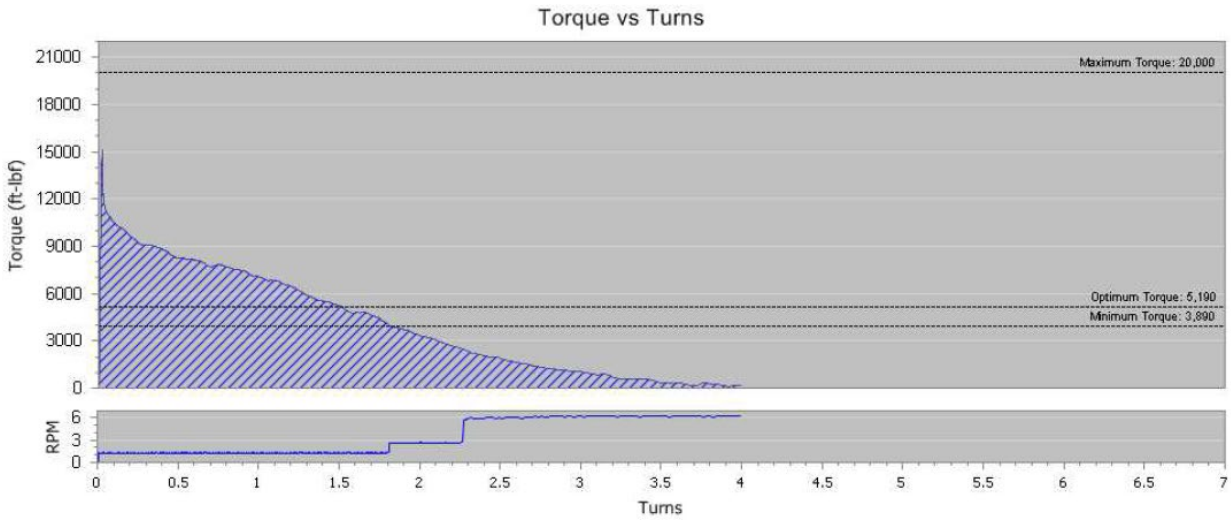

Figure 156: C019A Torque Turn Plot

The box and pin threads on the field side of the connections were examined before and after cleaning. The threads were cleaned using a degreaser and brushes. Except for C008A, the threads appeared clean and defect-free. Figure 157 shows an example of relatively clean threads (C007A).

Figure 158 shows the galling observed on the threads of C008A. The galling could explain the high torque observed in the torque turn plot (Figure 155) and the anomaly at 1.65 turns.

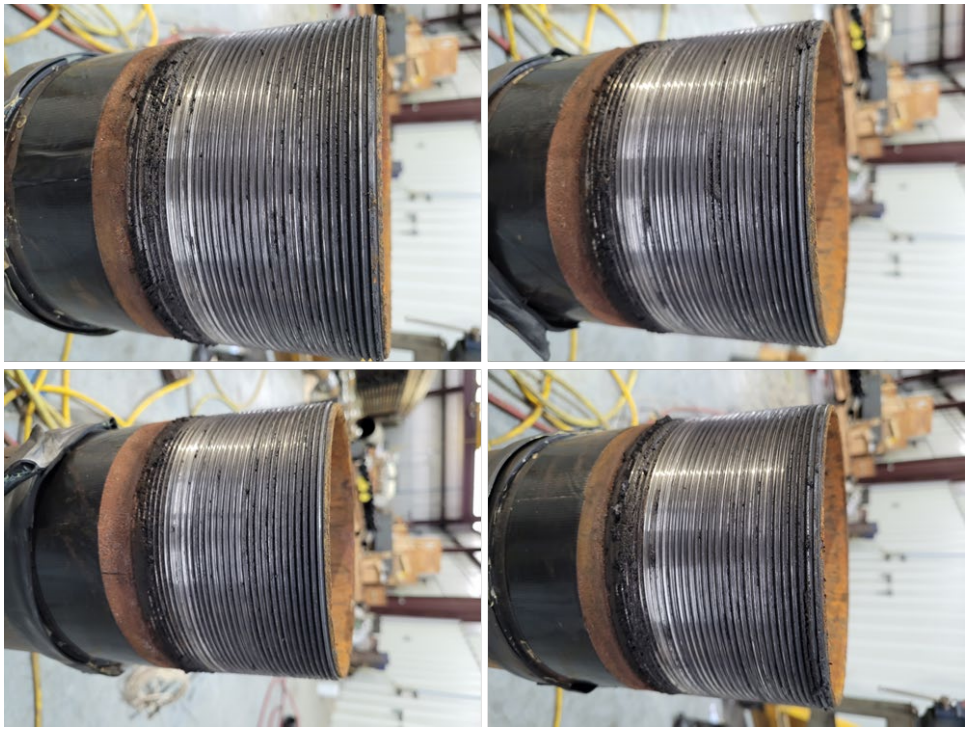

Figure 157: Connection C007A Pin Threads

Figure 158: Galling on C008A Pin Threads

8.4 Conclusions

Research shows that API LTC connections are prone to leak gas due to their reliance on thread dope to form a complete seal, however; LTC connections are commonly used in the oil and gas industry. Blade tested 19 out of 33 connections extracted from the #2244 well. The C007A connection leaked. The leaking connection was tested twice, once with a single boot and again with a double boot. The connection reached a peak leak rate of 325 SCC/minute at 2,500 psi, followed by a declining leak rate during the single boot test. The double boot test found that only the field side was leaking and measured a steady leak rate of 69.4 SCC/minute at 3,200 psi.

Four of the tested connections, three non-leaking (C002A, C008A, and C019A), and one leaking (C007A) connection were broken out and visually inspected. All the breakout torques were higher than the maximum torque for API 7 in. 26 ppf N80 API LTC connections. C008A had the highest torque at 19,776 ft-lb.

The visual inspection found that C008A was the only connection with a thread defect, which may explain the higher breakout torque. The leaking connection was defect-free, suggesting that the cause of the leak may have been a leak path that formed due to the breakdown of the dope.

This testing shows that gas was leaking into the annulus.

9 Top Joint Corrosion Mechanism

The objective in this section is to trace the mechanism by which the top joints corroded in Rager Mountain. The failure analysis, as discussed in Section 7, established that the oxygen along with water and possibly under-deposit corrosion were the causes for the extensive corrosion in the top joint at well #2244. The intent is to assess the underlying causes for this mechanism to occur.

There are two possible sources of water and debris ingress into the annulus:

- Water and debris ingress through the open annulus valve.
- Water ingresses into the annulus from the surface casing shoe.

In this section, the hypothesis of water and debris ingress through open annulus valves is evaluated in detail using multiple data sources. The second possibility is briefly discussed later in this section.

Blade collected data during site surveys of the Rager Mountain wells. Section 6.1.2 discussed that top joint corrosion was present in 7 out of 12 wells. The intent of the site surveys was to find any similarities and differences that could explain why only some of the wells had top joint corrosion. This section describes the data collection process, the data, and interpretations.

9.1 Annulus Valve Height Survey

Blade visited nine Rager Mountains wells on March 25, 2023, to measure the height above ground of the annulus valves. These heights were taken using a standard tape measure with the ground level as zero and measured to the center of the annulus valve. Figure 159 shows the height measurement process at the #2254 well site. There were two annulus valves on the casing head directly opposite from each other. Two measurements were taken for each side. An annulus valve is shown on the left. It is in the open position. The picture on the right shows an annulus valve, also in the open position, but with a threaded pressure fitting. Typically, this pressure fitting does not permit the ingress of water and/or air; it is intermittently used for checking annulus pressure.

Figure 159: Well #2254, Annulus Valve Height Measurements, March 25, 2023, Open Side (Left) and Pressure Fitting Side (Right)

Table 29 shows the annulus valve height measurements for each well in inches above ground level. There were two measurements for each valve. The first number is the open valve height, and the second number is height to the pressure fitting. The average height of all valves was 8.7 in. The minimum was 3.5 in., and the maximum was 20.5 in. The column on the right shows the HRVRT top joint wall loss as reported in the 2022 logs. Top joint corrosion was discussed in Section 6.1.2.

The wells that have top joint wall loss have varying heights of annulus valves (e.g., 4.5 – 18.5 in.). Blade did not find any direct or simple correlation from annulus valve height to amount of top joint corrosion. Blade did find local pooling adjacent to the wellhead (Figure 159), discussed later in this section.

Table 29: Height of Annulus Valves Above Ground Level

Well Number	Elevation above Ground Level of Two Annulus Valves (in.)	Top Joint Wall Loss, HRVRT 2022, (% WT)
2244	Not measured	Not available
2245	9.5, 10	23
2246	20.5, 17	0
2247	18.5, 18.5	32
2248	7.5, 8.5	42
2249	9, 9	0
2250	6.5, 3.5	0
2251	7, 4.5	49
2252	4, 5	0
2253	6.5, 4	37
2254	7.5, 8	45
2255	4.5, 4	0

9.2 Well Surface Drainage Analysis

Blade investigated the probability of ingress of water from natural sources (e.g., precipitation). To assess this, Blade conducted a drainage survey using either DEP photographs or actual site drainage measurements. DEP photographs were used to evaluate drainage for #2244, #2251, and #2248 because the surface had been disturbed for rig work and other equipment prior to our onsite assessment.

Figure 160 shows pictures of the #2244 wellhead at different dates by DEP inspectors (discussed in Section 4.3.2). The inset picture ‘A’ was taken on February 13, 2020. Three noteworthy observations are seen in this picture. The first is the ground cover is primarily grass and natural vegetation. The second is the proximity of the annulus valves to the ground. The third is the dark circular area around and to the right of the wellhead. Blade’s interpretation is that this is an area of water pooling.

Inset picture ‘B’, taken on September 22, 2021, shows the wellhead with annulus valves that is different from ‘C’ and ‘D’, taken on June 9, 2022. Sometime between these dates, the valves were changed. Additionally, the ground cover has changed from natural cover to rocks. The annulus valve in ‘D’ is roughly at ground level. The inset picture ‘E’ was taken on November 7, 2022. The gas was blowing out at ground level through the open annulus valve. Blade’s interpretation is that the ingress of water and surrounding organic and inorganic material (e.g., grass, soil, etc.) into the annulus valve was highly likely.

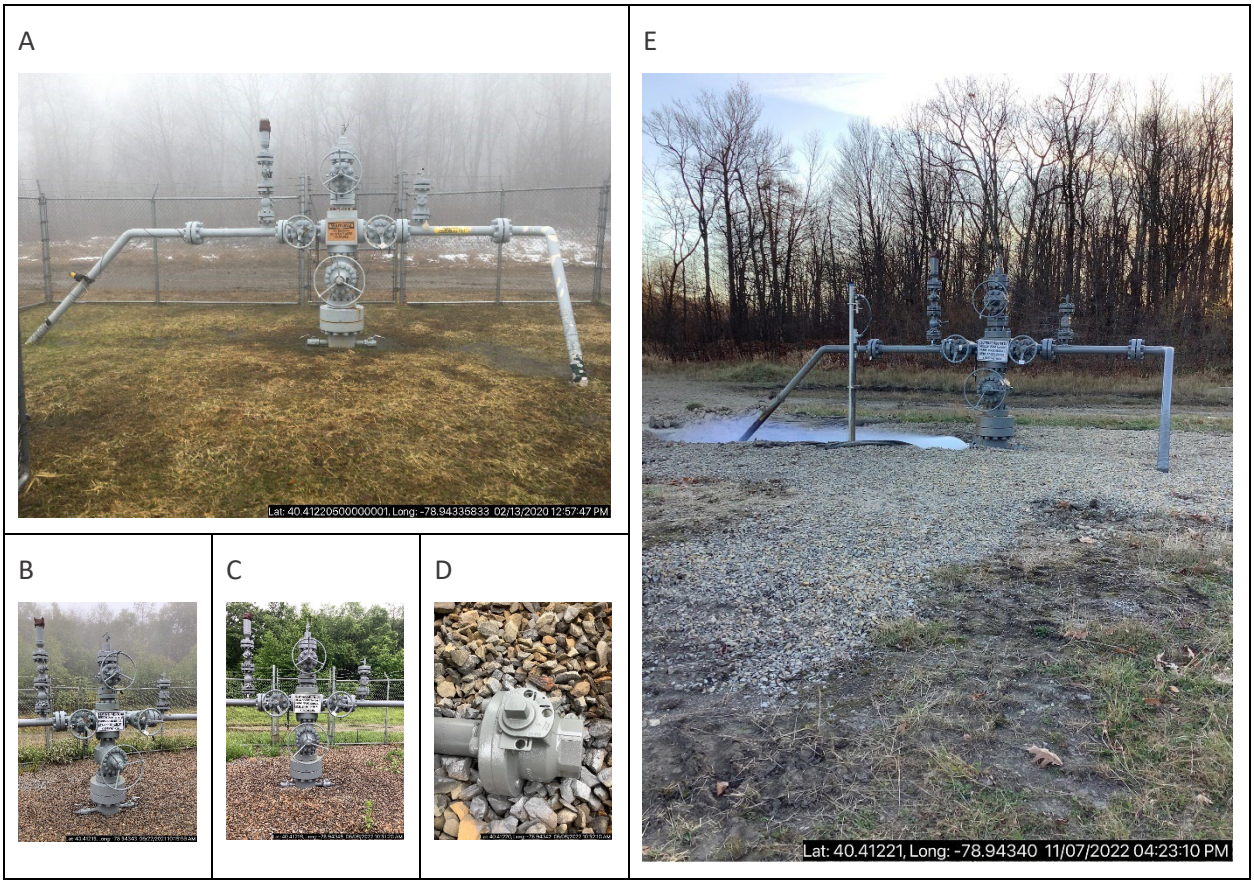

Figure 160: Well #2244 Wellhead, Tree, Annulus Valve at Various Dates [DEP]

Figure 161 and Figure 162 show pictures of the #2248 and #2251 well sites, respectively, at different dates by DEP inspectors. No indications of local pooling were observed. However, the ground conditions changed over time from grass to gravel/rock. No snow is located near the wellhead. Blade's interpretation is that warm withdrawal gas has warmed the wellhead and adjacent ground. Blade's opinion is that at times of significant snowfall or large snow drifts, this warmth could melt adjacent snow and make it possible for the water to enter the annulus through the open valve.

Figure 161: Well #2248 December 10, 2020, Left; October 26, 2023, Middle and Right [DEP]

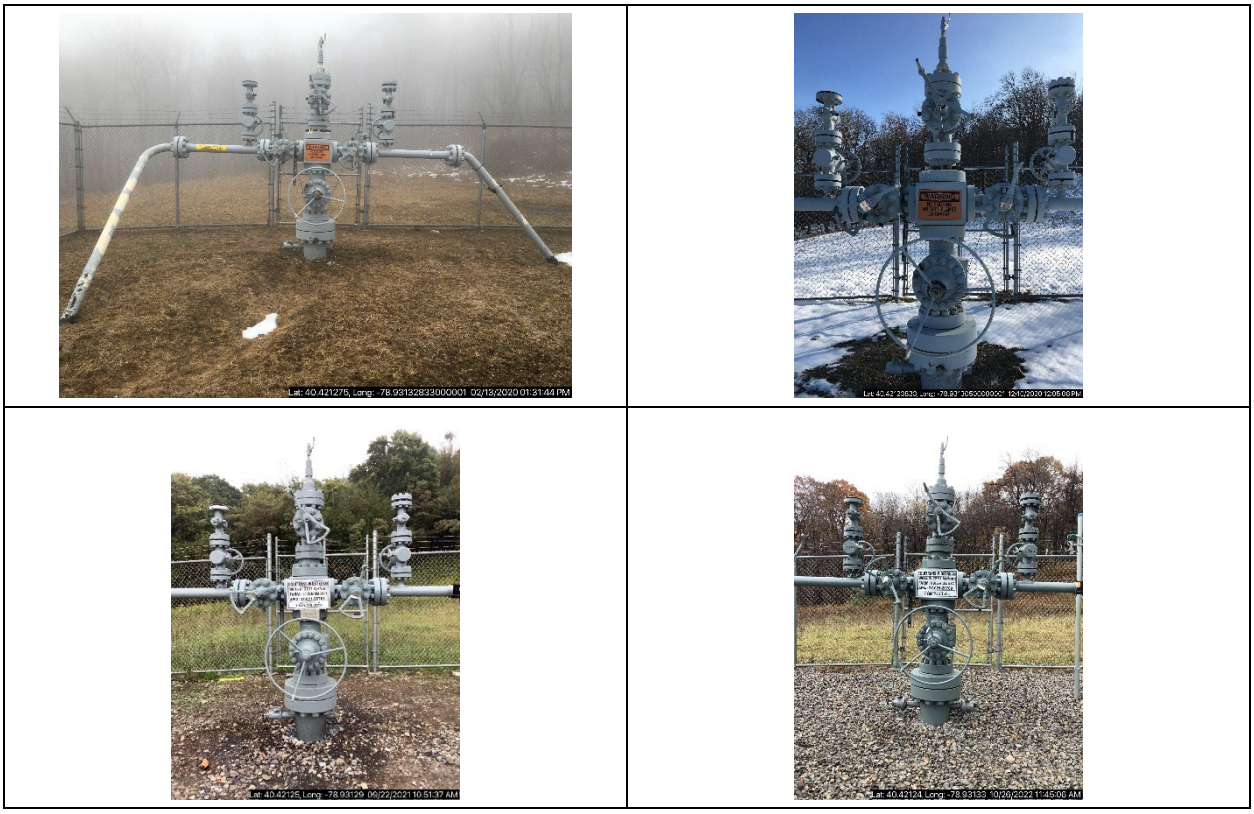

Figure 162: Well #2251 Dates Clockwise from Top Left, 2/13/2020, 12/10/2020, 9/22/2021, 10/26/2022 [DEP]

Because the other nine wells did not have the surface disturbed post incident, Blade worked with Equitrans to conduct a laser level survey. Figure 163 shows the survey being conducted by an Equitrans contractor per Blade guidelines at the #2254 wellsite. Elevation measurements were taken in the cardinal directions at a radius of 10 ft from the wellhead. The wellhead was considered the reference elevation (0 ft).

Figure 163: Well #2254 Laser Level Survey

Figure 164 shows the results of the survey in a color contour plot.

The y-axis and x-axis are in feet. The z-axis is elevation, where low spots are dark blue and high spots are light yellow. The contour range is from –0.8 to 0.8 ft elevation.

The wellhead orientation is depicted at the center of each plot. The side of the open valve is labeled. Some of these wells had relatively flat terrain. More contour lines represent terrain that is sloping more than wells that have fewer contour lines. Well #2245 has more contour lines and is sloped more than #2255, which is an example of a flat terrain well.

Two locations, namely #2253 and #2254, show the wellhead in a low spot, which is denoted by dark blue circles. As discussed in Section 6.1.2, these two wells showed top joint corrosion. These two wells had annulus valve heights of 4 – 8 in. Blade's interpretation is that these two wells with below–average annulus valve heights and in a low drainage spot correlate with ingress of water through the open annulus valve, resulting in top joint corrosion.

Well #2255, despite a low annulus valve height, has a constant low spot, so no flowing water or pooling of water may be feasible. This may explain the lack of top joint corrosion. Similarly, #2252 has a flat region around the wellhead despite low annulus valve height.

Well #2246 has a flatter terrain around the valve and a higher annulus valve height, thus enabling no water ingress and no top joint corrosion.

Finally, #2245 and #2247 exhibit some low levels of top joint corrosion. The valve height is high, but the drainage changes around the well and there may be movement locally.

The wells that have top joint wall loss have annulus valve heights of 4.5 – 18.5 in. Blade found only +/– 0.8 ft elevation changes. Blade's interpretation is that based on the laser level survey, locally pooled water would not be able to reach and enter *all* annulus valves, but entry into the lower valves is definitely feasible.

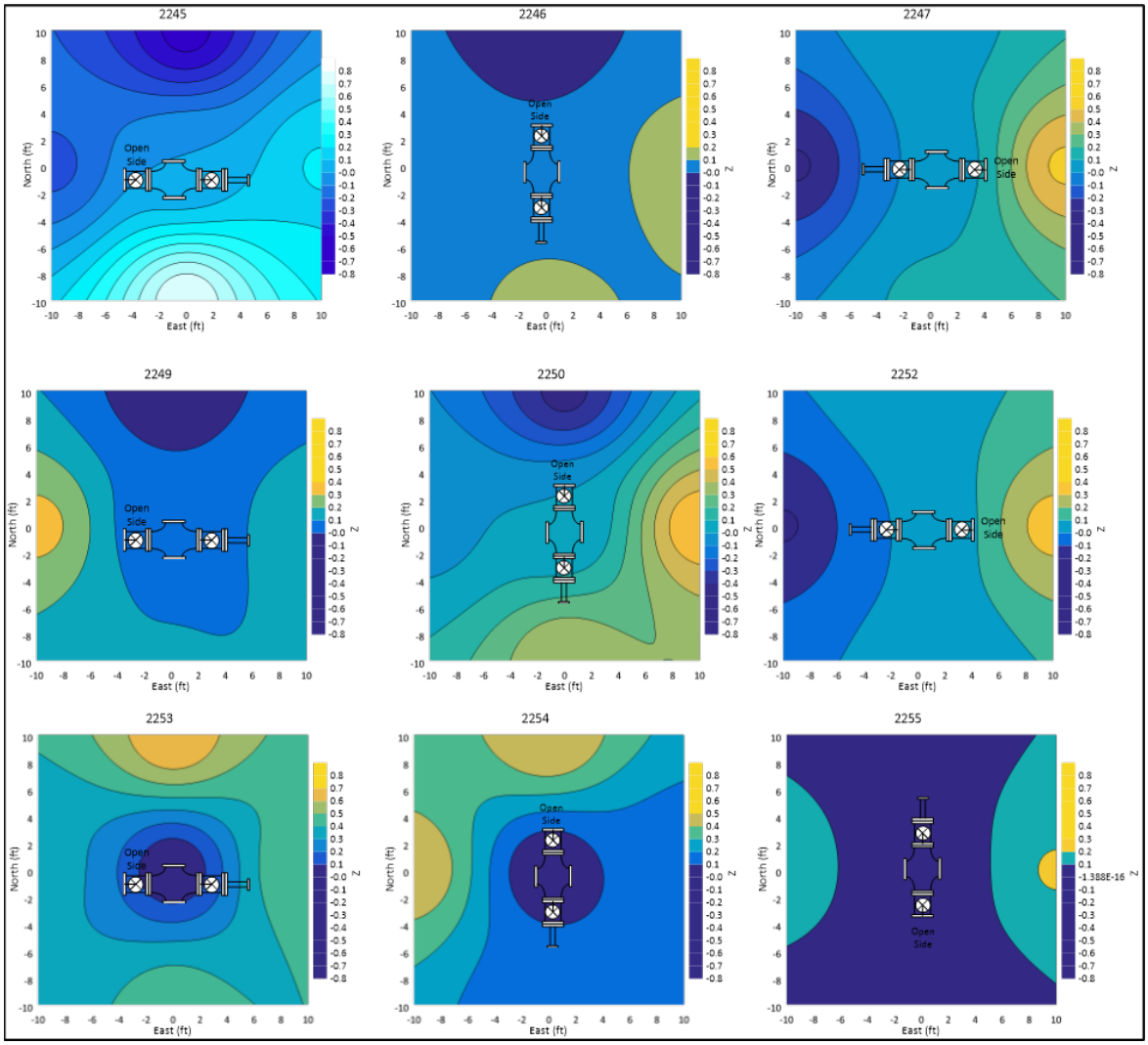

Figure 164: 10 ft x 10 ft Drainage Surveys for Nine Rager Mountain Wells, High Spot (Yellow), Low Spot (Blue)

During the site visits, Blade inspected the annulus valves. At Blade's request, Equitrans removed the annulus valves for further inspection of the annulus (the area adjacent to the casing and within the casing head). Figure 165 shows pictures of the annulus valves, material found in the annulus and the casing. The material found was mostly organic—primarily small dry fibrous, hay-like, woody debris. Mouse droppings were found only at the entrance of the annulus valve. Blade's opinion is that if mice brought in this organic material, droppings would be mixed with the debris. No droppings were found in the debris Blade's interpretation is that this organic matter was wind-blown or carried in by local pooling from intense precipitation.

Figure 165: Material Found in the Annulus

9.3 Integration and Interpretation

The primary source of water and debris ingress is the open annulus valve. PNG left the Rager Mountain annulus valves open. The PADEP inspected and recorded the position of these valves in monthly inspection reports. PNG provided Equitrans information regarding the Rager Mountain DEP inspections, and suggesting the DEP wanted annulus valves left open, i.e., “Annuals (sic) Valve Position (Wants them all Open – If Not need to explain why)” [6]. Equitrans maintained the previously established open annulus valve position at Rager Mountain.

The top joint corrosion was observed in #2244 where the 7 in. casing is uncemented from the cement stage tool to 2,940 feet. Wells #2251 and #2248 exhibited top joint corrosion and they are partially cemented. The top joint corrosion seems to affect wells independently of the quality of cement behind the production casing. Further, the presence of corrosion was associated with water and debris. The debris ingress would only be possible through the open annulus.

Consequently, the aqueous environment entering the annulus through the surface casing shoe appears improbable. Extensive debris was noted around the region of top joint corrosion in #2248 and #2251, and this debris is localized on the top region of the casing. An aqueous environment from the shoe cannot be responsible for the debris on the casing. Consequently, the totality of evidence of annulus valve pictures,

drainage analysis, and the nature of the top joint corrosion all point to the open valve being the primary pathway for water, air (oxygen), and organic and inorganic matter.

The water enters the annulus along with the debris. As the water drains or evaporates, the wet organic and inorganic matter (debris) remains on the production casing wall. The wet and dry cycles continue to introduce oxygen into the annulus environment, and further, the debris matter on the production casing facilitates the under-deposit corrosion. The same phenomena would be operable on the surface casing ID; however, the temperature would be significantly lower on the surface casing and result in a lower corrosion rate.

10 Magnetic Integrity Logging Limitations

10.1 Laser Scan Data vs. HR Vertilog (#2251 and #2248)

Equitrans sent the top joints of wells #2248 and #2251 to Blade in May 2023. Blade used a commercially available laser scanner (Creaform's HandySCAN 700) to acquire high-resolution 3D data of the corroded areas. The laser scan data was analyzed using Creaform's Pipecheck software. Figure 166 and Figure 237 (Appendix A.7) show the results of the laser scan analysis for wells #2248 and #2251, respectively. In each figure, the upper portion of (A) shows orange bars with blue numbers representing the deepest feature per foot. The y-axis is defect penetration in terms of percent wall thickness, and the x-axis is well depth in feet.

The deepest corrosion features for wells #2248 and #2251 were 55.5% and 65.2% NWT, respectively. Blade typically considers the accuracy of the laser scan depth measurements as +/– 5% compared to a manual pit gauge. Below the bar chart is a plot of blue dots showing individual pits. Each blue dot is the peak depth of each corrosion defect that is greater than 10% NWT. The bottom of (A) is a color contour plot showing the defect dimensions (length and width) in varying degrees of yellow to red; each color represents a range of corrosion depth.

In the color map, the green color reflects the 10% NWT threshold used in the analysis representing areas where the pipe is defect-free or has defects < 10% NWT. The y-axis is the clock position from 0 to 12 o'clock. The distribution of defects is circumferential and not along a specific clock position. The deepest defects (red shaded boxes) are approximately in the middle of the corroded areas. The figure's lower portion (B) shows the view from Baker Hughes Insight software (December 2022 HRVRT logs). The HRVRT shows a similar location of the corrosion as the laser scan data. The size comparison is discussed in Figure 166.

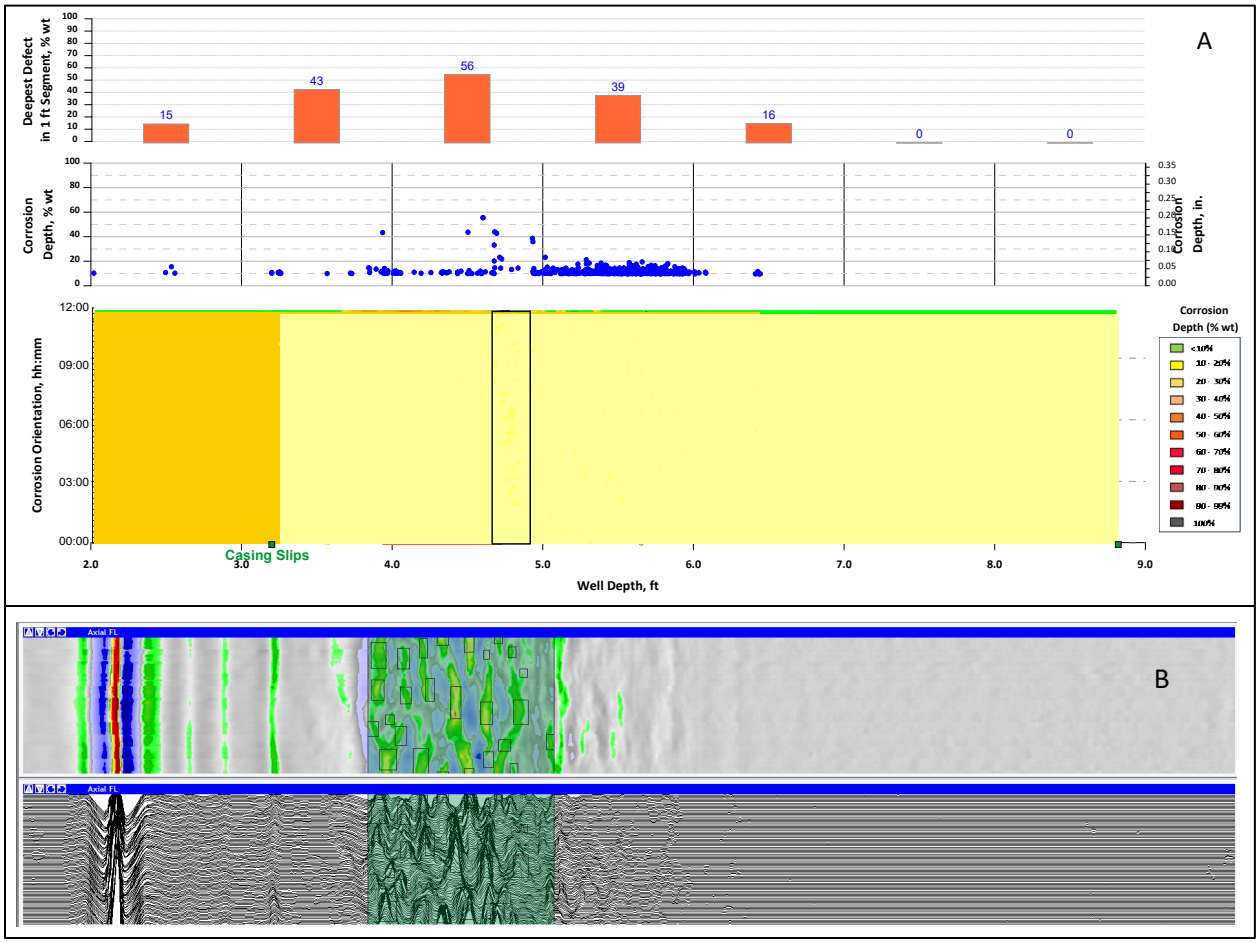

Figure 166: Laser Scan (A) and HRVRT (B) Data for the Top Joint of Well #2248

Appendix A.7 shows the laser scan defects denoted by shaded boxes (showing the length and width of the corrosion pits) and blue numbers (indicating the corrosion peak depths). In the same way, the red non-filled rectangles with black numbers are from the HRVRT metal loss (ML) features table. The defects have been shifted in well depth so that the indications from the casing slips are aligned. The orientation (i.e., clock position) has been rotated so the features match. There is generally good agreement; however, some boxes overlap while others do not. The cause of the misalignments is the difference between how the Pipecheck software and the HRVRT tool cluster defects.

Figure 167 shows Blade's feature-matching results of the laser scan and the HRVRT defects for wells #2248 and #2251 (December 2022). The tables on the right show that the HRVRT defects (denoted by black text) were matched to the corresponding measurements from the laser scan data. The right column (NDE Depth) is the laser scan data (denoted by blue text). The plots on the left are called unity plots, which are visual representations comparing one data set to another.

The y-axis is the HRVRT depth, and the x-axis is the more accurate laser scan depth. Both depths are in a percentage of the wall thickness. Points on the unity line (diagonal line with the origin at the bottom left corner) represent penetrations from the HRVRT that are identical to the laser scan values. Additional lines corresponding to 10, 15, and 20% wall thickness are shown above and below the central diagonal line. The HRVRT defects from wells #2248 and #2251 are within 16% of the laser scan data. The laser scan data reported deeper penetrations in 9 of the 15 defects. HRVRT reported deeper penetrations in 4 of the 15 defects, and 2 of the 15 defects were almost identical.

Blade's overall assessment of the HRVRT tool is that it performed reasonably well, considering the small dataset. At the time of writing, the top joint of well #2254 had been recovered but not laser scanned. The top joint of well #2253 has also been recovered and replaced. Data from these joints can be used to refine this assessment further.

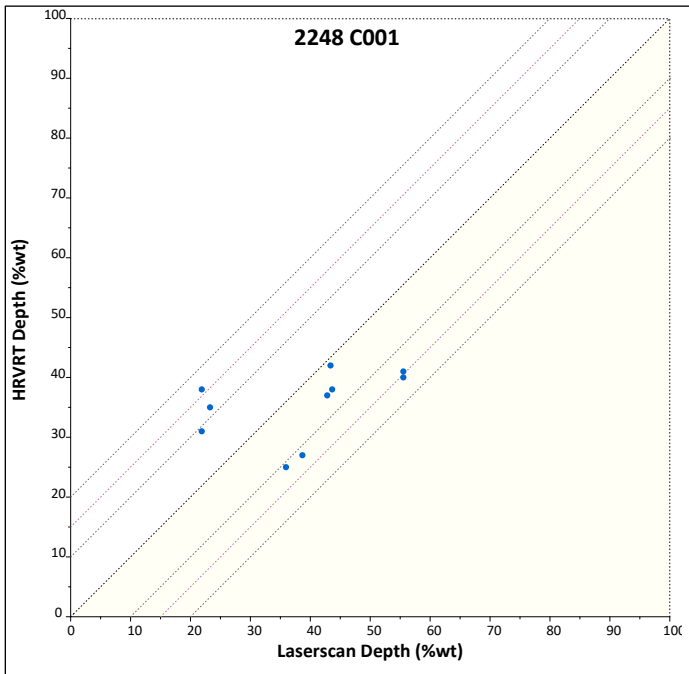

Log Depth	Identifier	Dim Class	ML-Length	ML-Width	ML-Depth	NDE Depth (%wt)
3.96	MLCB-1-1	CIGR	0.946	2.186	31	Within a cluster
4	MLCB-1-2	CIGR	1.156	3.06	35	Within a cluster
4	MLCB-1-3	GENE	1.367	3.81	31	Within a cluster
4.08	MLCB-1-4	GENE	1.588	3.123	42	43.4
4.09	MLCB-1-5	PITT	0.841	1.374	32	Within a cluster
4.18	MLCB-1-6	CIGR	1.156	2.81	32	Within a cluster
4.2	MLCB-1-7	CIGR	1.051	3.037	23	Within a cluster
4.22	MLCB-1-8	CIGR	1.051	2.477	26	Within a cluster
4.34	MLCB-1-9	GENE	1.472	3.878	33	Within a cluster
4.36	MLCB-1-10	CIGR	0.736	2.804	24	Within a cluster
4.4	MLCB-1-11	CIGR	0.847	3.372	27	Within a cluster
4.51	MLCB-1-12	CIGR	1.059	2.81	42	Within a cluster
4.61	MLCB-1-13	CIGR	0.946	4.809	37	Within a cluster
4.71	MLCB-1-14	CIGR	0.946	4.299	38	43.6
4.85	MLCB-1-15	CIGR	1.156	3.31	41	55.5
4.85	MLCB-1-16	CIGR	0.529	1.262	38	21.9
4.87	MLCB-1-17	CIGR	0.953	2.243	40	55.5
4.95	MLCB-1-18	CIGR	0.736	2.056	37	42.8
4.99	MLCB-1-19	PITT	1.164	1.686	35	23.3
5.05	MLCB-1-20	CIGR	0.736	1.495	31	21.9
5.07	MLCB-1-21	CIGR	0.736	1.561	27	38.7
5.12	MLCB-1-22	GENE	1.367	3.552	27	Within a cluster
5.14	MLCB-1-23	PITT	0.736	1.187	25	35.9
5.35	MLCB-1-24	CIGR	0.736	2.337	27	

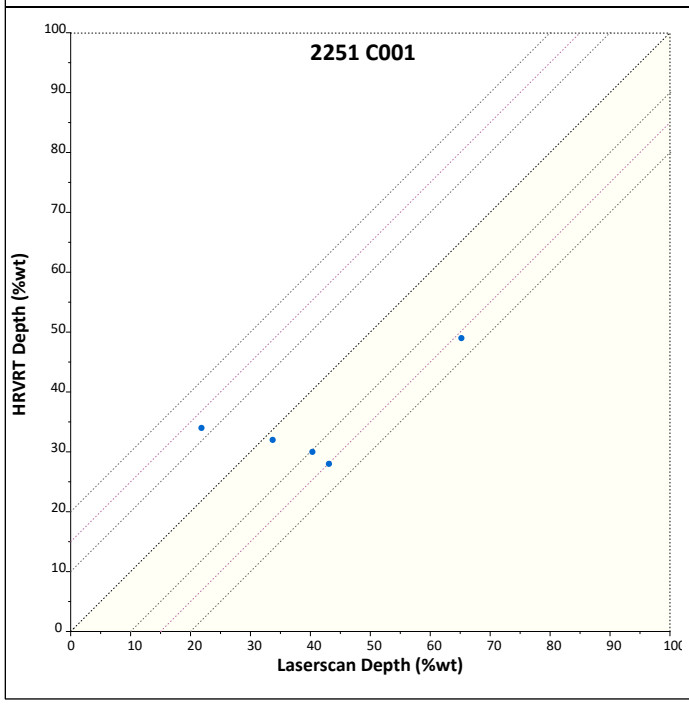

Log Depth	Identifier	Dim Class	ML-Length	ML-Width	ML-Depth	NDE Depth (%wt)
4.31	MLCB-1-1	GENE	1.807	2.623	28	43.1
4.61	MLCB-1-2	PITT	1.13	1.561	20	Within a cluster
4.75	MLCB-1-3	GENE	1.234	2.186	34	21.8
4.85	MLCB-1-4	CIGR	0.673	2.061	32	33.7
4.86	MLCB-1-5	PITT	1.122	1.686	30	Within a cluster
4.99	MLCB-1-6	PITT	1.009	1.749	49	65.2
5.21	MLCB-1-7	PITT	0.897	1.249	30	40.3

Figure 167: HRVRT Versus Laser Scan Data for Wells #2248 (Top) and #2251 (Bottom)

The defect profiles of #2248 and #2251 are distinctly different from #2244, as discussed in Section 10.2.

10.2 Corrosion Profiles in Well #2244

The corrosion area associated with well #2244 was measured in Blade's laboratory using a 3D laser scan, manual pit gauges, and manual 90° ultrasonic (UT) gauges. Figure 168 is a schematic of the observed corrosion profiles, which have the following characteristics:

- Axially long corroded areas with localized axial slotting features and small, deep pits
- Fully circumferential (360° around the casing tubular) and deep metal loss
- A relatively smooth corrosion profile (non-abrupt corrosion depth changes) along the casing axial length

It is well known in the NDE industry that such profiles are challenging for magnetic flux leakage (MFL) technology. The pipeline industry has studied this topic extensively. Blade has experience testing and evaluating MFL technologies for transmission pipelines [58]. Logging tools will exhibit similar technological limitations as the pipeline inline inspection (ILI) tools. Localized pitting or pinholes with general corrosion and wide-area wall loss sizing are a challenge for magnetic logging tools. These tools will also exhibit sizing challenges for axially and circumferentially smooth morphology, which was typical for #2244.

All three limitations are related to the physics of the MFL principles. Consequently, using the corrosion dimensions from the logging results will have limited failure pressure estimation and corrosion growth evaluation (by run comparison) capabilities.

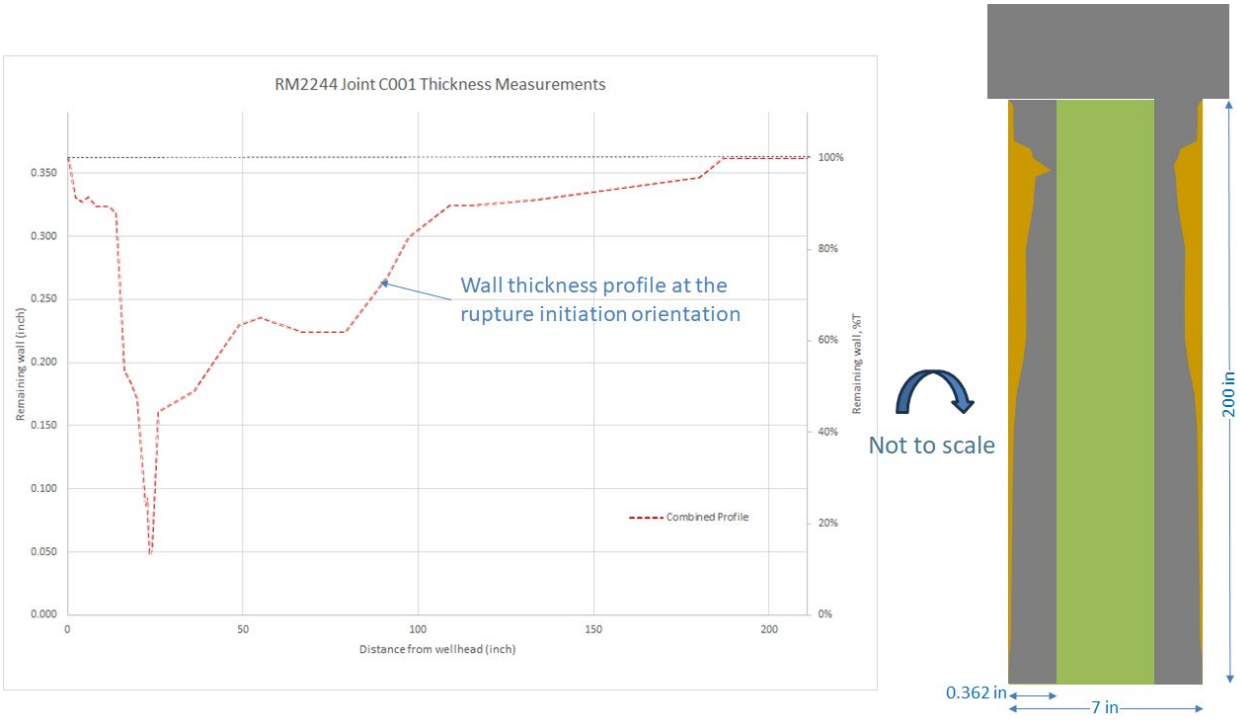

Figure 168: Corrosion Profiles for Well #2244

The corrosion sizing error measured in #2248 and #2251 was approximately 16% of NWT, as discussed in Section 10.1. The nature and morphology of corrosion in #2244 is distinctly different than the other two wells, as shown in Figure 169. The figure compares the corrosion wall loss % for the three well's top joints. The wall loss for #2244 shows a gradual change from approximately 13 ft to 4 ft where the wall thickness changes from nominal wall at 13 ft to almost 60% at 4.2 ft. From 4.2 ft to 3.6 ft, the wall

loss increases to over 80%. This is compared to #2248 and #2251 where the wall loss consists of pits (localized corrosion) with a maximum wall loss of approximately 60%. The uniform general corrosion that occurred in #2244 was not found in #2248 and #2251. The presence of general corrosion impacts the magnetic tool prediction, and the error in corrosion depth would be significantly greater than 16% NWT.

The implication of this assessment is that the limitations of magnetic tool technology affect their ability to quantify such defects, and consequently limit their ability to play a role in corrosion mitigation.

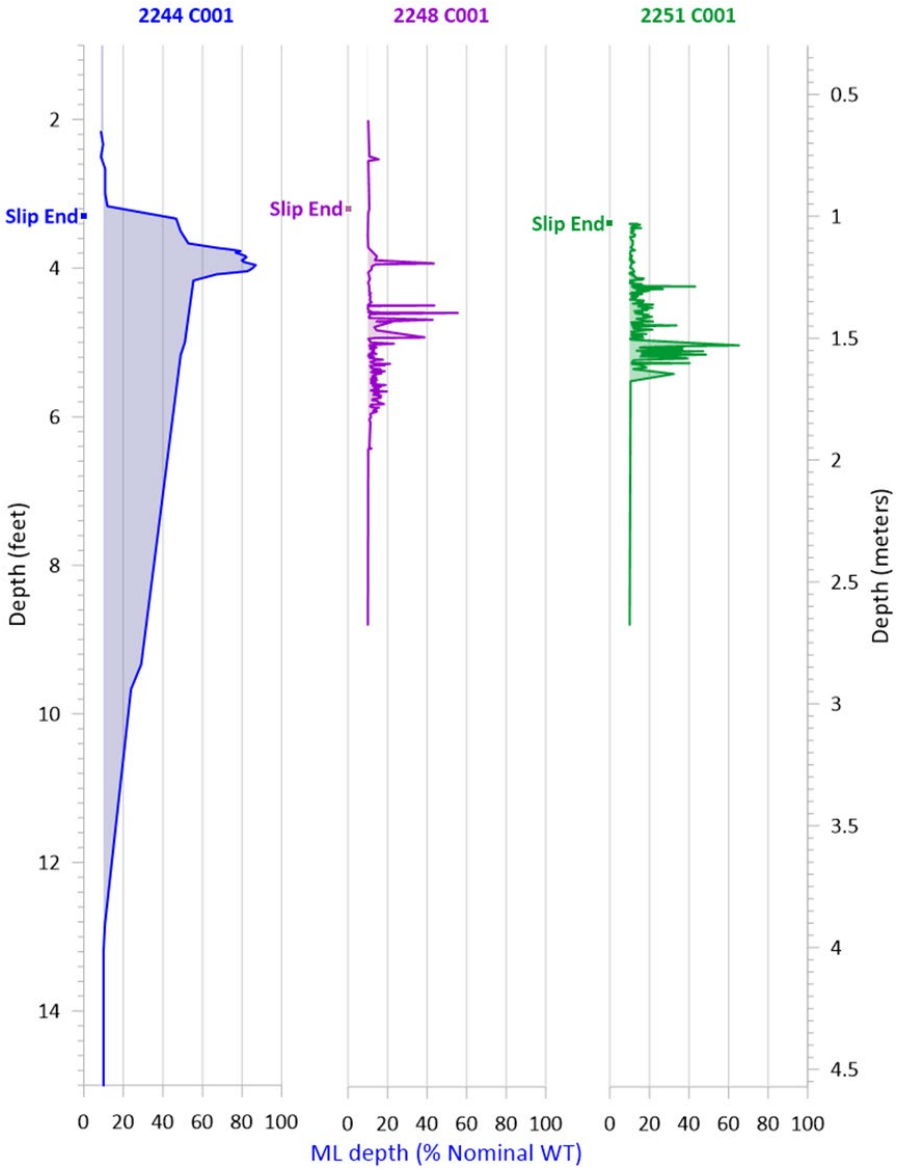

Figure 169: Laser Scan Depiction of the Corrosion on #2244, #2248, and #2251 as a Function of Depth

11 Internal Corrosion Threat

Multiple Rager Mountain wells exhibit internal corrosion, especially at the bottom of these wells. This was evidenced by the logging results, and the understanding of the reservoir that revealed a tendency to produce formation water towards the end of withdrawal season in some Rager Mountain wells.

11.1 Logging Results

Three wells demonstrated substantial internal corrosion features towards the bottom of the production casing and are evaluated here. Figure 170, Figure 171, and Figure 173 show the location, corrosion depth, corrosion growth estimate, and signal view from the HRVRT logs in 2016 and 2022 for the #2245, #2246, and #2253 wells, respectively.

The upper portion of each figure shows the location of the metal loss in the well by defect type. The y-axis is the depth of the well in feet. The left two tracks show the metal loss (ML) in terms of percentage of wall thickness for 2022 and 2016. The next two tracks show corrosion orientation, and the right-hand track shows the wall loss. Blue dots represent internal metal loss, and pink dots represent external metal loss. For these three plots, only the deeper portions of the well are shown.

For the #2245 well (Figure 170), internal corrosion is present at approximately 7,200 – 7,300 ft. External corrosion is not typically present at these depths. As shown in Figure 170, the internal corrosion depth and location have generally remained unchanged. There is very little evidence of corrosion growth. The bottom of each figure shows a signal view of a small portion of the log. This image shows the depth of the well on the x-axis; the flux leakage lines are shown horizontally.

Defects are shown in green boxes with numbers representing metal loss as a percentage of wall thickness. Some defects appear to grow between logs and are denoted by red triangles on the Depth Change track. Other defects appear to shrink and are denoted by green triangles. On an overall basis for the #2245 well, the corrosion does not appear to be growing. However, if one just focuses on the anomalies that exhibit growth, the average is around 4 mpy, with the maximum around 13 mpy.

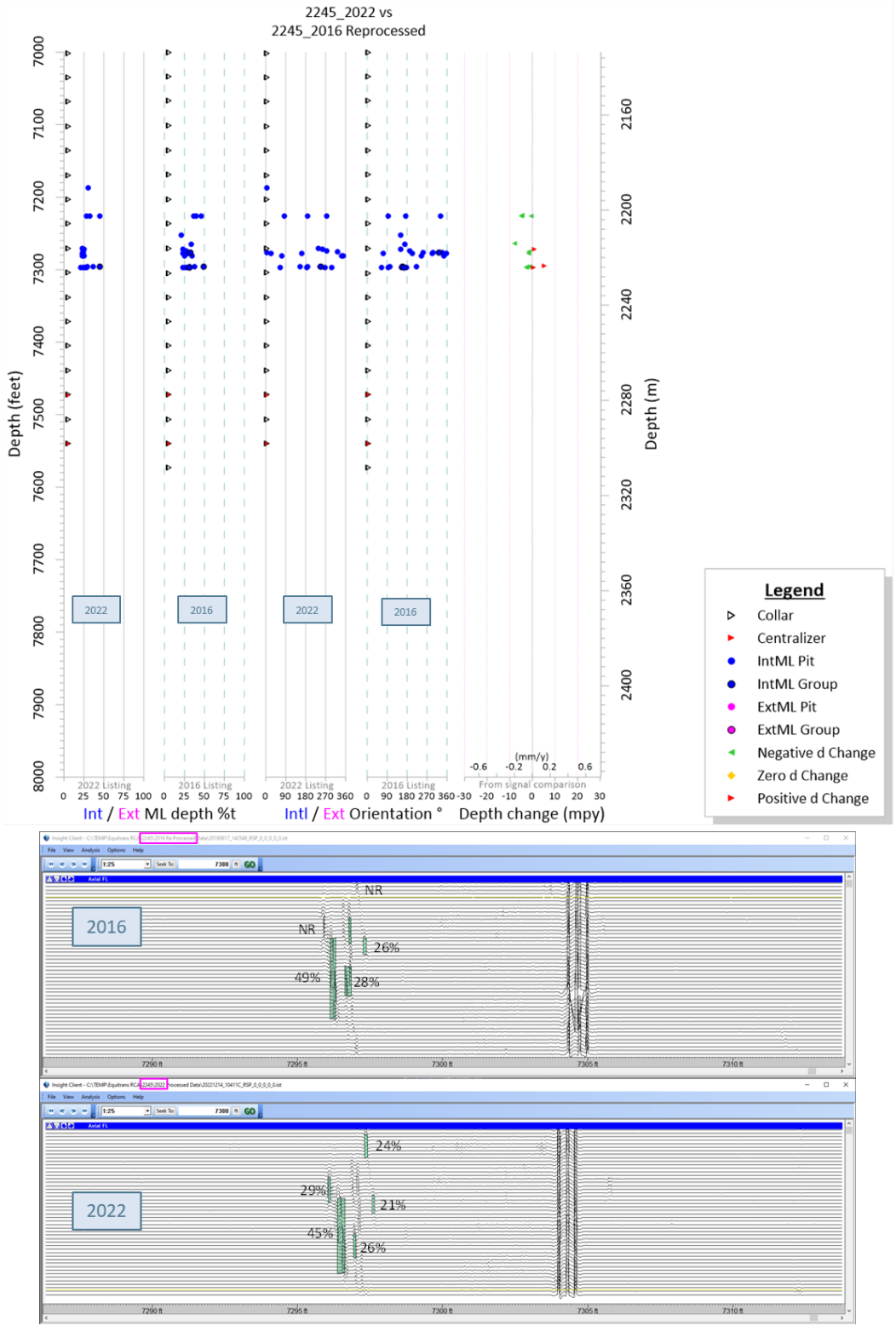

Figure 170: Internal Corrosion, Well #2245

Well #2246 has extensive internal corrosion from 6,000 to approximately 7,600 ft over a larger region of the casing. It is important to note that #2246 is an observation well, and as shown in Figure 172, the shut-in pressures of #2246 do not mimic the other storage wells starting in the years 2017 – 2018. This behavior is reflective of significant water at the bottom of well #2246, starting in years 2017 and 2018. This would have contributed to the internal corrosion at #2246. As shown in Figure 171, the defect depths are high, and corrosion rates range from zero to approximately 29 mpy. The average corrosion rate is approximately 5 mpy. Numerous defects exist that are not growing.

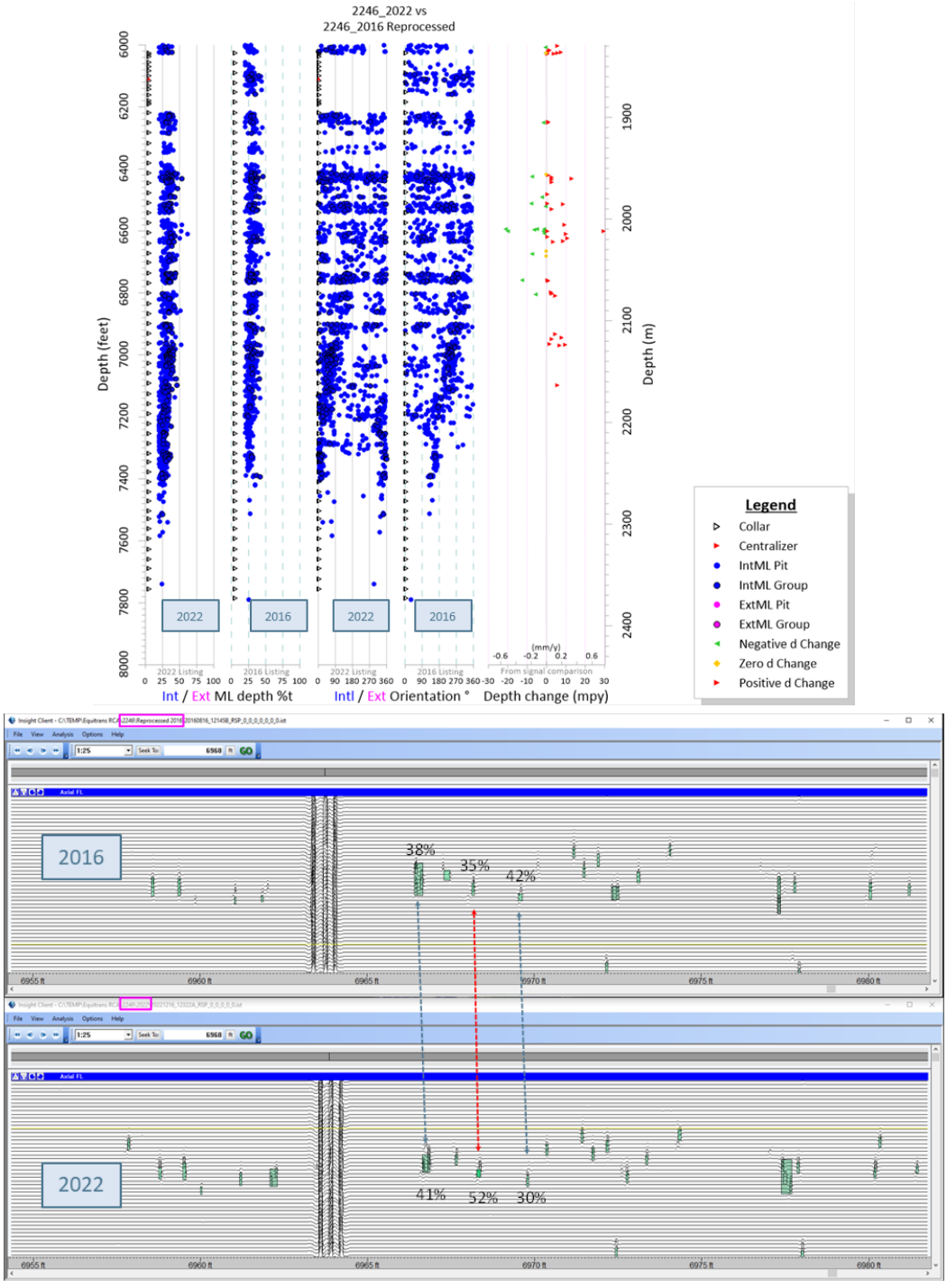

Figure 171: Internal Corrosion, Well #2246

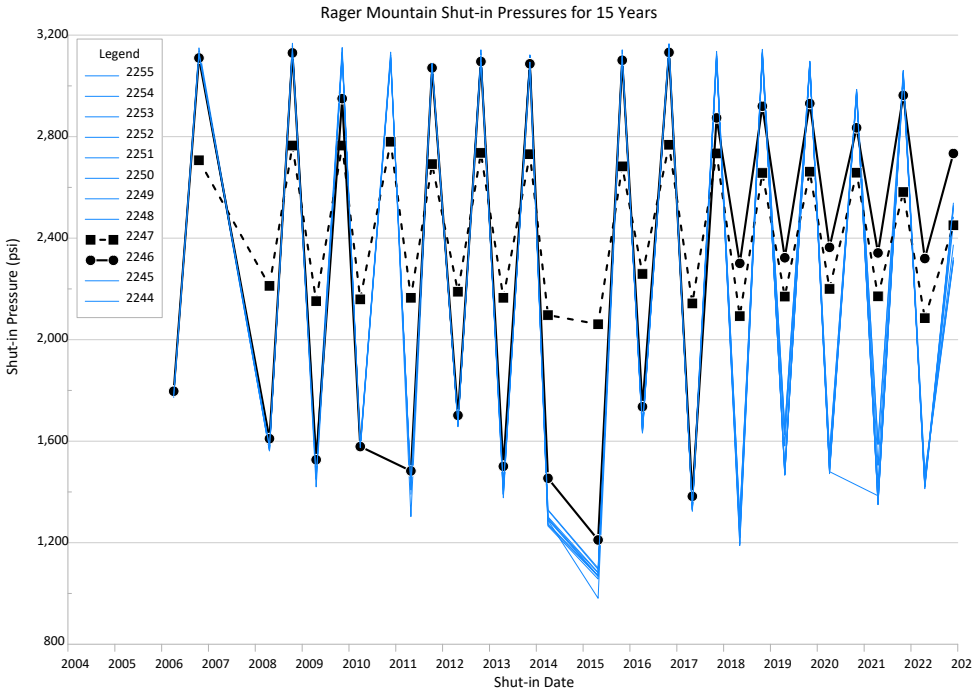

Figure 172: Shut-in Pressures for all Wells, Including the Observation Wells.

For the #2253 well, logging data from December 2022 was missing because the HRVRT log did not reach the bottom of the well. A cleanout using a mill and motor on coiled tubing (CT) was performed in late July 2023. After the well was cleaned out, HRVRT and caliper log data were acquired. A large region of internal corrosion exists from 7,350 to 7,650 feet.

The nature and extent of corrosion did not change between 2016 and 2023, as shown in Figure 173. The corrosion rate could not be estimated in this region because of the large amount of localized corrosion. Further, a comparison was made with the multi-finger caliper data as shown in Figure 174, confirming no generalized wall thinning, but more of a pitting corrosion that did not appear to have grown between 2016 and 2022.

This well was drilled as a storage well in 2010, and the log in 2016 showed extensive internal corrosion, as shown in Figure 173. Reports of water production in this well seem to indicate water is trapped within the crest of a structure. The water production may have been exhausted after a period of gas withdrawal. The log data does not indicate any growth in the 2022 log data.

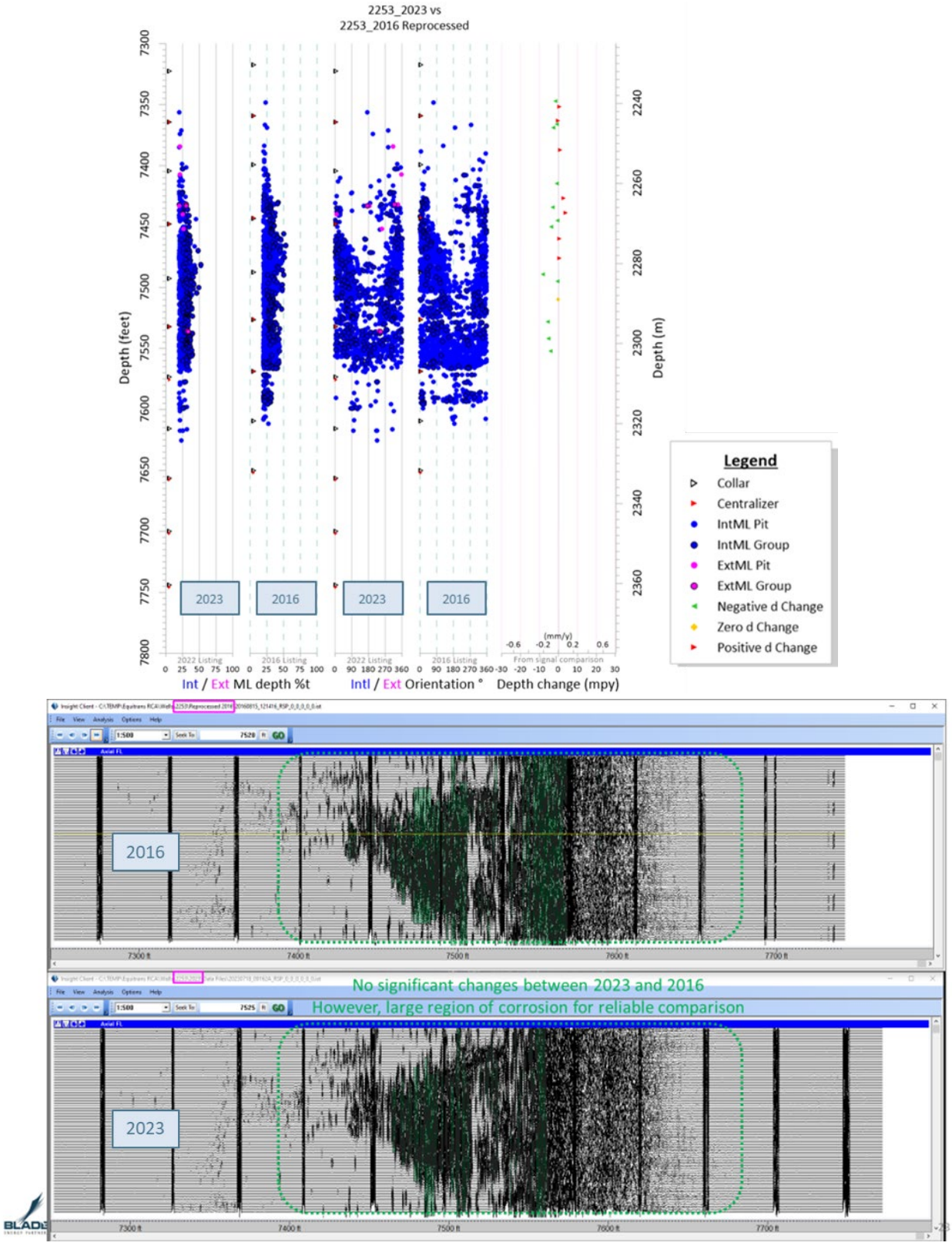

Figure 173: Internal Corrosion, Well #2253

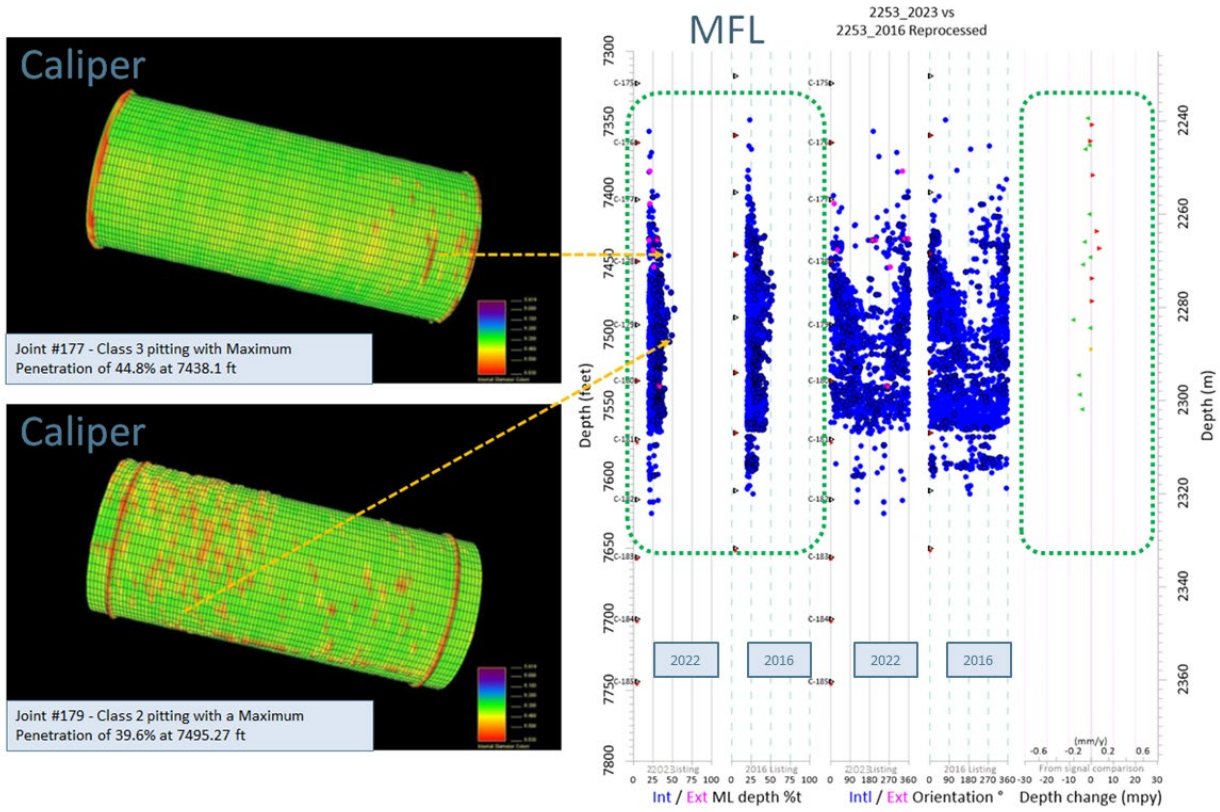

Figure 174: Internal Corrosion—HRVRT Log Compared with Caliper for #2253-July 2023 Logs

11.2 Corrosion Modeling

The intent of this section is to estimate the internal corrosion rate using gas and brine composition, pressure, and temperature profiles. A commercially available thermodynamic software called OLI was used to establish corrosion tendencies.

Analysis of gas samples collected from Rager Mountain wells on May 22, 2023, was used for establishing the gas composition for modeling (Table 30). Well #2245 gas composition was used as input, along with the highest CO_2 concentration of 0.32%. Another crucial input was the brine composition. The pond data was available, as shown in Table 31.

The brine concentration was used as input to the model for reconciliation. Oxygen was not input to the model because no oxygen was expected from the formation. The analysis did not include bicarbonate, but formation water typically contains brine, and a concentration of 200 ppm was assumed here. Two separate models were run with and without bicarbonate.

Table 30. Gas Samples Collected from Rager Mountain Wells [59]

Gas Samples Composition					
RL Laughlin Lab No.	Sample Name	Sample Date	Sample Time	Field Name	CO_2 %
12467-1	RAG 2244 Vent	5/22/2023	3:45	Rager Storage Field	0.008
12467-2	RAG 2245 Vent	5/22/2023	9:45	Rager Storage Field	0.025
12467-3	RAG 2245 Wellhead	5/22/2023	15:15	Rager Storage Field	0.31
12467-4	RAG 2246 Vent	5/22/2023	12:00	Rager Storage Field	0.018
12467-5	RAG 2246 Wellhead	5/22/2023	10:45	Rager Storage Field	0.32
12467-6	RAG 2247 Vent	5/22/2023	10:15	Rager Storage Field	0.038
12467-7	RAG 2247 Wellhead	5/22/2023	11:50	Rager Storage Field	0.31
12467-8	RAG 2248 Vent	5/22/2023	9:45	Rager Storage Field	nd
12467-9	RAG 2248 Wellhead	5/22/2023	8:40	Rager Storage Field	nd
12467-10	RAG 2249 Vent	5/22/2023	9:20	Rager Storage Field	0.013
12467-11	RAG 2249 Wellhead	5/22/2023	15:15	Rager Storage Field	0.32
12467-12	RAG 2250 Vent	5/22/2023	14:20	Rager Storage Field	0.040
12467-13	RAG 2250 Wellhead	5/22/2023	14:30	Rager Storage Field	0.31
12467-14	RAG 2251 Vent	5/22/2023	13:40	Rager Storage Field	0.14
12467-15	RAG 2251 Wellhead	5/22/2023	13:45	Rager Storage Field	0.26
12467-16	RAG 2252 Vent	5/22/2023	13:25	Rager Storage Field	0.20
12467-17	RAG 2252 Wellhead	5/22/2023	14:00	Rager Storage Field	0.31
12467-18	RAG 2253 Vent	5/22/2023	14:20	Rager Storage Field	0.32
12467-19	RAG 2253 Wellhead	5/22/2023	12:55	Rager Storage Field	0.31
12467-20	RAG 2254 Vent	5/22/2023	10:15	Rager Storage Field	0.14
12467-21	RAG 2254 Wellhead	5/22/2023	13:10	Rager Storage Field	0.32
12467-22	RAG 2255 Vent	5/22/2023	14:50	Rager Storage Field	0.020
12467-23	RAG 2255 Wellhead	5/22/2023	15:00	Rager Storage Field	0.29

Table 31. Concentration of the Chemical Constituents in Equitrans Rager Mtn. Pond [60]

Laboratory Sample ID: AWD4670-01 (Water/Grab)

Analyte	Result	MDL	RL	Units	Date / Time Analyzed	Analytical Method	* Analyst	Note
Analyses to be performed immediately upon sampling. See Definition indicated by: #								
# pH @ 22.7°C	5.62			pH Units	04/27/22 11:05	SM 4500-H+B-11	jal	
Conventional Chemistry Parameters by SM/EPA Methods								
Biochemical Oxygen Demand	234		20.0	mg/l	04/22/22 21:30	SM(20) 5210B-97	drw	D6
Chloride	6500		500	mg/l	04/28/22 18:34	EPA 300.0/2.1	bdw	
Chemical Oxygen Demand	980		150	mg/l	04/25/22 19:50	HACH 8000	dmm	
Nitrate as N	<2.000		2.000	mg/l	04/22/22 16:26	EPA 300.0/2.1	bdw	
Nitrite as N	<0.400		0.400	mg/l	04/22/22 16:26	EPA 300.0/2.1	bdw	
Total Dissolved Solids	9890		100	mg/l	04/25/22 15:50	SM 2540C-11	ark	
Total Suspended Solids	23.6		1.60	mg/l	04/22/22 10:28	SM 2540D-11	ark	K
Total Kjeldahl Nitrogen	6.380		1.000	mg/l	05/05/22 00:46	SM 4500NorgC-11/ASTMD6919-09	mmd	
Physical Parameters by APHA/ASTM/EPA Methods								
Ammonia as N	3.474		0.2000	mg/l	04/29/22 21:33	ASTM D6919-09	AKP	

The pressure ranges from 1,450 psi (100 bar)–3,500 psi (241.3 bar). The separator is at a temperature of 46°F and inlet pressure of 2,000 psi. The corrosion is considered to occur during the withdrawal season, when a water-to-gas ratio is a maximum of 300 bbl/D: 47 MMscf/D, i.e., 6.4 bbl/MMscf/D.

The OLI model is shown in Figure 175. The brine (bbl/d) is mixed with the gas (MMscf/D) in the ratio of 0.1:10, a conservative estimate, and mixed at the separator conditions of 46°F and 2,000 psi. The liquid phase is separated, and the corrosion rate is calculated for a temperature range of 75°F to 200°F.

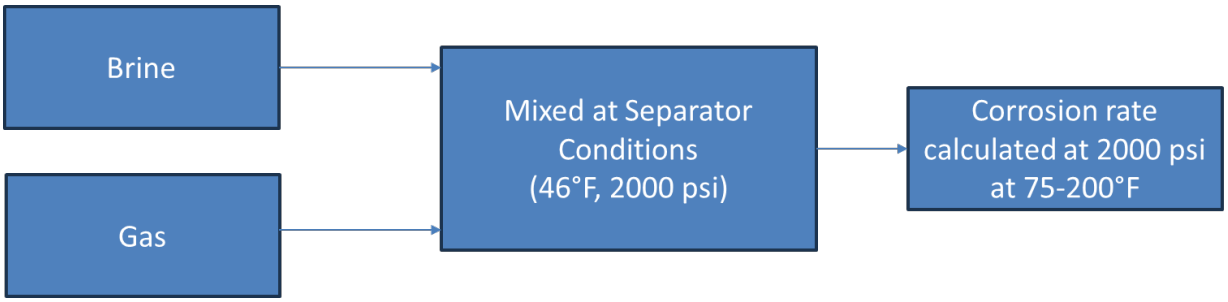

Figure 175. OLI Model – Brine without Bicarbonate – for Corrosion Rate Calculation

Table 32 shows the reconciled gas composition. The CO_2 mole % is 0.32%.

Table 32. Reconciled Gas Composition

Component	mole%	Reconciled (mole %)
Nitrogen	0.46	0.46
Carbon dioxide	0.32	**0.32**
Methane	96.07	95.79
Ethane	2.77	2.76
Propane	0.25	0.25
Isobutane	0.03	0.03
n-Butane	0.04	0.04
Isopentane	0.02	0.02
n-Pentane	0.01	0.01
n-Hexane	0.03	0.03

Table 33 lists the reconciled brine concentration used for the model. The chloride concentration is 6,500 mg/L.

Table 33. Reconciled Brine Composition

Brine Composition		
Cations (mg/L)	Input	Reconciled
Sodium (+1)	1,000	4,215
Anions (mg/L)	Input	Reconciled
Chloride ion (–1)	6,500	6,500

The maximum corrosion rate is 4.2 mm/yr at 165°F (Figure 176). The pH is in the range of 4.1 – 4.3.

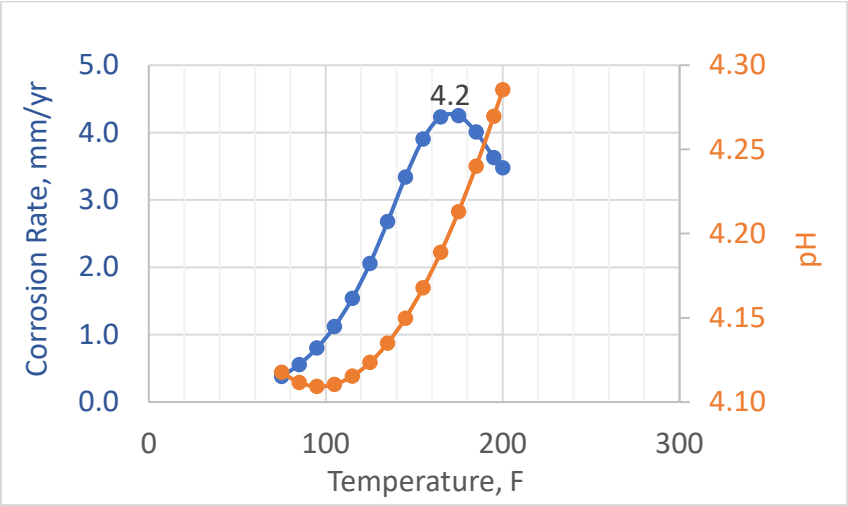

Figure 176. Corrosion Rate and pH as a Function of Temperature—Brine without Bicarbonate

The brine with bicarbonate is mixed with gas at the separator conditions of 46°F and 2,000 psi. The corrosion rate is calculated using the liquid phase from a temperature of 75°F to 200°F.

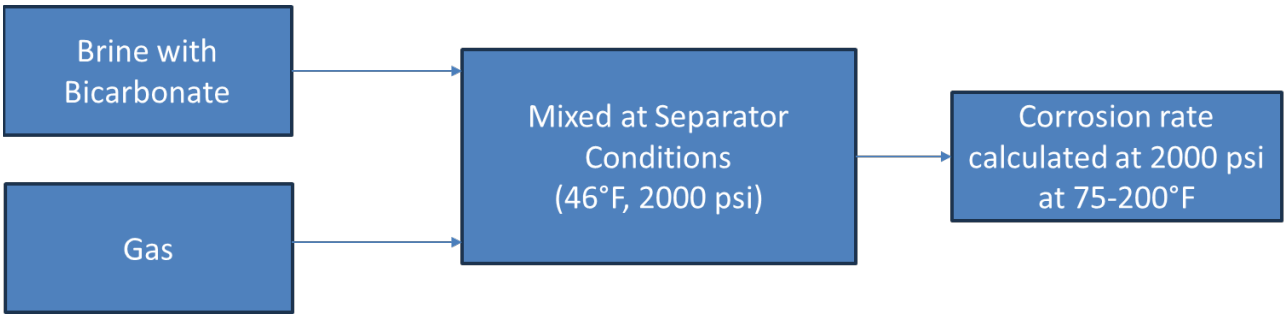

Figure 177. OLI Model – Brine with Bicarbonate – for Corrosion Rate Calculation

Table 34 lists the reconciled brine components used in the OLI model. The sodium ion is 4,290 ppm, chloride is 6,500 ppm, and bicarbonate is 200 ppm.

Table 34. Reconciled Brine Composition

Brine		
Cations (mg/L)	**Input**	**Reconciled**
Sodium (+1)	1,000	4,290
Anions (mg/L)		
Chloride ion (–1)	6,500	6,500
Bicarbonate (–1)	200	200

The maximum corrosion rate is 2 mm/yr at 185°F. The pH is in the range of 5.6 – 5.7. The corrosion rate decreased after bicarbonate inclusion. The maximum corrosion rate without bicarbonate is 4.2 mm/yr, and with bicarbonate is 2.0 mm/yr.

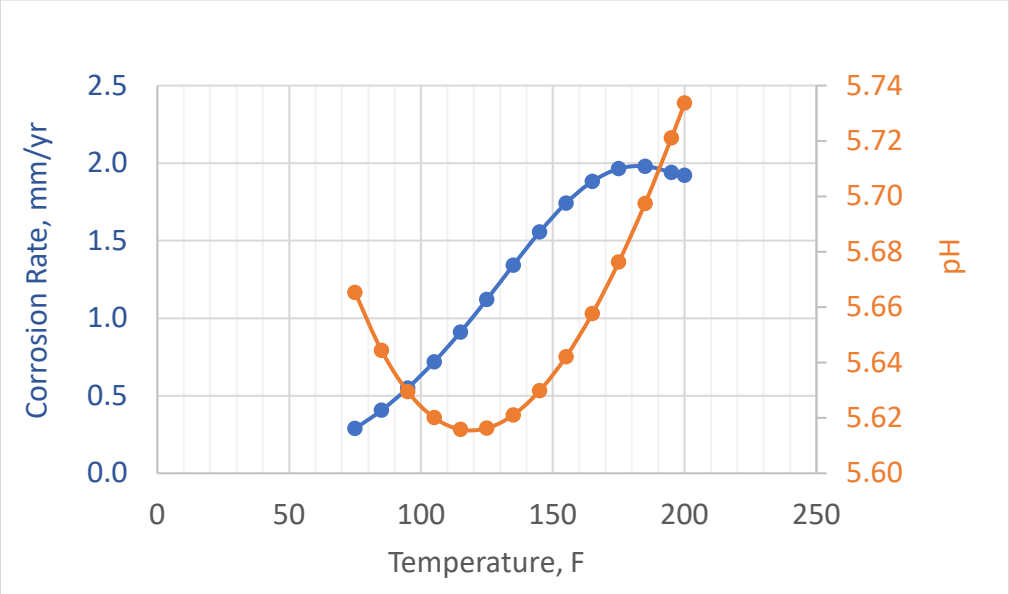

Figure 178. Corrosion Rate and pH as a Function of Temperature – Brine with Bicarbonate.

The corrosion mechanism is considered operative primarily during the withdrawal season. This is reflected in the analysis in Table 35.

11.3 Implications

11.3.1 Wells #2245, #2246, #2253

The maximum corrosion rate from log comparison for #2246 was 29 mpy, whereas the modeling showed 23 to 36, depending (considering a five-month withdrawal period) on the temperature, as shown in Table 35. The modeling shows the higher-end corrosion rates, and because the corrosion rate in the presence of bicarbonate was closer to maximum from logging, that was used to predict wall thickness.

Table 35: Remaining Wall Thickness by Year Based on Bicarbonate Corrosion Model Predictions

Well	OD (in.)	Wt (ppf)	NWT (in.)	Log Metal Loss (%)	Temp (°F)	Annual WT Loss (in.)	Remaining Wall Thickness by Year					
							2022	2023	2024	2025	2026	2027
2245	5.5	17	0.304	45%	132	0.023	0.167	0.144	0.120	0.097	0.074	0.050
2246	5.5	17	0.304	62%	168	0.036	0.116	0.080	0.044	0.008	—	—
2253	7	26	0.362	52%	154	0.032	0.174	0.142	0.109	0.077	—	—

Well #2246 has the highest corrosion rate and exhibits growth between the 2016 and 2022 log runs. The modeling predictions are broadly in line with logging data. Short-term and longer-term actions to mitigate should be considered. This will be further discussed in the next section. It is important that all indications of internal corrosion require consideration of quarterly batch treating the wells with inhibitors. There is a possibility that these internal corrosion defects grow despite the batch treatments, it is recommended that these three wells be logged by the end of 2025. After the next log the batch treatment effectiveness should be quantified, and logging frequency should be accordingly adjusted.

11.3.2 Well #2244

An internal corrosion anomaly was identified during the 2016 log run. The anomaly appears to reflect a pitting corrosion, as shown in Figure 179 with an approximate depth of 44% NWT. It is important to log this anomaly to determine if the corrosion is growing or not. This is a high deliverability well, and internal corrosion should not have grown, however confirmation of this is necessary especially in the absence of a 2022 log for this well.

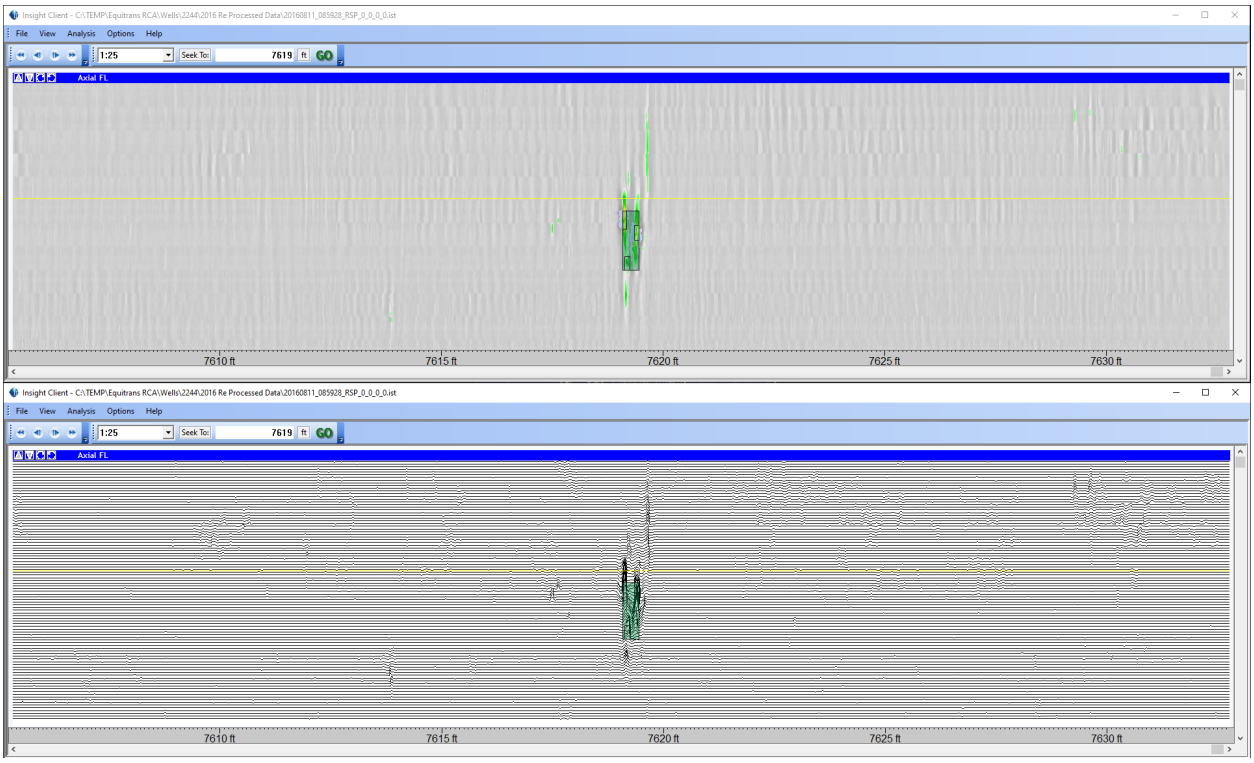

Figure 179: Well #2244, Raw Signal with Grey Scale and Flux Lines Showing the Internal Defect at around 7,618 ft.

12 Well #2244 Flow Rate Analysis

Flow rate estimates with flowing pressure and temperature estimates are useful for the root cause analysis. This flow assurance work estimated the flow rate from well #2244 by two flow paths:

- Flow rate from bottomhole inflow up to the measured annulus pressure
- Flow rate at surface from the measured annulus pressure to the atmosphere via the annulus valve

The annulus valve was attached to the 9 5/8 in. casing head via a threaded nipple. Figure 180 shows the annulus valve. The minimum ID through this annulus valve and nipple was 1.67 in.

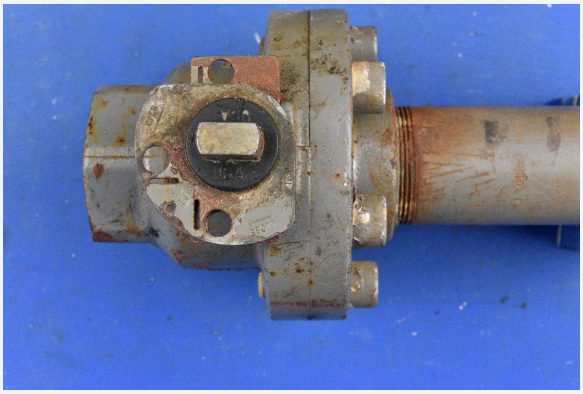

Figure 180: Annulus Valve

Figure 181 shows the two flow paths for the estimated rates. This work used Petroleum Experts PROSPER[i] application for well modeling. For both flow paths, the flow rates were estimated using the annulus pressures measured in the morning before any well work was done that day. The procedure assumed that the well blowout cleaned out any fluids in the paths from the previous day workovers/kill attempts—only gas flowed at that time.

[i] https://www.petex.com/products/ipm-suite/prosper/

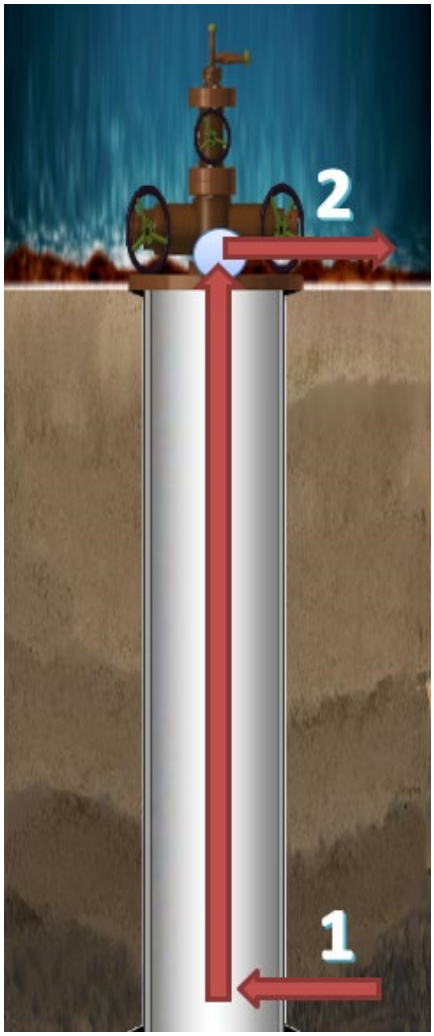

Figure 181: Flow Rate Estimate Paths

Flow Path 1, bottomhole to surface rate calculation process:

a. Used storage gas composition.
b. Used measured annulus pressure.
c. Modeled Inflow Performance Relationship (IPR) matched to a PLT and a falloff test.
d. Modeled Vertical Lift Profile (VLP) correlated from the well schematic.
e. Predicted choke inlet gas rate and temperature.

Flow Path 2, surface to atmospheric rate calculation process:

a. Used storage gas composition.
b. Used measured annulus pressure and Flow Path 1 estimated temperature.
c. Modeled the Elf choke calculation.
d. Estimated choke outlet gas rate and temperature.

Table 36 lists the storage gas composition. The high percentage of methane dominates the calculations, leaving the exact percentages of the remaining components not as significant in determining rates.

Table 36: Rager Well #2244 Storage Gas Composition During Blowout

Component	Molecular Weight	Mole Percent
CO_2	44	0.12
N_2	28	0.32
C1	16	96.30
C2	30	2.78
C3	44	0.22
C4+	72	0.26

Table 37 lists the measured annulus pressures for Flow Paths 1 and 2. Only the annulus pressures measured at the start of the workday were used to avoid possible contamination from the day's work. It was assumed that overnight, until the well was killed, the gas would have removed any fluids entering the well during the day.

Table 37: Rager Well #2244 Annulus Pressure vs. Time

Date	Time	Annulus Pressure (psig)
11/06/2022	00:00	—
11/07/2022	00:00	—
11/08/2022	11:23	1,311.1
11/09/2022	07:00	1,253.9
11/10/2022	07:00	1,200
11/11/2022	07:00	1,100
11/12/2022	07:00	1,100
11/13/2022	07:10	1,090
11/14/2022	07:00	1,077
11/15/2022	07:00	1,190
11/16/2022	07:00	1,142
11/17/2022	07:00	1,115
11/18/2022	07:00	—

Table 38 shows the drainage area average pressure used for well #2244 during the blowout. The work assumed that average pressures could be estimated from the monitoring pressures of wells #2250 and #2254. Wellhead pressures were converted to bottomhole using PROSPER. Well #2244's average pressure was set to the average bottomhole pressure of wells #2250 and #2254.

Table 38: Rager Well #2244 Drainage Area Average Pressure During Blowout

Date	Time	#2250 WHP (psig)	#2250 BHP Calc (psig)	#2254 WHP (psig)	#2254 BHP Calc (psig)	#2244 P-Res (psig)
11/06/2022	00:00	2,940	3,515	2,870	3,427	3,471

Date	Time	#2250 WHP (psig)	#2250 BHP Calc (psig)	#2254 WHP (psig)	#2254 BHP Calc (psig)	#2244 P-Res (psig)
11/07/2022	00:00	2,880	3,445	2,810	3,358	3,402
11/08/2022	11:23	2,830	3,387	2,750	3,288	3,338
11/09/2022	07:00	2,790	3,341	2,690	3,218	3,280
11/10/2022	07:00	2,730	3,271	2,630	3,148	3,209
11/11/2022	07:00	2,670	3,201	2,570	3,078	3,139
11/12/2022	07:00	2,610	3,131	2,510	3,007	3,069
11/13/2022	07:10	2,550	3,060	2,460	2,948	3,004
11/14/2022	07:00	2,500	3,001	2,410	2,948	2,975
11/15/2022	07:00	2,430	2,919	2,340	2,807	2,863
11/16/2022	07:00	2,360	2,836	2,280	2,736	2,786
11/17/2022	07:00	2,290	2,753	2,210	2,652	2,702
11/18/2022	07:00	—	—	—	—	2,619

12.1 Flow Path Models

12.1.1 Flow Path 1 Model: Bottomhole to Surface

This work estimated well #2244's injection/withdrawal rates at bottomhole conditions based on the formation volume around the well where gas is injected/withdrawn. The properties required are:

- An effective permeability-thickness of the formation, and
- The average pressure of the injection/withdrawal volume of investigation.

This work determined the inflow performance properties for the well based on the report by Eastern Reservoir Services titled "Well Test Report, 3369 Read 1, Dominion Peoples," June 2003. This report covered a production logging tool (PLT) and injection falloff test. Figure 182, copied from the report, shows that the gas was injected into 16 feet of the Oriskany formation, and Figure 183, also copied form the report, shows the summary of the falloff test.

7698' to 7740'	Less than 1% of Total gas flow
7740' to 7780'	Less than 1% of Total gas flow
7780' to 7796'	More than 99% of Total gas flow 16' Oriskany

Figure 182: Well Test Report—PLT Injection Gas Distribution

Initial wellhead pressure	2222 Psig		Initial bottomhole inj. pressure	2673 Psig
Final wellhead flowing pressure	2222 Psig		Final bottomhole flowing press.	N/a
Final wellhead fall-off press.	2196 Psig		Final bottomhole shut-in press.	2652 Psig
Av. bottomhole flowing temp.	122.5 degF		Max. bottomhole temp.	126 degF
Fluid top at start of test (measured from master valve)	No fluid		Fluid top at end of test (measured from master valve)	No fluid
TD measurement (from master valve)	7800'		Maximum interference observed	N/a
Injection rate prior shut-in =		11117 Mscf/d		

Figure 183: #2244 Well Test Report—Falloff Summary

Figure 184 shows, using Petroleum Experts PROSPER, the Jones Reservoir model inflow match of the test data. The effective permeability is 210 mD for the 16 feet of formation.

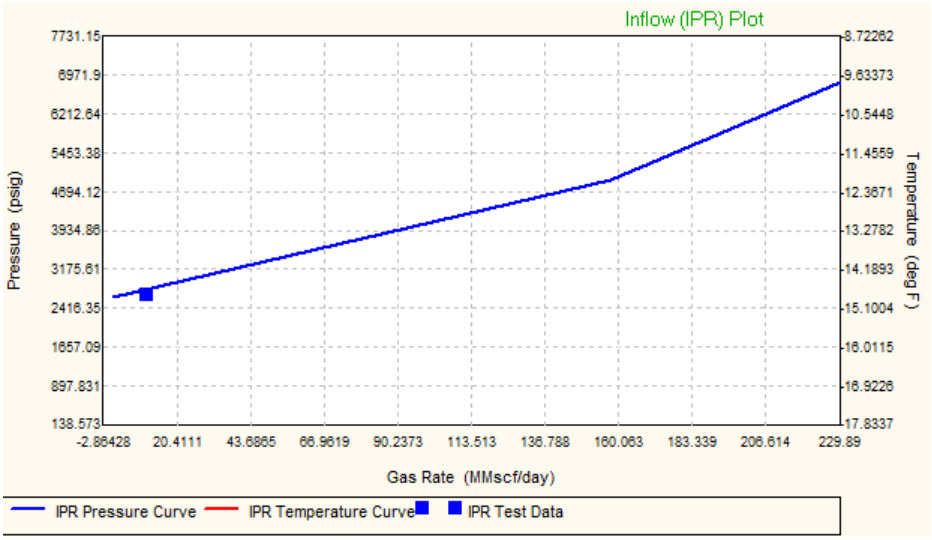

Figure 184: #2244 Well Test – Falloff Match

Figure 185 shows, using Petroleum Experts PROSPER, the Petroleum Experts 5 tubing correlation accurately predicts bottomhole test pressure from wellhead test pressure. This work used this tubing correlation for all modeling.

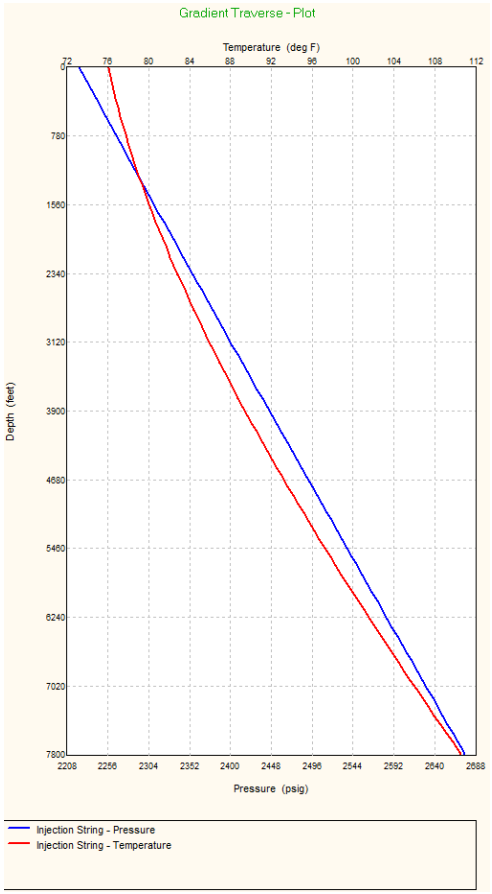

Figure 185: #2244 Well Test – Gradient Traverse

12.1.2 Flow Path 2 Model: Surface to Atmospheric

This work used Petroleum Experts implementation of the ELF Choke Model. This model is based on Perkin's (SPE20633) approach along with discharge coefficients determined by ELF at the Tulsa University Artificial Lift Project. The following explanation is from Petroleum Experts PROSPER help file.

The equations used are derived from the general energy equation that describes isentropic flow of multiphase mixtures through chokes. The flow equations developed by Perkin's are valid for critical and subcritical flow and have been compared against 1,432 sets of literature data points. The original model makes the following assumptions:

- The temperature varies with position, but at any point all phases are at the same temperature.
- The velocity varies with position, but at any point all components are moving with the same velocity.
- The gas compressibility factor is constant.
- The liquids have negligible compressibility compared to gas.
- The elevation changes are negligible.
- That the flow process is adiabatic and frictionless.

12.2 Flow Path Calculations

Table 39 shows the Flow Path 1 calculations using the PROSPER model. The method iteratively combines the inflow and gradient calculations to honor bottomhole Joule Thompson (JT) effects at blowout conditions. Annulus pressures were not available for the initial days and final day, so estimates for these days were extrapolations.

Table 39: Rager Well #2244 Flow Path 1 Calculations

Date	Time	P,wh,an (psig)	P,res,bh (psig)	Q, BH (MMscf/D)	P, BH (psig)	T, BH (°F)	T, WH (°F)	Q, Cum (BCF)
11/06/2022	00:00	—	3,471	106.1	—	—	—	0.000
11/07/2022	00:00	—	3,402	105.3	—	—	—	0.106
11/08/2022	11:23	1,311.1	3,338	104.4	1,848	83.0	53.1	0.211
11/09/2022	07:00	1,253.9	3,280	103.5	1,785	81.3	51.1	0.316
11/10/2022	07:00	1,200	3,209	101.9	1,721	79.8	49.5	0.419
11/11/2022	07:00	1,100	3,139	101.6	1,618	76.0	45.2	0.521
11/12/2022	07:00	1,100	3,069	98.5	1,602	77.3	47.1	0.623
11/13/2022	07:10	1,090	3,004	95.8	1,579	78.0	48.3	0.721
11/14/2022	07:00	1,077	2,975	94.9	1,561	77.9	48.3	0.817
11/15/2022	07:00	1,190	2,863	86.2	1,639	85.9	58.1	0.912
11/16/2022	07:00	1,142	2,786	84.2	1,579	85.0	57.4	0.998
11/17/2022	07:00	1,115	2,702	81.1	1,536	85.4	58.4	1.082
11/18/2022	07:00	—	2,619	77.9	—	—	—	1.164

Table 40 shows the Flow Path 2 calculations setting the temperature of the gas upstream of the choke to be the Flow Path 1 temperature estimate. Note that temperatures below 32°F were likely only downstream of the annular choke, and upstream in the well itself, temperatures were above 32°F.

Table 40: Rager Well #2244 Flow Path 2 Calculations

Date	Time	P,wh,an (psig)	T, WH (°F)	Q, CHK (MMscf/D)	T, CHK (°F)	Q, Cum (BCF)
11/06/2022	00:00	—	—	103.1	—	0.000
11/07/2022	00:00	—	—	99.1	—	0.103
11/08/2022	11:23	1,311.1	53.1	95.0	20.3	0.202
11/09/2022	07:00	1,253.9	51.1	90.9	19.0	0.297
11/10/2022	07:00	1,200	49.5	87.0	18.2	0.388
11/11/2022	07:00	1,100	45.2	79.9	15.3	0.475
11/12/2022	07:00	1,100	47.1	79.7	17.4	0.555
11/13/2022	07:10	1,090	48.3	78.7	19.0	0.635
11/14/2022	07:00	1,077	48.3	77.7	19.3	0.713
11/15/2022	07:00	1,190	58.1	84.9	28.1	0.791
11/16/2022	07:00	1,142	57.4	81.4	28.2	0.876

Date	Time	P,wh,an (psig)	T, WH (°F)	Q, CHK (MMscf/D)	T, CHK (°F)	Q, Cum (BCF)
11/17/2022	07:00	1,115	58.4	79.2	29.9	0.957
11/18/2022	07:00	—	—	76.6	—	1.037

Table 41 summarizes the rates from flow paths 1 and 2 and their differences. The differences are gas that leaked from the well other than across the annulus choke. There was approximately 0.125 BCF difference between the two methods.

Table 41: Rager Well #2244 Flow Path Differences

Date	Time	Q,BH (MMscf/D)	Q,BH,cum (BCF)	Q,CHK (MMscf/D)	Q,CHK,cum (BCF)	Q,Diff (MMscf/D)	Q,Diff,cum (BCF)
11/06/2022	00:00	106.1	0.000	103.1	0.000	3.0	0.000
11/07/2022	00:00	105.3	0.106	99.1	0.103	6.2	0.006
11/08/2022	11:23	104.4	0.211	95.0	0.202	9.4	0.016
11/09/2022	07:00	103.5	0.316	90.9	0.297	12.6	0.028
11/10/2022	07:00	101.9	0.419	87.0	0.388	14.9	0.043
11/11/2022	07:00	101.6	0.521	79.9	0.475	21.7	0.065
11/12/2022	07:00	98.5	0.623	79.7	0.555	18.8	0.084
11/13/2022	07:10	95.8	0.721	78.7	0.635	17.1	0.101
11/14/2022	07:00	94.9	0.817	77.7	0.713	17.2	0.118
11/15/2022	07:00	86.2	0.912	84.9	0.791	1.3	0.119
11/16/2022	07:00	84.2	0.998	81.4	0.876	2.8	0.122
11/17/2022	07:00	81.1	1.082	79.2	0.957	1.9	0.124
11/18/2022	07:00	77.9	1.164	76.6	1.037	1.3	0.125

Figure 186 charts the rates calculated from Flow Path 1 and Flow Path 2 and the differences. The methods compared favorably earlier in time.

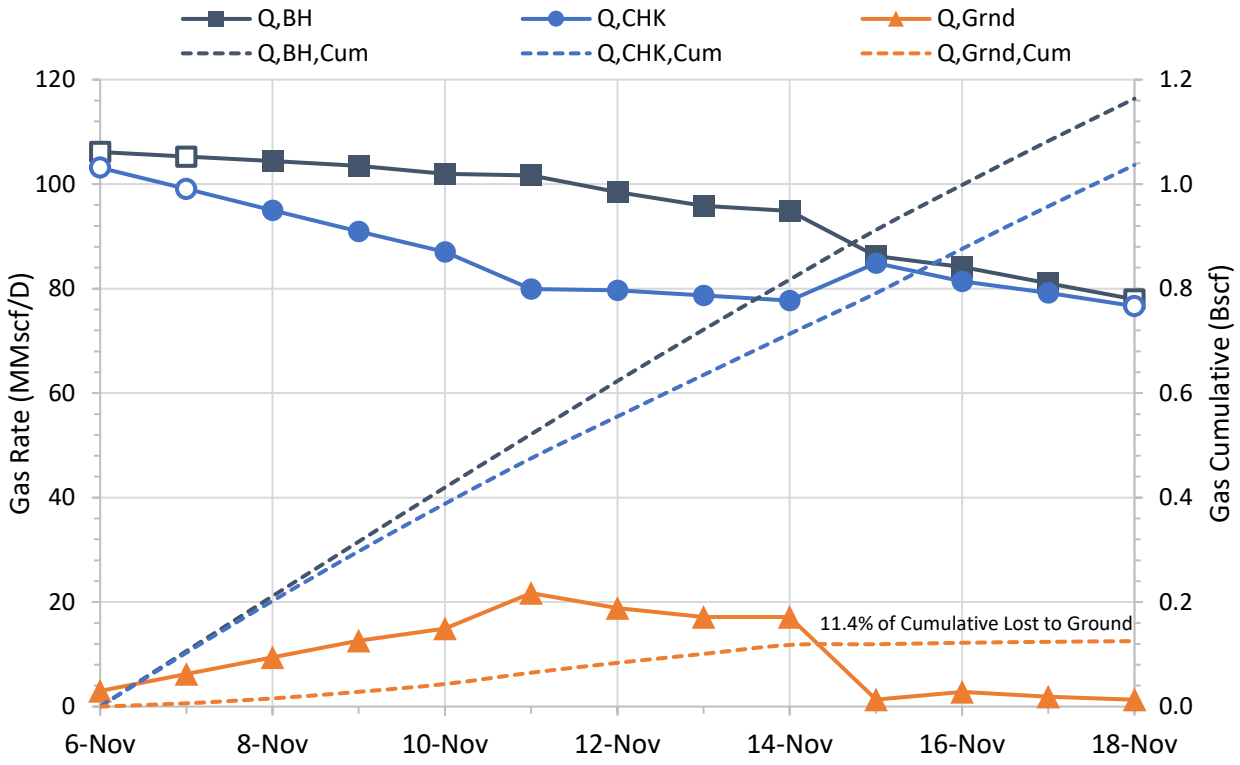

Figure 186: Rager Well #2244 Flow Rate Estimates during Blowout

13 Well #2244 Well Kill Discussion

Blade was asked to review the kill operations and modeling as part of the root cause analysis. The findings are included in the following sections.

13.1 Kill Operations Summary

Table 42 shows a summary of the Cudd Well Control daily reports (verbatim with minor editing for clarity) for the #2244 well. The summary results of the kill attempts are as follows:

- November 11, unable to run the 2 in. coiled tubing below the wellhead
- November 14, unsuccessful using 2 in. OD coiled tubing
- November 17, unsuccessful using 2 3/8 in. OD coiled tubing, flow was stopped, well went on a vacuum and after approximately 12 hours started flowing
- November 19, successful using 2 3/8 in. OD coiled tubing, set mechanical plugs and a cement plug

Table 42: #2244 Cudd Daily Reports Summary

Date	Operations
November 6, 2022	Cudd personnel mobilized from Muncy, PA. Initial assessment by Cudd. Mobilized personnel from Houston.
November 7, 2022	Cudd Houston personnel arrived. Meetings with Equitrans. Sourcing equipment and services. Closed master valve. Prepared venturi tube. Removed fence. Dirt work for water management. Spotted two frac tanks.
November 8, 2022	Continued dirt work. Spot equipment and rig up deluge system. Flowing 9 5/8 in. x 7 in. annulus pressure 1,311 psi. Stage coiled tubing unit and pump truck to location. Spotted four frac tanks for fresh water and brine. Rig up for crane. Modified venturi tube. Filling frac tanks.
November 9, 2022	Annulus pressure 1,254 psi. Filling frac tanks. Planning dynamic kill procedure. Clearing road for coiled tubing unit and crane. Installed windsocks. Torque up 7 1/16 in. valve, spools, and flow cross. Meet with Equitrans to discuss calculated AOF. Set up monitor and staged venturi tube. Set up gas monitors. Waiting on 220 bbl of brine.
November 10, 2022	Annulus pressure 1,200 psi. Set up gas monitoring. Installed venturi tube. Removed swab valve. Installed 7 1/16 in. valve and flow cross. Installed coiled tubing BOP. Rig up iron to pump truck, choke manifold, and flow back tank. Pressure test equipment.
November 11, 2022	Annulus pressure 1,100 psi. Test BOP and lines. RIH with CT. Unable to get past 26 ft below the injector, stopping point approximately at the 2 in. outlet on the starting head. Pumped fresh water at 3 bpm. Returns to surface immediately. Water started to freeze in the venturi tube. Shut down pumps and CTU. Lined up coiled tubing to flow back. Gas flow back from 9 5/8 in. x 13 3/8 in. annulus. Shut down and cleared the location. Ordered camera to arrive tomorrow.

Date	Operations
November 12, 2022	Annulus pressure 1,100 psi. Venturi tube iced up because of rainwater. Removed ice blocks from the venturi tube. Same amount of gas leaking from 13 3/8 in. x 9 5/8 in. annulus. Rigged up impression block and ran to obstruction. Filling frac tanks with brine. Rigged up coiled tubing with camera. Camera was inconclusive. Flow well through 7 in. to flowback to clear wellhead. Attempted second run with the camera, unsuccessful. Ordered wireline for camera. Prepare for wireline run.
November 13, 2022	Annulus pressure 1,090 psi. Test camera. Venturi tube iced up. Rigged up wireline to run camera. Communication problems with camera on wireline. Camera not working. Installed additional 7 1/16 in. valve above wellhead flow cross.
November 14, 2022	Annulus pressure 1,077 psi. Make up BHA with 4.375 in. mill. Tag obstruction. Milling with 2.5 bpm. Inspected mill. Made 1.8 ft. Ran 3 1/2 in. mill. Cleared obstruction and continued to 50 ft. Ran bull nose and RIH to 7,700 ft. Start dynamic kill procedure. Kill was unsuccessful. Pull out of the hole.
November 15, 2022	Annulus pressure 1,190 psi. Purge 2 in. CT with N2. Fill tanks with 11 ppg brine. Bring in 2 3/8 in. CTU and rig up. Rig up CTU.
November 16, 2022	Annulus pressure 1,142 psi. Nipple up BOP. Moving 11 ppg fluid to location.
November 17, 2022	Annulus pressure 1,115 psi. Run dynamic kill simulator. Pressure test BOP and iron. Start dynamic kill. Kill well at 9 bpm. Pump 1 bpm to keep well full. POH while pumping 3 bpm. Reduced rate to 1 bpm. Well on vacuum taking 2 bpm at midnight.
November 18, 2022	Annulus pressure 1,000 psi. Monitoring well. Well on vacuum taking 2.5 bpm at midnight. Well started flowing. Pumping at 2 bpm. Shut down equipment. Evacuate personnel. Ordered additional brine. RIH to 7,600 ft. No obstructions. POH. Filling frac tanks.
November 19, 2022	Annulus pressure 950 psi. RU CT with wash nozzle. RIH to 7,700 ft at 1 bpm. Pump rate 3 bpm while POH. Make up well control plug assembly. RIH with plug assembly to 5,986 ft. Attempted to pump down the backside to get plug deeper. Set plug at 5,978 ft. POH. RIH with second plug. Set plug at 5,875 ft. POH.
November 20, 2022	Annulus pressure 0 psi. Make up cast iron bridge plug. Set CIBP at 5,830 ft. Mix and pump 10 bbl of cement. Place cement plug above the CIBP. RD CTU. Secured well.
November 21, 2022	Load out equipment. NU swab valve on wellhead. Final report.

13.2 Kill Modeling

This section presents a thorough analyses of all kill attempts and a sensitivity study of different kill operation parameters using the Drillbench Blowout module [61]—a fully transient, two-phase flow model regarded as a benchmark in the oil and gas industry. Each kill analysis uses as its starting point the flow conditions identified in the Flow Rate Analysis section. This is followed by comparing the simulations with field operations with as much detail as was available. These case studies, together with the sensitivity analysis, enable an understanding of why certain kill attempts were unsuccessful and what could have been done differently to successfully kill well #2244 at an earlier stage.

13.2.1 Modeling Assumptions and Limitations

Despite being a powerful tool, Drillbench has some limitations that cannot be overridden. Furthermore, some simplifying assumptions were also used to increase the efficiency of the model. Without some of these simplifications, the models would become computationally expensive and impractical to use. The

assumptions and limitations of the model are listed in the paragraphs below and are summarized in Figure 187.

Drillbench limitations:

- Minimum grid size: 1 meter (3.28 ft)
- BOP is installed at the time of the blowout
- Minimum BOP choke line length: 20 m (65.6 ft)
- The well must be filled with liquid before blowout conditions can be established.
- The coiled tubing position is static; that is, it cannot be running in or out of the hole during simulation.

Well geometry:

- A 10 ft. grid was used to model the well.
- When building preliminary models, observations showed that using the minimum choke line length of 65.6 ft caused Drillbench to run at an impractical, slow pace. Trial-and-error revealed that setting the choke line length equal to 80 ft provided the best compromise in terms of accuracy and model efficiency.
- The 7 in. casing failure cannot be modeled efficiently due to the short length (approximately 2 ft) of the top part. Modeling such a short section would result in an inefficient and time-consuming model. Therefore, the flow area change from the 7 in. pipe to the 7 × 9 5/8 in. annulus had to be ignored as part of the wellbore flow path. The annulus flow was modeled by making the choke line ID equal to the equivalent diameter of the 7 × 9 5/8 in. annular space, that is 5.530 in.
  - The choke line ID of 5.530 in. is the equivalent to the total flow area of the 7 × 9 5/8 in. annulus. With this assumption, the flow path pressure profile can be simulated while accounting for the change in flow area and minimizing frictional pressure losses because the 5.530 in. ID is reasonably large, especially if considered that it only extends to a length of 80 ft. In fact, simulations showed that the 80 ft-long choke line in the model adds less than 6 psi to the total pressure loss, that is, less than 0.65 % of the lowest flowing wellhead pressure (FWHP) during the blowout.
- The choke is downstream of the choke line. To maximize the blowout potential, the choke ID was set to be equal to the choke line ID (5.530 in.). When the blowout condition is reached and only gas flows out of the well, the choke opening can be manipulated to represent the 2 in. annulus valve restriction seen in the field.

Coiled tubing:

- The actual dimensions of 2 in. and 2 3/8 in. coiled tubing were used in the simulations. The details of the coil tubing (CT) strings are summarized in Table 43.

Table 43: Coiled Tubing Dimensions (from the free end to the core end)

Coiled Tubing OD (in.)	Length (ft)	Cumulative Length (ft)	Wall Thickness (in.)	ID (in.)
2	5,199	5,199	0.147	1.760
	790	5,989	0.166	1.668
	835	6,824	0.193	1.614

Coiled Tubing OD (in.)	Length (ft)	Cumulative Length (ft)	Wall Thickness (in.)	ID (in.)
	11,810	18,634	0.213	1.574
2.375	10,000	10,000	.0204	1.967

Kill fluids:

- The viscosities of the 10 and 11 ppg brines used in the kill operations were estimated using the $CaCl_2$ Brine correlations from Ortego and Vollmer (2004) "Viscosities for Completion Fluids at Temperature and Density"—SPE 86506.
- Additionally, theoretical 12 and 14 ppg $CaCl_2/CaBr_2$ brines were used in the sensitivity analysis. Their viscosities were also derived from the correlations in Ortego and Vollmer (2004).
- In the sensitivity analysis, 10, 11, 12, and 14 ppg synthetic-based muds (SBM) were used for performance comparison. The rheology of these SBMs were based on experience and actual field measurements.
- Viscosity values are summarized in Table 44 for brine and SBM.

Table 44: Kill Fluid Viscosities at Kill Rate

Kill Fluid	Density (ppg)	Viscosity (cP)
Brine	10	2.1
	11	3.8
	12	8.9
	14	26
SBM	10	18
	11	22
	12	25
	14	30

Reservoir conditions:

- A linear productivity index (PI) was assumed from the Flow Rate Analysis section.
- Reservoir pressure and temperature were also obtained from the Flow Rate Analysis section.
- The reservoir fluid was a dry gas with a specific gravity of 0.575. No water or oil was produced with this fluid.
- The reservoir liquid injectivity index (II) was unknown. The well kill reports showed the well was on a vacuum, with a reported rate of 2.5 bpm after the flow stopped on November 17. An estimated II of 25 bpd/psi was assumed in the kill models.

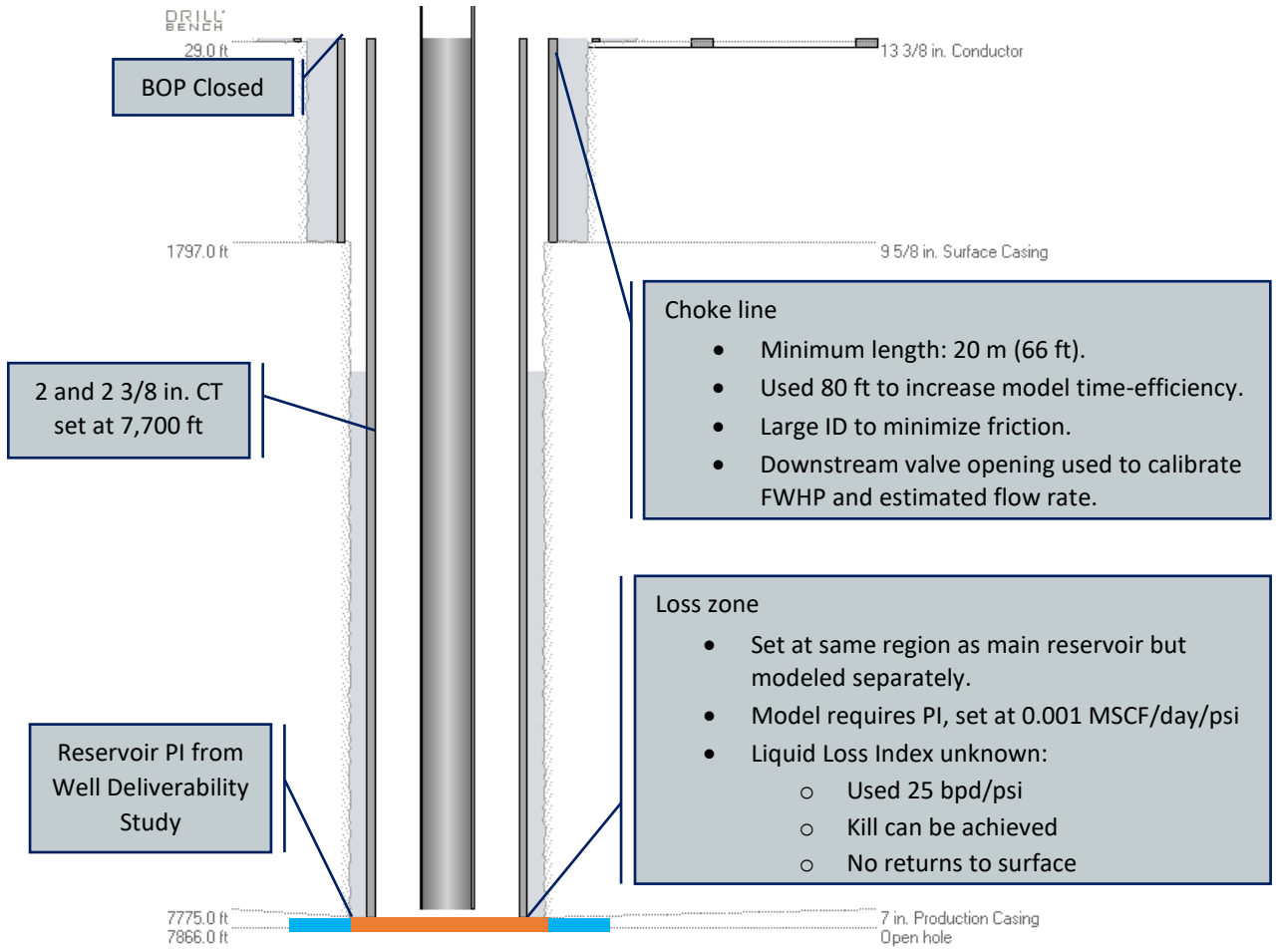

Figure 187: Well #2244 Kill Model and Summary of Assumptions

13.2.2 Kill Simulation

Understanding what happened during a kill attempt was fundamental for assessing the current state of well #2244 and for planning future operations and contingency scenarios on the same field. Therefore, running simulations representing each kill attempt, whether they were successful or not, was important to paint a full picture of the blowout event.

This section presents the results of the simulation work run with the Drillbench Blowout module, an industry standard and reliable tool that is capable of simulating fully transient, multiphase events like the loss of well control.

A total of four kill attempts were identified in the daily reports and meeting minutes. Table 45 provides a list of the attempts and their main driving parameters for simulation purposes. More detailed information about what happened during these kill attempts are provided in later in this section.

Table 45: List of Identified Kill Attempts and Respective Driving Parameters

Kill Attempt	Date	Coiled Tubing OD (in.)	Brine Kill Fluid Density (ppg)	CT Depth (ft)	Pump Rate (bpm)	Stopped Gas Influx
#1	11-Nov-2022	2	10	0	3	No
#2	14-Nov-2022	2	10	7,700	5	No
#3	17-Nov-2022	2 3/8	11	7,700	9	Yes
#4	19-Nov-2022	2 3/8	11	7,700	9.8	Yes

Each kill attempt was simulated following this procedure:

1. Calibrate the model (procedure described in Section -31681.0.0) to estimate the choke opening, which will be used in the next steps.
2. Use the calibrated model and set the CT at the desired depth. Set the BOP and choke open at 100%.
3. Run the simulation until all “blowout initiator” fluid is unloaded from the well (90 – 120 minutes of simulated time).
4. Close the BOP and set the choke opening to the calibrated value.
5. Let the well flow for 30 – 60 minutes until a steady state is reached.
6. Start the injection of kill fluid at the desired pump rate.

Model Calibration

The kill simulation implies that the coiled tubing is inside the well. However, before running the CT in the well, gas from the reservoir was flowing unrestricted up the 7 in. casing to the parted section on the top of the well. From there, it changed paths to the 7 × 9 5/8 in. annulus for a short length (approximately 2 ft), and then vented to the atmosphere through a 2 in. valve. Because the estimates of gas flow rate and actual casing pressure measurements were made under these conditions, this scenario must be used as a reference for calibrating the reservoir-well flow model prior to the killing attempt.

The model calibration uses the same well geometry and assumptions discussed in Section 13.2.1, with the only exception being the coiled tubing, which in this scenario is removed from the well. The goal of calibrating the blowout model is to match the flowing wellhead pressure (FWHP, or flowing casing pressure) with the measured field value and then compare Drillbench’s gas flow rate with the values obtained in the Flow Rate Analysis study. The FWHP is matched by changing the choke opening. This represents the 2 in. valve restriction on the actual well #2244.

The blowout model calibration starts with a well full of liquid (the blowout initiator fluid, described in the previous section) that must first be unloaded. After this fluid is completely removed from the well, fine tuning of the model is possible. The calibration process is summarized in the steps below, and the results are shown in Table 46.

1. Set reservoir pressure and productivity index.
2. Open the wellhead to atmosphere (choke 100% open).
3. Wait for the well to unload.

4. When no liquid remains in the well (liquid holdup = 0 at all depths), change the choke opening until the wellhead pressure matches the measured field value.
    a. It is important to highlight that the flowing casing/wellhead pressure measurements have discrepancies for kill attempts #1, #2, and #3. Based on the findings of the Flow Rate Analysis study and on the simulations carried out here, a decision was made to use the pressure measurement values shown in Table 37.
    b. The sections0 through 0, while discussing each simulation, will show the measurement discrepancies and indicate which ones were used as reference.
5. Check whether gas flow rate out of the well is within 5% difference from the Well Deliverability study.
6. Check whether flowing bottomhole pressure is within 5% difference from the Well Deliverability study.

Table 46: Calibration of Blowout Model Preceding Kill Simulations

Kill Atmpt	Meas WHP (psi)	Res Press (psi)	Productivity Index (MMscf/D/psi)	Choke Open (%)	Calibration Criteria: Blowout Flow Rate (max relative difference)			Calibration Criteria: FBHP (Max relative difference)		
					Est. (MMsf/D)	Drillbench	Rel. Diff.	Est. (psi)	Drillbench	Rel. Diff.
#1	1,100	3,139	66.8	8.6	101.6	98.8	–2.8	1,618	1,661	2.7
#2	1,077	2,975	67.1	8.3	94.9	92.5	–2.5	1,561	1,599	2.5
#3	1,115	2,702	69.5	7.0	81.1	78.7	–2.9	1,536	1,572	2.3
#4	950	2,579	57.0	7.3	71.7	69.8	–2.6	1,320	1,355.9	2.7

Kill Attempt #1—Simulation Results and Discussion

The first kill attempt did not actually try to kill the well because operations had to be stopped before the attempt could be initiated. Nonetheless, it provided an additional datapoint, which was beneficial for the model calibration and kill simulation procedure. This kill attempt took place on November 11, 2022, when an attempt was made to enter the well with a 2 in. coiled tubing. The CT could not pass through the wellhead area due to an obstruction. It was estimated that the bottom of the CT was at the same level as the 2 in. valve through which the gas was flowing.

This geometry is not replicable with Drillbench's Blowout module because the CT was not actually inside the well. Therefore, to simulate liquid being injected into the well through the CT, the bottom of the CT was set at a 50 ft depth. This depth was short enough that the impact on friction losses would be minimal, while also allowing the model to run efficiently (attempts were made to set the CT at a shallower depth, but that increased the simulation time considerably, making it impractical). Using the blowout calibration procedure, a steady-state blowout flow rate was established during the model calibration within 2.8% of the estimated rate while matching the 1,110 psi FWHP precisely.

After calibrating the model, the CT was set at 50 ft and the blowout model restarted. It ran until the well was completely unloaded. The BOP was then shut in, bringing the choke to an 8.6% opening which enabled the well to flow freely for 60 minutes. This was enough time to bring the well to a steady-state condition with the CT in place. At that time, pumping of the 10 ppg brine started at 3 bpm (average reported value). The result of the simulation is in Figure 188.

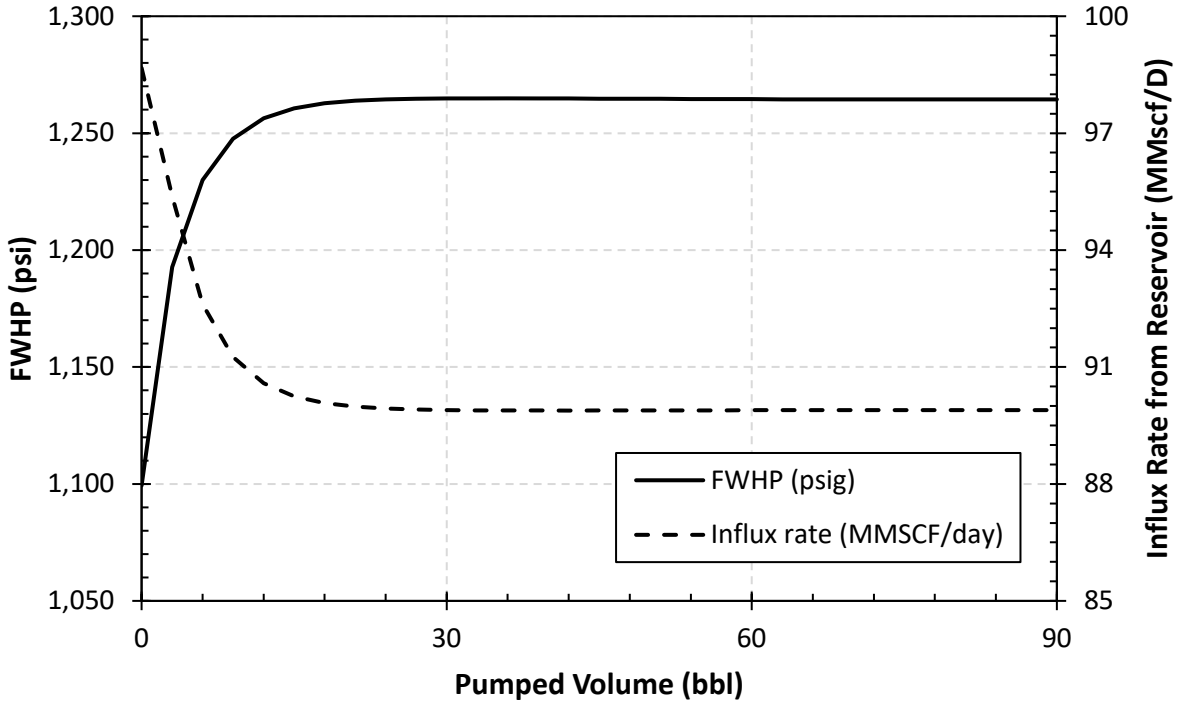

Figure 188: Kill Attempt #1 Simulation Result – FWHP in psi vs. Cumulative Pumped Volume

It is clear from the graph in Figure 188 that the well cannot be killed with the simulated geometry, kill fluid, and flow rates. In fact, the introduction of brine at that rate and depth only increases the FWHP by approximately 165 psi and the influx from the reservoir decreases by less than 9 MMscf/D.

Kill Attempt #2—Simulation Results and Discussion

In the second kill attempt, the 2 in. CT was run into the well to a 7,700 ft depth. At that depth, the 10 ppg brine was pumped at the reported average of 5.0 bpm and the kill was unsuccessful. As mentioned earlier, two distinct FWHP measurements existed before running the CT in the hole. The first registered 1,077 psi and the other recorded 1,500 psi. Here, the former value was adopted as reference because it results in flow rates consistent with the estimated values. Unfortunately, the recorded FWHP during the kill uses the later measure as reference, forcing a comparison of the results of the simulation and field measurements using a normalized pressure. The normalized pressure value is the ratio between the pressure reading at any time after the start of the kill and the pressure at the wellhead just prior to the start of a kill.

The result of the simulated kill is compared to field measurements in Figure 189. Please note that the black lines show the FWHP and gas influx from the reservoir (solid and dashed, respectively) assuming a constant 5 bpm pump rate throughout the entire kill procedure. The simulation shows that pumping at a constant 5 bpm rate, the FWHP was expected to decrease by approximately 4%; however, field observations showed that wellhead pressure remained nearly constant.

We then ran a second simulation using a reduced pump rate of 3.5 bpm, plotted in red in Figure 189. The 3.5 bpm simulation shows that the FWHP remains constant after some initial pressure oscillation, which is more consistent with the field observation. A possible explanation for this behavior is that the reported 5 bpm average only happens after bringing the pumps up to speed, and that “average” does not include the pumped volume while tripping the CT in the hole nor while ramping up the pump to the desired rate.

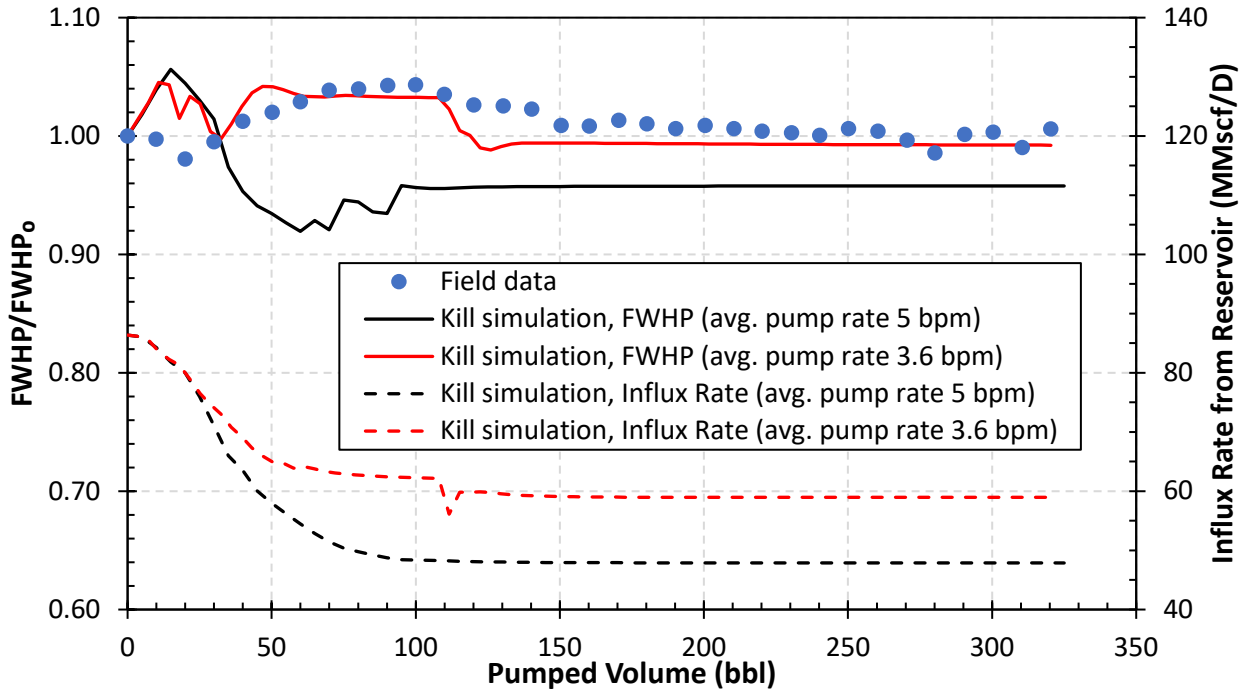

Figure 189: Kill Attempt #2 Simulation Results – Normalized FWHP vs. Cumulative Pumped Volume

Kill Attempt #3—Simulation Results and Discussion

In the third kill attempt, two significant changes happened when compared to the previous attempts:

1. The use of a larger OD coiled tubing (2 3/8 in.) not only allowed for higher pump rates, it also slightly decreases the equivalent flow area diameter by 2.3%. While this seems insignificant, it is important to highlight that frictional losses in a pipe are inversely proportional to the 5th power of the diameter, meaning that with the larger CT the frictional pressure drop in the annular space between the 7 in. casing and the CT itself will increase by an estimated 20.5%.
2. The kill fluid weight was increased from 10 to 11 ppg. The increase in density meant that the gas-liquid hydrostatic at the bottom of the well would also increase, which should help in the kill process. Furthermore, an increase in density of a $CaCl_2$ brine implies in an increase in viscosity. While the viscosity value remains low, the relative change is significant (from 2.1 to 3.8 cP, an approximate 80% increase). This is an added benefit to the kill as the total frictional pressure in the annulus will increase while pumping the brine.

Similar to what was presented in the discussion of kill attempt #2, in this case there was also a discrepancy in the measured values of FWHP. Two values were recorded, one at 1,115 psi and the other at 1,400 psi. Field data after kill again uses the later value; however, our analysis indicate that the former is more consistent with the estimated gas flow rate. For that reason, here again we are forced to compare the simulated and measured FWHP using a normalized pressure.

In line with what was discussed in the kill attempt #2, presented here are two simulation results. The black lines in Figure 190 represent the kill process with the reported average pump rate of 9.0 bpm. The red lines represent the FWHP and reservoir gas influx based on an estimated pump ramp up. The pump ramp up is not exact but was approximated based on the field data shown in Figure 191.

The data reported in Figure 191 establish the total 11 ppg brine volume pumped at 8.3 and 9.4 bpm. Changes by trial-and-error activity showed that using 3 and 3.5 bpm stages in the ramp up provided a good approximation to the field measurements.

As shown by the dashed lines in Figure 190, kill attempt #3 was able to stop the influx from the reservoir. However, the well was losing fluid and reported as, “well on vacuum” with an approximate loss rate of 2.5 bpm of brine. This loss rate doubled unexpectedly during the night following the kill attempt #3. There were practical limitations of transporting and unloading kill fluids and despite having a significant amount of kill fluid staged on site, the crew did not have enough to keep the reservoir from flowing again.

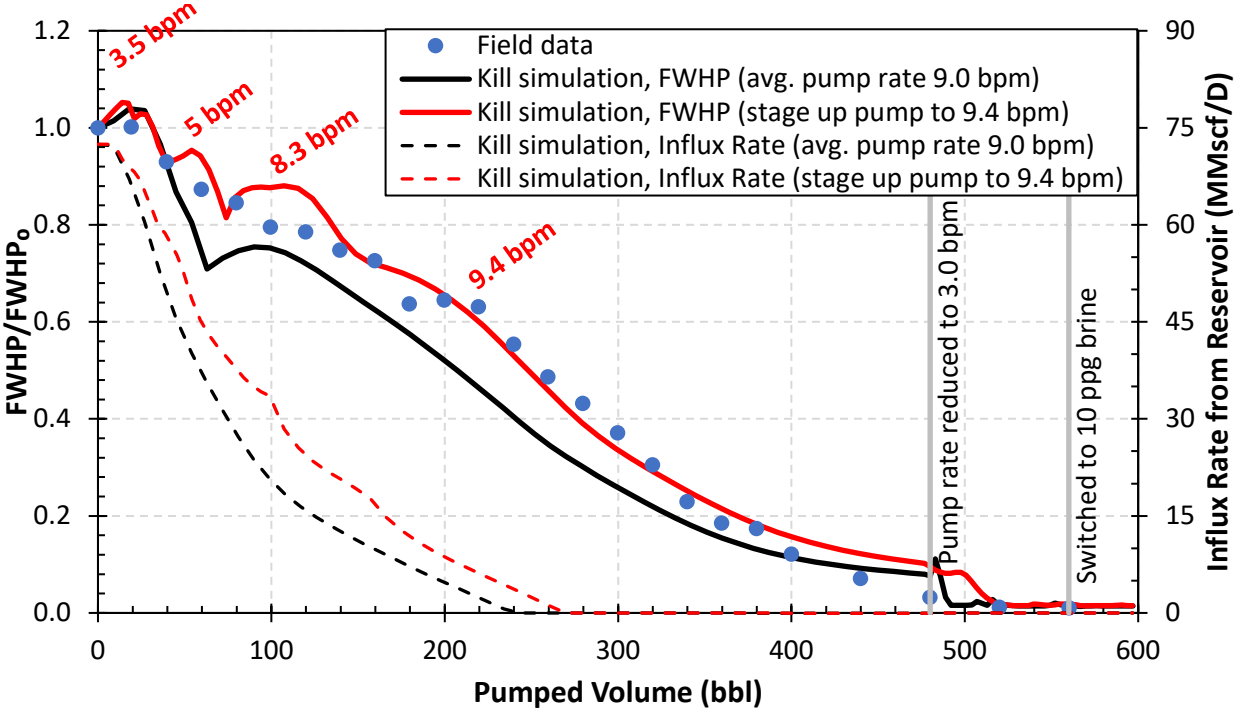

Figure 190: Kill Attempt #3 Simulation Results – Normalized FWHP vs. Cumulative Pumped Volume

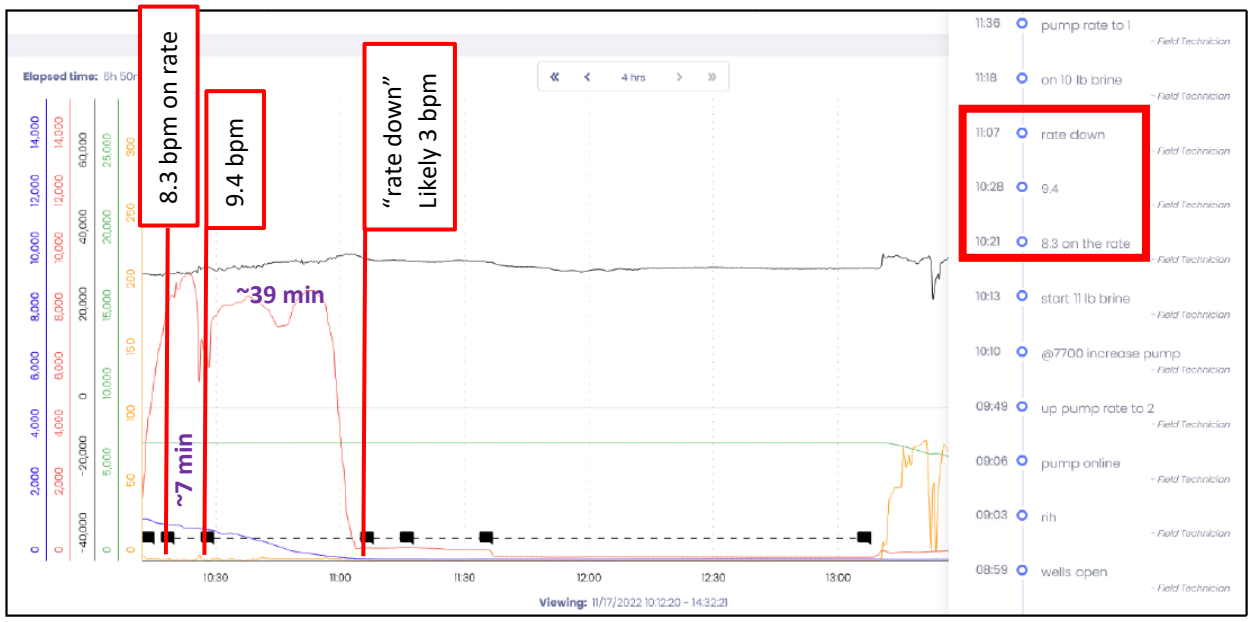

Figure 191: Field Data Provides Better Input for Simulated Pump Ramp Up During Kill

Kill Attempt #4—Simulation Results and Discussion

In the fourth, and last, kill attempt the well was successfully killed with a 2 3/8 in. coiled tubing by pumping 11 ppg $CaCl_2$ brine. Contrary to the previous attempts, the reported casing flowing pressures from the two different sources provided very similar measurements, with the FWHP approximately equal to 950 psi before the CT was run in the hole. This allows for a better comparison between simulated and field data, except that it provides no detailed information on pump rates and pressures and only one reported average pump rate during the kill, i.e., 9.8 bpm.

Figure 192 shows the recorded field data in blue circles and the simulated kill using the reported average pump rate of 9.8 bpm in black bold line. The simulation shows the influx from the reservoir stops just after 200 bbl, whereas FWHP drops to zero at 580 bbl, approximately 70 bbl prior to what the field data indicates.

Due to the discrepancy between the field data and the simplified, constant rate simulation (black line) in Figure 192, a decision was made to replicate what was seen on the field based on some realistic assumptions:

- According to records, the coiled tubing is run in hole starting at 08:35 and reaches 7,700 ft depth at 09:32 (58 minutes total). A low pump rate of 1 bpm is reported while RIH. Therefore, the new simulation set the pump rate to 1 bpm for the first 60 bbl.
- The kill procedure states that the pumps should be brought up to maximum rate slowly. Five different regions from the field data were identified based on pressure-pumped volume slopes: 60 – 100, 100 – 200, 200 – 300, 300 – 400, and 400 – 540 bbl.
  - An assumption was that the last range (400 – 540 bbl) corresponds to the 9.8 bpm flow rate.
  - The pump rates for the other regions were determined by trial-and-error.
- After 540 bbl, the pump schedule followed what is indicated by the vertical gray lines, originally obtained from the daily operations reports.

These assumptions enabled a re-creation of a pump schedule resulting in simulated pressures that matched the field data very closely, as indicated by the solid red line in Figure 192.

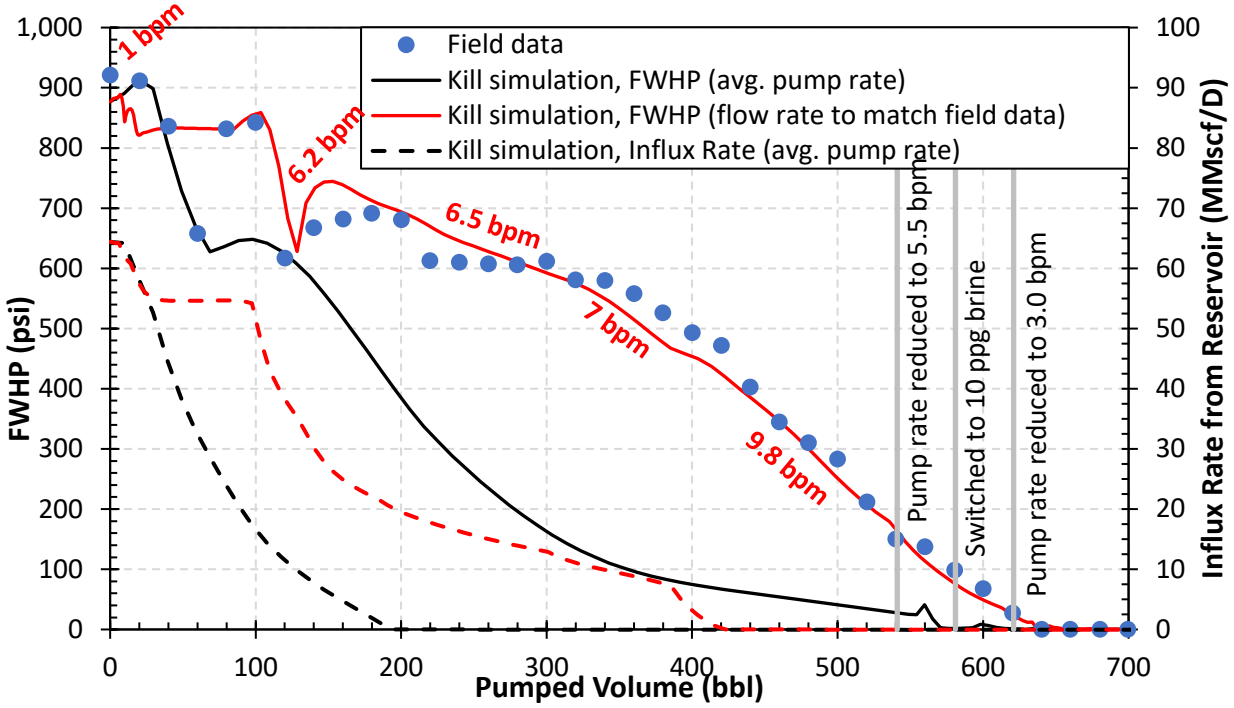

Figure 192: Kill Attempt #4 Simulation Results – FWHP vs. Cumulative Pumped Volume

13.3 Kill Analysis Conclusions

A review of the well control service provider (Cudd) daily reports, discussions with Equitrans personnel who were involved in the kill operations, interviews with Cudd personnel, and modeling led to the conclusion that the kill operations were conducted in an efficient manner. The well was killed and the reservoir was isolated with plugs on day 14 after the leak occurred. Overall, Blade's assessment was that the kill operations went largely as planned.

A couple of days were spent attempting to run a downhole camera. First, a memory camera run on the CT was unsuccessful because of cloudy fluid in the wellhead area. The disadvantage of a memory camera is the lack of depth control and no real-time video. The camera run was to help determine the cause of the obstruction that prevented running the coil deeper than the wellhead depth. A second camera run was attempted on eline. This attempt failed apparently because the eline or the connection to the camera was bad. After the camera run attempts failed, the obstruction was cleared with a motor and a mill. The kill attempts then proceeded.

The first attempt to kill the well using 2 in. coiled tubing was made because the 2 in. CT was immediately available. There was a chance that the 2 in. CT would work and reduce the volume of gas leaked to the atmosphere. Although Blade's modeling shows the kill attempt with 2 in. coil had little chance of success, modeling results are not always accurate and can under- or over-predict success because of uncertainties in the model and model input data. Therefore, Blade concurs with the decision to attempt the kill with 2 in. CT, while waiting for the availability of 2 3/8 in. coil tubing. A benefit of running the 2 in. CT at the time was to find and remove the obstruction and to confirm that the coil could be conveyed to the bottom of the well, even if the attempt was unsuccessful. This proved to be the case, and the well was later killed

with the 2 3/8 in. CT. One learning from kill attempt #3 and #4 was to be prepared to pump LCM pills in case of such losses.

13.3.1 Sensitivity Analysis

The goal of this sensitivity analysis was to investigate the conditions necessary to kill the well at the earliest reasonable time. Based on the actual response to the blowout, the date of the first kill attempt, November 11, 2022, was chosen as the earliest opportunity to kill well #2244. Therefore, all simulations concerning this study assume the estimated conditions at that time (see Table 46):

- Flow rate: 101.6 MMscf/D
- FWHP = 1,100 psi
- Reservoir pressure = 3,139 psi

The analysis focused on the effects of the following factors on the kill operation:

- **Coiled tubing size**: Two CT sizes were used, based on what was more readily available at the time of the well #2244 blowout, i.e., 2 and 2 3/8 in. Coiled tubing IDs are reported in Table 43.
- **Fluid type:** Aside from brines, the use of synthetic-based mud is also considered. These fluids not only differ in their chemistry, but they also have different rheological properties.
  - As mentioned earlier, the rheological properties of the brines were obtained using the data published on Ortego and Vollmer (2004) "Viscosities for Completion Fluids at Temperature and Density"—SPE 86506.
    - $CaCl_2$ brines for densities lower than 12 ppg were assumed.
    - For brines with densities higher than or equal to 12 ppg, $CaCl_2/CaBr_2$ was assumed.
  - The rheological properties of the SBM were based on experience and measured data in Blade's database.
- **Fluid density:** The most important parameter determining the pressure at the bottom of the well. The investigation considered four different fluid densities: 10, 11, 12, and 14 ppg.
- **Kill rate:** The rate at which the kill fluid was pumped downhole. The higher the rate, the easier it would be to kill the well; however, high rates induce high frictional pressure losses and high pump pressures, which may make the entire operation unfeasible.

Table 47 summarizes the results of this modeling study and highlights in green the conditions where the influx from the reservoir could be stopped. Only under two conditions was the kill successful and feasible. This condition consisted of pumping 14 ppg $CaCl_2/CaBr_2$ brine or 14 ppg SBM at 7.5 gpm through a 2 3/8 in. coiled tubing (see Table 43). It is also important to keep in mind that the results on Table 47 reflect the flow conditions on November 11, 2023. By the time the well was killed on November 19, 2022, the estimated reservoir pressure had reduced by approximately 560 psi (17.8 %) and the gas flow rate decreased by approximately 30 MMscf/D (29.5 %), which played favorably towards the actual kill.

Table 47: Sensitivity Analysis Results Showing Failed and Successful Kill Scenarios as Well as Estimated Pump Pressures Necessary to Achieve a Kill on November 11, 2022.

Kill Fluid	Density (ppg)	Viscosity (cP)	Pump Rate (bpm)						
			2 in. Coiled Tubing			2 3/8 in. Coiled Tubing			
			2.5	5.0	7.5	5.0	7.5	10.0	12.5
Brine	10	2.1							
	11	3.8							
	12	8.9							
	14	26							
SBM	10	18							
	11	22							
	12	25							
	14	30							

Failed to stop influx from reservoir
Successfully stopped influx from reservoir (pumped volume ≤ 1,000 bbl)
Pump pressure exceeded max surface pressure

The sensitivity analysis results shown in Table 47 are based on the flow conditions of November 11, 2022. A complementary study was conducted using the same reference date. However, instead of looking at the impact of different kill operational parameters, this new analysis investigated the maximum reservoir influx rate that could have been stopped if the surface conditions at the time of the blowout remained the same, that is, FWHP = 1,100 psi.

For this new analysis, the assumption was that no obstruction was found at wellhead and the CT was able to reach the target depth of 7,700 ft. Furthermore, the analysis only focused on the brines listed in Table 44 and left the SBM out of the analysis. Two different coiled tubing sizes (2 and 2 3/8 in.) were considered, but the analysis was only focused on how the different ODs affected the kill.

Contrary to the previous sensitivity, the analysis was not interested in pump pressure limits, but focuses only on the success or failure of the kill attempt. Because the pump pressure limits also depend on the lengths and IDs of the coiled tubing used on a kill job, the conclusion was that including such parameters on this sensitivity analysis would add an unnecessary and challenging layer of complexity and was unlikely to bring any real benefit.

The analysis was performed by varying the well deliverability and choke opening such that the total amount of gas flow into the well would be reduced while keeping reservoir and flowing casing pressures the same. When these conditions were established, the kill was simulated.

The results of this parametric analysis are shown in Table 48. As it can be inferred from the table, given the condition on November 11, 2022, it would have been possible to kill the well with the 2 in. CT if the influx from the reservoir was 20 MMscf/D or less. At 40 MMscf/D a larger CT size or heavier fluid would be necessary to stop influx from the reservoir. As expected, the most effective combination of coiled tubing size and brine density to kill the well was a 2 3/8 in. CT with 14 ppg brine. However, it could be argued that using the same 2 3/8 in. CT with either an 11 or 12 ppg brine would provide reasonable and less extreme conditions necessary to kill the well.

Table 48: Sensitivity Analysis Showing the Minimum Kill Rate Necessary to Stop Different Rates of Influx from the Reservoir.

Brine Density (ppg)	Influx from Reservoir (MMscf/day)	Pump Rate (bpm)									
		2 in. CT					2 3/8 in. CT				
		1	2	3	4	5	2	4	6	8	10
10	20										
	40										
	60										
	80										
	100										
11	20										
	40										
	60										
	80										
	100										
12	20										
	40										
	60										
	80										
	100										
14	20										
	40										
	60										
	80										
	100										

14 Gas Migration

Equitrans collected lower explosive limit (LEL) and annulus pressure readings in Rager Mountain wells after the blowout. Diagnostic logging was performed to determine the source of the annulus gas. This section contains a discussion of the data and interpretations.

14.1 Noise Logs

Noise logs were run in three wells, namely #2244, #2248, and #2251. Figure 193 shows the log comparisons for these wells. Noise was detected in #2244 and #2248 in December 2022, at approximately 3,000 ft; denoted by a purple rectangle in Figure 193. Noise was observed at #2251 but was associated to the leakage of temporary plugs. This plug leakage was later confirmed with a subsequent noise log on January 17, 2023 (not shown). Figure 194 shows a comparison of two noise logs run for the #2248. The two logs are separated in time and have different wellbore fluids. The December 20, 2022, log was performed in gas while the April 27, 2023, was performed with the well filled with water. Both logs have a common noise interval of approximately 3,000 ft. Additional noise is found in the second log.

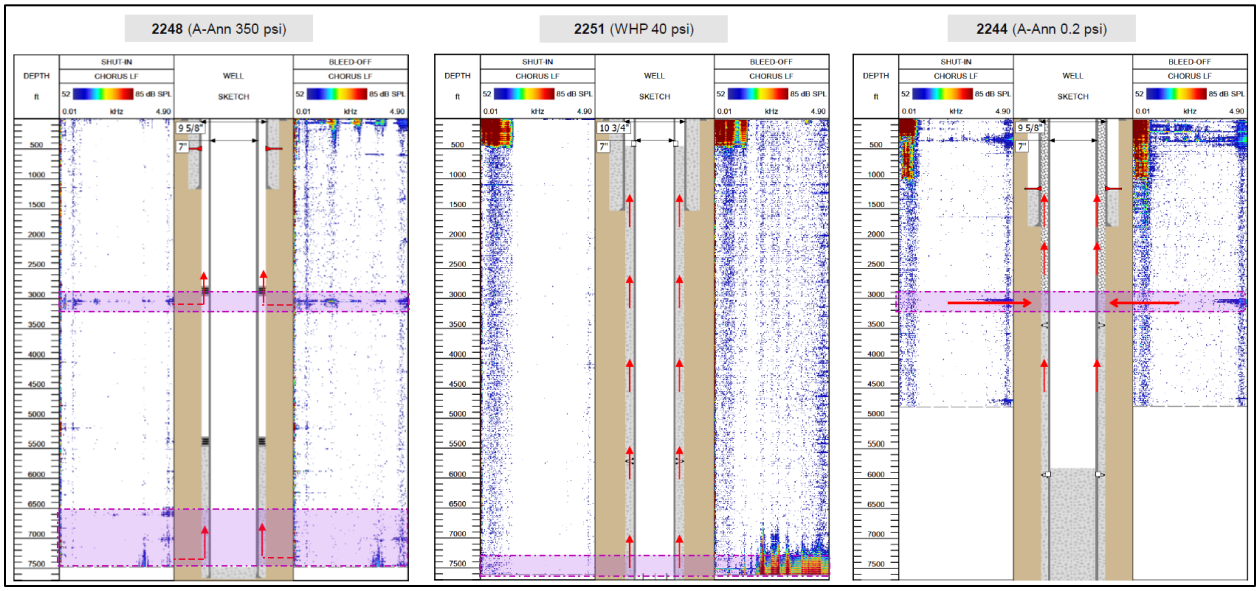

Figure 193: Noise Log Comparison for Well #2244, #2251, and #2248

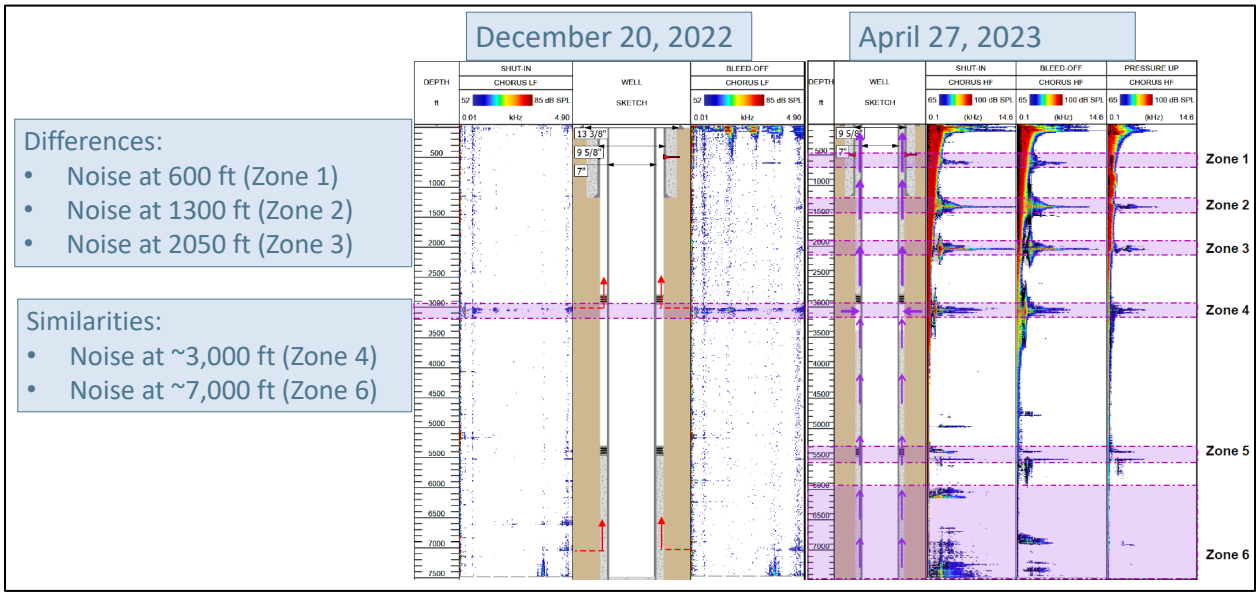

Figure 194: Noise Log Comparison for Well #2248

14.2 Gas Migration Discussion

Exponent, Inc. (Exponent) was contracted by Equitrans to develop a Conceptual Site Model to analyze the transport and location of storage gas that may have leaked into underground zones during the November 2022 gas release from well #2244. Exponent was tasked with a detailed analysis of the gas extracted from the casing and annuli from all Rager Mountain wells, other near field observations, and a detailed geological assessment. The information in this section is from work by Exponent. Exponent prepared a report that is included in the appendix (A.11).

Exponent has developed a conceptual site model of the Rager Mountain Field. Figure 195 shows the model cross section from southwest to northeast. The deeper overburden section is a low-permeability shale. A sand layer is common to the Rager Mountain wells at approximately 3,000 ft. The Balltown and Speechley interbedded sand layer was identified and cited in logs in wells #2244 and #2252. The interbedded sand and the prevalence of uncemented production casing at approximately 3,000 ft creates a path for gas to migrate away from #2244. The arrows in the figure indicate possible pathways for gas to travel away from #2244.

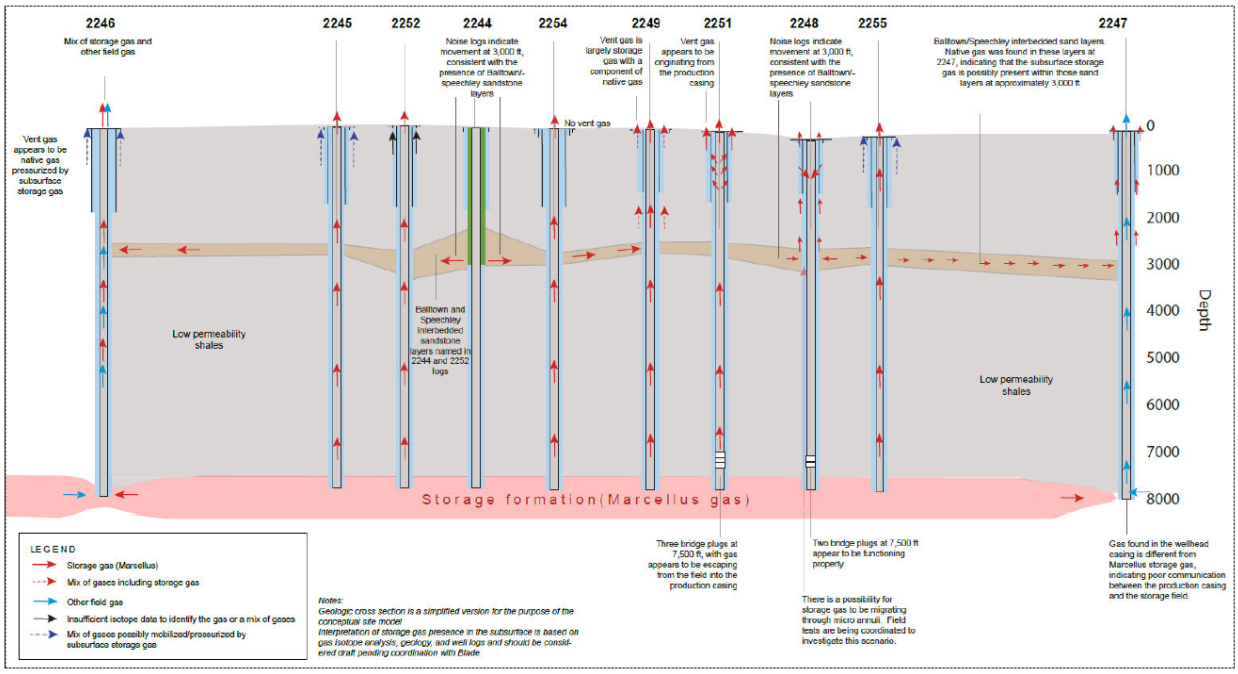

Figure 195: Exponent Rager Conceptual Site Model

Soil and residential water well samples were collected for testing in the area surrounding the Rager Mountain field. Figure 196 shows a map of Rager Mountain wells and sampling locations. Exponent analyzed the sampling reports and provided the following interpretation:

- Sampled 24 water wells in 23 different properties for dissolved gas. Dissolved gas was not found in any of the wells (i.e., the maximum dissolved gas concentrations was 0.016 mg/l, over two orders of magnitude lower than the Pennsylvania action level of 7 mg/l).
- Conducted a soil gas survey of the 23 different residential properties and found no gas in the soil.
- Screened soil gas south of the storage field, along highway 403 (Cramer Pike) and found no gas.

Exponent analyzed the pressure and composition of the gas in the annuli of the Rager Mountain wells. Exponent's interpretation was, as follows:

- Vent gases found in wells #2249, #2251, #2248, and #2247 resemble storage gas, based on the carbon isotope in methane, ethane, and propane.
- Annuli gases resembled storage gas in wells located north of #2244 (except for well #2255).
- Annuli gases resembled a mixture of gas in the wells located south of #2244.
- Overall, it appears the subsurface storage gas has migrated to the north at low volumes, as evidenced by the discontinuous and less distinct interbedded sandstone/shale layers, and the presence of storage gas at low pressures in observation well #2247.

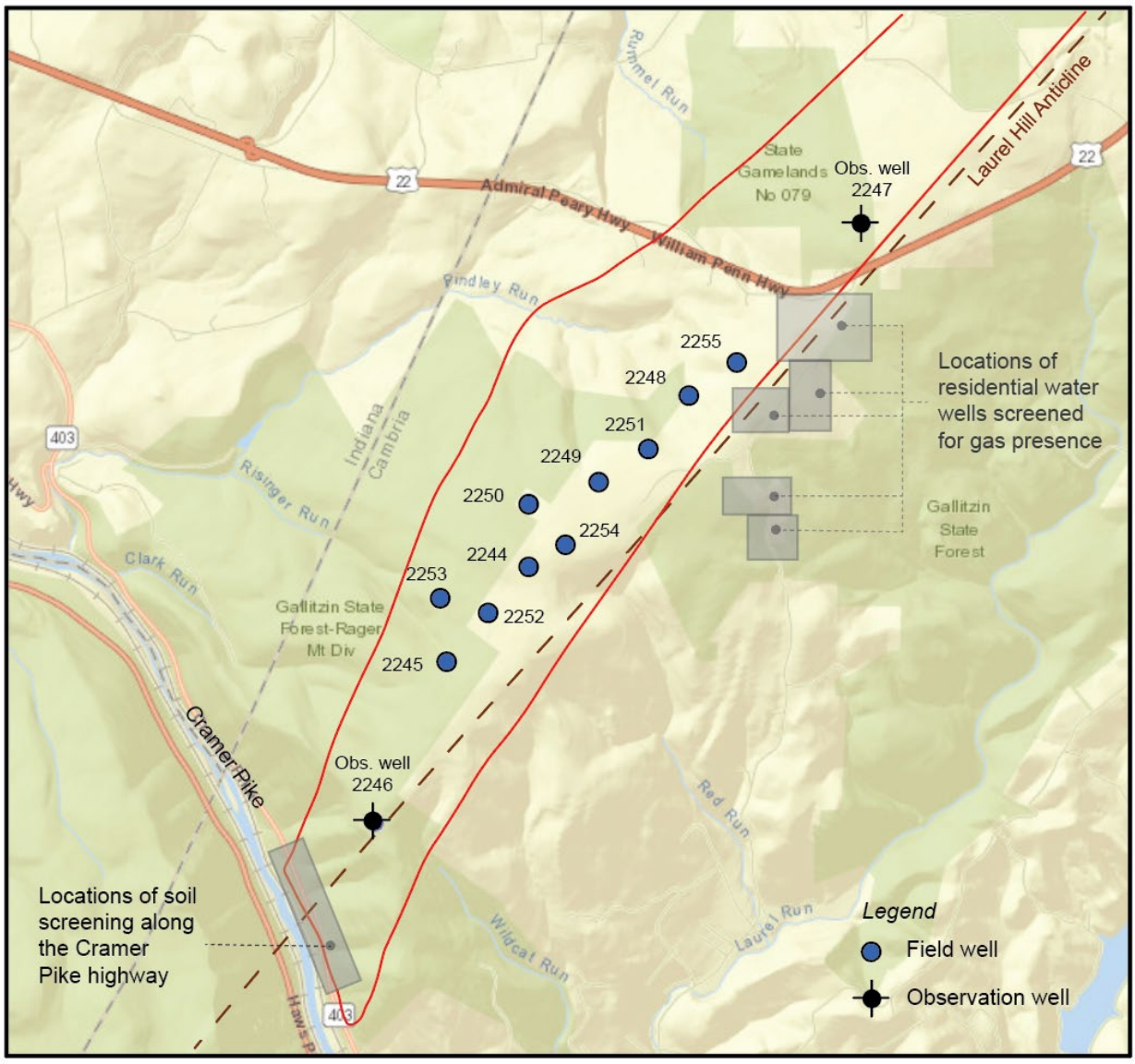

Figure 196: Rager Mountain Well and Sampling Locations

14.3 Implications

Some of the wells at Rager Mountain, including #2248 and #2251, exhibited annulus gas and there was a tendency to build up annulus pressure. The annulus gas does not pose an integrity risk following the mitigation of top joint corrosion through annulus relief valve and periodic annulus gelling. Periodic logging will further identify any corrosion issues and provide an opportunity to mitigate as necessary. Well #2248 appears to have production casing that is leaking and is a candidate for a tubing-packer or other completion options. Well #2251 was worked over to replace the corroded top joint. Despite a successful pressure test on #2251, it exhibited communication between the casing and the annulus and options to mitigate the leak need to be evaluated.

The annulus gas should be monitored and periodically tested. There are no integrity consequences, but threat assessments should be ongoing, using all available data.

The gas migration is contained downhole either at approximately 3,000 feet or possibly at the shoe. This gas does not broach at surface or enter the shallow aquifers per the Exponent study.

15 Root Cause Analysis

The details of the casing failure, the work to recover the failed casing pieces, the analysis of the corroded casing, analysis of Equitrans procedures, analysis of logging data, and kill analysis have been covered in the previous sections of this report. The next step in the process is to integrate all data, analyses, reviews, and conclusions from previous sections to get an understanding of all causes and identify the root causes.

15.1 Root Cause Analysis Process Background

A root cause analysis (RCA) is a systematic process used for identifying the root causes of problems or events and defining methods for responding to and preventing them. In other words, this process helps companies learn from past events and develop plans to improve safety and reliability. The goal of an RCA is to analyze problems or events to identify:

- What happened.
- How it happened.
- Why it happened.
- What actions are needed to prevent reoccurrence.

There are many different methods and philosophies for conducting an RCA, such as 5-Why's, Fish-Bone Diagram, Fault Tree, Management Oversight, and Risk Tree Analysis, depending on the industry and type of problems being investigated. However, most of them use preconceived or pre-defined categories of causes.

Blade selected the Apollo Root Cause Analysis (ARCA) approach because it is a structured, evidenced-based process that makes no assumptions about possible causes [1]. The ARCA companion RealityCharting software was used to develop a cause-and-effect chart, identify the root causes, and develop solutions. This methodology has been used in the energy, chemical, and aerospace industries.

The ARCA process starts with defining a primary effect, that is, the effect that should be prevented from occurring. The next step is to determine the causes of the primary effect. An *effect* has at least two causes in the form of conditions and actions, and together they become a causal set (Figure 197). Conditional causes are static causes that exist over time prior to the action.

Action causes are causes that interact with conditions to cause an effect. In other words, the condition must already exist for the action to cause the effect, and the condition and the action must exist at the same time for the effect to occur. For example, think of a fire as an effect. The conditions (i.e., the static causes) for that fire to happen would be a source of oxygen and fuel. The action (i.e., what interacts with the conditions) for that fire to happen would be the addition of a heat source. The action plus the conditions would result in a fire, and the absence of any of the conditions would not result in a fire regardless of the action.

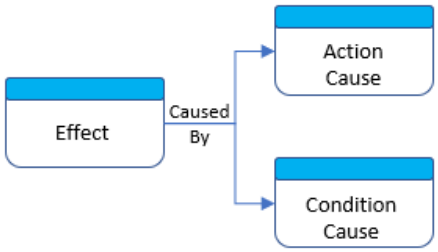

Figure 197: Causal Set

Next, the question *what was this caused by?* or *why did this happen?* is asked for each of the action and condition causes. The causes in essence, become effects, and new action and condition causes are determined for each effect. This process of continuously asking what or why and determining causes for each effect is repeated and develops into a cause path until an end point is reached (Figure 198). A valid end point is defined as an effect that is caused by a desired condition (e.g., the pursuit of a goal), a lack of control (e.g., a legal requirement), or some other more relevant or productive cause path. During this process, the evidence supporting each cause must be identified.

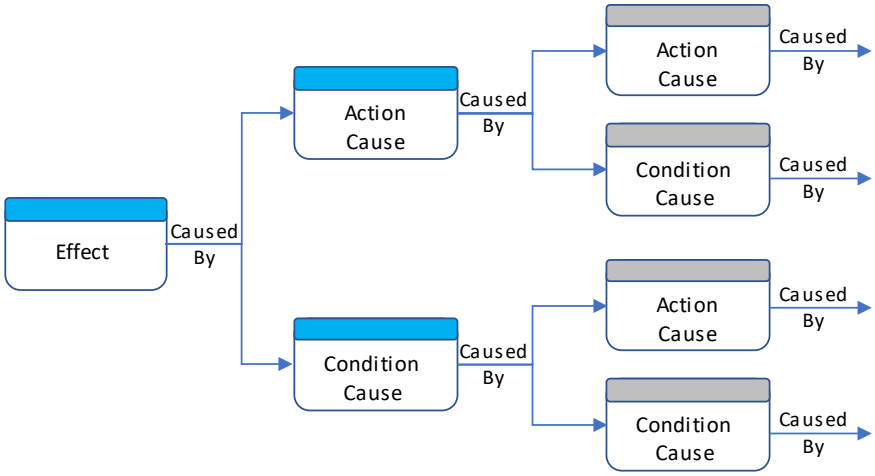

Figure 198: Casual Flowchart Development

When the causal flowchart is complete, the root causes are identified and solutions to mitigate or prevent them are developed. The criteria for developing solutions are:

- Preventing recurrence
- Being within one's control
- Meeting one's goals and objectives
- Preventing other problems

A team consisting of Blade investigators involved in all aspects of the RCA project was assembled to execute the structured ARCA. An external facilitator, trained in ARCA, was engaged as the process evolved and was finalized.

The primary effect of the #2244 casing leak was 14 days of uncontrolled hydrocarbon release. This primary effect was used as the starting point for the RCA analysis.

15.2 Root Cause Analysis Results

The first step in the RCA process was to determine the primary effect of the November 6, 2022, Rager Mountain well #2244 incident. As of November 2022, external corrosion in the top joints and/or casing has been mitigated 10 times in 7 wells, including #2244. The casing that was replaced in 1993 in #2244 corroded, causing the casing wall thickness to be reduced to the point of rupture and parting because of the internal gas pressure.

When the casing ruptured, gas escaped the 7 in. casing and vented at surface through the open 2 in. annulus valve for 14 days until the well was killed and plugs were set in the casing to create a pressure barrier between the gas storage reservoir and the atmosphere. This is the primary effect.

The RCA effort focused on determining why this primary effect occurred and what could have been done to prevent it. Further, the intent of identifying root causes and implementable solutions is to prevent reoccurrence of similar or other well integrity issues in the Rager Mountain Field.

Figure 199 shows the five causes for the primary effect:

- The ruptured 7 in. casing was the cause of the uncontrolled gas release. The 7 in. casing was the primary pressure barrier in well #2244. When it failed, the gas was free to leak into the 9 5/8 in. x 7 in. casing annulus. The wellhead was equipped with an open 2 in. annulus valve that allowed the gas to vent to the atmosphere.
- The presence of storage gas, a desired business condition, was in place as part of the gas storage business. Gas was injected and stored in the reservoir for future withdrawal to meet gas market demand.
- The Rager Mountain gas storage field was shut in for a semi-annual inventory verification test at the time of the leak. The gas pressure of 3,085 psi resulted from the gas that was injected during the injection season, which was a desired condition. This condition was terminated by the action and condition shown in the figure because these were desired conditions.
- The 7 in. casing was the primary and only pressure barrier to contain the gas. When the 7 in. casing ruptured, no secondary barrier was present to contain the pressure and prevent the leak into the atmosphere.
- The well was killed in 14 days by running coiled tubing to the bottom of the well and pumping kill weight fluid to create a column of fluid with a hydrostatic pressure greater than the reservoir pressure, stopping the gas flow to surface. Mechanical plugs were set in the casing to prevent gas flow up the casing and to prevent fluid losses to the highly fractured reservoir formation.

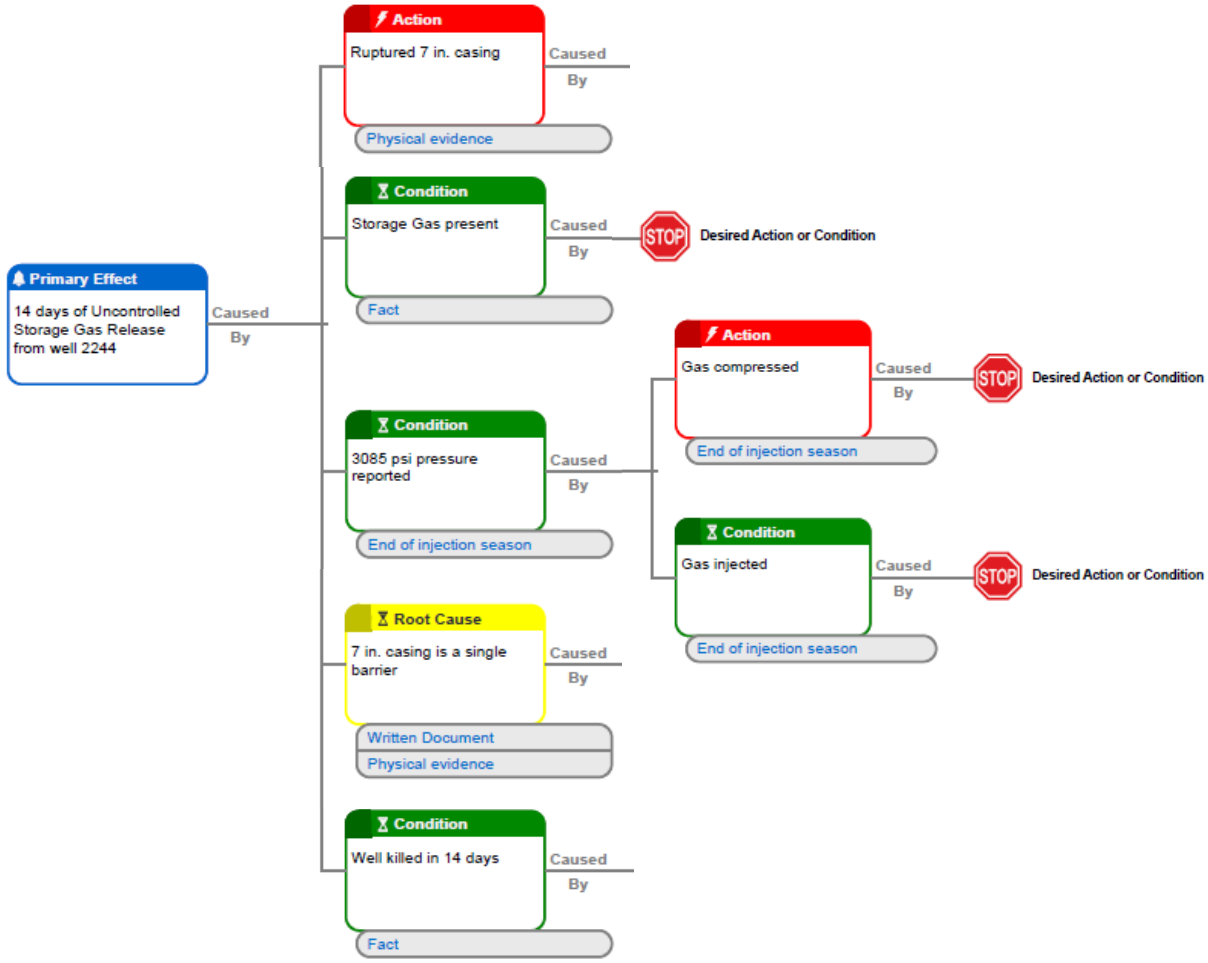

Figure 199: Causes of the Primary Effect

The next step was to explore the causes for each of the unterminated effects to determine what caused them and why. This process continued until identification of causes was no longer possible. Figure 200 shows the image of the completed RCA chart, which illustrates the overall structure and causal branches corresponding to the causes discussed previously.

While the chart is not readable in the figure, it shows the many branches that make up the various legs of actions and conditions. The details of the branches are shown in subsequent figures and discussed. Appendix A.13.1 includes a separate file that can be printed on larger paper size.

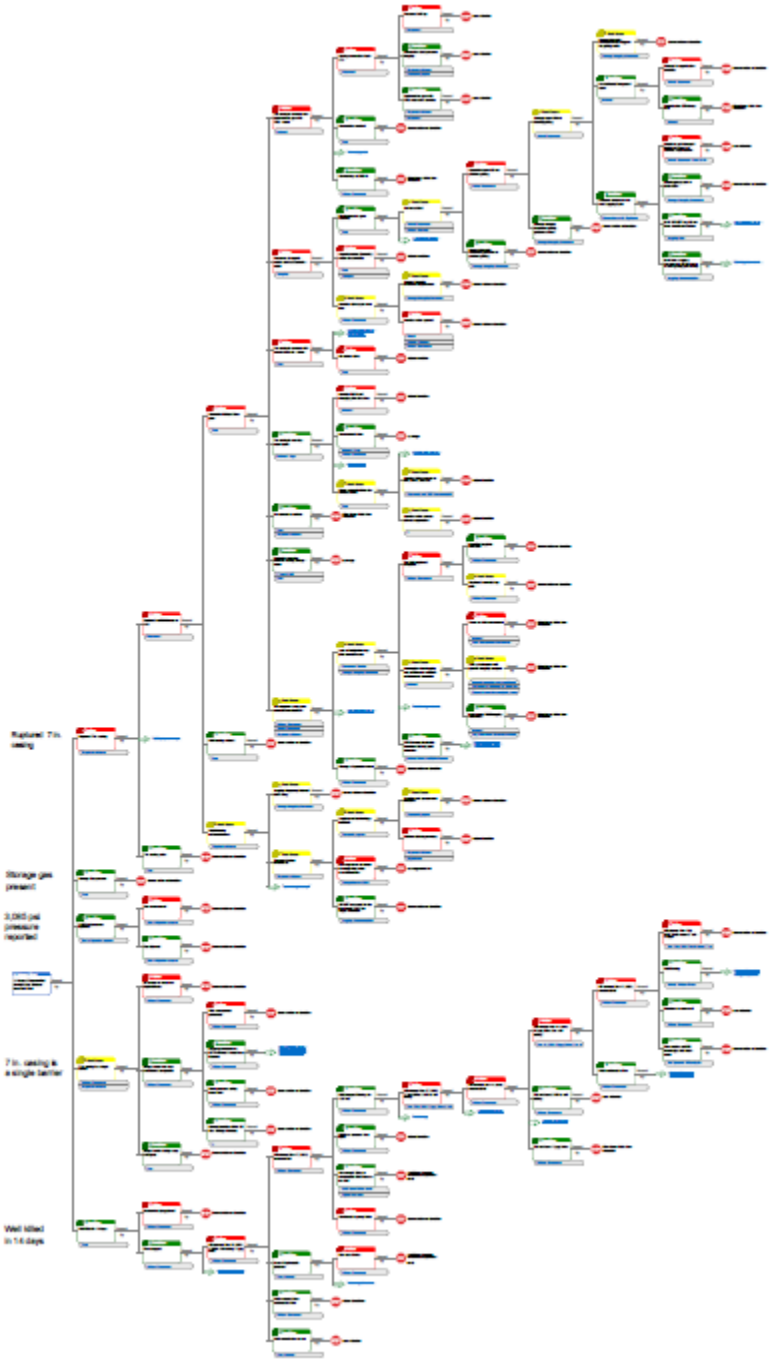

Figure 200: RealityCharting Root Cause Analysis Flowchart

15.2.1 Ruptured 7 in. Casing

Figure 201 shows the branch with the causes of the ruptured 7 in. casing. It was caused by the reduced wall thickness to 16% of nominal wall based on physical measurements of the recovered failed casing. The remaining wall was insufficient to contain the internal pressure of 3,085 psi, resulting in the casing rupture and parting just below the wellhead.

The wall thickness was reduced because corrosion on the 7 in. casing initiated and continued to grow. Casing corrosion and corrosion growth can be caused due to several possible conditions, including contact with a mixture of hydrocarbon gas, CO2, and water, the presence of organic and inorganic matter with bacteria and water, contact with oxygen from the air and water, and wet-dry cycles such as the water level rising and falling in the 9 5/8 in. x 7 in. annulus. The water level in the annulus can change because of water entering through the open annulus valve or by fluid entering or leaving through the open surface casing shoe.

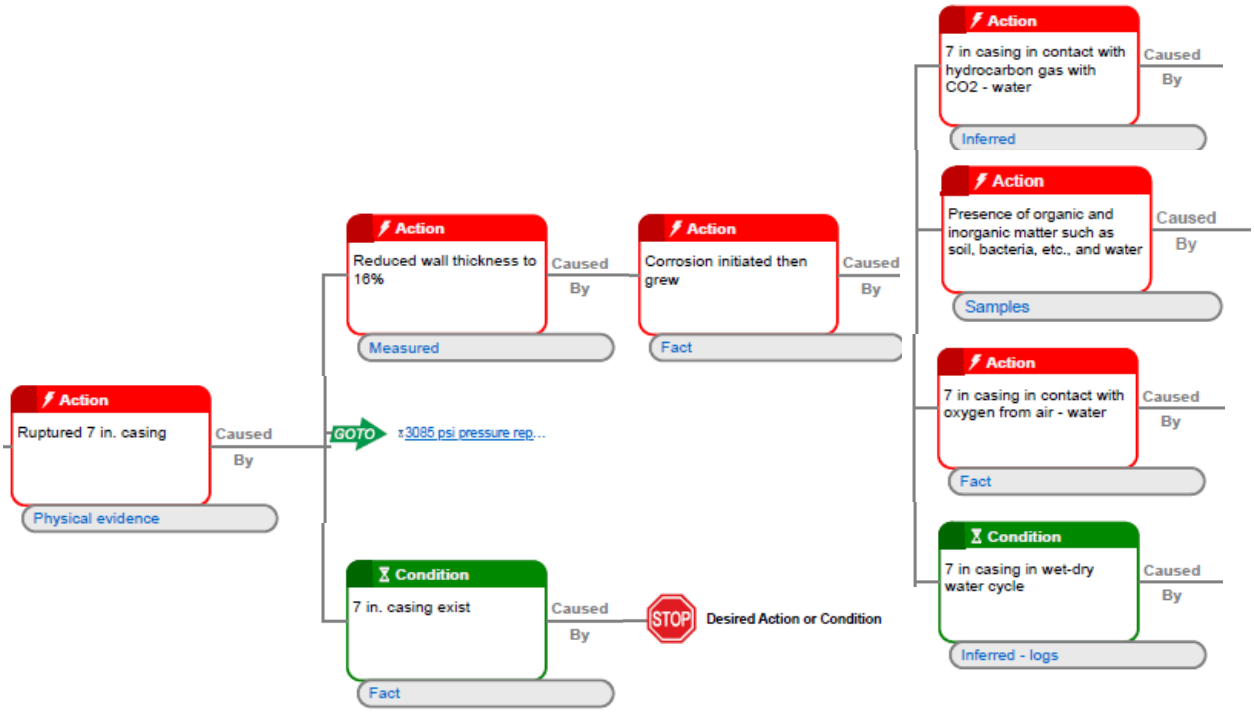

Figure 201: Ruptured 7 in. Casing Causes

Figure 202 shows the branch with causes for the reduction in wall thickness. A cause of external corrosion is exposure of the casing a low pH aqueous environment created by CO_2 from hydrocarbon gas entering the fluid in the annulus of a well. The annulus fluid is water from degraded drilling fluid or water that has entered the annulus through the open annulus valve. Gas with CO_2 can enter the annulus through a leaking casing connection.

Connections from well #2244 were left in the as-made-up condition when the casing was extracted from the well and tested in a laboratory. One connection out of 19 connections tested leaked at a rate of 325 cc/minute at 3,000 psi internal pressure. American Petroleum Institute (API) long thread and coupled (LTC) casing connections are used in all Rager Mountain wells. API LTC connections are prone to leak under gas service conditions [55] [56] [54].

The sealing mechanism for LTC connections is a thread compound that is applied before the connection is made up. Thread compound is grease based with solid particles including lead, tin, zinc, and Teflon. The solid particles plug the gaps in the thread roots and crests to provide a seal. When the thread compound is exposed to dry gas the grease base dries out. An LTC connection's ability to maintain pressure integrity depends on the thread cleanliness, how the thread compound was applied, and how the joint was made up (makeup torque and turns).

API RP 1171 Functional Integrity of *Natural Gas Storage in Depleted Hydrocarbon Reservoirs and Aquifer Reservoirs* [62] rates LTC connections at moderate sealability and low tensile strength. Proprietary metal-to-metal seal connections are rated high for sealability and tensile strength.

Another factor related to leaks of gas and CO_2 is the top of cement (TOC). Connection leaks above the top of cement allow leaked gas and CO_2 to contaminate the annulus fluid. CO_2 and water result in a low pH fluid that causes corrosion. CO_2 corrosion played a role in corrosion in #2244, however did not impact the top joint corrosion in #2248 and #2251. The connection selected for #2244 casing was LTC and the low TOC was caused by an operational problem with a cement stage tool when the upper part of the casing was replaced in 1993. This resulted in the TOC at approximately 2,940 ft.

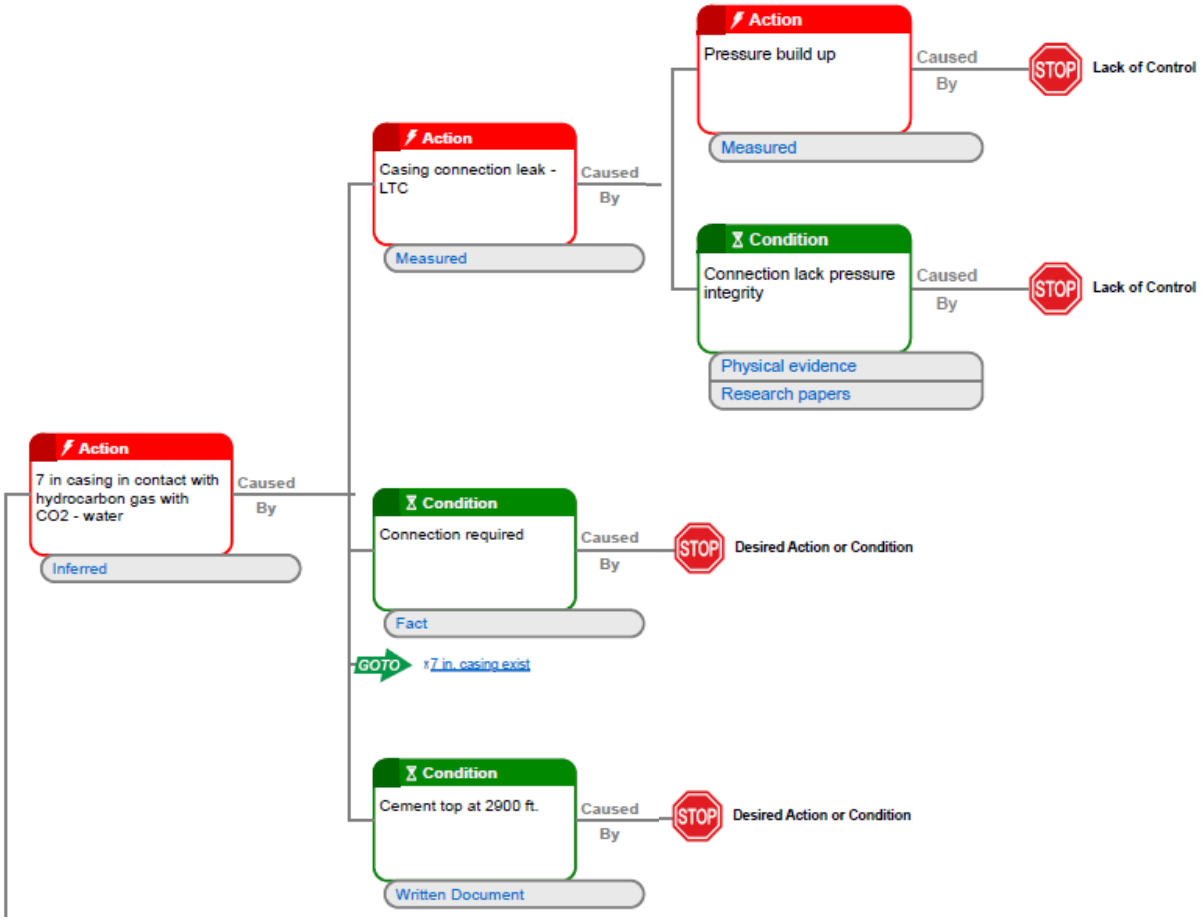

Figure 202: 7 in. Casing in Contact with Hydrocarbon Gas with CO_2 and Water

Figure 203 shows another possible cause of corrosion and growth of corrosion is the presence of organic and inorganic matter such as bacteria, soil, water, etc. Organic matter (grass, leaves, etc.) was found in the annuli of several wells by Blade. The annulus valves were removed for a visual inspection of the annulus condition. Such an agglomeration of organic and inorganic matter on the OD of the production casing can result in under-deposit corrosion. This mechanism played a significant role in the 7 in. casing corrosion in #2244. Further, this environment may enable bacteria to grow. Testing during this project demonstrated that bacteria played a minor role in the corrosion.

Equitrans has a protocol in the Storage Integrity Management document to identify wells for gelling. The treatment of gelling well annuli in the Rager Mountain Field was not conducted. Another important cause

was the open annulus valve that allowed the organic and inorganic matter to enter the annulus. The lack of gelling and the open annulus valve are root causes of the casing failure.

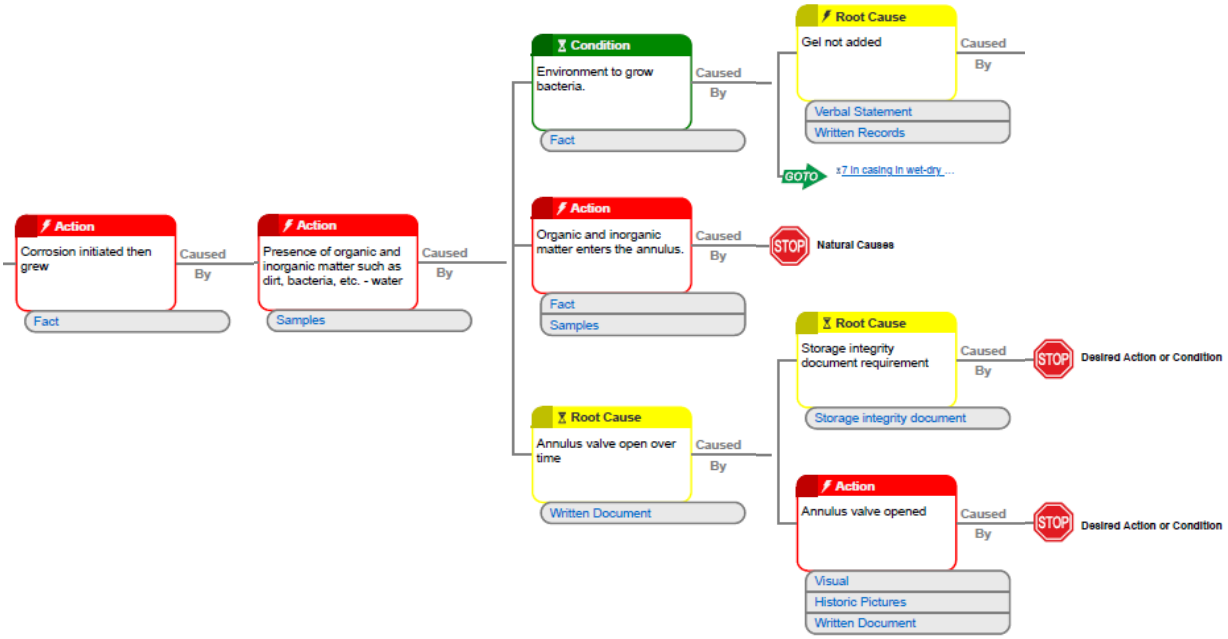

Figure 203: Presence of Organic and Inorganic Matter in the Annulus

Rager Mountain storage wells were not gelled, and this was confirmed by Equitrans. The 2022 Storage Integrity Management document specifies in Section 6.5 that Storage Integrity will select wells to be gelled, based on surveillance logging results (Figure 204).

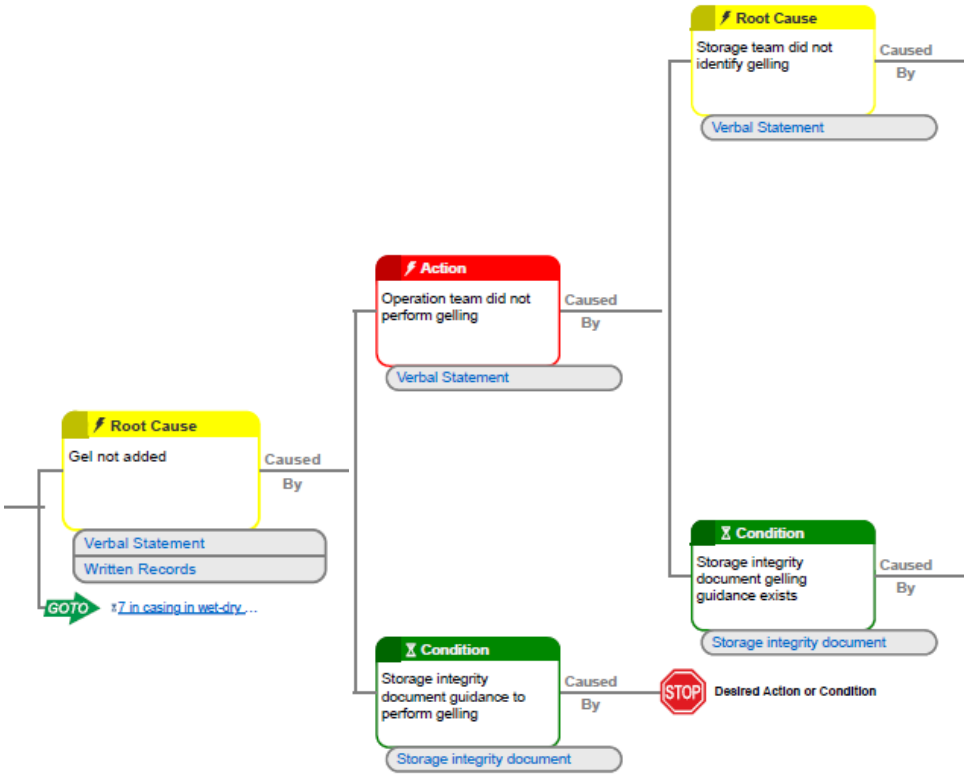

Figure 204: Gel Not Added to the Annulus

Figure 205 shows the causes associated with the failure to identify wells for gelling. A review of the records and discussion with Equitrans personnel indicate that all Rager Mountain wells were informally considered for gelling. Despite informally considering gelling, after a review of the 2016 HRVRT logs, it was never formally documented or communicated, nor was it executed. During this time, the Equitrans Storage team experienced leadership and organizational changes.

The Storage Integrity Management document states that Storage Integrity will select wells for gelling based on surveillance logging results, there are no criteria for gelling. One of the causes for lack of gelling is the lack of clearly documented criteria. It also appears based on discussions with Equitrans teams a decision was then made to delay the gelling, based on 2016 logging, until the next logging cycle. There is no clear evidence or documentation of the decisions to gel, not gel, or to postpone gelling to the next logging cycle.

There are three functional teams, Well Integrity, Operations, and Gas Systems that have a role in storage well integrity threats. For example, well #2244 is the oldest and has the highest deliverability at Rager Mountain field. Further, based on surface sideline temperature data and anecdotal operations data the sideline is consistently hotter than the other wells in the field. The hotter conditions result in a higher corrosion rate. The operational behavior of a well, along with the reservoir and well prognosis should be part of the well integrity decision making. The absence of an integrated team, consisting of Gas Systems, Operations, and Integrity, contributed to the lack of mitigation of some of the possible threats. Another example, some wells exhibit higher water production during withdrawal and those wells automatically should be part of a downhole corrosion mitigation program. This presence of water may be apparent to

Gas Systems and/or Operations but is essential for the Well Integrity team to understand and identify and mitigate this threat.

The Gas Systems, Operations, and Integrity groups together would have an effective insight into all aspects of wells and ensure all integrity threats are proactively identified and mitigated. A functional structure ensures a higher level of expertise, and a cross-functional team would work across disciplines to deliver an effective and efficient solution.

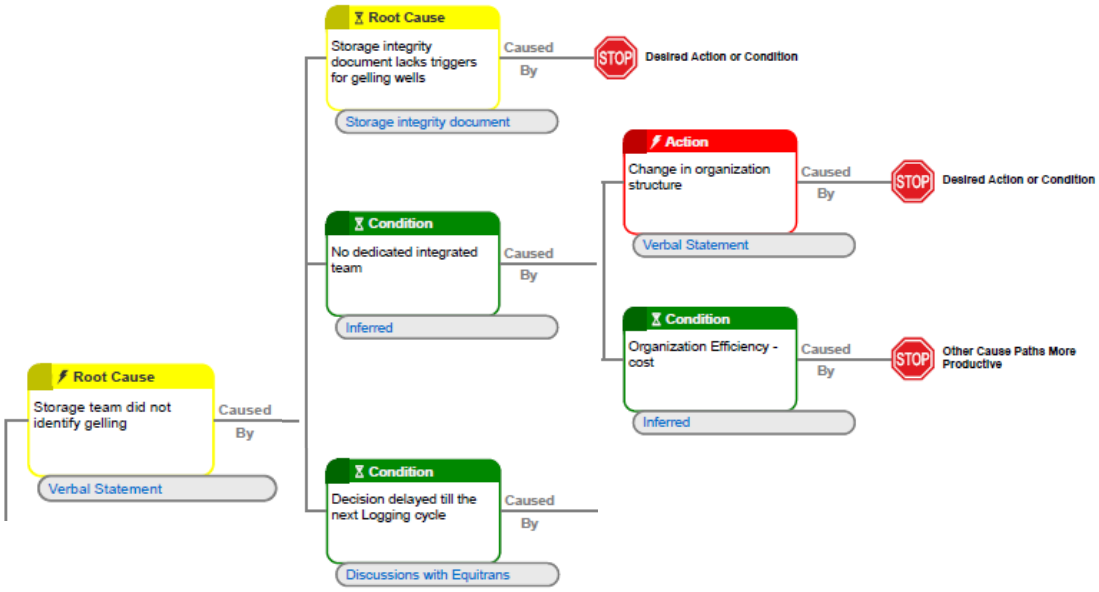

Figure 205: Wells Not Identified for Gelling

Figure 206 shows the causes of the delay in identifying wells for gelling. Logging data was being evaluated to determine the annulus fluid levels for planning of gel volumes. The next logging cycle was planned based on the seven-to-ten-year cycle prescribed in the Storage Integrity Management document. The 2016 HRVRT logging program did not show significant defects. Based on discussions with the previous operator, Equitrans did anticipate the Rager Mountain wells to exhibit significant corrosion. During one of the discussions with Equitrans it was stated that gelling was delayed to the next logging cycle. Further, in 2019 there was an informal criterion for gelling based on the GRNT log data.

The 2016 logs did not show any significant external anomalies. An internal casing patch was set in well #2246 to isolate an 88% internal indication at 6,158 ft in 2017. The logging tools and technology inaccurately sized the defects in 2016. The Baker Hughes logging summaries did not identify the need for inhibited fluid or gelling the annulus. This lack of external defect identification was different from the logging summaries from previous logging campaigns where Baker Hughes recommended that some wells should have inhibitor added to the annulus. It should be noted that the logging technology changed to the high-resolution Vertilog (HRVRT) in 2016.

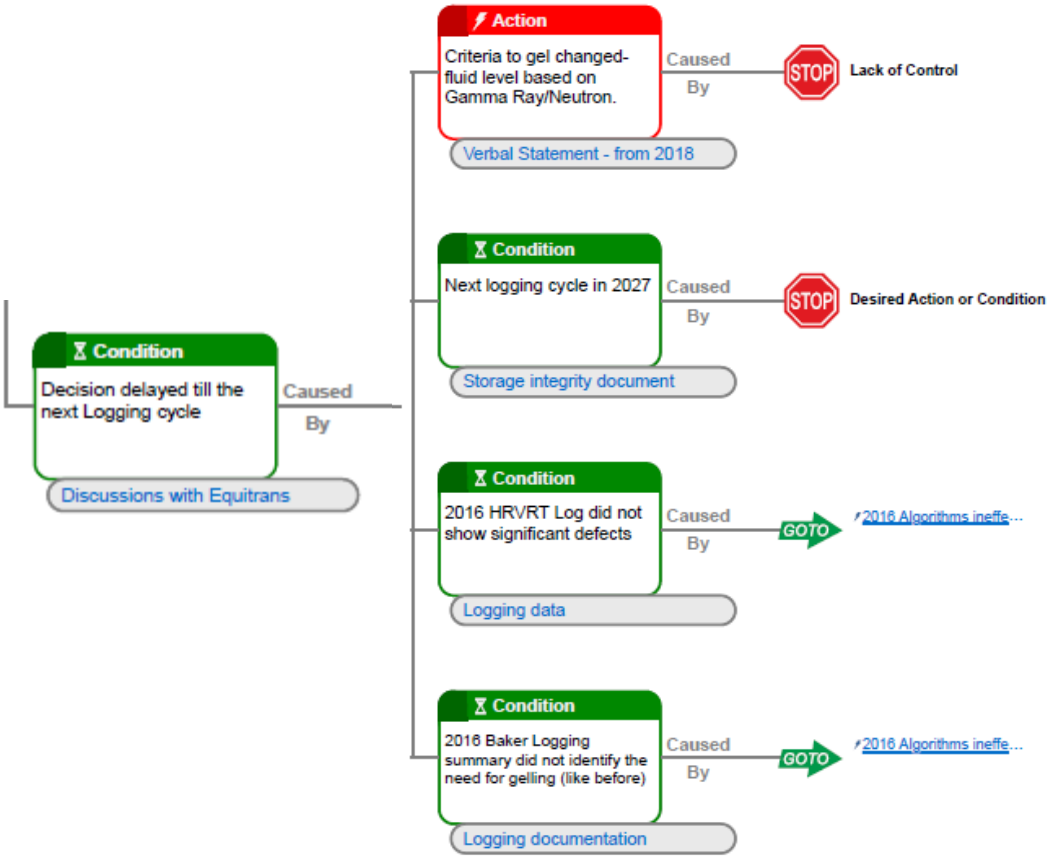

Figure 206: Gelling Decision Delayed

Operating wells with open annulus valves are required by the Storage Integrity Management document and was part of the recommendation from PNG [6]. The root cause for the top joint corrosion is the open annulus valves. Consideration needs to be given to operating wells in a manner that prevents the ingress of water and other contaminates into the annulus that have been identified as the cause for external corrosion on the 7 in. casing adjacent to the annulus valves (Figure 207).

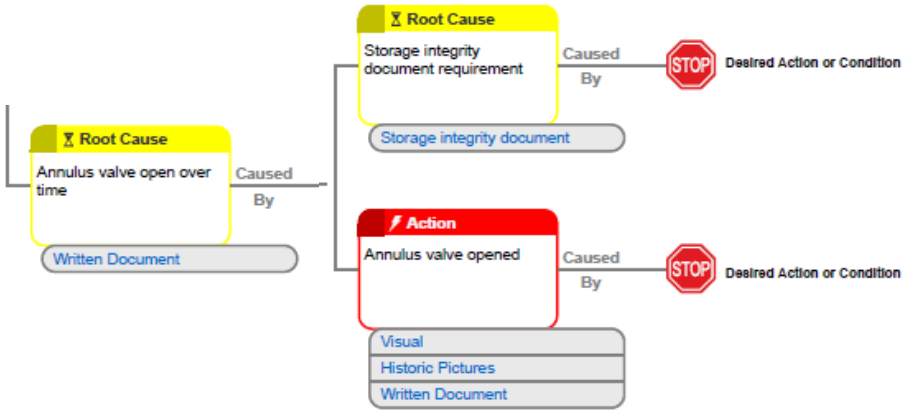

Figure 207: Open Annulus Valve

Figure 208 shows the branch where oxygen can cause the initiation of corrosion and contribute to its growth. This was the one of the major sources of corrosion in #2244. Another condition that results in corrosion and its growth is oxygen corrosion caused by the open annulus valves, resulting in annulus fluid exposure to air and oxygen. Oxygen is one of the most important causes for the top joint corrosion. Oxygen, along with the inorganic and organic soil that may adhere to the pipe surface, would further enhance the corrosion through a mechanism known as under-deposit corrosion.

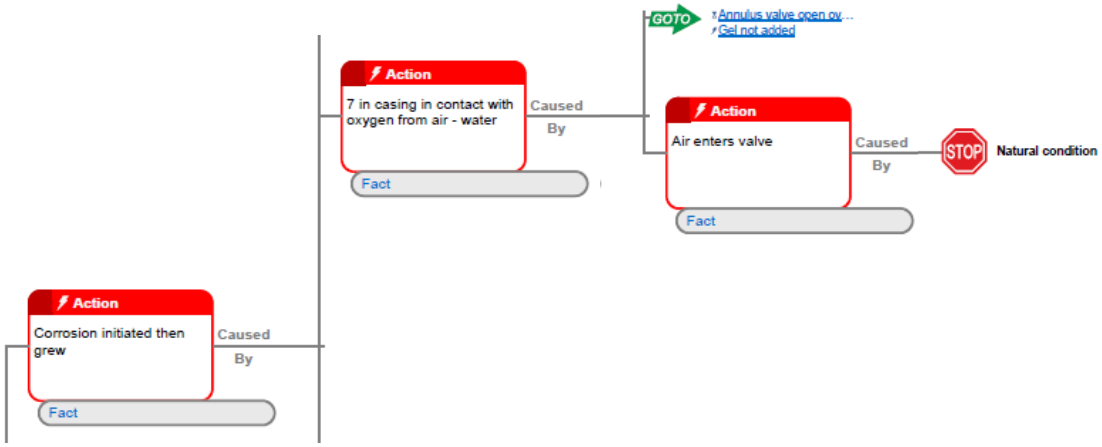

Figure 208: 7 in. Casing in Contact with Oxygen from Air and Water

Figure 209 shows the cause of corrosion because of wet-dry cycles exposure to the 7 in. casing OD. This cycling is caused by the annulus fluid level changing because of the open surface casing shoe at 1,794 ft in #2244. The cement top in #2244 is at 2,940 ft. Wet-dry cycles are also caused by water entering and exiting through the open annulus valve. The open valve allows water to enter from blowing rain, snow, and sleet. Water vapor can exit the open annulus valve when the well is on withdrawal and evaporation is high because of wellbore heat-up.

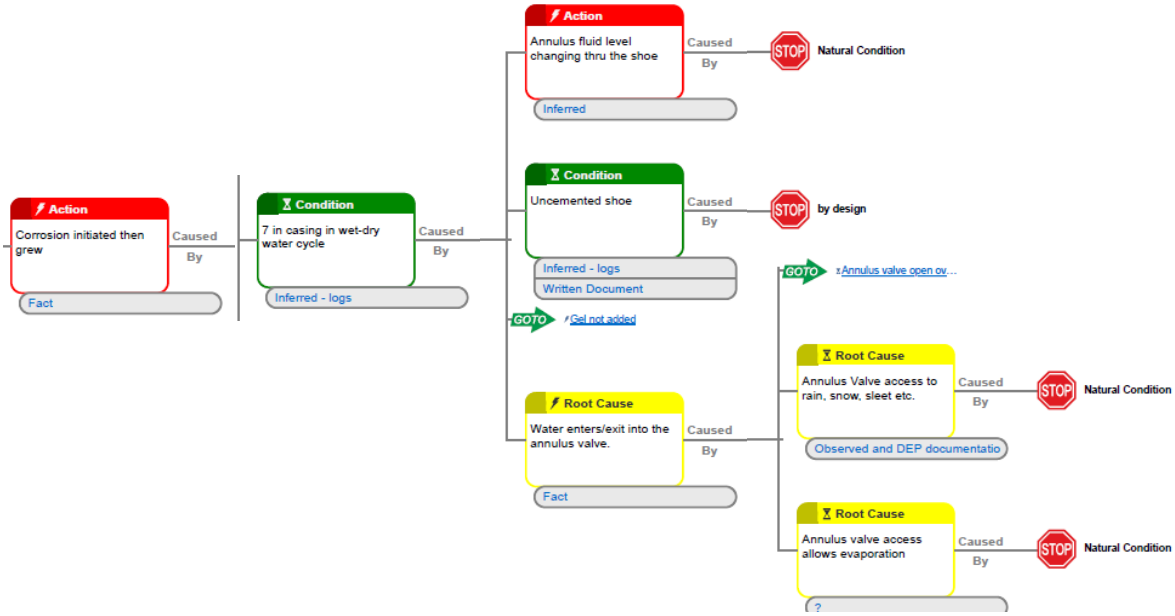

Figure 209: 7 in. Casing in Wet–Dry Water Cycles

Figure 210 shows three conditions related to corrosion initiation and growth. No cement to surface allows operating the well with fluid in the annulus that can become contaminated with CO_2 from casing leaks and bacteria. Galvanic corrosion between the surface and production casing is a condition that cannot be avoided. However, galvanic corrosion is not considered a problem because the two casing materials are very similar in chemistry.

The greater concern is the lack of mitigation of the top joint corrosion mechanism. Replacement of the upper sections of uncemented casing and change-out of top joints by the previous operator occurred 10 times. The perception based on a review of the records is that replacing the corroded joints was performed to mitigate the problem. However, the associated mechanism of corrosion was not investigated.

Ownership and operatorship changed in 2013 when Equitrans became the operator. There was transfer of well integrity issues from PNG to Equitrans. Consequently, Equitrans had an understanding that corrosion was an issue at Rager Mountain and ran inspection logs in 2016; but the log results, exhibiting no significant corrosion, did not raise any concerns about wall loss.

There was some loss in domain knowledge and possibly transfer of knowledge regarding Rager Mountain during the change in operatorship. During the review of the Rager Mountain well data, gaps existed in well data, especially the three new wells. The change in operatorship may have played a role in the lack of mitigation of the corrosion mechanism.

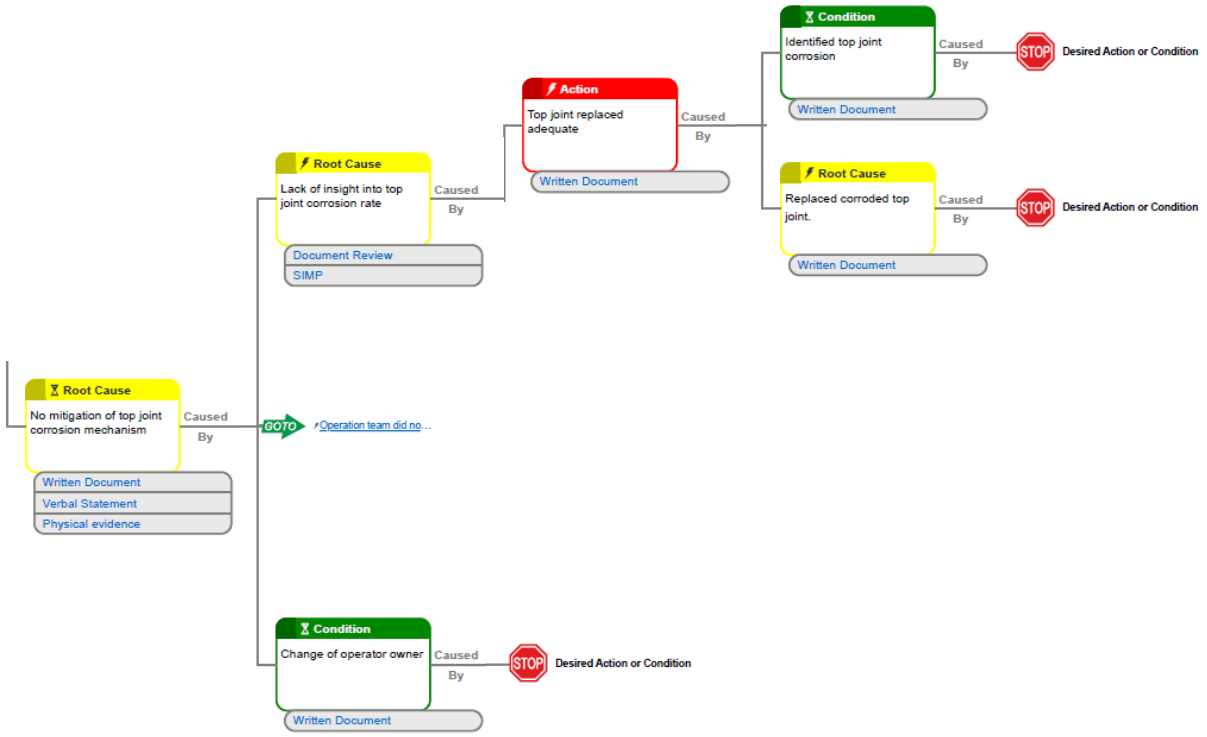

Figure 210: No Mitigation of Top Joint Corrosion

Figure 211 shows the causes of how the severity of external corrosion was not identified using the existing well integrity process as described in the Storage Integrity Management document. When Equitrans became the operator, they reviewed the records and were aware of the historical joint replacement. The physical evidence of recovered corroded casing was not available to Equitrans. Equitrans proceeded to operate the field based on the assumption that surveillance logging was sufficient to monitor and manage corrosion.

Surveillance logging is addressed in the Storage Integrity Management document. However, the wall loss criteria for action to be taken is set at identification of Class 4 features. Class 4 is 61–100% wall loss. The Storage Integrity Management specifies that a Class 4 feature requires prompt evaluation of the potential risk and mitigative steps to occur.

The criteria for Class 4 action first appeared in the 2017 Storage Integrity Management document. It is not documented or clear what the basis is for Class 4 being the trigger for action. It is also documented in the Storage Integrity Management documents that 17 of the 18 gas storage fields operated by Equitrans have a maximum shut-in wellhead pressure of 1,000 psi or less. The Rager Mountain shut-in wellhead pressure is 3,200 psi, so it is an outlier compared to the other fields. The current criteria of Class 4 wall loss for action for Rager Mountain wells is perhaps too high based on the #2244 event and the logging challenges.

The recommended criterion for action is Class 2 features for Rager Mountain based on the elevated SIWHP and the uncertainty associated with inspection log results. If the inspection log results identify a Class 2 feature, options to confirm integrity include a caliper log and an ultrasonic log, depending on whether the feature is OD or ID. Another confirmation is a pressure integrity test. Equitrans has an SOP for a pressure test that can be used. The well design should be evaluated with the actual remaining wall thickness to ensure the design is adequate with a burst safety factor greater than the design factor.

Equitrans has a risk assessment program in place. The risk assessment process has an input for well deliverability, however the absolute open flow (AOF) of Rager Mountain wells were not included in the assessment. This would have raised the consequence due to #2244 being a very high rate withdrawal well. In addition to risk assessment, the focus should be on individual well integrity analysis. Logging data should be the beginning of the integrity assessment; additional analysis of incorporating tool error and understanding the cause of the corrosion or the other threats are essential to well integrity management.

Additional resources may be required to supplement the well integrity team to ensure a detailed review of well integrity threat and risk assessment. A gelling program and batch treating for internal corrosion needs attention in addition to external corrosion.

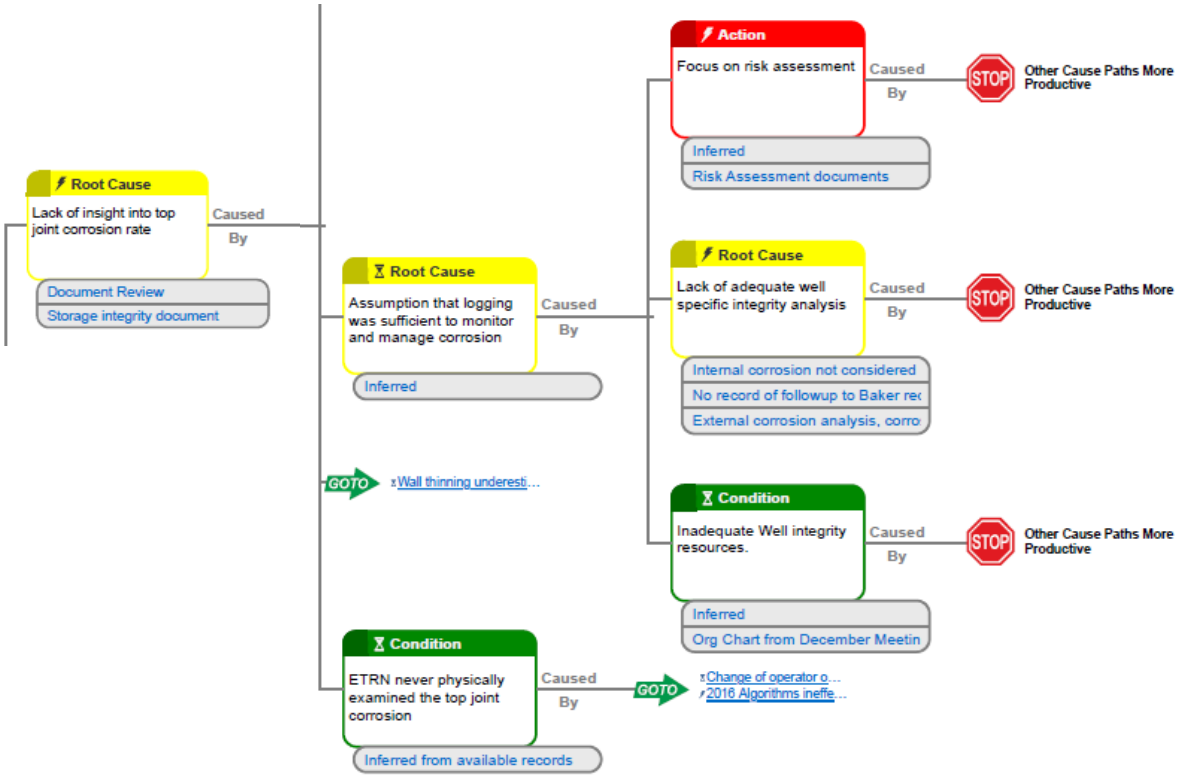

Figure 211: Lack of Insight into Top Joint Corrosion Rate

Figure 212 shows the causes of the wall thinning that was underestimated in well #2244 based on the 2016 log data. The wall loss underestimation was due to the under sizing of defects in #2244. The first clear indication that the defect was undersized in 2016 was the modified algorithm that was applied in 2022. The 2016 logs were reprocessed using the 2022 modified algorithm, and the estimated wall loss was increased in #2244 from 25% to 40%; the reprocessing was conducted after the #2244 incident. Further, as discussed in the report, the nature of the corrosion in #2244 further exacerbates the logging tool's ability to size the anomalies.

The limitation of inspection tool technology and analysis needs to be recognized. MFL inspection tools such as the HRVRT have the disadvantage of underestimating the wall thickness when general corrosion causes wall loss uniformly and gradually. The increased logging frequency may be utilized to overcome underestimation of wall loss.

Finally, the re-inspection frequency should be based on the anticipated corrosion rate; however, if the corrosion mechanism is mitigated, then the tool frequency can be longer. Here, an inspection earlier than planned might have identified these defects in a timely fashion.

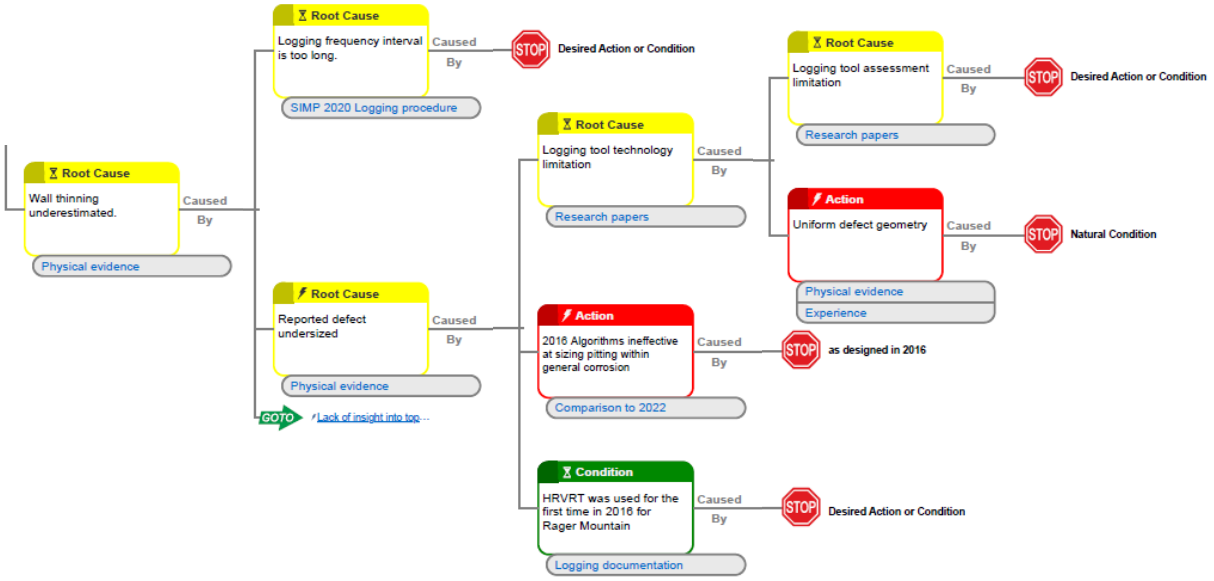

Figure 212: Lack of Insight into Top Joint Corrosion Rate

15.2.2 7 in. Casing is a Single Barrier

Figure 213 shows the branch covering the single-barrier issues. Well #2244 was operated as a single barrier well. The other 11 wells in the Rager Mountain Field are also single-barrier wells with 7 in. or 5 1/2 in. casing set near the top of the reservoir. An open hole below the casing shoe connects the reservoir to the casing. An operational advantage of a single barrier well is being able to run an MFL inspection log without killing the well and filling the casing with a liquid.

The US gas storage industry has successfully used single-barrier wells. With appropriate threat management single-barrier wells are an effective and efficient way to operate gas storage fields.

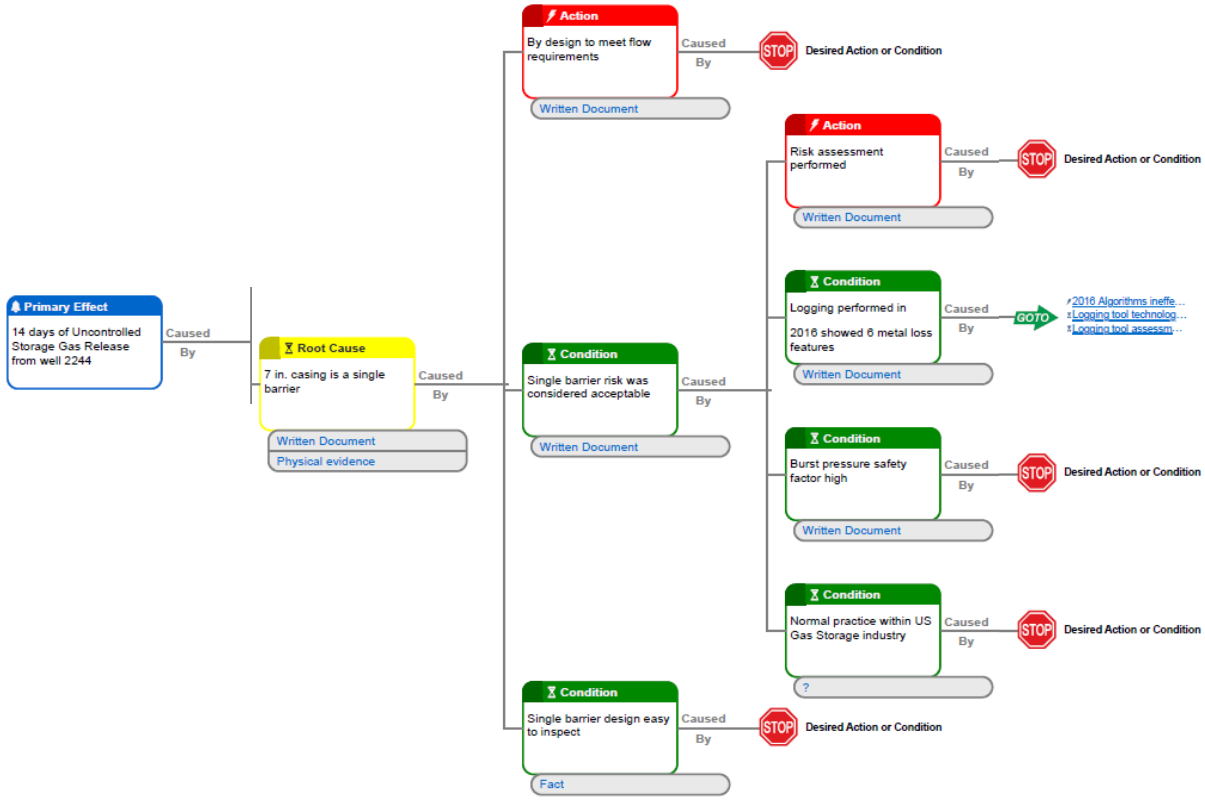

Figure 213: 7 in. Casing is a Single Barrier

15.2.3 Well Killed in 14 Days

Figure 214 shows the successful kill attempt on November 19, 2022. The casing leak in well #2244 occurred on November 6, 2022, and the flow to surface was stopped by killing the well with fluid and setting mechanical plugs 14 days later, on November 19. The kill attempt on November 19 was successful after running 2 3/8 in. coiled tubing to 7,700 ft and pumping 11 ppg brine fluid. The well was on a vacuum and taking fluid after the well was killed. The first well control plug was run on CT did not set. A second well control plug was run and set at 5,875 ft. The following day, November 20, a cast iron bridge plug (CIBP) was set in the 7 in. casing at 5,830 ft. A 10 bbl cement plug was set above the CIBP. Cudd Well Control personnel were released after setting the cement plug. The reason for the kill attempt on November 19, 2022, was the unsuccessful kill on November 17, 2022.

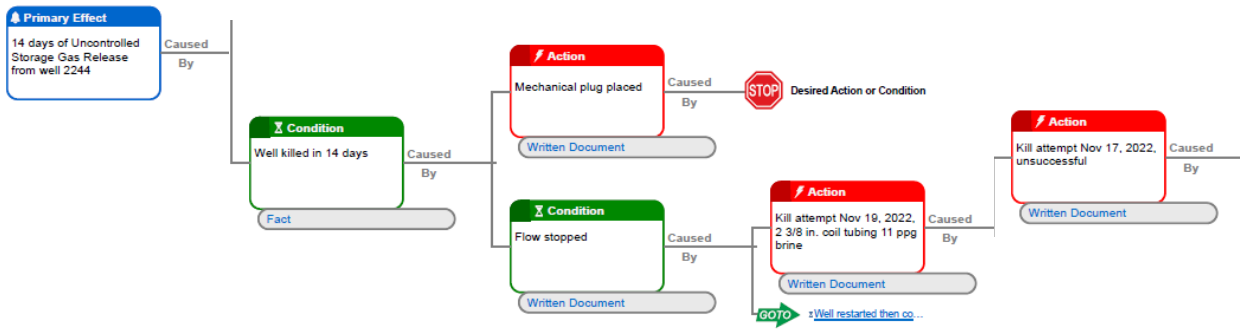

Figure 214: Well #2244 was Killed in 14 Days

Figure 215 covers the kill attempt on November 17, 2022, that was caused by an unsuccessful kill attempt on November 14. Kill modeling was conducted prior to the kill attempt on November 17, using the current reservoir pressure and flowing annulus pressure. The November 17, kill attempt resulted in stopping the flow for 12.5 hours. However, the well was on a vacuum. Kill weight fluid was pumped in the well to maintain a fluid column in the casing, but during the night the loss rate increased and an insufficient amount fluid was available to compensate for the fluid losses to the well. This resulted in the well starting to flow. The well was allowed to flow while additional brine was ordered in preparation for the next kill attempt.

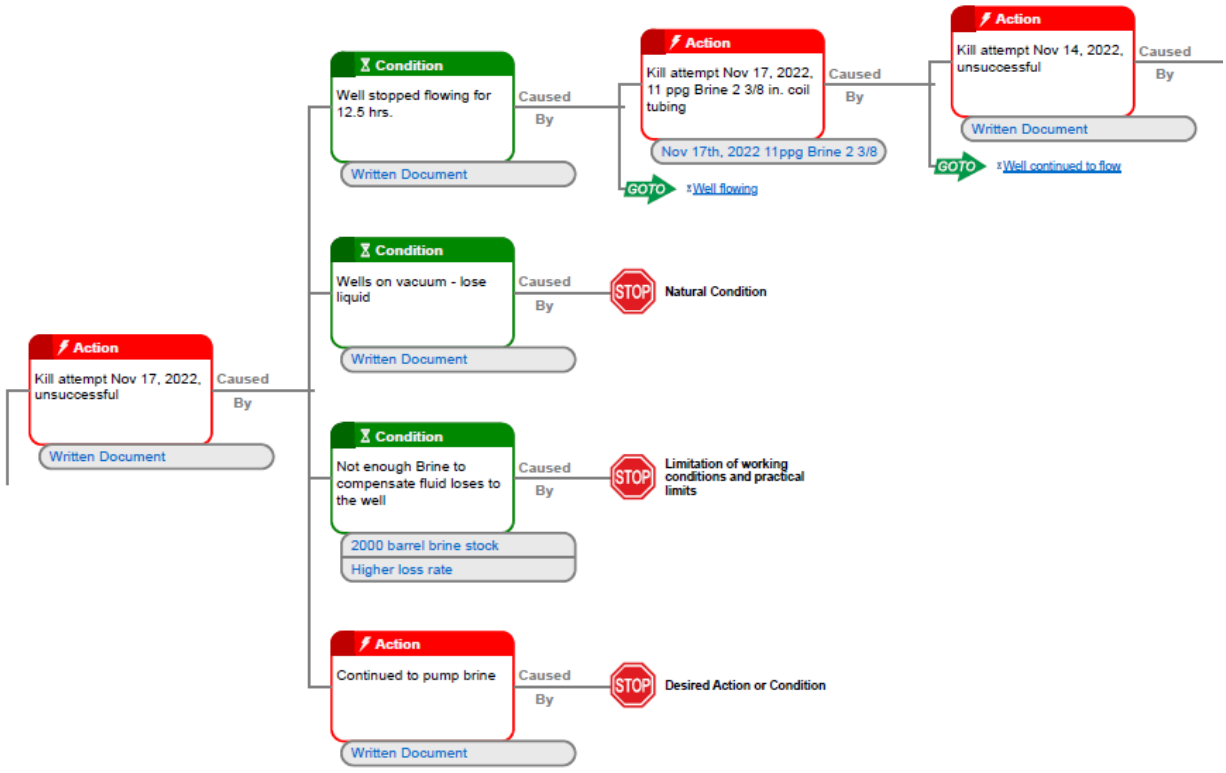

Figure 215: Well #2244 Kill Attempt November 17, 2022

A 2 in. coil tubing unit was available at the time and was evaluated for the kill operation. Internal meeting notes indicate there was belief that the 2 in. coil was big enough to pump at a sufficient rate to kill the well. Efforts were underway to procure a larger coil tubing at the same time as a contingency.

The unsuccessful kill attempt on November 14 was caused by attempting the kill using 2 in. OD coiled tubing and pumping 10 ppg brine. The combination of high friction pressure caused by the 2 in. OD coil and the extra length of coil and the 10 ppg kill fluid resulted in the unsuccessful kill. The reported average pump rate was 5 bpm. The rate was limited by the friction pressure caused by pumping through 18,600 ft of 2 in. coiled tubing. The pump rate of 5 bpm and 10 ppg fluid was insufficient to create a fluid column with sufficient hydrostatic pressure in the casing to overcome the flowing bottom hole pressure, and the well was not killed. The 2 in. coiled tubing with a length of 18,600 ft was available at the time but proved to be inadequate for the kill operation. Attempting the kill with the 2 in. CT had the benefit of finding the obstruction in the well that was removed with a motor and mill run. Following the November 14, kill attempt a 2 3/8 in. OD coiled tubing was sourced and used for subsequent kill attempts. Figure 216 shows the causes and conditions.

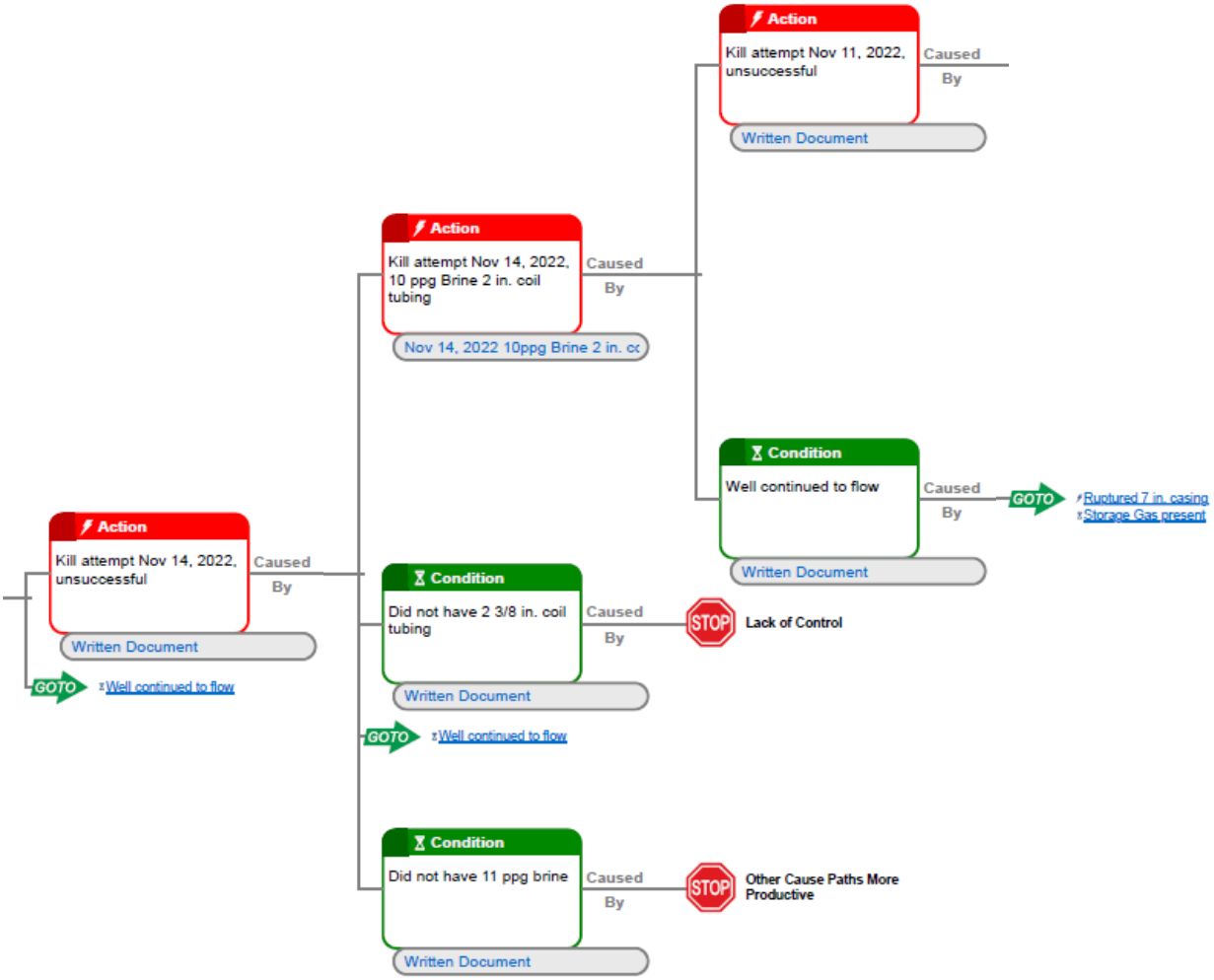

Figure 216: Well #2244 Kill Attempt November 14, 2022

The kill attempt on November 11, 2022, was unsuccessful because of a blockage in the well that prevented running the CT below the wellhead. The kill attempt was aborted, and measures were taken to determine what caused the obstruction and to remove the blockage for the next kill attempt (Figure 217).

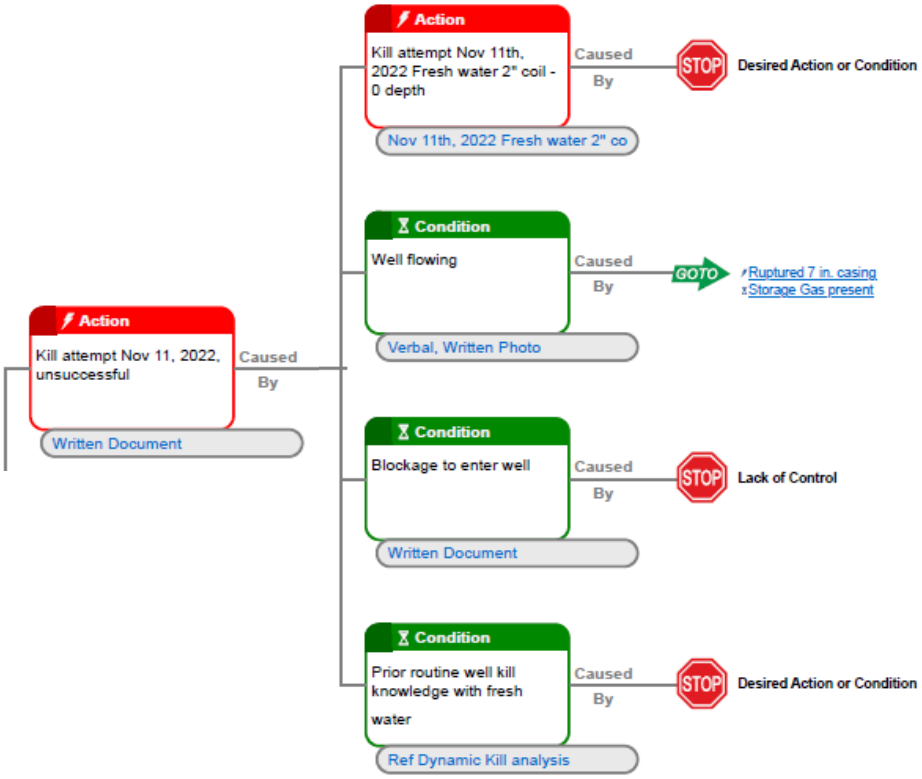

Figure 217: Well #2244 Kill Attempt November 11, 2022

Figure 218 shows the remaining causes of the successful kill on November 19, 2022. A previous kill operation failed because of an insufficient amount of brine to maintain a sufficient fluid column in the well. There were six brine tanks on location and were considered adequate; however, #2244 consumed substantially larger quantity of brine following the kill operation on November 17, 2022. The well flow restarted. The preferred plug was not available at the conclusion of the November 17, kill operation.

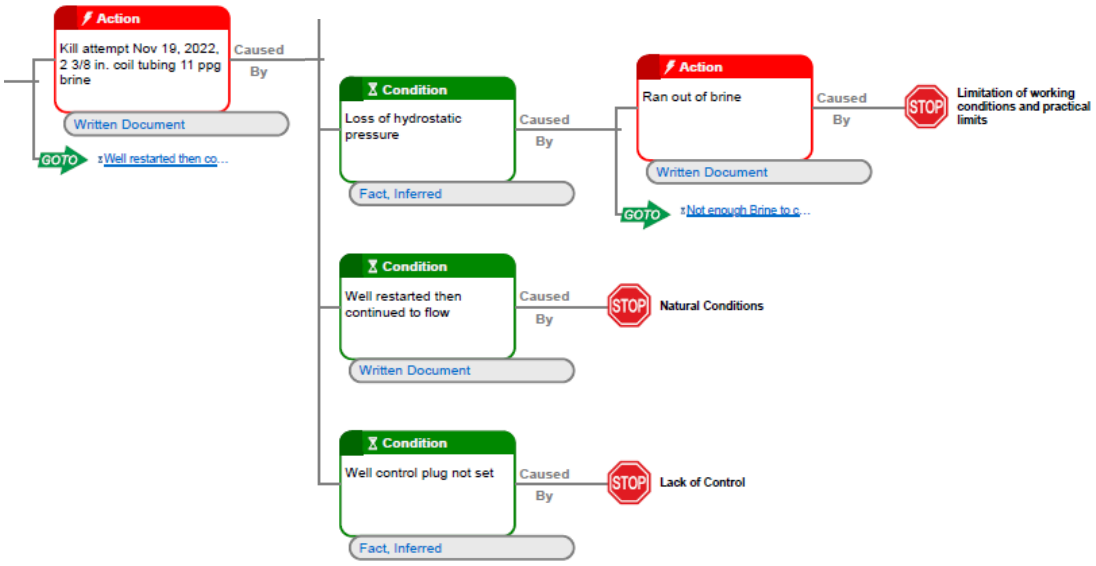

Figure 218: November 19, 2022, Success Kill, Other Causes

15.3 Root Causes

There are numerous root causes as shown in Figure 200; however, many of them are similar in nature. The root causes for the uncontrolled release of hydrocarbon in well #2244 for fourteen days have been consolidated into the following bullets:

- The 7 in. casing was a single barrier to hydrocarbon gas. Rager Mountain wells are single-barrier well designs with the casing as the primary and only barrier. Well #2244 was a prolific well and flowed at high rates.
- The top joint corrosion mechanism was not mitigated by gelling the annulus. Equitrans lacked specific triggers for gelling in the Storage Integrity Management document. Internal documentation indicates that gelling was informally considered but was not executed. Consequently, these guidelines and procedures were not implemented.
- The annulus valve was left open. This allowed ingress of fluids (water, air) and solids (organic and inorganic) and possibly egress through evaporation and otherwise. This resulted in wet-dry cycles and adherent solids on the casing causing oxygen and under-deposit corrosion of the 7 in. casing.
- Based on the available data, the corrosion mechanism was not investigated or examined by the previous operator, despite replacing the top joints in multiple Rager Mountain wells. No reports were found that showed analysis or evaluation of the top joints and casing that were replaced during the life of the field. The apparent mitigation for corroded top joints was to replace joints rather than prevent corrosion.

- Surveillance logging was considered adequate to monitor and mitigate corrosion. This approach assumes that the logging technology is adequate to quantify the corrosion and assumes that the frequency is adequate to detect and mitigate the corrosion. The tool technology is inadequate to characterize general corrosion with pitting. Further, the frequency of logging was changed from 10 years, then to 12 years, then to 15 years, and finally to 7 years through the various versions of the Equitrans Storage Integrity Management Program documents. This did not appear to be based on any estimate of corrosion rate, either through modeling or empirical logging data.

15.4 Solutions

The objective of a root cause analysis is to identify the root causes and develop solutions that meet certain criteria. The root cause analysis identified eight solutions that meet the following criteria:

- The solution prevents recurrence of the problem or failure.
- The solution can be implemented and is within the operating company control.
- The solution meets the goals and objectives.
- The solution does not cause or create other problems.

The list of solutions that will eliminate the root causes are:

- Gelling should be a routine maintenance action that is intended to manage corrosion in the annuli that is independent of the results of surveillance logging. Surveillance logging should be used to confirm the gelling is effective and results in corrosion rates that are acceptable for long-term pressure integrity. In addition to procedures, there should be clear accountability for well integrity decisions, especially during organizational changes. The current structure provides for this.
- Identify all possible threats to the wells and field and ensure individual threat management for each well. Well integrity considerations should also include downhole internal corrosion control that involves a way to mitigate against internal corrosion, log evaluation, and water management. Other log types such as ultrasonic, should be considered to confirm flux-leakage log results if general corrosion is suspected.
- Modify the annulus valve arrangement to install a relief valve, gel the annulus, monitor annulus pressure, and consequently mitigate the top joint *corrosion mechanism* at the Rager Mountain facility.
- Establish a logging frequency based on corrosion analysis, strength, load, and corrosion rate estimates (either historical logs or mechanistic). Use recovered top joint corroded casing to calibrate the inspection logging results.
- Evaluate a tubing-packer completion as a solution where casing integrity is compromised due to cementing issues or corrosion or other threats cannot be mitigated.

As part of the RCA process, additional solutions were identified that would not have directly prevented this incidence, however, they are valuable and will enhance the well integrity program and prevent well integrity type events at Rager Mountain. The proposed solutions are for longer term consideration and do not impact the short term requirements to get the Rager Mountain field back into operation. These solutions are:

- Acknowledging the challenge of surface casing corrosion at Rager Mountain, especially external casing corrosion, A recommendation is to evaluate and implement, if appropriate, external

cathodic protection to protect the surface casing from aquifer or groundwater surface casing corrosion.

- Developing a broad well control plan that has individual well deliverability for all Rager Mountain wells and identifies range of kill fluid densities, pump rates, and a logistics plan. This recommendation includes identifying general requirements for well control equipment and potential suppliers in the region.
- Establishing a cross-functional team between Gas Systems, Integrity, and Operations. A cross-functional team is recommended to evaluate and understand the business value of each well based on well performance. Log evaluation and recommendations to deal with corrosion should involve the teams responsible for well deliverability and operations in addition to well integrity. The team should review the utility of each well and make recommendations regarding keeping wells in service, plugging wells, etc. Other log types, such as ultrasonic, should be considered to confirm flux-leakage log results if general corrosion is suspected. In addition, because some wells exhibit water, they need to assess carefully independent of previous logging results.
- Assigning additional resources to address downhole integrity challenges in an effective manner. All logging data should be analyzed beyond the initial logging vendor assessment for trends and changes over time. Further corrosion mechanisms should be identified to mitigate.
- Maintaining up-to-date wellbore schematics with details of the casing size, weight, grade, and connection, etc., and the completion depth by well. In addition, include a directional survey for each well for relief well planning.
- Cementing to surface all casing strings in new wells. Blade has reviewed the Design and Construction Standard for well construction and the Equitrans standard calls for cementing casing strings to surface. New well designs should also include metal-to-metal connections for tubing and casing exposed to gas to ensure pressure integrity.

16 Mitigation

Blade has worked with Equitrans throughout the RCA process to identify actions to mitigate the corrosion threats and prepare the Rager Mountain facility for injection.

The RCA determined that a root cause of the casing failure in #2244 in November 2022, was corrosion caused by water and organic matter entering the annulus through the open annulus valves. A corrosion management program is recommended to mitigate the corrosion mechanisms.

A recommendation for all Rager Mountain wells is to install a valve arrangement that allows the annulus to vent to avoid excess annulus pressure and to prevent the ingress of water and air. Real-time monitoring of the annulus pressure is recommended to confirm the valve arrangement is working as designed. A gelling program to add a fluid with corrosion inhibitors and biocide to the annulus is recommended.

Several Rager Mountain wells have been worked over in 2023 in addition to the recovery of failed casing in #2244. The upper section of 7 in. casing in well #2244 has been replaced. The well is currently shut-in with plugs that were set after the well was killed. Plans for #2244 are being evaluated. An option for #2244 is to drill out the plugs and run casing inspection logs. Depending on the log results, the well can be recompleted or plugged and abandoned.

A program was undertaken to replace the upper joint of corroded casing in wells where shallow external corrosion has been identified by casing inspection logs. In addition to #2244, wells with top joints replaced in 2023 include #2248, #2251, #2254, and #2253.

The casing in well #2248 was pressure tested after the joint was replaced and there is a leak in the 7 in. casing. The follow-up recommendation for #2248 is to install a tubing-packer completion for injection and withdrawal purposes.

The casing in well #2251 was pressure tested with nitrogen according to Equitrans standard operating procedures and the test was considered successful. However, an annulus shut-in test shows communication between the 7 in. casing and the annulus. The well needs to be evaluated for options to isolate the leak and returned the well to service.

Some wells have internal corrosion in the lower part of the well, possibly caused by water. Batch treating with a corrosion inhibitor is recommended to manage and possibly mitigate the corrosion. Follow-up inspection logging will be needed to monitor the corrosion.

Well #2246 appears to have significant internal corrosion. It is recommended that the well be batch treated with corrosion inhibitors and monitored through logging longer term and consideration given to mitigation that could include a tubing-packer completion or other options.

Table 49 shows a summary of the upper and lower corrosion, the current status, and the recommendations for preparing each well for injection start-up. An annulus valve arrangement is recommended to prevent water, air, and organic matter from entering and exiting the annulus. The valve arrangement requirements include a relief valve, a valve for adding gelling fluid to the annulus, and a connection for real time pressure monitoring. The wells are all shut-in as of the date of this report.

Wells #2244, #2248, and #2251 are in a safe condition with deep plug barriers and can be suspended in the current state while plans for these wells are finalized. Field injection can be restarted in other wells when the pre-injection mitigation steps are completed.

Table 49: Rager Mountain Field Pre-injection Mitigation Recommendations

Well	Upper External Corrosion	Lower Internal Corrosion	Current Status	Mitigation Recommendations Pre-injection
2244	Heavy (before joint replacement)	Light	Cement and bridge plugs. 7 in. casing replaced to 1,488 ft	Relief valve (1) and annulus corrosion inhibitor program Clean out plugs, inspect casing, set deep plugs while considering the recompletion or P & A (2)
2245	Mild	Mild/Heavy	Shut-in Reanalysis of HRVRT	Relief valve (1) and annulus corrosion inhibitor program Batch treat for internal corrosion.
2246	—	Heavy	Shut-in	Relief valve (1) and annulus corrosion inhibitor program Batch Treat Casing with corrosion inhibitor
2247	Mild	—	Shut-in	Relief valve (1) and annulus corrosion inhibitor program
2248	Heavy (before joint replacement)	—	Top joint replaced 2023. Casing leak.	Relief valve (1) and annulus corrosion inhibitor program Remove RBP. Tubing-packer completion (2)
2249	—	—	Shut-in	Relief valve (1) and annulus corrosion inhibitor program
2250	—	—	Shut-in	Relief valve (1) and annulus corrosion inhibitor program
2251	Heavy (before joint replacement)	—	RBP Top joint replaced 2023 Casing leak.	Relief valve (1) and annulus corrosion inhibitor program Remove RBP. Evaluate recompletion options. (2)
2252	Mild	—	Shut-in	Relief valve (1) and annulus corrosion inhibitor program
2253	Mild/Heavy (before joint replacement)	Mild/Heavy	RBP Replaced top joint 2023	Relief valve (1) and annulus corrosion inhibitor program Batch treat for internal corrosion. Remove RBP return to service.
2254	Heavy (before joint replacement)	—	RBP Replaced top joint 2023	Remove RBP return to service. Relief valve (1) and annulus corrosion inhibitor program
2255	Mild	—	Shut-in	Relief valve (1) and annulus corrosion inhibitor program

Note: (1) Proposed annulus relief valve arrangement.

Note: (2): Well can be left shut in safely while starting up field injection in the other wells.

Table 50 shows the current well status and recommendations to mitigate corrosion for long term injection and withdrawal service by well. There are three wells that exhibit internal corrosion features that should be mitigated through batch treatments with corrosion inhibitors. HRVRT logging should be conducted by the end of 2025 to assess the inhibitor effectiveness in #2245, #2246, and #2253. Logging frequency after that period should be based on quantified analysis of the corrosion logs and the batch treatment.

Table 50:Rager Mountain Field Long Term Corrosion Management

Well	Upper External Corrosion	Lower Internal Corrosion	Current Status	Mitigation Recommendation Long Term
2244	Heavy (before joint replacement)	Mild	Cement and bridge plugs. 7 in. casing replaced to 1,488 ft	Batch treat for internal corrosion. Monitor corrosion.
2245	Mild	Mild/Heavy	Shut-in Reanalysis of HRVRT	Batch treat for internal corrosion. Monitor corrosion. (3)
2246	—	Heavy	Shut-in	Batch treat for internal corrosion. Monitor corrosion. (3)
2247	Mild	—	Shut-in	Monitor corrosion.
2248	Heavy (before joint replacement)	—	Top joint replaced 2023. Casing leak.	Monitor corrosion.
2249	—	—	Shut-in	Monitor corrosion.
2250	—	—	Shut-in	Monitor corrosion.
2251	Heavy (before joint replacement)	—	RBP Top joint replaced 2023 Casing leak.	Monitor corrosion.
2252	Mild	—	Shut-in	Monitor corrosion.
2253	Mild/Heavy (before joint replacement)	Mild/Heavy	RBP Replaced top joint 2023	Batch treat for internal corrosion. Monitor corrosion. (3)
2254	Heavy (before joint replacement)	—	RBP Replaced top joint 2023	Monitor corrosion.
2255	Mild	—	Shut-in	Monitor corrosion.

Note: (3) HRVRT Logging should be conducted by the end of 2025 to assess the state of the internal corrosion.

17 Nomenclature

17.1 Abbreviations and Acronyms

Term	Definition
AOF	Absolute open flow
API	American Petroleum Institute
ASME	American Society of Mechanical Engineers
BCF	Billion cubic feet
BHA	Bottom hole assembly
CIBP	Cast iron bridge plug
CAM	Conceptual Site Model
CTU	Coiled tubing unit
DBTT	Ductile brittle transition temperature
DEP	Pennsylvania Department of Environmental Protection
DSPA	Double-studded packoff adapter
DV	Diverter Valve (cement stage tool)
Eline	Electric (logging) line
GR	Gamma Ray
GRNT	Gamma Ray Neutron Temperature
HRVRT	High Resolution Vertilog
ID	Inside diameter
IDGC	Inside diameter general corrosion
ILI	Inline Inspection
I–W/D	Injection/Withdrawal
LEL	Lower Explosive Limit
LTC	Long threaded and coupled
MFL	Magnetic flux leakage
MIC	Microbiologically induced corrosion
NWT	Nominal wall thickness
OD	Outside diameter
PHMSA	Pipeline and Hazardous Material Safety Administration
PLT	Production Logging Tool
PNG	Peoples Natural Gas
POF	Pipeline Operators Forum
RBP	Retrievable Bridge Plug
RTU	Remote Terminal Unit
SCC	Standard cubic centimeter
SEM	Scanning electron microscope

Term	Definition
SENB	Single-edge notch bend
SIMP	Storage Integrity Management Plan
SRB	Sulfate reducing bacteria
UT	Ultrasonic testing
WT	Wall thickness

18 References

[1] D. L. Gano, RealityCharting - Seven Steps To Effective Problem-Solving and Strategies for Personal Success, Richland, Washington: Apollonian Publications, 2011.

[2] Blade Energy Partners, "Rager Mtn Well 2244 Handling Protocol Feb 23 2023.pdf," 2023.

[3] Equitrans, "Email - Rager Storage pigging complete, Rager 5 Day Shut-In," November 2, 2022.

[4] PA DEP, "78.402 Inspections by the gas storage operator," 2023. [Online]. Available: https://www.pacodeandbulletin.gov/Display/pacode?file=/secure/pacode/data/025/chapter78/s78.402.html&d=reduce.

[5] Equitrans, "Item 1: Timeline of Events and Meeting Pertaining to Emergency Response and Remediation of the Incident," 2022.

[6] PNG, "FW PNG Storage - DEP Inspections-RAGER.msg," Email from PNG to Equitrans, November 20, 2012.

[7] PNG, "Letter to Department of Environmental Resources June 30. 1993 2244 well pocket scan.pdf pgs 90-91".

[8] Equitrans, "Equitrans Probablistic Risk Assessment updated Oct22.xlsx," 2022.

[9] AGA INGAA, "GUIDANCE - Risk based evaluation and treatment DRAFT.docx".

[10] AGA INGAA, "JITF Risk Management Process Initiative - AGA-INGAA Presentation - Nowaczewski .pptx," 2018.

[11] Equitrans, "2022 Risk Assessment.pptx".

[12] M. Gao and R. Krishnamurthy, "Failure Analyses and Consequent Mitigation: Case Studies," in *PPIM Paper #109*, Houston, TX, 2023.

[13] W. Zhang, D. Young, B. Brown, C. Shafer, F. Lu and E. Anyanwu, "An in-situ Raman study on the oxidation of mackinawite as a corrosion product layer formed on mild steel im marginally sour environments," *Corrosion Science,* vol. 188, 2021.

[14] J. A. Bourdoiseau, M. Jeannin, C. Remazeilles and P. Refait, "Characterization of mackinawite by Raman spectroscopy: Effects of crystallization, drying, and oxidation," *Corrosion Science,* vol. 50, pp. 3247-3255, 2008.

[15] "API 579-1/ASME FFS-1 Fitness For Service," ASME, June 2016.

[16] ASTM E1820, *Standard Test Method for Measurement of Fracture Toughness,* West Conshohocken, PA: ASTM, 2011.

[17] L. Shengxi and L. H. Hihara, "A Micro-Raman Spectroscopic Study of Marine Atmospheric Corrosion of Carbon Steel: The Effect of Akaganeite," *Journal of The Electrochemical Society,* vol. 162, no. 9, pp. C495-C502, 2015.

[18] M. Morcillo, D. Fuente, I. Diaz and H. Cano, "Atmospheric Corrosion of Mild Steel," *Revista de Metalurgia,* vol. 47, no. 5, pp. 426-444, 2011.

[19] S. Nasrazadani and A. Raman, "Formation and Transformation of Magnetite (Fe3O4) on Steel Surfaces Under Continuous and Cyclic Water Fog Testing," *Corrosion,* vol. 49, no. 4, 1993.

[20] M. Madani and R. D. Granata, "Study of Akaganeite in Weathering Steel Corrosion Products and Distance From Ocean in South Florida," *Corrosion,* Vols. NACE-2018-11337, 2018.

[21] S. M. Cambier, D. Verreault and G. S. Frankel, "Raman Investigation of Anodic Undermining of Coated Steel During Environmental Exposure," *Corrosion,* vol. 70, no. 12, pp. 1219-1229, 2014.

[22] N. Buzgar and A. I. Apopei, "The Raman Study of Certian Carbonates," Universitatea Alexandru load Cuza, 2014.

[23] *NACE TM0194-94: Field Monitoring of Bacterial Growth in Oil and Gas Systems,* Houston, TX: NACE, 1994.

[24] *NACE TM0212-2018: Detection, Testing, and Evaluation of Microbiologically Influenced Corrosion on Internal Surfaces of Pipelines,* Houston, TX: NACE International, 2018.

[25] *NACE TM0106-2016: Detection, Testing and Evaluation of Microbiologically Influenced Corrosion (MIC) on External Surfaces of Buried Pipelines,* Houston, TX: NACE International, 2016.

[26] B. Little and J. Lee, Microbiologically Influenced Corrosion, Hoboken, NJ: Wiley & Sons, 2007.

[27] B. J. Little and J. S. Lee, "Microbiologically Influenced Corrosion," in *Oil and Gas Pipelines Integrity and Safety Handbook*, Hoboken, NJ, John Wiley & Sons, 2015, pp. 387-398.

[28] H. Herro, "MIC Myths- Does Pitting Cause MIC?," in *Corrosion*, San Diego, CA, 1998.

[29] J. S. Lee and B. J. Little, "Diagnosing Microbiologically Influenced Corrosion," in *Microbiologically Influenced Corrosion in the Upstream Oil and Gas Industry*, Boca Raton, FL, CRC Press, 2017, pp. 157-175.

[30] B. Little, J. Lee and R. Ray, "Diagnosing Microbiologically Influenced Corrosion: A State-of-the-Art Review," *Corrosion,* vol. 62, no. 11, pp. 1006-1017, 2006.

[31] C. Rodriguez, J. Hook and S. Underwood, "Sucessful Treatment of a Corrosive Acetic Acid Producing Halophile that is Averse to Culture Media," in *CORROSION*, 2021.

[32] B. Little, P. Wagner and Z. Lewandowski, "The Role of Biomineralization in Microbiologically Influenced Corrosion," in *Corrosion*, San Diego, CA, 1998.

[33] H. Almahadmedh, J. Spear, D. Olson, C. Williamson and B. Mishra, "Identification of Microorganisms and Their Effects on Corrosion of Carbon Steels Pipelines," in *Corrosion*, Houston, TX, 2011.

[34] J. Larsen, K. Rasmussen, H. Pedersen, K. Sorensen, T. Lundgaard and T. Skovhus, "Consortia of MIC Bacteria and Archaea Causing Pitting Corrosion in Top Side Oil Production Facilities," in *Corrosion*, San Antonio, TX, 2010.

[35] T. Rao, T. Sairam and K. N. B. Viswanathan, "Carbon Steel Corrosion by Iron Oxidising and Sulphate Reducing Bacteria in Freshwater Cooling System," *Corrosion Science,* vol. 42, pp. 1417-1431, 2000.

[36] D. Pope, *Microbiologically Influenced Corrosion (MIC): Methods of Detection in the Field,* Chicago, IL: Gas Research Institue, 1990.

[37] L. N. Strickland, R. T. Fortnum and B. W. Du Bose, "A Case History of Microbiologically Influenced Corrosion in the Lost Hills Oilfield, Kern County, California," in *Corrosion*, Denver, CO, 1996.

[38] Blade Energy Partners, "Root Cause Analysis of Uncontrolled Hydrocarbon Release from Aliso Canyon SS-25," 17 May 2019. [Online]. Available: https://files.cpuc.ca.gov/News_and_Outreach/SS-25%20RCA%20Final%20Report%20May%2016,%202019.pdf. [Accessed 14 July 2023].

[39] R. Baboian, Galvanic Corrosion, ASM Handbook 13A – Corrosion: Fundamentals Testing and Protection, Materials Park, OH: ASM International, 2003.

[40] R. J. Landrum, Fundamentals of Designing for Corrosion Control, Houston, TX: National Association of Corrosion Engineers, 2012.

[41] M. Noecker, D. W. Greenman and N. Beamer, "Water Resources of the Pittsburgh Area, Pennsylvania," Geological Survey, Washington, DC, 1954.

[42] D. Jones, Principles and Prevention of Corrosion, Upper Saddle River, NJ: Prentice-Hall, 1996.

[43] Baker Hughes, "Gamma Ray Neutron Differential Temperature - EQT 2244 Rager Mountain Storage Cambria," 2016.

[44] F. Speller, "Corrosion, Causes and Preventation," McGraw-Hill, 1951, p. 168.

[45] G. Schmitt, G. Karbasi, S. Nesic, R. H. B. Kinsella and B. Brown, "Pitting in Water/Hydrocarbon Boundary Region of Pipelines – Effect of Corrosion Inhibitors," in *Corrosion*, Orlando, FL, 2013.

[46] *2023-02-16 Gas Sample Summary.xls,* 2023.

[47] J. R. Vera, D. Daniels and M. H. Achour, "Under Deposit Corrosion in Oil and Gas Industry: A Review of Mechanisms, Testing and Mitigation," in *Corrosion*, Salt Lake City, Utah, 2012.

[48] Z. B. Wang, L. Pang and Y. G. Zheng, "A review of under-deposit corrosion of pipelines in oil and gas fields: Testing methods, corrosion mechanisms and mitigation strategies," *Corrosion Communications,* vol. 7, pp. 70-81, 2022.

[49] X. Wang and R. Melchers, "Long-term under-deposit pitting corrosion of carbon steel pipes," *Ocean Engineering,* vol. 133, pp. 231-243, 2017.

[50] C. Kagarise, J. Vera and R. Eckert, "The Importance of Deposit Characterization in Mitigating UDC and MIC in Dead Legs," in *Corrosion*, New Orleans, LA, 2017.

[51] P. K. Shukla and S. Naraian, "Under-Deposit Corrosion in a Sub-Sea Water Injection Pipeline – A Case Study," in *Corrosion*, New Orleans, LA, 2017.

[52] L. Pang, Z. Wang, Y. Zheng, X. Lai and X. Han, "On the localised corrosion of carbon steel induced by the in-situ local damage of porous corrosion products," *Journal of Materials Science and Technology,* vol. 54, pp. 95-104, 2020.

[53] L. Pang, Z. Wang, W. Emori and Y. Zheng, "Under-Deposit Corrosion of Carbon Steel Beneath Full Coverage of CaCO3 Deposit Layer under Different Atmospheres," *Journal of Materials Engineering and Performance,* vol. 30, pp. 7552-7563, 2021.

[54] Oilfield Team, "API 8-rd Connections," [Online]. Available: https://oilfieldteam.com/en/a/learning/API-8-rd-Connections. [Accessed 01 June 2023].

[55] W. T. Asbill, P. D. Pattillo and W. M. Rogers, "Investigation fo API 8 Round Casing Connection Performance - Part III: Sealability and Torque," *Transactions of the ASME,* vol. 106, pp. 144-152, 1984.

[56] J. C. M. Uribe, R. Carrazedo and A. T. Beck, "Leakage Resistance Envelopes of API 8 Round Casing Connection using FE Analysis," *Latin American Journal of Solids and Structures,* no. 162, 2019.

[57] C. Teodoriu and M. Badicioiu, "Sealing Capacity of API Connections - Tehoretical and Experimental Results," *SPE Drilling & Completion,* pp. 96-103, 2009.

[58] P. Cazenave, K. Jimenez, S. Tandon and R. Krishnamurthy, "Improving In-Line Inspectoin Sizing Accuracy," PRCI Project NDE-4-19F, PRCI Report PR-328-203803-R01, 2023.

[59] "2023-05-03 Representative Wellhead Gas Composition from 11978 Samples.xlsx".

[60] "AWD4670 Rager Mtn Pond.pdf".

[61] SLB, "Drillbench," [Online]. Available: https://www.software.slb.com/products/drillbench/drillbench-dynamic-well-control. [Accessed 2023].

[62] American Petroleum Institute, "API RP 1171, Functional Integrity of Natural Gas Storage in Depleted Hydrocarbon Reservoirs and Aquifer Reservoirs," Washington, DC, November 2022.

[63] ASTM E23, *Standard Test Methods for Notched Bar Impact Testing of Metallic Materials,* West Conshohocken, PA: ASTM, 2007.

[64] ASTM E1823, *Standard Terminology Relating to Fatigue and Fracture Testing,* West Conshohocken: ASTM, 2000.

[65] *Specification for Casing and Tubing,* API 5CT, 2011.

[66] T. L. Anderson, Fracture Mechanics Fundamentals and Applications, 2nd ed., Boca Raton, FL: CRC Press, 2004.

[67] X.-K. Zhu and J. A. Joyce, "Review of Fracture Toughness (G, K, J, CTOC, CTOA) Testing and Standardization," *Engineering Fracture Mechanics,* vol. 85, pp. 1-46, May 2012.

19 Appendices

Page intentionally left blank

Appendix A Detailed Information

Page intentionally left blank

A.1 Well Summary

Well	Well Type (Injection or Obs.)	Year Drilled	Surface hole fluid (While drilling)	Surf Casing OD (in.)	Surf Casing Depth (ft)	Prod Hole Fluid (While drilling)	Production Casing OD (in.)	Prod Casing Depth (ft)	Prod Casing Wt. (ppf)	Prod Casing Grade	Casing MIYP (psi)	DV Tool Part of Original Completion?	DV Tool Depth (ft)	Total Depth (ft)
2244	Inj	1965	Foam	9.625	1,794	Air	7	7,701	26	N80	7,240	No		7,866
2245	Inj	1965	Not stated	8.625	1,657	Not stated	5.5	7,692	20/17	P110/J55	12,640/5,320	No		7,874
2246	Obs	1966	Air	8.625	1,780	Air and Foam	5.5	7,872	17	N80	7,740	No		8,031
2247	Obs	1967	Foam	9.625	1,305	Air	7	7,927	26	N80	7,240	No		8,100
2248	Inj	1968	Not stated	9.625	1,178	Not stated	7	7,592	26	N80	7,240	No		7,681
2249	Inj	1971	Foam	9.625	1,325	Air	7	7,738	26	N80/P110	7,240	Yes	5,005	7,920
2250	Inj	1974	Foam	9.625	1,262	Air	7	7,800	26	N80	7,240	Yes	4,999	8,000
2251	Inj	1989	Air and Foam	10.75	1,533	Air	7	7,758	26	P110	9,960	Yes	5,719	8,051
2252	Inj	1989	Air and Fluid	10.75	1,747	Air	7	7,704	26	P110	9,960	Yes	5,613	7,869
2253	Inj	2010	Air and Foam	9.625	1,664	Air and Fluid	7	7,809	26	N80	7,240	No		8,054
2254	Inj	2010	Air and Foam	9.625	1,670	Air and Fluid	7	7,835	26	N80	7,240	No		8,156
2255	Inj	2011	Not stated	9.625	1,541	Not stated	7	7,693	26	N80	7,240	No		7,960

A.2 Historical Events for Well #2244

Table 51: Pre-Incident Well Operations Records for Well #2244 (Chronological Order)

Row	Date	Description	Reference
		Original Drilling	
1	September 12, 1965	Spudded 12 1/4 in. conductor hole. Fox Drilling.	2244 well pocket scan 7.pdf page 198
2	September 13, 1965	Drilled 12 1/4 in. hole to 57 ft. Open hole to 17 1/2 in. to 42 ft.	2244 well pocket scan 7.pdf page 198
3	September 14, 1965	Ran and cemented 13 3/8 in. conductor at 40 ft. Cement to surface. WOC.	2244 well pocket scan 7.pdf page 198
4	September 15, 1965	NU WH. Drilled to 70 ft with air and soap.	2244 well pocket scan 7.pdf page 198
5	September 16, 1965	Drilling 12 1/4 in. hole to 195 ft with foam.	2244 well pocket scan 7.pdf page 199
6	September 17, 1965	Drilling 12 1/4 in. hole to 410 ft with foam.	2244 well pocket scan 7.pdf page 199
7	September 18, 1965	Drilling 12 1/4 in. hole to 668 ft with foam.	2244 well pocket scan 7.pdf page 199
8	September 19, 1965	Drilling 12 1/4 in. hole to 1,110 ft with foam.	2244 well pocket scan 7.pdf page 199
9	September 20, 1965	Drilling 12 1/4 in. hole to 1,524 ft with foam.	2244 well pocket scan 7.pdf page 200
10	September 21, 1965	Drilling 12 1/4 in. hole to 1,800 ft with foam. POH. Run 9 5/8 in. 36 ppf J55 STC casing.	2244 well pocket scan 7.pdf page 200
11	September 22, 1965	Finish running casing. Cement 9 5/8 in. casing with 30 sx gel and 150 cu ft regular cement with 2% CaCl2. No cement to surface. WOC. NU WH. Shoe at 1,794 ft.	2244 well pocket scan 7.pdf page 200
12	September 23, 1965	NU WH. RIH and drill shoe joint. Blew water and started drying hole.	2244 well pocket scan 7.pdf page 201
13	September 24, 1965	Drilling to 2,300 ft. Dry and dusting.	2244 well pocket scan 7.pdf page 201
14	September 25, 1965	Drilling to 3,010 ft. Dry and dusting.	2244 well pocket scan 7.pdf page 201
15	September 26, 1965	Drilling to 3,760 ft. Dry and dusting.	2244 well pocket scan 7.pdf page 202
16	September 27, 1965	Drilling to 4,500 ft. Dry and dusting.	2244 well pocket scan 7.pdf page 202
17	September 28, 1965	Drilling to 5,350 ft. Dry and dusting.	2244 well pocket scan 7.pdf page 202
18	September 29, 1965	Drilling 8 3/4 in. hole to 5,930 ft. Dry and dusting.	2244 well pocket scan 7.pdf page 202
19	September 30, 1965	Drilling 8 3/4 in. hole to 6,400 ft. Dry and dusting.	2244 well pocket scan 7.pdf page 204

Row	Date	Description	Reference
20	October 1, 1965	Drilling 8 3/4 in. hole to 6,620 ft. Dry and dusting.	2244 well pocket scan 7.pdf page 204
21	October 2, 1965	Drilling 8 3/4 in. hole to 6,920 ft. Dry and dusting.	2244 well pocket scan 7.pdf page 203
22	October 3, 1965	Drilling 8 3/4 in. hole to 7,300 ft. Dry and dusting.	2244 well pocket scan 7.pdf page 203
23	October 4, 1965	Drilling 8 3/4 in. hole to 7,654 ft. Top of chert at 7,652 ft. LD DP. Prep to log.	2244 well pocket scan 7.pdf page 205
24	October 5, 1965	POH with DP. Stuck pipe at 6,450 ft. Worked free. Ran SLB directional survey from TD to 1,794 ft. Gamma ray Density logs from 4,000 ft to surface. RIH with DP. Corrected depth to 7,696 ft. C&C hole. POH LD DP. Running 7 in. casing.	2244 well pocket scan 7.pdf page 205
25	October 6, 1965	Finish running 7 in. casing. Cemented casing at 7,701 ft with 200 sx 50:50 Pozmix A.	2244 well pocket scan 7.pdf page 206
26	October 7, 1965	NU WH.	2244 well pocket scan 7.pdf page 206
27	October 8, 1965	Wait on 3 1/2 in. DP.	2244 well pocket scan 7.pdf page 206
28	October 9, 1965	Wait on 3 1/2 in. DP.	2244 well pocket scan 7.pdf page 206
29	October 10, 1965	Wait on 3 1/2 in. DP.	2244 well pocket scan 7.pdf page 206
30	October 11, 1965	Wait on 3 1/2 in. DP.	2244 well pocket scan 7.pdf page 206
31	October 12, 1965	Wait on 3 1/2 in. DP.	2244 well pocket scan 7.pdf page 206
32	October 13, 1965	MU 6 1/8 in. bit and BHA. Pick up DP. Pressure test casing to 3,000 psi.	2244 well pocket scan 7.pdf page 207
33	October 14, 1965	Drill cement and clean hole. MU core bbl.	2244 well pocket scan 7.pdf page 207
34	October 15, 1965	RIH with core bbl. Cored 7,701 – 7,708 ft. POH. LD CB. TIH with reamer and bit. Ream and drill to 7,723 ft.	2244 well pocket scan 7.pdf page 208
35	October 16, 1965	Drill 6 1/8 in. hole to 7,800 ft with water. Top of Oriskany 7,796 ft. POH.	2244 well pocket scan 7.pdf page 209
36	October 17, 1965	[part of daily report missing] Coring Oriskany at 7,810 ft, 75 bbl fluid gain (well flowed) shut well in. Increase mud weight to kill well.	2244 well pocket scan 7.pdf page 210
37	October 18, 1965	Total Depth 7,810 ft. Weight up mud.	2244 well pocket scan 7.pdf page 210
38	October 19, 1965	Pump and kill well. Lost returns. Bleed off annulus pressure. Pulled 65 stands, well flowed. Bled casing pressure. Repair valves. Lay flow line.	2244 well pocket scan 7.pdf page 210

Row	Date	Description	Reference
39	October 20, 1965	[part of daily report missing] POH with core. Flow well at 8,245 Mcfd.	2244 well pocket scan 7.pdf page 211
40	October 21, 1965	Flowed well. 8,200 MCFD. Removed core from CB. LD DP. ND BOP.	2244 well pocket scan 7.pdf page 211
41	October 22, 1965	LD DP. RD.	2244 well pocket scan 7.pdf page 211
42	October 23, 1965	LD DP. RD. Released rig.	2244 well pocket scan 7.pdf page 211
43			
44		Drill Deeper - 1967	2244 021-20005 CR and Loc Plat, VINTONDALE, GEORGE L READE 1.pdf page 2
45	May 1, 1967	Prep to move.	2244 well pocket scan 7.pdf page 216
46	May 2, 1967	MIRU	2244 well pocket scan 7.pdf page 214
47	May 3, 1967	RU and kill well.	2244 well pocket scan 7.pdf page 214
48	May 4, 1967	Kill well.	2244 well pocket scan 7.pdf page 214
49	May 5, 1967	Kill well.	2244 well pocket scan 7.pdf page 214
50	May 6, 1967	ND tree, NU BOP. Well flowed.	2244 well pocket scan 7.pdf page 215
51	May 7, 1967	ND tree, NU BOP. Well flowed. RIH and set bridge plug at 7,580 ft.	2244 well pocket scan 7.pdf page 215
52	May 8, 1967	RIH with 6 1/8 in. bit. Well flowed. Kill well. RIH with DP.	2244 well pocket scan 7.pdf page 216
53	May 9, 1967	Finish PU 3 1/2 in. DP and RIH to 7,750 ft. C&C. Drill on bridge plug at 7,580 ft.	2244 well pocket scan 7.pdf page 212
54	May 10, 1967	Drill on BP at 7,810 ft. Drilling at 7,814 ft.	2244 well pocket scan 7.pdf page 212
55	May 11, 1967	Drilled to 7,844 ft 6 1/8 in. hole.	2244 well pocket scan 7.pdf page 212
56	May 12, 1967	Drilled to 7,866 ft 6 1/8 in. hole. Lost circulation. Mix mud. Established circulation.	2244 well pocket scan 7.pdf page 218
57	May 13, 1967	C&C. Lost circulation. Establish circulation.	2244 well pocket scan 7.pdf page 218
58	May 14, 1967	C&C. Stuck pipe at 7,830 ft. Spotted fluid. Worked pipe free. POH.	2244 well pocket scan 7.pdf page 218
59	May 15, 1967	POH LD DP. Change rams. Run 2 3/8 in. tubing.	2244 well pocket scan 7.pdf page 219

Row	Date	Description	Reference
60	May 16, 1967	Finish running 2 3/8 in. tubing. Landed tubing. ND BOP. NU tree. Ran Gamma ray log 7,852 to 3,000 ft. Released rig.	2244 well pocket scan 7.pdf page 219
61	May 17, 1967	RD.	2244 well pocket scan 7.pdf page 220
62	May 18, 1967	Acidize well and flow well. Acid frac? Discussed 6/8/2023 team meeting. See frac done in 1968. Check for records.	2244 well pocket scan 7.pdf page 220
63	May 19, 1967	Flowed well.	2244 well pocket scan 7.pdf page 223
64			
65	1971	Conversion to gas storage	Assumed from Doc 003
66			
67		Workover to Replace Casing	
68	May 5, 1993	Prep	2244 well pocket scan 5.pdf page 38
69	May 6, 1993	Haul in brine and fresh water.	2244 well pocket scan 5.pdf page 39
70			
71		Complete RU. Kill well. ND WH. Install BOP. Pull tubing.	2244 well pocket scan 5.pdf page 40
72	May 13, 1993	Pull 2 3/8 in. tubing. Set WL bridge plug at 7,624 ft. RIH with tubing and spot sand on BP. Log well. [CBL-VDL]	2244 well pocket scan 5.pdf page 41
73	May 14, 1993	Finish logging. ND BOP and WH. Weld on pulling nipple. Pulled slips. Ran free point, free at 2,500 ft. Cut off head. Ran free point, free at 6,000 ft.	2244 well pocket scan 5.pdf page 42
74	May 15, 1993	RIH with DP and cutter. Make cut at 5,945 ft. POH. Work casing to 200,000 lb. Call out free point.	2244 well pocket scan 5.pdf page 43
75	May 16, 1993	Ran FP. Pipe free above and below the cut. TIH with cutter. Cut at 5,959 ft. POH cutter. Pulling 7 in. casing.	2244 well pocket scan 5.pdf page 44
76	May 17, 1993	Finish pulling 7 in. casing. Run SLB log [9 5/8 in. Multifrequency Electromagnetic Thickness Log] Welding to raise wellhead. Nipple up. RIH with bridge plug [9 5/8 in.] and set at 1,555 ft. Spot sand on BP. Perforated 8 holes at 1,180 ft. Hook up to circulate. Work on leaks at collar.	2244 well pocket scan 5.pdf page 45
77	May 18, 1993	Fix collar leaks and start cement squeeze. WOC. Good cement returns. NU. TIH to drill out cement.	2244 well pocket scan 5.pdf page 46
78	May 19, 1993	TIH. Tag cement at 988 ft. DO cement to 1,200 ft. TIH and CO sand. TIH and recover BP. TIH to 5,800 ft. CO to 5,949 ft.	2244 well pocket scan 5.pdf page 47
79	May 20, 1993	CO to 5,949 ft. Drag with hole caving. Mix and pump 450 bbl gel. Displace salt water to pit. POH. Run caliper	2244 well pocket scan 5.pdf page 48

Row	Date	Description	Reference
		log. POH with log. Start running 7 in. casing. Hydro-Test connection with H-N2 gas to 4,000 psi.	2244 well pocket scan 5.pdf page 23
80	May 21, 1993	Running 7 in. casing. Latch into casing with patch. ND and set slips. Cut off casing. NU BOP. TIH with Halliburton tool to cement first stage.	2244 well pocket scan 5.pdf page 49
81	May 22, 1993	Pump first stage. Pull up to second stage to circulate. Could not seal at BOP. WOC. Order new 3 1/2 in. rams. Install new 3 1/2 in. rams. Ran cement top log. TOC 3,470 ft, 26 ft below stage collar. TIH with Halliburton tool and DP.	2244 well pocket scan 5.pdf page 50
82	May 23, 1993	Pump through stage tool at 2,700 psi. No circulation. Shut stage tool. POH. TIH with 6 1/8 in. bit. TOC at 5.865 ft. Drill 10 ft of cement. CO and circulate and condition hole to 7,479 ft. POH.	2244 well pocket scan 5.pdf page 51
83	May 24, 1993	Finish POH. Ran SLB log [CBL-VDL] TOC at 2,950 ft. TIH with Halliburton tool. Squeeze 50 sx behind the stage tool. POH. TIH with 6 1/8 in. bit.	2244 well pocket scan 5.pdf page 52
84	May 25, 1993	WOC. No cement to drill. RIH to 7,590 ft. POH. RIH with magnet and boot basket. CO from 7,590 – 7,596 ft. POH.	2244 well pocket scan 5.pdf page 53
85	May 26, 1993	POH. Recovered tong die and metal. LD DP. RD	2244 well pocket scan 5.pdf page 54
86	May 27, 1993	Install new wellhead. Set BP and test WH.	2244 well pocket scan 5.pdf page 55
87			
88	June 2, 1993	Remove top flange. RU Otis. Retrieved BP at 1,000 ft. TIH to retrieve second BP. Could not get past 5,952 ft. TIH to top of sand at 5,590 ft. TOH.	2244 well pocket scan 5.pdf page 56
89	June 3, 1993	TIH with jetting tool and N2 foam. Jet out fluid and sand to 7,607 ft. Pick up catch tool. TIH, catch plug and TOH. Did not retrieve plug.	2244 well pocket scan 5.pdf page 57
90	June 4, 1993	TIH and jet. TOH. TIH with baker 7 in. BP retrieving tool. Load hole with 105 bbl of brine to equalization. TOH. Lost tools in the hole.	2244 well pocket scan 5.pdf page 58
91	June 5, 1993	TIH with 6 in. impression block to 7,330 ft. POH. No marks on IB. TIH with IB to 7,330 ft. POH. Small mark in IB.	2244 well pocket scan 5.pdf page 59
92	June 6, 1993	Shut Down	2244 well pocket scan 5.pdf page 59
93	June 7, 1993	Shut Down	2244 well pocket scan 5.pdf page 59
94	June 8, 1993	Haul brine.	2244 well pocket scan 5.pdf page 60
95			

Row	Date	Description	Reference
96	June 16, 1993	RU Otis Camera.	2244 well pocket scan 5.pdf page 61
97			
98	July 19, 1993	Cudd on site. Unload and RU. [Snubbing unit?]	2244 well pocket scan 5.pdf page 62
99	July 20, 1993	RU Cudd Pressure Control	2244 well pocket scan 5.pdf page 63
100	July 21, 1993	Pressure test BOP. RIH with fishing tools.	2244 well pocket scan 5.pdf page 64
101	July 22, 1993	RIH.	2244 well pocket scan 5.pdf page 65
102	July 23, 1993	TIH. On fish, fish fell away at 7,330 ft. Chased to 7,743 ft. POH.	2244 well pocket scan 5.pdf page 66
103	July 24, 1993	POH. Did not recover fish.	2244 well pocket scan 5.pdf page 67
104	July 25, 1993	Shut down.	2244 well pocket scan 5.pdf page 68
105	July 26, 1993	Shut down.	2244 well pocket scan 5.pdf page 68
106	July 27, 1993	Ran Otis camera to look at lost tools.	2244 well pocket scan 5.pdf page 69
107	July 28, 1993	RD camera. Install Tri-state drag tooth guide. Start TIH. Could not enter 7 in. casing.	2244 well pocket scan 5.pdf page 70
108	July 29, 1993	TIH with tools to fish.	2244 well pocket scan 5.pdf page 71
109	July 30, 1993	Fishing. Start POH.	2244 well pocket scan 5.pdf page 72
110	July 31, 1993	TOH. Did not get bridge plug.	2244 well pocket scan 5.pdf page 73
111	August 1, 1993	TIH with fishing tools.	2244 well pocket scan 5.pdf page 74
112	August 2, 1993	TIH to fish.	2244 well pocket scan 5.pdf page 75
113	August 3, 1993	TOH. Recovered tools [bridge plug].	2244 well pocket scan 5.pdf page 76
114	August 4, 1993	Rig down.	2244 well pocket scan 5.pdf page 77
115			
116	August 23, 1993	Install valve and test.	2244 well pocket scan 5.pdf page 78
117			
118		Change Master Valve	

Row	Date	Description	Reference
119	July 14, 2004	MIRU Baker Atlas. RIH with 6.00 in. gauge ring junk basket. Set down on master valve then fell through. POOH gauge ring.	001 2244 Wellpocket schematic of 1993 repair pg7.pdf page 4
120			
121	August 17, 2004	MIRU Baker Atlas WL and crane truck. MU 6.12 in. gauge ring on 5.75 in junk basket. NU lubricator. Could not get through master valve. Turned down gauge ring to 6.000 in. RIH GR-JB to 6,500 ft. POH. RIH with Baker 7 in. RBP. Set RBP at 6,445 ft. POH with setting tool. Bled gas off casing through lubricator. Fill casing with 10 ppg brine. SDFN.	001 2244 Wellpocket schematic of 1993 repair pg7.pdf page 3
122	August 18, 2004	Top off casing with brine water. ND studded cross and master valve. NU new 7 1/16 in 5000 psi MV. NU studded cross. Shut well in.	001 2244 Wellpocket schematic of 1993 repair pg7.pdf page 2
123	August 20, 2004	MI Halliburton Coil tubing, crane, and pump truck. NU 7 1/16 in. flow tee. NU and test connector and BOP. RIH with retrieving tool. RIH pumping N2 to unload brine. Shut well in and pressure test annulus to 3,000 psi [CT x casing annulus?]. Bleed pressure to 1,035 psi. Attempt to latch plug. Could not get on plug. Pressured up tubing to annulus pressure. Latched plug. Bled CT to 500 psi. Annulus pressure dropped to 2,266 psi. Unset BP and POH. NU 4 1/16 in. 5,000 psi swab valve. Flow well to unload N2. Shut well in. Move off.	001 2244 Wellpocket schematic of 1993 repair pg7.pdf page 1

Table 52: Pre-Incident Maintenance Records (Maximo) for Well #2244 (Chronological Order)

Work Order Number	Description	Status	Date and Time Completed
1632627	Inspect Well - Rager Mtn - RAG2244 - (PNG4469)	CLOSE	2013-12-18, 12:00:00 AM
1639741	Inspect Well - Rager Mtn - RAG2244 - (PNG4469)	CLOSE	2014-01-17, 12:00:00 AM
1660602	Inspect Well - Rager Mtn - RAG2244 - (PNG4469)	CLOSE	2014-02-10, 12:00:00 AM
1679416	GForms AdHoc - General WO	CLOSE	2014-02-21, 12:00:00 AM
1681738	Inspect Well - Rager Mtn - RAG2244 - (PNG4469)	CLOSE	2014-03-05, 12:00:00 AM
1700572	Echo Metering - Rager Mtn - RAG2244 - (PNG4469)	CLOSE	2014-04-01, 12:00:00 AM
1684913	Shut-In Testing - Rager Mtn - RAG2244 - (PNG4469)	CLOSE	2014-04-02, 12:00:00 AM
1705879	Inspect Well - Rager Mtn - RAG2244 - (PNG4469)	CLOSE	2014-04-07, 12:00:00 AM
1727313	Inspect Well - Rager Mtn - RAG2244 - (PNG4469)	CLOSE	2014-05-09, 12:00:00 AM
1745671	Inspect Well - Rager Mtn - RAG2244 - (PNG4469)	CLOSE	2014-06-02, 12:00:00 AM
1762552	Inspect Well - Rager Mtn - RAG2244 - (PNG4469)	CLOSE	2014-07-03, 12:00:00 AM
1778825	Inspect Well - Rager Mtn - RAG2244 - (PNG4469)	CLOSE	2014-08-06, 12:00:00 AM
1797625	GForms AdHoc - Field Investigation	CLOSE	2014-09-04, 12:00:00 AM

Work Order Number	Description	Status	Date and Time Completed
1793881	Inspect Well - Rager Mtn - RAG2244 - (PNG4469)	CLOSE	2014-09-08, 12:00:00 AM
1808958	Inspect Well - Rager Mtn - RAG2244 - (PNG4469)	CLOSE	2014-10-02, 12:00:00 AM
1818869	GForms AdHoc - Field Investigation	CLOSE	2014-10-21, 12:00:00 AM
1823760	Inspect Well - Rager Mtn - RAG2244 - (PNG4469)	CLOSE	2014-11-06, 12:00:00 AM
1795683	Shut-In Testing - Rager Mtn - RAG2244 - (PNG4469)	CLOSE	2014-11-11, 12:00:00 AM
1811036	Echo Metering - Rager Mtn - RAG2244 - (PNG4469)	CLOSE	2014-11-11, 12:00:00 AM
1831594	GForms AdHoc - General WO	CLOSE	2014-11-19, 12:00:00 AM
1833338	GForms AdHoc - Field Investigation	CLOSE	2014-11-20, 12:00:00 AM
1833436	GForms AdHoc - General WO	CLOSE	2014-11-25, 12:00:00 AM
1835909	Inspect Well - Rager Mtn - RAG2244 - (PNG4469)	CLOSE	2014-12-02, 12:00:00 AM
1840589	GForms AdHoc - General WO	CLOSE	2014-12-05, 12:00:00 AM
1840782	GForms AdHoc - General WO	CLOSE	2014-12-09, 12:00:00 AM
1846481	GForms AdHoc - General WO	CLOSE	2014-12-29, 12:00:00 AM
1849068	Inspect Well - Rager Mtn - RAG2244 - (PNG4469)	CLOSE	2015-01-05, 12:00:00 AM
1853390	GForms AdHoc - General WO	CLOSE	2015-01-07, 12:00:00 AM
1856889	GForms AdHoc - General WO	CLOSE	2015-01-14, 12:00:00 AM
1858810	GForms AdHoc - General WO	CLOSE	2015-01-21, 12:00:00 AM
1864036	Inspect Well - Rager Mtn - RAG2244 - (PNG4469)	CLOSE	2015-02-04, 12:00:00 AM
1873952	GForms AdHoc - General WO	CLOSE	2015-02-24, 12:00:00 AM
1877110	Inspect Well - Rager Mtn - RAG2244 - (PNG4469)	CLOSE	2015-03-11, 12:00:00 AM
1897804	GForms AdHoc - General WO	CLOSE	2015-04-02, 12:00:00 AM
1894727	Inspect Well - Rager Mtn - RAG2244 - (PNG4469)	CLOSE	2015-04-23, 12:00:00 AM
1881042	Shut-In Testing - Rager Mtn - RAG2244 - (PNG4469)	CLOSE	2015-04-28, 12:00:00 AM
1906222	Echo Metering - Rager Mtn - RAG2244 - (PNG4469)	CLOSE	2015-04-28, 12:00:00 AM
1907102	GForms AdHoc - Pipeline Maintenance	CLOSE	2015-04-28, 12:00:00 AM
1909291	Inspect Well - Rager Mtn - RAG2244 - (PNG4469)	CLOSE	2015-05-07, 12:00:00 AM
1926408	GForms AdHoc - General WO	CLOSE	2015-05-28, 12:00:00 AM
1925225	Inspect Well - Rager Mtn - RAG2244 - (PNG4469)	CLOSE	2015-06-08, 12:00:00 AM
1930838	GForms AdHoc - Surface Upkeep	CLOSE	2015-06-08, 12:00:00 AM
1940290	Inspect Well - Rager Mtn - RAG2244 - (PNG4469)	CLOSE	2015-07-15, 12:00:00 AM
1954203	Inspect Well - Rager Mtn - RAG2244 - (PNG4469)	CLOSE	2015-08-06, 12:00:00 AM
1960816	GForms AdHoc - General WO	CLOSE	2015-08-13, 12:00:00 AM
1969926	Inspect Well - Rager Mtn - RAG2244 - (PNG4469)	CLOSE	2015-09-03, 12:00:00 AM
1984422	Inspect Well - Rager Mtn - RAG2244 - (PNG4469)	CLOSE	2015-10-06, 12:00:00 AM
1997225	GForms AdHoc - General WO	CLOSE	2015-10-27, 12:00:00 AM
2000374	Inspect Well - Rager Mtn - RAG2244 - (PNG4469)	CLOSE	2015-11-02, 12:00:00 AM

Work Order Number	Description	Status	Date and Time Completed
1969971	Shut-In Testing - Rager Mtn - RAG2244 - (PNG4469)	CLOSE	2015-11-02, 12:00:00 AM
1994902	Echo Metering - Rager Mtn - RAG2244 - (PNG4469)	CLOSE	2015-11-06, 12:00:00 AM
2013037	Inspect Well - Rager Mtn - RAG2244 - (PNG4469)	CLOSE	2015-12-03, 12:00:00 AM
2026830	Inspect Well - Rager Mtn - RAG2244 - (PNG4469)	CLOSE	2016-01-04, 12:00:00 AM
2033733	GForms AdHoc - General WO	CLOSE	2016-01-11, 12:00:00 AM
2042197	Inspect Well - Rager Mtn - RAG2244 - (PNG4469)	CLOSE	2016-02-05, 12:00:00 AM
2051675	GForms AdHoc - General WO	CLOSE	2016-02-18, 12:00:00 AM
2057436	Inspect Well - Rager Mtn - RAG2244 - (PNG4469)	CLOSE	2016-03-03, 12:00:00 AM
2067877	GForms AdHoc - General WO	CLOSE	2016-03-15, 12:00:00 AM
2069155	GForms AdHoc - General WO	CLOSE	2016-03-18, 12:00:00 AM
2076761	Inspect Well - Rager Mtn - RAG2244 - (PNG4469)	CLOSE	2016-04-04, 12:00:00 AM
2060589	Shut-In Testing - Rager Mtn - RAG2244 - (PNG4469)	CLOSE	2016-04-08, 12:00:00 AM
2083814	GForms AdHoc - General WO	CLOSE	2016-04-11, 12:00:00 AM
2084274	GForms AdHoc - Field Investigation	CLOSE	2016-04-13, 12:00:00 AM
2091908	Inspect Well - Rager Mtn - RAG2244 - (PNG4469)	CLOSE	2016-05-09, 12:00:00 AM
2105875	Inspect Well - Rager Mtn - RAG2244 - (PNG4469)	CLOSE	2016-06-09, 12:00:00 AM
2125244	Inspect Well - Rager Mtn - RAG2244 - (PNG4469)	CLOSE	2016-07-07, 12:00:00 AM
2138405	Inspect Well - Rager Mtn - RAG2244 - (PNG4469)	CLOSE	2016-08-05, 09:05:00 AM
2150323	Inspect Well - Rager Mtn - RAG2244 - (PNG4469)	CLOSE	2016-09-13, 10:05:00 AM
2160571	Inspect Well - Rager Mtn - RAG2244 - (PNG4469)	CLOSE	2016-10-11, 09:29:00 AM
2152304	Shut-In Testing - Rager Mtn - RAG2244 - (PNG4469)	CLOSE	2016-11-01, 09:41:00 AM
2170378	Inspect Well - Rager Mtn - RAG2244 - (PNG4469)	CLOSE	2016-11-09, 09:14:00 AM
2181405	General Operations Rager wells	CLOSE	2016-12-05, 03:33:00 PM
2179362	Inspect Well - Rager Mtn - RAG2244 - (PNG4469)	CLOSE	2016-12-09, 11:55:00 AM
2188306	Inspect Well - Rager Mtn - RAG2244 - (PNG4469)	CLOSE	2017-01-03, 09:18:00 AM
2198142	Inspect Well - Rager Mtn - RAG2244 - (PNG4469)	CLOSE	2017-02-02, 10:09:00 AM
2200574	Odorizer Inspection	CLOSE	2017-02-02, 02:35:00 PM
2201414	Odorizer Inspection	CLOSE	2017-02-06, 09:00:00 AM
2202351	General Operations	CLOSE	2017-02-09, 03:40:00 PM
2208761	Inspect Well - Rager Mtn - RAG2244 - (PNG4469)	CLOSE	2017-03-02, 09:39:00 AM
2222056	Inspect Well - Rager Mtn - RAG2244 - (PNG4469)	CLOSE	2017-04-11, 09:24:00 AM
2234844	Inspect Well - Rager Mtn - RAG2244 - (PNG4469)	CLOSE	2017-05-02, 08:25:00 AM
2212064	Shut-In Testing - Rager Mtn - RAG2244 - (PNG4469)	CLOSE	2017-05-02, 09:10:00 AM
2246267	Inspect Well - Rager Mtn - RAG2244 - (PNG4469)	CLOSE	2017-06-12, 09:33:00 AM
2258939	Inspect Well - Rager Mtn - RAG2244 - (PNG4469)	CLOSE	2017-07-05, 08:35:00 AM
2270761	Inspect Well - Rager Mtn - RAG2244 - (PNG4469)	CLOSE	2017-08-03, 09:42:00 AM

Work Order Number	Description	Status	Date and Time Completed
2283293	Inspect Well - Rager Mtn - RAG2244 - (PNG4469)	CLOSE	2017-09-12, 10:47:00 AM
2292027	General Operations	CLOSE	2017-09-28, 10:57:00 AM
2293610	Inspect Well - Rager Mtn - RAG2244 - (PNG4469)	CLOSE	2017-10-04, 09:54:00 AM
2304235	Inspect Well - Rager Mtn - RAG2244 - (PNG4469)	CLOSE	2017-11-02, 08:39:00 AM
2285256	Shut-In Testing - Rager Mtn - RAG2244 - (PNG4469)	CLOSE	2017-11-07, 08:21:00 AM
2308689	General Operations	CLOSE	2017-11-13, 10:08:00 AM
2313249	Inspect Well - Rager Mtn - RAG2244 - (PNG4469)	CLOSE	2017-12-05, 08:27:00 AM
2324043	Inspect Well - Rager Mtn - RAG2244 - (PNG4469)	CLOSE	2018-01-09, 07:54:00 AM
2335195	Inspect Well - Rager Mtn - RAG2244 - (PNG4469)	CLOSE	2018-02-12, 08:02:00 AM
2345942	Inspect Well - Rager Mtn - RAG2244 - (PNG4469)	CLOSE	2018-03-05, 08:06:00 AM
2363803	Inspect Well - Rager Mtn - RAG2244 - (PNG4469)	CLOSE	2018-04-04, 09:04:00 AM
2349755	Shut-In Testing - Rager Mtn - RAG2244 - (PNG4469)	CLOSE	2018-05-07, 09:20:00 AM
2382722	Inspect Well - Rager Mtn - RAG2244 - (PNG4469)	CLOSE	2018-05-07, 10:30:00 AM
2396647	Inspect Well - Rager Mtn - RAG2244 - (PNG4469)	CLOSE	2018-06-06, 10:35:00 AM
2410330	Inspect Well - Rager Mtn - RAG2244 - (PNG4469)	CLOSE	2018-07-06, 09:45:00 AM
2425041	Inspect Well - Rager Mtn - RAG2244 - (PNG4469)	CLOSE	2018-08-16, 08:17:00 AM
2438779	Inspect Well - Rager Mtn - RAG2244 - (PNG4469)	CLOSE	2018-09-14, 10:04:00 AM
2450997	Inspect Well - Rager Mtn - RAG2244 - (PNG4469)	CLOSE	2018-10-02, 09:54:00 AM
2440792	Shut-In Testing - Rager Mtn - RAG2244 - (PNG4469)	CLOSE	2018-10-30, 12:22:00 PM
2463768	Inspect Well - Rager Mtn - RAG2244 - (PNG4469)	CLOSE	2018-11-14, 08:49:00 AM
2473238	Inspect Well - Rager Mtn - RAG2244 - (PNG4469)	CLOSE	2018-12-03, 10:46:00 AM
2477153	General Operations	CLOSE	2018-12-13, 02:39:00 PM
2481121	Inspect Well - Rager Mtn - RAG2244 - (PNG4469)	CLOSE	2019-01-03, 08:43:00 AM
2485031	General Operations	CLOSE	2019-01-04, 02:54:00 PM
2492468	Inspect Well - Rager Mtn - RAG2244 - (PNG4469)	CLOSE	2019-02-12, 08:26:00 AM
2501604	Inspect Well - Rager Mtn - RAG2244 - (PNG4469)	CLOSE	2019-03-12, 07:47:00 AM
2513540	Inspect Well - Rager Mtn - RAG2244 - (PNG4469)	CLOSE	2019-04-12, 08:27:00 AM
2504691	Shut-In Testing - Rager Mtn - RAG2244 - (PNG4469)	CLOSE	2019-04-23, 08:29:00 AM
2525346	Inspect Well - Rager Mtn - RAG2244 - (PNG4469)	CLOSE	2019-05-10, 08:24:00 AM
2535786	Inspect Well - Rager Mtn - RAG2244 - (PNG4469)	CLOSE	2019-06-04, 10:41:00 AM
2546446	Inspect Well - Rager Mtn - RAG2244 - (PNG4469)	CLOSE	2019-07-03, 09:21:00 AM
2560073	Inspect Well - Rager Mtn - RAG2244 - (PNG4469)	CLOSE	2019-08-08, 11:09:00 AM
2572687	Inspect Well - Rager Mtn - RAG2244 - (PNG4469)	CLOSE	2019-09-13, 09:29:00 AM
2582986	Inspect Well - Rager Mtn - RAG2244 - (PNG4469)	CLOSE	2019-10-03, 08:45:00 AM
2574084	Shut-In Testing - Rager Mtn - RAG2244 - (PNG4469)	CLOSE	2019-11-04, 08:40:00 AM
2593603	Inspect Well - Rager Mtn - RAG2244 - (PNG4469)	CLOSE	2019-11-04, 12:20:00 PM

Work Order Number	Description	Status	Date and Time Completed
2602886	Inspect Well - Rager Mtn - RAG2244 - (PNG4469)	CLOSE	2019-12-18, 01:30:00 PM
2611534	Inspect Well - Rager Mtn - RAG2244 - (PNG4469)	CLOSE	2020-01-09, 10:30:00 AM
2622558	Inspect Well - Rager Mtn - RAG2244 - (PNG4469)	CLOSE	2020-02-10, 09:30:00 AM
2632861	Inspect Well - Rager Mtn - RAG2244 - (PNG4469)	CLOSE	2020-03-16, 11:00:00 AM
2636085	Shut-In Testing - Rager Mtn - RAG2244 - (PNG4469)	CLOSE	2020-04-06, 02:30:00 PM
2646708	Inspect Well - Rager Mtn - RAG2244 - (PNG4469)	CLOSE	2020-04-27, 11:00:00 AM
2661883	Inspect Well - Rager Mtn - RAG2244 - (PNG4469)	CLOSE	2020-05-15, 11:00:00 AM
2674303	Inspect Well - Rager Mtn - RAG2244 - (PNG4469)	CLOSE	2020-06-16, 11:30:00 AM
2685011	Inspect Well - Rager Mtn - RAG2244 - (PNG4469)	CLOSE	2020-07-23, 04:00:00 PM
2699324	Inspect Well - Rager Mtn - RAG2244 - (PNG4469)	CLOSE	2020-08-07, 12:00:00 PM
2709616	Inspect Well - Rager Mtn - RAG2244 - (PNG4469)	CLOSE	2020-09-18, 10:30:00 AM
2720035	Inspect Well - Rager Mtn - RAG2244 - (PNG4469)	CLOSE	2020-10-16, 02:00:00 PM
2710955	Shut-In Testing - Rager Mtn - RAG2244 - (PNG4469)	CLOSE	2020-11-03, 09:00:00 AM
2730641	Inspect Well - Rager Mtn - RAG2244 - (PNG4469)	CLOSE	2020-11-04, 11:30:00 AM
2739181	Inspect Well - Rager Mtn - RAG2244 - (PNG4469)	CLOSE	2020-12-10, 11:00:00 AM
2749281	Inspect Well - Rager Mtn - RAG2244 - (PNG4469)	CLOSE	2021-01-22, 10:00:00 AM
2760218	Inspect Well - Rager Mtn - RAG2244 - (PNG4469)	CLOSE	2021-02-18, 02:00:00 PM
2769339	Inspect Well - Rager Mtn - RAG2244 - (PNG4469)	CLOSE	2021-03-04, 01:30:00 PM
2781800	Inspect Well - Rager Mtn - RAG2244 - (PNG4469)	CLOSE	2021-04-19, 11:00:00 AM
2772671	Shut-In Testing - Rager Mtn - RAG2244 - (PNG4469)	CLOSE	2021-04-19, 03:45:00 PM
2795490	Inspect Well - Rager Mtn - RAG2244 - (PNG4469)	CLOSE	2021-05-04, 10:30:00 AM
2813845	Inspect Well - Rager Mtn - RAG2244 - (PNG4469)	CLOSE	2021-06-11, 01:00:00 PM
2826818	Inspect Well - Rager Mtn - RAG2244 - (PNG4469)	CLOSE	2021-07-08, 01:30:00 PM
2841545	Inspect Well - Rager Mtn - RAG2244 - (PNG4469)	CLOSE	2021-08-20, 11:30:00 AM
2854927	Inspect Well - Rager Mtn - RAG2244 - (PNG4469)	CLOSE	2021-09-03, 10:30:00 AM
2867403	Inspect Well - Rager Mtn - RAG2244 - (PNG4469)	CLOSE	2021-10-20, 10:30:00 AM
2857696	Shut-In Testing - Rager Mtn - RAG2244 - (PNG4469)	CLOSE	2021-11-02, 09:00:00 AM
2878079	Inspect Well - Rager Mtn - RAG2244 - (PNG4469)	CLOSE	2021-11-02, 02:45:00 PM
2887508	Inspect Well - Rager Mtn - RAG2244 - (PNG4469)	COMP	2021-12-22, 10:30:00 AM
2896105	Inspect Well - Rager Mtn - RAG2244 - (PNG4469)	COMP	2022-01-21, 08:30:00 AM
2909263	Inspect Well - Rager Mtn - RAG2244 - (PNG4469)	COMP	2022-02-18, 07:30:00 AM
2921306	Inspect Well - Rager Mtn - RAG2244 - (PNG4469)	COMP	2022-03-18, 08:30:00 AM
2923799	Shut-In Testing - Rager Mtn - RAG2244 - (PNG4469)	COMP	2022-04-13, 02:30:00 PM
2922114	Well Valve RAG2244, Isolation Test, I/W	COMP	2022-04-18, 09:30:00 AM
2933790	Inspect Well - Rager Mtn - RAG2244 - (PNG4469)	COMP	2022-04-19, 12:00:00 PM
2945424	Inspect Well - Rager Mtn - RAG2244 - (PNG4469)	COMP	2022-05-24, 07:30:00 AM

Work Order Number	Description	Status	Date and Time Completed
2957512	Inspect Well - Rager Mtn - RAG2244 - (PNG4469)	COMP	2022-06-24, 09:30:00 AM
2968687	Inspect Well - Rager Mtn - RAG2244 - (PNG4469)	COMP	2022-07-22, 12:30:00 PM
2982168	Inspect Well - Rager Mtn - RAG2244 - (PNG4469)	COMP	2022-08-30, 10:00:00 AM
2993786	Inspect Well - Rager Mtn - RAG2244 - (PNG4469)	COMP	2022-09-16, 10:30:00 AM
3003439	Inspect Well - Rager Mtn - RAG2244 - (PNG4469)	COMP	2022-10-26, 10:30:00 AM
3011950	Shut-In Testing - Rager Mtn - RAG2244 - (PNG4469)	COMP	2022-11-01, 04:00:00 PM

A.3 Listing of Rager Mountain Logs

Table 53: Rager Mountain Logs (Chronological Order)

Item	Well #	Date	Description	Type
1	2244	October 4, 1965	Continuous Directional	O
2	2244	October 4, 1965	Formation Density Log Gamma Ray	F
3	2245	December 18, 1965	Sand Surveys Inc. - Gamma Ray, Temperature Log	F
4	2246	October 5, 1966	Schlumberger - Directional Log	O
5	2244	May 17, 1967	Correlation Gamma Ray CCL	F
6	2244	May 17, 1967	Gamma Ray CCL	F
7	2247	October 9, 1967	Gamma Ray Caliper Temperature	F
8	2248	August 16, 1968	Gamma Ray	F
9	2248	August 16, 1968	Cement Bond Temperature	C
10	2249	April 21, 1971	Gamma Ray Openhole Caliper CCL	F
11	2248	May 12, 1971	Sand Surveys Gamma Ray Collar Log	F
12	2246	May 29, 1971	Schlumberger - Gamma Ray	F
13	2246	May 29, 1971	Schlumberger - Pipe Inspection Log	I
14	2245	June 4, 1971	Cement Bond	C
15	2245	June 21, 1971	Sand Surveys Inc. - Gamma Ray, CCL	F
16	2249	August 8, 1971	Halliburton Fracometer Log	F
17	2250	April 2, 1974	Schlumberger Neutron	F
18	2250	April 2, 1974	Schlumberger Induction-Electrical	F
19	2250	April 2, 1974	Cement Bond	C
20	2250	April 2, 1974	Schlumberger Formation Density Gamma-Gamma	F
21	2250	April 2, 1974	Neutron Porosity Log	F
22	2249	July 13, 1978	Birdwell Gamma Ray Temperature	L
23	2245	July 13, 1978	Birdwell - Gamma Ray, Temperature	L
24	2249	July 14, 1978	Birdwell Gamma Ray Neutron Wellbore Sibilation	L
25	2248	July 17, 1978	Birdwell Gamma Ray Neutron Temperature	L

Item	Well #	Date	Description	Type
26	2245	July 20, 1978	Birdwell - Temperature, Gamma Ray-Neutron	L
27	2244	July 24, 1978	Gamma Ray Neutron Temperature	L
28	2250	July 25, 1978	Birdwell Gamma Ray Neutron Sibilation	L
29	2249	December 27, 1978	Schlumberger Temperature Log	L
30	2244	December 17, 1984	Temperature Log	L
31	2244	December 17, 1984	Gamma Ray Neutron	L
32	2250	December 18, 1984	Schlumberger Temperature Log	L
33	2250	December 18, 1984	Schlumberger Gamma Ray Neutron Log	L
34	2245	December 20, 1984	Schlumberger - Temperature Log	L
35	2245	December 20, 1984	Schlumberger - Gamma Ray Temperature Log	L
36	2248	December 21, 1984	Schlumberger Temperature Log	L
37	2248	December 21, 1984	Schlumberger Gamma Ray Neutron Log	L
38	2249	December 28, 1984	Schlumberger Gamma Ray Neutron Log	L
39	2247	January 4, 1985	Gamma Ray Neutron Log	L
40	2247	January 4, 1985	Temperature Log	L
41	2247	January 4, 1985	Gamma Ray Neutron Log	L
42	2245	September 18, 1986	Western Atlas - Gamma Ray-Neutron Temperature	L
43	2244	January 25, 1989	Pressure Drawdown Survey	F
44	2245	January 26, 1989	Schlumberger - Pressure Drawdown Survey	F
45	2248	January 27, 1989	Schlumberger Pressure Drawdown Survey	F
46	2252	June 29, 1989	Segmented Bond Log Gamma Ray	C
47	2251	July 30, 1989	Schlumberger Caliper Gamma Ray	C
48	2251	August 3, 1989	Titan Cement Top Log	C
49	2251	August 5, 1989	Schlumberger Cement Scan Log	C
50	2251	August 5, 1989	Schlumberger Cement Bond Log Variable Density	C
51	2251	August 6, 1989	Schlumberger Cement Evaluation Log	C
52	2251	August 8, 1989	Schlumberger Compensated Neutron Litho-density	F
53	2251	August 8, 1989	Schlumberger Cyberlook	F
54	2251	August 16, 1989	Titan Tracer Log	L
55	2252	August 20, 1989	Cement Scan Log	C
56	2252	August 20, 1989	Cement Bond Log Variable Density	C
57	2252	August 20, 1989	Cement Evaluation Log	C
58	2251	October 10, 1989	Titan Gamma Ray/P.D.C.	L
59	2250	October 18, 1989	Titan Gamma Ray P.D.C.	L
60	2245	October 18, 1989	Titan Wireline Services - Gamma Ray/P.D.C.	L
61	2251	November 15, 1989	Schlumberger Temperature	L
62	2251	November 16, 1989	Schlumberger Acoustic Spectrum Log	F

Item	Well #	Date	Description	Type
63	2251	November 17, 1989	Schlumberger Gamma Ray Neutron Log	L
64	2251	November 21, 1989	Schlumberger Electromagnetic Thickness	I
65	2252	November 29, 1989	Combined Temperature Neutron Log	L
66	2252	November 29, 1989	Temperature	L
67	2252	November 30, 1989	Acoustic Spectrum	F
68	2252	December 1, 1989	Electromagnetic Thickness Log	I
69	2250	December 8, 1989	Schlumberger Variable Density	C
70	2250	December 8, 1989	Schlumberger Cement Evaluation Log	C
71	2250	December 27, 1989	Schlumberger Electromagnetic Thickness	I
72	2244	October 24, 1990	Magnelog Gamma Ray	I
73	2244	October 24, 1990	Gamma Ray Neutron Temperature	L
74	2245	October 29, 1990	Western Atlas - Temperature/Neutron/Gamma Ray/CCL	L
75	2245	October 29, 1990	Western Atlas - Magnelog Gamma Ray	I
76	2249	October 30, 1990	Western Atlas Magnelog Gamma Ray	I
77	2249	October 30, 1990	Western Atlas Temperature Neutron Gamma Ray CCL	L
78	2247	October 31, 1990	Magnelog Gamma Ray	I
79	2247	October 31, 1990	Temperature Neutron Gamma Ray CCL	L
80	2248	November 1, 1990	Western Atlas Temperature Neutron/Gamma Ray/CCL	L
81	2246	November 2, 1990	Western Atlas - Magnelog	I
82	2246	November 29, 1990	Western Atlas - BAL Gamma Ray	F
83	2246	November 29, 1990	Western Atlas - Magnelog	I
84	2246	December 9, 1990	Titan Wireline Services - Caliper	I
85	2246	May 3, 1991	Western Atlas - Magnelog	I
86	2246	May 3, 1991	Western Atlas - Temperature Log	L
87	2246	May 3, 1991	Western Atlas - Neutron Gamma Ray	L
88	2245	April 25, 1992	Schlumberger - High Resolution Temperature Survey Gamma Ray-CCL	L
89	2245	April 27, 1992	Schlumberger - Plug Record, Caliper-Gamma Ray, Casing Collars	O
90	2245	May 4, 1992	Schlumberger - Bridge Plug Record	O
91	2245	May 4, 1992	Schlumberger - Temperature Survey	L
92	2245	May 12, 1992	Schlumberger - Cement Evaluation Quicklook	C
93	2245	May 12, 1992	Schlumberger - Cement Evaluation, Gamma Ray, Casing Collars	C
94	2245	May 12, 1992	Schlumberger - Cement Bond Log Variable Density	C
95	2245	May 12, 1992	Schlumberger - Multifrequency Electromagnetic Thickness Survey	I
96	2244	May 13, 1993	Cement Bond Log Variable Density	C
97	2244	May 13, 1993	Plug Setting Record	O

Item	Well #	Date	Description	Type
98	2244	May 13, 1993	Cement Bond Log Variable Density (old 7 in. casing)	C
99	2244	May 13, 1993	Multifrequency Electromagnetic Thickness Log	I
100	2244	May 15, 1993	CCL Log	O
101	2244	May 17, 1993	Multifrequency Electromagnetic Thickness Log (9 5/8 in. casing)	I
102	2244	May 17, 1993	Cement Bond Log Variable Density (9 5/8 in. casing)	C
103	2244	May 20, 1993	Caliper CCL Log (open hole 7 in. stub to 9 5/8 in. shoe)	O
104	2244	May 22, 1993	Cement Top Log (first stage cement top)	C
105	2244	May 24, 1993	Cement Bond Log Variable Density	C
106	2244	May 24, 1993	Cement Quick Look	C
107	2244	May 24, 1993	Cement Evaluation Gamma Ray CCL	C
108	2248	April 26, 1994	Schlumberger Cement Bond Log Variable Density Log	C
109	2248	May 15, 1994	Schlumberger Cement Top Log	C
110	2248	May 23, 1994	Schlumberger Cement Evaluation Quicklook	C
111	2248	May 23, 1994	Schlumberger Cement Evaluation with Gamma Ray-CCL	C
112	2248	May 23, 1994	Schlumberger Cement Bond Log Variable Density Log	C
113	2247	May 31, 1995	SBT Gamma Ray Run 1	C
114	2247	May 31, 1995	MC-Vertilog Evaluation (7 in. Casing Pulled 6/95)	I
115	2247	May 31, 1995	Vertilog	I
116	2247	May 31, 1995	SBT Cement Map	C
117	2247	June 7, 1995	Vertilog	I
118	2247	June 7, 1995	MC-Vertilog Evaluation (9 5/8 in. Casing)	I
119	2247	June 7, 1995	SBT Gamma Ray	C
120	2247	June 7, 1995	SBT Cement Map (9 5/8 in. Casing)	C
121	2247	June 10, 1995	4-Arm Caliper Gamma Ray	O
122	2247	June 15, 1995	SBT Gamma Ray Run 2	C
123	2247	June 15, 1995	Magnelog	I
124	2246	September 11, 1996	Western Atlas - Gamma Ray-Neutron Temperature	L
125	2246	September 12, 1996	Western Atlas - Multi-Channel Vertilog	I
126	2245	September 18, 1996	Western Atlas - Gamma Ray-Neutron Temperature	L
127	2245	September 18, 1996	Western Atlas - Multi-Channel Vertilog	I
128	2251	September 19, 1996	Western Atlas Gamma Ray Neutron Temperature	L
129	2251	September 20, 1996	Western Atlas Multi-Channel Vertilog	I
130	2247	September 30, 1996	Gamma Ray Neutron Temperature	L
131	2248	October 1, 1996	Western Atlas - Gamma Ray Neutron Temperature	L
132	2252	October 3, 1996	Multi-Channel Vertilog	I
133	2249	October 7, 1996	Western Atlas Gamma Ray Neutron Temperature	L
134	2250	October 9, 1996	Western Atlas Neutron Gamma Ray	L

Item	Well #	Date	Description	Type
135	2250	October 10, 1996	Western Atlas Multi-Channel Vertilog	I
136	2244	October 23, 1997	Junk Catcher 5.971 in. Gauge Ring	O
137	2249	May 29, 1998	Schlumberger Junk Basket Gauge Ring Set RBP	O
138	2252	June 21, 1999	Gamma Ray Neutron Temperature	L
139	2252	July 22, 1999	Digital Vertilog	I
140	2252	July 23, 1999	Digital Magnelog	I
141	2252	July 23, 1999	4-Arm Caliper Log Gamma Ray Log	I
142	2252	July 23, 1999	Digital Magnelog	I
143	2244	November 13, 2001	Gamma Ray Neutron Temperature	L
144	2252	November 14, 2001	Gamma Ray Neutron Temperature	L
145	2252	November 15, 2001	Micro Vertilog	I
146	2249	November 16, 2001	Baker Hughes MicroVertilog	I
147	2249	November 16, 2001	Baker Hughes Gamma Ray Neutron Temperature	L
148	2246	November 19, 2001	Baker Hughes - Gamma Ray Neutron Temperature	L
149	2246	November 20, 2001	Baker Hughes - MicroVertilog	I
150	2248	November 26, 2001	Baker Hughes Gamma Ray Neutron Temperature	L
151	2248	November 27, 2001	Baker Hughes Micro Vertilog	I
152	2247	November 27, 2001	Gamma Ray Neutron Temperature	L
153	2247	November 28, 2001	Micro Vertilog	I
154	2250	December 3, 2001	Baker Hughes Gamma Ray Neutron Temperature	L
155	2250	December 3, 2001	Baker Hughes MicroVertilog	I
156	2251	December 4, 2001	Baker Hughes Gamma Ray Neutron Temperature	L
157	2251	March 15, 2002	Baker Hughes Digital Vertilog	I
158	2244	March 15, 2002	Digital Vertilog Evaluation	I
159	2245	April 22, 2002	Baker Hughes - MicroVertilog	I
160	2245	April 23, 2002	Baker Hughes - Gamma Ray-Neutron Temperature	L
161	2248	June 23, 2003	Eastern Reservoir Services Injection Profile Log	F
162	2244	June 24, 2003	Eastern Reservoir Services - Injection Profile Log	F
163	2245	June 25, 2003	Eastern Reservoir Services - Injection Profile Log	F
164	2252	June 26, 2003	Eastern Reservoir Services - Injection Profile Log	F
165	2249	June 27, 2003	Eastern Reservoir Services - Injection Profile Log	F
166	2251	June 28, 2003	Eastern Reservoir Services Injection Profile Log	F
167	2250	June 29, 2003	Eastern Reservoir Services Injection Profile Log	F
168	2251	April 20, 2004	Baker Hughes Digital Vertilog	I
169	2248	June 24, 2004	Baker Hughes Plug Setting Record	O
170	2248	July 6, 2004	Baker Hughes - Segmented Bond Log Gamma Ray	C
171	2251	July 14, 2004	Baker Hughes Plug Setting Record	O

Item	Well #	Date	Description	Type
172	2251	July 15, 2004	Baker Hughes Segmented Bond Log Gamma Ray	C
173	2251	July 30, 2004	Baker Hughes Digital Vertilog	I
174	2244	August 17, 2004	Plug Setting Record	O
175	2245	September 14, 2005	Baker Hughes - MicroVertilog	I
176	2248	October 20, 2005	Baker Hughes Plug Setting Record	O
177	2247	August 31, 2006	Micro Vertilog	I
178	2248	April 14, 2008	Baker Hughes Plug Setting Record	O
179	2246	October 13, 2009	Baker Hughes - Gamma Ray Neutron Temperature	L
180	2246	October 13, 2009	Baker Hughes - MicroVertilog	I
181	2249	October 19, 2009	Baker Hughes MicroVertilog	I
182	2249	October 19, 2009	Baker Hughes Gamma Ray Neutron Temperature	L
183	2248	October 20, 2009	Baker Hughes Gamma Ray Neutron Temperature	L
184	2248	October 21, 2009	Baker Hughes Micro Vertilog	I
185	2247	October 21, 2009	Micro Vertilog	I
186	2247	October 22, 2009	Gamma Ray Neutron Temperature	L
187	2254	November 30, 2010	LWD Gamma Ray	F
188	2253	January 10, 2011	LWD Gamma Ray	F
189	2255	July 6, 2011	Baker Hughes CCL	O
190	2255	July 6, 2011	Baker Hughes Segmented Bond Tool Gamma Ray	C
191	2255	July 6, 2011	Baker Hughes Compensated Z-Densilog Neutron Gamma Ray Caliper	F
192	2244	August 10, 2016	Gamma Ray Neutron Temperature	L
193	2252	August 11, 2016	Gamma Ray Neutron Temperature	L
194	2244	August 11, 2016	Baker Hughes HR Vertilog	I
195	2252	August 12, 2016	HR Vertilog	I
196	2253	August 15, 2016	HR Vertilog	I
197	2253	August 15, 2016	Gamma Ray Neutron Temperature	L
198	2246	August 16, 2016	Baker Hughes - Gamma Ray Neutron Temperature	L
199	2246	August 16, 2016	Baker Hughes - HR Vertilog	I
200	2245	August 17, 2016	Baker Hughes - HR Vertilog	I
201	2245	August 17, 2016	Baker Hughes - Gamma Ray-Neutron Temperature	L
202	2254	August 22, 2016	Gamma Ray Neutron Delta Temperature	L
203	2254	August 22, 2016	Baker Hughes HR Vertilog	I
204	2250	August 23, 2016	Baker Hughes Gamma Ray Neutron Temperature	L
205	2250	August 23, 2016	Baker Hughes HR Vertilog	I
206	2249	August 24, 2016	Baker Hughes HR Vertilog	I
207	2249	August 24, 2016	Baker Hughes Gamma Ray Neutron Temperature	L
208	2251	August 25, 2016	Baker Hughes Gamma Ray Neutron Temperature	L

Item	Well #	Date	Description	Type
209	2251	August 25, 2016	Baker Hughes HR Vertilog	I
210	2248	August 26, 2016	Baker Hughes HR Vertilog	I
211	2248	August 26, 2016	Baker Hughes Gamma Ray Neutron Temperature	L
212	2255	August 29, 2016	Baker Hughes Gamma Ray Neutron Temperature	L
213	2255	August 29, 2016	Baker Hughes HR Vertilog	I
214	2247	August 30, 2016	Gamma Ray Neutron Temperature	L
215	2247	August 30, 2016	HR Vertilog	I
216	2247	August 30, 2016	Gamma Ray Neutron Temperature	L
217	2247	November 22, 2022	HR Vertilog	I
218	2247	November 22, 2022	Gamma Ray Neutron Temperature	L
219	2255	November 23, 2022	Baker Hughes Gamma Ray Neutron Temperature	L
220	2255	November 29, 2022	Baker Hughes HR Vertilog	I
221	2251	November 30, 2022	Baker Hughes Gamma Ray Neutron Temperature	L
222	2251	December 1, 2022	Baker Hughes HR Vertilog	I
223	2248	December 1, 2022	Baker Hughes Gamma Ray Neutron Temperature	L
224	2249	December 2, 2022	Baker HRVRT	I
225	2249	December 5, 2022	Baker Hughes Gamma Ray Neutron Temperature	L
226	2248	December 6, 2022	Baker Hughes HRVRT	I
227	2250	December 7, 2022	Baker Hughes Gamma Ray Neutron Temperature	L
228	2250	December 9, 2022	Baker Hughes HR Vertilog	I
229	2253	December 12, 2022	Baker Hughes - Gamma Ray-Neutron Temperature	L
230	2253	December 13, 2022	HR Vertilog	I
231	2245	December 13, 2022	Baker Hughes - Gamma Ray-Neutron Temperature	L
232	2254	December 14, 2022	Gamma Ray Neutron Temperature	L
233	2252	December 14, 2022	Nine Energy Gamma Ray Neutron Temperature CCL	L
234	2252	December 14, 2022	Nine Weatherford Fluxview Analysis	I
235	2245	December 14, 2022	Baker Hughes - HR Vertilog	I
236	2245	December 14, 2022	Baker Hughes HR Vertilog	I
237	2254	December 16, 2022	Baker Hughes HR Vertilog	I
238	2246	December 16, 2022	Gamma Ray Neutron Temperature	L
239	2246	December 16, 2022	Baker Hughes HR Vertilog	I
240	2248	December 19, 2022	TGT Chorus Log	L
241	2252	December 20, 2022	Baker Hughes HR Vertilog	I
242	2252	December 20, 2022	Gamma Ray Neutron Temperature	L
243	2251	December 28, 2022	TGT Chorus Log	L
244	2244	December 29, 2022	TGT Chorus Log	L
245	2248	January 9, 2023	Baker Hughes Imaging Caliper Log	I

Item	Well #	Date	Description	Type
246	2251	January 17, 2023	TGT Chorus Log	L
247	2248	January 18, 2023	Schlumberger Isolation Scanner Log	I
248	2251	January 19, 2023	Schlumberger Isolation Scanner	I
249	2244	March 6, 2023	Isolation Scanner	I
250	2244	March 13, 2023	56 Arm Imaging Caliper	I
251	2244	March 13, 2023	Gamma Ray Neutron Temperature	L
252	2244	March 18, 2023	I-CAL Caliper	I
253	2248	April 27, 2023	TGT Chorus Log	L
254	2248	April 28, 2023	Baker INTeX cement evaluation log	C
255	2254	May 30, 2023	Baker INTeX cement evaluation log	C

A.4 Baker Hughes Log Assessment

Baker Hughes analysts have provided one-page logging summaries along with recommendations by well from 1996 to 2016. Figure 219 shows the logging summary for well #2244 in 2001. Blade annotated this figure with blue numbers from 1–9 comments include:

1. Annulus fluid level was observed at 187 ft. Blade observed minor pitting at this depth after physically examining the 7 in. casing after extraction. This minor pitting was observed in the 2016 HRVRT log.
2. Gas was observed at various locations within the 7 in. x 9 5/8 in. annulus.
3. No temperature anomalies were observed, indicating no leak.
4. OD corrosion exists at several top joints. A 33% penetration was indicated at 59 ft. Blade did not find this corrosion nor did the log show it in 2016. During logging of the 9 5/8 in. casing, significant metal loss was observed at 66 ft. The logging tool used here was the Digital Vertilog, which is a smaller but older logging tool. The then-current generation of Baker Hughes' casing inspection tool was the MicroVertilog, but it was unable to pass the wellhead.
5. Corrosion was associated to the annulus fluid level.
6. The inhibitor was mentioned.
7. It is not clear if the logging frequency was known to the author.
8. A handwritten note said the next log would be run in 2006, five years later. This was not performed.
9. The Baker Hughes analyst was Mr. Dale Cole. Mr. Cole was on Rager Mountain logging summaries from 1996–2009.

Figure 220 shows the logging summary for well #2244 in 2016. Again, Blade annotated this figure with blue numbers from 1–9 and it is discussed below:

1. The annulus fluid is observed to be 11 ft.
2. This temperature instability is noted frequently on logging summaries and is occasionally noted as related to a short shut-in period and where temperatures have not stabilized.
3. Gas is observed in the annulus again at similar depths as mentioned in 2001.
4. Six defects are observed exceeding 20%. Only one is external.
5. The most significant defect by depth is at 7,575 ft with 30% metal loss in terms of percentage of wall thickness.
6. A cluster of defects is observed at 7,619 ft.
7. The external defect at 10 ft is reported to be 25% maximum penetration.
8. It is not clear whether Baker Hughes knew the Equitrans normal re-log schedule.

Table 54 shows a summary of all Baker Hughes logging summaries available from 1996 to 2016[ii]. There are some observations, as follows:

- Annulus liquid levels did not change significantly for some wells:

[ii] Verbatim with minor editing for clarity

  - Well #2246 had the following annulus liquid levels: 455 ft (1996), 450 ft (2001), 442 ft (2009), and 447 ft (2016).
  - Well #2252 had the following annulus liquid levels: 674 ft (1996), 664 ft (2001), and 634 ft (2016).
- Gas was observed in the annulus in a few wells: #2244, #2245, #2247, #2249, #2250, #2252.
- Inhibitor or biocide was mentioned in four logging summaries.
- Well #2251 had fast-growing top joint corrosion from 51% in March 2002 to 83.6% in April 2004.

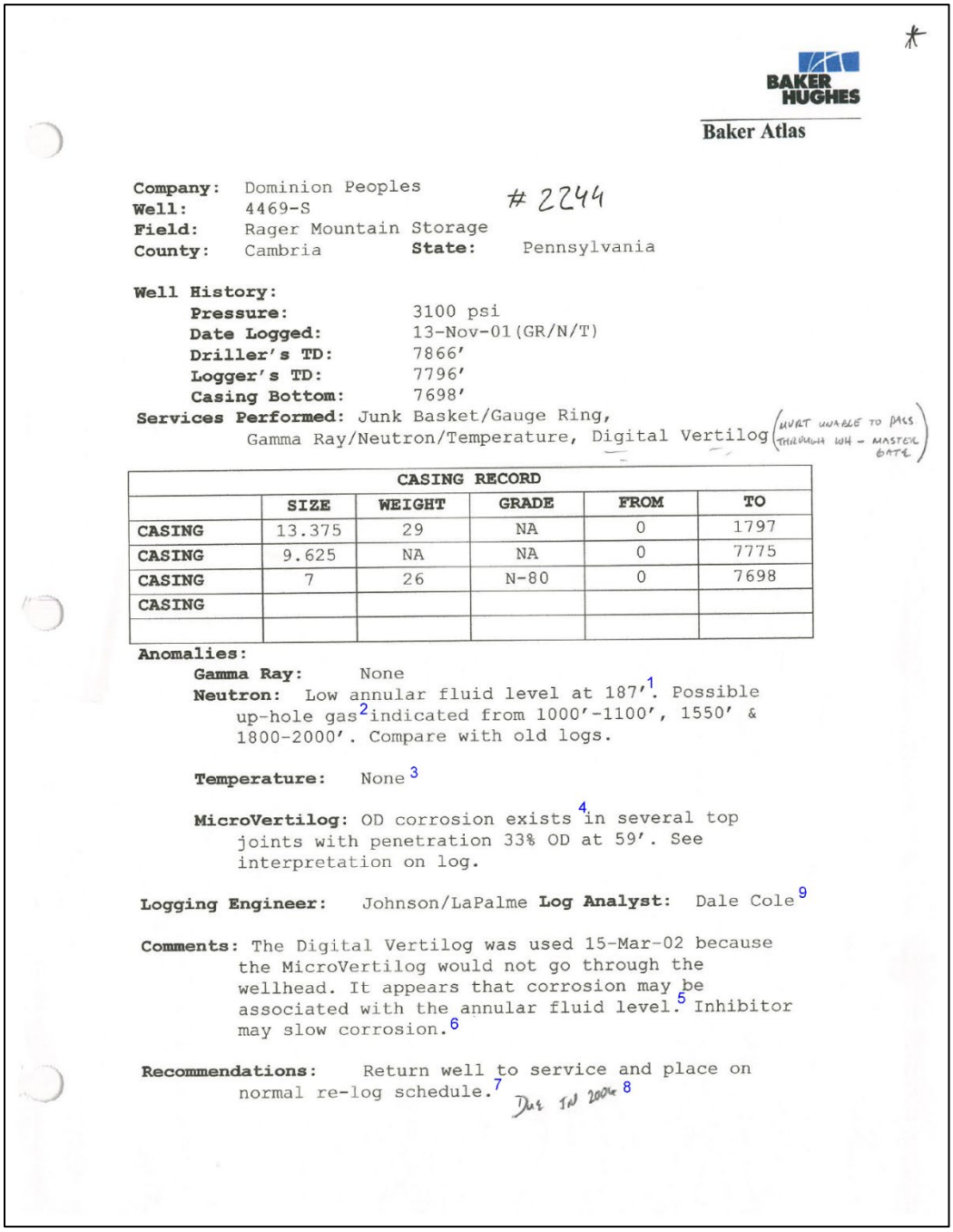

BAKER HUGHES

Baker Atlas

Company: Dominion Peoples
Well: 4469-S # 2244
Field: Rager Mountain Storage
County: Cambria **State:** Pennsylvania

Well History:
Pressure: 3100 psi
Date Logged: 13-Nov-01 (GR/N/T)
Driller's TD: 7866'
Logger's TD: 7796'
Casing Bottom: 7698'
Services Performed: Junk Basket/Gauge Ring, Gamma Ray/Neutron/Temperature, Digital Vertilog (UNIT UNABLE TO PASS THROUGH WH - MASTER GATE)

CASING RECORD					
	SIZE	WEIGHT	GRADE	FROM	TO
CASING	13.375	29	NA	0	1797
CASING	9.625	NA	NA	0	7775
CASING	7	26	N-80	0	7698
CASING					

Anomalies:
Gamma Ray: None
Neutron: Low annular fluid level at 187'[1]. Possible up-hole gas[2] indicated from 1000'-1100', 1550' & 1800-2000'. Compare with old logs.

Temperature: None[3]

MicroVertilog: OD corrosion exists[4] in several top joints with penetration 33% OD at 59'. See interpretation on log.

Logging Engineer: Johnson/LaPalme **Log Analyst:** Dale Cole[9]

Comments: The Digital Vertilog was used 15-Mar-02 because the MicroVertilog would not go through the wellhead. It appears that corrosion may be associated with the annular fluid level.[5] Inhibitor may slow corrosion.[6]

Recommendations: Return well to service and place on normal re-log schedule.[7] Due in 2004[8]

Figure 219: Baker Hughes 2001 Logging Summary for Well #2244

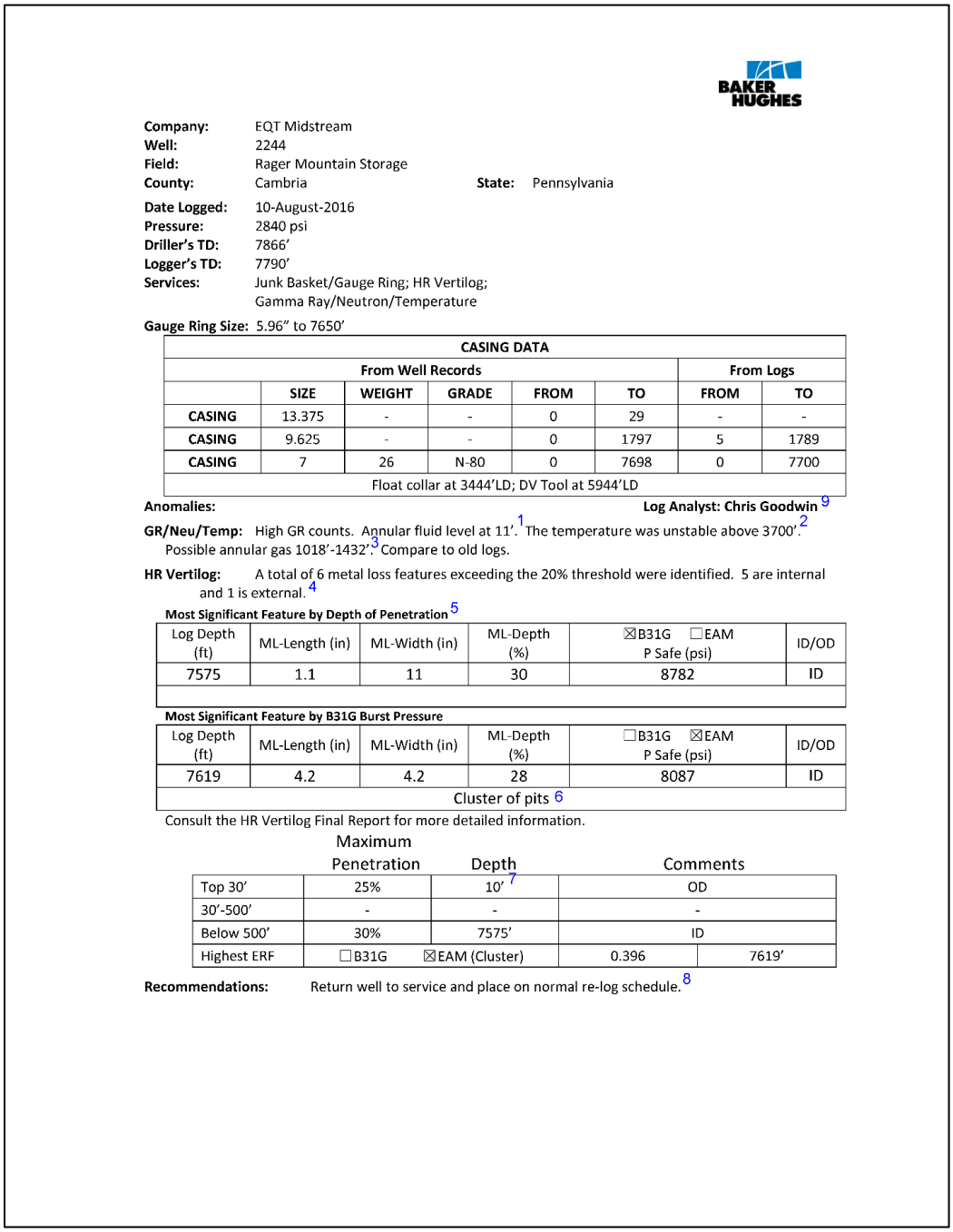

Company: EQT Midstream
Well: 2244
Field: Rager Mountain Storage
County: Cambria **State:** Pennsylvania

Date Logged: 10-August-2016
Pressure: 2840 psi
Driller's TD: 7866'
Logger's TD: 7790'
Services: Junk Basket/Gauge Ring; HR Vertilog; Gamma Ray/Neutron/Temperature

Gauge Ring Size: 5.96" to 7650'

CASING DATA							
	From Well Records					From Logs	
	SIZE	WEIGHT	GRADE	FROM	TO	FROM	TO
CASING	13.375	-	-	0	29	-	-
CASING	9.625	-	-	0	1797	5	1789
CASING	7	26	N-80	0	7698	0	7700
Float collar at 3444'LD; DV Tool at 5944'LD							

Anomalies: **Log Analyst: Chris Goodwin** [9]

GR/Neu/Temp: High GR counts. Annular fluid level at 11'.[1] The temperature was unstable above 3700'.[2] Possible annular gas 1018'-1432'.[3] Compare to old logs.

HR Vertilog: A total of 6 metal loss features exceeding the 20% threshold were identified. 5 are internal and 1 is external.[4]

Most Significant Feature by Depth of Penetration[5]

Log Depth (ft)	ML-Length (in)	ML-Width (in)	ML-Depth (%)	☒B31G ☐EAM P Safe (psi)	ID/OD
7575	1.1	11	30	8782	ID

Most Significant Feature by B31G Burst Pressure

Log Depth (ft)	ML-Length (in)	ML-Width (in)	ML-Depth (%)	☐B31G ☒EAM P Safe (psi)	ID/OD
7619	4.2	4.2	28	8087	ID
Cluster of pits [6]					

Consult the HR Vertilog Final Report for more detailed information.

	Maximum Penetration	Depth	Comments	
Top 30'	25%	10' [7]	OD	
30'-500'	-	-	-	
Below 500'	30%	7575'	ID	
Highest ERF	☐B31G ☒EAM (Cluster)		0.396	7619'

Recommendations: Return well to service and place on normal re-log schedule.[8]

Figure 220: Baker Hughes 2016 Logging Summary for Well #2244

Table 54: Summary of Baker Hughes Assessments, 1996 – 2016

Well	Year	Neutron, Temperature, Gamma Ray Comments	Casing Inspection Tool	Casing Inspection Comments	Comments and Recommendations
2244	2001	Low annular fluid level at 187 ft. Possible up-hole gas indicated from 1,000–1,100 ft, 1,550 ft, and 1,800–2000 ft.	Digital Vertilog	OD corrosion exists in several top joints with penetration 33% at 59 ft.	The Digital Vertilog was used March 15, 2015, because the MicroVertilog could not go through the wellhead. It appears that corrosion may be associated with the annular fluid level. Inhibitor may slow corrosion. Return well to service and place on normal re-log schedule.
	2016	High GR counts. Annular fluid level at 11 ft. The temperature was unstable above 3,700 ft. Possible annular gas 1,018–1,432 ft. compared to old logs.	HR Vertilog	A total of six metal loss features exceeding the 20% threshold were identified. Five are internal and one is external. 25% at 10 ft.	Return well to service and place on normal re-log schedule.
2245	1996	High counts near surface (100–300 ft)	MC Vertilog		Plan to rework or replace well. Re-log first.
	2002	Annular fluid level at 20 ft. Possible up-hole gas indicated at 120 ft, 110–270 ft, 650 ft, and 870 ft. Gas response same as 1996 logs.	MicroVertilog	39% at 5.8 ft. Corrosion from 5,635–5,680 ft with maximum penetration of 58%. Corrosion cell from 7,200–7,300ft (45%). 57% IDGC at 7,585 ft (these appear to be internal damage from drilling out cement).	Compare the neutron response to old logs to see if gas indications noted above are new. Return well to service and place on accelerated re-log schedule to monitor corrosion noted above. Re-log in 2005 for shallow corrosion.
	2005	Not run	MicroVertilog	97% General OD corrosion just above the DV tool at 5,651 ft. The corrosion in this area has grown significantly since the last log in 2002. There appears to be growth in internal corrosion in the	The interpretation procedure has changed for casing inside surface pipe since 2002. The corrosion is not as bad as it was in 2002 due to the casing correction factor. Return well to service and place on

Well	Year	Neutron, Temperature, Gamma Ray Comments	Casing Inspection Tool	Casing Inspection Comments	Comments and Recommendations
				Upper portion of the well.	Accelerated re-log schedule.
	2016	Annular fluid level at 36 ft. Possible annular gas 118–141 ft, 157–184 ft, 186–242 ft, 252–282 ft. and 860 ft–881 ft.	HR Vertilog	A total of 30 metal loss features exceeding the 20% threshold were identified. Twenty-eight are internal and two are external.	Return well to service and place on normal re-log schedule.
2246	1996	Annulus fluid 455 ft.	MC Vertilog		Significant amount of general internal corrosion in lower string of 5 1/2 in.
	2001	Annulus fluid 450 ft.	MicroVertilog	73% IDGC at 6,157 ft and 62% at 6,735 ft are the only class 4 defects.	60% ODGC at 1 ft needs to be investigated. It could be hardware and may be above ground. If corrosion is present, then the logging program should be accelerated or the well repaired. Due in 2006. Top Joint Replaced 2001, 35–40% actual.
	2009	Annular fluid level at 442 ft. Borehole fluid level at 7,958 ft.	MicroVertilog	80% IDGC at 6,119 ft and 6,178 ft. 80% IDIP at 6,990 ft. Significant internal corrosion found from 5,500 ft to TD. Well may need to be treated with biocide.	DV tools located at 3,982–3,986 ft and 5,961–5,965 ft. May want to check cementing records to see that the well is cemented below 5,500 ft. Return well to service and place on accelerated re-log schedule. Run the HRVRT next logging cycle to better describe the defects.

Well	Year	Neutron, Temperature, Gamma Ray Comments	Casing Inspection Tool	Casing Inspection Comments	Comments and Recommendations
	2016	Annular fluid level at 447 ft.	HR Vertilog	A total of 807 metal loss features exceeding the 20% threshold were identified. 703 are internal and 104 are external.	88% at 6,158 ft. This feature appears to be the result of drilling induced metal loss, possibly overstated. Return well to service and place on accelerated re-log schedule.
2247	1996	None	MC Vertilog		
	2001	Annulus fluid 16 ft.	MicroVertilog	82% ODGC at 9.8 ft. Otherwise, the casing is in good condition.	Special consideration needs to be given to the 82% ODGC at 9.8 ft. The uniformity of this defect indicates it could be mechanical in nature. Mechanical damage usually results in overstated of penetrations. Return well to service and place on accelerated re-log schedule or repair top joint. Re-log 2004
	2003	-	MicroVertilog	The only Class 4 defect is 74% ODGC at 10 ft. It may be the result of a mechanical defect. There are several Class 3 pits. 55% ODIP at 6,346 ft and 42% at 6,762 ft are the only Class 3 OD. Otherwise, the casing is in good condition.	The 74% at 10 ft appears to unchanged from two years earlier, which strengthens the possibility of mechanical damage rather than corrosion. Return well to service and place on normal re-log schedule.
	2004	-	MicroVertilog	The only Class 4 defect is 83% ODGC at 9.49 ft. It may be the result of a mechanical defect. Otherwise, the casing is in good condition.	The 83% defect was 74% in prior years. The difference is due to using 26# J-55 rather than 26# K-55 charts. The defect appears to be unchanged from last year and two years earlier. which strengthens the possibility of

Well	Year	Neutron, Temperature, Gamma Ray Comments	Casing Inspection Tool	Casing Inspection Comments	Comments and Recommendations
					mechanical damage rather than corrosion. Return well to service and place on normal re-log schedule.
	2006	-	MicroVertilog	46% IDIP at 6,713 ft, 45% ODIP at 5,925 ft and 44% IDIP at 4,901 ft. Otherwise the rest of the casing is Class 2 or better.	Return well to service and place on normal re-log schedule.
	2009	Annular fluid level is at 7 ft. Annular gas indicated from 40–52 ft. It may be due to enlarged hole drilled for the 13.375 in. surface casing. Also, there is possible annular gas at 470 ft. compared to old log data.	MicroVertilog	50% ODIP at 4.14 ft. Most of the downhole corrosion is internal indicating that the well may need to be treated with biocide. Otherwise, the casing is in good condition. See interpretation on log.	The annular space needs to be filled with inhibitor to stop the corrosion in the top joint. There is a DV tool located at 4,150–4,155 ft. Return well to service and place on accelerated re-log schedule to monitor the effectiveness of the inhibitor.
	2016	Annular fluid level at 58 ft. Possible annular gas 469–476 ft. compared to old logs.	HR Vertilog	A total of 0 metal loss features exceeding the 20% threshold were identified.	Return well to service and place on normal re-log schedule.
2248	1996	None	MC Vertilog	27% ODIP 4,899 ft.	Place on normal re-log schedule.
	2003	-	MicroVertilog	No Class 4 defects. 57% ODGC at 10 ft. 56% at 5,456 ft. 47% ODIP at 6,025 ft, and 54% ODGC at 6,837 ft. Otherwise the casing is in good condition.	The 57% ODGC at 10 ft appears to have increased in two years. The scatter of the defect increases the possibility that it is corrosion rather than mechanical. Top joint may need repair soon. Return well to service and place on accelerated re-log schedule until repairs are made.

Well	Year	Neutron, Temperature, Gamma Ray Comments	Casing Inspection Tool	Casing Inspection Comments	Comments and Recommendations
	2009	Annular fluid level is at 14 ft.	MicroVertilog	47% ODGC at 3.98 ft. Otherwise the casing is in very good condition. There is an internal casing patch at 5,420 ft. The MVRT was started above the patch because of concerns about sticking. See interpretation on log.	The annular space needs to be filled with inhibitor to stop the corrosion in the top joint. There is a DV tool located at 2,881–2,886 ft. Return well to service and place on accelerated re-log schedule to monitor the effectiveness of the inhibitor on the top joint.
	2016	Annular fluid level at 14 ft.	HRVRT	A total of seven metal loss features exceeding the 20% threshold were identified. All are external. 37% on OD at 3 ft.	Return well to service and place on normal re-log schedule.
2249	1996	None	-		
	2001	None	MicroVertilog	Nothing greater than Class 3.	Return well to service and place on normal re-log schedule. Due in 2006.
	2009	Possible annular gas from 5,055–5,286 ft. The cooling at 6,355 ft could indicate a leak. The Neutron does not show an annular gas build-up in this area.	MicroVertilog	44% IDIP at 1,473 ft. Otherwise the casing is in very good condition.	The Junk Catcher/Gauge Ring sat down and stuck at 4,240 ft. This prevented getting a MVRT below 4,240 ft. May want to clean well out and run casing inspection deeper in the well to investigate the cooling area at 6,355 ft.
	2016	Annular fluid level at 7 ft. Possible annular gas 5,032–5,284 ft. Temperature change near 5,300ft.	HR Vertilog	A total of 0 metal loss features exceeding the 20% threshold were identified.	Return well to service and place on normal re-log schedule.
2250	1996	Casing Fluid at 1,580 ft.	MC Vertilog		Well was killed due to having to replace master gate.

Well	Year	Neutron, Temperature, Gamma Ray Comments	Casing Inspection Tool	Casing Inspection Comments	Comments and Recommendations
	2001	Annulus fluid level at 26 ft.	MicroVertilog	Nothing greater than Class 3.	Return well to service and place on normal re-log schedule. Due in 2006.
	2016	Annular fluid level at 18 ft. Possible annular gas 5,046–5,201 ft. Temperature changes near 5,360 ft.	HR Vertilog	A total of one metal loss feature exceeding the 20% threshold was identified. It is internal. 29% ID at 3,704 ft.	Return well to service and place on normal re-log schedule.
2251	1996	None	MC Vertilog		
	2001	Low annular fluid level at 94 ft.	Digital Vertilog	74% for the N-80 -No, (51% if P-110 - Yes) at 88 ft. Otherwise, no defects in the casing greater than Class 3.	The digital Vertilog was used March 15, 2002, because the MicroVertilog could not go through the wellhead. This well should be repaired soon. It appears that corrosion is associated with annular fluid level. Inhibitor may slow corrosion until repaired. Return well to service and place on accelerated re-log schedule to monitor corrosion cell at 88 ft until repairs are made. Re-logged in 2004. Cement Top approximately 458 ft.
	2004	-	MicroVertilog	The defect at 88.7 ft has shown significant increase in just two years. Using the 26# P-110 chart for interpretation it is at 83.6% penetration (from 73% in 2002 using J-55 chart). Using the J-55 chart for this log it would be at 100% penetration.	255 gal of methanol was pumped to wash out the hydrates starting at 43 ft. Unable to get below 586 ft. The defect at 88ft shows an increase of about 25% compared to the 2002 log. The penetration was lessened by using the P-110 chart rather than the J-55 chart that was use in 2002.

Well	Year	Neutron, Temperature, Gamma Ray Comments	Casing Inspection Tool	Casing Inspection Comments	Comments and Recommendations
	2016	Annular fluid level at 40 ft.	HR Vertilog	A total of one metal loss feature exceeding the 20% threshold was identified. It is external. 45% OD at 1.89 ft.	Return well to service and place on accelerated re-log schedule.
2252	1996	High counts from surface to 674 ft.	MC Vertilog		Check annulus for presence of gas.
	2001	Low annular fluid level at 664 ft.	MicroVertilog	62% ODOP at 6,320 ft. Otherwise no defects in the casing greater than low Class 3 (less than 50%).	May want to do something about the low annular fluid level to slow corrosion. Return well to service and place on normal re-log schedule.
	2016	Annular fluid level at 634 ft. Possible annular gas at 894–898 ft, 1,581–1598 ft.	HR Vertilog	A total of 0 metal loss features exceeding the 20% threshold were identified.	Return well to service and place on normal re-log schedule.
2253	N/A	-	-	-	-
2254	N/A	-	-	-	-
2255	N/A	-	-	-	-

A.5 Metal Loss Overview

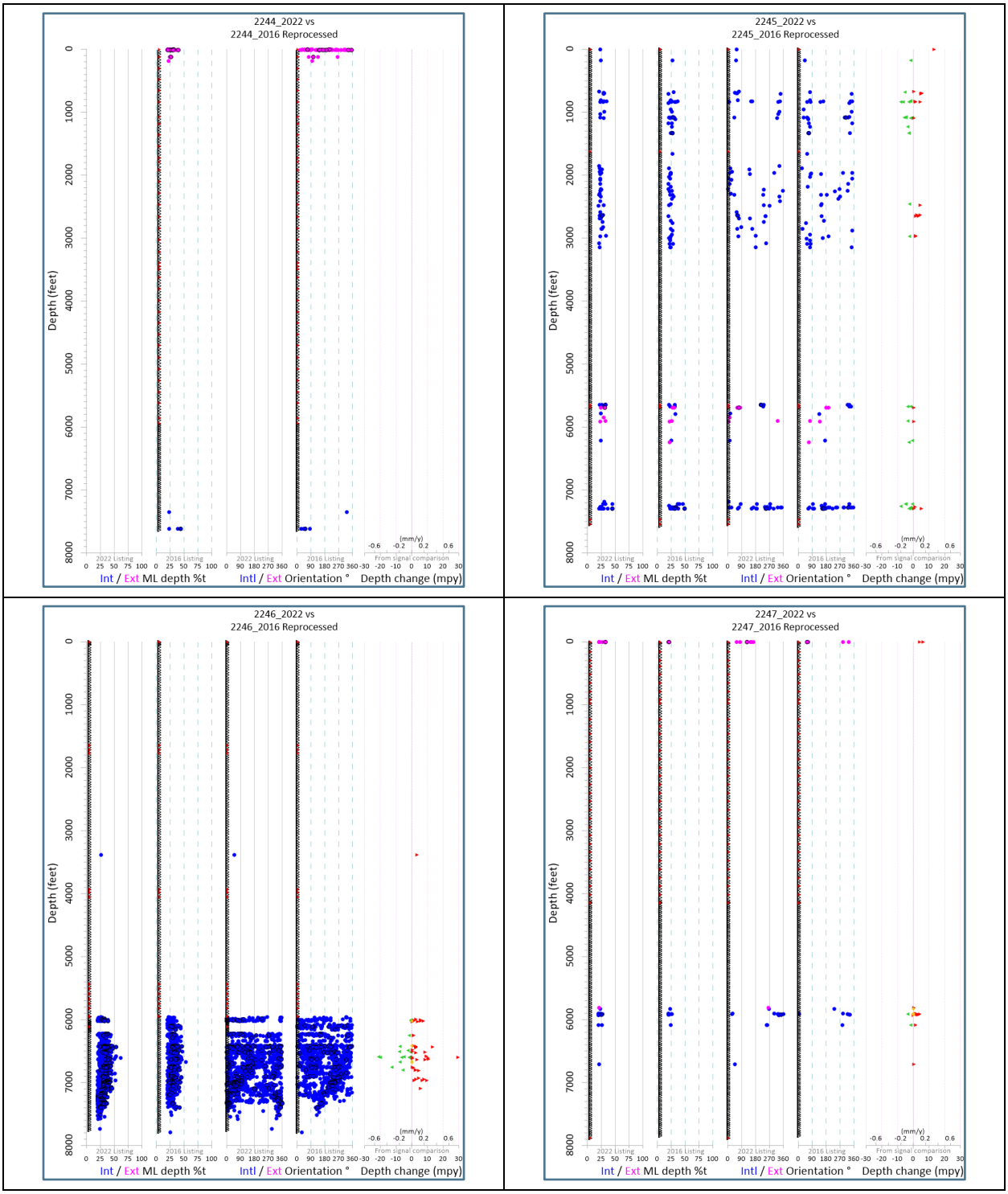

Figure 221: #2244, #2245, #2246, #2247

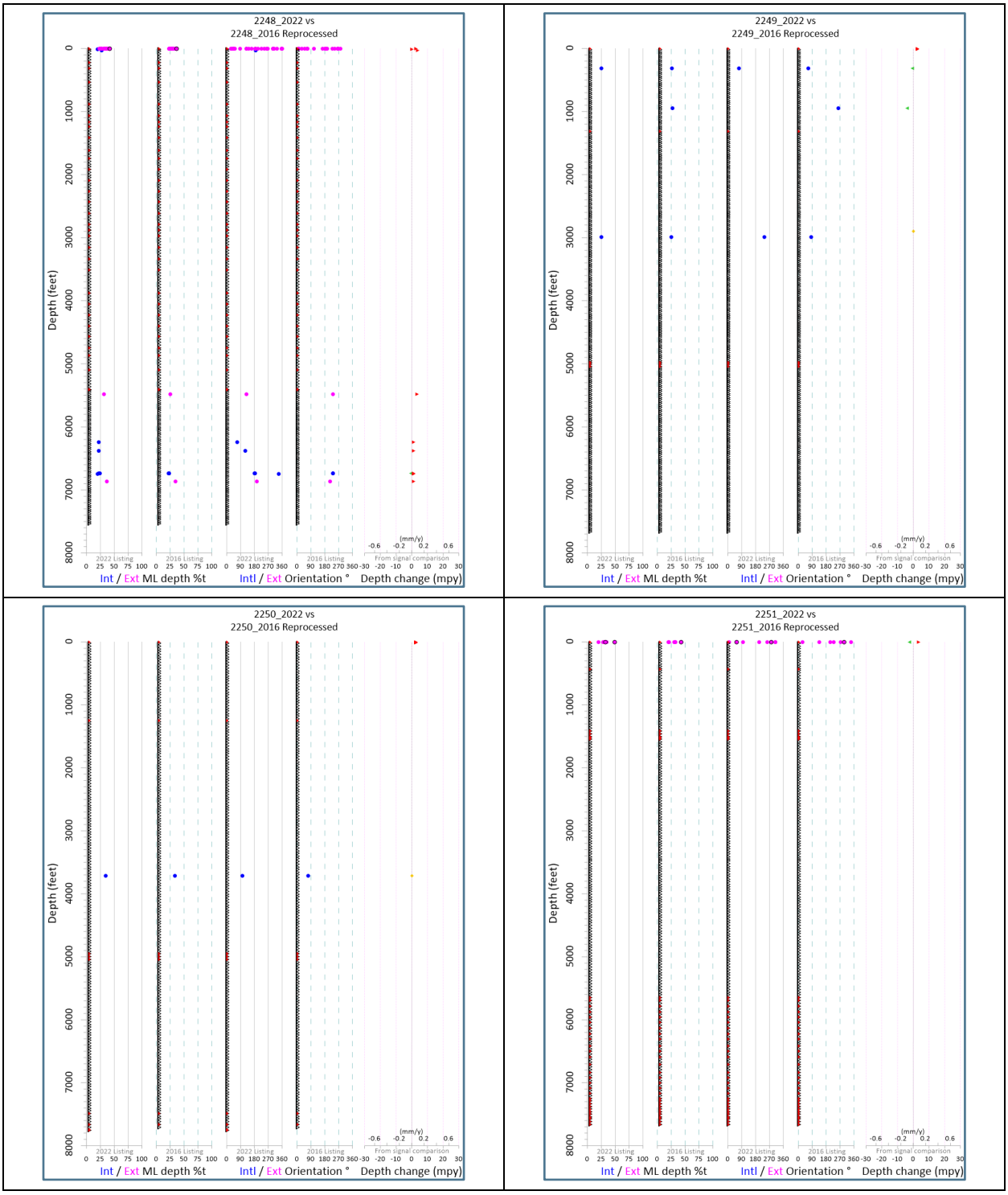

Figure 222: #2248, #2249, #2250, #2251

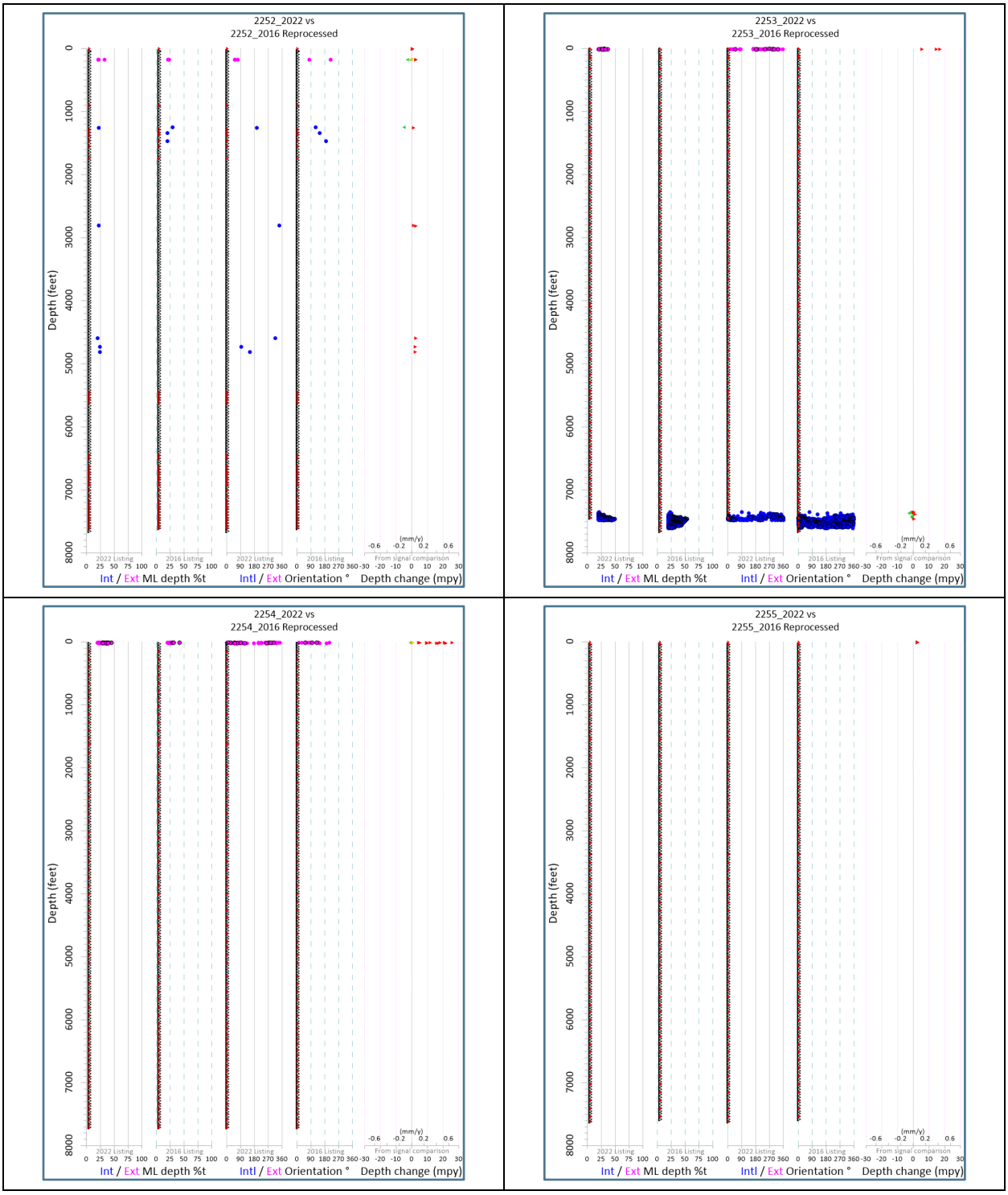

Figure 223: #2252, #2253, #2254, #2255

A.6 Comparison of Baker Hughes HR Vertilog 2016 (Reprocessed) and 2022 at Top Joint

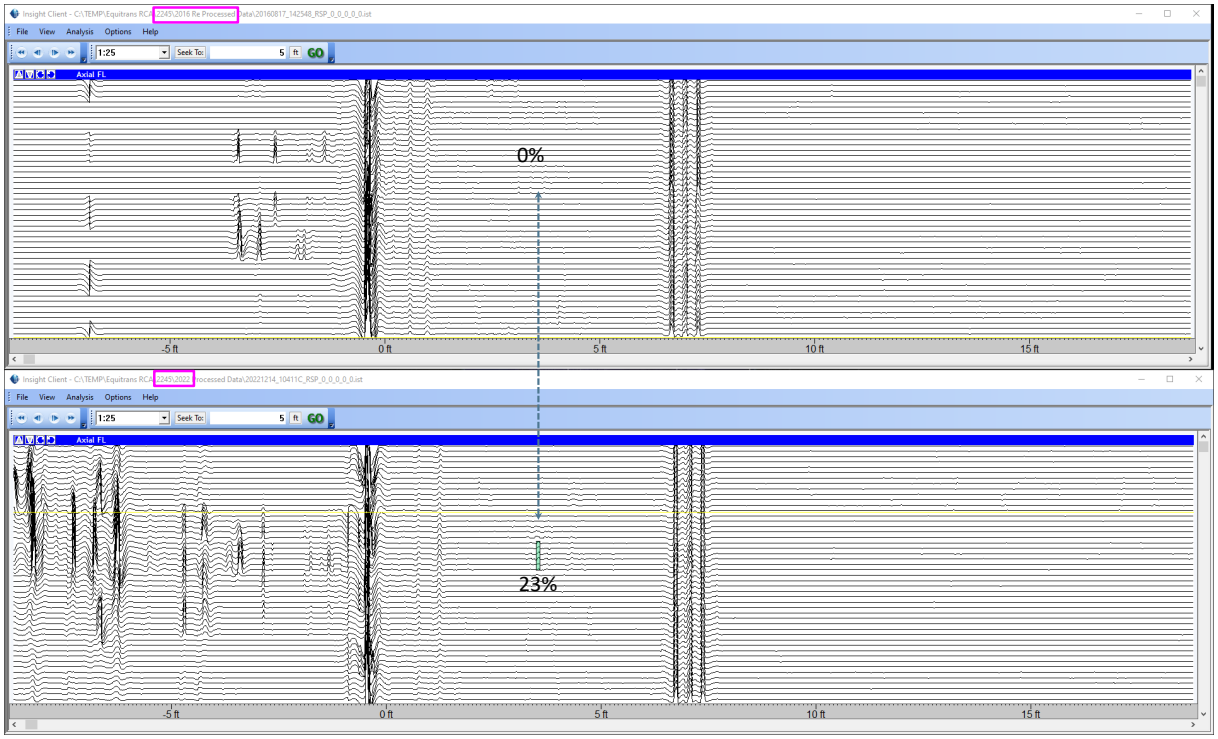

Figure 224: #2245 HR Vertilog 2016 (Above) and 2022 (Below)

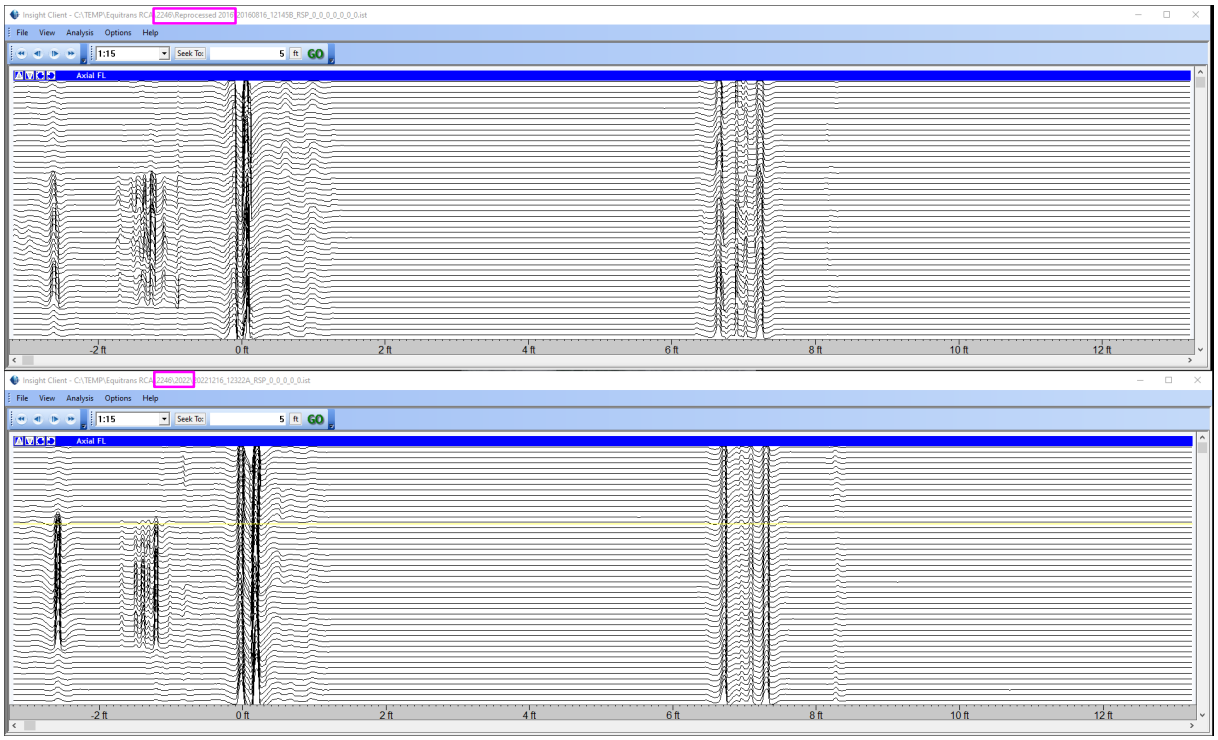

Figure 225: #2246 HR Vertilog 2016 (Above) and 2022 (Below)

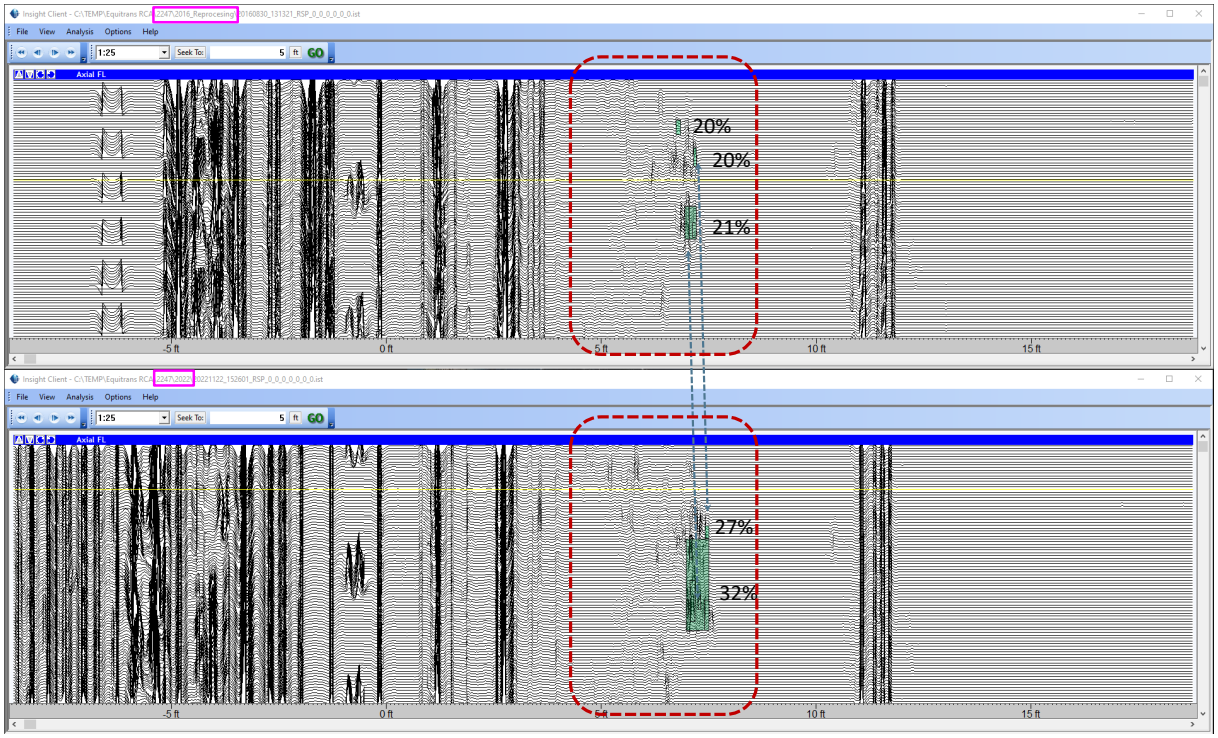

Figure 226: #2247 HR Vertilog 2016 (Above) and 2022 (Below)

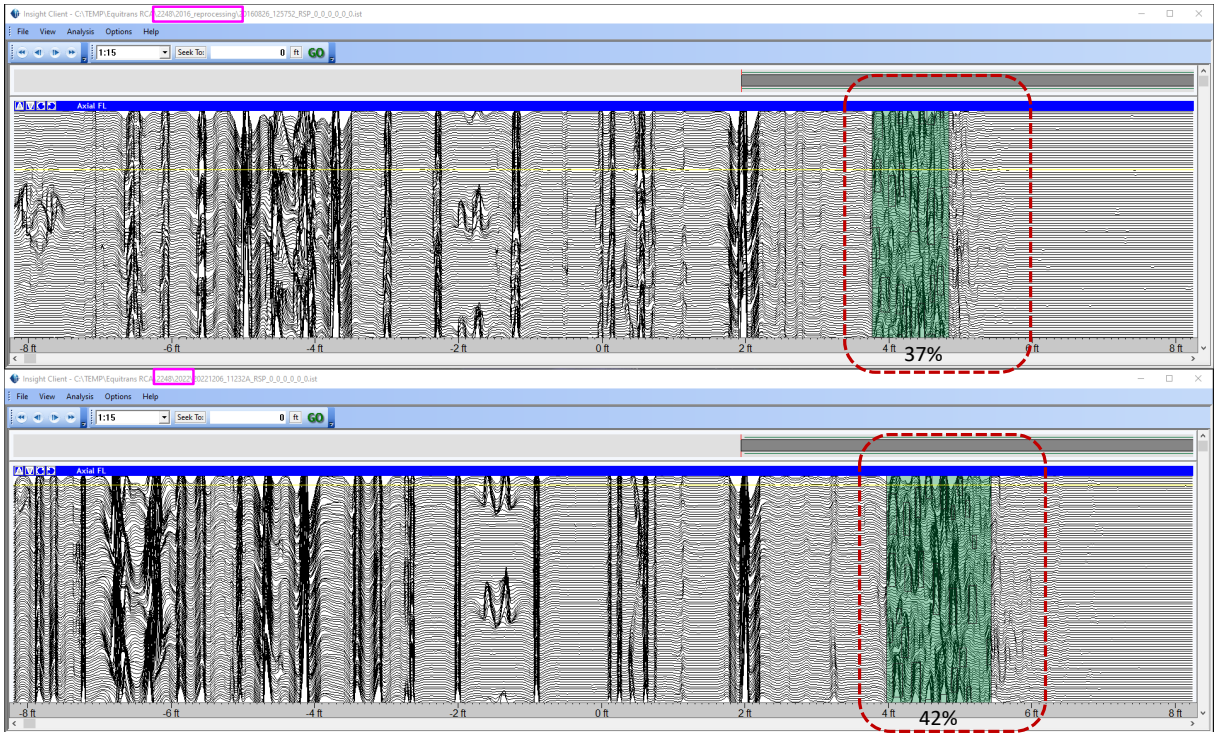

Figure 227: #2248 HR Vertilog 2016 (Above) and 2022 (Below)

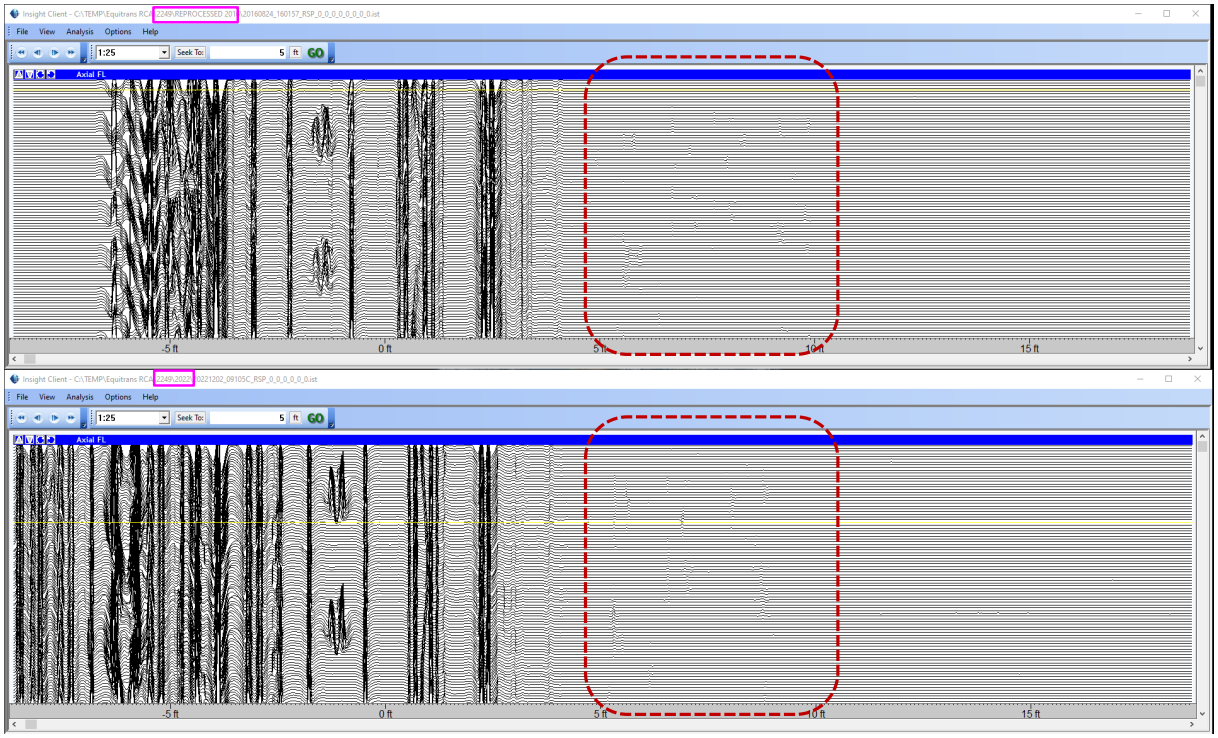

Figure 228: #2249 HR Vertilog 2016 (Above) and 2022 (Below)

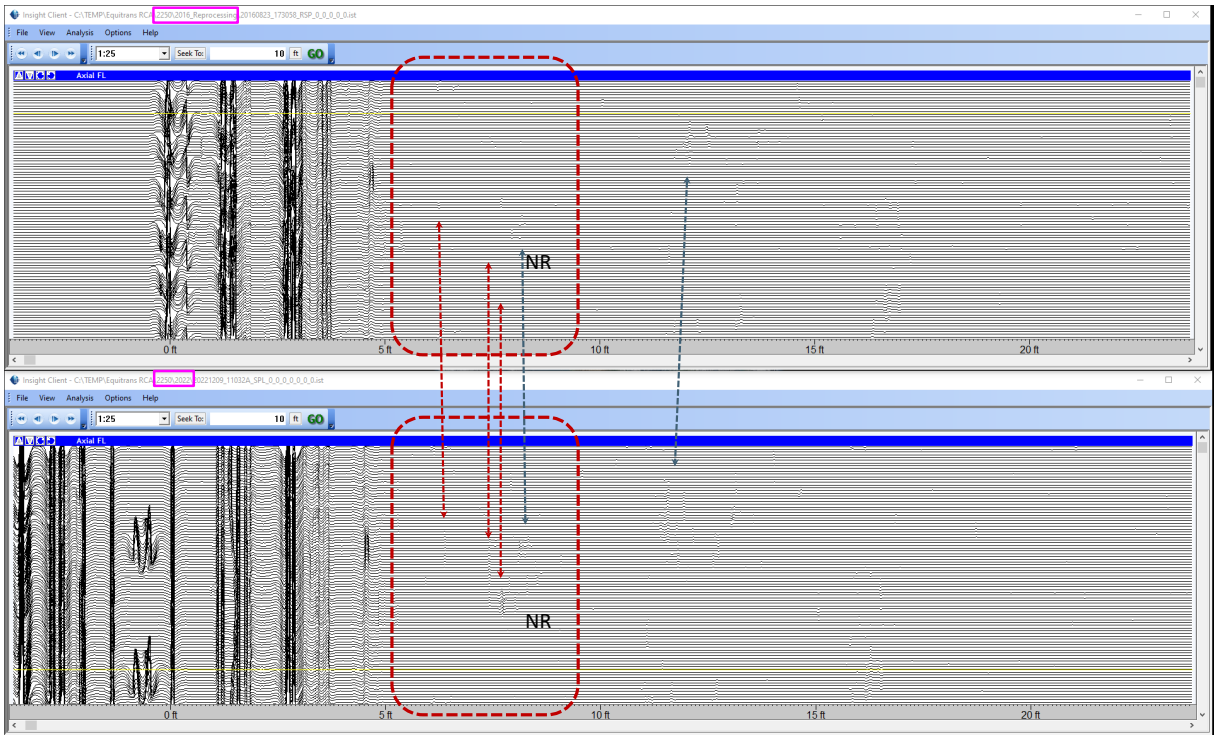

Figure 229: #2250 HR Vertilog 2016 (Above) and 2022 (Below)

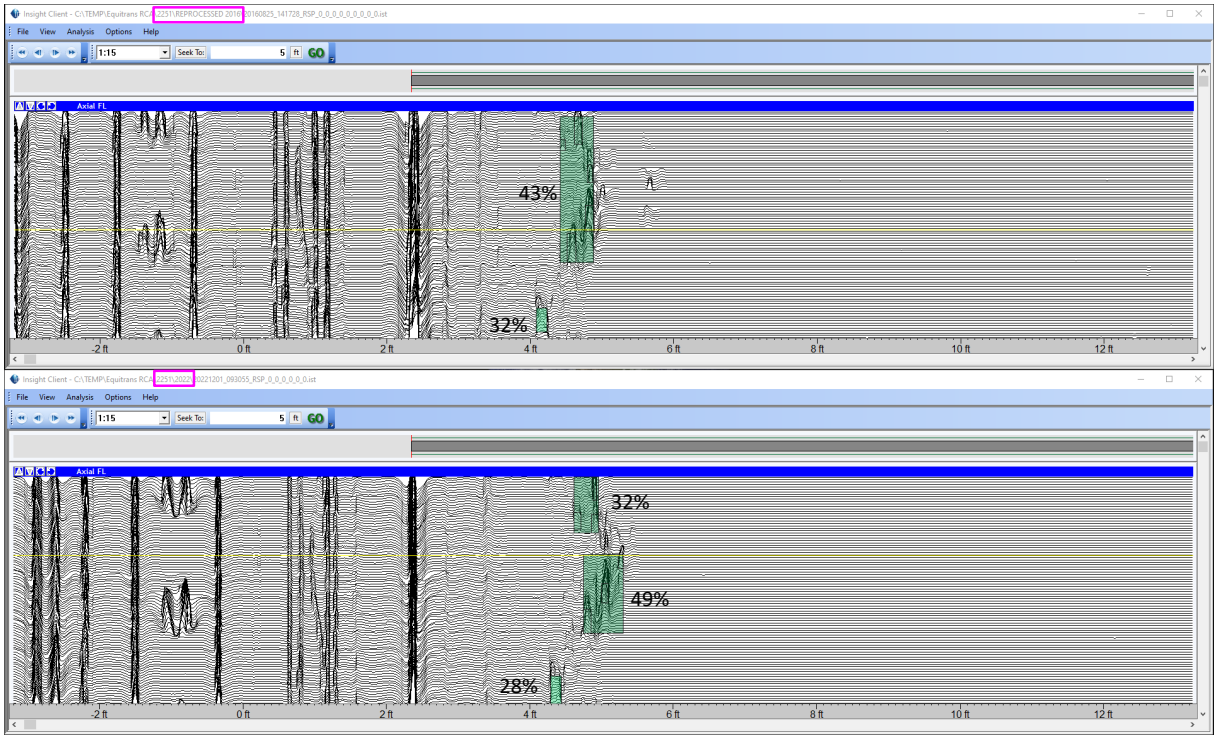

Figure 230: #2251 HR Vertilog 2016 (Above) and 2022 (Below)

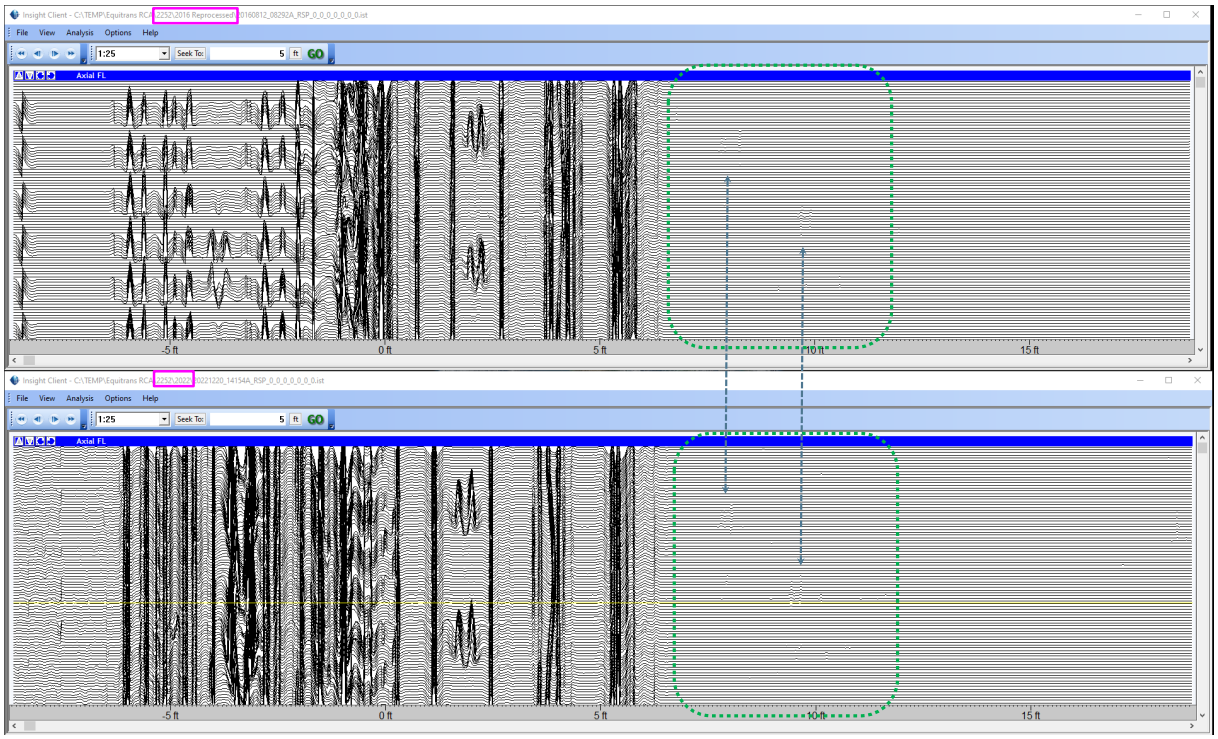

Figure 231: #2252 HR Vertilog 2016 (Above) and 2022 (Below)

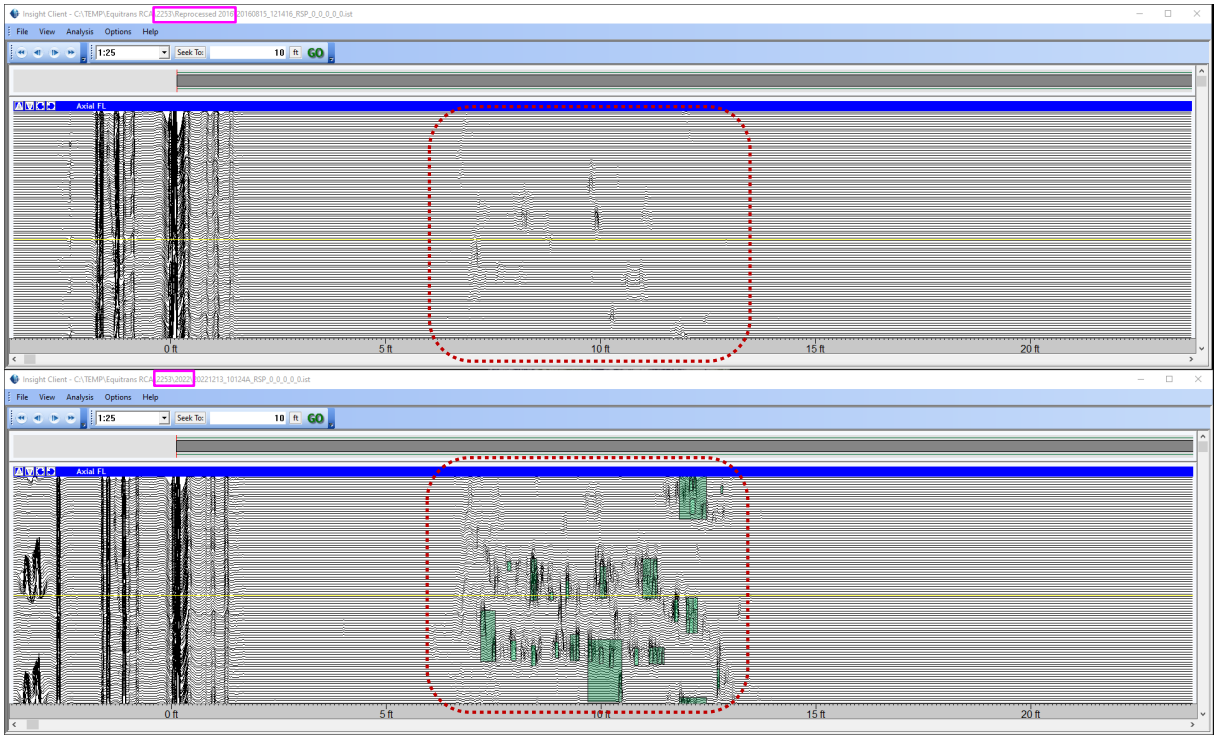

Figure 232: #2253 HR Vertilog 2016 (Above) and 2022 (Below)

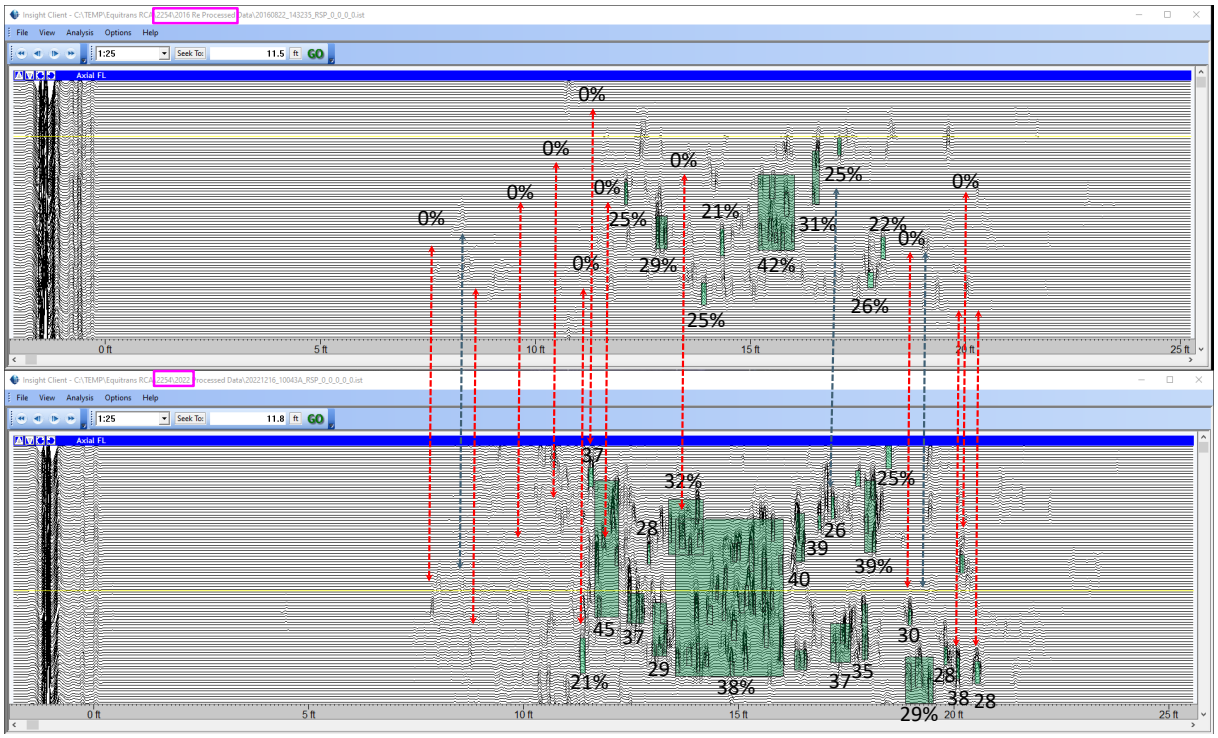

Figure 233: #2254 HR Vertilog 2016 (Above) and 2022 (Below)

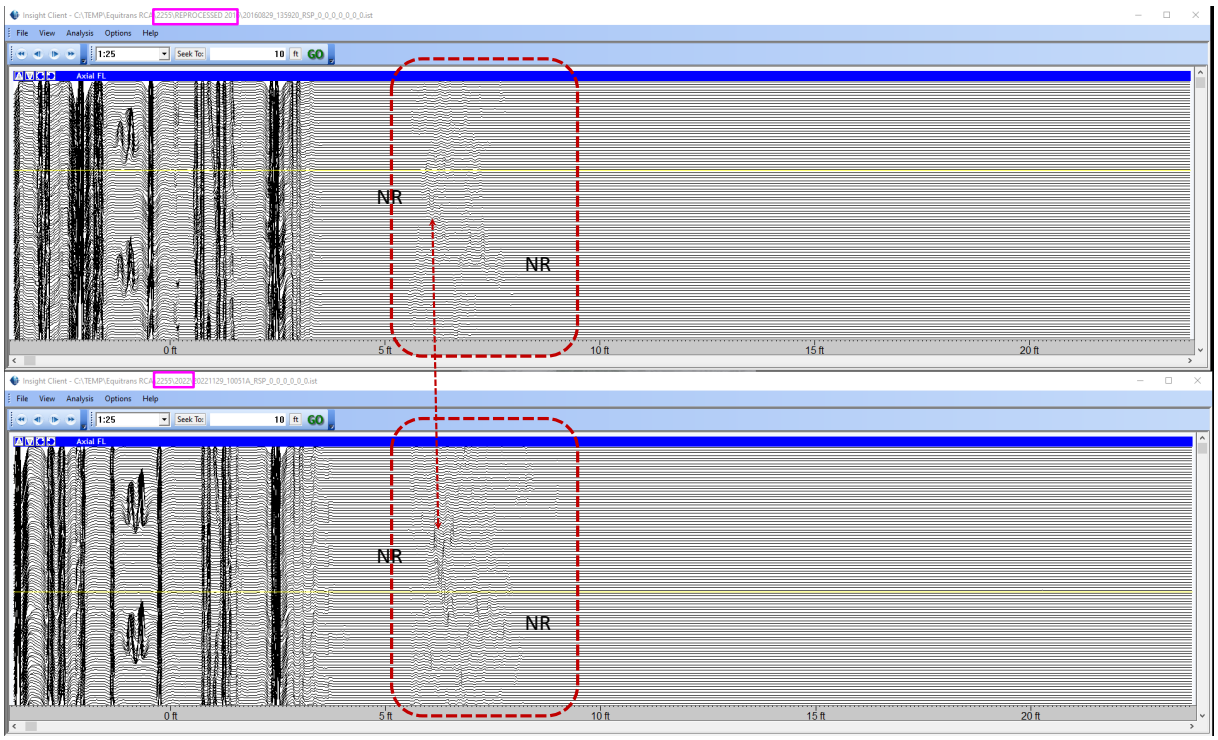

Figure 234: #2255 HR Vertilog 2016 (Above) and 2022 (Below)

A.7 Comparison of Laser Scan Data to HR Vertilog Data

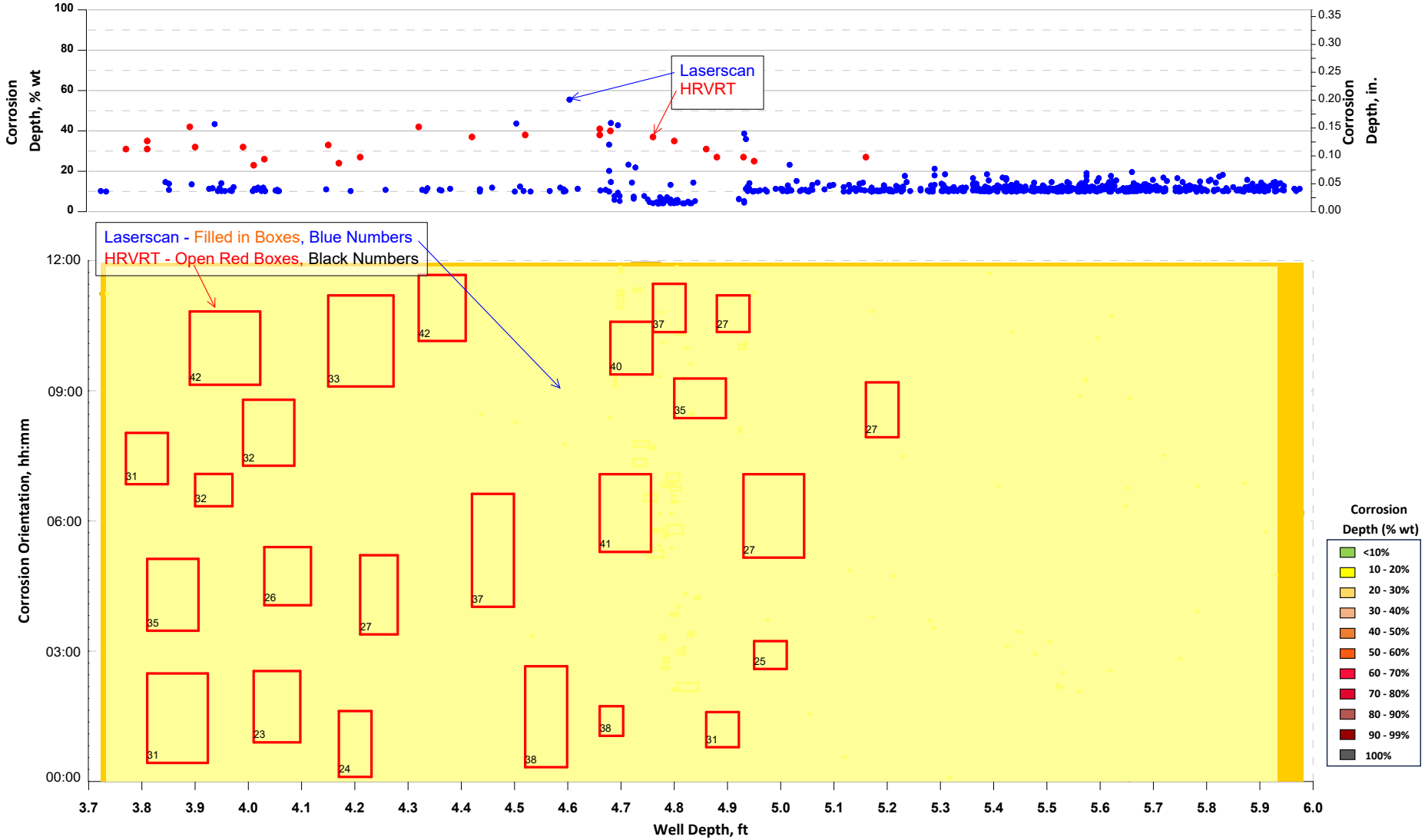

Figure 235: Laser Scan Data and HRVRT Data, Well #2248

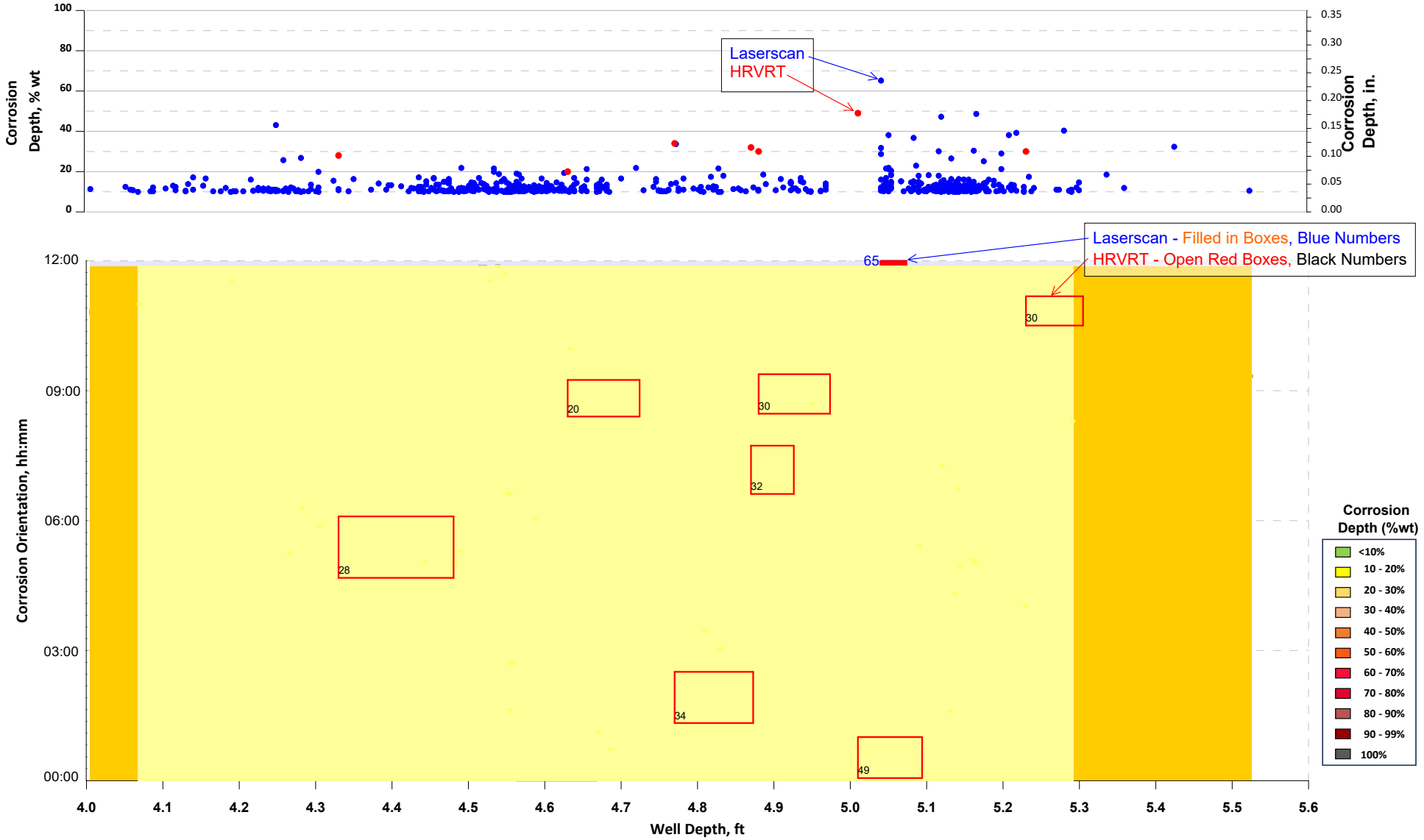

Figure 236: Laser Scan Data and HRVRT Data, Well #2251

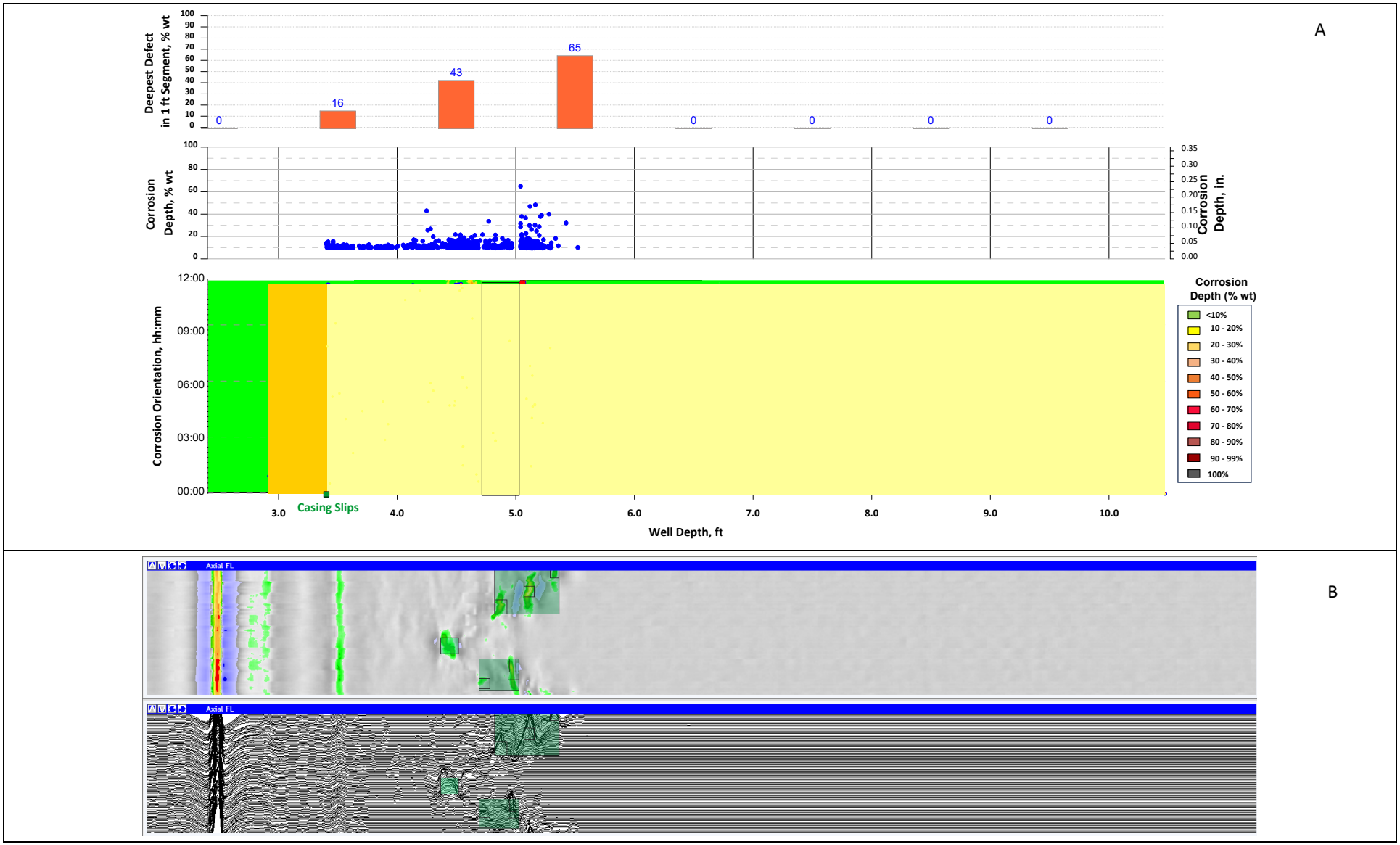

Figure 237: Top Joint of #2251, Laser Scan Data (A), HRVRT Insight Viewer (B)

A.8 Well Summary

Well	Well Type (Injection or Obs)	Year Drilled	Surf hole fluid (While drilling)	Surf Casing OD (in.)	Surf Csg Depth (ft)	Prod Hole Fluid (While drilling)	Prod Casing OD (in.)	Prod Casing Depth (ft)	Prod Casing Wt. (ppf)	Prod Casing Grade	Casing MIYP (psi)	DV Tool Part of Original Compl?	DV Tool Depth (ft)	Total Depth (ft)
2244	Inj	1965	Foam	9.625	1,794	Air	7	7,701	26	N80	7,240	No		7,866
2245	Inj	1965	Not stated	8.625	1,657	Not stated	5.5	7,692	20/17	P110/J55	12,640/5,320	No		7,874
2246	Obs	1966	Air	8.625	1,780	Air and Foam	5.5	7,872	17	N80	7,740	No		8,031
2247	Obs	1967	Foam	9.625	1,305	Air	7	7,927	26	N80	7,240	No		8,100
2248	Inj	1968	Not stated	9.625	1,178	Not stated	7	7,592	26	N80	7,240	No		7,681
2249	Inj	1971	Foam	9.625	1,325	Air	7	7,738	26	N80/P110	7,240	Yes	5,005	7,920
2250	Inj	1974	Foam	9.625	1,262	Air	7	7,800	26	N80	7,240	Yes	4,999	8,000
2251	Inj	1989	Air and Foam	10.75	1,533	Air	7	7,758	26	P110	9,960	Yes	5,719	8,051
2252	Inj	1989	Air and Fluid	10.75	1,747	Air	7	7,704	26	P110	9,960	Yes	5,613	7,869
2253	Inj	2010	Air and Foam	9.625	1,664	Air and Fluid	7	7,809	26	N80	7,240	No		8,054
2254	Inj	2010	Air and Foam	9.625	1,670	Air and Fluid	7	7,835	26	N80	7,240	No		8,156
2255	Inj	2011	Not stated	9.625	1,541	Not stated	7	7,693	26	N80	7,240	No		7,960

A.9 DEP Office of Oil and Gas Management Inspection Document Review

Table 55: A.8 DEP Office of Oil and Gas Management Inspection Document Review -Equitrans

Date accessed: 4/28/2023 12:47:42 PM

Inspections from 1/1/1990 to 4/28/2023

County: 11 - Cambria

Municipality: All

Region: All

Operator: EQUITRANS LP (27639)

Inspection Id	Inspection Date	Inspection Type	Inspection Category	Inspection Result	Inspector	Client Id	Operator	Ogo	Primary Facility Id	Farm	Permit	County
2308492	09/30/2014	Site Restoration	PF	No Violations Noted	KUHNS, SUSAN	27639	EQUITRANS LP	OGO-36770	17832	GEORGE L READE 1	021-20005	Cambria
2316347	10/21/2014	Routine/Complete Inspection	PF	No Violations Noted	WYRWAS, PAUL	27639	EQUITRANS LP	OGO-36770	17832	GEORGE L READE 1	021-20005	Cambria
2316351	10/21/2014	Routine/Complete Inspection	PF	No Violations Noted	WYRWAS, PAUL	27639	EQUITRANS LP	OGO-36770	17832	GEORGE L READE 1	021-20005	Cambria
2316356	10/21/2014	Routine/Complete Inspection	PF	No Violations Noted	WYRWAS, PAUL	27639	EQUITRANS LP	OGO-36770	17832	GEORGE L READE 1	021-20005	Cambria
2316357	10/21/2014	Routine/Complete Inspection	PF	No Violations Noted	WYRWAS, PAUL	27639	EQUITRANS LP	OGO-36770	17832	GEORGE L READE 1	021-20005	Cambria
2316358	10/21/2014	Routine/Complete Inspection	PF	No Violations Noted	WOODS, MATTHEW	27639	EQUITRANS LP	OGO-36770	17832	GEORGE L READE 1	021-20005	Cambria
2316360	10/21/2014	Routine/Complete Inspection	PF	No Violations Noted	VIRRUET, IVAN	27639	EQUITRANS LP	OGO-36770	17832	GEORGE L READE 1	021-20005	Cambria
2316362	10/21/2014	Routine/Complete Inspection	PF	No Violations Noted	SMALL, CURTIS	27639	EQUITRANS LP	OGO-36770	17832	GEORGE L READE 1	021-20005	Cambria
2316363	10/21/2014	Routine/Complete Inspection	PF	No Violations Noted	VIRRUET, IVAN	27639	EQUITRANS LP	OGO-36770	17832	GEORGE L READE 1	021-20005	Cambria
2316364	10/21/2014	Routine/Complete Inspection	PF	No Violations Noted	VIRRUET, IVAN	27639	EQUITRANS LP	OGO-36770	17832	GEORGE L READE 1	021-20005	Cambria
2316365	10/21/2014	Routine/Complete Inspection	PF	No Violations Noted	VIRRUET, IVAN	27639	EQUITRANS LP	OGO-36770	17832	GEORGE L READE 1	021-20005	Cambria
2316366	10/21/2014	Routine/Complete Inspection	PF	No Violations Noted	VIRRUET, IVAN	27639	EQUITRANS LP	OGO-36770	17832	GEORGE L READE 1	021-20005	Cambria
2316368	10/21/2014	Routine/Complete Inspection	PF	No Violations Noted	VIRRUET, IVAN	27639	EQUITRANS LP	OGO-36770	17832	GEORGE L READE 1	021-20005	Cambria
2421479	10/27/2015	Routine/Complete Inspection	PF	No Violations Noted	NAJEWICZ, JUSTIN	27639	EQUITRANS LP	OGO-36770	17832	GEORGE L READE 1	021-20005	Cambria
2421481	10/27/2015	Routine/Complete Inspection	PF	No Violations Noted	VIRRUET, IVAN	27639	EQUITRANS LP	OGO-36770	17832	GEORGE L READE 1	021-20005	Cambria
2421482	10/27/2015	Routine/Complete Inspection	PF	No Violations Noted	MARSCH, AMANDA	27639	EQUITRANS LP	OGO-36770	17832	GEORGE L READE 1	021-20005	Cambria

2421486	10/27/2015	Routine/Complete Inspection	PF	No Violations Noted	MARSCH, AMANDA	27639	EQUITRANS LP	OGO-36770	17832	GEORGE L READE 1	021-20005	Cambria
2421495	10/27/2015	Routine/Complete Inspection	PF	No Violations Noted	VIRRUET, IVAN	27639	EQUITRANS LP	OGO-36770	17832	GEORGE L READE 1	021-20005	Cambria
2421496	10/27/2015	Routine/Complete Inspection	PF	No Violations Noted	MARSCH, AMANDA	27639	EQUITRANS LP	OGO-36770	17832	GEORGE L READE 1	021-20005	Cambria
2421498	10/27/2015	Routine/Complete Inspection	PF	No Violations Noted	MARSCH, AMANDA	27639	EQUITRANS LP	OGO-36770	17832	GEORGE L READE 1	021-20005	Cambria
2421499	10/27/2015	Routine/Complete Inspection	PF	No Violations Noted	VIRRUET, IVAN	27639	EQUITRANS LP	OGO-36770	17832	GEORGE L READE 1	021-20005	Cambria
2421502	10/27/2015	Routine/Complete Inspection	PF	No Violations Noted	MARSCH, AMANDA	27639	EQUITRANS LP	OGO-36770	17832	GEORGE L READE 1	021-20005	Cambria
2421503	10/27/2015	Routine/Complete Inspection	PF	No Violations Noted	MARSCH, AMANDA	27639	EQUITRANS LP	OGO-36770	17832	GEORGE L READE 1	021-20005	Cambria
2421504	10/27/2015	Routine/Complete Inspection	PF	No Violations Noted	MARSCH, AMANDA	27639	EQUITRANS LP	OGO-36770	17832	GEORGE L READE 1	021-20005	Cambria
2532329	10/27/2016	Routine/Complete Inspection	PF	No Violations Noted	MARSCH, AMANDA	27639	EQUITRANS LP	OGO-36770	17832	GEORGE L READE 1	021-20005	Cambria
2532330	10/27/2016	Routine/Complete Inspection	PF	No Violations Noted	VIRRUET, IVAN	27639	EQUITRANS LP	OGO-36770	17832	GEORGE L READE 1	021-20005	Cambria
2532331	10/27/2016	Routine/Complete Inspection	PF	No Violations Noted	VIRRUET, IVAN	27639	EQUITRANS LP	OGO-36770	17832	GEORGE L READE 1	021-20005	Cambria
2532332	10/27/2016	Routine/Complete Inspection	PF	No Violations Noted	MARSCH, AMANDA	27639	EQUITRANS LP	OGO-36770	17832	GEORGE L READE 1	021-20005	Cambria
2532334	10/27/2016	Routine/Complete Inspection	PF	No Violations Noted	VIRRUET, IVAN	27639	EQUITRANS LP	OGO-36770	17832	GEORGE L READE 1	021-20005	Cambria
2532336	10/27/2016	Routine/Complete Inspection	PF	No Violations Noted	VIRRUET, IVAN	27639	EQUITRANS LP	OGO-36770	17832	GEORGE L READE 1	021-20005	Cambria
2532337	10/27/2016	Routine/Complete Inspection	PF	No Violations Noted	VIRRUET, IVAN	27639	EQUITRANS LP	OGO-36770	17832	GEORGE L READE 1	021-20005	Cambria
2532338	10/27/2016	Routine/Complete Inspection	PF	No Violations Noted	VIRRUET, IVAN	27639	EQUITRANS LP	OGO-36770	17832	GEORGE L READE 1	021-20005	Cambria
2532339	10/27/2016	Routine/Complete Inspection	PF	No Violations Noted	VIRRUET, IVAN	27639	EQUITRANS LP	OGO-36770	17832	GEORGE L READE 1	021-20005	Cambria
2532340	10/27/2016	Routine/Complete Inspection	PF	No Violations Noted	MARSCH, AMANDA	27639	EQUITRANS LP	OGO-36770	17832	GEORGE L READE 1	021-20005	Cambria
2532341	10/27/2016	Routine/Complete Inspection	PF	No Violations Noted	VIRRUET, IVAN	27639	EQUITRANS LP	OGO-36770	17832	GEORGE L READE 1	021-20005	Cambria
2532343	10/27/2016	Routine/Complete Inspection	PF	No Violations Noted	MARSCH, AMANDA	27639	EQUITRANS LP	OGO-36770	17832	GEORGE L READE 1	021-20005	Cambria
2624201	08/02/2017	Plugging (Includes Plugged/Mined Through)	PF	No Violations Noted	VIRRUET, IVAN	27639	EQUITRANS LP	OGO-36770	17832	GEORGE L READE 1	021-20005	Cambria
2649650	10/19/2017	Routine/Complete Inspection	PF	No Violations Noted	VIRRUET, IVAN	27639	EQUITRANS LP	OGO-36770	17832	GEORGE L READE 1	021-20005	Cambria
2649654	10/19/2017	Routine/Complete Inspection	PF	No Violations Noted	MARSCH, AMANDA	27639	EQUITRANS LP	OGO-36770	17832	GEORGE L READE 1	021-20005	Cambria
2649659	10/19/2017	Routine/Complete Inspection	PF	No Violations Noted	VIRRUET, IVAN	27639	EQUITRANS LP	OGO-36770	17832	GEORGE L READE 1	021-20005	Cambria

2649663	10/19/2017	Routine/Complete Inspection	PF	No Violations Noted	MARSCH, AMANDA	27639	EQUITRANS LP	OGO-36770	17832	GEORGE L READE 1	021-20005	Cambria
2649677	10/19/2017	Routine/Complete Inspection	PF	No Violations Noted	MARSCH, AMANDA	27639	EQUITRANS LP	OGO-36770	17832	GEORGE L READE 1	021-20005	Cambria
2649703	10/19/2017	Routine/Complete Inspection	PF	No Violations Noted	VIRRUET, IVAN	27639	EQUITRANS LP	OGO-36770	17832	GEORGE L READE 1	021-20005	Cambria
2649708	10/19/2017	Routine/Complete Inspection	PF	No Violations Noted	VIRRUET, IVAN	27639	EQUITRANS LP	OGO-36770	17832	GEORGE L READE 1	021-20005	Cambria
2649730	10/19/2017	Routine/Complete Inspection	PF	No Violations Noted	MARSCH, AMANDA	27639	EQUITRANS LP	OGO-36770	17832	GEORGE L READE 1	021-20005	Cambria
2649733	10/19/2017	Routine/Complete Inspection	PF	No Violations Noted	VIRRUET, IVAN	27639	EQUITRANS LP	OGO-36770	17832	GEORGE L READE 1	021-20005	Cambria
2649738	10/19/2017	Routine/Complete Inspection	PF	No Violations Noted	MARSCH, AMANDA	27639	EQUITRANS LP	OGO-36770	17832	GEORGE L READE 1	021-20005	Cambria
2649745	10/19/2017	Routine/Complete Inspection	PF	No Violations Noted	MARSCH, AMANDA	27639	EQUITRANS LP	OGO-36770	17832	GEORGE L READE 1	021-20005	Cambria
2649758	10/19/2017	Routine/Complete Inspection	PF	No Violations Noted	CLARK, ADAM	27639	EQUITRANS LP	OGO-36770	17832	GEORGE L READE 1	021-20005	Cambria
2710895	03/27/2018	Routine/Complete Inspection	PF	No Violations Noted	CLARK, ADAM	27639	EQUITRANS LP	OGO-36770	17832	GEORGE L READE 1	021-20005	Cambria
2787094	10/09/2018	Routine/Complete Inspection	PF	No Violations Noted	CLARK, ADAM	27639	EQUITRANS LP	OGO-36770	17832	GEORGE L READE 1	021-20005	Cambria
2787103	10/09/2018	Routine/Complete Inspection	PF	No Violations Noted	CLARK, ADAM	27639	EQUITRANS LP	OGO-36770	17832	GEORGE L READE 1	021-20005	Cambria
2787108	10/09/2018	Routine/Complete Inspection	PF	No Violations Noted	CLARK, ADAM	27639	EQUITRANS LP	OGO-36770	17832	GEORGE L READE 1	021-20005	Cambria
2787114	10/09/2018	Routine/Complete Inspection	PF	No Violations Noted	CLARK, ADAM	27639	EQUITRANS LP	OGO-36770	17832	GEORGE L READE 1	021-20005	Cambria
2787145	10/09/2018	Routine/Complete Inspection	PF	No Violations Noted	CLARK, ADAM	27639	EQUITRANS LP	OGO-36770	17832	GEORGE L READE 1	021-20005	Cambria
2787159	10/09/2018	Routine/Complete Inspection	PF	No Violations Noted	FOULK, SAMANTHA	27639	EQUITRANS LP	OGO-36770	17832	GEORGE L READE 1	021-20005	Cambria
2787161	10/09/2018	Routine/Complete Inspection	PF	No Violations Noted	FOULK, SAMANTHA	27639	EQUITRANS LP	OGO-36770	17832	GEORGE L READE 1	021-20005	Cambria
2787163	10/09/2018	Routine/Complete Inspection	PF	No Violations Noted	FOULK, SAMANTHA	27639	EQUITRANS LP	OGO-36770	17832	GEORGE L READE 1	021-20005	Cambria
2787167	10/09/2018	Routine/Complete Inspection	PF	No Violations Noted	FOULK, SAMANTHA	27639	EQUITRANS LP	OGO-36770	17832	GEORGE L READE 1	021-20005	Cambria
2787169	10/09/2018	Routine/Complete Inspection	PF	No Violations Noted	CLARK, ADAM	27639	EQUITRANS LP	OGO-36770	17832	GEORGE L READE 1	021-20005	Cambria
2787173	10/09/2018	Routine/Complete Inspection	PF	No Violations Noted	KUHNS, SUSAN	27639	EQUITRANS LP	OGO-36770	17833	MAUDE EMMA BOLE ET AL 1	021-20006	Cambria
2787175	10/09/2018	Routine/Complete Inspection	PF	No Violations Noted	WYRWAS, PAUL	27639	EQUITRANS LP	OGO-36770	17833	MAUDE EMMA BOLE ET AL 1	021-20006	Cambria
2998009	02/13/2020	Routine/Complete Inspection	PF	No Violations Noted	WYRWAS, PAUL	27639	EQUITRANS LP	OGO-36770	17833	MAUDE EMMA BOLE ET AL 1	021-20006	Cambria
2998181	02/13/2020	Routine/Complete Inspection	PF	No Violations Noted	WYRWAS, PAUL	27639	EQUITRANS LP	OGO-36770	17833	MAUDE EMMA BOLE ET AL 1	021-20006	Cambria

2998191	02/13/2020	Routine/Complete Inspection	PF	No Violations Noted	WYRWAS, PAUL	27639	EQUITRANS LP	OGO-36770	17833	MAUDE EMMA BOLE ET AL 1	021-20006	Cambria
2998196	02/13/2020	Routine/Complete Inspection	PF	No Violations Noted	WYRWAS, PAUL	27639	EQUITRANS LP	OGO-36770	17833	MAUDE EMMA BOLE ET AL 1	021-20006	Cambria
2998202	02/13/2020	Routine/Complete Inspection	PF	No Violations Noted	VIRRUET, IVAN	27639	EQUITRANS LP	OGO-36770	17833	MAUDE EMMA BOLE ET AL 1	021-20006	Cambria
2998184	02/18/2020	Routine/Complete Inspection	PF	No Violations Noted	SMALL, CURTIS	27639	EQUITRANS LP	OGO-36770	17833	MAUDE EMMA BOLE ET AL 1	021-20006	Cambria
2998188	02/18/2020	Routine/Complete Inspection	PF	No Violations Noted	VIRRUET, IVAN	27639	EQUITRANS LP	OGO-36770	17833	MAUDE EMMA BOLE ET AL 1	021-20006	Cambria
3120299	12/10/2020	Routine/Complete Inspection	PF	No Violations Noted	VIRRUET, IVAN	27639	EQUITRANS LP	OGO-36770	17833	MAUDE EMMA BOLE ET AL 1	021-20006	Cambria
3120306	12/10/2020	Routine/Complete Inspection	PF	No Violations Noted	VIRRUET, IVAN	27639	EQUITRANS LP	OGO-36770	17833	MAUDE EMMA BOLE ET AL 1	021-20006	Cambria
3120312	12/10/2020	Routine/Complete Inspection	PF	No Violations Noted	VIRRUET, IVAN	27639	EQUITRANS LP	OGO-36770	17833	MAUDE EMMA BOLE ET AL 1	021-20006	Cambria
3120318	12/10/2020	Routine/Complete Inspection	PF	No Violations Noted	VIRRUET, IVAN	27639	EQUITRANS LP	OGO-36770	17833	MAUDE EMMA BOLE ET AL 1	021-20006	Cambria
3120338	12/10/2020	Routine/Complete Inspection	PF	No Violations Noted	VIRRUET, IVAN	27639	EQUITRANS LP	OGO-36770	17833	MAUDE EMMA BOLE ET AL 1	021-20006	Cambria
3120344	12/10/2020	Routine/Complete Inspection	PF	No Violations Noted	VIRRUET, IVAN	27639	EQUITRANS LP	OGO-36770	17833	MAUDE EMMA BOLE ET AL 1	021-20006	Cambria
3120349	12/10/2020	Routine/Complete Inspection	PF	No Violations Noted	VIRRUET, IVAN	27639	EQUITRANS LP	OGO-36770	17833	MAUDE EMMA BOLE ET AL 1	021-20006	Cambria
3120367	12/10/2020	Routine/Complete Inspection	PF	No Violations Noted	VIRRUET, IVAN	27639	EQUITRANS LP	OGO-36770	17833	MAUDE EMMA BOLE ET AL 1	021-20006	Cambria
3120374	12/10/2020	Routine/Complete Inspection	PF	No Violations Noted	VIRRUET, IVAN	27639	EQUITRANS LP	OGO-36770	17833	MAUDE EMMA BOLE ET AL 1	021-20006	Cambria
3120429	12/10/2020	Routine/Complete Inspection	PF	No Violations Noted	VIRRUET, IVAN	27639	EQUITRANS LP	OGO-36770	17833	MAUDE EMMA BOLE ET AL 1	021-20006	Cambria
3120440	12/10/2020	Routine/Complete Inspection	PF	No Violations Noted	VIRRUET, IVAN	27639	EQUITRANS LP	OGO-36770	17833	MAUDE EMMA BOLE ET AL 1	021-20006	Cambria
3120467	12/10/2020	Routine/Complete Inspection	PF	No Violations Noted	KUHNS, SUSAN	27639	EQUITRANS LP	OGO-36770	17835	CHARLES MILLER 4500	021-20008	Cambria
3177400	04/15/2021	Routine/Complete Inspection	PF	No Violations Noted	WYRWAS, PAUL	27639	EQUITRANS LP	OGO-36770	17835	CHARLES MILLER 4500	021-20008	Cambria
3257377	09/22/2021	Routine/Complete Inspection	PF	No Violations Noted	WYRWAS, PAUL	27639	EQUITRANS LP	OGO-36770	17835	CHARLES MILLER 4500	021-20008	Cambria
3257382	09/22/2021	Routine/Complete Inspection	PF	No Violations Noted	WYRWAS, PAUL	27639	EQUITRANS LP	OGO-36770	17835	CHARLES MILLER 4500	021-20008	Cambria
3257393	09/22/2021	Routine/Complete Inspection	PF	No Violations Noted	WYRWAS, PAUL	27639	EQUITRANS LP	OGO-36770	17835	CHARLES MILLER 4500	021-20008	Cambria
3257398	09/22/2021	Routine/Complete Inspection	PF	No Violations Noted	WOODS, MATTHEW	27639	EQUITRANS LP	OGO-36770	17835	CHARLES MILLER 4500	021-20008	Cambria

3257405	09/22/2021	Routine/Complete Inspection	PF	No Violations Noted	VIRRUET, IVAN	27639	EQUITRANS LP	OGO-36770	17835	CHARLES MILLER 4500	021-20008	Cambria
3257416	09/22/2021	Routine/Complete Inspection	PF	No Violations Noted	SMALL, CURTIS	27639	EQUITRANS LP	OGO-36770	17835	CHARLES MILLER 4500	021-20008	Cambria
3257420	09/22/2021	Routine/Complete Inspection	PF	No Violations Noted	VIRRUET, IVAN	27639	EQUITRANS LP	OGO-36770	17835	CHARLES MILLER 4500	021-20008	Cambria
3257479	09/22/2021	Routine/Complete Inspection	PF	No Violations Noted	VIRRUET, IVAN	27639	EQUITRANS LP	OGO-36770	17835	CHARLES MILLER 4500	021-20008	Cambria
3257522	09/22/2021	Routine/Complete Inspection	PF	No Violations Noted	VIRRUET, IVAN	27639	EQUITRANS LP	OGO-36770	17835	CHARLES MILLER 4500	021-20008	Cambria
3257535	09/22/2021	Routine/Complete Inspection	PF	No Violations Noted	VIRRUET, IVAN	27639	EQUITRANS LP	OGO-36770	17835	CHARLES MILLER 4500	021-20008	Cambria
3257550	09/22/2021	Routine/Complete Inspection	PF	No Violations Noted	VIRRUET, IVAN	27639	EQUITRANS LP	OGO-36770	17835	CHARLES MILLER 4500	021-20008	Cambria
3257555	09/22/2021	Routine/Complete Inspection	PF	No Violations Noted	VIRRUET, IVAN	27639	EQUITRANS LP	OGO-36770	17835	CHARLES MILLER 4500	021-20008	Cambria
3375534	06/09/2022	Routine/Complete Inspection	PF	No Violations Noted	VIRRUET, IVAN	27639	EQUITRANS LP	OGO-36770	17835	CHARLES MILLER 4500	021-20008	Cambria
3375948	06/10/2022	Routine/Complete Inspection	PF	No Violations Noted	VIRRUET, IVAN	27639	EQUITRANS LP	OGO-36770	17835	CHARLES MILLER 4500	021-20008	Cambria
3375975	06/10/2022	Routine/Complete Inspection	PF	No Violations Noted	VIRRUET, IVAN	27639	EQUITRANS LP	OGO-36770	17835	CHARLES MILLER 4500	021-20008	Cambria
3377298	06/10/2022	Routine/Complete Inspection	PF	No Violations Noted	VIRRUET, IVAN	27639	EQUITRANS LP	OGO-36770	17835	CHARLES MILLER 4500	021-20008	Cambria
3447287	10/26/2022	Routine/Complete Inspection	PF	No Violations Noted	VIRRUET, IVAN	27639	EQUITRANS LP	OGO-36770	17835	CHARLES MILLER 4500	021-20008	Cambria
3447303	10/26/2022	Routine/Complete Inspection	PF	No Violations Noted	VIRRUET, IVAN	27639	EQUITRANS LP	OGO-36770	17835	CHARLES MILLER 4500	021-20008	Cambria
3447310	10/26/2022	Routine/Complete Inspection	PF	No Violations Noted	VIRRUET, IVAN	27639	EQUITRANS LP	OGO-36770	17835	CHARLES MILLER 4500	021-20008	Cambria
3447316	10/26/2022	Routine/Complete Inspection	PF	No Violations Noted	VIRRUET, IVAN	27639	EQUITRANS LP	OGO-36770	17835	CHARLES MILLER 4500	021-20008	Cambria
3447325	10/26/2022	Routine/Complete Inspection	PF	No Violations Noted	VIRRUET, IVAN	27639	EQUITRANS LP	OGO-36770	17835	CHARLES MILLER 4500	021-20008	Cambria
3447345	10/26/2022	Routine/Complete Inspection	PF	No Violations Noted	VIRRUET, IVAN	27639	EQUITRANS LP	OGO-36770	17835	CHARLES MILLER 4500	021-20008	Cambria
3447615	10/26/2022	Routine/Complete Inspection	PF	No Violations Noted	VIRRUET, IVAN	27639	EQUITRANS LP	OGO-36770	17835	CHARLES MILLER 4500	021-20008	Cambria
3447622	10/26/2022	Routine/Complete Inspection	PF	No Violations Noted	VIRRUET, IVAN	27639	EQUITRANS LP	OGO-36770	17835	CHARLES MILLER 4500	021-20008	Cambria
3447638	10/26/2022	Routine/Complete Inspection	PF	No Violations Noted	WOODS, MATTHEW	27639	EQUITRANS LP	OGO-36770	17835	CHARLES MILLER 4500	021-20008	Cambria
3447642	10/26/2022	Routine/Complete Inspection	PF	No Violations Noted	KUHNS, SUSAN	27639	EQUITRANS LP	OGO-36770	17836	GEORGE W GRIFFITH 1	021-20009	Cambria
3447645	10/26/2022	Routine/Complete Inspection	PF	No Violations Noted	WYRWAS, PAUL	27639	EQUITRANS LP	OGO-36770	17836	GEORGE W GRIFFITH 1	021-20009	Cambria
3447680	10/26/2022	Routine/Complete Inspection	PF	No Violations Noted	WYRWAS, PAUL	27639	EQUITRANS LP	OGO-36770	17836	GEORGE W GRIFFITH 1	021-20009	Cambria

Table 56: A.8 DEP Office of Oil and Gas Management Inspection Document Review -Peoples Natural Gas

Date accessed: 4/28/2023 12:47:42 PM

Inspections from 1/1/1990 to 4/28/2023

County: 11 - Cambria

Municipality: All

Region: All

Operator: PEOPLES NATURAL GAS CO LLC (189839)

Filtered list – "Violations Noted"

Inspection Id	Inspection Date	Inspection Type	Inspection Category	Inspection Result	Inspector	Client Id	Operator	Ogo	Primary Facility Id	Farm	Permit	County
212692	09/12/1990	Routine/Complete Inspection	PF	Violation(s) Noted	HUMMEL, THOMAS	189839	PEOPLES NATURAL GAS CO LLC	OGO-39243	17832	GEORGE L READE 1	021-20005	Cambria
213115	12/11/1990	Routine/Complete Inspection	PF	Violation(s) Noted	HOOVER, RICKEY	189839	PEOPLES NATURAL GAS CO LLC	OGO-39243	17832	GEORGE L READE 1	021-20005	Cambria
213137	12/27/1990	Routine/Complete Inspection	PF	Violation(s) Noted	WYRWAS, PAUL	189839	PEOPLES NATURAL GAS CO LLC	OGO-39243	17832	GEORGE L READE 1	021-20005	Cambria
216965	08/03/1995	Bond Release	PF	Violation(s) Noted	HUMMEL, THOMAS	189839	PEOPLES NATURAL GAS CO LLC	OGO-39243	17836	GEORGE W GRIFFITH 1	021-20009	Cambria
1967669	04/19/2011	Routine/Complete Inspection	PF	Violation(s) Noted	HOOVER, RICKEY	189839	PEOPLES NATURAL GAS CO LLC	OGO-39243	18612	PEOPLES NATURAL GAS 1	021-20789	Cambria
1981538	06/14/2011	Routine/Complete Inspection	PF	Violation(s) Noted	HUMMEL, THOMAS	189839	PEOPLES NATURAL GAS CO LLC	OGO-39243	18613	GEORGE L. READE 4	021-20790	Cambria
2002460	09/01/2011	Routine/Complete Inspection	PF	Violation(s) Noted	HUMMEL, THOMAS	189839	PEOPLES NATURAL GAS CO LLC	OGO-39243	18613	GEORGE L. READE 4	021-20790	Cambria
2002465	09/01/2011	Routine/Complete Inspection	PF	Violation(s) Noted	HUMMEL, THOMAS	189839	PEOPLES NATURAL GAS CO LLC	OGO-39243	18613	GEORGE L. READE 4	021-20790	Cambria
2002466	09/01/2011	Routine/Complete Inspection	PF	Violation(s) Noted	HUMMEL, THOMAS	189839	PEOPLES NATURAL GAS CO LLC	OGO-39243	18613	GEORGE L. READE 4	021-20790	Cambria

A.10 Material Testing

A.10.1 Chemistry

A sample obtained from well #2244 joint C001B was analyzed using optical emission spectroscopy. Table 57 shows the results of the material composition analysis. API 5CT does not have composition limits for the alloying elements of carbon steel N80, except for phosphorus and sulfur. The values obtained for phosphorus and sulfur are within the specified limits of API 5 CT.

Table 57: Composition of N80 Material from Well #2244 and API Specification Limits in Wt%

	C	Mn	P	S	Si	Ni	Cr	Mo	Cu	Al	V	Nb	Ti	Fe
N80 from #2244	0.23	1.06	0.013	0.006	0.31	0.08	0.40	0.06	0.13	0.02	<0.01	<0.01	0.05	Bal.
API 5CT Specification			Max 0.03	Max 0.03										

A.10.2 Microstructure

Samples taken from the longitudinal orientation and transverse orientation of the 7 in. casing were prepared by successive grinding in 120 µm, 75 µm, and 35 µm pads. The samples were then polished using 9 µm, 3 µm, and 0.25 µm diamond suspension. The specimens were etched in 2% Nital solution to reveal the microstructure. Figure 238 shows the microstructure of N80 along the longitudinal and transverse orientations. The microstructure of N80 material is made up of lath-like features. Literature indicates that N80 can be composed of bainitic microstructure and martensitic microstructure.

Higher-magnification images were obtained using SEM to verify the microstructure of the 7 in. casing. Figure 239 shows the images taken at 10,000x using 15KV and 2KV accelerating voltage. The images confirm that the microstructure of the 7 in. casing is bainitic. There is no needle-like feature that would indicate presence of martensitic microstructure.

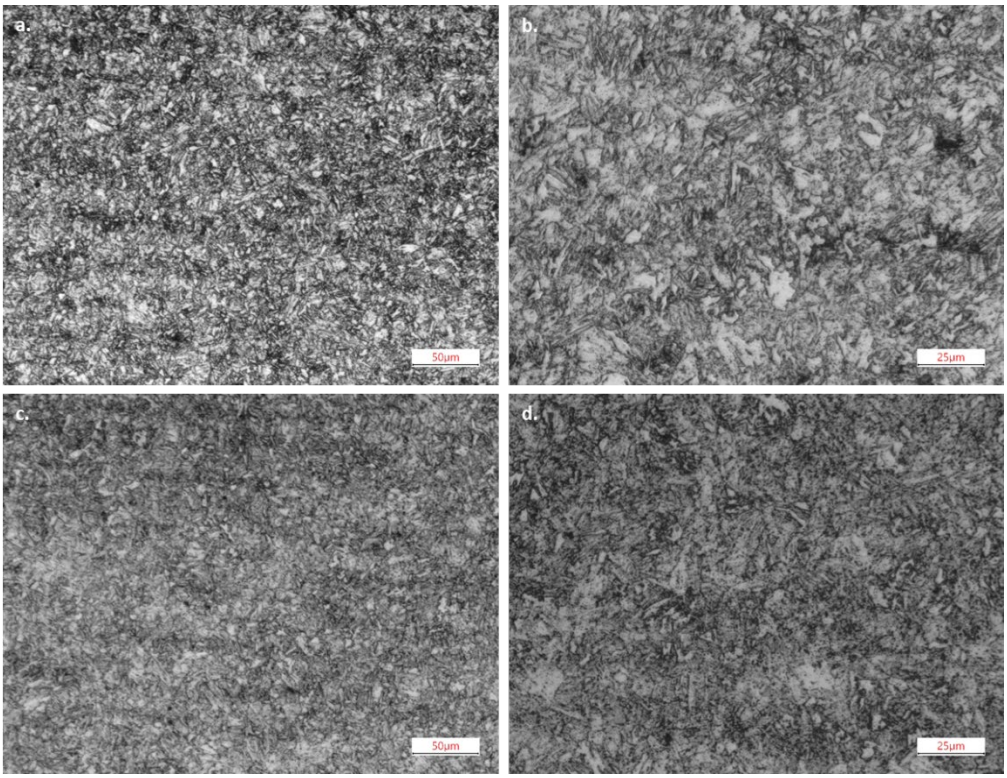

Figure 238: Microstructure Along the Longitudinal Orientation (a, b) and Transverse Orientation (c, d) Taken at 200x (a, c) and 400x (b, d)

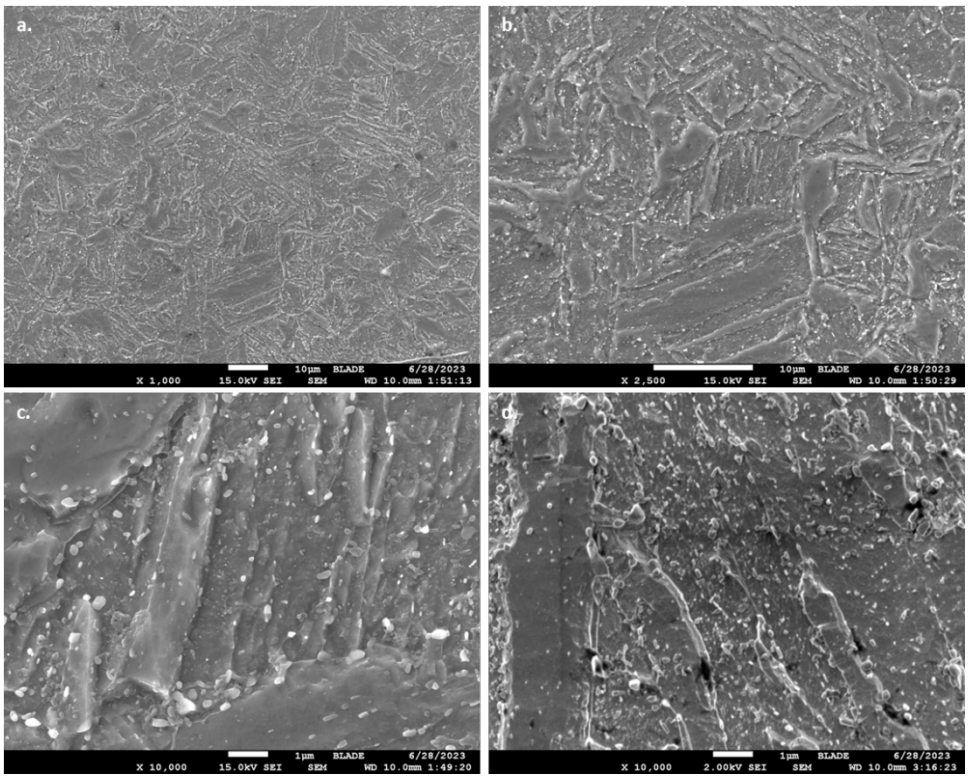

Figure 239: Higher-Magnification SEM Image of N80 Specimen Taken at 15 KV (a, b, c) and 2 KV (d) Accelerating Voltage

A.10.3 Grain Size

To determine the grain size of the 7 in. casing, Element polished the sample for metallography and heat treated the specimens prior to etching with super picral solution (Figure 240). Super picral reacts with the prior austenite grain boundary. The grain size of the prior austenite was determined based on the specifications provided in ASTM E112. The specimens from longitudinal and transverse orientations both have an average grain size equivalent to ASTM No. 9. This means that the average grain diameter is 15.9 µm, and the average grain area is 252 μm^2.

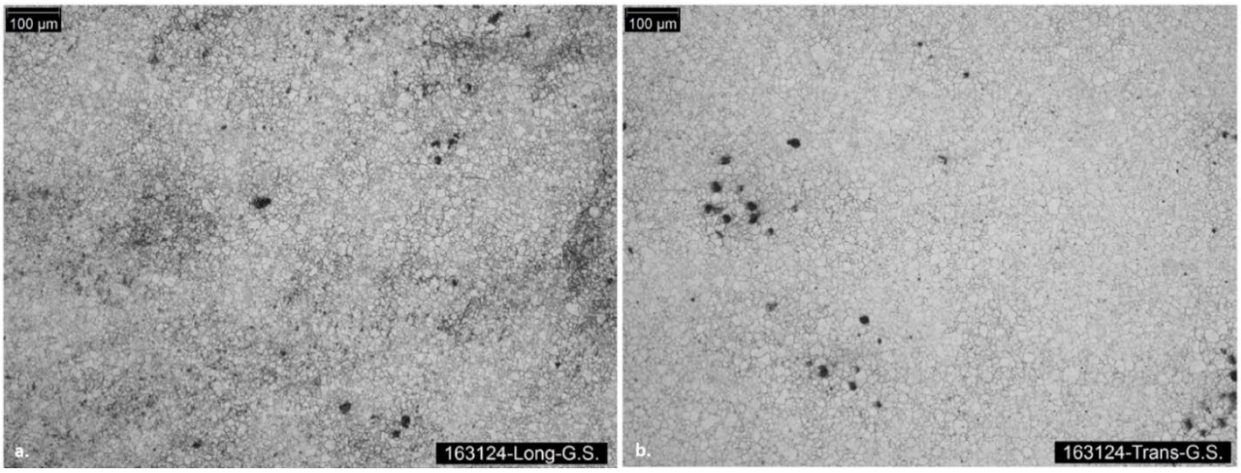

Figure 240: N80 Etched in Super Picral Showing Microstructure Along a. Longitudinal Orientation and b. Transverse Orientation

A.10.4 Hardness

The hardness measurements for the 7 in. casing were performed in accordance with ASTM E92 specification. The Vickers hardness measurements were obtained using a 10 kgf load, and measurements were taken in four quadrants of the 7 in. casing ring. Triplicate measurements were taken near the OD, in the midwall, and near the ID of the sample. The average Vickers hardness number is 230 HVN. Results of the hardness measurements also confirm that the N80 microstructure is not martensite because the hardness values are low compared to reported hardness values of martensite in the literature (approximately 900 to 1,000 HVN).

Table 58: Hardness Measurements Using Vickers 10 kgf Load

	1	2	3	Average (HV)
Quadrant 1				
OD	231	230	232	231
Midwall	230	231	230	230
ID	232	230	231	231
Quadrant 2				
OD	228	228	230	229
Midwall	228	229	228	228
ID	232	228	229	230
Quadrant 3				
OD	230	231	230	230
Midwall	230	231	232	231
ID	231	233	232	232
Quadrant 4				
OD	230	230	230	230

	1	2	3	Average (HV)
Midwall	232	233	231	232
ID	232	230	231	231

Additional hardness measurements were obtained from the metallography samples taken from the longitudinal and transverse orientations. The hardness values were determined using 0.5 kgf load. The values obtained from the metallography samples are slightly lower than the hardness measurements obtained from the 7 in. casing ring; however, the hardness measurements between the specimens are within range (218 to 233).

Table 59: Hardness Measurements Using Vickers 0.5 kgf Load

	1	2	3	Average (HV)
Longitudinal				
OD	218.1	222.4	225.6	222.0
Midwall	224.4	216.3	220.6	220.4
ID	226.3	221.8	225.6	224.6
Transverse				
OD	223.1	224.4	225.6	224.4
Midwall	223.7	231.6	230.2	228.5
ID	225.6	227.6	220.6	225.8

A.10.5 Tensile

Tensile tests were performed in accordance with ASTM A370. Dog bone specimens were taken in the longitudinal and transverse direction of the 7 in. casing. The gauge length of the specimens is 2.0 in. The transverse samples were flattened, but there was no subsequent heat treatment performed after the samples were flattened. The samples were tested in ambient laboratory conditions.

Table 60: Results of Flattening Tensile Test

	0.20% YS (psi)	0.5% EUL (psi)	UTS (psi)	% Elongation
Longitudinal				
1	87,000	87,500	102,000	28.4
2	85,500	85,500	102,000	29.3
3	89,000	88,500	104,000	32.0
Average	**87,167**	**87,167**	**102,667**	**29.9**
Transverse				
1	75,000	76,500	102,000	25.9
2	81,000	76,500	103,000	26.2
3	79,000	80,000	103,000	26.6
Average	**78,333**	**77,667**	**102,667**	**26.2**

Tensile tests were performed using subsize round bar specimens to remove the effects of flattening especially on the transverse direction. These additional tests were completed at Element.

Table 61: Results of Round Bar Tensile Test

	0.20% YS (psi)	0.5% EUL (psi)	UTS (psi)	% Elongation
Longitudinal				
1	89,000	88,500	106,000	25.9
2	90,500	90,500	106,000	25.3
3	90,500	90,500	106,000	24.6
Average	**90,000**	**89,833**	**106,000**	**25.3**
Transverse				
1	89,000	89,000	106,000	22.0
2	90,000	89,500	106,000	21.9
3	90,000	90,000	107,000	23.4
Average	**89,667**	**89,500**	**106,333**	**22.4**

Additional tests were completed using subsize round bar specimens to obtain the critical strain of the N80 material in the longitudinal and transverse orientation. Table 62 lists the results of the tensile test using subsize specimens. There is a slight variation on the yield strength of N80 material when Table 60 is compared to Table 61 and Table 62. This can be due to the flattening procedure performed. The samples were not heat-treated after the flattening procedure was completed. There is minimal difference between the yield and UTS values between Table 61 and Table 62.

Table 62: Results of Critical Strain Determination Using Round Bar Specimen

Specimen	Modulus (psi)	Yield Stress		UTS	Critical Strain		% Elongation	% RIA
		0.2% Yield (psi)	0.5% EUL (psi)		True Strain	True Stress (psi)		
Longitudinal								
643	26,396,784	92,484	93,463	106,705	0.6577	164,687	23.19	70.07
644	29,919,063	92,342	92,438	106,310	0.6522	164,556	22.23	69.67
645	27,107,914	91,844	94,754	105,368	0.6367	161,706	23.31	68.90
Average	**27,807,920**	**92,224**	**93,552**	**106,128**	**0.6489**	**163,649**	**22.91**	**69.55**
Transverse								
648	32,678,300	92,129	92,213	105,644	0.5584	156,098	24.22	63.80
649	29,303,221	90,381	90,392	105,489	0.5581	155,934	22.82	63.67
650	35,645,324	92,229	92,333	105,807	0.5584	157,024	22.68	63.35
Average	**32,542,282**	**91,580**	**91,646**	**105,647**	**0.5583**	**156,352**	**23.24**	**63.61**

A.10.6 Impact Testing

The goals of impact testing are to determine the amount of energy absorbed during fracture of a standard specimen and to determine the ductile brittle transition temperature (DBTT). A third-party laboratory (Element) conducted impact testing on C001 joint extracted from well #2244. Impact testing was performed at various temperatures to obtain the DBTT. The Charpy V-notch method was employed in accordance with ASTM E23 [63]. The striker radius was 8mm.

The specimens for impact testing were obtained from C001B-2E. Because the nominal thickness of the 7 in. casing is only 0.362 in. (9.2 mm), the Charpy specimens need to be half-size. Charpy specimen dimensions are 10 mm x 5 mm with a 2 mm notch. Figure 241 shows the full-size dimension and the half-size dimension of Charpy specimens. Figure 242 shows the nomenclature for specimen orientation based on ASTM E1823 [64] (fracture mechanics) and API 5CT [65] (CVN for tubulars). Transverse and longitudinal Charpy orientations from API 5CT [65] correspond with the C-L and L-C ASTM E1823 [64] orientations, respectively.

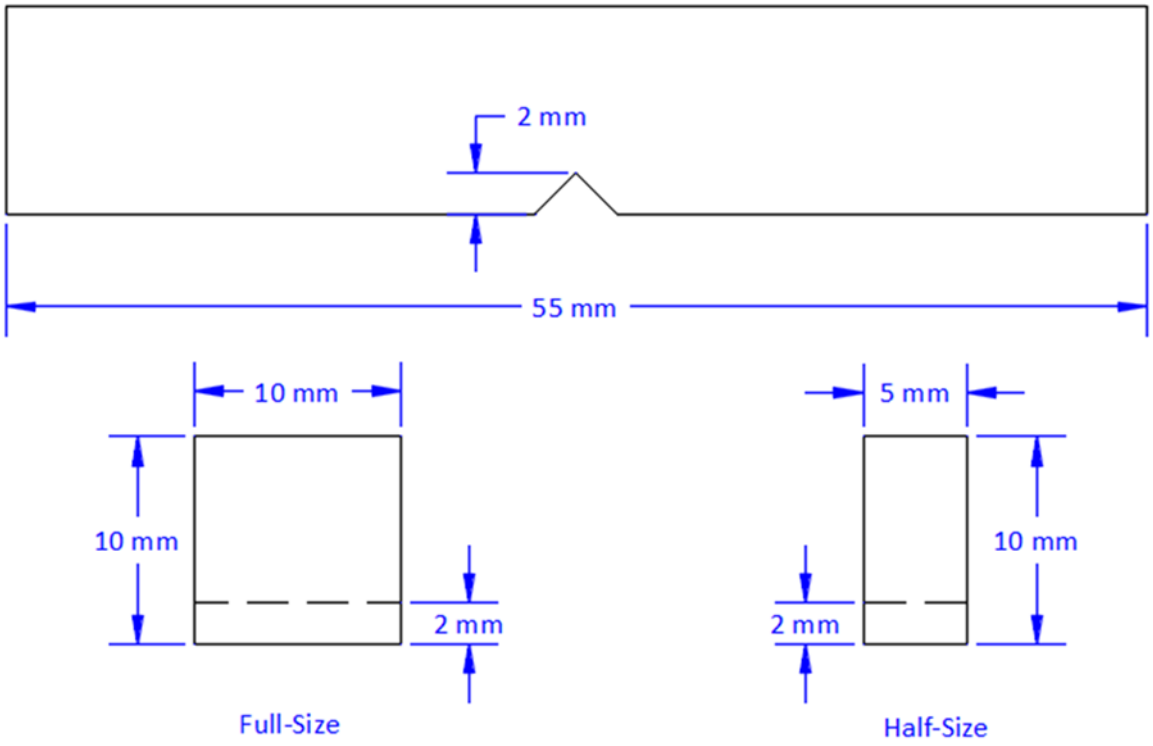

Figure 241: ASTM E23 CVN Specimen Dimensions

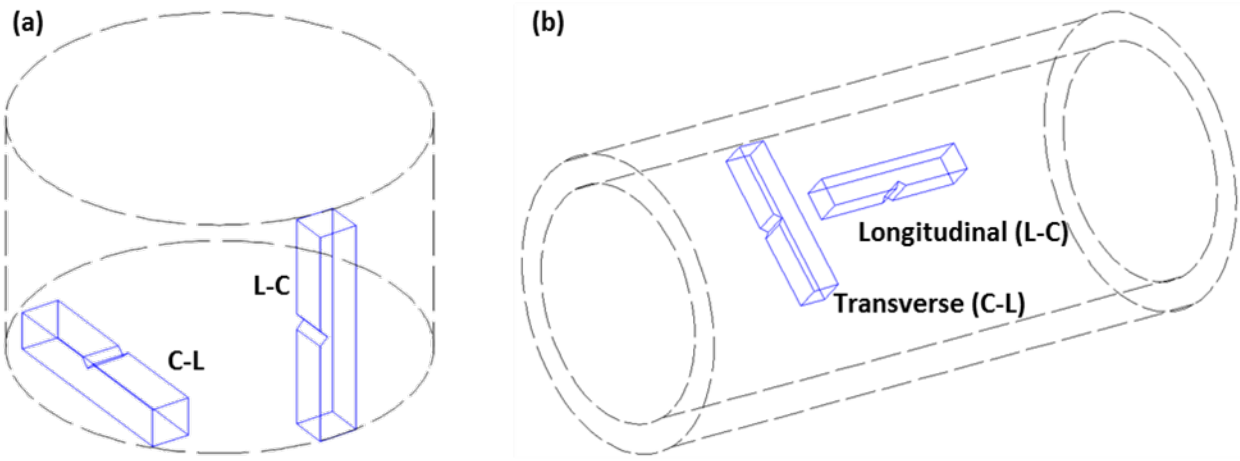

Figure 242: (a) ASTM E1823 Crack Plane Orientation [64] and (b) API 5CT CVN Orientations [65]

All the reported values herein are obtained using half-size specimens. No further conversion was obtained. Figure 243 shows the curve fit for the DBTT using specimens obtained from longitudinal and transverse orientations. The estimated DBTT for the longitudinal orientation using half-size specimen is –84°C (–119°F), and the estimated DBTT for the transverse orientation using half-size specimen is –70°C (–96°F). The half-size toughness values at 0°C (32°F) are 50 ft-lb and 30.3 ft-lb for longitudinal orientation and transverse orientation, respectively. This indicates that at the estimated failure temperature of 40°F, the failure will occur in a ductile manner.

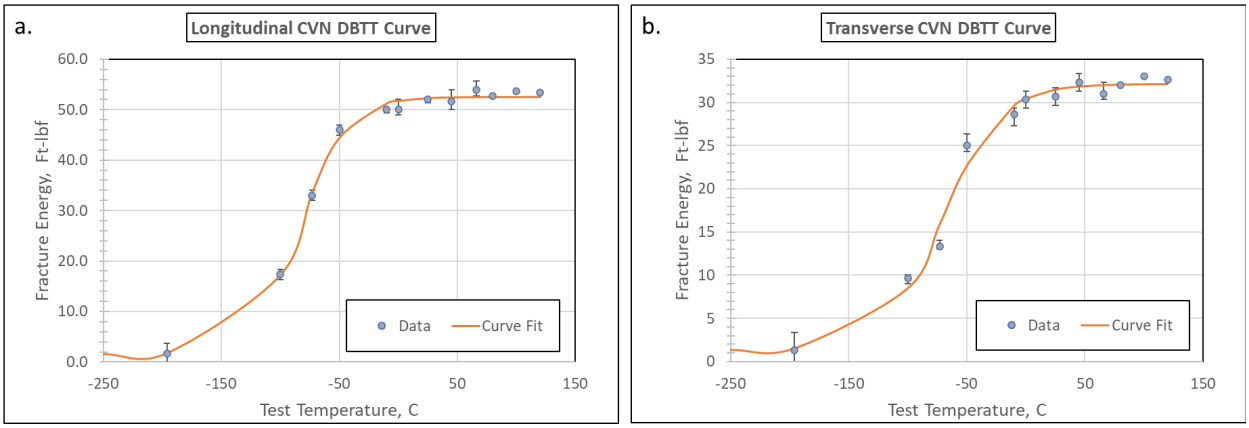

Figure 243: Ductile Brittle Transition Temperature Curve Using Fracture Energy Values of Half-Size a. Longitudinal and b. Transverse Specimens

Table 63: Toughness Values at Various Impact Temperatures

Temp. (°C)	Temp. (°F)	Longitudinal Energy Absorbed (ft-lb)			Longitudinal Average (ft-lb)	Transverse Energy Absorbed (ft-lb)			Transverse Average (ft-lb)
–196	–321	1	2	2	1.7	2	1	1	1.3
–100	–148	22	16	14	17.3	10	10	9	9.7
–73	–99	29	39	31	33.0	14	12	14	13.3

Temp. (°C)	Temp. (°F)	Longitudinal Energy Absorbed (ft-lb)			Longitudinal Average (ft-lb)	Transverse Energy Absorbed (ft-lb)			Transverse Average (ft-lb)
–50	–58	44	46	48	46.0	25	27	23	25.0
–10	14	50	49	51	50.0	29	29	28	28.7
0	32	49	51	50	50.0	30	30	31	30.3
25	77	53	52	51	52.0	30	32	30	30.7
45	113	52	51	52	51.7	33	31	33	32.3
66	150	56	53	53	54.0	31	32	30	31.0
80	176	53	52	53	52.7	32	33	31	32.0
100	212	52	53	56	53.7	34	33	32	33.0
120	248	55	52	53	53.3	34	32	32	32.7

The percent shear for the longitudinal and transverse Charpy specimens are plotted in Figure 244. The blue dots are the plotted values from Charpy impact testing listed in Figure 243. The orange curve was obtained by curve fitting. The estimated DBTT using the percent shear values are –89.5°C (–129°F) and –71.1°C (–94°F) for longitudinal and transverse orientation, respectively. These values are not far from the estimated DBTT from the fracture energy values. From the values listed in Figure 244, the temperature at which 50% shear occur is between –73 and –100°C for longitudinal orientation, and approximately –73°C for transverse orientation.

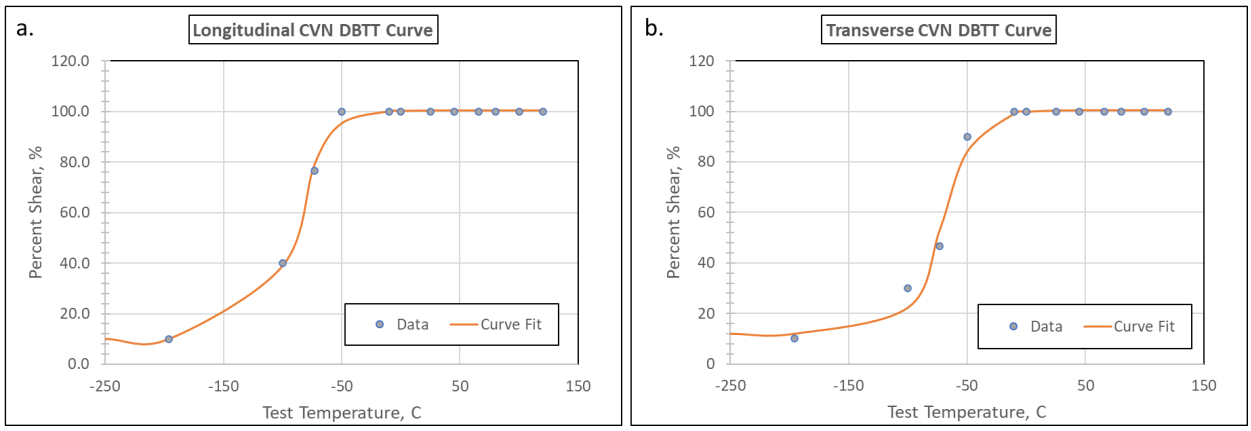

Figure 244: Ductile Brittle Transition Temperature Curve Using Percent Shear Values of Half-Size a. Longitudinal and b. Transverse Specimens

Table 64: Percent Shear at Various Impact Temperatures

Temp. (°C)	Temp. (°F)	Longitudinal % Shear			Longitudinal Average % Shear	Transverse % Shear			Transverse Average % Shear
–196	–321	10	10	10	10.0	10	10	10	10.0
–100	–148	50	40	30	40.0	30	30	30	30.0
–73	–99	70	90	70	76.7	50	40	50	46.7

Temp. (°C)	Temp. (°F)	Longitudinal % Shear			Longitudinal Average % Shear	Transverse % Shear			Transverse Average % Shear
–50	–58	100	100	100	100.0	90	90	90	90.0
–10	14	100	100	100	100.0	100	100	100	100.0
0	32	100	100	100	100.0	100	100	100	100.0
25	77	100	100	100	100.0	100	100	100	100.0
45	113	100	100	100	100.0	100	100	100	100.0
66	150	100	100	100	100.0	100	100	100	100.0
80	176	100	100	100	100.0	100	100	100	100.0
100	212	100	100	100	100.0	100	100	100	100.0
120	248	100	100	100	100.0	100	100	100	100.0

A.10.7 Fracture Toughness

K_{IC} and J_{IC} are quantitative measurements of a material's resistance to cracking. K_{IC} is a fracture parameter used when a material behaves in a linear elastic manner prior to failure. The plastic zone ahead of a crack must remain small when compared to specimen dimensions for K_{IC} to be valid. K_{IC} represents the critical point of unstable crack growth under Mode I loading [66]. J_{IC} is a fracture parameter that accounts for elastic-plastic material behavior. J_{IC} is determined by the resistance curve of a material. Most ductile materials exhibit a rising resistance curve. This means that the resistance of a material to crack propagation increases with crack growth. The crack driving force also increases with crack growth. J_{IC} is the initiation toughness near the onset of stable crack growth [67].

Fracture toughness was determined using single-edge notch bend (SENB) specimens in L-C orientation (see Figure 245). The goal of fracture toughness testing is to determine the instability of circumferential parting. The L-C oriented specimens were used in the tests, where loading is along the longitudinal direction and cracking is along the circumferential direction. Figure 245 shows the dimensions of the specimen used in the tests. The notch in SENB specimens is in the circumferential orientation. The tests to obtain the J-da (J-R test) were conducted in accordance with ASTM E1820 [16].

Blade conducted the fracture toughness testing at Element. The tests were performed at ambient laboratory condition and at 40°F in triplicates. For the ambient temperature testing, only two replicates are valid. Figure 246 shows the J-R curves for the valid tests. Table 65 lists the results of the valid fracture toughness tests. Because the specimens did not fail by cleavage, the values of J_Q and K_Q that were measured at the last unloading were taken and qualified as J_{IC} and K_{IC}, respectively. The average K_{IC} value was used for crack instability analysis.

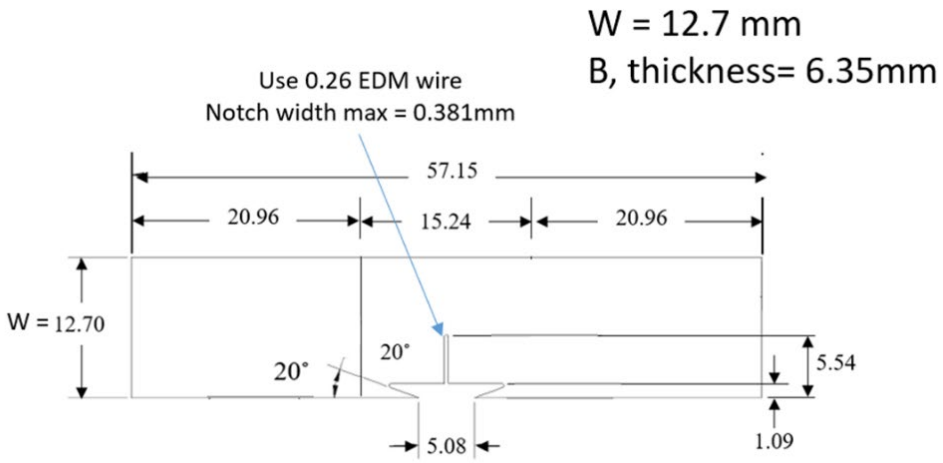

Figure 245: Dimensions of the SENB Specimens Used in the Fracture Toughness Test

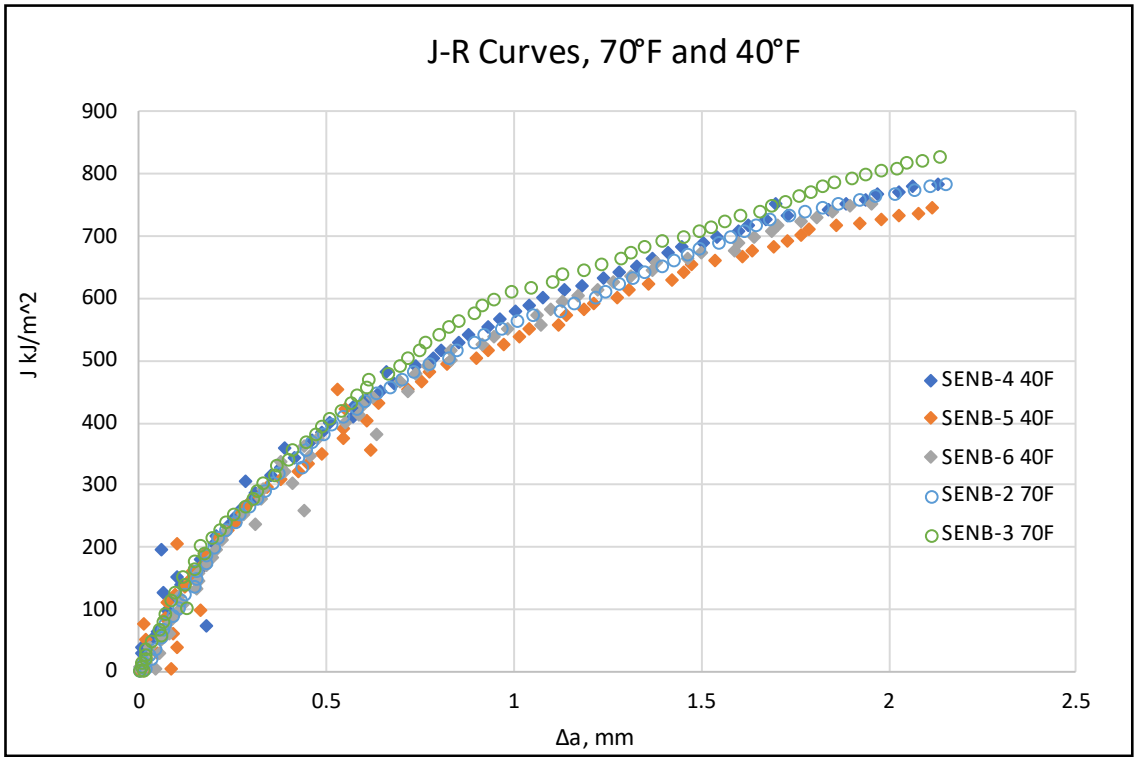

Figure 246: J-R Curves for the Tests Performed at 70°F and 40°F

Table 65: Fracture Toughness Results Summary

Sample	Temperature	Plane Strain, J_Q, KJ/m² (ksi.in.)	Stress Intensity Factor, K_Q, MPa√m (ksi√in.)
SENB 2	70°F	377 (2.15)	293 (267)
SENB 3	70°F	402 (2.30)	302 (275)

Sample	Temperature	Plane Strain, J_Q, KJ/m^2 (ksi.in.)	Stress Intensity Factor, K_Q, MPa√m (ksi√in.)
Average	**70˚F**	**390 (2.23)**	**298 (271)**
SENB 4	40°F	383 (2.19)	295 (269)
SENB 5	40°F	354 (2.02)	284 (258)
SENB 6	40°F	341 (1.95)	278 (253)
Average	**40˚F**	**359 (2.05)**	**286 (260)**

A.11 Exponent Report

Exponent®

Conceptual Site Model

Subsurface Storage Gas Migration and Fate Following the Rager Mountain Gas Leak Incident

Tarek Saba, Ph.D.
Kathryn Murdock, Ph.D.
Brun Hilbert, Ph.D.

Exponent®

Conceptual Site Model

Subsurface Storage Gas Migration and Fate Following the Rager Mountain Gas Leak Incident

Tarek Saba, Ph.D.
Kathryn Murdock, Ph.D.
Brun Hilbert, Ph.D.

August 23, 2023

© Exponent, Inc.

Table of Contents

		Page
List of Figures		**ii**
Acronyms and Abbreviations		**iii**
1	**Introduction and Objective**	**1**
2	**Conceptual Site Model Summary**	**3**
3	**Geology**	**7**
3.1	Summary	7
3.2	Facility Geology	8
3.3	Balltown and Speechley Sandstones	9
4	**Well Casing Gas Pressures and Isotope Analysis Results**	**11**
4.1	Background: Stable Isotope Analysis	11
4.2	Production Casing (i.e., Wellhead) Gas Isotope Results	12
4.2.1	Field wells production casings gas is storage gas	12
4.2.2	In Obs. Well 2247, production casing gas is composed of field gas different from storage gas, while in Obs. Well 2246, production casing gas appears to be a mix of storage gas and other field gas	13
4.3	Vent Gas Isotope Results	15
5	**Residential Water Wells and Soil Survey to Investigate the Presence of Gases**	**23**
5.1	Residential Property Water Well Sampling and Results	23
5.2	Soil Gas Screening and Results	23

Attachment 1 – Residential Area and Cramer Highway Sample Locations and Analysis Results

List of Figures

		Page
Figure 1.	Rager Mountain gas storage field well locations.	2
Figure 2.	CSM for the transport and fate of subsurface storage gas.	6
Figure 3.	Geologic cross section of the Facility.	8
Figure 4.	Rager Field wellhead gases have consistent isotopic signature (i.e., C_1, C_2, and C_3).	13
Figure 5.	Obs. Well 2247 production casing contains gas different from the field storage gas.	14
Figure 6.	Obs. Well 2246 production casing contains gas that appears to be a mix of storage gas and the gas found in the production casing of Obs. Well 2247.	15
Figure 7.	Obs. Well 2247 gas isotope results indicates the presence of storage gas in the vent, albeit at low pressures, consistent with less discontinuous and less distinct Balltown and Speechley sandstone formations moving father to the north from Field Well 2244.	16
Figure 8.	Field Well 2249 gas isotope results indicate the presence of storage gas in the vent mixed with other native gases. Storage gas likely migrated through the Balltown and Speechley sandstone layers present between Field Wells 2244 and 2249.	17
Figure 9.	Field Well 2251 vent gas and production casing storage gas are an isotopic match.	18
Figure 10.	Field Well 2248 vent and production casing gases are storage gas.	19
Figure 11.	Field Well 2248 noise log results from December 19, 2022, demonstrating potential migration pathway at 3,000 ft, consistent with the geology information regarding the Balltown and Speechley interbedded sandstone layers (Source: EQTRNS).	20
Figure 12.	Field Well 2248 noise log results from April 25, 2023, demonstrating a potential migration pathway at 3,000 ft, consistent with the geology information regarding the Balltown and Speechley interbedded sandstone layers (Source: EQTRNS).	21
Figure 13.	Field Wells 2245 and 2255 and Obs. Well 2246 vent gases are different from storage gas.	22

Acronyms and Abbreviations

API	American Petroleum Institute
bgs	below ground surface
C_1	carbon isotope in methane
C_2	carbon isotope in ethane
C_3	carbon isotope in propane
CSM	conceptual site model
EQTRNS	Equitrans Midstream Corporation
Facility	The Rager Mountain gas storage facility located in Jackson Township, Pennsylvania.
ft	feet
mg/L	milligrams per liter
Obs. Well	observation well
psi	pounds per square inch

1 Introduction and Objective

The Rager Mountain gas storage facility (hereafter, the Facility) is located in Jackson Township, Pennsylvania. Equitrans Midstream Corporation (EQTRNS) owns and operates the Facility. Natural gas (i.e., Marcellus gas) is injected into and withdrawn from field gas wells for the purpose of storage and extraction in a formation located approximately 7,000 feet (ft) below ground surface (bgs) (*see* Figure 1 for the Facility and field gas well locations). On November 6, 2022, a well casing failure and uncontrolled storage gas flow occurred at Field Well 2244. As a result of the incident, part of the uncontrolled storage gas flow is believed to have escaped into subsurface formations where it migrated and entered some of the surrounding field wells and potentially entered field observation wells (obs. wells) located north and south of the Facility (*see* Figure 1).

The incident prompted several investigations and analysis of existing data and information, such as:

- Collection of gas samples from field well and obs. well production casings and annuli casings for gas composition and isotope analysis to determine the types of gases present at the sampled well locations (e.g., storage gas, native gases, mixtures of gases).
- Pressure monitoring of annuli and production casing pressures to determine whether there is a migrating gas front.
- Well casing logs (e.g., noise, temperature, neutron, gamma logs).
- Soil screening and residential water well sampling at several locations (e.g., residential properties, soil along Cramer Pike [Highway 403]) to determine whether there are migrating gases in soils or water wells.

Exponent experts (Drs. Tarek Saba, Kathryn Murdock, and Brun Hilbert) were retained by EQTRNS to analyze available gas isotope data, geology information, and information related to mechanical integrity. The purpose of the analysis was to develop a conceptual site model (CSM) of the transport and fate of storage gas potentially present in the subsurface that resulted from the incident on November 6, 2022.

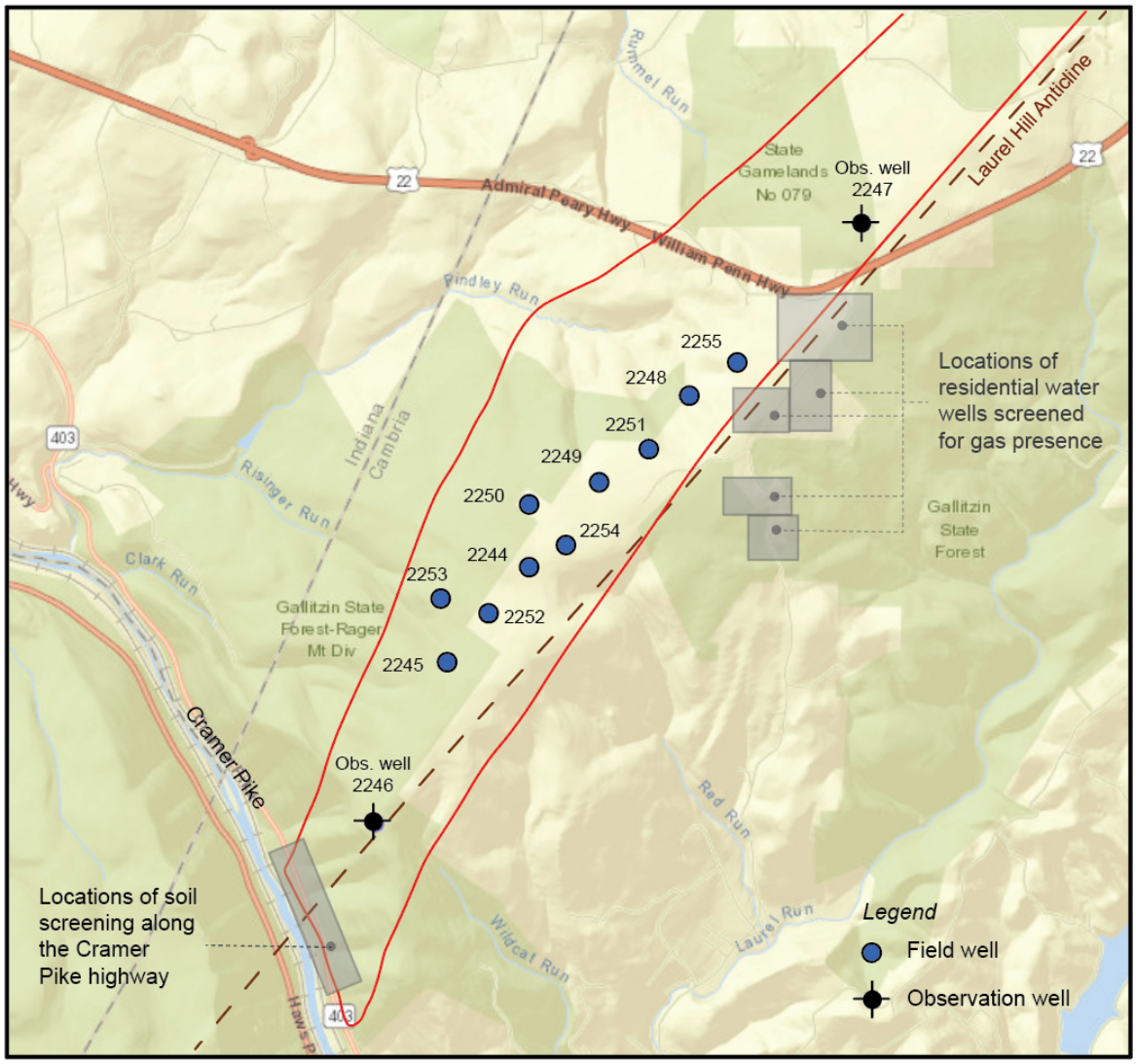

Figure 1. Rager Mountain gas storage field well locations.

2 Conceptual Site Model Summary

Figure 2 presents a cross section depicting the transport and fate of subsurface storage gas, based on multiple lines of evidence, including:

Geology Well logs indicate the presence of an interbedded sandstone and shale layers (Balltown and Speechley) that are most clear around Field Well 2244 at a depth of approximately 3,000 ft and become more discontinuous and less distinct as one moves father to the north and south of the well. The interbedded sandstone/shale layers are believed to have the ability to provide a migration pathway for the subsurface storage gas to transport to the north and south of Field Well 2244 (consistent with noise logs), albeit at low volumes with increasing distance from the well.

Gas Isotope Production casing gas samples subjected to isotope analysis demonstrated the presence of storage gas in all the field well casings, consistent with the fact that the production casings are directly connected to the storage field formation (Field wells 2245, 2252, 2254, 2249, 2251, and 2255). The Obs. Well 2247 production casing contains field gas different from storage gas, while Obs. Well 2246 appears to contain a mix of storage gas and other field gas.

Annuli (vent) gases resembled storage gas in wells located north of Field Well 2244 (with the exception of Field Well 2255) and were a mix of gases in wells located south of Feld Well 2244.

Gas Pressure Starting on May 23, 2023, annuli casings were left open for all wells except Field Well 2255 and Obs. Wells 2246 and 2247. The purpose was to monitor pressure build up in the closed annuli under a steady state condition. At the most northern well (Obs. Well 2247), vent gas pressure appeared to be steady or slowly increasing with time, consistent with the presence of discontinuous and less distinct interbedded sandstone/shale layers to the north of Field Well 2244. In the most southern well (Obs. Well 2246), vent gas pressure build up was at a

faster rate, reaching approximately 200 pound per square inch (psi) in July 2023. The vent gases in Obs. Well 2246 (and the other wells south of Field Well 2244), however, are a mix of gases, as opposed to storage gas, indicating that subsurface storage gas migration to the south increased native gas pressures.

Well Logs Noise logs at Field Wells 2244 and 2248, indicate the presence of gas at a depth of approximately 3,000 ft, consistent with the geology information regarding the presence of the Balltown and Speechley interbedded sandstone/shale layers at the same depth range.

Mechanical The well integrity analysis indicated casing or bridge plug issues, or both, at two field wells:

For Field Well 2251, it appears that the three retrievable bridge plugs installed at approximately 7,500 ft are leaking, and storage gas is escaping to the production casing. In addition, it appears the production casing is in communication with the annulus casing, consistent with the synchronized gas pressure in the production and annulus casing. In coordination with Exponent, EQTRNS has been addressing this issue.

For Field Well 2248, it appears that subsurface storage gas has migrated into the annulus space, as evidenced by the presence of storage gas in the vent gas. In addition, it appears that storage gas has migrated from the annulus space into the production casing, as evidenced by the synchronized higher vent gas pressure and the gas pressure in the production casing. Exponent has been working with EQTRNS to ensure that Field Well 2248 will be in a good working condition.

Overall, it appears that subsurface storage gas has migrated to the north at low volumes, as evidenced by the discontinuous and less distinct interbedded sandstone/shale layers, and the presence of storage gas at low pressures in Obs. Well 2247 vent gas.

Activities in areas adjacent to the Facility included:

- Sampling of 24 water wells in 23 different residential properties for dissolved gas (*see* Figure 2). Dissolved gas was not found in any of the wells (i.e., the maximum dissolved gas concentrations was 0.016 milligrams per liter [mg/L], over two orders of magnitude lower than the Pennsylvania action level of 7 mg/L).
- Conducting a soil gas survey of the 23 different residential properties, which found no gas in the soil.
- Screening soil gas south of the storage field, along Cramer Pike (Highway 403), which found no gas.

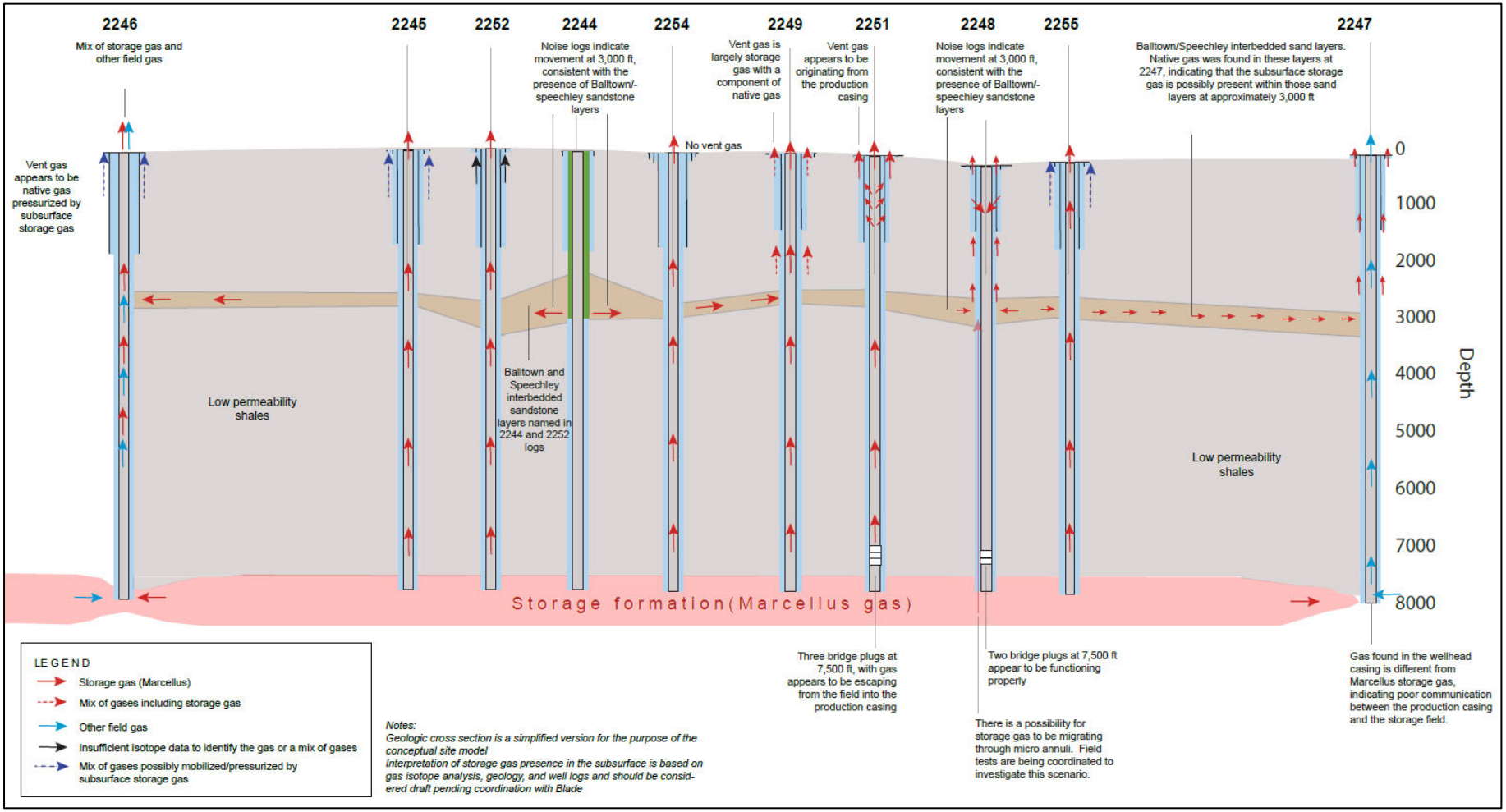

Figure 2. CSM for the transport and fate of subsurface storage gas.

3 Geology

3.1 Summary

Geologic information used for the CSM was derived from well drilling field notes, well completion records, and gamma ray logs where available. Additional information regarding the nature of subsurface geological formation and characteristics of various lithological formations was used to supplement the available data.

While surficial rocks are sandy in nature, most of the geologic formations in the Facility area are low permeability shales or contain significant amounts of shales. Sandstone layers, called Balltown and Speechley sandstones, were identified in Field Wells 2244 and 2252, and they represent the clearest sandstones in the Facility area, based on the gamma ray logs and well log descriptions. The Balltown and Speechley sandstones could allow for subsurface gas migration because of their relatively higher permeability compared to shales. The Balltown and Speechley sandstone layers are found at about 3,000 ft bgs in both Field Wells 2244 and 2252, and using the gamma logs, can be traced north and south at approximately the same depth. Gamma logs indicate the sandstone layers become highly interbedded with shale to the north and south from Field Wells 2244 and 2252, which would likely provide less pathways for subsurface gas to move at that depth.

Historical well logs indicate the presence of native gas in Obs. Well 2247 at 2,895 ft bgs, at approximately the depth of the Balltown and Speechley layers. Notably, there was no indication of upward migration of the native gas through the overlying rock, suggesting the shales found above the sandstone layer are relatively impermeable. Below are additional details.

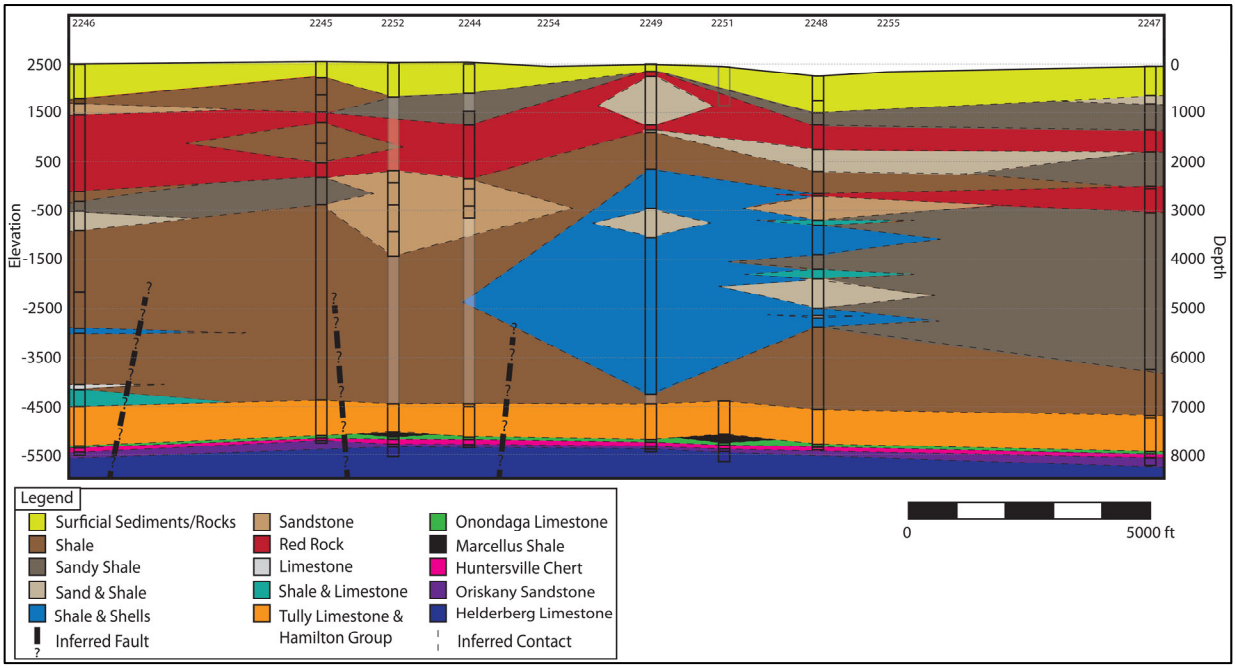

Figure 3. Geologic cross section of the Facility.

3.2 Facility Geology

The Facility geology is a series of sandstones and shales down to a depth of approximately 7,000 ft bgs. At or around 7,000 ft bgs, Tully Limestone is identified in well logs, followed by the Marcellus Shale or Hamilton Group, Onondaga Formation, Huntersville Chert, Oriskany Sandstone, and finally the Helderberg Limestone Group at or around 8,000 ft bgs. Originally, the field gas wells were drilled with the purpose of achieving the target formations below the Tully Limestone, therefore the majority of the available records focused on identifying lithological changes below 6,000 ft bgs.

Some of the well logs indicate the formations above the original target depths, and these include "Big Lime" and "Big Injun"—now identified as part of the Greenbrier and Pocono Formations, respectively[1]—as well as Murrysville sandstone, Speechley sandstone, Balltown sandstone, and

[1] Brezinski, D. K., 1999. Part II, Stratigraphy and Sedimentary Tectonics, Chapter 9: Mississippian, in Shultz, C. H. (ed.), The Geology of Pennsylvania: Pennsylvania Bureau of Topographic and Geologic Survey Special Publication 1, pp. 138-147.

Bradford sandstone. Most of the formation names used in the well logs are informal drillers' names and can be correlated to formal named geologic units or portions of those units.

Descriptions of geologic units vary greatly across the state, and with the addition of informal drillers' names, the correlations become more complex. The depth of interest based on the noise logs for the wells is generally around 3,000 ft bgs. Based on the well logs, this corresponds to a series of sandstones and shales that are highly interbedded to the north, with thicker sections of sandstone towards the middle of the storage field that become interbedded again in the southern section. This is confirmed with the gamma ray logs from each of the wells. Studies of gamma ray logs in similar stratigraphy as that found near Rager Mountain have shown sandstones are usually indicative of counts less than an American Petroleum Institute (API) value of 80, and shales greater than 80 API.[2]

3.3 Balltown and Speechley Sandstones

At 2,385 ft, Field Well 2244 logs name the Speechley sandstone.[3] At 2,500 and 2,900 ft bgs, Field Wells 2244 and 2252 specifically name the Balltown and Bradford sandstones, respectively.[4,5] The Balltown and Speechley sandstones are of particular interest because they have been shown to be shallow reservoirs for gas, and were noted in Obs. Well 2247.[6,7,8] The Balltown and Speechley sandstones are part of the Bradford Group.[9] Both sandstones are

---

2 Coughlin, M. F., 2009. "Subsurface mapping and reservoir analysis of the Upper Devonian Venango and Bradford groups in Westmoreland County, Pennsylvania." *Graduate Theses, Dissertations, and Problem Reports*, West Virginia University, 4452.

3 2244 well pocket scan 8.

4 2244 well pocket scan 8.

5 2252 well pocket scan 4.

6 Coughlin, M. F., 2009. "Subsurface mapping and reservoir analysis of the Upper Devonian Venango and Bradford groups in Westmoreland County, Pennsylvania." *Graduate Theses, Dissertations, and Problem Reports*, West Virginia University, 4452.

7 Behling, M. C., S. Pool, D. G. Patchen, and J. A. Harper, 2008. "Improving the Availability and Delivery of Critical Information for Tight Gas Resource Development in the Appalachian Basin." West Virginia University Research Corporation.

8 2247 well pocket scan 7.

9 Coughlin, M. F., 2009. "Subsurface mapping and reservoir analysis of the Upper Devonian Venango and Bradford groups in Westmoreland County, Pennsylvania." *Graduate Theses, Dissertations, and Problem Reports*, West Virginia University, 4452.

described as lenticular in shape; Balltown is slightly more continuous over larger areas than the shallower Speechley above it. Above the Balltown and Speechley layers is “Red Rock,” which is likely the red beds of the Catskill formation—a highly interbedded shale and siltstone. Below the Balltown and Speechley layers, the well logs identify mostly shale, with some limestone or shells. Overall, the Balltown and Speechley sandstone layers in Field Wells 2244 and 2252, and the interbedded sand reservoir in Obs. Wells 2246 and 2247 appear sandwiched between less permeable layers located above 2,000 ft bgs and below 3,500 ft bgs.

4 Well Casing Gas Pressures and Isotope Analysis Results

In January and May 2023, EQTRNS sampled gases found in the production and annuli (i.e., vent gas) casings of the field wells and the two obs. wells located to the north and south of the field. The gas samples were analyzed for composition and isotope analyses. The purpose of the analyses was to identify the type of gases present in the casings, whether it was storage gas, native gas, or a mixture of gases. Below is a discussion of the gas sampling data.

4.1 Background: Stable Isotope Analysis

Most elements (e.g., carbon) occur in nature as mixtures of stable isotope forms. For example, most carbon atoms (approximately 99% of carbons) are called carbon 12 (^{12}C), which has 6 electrons, and a nucleus containing 6 protons and 6 neutrons (hence the name carbon 12). The remaining approximately 1% of all carbon atoms are called carbon 13 (^{13}C isotope) and have one extra neutron in the nucleus (total of 7 neutrons and 6 protons). ^{13}C is therefore "heavier" than ^{12}C. The ratio of one isotope to another varies according to the source organic matter from which the methane gas is formed. As such, the ratio of ^{13}C/^{12}C has been proven to be an effective discriminator in identifying natural gases (i.e., methane, ethane, propane) from different sources (e.g., Coleman 1994;[10] Hoefs 1997;[11] Saba and Boehm 2012[12]).

Stable-isotope data are expressed as the ratio (^{13}C/^{12}C) in a sample compared to a standard. For example, the stable carbon isotope of methane in a gas sample compared to a standard is calculated as:

$$\delta^{13}C_1(in\ per\ mil\ or\ ‰, one\ part\ per\ thousand) = \frac{\left[\left(^{13}C/^{12}C\right)_{gas\ sample} - \left(^{13}C/^{12}C\right)_{standard}\right]}{\left(^{13}C/^{12}C\right)_{standard}}$$

[10] Coleman, D. 1994. "Advances in the use of geochemical fingerprinting for gas identification." Presented at the American Gas Association Operations Conference, San Francisco, CA. May 9-11.

[11] Hoefs, J. "Stable isotope geochemistry," 4th ed. Berlin, Springer-Verlag, 1997, 201 p.

[12] Saba T, Boehm PD. 2012. Use of natural gas compositional tracers to investigate gas migration from a storage field. Environmental geosciences, V. 19., No. 2. pp. 63-74. June.

In the gas isotope analysis below, the focus is on carbon isotope in methane ($\delta^{13}C_1$), ethane ($\delta^{13}C_2$), and propane ($\delta^{13}C_3$).

4.2 Production Casing (i.e., Wellhead) Gas Isotope Results

4.2.1 Field wells production casings gas is storage gas

Based on the gas isotope analysis, the gas present in field production casings is storage gas (i.e., Field Wells 2245, 2252, 2254, 2249, 2251, 2248, and 2255) (*see* Figure 4), as evidenced by:

- The consistent values of $\delta^{13}C_1$, $\delta^{13}C_2$, and $\delta^{13}C_3$ in the gas samples over the two gas sampling periods, and
- The similarity of the isotopic pattern with Marcellus gas (i.e., note the slight isotopic reversal in the C_1 compared to C_2).[13]

The presence of storage gas in the production casings is expected, considering the field cyclic operations of injection and withdrawal of Marcellus storage gas.

[13] Isotope reversal is indicated where $\delta^{13}C_1$ is heavier (less negative) than $\delta^{13}C_2$ in the same gas sample. The presence of a reversal in the storage gas sample is a characteristic of Marcellus gas.

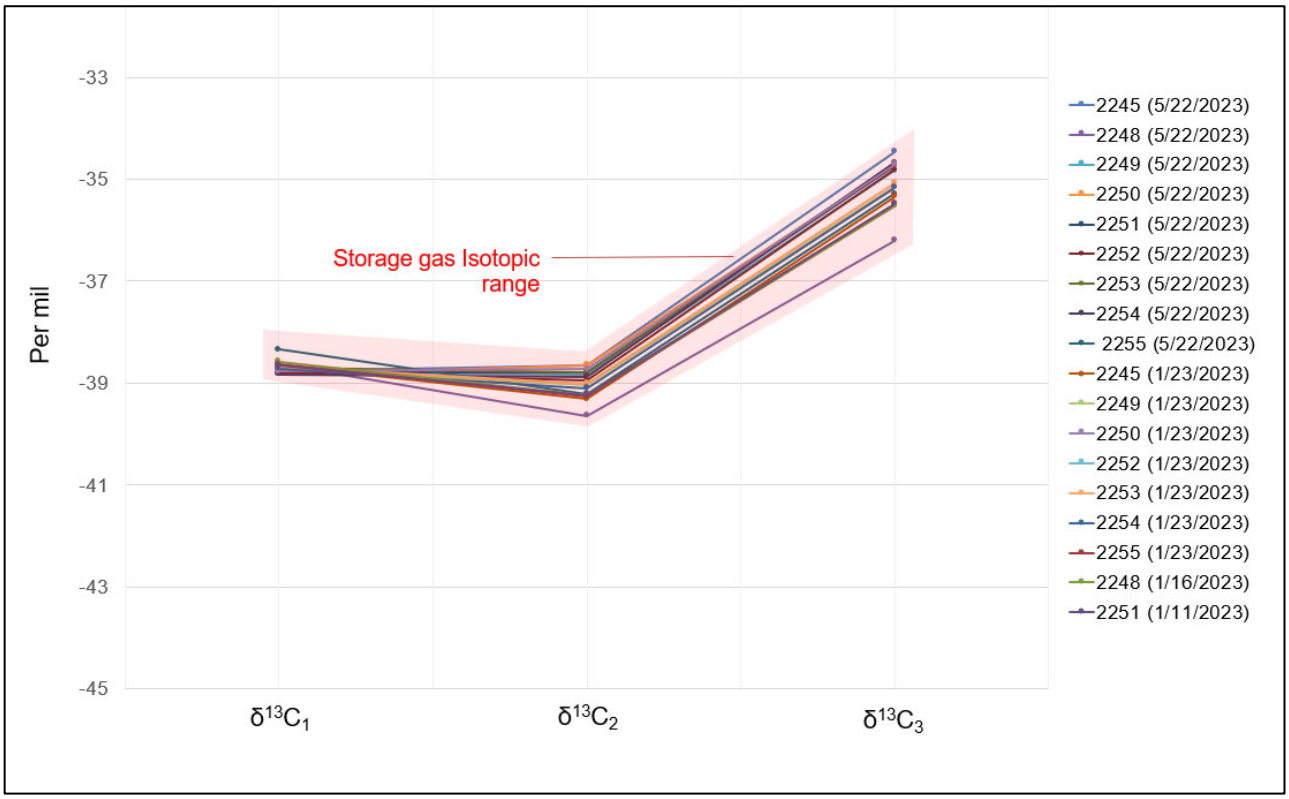

Figure 4. Rager Field wellhead gases have consistent isotopic signature (i.e., C_1, C_2, and C_3).

4.2.2 In Obs. Well 2247, production casing gas is composed of field gas different from storage gas, while in Obs. Well 2246, production casing gas appears to be a mix of storage gas and other field gas.

Obs. Well 2247: Located north of the Rager Field, the production casing gas was different from storage gas, indicating that the production casing is not in clear communication with the storage field formation—possibly a reflection of the field pinching out at that location. The origin of Obs. Well 2247 production gas is possibly field gas from the same storage field formation depth. Production casing gas pressure was approximately 2,050 psi as of July 22, 2023 (*see* Figure 5).

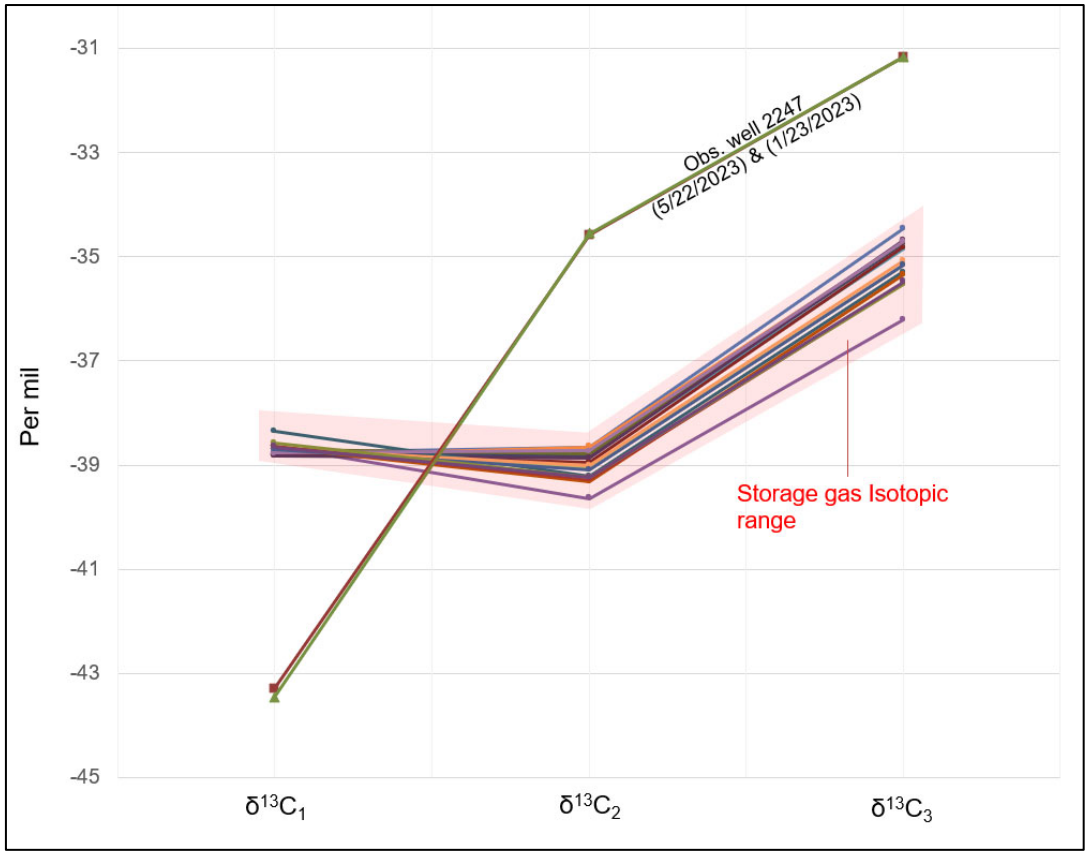

Figure 5. Obs. Well 2247 production casing contains gas different from the field storage gas.

Obs. Well 2246: Located south of the Rager Field, the production casing gas appears to be a mix of storage gas and the other field gas found in Obs. Well 2247. Comparing the two obs. wells together, it appears that Obs. Well 2246 has better communication with the storage field formation than Obs. Well 2247. Gas pressure in Obs. Well 2246 production casing was approximately 1,910 psi as of July 22, 2023.

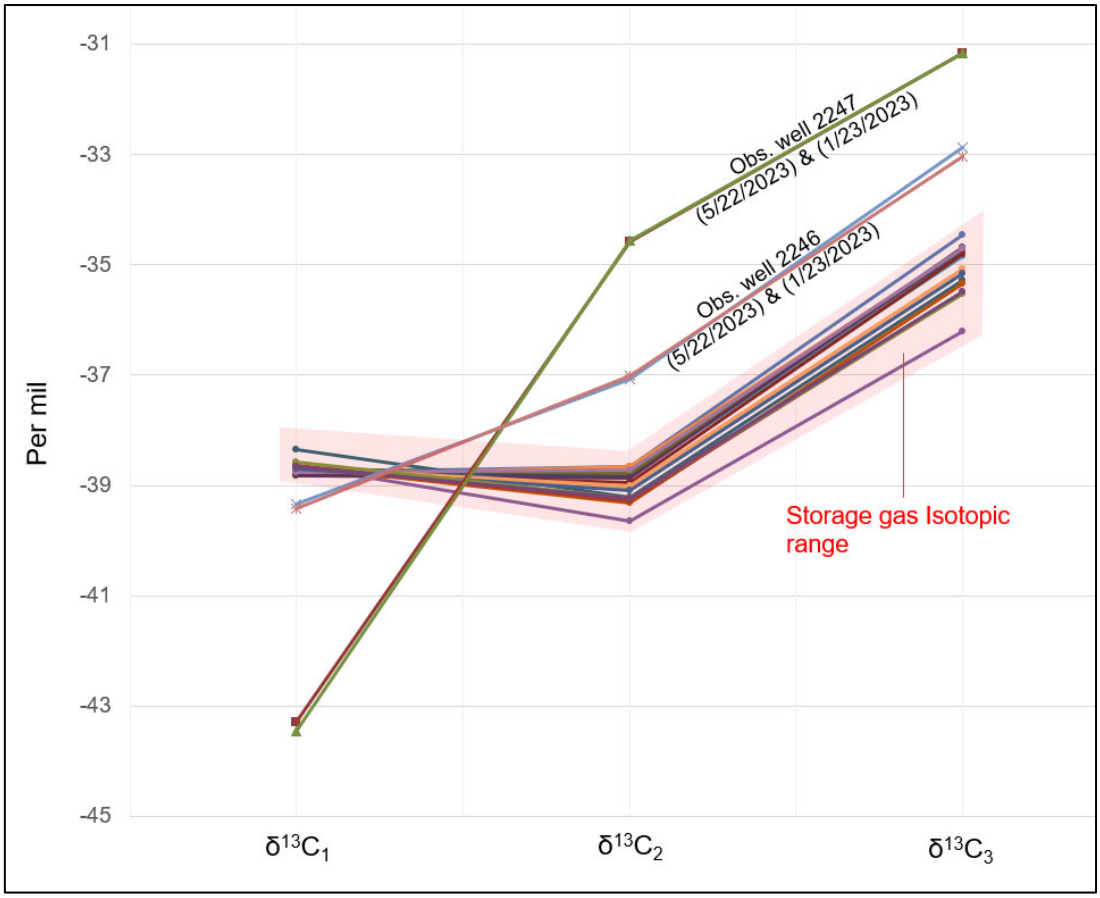

Figure 6. Obs. Well 2246 production casing contains gas that appears to be a mix of storage gas and the gas found in the production casing of Obs. Well 2247.

4.3 Vent Gas Isotope Results

Obs. Well 2247: Vent gas resembles storage gas (i.e., $\delta^{13}C_2$ and $\delta^{13}C_3$) with the $\delta^{13}C_1$ lighter than that for storage gas, likely resulting from the fractionation effect of subsurface storage gas migration from Field Well 2244 to Obs. Well 2247 (*see* Figure 7). The isotopic differences between wellhead gas and vent gas do not support communication between the two casings. Storage gas appearing in the Obs. Well 2247 vent is consistent with subsurface storage gas migration, which is likely to be occurring along the Balltown/Speechley interbedded sandstones (discussed in Section 3). At Obs. Well 2247, vent gas pressure had been steadily increasing and appears to have stabilized (at least temporarily) at approximately 100 psi as of July 22, 2023 (recall that the annulus valve had been closed at Obs. Well 2247 starting in May 2023). The

relatively lower vent pressure at 100 psi[14] is consistent with the observation of the Balltown and Speechley sandstone formations becoming less continuous and less distinct as one moves farther to the north from Field Well 2244—indicating less transmissive pathways in a north direction from Field Well 2244 to Obs. Well 2247.

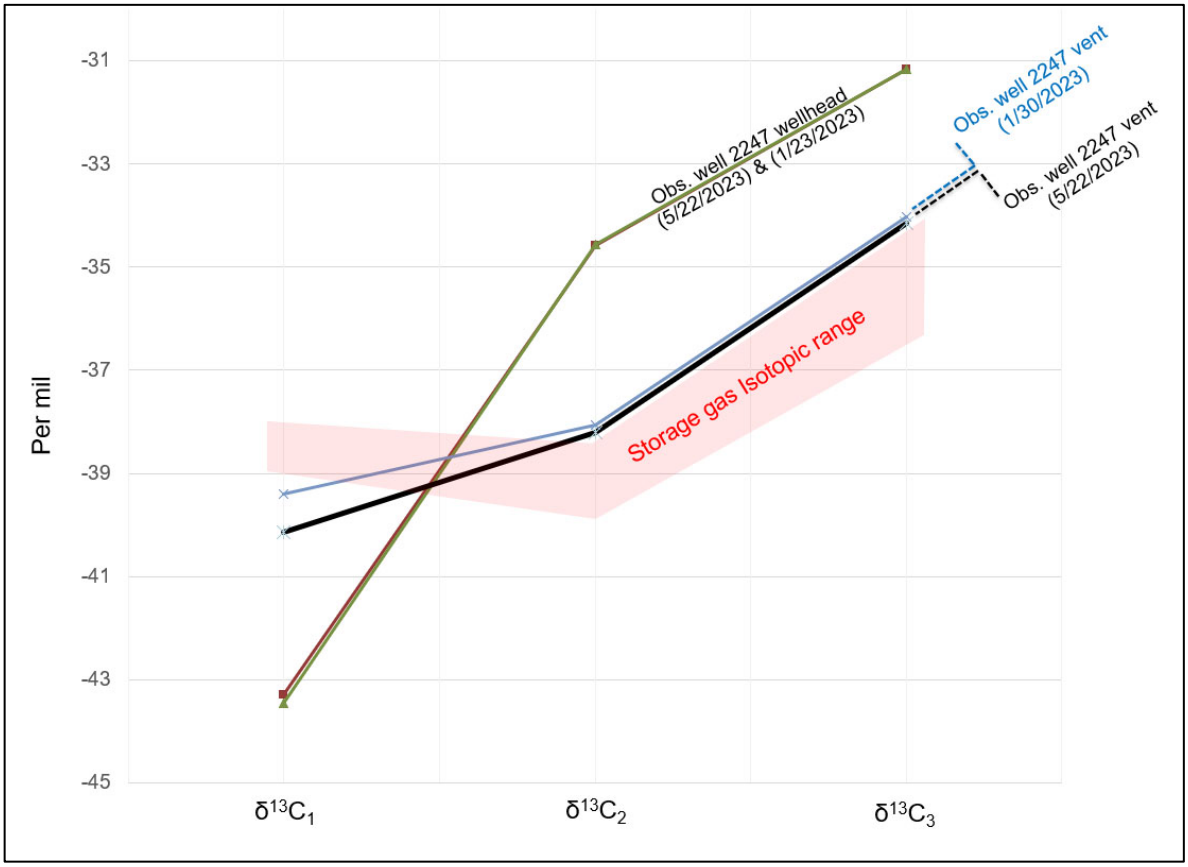

Figure 7. Obs. Well 2247 gas isotope results indicates the presence of storage gas in the vent, albeit at low pressures, consistent with less discontinuous and less distinct Balltown and Speechley sandstone formations moving father to the north from Field Well 2244.

Field Well 2249: Vent gas appears to contain storage gas mixed with other native gases. Figure 8 presents the isotopes for production and vent gases from Field Well 2249. Field Well 2249 vent and production gases do not perfectly match, which does not support a

[14] Compared to, for example, Obs. Well 2246 vent gas pressure at 200 psi as of July 22, 2023.

communication between the two casings, and which means that the presence of vent gas resembling storage gas, in part, is likely the result of subsurface storage gas migration.

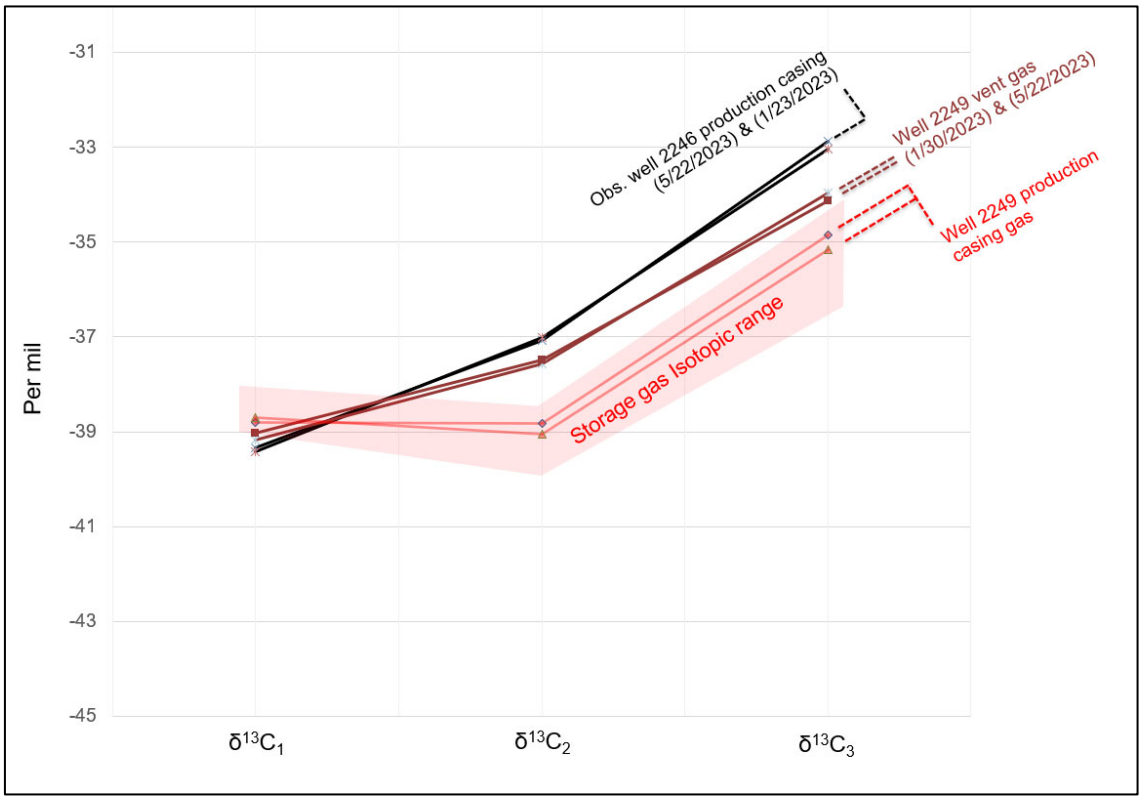

Figure 8. Field Well 2249 gas isotope results indicate the presence of storage gas in the vent mixed with other native gases. Storage gas likely migrated through the Balltown and Speechley sandstone layers present between Field Wells 2244 and 2249.

Field Well 2251: Vent gas matches storage gas (*see* Figure 9). From a mechanical integrity standpoint, it appeared that the production casing and the annulus casing were in communication, which resulted in production casing storage gas migrating to the annulus casing and appearing in the vent gas.[15]

[15] In May 2023, pressure tests for Field Well 2251 indicated that as the casing pressure increased, annulus pressure tracked the casing pressure when the annulus vent was closed. When the casing was shut-in starting in May 2023, casing pressure increased from 692 psi (on June 6, 2023) to 1,067 psi (on June 20, 2023), indicating that the plug in the well may had been slowly leaking.

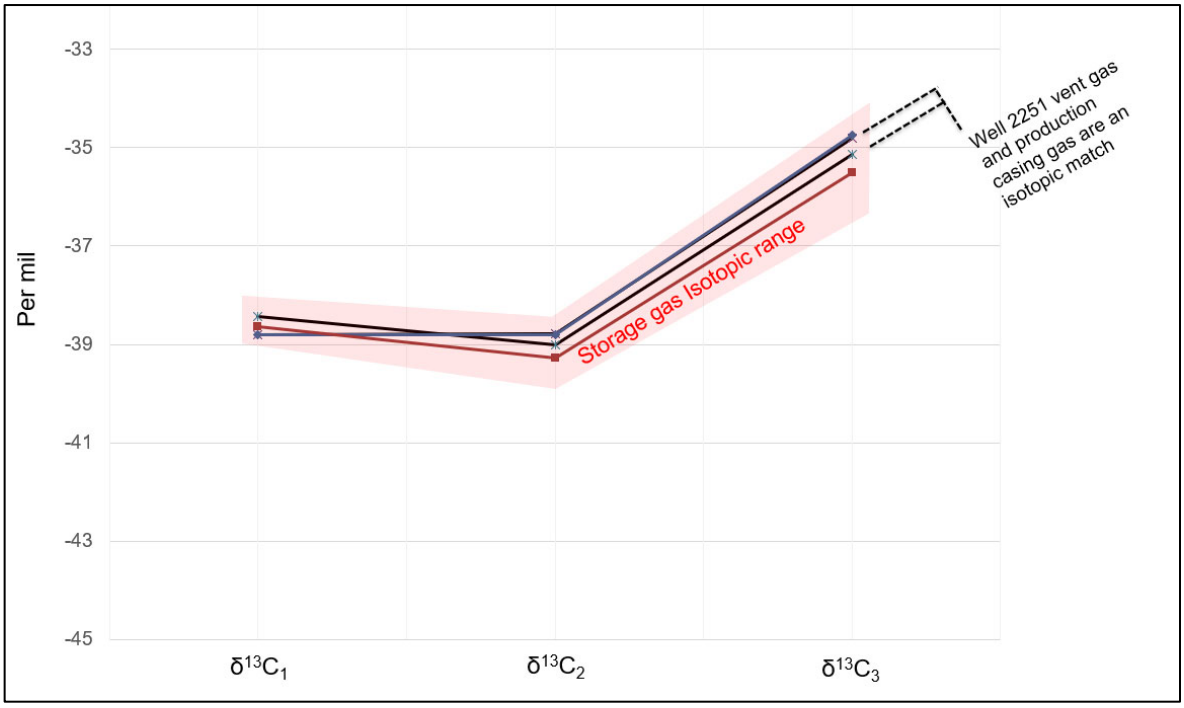

Figure 9. Field Well 2251 vent gas and production casing storage gas are an isotopic match.

Field Well 2248: Vent gas resembled storage gas (*see* Figure 10). From a mechanical integrity standpoint, subsurface storage gas appears to have migrated to the annulus casing, and then migrated to the production casing (*see* the Blade 2023 report for additional information).[16] The subsurface storage gas most likely migrated through the interbedded Speechley and Balltown sandstones. A noise log for Field Well 2248 demonstrated movement at 3,000 ft (*see* Figures 11 and 12), consistent with geology information regarding the presence of the interbedded Balltown and Speechley sandstone layers that likely provided a migration pathway for the subsurface gas.

[16] Briefly, on December 8, 2022, during logging of Field Well 2248, EQTRNS identified integrity issues with the well and began operations to temporarily plug it. Two retrievable bridge plugs were installed in the well (at 7,479 ft and 7,511 ft). From March to April 2023, workover was performed on this well. When production and annulus casing vents were shut, gas pressure in the production casing and annulus casing tracked together, with annulus pressure higher than the casing pressure. Casing pressure remained nearly 0 psi after the casing and annulus bled down at the end of May 2023.

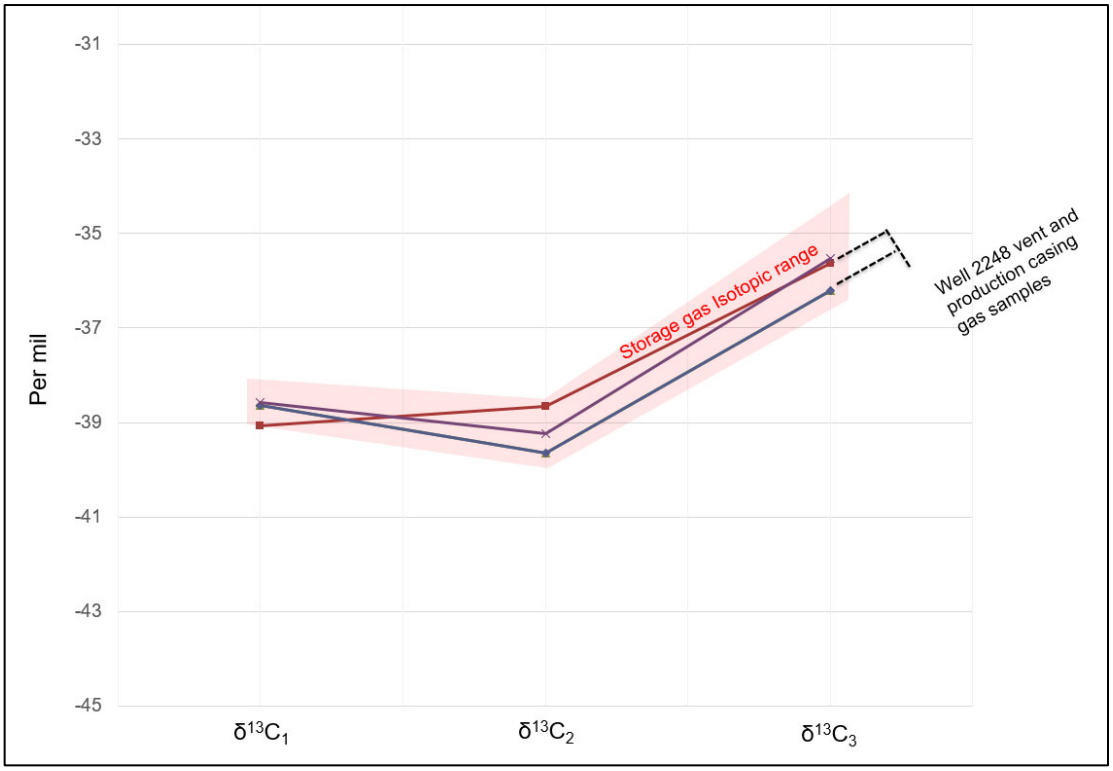

Figure 10. Field Well 2248 vent and production casing gases are storage gas.

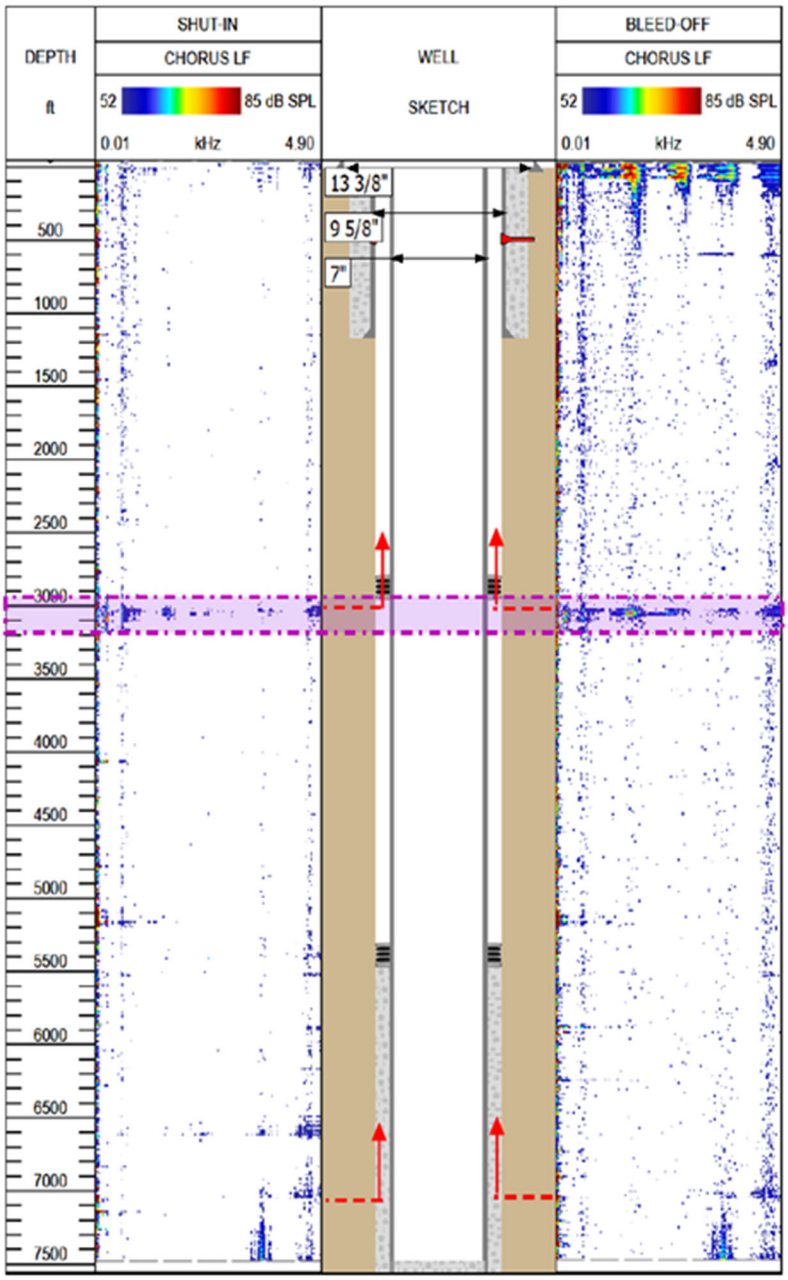

Figure 11. Field Well 2248 noise log results from December 19, 2022, demonstrating potential migration pathway at 3,000 ft, consistent with the geology information regarding the Balltown and Speechley interbedded sandstone layers (Source: EQTRNS).

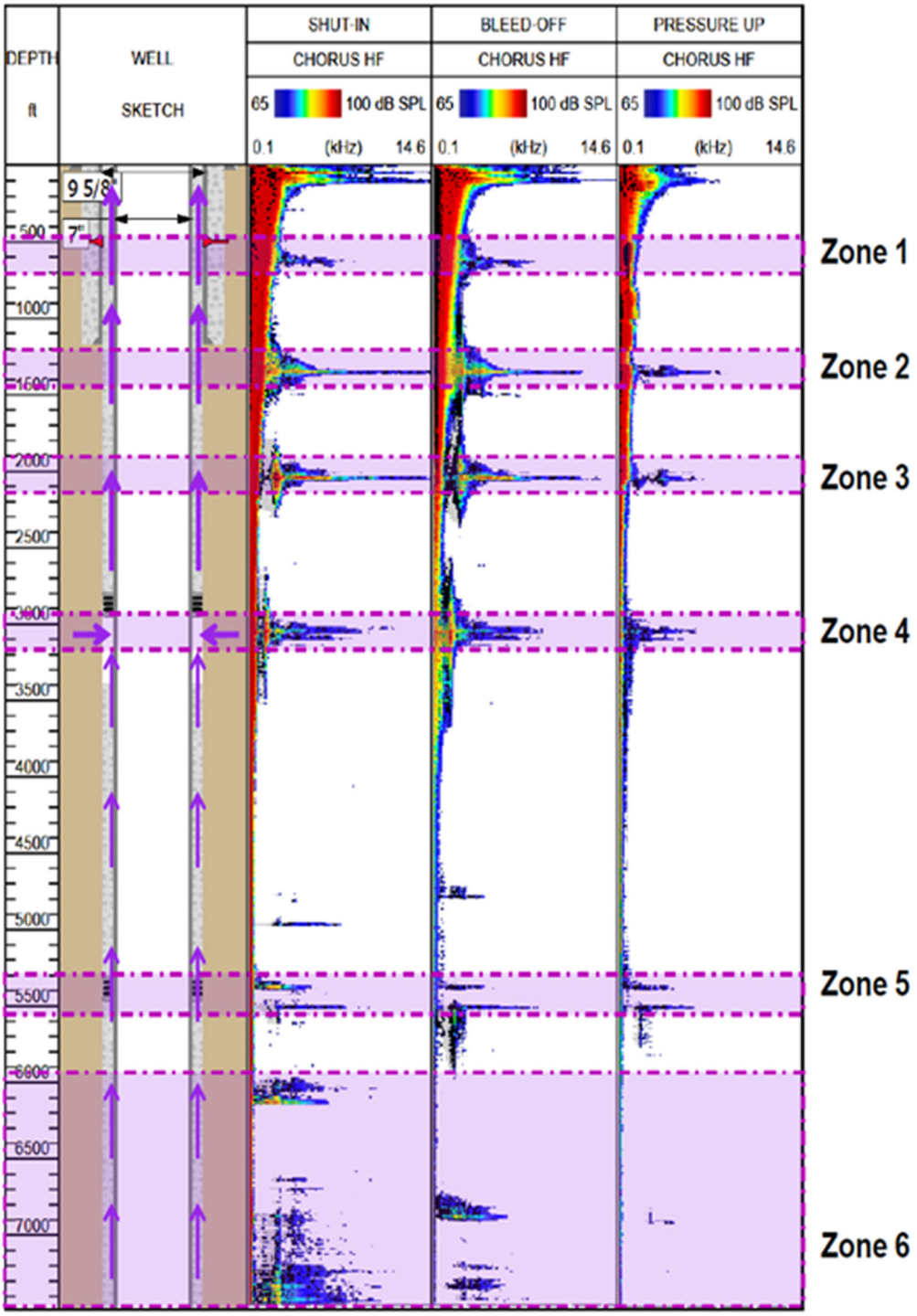

Figure 12. Field Well 2248 noise log results from April 25, 2023, demonstrating a potential migration pathway at 3,000 ft, consistent with the geology information regarding the Balltown and Speechley interbedded sandstone layers (Source: EQTRNS).

Field Wells 2245 and 2255 and Obs. Well 2246: Vent gases in these wells have somewhat similar isotopic patterns and are likely a mixture of gases that were collectively different from storage gas (*see* Figure 13). The exact composition of the vent gases is not clear—possibly native gases (and unknown if there is a percentage of storage gas in them). The mixtures of gases are possibly mobilized/pressurized by subsurface storage gas migration, an explanation consistent with increasing vent gas pressure in Obs. Well 2246 (from approximately 140 psi July 1, 2023, to approximately 200 psi on July 22, 2023).

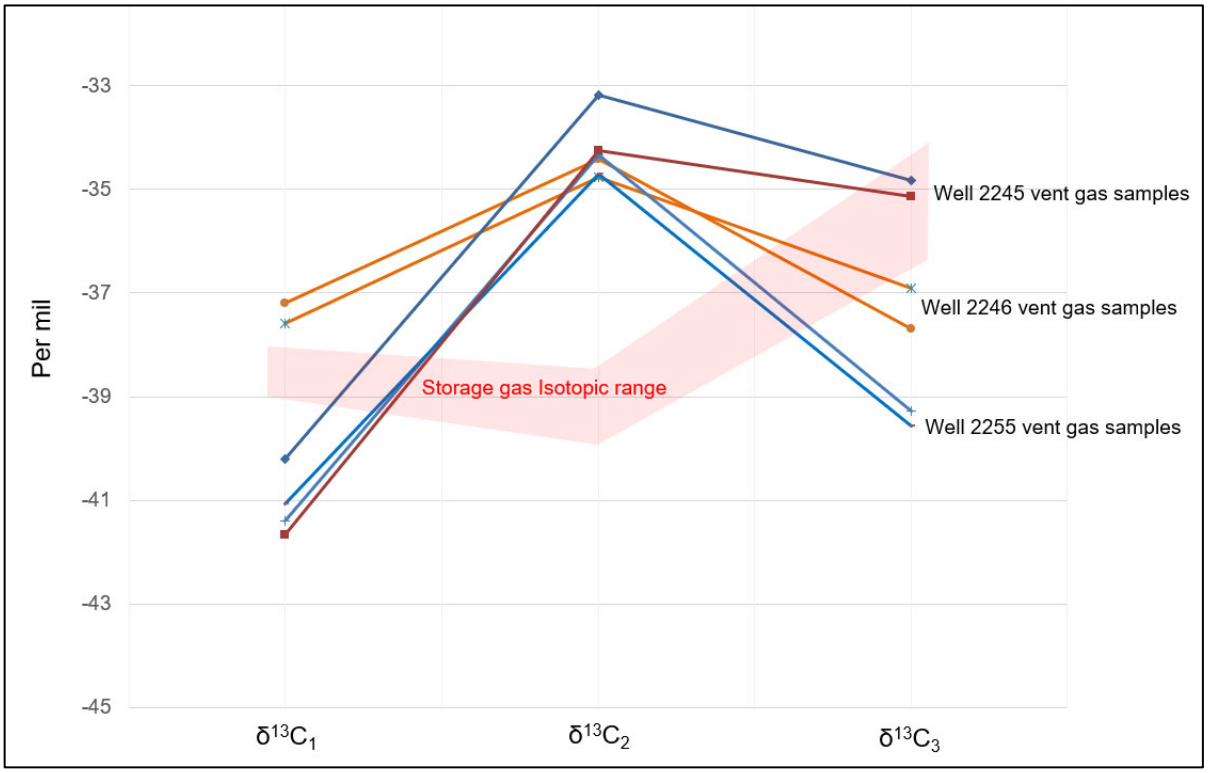

Figure 13. Field Wells 2245 and 2255 and Obs. Well 2246 vent gases are different from storage gas.

5 Residential Water Wells and Soil Survey to Investigate the Presence of Gases

Residential water wells adjacent to the facility were sampled for the presence of gases in the wells, and residential soils were screened for the presence of gas (the engineering company Civil and Environmental Consultants, CEC, conducted the sampling). In addition, soils along Cramer Pike ([Highway 403]) were also screened for gas. Figure 1 presents an overview of the screened area locations, while Attachment 1 presents the residential soil screening locations for each property. In summary, gases were not found in any of the screened areas, indicating that subsurface storage gas in the Facility has not migrated to nearby areas.

5.1 Residential Property Water Well Sampling and Results

For the residential property wells, water samples were collected before any treatment filters or systems. Water samples were analyzed under three different testing protocols and collected in the following order: (1) dissolved gasses, (2) total petroleum hydrocarbons, and (3) cations, anions, and general chemistry. Dissolved methane concentrations were a maximum of 0.016 mg/L (over two orders of magnitude below the action level of 7 mg/L).

5.2 Soil Gas Screening and Results

A shallow soil gas survey was conducted at each property and along Cramer Pike highway. Standard operating procedures prescribed up to 10 bar hole locations to a depth of 3 ft, if possible. Each testing hole was screened for methane soil gas, with maximum and sustained methane levels recorded. No gas was found in any of the screened soil locations.

Attachment 1

Residential Area and Cramer Highway Sample Locations And Analysis Results

P:\330-000\333-305\-GIS\Maps\EN04_Property_Report\333305_EN04_FIG1_Overview_Map.mxd 7/27/2023 1:13 PM (ssmall)

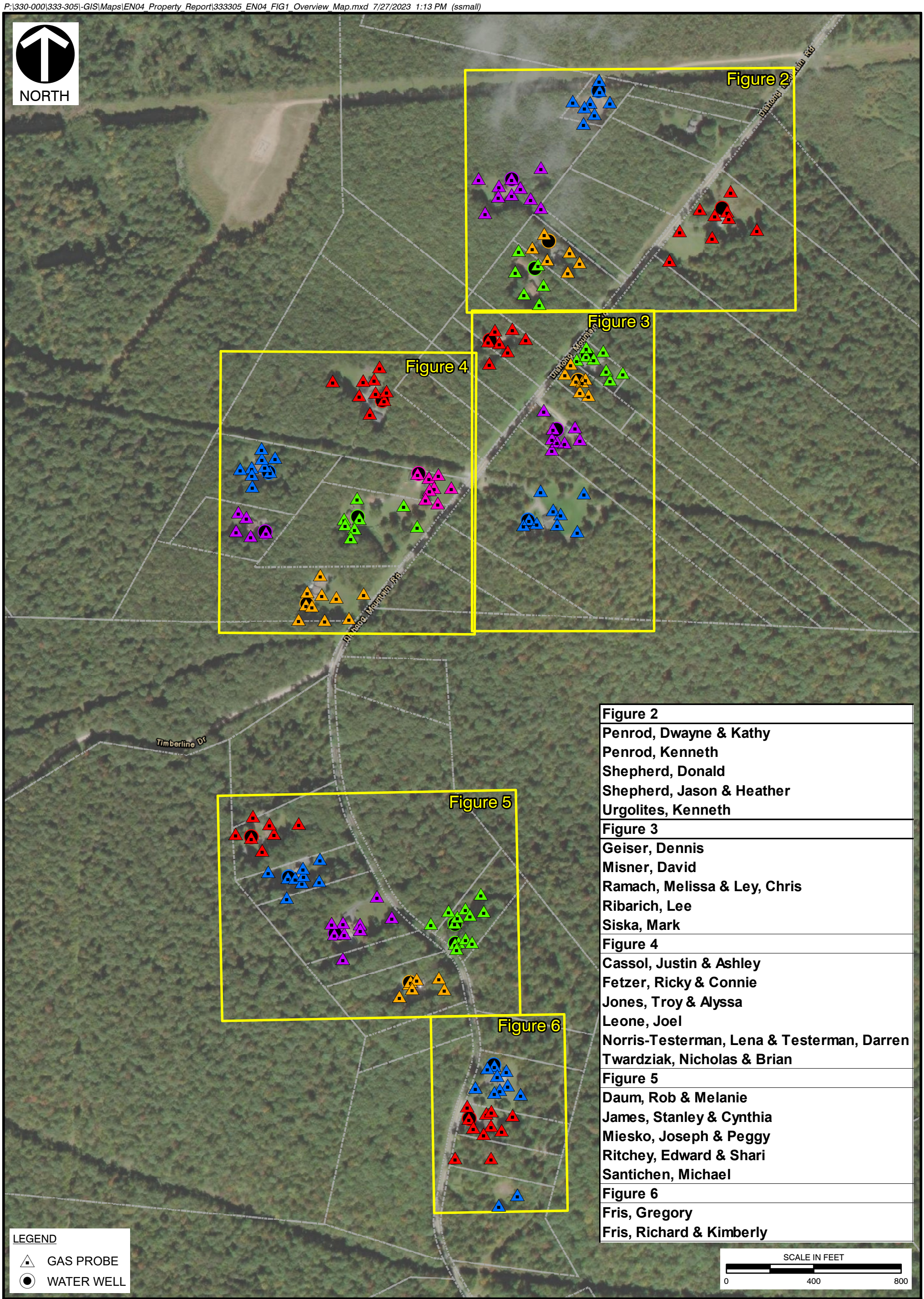

Figure 2
Penrod, Dwayne & Kathy
Penrod, Kenneth
Shepherd, Donald
Shepherd, Jason & Heather
Urgolites, Kenneth
Figure 3
Geiser, Dennis
Misner, David
Ramach, Melissa & Ley, Chris
Ribarich, Lee
Siska, Mark
Figure 4
Cassol, Justin & Ashley
Fetzer, Ricky & Connie
Jones, Troy & Alyssa
Leone, Joel
Norris-Testerman, Lena & Testerman, Darren
Twardziak, Nicholas & Brian
Figure 5
Daum, Rob & Melanie
James, Stanley & Cynthia
Miesko, Joseph & Peggy
Ritchey, Edward & Shari
Santichen, Michael
Figure 6
Fris, Gregory
Fris, Richard & Kimberly

REFERENCE

ESRI WORLD IMAGERY / ARCGIS MAP SERVICE: HTTP://GOTO.ARCGISONLINE.COM/MAPS/WORLD_IMAGERY, ACCESSED 7/27/2023, IMAGERY DATE: 2014.

CAMRBIA COUNTY, PA PARCELS, REAL ESTATE PORTAL USA, LLC, UPDATED 2019-Q1.

SCREENING AND SAMPLING LOCATIONS: REFERENCE EACH SUBFIGURE FOR COLOR LEGEND AND CORRESPONDING PARCEL.

Civil & Environmental Consultants, Inc.
700 Cherrington Parkway - Moon Township, PA 15108
412-429-2324 •800-365-2324
www.cecinc.com

EQUITRANS MIDSTREAM CORPORATION
RAGER MOUNTAIN GAS STORAGE AREA
JACKSON TOWNSHIP, CAMBRIA COUNTY, PENNSYLVANIA

RESIDENTAL SURVEY - WATER WELL & SOIL GAS PROBE LOCATIONS: SHEET OVERVIEW

DRAWN BY:	NTP / SRS	CHECKED BY:	DRAFT	APPROVED BY:	* Hand signature on file DRAFT	FIGURE NO:	1
DATE:	7/27/2023	SCALE:	1 " = 400 '	PROJECT NO:	333-305		

NORTH

34-017. -142.001
(SHEPHERD, JASON & HEATHER)

34-017. -142.000
(SHEPHERD, DONALD)

34-017. -133.000
(PENROD, DWAYNE & KATHY)

34-017. -132.000
(PENROD, KENNETH)

34-017. -117.000
(URGOLITES, KENNETH)

Dishong Mountain Rd

SCALE IN FEET
0 125 250

LEGEND

- 34-017.-142.001: SHEPHERD, JASON & HEATHER
- 34-017.-142.000: SHEPHERD, DONALD
- 34-017.-133.000: PENROD, DWAYNE & KATHY
- 34-017.-132.000: PENROD, KENNETH
- 34-017.-117.000: URGOLITES, KENNETH
- GAS PROBE
- WATER WELL
- SUBJECT PARCELS
- CAMBRIA COUNTY PARCELS

REFERENCE

ESRI WORLD IMAGERY / ARCGIS MAP SERVICE: HTTP://GOTO.ARCGISONLINE.COM/MAPS/WORLD_IMAGERY, ACCESSED 7/27/2023, IMAGERY DATE: 2014.

CAMBRIA COUNTY, PA PARCELS, REAL ESTATE PORTAL, USA, LLC, UPDATED 2019-Q1.

Civil & Environmental Consultants, Inc.
700 Cherrington Parkway - Moon Township, PA 15108
412-429-2324 · 800-365-2324
www.cecinc.com

EQUITRANS MIDSTREAM CORPORATION
RAGER MOUNTAIN GAS STORAGE AREA
JACKSON TOWNSHIP, CAMBRIA COUNTY, PENNSYLVANIA

RESIDENTAL SURVEY - WATER WELL & SOIL GAS PROBE LOCATIONS: SUBJECT PARCELS

DRAWN BY:	NTP / SRS	CHECKED BY:	DRAFT	APPROVED BY: * Hand signature on file	DRAFT
DATE:	7/27/2023	SCALE:	1 " = 125 '	PROJECT NO:	333-305

FIGURE NO: 2

P:\330-000\333-305\GIS\Maps\EN04_Property_Report\333305_EN04_FIG2_Sample_Locations_Map.mxd 7/27/2023 1:54 PM (ssmall)

NORTH

34-017. -134.000
(SISKA, MARK)

34-017. -119.004
(MISNER, DAVID)

34-017. -119.003
(GEISER, DENNIS)

34-017. -119.005
(RAMACH, MELISSA & LEY, CHRIS)

34-017. -120.000
(RIBARICH, LEE)

Dishong Mountain Rd

SCALE IN FEET
0 120 240

LEGEND

- 34-017.-120.000: RIBARICH, LEE
- 34-017.-119.005: RAMACH, MELISSA & LEY, CHRIS
- 34-017.-119.004: MISNER, DAVID
- 34-017.-119.003: GEISER, DENNIS
- 34-017.-134.000: SISKA, MARK
- GAS PROBE
- WATER WELL
- SUBJECT PARCELS
- CAMBRIA COUNTY PARCELS

REFERENCE

ESRI WORLD IMAGERY / ARCGIS MAP SERVICE: HTTP://GOTO.ARCGISONLINE.COM/MAPS/WORLD_IMAGERY, ACCESSED 7/27/2023, IMAGERY DATE: 2014.

CAMRBIA COUNTY, PA PARCELS, REAL ESTATE PORTAL USA, LLC, UPDATED 2019-Q1.

Civil & Environmental Consultants, Inc.
700 Cherrington Parkway - Moon Township, PA 15108
412-429-2324 · 800-365-2324
www.cecinc.com

EQUITRANS MIDSTREAM CORPORATION
RAGER MOUNTAIN GAS STORAGE AREA
JACKSON TOWNSHIP, CAMBRIA COUNTY, PENNSYLVANIA

RESIDENTIAL SURVEY - WATER WELL & SOIL GAS PROBE LOCATIONS: SUBJECT PARCELS

DRAWN BY:	NTP / SRS	CHECKED BY:	DRAFT	APPROVED BY: * Hand signature on file	DRAFT
DATE:	7/27/2023	SCALE:	1 " = 120 '	PROJECT NO:	333-305

FIGURE NO: 3

P:\330-000\333-305\GIS\Maps\EN04_Property_Report\333305_EN04_FIG3_Sample_Locations_Map.mxd 7/27/2023 1:55 PM (ssmall)

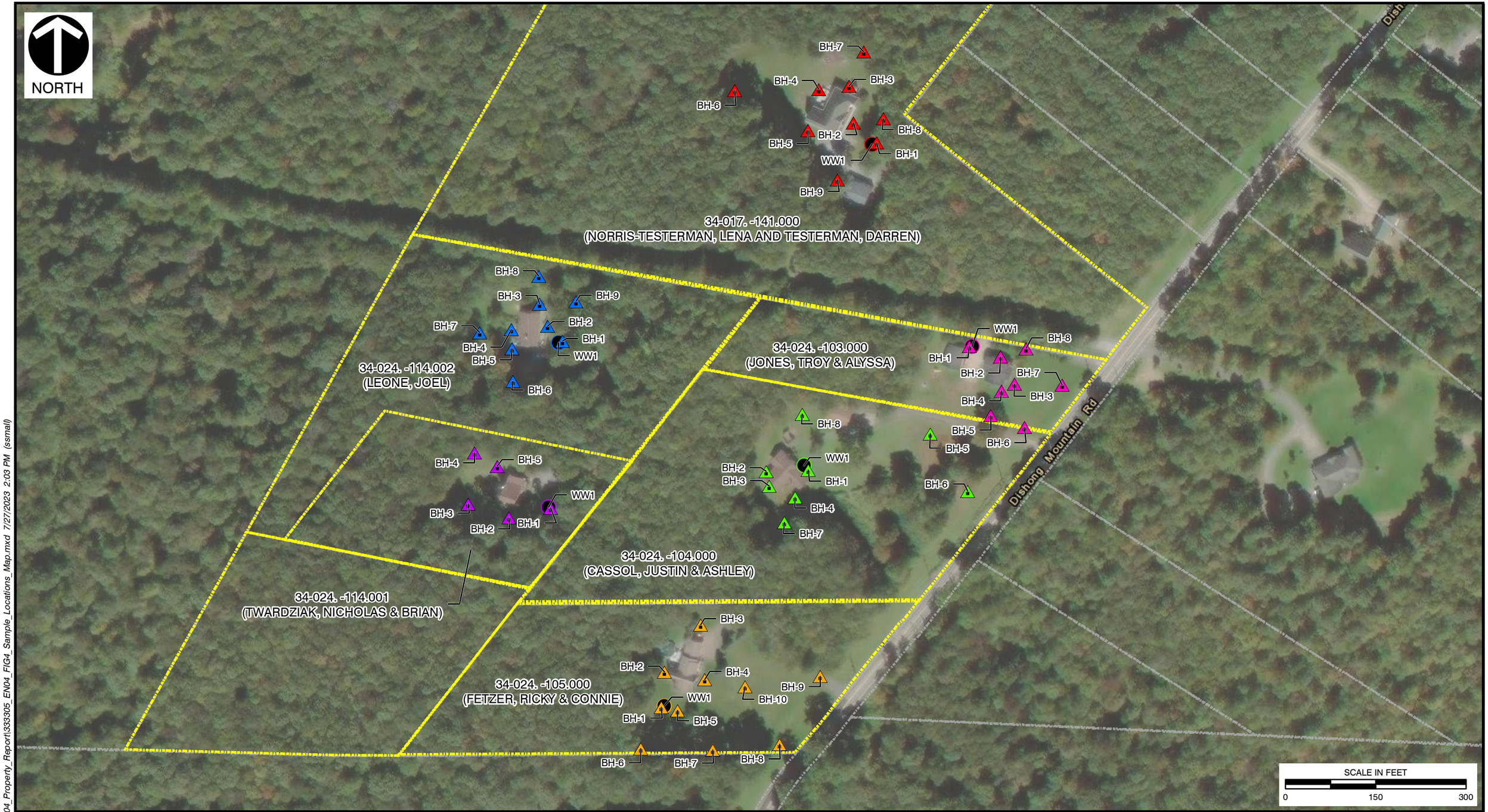

LEGEND

- 34-024.-114.002: LEONE, JOEL
- 34-024.-114.001: TWARDZIAK, NICHOLAS & BRIAN
- 34-024.-104.000: CASSOL, JUSTIN & ASHLEY
- 34-024.-105.000: FETZER, RICKY & CONNIE
- 34-017.-141.000: NORRIS-TESTERMAN, LENA
- 34-024.-103.000: JONES, TROY & ALYSSA
- GAS PROBE
- WATER WELL
- SUBJECT PARCELS
- CAMBRIA COUNTY PARCELS

REFERENCE

ESRI WORLD IMAGERY / ARCGIS MAP SERVICE: HTTP://GOTO.ARCGISONLINE.COM/MAPS/WORLD_IMAGERY, ACCESSED 7/27/2023, IMAGERY DATE: 2014.

CAMBRIA COUNTY, PA PARCELS, REAL ESTATE PORTAL, USA, LLC, UPDATED 2019-Q1.

Civil & Environmental Consultants, Inc.
700 Cherrington Parkway - Moon Township, PA 15108
412-429-2324 · 800-365-2324
www.cecinc.com

DRAWN BY:	NTP / SRS	CHECKED BY:	DRAFT	APPROVED BY: * Hand signature on file	DRAFT
DATE:	7/27/2023	SCALE:	1 " = 150 '	PROJECT NO:	333-305

EQUITRANS MIDSTREAM CORPORATION RAGER MOUNTAIN GAS STORAGE AREA JACKSON TOWNSHIP, CAMBRIA COUNTY, PENNSYLVANIA

RESIDENTAL SURVEY - WATER WELL & SOIL GAS PROBE LOCATIONS: SUBJECT PARCELS

FIGURE NO: 4

P:\330-000\333-305\-GIS\Maps\EN04_Property_Report\333305_EN04_FIG4_Sample_Locations_Map.mxd 7/27/2023 2:03 PM (ssmall)

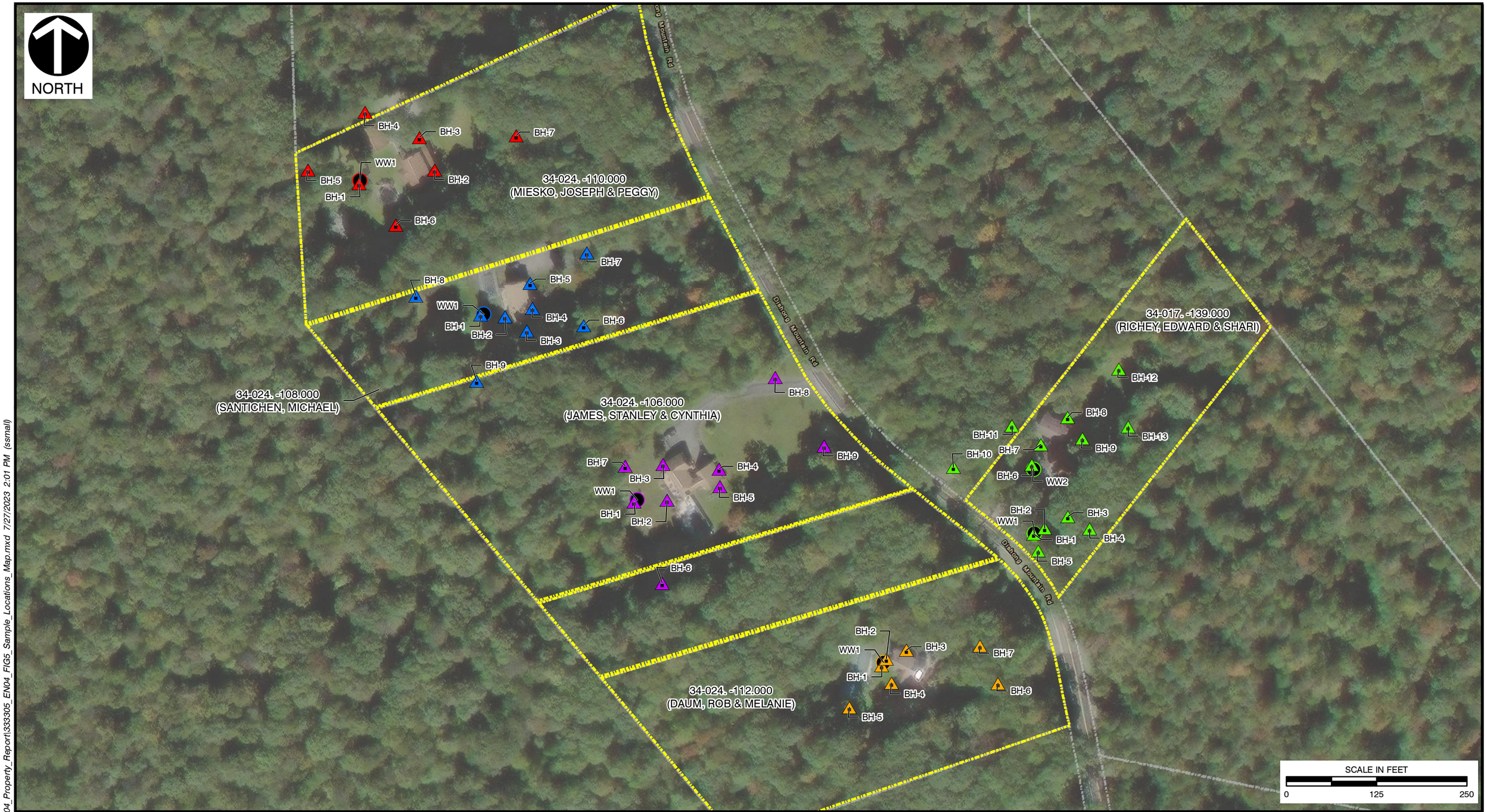

P:\330-000\333-305\-GIS\Maps\EN04_Property_Report\333305_EN04_FIG5_Sample_Locations_Map.mxd 7/27/2023 2:01 PM (ssmall)

LEGEND

- 34-024.-108.000: SANTICHEN, MICHAEL
- 34-024.-106.000: JAMES, STANLEY & CYNTHIA
- 34-017.-139.000: RICHEY, EDWARD & SHARI
- 34-024.-112.000: DAUM, ROB & MELANIE
- 34-024.-110.000: MIESKO, JOSEPH & PEGGY
- GAS PROBE
- WATER WELL
- SUBJECT PARCELS
- CAMBRIA COUNTY PARCELS

REFERENCE

ESRI WORLD IMAGERY / ARCGIS MAP SERVICE: HTTP://GOTO.ARCGISONLINE.COM/MAPS/WORLD_IMAGERY, ACCESSED 7/27/2023, IMAGERY DATE: 2014.

CAMBRIA COUNTY, PA PARCELS, REAL ESTATE PORTAL USA, LLC, UPDATED 2019-Q1.

Civil & Environmental Consultants, Inc.
700 Cherrington Parkway - Moon Township, PA 15108
412-429-2324 · 800-365-2324
www.cecinc.com

DRAWN BY:	NTP / SRS	CHECKED BY:	DRAFT	APPROVED BY: * Hand signature on file	DRAFT
DATE:	7/27/2023	SCALE:	1 " = 125 '	PROJECT NO:	333-305

EQUITRANS MIDSTREAM CORPORATION
RAGER MOUNTAIN GAS STORAGE AREA
JACKSON TOWNSHIP, CAMBRIA COUNTY, PENNSYLVANIA

RESIDENTAL SURVEY - WATER WELL & SOIL GAS PROBE LOCATIONS: SUBJECT PARCELS

FIGURE NO: 5

NORTH

WW1
BH-3
BH-4
BH-8
BH-7
BH-5
BH-9
BH-6
BH-10
BH-11

34-017. -127.000
(FRIS, RICHARD & KIMBERLY)

BH-7
BH-3
BH-2
WW1
BH-8
BH-1
BH-4
BH-6
BH-9
BH-5

34-017. -126.000
(FRIS, GREGORY)

BH-11
BH-10

34-017. -128.000
(FRIS, GREGORY)

34-017. -125.000
(FRIS, RICHARD & KIMBERLY)

BH-2
BH-1

SCALE IN FEET
0 90 180

P:\330-000\333-305\-GIS\Maps\EN04_Property_Report\333305_EN04_FIG6_Sample_Locations_Map.mxd 7/27/2023 2:01 PM (ssmall)

LEGEND

- 34-017.-127.000: FRIS, RICHARD & KIMBERLY
- 34-017.-126.000: FRIS, GREGORY
- GAS PROBE
- WATER WELL
- SUBJECT PARCELS
- CAMBRIA COUNTY PARCELS

REFERENCE

ESRI WORLD IMAGERY / ARCGIS MAP SERVICE:
HTTP://GOTO.ARCGISONLINE.COM/MAPS/WORLD_IMAGERY,
ACCESSED 7/27/2023, IMAGERY DATE: 2014.

CAMBRIA COUNTY, PA PARCELS,
REAL ESTATE PORTAL USA, LLC, UPDATED 2019-Q1.

Civil & Environmental Consultants, Inc.
700 Cherrington Parkway - Moon Township, PA 15108
412-429-2324 · 800-365-2324
www.cecinc.com

EQUITRANS MIDSTREAM CORPORATION
RAGER MOUNTAIN GAS STORAGE AREA
JACKSON TOWNSHIP, CAMBRIA COUNTY, PENNSYLVANIA

RESIDENTAL SURVEY - WATER WELL &
SOIL GAS PROBE LOCATIONS: SUBJECT PARCELS

DRAWN BY:	NTP / SRS	CHECKED BY:	DRAFT	APPROVED BY: * Hand signature on file	DRAFT
DATE:	7/27/2023	SCALE:	1 " = 90 '	PROJECT NO:	333-305

FIGURE NO: 6

TABLE 1
SUMMARY OF LABORATORY ANALYTICAL RESULTS
RESIDENTIAL SURVEY - WATER WELLS
RAGER MOUNTAIN GAS STORAGE AREA
JACKSON TOWNSHIP, CAMBRIA COUNTY, PENNSYLVANIA
EQUITRANS MIDSTREAM CORPORATION

Sample Location:	D and K Penrod WW1	K Penrod WW1	D Misner WW1	K Urgolites WW1	R and K M Fris WW1	G Fris WW1	R and C Fetzer WW1	M and V Santichen WW1	D Shepherd WW1	J and H Shepherd WW1	M Ramach & C Ley WW1	L Norris-Testerman & D Testerman WW1	Groundwater Screening Criteria [1]		
Lab ID:	AXF3634-01	AXF3631-01	AXF3768-04	AXF3768-03	AXF3768-02	AXF3768-01	AXF4193-01	AXF4193-02	AXF4374-01	AXF4378-01	AXF4376-01	AXF4933-01	MSC_{GW} [2]	EPA SMCL [3]	Other Screening Criteria
Sample Date:	6/14/2023	6/14/2023	6/15/2023	6/15/2023	6/15/2023	6/15/2023	6/16/2023	6/16/2023	6/19/2023	6/19/2023	6/19/2023	6/20/2023			
Petroleum Hydrocarbons (mg/l)															
Gasoline Range Organics	< 0.0675 I	< 0.0675	< 0.0675	< 0.0675	< 0.0675	< 0.0675	< 0.0675	< 0.0675	< 0.0675	< 0.0675	< 0.0675	< 0.0675	nse	nse	nse
Metals (mg/l)	--														
Barium (total)	**0.112**	**0.155**	**0.197**	**0.387**	**0.714**	**0.0748**	**0.0378**	**0.237**	**0.0372**	**0.792**	**0.542**	**0.147**	nse	nse	nse
Barium (dissolved)	**0.114**	**0.148**	**0.204**	**0.410**	**0.723**	**0.0713**	**0.0344**	**0.229**	**0.0343**	**0.751**	**0.506**	**0.137**	**2**	nse	nse
Boron (total)	< 0.0565 LK	< 0.0565 LK	< 0.0565	< 0.0565	< 0.0565	< 0.0565	< 0.0565	< 0.0565	0.0585 F, J	0.0660 F, J	0.0677 F, J	< 0.0565	nse	nse	nse
Boron (dissolved)	< 0.0565	< 0.0565	< 0.0565	< 0.0565	< 0.0565	< 0.0565	< 0.0565	< 0.0565	< 0.0565	< 0.0565	< 0.0565	< 0.0565	**6**	nse	nse
Cadmium (total)	< 0.00160	< 0.0016	< 0.0016	< 0.0016	< 0.0016	< 0.0016	< 0.0016	< 0.0016	< 0.0016	< 0.0016	< 0.0016	< 0.0016	nse	nse	nse
Cadmium (dissolved)	< 0.00160	< 0.0016	< 0.0016	< 0.0016	< 0.0016	< 0.0016	< 0.0016	< 0.0016	< 0.0016	< 0.0016	< 0.0016	< 0.0016	**0.005**	nse	nse
Calcium (total)	**3.16**	**1.44**	**3.57**	**7.77**	**25.9 T**	**2.33**	**3.40**	**28.0 T**	**2.00**	**23.8 T**	**16.1**	**19.2**	nse	nse	nse
Calcium (dissolved)	**3.17**	**1.43**	**3.50**	**7.96**	**25.5 T**	**2.16**	**3.37**	**27.7 T**	**1.90**	**23.4 T**	**15.4**	**20.2 T**	nse	nse	nse
Iron (total)	**0.369**	**38.2 T**	**2.71**	**31.3 T**	**2.65**	**3.58**	**8.28 T**	**1.44**	< 0.185	**3.03**	**0.274**	**18.3 T**	nse	nse	nse
Iron (dissolved)	**0.358**	**7.63 T**	**1.92**	**8.63 T**	< 0.185	**0.731**	**3.24**	**0.467**	< 0.185	< 0.185	< 0.185	**15.9 T**	nse	**0.3**	nse
Magnesium (total)	**1.16**	**0.954**	**2.21**	**2.03**	**4.12**	**1.33**	**3.16**	**2.86**	**1.01**	**2.62**	**3.35**	**1.36**	nse	nse	nse
Magnesium (dissolved)	**1.18**	**0.925**	**2.19**	**2.12**	**4.13**	**1.23**	**3.10**	**2.87**	**0.984**	**2.69**	**3.40**	**1.45**	nse	nse	nse
Manganese (total)	**0.516**	**0.876**	**1.65**	**1.64**	**0.541**	**0.386**	**1.91**	**0.212**	**0.183**	**0.0444**	**0.275**	**1.16**	nse	nse	nse
Manganese (dissolved)	**0.501**	**0.821**	**1.57**	**1.62**	**0.0306**	**0.335**	**1.89**	**0.195**	**0.182**	< 0.0124	**0.278**	**1.19**	**0.3**	**0.05**	nse
Potassium (total)	**0.998**	**0.737**	**0.919**	**1.48**	**2.18**	**0.481**	**1.44**	**1.92**	**0.820**	**2.92**	**2.85**	**0.837**	nse	nse	nse
Potassium (dissolved)	**1.09**	**0.701**	**0.933**	**1.55**	**2.17**	**0.466**	**1.42**	**1.93**	**0.776**	**3.01**	**2.82**	**0.950**	nse	nse	nse
Sodium (total)	**1.62**	< 0.793	**11.8**	**1.43**	< 0.793	< 0.793	< 0.793	< 0.793	**2.05**	< 0.793	**11.6**	< 0.793	nse	nse	nse
Sodium (dissolved)	**1.71**	< 0.793	**11.4**	**1.53**	< 0.793	< 0.793	< 0.793	< 0.793	**2.06**	< 0.793	**11.9**	0.972 J	nse	nse	nse
Strontium (total)	**0.0390**	0.0147 J	**0.0221**	**0.0553**	**0.538**	**0.0206**	0.0112 J	**0.0987**	0.0128 J	**0.517**	**0.391**	**0.0354**	nse	nse	nse
Strontium (dissolved)	**0.0383**	0.0149 J	0.0198 J	**0.0548**	**0.521**	0.0186 J	0.0104 J	**0.0947**	0.0123 J	**0.504**	**0.370**	**0.0410**	**4**	nse	nse
Sulfur (total)	**4.00**	**2.10**	< 0.176	**0.729**	**1.73**	**3.23**	**1.27**	**0.845**	**1.95**	**0.798**	**0.971**	0.332 J	nse	nse	nse
Wet Chemistry/Other (mg/l)	--														
Bromide	< 0.072	< 0.072	< 0.072	< 0.072	< 0.072	< 0.072	< 0.072	< 0.072	< 0.072	< 0.072	< 0.072	< 0.072	nse	nse	nse
Chloride	**3.66**	**3.00**	**45.3**	**23.7**	1.12 J	1.04 J	**6.22**	**2.32**	**2.33**	**3.34**	**36.4**	1.94 J	nse	**250**	nse
Fluoride	< 0.099	< 0.099	< 0.099	0.49 J	0.452 J	< 0.099	0.568 J	0.523 J	< 0.099	0.551 J	0.506 J	< 0.099	**4**	nse	nse
Phosphorus	< 0.00717	< 0.0143	**0.023**	**0.89**	**0.041**	< 0.00717	**0.221**	**0.031**	< 0.00717	**0.092**	0.008 J	**0.0710**	nse	nse	nse
Silica (as SiO_2)	**4.99**	2.01 J	**6.46 I, K**	**7.92**	**4.81 E**	**7.00**	**4.46 E**	**6.60 E**	**4.74 E**	**4.49 E**	**6.29 E**	7.18 J	nse	nse	nse
Sulfate (as SO_4)	**12.5**	**6.33**	0.712 J	**2.09**	**5.70**	**10.4**	**4.18**	**2.78**	**6.08**	**3.16**	**3.33**	1.37 J	nse	**250**	nse
Sulfide	< 0.600	< 0.60	< 0.60	< 0.60	< 0.60	< 0.60	< 0.6	< 0.6	< 0.6	**1.0**	< 0.6	< 0.6	nse	nse	nse
pH (SU)	**4.94**	**5.78**	**3.78**	**5.12**	**6.71**	**5.39**	**6.54**	**6.87**	**5.59**	**6.99**	**6.35**	**6.51**	nse	**6.5-8.5**	nse
Total Dissolved Solids (TDS)	< 18.0	**30.0**	**44.0**	**48.0**	**48.0**	**26.0**	**70.0**	**64.0**	**20.0**	**20.0**	**84.0**	**114 K**	nse	**500**	nse
Total Suspended Solids (TSS)	< 1.60 G	**8.67 G**	< 1.60 G	**96.0 G**	**12.4 G**	**3.60 G**	**11.0**	**4.80**	< 1.60 G	**4.80 G**	< 1.60 G	**7.00**	nse	nse	nse
Alkalinity (mg $CaCO_3$/L)	--														
Alkalinity, Bicarbonate (calculated)	< 9.24	9.50 J	< 9.24	< 9.24	**75.4**	< 9.24	14.3 J	**78.4**	< 9.24	**67.9**	**25.2**	**55.4**	nse	nse	nse
Alkalinity, Carbonate (calculated)	< 9.24	< 9.24	< 9.24	< 9.24	< 9.24	< 9.24	< 9.24	< 9.24	< 9.24	< 9.24	< 9.24	< 9.24	nse	nse	nse
Alkalinity, Hydroxide	< 20.0	< 20.0	< 20.0	< 20.0	< 20.0	< 20.0	< 20.0	< 20.0	< 20.0	< 20.0	< 20.0	< 20.0	nse	nse	nse
Alkalinity, Total	< 20.0	< 20.0	< 20.0 F	< 20.0 F	**75.4**	< 20.0	< 20.0	**78.4**	< 20.0	**67.9**	**25.2**	**55.4**	nse	nse	nse
Gas (%)															
Hydrogen (H_2)	ND	ND	ND	ND	ND	ND	ND	ND	ND	ND	ND	ND	na	na	nse
Argon (Ar)	**1.3**	**1.55**	**1.49**	**1.01**	**1.85**	**1.55**	**1.62**	**1.62**	**1.48**	**1.61**	**1.39**	**1.66**	na	na	nse
Oxygen (O_2)	**22.38**	**2.94**	**9.23**	**17.67**	**10.45**	**10.92**	**6.96**	**15.61**	**28.31**	**18.83**	**22.98**	**1.38**	na	na	nse
Carbon Dioxide (CO_2)	**14.8**	**21.78**	**24.82**	**3.91**	**7.70**	**8.72**	**17.80**	**11.00**	**6.69**	**10.31**	**17.30**	**22.21**	na	na	nse
Nitrogen (N_2)	**61.52**	**73.72**	**64.45**	**77.41**	**79.99**	**78.81**	**73.60**	**71.76**	**63.5**	**69.25**	**58.32**	**74.74**	na	na	nse
Carbon Monoxide (CO)	ND	ND	ND	ND	ND	ND	ND	ND	ND	ND	ND	ND	na	na	nse
Methane (C_1)	**0.0013**	**0.0082**	**0.0116**	**0.0030**	**0.0041**	**0.0011**	**0.0130**	**0.0100**	**0.00080**	ND	**0.002**	**0.005**	na	na	nse
Ethane (C_2)	ND	ND	ND	ND	ND	ND	ND	ND	ND	ND	ND	ND	na	na	nse
Ethylene (C_2H_4)	**0.0008**	ND	**0.0011**	ND	ND	ND	ND	ND	ND	ND	ND	ND	na	na	nse
Propane (C_3)	ND	ND	ND	ND	ND	ND	ND	ND	ND	ND	ND	ND	na	na	nse
Propylene (C_3H_6)	ND	ND	ND	ND	ND	ND	ND	ND	ND	ND	ND	ND	na	na	nse
Iso-butane (iC_4)	ND	ND	ND	ND	ND	ND	ND	ND	ND	ND	ND	ND	na	na	nse
N-butane (nC_4)	ND	ND	ND	ND	ND	ND	ND	ND	ND	ND	ND	ND	na	na	nse
Iso-pentane (iC_5)	ND	ND	ND	ND	ND	ND	ND	ND	ND	ND	ND	ND	na	na	nse
N-pentane (nC_5)	ND	ND	ND	ND	ND	ND	ND	ND	ND	ND	ND	ND	na	na	nse
Hexanes (C_{6+})	**0.0021**	**0.0029**	**0.0016**	**0.0004**	**0.0030**	**0.0015**	**0.0026**	**0.0029**	**0.0017**	**0.0036**	**0.0052**	**0.0051**	na	na	nse
Dissolved Gases (mg/L)															
Methane (CH_4)	**0.0003**	**0.0016**	**0.0022**	**0.0034**	**0.0007**	**0.0003**	**0.0025**	**0.0019**	0.0002	< 0.0002	**0.0004**	**0.00095**	nse	nse	**7** [4]
Ethane (C_2H_6)	< 0.0002	< 0.0002	< 0.0002	< 0.0003	< 0.0002	< 0.0002	< 0.0003	< 0.0003	< 0.0002	< 0.0002	< 0.0003	< 0.0002	nse	nse	nse
Propane (C_3H_8)	< 0.0003	< 0.0003	< 0.0003	< 0.0004	< 0.0003	< 0.0003	< 0.0004	< 0.0004	< 0.0003	< 0.0003	< 0.0004	< 0.0003	nse	nse	nse
Dilution Factor															
Helium	**0.76**	**0.79**	**0.81**	**0.11**	**0.83**	**0.73**	**0.85**	**0.86**	**0.76**	**0.83**	**0.85**	**0.84**	nse	nse	nse
Field Readings															
pH (SU)	**5.08**	**5.74**	**1.57**	**5.67**	**6.29**	**4.24**	**6.16**	**6.11**	**4.23**	**5.69**	**4.39**	**5.14**	nse	**6.5-8.5**	nse
Temperature (degrees C)	**14.3**	**10.97**	**15.70**	**11.78**	**13.56**	**13.5**	**11.33**	**11.25**	**15.2**	**13.3**	**10.32**	**10.52**	nse	nse	nse
Specific Conductance (uS/cm)	**57**	**52**	**188**	**117**	**149**	**37**	**61**	**142**	**53**	**148**	**188**	**159**	nse	nse	nse
Total Dissolved Solids (mg/l)	**37**	**34**	**123**	**76**	**90**	**24**	**4.0**	**9.3**	**3.5**	**9.6**	**12.2**	**10.4**	nse	**500**	nse
Oxidation Reduction Potential (ORP)	**293.9**	**150.1**	**304.8**	**160**	**233.1**	**228**	**132.1**	**158.7**	**251.6**	**145**	**241.7**	**38.9**	nse	nse	nse
Dissolved Oxygen (mg/L)	**6.82**	**2.27**	**5.16**	**2.06**	**2.25**	**42.4**	**1.74**	**4.30**	**9.34**	**5.61**	**8.34**	**2.46**	nse	**250**	nse
Turbidity (NTU)	**1.68**	**513**	**3.84**	**173**	**25.1**	**24.8**	**67.8**	**18.5**	**2.47**	**75.3**	**2.75**	**10.1**	nse	nse	nse

Notes:

1. In order to reduce potential for "sediment bias", only dissolved metals results were used when comparing sampling results against groundwater screening criteria.
2. Medium Specific Concentration for groundwater (MSC_{GW}) from the Pennsylvania Land Recycling and Environmental Remediation Standards Act (Act 2) (Tables 1 and 2). Values assume a residential used aquifer with TDS ≤ 2,500 mg/L. MSCs are the November 20, 2021 revised values.
3. Secondary Maximum Contaminant Level (SMCL) under USEPA's Drinking Water Regulation Standard. SMCLs are non-health related guidelines regulating contaminants that may cause aesthetic issues (such as undesireable taste, odor or color) in drinking water.
4. Pennsylvania Department of Environmental Protection has set a methane contamination action level of 7 mg/L.

Bold - Indicates analyte was detected.
"--" Denotes constituent not analyzed.
"nse" Denotes no standard has been established.
"na" Indicates constituent is Not Applicable
< - Analysis has been reported to the Method Detection Level (MDL).
ND - Analyte not detected by Isotech.
J - Detected between the Method Detection Limit (MDL) and the Reporting Limit (RL); therefore, the result is an estimated value.
Indicates an exceedance of a health-based MSC_{GW}
Indicates an exceedance of a cosmetic/aesthetics-based SMCL
Indicates an exceedance of both a health-based MSC_{GW} and SMCL.

Qualifiers

E: A Continuing Calibration Verification (CCV) analyzed with the analytical batch recovered below the acceptance range for th e noted analyte.
F: The Laboratory Control Sample (LCS) analyzed with this preparation batch recovered above the acceptance range for the note d analyte.
G: The Laboratory Control Sample (LCS) analyzed with this preparation batch recovered below the acceptance range for the note d analyte.
I: The spike recovery was below the acceptance range for the Matrix Spike (MS) and/or Matrix Spike Duplicate (MSD) sample ana lyzed with the preparation batch.
L: The noted analyte was detected in the method blank.
K: The RPD result exceeded the quality control limits for the duplicate, Laboratory Control Sample Duplicate (LCSD), or Matri x Spike Duplicate (MSD) sample analyzed with the preparation batch.
L: The noted analyte was detected in the method blank.

TABLE 1
SUMMARY OF LABORATORY ANALYTICAL RESULTS
RESIDENTIAL SURVEY - WATER WELLS
RAGER MOUNTAIN GAS STORAGE AREA
JACKSON TOWNSHIP, CAMBRIA COUNTY, PENNSYLVANIA
EQUITRANS MIDSTREAM CORPORATION

Sample Location:	J Leone WW1	J Leone WW1	J and P Miesko WW1	N and B Twardziak WW1	T and A Jones WW1	D Geisner WW1	S and C James WW1	E and S Ritchey WW1	E and S Ritchey WW2	L Ribarich WW1	J and A Cassol WW1	M Siska WW1	R and M Daum WW1	Groundwater Screening Criteria [1]		
Lab ID:	AXF4925-01	AXF5318-01	AXF4930-01	AXF4928-01	AXF5323-01	AXF5321-01	AXF5329-01	AXF5740-01	AXF5740-02	AXF5737-01	AXF5739-01	AXF5868-01	AXF5881-01	MSC_{GW} [2]	EPA SMCL [3]	Other Screening Criteria
Sample Date:	6/20/2023	6/21/2023	6/20/2023	6/20/2023	6/21/2023	6/21/2023	6/21/2023	6/22/2023	6/22/2023	6/22/2023	6/22/2023	6/23/2023	6/23/2023			
Petroleum Hydrocarbons (mg/l)																
Gasoline Range Organics	< 0.0675	--	< 0.0675	< 0.0675	< 0.0675	< 0.0675	< 0.0675	< 0.0675	< 0.0675	< 0.0675	< 0.0675	< 0.0675	< 0.0675	nse	nse	nse
Metals (mg/l)																
Barium (total)	--	**0.0904**	**0.0526**	**0.114**	**0.199**	**0.0995**	**0.0734**	**0.0407**	**0.0634**	**0.616**	**0.195**	**0.147**	**0.0548**	nse	nse	nse
Barium (dissolved)	**0.0818**	--	**0.0462**	**0.103**	**0.171**	**0.0852**	**0.0654**	**0.0389**	**0.0638**	**0.624**	**0.198**	**0.146**	**0.0483**	**2**	nse	nse
Boron (total)	--	< 0.0565	< 0.0565	< 0.0565	< 0.0565	< 0.0565	< 0.0565	< 0.0565	< 0.0565	< 0.0565	< 0.0565	< 0.0565	< 0.0565	nse	nse	nse
Boron (dissolved)	< 0.0565	--	< 0.0565	< 0.0565	< 0.0565	< 0.0565	< 0.0565	< 0.0565	< 0.0565	< 0.0565	< 0.0565	< 0.0565	< 0.0565	**6**	nse	nse
Cadmium (total)	--	< 0.0016	< 0.0016	< 0.0016	< 0.0016	< 0.0016	< 0.0016	< 0.0016	< 0.0016	< 0.0016	< 0.0016	< 0.0016	< 0.0016	nse	nse	nse
Cadmium (dissolved)	< 0.0016	--	< 0.0016	< 0.0016	< 0.0016	< 0.0016	< 0.0016	< 0.0016	< 0.0016	< 0.0016	< 0.0016	< 0.0016	< 0.0016	**0.005**	nse	nse
Calcium (total)	--	**2.94**	**2.02**	**12.0**	**10.1**	**5.21**	**2.08**	**2.01**	**4.46**	**6.72**	**2.23**	**4.39**	**1.12**	nse	nse	nse
Calcium (dissolved)	**2.66**	--	**1.97**	**12.8**	**9.28**	**4.78**	**2.03**	**1.94**	**4.41**	**6.77**	**2.27**	**5.27**	**0.954**	nse	nse	nse
Iron (total)	--	< 0.185	**1.97**	**0.617**	< 0.185	< 0.185	**6.90 T**	**8.13 T**	< 0.185	**26.6 T**	**10.3 T**	**2.33**	< 0.185	nse	nse	nse
Iron (dissolved)	< 0.185	--	< 0.185	< 0.185	< 0.185	< 0.185	**5.42 T**	**7.63 T**	< 0.185	**26.2 T**	**9.51 T**	**1.96**	< 0.185	nse	**0.3**	nse
Magnesium (total)	--	**1.37**	**2.05**	**2.44**	**1.64**	**2.56**	**1.64**	**1.67**	**1.39**	**2.25**	**1.48**	**2.57**	**0.373**	nse	nse	nse
Magnesium (dissolved)	**1.28**	--	**1.92**	**2.40**	**1.42**	**2.27**	**1.52**	**1.71**	**1.49**	**2.43**	**1.61**	**2.76**	**0.321**	nse	nse	nse
Manganese (total)	--	**0.190**	**0.125**	**0.255**	**0.285**	**0.755**	**1.19**	**1.61**	**0.242**	**1.58**	**1.26**	**1.61**	**0.170**	nse	nse	nse
Manganese (dissolved)	**0.190**	--	**0.0992**	**0.237**	**0.265**	**0.710**	**1.18**	**1.49**	**0.233**	**1.53**	**1.22**	**1.54**	**0.126**	**0.3**	**0.05**	nse
Potassium (total)	--	**0.812**	**0.981**	**1.47**	**1.43**	**0.936**	**0.743**	**0.464**	**0.539**	**1.74**	**1.15**	**0.849**	0.372 J	nse	nse	nse
Potassium (dissolved)	**0.786**	--	**0.994**	**1.44**	**1.27**	**0.897**	**0.719**	**0.451**	**0.543**	**1.80**	**1.14**	**0.946**	**0.412**	nse	nse	nse
Sodium (total)	--	< 0.793	< 0.793	< 0.793	< 0.793	**28.7**	< 0.793	< 0.793	**26.3**	0.942 J	< 0.793	**26.2**	**22.4**	nse	nse	nse
Sodium (dissolved)	< 0.793	--	< 0.793	**1.20**	< 0.793	**26.2**	< 0.793	< 0.793	**26.5**	0.951 J	< 0.793	**26.6**	**21.7**	nse	nse	nse
Strontium (total)	--	0.0175 J	0.0143 J	**0.0201**	**0.0711**	**0.0471**	0.00708 J	0.00536 J	0.0195 J	**0.127**	**0.0241**	**0.0288**	0.00759 J	nse	nse	nse
Strontium (dissolved)	0.018 J	--	0.0154 J	**0.0259**	**0.0674**	**0.0453**	0.00837 J	0.00433 J	0.0185 J	**0.127**	**0.0234**	**0.0285**	0.00535 J	**4**	nse	nse
Sulfur (total)	--	**3.61**	0.3300 J	**0.750**	**0.709**	**3.36**	0.193 LK, J	**1.17**	**4.34**	0.423 J	**0.726**	**0.782**	**3.24**	nse	nse	nse
Wet Chemistry/Other (mg/l)																
Bromide	< 0.072	--	< 0.072	< 0.072	< 0.072	< 0.072	< 0.072	< 0.072	< 0.072	< 0.072	< 0.072	< 0.072	< 0.072	nse	nse	nse
Chloride	1.24 J	--	**2.06**	1.65 J	**2.21**	**48.7**	1.87 J	**2.69**	**44.9**	**28.4**	1.92 J	**59.5**	1.01 J	nse	**250**	nse
Fluoride	< 0.099	--	< 0.099	0.559 J	0.408 J	< 0.099	< 0.099	< 0.099	0.393 J	0.465 J	0.435 J	< 0.099	0.414 J	**4**	nse	nse
Phosphorus	--	< 0.00717	< 0.00717	**0.012**	< 0.00717	< 0.00717	< 0.00717	< 0.00717	< 0.00717	**0.224**	**0.041**	< 0.00717	< 0.00717	nse	nse	nse
Silica (as SiO_2)	**4.50 E**	--	**6.18 E**	**6.18 E**	**5.63**	**5.20 I**	7.18 J	1.82 J	**4.72 I**	2.94 J	2.59 J	1.47 J	**3.71**	nse	nse	nse
Sulfate (as SO_4)	**11.8**	--	1.67 J	**2.91**	**2.44**	**10.5**	1.18 J	**3.98**	**13.8**	1.6 J	**2.82**	**2.54**	**9.78**	nse	**250**	nse
Sulfide	--	< 0.6	< 0.6	< 0.6	< 0.6	< 0.6	< 0.6	< 0.6	< 0.6	< 0.6	< 0.6	< 0.6	< 0.6	nse	nse	nse
pH (SU)	**5.18**	--	**6.24**	**6.65**	**6.37**	**5.37**	**6.34**	**6.32**	**4.83**	**5.75**	**6.20**	**4.02**	**6.74**	nse	**6.5-8.5**	nse
Total Dissolved Solids (TDS)	**52.0**	--	< 18.0	< 18.0	**44.0 K**	**246**	< 18.0	< 18.0	**38.0**	< 18.0	< 18.0	**78.0**	**64.0**	nse	**500**	nse
Total Suspended Solids (TSS)	--	**1.60 L**	**3.60**	**2.40 K**	**4.00 L**	< 1.60 L	**24.0 L**	< 1.60 G, L	< 1.60 G, L	**8.00 G, L**	**3.20 G, L**	**4.40**	**4.40 K**	nse	nse	nse
Alkalinity (mg $CaCO_3$/L)																
Alkalinity, Bicarbonate (calculated)	< 9.24	--	10.3 J	**36.3**	**30.1**	< 9.24	15.50 J	**20.3**	< 9.24	9.54 J	16.9 J	< 9.24	**40.9**	nse	nse	nse
Alkalinity, Carbonate (calculated)	< 9.24	--	< 9.24	< 9.24	< 9.24	< 9.24	< 9.24	< 9.24	< 9.24	< 9.24	< 9.24	< 9.24	< 9.24	nse	nse	nse
Alkalinity, Hydroxide	< 20.0	--	< 20.0	< 20.0	< 20.0	< 20.0	< 20.0	< 20.0	< 20.0	< 20.0	< 20.0	< 20.0	< 20.0	nse	nse	nse
Alkalinity, Total	< 20.0	--	< 20.0	**36.3**	**30.1**	< 20.0	< 20.0	**20.3**	< 20.0	< 20.0	< 20.0	< 20.0	**40.9**	nse	nse	nse
Gas (%)																
Hydrogen (H_2)	ND	--	ND	ND	ND	ND	ND	ND	ND	ND	ND	ND	ND	na	na	nse
Argon (Ar)	**1.44**	--	**1.01**	**1.43**	**1.29**	**1.35**	**1.55**	**1.70**	**1.43**	**1.50**	**1.43**	**1.27**	**1.42**	na	na	nse
Oxygen (O_2)	**25.57**	--	**21.49**	**21.49**	**17.63**	**22.36**	**7.44**	**6.40**	**24.21**	**6.29**	**9.66**	**9.98**	**24.95**	na	na	nse
Carbon Dioxide (CO_2)	**12.74**	--	**2.33**	**16.74**	**26.93**	**21.72**	**18.81**	**16.29**	**13.44**	**20.19**	**20.51**	**28.46**	**11.15**	na	na	nse
Nitrogen (N_2)	**60.25**	--	**75.17**	**60.33**	**54.14**	**54.57**	**72.20**	**75.61**	**60.92**	**71.94**	**68.39**	**60.29**	**62.48**	na	na	nse
Carbon Monoxide (CO)	ND	--	ND	ND	ND	ND	ND	ND	ND	ND	ND	ND	ND	na	na	nse
Methane (C_1)	**0.0017**	--	ND	**0.0027**	**0.0028**	**0.0024**	**0.0019**	ND	ND	**0.0764**	**0.0075**	**0.0014**	ND	na	na	nse
Ethane (C_2)	ND	--	ND	ND	ND	ND	ND	ND	ND	ND	ND	ND	ND	na	na	nse
Ethylene (C_2H_4)	ND	--	ND	ND	ND	ND	ND	ND	ND	ND	ND	ND	ND	na	na	nse
Propane (C_3)	ND	--	ND	ND	ND	ND	ND	ND	ND	ND	ND	ND	ND	na	na	nse
Propylene (C_3H_6)	ND	--	ND	ND	ND	ND	ND	ND	ND	ND	ND	ND	ND	na	na	nse
Iso-butane (iC_4)	ND	--	ND	ND	ND	ND	ND	ND	ND	ND	ND	ND	ND	na	na	nse
N-butane (nC_4)	ND	--	ND	ND	ND	ND	ND	ND	ND	ND	ND	ND	ND	na	na	nse
Iso-pentane (iC_5)	ND	--	ND	ND	ND	ND	ND	ND	ND	ND	ND	ND	ND	na	na	nse
N-pentane (nC_5)	ND	--	ND	ND	ND	ND	ND	ND	ND	ND	ND	ND	ND	na	na	nse
Hexanes (C_{6+})	**0.0028**	--	**0.0007**	**0.0034**	**0.0028**	**0.0024**	**0.0025**	**0.0019**	**0.0017**	**0.0021**	**0.0027**	**0.0009**	**0.0013**	na	na	nse
Dissolved Gases (mg/L)																
Methane (CH_4)	**0.0003**	--	< 0.0002	**0.00057**	**0.00065**	**0.00052**	**0.0004**	< 0.0002	< 0.0002	**0.016**	**0.0016**	**0.0003**	< 0.0003	nse	nse	7 [4]
Ethane (C_2H_6)	< 0.0002	--	< 0.0002	< 0.0003	< 0.0003	< 0.0003	< 0.0003	< 0.0002	< 0.0002	< 0.0002	< 0.0003	< 0.0002	< 0.0003	nse	nse	nse
Propane (C_3H_8)	< 0.0003	--	< 0.0003	< 0.0004	< 0.0004	< 0.0004	< 0.0004	< 0.0003	< 0.0003	< 0.0003	< 0.0004	< 0.0003	< 0.0004	nse	nse	nse
Dilution Factor																
Helium	**0.82**	--	**0.28**	**0.85**	**0.82**	**0.83**	**0.84**	**0.84**	**0.83**	**0.81**	**0.85**	**0.78**	**0.85**	nse	nse	nse
Field Readings																
pH (SU)	**4.12**	**4.3**	**5.54**	**4.37**	**4.72**	**3.55**	**3.92**	**4.92**	**3.73**	**5.00**	**4.73**	**4.69**	**4.63**	nse	**6.5-8.5**	nse
Temperature (degrees C)	**10.02**	**15.01**	**15.16**	**13.01**	**16.52**	**10.8**	**12.85**	**11.29**	**11.25**	**11.28**	**11.41**	**13.23**	**11.50**	nse	nse	nse
Specific Conductance (uS/cm)	**46**	**45**	**36**	**86**	**73**	**198**	**51**	**64**	**203**	**167**	**67**	**239**	**101**	nse	nse	nse
Total Dissolved Solids (mg/l)	**3.0**	**3.0**	**2.3**	**56**	**4.7**	**12.9**	**3.3**	**4.1**	**13.2**	**10.9**	**4.4**	**15.5**	**6.6**	nse	**500**	nse
Oxidation Reduction Potential (ORP)	**155.6**	**243.3**	**180.7**	**244.5**	**225.3**	**307.9**	**240.7**	**122.8**	**161.5**	**133.9**	**113.1**	**220.6**	**236.5**	nse	nse	nse
Dissolved Oxygen (mg/L)	**8.78**	**8.5**	**5.24**	**5.11**	**6.15**	**9.45**	**1.76**	**2.36**	**9.60**	**2.02**	**1.97**	**3.71**	**8.92**	nse	**250**	nse
Turbidity (NTU)	**1.68**	**0.79**	**17.7**	**20.1**	**2.32**	**0.9**	**20.3**	**3.46**	**0.40**	**8.67**	**9.43**	**0.40**	**0.93**	nse	nse	nse

Notes:

1. In order to reduce potential for "sediment bias", only dissolved metals results were used when comparing sampling results against groundwater screening criteria.
2. Medium Specific Concentration for groundwater (MSC_{GW}) from the Pennsylvania Land Recycling and Environmental Remediation Standards Act (Act 2) (Tables 1 and 2). Values assume a residential used aquifer with TDS ≤ 2,500 mg/L. MSCs are the November 20, 2021 revised values.
3. Secondary Maximum Contaminant Level (SMCL) under USEPA's Drinking Water Regulation Standard. SMCLs are non-health related guidelines regulating contaminants that may cause aesthetic issues (such as undesireable taste, odor or color) in drinking water.
4. Pennsylvania Department of Environmental Protection has set a methane contamination action level of 7 mg/L.

Bold - Indicates analyte was detected.
"--" Denotes constituent not analyzed.
"nse" Denotes no standard has been established.
"na" Indicates constituent is Not Applicable
< - Analysis has been reported to the Method Detection Level (MDL).
ND - Analyte not detected by Isotech.
J - Detected between the Method Detection Limit (MDL) and the Reporting Limit (RL); therefore, the result is an estimated value.
Indicates an exceedance of a health-based MSC_{GW}
Indicates an exceedance of a cosmetic/aesthetics-based SMCL
Indicates an exceedance of both a health-based MSC_{GW} and SMCL.

Qualifiers

E: A Continuing Calibration Verification (CCV) analyzed with the analytical batch recovered below the acceptance range for th e noted analyte.
F: The Laboratory Control Sample (LCS) analyzed with this preparation batch recovered above the acceptance range for the note d analyte.
G: The Laboratory Control Sample (LCS) analyzed with this preparation batch recovered below the acceptance range for the note d analyte.
I: The spike recovery was below the acceptance range for the Matrix Spike (MS) and/or Matrix Spike Duplicate (MSD) sample ana lyzed with the preparation batch.
L: The noted analyte was detected in the method blank.
K: The RPD result exceeded the quality control limits for the duplicate, Laboratory Control Sample Duplicate (LCSD), or Matri x Spike Duplicate (MSD) sample analyzed with the preparation batch.
L: The noted analyte was detected in the method blank.

A.12 Microbiological Analysis Reports

Project Report

Well 2244
Microbial Population Analysis of Organisms Associated with the Rager Mountain Gas Storage Failure

Prepared for
Ravi M. Krishnamurthy
Blade Energy Partners

Prepared by:
Elizabeth Summer, PhD
Ecolyse, Inc
11142 Hopes Creek Road
College Station, Texas 77845

Well 2244 MPN and Genetic Analysis

FINAL REPORT

June 20, 2023

Well 2244 Microbiological Analysis: Statement of Findings

Microbiological analysis was conducted on well pad soil, 7" casing OD scale, and annulus fluid samples collected from well 2244 in Feb - March 2023. These results represent the microbial population at the time of sampling. At the time of sampling, APB, SRB/sulfidogens, and IRB could be detected in the scale collected from the OD of the well 2244 7" casing, as well as in annulus fluids originating from the lower ~700' of the well. There was marked vertical distribution of corrosion associated organisms, with casing joint C001 having a population of organisms not typically associated with severe MIC. In contrast, the scale from the lower casing joints as well as annulus fluids from lower parts of the well, contained high levels of the potentially problematic, corrosion-associated organism, Halanaerobium. Because the most problematic organisms were not abundant in samples from the C001 casing joint around the fracture point, these results do not directly implicate MIC in the corrosion event, although a role of MIC was not conclusively eliminated. It should be noted that MIC is nuanced and complex, and there are other mechanisms that were not evaluated in the study, in particular the role of Eukaryotes such as aerobic, acid producing fungi.

The most important findings were:
1. Failure Joint C001A and C001B: APB, IRB, and sulfidogens were present in the scale collected from C001 above and below the failure joint, as determined by MPN. The most abundant organism identified directly on the surface of casing joint C001 was Ralstonia, which is not typically a corrosion associated, as well as unclassified bacteria. Of all the casing joints, C001 had experienced the most perturbations, both because of the leak itself and because of the efforts it took to shutdown the leak, and the impact of these activities on the microbial profile needs to be considered.

2. Lower casing joints C002 to C034: APB, IRB, and sulfidogens were present in scale collected from lower casing joints C002 to C034. These included many spore-forming sulfidogens. 24% of the population on the surface of casing joints C015-C034 was the problematic organism, Halanaerobium.

3. Annulus Fluids: Clear, colorless annulus fluids from the top ~800' of the well contained negligible levels of microorganisms, while the black viscous liquids from the bottom ~700' of the well were enriched (24%) in the problematic organism, Halanaerobium. This indicates that was a clear separation in annulus fluids from the top and bottom of the well, with the most problematic organism primarily located in the bottom of the well. The clear fluids at the top of the well were most likely introduced after the leak.

4. Soils from around the well pad contained sulfidogens, APB, and IRB, however the predominant organisms were different from those in casing scale and annulus fluid samples. For example, the predominant IRB in the soil was Rhodoferax, which was not present in any of the casing or annulus fluid samples. This indicates that the data from casing and annulus fluids were not contaminated by soil

M 979-694-6500 ● F 979-694-6511 ● 11142 Hopes Creek Road ● College Station, Texas 77845 ● www.ecolyse.com

Table of Contents

Well 2244 Microbiological Analysis: Statement of Findings pg 2
Summarized Microbiological Data Results and Analysis pg 4
Well 2244 Population Analysis: Detailed Methods and Results pg 8
Project Results: MPN Culture-Based Bacterial Diversity Analysis pg 11
Project Results: Bacterial Diversity Analysis by Genetic Approaches **pg 15**

Appendix A. List of Samples
Appendix B. Full list of all organisms identified in well 2244 samples
Appendix C. Detailed Methods
Appendix D. References

List of Abbreviations

Abbreviation	Definition
APB	Acid Producing Bacteria
COC	Chain of Custody
DNA	Deoxyribonucleic Acid
GHB	General Heterotrophic Bacteria
g	gram
H_2S	Hydrogen Sulfide
ID	Pipe Inner Diameter
IRB	Iron Reducing Bacteria
KCl	Potassium Chloride
<LOD	Below limit of detection
MIC	Microbiologically Influenced Corrosion
ml	milliliter
MPB	Modified Postgate's B media, for growth of SRB
MPN	Most Probable Number
NACE	National Association of Corrosion Engineers
NRB	Nitrate Reducing Bacteria
OD	Pipe Outer Diameter
O&G	Oil and Gas
OTU	Operational Taxonomic Unit
PBS	Phosphate Buffered Saline
PRD	Phenol Red Dextrose Media (for determination of APB)
qPCR	Quantitative polymerase chain reaction
RCA	Root Cause Analysis
Sp.	Species, the most narrowly defined taxa or taxonomic grouping
SRB	Sulfate Reducing Bacteria, these produce H2S.

Summarized Microbiological Data Results and Analysis

1. Well 2244 Failure Joints C001A and C001B

Sample Collection Notes: Scale samples were collected from the surface of C001A (above the failure point) and C001B (below the failure point) in early March, 2023. **See Table 1 for list of samples.** Between the time of casing failure in November 2022 and the time of sampling in early March 2023, the C001 casing had undergone significant manipulations. These manipulations were unavoidable as they were part of the well shutdown process, and which included addition of compounds and chemicals, as well as physical treatments . Because of this, data from C001A and C001B need to be considered with this in mind.

C001 outer surface was markedly flaky, with kg of material could have easily been removed for analysis. As microbial quantification data is provided in "cells per g", the gross amount of bacteria present on the surface of the failure casing joints is quite a bit higher than in lower casing joints from the same well.

a. **Well 2244 Failure Joint C001A and C001B MPN Data Interpretation**: **See Tables 2, 3, and 4**.
   i. MPN is the "NACE Standard" culture-based population analysis.
   ii. MPN Data reveled that the scale from the OD of 7" casing joints C001A and C001B both contained significant populations of APB, GHB, SRB, and IRB.
   iii. Typical levels were GHB (~10^6) APB (~10^5) SRB (~10^3) IRB (~10^2) cells per g.
   iv. Values for each population were higher by up to 2 log orders in C001A than in C001B scale
   v. Populations of microorganisms containing APB and SRB in particular are consistent with known cases and mechanisms of MIC .
   vi. While consistent with MIC, MPN data alone is insufficient to make an MIC diagnosis, especially as levels were not particularly high.
   vii. Making a confirmed diagnosis of MIC requires more supporting evidence then just MPN data.

b. **Well 2244 Failure Joint C001A and C001B qPCR Data Interpretation**. **See Tables 5**
   i. qPCR is a quantitative molecular approach to quantify organisms in a sample that relies on DNA isolation from sample material.
   ii. Results of qPCR analysis of DNA isolated from C001A and C001B, and well 2244 scale samples in general, were variable, unlike results for the liquid and soils samples as well as all other samples collected from other locations within the Rager Mountain complex (**See Table 5 and accompanying reports for wells 2248, 2251, and the Compressor Station**). The reason for this is unknown but is possible due to most bacteria being in the form of spores, and not vegetative cells in the sample, as it is more difficult to isolate DNA from spores especially when combined with metal scale. Alternatively, there might have inhibition of DNA extraction by compounds introduced into the well during leak control.
   iii. Where data was obtained, overall, for most samples from Rager Mountain, qPCR indicated a microbial load from 1 to 3 log orders higher than what was detected by MPN analysis.

c. Well 2244 Failure Joint C001A and C001B Metagenomic Population Analysis Interpretation. See Tables 6, 7, 8, 9, 10, 11, 12, and Appendix B)
   i. The population profile was determined directly from C001B scale. This population was dominated by biodegrading organism, Ralstonia (51%) and unclassified organisms (31%).
   ii. Sulfidogens were identified in the sample, however no IRB were. Because MPN results indicated IRB levels were several log orders less then GHB levels, higher sequence coverage might be needed to achieve a >99% chance of seeing IRB in the dataset.
   iii. The population of bacteria from casing joints C001A and C001B also elucidated by analysis of organisms in the MPN cultures established from scale from these casing joints.
   iv. Over 97% of the viable, culturable organisms were found to be spore-forming genera, including Bacillus, Clostridium, Geosporobacter, and Desulfosporosinus.
   v. The predominant IRB was determined to be spore-forming Geosporobacter
   vi. Predominant sulfidogens in the sample include spore forming Desulfosporosinus and Desulfitobacterium.

vii. The predominance of spore-forming organisms in the culture data set suggests that bacteria in the sample were in the form of spores, which are resistant to DNA isolation methods, especially when combined with high levels of metal scale.
viii. The predominant acid-producing genera identified was Trichococcus, however it is likely that the Bacillus isolate growing in the PRD culture media is also an acid forming bacteria, a trait present in a few, but not the majority, of Bacillus strains.
ix. Halanaerobium, a known corrosion-associated organism, whose abundance is elevated in the annulus fluid samples, was present in a very low abundance (0.002% of the population) in both the cultured and uncultured dataset.

d. **Well 2244 Failure Joint C001A and C001B Conclusions of Population Analysis**
i. Scale samples from failure joints C001A and C001B contained APB, SRB, and IRB, and these phenotypes were correlated to organisms identified genetically in the samples.
ii. Many of these were from spore-forming genera.
iii. The organism of most concern, Halanaerobium, which was elevated in lower casing joints and in the annulus fluids, was present only at extremely low levels on the surface of C001. However, it should be considered that levels were impacted by the well shutdown process and / or that levels could fluctuate throughout the year based on changing water levels.
iv. At the time of sampling, the microbial profile of C001A and C001B contained some organisms associated with MIC, notably APB and SRB, but additional data would be needed to link these with the corrosion event.
v. This data needs to be interpreted in the context of the manipulations the casing experienced during the well shut-down process, which may have greatly impacted the microbial population.

2. Well 2244 Lower Casing Joints C002 to C034

Sample Collection Notes: Casing Joints C002 to C034 were extracted from well 2244 between 3/9/23 and 3/11/23 and scale was removed for analysis. Most of the surface of the lower joints showed little evidence of corrosion, and only minimal amount of material could be removed for analysis. More solids and scale was accumulated on and around the lips of the collar. An effort was made to collect and analyze material separately from the “collar” and the “body” of the casing joints, although this distinction turned out to not be important to the final conclusions of the project.

a. Well 2244 Lower Casing Joints C002 to C034 MPN Interpretation: See Tables 2, 3, and 4.
i. MPN Data reveled that the scale from the OD of all 21 samples collected from well 2244 7” lower casing Joints C002 to C034 contained significant, but not excessive, populations of APB, GHB, SRB, and IRB.
ii. Overall, levels of GHB > APB > SRB > IRB.
iii. Lowest values were obtained for the lowest casing joints, C023 to C034
iv. Populations of microorganisms containing APB and SRB in particular are consistent with known cases and mechanisms of MIC
v. Many of the lower casing joints showed little evidence of corrosion, and had minimal scale that could be removed.

b. Well 2244 Lower Casing Joints C002 to C034 qPCR Interpretation. See Tables 5
i. qPCR is a quantitative molecular approach to quantify organisms in a sample that relies on DNA isolation from sample material.
ii. Similar to results of qPCR analysis of DNA isolated from C001, results from well 2244 lower casing joints were variable, unlike results for the liquid and soils samples as well as all other samples collected from other locations within the complex (**See Table 5**). The reason for this is unknown.
iii. The reason for qPCR failure is possibly due to the presence of a high concentration of spore-forming bacteria in the samples, based on analysis of the organisms that grew up in the MPN culture vials. Spores mixed with a large excess of metal scale presents additional challenges to DNA isolation and analysis.

iv. Overall, for most samples from Rager Mountain, qPCR indicated a microbial load from 1 to 3 log orders higher than what was detected by MPN analysis.
v.

c. Well 2244 Lower Casing Joints C002 to C034 Metagenomic Population Analysis Interpretation. See Tables 6, 7, 8, 9, 10, 11, 12, and Appendix B)

i. The population of bacteria from lower casing joints C002 to C0234 that were growing in the MPN culture medias was elucidated using a 16S amplicon metagenomic approach.
ii. Upwards of 70% of the organisms were novel, unclassified organisms
iii. The most prevalent of the unclassified organisms was classified as a member of Phylum Firmicutes, Class Clostridia. This class includes primarily anaerobic and often spore-forming organisms. Members of class Clostridia are quite divers, and includes sulfidogens, IRB, pathogens, GHB, APB. Additional work is required to elucidate the metabolic capacity of this organism from well 2244, although it is tempting to speculate it is a spore-forming sulfidogen based on its presence in the MPB culture bottles that tested positive for sulfidogenisis.
iv. Similar to C001, predominant IRB was determined to be spore-forming Geosporobacter
v. Similar to C001, predominant sulfidogens in the samples included spore forming Desulfosporosinus and Desulfitobacterium.
vi. The predominant acid-producing genera identified was Trichococcus, although Acetobacterium was also present in the cultures.
vii. Halanaerobium, a known corrosion-associated organism, whose abundance is elevated in the annulus fluid samples, was present at a low abundance in the cultured dataset. Halanaerobium contributed to over 43% of the population of bacteria in the C023 – C034 collar raw sample dataset, and 5% of the collar material from C015 to C022.

d. Well 2244 Lower Casing Joints C002 to C034 Conclusions of Population Analysis

i. As was seen for C001, the lower casing joints all contained significant levels of APB, SRB, and IRB, and these phenotypes were correlated to organisms identified genetically in the samples.
ii. Many of these were from spore-forming genera.
iii. The organism of most concern, Halanaerobium, was present at a very high level, 43%, in the material accumulating on the collar of lower casing joints casing joints C023 – C034.
iv. The presence of elevated levels of Halanaerobium is associated with corrosion in many O&G operations.
v. Because the Halanaerobium was not prevalent in the upper casing joints, it isn't obvious how the presence of Halanaerobium in the lower portions of the well is related to the failure event.

3. Well 2244 Annulus Fluids Summary of Results

Sample Collection Notes: Annulus fluids, from between the 7" and 9 5/8" casing, were pumped out of well 2244 on 3/8/23. To do this, water was pumped in from a source tank to push the annulus fluids out. Liquids were collected in 500 ml bottles, such that a sample was taken every 0.51 to 2.97 barrels of fluids, corresponding to a depth of 0 to 1675 ft. The first 11 samples that were collected, corresponding to the top most 700 ft of the well, were very clear and colorless. In contrast, samples collected from below this, down to a depth of around 1475 ft, consisted of strikingly black sludge like material, with an aroma similar to materials from anaerobic digestors. The last sample, at a depth of around 1675 ft, was lighter, suggesting that the bolus of dark black liquid was ending. The excess waters flowed into a holding tank, and the next day this tank was covered by a thick layer of foam that appeared to be microbial in composition. Samples of clear and black annulus fluids, along with the input waters used to pump out the annulus fluids, as well as material from the output holding tank, were analyzed.

e. Well 2244 Annulus Fluids MPN Interpretation: See Tables 2, 3, 4

i. MPN is the "NACE Standard" culture-based population analysis.
ii. MPN Data reveled that water from the input tank being used to push annulus fluids out had almost no bacteria.

iii. MPN Data reveled that the clear annulus fluids, from the top ~700 ft of the well, contained negligible levels of bacteria, less than 10^3 viable bacteria per ml for the most abundant type, GHB.
iv. The black annulus fluids contained significant, but not excessive, populations of APB, GHB, SRB, and IRB.
v. The levels of each type were on the order of GHB (10^4) APB (10^3) SRB (10^3) IRB (10^3) viable bacteria per ml.

f. Well 2244 Annulus Fluids qPCR Interpretation. See Tables 5

i. qPCR is a quantitative molecular approach to quantify organisms in a sample that relies on DNA isolation from sample material.
ii. qPCR results correlated well with MPN results. The clear annulus fluids from the top ~700 ft of the well contained negligible bacteria, while the black annulus fluids and output tank had 2 to 3 log orders higher microbial load then was indicated by MPN analysis.
iii. Taken together, these results indicate that microbial activity at the top of the well was several log orders reduced as compared to lower portions of the well, and the transition from low microbial activity to high microbial activity took place around the 700 foot depth mark.

g. Well 2244 Annulus Fluids Metagenomic Population Analysis Interpretation. See Tables 6, 7, 8, 9, 10, 11, 12, and Appendix B)

i. Population profiles for the black annulus fluids and output tank were elucidated from DNA isolated from the raw samples.
ii. The profiles of the 3 raw samples that were elucidated were nearly identical, suggesting liquids had a fairly homogenous population. .
iii. 35% of the organisms in the sample were unclassified organisms, of which over half originated from an unclassified archaea.
iv. Similar to the scale samples, the predominant IRB was determined to be spore-forming Geosporobacter
v. Halanaerobium, a known sulfidogenic corrosion-associated organism, contributed to 24% of the population of bacteria in the annulus fluid.
vi. While Halanaerobium was the most abundant sulfidogen, the annulus fluids contained over 28 sulfidogenic species.

h. **Well 2244 Annulus Fluids Conclusions of Population Analysis**

i. The microbial population of the annulus of well 2244 showed a pronounced and distinct vertical distribution.
ii. Fluids from the top ~ 700 ft of the well showed little microbial activity. These fluids were clear and colorless. Both MPN data and qPCR data indicated a very low microbial load.
iii. The bottom ~800 ft of the sample depth, in contrast, had a noticeable microbial population, with the liquids being black and sludge-like, with the appearance of anaerobic digestor materials.
iv. The black liquids from below 700 foot contained significant levels of APB, SRB, and IRB, and these phenotypes were correlated to organisms identified genetically in the samples.
v. Halanaerobium, was the most abundant organism in the annulus fluids, at 24% of the population.
vi. The presence of elevated levels of Halanaerobium is associated with corrosion in O&G operations.

Well 2244 Population Analysis: Detailed Methods and Results

Well 2244 Sample Information

- For well 2244, 46 sample sets were collected and analyzed.
- These samples included:
    - Well 2244 pad area soil pre-samples were collected on Feb 16 2023 Soil" refers to rock, dirt, and mud collected around wellsite
    - Well 2244 wellhead master valve and tree had been previously removed from the well and stored in the Compressor Station. The wellhead tree and master valve ID scale, grease, and solids samples are indicated by a "W0" and were collected on 3/3/23
    - Well 2244 casing joint C001 was stored in the compressor station. C001 OD scale samples were collected from the surface of C001A (above the failure point) and C001B (below the failure point) March, 5 and March 6 2023. **See Table 1 for list of samples.** The C001A and C001B sections showed extreme evidence of corrosion, as they were covered with easily removable metal flakes and scale. While a lot of material could be collected, it needs to be considered that the area around the failure had experienced a great deal of manipulations to plug the leak. Because of this, data from C001A and C001B need to be considered with this in mind.
    - 7" casing joints C002 to C034 OD scale samples were collected off the casing surface as they were extracted from the well, between 3/3/23 and 3/6/23
        - OD scale samples were further categorized as those originating around the collar and those on the long body of the casing joint.
        - Note that rather than separating casing joints at the collar, the casing joints were cut about 2' above each collar
        - Collar sample originated predominantly from solids materials accumulated on the lip of the collar.
    - Annulus liquids from between the 7" and 9 5/8" casing, pumped out on 3/8/23.
        - Annulus liquids were pumped to a depth of 1675 ft
        - In order to push liquids out of the well, clear fresh water from an injection tank were pumped into the well.
        - Waters were pumped into a holding tank
        - At regular intervals, as defined by pump strokes, a 500 ml bottle was filled with liquids
        - In all 20 samples were collected during the pumping process
        - The first 11 samples, corresponding to regular intervals down to ~700', were extremely clear and colorless.
        - The next 8 samples, corresponding to regular intervals down to around 1500', were extremely black and viscous, similar in appearance and aroma to anaerobic digestor material.
        - The final sample was clearer than the previous samples, suggesting that it was mixed annulus fluids and injection tank fluids.
        - In addition to the 20 annulus fluid samples, liquid from the output tank where all the pumped out fluids were mixed, as well as the clean input tank waters, were collected and analyzed.
- "Scale" refers to all solids scraped off of the casing surface. These include metal flakes.
- "Grease" and "Slime" were collected but were of no relevance to the larger project conclusions.
- Table 1 provides an overview of well 2244 samples
- Appendix A provides more details on each sample.

Table 1. Well 2244 Sample Overview					
Pool	Sample Date	Well	Sample Description	Type	Quantity
1	2/16/23	2244	Well 2244 Soils around well pad	Soil	211.0 g
4	3/3/23	2244	Well 2244 W06 W03 Master Valve ID Solids	S	34.7 g
5	3/3/23	2244	Well 2244 W02 Crown Valve ID Solids	S	22.5 g
6	3/3/23	2244	Well 2244 W04 W05 Wing Valve ID Solids	S	16.0 g
7	3/3/23	2244	Well 2244 W04 W05 Wing Valve ID Grease	G	73.0 g
8	3/5/23	2244	Well 2244 7" C001 OD Scale below seal ring	S	137.7 g
9	3/5/23	2244	Well 2244 7" C001A OD Scale	S	7.2 g
10	3/5/23	2244	Well 2244 7" C001A OD Scale	S	10.6 g
11	3/5/23	2244	Well 2244 7" C001A scale below slip	S	11.4 g
12	3/6/23	2244	Well 2244 7" C001B OD Scale	S	14.9 g
13	3/6/23	2244	Well 2244 7" C001B OD Scale	S	33.7 g
14	3/6/23	2244	Well 2244 7" C001B OD Scale	S	26.0 g
15	3/6/23	2244	Well 2244 7" C001B OD Scale	S	11.7 g
16	3/6/23	2244	Well 2244 7" C001B OD Scale	S	23.1 g
17	3/8/23	2244	Well 2244 Annulus Fluid Clear – 0 to 89’	L	2000 ml
18	3/8/23	2244	Well 2244 Annulus Fluid Clear– 89 to 406’	L	2000 ml
19	3/8/23	2244	Well 2244 Annulus Fluid Clear– 406 to 706’	L	1500 ml
20	3/8/23	2244	Well 2244 Annulus Fluid Black– 706 to 1106’	L	2000 ml
21	3/8/23	2244	Well 2244 Annulus Fluid Black– 1106 to 1475’	L	2000 ml
22	3/8/23	2244	Well 2244 Annulus Fluid Gray -1475-1675’	L	500 ml
23	3/8/23	2244	Well 2244 Water from Injection Tank	L	500 ml
24	3/8/23	2244	Well 2244 Overshot Material Solids	S	96.0 g
25	3/8/23	2244	Well 2244 7" C001C OD Scale	S	96.1 g
26	3/8/23	2244	Well 2244 7" C001C OD Scale	S	28.7 g
27	3/9/23	2244	Well 2244 Fluids Foam Output Tank	L	500.0
28	3/9/23	2244	Well 2244 7" C002 to C003 OD Scale	S	81.4 g
29	3/9/23	2244	Well 2244 Centralizer	S	59.2 g
30	3/9/23	2244	Well 2244 7" C004 OD Scale, all	S	34.4 g
31	3/9/23	2244	Well 2244 7" C005 OD Scale, all	S	63.2 g
32	3/9/23	2244	Well 2244 7" C006, to C007 Body Scale	S	17.3 g
33	3/9/23	2244	Well 2244 7" C006, to C007 Collar Scale	S	70.0 g
34	3/9/23	2244	Well 2244 7" C008 to C014 Body Scale	S	14.8 g
35	3/9/23	2244	Well 2244 7" C008 to C014 Collar Scale	S	178.6 g
36	3/9/23	2244	Well 2244 7" C015 to C022 Body Scale	S	14.0 g
37	3/9/23	2244	Well 2244 7" C015 to C022 Collar Scale	S	170.7 g
38	3/11/23	2244	Well 2244 7" C023, C024 Body Scale	S	13.2 g
39	3/11/23	2244	Well 2244 7" C023, C024 Collar Scale	S	28.2 g
40	3/11/23	2244	Well 2244 7" C025, C026, C027 Body Scale	S	5.3 g
41	3/11/23	2244	Well 2244 7" C025, C026, C027 Collar Scale	S	29.9 g
42	3/11/23	2244	Well 2244 7" C028 to C034, Body Scale	S	8.4 g
43	3/11/23	2244	Well 2244 7" C028 Collar Scale	S	7.6 g
44	3/11/23	2244	Well 2244 7" C029 Collar Scale	S	23.8 g
45	3/11/23	2244	Well 2244 7" C030 to C034, Collar Scale	S	77.2 g
46	3/12/23	2244	Well 2244 9 5/8 ID scrape 0-200 ft Scale	S	355.2 g
47	3/13/23	2244	Well 2244 9 5/8 ID scrape 0-1475 ft Scale	S	44.5 g
48	3/11/23	2244	Well 2244 "slime" 7" C029	S	11.9 g

Well 2244 Samples for Microbial Analysis. Sample types are Soil, L liquid, S solid, G grease. Soil refers to dirt and rocks collected from the well pads. Scale refers to dry metal flakes and solids removed from the surface of the casing joints. For scale samples from well 2244 7” casing, samples originating from the “Body” and “Collar” of each joint were collected and analyzed separately. Body refers to the majority of the length of casing (~36’) starting around 1’ below the collar. Collar refers to scale accumulated on the collar lip and surface, along with some scale above and below the collar. Liquids Samples details: Liquids are the annulus fluid samples that were pushed out of the well on 3/8/23. The approximate depth in the well was estimated from the flow rate and annulus volume. There were two distinct types of annulus fluids: clear / colorless liquids from the shallow parts of the well and black / viscous / aromatic fluids from the deeper part of the well. The ”water from injection tank” was a sample of the water being pumped into the well in order to push liquids out of annulus. “Fluids and foam: output tank” was a sample of the microbial foam and liquid growing the surface of the collection tank were all the liquids being pushed out of well 2244 were being mixed, Amount of material collected is provided in ml or g. Appendix A contains more details on each sample.

Methods Used for Microbial Population Profiles Evaluation

- Testing microbial populations for corrosion potential is based on recommendations and guidelines established by NACE (National Association of Corrosion Engineers),.
- NACE Standard Test Methods include those described in the following documents:

NACE ID	Item	Standard Test Method
TM0194	21224	Field Monitoring of Bacterial Growth in Oil and Gas Systems
TM0212	21260	Detection, Testing, and Evaluation of Microbiologically Influenced Corrosion on Internal Surfaces of Pipeline
TM0106	21248	Detection, Testing, and Evaluation of Microbiologically Influenced Corrosion (MIC) on External Surfaces of Buried Pipeline

- NACE recognizes that the subsurface and infrastructure systems being sampled vary greatly with respect to accessibility, as well as physical, chemical, and biological traits, and thus it is impossible to give an exact list of methods or protocols that must be followed absolutely.
- Guidelines must be adapted to any given situation and system.
- In recognition of these guidelines, a conservative, combined approach was adopted for the Rager Mountain project.
- The approach used included the most traditional and well-established method (triplicate MPN set up in standard medias for APB, SRB, IRB and GHB) method, along with two more advanced approaches (qPCR and amplicon metagenomics)
- **Interpretation of results:** Microbiological data does not provide simple "action level" "cut-off concentrations" data. MIC is a highly complex problem, impacted not only by the numbers and extreme diversity of organisms, but their metabolic activity levels, and fluctuations in environmental physio-chemical conditions (for example, nutrients, temperature, water levels, water circulation, chemical treatments).
- As noted in **NACE TM0194-94 statement of interpretation of MPN data:**

1.1.8 The simple presence of bacteria in a system does not necessarily indicate that they are causing a problem. In addition, bacterial populations causing problems in one situation, or system, may be harmless in another. Therefore, "action" concentrations for bacterial contamination cannot be given. Rather, bacterial population determination are one more diagnostic tool useful in assessing oilfield problems.

Project Results: MPN Culture-Based Bacterial Diversity Analysis

1. Triplicate, Culture -Based MPN Method

MPN stands for "Most Probably Number" and is a culture-based method for the quantification of specific types of bacteria in a sample. The data generated is in terms of "bacteria per ml" or "bacteria per g" of sample, where "bacterial types" are members of a phenotypic group rather than a taxonomic group. The identity of the organisms quantified is based on the use of the selective indicator artificial growth media used to set up the assay. Indicator medias contain a substrate that undergoes a visible chemical change when certain types of bacteria grow in them, for example, addition of a pH indicator will provide strong visual evidence for the growth of acid producing bacteria that have dropped the media pH. Selective medias contain substrates and conditions that promote the growth of certain types of bacteria, for example, anaerobic conditions and addition of sulfate promotes the growth of sulfate reducing bacteria.

MPN Method Advantages

- Minimal sample manipulation is required to set up assay.
- Easy to interpret results
- Low-tech and easy to set up in the field.
- Determines the number of live, culturable bacteria in the sample.
- Provides experimental phenotypic data.
- Traditional method, recommended by NACE as a standard method.
- Historical approach that is widely used in throughout the industry.

- Can be used for the analysis of anaerobic organisms..

Figure 1 shows what the indicator, selective medias used in this study look like:

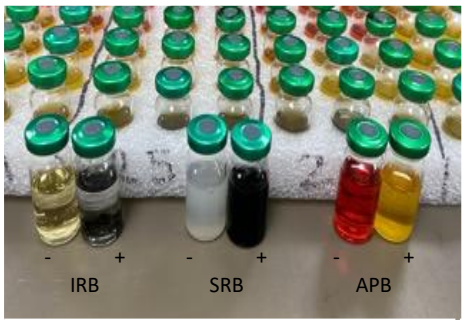

A. How + plus and - minus bacterial growth appears in 3 selective indicator medias used for this project: IRB (iron reducing bacteria), MPB (SRB: sulfate reducing bacteria), PRD (APB: acid producing bacteria)

B. Triplicate MPN set-up for 4 samples (samples 24, 25, 26, 27). There are 3 dilution series columns set up in parallel for each sample, so 24 media bottles are inoculated per sample.

Figure 1. MPN microbial culture vials.

MPN Method Disadvantages

- There are well-known limitations inherent in culture-based analysis,
- **NACE TM0194 describes some of these limitations (direct quote):**
  - *3.1.1 Bacterial culturing in artificial growth media is accepted as the standard technique for the estimation of bacteria numbers. However, users should be aware of the limitations of the culture technique:*
  - *3.1.1.1 Any culture medium grows only those bacteria able to use the nutrients provided.*
  - *3.1.1.2 Culture medium conditions (pH, osmotic balance, redox potential, etc.) prevent the growth of some bacteria and enhance the growth of others.*
  - *3.1.1.3 Conditions induced by sampling and culturing procedures, such as exposure to oxygen, may hamper the growth of strict anaerobes.*
  - *3.1.1.4 Only a small percentage of the viable bacteria in a sample can be recovered by any single medium; i.e., culture media methods may underestimate the number of bacteria in a sample.*
  - *3.1.1.5 Some bacteria cannot be grown on culture media at all.*

Well 2244 – Culture-Based MPN Enumeration of APB, GHB, SRB, and IRB

- MPN analysis was set up with 46 well 2244 sample pools, in 3 medias each (PRD, MPB, IRB)
- These 3 medias provide quantitative data for 4 metabolic categories: APB, GHB, SRB, IRB
- As per NACE standards, readings were taken weekly for 4 weeks.
- Resulting values were converted to microbial cells per g or ml of starting material, after accounting for the initial dilution of the sample used to inoculate the first bottle in each dilution series.
- Resulting values were converted to microbial cells per g or ml of starting material, after accounting for the initial dilution of the sample used to inoculate the first bottle in each dilution series.
- Table 2 shows the results of MPN analysis, after 4 weeks of growth, for all 46 well 2244 samples.

Table 2. Well 2244: Results of MPN Analysis							
#	Well	Sample Description	Type	APB	GHB	IRB	SRB
2.A Well 2244 Well site soils and Well head tree samples							
1	2244	Well 2244 Soils	S	6E+07	9E+08	3E+07	3E+04
7	2244	Well 2244 Tree Grease W04 W05	G	2E+01	2E+03	5E+00	6E+00
5	2244	Well 2244 Tree Scale W02 Crown Valve Solids	S	3E+01	5E+01	4E+00	<LOD
6	2244	Well 2244 Tree Scale W04 W05 Solids	S	5E+02	9E+02	<LOD	<LOD
4	2244	Well 2244 Tree Scale W06 W03 Master Valve Solids	S	2E+01	2E+02	7E+00	4E+01
2.B Well 2244 7' Casing OD Scale samples							
9	2244	Well 2244 Scale 7" C001A OD above failure	S	4E+03	1E+04	2E+02	7E+01
10	2244	Well 2244 Scale 7" C001A OD above failure	S	9E+05	2E+07	2E+04	2E+04
8	2244	Well 2244 Scale 7" C001A OD below seal ring	S	6E+05	3E+07	3E+03	6E+04
11	2244	Well 2244 Scale 7" C001A Scale from Slips	S	2E+05	1E+06	2E+04	2E+04
12	2244	Well 2244 Scale 7" C001B OD 1' to 12' from cut end	S	3E+05	3E+05	3E+03	2E+04
15	2244	Well 2244 Scale 7" C001B OD 102" to 117" from cut end	S	2E+04	3E+04	8E+02	4E+03
16	2244	Well 2244 Scale 7" C001B OD 12' to 14' from cut end	S	7E+04	7E+04	7E+01	2E+03
13	2244	Well 2244 Scale 7" C001B OD 68" to 84 " from cut end	S	2E+04	2E+04	9E+01	1E+03
14	2244	Well 2244 Scale 7" C001B OD 84" to 94" from cut end	S	4E+04	2E+04	4E+02	9E+03
25	2244	Well 2244 Scale 7" C001C OD solids 0 - 5'	S	3E+04	3E+04	3E+02	6E+03
26	2244	Well 2244 Scale 7" C001C OD solids 5' - 12'	S	1E+04	2E+05	2E+02	7E+03
24	2244	Well 2244 Scale 7" C001C Overshot Material	S	8E+04	8E+04	8E+02	6E+03
28	2244	Well 2244 Scale Body and Collar OD 7" C002 C003	S	3E+04	3E+04	1E+02	9E+02
29	2244	Well 2244 Scale Centralizer OD 7" C004	S	8E+03	5E+05	1E+02	5E+02
30	2244	Well 2244 Scale 7" C004 OD All	S	1E+04	1E+05	8E+01	1E+03
31	2244	Well 2244 Scale 7" C005 OD All	S	1E+04	1E+05	2E+02	2E+04
32	2244	Well 2244 Scale Body 7" C006 to C007 OD	S	1E+04	8E+05	8E+03	4E+03
33	2244	Well 2244 Scale Collar 7" C006 to C007 OD	S	1E+04	5E+05	1E+03	2E+04
34	2244	Well 2244 Scale Body 7" C008 to C014 OD	S	9E+04	1E+06	2E+03	9E+03
35	2244	Well 2244 Scale Collar 7" C008 to C014 OD	S	9E+03	9E+04	2E+03	6E+03
36	2244	Well 2244 Scale Body 7" C015 to C022 OD	S	1E+03	8E+04	2E+03	2E+03
37	2244	Well 2244 Scale Collar 7" C015 to C022 OD	S	3E+04	3E+04	2E+03	5E+03
38	2244	Well 2244 Scale Body 7" C023 C024 OD	S	2E+04	3E+05	2E+03	3E+04
39	2244	Well 2244 Scale Collar 7" C023 C024 OD	S	3E+04	6E+04	1E+03	3E+03
40	2244	Well 2244 Scale Body 7" C025 C026 C027 OD	S	3E+03	6E+03	3E+01	3E+02
41	2244	Well 2244 Scale Collar 7" C025 C026 C027 OD	S	1E+04	4E+04	9E+01	4E+03
42	2244	Well 2244 Scale Body 7" C028 to C034 OD	S	1E+03	7E+03	2E+01	1E+03
43	2244	Well 2244 Scale Collar 7" C028 OD	S	1E+03	1E+04	1E+02	1E+03
44	2244	Well 2244 Scale Collar 7" C029 OD	S	4E+03	7E+03	4E+02	2E+03
48	2244	Well 2244 Slime 7" C029 OD	S	9E+02	5E+03	2E+02	5E+02
45	2244	Well 2244 Scale Collar 7" C030 to C034 OD	S	1E+04	2E+04	3E+03	3E+03
46	2244	Well 2244 Scale 9 5/8 ID scrape 0-200 ft	S	2E+04	3E+05	2E+02	4E+03
47	2244	Well 2244 Scale 9 5/8 ID scrape 0-1475 ft	S	1E+04	1E+05	8E+02	6E+03
2.C Well 2244 Annulus Fluid Samples							
17	2244	Well 2244 Annulus Fluid Clear – 0 to 89'	L	4E+02	8E+02	1E+01	1E+01
18	2244	Well 2244 Annulus Fluid Clear– 89 to 406'	L	1E+02	5E+02	2E+01	2E+01
19	2244	Well 2244 Annulus Fluid Clear– 406 to 706'	L	3E+01	6E+02	2E+01	6E+00
20	2244	Well 2244 Annulus Fluid Black– 706 to 1106'	L	2E+04	2E+04	1E+04	2E+04
21	2244	Well 2244 Annulus Fluid Black– 1106 to 1475'	L	5E+03	2E+04	2E+03	1E+03
22	2244	Well 2244 Annulus Fluid Gray -1475-1575'	L	2E+03	2E+03	5E+02	5E+02
23	2244	Well 2244 Annulus Fluids Injection Tank source clear	L	2E+00	5E+00	<LOD	<LOD
27	2244	Well 2244 Annulus Fluids Output Tank Foam 16 hr	L	1E+05	5E+05	2E+03	1E+04

MPN Results Table Legend. Results of population analysis by triplicate MPN method. Values are the culturable bacteria per g of each sample, set up in triplicate, after 28 days of growth. SRB: Sulfate-Reducing Bacteria. APB: Acid Producing Bacteria, GHB: General Heterotrophic Bacteria, IRB: Iron Reducing Bacteria, Yellow are >10^6, Red are between 10^4 - 10^6, Green are between 10^3 - 10^4, White are <10^3, Grey <LOD indicates "below limit of detection", e.g. no growth

M 979-694-6500 ● F 979-694-6511 ● 11142 Hopes Creek Road ● College Station, Texas 77845 ● www.ecolyse.com

Well 2244 MPN Analysis Overall Results (Table 3)

- The most striking result from MPN analysis was how widely distributed APB, IRB and SRB among samples collected from well 2244
- Out of 46 samples collected from well 2244:
  - All 46 tested positive for the presence of APB.
  - All 46 tested positive for the presence of GHB
  - 44 tested positive for the presence of IRB
  - 43 tested positive for the presence of SRB.
- The average cell density in all media types was 3.7E+03 cells/g,
  - Range of no growth to up to 9E+08 cells/g.
- GHB exhibited the highest overall average cell density, at 4.1E+04 cells/g
- IRB exhibited the lowest overall average cell density, at 3.9E+02 cells/g

Table 3. Well 2244 MPN Culture Based Microbial Density. Overall Summary of Results.

Media Type	APB	GHB	IRB	MPB	*Summary*
# Samples Positive	46 of 46	46 of 46	44 of 46	43 of 46	46 of 46
Average cells/g	8.5E+03	4.1E+04	3.9E+02	1.4E+03	*3.7E+03*
Highest cell density cells/g and sample	6E+07 Soil	9E+08 Soil	3E+07 Soil	6E+04 Soil	*9E+08 Soil*
Lowest cell density cells/g and sample	2E+00 Well head, Injection Tank Water	5E+00 Well head, Injection Tank Water	<LOD Well head, Injection Tank Water	<LOD Well head, Injection Tank Water	*<LOD Well head, Injection Tank Water*

Well 2244 MPN Analysis Results by Sample Type (Figure 2 and Table 4)

- Data from samples originating from the same sample type were averaged (Fig. 2 and Table 4)

Soil Sample

- Soil had the highest average cell density in all media types, and was the only sample for which IRB levels exceeded SRB levels. Because none of the casing scale samples showed an elevation in IRB over SRB, it suggests that soil contamination did not impact the analysis of the casing scale samples.

Well Head and Casing Scale Samples

- Well head master valve and tree had negligible microbial activity.
  - At the time of sample collection, the master valve and tree had been stored for some length of time in the compressor station.
- All casing joints had significant levels of APB, GHB, SRB, and IRB,
- Variations in levels were upwards of 2 log orders between each sample group.
- Samples from joint C001A had the highest microbial load out of the casing samples
- Casing joint C025 to C034 had the lowest microbial load of all the casing samples

Annulus Fluid Samples

- The source water used to flood the annulus during the annulus fluid pumping process had zero detectable IRB and SRB, and almost zero GHB and APB.
- The clear annulus fluid samples from the top 700' of the annulus had less than 1000 cells per ml, although there was evidence of all metabolic types.
  - This would have been the liquid closest to the failure casing joint and was the liquid pumped into the system during the blowout killing process.
- The black annulus fluids from the bottom 700' of the well had the highest microbial load
- The material from the output tank had the highest microbial load, and had the appearance of

fresh microbial foam, indicating that mixing of annulus liquids promoted microbial growth.

Figure 2 and Table 4

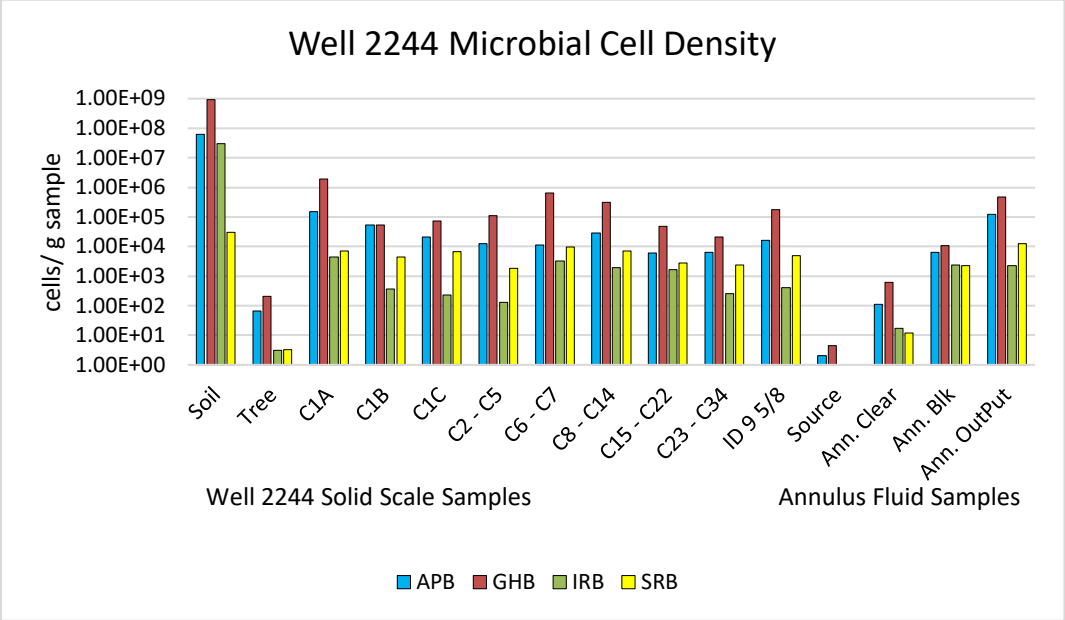

Figure 2: Graph of Data in Table 4

Table 4. MPN Culture Based Microbial Density Wells 2244. Summary of Results.						
4.A Solids: Soil and Scale Samples						
Sample Group	Sample Description	Type	APB	GHB	IRB	MPB
1	Well 2244 Soils, All	S	6E+07	9E+08	3E+07	3E+04
4, 5, 6	Well 2244 Scale Master Valve & Tree	S	6E+01	2E+02	3E+00	3E+00
8, 9, 10, 11	Well 2244 Scale 7" C001A All	S	2E+05	2E+06	4E+03	7E+03
12, 13, 14, 15, 16	Well 2244 Scale 7" C001B All	S	5E+04	5E+04	4E+02	5E+03
25, 26	Well 2244 Scale 7" C001C All	S	2E+04	7E+04	2E+02	7E+03
28, 29, 30, 31	Well 2244 Scale 7" C002, C003, C004, C005 ALL	S	1E+04	1E+05	1E+02	2E+03
32, 33	Well 2244 Scale 7" C006, C007 All	S	1E+04	6E+05	3E+03	9E+03
34, 35	Well 2244 Scale 7" C008 to C014 All	S	3E+04	3E+05	2E+03	7E+03
36, 37	Well 2244 Scale 7" C015 to C022 All	S	6E+03	5E+04	2E+03	3E+03
38, 40, 42, 39, 41, 43, 44, 45	Well 2244 Scale 7" C023 to C034, All	S	6E+03	2E+04	3E+02	2E+03
46, 47	Well 2244 Scale 9 5/8 ID scrape ALL	S	2E+04	2E+05	4E+02	5E+03
4.B Fluids: Annulus fluid samples						
Sample Group	Sample Description	Type	APB	GHB	IRB	MPB
23	Well 2244 Annulus Fluid Injection Source Tank	F	2E+00	5E+00	<LOD	<LOD
17, 18, 19	Well 2244 Annulus Fluid Clear	F	1E+02	6E+02	2E+01	1E+01
20, 21, 22	Well 2244 Annulus Fluid Black	F	6E+03	1E+04	2E+03	2E+03
27	Well 2244 Annulus Fluid Output Tank, 16 hrs.	F	1E+05	5E+05	2E+03	1E+04

Table 4. Microbial Density Wells 2244. Summary of Results. Averages were calculated from Ln for each sample group. Results of population analysis by triplicate MPN method. Values are the culturable bacteria per g of each sample, set up in triplicate, after 28 days of growth. SRB: Sulfate-Reducing Bacteria. APB: Acid Producing Bacteria, GHB: General Heterotrophic Bacteria, IRB: Iron Reducing Bacteria, Red are >10^6, Yellow 10^4 - 10^6, Green are 10^3 - 10^4, White are <10^3, Grey <LOD are "below limit of detection", e.g. no growth

Project Results: Bacterial Diversity Analysis by Genetic Approaches

- qPCR and Amplicon Metagenomics are two approaches that rely on DNA isolation from a sample
- Isolated DNA is used for two types of analysis: qPCR and Amplicon Metagenomics
- qPCR provides quantitative data on total microbial load per g or ml sample
- Amplicon metagenomics provides identification of the types of microbes in a sample
- Information gathered includes the types of bacteria and the % in the population
- Amplicon metagenomics and qPCR do not differentiate between live and dead cells
- The identity of the species in the sample is used to predict the physiological or metabolic role that organism might have in the environment
- The prediction is done by comparing the organisms identified to the research on that type of organism, available in the scientific literature
- Not every organism has been studied enough to understand its metabolism
- Following traits assigned to identified bacteria and archaea where possible:
    - **Sulfidogen**-includes all bacteria that can produce sulfide or H_2S as a metabolic byproduct. This includes "true" SRB as well as TRB (thiosulfate-reducing bacteria) SuRB(sulfur-reducing bacteria) and peptide-fermenting bacteria (such as some Clostridia)
    - **SRB**-(sulfate-reducing bacteria) "true" SRB, utilize sulfate as respiratory electron acceptor and produce sulfide as a metabolic byproduct
    - **APB**-(acid-producing bacteria) these make organic and/or inorganic acids. Not all APB result in a lowering of ambient pH. Organisms that produce inorganic acids are often acidophilic, and grow at very low corrosive pH.
    - **IRB**-(iron-reducing bacteria) many are strongly corrosive
    - **NRB**-(nitrate-reducing bacteria) many bacteria are nitrate reducers. Of particular relevance to the O&G industry are the NRSOB (nitrate-reducing sulfur-oxidizing bacteria) promoted by nitrate injections.
    - **Biodeg**-biodegrading bacteria. These bacteria are capable of breaking down unusual substrates such as O&G hydrocarbons **(HC),** petrochemicals, cellulose, toxic chemicals etc.
    - **Methanogen** – Archaea that produce methane as a metabolic byproduct under anaerobic growth
    - **Methylotroph**- Utilize reduced one-carbon compounds, such as methanol or methane, as the carbon source for their growth; and multi-carbon compounds that contain no carbon-carbon bonds, such as dimethyl ether and dimethylamine.
    - **Phototroph**- photosynthetic organisms, these include both aerobes and anaerobes.
- Percent of population, and number of unique microbial types (species) are provided as results

Well 2244 qPCR Analysis

DNA Isolation and qPCR from Well 2244 Samples

All individual well 2244 solid and liquid samples listed in Table 1 were subject to multiple rounds of DNA isolations. Multiple approaches were used, including elution of materials off of the solids with sterile PBS buffer followed by concentration by filtration or centrifugation, direct isolation from solids (e.g. resuspending solid material direction in the lysis buffer solution), as well as filtration and centrifugation of annulus liquids. When materials from some samples became limiting, these were combined with other sample from the same sample type (for example, well 2244 clear annulus liquids or well 2244 lower casing joints). In all, over 100 DNA extractions attempts were made using raw samples. Genetic data from well 2244 samples were inconsistent, with DNA from only 6 extraction efforts yielding population profile results (Table 5). In stark contrast, the same processes were used to extract DNA from well 2248, 2251, and compressor station samples, and these resulted in qPCR and sequence library results as expected (Table 6, and see accompanying report OG230510 Well 2248, Compressor station, and Well 2251 population analysis).

It should be noted that while isolation of DNA from materials such as cultures, tissues, such as cheek swabs, blood, high biological content soils, are reasonably standardized processes with a high % of success. In contrast, isolation of DNA from crude environmental samples, especially those consisting primarily of inorganic material such as metal scales or strong chemicals, is not standardized and it is

expected that there can be variability in % recovery of DNA. When this happens, it can provide additional insight as to the composition of either the microbial content, or the physical content, of the sample.

TABLE 5. RM Well 2244 Well 2248, Well 2251, and Compressor Station qPCR Results

DNA ID	DNA Template	Seq Data?	qPCR Cells per g	MPN Cells per g
5.A Well 2244 Soil and Fluid Samples				
OG230207-001	2244 Well Pad Soil Pool 1 : BLRM230216-001,	YES	2.02E+10	9.0E+08
OG230305-003	Well 2244 Annulus Fluids Black Gray (7" - 9 5/8") Pool 22	YES	3.71E+05	2.0E+03
OG230305-004	Well 2244 Annulus Fluids Output Tank Foam 16 hr Pool 27	YES	1.38E+06	5.0E+05
OG230305-002	Well 2244 Annulus Fluids Black Viscous (7" - 9 5/8") Pool 20	YES	2.32E+06	2.0E+04
OG230305-008	Well 2244 Annulus Fluids Clear (7" - 9 5/8") Pool 17	no	<LOD	8.0E+02
OG230305-009	Well 2244 Annulus Fluids Clear (7" - 9 5/8") Pool 18	no	<LOD	8.0E+02
OG230305-010	Well 2244 Annulus Fluids Clear (7" - 9 5/8") Pool 19	no	<LOD	6.0E+02
5.B Well 2244 Casing Scale Samples				
OG230401-001	Well 2244 Master Valve, Tree Combined Pool 04, 5, 6, 7	no	<LOD	2.00E+03
OG230305-001	Well 2244 C001A OD below seal ring Pool 08	no	<LOD	3.00E+07
OG230305-007	Well 2244 C001B OD 68" to 84 " Pool 13	YES	<LOD	2.00E+04
OG230401-003	Well 2244 C002 - C005, Solids, All Pool 28, 29, 30, 31	no	2.63E+08	5.00E+05
OG230401-004	Well 2244 C006 - C022 Body Pool 32, 34, 36	no	<LOD	1.00E+06
OG230401-005	Well 2244 C006 - C022 Collar Pool 33, 35, 37	no	1.86E+08	5.00E+05
OG230305-006	Well 2244 C015 to C022 Collar Pool 37	YES	<LOD	3.00E+04
OG230401-006	Well 2244 C023 - C034 Body Pool 38, 40, 42	no	<LOD	3.00E+05
OG230401-007	Well 2244 C023 - C034 Collar Pool 39, 41, 43, 44, 45	YES	2.12E+08	6.00E+04
OG230401-008	Well 2244 9 5/8 ID Scrape, All Pool 46, 47	no	3.67E+08	3.00E+05
5.C Compressor Station Pond and Separator fluids				
OG230409-001	Compressor Station pond sample, clear	Yes	6.43E+04	2E+05
OG230409-002	Compressor Station pond sample, emulsion	Yes	3.14E+05	5E+07
OG230409-004	Compressor station separator fluid, Black.	Yes	6.23E+04	1E+02
OG230409-005	Compressor station separator fluid, Clear.	no	<LOD	8E+01
5.D Well 2248 Soil, Scale, and Fluid				
OG230207-002	Well 2248 Soils	Yes	2.3E+10	1E+08
OG230409-006	Well 2248, 7" C001 OD Scale sample	Yes	2.54E+07	8E+05
OG230406-001	Well 2248, 7" C001 OD Scale Sample	Yes	5.24E+07	1E+06
OG230406-003	Well 2248, 7" C001 OD Scale, 4 - 5 lbs	Yes	5.68E+07	1E+07
OG230406-002	Well 2248, 7" C001 Scale Sample Couplings	Yes	5.57E+08	3E+05
OG230409-003	Well 2248, Annulus Liquid Sample	Yes	1.03E+06	8E+04
OG230406-004	Well 2248, OD Scale, Conductor	Yes	2.64E+06	9E+07
OG230406-005	Well 2248, uppermost 9 5/8" casing ID scrape	Yes	8.35E+05	2E+05
5.E Well 2251 Soil and Scale				
OG230207-003	Well 2251 Soils	Yes	9.6E+09	2E+09
OG230406-008	Well 2251, 7" casing OD, C001 10'6" from top	no	<LOD	3E+02
OG230406-006	Well 2251, 7" casing OD, C001 top of joint	no	<LOD	1E+02
OG230406-007	Well 2251, 7" casing OD, C001 top of joint	no	<LOD	3E+01

Results of qPCR quantification of total microbes in samples from well 2244, well 2248, and Compressor Station Liquids. qPCR results, in microbial cells per g or ml sample, are provided. <LOD indicates “below the limit of detection”. These same DNA were subject to 16S amplicon metagenomics, and “Sequence Data” indicates if data was obtained from sequence analysis. The concentration of GHB in the sample, taken from MPN analysis, Table 2, is also provided for comparison.

The data for qPCR is provided in Table 5, along with the cells per g as calculated by MPN, using the highest values for component samples.

Evaluation of qPCR results, taken together with the success of DNA analysis and MPN leads to several observations:

1. Sequence library data was obtained for 7 samples: three annulus fluid samples, the soil sample, and 3 scale samples.

Results from Annulus fluid samples, and the Soil sample: there was good agreement between qPCR and MPN data for annulus fluids and soil samples in that the fluid and soil samples with the highest qPCR

results >LOD yielded DNA sequence data, and these represented the samples with the highest microbial content as determined by MPN.

2. For the fluid and soil samples, the microbial content as detected by qPCR was 1 to 3 log orders higher than what was observed in MPN cultures.
    a. NACE TM0194 describes why bacteria may not grow in culture
    b. This is a common observation; typical estimates are that MPN analysis underestimates total microbial load in samples.
        i. The medias used are not 100% inclusive, they do not support the growth of all microbes.
        ii. Because cells can adhere to each other or attach to solids, it isn't possible to accurately dilute microbes in some samples, which leads to an under estimation, eg, if 100 cells are stuck to a piece of metal, it will only be counted as "1' in MPN dilution.
        iii. Some bacterial types grow as filaments and so an accurate dilution isn't possible.
3. Taken together, the qPCR data indicates the level of bacteria in the black annulus fluids was likely to be 3 or 4 log orders higher than in the clear annulus fluids.
4. The clear annulus fluids were predominantly the liquids injected in the leak control process, while the black annulus fluids more likely has the typical composition of the annulus during regular operations.

Results from Well 2244 Scale Samples: In contrast to the fluid and soil sample data, the results of qPCR and DNA sequence library generation was quite variable.

1. There were multiple scale samples with significant microbial population, as determined by MPN, did not yield any DNA for analysis (Table 2 and Table 5). This includes all samples from Table 2 with MPN values > 1.0+E05 that are not included in Table 5.
2. For several casing scale samples, no sequence data was obtained, even though qPCR and MPN results both indicate there were enough bacteria, and enough isolated DNA, to generate a sequence library. Because qPCR is an assay that is much less involved than generating a DNA sequence library, and so while the DNA quality and yield might be high enough for qPCR, it was not of sufficient quality to generate a sequence library.
3. For two samples, sequence library data was generated, but the qPCR results were not generated. *This is a technical anomaly and is being followed up on.*
4. In contrast to Well 2244, samples from other locations at Rager Mountain, including soils, scales, and fluids from wells 2248, 2251, and the compressor station, did not offer any unusual challenges to DNA isolation and analysis (Table 5). For these samples, there was almost 100% agreement between MPN, qPCR, and DNA sequence data (see accompanying report for full details).
5. When so many samples show inconsistencies, it indicates something fundamentally different about the conditions of well 2244. One possibility is that the might contain a chemical that somewhat reduces DNA isolation efficiency.

The take home conclusions from qPCR include:

1. DNA isolation efficiency was reduced in well 2244 samples, as compared to samples from wells 2248 and 2251, leading to most well 2244 samples yielding inconsistent DNA analysis results.
a. Possible due to inhibitors in the clear annulus fluid that all joints were exposed to at some point in the extraction process.
2. For samples where results were generated, the microbial load was determined to be several log orders higher than what is reflected by MPN analysis, this is an expected result.
3. The scale samples that yielded qPCR data contained around 10^8 cells per g of scale, which is a significant microbial load.

Well 2244 Population Profile by amplicon metagenomics

Isolation of additional DNA templates from the MPN culture vials

While determining the population of a sample directly from the raw sample is the most ideal analysis, another approach to elucidating the type of bacteria in a sample is to analyze the organisms that grow up in culture. Analysis of cultured organisms has been used extensively in the scientific literature. DNA isolated from microbial cultures is typically a suitable template for downstream molecular analysis. There are several reasons for this including:

1. DNA yields from metabolically active cells, such as those in a fresh culture, are typically higher than from stationary stage cells, as is often the case for environmental bacteria.
2. Bacteria in culture often grow to a much higher density then they were in the environment, due to the increased nutrient content of the culture media.
3. Sample physical and chemical components that inhibit DNA analysis are diluted out.

There are major disadvantages to using the cultured organisms for population analysis.

1. Although the organisms growing in culture were present in the starting sample, their relative abundance is likely to change dramatically.
2. There is likely to be a loss of species diversity, as not all organisms present in the original sample will grow in the culture media.

TABLE 6. Well 2244 Casing Scale Culture DNA Yields

Component Samples	DNA ID	Source	DNA ng/ul	Sequence Data?
Well 2244 Casing C001 Solids, all , Samples 8, 9, 10, 11, 12, 13, 14, 15, 16, 25, 26	OG230402-001	PRD	37	Yes
	OG230402-002	MPB	14.2	Yes
	OG230402-003	IRB	4.3	Yes
Well 2244 Casing C002 - C005, Solids, Collar, Samples 28, 29, 30, 31	OG230402-004	PRD	19.8	Yes
	OG230402-005	MPB	10.5	Yes
	OG230402-006	IRB	3.1	Yes
Well 2244 Casing C006 - C022 Solids, Body, Samples 32, 34, 36	OG230402-007	PRD	20	Yes
	OG230402-008	MPB	7.3	Yes
	OG230402-009	IRB	42.5	Yes
Well 2244 Casing C006 - C022 Solids, Collar, Samples 33, 35, 37	OG230402-010	PRD	25.3	Yes
	OG230402-011	MPB	16.2	Yes
	OG230402-012	IRB	6	Yes
Well 2244 Casing C023 - C034 Solids, Body, Samples 38, 40, 42	OG230402-013	PRD	24.3	Yes
	OG230402-014	MPB	9.4	Yes
	OG230402-015	IRB	4.8	Yes
Well 2244 Casing C023 - C034 Solids, Collar, Samples 39, 41, 43, 44, 45	OG230402-016	PRD	25.1	Yes
	OG230402-017	MPB	12.8	Yes
	OG230402-018	IRB	7.7	Yes
Well 2244 9 5/8 Casing ID Scrape, 0-1475', Samples Pools 46, 47	OG230402-019	PRD	15.1	Yes
	OG230402-020	MPB	14.8	Yes
	OG230402-021	IRB	19.3	Yes

DNA yields from well 2244 casing scale cultures. DNAs were isolated from mixtures of cultures set up with indicated samples, in the indicated medias. Each "OG" number indicates an individual DNA preparation generated from a mix of cultures originating from the indicated component well 2244 casing scale samples (See Table 4 for sample details) that was set up in the indicated type of media. The DNA yield, in ng/ul are provided. All culture DNA resulted in 16S amplicon metagenomic library sequence data.

However, because of the significant challenges to isolating DNA directly from the well 2244 samples, DNA isolated from MPN cultures was chosen as the "next best source" of population data.

- DNA was isolated from well 2244 casing scale sample cultures only (i.e. not cultures set up from soil, tree, or fluid samples).
- DNA was isolated separately from each of the 3 media types (PRD, MPB, IRB) such that for every sample to be analyzed, 3 DNA isolations and analysis had to be conducted.
- The 32 well 2244 casing scale samples as described in Table 2 were condensed into 7 sample pools, such that 21 DNA extracts were isolated (7 sample pools X 3 medias each).
- All 21 of these DNA samples yielded sequence data (Table 6).

Well 2244 Microbial Diversity Analysis by Amplicon Metagenomics

The microbial population of population profiles were determined for 28 DNA templates isolated from well 2244 soil, scale, and annulus fluids (Table 7). 21 of the sequences were obtained from DNA extracted from casing scale samples cultures and 8 were extracted directly from the raw sample material.

- Between 4232 and 72738 sequences were analyzed from each sample, for a total of 882588 sequences in all.
- These correlated to between 18 and 279 species in each sample, for a total of 555 species in all.
    - This value doesn't include the full breakdown of the number of organisms with an "unclassified" annotation, and so is an underestimation.
- Soils and annulus fluids had the highest diversity, at over 200 species each
- Scale sample cultures contained between 18 to 42 species each
- These values are neither extremely high nor extremely low for these types of samples

Table 7 provides an overall summary of population profile data from all well 2244 samples.

Table 7. Well 2244 Microbial Population Profile Analysis: Overview of all DNA sequence data sets

Seq ID	OG230207-001	OG230402-001	OG230402-002	OG230402-003	OG230402-004	OG230402-005	OG230402-006	OG230402-007	OG230402-008	OG230402-009
Sample	W2244 Soils	W2244 C001 A PRD	W2244 C01 A MPB	W2244 C01 A IRB	W2244 C02 - C05 A PRD	W2244 C02 - C05 A MPB	W2244 C02 - C05 A IRB	W2244 C06 - C22 B, PRD	W2244 C06 - C22 B MPB	W2244 C06 - C22 B IRB
# Seq	56739	24788	22964	15844	27335	20249	23206	28545	23371	4232
# Spp	279	20	43	42	25	29	31	24	22	31
Seq ID	OG230402-010	OG230402-011	OG230402-012	OG230402-013	OG230402-014	OG230402-015	OG230402-016	OG230402-017	OG230402-018	OG230402-019
Sample	W2244 C06 - C22 C PRD	W2244 C06 - C22 C MPB	W2244 C06 - C22 C IRB	W2244 C23 - C34 B PRD	W2244 C23 - C34 B MPB	W2244 C23 - C34 B IRB	W2244 C23 - C34 C, PRD	W2244 C23 - C34 C MPB	W2244 C23 - C34 C IRB	W2244 9 5/8 ID A PRD
# Seq	23485	27163	28184	28672	24298	23553	21088	16651	32278	28536
# Spp	18	32	33	25	22	35	23	22	35	21
Seq ID	OG230402-020	OG230402-021	OG230508-001	OG230508-002	OG230508-003	OG230508-004	OG230508-005	OG230508-006	***Total Population Overview 29 Well 2244 Samples***	
Sample	W2244 95/8 ID MPB	W2244 9 5/8 ID IRB	W2244 Ann. Fl. Black	W2244 Ann. Fl. Grey	W2244 Ann. Fl. Output	W2244 C15 - C22 Scale	W2244 Scale C01B OD	W2244 Scale C23 - C34		
# Seq	29592	25137	72738	42038	72438	37834	63261	38369	***882588 sequences***	
# Spp	21	40	231	133	203	59	42	142	***555 species****	

Well 2244 Population Breakdown: Number of sequences analyzed and the number of species identified in each sample. # Seq is the number of sequences analyzed from each sample. # Spp is the number of unique species identified in the sample, not including "unclassified" organisms. Samples with "PRD" "MPB" and "IRB" in the sample name are the scale sample MPN cultures from the corresponding media. Ann. Fl. Are annulus fluid samples, B are casing body samples, C casing collar samples.

Well 2244 microbial population: Functional Trait Profiles

Each of the species identified in the samples was assigned a "Functional Trait Profile" that includes select metabolic, physiological, ecological, and taxonomic tags. Note that the functional trait % of population adds up to over 100%, because organisms can have more than 1 functional trait assigned (eg, some GHB, sulfidogens, and IRB are also spore-forming).

The trait profile tags are generated by analysis of the published scientific literature for that species, or closely related species (when relevant). The trait assignment database in inherently incomplete, because not every organism has been subject to the same degree of experimental investigation, and so the information is not known.

Some traits have a high confidence, because the majority of organisms of that genera exhibit that trait. For example, assigning the tag of "Anaerobe, Sulfidogen, SRB" to any Desulfovibrio species has a high confidence because all known Desulfovibrio isolates are anaerobic, sulfidogenic SRB. In contrast, some traits are present in only a few isolates of a given genera, or even species, and so just because one genera or species has that trait it can't be assigned confidently to all members. One trait that is straightforward from some genera, but difficult for others, is the important trait of acid production. It is straightforward to assign APB to some organisms, such as Acetobacter and Acetobacterium. But, in some cases such as Bacillus some species produce enough organic acids and reduce the pH of the environment, but Bacillus species also increases the pH during sporulation. Acids can also be produced by some alkaliphilic organisms growing at a high pH, for example alkaliphilic LAB, including Marinilactibacillus, Halolactibacillus, and Alkalibacterium spp, live in an alkaline environment. Because of the nuances, for some species, the important trait of "APB" is not automatically tagged.

Despite these nuances and limitations, "Trait Profile" analysis is the best way to correlate the identity of the organisms in a sample to insight as to what the organisms identified in a sample are actually doing. Table 8 provides the functional trait overview for each of the samples sequenced from well 2244. Only the traits with the highest % of the population of each sample are included.

Summary of 8 most represented functional traits for well 2244:

1. **Acid producing bacteria, APB** APB here includes only the most robustly assigned APB: 21.1 % of all organisms, 26 species
2. **Biodegrading organisms, BioD**, "Biodegrading" is a trait assigned to organisms capable of degrading difficult, specialized, or unusual substrates of natural and xenobiotic origin: 29% of all organisms, 101 species
3. **GHB General Heterotrophic Bacteria**, the values provided are an underestimation because this trait could also be assigned to most common APB and Biodegrading organisms : 28.0% of all organisms and 65 species
4. **Halophiles, Halo, Salt tolerant organisms**, 7.52% of all organisms with 25 species
5. **Iron Reducing Bacteria, IRB**, Capable of iron reduction, 5% of all organisms with 11 species
6. **Spore-forming organisms, Spore** Form chemical, heat, radiation resistant spores under conditions of stress: 38.2% of all organisms with 47 species
7. **Sulfide, Sulfidogens, H2S**, Hydrogen sulfide producing organisms, includes SRB, TRB, SuRB, and peptide fermenting organisms: 15.1% of all organisms with 45 species
8. **Unclassified, UnCl**, includes organisms that could not be assigned Genus level designation: 20.76% of all organisms, approximately 100 different types organisms received this classification (see table 19 for details of these)

- Looking at well 2244 as a whole, APB, Sulfidogens, and IRB were widespread throughout the well, which was consistent with MPN results.
- The high % of "unknown organisms in most samples means that some trait values are under estimated, because the unknown organisms might exhibit the indicated trait.
- The most unexpected finding was the predominance of spore forming organisms in well 2244 samples.

Table 8. Well 2244 Microbial Population Profile Analysis: Selected Traits Relative Abundance and Number Species

Seq ID	OG230207-001	OG230402-001	OG230402-002	OG230402-003	OG230402-004	OG230402-005	OG230402-006	OG230402-007	OG230402-008	OG230402-009
Sample	W2244 Soils	W2244 C001 A PRD	W2244 C01 A MPB	W2244 C01 A IRB	W2244 C02-C05 A PRD	W2244 C02-C05 A MPB	W2244 C02-C05 A IRB	W2244 C06-C22 B, PRD	W2244 C06-C22 B MPB	W2244 C06-C22 B IRB
APB	1.09%7	0.08%2	10.8%7	2.3%5	0.1%2	22.8%3	18.0%4	0.10%1	0.04%2	0.1%3
BioD	31.3%57	84.4%7	20%12	11.9%11	89.1%7	17.4%7	18.5%9	86.6%6	4.6%6	7.4%6
GHB	18.7%36	87.7%6	31.1%9	14.8%6	76.2%8	1.23%6	25.1%10	99.3%7	6.6%5	8.0%8
Halo	0.041%4	0%0	0.01%2	21.4%5	0.004%1	0.02%2	0.03%1	0%0	0.1%1	1.8%4
IRB	9.53%9	0.01%1	0.1%1	26.2%1	0.004%1	0.04%1	46.8%1	0.01%1	10.4%1	79.6%1
Spore	0.5%8	97.6%11	74%16	51.0%16	99.1%13	53.8%12	72.1%10	99.7%10	28.4%11	89.%11
Sulfide	0.5%12	0%0	42.1%8	30.9%13	0.01%3	50.7%7	2.2%4	0.01%1	11.5%6	4.3%9
UnCl	32.8%x	0.03%x	10.7%x	22.0%x	0.1%x	24.8%x	2.6%x	0.04%x	70.5%x	3.9%x
Seq ID	OG230402-010	OG230402-011	OG230402-012	OG230402-013	OG230402-014	OG230402-015	OG230402-016	OG230402-017	OG230402-018	OG230402-019
Sample	W2244 C06-C22 C PRD	W2244 C06-C22 C MPB	W2244 C06-C22 C IRB	W2244 C23-C34 B PRD	W2244 C23-C34 B MPB	W2244 C23-C34 B IRB	W2244 C23-C34 C, PRD	W2244 C23-C34 C MPB	W2244 C23-C34 C IRB	W2244 9 5/8 ID A PRD
APB	0.01%1	29.1%5	85.5%6	0.43%3	0.03%2	36.%4	10.0%3	13.6%2	84.6%5	29.3%2
BioD	46.6%6	5.8%6	3.7%10	98.7%6	9.3%7	8.25%8	76.0%5	0.5%6	2.9%8	69.9%8
GHB	98.4%7	37.5%5	5.72%7	97.9%7	50.4%5	9.99%9	87.8%7	15.7%6	4.7%8	69.8%6
Halo	0%0	0.05%2	0.03%4	0.01%1	0.51%1	0.153%2	0.02%1	0%0	0.7%3	0%0
IRB	0.03%1	0.004%1	3.16%1	0.01%1	0%0	34.4%1	0.01%1	0.04%1	4.1%1	0%0
Spore	98.6%10	59.8%12	8.7%10	99.3%12	74.1%11	47.1%8	88.6%9	16.8%9	9.17%11	37.9%9
Sulfide	0.004%1	22.3%8	0.05%7	0.02%3	16.0%6	3.83%5	0.02%1	0.6%2	1.1%7	0.02%3
UnCl	0.2%x	8.3%x	4.68%x	0.02%x	19.6%x	12.4%x	0.05%x	67.9%x	4.1%x	0.2%x
Seq ID	OG230402-020	OG230402-021	OG230508-001	OG230508-002	OG230508-003	OG230508-004	OG230508-005	OG230508-006	***Total Well 2244 Population Overview 29 Samples***	
Sample	W2244 9 5/8 ID A MPB	W2244 9 5/8 ID A IRB	W2244 Ann. Fl. Black	W2244 Ann. Fl. Grey	W2244 Ann. Fl. Output	W2244 C15-C22 Scale	W2244 Scale C01B OD	W2244 Scale C23-C34		
APB	44.2%4	56.5%5	16%13	46.6%6	19.8%13	5.2%3	1.6%4	46.1%5	***21.1 %26 species***	
BioD	0.05%5	10.0%14	7.8%52	6.1%35	7.1%50	41.7%18	60.2%13	7.24%36	***29%101 species***	
GHB	0.6%5	29.6%10	8.0%29	6.3%19	7.7%24	6.5%10	3.6%9	5.36%22	***28.0%65 species***	
Halo	0.003%1	0.06%3	14.8; 15	45.0%11	18.6; 17	5.61%3	0.006%2	44.3%13	***7.52%25 species***	
IRB	0.6%1	5.1%1	3.0%7	0.7%3	2.1%5	2.1%2	0%0	2.71%5	***5%11 species***	
Spore	1.2%5	33.2%9	23%26	18.1; 16	23.0%27	5.5%6	1.9%3	15.2%14	***38.2%47 species***	
Sulfide	0.5%3	1.3%6	31%28	52.6%18	34.4%26	5.7%5	0.2%3	53.9%16	***15.1%45 species***	
UnCl	17.5%x	6.7%x	42.9%x	21.8%x	42.5%x	31.0%x	20.2%x	24.6%x	***20.76%x species***	

Overview of results of population profile by 16S amplicon metagenomics: **Selected** physiological traits relative abundance and number of species. In each cell, the first number is % of total population, yellow are >10%. The second Number is number of species. Traits: APB (acid producing bacteria), BioD (biodegrading organism) GHB (General Heterotrophic Bacteria), Halo (salt tolerant halophiles), IRB (Iron Reducing Bacteria), Spore (spore-forming bacteria), Sulfide: Sulfidogen (Hydrogen Sulfide Producing (includes SRB, TRB, SuRB and some peptide fermentation bacteria), UnCl, *Unclassified organisms did not closely match an organism with a full taxonomic annotation. This category includes multiple different types of organisms with different physiological characteristics, and will be elaborated on later.* ***Note that for Physiological, Metabolic, Traits of Interest, the % add up to more than 100 because organisms have more than one trait (e.g. Some sulfidogens, APB, GHB, and IRB are spore-forming).***

Well 2244 microbial population: Class Level Taxonomic Profiles

A higher-level profile of bacteria identified in well 2244 can be obtained by evaluating the most abundant organisms at a Class level designation (Table 9).

The Classes with the highest number of individual species were calculated for each sample (Table 9)

250 species, encompassing 11.9% of all organisms, were included in class Alphaproteobacteria, Gammaproteobacteria and Betaproteobacteria. These are three distinct Gram – classes, each containing a rich diversity of biodegrading and general heterotrophic organisms, includes many aerobes and facultative anaerobes and some anaerobes.

32 species, encompassing 0.7% of all organisms, were included in class Deltaproteobacteria, a Gram - lineage including many important anaerobic sulfidogens and iron reducing bacteria. The “classic” SRB such as Desulfovibrio belongs to the class Deltaproteobacteria. These are typically non-spore forming.

46 species, encompassing 0.7% of all organisms, were included in class Actinobacteria, a class characterized by having an unusual cell wall composition, and includes many common soil and water dwelling organisms

81 species, encompassing 30% of all organisms, were included in class Clostridia, a large and diverse class of Gram +, primarily strictly anaerobic, commonly spore forming organisms. Class Clostridia includes the anaerobic spore forming sulfidogens.

31.1% 48 species, encompassing 31.1% of all organisms were included in class Bacilli Bacillus is a large and diverse class of Gram +, frequently spore forming organism. Many are strict aerobes.

20% of all organisms were not assigned to a specific class and are listed as “unclassified”. The identity of these was further elucidated (see Table 19)

Table 9. Well 2244 Microbial Population Profile Analysis: Selected Classes: Relative Abundance and Number Species

Seq ID	OG23020 7-001	OG23040 2-001	OG2304 02-002	OG23040 2-003	OG23040 2-004	OG2304 02-005	OG2304 02-006	OG2304 02-007	OG230 402-008	OG23 0402-009
Taxonomic Class	W2244 Soils	W2244 C001 A PRD	W2244 C01 A MPB	W2244 C01 A IRB	W2244 C02-C05 A PRD	W2244 C02-C05 A MPB	W2244 C02-C05 A IRB	W2244 C06-C22 B, PRD	W2244 C06-C22 B MPB	W224 4 C06-C22 B IRB
Unclassified	32.8%x	0.03%x	10.7%x	22.0%x	0.11%x	24.8%x	2.64%x	0.04%x	70.5%x	3.9%x
GammaP	19.6%30	0.01%1	0.03%4	0.04%2	0.01%2	0.02%1	0.004%1	0.01%1	0.01%2	<.1%1
BetaP	18.8%29	0.02%3	0.04%3	0.01%2	0%0	0.03%2	0.02%3	0.04%6	0.01%1	<.1%1
AlphaP	4.33%56	0%0	0.02%2	0%0	0.01%2	0.01%2	0%0	0.004%1	0%0	<.1%3
DeltaP	1.89%24	0%0	0%0	0%0	0%0	0%0	0%0	0%0	0%0	0%0
Actinobacteria	1.44%22	0.01%1	0%0	0%0	0%0	0%0	0.004%1	0.01%1	0%0	0%0
Clostridia	0.70%12	13.1%4	74.1%19	74.4%26	7.52%6	53.0%11	61.7%11	12.7%4	28.0%9	92%16
Bacilli	0.51%8	86.9%10	11.9%11	3.43%7	92.3%12	22.1%9	33.2%10	87.1%8	1.3%5	3.6%5
Seq ID	OG23040 2-010	OG23040 2-011	OG2304 02-012	OG23040 2-013	OG23040 2-014	OG2304 02-015	OG2304 02-016	OG2304 02-017	OG230 402-018	OG23 0402-019
Taxonomic Class	W2244 C06-C22 C PRD	W2244 C06-C22 C MPB	W2244 C06-C22 C IRB	W2244 C23-C34 B PRD	W2244 C23-C34 B MPB	W2244 C23-C34 B IRB	W2244 C23-C34 C, PRD	W2244 C23-C34 C MPB	W2244 C23-C34 C IRB	W224 4 9 5/8 ID A PRD
Unclassified	0.2%x	8.397%x	4.68%x	0.024%x	19.61%x	12.4%x	0.052%x	67.9%x	4.1%x	0.2%x
GammaP	0.01%1	0.01%2	0.03%2	0.01%2	0.01%1	0.03%1	0%0	0.01%1	0.01%1	32%3
BetaP	0.03%2	0.02%1	0%0	0.003%1	0.02%2	0.10%3	0.01%2	0.06%4	0%0	<.1%1
AlphaP	0%0	0.04%4	0%0	0.003%1	0%0	0.01%1	0.01	0%0	0.01%2	0%0
DeltaP	0%0	0%0	0%0	0%0	0%0	0%0	0%0	0%0	0%0	0%0
Actinobacteria	0.01%1	0%0	0%0	0%0	0%0	0.01%2	0%0	0.01%1	0%0	0%0
Clostridia	51.8%5	68.4%13	9.2%16	0.06%7	72.2%12	45.3%15	11.7%5	29.9%6	9.1%14	<.1%4
Bacilli	47.9%8	20.7%8	86.1%10	99.9%10	8.2%6	40.9%8	88.2%11	1.7%7	86.%12	67%11
Seq ID	OG23040 2-020	OG23040 2-021	OG2305 08-001	OG23050 8-002	OG23050 8-003	OG2305 08-004	OG2305 08-005	OG2305 08-006	***Total***	
Taxonomic Class	W2244 9 5/8 ID A MPB	W2244 9 5/8 ID A IRB	W2244 Ann. Fl. Black	W2244 Ann. Fl. Grey	W2244 Ann. Fl. Output	W2244 C15-C22 Scale	W2244 Scale C01B OD	W2244 Scale C23-C34	***Well 2244 Population Overview : 29 Samples***	
Unclassified	17.5%x	6.71%x	42.9%x	21.8%x	42.5%x	31.0%x	20.2%x	24.6%x	20.8% x species	
GammaP	0.03%2	0.21%3	1.3%20	1.37%18	0.77%22	5.6%10	3.1%5	2.4%18	3.1% 60 species	
BetaP	0.12%2	0.02%2	0.7%18	2.29%15	0.81%17	33.0%10	60.8%11	1.6%11	7.3% 47 species	
AlphaP	0%0	0.01%2	3.3%36	1.16%17	2.13%28	7.5%11	4.2%4	1.3%22	1.5% 86 species	
DeltaP	0%0	0%0	3.0%11	1.29%5	1.68%6	1.1%2	0.1%1	1.1%7	0.7% 32 species	
Actinobacteria	0%0	0%0	2.0%26	1.65%16	1.87%24	3.7%5	0.02%4	2.0%9	0.7% 46 species	
Clostridia	20.7%6	28.4%14	37.4%50	56.4%25	40.2%44	7.3%6	0.2%4	59.3%27	30.0% 81 species	
Bacilli	25.3%6	64.3%11	3.8%22	9.1%8	4.6%20	4.0%4	3.5%5	3.6%14	31.1% 48 species	

Overview of results of population profile by 16S amplicon metagenomics: **Selected** taxonomic classes, relative abundance in the sample and number of species belonging to that class. In each cell, the first number is % of total population, yellow are >10%. GammaP, BetaP, AlphaP and DeltaP are Gammaproteobacteria, Betaproteobacteria, Alphaproteobacteria, and Deltaproteobacteria, respectively. ***Note that for taxonomic classification, the % will add up to 100 at most, because organisms belong to only one class. Because this table only shows the most abundant Classes, and not the many minorly represented classes, these values might be less than 100%.*** *Unclassified organisms did not closely match an organism with a full taxonomic annotation. This category includes multiple different types of organisms and will be elaborated on later.*

Well 2244 microbial population: Most Abundant Species

In all, 555 species of bacteria, not including "unclassified" organisms were identified in the 28 sequence data sets (see Appendix B, All Species).

Most, 480 species, were low abundance organisms, present at less than 1% of all samples they were found in, while 18 of the species were present at greater than 10% of at least one of the samples they were found in (Appendix A).

The most abundant organisms identified in well 2244 were identified from the full list of all organisms in all 28 samples (Appendix A).

As expected, for the cultured samples, the profile from a given sample was quite different in each of the different media types, which is a function of the selective nature of each media. However, it should be noted that all bacteria that grew in each media had to be present in the original starting sample, although the relative proportions isn't known. Regardless of the altered relative abundance, the combined population profiles from the 3 cultures set up for each sample provides the identity of at least some organisms present in the starting sample.

Data for the different sample types were combined into 7 groups, and values for the most abundant organisms averaged (Table 10):

Sample Pool		Sample Description	Sequence ID
1.	1. 2244 Soils, DIRECT	Well 2244 Soils, MG 1 Pool 1	OG230207-001
2.	2244 C001 Scale, All, Culture	Well 2244 C001 Solids, All, PRD	OG230402-001
		Well 2244 C001 Solids, All, MPB	OG230402-002
		Well 2244 C001 Solids, all, IRB	OG230402-003
3.	2244 C001B Scale DIRECT	Pool 13 Well 2244 Scale C001B OD	OG230508-005
4.	2244, C002 - C034, Scale, All Cultures	Well 2244 C002 - C005 Solids, PRD	OG230402-004
		Well 2244 C002 - C005 Solids, MPB	OG230402-005
		Well 2244 C002 - C005 Solids, IRB	OG230402-006
		Well 2244 C006 - C022 Body, PRD	OG230402-007
		Well 2244 C006 - C022 Body, MPB	OG230402-008
		Well 2244 C006 - C022 Body, IRB	OG230402-009
		Well 2244 C006 - C022 Collar, PRD	OG230402-010
		Well 2244 C006 - C022 Collar, MPB	OG230402-011
		Well 2244 C006 - C022 Collar, IRB	OG230402-012
		Well 2244 C023 - C034 Body, PRD	OG230402-013
		Well 2244 C023 - C034 Body, MPB	OG230402-014
		Well 2244 C023 - C034 Body, IRB	OG230402-015
		Well 2244 C023 - C034 Collar, PRD	OG230402-016
		Well 2244 C023 - C034 Collar, MPB	OG230402-017
		Well 2244 C023 - C034 Collar, IRB	OG230402-018
5.	2244 C015 - C034, Scale DIRECT	Pool 37 Well 2244 Scale C015 - C022 Collar	OG230508-004
		MG08 Well 2244 Scale C023 - C034 Collar	OG230508-006
6.	2244 9 5/8 ID Solids, Culture	Well 2244 9 5/8 ID Solids, PRD	OG230402-019
		Well 2244 9 5/8 ID Solids, MPB	OG230402-020
		Well 2244 9 5/8 ID Solids, IRB	OG230402-021
7.	2244 Annulus Fluid, DIRECT	Pool 20 Well 2244 Annulus Fluids Black	OG230508-001
		Pool 22 Well 2244 Annulus Fluids Grey	OG230508-002
		Pool 27 Well 2244 Annulus Fluids Output Tank	OG230508-003

The populations were evaluated, within the context of most prevalent organisms and corrosion associated organisms (Table 10).

1. Soil samples were dominated by unclassified organisms and Perlucidibaca and Flavobacterium, the later of which are not of any specific concern in the context of MIC. The predominant soil IRB was Rhodoferax, which was not identified in any of the casing or annulus fluid samples. APB and SRB, although present, were minor components of the population.

2. C001 casing scale cultures combined data set (includes C001A and C001B) was dominated by spore forming Bacillus and Clostridium sp. The predominant IRB was Geosporobacter, a spore forming member of Class Clostridia. The predominant APB was the filamentous Trichococcus, but it is likely, however, that the Bacillus sp is also acid forming due to it's abundance in the PRD culture. The dominant sulfidogens were spore-forming members of class Clostridia, such as Desulfosporosinus and Desulfitobacterium.

3. C001B direct isolated data set was dominated by the Alphaproteobacteria, Ralstonia, an organism that is not generally implicated in corrosion in the field. Sulfidogens, primarily spore forming, were Dethiobacter. An IRB was not identified. This is consistent with MPN analysis which showed IRB were at least 3 log orders less than GHB (see table 2 MPN results all samples), and so are represented by low abundance organisms in the sequence data set, not all of which will be present in the dataset at the project sequence coverage. APB including Acetobacterium, Halanaerobium and Trichococcus were all present, albeit at a very low abundance. It may be that the Bacillus isolates in the sample are acid producing.

4. C002 to C034 casing scale cultures were dominated by the spore-forming IRB, Geosporobacter, the APB, Trichococcus, Bacillus sp. and unclassified organisms. Sulfidogens were diverse, and included spore-forming SRB and SuRB such as Desulfosporosinus and Desulfitobacterium. APB included Trichococcus and Acetobacterium.

5. C015 – C034 direct isolation dataset. Significantly dominated (24%) by Halanaerobium, a non-spore forming sulfidogen and APB that is associated with corrosion in O&G systems. Other sulfidogens in the data set were alkaline tolerant, spore forming Dethiobacter and Desulfitibacter. The predominant IRB was the spore forming organism, Geosporobacter. The APB Acetobacterium was also present.

6. 9 5/8" ID scrape culture data set. Dominated by APB including Trichococcus and Acetobacterium as well as the Bacillus sp. and unclassified organisms. The predominant IRB was the spore-forming IRB, Geosporobacter. Sulfidogens such as Dethiobacter and Desulfitobacterium were present.

7. Annulus Fluids direct isolation data set was similar to that of 5 (C015 – C034 direct isolation dataset), with Halanaerobium and unclassified organisms dominating the dataset. The predominant IRB was the spore-forming IRB, Geosporobacter. The alkaliphilic, spore-forming sulfidogen, Dethiobacter alkaliphilus, was also abundant in the sample.

Population Profile overall conclusion.
Sulfidogens, IRB, and APB were identified in all parts of well 2244, from soils, to casing joints, to annulus fluids. However, there was vertical distribution in abundance, with organisms of least concern in scale from C001, and organisms of most concern in lower levels of the well.

Overall, the population of bacteria with the profile of that found on the casing surface of C001 is not similar to populations of bacteria predicted to mediate the catastrophic level of corrosion on C001.

In contrast, the lower casing joints, C015 – C034, and the annulus fluids both characterized by extremely elevated (24%) levels of Halanaerobium. Halanaerobium is an organism associated with MIC in various oil and gas wells, and it's presence is of concern. Given that the corrosion event was in a region of the well where Halanaerobium was only a minor component, it is not apparent that Halanaerobium was responsible for the corrosion event.

Table 10. Top 21 most abundant organisms in Well 2244 soil, scale, and annulus fluid samples, data combined by sample type

Species	1. 2244 Soils, DIRECT	2. 2244 C001 Scale, All, Culture	3. 2244 C001B Scale DIRECT	4. 2244, C002 - C034, Scale Culture	5. 2244 C015 - C034, Scale DIRECT	6. 2244 9 5/8 ID Solids, Culture	7. 2244 Annulus Fluid, DIRECT	Select Traits of Interest: Metabolic, Physiological, Ecological, Taxonomic
Unclassified	29.793	7.280	16.756	14.504	27.579	7.855	35.646	Polyphyletic (not uniform); Unknown; Varies
Bacillus sp	0.081	22.867	1.898	21.734	2.011	15.277	2.398	Bacilli; BioDeg; Diverse; Firmicutes; GHB; Spore
Trichococcus sp	0.300	3.559	0.002	18.040	0.727	36.630	1.700	Activated Sludge; APB; Facultative Anaerobe; Ferm; Filamentous; Firmicutes; Lactobacillales; Wastewater
Halanaerobium sp	0.000	0.003	0.002	0.008	24.056	0.004	24.238	Anaerobe; APB; Clostridia; Ferm; Firmicutes; Halophile; MIC; SRB-Promoting; Sulfidogen; SuRB; TRB
Ralstonia sp	0.011	0.008	51.137	0.013	13.083	0.010	0.678	Betaproteobacteria; BioDeg; BioDeg HC
Geosporobacter sp	0.014	8.743	0.000	11.930	1.846	1.935	1.656	Anaerobe; Clostridia; Ferm; Firmicutes; IRB; Spore
Clostridium sp	0.282	14.581	0.000	7.564	1.172	6.435	3.293	Anaerobe; Clostridia; Diverse; Ferm; Firmicutes; GHB; Spore
Lysinibacillus sp	0.000	3.423	0.000	6.070	0.030	0.103	0.000	Aerobe; Bacilli; BioDeg; Bioremediation; Firmicute; Firmicutes; GHB; Metal tolerant; Soil; Spore
Clostridium botulinum	0.000	3.580	0.005	6.004	0.000	0.000	0.010	Anaerobe; Clostridia; Ferm; Firmicutes; Pathogen; Spore
Desulfosporosinus sp	0.058	8.900	0.000	4.636	0.179	0.005	0.289	Anaerobe; Clostridia; Firmicutes; Spore; SRB; Sulfidogen
Dethiobacter alkaliphilus	0.000	0.000	0.003	0.004	1.930	0.001	8.152	Alkaliphile; Anaerobe; Clostridia; Firmicutes; Spore; Sulfidogen; SuRB; TRB
Acetobacterium sp	0.000	0.001	0.000	1.647	0.768	6.667	0.977	Acetogen; Anaerobe; APB; Clostridia; Firmicutes
Soehngenia sp	0.000	0.004	0.000	0.178	0.141	12.082	0.979	Ferm; Firmicutes; Tissierellia
Desulfitobacterium sp	0.000	5.181	0.000	1.907	0.159	0.003	0.203	Anaerobe; BioDeg halogenated organic compounds; Clostridia; Ferm; Firmicutes; Metal Reduction; NiF; SIRB; Spore; Sulfidogen; SuRB; TRB
Pseudomonas sp	2.178	0.004	1.421	0.002	0.212	10.755	0.111	Aerobe; BioDeg; Gammaproteobacteria; GHB; Varies; Versatile; Widespread
Desulfitibacter alkalitolerans	0.000	0.000	0.000	0.000	1.846	0.000	3.188	Alkaliphile; Anaerobe; Clostridia; Firmicutes; Spore; Sulfidogen; SuRB; TRB
Perlucidibaca sp	12.039	0.000	0.000	0.000	0.000	0.000	0.000	Gammaproteobacteria; GHB
Flavobacterium sp	10.079	0.000	0.000	0.000	0.608	0.000	0.208	Aerobe; Bacteroidetes; BioDeg; BioDeg HC; Water
Paenibacillus sp	0.000	3.098	0.000	1.403	0.007	0.079	0.019	Bacilli; BioDeg; BioDeg EPS; BioDeg PAH; Dendritiformis colonies; Facultative Anaerobe; Firmicute; Firmicutes; Spore
Methanobacterium sp	0.000	0.000	0.000	0.000	0.207	0.000	2.619	Anaerobe; Archaea; Methanogen
Rhodoferax sp	8.123	0.000	0.000	0.000	0.000	0.000	0.000	Betaproteobacteria; IRB

Top 21 (out of 555) most abundant organism identified in well 2244 samples. The value is the % of the total population. Yellow are >10% of the population, Blue are 1 – 10% of the population, White are <1%, Gray are 0%, not identified in sample. Data with multiple sequence IDs are the averages for those samples. Direct is data from raw samples. Under traits, sulfidogens are indicated in red, IRB are indicated in green, and archaea in yellow. Trait Details: Polyphyletic (is not a homogenous grouping and includes multiple species) Unknown (traits are not known), Varies (likely to have multiple different traits), BioDeg (biodegrading organism capable of utilization of specialized substrates) GHB (general heterotrophic bacteria), Activated Sludge (present in activated sludge), Spore (spore-forming organism), APB (acid producing bacteria), Anaerobe / Aerobe (growth in absence or presence of oxygen, respectively), IRB (iron reducing bacteria), Acetic Acid and Acetogen (production of acids), Metal T (metal tolerant), Sulfidogen (produces H2S, can be by SuRB (sulfur reduction), TRB (thiosulfate reduction) SRB (sulfate reduction), MIC (known association with microbiological influenced corrosion)

Well 2244 Samples Unclassified Organisms

- A common theme of population analysis from well 2244 was the high percentage of unclassified organisms in almost all samples.
- For most samples from well 2244, “Unclassified” organisms represented a significant proportion of the population.
- Values ranged from less than 1% of the sample, to almost 70%.
- The number of possible organisms represented by “unclassified” annotations was determined.
- At least 100 unique organisms were classified as “unclassified”.
- Between 2 and 78 unclassified organisms were present in the samples, with the soil sample containing the most, at 78.
- Almost all of these were taxa present only in the soil sample, and almost all of these were “low abundance”, that is present at less than 1% of the sample (data not shown).
- A list of the 19 most abundant “unclassified” organisms is provided in Table 11.

The most relevant unclassified organisms are:

1. Unclassified Clostridia, present in all but 2 datasets, and particularly elevated in the MPB cultures set up with well 2244 scale at 2% to 56% of the sample. Possibly a sulfidogen whose growth is promoted by the selective MPB media
2. Unclassified Archaea, present in most datasets, and particularly elevated in the 3 annulus fluid data sets, as well as the two lower casing joints direct sequence datasets. Possibly a widespread Archaea that is resistant to culturing.
3. Unclassified Bacteria, present in most data sets including all of the direct sequencing datasets, soil and C001B in particular, as well as in the IRB culture datasets. However, additional experimental data would be required before calling this an IRB.
4. Uncultured Clostridiales present in most samples, in particular the IRB datasets, the annulus fluids, and the lower casing joint direct sequencing datasets.
5. Unclassified Peptococcaceae, particularly elevate in MPB cultures from casing joint C006 – C022 scale. Peptococcaceae are obligate anaerobes, and includes genera of spore-forming sulfidogens such as Desulfotomaculum.

Overall, it is apparent unclassified organisms, for which classification to the Genus species level was not possible, might include APB, SRB, and IRB. However, experimental data is required to verify this.

M 979-694-6500 ● F 979-694-6511 ● 11142 Hopes Creek Road ● College Station, Texas 77845 ● www.ecolyse.com

Table 11. Well 2244. Most abundant Unclassified Organisms in soil, scale, and annulus fluids

Taxonomy					Sample Details	well 2244 Soil	well 2244 Scal PRD C001	well 2244 Scal MPB C001	well 2244 Scal IRB C001	well 2244 Scal PRD C002-5	well 2244 Scal MPB C002-5	well 2244 Scal IRB C002-5	well 2244 Scal PRD C006-22 B	well 2244 Scal MPB C006-22 B	well 2244 Scal IRB C006-22 B	well 2244 Scal PRD C006-22 C	well 2244 Scal MPB C006-22 C	well 2244 Scal IRB C006-22 C	well 2244 Scal PRD C023-34 B	well 2244 Scal MPB C023-34 B	well 2244 Scal IRB C023-34 B	well 2244 Scal PRD C023-34 C	well 2244 Scal MPB C023-34 C	well 2244 Scal IRB C023-34 C	well 2244 Scal PRD 9 5/8 ID	well 2244 Scal MPB 9 5/8 ID	well 2244 Scal IRB 9 5/8 ID	well 2244 Scal C023-34 C	well 2244 Scal C015-22 C	well 2244 Scal C001 B	well 2244 Fluid Ann. Output	well 2244 Fluid Ann. Gray	well 2244 Fluid Ann. Blk
Kingdom	Phylum	Class	Order	Family	Species	OG230207-001	OG230402-001	OG230402-002	OG230402-003	OG230402-004	OG230402-005	OG230402-006	OG230402-007	OG230402-008	OG230402-009	OG230402-010	OG230402-011	OG230402-012	OG230402-013	OG230402-014	OG230402-015	OG230402-016	OG230402-017	OG230402-018	OG230402-019	OG230402-020	OG230402-021	OG230401-007	OG230305-006	OG230305-007	OG230305-004	OG230305-003	OG230305-002
Bacteria	Firmicutes	Clostridia	Unclassified	Unclassified	Unclassified	0.35	0	2.76	0.85	0	14.3	0.23	0.01	55.9	0.4	0.01	8.09	0.05	0.01	14.5	0.05	0.02	56.1	0.03	0	16.5	0.02	0.82	1.61	0	1.1	0.75	1.36
Archaea	Unclassified	Unclassified	Unclassified	Unclassified	Unclassified	0.36	0	0.01	0	0	0	0	0	0	0	0	0	0.01	0.01	0	0.01	0	0	0.01	0.01	0	0.01	7.35	16.7	0	21.8	10.5	20.9
Bacteria	Unclassified	Unclassified	Unclassified	Unclassified	Unclassified	13.8	0.02	1.72	4.68	0.11	0.11	0.44	0.02	0.13	1.59	0.16	0	0.83	0	0.02	1.47	0.06	0	0.09	0	0	3.43	4.77	1.09	6.13	4.83	3.07	5.2
Bacteria	Firmicutes	Erysipelotrichia	Erysipelotrichales	Unclassified	Unclassified	0	0	0	0	0	10.8	0	0	0	0.05	0	0	1.43	0	0	0	0	8.95	0.63	0	0.6	2.17	3.95	0.17	0	3.93	2.5	5.53
Bacteria	Firmicutes	Clostridia	Clostridiales	Unclassified	Unclassified	0.01	0.01	0.2	9.31	0	0	1.02	0	0	0.75	0	0	0.8	0	0	6.95	0	2.63	2.07	0	0	0.07	4.39	0.71	0	4.47	1.13	2.73
Bacteria	Firmicutes	Clostridia	Clostridiales	Peptococcaceae	Unclassified	0	0	1.1	0	0	0	0	0	14.1	0	0	0	0	0	4.78	0.01	0	0	0.02	0	0.01	0.02	0.22	0	0	0.1	0	0.18
Bacteria	Actinobacteria	Coriobacteriia	Coriobacteriales	Coriobacteriaceae	Unclassified	0	0	0	0	0	0	0	0	0	0	0	0	0	0	0	0	0	0	0	0	0	0	0.48	1.94	0	2.66	1.5	3.04
Bacteria	Firmicutes	Unclassified	Unclassified	Unclassified	Unclassified	0.01	0	1.19	0.06	0	0	0.05	0	0	0.05	0	0	0.09	0	0	2.71	0	0	0.04	0	0	0.01	0.94	0.09	0	1.77	0.66	0.94
Bacteria	Bacteroidetes	Sphingobacteriia	Sphingobacteriales	Unclassified	Unclassified	0.41	0	0.01	0.02	0	0	0	0	0	0.02	0	0.01	0.01	0	0	0	0	0	0	0	0	0	0.12	2.49	4.91	0	0.36	0
Bacteria	Proteobacteria	Deltaproteobacteria	Unclassified	Unclassified	Unclassified	0.26	0	0	0	0	0	0	0	0	0	0	0.01	0.04	0	0	0.99	0	0	0.98	0.01	0.01	0.02	0.29	0.72	0	0.45	0.27	0.83
Bacteria	Proteobacteria	Gammaproteobacter	Pseudomonadales	Unclassified	Unclassified	4.7	0	0	0	0	0	0	0	0	0	0	0	0	0	0	0	0	0	0	0	0	0	0	0	0	0.03	0	0.02
Bacteria	Proteobacteria	Alphaproteobacteria	Rhizobiales	Unclassified	Unclassified	0.08	0	0	0	0	0	0	0	0	0	0	0	0	0	0	0	0	0	0	0	0	0	0.43	2.29	0	0.5	0.27	1.01
Bacteria	Proteobacteria	Unclassified	Unclassified	Unclassified	Unclassified	1.32	0	0	0	0	0	0	0	0	0	0	0	0	0	0	0	0	0	0	0	0	0	0.15	0	1.77	0.01	0	0.12
Bacteria	Proteobacteria	Alphaproteobacteria	Rhodobacterales	Unclassified	Unclassified	0	0	0	0	0	0	0	0	0	0	0	0	0	0	0	0	0	0	0	0	0	0	0	0	2.37	0	0	0
Bacteria	Chlamydiae	Unclassified	Unclassified	Unclassified	Unclassified	0	0	0	0	0	0	0	0	0	0	0	0	0	0	0	0	0	0	0	0	0	0	0.01	1.95	0	0.02	0	0.02
Bacteria	Verrucomicrobia	Verrucomicrobiae	Verrucomicrobiales	Unclassified	Unclassified	1.88	0	0	0	0	0	0	0	0	0	0	0	0	0	0	0	0	0	0	0	0	0	0	0	0	0	0	0.01
Bacteria	Bacteroidetes	Unclassified	Unclassified	Unclassified	Unclassified	0.65	0	0	0	0	0	0	0	0	0.02	0	0	0	0	0	0	0.01	0	0	0	0	0	0.2	0.24	0.2	0.02	0.14	0.09
Bacteria	Verrucomicrobia	Unclassified	Unclassified	Unclassified	Unclassified	0.24	0	0	0	0	0	0	0	0	0	0	0	0	0	0	0	0	0	0	0	0	0	0	0	0.93	0.02	0	0.01
Bacteria	Acidobacteria	Acidobacteriia	Acidobacteriales	Unclassified	Unclassified	1.14	0	0	0	0	0	0	0	0	0	0	0	0	0	0	0	0	0	0	0	0	0	0	0	0	0	0.05	0
					%	29.6	0.03	6.99	14.9	0.13	25.2	1.75	0.03	70.2	3.69	0.17	8.12	3.25	0.03	19.3	12.4	0.09	67.7	3.87	0.19	17.1	5.75	24.5	30.4	16.7	42.5	21.4	42.8
					# Taxa	78	3	9	10	5	5	7	3	3	8	2	5	8	6	5	9	7	3	9	5	6	9	22	15	8	29	19	41

Table Legend: Expanded taxonomic lineages of “Unclassified” organisms. “Unclassified” is a designation provided to sequences whose closest matches in the public database lacks taxonomic information. Unclassified is a polyphyletic term, and may include numerous different types of organisms. This table provides more details on the diversity of unclassified organisms, showing the top most abundant members, with expanded lineages, where the highest level at which unclassified is designated are indicated in red. Values are % of the population, yellow indicates >10%, green are 1 to 10%, white are <1%, >0%, Gray are 0% (not identified in the sample).
For sample details, orange is the soil sample, blue-green are data sets obtained from sequencing DNA extracted from the cultured scale samples, yellow are the data sets obtained from sequencing DNA extracted directly from scale samples, and green are the black annulus liquid samples.
The bottom two rows (% and # Taxa) indicate the total % of all unclassified for that sample, and the number of different unclassified organisms.

Well 2244 Sulfidogenic Organisms

Samples from Well 2244 contained 47 sulfidogenic taxa, which is almost 8.4% of all taxa (Table 12). Most, 31, were spore-forming organisms from the Class Clostridia, while 9 were from Class Deltaproteobacteria. Several are alkaliphilic, and some are metal-reducing.

Table 12. Well 2244 all sulfidogenic organisms identified in the samples

Alkaliphilus crotonatoxidans	Alkaliphile; Anaerobe; Halophile; Clostridia; Firmicutes; Peptide Ferm; Spore; Sulfidogen
Alkaliphilus halophilus	Alkaliphile; Anaerobe; Halophile; Clostridia; Firmicutes; Peptide Ferm; Spore; Sulfidogen
Alkaliphilus oremlandii	Alkaliphile; Anaerobe; Halophile; Clostridia; Firmicutes; Peptide Ferm; Spore; Sulfidogen
Alkaliphilus sp	Alkaliphile; Anaerobe; Halophile; Clostridia; Firmicutes; Peptide Ferm; Spore; Sulfidogen
Citrobacter sp	Aerobe; Biofilm; Gammaproteobacteria; MIC; NRB; Sulfidogen
Clostridium celerecrescens	Anaerobe; Clostridia; Firmicutes; Spore; SRB; Sulfidogen
Desulfitibacter alkalitolerans	Alkaliphile; Clostridia; Firmicutes; Anaerobe; Spore; Sulfidogen; SuRB; TRB
Desulfitispora sp	Alkaliphile; Anaerobe; Halophile; Clostridia; Firmicutes; Spore; Sulfidogen; TRB
Desulfitobacterium aromaticivorans	Anaerobe; BioDeg; Metal Reduction; Clostridia; Firmicutes; Spore; Sulfidogen; SuRB; TRB
Desulfitobacterium dehalogenans	Anaerobe; BioDeg; Metal Reduction; Clostridia; Firmicutes; Spore; Sulfidogen; SuRB; TRB
Desulfitobacterium dichloroeliminans	Anaerobe; BioDeg; Metal Reduction; Clostridia; Firmicutes; Spore; Sulfidogen; SuRB; TRB
Desulfitobacterium sp	Anaerobe; BioDeg; Metal Reduction; Clostridia; Firmicutes; Spore; Sulfidogen; SuRB; TRB
Desulfobacter sp	Anaerobe; Deltaproteobacteria; SRB; Sulfidogen
Desulfobulbus sp	Anaerobe; Deltaproteobacteria; SRB; Sulfidogen
Desulfomonile sp	Anaerobe; BioDeg; Deltaproteobacteria; SRB; Sulfidogen
Desulfonosporus sp	Anaerobe; Clostridia; Firmicutes; Spore; SRB; Sulfidogen
Desulforegula sp	Anaerobe; Deltaproteobacteria; SRB; Sulfidogen
Desulfosporosinus burensis	Anaerobe; Clostridia; Firmicutes; Spore; SRB; Sulfidogen
Desulfosporosinus sp	Anaerobe; Clostridia; Firmicutes; Spore; SRB; Sulfidogen
Desulfotomaculum aeronauticum	Anaerobe; Clostridia; Firmicutes; Spore; SRB; Sulfidogen
Desulfotomaculum defluvii	Anaerobe; Clostridia; Firmicutes; Spore; SRB; Sulfidogen
Desulfotomaculum geothermicum	Anaerobe; Clostridia; Firmicutes; Spore; SRB; Sulfidogen
Desulfotomaculum reducens	Anaerobe; Clostridia; Firmicutes; Spore; SRB; Sulfidogen
Desulfotomaculum sp	Anaerobe; Clostridia; Firmicutes; Spore; SRB; Sulfidogen; Thermophile
Desulfovibrio alaskensis	Anaerobe; Deltaproteobacteria; Oilfield; SRB; Sulfidogen
Desulfovibrio desulfuricans	Anaerobe; Deltaproteobacteria; SRB; Sulfidogen
Desulfovibrio sp	Anaerobe; Deltaproteobacteria; SRB; Sulfidogen
Desulfuromonas sp	Anaerobe; Deltaproteobacteria; IRB; Sulfidogen; SuRB
Dethiobacter alkaliphilus	Alkaliphile; Anaerobe; Clostridia; Firmicutes; Spore; Sulfidogen; TRB
Dethiosulfatibacter sp	Anaerobe; Clostridia; Firmicutes; Spore; Sulfidogen; SuRB; TRB
Fusibacter paucivorans	Anaerobe; Clostridia; Firmicutes; Sulfidogen; SuRB; TRB
Fusibacter sp	Anaerobe; Clostridia; Firmicutes; Sulfidogen; SuRB; TRB
Garciella sp	Clostridia; Firmicutes; NRB; Oilfield; Sulfidogen; TRB
Geotoga sp	Sulfidogen; SuRB; Thermophile; Thermotogae
Halanaerobium saccharolyticum	Anaerobe; APB; Clostridia; Ferm; Firmicutes; Halophile; MIC; SRB-Promoting; Sulfidogen; TRB
Halanaerobium sp	Anaerobe; APB; Clostridia; Ferm; Firmicutes; Halophile; MIC; SRB-Promoting; Sulfidogen; TRB
Limnobacter sp	Betaproteobacteria; Sulfidogen; TRB
Moorella sp	Acetogen; Anaerobe; APB; Clostridia; Ferm; Firmicutes; NRB; Spore; Sulfidogen; TRB
Moorella thermoacetica	Acetogen; Anaerobe; APB; Clostridia; NRB; Spore; Sulfidogen; TRB
Shewanella sp	Facultative Anaerobe; Gammaproteobacteria; IRB; Sulfidogen; TRB
Spirochaeta sp	Anaerobe; Ferm; H2S resistant; Halophile; Sulfidogen; TRB
Syntrophobacter sp	BioDeg HC; Deltaproteobacteria; Methanogen Syntroph; SRB; Sulfidogen
Thermoanaerobacter italicus	Anaerobe; Clostridia; Ferm; Firmicutes; Sulfidogen; Thermophile; TRB
Thermoanaerobacter sp	Anaerobe; Clostridia; Ferm; Firmicutes; Sulfidogen; Thermophile; TRB
Thermoanaerobacterium saccharolyticum	Anaerobe; APB; Clostridia; Firmicutes; NRB; Spore; Sulfidogen; Thermophile; TRB
Thermoanaerobacterium thermosaccharolyticum	Anaerobe; APB; Clostridia; Firmicutes; NRB; Spore; Sulfidogen; Thermophile; TRB

All sulfidogenic organisms identified in well 2244 samples. Sulfidogens are defined as H2S producing, which can be by any of the following mechanisms: SRB (sulfate reducing bacteria), TRB (thiosulfate reducing bacteria), SuRB (sulfur reducing bacteria), Peptide Fermenting (production of H2S through peptide fermentation). Additional traits indicated are IRB (iron reducing bacteria) Ferm (fermentation), Spore (spore forming), Halophile (salt tolerant), APB (acid producing), MIC (microbiological influenced corrosion associated), Alkaliphile (growth at high pH).

Appendix A
Well 2244, 2248, 2251 Sample List

Pool	BLRM Sample ID	Corresponding Blade Sample ID	Sample Description: Source Well, Casing Joint, Sample Type	Sample Date	Quantity g or ml
1	BLRM230216-001	RM-2244-S001, RM-2244-S002, RM-2244-S003	Well 2244 Soils (3 soil sample composite)	2/16/23	211.0
2	BLRM230216-002	RM-2248-S001	Well 2248 Soils	2/16/23	359.0
3	BLRM230216-003	RM-2251-S001, RM-2251-S002	Well 2251 Soils (2 soil sample composite)	2/16/23	162.0
4	BLRM230303-001	RM-2244-W06-S1	Well 2244 Scale W06 Master Valve	3/3/23	17.3
4	BLRM230303-002	no sample ID	Well 2244 Scale W03 - Flowcross	3/3/23	2.74
4	BLRM230303-003	no sample ID	Well 2244 Scale W03 - Flowcross Wing Side	3/3/23	14.67
5	BLRM230303-005	no sample ID	Well 2244 Scale W02 Crown Valve Freeable Solids	3/3/23	22.49
6	BLRM230303-007	no sample ID	Well 2244 Scale W04 - Southside Wing Valve Brown Solids	3/3/23	15.03
6	BLRM230303-008	no sample ID	Well 2244 Scale W05 - Wing Valve Solids	3/3/23	1.01
7	BLRM230303-004	no sample ID	Well 2244 Grease W02 Crown Valve	3/3/23	27.15
7	BLRM230303-006	no sample ID	Well 2244 Grease + Solids W04 - Southside Wing Valve	3/3/23	30.86
7	BLRM230303-009	no sample ID	Well 2244 Grease W05 - Wing Valve	3/3/23	15.01
8	BLRM230305-001	RM-2244-C001A-S1	Well 2244 Scale 7" C001A OD below seal ring	3/5/23	137.7
9	BLRM230305-002	RM-2244-C001A-S2	Well 2244 Scale 7" C001A OD above failure	3/5/23	4.85
9	BLRM230305-003	RM-2244-C001A-S3	Well 2244 Scale 7" C001A ID above failure	3/5/23	1.65
9	BLRM230305-004	RM-2244-C001A-S4	Well 2244 Scale 7" C001A Scale from slips	3/5/23	0.74
10	BLRM230305-005	RM-2244-C001A-S5	Well 2244 Scale 7" C001A OD above failure	3/5/23	10.59
11	BLRM230305-006	RM-2244-C001A-S6	Well 2244 Scale 7" C001A Scale from Slips	3/5/23	11.44
12	BLRM230306-001	RM-2244-C001B-S1	Well 2244 Scale 7" C001B OD 1' to 3' from cut end	3/6/23	8.9
12	BLRM230306-002	RM-2244-C001B-S2	Well 2244 Scale 7" C001B OD 42" to 60" from cut end	3/6/23	6
13	BLRM230306-003	RM-2244-C001B-S3	Well 2244 Scale 7" C001B OD 68" to 84 " from cut end	3/6/23	33.7
14	BLRM230306-004	RM-2244-C001B-S4	Well 2244 Scale 7" C001B OD 84" to 94" from cut end	3/6/23	26
15	BLRM230306-005	RM-2244-C001B-S5	Well 2244 Scale 7" C001B OD 102" to 117" from cut end	3/6/23	11.71
16	BLRM230306-006	RM-2244-C001B-S6	Well 2244 Scale 7" C001B OD 120" from cut end	3/6/23	17.26
16	BLRM230306-007	RM-2244-C001B-S7	Well 2244 Scale 7" C001B OD 14' from cut end	3/6/23	5.86
17	BLRM230308-001	RM-2244-L01	Well 2244 Annulus Fluids Clear (7" - 9 5/8")	3/8/23	500
17	BLRM230308-002	RM-2244-L02	Well 2244 Annulus Fluids Clear (7" - 9 5/8")	3/8/23	500
17	BLRM230308-003	RM-2244-L03	Well 2244 Annulus Fluids Clear (7" - 9 5/8")	3/8/23	500
17	BLRM230308-004	RM-2244-L04	Well 2244 Annulus Fluids Clear (7" - 9 5/8")	3/8/23	500
18	BLRM230308-005	RM-2244-L05	Well 2244 Annulus Fluids Clear (7" - 9 5/8")	3/8/23	500

Pool	BLRM Sample ID	Corresponding Blade Sample ID	Sample Description: Source Well, Casing Joint, Sample Type	Sample Date	Quantity g or ml
18	BLRM230308-006	RM-2244-L06	Well 2244 Annulus Fluids Clear (7" - 9 5/8")	3/8/23	500
18	BLRM230308-007	RM-2244-L07	Well 2244 Annulus Fluids Clear (7" - 9 5/8")	3/8/23	500
18	BLRM230308-008	RM-2244-L08	Well 2244 Annulus Fluids Clear (7" - 9 5/8")	3/8/23	500
19	BLRM230308-009	RM-2244-L09	Well 2244 Annulus Fluids Clear (7" - 9 5/8")	3/8/23	500
19	BLRM230308-010	RM-2244-L10	Well 2244 Annulus Fluids Clear (7" - 9 5/8")	3/8/23	500
19	BLRM230308-011	RM-2244-L11	Well 2244 Annulus Fluids Clear (7" - 9 5/8")	3/8/23	500
20	BLRM230308-012	RM-2244-L12	Well 2244 Annulus Fluids Brown (7" - 9 5/8")	3/8/23	500
20	BLRM230308-013	RM-2244-L13	Well 2244 Annulus Fluids Black Viscous (7" - 9 5/8")	3/8/23	500
20	BLRM230308-014	RM-2244-L14	Well 2244 Annulus Fluids Black Viscous (7" - 9 5/8")	3/8/23	500
20	BLRM230308-015	RM-2244-L15	Well 2244 Annulus Fluids Black Viscous (7" - 9 5/8")	3/8/23	500
21	BLRM230308-016	RM-2244-L16	Well 2244 Annulus Fluids Black Viscous (7" - 9 5/8")	3/8/23	500
21	BLRM230308-017	RM-2244-L17	Well 2244 Annulus Fluids Black Viscous (7" - 9 5/8")	3/8/23	500
21	BLRM230308-018	RM-2244-L18	Well 2244 Annulus Fluids Black Viscous (7" - 9 5/8")	3/8/23	500
21	BLRM230308-019	RM-2244-L19	Well 2244 Annulus Fluids Black Viscous (7" - 9 5/8")	3/8/23	500
22	BLRM230308-020	RM-2244-L20	Well 2244 Annulus Fluids Gray (7" - 9 5/8")	3/8/23	500
23	BLRM230308-021	RM-2244-L21	Well 2244 Annulus Fluids Injection Tank source, clear	3/8/23	500
24	BLRM230308-022	RM-2244-C001C-S1	Well 2244 Scale 7" C001C Overshot Material	3/8/23	95.95
25	BLRM230308-023	RM-2244-C001C-S2	Well 2244 Scale 7" C001C OD solids, 0 - 5'	3/8/23	96.06
26	BLRM230308-024	RM-2244-C001C-S3	Well 2244 Scale 7" C001C OD solids, 5' - 8'	3/8/23	25.27
26	BLRM230308-025	RM-2244-C001C-S4	Well 2244 Scale 7" C001C OD solids, 8 - 12'	3/8/23	3.47
27	BLRM230309-002	RM-2244-L22	Well 2244 Annulus Fluids Output Tank Foam, 16 hr	3/9/23	500
28	BLRM230309-003	RM-2244-C002-S1, RM-2244-C002-S2	Well 2244 Scale OD 7" Body and Collar C002	3/9/23	2.1
28	BLRM230309-004	RM-2244-C003-S1, RM-2244-C003-S2	Well 2244 Scale OD 7" Body and Collar C003	3/9/23	79.33
29	BLRM230309-005	RM-2244-C004-S1	Well 2244 Scale OD 7" Centralizer C004	3/9/23	59.19
30	BLRM230309-006	RM-2244-C004-S2	Well 2244 Scale OD 7" Body and Collar C004	3/9/23	34.4
31	BLRM230309-007	RM-2244-C005-S1	Well 2244 Scale OD 7" Body and Collar C005	3/9/23	63.17
32	BLRM230309-008	RM-2244-C006-S1	Well 2244 Scale OD 7" Body C006	3/9/23	15.36
32	BLRM230309-010	RM-2244-C007-S1	Well 2244 Scale OD 7" Body C007	3/9/23	1.92
33	BLRM230309-009	RM-2244-C006-S2	Well 2244 Scale OD 7" Collar C006	3/9/23	30.43
33	BLRM230309-011	RM-2244-C007-S2	Well 2244 Scale OD 7" Collar C007	3/9/23	39.56

Appendix A
Well 2244, 2248, 2251 Sample List

Pool	BLRM Sample ID	Corresponding Blade Sample ID	Sample Description: Source Well, Casing Joint, Sample Type	Sample Date	Quantity g or ml
34	BLRM230309-012	RM-2244-C008-S1, RM-2244-C009-S1, RM-2244-C010-S1	Well 2244 Scale OD 7" Body C008, C009, C010	3/9/23	6.62
34	BLRM230309-014	RM-2244-C011-S1, RM-2244-C012-S1	Well 2244 Scale OD 7" Body, C011, C012, C013, C014	3/9/23	8.14
35	BLRM230309-013	RM-2244-C008-S2, RM-2244-C009-S2, RM-2244-C010-S2	Well 2244 Scale OD 7" Collar, C08, C09, C10	3/9/23	77.65
35	BLRM230309-015	RM-2244-C011-S2, RM-2244-C012-S2	Well 2244 Scale OD 7" Collar, C011, C012, C013, C014	3/9/23	100.97
36	BLRM230309-016	no sample ID	Well 2244 Scale OD 7" Body, C015, C016, C017	3/9/23	5.85
36	BLRM230309-018	no sample ID	Well 2244 Scale OD 7" Body, C018, C019, C020, C021, C022	3/9/23	8.15
37	BLRM230309-017	no sample ID	Well 2244 Scale OD 7" Collar, C015, C016, C017	3/9/23	69.11
37	BLRM230309-019	no sample ID	Well 2244 Scale OD 7" Collar, C018, C019, C020, C021, C022	3/9/23	101.58
38	BLRM230311-001	no sample ID	Well 2244 Scale OD 7" Body, C023	3/11/23	9.42
38	BLRM230311-003	no sample ID	Well 2244 Scale OD 7" Body, C024	3/11/23	3.82
39	BLRM230311-002	no sample ID	Well 2244 Scale OD 7" Collar, C023	3/11/23	13.15
39	BLRM230311-004	no sample ID	Well 2244 Scale OD 7" Collar, C024	3/11/23	15.07
40	BLRM230311-005	no sample ID	Well 2244 Scale OD 7" Body, C025	3/11/23	2.25
40	BLRM230311-007	no sample ID	Well 2244 Scale OD 7" Body, C026	3/11/23	1.65
40	BLRM230311-009	no sample ID	Well 2244 Scale OD 7" Body, C027	3/11/23	1.35
41	BLRM230311-006	no sample ID	Well 2244 Scale OD 7" Collar, C025	3/11/23	5.96
41	BLRM230311-008	no sample ID	Well 2244 Scale OD 7" Collar, C026	3/11/23	10.8
41	BLRM230311-010	no sample ID	Well 2244 Scale OD 7" Collar, C027	3/11/23	13.13
42	BLRM230311-011	no sample ID	Well 2244 Scale OD 7" Body, C028	3/11/23	1.02
42	BLRM230311-014	no sample ID	Well 2244 Scale OD 7" Body, C029	3/11/23	2.46
42	BLRM230311-016	no sample ID	Well 2244 Scale OD 7" Body, C030, C031, C032, C033, C034	3/11/23	4.89
43	BLRM230311-012	no sample ID	Well 2244 Scale OD 7" Collar, C028	3/11/23	7.63
44	BLRM230311-015	no sample ID	Well 2244 Scale OD 7" Collar, C029	3/11/23	23.76

Pool	BLRM Sample ID	Corresponding Blade Sample ID	Sample Description: Source Well, Casing Joint, Sample Type	Sample Date	Quantity g or ml
45	BLRM230311-017	no sample ID	Well 2244 Scale OD 7" Collar, C030, C031, C032, C033, C034	3/11/23	77.24
46	BLRM230312-001	RM-2244-Scraper-001	Well 2244 Scale 9 5/8 ID scrape 0-200 ft	3/12/23	355.2
47	BLRM230313-001	RM-2244-Scraper-001	Well 2244 Scale 9 5/8 ID scrape 0-1475 ft	3/13/23	44.52
48	BLRM230309-020, BLRM230311-013	no sample ID	Well 2244 Slime on OD	3/11/23	11.87
49	BLRM230317-001	no sample ID	Well 2248 Scale Annulus valve Solids	3/17/23	0.8
50	BLRM230317-002	no sample ID	Well 2248 Scale Annulus valve Solids	3/17/23	0.8
51	BLRM230326-001	no sample ID	Well 2248 Fluids Annulus Liquid Sample	3/26/23	500
52	BLRM230326-002	RM-2248-C001-S1	Well 2248, C001 Scale Sample OD	3/26/23	190
53	BLRM230326-003	RM-2248-C001-S2	Well 2248, C001 Scale Sample Couplings	3/26/23	28.2
54	BLRM230326-004	no sample ID	Well 2248, C001 OD Scale, 4 - 5 lbs	3/26/23	2360
55	BLRM230326-005	no sample ID	Well 2248 Scale OD Scale, Conductor	3/26/23	91.5
56	BLRM230328-001	2248-C001-S4	Well 2248 Scale C001 Scale OD sample	3/28/23	7.5
57	BLRM230328-002	no sample ID	Compressor Station Seperator Fluid, Black. Chemical smell	3/28/23	200
58	BLRM230328-003	no sample ID	Compressor Station Seperator Fluid, Clear. Chemical smell	3/28/23	200
59	BLRM230329-001	RM-2248-958-S1	Well 2248 Scale Uppermost 9 5/8" casing ID scrape	3/29/23	70.8
60	BLRM230401-001	RM-Pond-L1	Compressor Station Fluid pond sample, clear	4/1/23	500
61	BLRM230401-002	RM-Pond-L2	Compressor Station Fluid pond sample, emulsion	4/1/23	500
62	BLRM230403-001	RM-2251-C001-S01	Well 2251 Scale 7" OD, C001 top of joint	4/3/23	23.2
63	BLRM230403-002	RM-2251-C001-S02	Well 2251 Scale 7" OD, C001 top of joint	4/3/23	508.5
64	BLRM230403-003	RM-2251-C001-S03	Well 2251 Scale 7" OD, C001 10'6" top of cement	4/3/23	9.2

Table Well 2244, 2248, 2251 Samples. Pool Numbers are the combined sample pools used for analysis. BLRM numbers are "Blade Rager Mountain" sample identification numbers indicating year, month, day of collection. Sampling locations are CS (compressor station) where the 2244 master valve and tree and C001 7" casing fracture pieces were moved to after extraction from well site. Sample Types are: S (solid, scale), L (liquid/ fluids), G (grease). Most samples were collected from the OD surface of the 7" casing. Casing joints are sequentially numbered C001 to C034, with C001 being the failure facture site casing joint attached to the master valve and tree, at the surface, all the way down to casing joint C034 approximately 1364 ft below the surface. "Collar" samples were from the accumulated material around the lip of the casing collar, plus or minus 1 - 2', and "Body" samples were collected from the remaining length of casing joint (most of the length of the casing, 36 ft). A few were ID surfaces from the 9 5/8" casings. W0 samples were collected from the master valve and tree removed from well 2244. Most liquid samples were annular fluids, pumped out from the space between the 7" casing and the 9 5/8 inch casing, except for the sample collected from the input water strage tank and the output catch tank (taken ~16 hours after pumping annular fluids into it). Additionally, fluid samples from the separator and pond were provided. Quantity is either g for scale/solids/ grease or ml for fluids/ liquids.

Appendix B. Well 2244 Soil, Scale, Annulus Fluid Microbial Population
16S Amplicon Metagenomic Analysis
Samples collected March 2023

Sequence ID	OG230207-001	OG230402-001	OG230402-002	OG230402-003	OG230402-004	OG230402-005	OG230402-006	OG230402-007	OG230402-008	OG230402-009	OG230402-010	OG230402-011	OG230402-012	OG230402-013	OG230402-014	OG230402-015	OG230402-016	OG230402-017	OG230402-018	OG230402-019	OG230402-020	OG230402-021	OG230508-001	OG230508-002
Well 2244 Sample Description:	Soils Direct	C001 Scale, All, PRD	C001 Scale, All, MPB	C001 Scale, All, IRB	C002 - C005 Scale, PRD	C002 - C005 Scale, MPB	C002 - C005 Scale IRB	C006 - C022 Scale Body, PRD	C006 - C022 Scale Body, MPB	C006 - C022 Scale Body IRB	C006 - C022 Scale Collar, PRD	C006 - C022 Scale Collar, MPB	C006 - C022 Scale Collar IRB	C023 - C034 Scale Body, PRD	C023 - C034 Scale Body, MPB	C023 - C034 Scale Body IRB	C023 - C034 Scale Collar, PRD	C023 - C034 Scale Collar, MPB	C023 - C034 Scale Collar , IRB	9 5/8 ID Scale, PRD	9 5/8 ID Scale, MPB	9 5/8 ID Scale IRB	Pool 20 Annulus Fluids Black Direct	Pool 22 Annulus Fluids Grey Direct
Acetanaerobacterium elongatum	0	0	0	0.006	0	0	0	0	0	0	0	0	0	0	0	0	0	0	0.019	0	0	0	0	0
Acetivibrio sp	0	0	0	0.006	0	0	0	0	0	0	0	0	0	0	0	0	0	0	0	0	0	0	0.463	0.026
Acetobacterium sp	0	0	0.004	0	0	0	0.53	0	0	0	0	8.791	1.075	0.007	0.004	0	0.005	13.609	0.682	0	18.894	1.106	1.243	0.823
Acholeplasma sp	0	0	0	0	0	0	0	0	0	0	0	0	0	0	0	0	0	0	0	0	0	0	0.044	0
Acidobacterium sp	0.731	0	0	0	0	0	0	0	0	0	0	0	0	0	0	0	0	0	0	0	0	0	0.032	0.081
Acidovorax sp	0.331	0.004	0.004	0	0	0.01	0	0.011	0	0	0	0	0	0	0	0	0	0.006	0	0	0.112	0	0.012	0.131
Acinetobacter sp	2.138	0	0	0	0	0	0	0	0.009	0	0	0.004	0	0	0	0	0	0	0	0	0	0	0.045	0.093
Actinobacillus sp	0	0	0	0	0	0	0	0	0	0	0	0	0	0	0	0	0	0	0	0	0	0	0	0
Actinomadura sp	0	0	0	0	0	0	0	0	0	0	0	0	0	0	0	0	0	0	0	0	0	0	0	0
Actinomyces sp	0.055	0	0	0	0	0	0	0	0	0	0	0	0	0	0	0	0	0	0	0	0	0	0.016	0.014
Actinomycetospora sp	0.002	0	0	0	0	0	0	0	0	0	0	0	0	0	0	0	0	0	0	0	0	0	0	0
Aerococcus sp	0	0	0.004	0	0.011	0	0.004	0	0	0	0	0	0	0.059	0	0	0.057	0	0.043	0.168	0	0.072	0	0
Aeromonas sp	0	0	0	0	0	0	0	0	0	0	0	0	0	0	0	0	0	0	0	0	0	0	0.008	0.048
Afipia sp	0.002	0	0	0	0	0	0	0	0	0	0	0	0	0	0	0	0	0	0	0	0	0	0	0
Aggregicoccus edonensis	0.007	0	0	0	0	0	0	0	0	0	0	0	0	0	0	0	0	0	0	0	0	0	0	0
Agromyces sp	0.002	0	0	0	0	0	0	0	0	0	0	0	0	0	0	0	0	0	0	0	0	0	0	0
Algoriphagus sp	0.051	0	0	0	0	0	0	0	0	0	0	0	0	0	0	0	0	0	0	0	0	0	0	0
Alicyclobacillus ferrooxydans	0	0	0	0	0	0	0	0	0	0	0	0	0	0	0	0	0	0	0	0	0	0	0.025	0
Aliihoeflea sp	0	0	0	0	0	0	0	0	0	0	0	0	0	0	0	0	0	0	0	0	0	0	0.073	0.026
Alkalibacter sp	0	0	0	0	0	0	0	0	0	0	0	0	0.035	0	0	0	0	0	0	0	0	0.044	0.076	0.102
Alkalibacterium sp	0	0	0.004	0	0	0	0.013	0	0	0	0	0.007	0	0	0	0.017	0	1.153	0	0	0	0	0.208	0.285
Alkaliphilus crotonatoxidans	0	0	0	7.675	0	0	0	0	0	0	0	0	0.014	0	0	0.085	0	0	0	0	0	0	0.001	0.002
Alkaliphilus halophilus	0	0	0	0	0	0	0	0	0	0	0	0	0	0	0	0	0	0	0	0	0	0	0.008	0.007
Alkaliphilus oremlandii	0	0	0	0.069	0	0	0	0	0	1.489	0	0	0	0	0	0	0	0	0	0	0	0	0	0
Alkaliphilus sp	0	0	0.004	13.664	0	0.015	0	0	0	0.142	0	0.055	0.004	0	0.51	0	0	0	0.706	0	0	0.004	0.019	0
Alkanindiges illinoisensis	1.569	0	0	0	0	0	0	0	0	0	0	0	0	0	0	0	0	0	0	0	0	0	0	0
Alkanindiges sp	0.449	0	0	0	0	0	0	0	0	0	0	0	0	0	0	0	0	0	0	0	0	0	0	0
Altererythrobacter sp	0.079	0	0	0	0	0	0	0	0	0	0	0	0	0	0	0	0	0	0	0	0	0	0	0
Aminivibrio pyruvatiphilus	0	0	0	0	0	0	0	0	0	0	0	0	0	0	0	0	0	0	0.006	0	0	0.215	0.177	0.012
Aminobacter sp	0.026	0	0	0	0	0	0	0	0	0	0	0	0	0	0	0	0	0	0	0	0	0	0	0
Ammoniphilus sp	0	0	0	0	0	0	0	0	0	0	0	0	0	0	0	0	0	0	0	0	0	0	0.022	0
Amycolatopsis sp	0	0	0	0	0	0	0	0	0	0	0	0	0	0	0	0	0	0	0	0	0	0	0.005	0
Anaerobacterium chartisolvens	0	0	0	0	0	0	0	0	0	0	0	0	0	0	0	0	0	0	0	0	0	0	0.023	0.005
Anaerobranca horikoshii	0	0	0	0	0	0	0	0	0	0	0	0	0	0	0	0	0	0	0	0	0	0	0.007	0
Anaerolinea sp	0.023	0	0	0	0	0	0	0	0	0	0	0	0	0	0	0	0	0	0	0	0	0	0.043	0
Anaeromyxobacter dehalogenans	0	0	0	0	0	0	0	0	0	0	0	0	0	0	0	0	0	0	0	0	0	0	0.011	0
Anaeromyxobacter sp	0.044	0	0	0	0	0	0	0	0	0	0	0	0	0	0	0	0	0	0	0	0	0	0.045	0.036
Anaerophaga sp	0	0	0	0	0	0	0	0	0	0	0	0	0	0	0	0	0	0	0	0	0	0	0	0.017
Anaerosalibacter bizertensis	0	0	0.745	0	0	0	0	0	0.783	0	0	0	0	0	5.634	0	0	0	0	0	0	0	0	0
Anaerovorax sp	0.095	0	0	0	0	0	0	0	0	0	0	0	0	0	0	0	0	0	0	0	0	0	0.019	0
Aneurinibacillus migulanus	0	0	0	0	0	0	0	0	0	0	0	0	0	0	0	0	0	0	0	0	0	0	0.005	0
Aquabacterium sp	2.682	0	0	0	0	0	0	0	0	0	0	0	0	0	0	0	0	0	0	0	0	0.875	0.022	0
Aquamicrobium sp	0	0	0	0	0	0	0	0	0	0.024	0	0.007	0	0	0	0	0	0	0	0	0	0	0	0
Aquicella sp	0.011	0	0	0	0	0	0	0	0	0	0	0	0	0	0	0	0	0	0	0	0	0	0.07	0.105
Aquihabitans daechungensis	0.004	0	0	0	0	0	0	0	0	0	0	0	0	0	0	0	0	0	0	0	0	0	0	0
Arcobacter nitrofigilis	0	0	0	0	0	0	0	0	0	0	0	0	0	0	0	0	0	0	0	0	0	0	0.036	0
Arcobacter sp	0	0	0	0	0	0	0	0	0.004	0.071	0	0	0	0	0	0	0.019	0	0	0	0.003	0	0	0
Arenimonas aquatica	0.023	0	0	0	0	0	0	0	0	0	0	0	0	0	0	0	0	0	0	0	0	0	0	0
Arenimonas daechungensis	0.005	0	0	0	0	0	0	0	0	0	0	0	0	0	0	0	0	0	0	0	0	0	0	0
Arenimonas sp	0.254	0	0	0	0	0	0	0	0	0	0	0	0	0	0	0	0	0	0	0	0	0	0	0
Arhodomonas sp	0	0	0	0	0	0	0	0	0	0	0	0	0	0	0	0	0	0	0	0	0	0	0	0
Arthrobacter sp	0.679	0.008	0	0	0	0	0.004	0	0	0	0.009	0	0	0	0	0.004	0	0.006	0	0	0	0	0.07	0.266
Azoarcus sp	0.07	0	0	0	0	0	0	0	0	0	0	0	0	0	0	0	0	0	0	0	0	0	0	0
Azohydromonas lata	0.012	0	0	0	0	0	0	0	0	0	0	0	0	0	0	0	0	0	0	0	0	0	0	0
Azonexus hydrophilus	0	0	0	0	0	0	0	0	0	0	0	0	0	0	0	0	0	0	0	0	0	0	0.007	0
Azospirillum sp	0	0	0	0	0	0	0	0	0	0	0	0	0	0	0	0	0	0	0	0	0	0	0.016	0.021
Bacillus acidicola	0	0	0	0	0.004	0	0	0	0	0	0	0	0	0	0	0	0	0	0	0	0	0	0	0

Sequence ID	OG230508-003	OG230508-004	OG230508-005	OG230508-006	Selected Traits
Well 2244 Sample Description:	Pool 27 Annulus Fluids Tank Direct	Pool 37 C015 - C022 Scale C Direct	Pool 13 C001B OD Scale All Direct	MG08 C023 - C034 Scale C Direct	Metabolic, Taxonomic, Physiological, Ecological
Acetanaerobacterium elongatum	0	0	0	0	Clostridia; Firmicutes
Acetivibrio sp	0.342	0	0	0.034	BioDeg; Clostridia; Firmicutes; Plant biomass
Acetobacterium sp	0.866	0	0	1.535	Acetic Acid; Acetogen; Anaerobe; APB; Clostridia; Firmicutes
Acholeplasma sp	0	0	0	0.216	Facultative Anaerobe; GHB; Tenericutes
Acidobacterium sp	0	0	0	0	Acidobacteria; Acidophile; Aerobe; APB
Acidovorax sp	0.026	0.576	1.518	0.245	Anaerobe; Betaproteobacteria; Facultative; Facultative Anaerobe; Fe(II)OX; Green Rust; MIC; NRB
Acinetobacter sp	0.033	0.058	0	0.323	Aerobe; BioDeg; BioDeg HC; Gammaproteobacteria; Soil
Actinobacillus sp	0.011	0	0	0	
Actinomadura sp	0.012	0	0	0	Actinobacteria
Actinomyces sp	0.006	0	0	0	Actinobacteria; Ferm
Actinomycetospora sp	0	0	0	0	Actinobacteria
Aerococcus sp	0.004	0	0	0	Firmicutes; GHB; Lactobacillales
Aeromonas sp	0.004	0.428	0	0	Facultative Anaerobe; Gammaproteobacteria; GHB; Water
Afipia sp	0.004	0	0	0	Alphaproteobacteria; Biofilm; MIC
Aggregicoccus edonensis	0	0	0	0	
Agromyces sp	0	0	0	0	Actinobacteria; BioDeg
Algoriphagus sp	0	0	0	0	Bacteroidetes; BioDeg
Alicyclobacillus ferrooxydans	0.008	0	0	0	Acidophile; Aerobe; APB; Bacilli; Firmicutes; ISOX; Spore; Thermophile
Aliihoeflea sp	0.026	0	0	0.026	
Alkalibacter sp	0.069	0	0	0.018	Alkaliphile; BioDeg; Clostridia; Firmicutes
Alkalibacterium sp	0.28	0	0	0.039	Alkaliphile; Firmicutes; Lactobacillales
Alkaliphilus crotonatoxidans	0.032	0	0	0	Alkaliphile; Anaerobe; Clostridia; Firmicutes; Halophile; Peptide Ferm; Sulfidogen
Alkaliphilus halophilus	0.04	0	0	0	Alkaliphile; Anaerobe; Clostridia; Firmicutes; Halophile; Peptide Ferm; Spore; Sulfidogen
Alkaliphilus oremlandii	0	0	0	0	Alkaliphile; Anaerobe; Clostridia; Firmicutes; Halophile; Peptide Ferm; Sulfidogen
Alkaliphilus sp	0.121	0	0	0.01	Alkaliphile; Anaerobe; Clostridia; Firmicutes; Halophile; Peptide Ferm; Sulfidogen
Alkanindiges illinoisensis	0	0	0	0	Alkaliphile; BioDeg; BioDeg HC; Gammaproteobacteria; Oilfield
Alkanindiges sp	0	0	0	0	Alkaliphile; BioDeg; BioDeg HC; Gammaproteobacteria
Altererythrobacter sp	0	0	0	0	Alphaproteobacteria; CT
Aminivibrio pyruvatiphilus	0.033	0	0	0.073	Synergistetes
Aminobacter sp	0	0	0	0	Alphaproteobacteria
Ammoniphilus sp	0	0	0	0	Alkaliphile; Ammonium-dependent; Bacilli; Firmicutes; Halophile; Oxalotrophic
Amycolatopsis sp	0	0	0	0	Actinobacteria
Anaerobacterium chartisolvens	0.003	0	0	0	
Anaerobranca horikoshii	0	0	0	0	Anaerobe; Clostridia; Firmicutes
Anaerolinea sp	0.023	0	0	0.008	Anaerobe; BioDeg; Chloroflexi; Filamentous; Thermophile
Anaeromyxobacter dehalogenans	0	0	0	0	Anaerobe; Deltaproteobacteria; IRB; XRB
Anaeromyxobacter sp	0.022	0	0	0	Anaerobe; Deltaproteobacteria; IRB; XRB
Anaerophaga sp	0.007	0	0	0	Anaerobe; Bacteroidetes; Ferm; Thermophile
Anaerosalibacter bizertensis	0	0	0	0	
Anaerovorax sp	0.001	0	0	0	Anaerobe; Clostridia; Firmicutes
Aneurinibacillus migulanus	0	0	0	0	
Aquabacterium sp	0	0.003	0	0	Aerobe; BioDeg; MIC
Aquamicrobium sp	0	0	0	0	Aerobe; Alphaproteobacteria; Filters; Water
Aquicella sp	0.015	0	0	0.036	Gammaproteobacteria; Pathogen; Protazoan Pathogen
Aquihabitans daechungensis	0	0	0	0	Acidobacteria; Actinobacteria
Arcobacter nitrofigilis	0	0	0.005	0	Epsilonproteobacteria; Nitrate Injections; NRB; NRSOB; SOB
Arcobacter sp	0	0	0	0.013	Epsilonproteobacteria; Nitrate Injections; NRB; NRSOB; SOB
Arenimonas aquatica	0	0	0	0	Gammaproteobacteria; GHB
Arenimonas daechungensis	0	0	0	0	Gammaproteobacteria; GHB
Arenimonas sp	0	0	0	0	Gammaproteobacteria; GHB
Arhodomonas sp	0.026	0	0	0.013	Aerobe; Gammaproteobacteria; Halophile; Oilfield; Petroleum Reservoir Fluids
Arthrobacter sp	0.144	0	0	0.245	Actinobacteria; Aerobe; GHB; Soil
Azoarcus sp	0	0	0	0	Betaproteobacteria; BioDeg; NiF
Azohydromonas lata	0	0	0	0	Betaproteobacteria; BioDeg; NiF
Azonexus hydrophilus	0	0	0	0	Betaproteobacteria; NiF
Azospirillum sp	0	0	0	0	Alphaproteobacteria; NiF
Bacillus acidicola	0	0	0	0	Bacilli; Firmicutes; Spore

Sequence ID	OG230207-001	OG230402-001	OG230402-002	OG230402-003	OG230402-004	OG230402-005	OG230402-006	OG230402-007	OG230402-008	OG230402-009	OG230402-010	OG230402-011	OG230402-012	OG230402-013	OG230402-014	OG230402-015	OG230402-016	OG230402-017	OG230402-018	OG230402-019	OG230402-020	OG230402-021	OG230508-001	OG230508-002
Well 2244 Sample Description:	Soils Direct	C001 Scale, All, PRD	C001 Scale, All, MPB	C001 Scale, All, IRB	C002 - C005 Scale, PRD	C002 - C005 Scale, MPB	C002 - C005 Scale IRB	C006 - C022 Scale Body, PRD	C006 - C022 Scale Body, MPB	C006 - C022 Scale Body IRB	C006 - C022 Scale Collar, PRD	C006 - C022 Scale Collar, MPB	C006 - C022 Scale Collar IRB	C023 - C034 Scale Body, PRD	C023 - C034 Scale Body, MPB	C023 - C034 Scale Body IRB	C023 - C034 Scale Collar, PRD	C023 - C034 Scale Collar, MPB	C023 - C034 Scale Collar , IRB	9 5/8 ID Scale, PRD	9 5/8 ID Scale, MPB	9 5/8 ID Scale IRB	Pool 20 Annulus Fluids Black Direct	Pool 22 Annulus Fluids Grey Direct
Bacillus badius	0	0.004	0	0.069	0.201	0	0.073	0.158	0.009	0.047	0.072	0	0.004	0.014	0	0	0.398	0.006	0.009	0.007	0.003	0.02	0.014	0
Bacillus cereus	0	0.024	0	0	0.007	0	0	0.021	0	0	0.132	0	0	0.003	0	0	0.033	0	0.006	0.326	0	0	0	0
Bacillus hackensackii	0	0	0	0	0	0	0	0	0	0	0	0	0	0	0	0	0	0	0	0	0	0	0.003	0
Bacillus horti	0	0	0	0	0	0	0	0	0	0	0	0	0	0	0	0	0	0	0	0	0	0	0.008	0
Bacillus licheniformis	0	0.198	0	0	2.199	0.015	0	0.217	0	0	0.03	0.004	0	0.582	0.012	0	0.398	0	0	0.011	0	0.012	0	0
Bacillus malikii	0	0	0	0	0	0	0	0	0	0	0	0	0	0	0	0	0	0	0	0	0	0	0	0
Bacillus sp	0.081	66.359	0.74	1.502	43.783	0.835	2.232	83.724	0.924	2.41	36.832	0.063	0.976	85.805	8.091	1.371	56.7	0.048	2.218	37.209	0.014	8.609	2.895	1.139
Bacillus subtilis	0	0.678	0.004	0	0.011	0	0	0	0	0	0	0	0	0.841	0	0	0.024	0	0	0	0	0	0	0
Bacteriovorax sp	0.249	0	0	0	0	0	0	0	0	0	0	0	0	0	0	0	0	0	0	0	0	0	0	0.05
Bacteriovorax stolpii	0.033	0	0	0	0	0	0	0	0	0	0	0	0	0	0	0	0	0	0	0	0	0	0	0
Bacteroides graminisolvens	0	0	0	0	0	0	0	0	0	0	0	0	0	0	0	0	0	0	0	0	0	0	0.012	0
Bacteroides sp	0.109	0	0	0	0	0	0	0	0	0	0	0	0	0	0	0	0	0	0	0	0	0	0.011	0.107
Bdellovibrio bacteriovorus	0.002	0	0	0	0	0	0	0	0	0	0	0	0	0	0	0	0	0	0	0	0	0	0	0
Bdellovibrio sp	0.053	0	0	0	0	0	0	0	0	0	0	0	0	0	0	0	0	0	0	0	0	0	0.005	0
Beggiatoa sp	0.157	0	0	0	0	0	0	0	0	0	0	0	0	0	0	0	0	0	0	0	0	0	0	0
Beijerinckia sp	0.004	0	0	0	0	0	0	0	0	0	0	0	0	0	0	0	0	0	0	0	0	0	0.026	0
Bellilinea sp	0.002	0	0	0	0	0	0	0	0	0	0	0	0	0	0	0	0	0	0	0	0	0	0	0
Bergeyella sp	0	0	0	0	0	0	0.047	0	0	0	0	0	0	0	0	0	0	0	0	0	0	0	0	0
Blastochloris sp	0.007	0	0	0	0	0	0	0	0	0	0	0	0	0	0	0	0	0	0	0	0	0	0	0
Blastococcus sp	0.002	0	0	0	0	0	0	0	0	0	0	0	0	0	0	0	0	0	0	0	0	0	0.003	0
Blastomonas sp	0	0	0	0	0	0	0	0	0	0	0	0	0	0	0	0	0	0	0	0	0	0	0	0
Bosea sp	0.009	0	0	0	0	0	0	0	0	0	0	0	0	0	0	0	0	0	0	0	0	0	0.011	0
Brachybacterium sp	0	0	0	0	0	0	0	0	0	0	0	0	0	0	0	0	0	0	0	0	0	0	0.019	0.01
Bradyrhizobium sp	0.074	0	0	0	0	0	0	0	0	0	0	0	0	0	0	0	0	0	0	0	0	0	0.036	0.043
Brevibacillus sp	0	0	0	0	0	0	0	0.007	0	0	0	0	0	0	0	0	0	0	0	0	0	0	0	0
Brevibacterium sp	0	0	0	0	0	0	0	0	0	0	0	0	0	0	0	0	0	0	0	0	0	0	0	0
Brevundimonas sp	0.044	0	0	0	0	0	0	0	0	0	0	0	0	0	0	0	0	0	0	0	0	0	0	0.024
Brevundimonas viscosa	0	0	0	0	0	0	0	0	0	0	0	0	0	0	0	0	0	0	0	0	0	0	0	0
Burkholderia sp	0.07	0	0	0.006	0	0	0	0	0	0	0	0	0	0	0	0	0	0	0	0	0	0	0	0
Caenimonas sp	0.058	0	0	0	0	0	0	0	0	0	0	0	0	0	0	0	0	0	0	0	0	0	0	0
Caenispirillum sp	0	0	0.004	0	0	0	0	0	0	0	0	0.007	0	0	0	0	0	0	0	0	0	0	0	0
Caldilinea sp	0.007	0	0	0	0	0	0	0	0	0	0	0	0	0	0	0	0	0	0	0	0	0	0	0
Caloramator australicus	0	0	0	0	0	0	0	0	0	0	0	0	0	0	0	0	0	0	0	0	0	0	0.194	0.067
Candidatus Alysiosphaera europeae	0	0	0	0	0	0	0	0	0	0	0	0	0	0	0	0	0	0	0	0	0	0	0	0
Candidatus Captivus sp	0.007	0	0	0	0	0	0	0	0	0	0	0	0	0	0	0	0	0	0	0	0	0	0	0
Candidatus Desulforudis audaxviator	0	0	0	0	0	0	0	0	0	0	0	0	0	0	0	0	0	0	0	0	0	0	0.027	0
Candidatus Desulforudis sp	0.004	0	0	0	0	0	0	0	0	0	0	0	0	0	0	0	0	0	0	0	0	0	0	0
Candidatus Entotheonella palauensis	0.004	0	0	0	0	0	0	0	0	0	0	0	0	0	0	0	0	0	0	0	0	0	0	0
Candidatus Microthrix sp	0	0	0	0	0	0	0	0	0	0	0	0	0	0	0	0	0	0	0	0	0	0	0	0
Candidatus Mycoplasma haemobos	0	0	0	0	0	0	0	0	0	0	0	0	0	0	0	0	0	0	0	0	0	0	0	0
Candidatus Odyssella sp	0.026	0	0	0	0	0	0	0	0	0	0	0	0	0	0	0	0	0	0	0	0	0	0	0
Candidatus Protochlamydia amoebophila	0	0	0	0	0	0	0	0	0	0	0	0	0	0	0	0	0	0	0	0	0	0	0.037	0
Candidatus Protochlamydia sp	0	0	0	0	0	0	0	0	0	0	0	0	0	0	0	0	0	0	0	0	0	0	0	0.021
Candidatus Soleaferrea massiliensis	0.009	0	0	0.284	0	0	0	0	0	0	0	0	0	0	0	0	0	0	0	0	0	0	0	0
Candidatus Solibacter sp	0.007	0	0	0	0	0	0	0	0	0	0	0	0	0	0	0	0	0	0	0	0	0	0	0
Camobacterium maltaromaticum	0.005	0	0	0	0	0	0	0	0	0	0	0	0	0	0	0	0	0	0	0	0	0	0	0
Camobacterium sp	0	0	0	0	0	0	0	0	0	0	0	0	0	0	0	0	0	0	0	0	0	0	0.007	0
Caulobacter fusiformis	0.005	0	0	0	0	0	0	0	0	0	0	0	0	0	0	0	0	0	0	0	0	0	0	0
Caulobacter sp	0	0	0	0	0	0	0	0	0	0	0	0	0	0	0	0	0	0	0	0	0	0	0	0.057
Cellulomonas sp	0.004	0	0	0	0	0	0	0	0	0	0	0	0	0	0	0	0	0	0	0	0	0	0.43	0.495
Cellvibrio gandavensis	0.016	0	0	0	0	0	0	0	0	0	0	0	0	0	0	0	0	0	0	0	0	0	0	0
Cellvibrio sp	0.051	0	0	0	0	0	0	0	0	0	0	0	0	0	0	0	0	0	0	0	0	0	0	0
Cereibacter changlensis	0.005	0	0	0	0	0	0	0	0	0	0	0	0	0	0	0	0	0	0	0	0	0	0	0
Chelativorans multitrophicus	0	0	0	0	0	0	0	0	0	0	0	0	0	0	0	0	0	0	0	0	0	0	0.04	0.024
Chelativorans sp	0.002	0	0	0	0	0	0	0	0	0	0	0	0	0	0	0	0	0	0	0	0	0	0	0
Chitinophaga sp	0.07	0	0	0	0	0	0	0	0	0	0	0	0	0	0	0	0	0	0	0	0	0	0	0
Chlamydia sp	0	0	0	0	0	0	0	0	0	0	0	0	0	0	0	0	0	0	0	0	0	0	0	0

Sequence ID	OG230508-003	OG230508-004	OG230508-005	OG230508-006	Selected Traits
Well 2244 Sample Description:	Pool 27 Annulus Fluids Tank Direct	Pool 37 C015 - C022 Scale C Direct	Pool 13 C001B OD Scale All Direct	MG08 C023 - C034 Scale C Direct	Metabolic, Taxonomic, Physiological, Ecological
Bacillus badius	0.01	0	0	0	Bacilli; Firmicutes; Spore
Bacillus cereus	0	0	0	0	Bacilli; Biofilm; Firmicutes; MIC; Spore
Bacillus hackensackii	0	0	0	0	
Bacillus horti	0.006	0	0	0.37	Bacilli; Firmicutes; Spore
Bacillus licheniformis	0	0	0	0	Bacilli; Biosurfactant Producing; Firmicutes; MEOR; Spore
Bacillus malikii	0	0.457	0	0	
Bacillus sp	3.159	3.227	1.898	0.795	Bacilli; BioDeg; Diverse; Firmicutes; GHB; Spore
Bacillus subtilis	0	0	0	0	Bacilli; BioDeg; BioDeg HC; Biofilm; Biosurfactant Producing; Firmicutes; MIC; Spore
Bacteriovorax sp	0	0	0.054	0	Bacterial Predator; Deltaproteobacteria
Bacteriovorax stolpii	0	0	0	0	Bacterial Predator; Deltaproteobacteria
Bacteroides graminisolvens	0	0	0	0.013	Anaerobe; Bacteroidetes; BioDeg; Ferm
Bacteroides sp	0.019	0	0	0	Anaerobe; Bacteroidetes; BioDeg; Ferm
Bdellovibrio bacteriovorus	0	0	0	0	Bacterial Predator; Deltaproteobacteria
Bdellovibrio sp	0.011	0	0	0	Bacterial Predator; Deltaproteobacteria
Beggiatoa sp	0	0	0	0	Biofilm; Gammaproteobacteria; OX; SOB; White mats hydrocarbon seeps
Beijerinckia sp	0	0	0	0	Alphaproteobacteria
Bellilinea sp	0	0	0	0	Chloroflexi; Oilfield; Tilling pond
Bergeyella sp	0	0	0	0	Bacteroidetes; GHB
Blastochloris sp	0	0	0	0	Alphaproteobacteria
Blastococcus sp	0.008	0	0	0	Actinobacteria; Aerobe; Sediment; Stone; Unknown; Water
Blastomonas sp	0.019	0	0	0	Alphaproteobacteria; CT
Bosea sp	0.007	0	0	0	Alphaproteobacteria; GHB
Brachybacterium sp	0.019	0	0	0	Actinobacteria; BioDeg; BioDeg HC
Bradyrhizobium sp	0	0	0	0	Alphaproteobacteria; NiF
Brevibacillus sp	0	0	0	0	Aerobe; Bacilli; Firmicutes; GHB; Spore
Brevibacterium sp	0.004	0	0	0	Actinobacteria; BioDeg; BioDeg HC
Brevundimonas sp	0.035	0	0	0.018	Aerobe; Alphaproteobacteria; BioDeg; BioDeg HC; GHB
Brevundimonas viscosa	0.004	0	0	0	
Burkholderia sp	0	0	0	0	Aerobe; Betaproteobacteria; BioDeg; Soil
Caenimonas sp	0	0	0	0	Betaproteobacteria
Caenispirillum sp	0	0	0	0.018	Alphaproteobacteria; Phototroph
Caldilinea sp	0	0	0	0	Chloroflexi; Facultative; Filamentous; Thermophile
Caloramator australicus	0.28	0	0	0.042	Anaerobe; Clostridia; Ferm; Firmicutes; GHB; Thermophile
Candidatus Alysiosphaera europeae	0	0	0.879	0	
Candidatus Captivus sp	0	0	0	0	Unknown
Candidatus Desulforudis audaxviator	0.015	0	0	0	Clostridia; Firmicutes
Candidatus Desulforudis sp	0	0	0	0	Clostridia; Firmicutes
Candidatus Entotheonella palauensis	0	0	0	0	
Candidatus Microthrix sp	0.008	0	0	0	Filamentous
Candidatus Mycoplasma haemobos	0.008	0.116	0	0	
Candidatus Odyssella sp	0	0	0	0	
Candidatus Protochlamydia amoebophila	0	0	0	0	Chlamydiae
Candidatus Protochlamydia sp	0	0	0	0	Chlamydiae
Candidatus Soleaferrea massiliensis	0	0	0	0	Clostridia; Firmicutes
Candidatus Solibacter sp	0	0	0	0	Acidobacteria; Aerobe; Biofilm; GHB; NRB; Soil
Carnobacterium maltaromaticum	0	0	0	0.104	Firmicutes; Lactobacillales
Carnobacterium sp	0.029	0	0	0	Firmicutes; Lactobacillales
Caulobacter fusiformis	0	0	0	0	Aerobe; Alphaproteobacteria; GHB; Oligotroph
Caulobacter sp	0	0	0	0	Aerobe; Alphaproteobacteria; GHB; Oligotroph
Cellulomonas sp	0.422	0.743	0.009	1.191	Actinobacteria; Aerobe; BioDeg; BioDeg Cellulose; Facultative Anaerobe
Cellvibrio gandavensis	0	0	0	0	Aerobe; BioDeg; BioDeg Agar; BioDeg Cellulose; Gammaproteobacteria
Cellvibrio sp	0	0	0	0	Aerobe; BioDeg; BioDeg Agar; BioDeg Cellulose; Gammaproteobacteria
Cereibacter changlensis	0	0	0	0	Alphaproteobacteria; Phototroph
Chelativorans multitrophicus	0.003	0.537	0	0	Alphaproteobacteria
Chelativorans sp	0	0	0	0	Aerobe; Alphaproteobacteria
Chitinophaga sp	0	0	0	0	Aerobe; Bacteroidetes; BioDeg
Chlamydia sp	0.004	0	0	0	Chlamydiae; Endosymbiont; Parasite; Pathogen

Sequence ID	OG230207-001	OG230402-001	OG230402-002	OG230402-003	OG230402-004	OG230402-005	OG230402-006	OG230402-007	OG230402-008	OG230402-009	OG230402-010	OG230402-011	OG230402-012	OG230402-013	OG230402-014	OG230402-015	OG230402-016	OG230402-017	OG230402-018	OG230402-019	OG230402-020	OG230402-021	OG230508-001	OG230508-002
Well 2244 Sample Description:	Soils Direct	C001 Scale, All, PRD	C001 Scale, All, MPB	C001 Scale, All, IRB	C002 - C005 Scale, PRD	C002 - C005 Scale, MPB	C002 - C005 Scale IRB	C006 - C022 Scale Body, PRD	C006 - C022 Scale Body, MPB	C006 - C022 Scale Body IRB	C006 - C022 Scale Collar, PRD	C006 - C022 Scale Collar, MPB	C006 - C022 Scale Collar IRB	C023 - C034 Scale Body, PRD	C023 - C034 Scale Body, MPB	C023 - C034 Scale Body IRB	C023 - C034 Scale Collar, PRD	C023 - C034 Scale Collar, MPB	C023 - C034 Scale Collar , IRB	9 5/8 ID Scale, PRD	9 5/8 ID Scale, MPB	9 5/8 ID Scale IRB	Pool 20 Annulus Fluids Black Direct	Pool 22 Annulus Fluids Grey Direct
Chloracidobacterium sp	0.011	0	0	0	0	0	0	0	0	0	0	0	0	0	0	0	0	0	0	0	0	0	0	0
Chloroflexi bacterium	0	0	0	0	0	0	0	0	0	0	0	0	0	0	0	0	0	0	0	0	0	0	0.143	0.007
Chloroflexus sp	0.011	0	0	0	0	0	0	0	0	0	0	0	0	0	0	0	0	0	0	0	0	0	0.158	0.071
Chondromyces sp	0	0	0	0	0	0	0	0	0	0	0	0	0	0	0	0	0	0	0	0	0	0	0.029	0
Christensenella sp	0	0	0	0	0	0	0	0	0	0	0	0	0	0	0	0	0	0	0	0	0	0	0.01	0
Chromohalobacter sp	0	0	0	0	0	0	0	0	0	0	0	0	0	0	0	0	0	0	0	0	0	0	0.12	0.057
Chryseobacterium anthropi	0.021	0	0	0	0	0	0	0	0	0	0	0	0	0	0	0	0	0	0	0	0	0	0	0
Chryseobacterium sp	0.004	0	0	0	0	0	0	0	0	0	0	0	0	0	0	0	0	0	0	0	0	0	0	0
Citricoccus sp	0	0	0	0	0	0	0	0	0	0	0	0	0	0	0	0	0	0	0	0	0	0	0.012	0
Citrobacter sp	0	0	0	0	0	0	0	0	0	0	0	0	0	0	0	0	0	0	0	0	0	0	0.014	0
Cloacibacterium sp	0	0	0	0	0	0	0	0	0	0	0	0	0	0	0	0	0	0	0	0	0	0	0.03	0.069
Clostridium botulinum	0	10.501	0.24	0	7.401	0.01	0.03	12.258	4.574	0.118	51.429	2.618	0.028	0.003	0.008	0.03	11.537	0.012	0	0	0	0	0.029	0
Clostridium celerecrescens	0	0	1.376	7.403	0	0	0	0	0	0	0	0	0	0	0	0	0	0	0	0	0	0	0	0
Clostridium cylindrosporum	0	0	0.17	0.069	0	0	0	0	0	0	0	0	0	0	0	0	0	0	0	0	0	0	0	0
Clostridium fimetarium	0	0	0	0	0	0	0	0	0	0	0	0	0	0	0	0	0	0	0	0	0	0	0	0.024
Clostridium hungatei	0	0	0	0	0	0	0	0	0	0	0	0	0	0	0	0	0	0	0	0	0	0	0	0
Clostridium luticellarii	0	0	0	0	0	0	0	0	0	0	0	0	0	0	0	0	0	0	0	0	0	0	0	0
Clostridium malenominatum	0	0	0.292	0.063	0	0	0	0	0	0	0	0	0	0	8.178	0	0	0	0	0	0	0	0	0
Clostridium metallolevans	0	0	0	1.193	0	0	0	0	0	0	0	0	0	0	0	0	0	0	0	0	0	0	0	0
Clostridium sp	0.282	2.505	30.003	11.235	0.106	0.361	7.416	0.455	0.817	4.064	0.341	34.643	3.232	0.014	42.238	2.051	0.142	15.663	1.915	0.004	0	19.302	3.662	2.995
Clostridium tertium	0	0.04	0.113	0.688	0	1.783	0	0	0	0	0	0	0	0	0	0	0	0	0	0	0	0	0	0
Cohnella sp	0.004	0	0	0	0	0	0	0	0	0	0	0	0	0	0	0	0	0	0	0	0	0	0	0
Comamonas sp	0	0	0	0	0	0	0	0	0	0	0	0	0	0	0	0	0	0	0	0	0	0	0.034	0.117
Conexibacter sp	0.007	0	0	0	0	0	0	0	0	0	0	0	0	0	0	0	0	0	0	0	0	0	0.025	0.01
Corynebacterium kroppenstedtii	0	0	0	0	0	0	0	0	0	0	0	0	0	0	0	0	0	0	0	0	0	0	0	0.219
Cryobacterium sp	0.157	0	0	0	0	0	0	0	0	0	0	0	0	0	0	0	0	0	0	0	0	0	0	0
Curvibacter sp	0	0	0	0	0	0	0	0	0	0	0	0	0	0	0	0	0	0	0	0	0	0	0.008	0
Cyanobacterium sp	0.002	0	0	0	0	0	0	0	0	0	0	0	0	0	0	0	0	0	0	0	0	0	0	0
Cystobacter sp	0	0	0	0	0	0	0	0	0	0	0	0	0	0	0	0	0	0	0	0	0	0	0.03	0
Cytophaga hutchinsonii	0.016	0	0	0	0	0	0	0	0	0	0	0	0	0	0	0	0	0	0	0	0	0	0	0
Cytophaga sp	0.058	0	0	0	0	0	0	0	0	0	0	0	0	0	0	0	0	0	0	0	0	0	0.016	0
Dechloromonas sp	0.011	0	0	0.006	0	0	0	0.004	0	0	0	0	0	0	0	0	0	0.006	0	0	0	0	0.051	0.1
Defluviicoccus sp	0.005	0	0	0	0	0	0	0	0	0	0	0	0	0	0	0	0	0	0	0	0	0	0	0
Dehalobacter sp	0	0	0.009	0	0	0	0	0	0	0	0	0	0	0	0	0	0	0	0	0	0	0	0.043	0.067
Dehalococcoides sp	0.016	0	0	0	0	0	0	0	0	0	0	0	0	0	0	0	0	0	0	0	0	0	0.037	0
Denitrovibrio acetiphilus	0	0	0	0	0.011	0	0	0.011	0	0.024	0	0	0	0.007	0	0.008	0.005	0	0	0	0.003	0	0	0
Derxia sp	0.002	0	0	0	0	0	0	0	0	0	0	0	0	0	0	0	0	0	0	0	0	0	0	0
Desemzia incerta	0	0	0	0	0	0	0	0	0	0	0	0	0	0	0	0	0	0	0	0	0	0	0	0
Desulfitibacter alkalitolerans	0	0	0	0	0	0	0	0	0	0	0	0	0	0	0	0	0	0	0	0	0	0	4.391	1.456
Desulfitispora sp	0	0	0	0	0	0	0	0	0	0	0	0	0	0	0	0	0	0	0	0	0	0	0	0
Desulfitobacterium aromaticivorans	0	0	0	0	0	0	0	0	0	0	0	0	0	0	0	0	0	0	0	0	0	0	0	0
Desulfitobacterium dehalogenans	0	0	0	0	0	0	0	0	0	0	0	0	0	0	0	0	0	0	0	0	0	0	0.026	0
Desulfitobacterium dichloroeliminans	0	0	0	0.145	0	0	0	0	0	0	0	0	0	0	0	0	0	0	0	0	0	0	0	0
Desulfitobacterium sp	0	0	15.494	0.05	0	16.411	0.883	0	3.367	0.449	0	5.522	0.011	0	1.132	0.684	0	0	0.149	0.004	0	0.004	0.241	0.15
Desulfobacter sp	0.007	0	0	0	0	0	0	0	0	0	0	0	0	0	0	0	0	0	0	0	0	0	0	0
Desulfobulbus sp	0.011	0	0	0	0	0	0	0	0	0	0	0	0	0	0	0	0	0	0	0	0	0	0	0
Desulfomonile sp	0.025	0	0	0	0	0	0	0	0	0	0	0	0	0	0	0	0	0	0	0	0	0	0	0
Desulfonosporus sp	0	0	0	0.057	0	0	0.802	0	0	0.024	0	0	0	0	0	0	0	0	0.046	0	0	0	0.899	0.523
Desulforegula sp	0.012	0	0	0	0	0	0	0	0	0	0	0	0	0	0	0	0	0	0	0	0	0	0	0
Desulfosporosinus burensis	0	0	0.009	0	0	0.005	0	0	0	0	0	0.018	0	0	0	0.038	0	0	0	0	0	0	0	0
Desulfosporosinus sp	0.058	0	25.035	1.666	0.004	33.873	0.552	0.018	0.218	1.394	0.004	16.084	0.004	0.003	14.137	2.993	0	0	0.254	0.014	0	0	0.143	0.497
Desulfotomaculum aeronauticum	0	0	0	0.139	0	0	0	0	0	0.638	0	0	0	0	0	0	0	0	0	0	0	0	0.016	0
Desulfotomaculum defluvii	0	0	0.022	0	0	0.015	0	0	0	0	0	0.011	0	0	0.004	0	0	0	0	0	0	0	0	0
Desulfotomaculum geothermicum	0	0	0	0	0	0	0	0	0	0	0	0	0	0	0	0	0	0	0	0	0	0	0	0.007
Desulfotomaculum reducens	0	0	0.017	0	0	0.143	0	0	0.71	0	0	0.085	0	0	0.049	0	0	0.553	0	0	0.348	0	0	0
Desulfotomaculum sp	0	0	0.174	0.05	0	0.306	0	0	7.064	0	0	0.593	0	0	0.259	0	0	0.06	0	0	0.243	0	0.216	0.019
Desulfovibrio alaskensis	0	0	0	0	0	0	0	0	0	0	0	0	0	0	0	0	0	0	0	0	0	0	2.179	1.042

Sequence ID	OG230508-003	OG230508-004	OG230508-005	OG230508-006	Selected Traits
Well 2244 Sample Description:	Pool 27 Annulus Fluids Tank Direct	Pool 37 C015 - C022 Scale C Direct	Pool 13 C001B OD Scale All Direct	MG08 C023 - C034 Scale C Direct	Metabolic, Taxonomic, Physiological, Ecological
Chloracidobacterium sp	0	0	0	0	Acidobacteria; Microaerophile; Phototroph; Thermophile
Chloroflexi bacterium	0.036	0.016	0	0	
Chloroflexus sp	0.055	0	0	0	Anoxygenic Phototroph; Chloroflexi; FAP; Filamentous; Phototroph
Chondromyces sp	0	0	0	0	Deltaproteobacteria
Christensenella sp	0	0	0	0.021	Clostridia; Ferm; Firmicutes
Chromohalobacter sp	0.059	0	0	0.292	Fermented Foods; Gammaproteobacteria; Halophile; Pigmented
Chryseobacterium anthropi	0	0	0	0	Aerobe; Bacteroidetes; BioDeg; Food; Pigmented; Soil; Wastewater
Chryseobacterium sp	0	0	0	0	Aerobe; Bacteroidetes; BioDeg; Food; Pigmented; Soil; Wastewater
Citricoccus sp	0.011	0	0	0.044	Actinobacteria; BioDeg; Oligotroph
Citrobacter sp	0	0	0	0.029	Aerobe; Biofilm; Gammaproteobacteria; MIC; NRB; Sulfidogen
Cloacibacterium sp	0	0	0	0	Bacteroidetes; GHB
Clostridium botulinum	0	0	0.005	0	Anaerobe; Clostridia; Ferm; Firmicutes; GHB; Pathogen; Saprophyte; Spore
Clostridium celerecrescens	0	0	0	0	Anaerobe; Clostridia; Firmicutes; Spore; SRB; Sulfidogen
Clostridium cylindrosporum	0	0	0	0	Anaerobe; Clostridia; Firmicutes; Spore
Clostridium fimetarium	0	0	0	0	Anaerobe; Clostridia; Ferm; Firmicutes; Spore
Clostridium hungatei	0.026	0	0	0	Anaerobe; BioDeg; BioDeg Cellulose; Clostridia; Firmicutes; NRB; Soil
Clostridium luticellarii	0	0	0	0.021	Anaerobe; APB; Clostridia; Ferm; Firmicutes; Spore
Clostridium malenominatum	0	0	0	0	Anaerobe; Clostridia; Firmicutes; Spore; Varies
Clostridium metallolevans	0	0	0	0	
Clostridium sp	3.221	0.423	0	1.921	Anaerobe; Clostridia; Diverse; Ferm; Firmicutes; GHB; Saprophyte; Spore
Clostridium tertium	0	0	0	0	Anaerobe; APB; Clostridia; Firmicutes; Spore
Cohnella sp	0	0	0	0	Aerobe; Bacilli; BioDeg; BioDeg Cellulose; Firmicutes; Spore
Comamonas sp	0.011	0.835	0.041	0	Aerobe; Betaproteobacteria; BioDeg
Conexibacter sp	0.001	0	0	0	Actinobacteria; NRB
Corynebacterium kroppenstedtii	0	0	0	0	Actinobacteria; Aerobe; GHB
Cryobacterium sp	0	0	0	0	Actinobacteria
Curvibacter sp	0	0	0	0.047	Aerobe; Betaproteobacteria; GHB; Well Water
Cyanobacterium sp	0	0	0	0	Phototroph
Cystobacter sp	0	0	0	0	Deltaproteobacteria
Cytophaga hutchinsonii	0	0	0	0	Aerobe; Bacteroidetes; BioDeg; BioDeg Cellulose; Soil
Cytophaga sp	0	0	0	0	Aerobe; Bacteroidetes; BioDeg; BioDeg Cellulose; Soil
Dechloromonas sp	0.017	0.507	2.246	0	Anaerobe; Betaproteobacteria; NRB; PerRB
Defluviicoccus sp	0	0	0	0	Alphaproteobacteria
Dehalobacter sp	0.041	0	0	0.057	Anaerobe; BioDeg; BioDeg Dichlorobenzene; Clostridia; Firmicutes
Dehalococcoides sp	0.003	0	0	0	BioDeg; BioDeg TCE; BioDeg XRB; Bioremediation; Chloroflexi; Vinyl Chloride Reducing
Denitrovibrio acetiphilus	0	0	0	0	Deferribacteres; NRB; Oilfield
Derxia sp	0	0	0	0	Betaproteobacteria; NiF
Desemzia incerta	0	0	0	0.018	
Desulfitibacter alkalitolerans	3.718	0.069	0	3.623	Alkaliphile; Anaerobe; Clostridia; Firmicutes; Spore; Sulfidogen; SuRB; TRB
Desulfitispora sp	0.003	0	0	0	Alkaliphile; Anaerobe; Firmicutes; Haloalkaliphile; Halophile; Spore; Sulfidogen; TRB
Desulfitobacterium aromaticivorans	0.029	0	0	0	Anaerobe; BioDeg; Clostridia; Ferm; Firmicutes; Metal Reduction; Spore; Sulfidogen; SuRB; TRB
Desulfitobacterium dehalogenans	0.059	0	0	0	Anaerobe; BioDeg; Clostridia; Ferm; Firmicutes; Metal Reduction; Spore; Sulfidogen; SuRB; TRB
Desulfitobacterium dichloroeliminans	0	0	0	0	Anaerobe; BioDeg; Clostridia; Ferm; Firmicutes; Metal Reduction; Spore; Sulfidogen; SuRB; TRB
Desulfitobacterium sp	0.217	0.003	0	0.315	Anaerobe; BioDeg; Clostridia; Ferm; Firmicutes; Metal Reduction; Spore; Sulfidogen; SuRB; TRB
Desulfobacter sp	0	0	0	0	Anaerobe; Deltaproteobacteria; SRB; Sulfidogen
Desulfobulbus sp	0	0	0	0	Anaerobe; Deltaproteobacteria; SRB; Sulfidogen
Desulfomonile sp	0	0	0	0	Anaerobe; BioDeg; BioDeg Benzene; Deltaproteobacteria; SRB; Sulfidogen
Desulfonosporus sp	0.578	0	0	1.371	Anaerobe; Clostridia; Firmicutes; Spore; SRB; Sulfidogen
Desulforegula sp	0	0	0	0	Anaerobe; Deltaproteobacteria; SRB; Sulfidogen
Desulfosporosinus burensis	0	0	0	0	Anaerobe; Clostridia; Firmicutes; Spore; SRB; Sulfidogen
Desulfosporosinus sp	0.228	0	0	0.357	Anaerobe; Clostridia; Firmicutes; Spore; SRB; Sulfidogen
Desulfotomaculum aeronauticum	0	0	0	0	Anaerobe; Clostridia; Firmicutes; Spore; SRB; Sulfidogen
Desulfotomaculum defluvii	0	0	0	0	Firmicutes; Spore; SRB; Sulfidogen
Desulfotomaculum geothermicum	0.019	0	0	0	Anaerobe; Clostridia; Firmicutes; Spore; SRB; Sulfidogen
Desulfotomaculum reducens	0	0	0	0	Anaerobe; Clostridia; Firmicutes; Spore; SRB; Sulfidogen
Desulfotomaculum sp	0.226	0	0	0	Anaerobe; Clostridia; Firmicutes; Spore; SRB; Sulfidogen; Thermophile
Desulfovibrio alaskensis	1.346	0	0	0.626	Anaerobe; Deltaproteobacteria; Oilfield; SRB; Sulfidogen

Sequence ID	OG230207-001	OG230402-001	OG230402-002	OG230402-003	OG230402-004	OG230402-005	OG230402-006	OG230402-007	OG230402-008	OG230402-009	OG230402-010	OG230402-011	OG230402-012	OG230402-013	OG230402-014	OG230402-015	OG230402-016	OG230402-017	OG230402-018	OG230402-019	OG230402-020	OG230402-021	OG230508-001	OG230508-002
Well 2244 Sample Description:	Soils Direct	C001 Scale, All, PRD	C001 Scale, All, MPB	C001 Scale, All, IRB	C002 - C005 Scale, PRD	C002 - C005 Scale, MPB	C002 - C005 Scale IRB	C006 - C022 Scale Body, PRD	C006 - C022 Scale Body, MPB	C006 - C022 Scale Body IRB	C006 - C022 Scale Collar, PRD	C006 - C022 Scale Collar, MPB	C006 - C022 Scale Collar IRB	C023 - C034 Scale Body, PRD	C023 - C034 Scale Body, MPB	C023 - C034 Scale Body IRB	C023 - C034 Scale Collar, PRD	C023 - C034 Scale Collar, MPB	C023 - C034 Scale Collar , IRB	9 5/8 ID Scale, PRD	9 5/8 ID Scale, MPB	9 5/8 ID Scale IRB	Pool 20 Annulus Fluids Black Direct	Pool 22 Annulus Fluids Grey Direct
Desulfovibrio desulfuricans	0	0	0	0	0	0	0	0	0	0	0	0	0	0	0	0	0	0	0	0	0	0	0	0
Desulfovibrio sp	0.009	0	0	0	0	0	0	0	0	0	0	0	0	0	0	0	0	0	0	0	0	0	0.143	0.064
Desulfuromonas sp	0.041	0	0	0	0	0	0	0	0	0	0	0	0	0	0	0	0	0	0	0	0	0	0.393	0.1
Dethiobacter alkaliphilus	0	0	0	0	0.004	0	0	0	0	0.024	0	0.011	0.004	0.007	0	0.004	0	0	0.009	0	0	0.004	7.916	7.31
Dethiosulfatibacter sp	0	0	0	0	0	0	0	0	0	0	0	0	0	0	0	0	0	0	0	0	0	0	0.014	0.017
Devosia sp	0.06	0	0	0	0	0	0	0	0	0	0	0	0	0	0	0	0	0	0	0	0	0	0.029	0.124
Devosia submarina	0.002	0	0	0	0	0	0	0	0	0	0	0	0	0	0	0	0	0	0	0	0	0	0	0
Dietzia sp	0.048	0	0	0	0	0	0	0	0	0	0	0	0	0	0	0	0	0	0	0	0	0	0.447	0.228
Dokdonella ginsengisoli	0	0	0	0	0	0	0	0	0	0	0	0	0	0	0	0	0	0	0	0	0	0	0	0.01
Dokdonella sp	0	0	0	0	0	0	0	0	0	0	0	0	0	0	0	0	0	0	0	0	0	0	0.01	0.14
Dongia sp	0.018	0	0	0	0	0	0	0	0	0	0	0	0	0	0	0	0	0	0	0	0	0	0	0
Duganella sp	0.009	0	0	0	0	0	0	0	0	0	0	0	0	0	0	0	0	0	0	0	0	0	0	0
Dyadobacter alkalitolerans	0.002	0	0	0	0	0	0	0	0	0	0	0	0	0	0	0	0	0	0	0	0	0	0	0
Dyadobacter koreensis	0.004	0	0	0	0	0	0	0	0	0	0	0	0	0	0	0	0	0	0	0	0	0	0	0
Dyadobacter sp	0.028	0	0	0	0	0	0	0	0	0	0	0	0	0	0	0	0	0	0	0	0	0	0	0
Dysgonomonas sp	0	0	0	0	0	0	0	0	0	0	0	0	0	0	0	0	0	0	0	0	0	0	0.004	0
Ectothiorhodospira sp	0.004	0	0	0	0	0	0	0	0	0	0	0	0	0	0	0	0	0	0	0	0	0	0	0
Edaphobacter sp	0.005	0	0	0	0	0	0	0	0	0	0	0	0	0	0	0	0	0	0	0	0	0	0	0
Eggerthella sp	0	0	0	0	0	0	0	0	0	0	0	0	0	0	0	0	0	0	0	0	0	0	0.217	0.069
Egicoccus halophilus	0	0	0	0	0	0	0	0	0	0	0	0	0	0	0	0	0	0	0	0	0	0	0.058	0.007
Empedobacter sp	0	0	0	0	0	0	0	0	0	0	0	0	0	0	0	0	0	0	0	0	0	0	0	0
Emticicia sp	0.004	0	0	0	0	0	0	0	0	0	0	0	0	0	0	0	0	0	0	0	0	0	0	0
Ensifer adhaerens	0	0	0	0	0	0	0	0	0	0	0	0	0	0	0	0	0	0	0	0	0	0	0.025	0
Enteractinococcus fodinae	0	0	0	0	0	0	0	0	0	0	0	0	0	0	0	0	0	0	0	0	0	0	0.003	0
Enterococcus cecorum	0	0	0	0	0	0	0	0	0	0	0	0	0	0	0	0	0	0	0	0	0	0	0	0
Enterococcus columbae	0	0	0	0	0	0	0	0	0	0	0	0	0	0	0	0	0	0	0	0	0	0	0	0
Erysipelothrix sp	0.074	0	0	0	0	0	0	0	0	0	0	0	0	0	0	0	0	0	0	0	0.098	0	0.058	0.588
Erythrobacter mathurensis	0.002	0	0	0	0	0	0	0	0	0	0	0	0	0	0	0	0	0	0	0	0	0	0	0
Ethanoligenens harbinense	0	0	0	0	0	0	0	0	0	0	0	0	0	0	0	0	0	0	0	0	0	0	0.007	0
Ethanoligenens sp	0	0	0	0	0	0	0	0	0	0	0	0	0	0	0	0	0	0	0	0	0	0	0.023	0
Exiguobacterium sp	0.002	0	0	0	0	0	0	0	0	0	0	0	0	0	0	0	0	0	0	0	0	0	0	0
Ferribacterium sp	0.012	0	0	0	0	0	0	0	0	0	0	0	0	0	0	0	0	0	0	0	0	0	0	0
Ferruginibacter sp	0.236	0	0	0	0	0	0	0	0	0	0	0	0	0	0	0	0	0	0	0	0	0	0	0
Flavihumibacter sp	0.021	0	0	0	0	0	0	0	0	0	0	0	0	0	0	0	0	0	0	0	0	0	0	0
Flavisolibacter sp	0.032	0	0	0	0	0	0	0	0	0	0	0	0	0	0	0	0	0	0	0	0	0	0	0
Flavitalea sp	0.012	0	0	0	0	0	0	0	0	0	0	0	0	0	0	0	0	0	0	0	0	0	0	0
Flavobacterium glaciei	0.987	0	0	0	0	0	0	0	0	0	0	0	0	0	0	0	0	0	0	0	0	0	0	0.105
Flavobacterium sp	10.079	0	0	0	0	0	0	0	0	0	0	0	0	0	0	0	0	0	0	0	0	0	0.036	0.383
Flexibacter sp	0.363	0	0	0	0	0	0	0	0	0	0	0	0	0	0	0	0	0	0	0	0	0	0	0
Flexistipes sinusarabici	0	0	0	0	0	0	0	0	0	0	0	0	0	0	0	0	0	0	0	0	0	0	0	0
Fluviicoccus keumensis	0.005	0	0	0	0	0	0	0	0	0	0	0	0	0	0	0	0	0	0	0	0	0	0	0
Fluviicola sp	0.347	0	0	0	0	0	0	0	0	0	0	0	0	0	0	0	0	0	0	0	0	0	0	0
Fontibacter flavus	0	0	0	0	0	0	0	0	0	0	0	0	0	0	0	0	0	0	0	0	0	0	0.044	0
Formivibrio citricus	0	0	0	0	0	0	0	0	0	0	0	0	0	0	0	0	0	0	0	0	0	0	0	0
Frankia sp	0.002	0	0	0	0	0	0	0	0	0	0	0	0	0	0	0	0	0	0	0	0	0	0	0
Frigoribacterium sp	0.026	0	0	0	0	0	0	0	0	0	0	0	0	0	0	0	0	0	0	0	0	0	0	0
Fusibacter paucivorans	0	0	0	0	0	0	0	0	0	0	0	0	0	0	0	0	0	0	0	0	0	0	0	0
Fusibacter sp	0.148	0	0	0.006	0	0	0	0	0	0	0	0	0	0	0	0	0	0	0	0.004	0	1.265	0.022	0.021
Fusobacterium sp	0	0	0	0	0	0	0	0	0	0	0	0	0	0	0	0	0	0	0	0	0	0	0	0
Gaiella sp	0.002	0	0	0	0	0	0	0	0	0	0	0	0	0	0	0	0	0	0	0	0	0	0	0
Garciella sp	0	0	0	0	0	0	0	0	0	0	0	0	0	0	0	0	0	0	0	0	0	0	0.158	0.059
Gemella sp	0	0	0	0	0	0	0	0	0	0	0	0	0	0	0	0	0	0	0	0	0	0	0	0
Gemmata sp	0.009	0	0	0	0	0	0	0	0	0	0	0	0	0	0	0	0	0	0	0	0	0	0	0
Gemmatimonas sp	0.079	0	0	0	0	0	0	0	0	0	0	0	0	0	0	0	0	0	0	0	0	0	0	0
Gemmobacter sp	0.012	0	0	0	0	0	0	0	0	0	0	0	0	0	0	0	0	0	0	0	0	0	0	0
Geoalkalibacter sp	0.004	0	0	0	0	0	0	0	0	0	0	0	0	0	0	0	0	0	0	0	0	0	0	0
Geoalkalibacter subterraneus	0	0	0	0	0	0	0	0	0	0	0	0	0	0	0	0	0	0	0	0	0	0	0.023	0

Sequence ID	OG230508-003	OG230508-004	OG230508-005	OG230508-006	Selected Traits
Well 2244 Sample Description:	Pool 27 Annulus Fluids Tank Direct	Pool 37 C015 - C022 Scale C Direct	Pool 13 C001B OD Scale All Direct	MG08 C023 - C034 Scale C Direct	Metabolic, Taxonomic, Physiological, Ecological
Desulfovibrio desulfuricans	0	0	0	0.047	Anaerobe; Deltaproteobacteria; SRB; Sulfidogen
Desulfovibrio sp	0.127	0.389	0	0.039	Anaerobe; Deltaproteobacteria; SRB; Sulfidogen
Desulfuromonas sp	0.17	0	0	0.209	Anaerobe; Deltaproteobacteria; IRB; Sulfidogen; SuRB
Dethiobacter alkaliphilus	9.23	0	0.003	3.86	Alkaliphile; Anaerobe; Clostridia; Firmicutes; Spore; Sulfidogen; SuRB; TRB
Dethiosulfatibacter sp	0.028	0	0	0	Spore; Sulfidogen; SuRB; TRB
Devosia sp	0.037	0	0	0.044	Alphaproteobacteria; GHB; NiF
Devosia submarina	0	0	0	0	Aerobe; Sediments
Dietzia sp	0.374	0	0	0.287	Actinobacteria; Aerobe; BioDeg; GHB
Dokdonella ginsengisoli	0	0	0	0	Gammaproteobacteria
Dokdonella sp	0	0.338	0.971	0	Gammaproteobacteria
Dongia sp	0	0	0	0	Alphaproteobacteria
Duganella sp	0	0	0	0	Aerobe; Betaproteobacteria; GHB; Soil
Dyadobacter alkalitolerans	0	0	0	0	
Dyadobacter koreensis	0	0	0	0	Aerobe; Bacteroidetes; BioDeg
Dyadobacter sp	0.007	0	0	0.029	Aerobe; Bacteroidetes; BioDeg
Dysgonomonas sp	0	0	0	0.151	Bacteroidetes; BioDeg; Facultative Anaerobe; Ferm
Ectothiorhodospira sp	0	0	0	0	Anaerobe; Gammaproteobacteria; Halophile; Phototroph; Purple Sulfur Bacteria; Sulfide-Oxidizing
Edaphobacter sp	0	0	0	0	Acidobacteria; Aerobe; APB; GHB; Oligotroph; Soil
Eggerthella sp	0.179	0	0	0.042	Actinobacteria
Egicoccus halophilus	0.019	0	0	0.057	Actinobacteria; Alkaliphile; Halophile
Empedobacter sp	0	0.481	0	0	Bacteroidetes; GHB
Emticicia sp	0	0	0	0	Bacteroidetes; GHB
Ensifer adhaerens	0	0	0	0	Alphaproteobacteria
Enteractinococcus fodinae	0.008	0	0.005	0.029	Coal mine; Generalist; GHB; Soil
Enterococcus cecorum	0	0	1.604	0	APB; Facultative Anaerobe; Firmicutes; LAB; Lactobacillales
Enterococcus columbae	0.001	0	0.005	0	APB; Facultative Anaerobe; Firmicutes; LAB; Lactobacillales
Erysipelothrix sp	0.052	0	0	0.334	Erysipelotrichia; Facultative Anaerobe; Firmicutes; GHB; Pathogen
Erythrobacter mathurensis	0	0	0	0	
Ethanoligenens harbinense	0	0	0	0	Clostridia; Firmicutes
Ethanoligenens sp	0	0	0	0	
Exiguobacterium sp	0	0	0	0	APB; GHB
Ferribacterium sp	0	0	0	0	Betaproteobacteria
Ferruginibacter sp	0	0	0	0	Bacteroidetes; BioDeg
Flavihumibacter sp	0	0	0	0	
Flavisolibacter sp	0	0	0	0	Bacteroidetes; Industrial Wastewater
Flavitalea sp	0	0	0	0	Bacteroidetes
Flavobacterium glaciei	0	0	0	0	Aerobe; Bacteroidetes; Water
Flavobacterium sp	0.204	0	0	1.215	Aerobe; Bacteroidetes; BioDeg; BioDeg HC; Water
Flexibacter sp	0	0	0	0	Bacteroidetes; BioDeg; BioDeg HC; Oilfield
Flexistipes sinusarabici	0	0	0	0.021	Anaerobe; Deferribacteres; Ferm; GHB; Halophile; Possible Sulfidogen; Thermophile
Fluviicoccus keumensis	0	0	0	0	Facultative; Gammaproteobacteria
Fluviicola sp	0	0	0	0	Bacterioplankton; Bacteroidetes; GHB
Fontibacter flavus	0.046	2.159	0	0.078	Bacteroidetes
Formivibrio citricus	0	0	0	0.065	Betaproteobacteria
Frankia sp	0	0	0	0	Actinobacteria; NiF
Frigoribacterium sp	0	0	0	0	Actinobacteria
Fusibacter paucivorans	0	0	0	0.005	Anaerobe; Clostridia; Firmicutes; Sulfidogen; SuRB; TRB
Fusibacter sp	0	0	0.209	0	Anaerobe; Clostridia; Firmicutes; Sulfidogen; SuRB; TRB
Fusobacterium sp	0	0	0	0.021	Anaerobe; Fusobacteria; Pathogen
Gaiella sp	0	0	0	0	
Garciella sp	0.148	0	0	0.182	Clostridia; Firmicutes; NRB; Oilfield; Sulfidogen; TRB
Gemella sp	0.014	0	0	0	GHB
Gemmata sp	0	0	0	0	Planctomycetes; Unknown
Gemmatimonas sp	0	0	0	0	Gemmatimonadetes; GHB; Oligotroph
Gemmobacter sp	0	0	0	0	Alphaproteobacteria; BioDeg; Methyltroph
Geoalkalibacter sp	0	0	0	0	Anaerobe; Deltaproteobacteria; IRB; Thermophile
Geoalkalibacter subterraneus	0	0	0	0.06	Anaerobe; Deltaproteobacteria; IRB; Thermophile

Sequence ID	OG230207-001	OG230402-001	OG230402-002	OG230402-003	OG230402-004	OG230402-005	OG230402-006	OG230402-007	OG230402-008	OG230402-009	OG230402-010	OG230402-011	OG230402-012	OG230402-013	OG230402-014	OG230402-015	OG230402-016	OG230402-017	OG230402-018	OG230402-019	OG230402-020	OG230402-021	OG230508-001	OG230508-002
Well 2244 Sample Description:	Soils Direct	C001 Scale, All, PRD	C001 Scale, All, MPB	C001 Scale, All, IRB	C002 - C005 Scale, PRD	C002 - C005 Scale, MPB	C002 - C005 Scale IRB	C006 - C022 Scale Body, PRD	C006 - C022 Scale Body, MPB	C006 - C022 Scale Body IRB	C006 - C022 Scale Collar, PRD	C006 - C022 Scale Collar, MPB	C006 - C022 Scale Collar IRB	C023 - C034 Scale Body, PRD	C023 - C034 Scale Body, MPB	C023 - C034 Scale Body IRB	C023 - C034 Scale Collar, PRD	C023 - C034 Scale Collar, MPB	C023 - C034 Scale Collar , IRB	9 5/8 ID Scale, PRD	9 5/8 ID Scale, MPB	9 5/8 ID Scale IRB	Pool 20 Annulus Fluids Black Direct	Pool 22 Annulus Fluids Grey Direct
Geobacter lovleyi	0.004	0	0	0	0	0	0	0	0	0	0	0	0	0	0	0	0	0	0	0	0	0	0	0
Geobacter sp	1.077	0	0	0	0	0	0	0	0	0	0	0	0	0	0	0	0	0	0	0	0	0	0.124	0
Geodermatophilus sp	0.002	0	0	0	0	0	0	0	0	0	0	0	0	0	0	0	0	0	0	0	0	0	0	0
Georgenia sp	0	0	0	0	0	0	0	0	0	0	0	0	0	0	0	0	0	0	0	0	0	0	0.007	0
Geosporobacter sp	0.014	0.016	0.096	26.117	0.004	0.04	46.893	0.014	10.419	79.679	0.038	0.004	3.165	0.017	0	34.42	0.014	0.042	4.195	0	0.686	5.12	2.407	0.626
Geotoga sp	0	0	0	0	0	0	0	0	0	0	0	0	0	0	0	0	0	0	0	0	0	0	0.008	0
Gillisia sp	0	0	0	0	0	0	0	0	0	0	0	0	0	0	0	0	0	0	0	0	0	0	0	0
Gloeobacter sp	0	0	0	0	0	0	0	0	0	0	0	0	0	0	0	0	0	0	0	0	0	0	0	0.007
Gracilibacter sp	0.014	0	0	0.353	0	0	2.211	0	0	0.307	0.004	0	0.209	0	0	0.921	0	0	0.251	0	0.51	0.119	0.074	0
Granulibacter sp	0	0	0	0	0	0	0	0	0	0	0	0	0	0	0	0	0	0	0	0	0	0	0	0
Hahella chejuensis	0.041	0	0	0	0	0	0	0	0	0	0	0	0	0	0	0	0	0	0	0	0	0	0	0
Halanaerobium saccharolyticum	0	0	0	0	0	0	0	0	0	0	0	0	0	0	0	0	0	0	0	0	0	0	0.272	0.274
Halanaerobium sp	0	0	0.004	0.006	0.004	0	0	0	0	0.047	0	0.004	0.011	0.01	0	0	0.028	0	0.012	0	0.003	0.008	13.935	41.103
Haliangium sp	0.014	0	0	0	0	0	0	0	0	0	0	0	0	0	0	0	0	0	0	0	0	0	0	0
Halobacillus sp	0.004	0	0	0	0	0	0	0	0	0	0	0	0	0	0	0	0	0	0	0	0	0	0	0
Halolactibacillus halophilus	0	0	0	0	0	0	0	0	0	0	0	0	0	0	0	0	0	0	0	0	0	0	0.065	0.086
Halomonas sp	0	0	0	0	0	0	0	0	0	0	0	0	0	0	0	0	0	0	0	0	0	0	0.183	0.226
Halospirulina sp	0	0	0	0	0	0	0	0	0	0	0	0	0	0	0	0	0	0	0	0	0	0	0	0
Halothiobacillus neapolitanus	0	0	0.009	0	0	0	0	0	0	0	0	0.004	0	0	0	0	0	0	0	0.018	0	0	0	0
Herbaspirillum autotrophicum	0.085	0	0	0	0	0	0	0	0	0	0	0	0	0	0	0	0	0	0	0	0	0	0	0
Herbaspirillum sp	0.34	0	0	0	0	0	0	0	0	0	0	0	0	0	0	0	0	0	0	0	0	0	0.059	0.152
Herminiimonas sp	0.053	0	0	0	0	0	0	0	0	0	0	0	0	0	0	0	0	0	0	0	0	0	0	0
Herpetosiphon sp	0.007	0	0	0	0	0	0	0	0	0	0	0	0	0	0	0	0	0	0	0	0	0	0	0
Hirschia sp	0.004	0	0	0	0	0	0	0	0	0	0	0	0	0	0	0	0	0	0	0	0	0	0	0
Holophaga sp	0.099	0	0	0	0	0	0	0	0	0	0	0	0	0	0	0	0	0	0	0	0	0	0	0
Hongiella sp	0.011	0	0	0	0	0	0	0	0	0	0	0	0	0	0	0	0	0	0	0	0	0	0	0
Hyalangium sp	0.004	0	0	0	0	0	0	0	0	0	0	0	0	0	0	0	0	0	0	0	0	0	0	0
Hydrogenoanaerobacterium saccharovorans	0	0	0.261	0.095	0	0	0	0	0	0.142	0	0	0	0	0	0	0	0	0	0	0	0	0	0
Hydrogenoanaerobacterium sp	0	0	0	0.619	0	0	0.944	0	0	0	0	0	0.639	0	0	0.467	0	0	0.7	0	0	0	0	0
Hydrogenophaga sp	1.521	0	0	0	0	0	0	0	0	0	0	0	0	0	0	0	0	0	0	0	0	0	0.08	0.036
Hydrogenophilus sp	0	0	0	0	0	0	0	0	0	0	0	0	0	0	0	0	0	0	0	0	0	0	0	0
Hyphomicrobium nitrativorans	0	0	0	0	0	0	0	0	0	0	0	0	0	0	0	0	0	0	0	0	0	0	0.118	0
Hyphomicrobium sp	0.055	0	0	0	0	0	0	0	0	0	0	0	0	0	0	0	0	0	0	0	0	0	1.358	0.221
Hyphomicrobium sulfonivorans	0	0	0	0	0	0	0	0	0	0	0	0.004	0	0	0	0	0	0	0	0	0	0	0.008	0
Hyphomonas sp	0.016	0	0	0	0	0	0	0	0	0.024	0	0	0	0.003	0	0	0	0	0	0	0	0	0.036	0
Iamia sp	0.004	0	0	0	0	0	0	0	0.009	0	0	0	0	0	0	0	0	0	0	0	0	0	0	0
Ideonella sp	0.002	0	0	0	0	0	0	0	0	0	0	0	0	0	0	0	0	0	0	0	0	0	0	0
Idiomarina sp	0	0	0	0	0	0	0	0	0	0	0	0	0	0	0	0	0	0	0	0	0	0	0.007	0
Isosphaera sp	0	0	0	0	0	0	0	0	0	0	0	0	0	0	0	0	0	0	0	0	0	0	0.004	0
Janibacter sp	0	0	0	0	0	0	0	0	0	0	0	0	0	0	0	0	0	0	0	0	0	0	0.014	0
Janthinobacterium sp	0.368	0	0	0	0	0	0	0.004	0	0	0	0	0	0.003	0	0	0	0	0	0	0	0.004	0.043	0.021
Jeotgalicoccus coquinae	0	0	0	0	0	0	0	0	0	0	0	0	0	0	0	0	0	0	0	0	0	0	0.034	0
Jeotgalicoccus sp	0	0	0	0	0	0	0	0	0	0	0	0	0	0	0	0	0	0	0	0	0	0	0	0
Kaistia sp	0.004	0	0	0	0	0	0	0	0	0	0	0	0	0	0	0	0	0	0	0	0	0	0	0
Ktedonobacter sp	0.063	0	0	0	0	0	0	0	0	0	0	0	0	0	0	0	0	0	0	0	0	0	0	0
Lacibacter sp	0.06	0	0	0	0	0	0	0	0	0	0	0	0	0	0	0	0	0	0	0	0	0	0	0
Lacihabitans soyangensis	0.021	0	0	0	0	0	0	0	0	0	0	0	0	0	0	0	0	0	0	0	0	0	0	0
Larkinella insperata	0.002	0	0	0	0	0	0	0	0	0	0	0	0	0	0	0	0	0	0	0	0	0	0	0
Legionella jordanis	0	0	0	0	0	0	0	0	0	0	0	0	0	0	0	0	0	0	0	0	0	0	0	0
Legionella pneumophila	0	0	0	0	0	0	0	0	0	0	0	0	0	0	0	0	0	0	0	0	0	0	0.012	0
Legionella sp	0.051	0	0	0	0	0	0	0	0	0	0	0	0	0	0	0	0	0	0	0	0	0	0.088	0.076
Legionella wadsworthii	0	0	0	0	0	0	0	0	0	0	0	0	0	0	0	0	0	0	0	0	0	0	0.003	0
Leptolinea sp	0	0	0	0	0	0	0	0	0	0	0	0	0	0	0	0	0	0	0	0	0	0	0.01	0
Leptothrix sp	0.039	0	0	0	0	0	0	0	0	0	0	0	0	0	0	0	0	0	0	0	0	0	0.004	0.01
Leucobacter aridicollis	0	0	0	0	0	0	0	0.011	0	0	0	0	0	0	0	0.008	0	0	0	0	0	0	0	0
Leucobacter komagatae	0	0	0	0	0	0	0	0	0	0	0	0	0	0	0	0	0	0	0	0	0	0	0.06	0.031
Leucobacter sp	0	0	0	0	0	0	0	0	0	0	0	0	0	0	0	0	0	0	0	0	0	0	0	0

Sequence ID	OG2305008-003	OG2305008-004	OG2305008-005	OG2305008-006	Selected Traits
Well 2244 Sample Description:	Pool 27 Annulus Fluids Tank Direct	Pool 37 C015 - C022 Scale C Direct	Pool 13 C001B OD Scale All Direct	MG08 C023 - C034 Scale C Direct	Metabolic, Taxonomic, Physiological, Ecological
Geobacter lovleyi	0	0	0	0	Anaerobe; BioDeg; BioDeg HC; Biofilm; Deltaproteobacteria; IRB; Metal Reduction; Microbial Fuel Cell
Geobacter sp	0.007	0.669	0	0.125	Anaerobe; BioDeg; BioDeg HC; Biofilm; Deltaproteobacteria; IRB; Metal Reduction; Microbial Fuel Cell
Geodermatophilus sp	0	0	0	0	Actinomycete; Soil
Georgenia sp	0	0	0	0	Actinobacteria; BioDeg
Geosporobacter sp	1.935	1.483	0	2.208	Anaerobe; Clostridia; Ferm; Firmicutes; IRB; Spore
Geotoga sp	0	0	0	0	Sulfidogen; SuRB; Thermophile; Thermotogae
Gillisia sp	0.033	0	0	0	Bacteroidetes
Gloeobacter sp	0.015	0	0	0	Cyanobacteria; Phototroph
Gracilibacter sp	0.051	0	0	0	Clostridia; Ferm; Firmicutes; GHB
Granulibacter sp	0.01	0	0	0	Alphaproteobacteria
Hahella chejuensis	0	0	0	0	Gammaproteobacteria
Halanaerobium saccharolyticum	0.265	0.209	0	0	Anaerobe; APB; Clostridia; Ferm; Firmicutes; Halophile; MIC; SRB-Promoting; Sulfidogen; TRB
Halanaerobium sp	17.677	5.064	0.002	43.048	Anaerobe; APB; Clostridia; Ferm; Firmicutes; Halophile; MIC; SRB-Promoting; Sulfidogen; TRB
Haliangium sp	0	0	0	0	Deltaproteobacteria
Halobacillus sp	0	0	0	0	Alkaliphile; Bacilli; Firmicutes; Halophile; NRB
Halolactibacillus halophilus	0.061	0	0	0.206	Alkaliphile; Bacilli; Firmicutes; GHB; Halophile
Halomonas sp	0.086	0	0	0.216	Alkaliphile; BioDeg; BioDeg HC; Facultative Anaerobe; Gammaproteobacteria; Haloalkaliphile; Halophil
Halospirulina sp	0.007	0	0	0	Halophile; Phototroph
Halothiobacillus neapolitanus	0	0	0	0	Acidophile; Aerobe; APB; Filamentous; Gammaproteobacteria; ISOX; MIC; SOB
Herbaspirillum autotrophicum	0	0	0	0	Aerobe; Betaproteobacteria; NiF
Herbaspirillum sp	0.039	0	0	0.112	Aerobe; Betaproteobacteria; NiF
Herminiimonas sp	0	0	0	0	Betaproteobacteria; Heavy Metal
Herpetosiphon sp	0	0	0	0	Chloroflexi
Hirschia sp	0	0	0	0	Alphaproteobacteria
Holophaga sp	0	0	0	0	Acidobacteria; BioDeg; BioDeg HC
Hongiella sp	0	0	0	0	Bacteroidetes; GHB
Hyalangium sp	0	0	0	0	Deltaproteobacteria; Unknown
Hydrogenoanaerobacterium saccharovorans	0	0	0	0	Anaerobe; Clostridia; Ferm; Firmicutes; H2 producing
Hydrogenoanaerobacterium sp	0.015	0	0	0	Anaerobe; Clostridia; Ferm; Firmicutes; H2 producing
Hydrogenophaga sp	0.017	0.6	0.809	0	Aerobe; Betaproteobacteria; BioDeg; BioDeg HC
Hydrogenophilus sp	0	0	0	0.039	Aerobe; Betaproteobacteria; BioDeg; BioDeg HC
Hyphomicrobium nitrativorans	0.052	0.042	0	0	
Hyphomicrobium sp	0.653	1.811	0	0.435	Aerobe; Alphaproteobacteria; BioDeg; Methylotroph; Soil
Hyphomicrobium sulfonivorans	0.008	0	0	0	Aerobe; Alphaproteobacteria; BioDeg; Methylotroph; Soil
Hyphomonas sp	0	0	0	0.083	Alphaproteobacteria; Biofilm
Iamia sp	0	0	0	0	Actinobacteria
Ideonella sp	0	0	0	0	PerRB
Idiomarina sp	0.008	0	0	0	Aerobe; Gammaproteobacteria; GHB
Isosphaera sp	0	0	0	0	Planctomycetes
Janibacter sp	0.035	0	0	0	Actinobacteria; BioDeg; BioDeg HC
Janthinobacterium sp	0.113	0	0	0.383	Aerobe; Antimicrobial; Betaproteobacteria; Biofilm; Dark Violet; Natural Dye
Jeotgalicoccus coquinae	0	0	0.005	0	Faculatative Anaerobe; Fish sauce; Generalist; GHB; Halophile
Jeotgalicoccus sp	0	0	0	0.133	Bacilli; Faculatative Anaerobe; Firmicutes; Fish sauce; Generalist; GHB; Halophile
Kaistia sp	0	0	0	0	Alphaproteobacteria
Ktedonobacter sp	0	0	0	0	
Lacibacter sp	0	0	0	0	
Lacihabitans soyangensis	0	0	0	0	Bacteroidetes
Larkinella insperata	0	0	0	0	Aerobe; Sediments; Soil
Legionella jordanis	0.022	0	0	0	Aerobe; Gammaproteobacteria
Legionella pneumophila	0.004	0	0	0	Aerobe; Gammaproteobacteria; Pathogen
Legionella sp	0.048	0	0	0.076	Aerobe; Gammaproteobacteria
Legionella wadsworthii	0	0	0	0	Aerobe; Gammaproteobacteria
Leptolinea sp	0.004	0	0	0	Chloroflexi; Filamentous; GHB
Leptothrix sp	0.014	0.465	0	0	Aerobe; GHB
Leucobacter aridicollis	0	0	0	0	Actinobacteria; Aerobe; BioDeg; BioDeg chromium compounds; Biosurfactant Producing; Chromium tolo
Leucobacter komagatae	0.008	1.084	0.002	0	Actinobacteria; Aerobe; BioDeg; BioDeg chromium compounds; Biosurfactant Producing; Chromium tolo
Leucobacter sp	0	0.51	0	0	Actinobacteria; BioDeg

Sequence ID	OG230207-001	OG230402-001	OG230402-002	OG230402-003	OG230402-004	OG230402-005	OG230402-006	OG230402-007	OG230402-008	OG230402-009	OG230402-010	OG230402-011	OG230402-012	OG230402-013	OG230402-014	OG230402-015	OG230402-016	OG230402-017	OG230402-018	OG230402-019	OG230402-020	OG230402-021	OG230508-001	OG230508-002
Well 2244 Sample Description:	Soils Direct	C001 Scale, All, PRD	C001 Scale, All, MPB	C001 Scale, All, IRB	C002 - C005 Scale, PRD	C002 - C005 Scale, MPB	C002 - C005 Scale IRB	C006 - C022 Scale Body, PRD	C006 - C022 Scale Body, MPB	C006 - C022 Scale Body IRB	C006 - C022 Scale Collar, PRD	C006 - C022 Scale Collar, MPB	C006 - C022 Scale Collar IRB	C023 - C034 Scale Body, PRD	C023 - C034 Scale Body, MPB	C023 - C034 Scale Body IRB	C023 - C034 Scale Collar, PRD	C023 - C034 Scale Collar, MPB	C023 - C034 Scale Collar , IRB	9 5/8 ID Scale, PRD	9 5/8 ID Scale, MPB	9 5/8 ID Scale IRB	Pool 20 Annulus Fluids Black Direct	Pool 22 Annulus Fluids Grey Direct
Levilinea sp	0	0	0	0	0	0	0	0	0	0	0	0	0	0	0	0	0	0	0	0	0	0	0.016	0
Limnobacter sp	0.055	0	0	0	0	0	0	0	0	0	0	0	0	0	0	0	0	0	0	0	0	0	0	0
Lishizhenia sp	0.522	0	0	0	0	0	0	0	0	0	0	0	0	0	0	0	0	0	0	0	0	0	0	0
Litorilinea sp	0.005	0	0	0	0	0	0	0	0	0	0	0	0	0	0	0	0	0	0	0	0	0	0	0
Longilinea arvoryzae	0	0	0	0	0	0	0	0	0	0	0	0	0	0	0	0	0	0	0	0	0	0	0.03	0
Longilinea sp	0.007	0	0	0	0	0	0	0	0	0	0	0	0	0	0	0	0	0	0	0	0	0	0.014	0
Luteolibacter sp	0.019	0	0	0	0	0	0	0	0	0	0	0	0	0	0	0	0	0	0	0	0	0	0	0
Lysinibacillus sp	0	8.363	0.165	1.742	24.935	0.01	13.229	2.883	0.291	1.063	9.806	0.239	1.245	12.033	0.045	5.57	19.352	0.012	0.335	0.165	0	0.143	0	0
Lysobacter concretionis	0	0	0	0	0	0	0	0	0	0	0	0	0	0	0	0	0	0	0	0	0	0	0	0.019
Lysobacter sp	0.085	0	0	0	0	0	0	0	0	0	0	0	0	0	0	0	0	0	0	0	0	0	0	0
Malonomonas sp	0.004	0	0	0	0	0	0	0	0	0	0	0	0	0	0	0	0	0	0	0	0	0	0	0
Marinobacterium sp	0	0	0.004	0.013	0.004	0	0	0.011	0.004	0.024	0	0	0.014	0.007	0	0.034	0	0	0.006	0	0.024	0.016	0	0.021
Massilia sp	0.647	0	0	0	0	0	0	0	0	0	0	0	0	0	0	0	0	0	0	0	0	0	0.003	0.055
Megasphaera cerevisiae	0	0	0	0	0	0	0	0	0	0	0	0	0	0	0	0	0	0	0	0	0	0	0.029	0
Mesorhizobium albiziae	0.005	0	0	0	0	0	0	0	0	0	0	0	0	0	0	0	0	0	0	0	0	0	0	0
Mesorhizobium sp	0.039	0	0	0	0	0	0	0	0	0	0	0	0	0	0	0	0	0	0	0	0	0	0.069	0.014
Methanobacterium sp	0	0	0	0	0	0	0	0	0	0	0	0	0	0	0	0	0	0	0	0	0	0	2.888	1.737
Methylibium sp	0.308	0	0	0	0	0	0	0	0	0	0	0	0	0	0	0	0	0	0	0	0	0	0	0
Methylobacillus sp	0.074	0	0	0	0	0	0	0	0	0	0	0	0	0	0	0	0	0	0	0	0	0	0	0
Methylobacter sp	0.012	0	0	0	0	0	0	0	0	0	0	0	0	0	0	0	0	0	0	0	0	0	0	0
Methylobacterium sp	0	0	0	0	0	0	0	0	0	0	0	0	0	0	0	0	0	0	0	0	0	0	0.003	0
Methylocaldum sp	0	0	0	0	0	0	0	0	0	0	0	0	0	0	0	0	0	0	0	0	0	0	0.111	0.019
Methylocapsa aurea	0	0	0	0	0	0	0	0	0	0	0	0	0	0	0	0	0	0	0	0	0	0	0.012	0
Methylocapsa sp	0.004	0	0	0	0	0	0	0	0	0	0	0	0	0	0	0	0	0	0	0	0	0	0	0
Methylococcus sp	0	0	0	0	0	0	0	0	0	0	0	0	0	0	0	0	0	0	0	0	0	0	0.164	0.09
Methylocystis sp	0.007	0	0	0	0	0	0	0	0	0	0	0	0	0	0	0	0	0	0	0	0	0	0.473	0.178
Methylomonas sp	0	0	0	0	0	0	0	0	0	0	0	0	0	0	0	0	0	0	0	0	0	0	0.1	0
Methylophilus sp	1.889	0	0	0	0	0	0	0	0	0	0	0	0	0	0	0	0	0	0	0	0	0	0	0
Methylorosula polaris	0.004	0	0	0	0	0	0	0	0	0	0	0	0	0	0	0	0	0	0	0	0	0	0	0
Methylosinus sporium	0.007	0	0	0	0	0	0	0	0	0	0	0	0	0	0	0	0	0	0	0	0	0	0.021	0
Methylosinus trichosporium	0	0	0	0	0	0	0	0	0	0	0	0	0	0	0	0	0	0	0	0	0	0	0.25	0.014
Methyloversatilis sp	0	0	0	0	0	0	0	0	0	0	0	0	0	0	0	0	0	0	0	0	0	0	0.005	0.064
Microbispora sp	0	0	0	0	0	0	0	0	0	0	0	0	0	0	0	0	0	0	0	0	0	0	0.007	0
Micromonospora sp	0	0	0	0	0	0	0	0	0	0	0	0	0	0	0	0	0	0	0	0	0	0	0.04	0.01
Microvirga sp	0	0	0	0	0	0	0	0	0	0	0	0	0	0	0	0	0	0	0	0	0	0	0.005	0
Microvirga subterranea	0	0	0	0	0	0	0	0	0	0	0	0	0	0	0	0	0	0	0	0	0	0	0.051	0
Mobilitalea sibirica	0	0	0	0	0	0	0	0	0	0	0	0	0	0	0	0	0	0	0	0	0	0	0.018	0
Modestobacter sp	0.002	0	0	0	0	0	0	0	0	0	0	0	0	0	0	0	0	0	0	0	0	0	0	0
Mongoliitalea lutea	0	0	0	0	0	0	0	0	0	0	0	0	0	0	0	0	0	0	0	0	0	0	0	0
Moorella sp	0.051	0	0	0	0	0	0	0	0	0	0	0	0	0	0	0	0	0	0	0	0	0	0	0
Moorella thermoacetica	0	0	0	0	0	0	0	0	0	0	0	0	0	0	0	0	0	0	0	0	0	0	0.033	0
Moraxella sp	0	0	0	0	0	0	0	0	0	0	0	0	0	0	0	0	0	0	0	0	0	0	0	0
Morganella morganii	0	0	0	0	0	0	0	0	0	0	0	0	0	0	0	0	0	0	0	0	0	0	0	0
Mucilaginibacter auburnensis	0.002	0	0	0	0	0	0	0	0	0	0	0	0	0	0	0	0	0	0	0	0	0	0	0
Mycobacterium sp	0.078	0	0	0	0	0	0	0	0	0	0	0	0	0	0	0	0	0	0	0	0	0	0.445	0.136
Mycoplasma wenyonii	0	0	0	0	0	0	0	0	0	0	0	0	0	0	0	0	0	0	0	0	0	0	0.034	0.052
Nannocystis sp	0.009	0	0	0	0	0	0	0	0	0	0	0	0	0	0	0	0	0	0	0	0	0	0	0
Natronomonas sp	0.011	0	0	0	0	0	0	0	0	0	0	0	0	0	0	0	0	0	0	0	0	0	0	0
Neisseria sp	0	0	0	0	0	0	0	0	0	0	0	0	0	0	0	0	0	0	0	0	0	0	0	0
Nesterenkonia sp	0	0	0	0	0	0	0	0	0	0	0	0	0	0	0	0	0	0	0	0	0	0	0.034	0.059
Nevskia ramosa	0.004	0	0	0	0	0	0	0	0	0	0	0	0	0	0	0	0	0	0	0	0	0	0	0
Niabella sp	0	0	0	0	0	0	0	0	0	0	0	0	0	0	0	0	0	0	0	0	0	0	0	0
Niastella sp	0.004	0	0	0	0	0	0	0	0	0	0	0	0	0	0	0	0	0	0	0	0	0	0	0
Nitratireductor sp	0.011	0	0	0	0	0	0	0	0	0	0	0	0	0	0	0	0	0	0	0	0	0	0	0
Nitrosococcus sp	0.028	0	0	0	0	0	0	0	0	0	0	0	0	0	0	0	0	0	0	0	0	0	0	0
Nitrosomonas sp	0	0	0	0	0	0	0	0	0	0	0	0	0	0	0	0	0	0	0	0	0	0	0	0
Nitrosospira sp	0	0	0	0	0	0	0	0	0	0	0	0	0	0	0	0	0	0	0	0	0	0	0	0

Sequence ID	OG230508-003	OG230508-004	OG230508-005	OG230508-006	Selected Traits
Well 2244 Sample Description:	Pool 27 Annulus Fluids Tank Direct	Pool 37 C015 - C022 Scale C Direct	Pool 13 C001B OD Scale All Direct	MG08 C023 - C034 Scale C Direct	Metabolic, Taxonomic, Physiological, Ecological
Levilinea sp	0.026	0	0	0	Alaska; Chloroflexi; Oilfield; Produced Water
Limnobacter sp	0	0	0	0	Betaproteobacteria; Sulfidogen; TRB
Lishizhenia sp	0	0	0	0	
Litorilinea sp	0	0	0	0	
Longilinea arvoryzae	0	0	0	0	Chloroflexi
Longilinea sp	0.003	0	0	0.01	Anaerobe; Chloroflexi; Consortium Member; Filamentous; Methanogenic Community Member
Luteolibacter sp	0	0	0	0	Verrucomicrobia
Lysinibacillus sp	0	0	0	0.06	Aerobe; Bacilli; BioDeg; Bioremediation; Chromate reduction; Firmicute; Firmicutes; GHB; Insect Pathog
Lysobacter concretionis	0	0	0	0	BioDeg; Gammaproteobacteria
Lysobacter sp	0	1.084	0	0.042	BioDeg; BioDeg HC; Gammaproteobacteria
Malonomonas sp	0	0	0	0	Deltaproteobacteria; Ferm
Marinobacterium sp	0.006	0	0.011	0	Aerobe; BioDeg; Gammaproteobacteria; GHB
Massilia sp	0.025	0	0	0	Betaproteobacteria; BioDeg; Filamentous; Soil
Megasphaera cerevisiae	0.006	0	0	0.107	
Mesorhizobium albiziae	0	0	0	0	
Mesorhizobium sp	0.035	1.969	0	0.021	Alphaproteobacteria; NiF; Soil
Methanobacterium sp	3.233	0	0	0.414	Anaerobe; Archaea; Methanogen
Methylibium sp	0	0	0	0	Methylotroph
Methylobacillus sp	0	0	0	0	Betaproteobacteria; Methylotroph
Methylobacter sp	0	0	0	0	Gammaproteobacteria; Methylotroph
Methylobacterium sp	0.003	0.447	0	0	Aerobe; Alphaproteobacteria; Methylotroph
Methylocaldum sp	0.061	0.624	0	0	Gammaproteobacteria; Methylotroph
Methylocapsa aurea	0.012	0	0	0	
Methylocapsa sp	0	0	0	0	Alphaproteobacteria; Methylotroph
Methylococcus sp	0.011	0	0	0.292	Gammaproteobacteria; Methylotroph
Methylocystis sp	0.522	0	0	0.188	Alphaproteobacteria; Methylotroph
Methylomonas sp	0.068	0	0	0.216	Gammaproteobacteria; Methylotroph
Methylophilus sp	0	0	0	0	Betaproteobacteria; Methylotroph
Methylorosula polaris	0	0	0	0	
Methylosinus sporium	0	0	0	0	Alphaproteobacteria; Methylotroph
Methylosinus trichosporium	0.203	0.14	0	0	Alphaproteobacteria; Methylotroph
Methyloversatilis sp	0.021	0	0	0.018	Betaproteobacteria; Methylotroph
Microbispora sp	0	0	0	0	Actinobacteria; GHB
Micromonospora sp	0.032	0	0	0	
Microvirga sp	0	0	0	0.016	Alphaproteobacteria
Microvirga subterranea	0	0	0	0	Alphaproteobacteria
Mobilitalea sibirica	0	0	0	0.05	
Modestobacter sp	0	0	0	0	Aerobe; Alphaproteobacteria; Soil; Soil Crust
Mongoliitalea lutea	0	0	0	0.013	Alkaliphile; Bacteroidetes; Halophile
Moorella sp	0.011	0	0	0	Acetogen; Anaerobe; APB; Clostridia; Ferm; Firmicutes; NRB; Spore; Sulfidogen; Thermophile; TRB
Moorella thermoacetica	0.006	0	0	0	Acetogen; Anaerobe; APB; Clostridia; Ferm; Firmicutes; NRB; Spore; Sulfidogen; Thermophile; TRB
Moraxella sp	0	1.895	0	0	Gammaproteobacteria; Pathogen
Morganella morganii	0	0	0	0.008	Gammaproteobacteria
Mucilaginibacter auburnensis	0	0	0	0	
Mycobacterium sp	0.353	1.324	0	0.109	Actinobacteria; Environmental; Widespread
Mycoplasma wenyonii	0.015	3.058	1.959	0.076	Actinomycete; Pathogen
Nannocystis sp	0	0	0	0	Deltaproteobacteria
Natronomonas sp	0	0	0	0	Archaea
Neisseria sp	0.07	0	0	0	Betaproteobacteria
Nesterenkonia sp	0.058	0	0	0.005	Actinobacteria; BioDeg; BioDeg HC; CrIV RB; Halophile
Nevskia ramosa	0	0	0	0	Gammaproteobacteria; GHB
Niabella sp	0	0	3.348	0	Bacteroidetes
Niastella sp	0	0	0	0.005	Bacteroidetes
Nitratireductor sp	0	0	0	0	Alphaproteobacteria; Facultative Anaerobe; NRB
Nitrosococcus sp	0.011	0	0	0	Gammaproteobacteria; Halophile; NOB
Nitrosomonas sp	0	0	1.371	0	AOB; AOX; Betaproteobacteria
Nitrosospira sp	0	0	0	0.021	Aerobe; AOB; AOX; Betaproteobacteria

Appendix B. Well 2244 Soil, Scale, Annulus Fluid Microbial Population
16S Amplicon Metagenomic Analysis
Samples collected March 2023

Sequence ID	OG230207-001	OG230402-001	OG230402-002	OG230402-003	OG230402-004	OG230402-005	OG230402-006	OG230402-007	OG230402-008	OG230402-009	OG230402-010	OG230402-011	OG230402-012	OG230402-013	OG230402-014	OG230402-015	OG230402-016	OG230402-017	OG230402-018	OG230402-019	OG230402-020	OG230402-021	OG230508-001	OG230508-002
Well 2244 Sample Description:	Soils Direct	C001 Scale, All, PRD	C001 Scale, All, MPB	C001 Scale, All, IRB	C002 - C005 Scale, PRD	C002 - C005 Scale, MPB	C002 - C005 Scale IRB	C006 - C022 Scale Body, PRD	C006 - C022 Scale Body, MPB	C006 - C022 Scale Body IRB	C006 - C022 Scale Collar, PRD	C006 - C022 Scale Collar, MPB	C006 - C022 Scale Collar IRB	C023 - C034 Scale Body, PRD	C023 - C034 Scale Body, MPB	C023 - C034 Scale Body IRB	C023 - C034 Scale Collar, PRD	C023 - C034 Scale Collar, MPB	C023 - C034 Scale Collar , IRB	9 5/8 ID Scale, PRD	9 5/8 ID Scale, MPB	9 5/8 ID Scale IRB	Pool 20 Annulus Fluids Black Direct	Pool 22 Annulus Fluids Grey Direct
Nitrosovibrio sp	0.004	0	0	0	0	0	0	0	0	0	0	0	0	0	0	0	0	0	0	0	0	0	0	0
Nitrospira enrichment	0.007	0	0	0	0	0	0	0	0	0	0	0	0	0	0	0	0	0	0	0	0	0	0	0
Nitrospira sp	0.074	0	0	0	0	0	0	0	0	0	0	0	0	0	0	0	0	0	0	0	0	0	0	0
Nocardia nova	0	0	0	0	0	0	0	0	0	0	0	0	0	0	0	0	0	0	0	0	0	0	0	0
Nocardioides sp	0.025	0	0	0	0	0	0	0	0	0	0	0	0	0	0	0	0	0	0	0	0	0	0.054	0.005
Nocardiopsis sp	0	0	0	0	0	0	0	0	0	0	0	0	0	0	0	0	0	0	0	0	0	0	0.041	0
Nordella oligomobilis	0.002	0	0	0	0	0	0	0	0	0	0	0	0	0	0	0	0	0	0	0	0	0	0	0
Nordella sp	0.033	0	0	0	0	0	0	0	0	0	0	0	0	0	0	0	0	0	0	0	0	0	0	0
Noviherbaspirillum aurantiacum	0.333	0	0	0	0	0	0	0	0	0	0	0	0	0	0	0	0	0	0	0	0	0	0	0
Novosphingobium sp	0.28	0	0	0	0	0	0	0	0	0	0	0	0	0	0	0	0	0	0	0	0	0	0	0
Oceanirhabdus sediminicola	0	0	0	0	0	0	0.043	0	0	0	0	0	0.028	0	0	0	0	0	0.056	0	0	0.147	0	0
Oceanobacillus picturae	0	0	0	0	0	0	0	0	0	0	0	0	0	0	0	0	0	0	0	0	0	0	0	0
Ochrobactrum sp	0	0	0	0	0	0	0	0	0	0	0	0	0	0	0	0	0	0	0	0	0	0	0	0
Oerskovia sp	0.002	0	0	0	0	0	0	0	0	0	0	0	0	0	0	0	0	0	0	0	0	0	0	0
Ohtaekwangia sp	0.033	0	0	0	0	0	0	0	0	0	0	0	0	0	0	0	0	0	0	0	0	0	0	0
Opitutus sp	0.211	0	0	0	0	0	0	0	0	0	0	0	0	0	0	0	0	0	0	0	0	0	0	0
Ornithinimicrobium sp	0	0	0	0	0	0	0	0	0	0	0	0	0	0	0	0	0	0	0	0	0	0	0.003	0.01
Owenweeksia sp	0.023	0	0	0	0	0	0	0	0	0	0	0	0	0	0	0	0	0	0	0	0	0	0	0
Oxalobacter sp	0	0	0	0	0	0	0	0	0	0	0	0	0	0	0	0	0	0	0	0	0	0	0.049	0
Oxobacter pfennigii	0	0	0	1.168	0	0	1.362	0	0	3.426	0	0	0.021	0	0.004	0.501	0	0	0.13	0	0	0.064	0.038	0
Oxobacter sp	0	0	0	0	0	0	0	0	0	0.024	0	0	0	0	0	0.017	0	0	0	0	0	0	0.073	0
Paenalcaligenes hominis	0	0	0	0	0	0	0.004	0	0	0.047	0	0	0	0	0	0.004	0.005	0	0	0	0	0	0	0
Paenibacillus granivorans	0	0	0	0	0	0	0	0	0	0	0	0	0	0	0	0	0	0	0	0	0	0	0.003	0.031
Paenibacillus sp	0	9	0.274	0.019	20.443	0	0.06	0	0	0	0.004	0	0.043	0.007	0	0	0	0.45	0.034	0.228	0	0.008	0.021	0
Paludibacter sp	0.273	0	0	0	0	0	0	0	0	0	0	0	0	0	0	0	0	0	0	0	0	0	0	0.293
Papillibacter sp	0	0	0	0	0	0	0	0	0	0	0	0	0	0	0	0	0	0	0	0	0	0	0.021	0
Parabacteroides sp	0	0	0	0	0	0	0	0	0	0	0	0	0	0	0	0	0	0	0	0	0	0	0.224	0
Paracoccus denitrificans	0	0	0	0	0	0	0	0	0	0	0	0	0	0	0	0	0	0	0	0	0	0	0.005	0
Paracoccus sp	0	0	0	0	0	0	0	0	0	0	0	0	0	0	0	0	0	0	0	0	0	0	0.03	0.169
Paracraurococcus sp	0.002	0	0	0	0	0	0	0	0	0	0	0	0	0	0	0	0	0	0	0	0	0	0.003	0
Paraliobacillus quinghaiensis	0.005	0	0	0	0	0	0	0	0	0	0	0	0	0	0	0	0	0	0	0	0	0	0.047	3.211
Parvibaculum sp	0	0	0	0	0	0	0	0	0	0	0	0	0	0	0	0	0	0	0	0	0	0	0	0
Pasteuria sp	0.004	0	0	0	0	0	0	0	0	0	0	0	0	0	0	0	0	0	0	0	0	0	0	0
Patulibacter medicamentivorans	0	0	0	0	0	0	0	0	0	0	0	0	0	0	0	0	0	0	0	0	0	0	0	0
Patulibacter sp	0	0	0	0	0	0	0	0	0	0	0	0	0	0	0	0	0	0	0	0	0	0	0	0
Pedobacter daechungensis	0.004	0	0	0	0	0	0	0	0	0	0	0	0	0	0	0	0	0	0	0	0	0	0	0
Pedobacter luteus	0	0	0	0	0	0	0	0	0	0	0	0	0	0	0	0	0	0	0	0	0	0	0	0
Pedobacter metabolipauper	0	0	0	0	0	0	0	0	0	0	0	0	0	0	0	0	0	0	0	0	0	0	0.01	0
Pedobacter sp	1.079	0	0	0	0	0	0	0	0	0	0	0	0	0	0	0	0	0	0	0	0	0	0.033	0
Pedomicrobium sp	0.009	0	0	0	0	0	0	0	0	0	0	0	0	0	0	0	0	0	0	0	0	0	0	0
Pedosphaera parvula	0.004	0	0	0	0	0	0	0	0	0	0	0	0	0	0	0	0	0	0	0	0	0	0	0
Pedosphaera sp	0.011	0	0	0	0	0	0	0	0	0	0	0	0	0	0	0	0	0	0	0	0	0	0	0
Pelobacter sp	0.146	0	0	0	0	0	0	0	0	0	0	0	0	0	0	0	0	0	0	0	0	0	0	0
Pelotomaculum isophthalicicum	0	0	0	0	0	0	0	0	0	0	0	0	0	0	0	0	0	0	0	0	0	0	0	0
Pelotomaculum sp	0	0	0	0	0	0	0	0	0	0.047	0	0	0	0	0	0	0	0	0	0	0	0.02	0.063	0
Peredibacter starrii	0.1	0	0	0	0	0	0	0	0	0	0	0	0	0	0	0	0	0	0	0	0	0	0	0
Perlucidibaca sp	12.039	0	0	0	0	0	0	0	0	0	0	0	0	0	0	0	0	0	0	0	0	0	0	0
Petrobacter sp	0	0	0	0	0	0	0	0.007	0	0	0	0	0	0	0	0.017	0	0	0	0	0	0	0.007	0
Phenylobacterium sp	0.314	0	0	0	0	0	0	0	0	0	0	0	0	0	0	0	0	0	0	0	0	0	0.008	0
Phormidium sp	0.007	0	0	0	0	0	0	0	0	0	0	0	0	0	0	0	0	0	0	0	0	0	0	0
Phycisphaera sp	0.03	0	0	0	0	0	0	0	0	0	0	0	0	0	0	0	0	0	0	0	0	0	0	0
Phyllobacterium sp	0.004	0	0	0	0	0	0	0	0	0	0	0	0	0	0	0	0	0	0	0	0	0	0	0
Pigmentiphaga sp	0.004	0	0	0	0	0	0	0	0	0	0	0	0	0	0	0	0	0	0	0	0	0	0	0
Pirellula sp	0.023	0	0	0	0	0	0	0	0	0	0	0	0	0	0	0	0	0	0	0	0	0	0	0
Planctomyces sp	0.081	0	0	0	0	0	0	0	0	0	0	0	0	0	0	0	0	0	0	0	0	0	0	0
Planococcus sp	0	0	0	0	0	0.119	0	0	0	0	0	0	0.064	0	0	0.004	0.009	0	0.084	0.007	0.003	0.04	0.015	0
Polaromonas sp	3.19	0	0	0	0	0	0	0	0	0	0	0	0	0	0	0	0	0	0	0	0	0	0.007	0.031

Sequence ID	OG230508-003	OG230508-004	OG230508-005	OG230508-006	Selected Traits
Well 2244 Sample Description:	Pool 27 Annulus Fluids Tank Direct	Pool 37 C015 - C022 Scale C Direct	Pool 13 C001B OD Scale All Direct	MG08 C023 - C034 Scale C Direct	Metabolic, Taxonomic, Physiological, Ecological
Nitrosovibrio sp	0	0	0	0	Aerobe; AOB; AOX; Betaproteobacteria
Nitrospira enrichment	0	0	0	0	
Nitrospira sp	0	0	0	0	Nitrospinae; NOB
Nocardia nova	0.007	0	0	0	
Nocardioides sp	0.04	0	0	0.018	Actinobacteria; Filamentous
Nocardiopsis sp	0	0	0.005	0	Actinobacteria; Filamentous
Nordella oligomobilis	0	0	0	0	
Nordella sp	0	0	0	0	
Noviherbaspirillum aurantiacum	0	0	0	0	
Novosphingobium sp	0	0	0	0	Alphaproteobacteria; BioDeg
Oceanirhabdus sediminicola	0	0	0	0	Clostridia; Firmicutes
Oceanobacillus picturae	0.015	0	0	0	Bacilli; Firmicutes; Spore
Ochrobactrum sp	0	0	0	0.042	Alphaproteobacteria; NiF
Oerskovia sp	0	0	0	0	
Ohtaekwangia sp	0	0	0	0	Bacteroidetes
Opitutus sp	0	0	0	0	Ferm; Verrucomicrobia
Ornithinimicrobium sp	0.008	0	0	0	Actinobacteria
Owenweeksia sp	0	0	0	0	Bacteroidetes
Oxalobacter sp	0.044	0.005	0.006	0	Betaproteobacteria; Unknown
Oxobacter pfennigii	0.001	0	0	0	BioDeg; Clostridia; Firmicutes; Plant biomass
Oxobacter sp	0.036	0	0	0.063	Clostridia; Firmicutes
Paenalcaligenes hominis	0	0	0	0	Aerobe; Bacteroidetes; Betaproteobacteria; Bioreactor; Generalist; GHB
Paenibacillus granivorans	0	0	0	0	Bacilli; Facultative Anaerobe; Firmicutes; Spore
Paenibacillus sp	0.037	0	0	0.013	Bacilli; BioDeg; BioDeg EPS; BioDeg PAH; Dendritiformis colonies; Facultative Anaerobe; Firmicute; Fi
Paludibacter sp	0	0	0	0.021	Bacteroidetes; Ferm
Papillibacter sp	0.012	0	0	0.013	Clostridia; Firmicutes
Parabacteroides sp	0	0	0	0.164	Bacteroidetes; Unknown
Paracoccus denitrificans	0	0	0	0	Alphaproteobacteria; APB; BioDeg; Facultative Anaerobe; Mitochondrial Ancestor; NRB
Paracoccus sp	0.195	0	0	0.039	Alphaproteobacteria; APB; BioDeg; Facultative Anaerobe; Mitochondrial Ancestor; NRB
Paracraurococcus sp	0	0	0	0	Alphaproteobacteria; APB
Paraliobacillus quinghaiensis	0.126	0.333	0	0.266	Aerobe; Firmicutes; Halophile; Spore
Parvibaculum sp	0	0	1.506	0	Alphaproteobacteria; BioDeg; BioDeg HC
Pasteuria sp	0	0	0	0	Bacilli; Firmicutes
Patulibacter medicamentivorans	0.008	0	0	0	
Patulibacter sp	0.01	0	0	0	Actinobacteria
Pedobacter daechungensis	0	0	0	0	Bacteroidetes; BioDeg; Soil
Pedobacter luteus	0.048	0	0	0	Aerobe; Bacteroidetes; Soil
Pedobacter metabolipauper	0	0	0	0	
Pedobacter sp	0	0	0	0.05	Bacteroidetes; BioDeg; Soil
Pedomicrobium sp	0	0	0	0	Alphaproteobacteria
Pedosphaera parvula	0	0	0	0	Aerobe; Verrucomicrobia
Pedosphaera sp	0	0	0	0	Verrucomicrobia
Pelobacter sp	0	0	0	0	Anaerobe; Deltaproteobacteria; IRB
Pelotomaculum isophthalicicum	0.004	0	0	0	Anaerobe; BioDeg; Clostridia; Firmicutes; Syntroph
Pelotomaculum sp	0.059	0	0	0.016	Anaerobe; BioDeg; Clostridia; Firmicutes; Syntroph
Peredibacter starrii	0	0	0	0	Deltaproteobacteria; Ferm
Perlucidibaca sp	0	0	0	0	Gammaproteobacteria; GHB
Petrobacter sp	0	0	0.002	0	Aerobe; Betaproteobacteria; NRB; Oilfied; Oilfield; Thermophile
Phenylobacterium sp	0.007	0.14	0	0.013	Aerobe; Alphaproteobacteria; GHB
Phormidium sp	0	0	0	0	Cyanobacteria; Oilfield; Phototroph
Phycisphaera sp	0	0	0	0	Planctomycetes
Phyllobacterium sp	0	0	0	0	Alphaproteobacteria
Pigmentiphaga sp	0	0	0	0	Betaproteobacteria
Pirellula sp	0	0	0	0	Planctomycetes
Planctomyces sp	0	0.193	0	0	Planctomycetes
Planococcus sp	0.047	0	0	0	Bacilli; BioDeg; Firmicutes
Polaromonas sp	0	0	0	0	Betaproteobacteria; BioDeg; BioDeg HC

Sequence ID	OG230207-001	OG230402-001	OG230402-002	OG230402-003	OG230402-004	OG230402-005	OG230402-006	OG230402-007	OG230402-008	OG230402-009	OG230402-010	OG230402-011	OG230402-012	OG230402-013	OG230402-014	OG230402-015	OG230402-016	OG230402-017	OG230402-018	OG230402-019	OG230402-020	OG230402-021	OG230508-001	OG230508-002
Well 2244 Sample Description:	Soils Direct	C001 Scale, All, PRD	C001 Scale, All, MPB	C001 Scale, All, IRB	C002 - C005 Scale, PRD	C002 - C005 Scale, MPB	C002 - C005 Scale IRB	C006 - C022 Scale Body, PRD	C006 - C022 Scale Body, MPB	C006 - C022 Scale Body IRB	C006 - C022 Scale Collar, PRD	C006 - C022 Scale Collar, MPB	C006 - C022 Scale Collar IRB	C023 - C034 Scale Body, PRD	C023 - C034 Scale Body, MPB	C023 - C034 Scale Body IRB	C023 - C034 Scale Collar, PRD	C023 - C034 Scale Collar, MPB	C023 - C034 Scale Collar , IRB	9 5/8 ID Scale, PRD	9 5/8 ID Scale, MPB	9 5/8 ID Scale IRB	Pool 20 Annulus Fluids Black Direct	Pool 22 Annulus Fluids Grey Direct
Pontibacillus chungwhensis	0	0	0	0	0	0	0	0	0	0	0	0	0	0	0	0	0	0	0	0	0	0	0.001	0.09
Porphyrobacter sp	0	0	0	0	0	0	0	0	0	0	0	0	0	0	0	0	0	0	0	0	0	0	0	0
Prevotella sp	0	0	0	0	0	0	0	0	0	0	0	0	0	0	0	0	0	0	0	0	0	0	0	0
Prochlorococcus sp	0.004	0	0	0	0	0	0	0	0	0	0	0	0	0	0	0	0	0	0	0	0	0	0	0
Prolixibacter sp	0.791	0	0	0	0	0	0	0	0	0	0	0	0	0	0	0	0	0	0	0	0	0	0.015	0
Promicromonospora sp	0	0	0	0	0	0	0	0	0	0	0	0	0	0	0	0	0	0	0	0	0	0	0.018	0.002
Propionivibrio sp	0	0	0	0	0	0	0	0	0	0	0	0	0	0	0	0	0	0	0	0	0	0	0	0.017
Prosthecobacter algae	0.534	0	0	0	0	0	0	0	0	0	0	0	0	0	0	0	0	0	0	0	0	0	0	0
Prosthecobacter sp	0.319	0	0	0	0	0	0	0	0	0	0	0	0	0	0	0	0	0	0	0	0	0	0	0
Proteiniphilum sp	0	0	0	0	0	0.005	0	0	0	0	0	0	0	0	0	0	0	0	0.019	0	0	0.028	0.033	0
Pseudaminobacter salicylatoxidans	0	0	0	0	0	0	0	0	0	0	0	0	0	0	0	0	0	0	0	0	0	0	0.027	0
Pseudochrobactrum sp	0	0	0.017	0	0	0	0	0.004	0	0.024	0	0.022	0	0	0	0.008	0.009	0	0.003	0	0	0	0.005	0
Pseudofulvimonas gallinarii	0	0	0	0	0	0	0	0	0	0	0	0	0	0	0	0	0	0	0	0	0	0	0	0
Pseudolabrys sp	0.004	0	0	0	0	0	0	0	0	0	0	0	0	0	0	0	0	0	0	0	0	0	0.019	0
Pseudomonas balearica	0	0	0	0	0	0	0	0	0	0	0	0	0	0	0	0	0	0	0	0	0	0	0.007	0
Pseudomonas caeni	0	0	0	0	0	0	0	0	0	0	0	0	0	0	0	0	0	0	0	0	0	0	0	0
Pseudomonas sp	2.178	0	0.013	0	0.004	0.015	0	0	0	0	0	0	0	0.003	0.012	0	0	0	0	32.254	0	0.012	0.096	0.131
Pseudomonas stutzeri	0	0.008	0.004	0.032	0	0	0.004	0	0	0	0.013	0	0.014	0	0	0	0	0.012	0	0.028	0.01	0.179	0.194	0.183
Pseudomonas xinjiangensis	0.019	0	0	0	0	0	0	0	0	0	0	0	0	0	0	0	0	0	0	0	0	0	0	0
Pseudonocardia sp	0.007	0	0	0	0	0	0	0	0	0	0	0	0	0	0	0	0	0	0	0	0	0	0.021	0
Pseudorhodobacter sp	0.116	0	0	0	0	0	0	0	0	0	0	0	0	0	0	0	0	0	0	0	0	0	0	0
Pseudoxanthomonas sp	0.011	0	0	0	0	0	0	0	0	0	0	0	0	0	0	0	0	0	0	0	0	0	0	0.024
Psychrobacter sp	0	0	0	0	0	0	0	0	0	0	0	0	0	0	0	0	0	0	0	0	0	0	0.014	0.002
Ralstonia sp	0.011	0.008	0.017	0	0	0.015	0.013	0.007	0.009	0	0.021	0.015	0	0	0.008	0.076	0	0.036	0	0.014	0.003	0.012	0.22	1.463
Reyranella massiliensis	0.004	0	0	0	0	0	0	0	0	0	0	0	0	0	0	0	0	0	0	0	0	0	0	0
Rhabdobacter roseus	0.005	0	0	0	0	0	0	0	0	0	0	0	0	0	0	0	0	0	0	0	0	0	0	0
Rhizobacter sp	0.002	0	0	0	0	0	0	0	0	0	0	0	0	0	0	0	0	0	0	0	0	0	0	0
Rhizobium sp	0.046	0	0	0	0	0	0	0	0	0	0	0	0	0	0	0	0	0	0	0	0	0	0.034	0.069
Rhodobacter sp	0.002	0	0	0	0	0	0	0	0	0	0	0	0	0	0	0	0	0	0	0	0	0	0.029	0.043
Rhodobium sp	0.004	0	0	0	0	0	0	0	0	0	0	0	0	0	0	0	0	0	0	0	0	0	0	0
Rhodocista sp	0.041	0	0	0	0	0	0	0	0	0	0	0	0	0	0	0	0	0	0	0	0	0	0	0
Rhodococcus sp	0.321	0	0	0	0	0	0	0	0	0	0	0	0	0	0	0	0	0	0	0	0	0	0.037	0.021
Rhodocyclus sp	0	0	0	0	0	0	0	0	0	0	0	0	0	0	0	0	0	0	0	0	0	0	0.001	0.036
Rhodoferax sp	8.123	0	0	0	0	0	0	0	0	0	0	0	0	0	0	0	0	0	0	0	0	0	0	0
Rhodomicrobium sp	0.005	0	0	0	0	0	0	0	0	0	0	0	0	0	0	0	0	0	0	0	0	0	0	0
Rhodonellum psychrophilum	0	0	0	0	0	0	0	0	0	0	0	0	0	0	0	0	0	0	0	0	0	0	0	0
Rhodopirellula sp	0.012	0	0	0	0	0	0	0	0	0	0	0	0	0	0	0	0	0	0	0	0	0	0	0
Rhodoplanes sp	0.046	0	0	0	0	0	0	0	0	0	0	0	0	0	0	0	0	0	0	0	0	0	0.129	0.057
Rhodopseudomonas palustris	0	0	0	0	0	0	0	0	0	0	0	0	0	0	0	0	0	0	0	0	0	0	0.008	0
Rhodopseudomonas sp	0.812	0	0	0	0	0	0	0	0	0	0	0	0	0	0	0	0	0	0	0	0	0	0	0
Rhodovulum sp	0.016	0	0	0	0	0	0	0	0	0	0	0	0	0	0	0	0	0	0	0	0	0	0	0
Rikenella sp	0	0	0	0	0	0	0	0	0	0	0	0	0	0	0	0	0	0	0	0	0	0	0	0
Roseiflexus sp	0.009	0	0	0	0	0	0	0	0	0	0	0	0	0	0	0	0	0	0	0	0	0	0	0
Roseomonas lacus	0.004	0	0	0	0	0	0	0	0	0	0	0	0	0	0	0	0	0	0	0	0	0	0	0
Roseomonas sp	0.016	0	0	0	0	0	0	0	0	0	0	0	0	0	0	0	0	0	0	0	0	0	0.015	0
Rubellimicrobium sp	0.004	0	0	0	0	0	0	0	0	0	0	0	0	0	0	0	0	0	0	0	0	0	0	0
Rubrobacter sp	0.028	0	0	0	0	0	0	0	0	0	0	0	0	0	0	0	0	0	0	0	0	0	0.019	0
Runella sp	0.004	0	0	0	0	0	0	0	0	0	0	0	0	0	0	0	0	0	0	0	0	0	0	0
Saccharibacillus sp	0.104	0	0	0	0	0	0	0	0	0	0	0	0	0	0	0	0	0	0	0	0	0	0	0
Saccharofermentans sp	0	0	0	0	0	0	0	0	0	0	0	0	0	0	0	0	0	0	0	0	0	0	0.043	0
Saccharomonospora sp	0	0	0	0	0	0	0	0	0	0	0	0	0	0	0	0	0	0	0	0	0	0	0	0
Salinicoccus halodurans	0	0	0	0	0	0	0	0	0	0	0	0	0	0	0	0	0	0	0	0	0	0	0.012	0
Sandaracinus sp	0.007	0	0	0	0	0	0	0	0	0	0	0	0	0	0	0	0	0	0	0	0	0	0	0
Sanguibacter sp	0	0	0	0	0	0	0	0	0	0	0	0	0	0	0	0	0	0	0	0	0	0	0	0
Sanguibacter suarezii	0	0	0	0	0	0	0	0	0	0	0	0	0	0	0	0	0	0	0	0	0	0	0.023	0.029
Saprospira sp	0.15	0	0	0	0	0	0	0	0	0	0	0	0	0	0	0	0	0	0	0	0	0	0	0
Schlegelella sp	0	0	0	0	0	0	0	0	0	0	0	0	0	0	0	0	0	0	0	0	0	0	0.004	0.024

Sequence ID	OG230508-003	OG230508-004	OG230508-005	OG230508-006	Selected Traits
Well 2244 Sample Description:	Pool 27 Annulus Fluids Tank Direct	Pool 37 C015 - C022 Scale C Direct	Pool 13 C001B OD Scale All Direct	MG08 C023 - C034 Scale C Direct	Metabolic, Taxonomic, Physiological, Ecological
Pontibacillus chungwhensis	0	0	0	0.021	
Porphyrobacter sp	0	0	0	0.023	Alphaproteobacteria; BioDeg; Phototroph
Prevotella sp	0	0.066	0	0	Bacteroidetes; Gut
Prochlorococcus sp	0	0	0	0	Phototroph
Prolixibacter sp	0	0	0	0.01	Bacteroidetes
Promicromonospora sp	0.012	0	0	0	
Propionivibrio sp	0.004	0	0	0	Betaproteobacteria; BioDeg; BioDeg HC; BioDeg PAH; PerRB
Prosthecobacter algae	0	0	0	0	
Prosthecobacter sp	0	0	0	0	Verrucomicrobia
Proteiniphilum sp	0.01	0	0	0.07	Bacteroidetes; Ferm
Pseudaminobacter salicylatoxidans	0.012	0	0	0	Alphaproteobacteria
Pseudochrobactrum sp	0	0.003	0.022	0	Aerobe; Alphaproteobacteria; GHB
Pseudofulvimonas gallinarii	0	0	0	0.068	
Pseudolabrys sp	0.03	0	0	0	Alphaproteobacteria
Pseudomonas balearica	0	0	0	0	Aerobe; Biofilm; Gammaproteobacteria; GHB; NRB
Pseudomonas caeni	0	0.285	0	0	Denitrifying; Facultative Anaerobe; Gammaproteobacteria; NRB
Pseudomonas sp	0.105	0.011	1.421	0.412	Aerobe; BioDeg; Gammaproteobacteria; GHB; Varies; Versatile; Widespread
Pseudomonas stutzeri	0.117	0	0.009	0.193	Aerobe; BioDeg; BioDeg HC; Gammaproteobacteria; GHB; NRB
Pseudomonas xinjiangensis	0	0	0	0	Aerobe; Gammaproteobacteria; GHB
Pseudonocardia sp	0.021	0	0	0	Actinobacteria
Pseudorhodobacter sp	0	0	0	0	Alphaproteobacteria
Pseudoxanthomonas sp	0	0	0.667	0	BioDeg; BioDeg HC; Gammaproteobacteria
Psychrobacter sp	0.019	0	0	0.005	BioDeg; BioDeg HC; Gammaproteobacteria; Oilfield
Ralstonia sp	0.352	25.559	51.137	0.607	Betaproteobacteria; BioDeg; BioDeg HC
Reyranella massiliensis	0	0	0	0	Unknown
Rhabdobacter roseus	0	0	0	0	
Rhizobacter sp	0	0	0	0	NiF
Rhizobium sp	0.015	0.412	0	0.013	Alphaproteobacteria; NiF
Rhodobacter sp	0	0	2.447	0.029	Alphaproteobacteria; Anaerobe; NiF; Phototroph
Rhodobium sp	0	0	0	0	Alphaproteobacteria
Rhodocista sp	0	0	0	0	Alphaproteobacteria; Phototroph
Rhodococcus sp	0.048	0	0	0	Actinobacteria; BioDeg
Rhodocyclus sp	0.023	0.788	0.28	0	Betaproteobacteria; BioDeg
Rhodoferax sp	0	0	0	0	Betaproteobacteria; IRB
Rhodomicrobium sp	0	0	0	0	Alphaproteobacteria
Rhodonellum psychrophilum	0	0	0	0.036	Bacteroidetes
Rhodopirellula sp	0	0	0	0	Planctomycetes
Rhodoplanes sp	0.097	0	0	0.107	Alphaproteobacteria; Phototroph
Rhodopseudomonas palustris	0	0	0	0	Alphaproteobacteria; Phototroph
Rhodopseudomonas sp	0	0	0	0.044	Alphaproteobacteria; Phototroph
Rhodovulum sp	0	0	0	0	Alphaproteobacteria; Phototroph
Rikenella sp	0	0	2.428	0	Bacteroidetes; Ferm
Roseiflexus sp	0	0	0	0	Chloroflexi
Roseomonas lacus	0	0	0	0	Alphaproteobacteria
Roseomonas sp	0.039	0	0.264	0.026	Alphaproteobacteria; GHB
Rubellimicrobium sp	0	0	0	0	Alphaproteobacteria; GHB
Rubrobacter sp	0	0	0	0	Actinobacteria; BioDeg
Runella sp	0	0	0	0	Bacteroidetes
Saccharibacillus sp	0	0	0	0	
Saccharofermentans sp	0	0	0	0	Clostridia; Firmicutes
Saccharomonospora sp	0.017	0	0	0	Actinobacteria
Salinicoccus halodurans	0	0	0	0.055	Bacilli; Firmicutes
Sandaracinus sp	0	0	0	0	Deltaproteobacteria
Sanguibacter sp	0	0	0	0.034	Actinobacteria
Sanguibacter suarezii	0	0	0	0	
Saprospira sp	0	0	0	0	Bacterial Predator; Bacteroidetes
Schlegelella sp	0.008	0	0	0.018	Betaproteobacteria; Biofilm; Thermophile

Sequence ID	OG230207-001	OG230402-001	OG230402-002	OG230402-003	OG230402-004	OG230402-005	OG230402-006	OG230402-007	OG230402-008	OG230402-009	OG230402-010	OG230402-011	OG230402-012	OG230402-013	OG230402-014	OG230402-015	OG230402-016	OG230402-017	OG230402-018	OG230402-019	OG230402-020	OG230402-021	OG230508-001	OG230508-002
Well 2244 Sample Description:	Soils Direct	C001 Scale, All, PRD	C001 Scale, All, MPB	C001 Scale, All, IRB	C002 - C005 Scale, PRD	C002 - C005 Scale, MPB	C002 - C005 Scale IRB	C006 - C022 Scale Body, PRD	C006 - C022 Scale Body, MPB	C006 - C022 Scale Body IRB	C006 - C022 Scale Collar, PRD	C006 - C022 Scale Collar, MPB	C006 - C022 Scale Collar IRB	C023 - C034 Scale Body, PRD	C023 - C034 Scale Body, MPB	C023 - C034 Scale Body IRB	C023 - C034 Scale Collar, PRD	C023 - C034 Scale Collar, MPB	C023 - C034 Scale Collar , IRB	9 5/8 ID Scale, PRD	9 5/8 ID Scale, MPB	9 5/8 ID Scale IRB	Pool 20 Annulus Fluids Black Direct	Pool 22 Annulus Fluids Grey Direct
Sedimentibacter sp	0	0	3.732	7.227	0	0	0.78	0	0	0	0	0	1.355	0	0	0	0	0	0	0	0	0	0.019	0.247
Sediminibacterium sp	0.002	0	0	0	0	0	0	0	0	0	0	0	0	0	0	0	0	0	0	0	0	0	0	0
Segetibacter sp	0.002	0	0	0	0	0	0	0	0	0	0	0	0	0	0	0	0	0	0	0	0	0	0	0
Selenihalanaerobacter shriftii	0	0	0	0	0	0	0	0	0	0	0	0	0	0	0	0	0	0	0	0	0	0	0.021	0
Serratia sp	0	0	0	0	0	0	0	0	0	0	0	0	0	0	0	0	0	0	0	0	0	0	0	0.038
Shewanella sp	0.079	0	0	0	0	0	0	0	0	0	0	0	0	0	0	0	0	0	0	0	0	0	0.026	0
Simplicispira psychrophila	0.252	0	0	0	0	0	0	0	0	0	0	0	0	0	0	0	0	0	0	0	0	0	0	0
Simplicispira sp	0	0	0	0	0	0	0	0	0	0	0	0	0	0	0	0	0	0	0	0	0	0	0	0
Sinorhizobium sp	0.002	0	0	0	0	0	0	0	0	0	0	0	0	0	0	0	0	0	0	0	0	0	0	0
Skermanella sp	0.012	0	0	0	0	0	0	0	0	0	0	0	0	0	0	0	0	0	0	0	0	0	0	0
Skermanella stibiiresistens	0.002	0	0	0	0	0	0	0	0	0	0	0	0	0	0	0	0	0	0	0	0	0	0	0
Smaragdicoccus niigatensis	0.002	0	0	0	0	0	0	0	0	0	0	0	0	0	0	0	0	0	0	0	0	0	0	0
Soehngenia sp	0	0	0	0.013	0	0	2.392	0	0	0	0	0.004	0.004	0	0	0	0	0.264	0.012	0	36.226	0.02	0.866	1.028
Solirubrobacter sp	0.009	0	0	0	0	0	0	0	0	0	0	0	0	0	0	0	0	0	0	0	0	0	0.014	0
Sphaerobacter sp	0.004	0	0	0	0	0	0	0	0	0	0	0	0	0	0	0	0	0	0	0	0	0	0.019	0.026
Sphingobacterium sp	0.048	0	0	0	0	0	0	0	0	0	0	0	0	0	0	0	0	0	0	0	0	0	0.014	0.119
Sphingobium sp	0.345	0	0	0	0	0	0	0	0	0	0	0	0	0	0	0	0	0	0	0	0	0	0	0
Sphingobium yanoikuyae	0	0	0	0	0	0	0	0	0	0	0	0	0	0	0	0	0	0	0	0	0	0	0	0
Sphingomonas sp	0.479	0	0	0	0.007	0.005	0	0	0	0	0	0	0	0	0	0	0	0	0.003	0	0	0.004	0.038	0
Sphingopyxis sp	1.186	0	0	0	0	0	0	0	0	0	0	0	0	0	0	0	0	0	0	0	0	0	0.016	0
Sphingopyxis witflariensis	0.03	0	0	0	0	0	0	0	0	0	0	0	0	0	0	0	0	0	0	0	0	0	0	0
Spirochaeta sp	0	0	0	0.025	0	0.005	0.039	0	0.158	0.118	0	0	0.004	0	0	0.068	0	0	0.009	0	0	0.048	0.022	0.005
Spirosoma radiotolerans	0.002	0	0	0	0	0	0	0	0	0	0	0	0	0	0	0	0	0	0	0	0	0	0	0
Sporacetigenium mesophilum	0	0	0	1.527	0	0	0	0	0	0	0	0	0.674	0	0	3.031	0	0	0	0	0	0	0.008	0
Sporacetigenium sp	0.004	0	0	0	0	0	0	0	0	0	0	0	0	0	0	0	0	0	0	0	0	0	0	0
Sporobacter sp	0.004	0	0	0	0	0	0	0	0	0	0	0	0	0	0	0	0	0	0	0	0	0	0.004	0
Sporosalibacterium faouarense	0	0	0	0	0	0	0	0	0	0	0	0	0	0	0	0	0	0	0	0	0	0	0.011	0
Sporosarcina soli	0	0	0	0	0	0	0	0	0	0	0	0	0	0	0	0	0	0	0	0	0	0	0.005	0.057
Sporosarcina sp	0	0	0	0	0	0	0	0	0	0	0	0	0	0	0	0	0	0	0	0	0	0	0.045	0
Staphylococcus sciuri	0	2.154	0	0	0.552	0.005	0	0.004	0	0	1.043	0	0.004	0.098	0	0	1.219	0.006	0	0.004	0	0	0	0
Staphylococcus sp	0	0	0.009	0	0	0.04	0	0	0	0	0	0.011	0	0	0.008	0	0	0	0.003	0	0	0	0	0
Starkeya sp	0	0	0	0	0	0	0	0	0	0	0	0	0	0	0	0	0	0	0	0	0	0	0.143	0
Stenotrophomonas maltophilia	0	0	0	0	0	0	0	0	0	0	0	0	0	0	0	0	0	0	0	0	0	0	0	0
Stenotrophomonas sp	0	0	0	0	0	0	0	0	0	0	0	0	0	0	0	0	0	0	0	0	0	0	0	0.09
Steroidobacter agariperforans	0.002	0	0	0	0	0	0	0	0	0	0	0	0	0	0	0	0	0	0	0	0	0	0	0
Steroidobacter sp	0.203	0	0	0	0	0	0	0	0	0	0	0	0	0	0	0	0	0	0	0	0	0	0	0
Sterolibacterium sp	0.026	0	0	0	0	0	0	0	0	0	0	0	0	0	0	0	0	0	0	0	0	0	0	0
Streptococcus sp	0	0	0	0	0	0	0	0	0	0	0	0	0	0	0	0	0	0	0	0	0	0	0	0
Streptococcus thermophilus	0	0	0	0	0	0	0	0	0	0	0	0	0	0	0	0	0	0	0	0	0	0	0	0
Streptomyces sp	0.005	0	0	0	0	0	0	0	0	0	0	0	0	0	0	0	0	0	0	0	0	0	0.043	0
Sulfuricaulis limicola	0.002	0	0	0	0	0	0	0	0	0	0	0	0	0	0	0	0	0	0	0	0	0	0	0
Sulfurifustis variabilis	0.002	0	0	0	0	0	0	0	0	0	0	0	0	0	0	0	0	0	0	0	0	0	0	0
Sulfuritalea sp	1.179	0	0	0	0	0	0	0	0	0	0	0	0	0	0	0	0	0	0	0	0	0	0	0
Sulfurospirillum cavolei	0	0	0	0	0	0	0	0	0	0	0	0	0	0	0	0	0	0	0	0	0	0	0.026	0.029
Sulfurospirillum deleyianum	0	0	0.004	0	0	0	0	0	0	0	0	0.015	0	0	0	0	0	0.006	0	0.007	0	0.004	0	0
Sulfurospirillum sp	0	0	0	0	0.022	0.005	0	0.025	0.009	0	0	0	0.004	0.024	0	0.042	0.005	0	0.009	0	0	0.024	0	0.019
Sunxiuqinia sp	1.422	0	0	0	0	0	0	0	0	0	0	0	0	0	0	0	0	0	0	0	0	0	0	0.007
Symbiobacterium sp	0	0	0	0	0	0	0	0	0	0	0	0	0	0	0	0	0	0	0	0	0	0	0	0
Synechococcus sp	0.005	0	0	0	0	0	0	0	0	0	0	0	0	0	0	0	0	0	0	0	0	0	0.004	0
Syntrophobacter sp	0.014	0	0	0	0	0	0	0	0	0	0	0	0	0	0	0	0	0	0	0	0	0	0	0
Syntrophobotulus sp	0	0	0	0	0	0	0	0	0	0	0	0	0	0	0	0	0	0	0	0	0	0	0	0
Syntrophomonas sp	0.021	0	0	0	0	0	0	0	0	0	0	0	0	0	0	0	0	0	0	0	0	0	0	0
Syntrophomonas wolfei	0	0	0	0	0	0	0	0	0	0	0	0	0	0	0	0	0	0	0	0	0	0	0.007	0.074
Syntrophomonas zehnderi	0	0	0	0	0	0	0	0	0	0	0	0	0	0	0	0.013	0	0	0	0	0	0	0.003	0
Syntrophorhabdus sp	0	0	0	0	0	0	0	0	0	0	0	0	0	0	0	0	0	0	0	0	0	0	0	0
Syntrophus sp	0.019	0	0	0	0	0	0	0	0	0	0	0	0	0	0	0	0	0	0	0	0	0	0	0
Terrabacter sp	0.002	0	0	0	0	0	0	0	0	0	0	0	0	0	0	0	0	0	0	0	0	0	0	0

Sequence ID	OG2305008-003	OG2305008-004	OG2305008-005	OG2305008-006	Selected Traits
Well 2244 Sample Description:	Pool 27 Annulus Fluids Tank Direct	Pool 37 C015 - C022 Scale C Direct	Pool 13 C001B OD Scale All Direct	MG08 C023 - C034 Scale C Direct	Metabolic, Taxonomic, Physiological, Ecological
Sedimentibacter sp	0.004	0	0	0.055	BioDeg
Sediminibacterium sp	0	0	0	0	Bacteroidetes; GHB
Segetibacter sp	0	0	0	0	Bacteroidetes
Selenihalanaerobacter shriftii	0.05	0	0	0.209	Clostridia; Firmicutes
Serratia sp	0.001	0	0	0.029	Biofilm; Gammaproteobacteria; MIC
Shewanella sp	0.044	0	0	0.104	Facultative Anaerobe; Gammaproteobacteria; IRB; Sulfidogen; TRB
Simplicispira psychrophila	0	0	0	0	Betaproteobacteria
Simplicispira sp	0.007	0.003	0.978	0	Betaproteobacteria; HOX; Microaerophile
Sinorhizobium sp	0	0	0	0	Alphaproteobacteria; NiF
Skermanella sp	0	0	0	0	Alphaproteobacteria
Skermanella stibiiresistens	0	0	0	0	Alphaproteobacteria
Smaragdicoccus niigatensis	0	0	0	0	
Soehngenia sp	1.044	0	0	0.281	Ferm; Firmicutes; Tissierellia
Solirubrobacter sp	0.023	0	0	0	Actinobacteria
Sphaerobacter sp	0	0	0	0.01	Chloroflexi; Wastewater
Sphingobacterium sp	0.028	0	0	0.281	Aerobe; Bacteroidetes; BioDeg; GHB
Sphingobium sp	0.017	0	0	0	Aerobe; Alphaproteobacteria; BioDeg; BioDeg Herbacides; Soil
Sphingobium yanoikuyae	0	0	0	0.016	Aerobe; Alphaproteobacteria; BioDeg; BioDeg Herbacides; Soil
Sphingomonas sp	0	0.597	0	0.021	Aerobe; Alphaproteobacteria; BioDeg; BioDeg PAH; GHB; Marine
Sphingopyxis sp	0	0	0	0	Aerobe; Alphaproteobacteria; BioDeg; BioDeg HC
Sphingopyxis witflariensis	0	0	0	0	Aerobe; Alphaproteobacteria
Spirochaeta sp	0.048	0	0	0.096	Anaerobe; Ferm; H2; H2S resistant; Halophile; Spirochaetes; Sulfidogen; Thermophile; TRB
Spirosoma radiotolerans	0	0	0	0	
Sporacetigenium mesophilum	0.008	0	0	0	APB; Clostridia; Ferm; Firmicutes
Sporacetigenium sp	0	0	0	0	Alkaliphile; Anaerobe; Anaerobic Digester; Ferm; WWTP
Sporobacter sp	0.003	0	0	0	Clostridia; Firmicutes
Sporosalibacterium faouarense	0	0	0	0	Clostridia; Deep Subsurface; Firmicutes
Sporosarcina soli	0.011	0	0	0	Bacilli; Firmicutes
Sporosarcina sp	0.03	0	0	0	Bacilli; Firmicutes
Staphylococcus sciuri	0	0	0	0	Bacilli; Firmicutes; Skin
Staphylococcus sp	0	0	0	0	Bacilli; Firmicutes; Skin
Starkeya sp	0.076	0	0	0.013	Alphaproteobacteria
Stenotrophomonas maltophilia	0	0.579	0	0	Aerobe; BioDeg HC; Gammaproteobacteria; Sludge
Stenotrophomonas sp	0	0.248	0	0	Aerobe; BioDeg HC; Gammaproteobacteria; Sludge
Steroidobacter agariperforans	0	0	0	0	
Steroidobacter sp	0	0	0	0	BioDeg; Gammaproteobacteria
Sterolibacterium sp	0	0	0	0	Betaproteobacteria; BioDeg; NRB
Streptococcus sp	0.199	0	0	0	APB; Ferm; Firmicutes; LAB; Lactobacillales
Streptococcus thermophilus	0.007	0	0	0	APB; Ferm; Firmicutes; LAB; Lactobacillales
Streptomyces sp	0.029	0	0	0	Actinobacteria; Antibiotic Producing; BioDeg; Filamentous; Soil; Spore
Sulfuricaulis limicola	0	0	0	0	Acidophile; Aerobe; APB; Gammaproteobacteria; SOX
Sulfurifustis variabilis	0	0	0	0	
Sulfuritalea sp	0	0	0	0	Betaproteobacteria; Facultative Anaerobe; NRB; NRSOB; SOB
Sulfurospirillum cavolei	0.07	0	0	0.219	Epsilonproteobacteria; Facultative Anaerobe; NRB; NRSOB; Oilfield; SOB
Sulfurospirillum deleyianum	0	0	0	0	Epsilonproteobacteria; Facultative Anaerobe; NRB; NRSOB; Oilfield; SOB
Sulfurospirillum sp	0.03	0	0.016	0	Epsilonproteobacteria; Facultative Anaerobe; NRB; NRSOB; Oilfield; SOB
Sunxiuqinia sp	0	0	0	0	Bacteroidetes; GHB
Symbiobacterium sp	0.007	0	0	0.013	Clostridia; Firmicutes
Synechococcus sp	0	0	0	0	Phototroph
Syntrophobacter sp	0	0	0	0	BioDeg; BioDeg HC; Deltaproteobacteria; Methanogen Syntroph; SRB; Sulfidogen
Syntrophobotulus sp	0	0	0	0.005	Anaerobe; Clostridia; Ferm; Firmicutes
Syntrophomonas sp	0	0	0	0	Anaerobe; Clostridia; Firmicutes; Methanogen Syntroph; Sludge; Syntroph
Syntrophomonas wolfei	0	0	0	0	Anaerobe; Clostridia; Firmicutes; Methanogen Syntroph; Sludge; Syntroph
Syntrophomonas zehnderi	0	0	0	0	Anaerobe; Clostridia; Firmicutes; Methanogen Syntroph; Sludge; Syntroph
Syntrophorhabdus sp	0	0	0	0.018	Anaerobe; BioDeg HC; Deltaproteobacteria; Methanogen Syntroph; Sludge; Syntroph
Syntrophus sp	0	0	0	0	Anaerobe; BioDeg; BioDeg HC; Deltaproteobacteria; Sludge; Syntroph; Thermophile
Terrabacter sp	0	0	0	0	Actinobacteria; Aerobe; Air

Appendix B. Well 2244 Soil, Scale, Annulus Fluid Microbial Population
16S Amplicon Metagenomic Analysis
Samples collected March 2023

Sequence ID	OG230207-001	OG230402-001	OG230402-002	OG230402-003	OG230402-004	OG230402-005	OG230402-006	OG230402-007	OG230402-008	OG230402-009	OG230402-010	OG230402-011	OG230402-012	OG230402-013	OG230402-014	OG230402-015	OG230402-016	OG230402-017	OG230402-018	OG230402-019	OG230402-020	OG230402-021	OG230508-001	OG230508-002
Well 2244 Sample Description:	Soils Direct	C001 Scale, All, PRD	C001 Scale, All, MPB	C001 Scale, All, IRB	C002 - C005 Scale, PRD	C002 - C005 Scale, MPB	C002 - C005 Scale IRB	C006 - C022 Scale Body, PRD	C006 - C022 Scale Body, MPB	C006 - C022 Scale Body IRB	C006 - C022 Scale Collar, PRD	C006 - C022 Scale Collar, MPB	C006 - C022 Scale Collar IRB	C023 - C034 Scale Body, PRD	C023 - C034 Scale Body, MPB	C023 - C034 Scale Body IRB	C023 - C034 Scale Collar, PRD	C023 - C034 Scale Collar, MPB	C023 - C034 Scale Collar , IRB	9 5/8 ID Scale, PRD	9 5/8 ID Scale, MPB	9 5/8 ID Scale IRB	Pool 20 Annulus Fluids Black Direct	Pool 22 Annulus Fluids Grey Direct
Terriglobus sp	0.005	0	0	0	0	0	0	0	0	0	0	0	0	0	0	0	0	0	0	0	0	0	0	0
Terrimicrobium sacchariphilum	0	0	0	0	0	0	0	0	0	0	0	0	0	0	0	0	0	0	0	0	0	0	0	0
Terrimonas sp	0.025	0	0	0	0	0	0	0	0	0	0	0	0	0	0	0	0	0	0	0	0	0	0	0
Tetrasphaera sp	0.018	0	0	0	0	0	0	0	0	0	0	0	0	0	0	0	0	0	0	0	0	0	0	0
Thalassobacillus sp	0	0.048	0.022	0.013	0.07	0.064	0.026	0	0.047	0	0	0.044	0.004	0	0.012	0.017	0.005	0	0.012	0.004	0.01	0.004	0	0
Thauera sp	0	0	0	0	0	0	0	0	0	0	0	0	0	0	0	0	0	0	0	0	0	0	0.081	0.014
Thermacetogenium sp	0	0	0	0	0	0	0	0	0	0	0	0	0	0	0	0	0	0	0	0	0	0	0.128	0.112
Thermincola sp	0	0	0	0	0	0	0	0	0	0	0	0	0	0	0	0.013	0	0	0	0	0	0	0.236	0.083
Thermoanaerobacter italicus	0	0	0	0	0	0	0	0	0	0	0	0	0	0	0	0	0	0	0	0	0	0	0.049	0
Thermoanaerobacter sp	0	0	0	0	0	0	0	0	0	0	0	0	0	0	0	0	0	0	0	0	0	0	0.063	0
Thermoanaerobacterium saccharolyticum	0	0	0	0	0	0	0	0	0.043	0	0	0	0	0	0	0	0	0	0	0	0	0	0.03	0
Thermoanaerobacterium thermosaccharolyti	0	0	0	0	0	0	0	0	0	0	0	0	0	0	0	0	0	0	0	0	0	0	0.014	0
Thermomonas sp	0.106	0	0	0	0	0	0	0	0	0	0	0	0	0	0	0	0	0	0	0	0	0	0	0
Thiobacillus sp	0.033	0	0	0	0	0	0	0	0	0	0	0	0	0	0	0	0	0	0	0	0	0	0	0
Thioclava sp	0	0	0	0	0.004	0.005	0	0	0	0	0	0	0	0	0	0	0	0	0	0	0	0.004	0	0
Thioprofundum hispidum	0	0	0	0	0	0	0	0	0	0	0	0	0	0	0	0	0	0	0	0	0	0	0.004	0
Thiorhodospira sp	0.021	0	0	0	0	0	0	0	0	0	0	0	0	0	0	0	0	0	0	0	0	0	0	0
Tissierella sp	0	0	3.188	0.057	0	0	0	0	0	0.047	0	2.378	0	0.003	0	1.057	0	0	0	0	0	0	0.008	0
Tolumonas sp	0	0	0	0	0	0	0	0	0	0	0	0	0	0	0	0	0	0	0	0	0	0	0	0
Trichococcus collinsii	0	0	0.004	0.006	0	0	0.047	0	0	0.024	0	0	0.007	0	0	0.013	0	0	0.05	0	0	0.095	0	0
Trichococcus flocculiformis	0	0	0.157	0	0	0.227	0.03	0	0.004	0	0	0.074	0.021	0	0	0.089	0	0	0.214	0	0.007	0.008	0	0
Trichococcus sp	0.3	0.04	10.556	0.082	0.099	20.831	17.47	0.102	0	0.071	0.017	20.263	83.757	0.419	0.025	33.83	9.977	0.042	83.698	29.307	25.294	55.289	0.33	4.199
Tumeriella parva	0	0	0	0	0	0	0	0	0	0	0	0	0	0	0	0	0	0	0	0	0	0	0	0
Unclassified	29.793	0.032	6.976	14.832	0.113	24.831	1.862	0.042	70.528	3.97	0.2	8.397	3.328	0.024	19.619	12.491	0.052	67.996	4.102	0.221	17.505	5.84	42.891	21.561
Uncultured bacterium	0.046	0	0	0	0	0	0	0	0	0	0	0	0	0	0	0	0	0	0	0	0	0	0	0
Variovorax sp	0.03	0	0	0	0	0	0	0	0	0	0	0	0	0	0	0	0	0	0	0	0	0	0	0
Veillonella sp	0	0	0	0	0	0	0	0	0	0	0	0	0	0	0	0	0	0	0	0	0	0	0	0
Verrucomicrobium sp	0.333	0	0	0	0	0	0	0	0	0	0	0	0	0	0	0	0	0	0	0	0	0	0	0
Verrucosispora sp	0	0	0	0	0	0	0	0	0	0	0	0	0	0	0	0	0	0	0	0	0	0	0.168	0.112
Virgibacillus halotolerans	0	0	0	0	0	0	0	0	0	0	0	0	0	0	0	0	0	0	0	0	0	0	0	0
Virgibacillus sp	0	0	0	0	0	0	0	0	0	0	0	0	0	0	0	0	0	0	0	0	0	0	0.021	0
Vulcanibacillus modesticaldus	0	0	0	0	0	0	0	0	0	0	0	0	0	0	0	0	0	0	0	0	0	0	0.015	0
Vulgatibacter incomptus	0	0	0	0	0	0	0	0	0	0	0	0	0	0	0	0	0	0	0	0	0	0	0.005	0
Williamsia sp	0.005	0	0	0	0	0	0	0	0	0	0	0	0	0	0	0	0	0	0	0	0	0	0	0
Woodsholea maritima	0.005	0	0	0	0	0	0	0	0	0	0	0	0	0	0	0	0	0	0	0	0	0	0	0
Xanthobacter autotrophicus	0	0	0	0	0	0	0	0	0	0	0	0	0	0	0	0	0	0	0	0	0	0	0	0.012
Xanthobacter sp	0	0	0	0	0	0	0	0	0	0	0	0	0	0	0	0	0	0	0	0	0	0	0.098	0.067
Xanthomonas sp	0.004	0	0	0	0	0	0	0	0	0	0	0	0	0	0	0	0	0	0	0	0	0	0	0
Yaniella sp	0	0	0	0	0	0	0	0	0	0	0	0	0	0	0	0	0	0	0	0	0	0	0.014	0
Youngiibacter fragilis	0	0	0	0	0	0	0	0	0	0	0	0	0	0	0	0	0	0	0	0	0	1.209	0	0
Zavarzinella sp	0.014	0	0	0	0	0	0	0	0	0	0	0	0	0	0	0	0	0	0	0	0	0	0	0
Zoogloea sp	0	0.008	0.017	0	0	0	0.004	0.007	0	0	0.004	0	0	0	0.008	0	0.005	0.012	0	0	0	0	0.011	0.033

Appendix B. Well 2244 Soil, Scale, Annulus Fluid Microbial Population
16S Amplicon Metagenomic Analysis
Samples collected March 2023

Sequence ID	OG230508-003	OG230508-004	OG230508-005	OG230508-006	Selected Traits
Well 2244 Sample Description:	Pool 27 Annulus Fluids Tank Direct	Pool 37 C015 - C022 Scale C Direct	Pool 13 C001B OD Scale All Direct	MG08 C023 - C034 Scale C Direct	Metabolic, Taxonomic, Physiological, Ecological
Terriglobus sp	0	0	0	0	Acidobacteria; GHB
Terrimicrobium sacchariphilum	0	0	0	0.018	Anaerobe; Ferm; GHB; Verrucomicrobia
Terrimonas sp	0	0.74	0	0	Aerobe; Bacteroidetes; GHB
Tetrasphaera sp	0	0	0	0	Actinobacteria
Thalassobacillus sp	0	0	0	0	Bacilli; Firmicutes
Thauera sp	0.026	1.002	0	0.086	Betaproteobacteria; BioDeg; NRB
Thermacetogenium sp	0.065	0	0	0.026	Acetate Oxidizing; Anaerobe; Clostridia; Ferm; Firmicutes; Spore; Syntroph; Thermophile
Thermincola sp	0.413	0	0	0.237	
Thermoanaerobacter italicus	0	0	0	0	Anaerobe; Clostridia; Ethanologenic; Ferm; Firmicutes; Sulfidogen; Thermophile; TRB
Thermoanaerobacter sp	0.048	0	0	0	Anaerobe; Clostridia; Ethanologenic; Ferm; Firmicutes; Sulfidogen; Thermophile; TRB
Thermoanaerobacterium saccharolyticum	0.004	0	0	0	Anaerobe; APB; Clostridia; Firmicutes; NRB; Spore; Sulfidogen; Thermophile; TRB
Thermoanaerobacterium thermosaccharolyti	0	0	0	0	Anaerobe; APB; Clostridia; Firmicutes; NRB; Spore; Sulfidogen; Thermophile; TRB
Thermomonas sp	0	0	0	0	Aerobe; Gammaproteobacteria; GHB
Thiobacillus sp	0	0	0	0	Betaproteobacteria; NRB; NRSOB; SOB
Thioclava sp	0	0	0	0	Alphaproteobacteria; Facultative autotroph; SOB; Sulfur Vent
Thioprofundum hispidum	0.007	0	0	0	
Thiorhodospira sp	0	0	0	0	Anaerobe; Gammaproteobacteria; Phototroph; Purple Sulfur Bacteria
Tissierella sp	0	0	0	0	Anaerobe; Clostridia; Ferm; Firmicutes; Sludge
Tolumonas sp	0	0	0	0.029	Facultative Anaerobe; Ferm; Gammaproteobacteria; Toluene Production
Trichococcus collinsii	0	0	0	0	Activated Sludge; APB; Facultative Anaerobe; Ferm; Filamentous; Firmicutes; Lactobacillales; WWTP
Trichococcus flocculiformis	0	0	0	0	Activated Sludge; APB; Facultative Anaerobe; Ferm; Filamentous; Firmicutes; Lactobacillales; WWTP
Trichococcus sp	0.57	0.005	0.002	1.449	Activated Sludge; APB; Facultative Anaerobe; Ferm; Filamentous; Firmicutes; Lactobacillales; WWTP
Tumeriella parva	0	0	2.662	0	
Unclassified	42.485	30.568	16.756	24.59	Polyphyletic; Unknown; Varies
Uncultured bacterium	0	0	0	0	Unknown
Variovorax sp	0	0	0	0	Betaproteobacteria; BioDeg; BioDeg HC; BioDeg Phenol
Veillonella sp	0.007	0	0	0	Anaerobe; Ferm; Firmicutes; Negativicutes
Verrucomicrobium sp	0	0	0	0	Ferm; Verrucomicrobia
Verrucosispora sp	0.188	0.011	0	0	Actinobacteria
Virgibacillus halotolerans	0	0	0	0.021	
Virgibacillus sp	0.014	0	0	0	Bacilli; Firmicutes; Halophile; Spore
Vulcanibacillus modesticaldus	0.022	0	0	0	Bacilli; Firmicutes; NRB; Thermophile
Vulgatibacter incomptus	0	0	0	0	
Williamsia sp	0	0	0	0	Actinobacteria; Filamentous; Foam
Woodsholea maritima	0	0	0	0	Alphaproteobacteria
Xanthobacter autotrophicus	0.012	0	0	0	Alphaproteobacteria
Xanthobacter sp	0.001	1.438	0	0.047	Alphaproteobacteria
Xanthomonas sp	0	0	0	0	Aerobe; Biofilm; EPS; Gammaproteobacteria; Plant Pathogen
Yaniella sp	0	0	0	0	Actinobacteria
Youngiibacter fragilis	0	0	0	0	Anaerobe; Clostridia; Ferm; GHB; Methane Production Well; Methanogen Community Member
Zavarzinella sp	0	0	0	0	
Zoogloea sp	0.007	3.172	2.434	0	Betaproteobacteria; BioDeg; BioDeg HC; Biofilm; Facultative Anaerobe; Floc; Oilfield

Appendix B. Complete list of all organisms identified in well 2244 samples

Values are % of population. Yellow are > 10%, Green are 1 - 10%, Gray are 0%.

Under "Select Traits of Interest" sulfidogens are highlighted in red, archaea in yellow, IRB in green.

Trait Abbreviations: Acetogen (Acetate producing, via fermentation or CO2 fixation), Acidophile (Growth at low pH), Aerobe (Oxygen requiring), Alkaliphile (Growth at high pH), Anaerobe (Grows only under anoxic conditions), AOB (Ammonia Oxidizing Bacteria), AOX (Ammonia Oxidizing Bacteria), APB (Acid-Producing Bacteria), BioDeg (Biodegrading unusual substrates, catabolically versatile, with the ability to utilize a wide range of unusual substrates, such as pyridine, herbicides, chlorinated biphenyls, and oil), BioDeg HC (Petroleum Hydrocarbon-Degrading Bacteria), BioDeg PAH (Polyaromatic Hydrocarbon-Degrading Bacteria), BioDeg TCE (Trichloroethylene Degrading Bacteria), Biofilm (Biofilm Member), CrIV RB (hexavalent chromium reducing bacteria), Diverse (Exhibit metabolic diversity), EPS (Exopolysaccharide), Ethanologenic (Ethanol producing), Facultative (Grows under both aerobic and anaerobic conditions), FAP (Filamentous Anoxygenic Phototroph), Ferm (Fermentative), Filamentous (Forms long filaments), Floc (Wastewater floc-associated), GHB (General Heterotrophic Bacteria), Halophile (Salt tolerant), IRB (Iron-Reducing Bacterial), ISOX (inorganic sulfur oxidizing), LAB (Lactic Acid Bacteria), Methanogen (Archaea that produce methane), Methylotroph (Utilize methane, methanol, and other simple carbons), MIC (Microbial-Influenced Corrosion), NiF (Nitrogen Fixing), NOB (Nitrite Oxidizing Bacteria), NRB (Nitrate-Reducing Bacteria), NRSOB (Nitrate-Reducing Sulfur-Oxidizing Bacteria), Oilfield (Found in oilfield samples), Oligotroph (Growth under low nutrient conditions), OX (Oxidizing Bacteria), Pathogen (Disease-causing), PerRB (Perchlorate-Reducing Bacteria), PhotoT (Phototrophic, Photosynthetic), Phototroph (Phototrophic, Photosynthetic), Sludge (Component of WWTP Sludges), SOB (Sulfur-Oxidizing Bacteria), Soil (Found in soil), SOX (Sulfur-Oxidizing Bacteria), Spore (Spore-forming bacteria), SRB (SRB, Sulfate-Reducing Bacteria), Sulfidogen (Hydrogen Sulfide Producing (includes SRB, TRB, SuRB and some peptide fermentation bacteria),), SuRB (Sulfur Reducing Bacteria), Syntroph (Mutualistic sharing of metabolic byproducts), Thermophile (Growth above 50oC), TRB (Thiosulfate Reducing Bacteria), Wastewater (Wastewater Associated), WWTP (Wastewater Treatment Plant),

Sample descriptions that include PRD, MPB, and IRB are the results of sequencing DNA isolated from cultures established from the indicated samples in the indicated media.

All other data sets are from DNA isolated directly from the raw sample

Appendix C: Methods

Sample Collection

In all, 11 sets of samples, encompassing 109 individual samples, were collected between Feb 16, 2023 and April 3 2023. Sampling locations were sites within the Rager Mountain gas storage facility, Equitrans Midstream Corp, 555 Dishong Mountain Road, Johnstown PA 15906 USA. Sites within the facility included wells 2244, 2248, and 2251. Most samples were collected from well 2244 as it was the well involved in the failure event. Samples were predominantly of two types: solid scale material scraped from the outer diameter surface (OD) of the 7" casing joints and liquid annular fluids pumped from the annulus of the 7" and 9 5/8" casing. Additional samples included ID materials from 9 5/8 casing, soil from the surrounding area, grease on casing surface, material from the ID of the well head master valve and tree, as well as liquids collected in the compressor station and a pond. For scale samples, 2" disposable plastic putty knives were used to debride surface scale and solids, care was taken to use a new putty knife for each sample. Solids were stored in sterile Whirl-Pak bags (18 oz, 4.5" X 9"). Liquid samples were collected and stored in 500 ml HDPE Nalgene bottles. After collection, all samples were stored in a refrigerator prior to overnight shipping from Pennsylvania to Texas for analysis.

MPN Analysis

For MPN analysis, each sample is initially diluted in 20 ml of sterile PBS. The quantity of starting material added to the initial dilution varied from sample to sample, depending on sample type and amount of available sample, and the variation in initial sample used is corrected for when determining the dilution factor to adjust the final values. From these 20 ml initial dilutions, 1 ml is used to inoculate each of the primary dilution series bottles, 3 per media type. Each primary dilution was subject to eightfold serial dilution. Selective media used for this project were Modified Postgate's B Broth (MPB) for the growth of Sulfate-Reducing Bacteria, Phenol Dextrose Red Broth (PRD) for the enumeration of acid-producing bacteria (APB) and general heterotrophic bacteria (GHB), and Iron-Reducing Broth (IRB) for the enumeration of iron-reducing bacteria. Dilutions were carried out in triplicate. All medias were at 1% salinity. Incubations were conducted at 30^{o}C. Growth was assayed every 7 days, for a total of 28 days. Growth was compared to the FDA Bacterial Analytical Manual appendix 2 to determine the most probable number. It should be noted that the MPN is an estimate of growth units or colony-forming units and not individual bacterial cells.

For the samples from Rager Mountain, in order set up MPN analysis, a measured amount (g or ml) of each sample was first suspended in 20 ml of sterile PBS buffer and vortexed vigorously for 1 minute. Heavy solids were allowed to gravity settle. 1 ml of this initial dilution was used to inoculate each of the first bottles in the dilution series, creating the initial inoculations, with each bottle containing 10 ml such that each dilution is 10X. The initial inoculations were then subject to 7 additional serial 10-fold dilutions as such: 1 ml was transferred to the next media bottle in the series, shaken to mix, then a new syringe was used to transfer 1 ml into the next media bottle in the series, etc, until 8 media bottles were inoculated in the dilution series. Each dilution series was set up in triplicate (3 times) and cultures are incubated for 28 days at 30 ^{o}C to allow for microbial growth). The presence of growth is recorded every week for 4 weeks at which time the number of positive bottles in a dilution series are used to calculate the starting concentration of bacteria in the initial inoculum, and this number adjusted based on the amount of starting material added to the initial 20 ml dilution used to inoculate the first bottles in the dilution series.

The following media types were chosen for this project, each provides information on a different phenotypic population:

Media	Full Name	Type of Organisms Detected
MPB	Modified Postgate's Medium B	Sulfidogen, SRB (sulfate reducing bacteria).
PRD	Phenol Red Dextrose	APB (acid producing bacteria) and GHB (general heterotrophic bacteria).
IRB	Iron Reducing Bacteria Media	IRB (iron reducing bacteria).

- **PRD** (phenol red dextrose) culture media is used for enumeration of **APB** (acid producing bacteria) and **GHB** (general heterotrophic bacteria).
  - APB convert the bright red media to bright yellow.
  - GHB appear as turbid growth in the red media.
  - All cultures positive for APB are considered positive for GHB.
- **MPB** (modified Postgate's B) culture media is used for enumeration of **SRB** (sulfate reducing bacteria). Although MPB is somewhat selected for SRB, other H2S producing sulfidogenic bacteria such as peptide fermenting organisms and thiosulfate reducing bacteria will sometime grow in MPB, and also generate a positive response.
  - **SRB and Sulfidogens** generate H2S, forming a black FeS precipitate.
- **IRB** (iron reducing bacteria) culture media is clear and slightly yellow-green, with no precipitate.
  - **IRB** Iron reducing organisms chelate the iron, resulting in a clear media with green precipitate.

A 1% salinity was used for all medias. Culturing temperature was set at 30ºC.
Final readings were taken after full 28 days of incubation.

DNA Isolation for qPCR and Amplicon Metagenomics

DNA isolated from the samples were used for both the qPCR and 16S amplicon metagenomics assays. Scale samples such as those from Rager Mountain are atypical samples for DNA isolation, as they consist mostly of non-biological material including possible inhibitors of the DNA isolation and downstream analysis steps. DNA isolations had to be performed multiple times to identify the approach that worked best for that individual sample. The most challenging part is separation of a bacterial fraction away from non-biological materials in the sample. For solid samples, a combination of extraction in sterile PBS buffer and centrifugation was used to isolate a bacterial fraction away from other material in the sample. For liquid samples, a combination of filtration (using sterile 0.2 micron polyethersulfone (PES) membrane filter units) and / or centrifugation. Centrifugation was performed either in 50 ml centrifuge tubes, centrifuged at 2000 g for 50 minutes, or in 2 ml sample tubes, centrifuged for 10,000 g for 15 minutes, depending on volume. Pellets, containing bacteria and additional sample solids, were resuspended in the DNA isolation buffer and processed. For samples with bacteria concentrated by filtration, after filtration the bacteria are trapped on the filter surface while sterile liquids flow through the filtrate reservoir. Bacteria on the surface of the membrane are eluted with sterile PBS buffer, and pelleted by centrifugation. Once a bacterial pellet fraction was prepared, total DNA was isolated using the Qiagen DNeasy UltraClean Microbial Kit (12224-250). Additionally, a "direct isolation" approach was used, in which sample was placed directly into the DNA isolation reagents without the initial bacterial concentration steps. This approach utilized the Qiagen DNeasy Soil DNA Isolation Kit (47014) and / or the Qiagen DNeasy PowerMax Soil DNA Isolation Kit (12988-10) methods, although DNA yields using these approaches were generally not sufficient for downstream analysis.

Primers for 16S qPCR microbial quantification:

515F-GTGCCAGCMGCCGCGGTAA
806R-GGACTACHVGGGTWTCTAAT.
16S probe TACAAGGCCCGGGAACGTATTCACCG
For qPCR, 2.5uL of Sample DNA was loaded into 10uL Quanta Perfecta Tough Mix (QuantaBio) and run on a Roche 480 LightCyler ® with the following cycling conditions: one cycle at 50ºC for 2 minutes, one cycle at 95ºC for 10 minutes, 35 cycles at 95ºC for 15 seconds and 60ºC for 1 minute, and finally, one cycle at 40ºC for 30 seconds. Results of qPCR were scored based on CT score (a positive result was recorded if the CT was ≤30 cycles, negative if CT>30 cycles)..

Amplicon Metagenomics

Illumina 2-step MiSeq
Samples were amplified for sequencing in a two-step process. The forward primer was constructed with (5'-3') the Illumina i5 sequencing primer (TCGTCGGCAGCGTCAGATGTGTATAAGAGACAG) and the indicated forward primer. The reverse primer was constructed with (5'-3') the Illumina i7 sequencing primer (GTCTCGTGGGCTCGGAGATGTGTATAAGAGACAG) and the indicated reverse primer. Amplifications were performed in 25 ul reactions with Qiagen HotStar Taq master mix (Qiagen Inc, Valencia, California), 1ul of each 5uM primer, and 1ul of template. Reactions were performed on ABI Veriti thermocyclers (Applied Biosystems, Carlsbad, California) under the following thermal profile: 95○C for 5 min, then 35 cycles of 94○C for 30 sec, 54○C for 40 sec, 72○C for 1 min, followed by one cycle of 72○C for 10 min and 4○C hold.
Products from the first stage amplification were added to a second PCR based on qualitatively determine concentrations. Primers for the second PCR were designed based on the Illumina Nextera PCR primers as follows: Forward - AATGATACGGCGACCACCGAGATCTACAC[i5index]TCGTCGGCAGCGTC and Reverse - CAAGCAGAAGACGGCATACGAGAT[i7index]GTCTCGTGGGCTCGG. The second stage amplification was run the same as the first stage except for 10 cycles.
Amplification products were visualized with eGels (Life Technologies, Grand Island, New York). Products were then pooled equimolar and each pool was size selected in two rounds using SPRIselect (BeckmanCoulter, Indianapolis, Indiana) in a 0.7 ratio for both rounds. Size selected pools were then run on a Fragment Analyzer (Advanced Analytical, Ankeny, Iowa) to assess the size distribution, quantified using the Qubit 3.0 fluorometer (Life Technologies), and loaded on an Illumina MiSeq (Illumina, Inc. San Diego, California) 2x300 flow cell at 10pM and sequenced.

Notes on Taxonomic and Metabolic Assignment
Organisms are referred to by the identity of the most closely matched organism in the database. However, this does not indicate 100% identity. In most cases, the most closely matched organisms are referred to as "uncultured organism" and as such there is no physiological or metabolic information for them. Organisms that fall below the cutoff for taxonomic assignment are listed as unclassified. Due to the unusual source of samples, a large number of organisms in the samples may unclassified. This indicates that they are novel organisms that have not been described in the scientific literature.
Metabolic assignments are inferred by the metabolic characteristics of the most closely related organism for which experimental data has been provided. Some metabolic groupings are overlapping and non-exclusive, e.g. many fermentative organisms generate organic acids or are capable of sulfidogenesis under some conditions. An overview of select metabolisms is provided in Appendix B.

Overview of Select Metabolic Processes

APB: Acid-Producing Bacteria
Acid-producing bacteria are of specific interest to the oilfield community as acid production directly and aggressively promotes corrosion. Several metabolic pathways result in the production of acids, including fermentation pathways that generate organic acids such as lactic acid and acetic acid, as well as those that generate inorganic acids such as sulfuric acid as a byproduct of the oxidation of inorganic sulfur compound. Not all fermentative pathways result in acidification of the surrounding environment. The identification of bacteria as acid producing does not necessarily indicate acidification of bulk fluids.

Biodeg: Biodegradation
Some bacterial genera and species have the capacity to utilize "atypical" or "unusual" substrates as carbon sources. These bacteria are loosely referred to as Biodeg, for "Biodegradation". The definition used here for "atypical or unusual substrates" with reference to bacterial metabolism includes compounds that most bacteria cannot utilize as a food source. Unusual compounds Biodeg organisms utilize include disinfectants, antibiotics, xenobiotics and detergents. Some degrade long chain polymers of sugars and carbohydrates, such as those found in cell wall materials. Others are able to degrade hydrocarbons. Hydrocarbons, including alkanes, alkenes, aromatic hydrocarbons, and waxes, are found naturally in great variety in crude oil and other petroleum compounds. Due to their structural diversity, most bacteria lack the capacity to utilize petroleum hydrocarbons as food sources. Each type of hydrocarbon-degrading microorganism is likely to be capable of metabolizing a few specific types of hydrocarbons.

IRB: Iron-Reducing Bacteria, Fe(III)RB
Some microbes can use Fe(III) as an electron acceptor, reducing it to Fe(II). Iron reduction has been observed under both acidophilic and neutrophilic conditions. Two common iron-reducing genera are Shewanella and Geobacter. In addition to IRB activity, Shewanella species produce chelators that solubilize Fe(III) oxides (Lovley et al, 2004). Shewanella are capable of growing in corrosive biofilms where they have been shown to remove the protective H2 film layer that normally protects iron surfaces from corrosion under anoxic conditions. should not be confused with iron oxidizing bacteria, which are aerobes responsible for a rust brown staining and slimy growth in surface waters.

NRB: Nitrate Reducing Bacteria
NRB reduce nitrates to nitrites, nitrous oxide, or nitrogen under anaerobic conditions in a process termed denitrification. Most are heterotrophic facultative anaerobic bacteria including such common bacteria as *Paracoccus, Pseudomonas, Alcaligenes,* and *Bradyrhizobioium*. A few bacteria use such reduction processes as hydrogen acceptor reactions and hence as a source of energy; in this case the end product is ammonia. Denitrification is a normal part of nitrogen cycling and not all NRB are of concern to O&G infrastructure.

A subcategory of NRB is the **NRSOB**: Nitrate-Reducing Sulfur-Oxidizing Bacteria are a specific subgroup of NRB whose levels are increased in reservoirs following nitrate injections (Gittel et al 2009; Grigoryan et al, 2008; Hubert and Voordouw, 2007). Growth of NRSOB suppresses the activity of SRB, and thus reducing sulfidogenisis. Some Epsilonproteobacteria can also oxidize petroleum sulfur compounds and utilize nitrate as an electron acceptor for growth, and thus may be considered hydrocarbon degrading. Massive dominance of related Epsilonproteobacteria has been observed in other petroleum samples, for example in formation waters from a Canadian oil sands reservoir containing severely biodegraded oil. (Kodama, Y and Kazuya Watanabe, 2003; Hubert et al, 2011). Sulfurospirillum are nitrate-reducing, sulfur oxidizing bacteria (NRSOB) members of the class Epsilonproteobacteria and are sometimes referred to as “Campylobacter” in older publications. The way in which nitrate addition can affect the SRB population involves several pathways. First, nitrate is a thermodynamically more favorable electron acceptor than sulfate, thus NRB have a competitive advantage. To emphasize the complexity of the metabolism in oilfield samples, it should be noted that under some conditions, these bacteria are also sulfidogens capable of reducing sulfur and thus producing H_2S (Finster K et al, 1997).

Sulfidogenesis: (e.g. SRB, TRB, SuRB)
The metabolic pathways of most interest to the oilfield community are those that generate significant levels of hydrogen sulfide (H_2S). In addition to inorganic processes, biogenic processes can generate significant levels of hydrogen sulfide, primarily through the action of sulfidogenic bacteria. Bacteria that evolve hydrogen sulfide are commonly referred to as “sulfidogens”. Sulfate-reducing bacteria (SRB) are particularly aggressive at sulfide production and are the group of bacteria most commonly implicated oil filed biogenic sulfide production (Barton et al, 2009). Hydrogen sulfide formation by sulfate-reducing bacteria (SRB) under strict anaerobic circumstances is a common problem in sediments, sewer systems, oil reservoirs and anaerobic effluents (Holmer & Storkholm, 2001; McComas et al., 2001). The emission of H_2S into the atmosphere of sewer systems does not only imply odor nuisances and possible health risks. It also induces the biological production of sulfuric acid in the aerobic zones, causing severe corrosion of the inner surface of concrete sewer structures (Sand, 1987; Vincke et al., 2002). Hence, preventive or curative actions are needed.

While SRB are traditionally associated with O&G system sulfide generation, sulfur- and thiosulfate-reducing bacteria (SuRB and TRB, respectively) can also generate significant levels of H_2S and contribute to corrosion and souring (Hulecki JC et al, 2009, Magot et al 1997, Agrawal et al, 2010). Compared to SRB, the TRB are harder to classify taxonomically, as they are members of bacterial genera that can include non-tSRB members. Examples of sulfidogenic TRB commonly found in oilfield samples include *Halanaerobium congolense*, as well as some *Thermoanaerobacter*, and *Spirochaeta*. Additionally, many common enteric bacteria are sulfidogenic, including *Citrobacter* and *Salmonella*.

Thermophiles:
A thermophile is an organism that can survive and often thrives in environments having relatively high temperatures ranging between 45 and 122 °C.

Methanogens:

Methanogens are Archaea that produce methane as a metabolic byproduct in anoxic conditions. Methanogens are found in different environments including wetlands (marsh gas), animal digestive tracts (methane production of cattle and in farts), and anaerobic digestor sludges of wastewater treatment systems. Some methanogens are extremophiles and can be found in hot springs, submarine hydrothermal vents as well as in the "solid" rock of the Earth's crust, kilometers below the surface. Methanogens are associated with microbial influenced corrosion. Hydrogenotrophic methanogens are believed to cause metal corrosion through cathodic depolarization, whereas the acetotrophic methanogens grow syntrophically with corrosion-causing SRB.

Appendix D References

1. Angelez-Chavez, C., Mora-Mendoza, J.L., Garcia-Esquivel, R., Padilla-Viveros, A.A., Perez, R., Flores, O. and Martinez, L. (2002) Microbiologically influenced corrosion by Citrobacter in sour gas pipelines. Mater Perform 41, 50-55.
2. Balch, W. E.; Schoberth, S.; Tanner, R. S.; Wolfe, R. S. (1977). Acetobacterium, a New Genus of Hydrogen-Oxidizing, Carbon Dioxide-Reducing, Anaerobic Bacteria. International Journal of Systematic Bacteriology 27 (4): 355.
3. Barton LL, Fauque GD. (2009) Biochemistry, physiology and biotechnology of sulfate-reducing bacteria. Adv Appl Microbiol. 68:41-98.
4. Bermont-Bouis D, Janvier M, Grimont PA, Dupont I, Vallaeys T. (2007) Both sulfate-reducing bacteria and Enterobacteriaceae take part in marine biocorrosion of carbon steel. J Appl Microbiol. 102:161-168.
5. Bermont-Bouis D, Janvier M, Grimont PA, Dupont I, Vallaeys T. (2007) Both sulfate-reducing bacteria and Enterobacteriaceae take part in marine biocorrosion of carbon steel. J Appl Microbiol. 102:161-168.
6. Boone DR, Whitman WB, Rouviere P (1994). "Diversity and taxonomy of methanogens". In JG Ferry, ed. Methanogenesis: Ecology, Physiology, Biochemistry & Genetics. Pp 35-80.
7. D'Ippolito S, de Castro RE, Herrera Seitz K. (2011) Chemotactic responses to gas oil of Halomonas spp. strains isolated from saline environments in Argentina. Rev Argent Microbiol. 43(2):107-10.
8. Dice, L.R., "Measures of the Amount of Ecologic Association Between Species," *Ecology* 26, 3, (1945): pp.297-302
9. Hubert CR Oldenburg TB, Fustic M, Gray ND, Larter SR, Penn K, Rowan AK, Seshadri R, Sherry A, Swainsbury R, Voordouw G, Voordouw JK, Head IM. (2012) Massive dominance of Epsilonproteobacteria in formation waters from a Canadian oil sands reservoir containing severely biodegraded oil. Environ Microbiol. 14(2):387-404.
10. Kryachko Y, Dong X, Sensen CW, Voordouw G. (2012) Compositions of microbial communities associated with oil and water in a mesothermic oil field. Antonie Van Leeuwenhoek. 101: 3, pp 493-506
11. Kwon S, Moon E, Kim TS, Hong S, Park HD. (2011) Pyrosequencing demonstrated complex microbial communities in a membrane filtration system for a drinking water treatment plant. Microbes Environ. 26(2):149-55.
12. Li XX, Yang T, Mbadinga SM, Liu JF, Yang SZ, Gu JD, Mu BZ. Responses of Microbial Community Composition to Temperature Gradient and Carbon Steel Corrosion in Production Water of Petroleum Reservoir. Front Microbiol. 2017 Dec 5;8:2379.
13. Lonergan DJ, Jenter HL, Coates JD, Phillips EJ, Schmidt TM, Lovley DR (1996) Phylogenetic analysis of dissimilatory Fe(III)-reducing bacteria. J Bacteriol. 178(8):2402-8.
14. Montoya D, Ar_valo C, Gonzales S, Aristizabal F, Schwarz WH. (2001) New solvent-producing Clostridium sp. strains, hydrolyzing a wide range of polysaccharides, are closely related to Clostridium butyricum. J Ind Microbiol Biotechnol. 27(5):329-35.
15. Pham,V.D., Hnatow,L.L., Zhang,S., Fallon,R.D., Jackson,S.C., Tomb,J.F., DeLong,E.F. and Keeler,S.J. (2009) Characterizing microbial diversity in production water from an Alaskan mesothermic petroleum reservoir with two independent molecular methods Environ. Microbiol. 11 (1), 176-187.
16. Rajasekar A, Anandkumar B, Maruthamuthu S, Ting YP, Rahman PK. (2010) Characterization of corrosive bacterial consortia isolated from petroleum-product-transporting pipelines. Appl Microbiol Biotechnol. 85(4):1175-88.
17. Ravot G, Ollivier B, Magot M, Patel B, Crolet J, Fardeau M, Garcia J. (1995) Thiosulfate reduction, an important physiological feature shared by members of the order thermotogales. Appl Environ Microbiol. 61(5):2053-5.
18. Vigneron A, Alsop EB, Chambers B, Lomans BP, Head IM, Tsesmetzis N. Complementary Microorganisms in Highly Corrosive Biofilms from an Offshore Oil Production Facility. Appl Environ Microbiol. 2016 Apr 4;82(8):2545-2554.
19. Vigneron A, Head IM, Tsesmetzis N. Damage to offshore production facilities by corrosive microbial biofilms. Appl Microbiol Biotechnol. 2018 Mar;102(6):2525-2533.
20. *Yan, Z., Zheng, X.-W., Chen, J.-Y., Han, J.-S. and Han, B.-Z. (2013), Effect of different Bacillus strains on the profile of organic acids in a liquid culture of Daqu. J. Inst. Brew., 119: 78-83.* https://doi.org/10.1002/jib.58 https://onlinelibrary.wiley.com/doi/epdf/10.1002/jib.58
21. Zhang T, Ye L, Tong AH, Shao MF, Lok S. (2011) Ammonia-oxidizing archaea and ammonia-oxidizing bacteria in six full-scale wastewater treatment bioreactors. Appl Microbiol Biotechnol. 91(4):1215-25.

Project Report

Microbial Population Analysis of Organisms Associated with the Rager Mountain Gas Storage Failure

Wells 2248
Soil, C001 Scale, Annulus Valve, Annulus Fluids

Prepared for
Ravi M. Krishnamurthy
Blade Energy Partners

Prepared by:
Elizabeth Summer, PhD
Ecolyse, Inc
11142 Hopes Creek Road
College Station, Texas 77845

Final Report

June 20, 2023

Well 2248 Microbiological Analysis: Statement of Findings

Microbiological analysis was conducted on well pad soil, 7" casing OD scale, annulus valve solids, and annulus fluid samples collected from well 2248 in Feb - March 2023. These results represent the microbial population at the time of sampling.
Results of MPN analysis: At the time of sampling, all samples from well 2248 contained APB, SRB, and IRB, with GHB and APB levels 3 to 4 log orders higher than SRB and IRB from the same samples.
Results of qPCR: qPCR results suggested that the total microbial load might be as much as 2- to 3- log orders higher then what was detected by MPN analysis.
Population Profile Analysis Population profile analysis supported the culture-based data. Aerobes and biodegrading organisms dominated each of the samples, and APB were a significant proportion of the population. Sulfidogens and IRB contributed to less than 1% of all species.
Summary of all data: Populations were dominated by aerobes and biodegrading organisms, at levels greater than 10^8 per g C001 scale. APB were also a significant proportion of the populations. In contrast, sulfidogens were present at a 3 log orders lower relative abundance.
APB and SRB are both corrosion associated microbial traits, however it was not directly demonstrated that the SRB and APB on the C001 casing scale are capable of causing corrosion. It should also be considered that MIC is complicated, and there are additional MIC mechanisms that were not evaluated for example aerobic acid producing Fungi.

Summarized Microbiological Data Analysis Results and Conclusions

1. **Well 2248 C001 Scale Samples**

8 samples from well 2248 were collected, including 4 scale samples from the OD of 7" casing C001 were collected in March, 2023. **See Table 1 for list of samples.**

a. **Well 2248 casing C001 MPN results**: **See Tables 2, 3, and 4**.
   i. MPN is the "NACE Standard" culture-based population analysis.
   ii. MPN Data reveled that the all samples scale from the OD of well 2248 7" casing joints C001 contained significant populations of APB, GHB, SRB, and IRB.
   iii. Overall, levels of culturable GHB > APB > SRB > IRB
      1. GHB levels in the C001 casing OD of around 10^6 cell per g, while levels of SRB and IRB were around 3 and 4 log orders less than that, respectively.

b. **Well 2248 casing C001 qPCR results**: **See Tables 5**.
   i. qPCR is a DNA based assay that is used to quantify bacteria in a DNA sample, results are provided in total bacterial cells per g.
   ii. qPCR assay of well 2248 C001 casing scale samples indicated that microbial levels are 2 log orders higher then what was detected by culture based MPN analysis
   iii. This supports a model in which microbial population is present on the surface of C001, and values from MPN analysis should be adjusted accordingly.

c. **Well 2248 casing C001 microbial population diversity analysis results**: **See Tables 6, 7, 8, 9**.
   i. Microbial profile was determined by amplicon metagenomics, in which tens of thousands of DNA sequence fragments are sequenced and identified based on similarity to known organisms
   ii. Well 2248 7" casing joint C001 OD population profile indicated that the sample was overwhelmingly dominated by aerobic biodegrading organisms.
   iii. Sulfidogens were present at <1% of the population.

Well 2248 Population Analysis: Detailed Methods and Results

Sample Information

- For well 2248, 10 samples were collected and analyzed.
- These samples included:
  - Well 2248 pad area soil pre-samples were collected on Feb 16 2023 Soil" refers to rock, dirt, and mud collected around wellsite ; 1 sample
  - Well 2248 annulus valve solid samples ; 2 small samples
  - Well 2248 annulus liquid sample ; 1 sample
  - Well 2248 7" casing joint C001 OD scale ; 4 samples
  - Well 2248 Conductor ; 1 sample
  - Well 2248 9 5/8 uppermost ID scrape ; 1 sample
- "Scale" refers to all solids scraped from surfaces. These were primarily metal flakes.
- Table 1 provides an overview of well 2248 samples, as well as details from wells 2251 and Compressor Station fluids whose results are elaborated on in an accompanying report.
- Appendix A provides more details on each sample.

Table 1. Well 2248, Well 2251, and Compressor Station Sample Overview

#	Sample Date	Well	Sample Description	Type	Quantity
1.A Well 2248 Well site soils, 7" casing OD, annulus fluids					
2	2/16/23	2248	Well 2248 Soils	Soil	359.0
49	3/17/23	2248	Well 2248, Annulus valve Solids	S	0.8 g
50	3/17/23	2248	Well 2248, Annulus valve Solids	S	0.8 g
51	3/26/23	2248	Well 2248, Annulus Liquids	L	~500 ml
52	3/26/23	2248	Well 2248, 7" C001 OD Scale	S	190 g
53	3/26/23	2248	Well 2248, 7" C001 Couplings Scale	S	28.2 g
54	3/26/23	2248	Well 2248, 7" C001 OD Scale (4 - 5 lbs)	S	2360 g
55	3/26/23	2248	Well 2248, OD Scale, Conductor	S	91.5 g
56	3/28/23	2248	Well 2248, 7" C001 OD Scale	S	7.5 g
59	3/29/23	2248	Well 2248, uppermost 9 5/8" casing ID	S	70.8 g
1.B Well 2251 Well site soil, 7" casing OD					
3	2/16/23	2251	Well 2251 Soils	Soil	162.0
62	4/01/23	2251	Well 2251, 7" casing OD, C001 top of joint	S	23.2 g
63	4/03/23	2251	Well 2251, 7" casing OD, C001 top of joint	S	508.5 g
64	4/03/23	2251	Well 2251, 7" casing OD, C001 10'6" from top	S	9.2 g
1.C Compressor Station Fluid Samples					
57	3/28/23	CS	Compressor station separator fluid, Black.	L	~200 ml
58	3/28/23	CS	Compressor station separator fluid, Clear.	L	~200 ml
60	4/01/23	CS	Compressor Station pond sample, Clear	L	500 ml
61	4/01/23	CS	Compressor Station pond sample, Emulsion	L	500 ml

Details of Samples used for MPN and DNA based microbial population analysis. Exact samples included in each pool are found in Appendix A. Collection date and well pad. Description of each sample includes well, OD or ID, casing joint, detail of sample type. Sample types are Soil, L liquid, S scale. Soil refers to dirt and rocks collected from the well pads. Scale refers to any solids originating on the surface of a casing joint or tree. S is Scale typically contains a large amount of metal flakes. Amount of material collected is provided in ml or g.

Methods Used for Microbial Population Profiles Evaluation

- Testing microbial populations for corrosion potential is based on recommendations and guidelines established by NACE (National Association of Corrosion Engineers),.
- NACE Standard Test Methods include those described in the following documents:

NACE ID	Item	Standard Test Method
TM0194	21224	Field Monitoring of Bacterial Growth in Oil and Gas Systems
TM0212	21260	Detection, Testing, and Evaluation of Microbiologically Influenced Corrosion on Internal Surfaces of Pipeline
TM0106	21248	Detection, Testing, and Evaluation of Microbiologically Influenced Corrosion (MIC) on External Surfaces of Buried Pipeline

- NACE recognizes that the subsurface and infrastructure systems being sampled vary greatly with respect to accessibility, as well as physical, chemical, and biological traits, and thus it is impossible to give an exact list of methods or protocols that must be followed absolutely.
- Guidelines must be adapted to any given situation and system.
- In recognition of these guidelines, a conservative, combined approach was adopted for the Rager Mountain project.
- The approach used included the most traditional and well-established method (triplicate MPN set up in standard medias for APB, SRB, IRB and GHB) method, along with two more advanced approaches (qPCR and amplicon metagenomics)
- **Interpretation of results:** Microbiological data does not provide simple “action level” “cut-off concentrations” data. MIC is a highly complex problem, impacted not only by the numbers and extreme diversity of organisms, but their metabolic activity levels, and fluctuations in environmental physio-chemical conditions (for example, nutrients, temperature, water levels, water circulation, chemical treatments).

NACE TM0194-94 statement of interpretation of MPN data:
1.1.8 The simple presence of bacteria in a system does not necessarily indicate that they are causing a problem. In addition, bacterial populations causing problems in one situation, or system, may be harmless in another. Therefore, “action” concentrations for bacterial contamination cannot be given. Rather, bacterial population determination are one more diagnostic tool useful in assessing oilfield problems**.**

Project Results: MPN Culture-Based Bacterial Diversity Analysis

1. Triplicate, Culture -Based MPN Method

MPN stands for “Most Probably Number” and is a culture-based method for the quantification of specific types of bacteria in a sample. The data generated is in terms of “bacteria per ml” or “bacteria per g” of sample, where “bacterial types” are members of a phenotypic group rather than a taxonomic group. The identity of the organisms quantified is based on the use of the selective indicator artificial growth media used to set up the assay. Indicator medias contain a substrate that undergoes a visible chemical change when certain types of bacteria grow in them, for example, addition of a pH indicator will provide strong visual evidence for the growth of acid producing bacteria that have dropped the media pH. Selective medias contain substrates and conditions that promote the growth of certain types of bacteria, for example, anaerobic conditions and addition of sulfate promotes the growth of sulfate reducing bacteria.

Figure 1 shows what the indicator, selective medias used in this study look like:

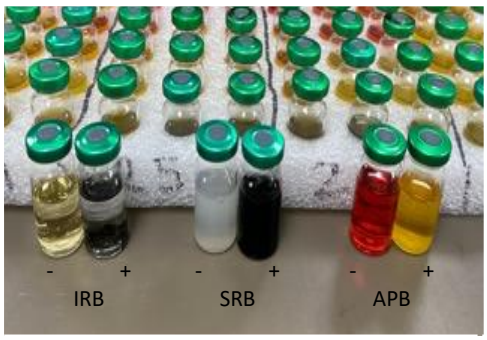

A. How + plus and - minus bacterial growth appears in 3 selective indicator medias used for this project: IRB (iron reducing bacteria), MPB (SRB: sulfate reducing bacteria), PRD (APB: acid producing bacteria)

B. Triplicate MPN set-up for 4 samples (samples 24, 25, 26, 27). There are 3 dilution series columns set up in parallel for each sample, so 24 media bottles are inoculated per sample.

Figure 1. MPN microbial culture vials.

MPN Method Advantages

- Minimal sample manipulation is required to set up assay.
- Easy to interpret results
- Low-tech and easy to set up in the field.
- Determines the number of live, culturable bacteria in the sample.
- Provides experimental phenotypic data.
- Traditional method, recommended by NACE as a standard method.
- Historical approach that is widely used in throughout the industry.
- Can be used for the analysis of anaerobic organisms.

MPN Method Disadvantages

- There are well-known limitations inherent in culture-based analysis,
- **NACE TM0194 describes some of these limitations (direct quote):**
  - *3.1.1 Bacterial culturing in artificial growth media is accepted as the standard technique for the estimation of bacteria numbers. However, users should be aware of the limitations of the culture technique:*
  - *3.1.1.1 Any culture medium grows only those bacteria able to use the nutrients provided.*
  - *3.1.1.2 Culture medium conditions (pH, osmotic balance, redox potential, etc.) prevent the growth of some bacteria and enhance the growth of others.*
  - *3.1.1.3 Conditions induced by sampling and culturing procedures, such as exposure to oxygen, may hamper the growth of strict anaerobes.*
  - *3.1.1.4 Only a small percentage of the viable bacteria in a sample can be recovered by any single medium; i.e., culture media methods may underestimate the number of bacteria in a sample.*
  - *3.1.1.5 Some bacteria cannot be grown on culture media at all.*

Well 2248 – Culture-Based MPN Enumeration of APB, GHB, SRB, and IRB

- MPN analysis was set up with 8 well 2248 samples, in 3 medias each (PRD, MPB, IRB)
- These 3 medias provide quantitative data for 4 metabolic categories: APB, GHB, SRB, IRB
  - **PRD** (phenol red dextrose) culture media is used for enumeration of **APB** (acid producing bacteria) and **GHB** (general heterotrophic bacteria).
    - APB convert the bright red media to bright yellow.
    - GHB appear as turbid growth in the red media.
    - All cultures positive for APB are considered positive for GHB.
  - **MPB** (modified Postgate's B) culture media is used for enumeration of **SRB** (sulfate reducing bacteria). Although MPB is somewhat selected for SRB, other H2S producing sulfidogenic

bacteria such as peptide fermenting organisms and thiosulfate reducing bacteria will sometime grow in MPB, and also generate a positive response.
    - **SRB and Sulfidogens** generate H2S, forming a black FeS precipitate.
  - **IRB** (iron reducing bacteria) culture media is clear and slightly yellow-green, with no precipitate.
    - **IRB** Iron reducing organisms chelate the iron, resulting in a clear media with green precipitate.
- As per NACE standards, readings were taken weekly for 4 weeks.
- Resulting values were converted to microbial cells per g or ml of starting material, after accounting for the initial dilution of the sample used to inoculate the first bottle in each dilution series.
- Resulting values were converted to microbial cells per g or ml of starting material, after accounting for the initial dilution of the sample used to inoculate the first bottle in each dilution series.
- Table 2 shows the results of after 4 weeks of growth, for all 8 well 2248 samples.
- Table 2 also provide results from wells 2251 and Compressor Station fluids, whose results are elaborated on in an accompanying report.

Table 2. Well 2248, Well 2251, and Compressor Station; Results of MPN Analysis

#	Well	Sample Description	Type	APB	GHB	IRB	SRB
2.A Well 2248 Well site soils, 7" casing OD, annulus fluids							
2	2248	Well 2248 Soils	Soil	3.8E+07	1.2E+08	1.8E+04	6.0E+03
49	2248	Well 2248, Annulus valve Solids	S	5.0E+04	1.0E+06	2.8E+01	5.0E+03
50	2248	Well 2248, Annulus valve Solids	S	3.5E+09	3.5E+09	3.8E+04	1.1E+05
51	2248	Well 2248, Annulus Liquids	L	7.5E+04	7.5E+04	2.5E+01	2.0E+01
52	2248	Well 2248, 7" C001 OD Scale	S	2.7E+04	1.0E+06	3.0E+01	1.7E+03
53	2248	Well 2248, 7" C001 Couplings Scale	S	2.7E+05	2.7E+05	1.5E+02	2.4E+04
54	2248	Well 2248, 7" C001 OD Scale (4 - 5 lbs)	S	5.6E+05	1.5E+07	5.6E+01	2.7E+03
55	2248	Well 2248, OD Scale, Conductor	S	9.1E+04	9.1E+07	1.5E+03	5.8E+02
56	2248	Well 2248, 7" C001 OD Scale	S	4.5E+04	7.5E+05	2.5E+01	9.5E+02
59	2248	Well 2248, uppermost 9 5/8" casing ID	S	7.6E+04	2.0E+05	2.0E+02	5.6E+02
2.B Well 2251 Well site soil, 7" casing OD							
3	2251	Well 2251 Soils	Soil	2.9E+07	1.6E+09	5.3E+03	1.8E+04
62	2251	Well 2251, 7" casing OD, C001 top of joint	S	2.5E+01	9.5E+01	<LOD	<LOD
63	2251	Well 2251, 7" casing OD, C001 top of joint	S	9.0E+00	2.5E+01	<LOD	<LOD
64	2251	Well 2251, 7" casing OD, C001 10'6" from top	S	9.5E+01	2.5E+02	<LOD	<LOD
2.C Compressor Station Fluid Samples							
57	CS	Compressor station separator fluid, Black.	L	6.0E+00	1.2E+02	2.5E+01	0.0E+00
58	CS	Compressor station separator fluid, Clear.	L	6.0E+00	7.5E+01	2.5E+01	0.0E+00
60	CS	Compressor Station pond sample, Clear	L	1.1E+01	2.0E+05	<LOD	<LOD
61	CS	Compressor Station pond sample, Emulsion	L	9.5E+02	4.5E+07	4.0E+01	1.5E+01

MPN Results Table Legend. Results of population analysis by triplicate MPN method. Values are the culturable bacteria per g of each sample, set up in triplicate, after 28 days of growth. SRB: Sulfate-Reducing Bacteria. APB: Acid Producing Bacteria, GHB: General Heterotrophic Bacteria, IRB: Iron Reducing Bacteria, Yellow are >10^6, Red are between 10^4 - 10^6, Green are between 10^3 - 10^4, White are <10^3, Grey <LOD indicates "below limit of detection", e.g. no growth

Well 2248 MPN Analysis Overall Results (Table 3)

- Out of 10 samples collected from well 2248:
  - All 10 tested positive for the presence of APB.
  - All 10 tested positive for the presence of GHB
  - All 10 tested positive for the presence of IRB
  - All 10 tested positive for the presence of SRB.
- The average cell density in all media types was 3.2E+04cells/g,
  - Range of 2.00E+01 to up to 3.5E+09 cells/g.
- GHB exhibited the highest overall average cell density, at 4.2E+06 cells/g
- IRB exhibited the lowest overall average cell density, at 2.5E+02 cells/g

Table 3. Well 2248 MPN Culture Based Microbial Density. Overall Summary of Results.

Media Type	APB	GHB	IRB	MPB	*Summary*
# Samples Positive	10 of 10	10 of 10	10 of 10	10 of 10	10 of 10
Average cells/g	4.8E+05	4.2E+06	2.5E+02	2.2E+03	*3.2E+04*
Highest cell density cells/g and sample	3.50E+09 Annulus Valve	3.50E+09 Annulus Valve	3.80E+04 Annulus Valve	1.10E+05 Annulus Valve	3.50E+09 Annulus Valve
Lowest cell density cells/g and sample	2.70E+04 7" OD Scale	7.50E+04 7" OD Scale	2.50E+01 7" OD Scale	2.00E+01 7" OD Scale	2.00E+01 7" OD Scale

Well 2248 MPN Analysis Results by Sample Type (Figure 2 and Table 4)

Soil Sample

- Soil was dominated by GHB and APB, with GHB having the highest density of 1.2E+08 cells per g
- Similar to well 2244 results, IRB levels exceeded SRB levels, although the difference was by less than 1 log order.
  - IRB were 1.8E+04 cells per g while IRB were 6.0E+03
  - In contrast, for C001 OD scale, IRB levels were almost 2 log orders less than SRB levels.

7" Casing C001 OD Scale Samples

- Surface of casing C001 was dominated by GHB, at 1.3E+06 cells per g
- APB levels were 1.2E+05 cells per g
- SRB and IRB, although present, were 3 to 4 log orders lower density than GHB
- SRB levels were 3.2E+03 while IRB levels were 5.0E+01 cells per g

Annulus Fluid Sample

- Annulus fluid sample was dominated by GHB and APB, at nearly identical around 7.5E+04 each
- IRB and SRB were 3 log orders lower, at 2.5E+01 and 2.0E+01 cells per g, respectively.

Annulus Valve Solids

- Annulus valve solid sample was dominated by similar levels of GHB and APB, at 1.3E+07 and 5.9E+07 cell per g, respectively.
- IRB and SRB were 3 and 4 log orders less, at 1.0E+03 and 2.3E+04 cells per g, respectively.

Conductor Solids

- Solids removed from the conductor contained the most marked difference in GHB and APB, wit 3 log orders lower APB relative to GHB.
- SRB and IRB were present, at 2 log orders lower density then APB.
- Similar to soils, IRB were slightly elevated relative to SRB

Figure 2 and Table 4. Well 2248 MPN Data Summarized by Sample Type

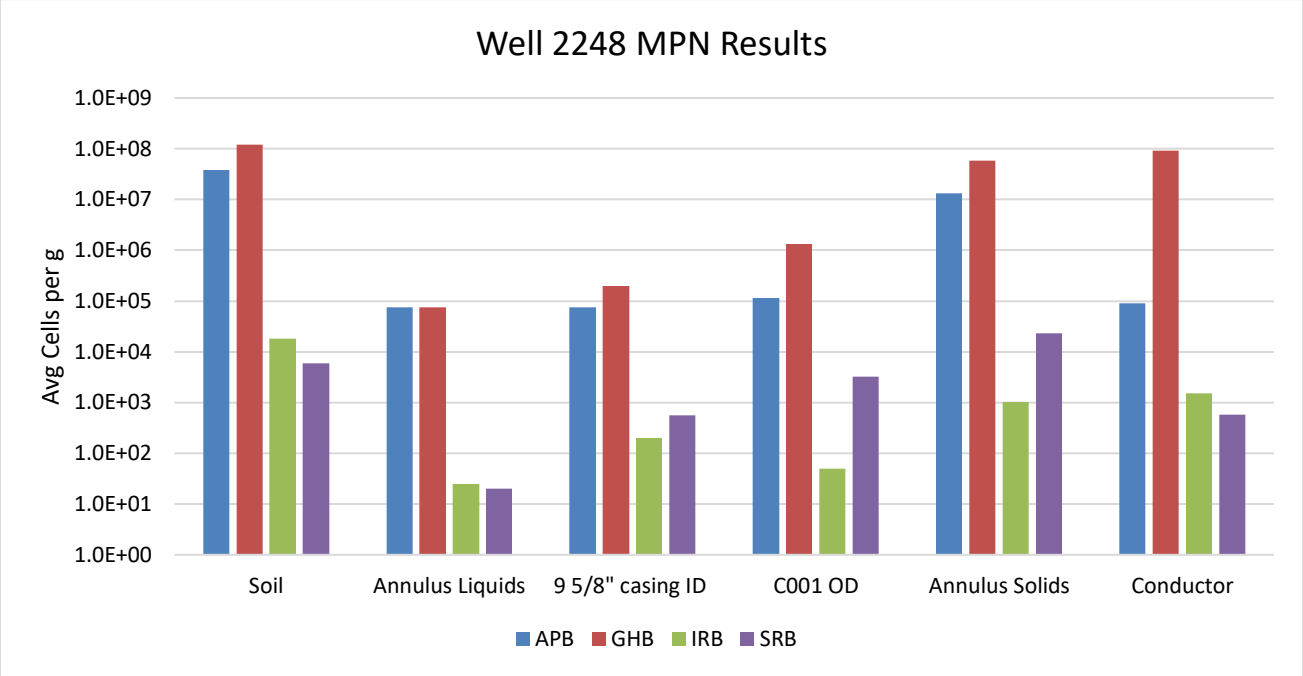

Figure 2. Graphical representation of data in Table 4.

Table 4. MPN Culture Based Microbial Density Wells 2248. Summary of Results.

Sample Group	Sample Type Description	Type	APB	GHB	IRB	SRB
2	Well 2248 Soils	Soil	3.8E+07	1.2E+08	1.8E+04	6.0E+03
51	Well 2248, Annulus Liquid Sample	L	7.5E+04	7.5E+04	2.5E+01	2.0E+01
59	Well 2248, uppermost 9 5/8" casing ID	S	7.6E+04	2.0E+05	2.0E+02	5.6E+02
52, 53, 54, 56	7" C001 OD Scale	S	1.2E+05	1.3E+06	5.0E+01	3.2E+03
49, 50	Annulus Valve Solids	S	1.3E+07	5.9E+07	1.0E+03	2.3E+04
55	Conductor	S	9.1E+04	9.1E+07	1.5E+03	5.8E+02

Table 4. Microbial Density Wells 2248. Summary of Results. Averages were calculated from Ln for each sample group. Results of population analysis by triplicate MPN method. Values are the culturable bacteria per g of each sample, set up in triplicate, after 28 days of growth. SRB: Sulfate-Reducing Bacteria. APB: Acid Producing Bacteria, GHB: General Heterotrophic Bacteria, IRB: Iron Reducing Bacteria, Yellow are >10^6, Red are 10^4 - 10^6, Green are 10^3 - 10^4, White are <10^3, Grey <LOD are "below limit of detection", e.g. no growth

Project Results: Bacterial Diversity Analysis by Genetic Approaches

- qPCR and Amplicon Metagenomics are two approaches that rely on DNA isolation from a sample
- Isolated DNA is used for two types of analysis: qPCR and Amplicon Metagenomics
- qPCR provides quantitative data on total microbial load per g or ml sample
- Amplicon metagenomics provides identification of the types of microbes in a sample
- Information gathered includes the types of bacteria and the % in the population
- Amplicon metagenomics and qPCR do not differentiate between live and dead cells
- The identity of the species in the sample is used to predict the physiological or metabolic role that organism might have in the environment
- The prediction is done by comparing the organisms identified to the research on that type of organism, available in the scientific literature
- Not every organism has been studied enough to understand its metabolism
- Following traits assigned to identified bacteria and archaea where possible:
    - **Sulfidogen**-includes all bacteria that can produce sulfide or H_2S as a metabolic byproduct. This includes "true" SRB as well as TRB (thiosulfate-reducing bacteria) SuRB(sulfur-reducing bacteria) and peptide-fermenting bacteria (such as some Clostridia)
    - **SRB**-(sulfate-reducing bacteria) "true" SRB, utilize sulfate as respiratory electron acceptor and produce sulfide as a metabolic byproduct
    - **APB**-(acid-producing bacteria) these make organic and/or inorganic acids. Not all APB result in a lowering of ambient pH. Organisms that produce inorganic acids are often acidophilic, and grow at very low corrosive pH.
    - **IRB**-(iron-reducing bacteria) many are strongly corrosive
    - **NRB**-(nitrate-reducing bacteria) many bacteria are nitrate reducers. Of particular relevance to the O&G industry are the NRSOB (nitrate-reducing sulfur-oxidizing bacteria) promoted by nitrate injections.
    - **Biodeg**-biodegrading bacteria. These bacteria are capable of breaking down unusual substrates such as O&G hydrocarbons **(HC),** petrochemicals, cellulose, toxic chemicals etc.
    - **Methanogen** – Archaea that produce methane as a metabolic byproduct under anaerobic growth
    - **Methylotroph**- Utilize reduced one-carbon compounds, such as methanol or methane, as the carbon source for their growth; and multi-carbon compounds that contain no carbon-carbon bonds, such as dimethyl ether and dimethylamine.
    - **Phototroph**- photosynthetic organisms, these include both aerobes and anaerobes.
- Percent of population, and number of unique microbial types (species) are provided as results

Well 2248 Genetic – Based Diversity Analysis –

DNA Isolation and qPCR from Well 2248 Samples (Table 5)

- For well 2248, DNA was isolated from 8 of the 10 solid and liquid samples listed in Table 1. DNA was not isolated from the 2 annulus valve samples, due to the small sample size (<1g per sample). The entire sample was utilized for MPN analysis.
- DNA was successfully extracted from the remaining 8 well 2248 samples.
- qPCR was conducted using "universal" primers that detect both bacteria and archaea.
- For all samples except sample 55, conductor scale, qPCR detected 1 to 3 log orders more microorganisms in the sample then was enumerated by MPN
- This is not unexpected, and indicates most organisms were either not viable, or did not grow in the 3 media types used for MPN
- Overall microbial levels at well 2248 ranged between 8.4E+05 to 2.3E+10 cells per g
  - Soils: Highest at 2.3E+10 cells per g
  - Annulus liquid: 1.0E+06 cells per g
  - C001 OD scale: 2.5E+07 to 5.6E+08 cells per g
  - 9 5/8" casing ID: 8.4E+05 cells per g
  - Conductor: 2.6E+06 cells per g
- All DNA extracts isolated from well 2248 samples resulted in sequence library data (next section)

TABLE 5. RM Well 2248, Well 2251, and Compressor Station qPCR Results

#	DNA ID	Sample Description	Type	Seq Data?	qPCR Cells /g	MPN Max Cells /g
5.A Well 2248 Well site soils, 7" casing OD, annulus fluids						
2	OG230207-002	Well 2248 Soils	Soil	Yes	2.3E+10	1.2E+08
49	nd*	Well 2248, Annulus valve Solids	S	nd*	nd*	1.0E+06
50	nd*	Well 2248, Annulus valve Solids	S	nd*	nd*	3.5E+09
51	OG230409-003	Well 2248, Annulus valve Liquid	L	Yes	1.0E+06	7.5E+04
52	OG230406-001	Well 2248, 7" C001 OD Scale	S	Yes	5.2E+07	1.0E+06
53	OG230406-002	Well 2248, 7" C001 Couplings Scale	S	Yes	5.6E+08	2.7E+05
54	OG230406-003	Well 2248, 7" C001 OD Scale (4 - 5 lbs)	S	Yes	5.7E+07	1.5E+07
55	OG230406-004	Well 2248, OD Scale, Conductor	S	Yes	2.6E+06	9.1E+07
56	OG230409-006	Well 2248, 7" C001 OD Scale	S	Yes	2.5E+07	7.5E+05
59	OG230406-005	Well 2248, uppermost 9 5/8" casing ID	S	Yes	8.4E+05	2.0E+05
5.B Well 2251 Well site soil, 7" casing OD						
3	OG230207-003	Well 2251 Soils	Soil	Yes	9.6E+09	1.6E+09
62	OG230406-006	Well 2251, 7" casing OD, C001 top of joint	S	no	<LOD	9.5E+01
63	OG230406-007	Well 2251, 7" casing OD, C001 top of joint	S	no	<LOD	2.5E+01
64	OG230406-008	Well 2251, 7" casing OD, C001 10'6" from top	S	no	<LOD	2.5E+02
5.C Compressor Station Fluid Samples						
57	OG230409-004	Compressor station separator fluid, Black.	L	Yes	6.2E+04	1.2E+02
58	OG230409-005	Compressor station separator fluid, Clear.	L	no	<LOD	7.5E+01
60	OG230409-001	Compressor Station pond sample, clear	L	Yes	6.4E+04	2.0E+05
61	OG230409-002	Compressor Station pond sample, emulsion	L	Yes	3.1E+05	4.5E+07

Results of qPCR quantification of total microbes in samples from well 2248, well 2251, and the compressor station liquids. qPCR results, in microbial cells per g or ml sample, are provided. <LOD indicates "below the limit of detection". These same DNA were subject to 16S amplicon metagenomics, and "Sequence Data" indicates of population profiles was obtained from the sample. Highlighted gray are samples that yielded population data. The data from MPN analysis is also provided, using values from Table 2. *nd is "not determined" due to insufficient amount of sample for both MPN and DNA isolation.

The take home conclusions from qPCR of well 2248 samples indicate include:

1. There was no reduction in DNA isolation efficiency for well 2248 samples,
2. All well 2248 samples yielded consistent DNA analysis results.
3. For samples where results were generated, the microbial load was determined to be several log orders higher than what is reflected by MPN analysis, this is an expected result.
4. Well 2248 microbial loads are not insignificant

Well 2248 Microbial Diversity Analysis by Amplicon Metagenomics Tables 6, 7, 8, 9, 10

The microbial population of population profiles were determined for 8 of the 10 samples collected from well 2248 (Table 6). The two samples for which no population profile was obtained was due to small sample size, all available sample was used for MPN analysis. Data was obtained from well 2248 soil, scale, and annulus fluids (Table 6.A).

- Between 51894 and 75871 sequences were analyzed from each sample, for a total of 514405 sequences in all.
- These correlated to between 157 and 428 species in each sample, for a total of 690 species in all.
    - This value doesn't include the full breakdown of the number of organisms with an "unclassified" annotation, and so is an underestimation.
- Soils and the conductor solids had the highest diversity, at 428 and 406 species each
- Casing C001 Scale samples were uniform, with between 157 to 174 species each

Table 6.A provides an overall summary of population profile data from well 2248 samples.

Table 6. Well 2248 Microbial Population Profile Analysis: Overview of all DNA sequence data sets

Seq ID	OG2302 07-002	OG2304 06-001	OG2304 06-002	OG2304 06-003	OG2304 06-004	OG2304 06-005	OG2304 09-003	OG2304 09-006	Total
Sample Details	s2 w2248 Soils	s52 w2248, C001 OD Scale	s53 w2248 C001 Coup.	s54 w2248, C001 OD Scale	s55 w2248, Cond. OD Scale	s59 w2248 95/8" ID Solids	s51 w2248, Annulus Liquids	s56 w2248 C001 OD Scale	8 Samples
6.A Number of sequences and Number Species									
# Seq	61183	66894	65903	55347	51894	75732	75871	61581	514405
# Spp	428	161	159	157	406	174	163	166	690
6.B Selected Traits Relative Abundance and Number Species									
Aerobe	20.2% 63	62.93% 41	71% 36	69.67% 38	42.09% 60	60.67% 40	56.78% 37	51.71% 36	54.93% 96
APB	2.48% 15	7.43% 5	8.39% 10	5.73% 8	2.79% 16	4.16% 10	10.01% 9	15.45% 9	8.58% 31
BioDeg	23.2% 72	17.63% 36	18.22% 29	14.88% 33	18.33% 70	36.44% 35	24.93% 32	20.24% 33	22.3% 107
GHB	12.0% 54	57.95% 30	50.61% 28	68.32% 31	34.82% 48	38.16% 28	56.02% 28	56.71% 29	46.98% 80
IRB	2.15% 9	0.034% 2	0.008% 1	0.005% 2	1.31% 8	0.042% 2	0.003% 1	0.002% 1	0.401% 11
Spore	1.21% 9	5.2% 11	2.17% 10	4.75% 11	1.09% 22	1.56% 11	5.2% 13	4.34% 14	3.24% 29
Sulfidogen	0.84 ; 14	0.36 ; 3	0.22 ; 4	0.31 ; 4	0.57 ; 12	0.39 ; 5	0.33 ; 4	0.84 ; 14	0.44 ; 23
6.C Selected Classes: Relative Abundance and Number Species									
Unclassified	36.8% 34	2.44% 6	2.46% 5	2.46% 5	25.59% 31	1.02% 7	5.68% 3	3.69% 4	9.29% 49
AlphaP	11.8% 84	43.02% 34	13.32% 38	28.84% 35	9.66% 84	61.12% 35	38.11% 32	39.97% 33	32.1% 128
BetaP	11.7% 34	18.07% 20	47.38% 13	40.70% 16	11.98% 37	2.01% 17	6.92% 18	3.69% 13	17.16% 58
GammaP	10.6% 35	1.56% 9	9.40% 9	4.27% 12	6.08% 42	6.58% 14	5.32% 11	4.38% 10	6.03% 62
Actinobacteria	10.5% 54	23.36% 39	18.71% 38	15.28% 36	32.39% 44	20.41% 38	26.79% 36	27.77% 37	21.88% 88
DeltaP	3.18% 38	0% 0	0.003% 2	0% 0	1.34% 22	0.01% 2	0.001% 1	0.006% 1	0.51% 41
Bacilli	0.83% 18	10.48% 22	7.93% 25	7.08% 22	2.74% 29	7.50% 23	15.27% 29	19.02% 28	9.15% 54
Clostridia	0.81% 12	0.42% 8	0.31% 9	0.56% 9	2.27% 20	0.54% 10	0.67% 9	0.51% 13	0.72% 40

Well 2248 Population Breakdown: 6.A Number of sequences analyzed (#Seq) and the number of species identified (#Spp) in each sample. 6.B.Selected physiological traits relative abundance and number of species. In each cell, the first number is % of total population, yellow are >10%. The second Number is number of species. Selected Traits: Aerobe (growth in oxygen), APB (acid producing bacteria), BioDeg (biodegrading organism) GHB (General Heterotrophic Bacteria), IRB (Iron Reducing Bacteria), Spore (spore-forming bacteria), Sulfide: Sulfidogen (Hydrogen Sulfide Producing (includes SRB, TRB, SuRB and some peptide fermentation bacteria), Note that for Selected Traits of Interest, the % add up to more than 100 because organisms have more than one trait (e.g. Some sulfidogens, APB, GHB, and IRB are spore-forming). 6.C Selected taxonomic classes with the highest number of associated species, relative abundance in the sample and number of species belonging to that class. In each cell, the first number is % of total population, yellow are >10%. GammaP, BetaP, AlphaP and DeltaP are Gammaproteobacteria, Betaproteobacteria, Alphaproteobacteria, and Deltaproteobacteria, respectively. Note that for taxonomic classification, the % will add up to 100 at most, because organisms belong to only one class. Unclassified organisms did not closely match an organism with a full taxonomic annotation. This category includes multiple different types of organisms and will be expanded on later.

Well 2248 microbial population: Functional Trait Profiles Table 6.B
Each of the species identified in the samples was assigned a "Functional Trait Profile" that includes select metabolic, physiological, ecological, and taxonomic tags. Note that the functional trait % of population adds up to over 100% because organisms can have more than 1 functional trait assigned (eg, some GHB are also APB and Biodegrading organisms).

The trait profile tags are generated by analysis of the published scientific literature for that species, or closely related species (when relevant). The trait assignment database in inherently incomplete, because not every organism has been subject to the same degree of experimental investigation, and so the information is not known. Despite nuances and limitations, "Trait Profile" analysis is the best way to correlate the identity of the organisms in a sample to insight as to what the organisms identified in a sample are actually doing.
Table 6.B provides the functional trait overview for each of the samples sequenced from well 2248. Only the traits with the highest % of the population of each sample are included.

Summary of 3 most represented functional traits for well 2248:

1. **Aerobe:** By far the most well represented functional trait was that of Aerobe, at 54% of all sequences with 96 different organisms. Values ranged from 20% in soil to 71% in the coupling scale sample.
2. **GHB:** Between 12% and 68% of all organisms, including most of the aerobes, were annotated as General Heterotrophic Bacteria.
3. **APB:** APB accounted for almost 9% of all organisms, with 31 species.
4. **BioDeg:** Biodegrading organisms accounted for between 17% and 36% of each sample, with 107 different types.

- APB were present in all samples, at between 2% and 9% of the population. This is consistent with MPN analysis, where GHB were slightly elevated as compared to APB. It is likely, however, that both GHB and APB are not fully accounted for in the annotation algorithm, which as stated is limited by available data for each organism.
- SRB and IRB were present, but low percentage of the populations. Sulfidogens did not account for even 1% of any one sample, and in most cases IRB levels were about 10% of sulfidogens. The exception was the conductor, which according to MPN results had higher IRB levels then SRB levels.
- Overall, data from diversity analysis was quite consistent with MPN analysis.
- Interestingly **Unclassified organisms**, a category that made up a significant proportion of the organisms from well 2244, were abundant in only two of the 8 samples from well 2248: the soil sample (36%) and the scale from the conductor (25%). This indicates that unknown organisms do not play as important a potential role in well 2248 scale and annulus samples.

Well 2248 microbial population: Class Level Taxonomic Profiles (Table 6.C)

- A higher-level profile of bacteria identified in well 2248 can be obtained by evaluating the most abundant organisms at a Class level designation (Table 7.C).
- The Classes with the highest number of individual species were calculated for each sample (Table 7.C)
- Particularly dominant Class included Alphaproteobacteria, Betaproteobacteria, Gammaproteobacteria, and Actinobacteria. Each of these are Classes include a large number of GHB, generalists, facultative and strict aerobes, as well as soil dwelling and biodegrading organisms.
- Class Clostridia and Deltaproteobacteria, two classes that include many strict anaerobes and sulfidogens, were not as well represented as in well 2244

Well 2248 microbial population: Most Abundant Species (Table 7)

- In all, 690 species of bacteria, not including "unclassified" organisms were identified in the 8 sequence data sets from well 2248 (see Appendix B, All Species).
- Of 690 organisms, 632 were "low abundance" organisms, that is present at less than 1% of all samples they were found in
- Of 690 organisms, 490 were present in only 1 or 2 samples
- Only 8 species were present at greater than 10% of at least one of the samples they were found in (Table 7 and Appendix A).
- This population profile, in which the majority of organisms are present in only 1 or 2 different samples, and at less than 1% of the sample population, is typical for natural populations of bacteria.
- The most abundant organisms were aerobic, GHB and not MIC associated, for example Pseudochrobactrum and Paenalcaligenes
- The most abundant and prevalent APB was Enteractinococcus fodinae, an organism initially isolated from a coal mine

Well 2248 Samples Unclassified Organisms (Table 8)

- All samples from well 2248 contained unclassified organisms, at between 1% and 36% of the sample
- Unlike well 2244, only 2 of 8 well 2248 samples were characterized by a high % of unclassified organisms.
- Unclassified organisms from well 2248 were examined in greater detail, by determining the number of individual types of organisms, and determining their taxonomic relationships.
- In all, there were 143 different types of unclassified organisms.
- The top organisms out of 143, different unclassified organisms are provided in Table 8
  - Top is defined as the most abundant, determined by the maximum value for any sample, as well as some particularly widespread organisms (present in many samples)
- Samples were not dominated by any one type, but instead several different organisms vied for the tope most abundant organisms.
- Population similarity between the soil sample and the conductor is apparent, as the unclassified organisms were largely shared between the two samples.
- Acidobacteria contributed to most of the unclassified organisms in the conductor and soil sample
  - As the name implied, Acidobacteria includes acid tolerant species
- Potential APB in the scale an annulus fluid samples includes Lachnospiraceae, a family including species of butyric acid producing anaerobes
- A few low abundance Deltaproteobacteria were identified, these are candidate IRB and SRB
- Fewer candidate SRB were identified in the scale and annulus fluid samples
- Overall, it is apparent unclassified organisms might include APB in particular
- There was less evidence for unclassified SRB, and IRB.
- However, experimental data is required to verify this.

Well 2248 Sulfidogenic and Iron Reducing Organisms (Table 9)

- Although sulfidogens did not compromise more than 1% of any sample, all samples from well 2248 contained sulfidogens (Table 10)
- In all, there 23 sulfidogenic taxa identified in samples from well 2248.
- Sulfidogens included SRB, TRB, and SuRB as well as peptide fermenting organisms.
- 9 were from the Class Clostridia,
  - 5 of these were spore-forming genera,
- 11 were from Class Deltaproteobacteria.
- Halanaerobium was present at a low % of the population in 2 samples.
- Similar to sulfidogens, IRB were present in all samples, but at very low abundance. The two most widespread IRB were Rhodoferax and Geosporobacter, similar to what was observed for well 2244.

Table 7. Well 2248 soil, scale, and annulus fluid samples, Top 20 most abundant organisms

Sequence ID	OG230207-002	OG230406-001	OG230406-002	OG230406-003	OG230409-006	OG230406-004	OG230406-005	OG230409-003	Metabolism
Species	s2 w2248 Soils	s52 w2248, C001 OD Scale	s53 w2248 C001 Coup.	s54 w2248, C001 OD Scale	s56 w2248 C001 OD Scale	s55 w2248, Cond. OD Scale	s59 w2248 9 5/8" ID Solids	s51 w2248, Annulus Liquids	Select Traits of Interest: Metabolic, Physiological, Ecological, Taxonomic
Unclassified	33.45	1.27	0.75	1.48	1.45	21.91	0.67	1.95	Polyphyletic; Unknown; Varies
Pseudochrobactrum sp	0.03	33.34	3.27	12.82	32.69	0.57	24.88	30.13	Aerobe; AlphaP; GHB
Paenalcaligenes hominis	0.00	8.42	19.68	31.41	1.26	0.83	0.78	5.04	Aerobe; Bacteroidetes; BetaP; Bioreactor; Generalist; GHB
Arthrobacter sp	2.04	0.61	0.49	0.49	0.64	27.60	0.12	1.12	Actinobacteria; Aerobe; GHB; Soil
Alcaligenes faecalis	0.00	6.04	21.26	1.36	0.90	0.06	0.35	0.32	Aerobe; Alkaliphile; BetaP; NRB
Falsochrobactrum ovis	0.00	0.83	8.07	11.48	0.49	0.36	0.20	0.64	Aerobe; AlphaP; Generalist; GHB
Hyphomicrobium sulfonivorans	0.00	0.65	0.09	0.39	0.34	0.23	11.33	0.44	Aerobe; AlphaP; BioDeg; Methylotroph; Soil
Hyphomicrobium sp	1.09	0.46	0.18	0.38	0.12	1.03	10.22	0.06	Aerobe; AlphaP; BioDeg; Methylotroph; Soil
Pseudomonas sp	0.29	1.15	9.33	4.03	3.90	0.31	2.41	5.23	Aerobe; BioDeg; GammaP; GHB; Varies; Versatile; Common
Enteractinococcus fodinae	0.09	5.11	5.36	3.79	7.67	0.04	2.16	4.91	APB, Coal mine; Generalist; GHB; Soil
Leucobacter aridicollis	0.02	2.70	2.80	2.14	3.03	0.01	1.16	6.50	Actinobacteria; Aerobe; BioDeg; BioDeg Chromium tolerant
Atopostipes sp	0.00	1.77	2.67	1.29	6.12	0.03	1.29	2.48	APB; Ferm; Firmicutes; LAB; Lactobacillales
Pusillimonas sp	0.00	1.95	3.12	5.86	0.32	0.26	0.12	0.91	AOX; BetaP
Mesorhizobium sp	0.24	0.67	0.24	0.51	0.54	0.15	5.08	0.40	AlphaP; NiF; Soil
Polaromonas sp	1.54	0.004	0.00	0.002	0.00	4.22	0.00	0.00	BetaP; BioDeg; BioDeg HC
Psychrobacter sp	0.01	0.00	0.00	0.00	0.00	0.32	3.96	0.00	BioDeg; BioDeg HC; GammaP; Oilfield
Timonella senegalensis	0.00	1.09	1.62	0.91	2.15	0.004	0.25	3.68	
Defluvibacter sp	0.00	2.41	0.44	1.30	2.12	0.08	3.52	2.96	Aerobe; AlphaP; Aquamicrobium; BioDeg; BioDeg chlorophenol; WWTP
Streptomyces sp	0.17	3.50	1.07	3.23	1.84	0.15	0.67	2.62	Actinobacteria; BioDeg; Filamentous; Soil; Spore
Trichococcus sp	0.05	0.64	0.60	0.39	1.08	0.69	0.58	3.46	Activated Sludge; APB; Facultative Anaerobe; Ferm; Filamentous; Firmicutes; Lactobacillales; Wastewater

Top 20 organism identified in well 2248 samples. The value is the % of the total population. Yellow are >10% of the population, Blue are 1 – 10% of the population, White are <1% Gray are 0% not identified in sample. Trait Details: Polyphyletic (is not a homogenous grouping and includes multiple species) Unknown (traits are not known), Varies (likely to have multiple different traits), BioDeg (biodegrading organism capable of utilization of specialized substrates) GHB (general heterotrophic bacteria), Activated Sludge (present in activated sludge), Spore (spore-forming organism), APB (acid producing bacteria), Anaerobe / Aerobe (growth in absence or presence of oxygen, respectively), GammaP, BetaP, AlphaP and DeltaP are Gammaproteobacteria, Betaproteobacteria, Alphaproteobacteria, and Deltaproteobacteria, respectively.

Table 8. Well 2248. Most abundant Unclassified Organisms in soil, scale, and annulus fluids

Taxonomic Lineage				Sequence ID	OG230207-002	OG230406-001	OG230406-002	OG230406-003	OG230406-004	OG230406-005	OG230409-003	OG230409-006
Kingdom	Phylum	Class	Order	Family	s2 w2248 Soils	s52 w2248, C001 OD Scale	s53 w2248 C001 Coup.	s54 w2248, C001 OD Scale	s55 w2248, Cond. OD Scale	s59 w2248 95/8" ID Solids	s51 w2248, Annulus Liquids	s56 w2248 C001 OD Scale
Bacteria	Unclassified	Unclassified	Unclassified	Unclassified	4.89	0.37	0.3	0.33	4.44	0.16	0.89	0.48
Bacteria	Acidobacteria	Acidobacteriia	Acidobacteriales	Unclassified	4.86	0	0	0	2.1	0	0	0
Bacteria	Acidobacteria	Acidobacteriia	Unclassified	Unclassified	3.65	0	0	0	1.68	0	0	0
Bacteria	Proteobacteria	Alphaproteobacteria	Rhizobiales	Unclassified	0.87	0.4	0.09	0.2	0.92	0.16	0.23	0.38
Bacteria	Bacteroidetes	Unclassified	Unclassified	Unclassified	0.52	0.35	0.14	0.79	0.34	0.05	0.62	0.35
Bacteria	Planctomycetes	Planctomycetia	Planctomycetales	Unclassified	1.67	0	0	0	1.23	0	0	0
Bacteria	Bacteroidetes	Sphingobacteriia	Sphingobacteriales	Unclassified	1.29	<.01	<.01	0	0.75	0.02	0	0.01
Bacteria	Proteobacteria	Unclassified	Unclassified	Unclassified	1.36	0	0.01	<.01	0.32	<.01	0.01	0
Bacteria	Proteobacteria	Deltaproteobacteria	Unclassified	Unclassified	1.31	0	0	0	0.33	0	0	0
Bacteria	Actinobacteria	Actinobacteria	Unclassified	Unclassified	0.81	0.09	0.12	0.05	0.4	0.08	0.01	0.02
Bacteria	Verrucomicrobia	Unclassified	Unclassified	Unclassified	1.01	0.01	0.01	<.01	0.31	0.03	0	0.01
Bacteria	Actinobacteria	Rubrobacteria	Rubrobacterales	Unclassified	0.29	<.01	0.01	0.01	0.26	0	0<.01	0.02
Bacteria	Firmicutes	Clostridia	Clostridiales	Lachnospiraceae	0	0.02	0.02	0.06	0.03	0.01	0.03	0.04
Bacteria	Firmicutes	Clostridia	Unclassified	Unclassified	<.01	<.01	0.02	<.01	0.02	0.02	0.01	0.04
Bacteria	Firmicutes	Clostridia	Clostridiales	Unclassified	0	<.01	0.01	0.01	<.01	0.01	0.02	0.03
Bacteria	Firmicutes	Bacilli	Bacillales	Unclassified	0.01	0.01	0.01	0.01	<.01	0	0.01	0.03
				% of population	36.2	2.44	2.46	2.47	25.1	1.02	5.68	3.69
				# of types	109	18	18	17	118	19	15	17

Table Legend: Most Abundant unclassified organisms, out of 143. All are unclassified at the Genus level. Expanded taxonomic lineages of "Unclassified" organisms. "Unclassified" is a designation provided to sequences whose closest matches in the public database lacks taxonomic information. Unclassified is a polyphyletic term, and may include numerous different types of organisms. This table provides more details on the diversity of unclassified organisms, showing the top most abundant types, with expanded lineages, where the highest level at which unclassified is designated are indicated in red. The value is the % of the total population. Yellow are >10% of the population, Blue are 1 – 10% of the population, White are <1% Gray are 0% not identified in sample.in the sample). <.01 indicates a valus >0, <.01The bottom two rows (% and # Taxa) indicate the total % of all unclassified for that sample, and the number of different unclassified organisms.

M 979-694-6500 ● F 979-694-6511 ● 11142 Hopes Creek Road ● College Station, Texas 77845 ● www.ecolyse.com

Table 9. Well 2248 sulfidogens soil, scale, and annulus fluids									
Species	OG230 207-002	OG230 406-001	OG230 406-002	OG230 406-003	OG23 0406-004	OG23 0406-005	OG230 409-003	OG230 409-006	Metabolism
Species	s2 w2248 Soil	s52 w2248 C001 OD Scale	s53 w2248 C001 Coup. Scale	s54 w2248 C001 OD Scale	s55 w2248 Cond. OD Scale	s59 w2248 9 5/8" ID Solids	s51 w2248, Annulus Liquids	s56 w2248 C001 OD Scale	
Alkaliphilus halophilus	0	0.003	0	0.023	0	0	0.012	0.005	Alkaliphile; Anaerobe; Clostridia; Firmicutes; Halophile; Peptide Ferm; Spore; Sulfidogen
Alkaliphilus sp	0	0.069	0.03	0.022	0	0.24	0.014	0.016	Alkaliphile; Anaerobe; Clostridia; Firmicutes; Halophile; Peptide Ferm; Sulfidogen
Citrobacter sp	0	0	0	0	0.008	0.011	0.008	0	Aerobe; Biofilm; GammaP; MIC; NRB; Sulfidogen
Desulfitobacterium sp	0	0	0	0	0.048	0	0	0	Anaerobe; BioDeg; BioDeg halogenated organic compounds; Clostridia; Ferm; Firmicutes; Metal Reduction; NiF; SIRB; Spore; Sulfidogen; SuRB; TRB
Desulfobacter sp	0.007	0	0	0	0	0	0	0	Anaerobe; DeltaP; SRB; Sulfidogen
Desulfobacterium sp	0	0	0	0	0.008	0	0	0	Anaerobe; BioDeg; BioDeg Benzene; DeltaP; SRB; Sulfidogen
Desulfobulbus sp	0.003	0	0	0	0.01	0	0	0	Anaerobe; DeltaP; SRB; Sulfidogen
Desulfocurvus sp	0.003	0	0	0	0	0	0	0	Anaerobe; DeltaP; Gas storage well; SRB; Sulfidogen
Desulfomonile sp	0.026	0	0	0	0	0	0	0	Anaerobe; BioDeg; BioDeg Benzene; DeltaP; SRB; Sulfidogen
Desulforegula sp	0.057	0	0	0	0.052	0	0	0	Anaerobe; DeltaP; SRB; Sulfidogen
Desulfosporosinus sp	0	0.294	0.18	0.266	0.156	0.099	0.419	0.299	Anaerobe; Clostridia; Firmicutes; Spore; SRB; Sulfidogen
Desulfotalea sp	0	0	0	0	0.108	0	0	0	Anaerobe; DeltaP; SRB; Sulfidogen
Desulfovibrio sp	0.015	0	0	0	0.017	0	0	0	Anaerobe; DeltaP; SRB; Sulfidogen
Fusibacter sp	0.002	0	0.002	0	0.006	0	0	0	Anaerobe; Clostridia; Firmicutes; Sulfidogen; SuRB; TRB
Halanaerobium sp	0	0	0	0.005	0	0.02	0	0	Anaerobe; APB; Clostridia; Ferm; Firmicutes; Halophile; Methanogen-Promoting; MIC; SRB-Promoting; Sulfidogen; SuRB; TRB
Limnobacter sp	0.059	0	0	0	0	0	0	0	BetaP; Sulfidogen; TRB
Moorella sp	0.569	0	0	0	0.075	0	0	0	Acetogen; Anaerobe; APB; Clostridia; Ferm; Firmicutes; NRB; Spore; Sulfidogen; Thermophile; TRB
Syntrophobacter sp	0.042	0	0	0	0	0	0	0	BioDeg; BioDeg HC; DeltaP; Methanogen Syntroph; SRB; Sulfidogen
Thermoanaerobacter sp	0.002	0	0	0	0	0	0	0	Anaerobe; Clostridia; Ethanologenic; Ferm; Firmicutes; Sulfidogen; Thermophile; TRB
Thermoanaerobacterium saccharolyticum	0	0	0.01	0	0.012	0.025	0.028	0.01	Anaerobe; APB; Clostridia; Firmicutes; NRB; Spore; Sulfidogen; Thermophile; TRB
Thermodesulfovibrio sp	0.003	0	0	0	0	0	0	0	Anaerobe; Nitrospinae; SRB; Sulfidogen; Thermophile
Anaeromyxobacter dehalogenans	0.003	0	0	0	0	0	0	0	Anaerobe; DeltaP; IRB; XRB
Anaeromyxobacter sp	0.121	0	0	0	0.081	0	0	0	Anaerobe; DeltaP; IRB; XRB

Table 9. Well 2248 sulfidogens soil, scale, and annulus fluids

Species	OG230 207-002	OG230 406-001	OG230 406-002	OG230 406-003	OG23 0406-004	OG23 0406-005	OG230 409-003	OG230 409-006	Metabolism
Species	s2 w2248 Soil	s52 w2248 C001 OD Scale	s53 w2248 C001 Coup. Scale	s54 w2248 C001 OD Scale	s55 w2248 Cond. OD Scale	s59 w2248 9 5/8" ID Solids	s51 w2248, Annulus Liquids	s56 w2248 C001 OD Scale	
Bacillus thermoamylovorans	0	0	0	0	0	0	0.003	0.002	Bacilli; Firmicutes; IRB; Spore; Thermophile
Desulfuromonas sp	0.049	0	0	0	0.073	0	0	0	Anaerobe; DeltaP; IRB; Sulfidogen; SuRB
Desulfuromusa sp	0.003	0	0	0	0	0	0	0	Anaerobe; DeltaP; IRB; Sulfidogen; SuRB
Geoalkalibacter sp	0.082	0	0	0	0.048	0	0	0	Anaerobe; DeltaP; IRB; Thermophile
Geobacter sp	0.289	0	0	0	0.154	0	0	0	Anaerobe; BioDeg; BioDeg HC; Biofilm; DeltaP; IRB; Metal Reduction;
Geosporobacter sp	0	0.001	0	0.002	0.017	0.026	0	0	Anaerobe; Clostridia; Ferm; Firmicutes; IRB; Spore
Geothrix sp	0.052	0	0	0	0.008	0	0	0	Acidobacteria; Anaerobe; IRB
Pelobacter sp	0.791	0	0	0	0.085	0	0	0	Anaerobe; DeltaP; IRB
Rhodoferax sp	0.758	0.033	0.01	0.004	0.848	0.016	0	0	BetaP; IRB

Sulfidogenic and IRB identified in well 2248 samples. The value is the % of the total population. Yellow are >10% of the population, Blue are 1 – 10% of the population, White are <1% Gray are 0% not identified in sample. Trait Details: Polyphyletic (is not a homogenous grouping and includes multiple species) Unknown (traits are not known), Varies (likely to have multiple different traits), BioDeg (biodegrading organism capable of utilization of specialized substrates) GHB (general heterotrophic bacteria), Activated Sludge (present in activated sludge), Spore (spore-forming organism), APB (acid producing bacteria), Anaerobe / Aerobe (growth in absence or presence of oxygen, respectively), GammaP, BetaP, AlphaP and DeltaP are Gammaproteobacteria, Betaproteobacteria, Alphaproteobacteria, and Deltaproteobacteria, respectively.

Pool	BLRM Sample ID	Corresponding Blade Sample ID	Sample Description: Source Well, Casing Joint, Sample Type	Sample Date	Quantity g or ml
49	BLRM230317-001	no sample ID	Well 2248 Scale Annulus valve Solids	3/17/23	0.8
50	BLRM230317-002	no sample ID	Well 2248 Scale Annulus valve Solids	3/17/23	0.8
51	BLRM230326-001	no sample ID	Well 2248 Fluids Annulus Liquid Sample	3/26/23	500
52	BLRM230326-002	RM-2248-C001-S1	Well 2248, C001 Scale Sample OD	3/26/23	190
53	BLRM230326-003	RM-2248-C001-S2	Well 2248, C001 Scale Sample Couplings	3/26/23	28.2
54	BLRM230326-004	no sample ID	Well 2248, C001 OD Scale, 4 - 5 lbs	3/26/23	2360
55	BLRM230326-005	no sample ID	Well 2248 Scale OD Scale, Conductor	3/26/23	91.5
56	BLRM230328-001	2248-C001-S4	Well 2248 Scale C001 Scale OD sample	3/28/23	7.5
57	BLRM230328-002	no sample ID	Compressor Station Seperator Fluid, Black. Chemical smell	3/28/23	200
58	BLRM230328-003	no sample ID	Compressor Station Seperator Fluid, Clear. Chemical smell	3/28/23	200
59	BLRM230329-001	RM-2248-958-S1	Well 2248 Scale Uppermost 9 5/8" casing ID scrape	3/29/23	70.8
60	BLRM230401-001	RM-Pond-L1	Compressor Station Fluid pond sample, clear	4/1/23	500
61	BLRM230401-002	RM-Pond-L2	Compressor Station Fluid pond sample, emulsion	4/1/23	500
62	BLRM230403-001	RM-2251-C001-S01	Well 2251 Scale 7" OD, C001 top of joint	4/3/23	23.2
63	BLRM230403-002	RM-2251-C001-S02	Well 2251 Scale 7" OD, C001 top of joint	4/3/23	508.5
64	BLRM230403-003	RM-2251-C001-S03	Well 2251 Scale 7" OD, C001 10'6" top of cement	4/3/23	9.2

Appendix A. Well 2248, 2251 and Compressor Station Samples. BLRM numbers are "Blade Rager Mountain" sample identification numbers indicating year, month, day of collection.

Sequence ID	OG230207-002	OG230406-001	OG230406-002	OG230406-003	OG230406-004	OG230406-005	OG230409-003	OG230409-006	Select Traits
Species	s2 w2248 Soil	s52 w2248 C001 OD Scale	s53 w2248 C001 Coup. Scale	s54 w2248 C001 OD Scale	s56 w2248 C001 OD Scale	s55 w2248 Cond. OD Scale	s59 w2248 9 5/8" ID Solids	s51 w2248, Annulus Liquids	Metabolism, Ecology, Physiology, Taxonomy
Acetivibrio sp	0.007	0	0	0	0	0	0	0.006	BioDeg; Clostridia; Firmicutes; Plant biomass
Acetobacterium sp	0	0	0	0	0	0.012	0	0	Acetic Acid; Acetogen; Anaerobe; APB; Clostridia; Firmicutes
Acetonema sp	0	0	0	0	0.085	0	0	0	
Achromobacter sp	0	0.306	0.052	0.159	0	0.073	0.078	0.432	Aerobe; BetaP; BioDeg; NRB; Soil
Acidimicrobium sp	0	0	0	0	0.037	0	0	0	Acidophile; Actinobacteria; APB; FeOX; SOB
Acidisphaera rubrifaciens	0.008	0	0	0	0	0	0	0	AlphaP
Aciditerrimonas sp	0.069	0	0	0	0.129	0	0	0	Acidophile; Actinobacteria; APB; FeOX; SOB
Acidobacterium sp	1.608	0	0	0	1.351	0	0	0	Acidobacteria; Acidophile; Aerobe; APB
Acidocella sp	0.005	0	0	0	0	0	0	0	Acidophile; AlphaP; APB
Acidothermus sp	0.016	0	0	0	0	0	0	0	Acidophile; Actinobacteria; APB; BioDeg Cellulose; Thermophile
Acidovorax sp	1.151	0	0	0	0	0	0	0	Anaerobe; BetaP; Facultative; Facultative Anaerobe; Fe(II)OX; Green Rust; MIC; NRB
Acinetobacter sp	1.299	0	0.003	0	0.283	0.02	0	0	Aerobe; BioDeg HC; GammaP; Soil
Actinomadura sp	0.002	0	0	0	0	0	0	0	Actinobacteria
Actinomyces sp	0.49	0	0	0	0.094	0	0	0	Actinobacteria; Ferm
Actinomycetospora sp	0.355	0	0	0	0	0	0	0	Actinobacteria
Actinoplanes abujensis	0.021	0	0	0	0	0	0	0	Actinomycete; Faculatative; Soil
Actinoplanes auranticolor	0	0	0	0	0.006	0.008	0	0	Actinobacteria
Actinoplanes friuliensis	0.078	0	0	0	0	0	0	0.013	
Actinotalea fermentans	0	0	0	0	0	0	0.083	0.078	Actinobacteria; BioDeg Cellulose
Adhaeribacter sp	0.023	0	0	0	0.017	0	0	0	Bacteroidetes; Biofilm; GHB
Advenella kashmirensis	0	0.031	0.003	0.013	0	0.001	0	0	

Sequence ID	OG230207-002	OG230406-001	OG230406-002	OG230406-003	OG230406-004	OG230406-005	OG230409-003	OG230409-006	Select Traits
Species	s2 w2248 Soil	s52 w2248 C001 OD Scale	s53 w2248 C001 Coup. Scale	s54 w2248 C001 OD Scale	s56 w2248 C001 OD Scale	s55 w2248 Cond. OD Scale	s59 w2248 9 5/8" ID Solids	s51 w2248, Annulus Liquids	Metabolism, Ecology, Physiology, Taxonomy
Aeromicrobium fastidiosum	0	0	0	0	0	0	0.008	0.016	
Aeromicrobium kazakhstani	0.029	1.026	0.326	0.334	0	3.371	0.453	0.766	Actinomycete; Aerobe; Generalist; GHB
Aeromicrobium panaciterrae	0.077	0	0	0	0	0	0	0	
Aeromicrobium sp	0.003	0.007	0.006	0.005	0.187	0	0	0	Actinobacteria
Aeromonas sp	0	0	0	0	0.01	0	0	0	Facultative Anaerobe; GammaP; GHB; Water
Aetherobacter rufus	0.003	0	0	0	0	0	0	0	
Afipia sp	0.018	0.004	0.003	0	0.037	0.017	0	0	AlphaP; Biofilm; MIC
Aggregicoccus edonensis	0.083	0	0	0	0	0	0	0	
Agreia sp	0	0	0	0	0	0	0.012	0.052	Actinobacteria
Agrobacterium vitis	0	0.001	0.003	0.005	0	0.011	0	0	AlphaP; NiF; Plant
Agromyces sp	0.005	0	0	0	0	0	0	0	Actinobacteria; BioDeg
Alcaligenes faecalis	0	6.039	21.262	1.355	0.058	0.345	0.316	0.904	Aerobe; Alkaliphile; BetaP; NRB
Alcaligenes sp	0	0.683	2.971	1.328	0.056	0.091	0	0	Aerobe; Alkaliphile; BetaP; NRB
Alicyclobacillus fastidiosus	0	0	0	0	0.006	0	0	0	Acidophile; Aerobe; APB; Bacilli; Firmicutes; ISOX; Spore; Thermophile
Alicyclobacillus sp	0	0	0	0	0.01	0	0	0	Acidophile; Aerobe; APB; Bacilli; Firmicutes; ISOX; Spore; Thermophile
Aliihoeflea aestuarii	0	0.003	0.002	0.009	0.033	0.001	0	0	AlphaP
Aliihoeflea sp	0	0	0	0	0	0	0.004	0.006	
Alkalilactibacillus ikkensis	0	0.034	0.038	0.036	0	0.046	0	0	
Alkalilimnicola sp	0	0	0	0	0.008	0	0	0	Alkaliphile; GammaP
Alkaliphilus halophilus	0	0.003	0	0.023	0	0	0.012	0.005	Alkaliphile; Anaerobe; Clostridia; Firmicutes; Halophile; Peptide Ferm; Spore; Sulfidogen
Alkaliphilus sp	0	0.069	0.027	0.022	0	0.24	0.014	0.016	Alkaliphile; Anaerobe; Clostridia; Firmicutes; Halophile; Peptide Ferm; Sulfidogen

Sequence ID	OG230207-002	OG230406-001	OG230406-002	OG230406-003	OG230406-004	OG230406-005	OG230409-003	OG230409-006	Select Traits
Species	s2 w2248 Soil	s52 w2248 C001 OD Scale	s53 w2248 C001 Coup. Scale	s54 w2248 C001 OD Scale	s56 w2248 C001 OD Scale	s55 w2248 Cond. OD Scale	s59 w2248 9 5/8" ID Solids	s51 w2248, Annulus Liquids	Metabolism, Ecology, Physiology, Taxonomy
Alkalispirillum sp	0	0	0	0	0.006	0	0	0	Alkaliphile; GammaP
Alkanindiges illinoisensis	0.234	0	0	0	0.112	0.007	0	0	Alkaliphile; BioDeg HC; GammaP; Oilfield
Alkanindiges sp	1.46	0	0	0	0.021	0	0	0	Alkaliphile; BioDeg HC; GammaP
Allobaculum sp	0	0	0.003	0	0	0	0	0.016	Erysipelotrichia; Firmicutes
Altererythrobacter sp	0.278	0	0	0	0.092	0	0	0	AlphaP; CT
Alterococcus agarolyticus	0.013	0	0	0	0	0	0	0	Verrucomicrobia
Amaricoccus sp	0.056	0	0	0	0.06	0	0.001	0	AlphaP; GHB
Amaricoccus tamworthensis	0.016	0	0	0	0.023	0	0	0	AlphaP
Aminobacter niigataensis	0	0.043	0.033	0.049	0.079	0.438	0	0	
Aminobacter sp	0.175	0.022	0.017	0.034	0.129	0.143	0.026	0.015	AlphaP
Amphibacillus sp	0	0	0	0	0	0	0.004	0.003	Bacilli; Firmicutes; GHB
Amycolatopsis sp	0	0.045	0.012	0.004	0	0.026	0.009	0.026	Actinobacteria
Amycolatopsis taiwanensis	0	0	0	0	0.006	0	0	0	
Anabaena sp	0	0	0	0	0.015	0	0	0	NiF; Phototroph
Anabaena variabilis	0.003	0	0	0	0	0	0	0	
Anaerolinea sp	0.065	0	0	0	0.019	0	0	0	Anaerobe; BioDeg; Chloroflexi; Filamentous; Thermophile
Anaeromyxobacter dehalogena	0.003	0	0	0	0	0	0	0	Anaerobe; DeltaP; IRB; XRB
Anaeromyxobacter sp	0.121	0	0	0	0.081	0	0	0	Anaerobe; DeltaP; IRB; XRB
Anaplasma sp	0	0	0	0	0.004	0	0	0	AlphaP
Ancylobacter sp	0.007	0	0	0	0.019	0	0	0	Aerobe; AlphaP; BioDeg
Anderseniella sp	0.026	0	0	0	0.1	0	0	0	Aerobe; AlphaP; GHB; Pigmented
Aquabacterium sp	1.144	0	0	0	0.449	0	0	0	Aerobe; BioDeg; MIC
Aquamicrobium aestuarii	0	0.132	0.093	0.15	0.017	0.57	0.19	0.216	
Aquicella sp	0.036	0	0	0	0.116	0	0	0	GammaP; Pathogen; Protazoan Pathogen
Aquihabitans daechungensis	0.121	0.006	0.005	0	0.023	0.007	0.004	0.005	Acidobacteria; Actinobacteria
Aquimonas sp	0.083	0	0	0	0	0	0	0	GammaP; GHB

Sequence ID	OG230207-002	OG230406-001	OG230406-002	OG230406-003	OG230406-004	OG230406-005	OG230409-003	OG230409-006	Select Traits
Species	s2 w2248 Soil	s52 w2248 C001 OD Scale	s53 w2248 C001 Coup. Scale	s54 w2248 C001 OD Scale	s56 w2248 C001 OD Scale	s55 w2248 Cond. OD Scale	s59 w2248 9 5/8" ID Solids	s51 w2248, Annulus Liquids	Metabolism, Ecology, Physiology, Taxonomy
Arcobacter sp	0	0	0.003	0.011	0	0	0	0	EpsilonP; Nitrate Injections; NRB; NRSOB; SOB
Arcobacter venerupis	0	0	0	0	0	0	0	0.005	EpsilonP; Injections; Nitrate; NRB; NRSOB; SOB
Arenimonas aquatica	0.266	0	0	0	0.181	0	0	0	GammaP; GHB
Arenimonas daechungensis	0.007	0	0	0	0	0	0	0	GammaP; GHB
Arenimonas sp	0.583	0	0	0	0.123	0	0	0	GammaP; GHB
Arthrobacter sp	2.043	0.607	0.49	0.486	27.595	0.115	1.123	0.641	Actinobacteria; Aerobe; GHB; Soil
Asaia sp	0	0	0	0	0.01	0	0	0	AlphaP
Asticcacaulis sp	0	0	0	0	0.013	0	0	0	AlphaP; Unknown
Atopostipes sp	0	1.768	2.669	1.29	0.029	1.293	2.477	6.12	APB; Ferm; Firmicutes; LAB; Lactobacillales
Aurantimonas sp	0.036	0.001	0.006	0	0.048	0.001	0	0	AlphaP; MnOX
Aureimonas altamirensis	0	0.235	0.035	0.078	0	0.559	0.174	0.296	AlphaP; GHB
Aureimonas ferruginea	0	0	0	0	0	0	0	0.032	
Azoarcus sp	0.065	0	0	0	0	0	0	0	BetaP; BioDeg; NiF
Azohydromonas lata	0.397	0	0	0	0	0	0	0	BetaP; BioDeg; NiF
Azomonas insignis	0	0	0	0.009	0	0	0	0	GammaP; NiF
Azospirillum sp	0.02	0	0	0	0.008	0	0	0	AlphaP; NiF
Bacillus clausii	0	0	0	0	0.019	0	0	0	Bacilli; Firmicutes; Spore
Bacillus gibsonii	0.003	0	0	0	0	0	0	0	
Bacillus hackensackii	0	0.01	0.003	0.007	0	0.03	0.005	0.015	
Bacillus horti	0	0	0	0	0.006	0	0	0	Bacilli; Firmicutes; Spore
Bacillus selenatarsenatis	0	0	0	0	0.017	0	0	0	
Bacillus sp	0.279	1.002	0.402	0.641	0.081	0.236	1.41	1.288	Bacilli; BioDeg; Diverse; Firmicutes; GHB; Spore
Bacillus thermoamylovorans	0	0	0	0	0	0	0.003	0.002	Bacilli; Firmicutes; IRB; Spore; Thermophile

Sequence ID	OG230207-002	OG230406-001	OG230406-002	OG230406-003	OG230406-004	OG230406-005	OG230409-003	OG230409-006	Select Traits
Species	s2 w2248 Soil	s52 w2248 C001 OD Scale	s53 w2248 C001 Coup. Scale	s54 w2248 C001 OD Scale	s56 w2248 C001 OD Scale	s55 w2248 Cond. OD Scale	s59 w2248 9 5/8" ID Solids	s51 w2248, Annulus Liquids	Metabolism, Ecology, Physiology, Taxonomy
Bacteriovorax sp	0.163	0	0	0	0.019	0	0	0	Bacterial Predator; DeltaP
Bacteriovorax stolpii	0.002	0	0	0	0.05	0	0	0	Bacterial Predator; DeltaP
Bacteroides sp	0	0	0	0	0.006	0	0.004	0	Anaerobe; Bacteroidetes; BioDeg; Ferm
Balneimonas sp	0.051	0	0	0	0	0	0	0	AlphaP
Bauldia consociata	0.011	0	0	0	0.013	0	0	0	
Bdellovibrio bacteriovorus	0.013	0	0	0	0	0	0.001	0.006	Bacterial Predator; DeltaP
Bdellovibrio exovorus	0.008	0	0	0	0	0	0	0	Bacterial Predator; DeltaP
Bdellovibrio sp	0.348	0	0.002	0	0.204	0.016	0	0	Bacterial Predator; DeltaP
Beggiatoa sp	0.747	0	0	0	0.628	0	0	0	Biofilm; GammaP; OX; SOB; White mats hydrocarbon seeps
Beijerinckia sp	0.034	0	0	0	0.11	0	0	0.002	AlphaP
Bellilinea sp	0.003	0	0	0	0	0	0	0	Chloroflexi; Oilfield; Tilling pond
Belnapia soli	0	0	0	0	0.008	0	0	0	Aerobe; AlphaP; Soil
Blastochloris sp	0.028	0	0	0	0	0	0	0	AlphaP
Blastococcus sp	0.098	0	0	0	0.029	0	0	0	Actinobacteria; Aerobe; Sediment; Stone; Unknown; Water
Blastomonas sp	0.003	0	0	0	0.023	0	0	0	AlphaP; CT
Blastopirellula sp	0.021	0	0	0	0	0	0	0	Planctomycetes
Blautia schinkii	0	0	0.015	0	0	0	0	0.015	
Blautia sp	0	0	0	0	0	0	0	0.013	BioDeg Cellulose; Clostridia; Ferm; Firmicutes
Bordetella sp	0	0.007	0.053	0.175	0.006	0.008	0.014	0.018	BetaP; Environmental; GHB
Bosea sp	0.052	0.262	0.05	0.164	0.123	0.734	0.389	0.309	AlphaP; GHB
Brachybacterium sp	0.025	0.737	0.827	0.376	0.004	0.283	0.783	1.207	Actinobacteria; BioDeg HC
Bradyrhizobium sp	0.955	0.106	0.05	0.099	0.38	0.668	0.079	0.083	AlphaP; NiF
Brevibacillus sp	0	0	0	0	0.025	0	0	0	Aerobe; Bacilli; Firmicutes; GHB; Spore
Brevibacterium sp	0.062	2.567	2.117	1.185	0.002	0.817	2.176	2.954	Actinobacteria; BioDeg HC
Brevundimonas sp	0.121	0.774	0.035	0.114	0.172	0.111	0.047	0.196	Aerobe; AlphaP; BioDeg HC; GHB

Sequence ID	OG230207-002	OG230406-001	OG230406-002	OG230406-003	OG230406-004	OG230406-005	OG230409-003	OG230409-006	Select Traits
Species	s2 w2248 Soil	s52 w2248 C001 OD Scale	s53 w2248 C001 Coup. Scale	s54 w2248 C001 OD Scale	s56 w2248 C001 OD Scale	s55 w2248 Cond. OD Scale	s59 w2248 9 5/8" ID Solids	s51 w2248, Annulus Liquids	Metabolism, Ecology, Physiology, Taxonomy
Burkholderia sp	0.371	0	0	0	0.143	0.012	0	0	Aerobe; BetaP; BioDeg; Soil
Burkholderia tropica	0	0.206	0.141	0.069	0.004	0.182	0.12	0.112	Aerobe; BetaP; BioDeg; Soil
Byssovorax sp	0.016	0	0	0	0.021	0	0	0	BioDeg Cellulose; DeltaP
Caedibacter sp	0	0	0	0	0.006	0	0	0	
Caenimonas sp	0.09	0	0	0	0	0	0.001	0	BetaP
Caldilinea sp	0.139	0	0	0	0.087	0	0	0	Chloroflexi; Facultative; Filamentous; Thermophile
Caldimonas hydrothermale	0.003	0	0	0	0	0	0	0	
Caldithrix sp	0	0	0	0	0.015	0	0	0	Anaerobe; Ferm; Thermophile
Camelimonas lactis	0	0.142	0.052	0.051	0.002	0.124	0.252	0.239	Aerobe; AlphaP
Candidatus Alysiosphaera euro	0.06	0	0	0	0	0	0	0	
Candidatus Brocadia carolinien	0	0	0	0	0	0	0.011	0.026	
Candidatus Burkholderia calva	0.02	0	0	0	0	0	0	0	BetaP
Candidatus Entotheonella pala	0.02	0	0	0	0	0	0	0	
Candidatus Koribacter sp	0.007	0	0	0	0	0	0	0	Acid Mine Drainage; Acidobacteria
Candidatus Metachlamydia lacu	0.08	0	0	0	0.048	0	0	0	Amoeba Symbiont; Chlamydiae; Symbiont
Candidatus Microthrix sp	0.013	0	0	0	0.004	0	0	0	Filamentous
Candidatus Odyssella sp	0	0	0	0	0.008	0	0	0	
Candidatus Protochlamydia am	0.011	0	0	0	0.021	0	0	0	Chlamydiae
Candidatus Protochlamydia sp	0.02	0	0	0	0.048	0	0	0	Chlamydiae
Candidatus Rhabdochlamydia	0	0	0	0	0.01	0	0	0	
Candidatus Solibacter sp	0.077	0	0	0	0.017	0	0	0	Acidobacteria; Aerobe; Biofilm; GHB; NRB; Soil
Carboxydothermus sp	0.011	0	0	0	0.025	0	0	0	Clostridia; Firmicutes
Carnobacterium maltaromaticur	0	0.012	0.003	0.002	0	0.013	0.795	0.183	Firmicutes; Lactobacillales
Carnobacterium sp	0	0.321	0.37	0.154	0.058	0.371	0.672	0.705	Firmicutes; Lactobacillales
Catellatospora sp	0.005	0	0	0	0	0	0	0	

Sequence ID	OG230207-002	OG230406-001	OG230406-002	OG230406-003	OG230406-004	OG230406-005	OG230409-003	OG230409-006	Select Traits
Species	s2 w2248 Soil	s52 w2248 C001 OD Scale	s53 w2248 C001 Coup. Scale	s54 w2248 C001 OD Scale	s56 w2248 C001 OD Scale	s55 w2248 Cond. OD Scale	s59 w2248 9 5/8" ID Solids	s51 w2248, Annulus Liquids	Metabolism, Ecology, Physiology, Taxonomy
Catellicoccus sp	0	0	0	0	0	0	0	0.008	
Caulobacter fusiformis	0.002	0	0	0	0	0	0	0	Aerobe; AlphaP; GHB; Oligotroph
Caulobacter sp	0.003	0	0	0	0.027	0	0	0	Aerobe; AlphaP; GHB; Oligotroph
Cellulomonas sp	0.078	0.039	0.077	0.051	0.154	0.079	0	0	Actinobacteria; Aerobe; BioDeg Cellulose; Facultative Anaerobe
Cellvibrio gandavensis	0.029	0	0	0	0	0	0	0	Aerobe; BioDeg Agar; BioDeg Cellulose; GammaP
Cellvibrio sp	0.029	0	0	0	0	0	0	0	Aerobe; BioDeg Agar; BioDeg Cellulose; GammaP
Cereibacter changlensis	0.008	0	0	0	0.012	0	0	0	AlphaP; Phototroph
Chitinophaga sp	0.369	0	0	0	0.162	0	0.001	0	Aerobe; Bacteroidetes; BioDeg
Chlamydia sp	0.041	0	0	0	0.031	0	0	0	Chlamydiae; Endosymbiont; Parasite; Pathogen
Chloracidobacterium sp	0.016	0	0	0	0	0	0	0	Acidobacteria; Microaerophile; Phototroph; Thermophile
Chloroflexus sp	0.09	0	0	0	0.127	0	0	0	Anoxygenic Phototroph; Chloroflexi; FAP; Filamentous; Phototroph
Chondromyces sp	0.033	0	0.002	0	0.077	0.003	0	0	DeltaP
Chroococcidiopsis sp	0.047	0	0	0	0	0	0	0	Phototroph
Chryseobacterium anthropi	0.023	0	0	0	0.042	0	0	0	Aerobe; Bacteroidetes; BioDeg; Food; Pigmented; Soil; Wastewater
Chryseobacterium jeonii	0	0	0	0	0	0	0.003	0	
Chryseobacterium luteum	0	0	0	0	0	0	0	0.003	
Citreicella sp	0	0	0	0	0	0	0.001	0	AlphaP
Citrobacter sp	0	0	0	0	0.008	0.011	0.008	0	Aerobe; Biofilm; GammaP; MIC; NRB; Sulfidogen
Clostridium algidixylanolyticum	0	0	0.003	0	0.006	0	0	0	Anaerobe; Clostridia; Firmicutes; Spore
Clostridium baratii	0.002	0	0	0	0	0	0	0	Anaerobe; Clostridia; Firmicutes; Spore

Sequence ID	OG230207-002	OG230406-001	OG230406-002	OG230406-003	OG230406-004	OG230406-005	OG230409-003	OG230409-006	Select Traits
Species	s2 w2248 Soil	s52 w2248 C001 OD Scale	s53 w2248 C001 Coup. Scale	s54 w2248 C001 OD Scale	s56 w2248 C001 OD Scale	s55 w2248 Cond. OD Scale	s59 w2248 9 5/8" ID Solids	s51 w2248, Annulus Liquids	Metabolism, Ecology, Physiology, Taxonomy
Clostridium botulinum	0	0.004	0	0.004	0.01	0.004	0.003	0.008	Anaerobe; Clostridia; Ferm; Firmicutes; GHB; Pathogen; Saprophyte; Spore
Clostridium colinum	0	0	0	0	0	0	0	0.003	
Clostridium cylindrosporum	0.005	0	0	0	0	0	0	0	Anaerobe; Clostridia; Firmicutes; Spore
Clostridium hydrogeniformans	0	0	0	0	0.01	0	0	0	
Clostridium luticellarii	0	0	0	0	0	0	0.001	0.003	Anaerobe; APB; Clostridia; Ferm; Firmicutes; Spore
Clostridium sp	0.085	0.042	0.055	0.231	0.316	0.111	0.187	0.123	Anaerobe; Clostridia; Diverse; Ferm; Firmicutes; GHB; Saprophyte; Spore
Clostridium sufflavum	0	0	0	0	0.008	0	0	0	Anaerobe; Clostridia; Firmicutes; Spore
Cohnella rhizosphaerae	0.002	0	0	0	0	0	0	0	
Cohnella sp	0.015	0.01	0.011	0.011	0.01	0.011	0.004	0.024	Aerobe; Bacilli; BioDeg Cellulose; Firmicutes; Spore
Comamonas sp	0	0	0	0	0	0	0.004	0	Aerobe; BetaP; BioDeg
Conexibacter sp	0.252	0.007	0.017	0.014	0.141	0.073	0.02	0.013	Actinobacteria; NRB
Conexibacter woesei	0	0	0	0.009	0	0	0.004	0.003	Actinobacteria
Coprococcus sp	0	0	0.008	0	0	0	0	0.006	Anaerobe; APB; Clostridia; Fecal; Ferm; Firmicutes
Coraliomargarita akajimensis	0.005	0	0	0	0	0	0	0	Verrucomicrobia
Corallococcus sp	0.379	0	0	0	0	0	0	0	DeltaP
Corynebacterium sp	0	0.078	0.053	0.119	0	0.022	0.036	0.097	Actinobacteria; Aerobe; GHB
Coxiella cheraxi	0.029	0	0	0	0.037	0	0	0	GammaP
Coxiella endosymbiont	0.033	0	0	0	0.048	0	0	0	Endosymbiont
Coxiella sp	0.031	0	0	0	0.019	0	0	0	GammaP
Criblamydia sequanensis	0	0	0	0	0.019	0	0	0	Chlamydiae
Croceicoccus sp	0	0	0	0	0.017	0	0	0	
Crocinitomix sp	0.01	0	0	0	0.008	0	0	0	Bacteroidetes; GHB
Cryobacterium sp	0.253	0.057	0.061	0.04	0.42	0.075	0	0	Actinobacteria

Sequence ID	OG230 207-002	OG230 406-001	OG230 406-002	OG230 406-003	OG230 406-004	OG230 406-005	OG230 409-003	OG230 409-006	Select Traits
Species	s2 w2248 Soil	s52 w2248 C001 OD Scale	s53 w2248 C001 Coup. Scale	s54 w2248 C001 OD Scale	s56 w2248 C001 OD Scale	s55 w2248 Cond. OD Scale	s59 w2248 9 5/8" ID Solids	s51 w2248, Annulus Liquids	Metabolism, Ecology, Physiology, Taxonomy
Cryptosporangium aurantiacum	0.011	0	0	0	0	0	0	0	
Cupriavidus sp	0.177	0	0	0	0.224	0	0	0	Aerobe; BetaP; BioDeg; GHB; Soil
Curvibacter fontanus	0	0	0	0	0.345	0	0	0	Aerobe; BetaP; GHB; Well Water
Cyanobacterium sp	0.078	0	0	0	0.027	0	0	0	Phototroph
Cytophaga hutchinsonii	0.093	0	0	0	0	0	0	0	Aerobe; Bacteroidetes; BioDeg Cellulose; Soil
Cytophaga sp	0.123	0.003	0	0	0.042	0	0	0	Aerobe; Bacteroidetes; BioDeg Cellulose; Soil
Dactylosporangium sp	0.002	0	0	0	0	0	0	0	Actinobacteria
Dechloromonas sp	0.108	0	0	0	0.096	0.033	0.134	0.005	Anaerobe; BetaP; NRB; PerRB
Defluvibacter sp	0	2.408	0.442	1.303	0.083	3.518	2.955	2.118	Aerobe; AlphaP; Aquamicrobium; BioDeg chlorophenol; WWTP
Defluviicoccus sp	0.005	0	0	0	0	0	0	0	AlphaP
Dehalobacter sp	0	0	0	0	0.008	0	0	0	Anaerobe; BioDeg Dichlorobenzene; Clostridia; Firmicutes
Dehalococcoides sp	0.016	0	0	0	0.092	0	0	0	BioDeg TCE; BioDeg XRB; Bioremediation; Chloroflexi; Vinyl Chloride Reducing
Dehalogenimonas sp	0.06	0	0	0	0.019	0	0	0	BioDeg
Deinococcus sp	0.018	0	0	0	0.008	0	0	0	Deinococcus-Thermus; polyextremophile; Radiation Resistant
Demequina sp	0	0.034	0.036	0.014	0.017	0.085	0	0	Actinobacteria; GHB
Derxia sp	0.307	0	0	0	0.006	0	0	0	BetaP; NiF
Desertibacter roseus	0	0	0	0	0.015	0	0	0	AlphaP
Desulfitobacterium sp	0	0	0	0	0.048	0	0	0	Anaerobe; BioDeg halogenated organic compounds; Clostridia; Ferm; Firmicutes; Metal Reduction; NiF; SIRB; Spore; Sulfidogen; SuRB; TRB

Sequence ID	OG230 207-002	OG230 406-001	OG230 406-002	OG230 406-003	OG230 406-004	OG230 406-005	OG230 409-003	OG230 409-006	Select Traits
Species	s2 w2248 Soil	s52 w2248 C001 OD Scale	s53 w2248 C001 Coup. Scale	s54 w2248 C001 OD Scale	s56 w2248 C001 OD Scale	s55 w2248 Cond. OD Scale	s59 w2248 9 5/8" ID Solids	s51 w2248, Annulus Liquids	Metabolism, Ecology, Physiology, Taxonomy
Desulfobacter sp	0.007	0	0	0	0	0	0	0	Anaerobe; DeltaP; SRB; Sulfidogen
Desulfobacterium sp	0	0	0	0	0.008	0	0	0	Anaerobe; BioDeg Benzene; DeltaP; SRB; Sulfidogen
Desulfobulbus sp	0.003	0	0	0	0.01	0	0	0	Anaerobe; DeltaP; SRB; Sulfidogen
Desulfocurvus sp	0.003	0	0	0	0	0	0	0	Anaerobe; DeltaP; Gas storage well; SRB; Sulfidogen
Desulfomonile sp	0.026	0	0	0	0	0	0	0	Anaerobe; BioDeg Benzene; DeltaP; SRB; Sulfidogen
Desulforegula sp	0.057	0	0	0	0.052	0	0	0	Anaerobe; DeltaP; SRB; Sulfidogen
Desulfosporosinus sp	0	0.294	0.182	0.266	0.156	0.099	0.419	0.299	Anaerobe; Clostridia; Firmicutes; Spore; SRB; Sulfidogen
Desulfotalea sp	0	0	0	0	0.108	0	0	0	Anaerobe; DeltaP; SRB; Sulfidogen
Desulfovibrio sp	0.015	0	0	0	0.017	0	0	0	Anaerobe; DeltaP; SRB; Sulfidogen
Desulfuromonas sp	0.049	0	0	0	0.073	0	0	0	Anaerobe; DeltaP; IRB; Sulfidogen; SuRB
Desulfuromusa sp	0.003	0	0	0	0	0	0	0	Anaerobe; DeltaP; IRB; Sulfidogen; SuRB
Devosia sp	0.181	0.007	0.014	0.022	0.069	0.044	0.008	0.003	AlphaP; GHB; NiF
Devosia submarina	0.021	0	0	0	0	0	0	0	Aerobe; Sediments
Devosia terrae	0	0.007	0.006	0.005	0.017	0.005	0	0	AlphaP; GHB; NiF
Dietzia sp	0.118	0.181	0.117	0.089	0.372	0.177	0.156	0.292	Actinobacteria; Aerobe; BioDeg; GHB
Dokdonella sp	0.018	0	0	0	0.004	0	0	0	GammaP
Dongia sp	0.111	0	0	0	0.006	0	0	0	AlphaP
Duganella sp	0.214	0	0	0	0	0	0	0	Aerobe; BetaP; GHB; Soil
Dyadobacter alkalitolerans	0.075	0	0	0	0	0	0	0	
Dyadobacter sp	0.02	0	0	0	0	0	0	0	Aerobe; Bacteroidetes; BioDeg

Sequence ID	OG230207-002	OG230406-001	OG230406-002	OG230406-003	OG230406-004	OG230406-005	OG230409-003	OG230409-006	Select Traits
Species	s2 w2248 Soil	s52 w2248 C001 OD Scale	s53 w2248 C001 Coup. Scale	s54 w2248 C001 OD Scale	s56 w2248 C001 OD Scale	s55 w2248 Cond. OD Scale	s59 w2248 9 5/8" ID Solids	s51 w2248, Annulus Liquids	Metabolism, Ecology, Physiology, Taxonomy
Ectothiorhodospira sp	0.007	0	0	0	0.044	0	0	0	Anaerobe; GammaP; Halophile; Phototroph; Purple Sulfur Bacteria; Sulfide-Oxidizing
Elioraea sp	0.01	0	0	0	0	0	0	0	
Elstera litoralis	0.011	0	0	0	0	0	0	0	Cyanobacteria; PhotoT; Phototrophic
Elusimicrobium sp	0.025	0	0	0	0.054	0	0	0	Elusimicrobia; Ultrabacterium
Emticicia sp	0.008	0	0	0	0	0	0	0	Bacteroidetes; GHB
Enteractinococcus fodinae	0.087	5.107	5.361	3.785	0.042	2.164	4.914	7.666	Coal mine; Generalist; GHB; Soil, APB
Enterococcus faecalis	0	0	0	0	0	0	0.008	0.01	APB; Facultative Anaerobe; Firmicutes; LAB; Lactobacillales
Enterorhabdus mucosicola	0	0	0	0.005	0	0	0.005	0	
Eoetvoesia caeni	0	0.003	0	0.002	0	0	0	0	
Eoetvoesia sp	0	0.013	0	0	0	0	0	0	BetaP
Erysipelothrix rhusiopathiae	0	0	0.003	0.004	0	0	0	0	Erysipelotrichia; Facultative Anaerobe; Firmicutes; GHB; Pathogen
Erythrobacter mathurensis	0.005	0	0	0	0	0	0	0	
Eubacterium coprostanoligenes	0	0.003	0.011	0.011	0	0.003	0.003	0	Acetic Acid; Acetogen; Anaerobe; APB; Butyrate; Clostridia; Ethanol; Firmicutes; SynGas
Eubacterium sp	0	0	0	0	0.015	0	0	0	Acetic Acid; Acetogen; Anaerobe; APB; Butyrate; Clostridia; Ethanol; Firmicutes; SynGas
Exiguobacterium sp	0.005	0	0	0	0.179	0	0	0	APB; GHB
Facklamia sp	0	0.601	0.495	0.103	0.01	0.209	0.859	0.917	Firmicutes; GHB; Lactobacillales
Falsochrobactrum ovis	0	0.828	8.071	11.478	0.364	0.202	0.643	0.494	Aerobe; AlphaP; Generalist; GHB
Ferribacterium sp	0.1	0	0	0	0.091	0	0.016	0	BetaP
Ferrimicrobium sp	0.026	0	0	0	0	0	0	0	Acidophile; Actinobacteria; APB; FeOX; SOB

Sequence ID	OG230207-002	OG230406-001	OG230406-002	OG230406-003	OG230406-004	OG230406-005	OG230409-003	OG230409-006	Select Traits
Species	s2 w2248 Soil	s52 w2248 C001 OD Scale	s53 w2248 C001 Coup. Scale	s54 w2248 C001 OD Scale	s56 w2248 C001 OD Scale	s55 w2248 Cond. OD Scale	s59 w2248 9 5/8" ID Solids	s51 w2248, Annulus Liquids	Metabolism, Ecology, Physiology, Taxonomy
Ferruginibacter sp	0.407	0	0	0	0	0	0	0	Bacteroidetes; BioDeg
Flavihumibacter sp	0.044	0	0	0	0	0	0	0	
Flavisolibacter sp	0.105	0	0	0	0.066	0	0	0	Bacteroidetes; Industrial Wastewater
Flavitalea sp	0.026	0	0	0	0.017	0	0	0	Bacteroidetes
Flavobacterium caeni	0.003	0	0	0	0	0	0	0	Aerobe; Bacteroidetes; BioDeg; Sludge
Flavobacterium cauense	0	0	0	0	0.035	0	0	0	Aerobe; Bacteroidetes; Water
Flavobacterium glaciei	0.111	0	0	0	0	0	0	0	Aerobe; Bacteroidetes; Water
Flavobacterium sp	1.548	0.018	0.008	0.031	0.767	0.009	0.445	0.237	Aerobe; Bacteroidetes; BioDeg HC; Water
Flavobacterium yanchengense	0	0.003	0	0	0	0.003	0	0	Aerobe; Bacteroidetes; BioDeg; Soil
Flexibacter flexilis	0.01	0	0	0	0	0	0	0	Bacteroidetes; BioDeg HC; Oilfield
Flexibacter sp	0.057	0	0	0	0.058	0	0	0	Bacteroidetes; BioDeg HC; Oilfield
Flexithrix dorotheae	0.003	0	0	0	0	0	0	0	Bacteroidetes
Fluviicola sp	0.016	0	0	0	0.015	0	0	0	Bacterioplankton; Bacteroidetes; GHB
Frankia sp	0.08	0	0	0	0.037	0	0	0	Actinobacteria; NiF
Frigoribacterium sp	0.196	0.022	0.029	0.007	0.012	0.251	0	0	Actinobacteria
Frondihabitans sp	0	0.094	0.044	0.023	0.019	0.172	0	0	
Fulvimonas yonginensis	0.007	0	0	0	0	0	0	0	
Fusibacter sp	0.002	0	0.002	0	0.006	0	0	0	Anaerobe; Clostridia; Firmicutes; Sulfidogen; SuRB; TRB
Fusobacterium nucleatum	0	0	0	0	0.008	0	0	0	Fusobacteria
Gaiella occulta	0	0	0	0	0.1	0	0	0	Actinobacteria; BioDeg
Gaiella sp	0.1	0	0	0	0.121	0.003	0	0	
Gallionella sp	0	0	0	0	0.01	0	0	0	BetaP; Biofilm
Gemella sp	0	0	0	0	0.004	0	0	0	GHB
Geminicoccus roseus	0.06	0	0	0	0.004	0	0	0	GHB
Gemmata sp	0.417	0	0	0	0.33	0	0	0	Planctomycetes; Unknown
Gemmatimonas sp	0.108	0	0	0	0.039	0	0	0	Gemmatimonadetes; GHB; Oligotroph

Sequence ID	OG230207-002	OG230406-001	OG230406-002	OG230406-003	OG230406-004	OG230406-005	OG230409-003	OG230409-006	Select Traits
Species	s2 w2248 Soil	s52 w2248 C001 OD Scale	s53 w2248 C001 Coup. Scale	s54 w2248 C001 OD Scale	s56 w2248 C001 OD Scale	s55 w2248 Cond. OD Scale	s59 w2248 9 5/8" ID Solids	s51 w2248, Annulus Liquids	Metabolism, Ecology, Physiology, Taxonomy
Gemmobacter sp	0.007	0	0	0	0	0	0	0	AlphaP; BioDeg; Methyltroph
Geoalkalibacter sp	0.082	0	0	0	0.048	0	0	0	Anaerobe; DeltaP; IRB; Thermophile
Geobacter sp	0.289	0	0	0	0.154	0	0	0	Anaerobe; BioDeg HC; Biofilm; DeltaP; IRB; Metal Reduction; Microbial Fuel Cell
Geodermatophilus sp	0.021	0	0	0	0	0	0	0	Actinomycete; Soil
Georgenia sp	0	0.386	0.326	0.222	0.035	0.58	0.403	0.646	Actinobacteria; BioDeg
Geosporobacter sp	0	0.001	0	0.002	0.017	0.026	0	0	Anaerobe; Clostridia; Ferm; Firmicutes; IRB; Spore
Geothermobacter sp	0.057	0	0	0	0	0	0	0	DeltaP
Geothrix sp	0.052	0	0	0	0.008	0	0	0	Acidobacteria; Anaerobe; IRB
Gloeobacter sp	0	0	0	0	0.01	0	0	0	Cyanobacteria; Phototroph
Gordonia sp	0.013	0.016	0.009	0.007	0	0.144	0.012	0.042	Actinobacteria; Aerobe; Filamentous; Foam; Wastewater
Gracilibacter sp	0.002	0	0	0	0.004	0	0	0	Clostridia; Ferm; Firmicutes; GHB
Haemophilus sp	0	0	0	0	0.01	0	0	0	GammaP; Pathogen
Hahella chejuensis	0	0	0	0	0.069	0	0	0	GammaP
Halanaerobium sp	0	0	0	0.005	0	0.02	0	0	Anaerobe; APB; Clostridia; Ferm; Firmicutes; Halophile; Methanogen-Promoting; MIC; SRB-Promoting; Sulfidogen; SuRB; TRB
Haliangium sp	0.144	0	0	0	0.152	0	0	0	DeltaP
Haliscomenobacter sp	0	0	0	0	0.006	0	0	0	Bacteroidetes; Filamentous
Haloactinobacterium album	0	0.021	0.015	0.02	0	0.005	0.038	0.026	
Halobacillus sp	0.002	0	0	0	0	0	0	0	Alkaliphile; Bacilli; Firmicutes; Halophile; NRB
Halochromatium sp	0	0	0	0	0	0	0.004	0	GammaP; Halophile; Phototroph; Purple Sulfur Bacteria

Sequence ID	OG230207-002	OG230406-001	OG230406-002	OG230406-003	OG230406-004	OG230406-005	OG230409-003	OG230409-006	Select Traits
Species	s2 w2248 Soil	s52 w2248 C001 OD Scale	s53 w2248 C001 Coup. Scale	s54 w2248 C001 OD Scale	s56 w2248 C001 OD Scale	s55 w2248 Cond. OD Scale	s59 w2248 9 5/8" ID Solids	s51 w2248, Annulus Liquids	Metabolism, Ecology, Physiology, Taxonomy
Halolactibacillus halophilus	0	0	0.009	0.005	0	0	0.02	0.063	Alkaliphile; Bacilli; Firmicutes; GHB; Halophile
Halomonas sp	0	0	0	0.004	0	0.004	0	0	Alkaliphile; BioDeg HC; Facultative Anaerobe; GammaP; Haloalkaliphile; Halophile; NRB
Halospirulina sp	0	0	0	0	0.042	0.017	0	0	Halophile; Phototroph
Halothiobacillus neapolitanus	0	0	0.003	0.004	0	0.005	0	0	Acidophile; Aerobe; APB; Filamentous; GammaP; ISOX; MIC; SOB
Hansschlegelia plantiphila	0	0	0	0	0.008	0	0	0	AlphaP
Hartmannibacter sp	0.008	0	0	0	0.006	0	0	0	
Herbaspirillum autotrophicum	0.026	0	0	0	0	0	0	0	Aerobe; BetaP; NiF
Herbaspirillum sp	1.285	0.024	0.014	0.02	0.983	0.148	0.041	0.112	Aerobe; BetaP; NiF
Herminiimonas sp	0.085	0.004	0.002	0	0.087	0	0.001	0.002	BetaP; Heavy Metal
Herpetosiphon sp	0.008	0	0	0	0	0	0	0	Chloroflexi
Hirschia sp	0.028	0	0	0	0.096	0	0	0	AlphaP
Holophaga sp	0.564	0	0	0	0.133	0	0	0	Acidobacteria; BioDeg HC
Holospora acuminata	0.008	0	0	0	0	0	0	0	
Homoserinibacter gongjuensis	0	0	0	0	0	0	0.005	0.015	
Hongiella sp	0.007	0	0	0	0	0	0	0	Bacteroidetes; GHB
Hyalangium sp	0.002	0	0	0	0	0	0	0	DeltaP; Unknown
Hydrogenophaga sp	1.04	0.332	0.083	0.289	1.65	0.149	0.067	0.486	Aerobe; BetaP; BioDeg HC
Hymenobacter gelipurpurascen	0	0	0	0	0.013	0	0	0	Bacteroidetes; BioDeg; GHB
Hymenobacter norwichensis	0.007	0	0	0	0	0	0	0	Bacteroidetes; BioDeg; GHB
Hymenobacter roseosalivarius	0.015	0	0	0	0	0	0	0	
Hymenobacter sp	0.059	0	0	0	0	0	0	0	Bacteroidetes; BioDeg; GHB
Hymenobacter tibetensis	0	0	0	0	0.025	0	0	0	
Hyphomicrobium nitrativorans	0	0	0	0	0.177	0	0	0	

Sequence ID	OG230207-002	OG230406-001	OG230406-002	OG230406-003	OG230406-004	OG230406-005	OG230409-003	OG230409-006	Select Traits
Species	s2 w2248 Soil	s52 w2248 C001 OD Scale	s53 w2248 C001 Coup. Scale	s54 w2248 C001 OD Scale	s56 w2248 C001 OD Scale	s55 w2248 Cond. OD Scale	s59 w2248 9 5/8" ID Solids	s51 w2248, Annulus Liquids	Metabolism, Ecology, Physiology, Taxonomy
Hyphomicrobium sp	1.09	0.457	0.182	0.383	1.025	10.215	0.061	0.115	Aerobe; AlphaP; BioDeg; Methylotroph; Soil
Hyphomicrobium sulfonivorans	0	0.65	0.091	0.39	0.227	11.327	0.44	0.344	Aerobe; AlphaP; BioDeg; Methylotroph; Soil
Hyphomonas sp	0.062	0	0	0	0.004	0	0	0	AlphaP; Biofilm
Iamia sp	0.095	0	0	0	0.085	0	0	0	Actinobacteria
Ideonella sp	0.015	0.001	0	0	0.04	0.001	0	0	PerRB
Ignavibacterium sp	0	0	0	0	0.019	0	0	0	Ignavibacteriae
Ilumatobacter sp	0.018	0	0	0	0.01	0	0	0	Actinobacteria
Intestinibacter sp	0.002	0	0	0	0	0	0	0	
Intestinimonas sp	0	0	0	0	0	0	0	0.008	
Isoptericola sp	0.013	0	0	0	0	0	0	0	
Isosphaera sp	0.008	0	0	0	0	0	0.003	0.005	Planctomycetes
Jahnella thaxteri	0.031	0	0	0	0	0	0	0	
Janibacter sp	0	0.009	0.011	0.009	0.838	0.003	0	0	Actinobacteria; BioDeg HC
Janthinobacterium sp	0.306	0	0	0	0	0	0.154	0	Aerobe; Antimicrobial; BetaP; Biofilm; Dark Violet; Natural Dye
Jatrophihabitans sp	0	0	0	0	0	0	0	0.002	
Jeotgalicoccus coquinae	0	0	0	0	0	0	2.769	3.017	Faculatative Anaerobe; Fish sauce; Generalist; GHB; Halophile
Jeotgalicoccus sp	0.011	2.195	1.387	1.22	0.025	1.092	0	0	Bacilli; Faculatative Anaerobe; Firmicutes; Fish sauce; Generalist; GHB; Halophile
Kaistia granuli	0	0.012	0.014	0.009	0.004	0.038	0.011	0.011	AlphaP
Kaistia sp	0.007	0	0	0	0	0	0	0	AlphaP
Kineosporia aurantiaca	0.087	0	0	0	0	0	0	0	Actinobacteria
Kineosporia rhamnosa	0.057	0	0	0	0	0	0	0	
Kitasatospora sp	0	0	0	0	0.054	0	0	0	Actinobacteria; Unknown

Sequence ID	OG230207-002	OG230406-001	OG230406-002	OG230406-003	OG230406-004	OG230406-005	OG230409-003	OG230409-006	Select Traits
Species	s2 w2248 Soil	s52 w2248 C001 OD Scale	s53 w2248 C001 Coup. Scale	s54 w2248 C001 OD Scale	s56 w2248 C001 OD Scale	s55 w2248 Cond. OD Scale	s59 w2248 9 5/8" ID Solids	s51 w2248, Annulus Liquids	Metabolism, Ecology, Physiology, Taxonomy
Kocuria sp	0	0.021	0.015	0.009	0.066	0.001	0	0	Actinobacteria; Biosurfactant Producing; Ferm; Halophile; NRB
Kofleria sp	0.005	0	0	0	0	0	0	0	DeltaP
Kouleothrix sp	0.028	0	0	0	0.006	0	0	0	Filamentous
Kribbella sp	0.008	0	0	0	0	0	0	0	Actinobacteria
Labrenzia sp	0	0	0	0	0.033	0	0	0	AlphaP
Lacibacter sp	0.137	0	0	0	0.064	0	0	0	
Lacibacterium sp	0.007	0	0	0	0	0	0	0	AlphaP
Lacihabitans soyangensis	0.007	0	0	0	0.013	0	0	0	Bacteroidetes
Lactobacillus animalis	0.028	0.022	0.071	0.02	0	0.036	0.017	0.224	APB; Firmicutes; LAB; Lactobacillales
Lactobacillus rodentium	0	0	0	0	0.006	0	0	0	
Lactobacillus sp	0.003	0	0.006	0	0	0	0	0	APB; Firmicutes; LAB; Lactobacillales
Larkinella insperata	0.036	0	0	0	0	0	0	0	Aerobe; Sediments; Soil
Lautropia sp	0	0	0	0	0.046	0	0	0	BetaP
Legionella adelaidensis	0	0	0	0	0.004	0	0	0	
Legionella beliardensis	0	0	0	0	0	0	0	0.005	Aerobe; GammaP
Legionella gresilensis	0.002	0	0	0	0	0	0	0	Aerobe; GammaP
Legionella quinlivanii	0	0	0	0	0.017	0	0	0	
Legionella sp	0.092	0.003	0	0.004	0.491	0.026	0.003	0.003	Aerobe; GammaP
Leptolyngbya sp	0.01	0	0	0	0	0	0	0	Cyanobacteria; dry biofilms; Phototroph
Leptothrix sp	0.049	0	0	0	0	0	0	0	Aerobe; GHB
Leptotrichia sp	0	0	0	0	0.013	0.007	0	0	Fusobacteria; Pathogen
Leucobacter aridicollis	0.02	2.703	2.8	2.136	0.013	1.155	6.495	3.03	Actinobacteria; Aerobe; BioDeg chromium compounds; Biosurfactant Producing; Chromium tolorant
Leucobacter sp	0	0.009	0.002	0	0	0	1.249	0.705	Actinobacteria; BioDeg
Levilinea sp	0	0	0	0	0.023	0	0	0	Alaska; Chloroflexi; Oilfield; Produced Water

Sequence ID	OG230 207-002	OG230 406-001	OG230 406-002	OG230 406-003	OG230 406-004	OG230 406-005	OG230 409-003	OG230 409-006	Select Traits
Species	s2 w2248 Soil	s52 w2248 C001 OD Scale	s53 w2248 C001 Coup. Scale	s54 w2248 C001 OD Scale	s56 w2248 C001 OD Scale	s55 w2248 Cond. OD Scale	s59 w2248 9 5/8" ID Solids	s51 w2248, Annulus Liquids	Metabolism, Ecology, Physiology, Taxonomy
Lewinella sp	0.005	0	0	0	0.021	0	0	0	Bacteroidetes; Filamentous; GHB
Limnobacter sp	0.059	0	0	0	0	0	0	0	BetaP; Sulfidogen; TRB
Limnohabitans sp	0	0	0	0	0	0	0	0.002	BetaP; GHB
Lishizhenia sp	0.824	0	0.003	0	0.592	0	0	0	
Litorilinea sp	0.075	0	0	0	0	0	0	0	
Loktanella atrilutea	0.018	0	0	0	0	0	0	0	Aerobe; AlphaP; GHB
Longilinea sp	0.007	0	0	0	0.012	0	0	0	Anaerobe; Chloroflexi; Consortium Member; Filamentous; Methanogenic Community Member
Luedemannella sp	0.002	0	0	0	0	0	0	0	
Luteolibacter cuticulihirudinis	0.003	0	0	0	0	0	0	0	Aerobe; Verrucomicrobia
Luteolibacter sp	0.015	0	0	0	0.029	0	0	0	Verrucomicrobia
Lysinibacillus massiliensis	0	0	0	0	0	0	0.003	0.003	Bacilli; Environmental; Firmicute; GHB; Spore
Lysinibacillus sphaericus	0	0.012	0.006	0	0.383	0.008	0	0	Bacilli; Firmicutes
Lysobacter sp	0.227	0	0	0.002	0.083	0	0	0	BioDeg HC; GammaP
Lysobacter spongiicola	0	0	0	0	0	0	0.005	0.008	
Malonomonas sp	0.005	0	0	0	0.008	0	0	0	DeltaP; Ferm
Maricaulis sp	0.02	0	0	0	0.025	0	0	0	AlphaP
Marinilactibacillus sp	0	0	0	0	0.027	0.012	0.001	0.005	Alkaliphile; Firmicutes; Halophile; LAB; Lactobacillales
Marinobacter sp	0	0.003	0.003	0	0	0	0.004	0.013	Aerobe; BioDeg HC; GammaP; NRB
Marinobacterium sp	0.025	0.036	0.006	0.018	0	0.003	0.025	0.003	Aerobe; BioDeg; GammaP; GHB
Marmoricola sp	0.029	0.001	0.002	0	0.183	0.008	0	0.016	Actinobacteria; GHB
Massilia sp	1.827	0	0	0	0.347	0	0.003	0	BetaP; BioDeg; Filamentous; Soil
Melioribacter sp	0.023	0	0	0	0	0	0	0	
Mesorhizobium albiziae	0.051	0	0	0	0	0	0	0	
Mesorhizobium sp	0.242	0.668	0.243	0.506	0.152	5.076	0.395	0.542	AlphaP; NiF; Soil

Sequence ID	OG230207-002	OG230406-001	OG230406-002	OG230406-003	OG230406-004	OG230406-005	OG230409-003	OG230409-006	Select Traits
Species	s2 w2248 Soil	s52 w2248 C001 OD Scale	s53 w2248 C001 Coup. Scale	s54 w2248 C001 OD Scale	s56 w2248 C001 OD Scale	s55 w2248 Cond. OD Scale	s59 w2248 9 5/8" ID Solids	s51 w2248, Annulus Liquids	Metabolism, Ecology, Physiology, Taxonomy
Methanobacterium sp	0	0	0	0	0	0.005	0	0	Anaerobe; Archaea; Methanogen
Methylibium petroleiphilum	0	0	0	0	1.817	0	0	0	Methylotroph
Methylibium sp	1.067	0.018	0.003	0.009	0.252	0.012	0	0	Methylotroph
Methylobacillus sp	0	0	0	0	0.027	0	0	0	BetaP; Methylotroph
Methylobacterium soli	0.013	0	0	0	0	0	0	0	
Methylobacterium sp	0.134	0.007	0.035	0.023	0.058	0.021	0.011	0.104	Aerobe; AlphaP; Methylotroph
Methylocapsa sp	0.041	0	0	0	0.019	0	0	0	AlphaP; Methylotroph
Methylococcus capsulatus	0	0	0	0	0.012	0	0	0	GammaP; Methylotroph
Methylocystis sp	0.116	0	0	0	0.131	0	0	0	AlphaP; Methylotroph
Methylohalomonas sp	0	0	0	0	0.008	0	0	0	
Methylomicrobium sp	0	0	0	0	0.015	0	0	0	BioDeg HC; GammaP; Methylotroph
Methylophilus sp	0.08	0	0	0	0.198	0	0	0	BetaP; Methylotroph
Methylorosula polaris	0.025	0	0	0	0	0	0	0	
Methylosinus sp	0.025	0	0	0	0	0	0	0	AlphaP; Methylotroph
Methylosinus sporium	0.033	0	0	0	0.05	0	0	0	AlphaP; Methylotroph
Methylosinus trichosporium	0	0	0	0	0.058	0	0	0	AlphaP; Methylotroph
Methyloversatilis sp	0	0	0	0.002	0.017	0	0	0	BetaP; Methylotroph
Micavibrio sp	0	0	0	0	0.029	0	0	0	Bacterial Predator
Microbacterium kitamiense	0	0.003	0	0.002	0	0.007	0.011	0.006	
Microvirga sp	0.008	0	0	0	0	0	0	0	AlphaP
Microvirga zambiensis	0.119	0.01	0.008	0.011	0.037	0.008	0.004	0.005	AlphaP
Mobilicoccus sp	0	0.003	0	0.007	0.06	0.055	0	0	
Modestobacter sp	0.01	0	0	0	0.01	0	0	0	Aerobe; AlphaP; Soil; Soil Crust
Moorella sp	0.569	0	0	0	0.075	0	0	0	Acetogen; Anaerobe; APB; Clostridia; Ferm; Firmicutes; NRB; Spore; Sulfidogen; Thermophile; TRB
Motilibacter peucedani	0.003	0	0	0	0	0	0	0	Actinobacteria; GHB
Mucilaginibacter auburnensis	0.007	0	0	0	0	0	0	0	

Sequence ID	OG230207-002	OG230406-001	OG230406-002	OG230406-003	OG230406-004	OG230406-005	OG230409-003	OG230409-006	Select Traits
Species	s2 w2248 Soil	s52 w2248 C001 OD Scale	s53 w2248 C001 Coup. Scale	s54 w2248 C001 OD Scale	s56 w2248 C001 OD Scale	s55 w2248 Cond. OD Scale	s59 w2248 9 5/8" ID Solids	s51 w2248, Annulus Liquids	Metabolism, Ecology, Physiology, Taxonomy
Mucilaginibacter pineti	0.01	0	0	0	0	0	0	0	
Mumia sp	0.059	0	0	0	0	0	0	0	
Mycobacterium sp	1.621	0.571	0.399	0.298	0.264	3.168	0.413	1.101	Actinobacteria; Environmental; Widespread
Myroides odoratus	0	0.012	0	0.013	0	0.016	0.003	0.023	Bacteroidetes
Myxococcus sp	0.002	0	0	0	0.021	0	0	0	DeltaP
Nakamurella flavida	0.239	0	0	0	0	0	0	0	
Nakamurella multipartita	0	0	0	0	0.056	0	0	0	
Nakamurella sp	0	0	0	0	0.012	0	0	0	Actinobacteria
Nannocystis sp	0.013	0	0	0	0.077	0	0	0	DeltaP
Natronomonas sp	0	0	0	0	0.017	0	0	0	Archaea
Neisseria sp	0	0	0	0	0.013	0.009	0	0	BetaP
Neochlamydia hartmannellae	0.007	0	0	0	0.023	0	0	0	Chlamydiae
Neochlamydia sp	0.023	0	0	0	0.029	0	0	0	Chlamydiae
Nevskia ramosa	0.028	0	0	0	0	0	0	0	GammaP; GHB
Niastella sp	0.083	0	0	0	0.297	0	0	0.003	Bacteroidetes
Nitratireductor sp	0.041	0	0	0	0.008	0	0	0	AlphaP; Facultative Anaerobe; NRB
Nitrobacter sp	0.039	0	0	0	0.01	0	0	0	AlphaP; NOB
Nitrosococcus sp	0.087	0	0	0	0.029	0	0	0	GammaP; Halophile; NOB
Nitrosomonas communis	0.003	0	0	0	0	0	0	0	AOB; AOX; BetaP
Nitrosospira sp	0.013	0	0	0	0.008	0	0	0	Aerobe; AOB; AOX; BetaP
Nitrosovibrio sp	0.028	0	0	0	0.092	0	0	0	Aerobe; AOB; AOX; BetaP
Nitrospira sp	0.523	0	0	0	0.224	0	0	0	Nitrospinae; NOB
Nocardia sp	0.042	0	0	0	0	0	0.003	0	Actinobacteria; Aerobe; Filamentous
Nocardioides dilutus	0	0	0	0	0.056	0	0	0	
Nocardioides ginsengagri	0.044	0	0	0	0	0	0	0	
Nocardioides halotolerans	0	0	0	0	0	0	0	0.002	
Nocardioides insulae	0	0	0	0	0.118	0	0	0	

Sequence ID	OG230207-002	OG230406-001	OG230406-002	OG230406-003	OG230406-004	OG230406-005	OG230409-003	OG230409-006	Select Traits
Species	s2 w2248 Soil	s52 w2248 C001 OD Scale	s53 w2248 C001 Coup. Scale	s54 w2248 C001 OD Scale	s56 w2248 C001 OD Scale	s55 w2248 Cond. OD Scale	s59 w2248 9 5/8" ID Solids	s51 w2248, Annulus Liquids	Metabolism, Ecology, Physiology, Taxonomy
Nocardioides sp	1.187	0.006	0.002	0.004	0.854	0.001	0.001	0.006	Actinobacteria; Filamentous
Nocardiopsis sp	0.06	2.739	2.39	1.346	0.004	2.592	2.366	2.567	Actinobacteria; Filamentous
Nordella oligomobilis	0.279	0	0	0	0.027	0	0	0	
Nordella sp	0.15	0	0	0	0.382	0	0	0	
Nostoc commune	0.01	0	0	0	0	0	0	0	Phototroph
Nostoc sp	0.005	0	0	0	0.033	0	0	0	Phototroph
Noviherbaspirillum aurantiacum	1.044	0	0	0	0	0	0	0	
Novosphingobium sp	0.237	0	0	0	0.01	0	0	0	AlphaP; BioDeg
Oceanobacillus chironomi	0	0.051	0.027	0.036	0	0.029	0.018	0.088	
Oceanobacillus chungangensis	0	0	0	0	0	0	0.003	0.021	
Oceanobacillus luteolus	0	0.105	0.105	0.061	0	0.044	0.059	0.196	
Oceanobacillus massiliensis	0	0.043	0.018	0.029	0	0.078	0.021	0.065	
Oceanobacillus sp	0	0.007	0.003	0.005	0	0	0	0.003	Bacilli; Ferm; Firmicutes; Halophile; Spore
Ochrobactrum grignonense	0	0.093	0.067	0.302	0	0.147	0	0	AlphaP; NiF
Ochrobactrum sp	0	1.413	0.264	0.446	0.013	1.256	1.223	1.129	AlphaP; NiF
Oerskovia sp	0.042	0.039	0.068	0.049	0	0.004	0.084	0.026	
Ohtaekwangia sp	0.53	0	0	0	0.172	0	0	0	Bacteroidetes
Opitutus sp	0.098	0	0	0	0.089	0	0	0	Ferm; Verrucomicrobia
Ornithinimicrobium sp	0	0	0	0	0	0	0.003	0	Actinobacteria
Owenweeksia sp	0.005	0	0	0	0	0	0	0	Bacteroidetes
Paenalcaligenes hominis	0	8.419	19.677	31.411	0.831	0.779	5.036	1.259	Aerobe; Bacteroidetes; BetaP; Bioreactor; Generalist; GHB
Paenibacillus assamensis	0.011	0	0	0	0.019	0	0	0	Bacilli; Facultative Anaerobe; Firmicutes; Spore
Paenibacillus harenae	0.007	0	0	0	0.01	0	0	0	
Paenibacillus macquariensis	0	0	0	0	0	0	0.005	0	

Sequence ID	OG230207-002	OG230406-001	OG230406-002	OG230406-003	OG230406-004	OG230406-005	OG230409-003	OG230409-006	Select Traits
Species	s2 w2248 Soil	s52 w2248 C001 OD Scale	s53 w2248 C001 Coup. Scale	s54 w2248 C001 OD Scale	s56 w2248 C001 OD Scale	s55 w2248 Cond. OD Scale	s59 w2248 9 5/8" ID Solids	s51 w2248, Annulus Liquids	Metabolism, Ecology, Physiology, Taxonomy
Paenibacillus sp	0.074	0.034	0.011	0.033	0.083	0.232	0.008	0.034	Bacilli; BioDeg EPS; BioDeg PAH; Dendritiformis colonies; Facultative Anaerobe; Firmicute; Firmicutes; Spore
Paenibacillus tianmuensis	0	0	0.003	0	0	0.009	0.004	0	
Paenochrobactrum sp	0	0.762	0.033	0.036	0	0.124	0.03	0.231	
Paludibacter sp	0	0	0	0	0.01	0	0.058	0.008	Bacteroidetes; Ferm
Panacagrimonas perspica	0.011	0	0	0	0	0	0	0	GammaP; GHB
Parachlamydia sp	0	0	0	0	0.025	0	0	0	Chlamydiae; Unknown
Paracoccus koreensis	0.002	0	0	0	0	0	0	0	AlphaP; APB; BioDeg; Facultative Anaerobe; Mitochondrial Ancestor; NRB
Paracoccus saliphilus	0.007	0	0	0	0	0	0	0	
Paracoccus sp	0	0	0.014	0.005	0.249	0	0.012	0.003	AlphaP; APB; BioDeg; Facultative Anaerobe; Mitochondrial Ancestor; NRB
Paracraurococcus ruber	0.005	0	0	0	0	0	0	0	AlphaP; APB
Paracraurococcus sp	0.092	0	0	0	0.004	0	0	0	AlphaP; APB
Paraliobacillus sp	0	0	0	0	0	0	0.007	0.052	
Parapedobacter koreensis	0	0	0	0.004	0	0	0	0	
Parasegetibacter luojiensis	0.016	0	0	0	0.008	0	0	0	Bacteroidetes
Parvibacter caecicola	0	0	0	0	0	0.003	0	0	
Parvibaculum sp	0	0	0	0	0.013	0	0	0	AlphaP; BioDeg HC
Parvularcula sp	0	0	0	0	0.01	0	0	0	AlphaP
Pasteuria sp	0.059	0	0	0	0.012	0	0	0	Bacilli; Firmicutes
Patulibacter medicamentivoran	0	0.106	0.026	0.051	0	0.145	0.028	0.047	
Patulibacter minatonensis	0.016	0.03	0.011	0.036	0.01	0.119	0.004	0.015	Actinobacteria
Patulibacter sp	0	0.046	0.049	0.06	0.002	0.165	0.029	0.084	Actinobacteria
Pedobacter sp	0.173	0.001	0	0	0.05	0.012	0.005	0.005	Bacteroidetes; BioDeg; Soil
Pedomicrobium manganicum	0.026	0	0	0	0	0	0	0	AlphaP
Pedomicrobium sp	0.134	0	0	0	0.195	0	0	0.002	AlphaP

Sequence ID	OG230207-002	OG230406-001	OG230406-002	OG230406-003	OG230406-004	OG230406-005	OG230409-003	OG230409-006	Select Traits
Species	s2 w2248 Soil	s52 w2248 C001 OD Scale	s53 w2248 C001 Coup. Scale	s54 w2248 C001 OD Scale	s56 w2248 C001 OD Scale	s55 w2248 Cond. OD Scale	s59 w2248 9 5/8" ID Solids	s51 w2248, Annulus Liquids	Metabolism, Ecology, Physiology, Taxonomy
Pedosphaera parvula	0.003	0	0	0	0.023	0	0	0	Aerobe; Verrucomicrobia
Pedosphaera sp	0.047	0	0	0	0.039	0	0	0	Verrucomicrobia
Pelagibacterium halotolerans	0	0.006	0.003	0.009	0.002	0.058	0	0	
Pelagibacterium sp	0	0.117	0.088	0.099	0	0.038	0.051	0.132	
Pelobacter sp	0.791	0	0	0	0.085	0	0	0	Anaerobe; DeltaP; IRB
Pelosinus fermentans	0	0	0	0	0.006	0	0	0	
Pelotomaculum sp	0	0	0	0	0.15	0	0	0	Anaerobe; BioDeg; Clostridia; Firmicutes; Syntroph
Peredibacter starrii	0.031	0	0	0	0	0	0	0	DeltaP; Ferm
Perlucidibaca sp	2.037	0	0	0	0.173	0	0	0	GammaP; GHB
Petrobacter sp	0	0.009	0	0	0.023	0	0.011	0.005	Aerobe; BetaP; NRB; Oilfied; Oilfield; Thermophile
Phaselicystis sp	0.013	0	0	0	0	0	0	0	
Phenylobacterium sp	0.229	0	0	0	0.044	0	0	0	Aerobe; AlphaP; GHB
Phycicoccus sp	0	0	0	0	0.146	0	0	0	
Phycisphaera sp	0.023	0	0	0	0	0	0	0	Planctomycetes
Phyllobacterium sp	0.003	0	0	0	0	0	0	0	AlphaP
Phytoplasma sp	0.028	0	0	0	0.01	0	0.003	0	Tenericutes
Pigmentiphaga sp	0.005	0	0	0	0	0	0	0	BetaP
Pirellula sp	0.301	0	0	0	0.172	0	0	0	Planctomycetes
Pirellula staleyi	0.002	0	0	0	0.037	0	0	0	Planctomycetes
Planctomyces sp	0.548	0	0	0	0.198	0	0	0	Planctomycetes
Planomicrobium sp	0	0.049	0.012	0.045	1.002	0.1	0	0	Bacilli; BioDeg; Firmicutes
Polaromonas sp	1.536	0.004	0	0.002	4.218	0.001	0	0	BetaP; BioDeg HC
Porphyrobacter sp	0	0	0	0	0.004	0	0	0	AlphaP; BioDeg; Phototroph
Porphyrobacter tepidarius	0.008	0	0	0	0	0	0	0	AlphaP; BioDeg; Phototroph
Prochlorococcus sp	0.016	0	0	0	0	0	0	0	Phototroph
Prolixibacter sp	0.01	0	0	0	0	0	0	0	Bacteroidetes

Sequence ID	OG230207-002	OG230406-001	OG230406-002	OG230406-003	OG230406-004	OG230406-005	OG230409-003	OG230409-006	Select Traits
Species	s2 w2248 Soil	s52 w2248 C001 OD Scale	s53 w2248 C001 Coup. Scale	s54 w2248 C001 OD Scale	s56 w2248 C001 OD Scale	s55 w2248 Cond. OD Scale	s59 w2248 9 5/8" ID Solids	s51 w2248, Annulus Liquids	Metabolism, Ecology, Physiology, Taxonomy
Propionivibrio sp	0	0.001	0	0	0.017	0	0	0	BetaP; BioDeg HC; BioDeg PAH; PerRB
Prosthecobacter algae	0.021	0	0	0	0	0	0	0	
Prosthecobacter sp	0.07	0	0	0	0.071	0	0	0	Verrucomicrobia
Prosthecomicrobium sp	0.002	0	0	0	0.01	0	0	0	AlphaP
Protochlamydia naegleriophila	0.002	0	0	0	0.006	0	0	0	Chlamydiae; Unknown
Providencia sp	0	0.007	0.006	0.002	0	0.005	0.003	0.021	GammaP; Unknown
Pseudochelatococcus contami	0	0.164	0.032	0.058	0.01	0.176	0.608	0.427	AlphaP; Metal Working Fluids
Pseudochrobactrum kiredjiania	0	0.161	0.027	0.061	0	0.104	0	0	Aerobe; AlphaP; GHB
Pseudochrobactrum sp	0.034	33.342	3.27	12.823	0.574	24.881	30.126	32.689	Aerobe; AlphaP; GHB
Pseudoclavibacter chungange	0	0.081	0.085	0.038	0.002	0.018	0	0	
Pseudofulvimonas gallinarii	0	0	0	0	0.021	0	0	0	
Pseudolabrys sp	0.057	0	0.002	0.002	0.083	0.007	0.003	0	AlphaP
Pseudomonas sp	0.291	1.148	9.326	4.031	0.31	2.412	5.225	3.902	Aerobe; BioDeg; GammaP; GHB; Varies; Versatile; Widespread
Pseudonocardia sp	0.335	0.223	0.208	0.136	0.139	1.54	0.241	0.512	Actinobacteria
Pseudonocardia spinosa	0.013	0	0	0	0	0	0	0	
Pseudonocardia tetrahydrofura	0	0	0.002	0	0.025	0	0.003	0.003	
Pseudophormidium sp	0.005	0	0	0	0	0	0	0	Phototroph
Pseudorhodobacter sp	0.244	0	0	0	0	0	0	0	AlphaP
Pseudorhodoferax caeni	0	0.004	0	0.011	0.214	0	0	0	BetaP; BioDeg
Pseudoxanthomonas sp	0.628	0	0	0	0	0	0	0	BioDeg HC; GammaP
Psychrobacter sp	0.011	0	0	0	0.318	3.961	0	0	BioDeg HC; GammaP; Oilfield
Pusillimonas sp	0.003	1.945	3.12	5.863	0.26	0.118	0.912	0.322	AOX; BetaP
Ralstonia sp	0.172	0	0	0	0.01	0.007	0	0	BetaP; BioDeg HC
Reyranella massiliensis	0.007	0	0	0	0	0	0	0	Unknown
Reyranella soli	0.005	0	0	0	0	0	0	0	
Reyranella sp	0.002	0	0	0	0.015	0	0	0	
Rhabdobacter roseus	0.01	0	0	0	0	0	0	0	

Sequence ID	OG230207-002	OG230406-001	OG230406-002	OG230406-003	OG230406-004	OG230406-005	OG230409-003	OG230409-006	Select Traits
Species	s2 w2248 Soil	s52 w2248 C001 OD Scale	s53 w2248 C001 Coup. Scale	s54 w2248 C001 OD Scale	s56 w2248 C001 OD Scale	s55 w2248 Cond. OD Scale	s59 w2248 9 5/8" ID Solids	s51 w2248, Annulus Liquids	Metabolism, Ecology, Physiology, Taxonomy
Rhizobium sp	0.358	0.048	0.008	0.029	0.06	0.194	0.082	0.063	AlphaP; NiF
Rhizomicrobium sp	0	0	0	0	0.008	0	0	0	AlphaP
Rhodobacter maris	0.046	0	0	0	0	0	0	0	
Rhodobacter sp	0.021	0	0	0	1.216	0	0	0	AlphaP; Anaerobe; NiF; Phototroph
Rhodobium sp	0.067	0	0	0	0.019	0	0	0	AlphaP
Rhodocista sp	0.116	0	0	0	0	0	0	0	AlphaP; Phototroph
Rhodococcus sp	1	0.025	0.046	0.018	0.191	0.04	0.017	0.089	Actinobacteria; BioDeg
Rhodocytophaga aerolata	0	0	0	0	0.006	0	0	0	Aerobe; Bacteroidetes
Rhodocytophaga sp	0.008	0	0	0	0	0	0	0	Aerobe; Bacteroidetes
Rhodoferax sp	0.758	0.033	0.008	0.004	0.848	0.016	0	0	BetaP; IRB
Rhodomicrobium sp	0.02	0	0	0	0.013	0	0	0	AlphaP
Rhodopirellula sp	0.111	0	0	0	0.042	0	0	0	Planctomycetes
Rhodoplanes sp	0.384	0	0	0	0.316	0	0.005	0.018	AlphaP; Phototroph
Rhodopseudomonas sp	0.959	0.093	0.023	0.058	0.006	0.263	0.254	0.125	AlphaP; Phototroph
Rhodovulum sp	0.039	0	0	0.004	0.05	0	0	0	AlphaP; Phototroph
Rickettsia sp	0	0	0	0	0.013	0	0	0	AlphaP
Rickettsiella endosymbiont	0	0.003	0.003	0	0.023	0.011	0	0	
Roseiflexus sp	0.038	0	0	0	0.004	0	0	0	Chloroflexi
Roseomonas lacus	0.011	0	0	0	0	0	0	0	AlphaP
Roseomonas sp	0.093	0	0	0	0.033	0	0	0	AlphaP; GHB
Roseomonas vinacea	0.015	0	0	0	0	0	0	0	AlphaP
Rothia sp	0	0	0	0	0	0.012	0	0	Actinobacteria; NiF
Ruania albidiflava	0	1.825	1.299	0.878	0.015	0.7	2.366	2.618	Actinomycete; Aerobe; Generalist; GHB
Rubellimicrobium sp	0.077	0	0	0	0.039	0	0	0	AlphaP; GHB
Rubrobacter sp	0.245	0	0	0	0.062	0	0	0	Actinobacteria; BioDeg
Rudanella lutea	0.003	0	0	0	0	0	0	0	
Ruminococcus albus	0	0	0	0	0	0	0	0.006	Anaerobe; BioDeg Cellulose; Clostridia; Ferm; Firmicutes

Sequence ID	OG230207-002	OG230406-001	OG230406-002	OG230406-003	OG230406-004	OG230406-005	OG230409-003	OG230409-006	Select Traits
Species	s2 w2248 Soil	s52 w2248 C001 OD Scale	s53 w2248 C001 Coup. Scale	s54 w2248 C001 OD Scale	s56 w2248 C001 OD Scale	s55 w2248 Cond. OD Scale	s59 w2248 9 5/8" ID Solids	s51 w2248, Annulus Liquids	Metabolism, Ecology, Physiology, Taxonomy
Ruminococcus flavefaciens	0	0	0	0.004	0	0	0	0	Anaerobe; BioDeg Cellulose; Clostridia; Ferm; Firmicutes
Ruminococcus sp	0	0.003	0	0	0	0	0	0	Anaerobe; BioDeg Cellulose; Clostridia; Ferm; Firmicutes
Runella sp	0.007	0	0	0	0.01	0	0	0	Bacteroidetes
Saccharibacillus sp	0.193	0	0	0	0	0	0	0	
Saccharopolyspora sp	0.007	0.066	0.085	0.049	0	0.017	0.169	0.188	Actinobacteria
Salana multivorans	0	0.001	0.002	0	0.006	0	0	0	Actinobacteria
Salibacter sp	0	0	0	0	0	0.018	0	0	Bacteroidetes
Sandaracinus amylolyticus	0.003	0	0	0	0	0	0	0	Aerobe; BioDeg Starch; DeltaP; GHB; Soil
Sandaracinus sp	0.263	0	0	0	0.013	0	0	0	DeltaP
Scytonema sp	0.021	0	0	0	0	0	0	0	
Sediminibacterium sp	0.003	0	0	0	0	0	0	0	Bacteroidetes; GHB
Segetibacter sp	0.002	0	0	0	0	0	0	0	Bacteroidetes
Serratia sp	0	0.019	0	0.013	0.002	0.03	0.004	0.044	Biofilm; GammaP; MIC
Shinella daejeonensis	0	0.025	0.006	0.02	0.058	0.044	0	0	
Silanimonas sp	0	0	0	0	2.093	0	0	0	GammaP; Unknown
Simkania sp	0	0	0	0	0.01	0	0	0	Chlamydiae
Simplicispira psychrophila	0.008	0	0	0	0	0	0	0	BetaP
Simplicispira sp	0	0.001	0.003	0.004	0.133	0	0	0	BetaP; HOX; Microaerophile
Singulisphaera acidiphila	0.01	0	0	0	0	0	0	0	Planctomycetes
Singulisphaera sp	0.062	0	0	0	0.012	0	0	0.005	Planctomycetes
Sinorhizobium sp	0.064	0	0	0	0	0	0.016	0.011	AlphaP; NiF
Skermanella sp	0.199	0	0	0	0.089	0	0	0	AlphaP
Skermanella stibiiresistens	0.007	0	0	0	0	0	0	0	AlphaP
Smaragdicoccus niigatensis	0.06	0	0	0	0.025	0	0	0	
Solibacter sp	0.047	0	0	0	0.013	0	0	0	Acidobacteria; Unknown

Sequence ID	OG230207-002	OG230406-001	OG230406-002	OG230406-003	OG230406-004	OG230406-005	OG230409-003	OG230409-006	Select Traits
Species	s2 w2248 Soil	s52 w2248 C001 OD Scale	s53 w2248 C001 Coup. Scale	s54 w2248 C001 OD Scale	s56 w2248 C001 OD Scale	s55 w2248 Cond. OD Scale	s59 w2248 9 5/8" ID Solids	s51 w2248, Annulus Liquids	Metabolism, Ecology, Physiology, Taxonomy
Solirubrobacter sp	0.302	0	0	0	0.123	0.005	0	0	Actinobacteria
Solitalea canadensis	0.007	0	0	0	0	0	0	0	Bacteroidetes
Solitalea koreensis	0	0	0	0	0.006	0	0	0	
Sorangium sp	0.007	0	0	0	0	0	0	0	DeltaP
Sphaerobacter sp	0.165	0.012	0.023	0.007	0.054	0.021	0.008	0.005	Chloroflexi; Wastewater
Sphaerobacter thermophilus	0	0	0.014	0.004	0	0.004	0.005	0.003	Chloroflexi
Sphingobacterium alimentarium	0	0.004	0.006	0.005	0	0	0.016	0.008	Aerobe; Bacteroidetes; BioDeg; GHB
Sphingobacterium nematocida	0	0.069	0.005	0.009	0	0.008	0	0.019	Aerobe; Bacteroidetes; Endophyte
Sphingobacterium paucimobilis	0.226	0	0	0	0.046	0	0	0	
Sphingobacterium psychroaqua	0	0.003	0	0	0	0.003	0	0	Aerobe; Bacteroidetes; BioDeg; GHB; Water
Sphingobacterium sp	0.101	0.004	0	0.009	0.008	0.001	0	0.005	Aerobe; Bacteroidetes; BioDeg; GHB
Sphingobacterium spiritivorum	0	0.007	0	0.004	0	0.025	0	0	Aerobe; Bacteroidetes; BioDeg; GHB
Sphingobium sp	0.396	0	0	0	0.206	0	0	0	Aerobe; AlphaP; BioDeg Herbacides; Soil
Sphingomonas sp	2.55	0	0.002	0	1.395	0	0.008	0.006	Aerobe; AlphaP; BioDeg PAH; GHB; Marine
Sphingopyxis sp	0.904	0	0	0	0.441	0	0	0.002	Aerobe; AlphaP; BioDeg HC
Spirosoma radiotolerans	0.029	0	0	0	0	0	0	0	
Spirosoma rigui	0.011	0	0	0	0	0	0	0	Bacteroidetes
Spirosoma sp	0.1	0	0	0	0	0	0	0	Bacteroidetes; Wastewater
Sporacetigenium mesophilum	0.003	0	0	0	0	0	0	0	APB; Clostridia; Ferm; Firmicutes
Sporacetigenium sp	0	0	0	0	0.006	0	0	0	Alkaliphile; Anaerobe; Anaerobic Digester; Ferm; WWTP
Sporichthya sp	0.011	0	0	0	0.015	0	0	0	Actinobacteria; BioDeg
Sporocytophaga sp	0	0	0	0	0.006	0	0	0	Bacteroidetes; BioDeg Cellulose
Sporomusa silvacetica	0	0	0	0	0.002	0.013	0	0	Anaerobe; APB; Firmicutes; Homoacetogen; Negativicutes; Spore

Sequence ID	OG230207-002	OG230406-001	OG230406-002	OG230406-003	OG230406-004	OG230406-005	OG230409-003	OG230409-006	Select Traits
Species	s2 w2248 Soil	s52 w2248 C001 OD Scale	s53 w2248 C001 Coup. Scale	s54 w2248 C001 OD Scale	s56 w2248 C001 OD Scale	s55 w2248 Cond. OD Scale	s59 w2248 9 5/8" ID Solids	s51 w2248, Annulus Liquids	Metabolism, Ecology, Physiology, Taxonomy
Sporosarcina sp	0.023	0.577	0.29	0.295	0.046	0.936	0.804	1.028	Bacilli; Firmicutes
Stakelama sediminis	0	0	0.003	0	0.048	0.004	0	0	
Staphylococcus equorum	0	0.022	0.014	0.016	0	0.008	0	0	Bacilli; Firmicutes; Skin
Staphylococcus lentus	0.034	1.257	0.768	0.667	0.04	0.916	0.754	2.394	
Stella sp	0.042	0	0	0	0	0	0	0	AlphaP; Prothecate
Stenotrophomonas maltophilia	0	0.333	0.05	0.164	0	0.071	0.033	0.351	Aerobe; BioDeg HC; GammaP; Sludge
Stenotrophomonas sp	0	0.015	0.005	0.022	0.006	0.015	0.008	0.039	Aerobe; BioDeg HC; GammaP; Sludge
Steroidobacter sp	0.389	0	0	0	0.123	0	0	0	BioDeg; GammaP
Sterolibacterium sp	0.144	0	0	0	0.021	0	0	0	BetaP; BioDeg; NRB
Streptococcus thermophilus	0	0	0	0	0.01	0	0	0	APB; Ferm; Firmicutes; LAB; Lactobacillales
Streptomyces sp	0.17	3.503	1.067	3.231	0.146	0.671	2.615	1.838	Actinobacteria; Antibiotic Producing; BioDeg; Filamentous; Soil; Spore
Streptosporangium sp	0	0	0	0	0.027	0	0.001	0	Actinobacteria; Alaska; Oilfield; Produced Water
Sulfuricurvum sp	0	0	0	0	0.067	0	0	0	BioDeg Oil; EpsilonP; NRB; NRSOB; Oilfield; SOB
Sulfuritalea hydrogenivorans	0	0	0	0	0.012	0	0	0	BetaP; Facultative Anaerobe; NRB; NRSOB; SOB
Sulfuritalea sp	0.018	0	0	0	0.01	0	0	0	BetaP; Facultative Anaerobe; NRB; NRSOB; SOB
Sulfurospirillum deleyianum	0	0	0	0	0.008	0.007	0	0	EpsilonP; Facultative Anaerobe; NRB; NRSOB; Oilfield; SOB
Sulfurospirillum sp	0.02	0.013	0.011	0.011	0	0.007	0.016	0.011	EpsilonP; Facultative Anaerobe; NRB; NRSOB; Oilfield; SOB
Sunxiuqinia sp	0.007	0	0	0	0	0	0	0	Bacteroidetes; GHB
Synechococcus sp	0.101	0	0	0	0.1	0	0	0	Phototroph

Sequence ID	OG230207-002	OG230406-001	OG230406-002	OG230406-003	OG230406-004	OG230406-005	OG230409-003	OG230409-006	Select Traits
Species	s2 w2248 Soil	s52 w2248 C001 OD Scale	s53 w2248 C001 Coup. Scale	s54 w2248 C001 OD Scale	s56 w2248 C001 OD Scale	s55 w2248 Cond. OD Scale	s59 w2248 9 5/8" ID Solids	s51 w2248, Annulus Liquids	Metabolism, Ecology, Physiology, Taxonomy
Syntrophobacter sp	0.042	0	0	0	0	0	0	0	BioDeg HC; DeltaP; Methanogen Syntroph; SRB; Sulfidogen
Syntrophomonas sp	0.123	0	0	0	0.04	0	0	0	Anaerobe; Clostridia; Firmicutes; Methanogen Syntroph; Sludge; Syntroph
Syntrophorhabdus sp	0	0	0	0	0.004	0	0	0	Anaerobe; BioDeg HC; DeltaP; Methanogen Syntroph; Sludge; Syntroph
Syntrophus sp	0.064	0	0	0	0.066	0	0	0	Anaerobe; BioDeg HC; DeltaP; Methanogen Syntroph; Sludge; Syntroph; Thermophile
Tahibacter aquaticus	0.047	0	0	0	0	0	0	0	
Taibaiella coffeisoli	0	0	0	0	0	0.011	0	0	
Taibaiella smilacinae	0	0.016	0.008	0.009	0	0.022	0.04	0.063	
Terrabacter sp	0.023	0	0	0	0	0	0	0	Actinobacteria; Aerobe; Air
Terriglobus sp	0.028	0	0	0	0	0	0	0	Acidobacteria; GHB
Terrimonas sp	0.155	0.001	0	0.002	0.345	0	0	0	Aerobe; Bacteroidetes; GHB
Tetragenococcus halophilus	0	0	0	0	0.017	0	0	0	Firmicutes; Lactobacillales
Tetragenococcus osmophilus	0	0	0	0	0	0	0.003	0	Firmicutes; Lactobacillales
Tetrasphaera sp	0.704	0	0	0	0	0	0.004	0.011	Actinobacteria
Thalassospira sp	0	0	0	0.004	0	0	0	0	AlphaP; BioDeg PAH
Thermaerobacter sp	0	0	0	0	0.008	0	0	0	Aerobe; Clostridia; Firmicutes; Sludge; Spore; Thermophile
Thermanaerothrix sp	0.007	0	0	0	0	0	0	0	Anaerobe; Chloroflexi; Thermophile
Thermincola sp	0	0	0	0	1.353	0.003	0	0	
Thermoanaerobacter sp	0.002	0	0	0	0	0	0	0	Anaerobe; Clostridia; Ethanologenic; Ferm; Firmicutes; Sulfidogen; Thermophile; TRB

Sequence ID	OG230207-002	OG230406-001	OG230406-002	OG230406-003	OG230406-004	OG230406-005	OG230409-003	OG230409-006	Select Traits
Species	s2 w2248 Soil	s52 w2248 C001 OD Scale	s53 w2248 C001 Coup. Scale	s54 w2248 C001 OD Scale	s56 w2248 C001 OD Scale	s55 w2248 Cond. OD Scale	s59 w2248 9 5/8" ID Solids	s51 w2248, Annulus Liquids	Metabolism, Ecology, Physiology, Taxonomy
Thermoanaerobacterium sacch	0	0	0.011	0	0.012	0.025	0.028	0.01	Anaerobe; APB; Clostridia; Firmicutes; NRB; Spore; Sulfidogen; Thermophile; TRB
Thermobacillus composti	0	0	0	0	0.004	0	0	0	Bacilli; Firmicutes; Thermophile
Thermobaculum sp	0	0	0	0	0.027	0	0	0	EpsilonP; Thermophile
Thermobifida sp	0.134	0	0	0	0.029	0	0	0	Actinobacteria; Thermophile
Thermodesulfovibrio sp	0.003	0	0	0	0	0	0	0	Anaerobe; Nitrospinae; SRB; Sulfidogen; Thermophile
Thermomicrobium sp	0.036	0.001	0.002	0	0	0	0	0	Chloroflexi; OX; Thermophile
Thermomonas sp	1.445	0	0	0.005	0.229	0	0	0	Aerobe; GammaP; GHB
Thioalkalivibrio sp	0.008	0	0	0	0.025	0	0	0	Aerobe; BioDeg HC; GammaP; Halophile; Microaerophile; NRB; NRSOB; SOB
Thiobacillus sp	0.105	0	0	0	0.01	0	0	0	BetaP; NRB; NRSOB; SOB
Thiobacter sp	0.06	0	0	0	0.087	0	0	0	SOB; Thermophile
Thiohalomonas sp	0	0	0	0	0.087	0	0	0	Halophile; Microaerophile; NRB; NRSOB; SOB
Thiohalospira sp	0.1	0	0	0	0.025	0	0	0	GammaP; Halophile; Microaerophile; SOB
Thioprofundum sp	0	0	0	0	0.031	0	0	0	Facultative Anaerobe; Filamentous; GammaP; NRB; NRSOB; SOB; Sulfide-Oxidizing
Thiorhodospira sp	0.276	0	0	0	0.064	0	0	0	Anaerobe; GammaP; Phototroph; Purple Sulfur Bacteria
Timonella senegalensis	0	1.085	1.622	0.912	0.004	0.252	3.677	2.153	
Tissierella creatinophila	0	0.112	0.127	0.266	0.01	0.012	0.286	0.119	Anaerobe; Clostridia; Ferm; Firmicutes; Sludge

Sequence ID	OG230207-002	OG230406-001	OG230406-002	OG230406-003	OG230406-004	OG230406-005	OG230409-003	OG230409-006	Select Traits
Species	s2 w2248 Soil	s52 w2248 C001 OD Scale	s53 w2248 C001 Coup. Scale	s54 w2248 C001 OD Scale	s56 w2248 C001 OD Scale	s55 w2248 Cond. OD Scale	s59 w2248 9 5/8" ID Solids	s51 w2248, Annulus Liquids	Metabolism, Ecology, Physiology, Taxonomy
Tissierella sp	0	0.142	0.127	0.21	0	0.055	0.216	0.18	Anaerobe; Clostridia; Ferm; Firmicutes; Sludge
Tolumonas sp	0	0	0	0	0.091	0	0	0	Facultative Anaerobe; Ferm; GammaP; Toluene Production
Tolypothrix sp	0	0	0	0	0.017	0	0	0	Phototroph
Tomitella biformata	0	0.036	0.05	0.031	0	0.022	0.061	0.084	
Trichococcus sp	0.054	0.638	0.601	0.39	0.686	0.578	3.461	1.077	Activated Sludge; APB; Facultative Anaerobe; Ferm; Filamentous; Firmicutes; Lactobacillales; Wastewater
Trichodesmium sp	0.015	0	0	0	0	0	0	0	Phototroph
Tumebacillus sp	0.015	0	0	0	0.021	0	0	0	
Turicibacter sp	0.034	0.001	0.003	0	0.017	0	0	0.011	Anaerobe; Erysipelotrichia; Firmicutes;
Unclassified	33.447	1.268	0.754	1.478	21.906	0.671	1.947	1.452	Polyphyletic; Unknown; Varies
Uncultured bacterium	0.322	0	0	0	0.008	0	0	0	Unknown
Undibacterium oligocarboniphil	0	0.003	0	0	0.023	0.038	0	0	
Undibacterium sp	0	0	0	0	0	0	0.004	0	BetaP; Unknown
Variibacter gotjawalensis	0.065	0	0	0	0	0	0	0	
Variovorax sp	0.194	0	0	0	0.852	0	0.007	0.036	BetaP; BioDeg HC; BioDeg Phenol
Vermiphilus pyriformis	0.007	0	0	0	0.048	0	0	0	Amoebae endosymbiont;
Verrucomicrobium sp	0.392	0	0	0	0.229	0	0	0	Ferm; Verrucomicrobia
Virgibacillus halotolerans	0.021	1.453	0.225	1.756	0.046	1.129	0.572	0.776	
Virgibacillus sp	0	0.294	0.423	0.3	0.033	0.133	0.507	0.703	Bacilli; Firmicutes; Halophile; Spore
Williamsia sp	0.402	0.006	0.005	0.002	0.015	0.013	0.003	0.021	Actinobacteria; Filamentous; Foam
Woodsholea maritima	0	0	0	0	0.135	0	0	0	AlphaP
Xanthobacter autotrophicus	0	0	0	0	0.056	0	0	0	AlphaP
Xanthobacter sp	0	0.013	0.006	0	0.013	0	0.007	0.006	AlphaP
Xanthomonas sp	0.075	0	0	0	0.085	0	0	0	Aerobe; Biofilm; EPS; GammaP; Plant Pathogen; Xantham guar gum

Sequence ID	OG230 207-002	OG230 406-001	OG230 406-002	OG230 406-003	OG230 406-004	OG230 406-005	OG230 409-003	OG230 409-006	Select Traits
Species	s2 w2248 Soil	s52 w2248 C001 OD Scale	s53 w2248 C001 Coup. Scale	s54 w2248 C001 OD Scale	s56 w2248 C001 OD Scale	s55 w2248 Cond. OD Scale	s59 w2248 9 5/8" ID Solids	s51 w2248, Annulus Liquids	Metabolism, Ecology, Physiology, Taxonomy
Xylanimonas sp	0	0.085	0.164	0.074	0	0.478	0.187	0.136	
Yaniella halotolerans	0	0.17	0.083	0.123	0	0.067	0.199	0.13	
Yaniella sp	0.011	0.254	0.076	0.112	0	1.493	0.154	0.224	Actinobacteria
Youngiibacter fragilis	0	0	0	0	0	0	0.008	0	Anaerobe; Clostridia; Ferm; GHB; Methanogen Community Member
Zavarzinella formosa	0.005	0	0	0	0	0	0	0	
Zavarzinella sp	0.067	0	0	0	0.067	0	0	0	

Appendix B. Complete list of all organisms identified in well 2248

Values are % of population. Yellow are > 10%, Green are 1 - 10%, Gray are 0%.

Trait Abreviations: Acetogen (Acetate producing, via fermentation or CO2 fixation), Acidophile (Growth at low pH), Aerobe (Oxygen requiring), Alkaliphile (Growth at high pH), Anaerobe (Grows only under anoxic conditions), AOB (Ammonia Oxidizing Bacteria), AOX (Ammonia Oxidizing Bacteria), APB (Acid-Producing Bacteria), BioDeg (Biodegrading unusual substrates, catabolically versatile, with the ability to utilize a wide range of unusual substrates, such as pyridine, herbicides, chlorinated biphenyls, and oil), BioDeg HC (Petroleum Hydrocarbon-Degrading Bacteria), BioDeg PAH (Polyaromatic Hydrocarbon-Degrading Bacteria), BioDeg TCE (Trichloroethylene Degrading Bacteria), Biofilm (Biofilm Member), Diverse (Exhibit metabolic diversity), EPS (Exopolysaccharide), Ethanologenic (Ethanol producing), Facultative (Grows under both aerobic and anaerobic conditions), FAP (Filamentous Anoxygenic Phototroph), Ferm (Fermentative), Filamentous (Forms long filaments), GHB (General Heterotrophic Bacteria), Halophile (Salt tolerant), IRB (Iron-Reducing Bacterial), ISOX (inorganic sulfur oxidizing), LAB (Lactic Acid Bacteria), Methanogen (Archaea that produce methane), Methylotroph (Utilize methane, methanol, and other simple carbons), MIC (Microbial-Influenced Corrosion), NiF (Nitrogen Fixing), NOB (Nitrite Oxidizing Bacteria), NRB (Nitrate-Reducing Bacteria), NRSOB (Nitrate-Reducing Sulfur-Oxidizing Bacteria), Oilfield (Found in oilfield samples), Oligotroph (Growth under low nutrient conditions), OX (Oxidizing Bacteria), Pathogen (Disease-causing), PerRB (Perchlorate-Reducing Bacteria), PhotoT (Phototrophic, Photosynthetic), Phototroph (Phototrophic, Photosynthetic), Sludge (Component of WWTP Sludges), SOB (Sulfur-Oxidizing Bacteria), Soil (Found in soil), Spore (Spore-forming bacteria), SRB (SRB, Sulfate-Reducing Bacteria), Sulfidogen (Hydrogen Sulfide Producing (includes SRB, TRB, SuRB and some peptide fermentation bacteria),), SuRB (Sulfur Reducing Bacteria), Syntroph (Mutualistic sharing of metabolic byproducts), Thermophile (Growth above 50oC), TRB (Thiosulfate Reducing Bacteria), Wastewater (Wastewater Associated), WWTP (Wastewater Treatment Plant),

Under "Select Traits of Interest" sulfidogens are highlighted in red, archaea in yellow, IRB in green.

GammaP, BetaP, AlphaP and DeltaP are Gammaproteobacteria, Betaproteobacteria, Alphaproteobacteria, and Deltaproteobacteria, respectively

Appendix C: Methods

Sample Collection

In all, 11 sets of samples, encompassing 109 individual samples, were collected between Feb 16, 2023 and April 3 2023. Sampling locations were sites within the Rager Mountain gas storage facility, Equitrans Midstream Corp, 555 Dishong Mountain Road, Johnstown PA 15906 USA. Sites within the facility included wells 2244, 2248, and 2251. Most samples were collected from well 2244 as it was the well involved in the failure event. Samples were predominantly of two types: solid scale material scraped from the outer diameter surface (OD) of the 7" casing joints and liquid annular fluids pumped from the annulus of the 7" and 9 5/8" casing. Additional samples included ID materials from 9 5/8 casing, soil from the surrounding area, grease on casing surface, material from the ID of the well head master valve and tree, as well as liquids collected in the compressor station and a pond. For scale samples, 2" disposable plastic putty knives were used to debride surface scale and solids, care was taken to use a new putty knife for each sample. Solids were stored in sterile Whirl-Pak bags (18 oz, 4.5" X 9"). Liquid samples were collected and stored in 500 ml HDPE Nalgene bottles. After collection, all samples were stored in a refrigerator prior to overnight shipping from Pennsylvania to Texas for analysis.

MPN Analysis

For MPN analysis, each sample is initially diluted in 20 ml of sterile PBS. The quantity of starting material added to the initial dilution varied from sample to sample, depending on sample type and amount of available sample, and the variation in initial sample used is corrected for when determining the dilution factor to adjust the final values. From these 20 ml initial dilutions, 1 ml is used to inoculate each of the primary dilution series bottles, 3 per media type. Each primary dilution was subject to eightfold serial dilution. Selective media used for this project were Modified Postgate's B Broth (MPB) for the growth of Sulfate-Reducing Bacteria, Phenol Dextrose Red Broth (PRD) for the enumeration of acid-producing bacteria (APB) and general heterotrophic bacteria (GHB), and Iron-Reducing Broth (IRB) for the enumeration of iron-reducing bacteria. Dilutions were carried out in triplicate. All medias were at 1% salinity. Incubations were conducted at 30^{o}C. Growth was assayed every 7 days, for a total of 28 days. Growth was compared to the FDA Bacterial Analytical Manual appendix 2 to determine the most probable number. It should be noted that the MPN is an estimate of growth units or colony-forming units and not individual bacterial cells.

For the samples from Rager Mountain, in order set up MPN analysis, a measured amount (g or ml) of each sample was first suspended in 20 ml of sterile PBS buffer and vortexed vigorously for 1 minute. Heavy solids were allowed to gravity settle. 1 ml of this initial dilution was used to inoculate each of the first bottles in the dilution series, creating the initial inoculations, with each bottle containing 10 ml such that each dilution is 10X. The initial inoculations were then subject to 7 additional serial 10-fold dilutions as such: 1 ml was transferred to the next media bottle in the series, shaken to mix, then a new syringe was used to transfer 1 ml into the next media bottle in the series, etc, until 8 media bottles were inoculated in the dilution series. Each dilution series was set up in triplicate (3 times) and cultures are incubated for 28 days at 30 ^{o}C to allow for microbial growth). The presence of growth is recorded every week for 4 weeks at which time the number of positive bottles in a dilution series are used to calculate the starting concentration of bacteria in the initial inoculum, and this number adjusted based on the amount of starting material added to the initial 20 ml dilution used to inoculate the first bottles in the dilution series.

The following media types were chosen for this project, each provides information on a different phenotypic population:

Media	Full Name	Type of Organisms Detected
MPB	Modified Postgate's Medium B	Sulfidogen, SRB (sulfate reducing bacteria).
PRD	Phenol Red Dextrose	APB (acid producing bacteria) and GHB (general heterotrophic bacteria).
IRB	Iron Reducing Bacteria Media	IRB (iron reducing bacteria).

- **PRD** (phenol red dextrose) culture media is used for enumeration of **APB** (acid producing bacteria) and **GHB** (general heterotrophic bacteria).
  - APB convert the bright red media to bright yellow.
  - GHB appear as turbid growth in the red media.
  - All cultures positive for APB are considered positive for GHB.
- **MPB** (modified Postgate's B) culture media is used for enumeration of **SRB** (sulfate reducing bacteria). Although MPB is somewhat selected for SRB, other H2S producing sulfidogenic bacteria such as peptide fermenting organisms and thiosulfate reducing bacteria will sometime grow in MPB, and also generate a positive response.
  - **SRB and Sulfidogens** generate H2S, forming a black FeS precipitate.
- **IRB** (iron reducing bacteria) culture media is clear and slightly yellow-green, with no precipitate.
  - **IRB** Iron reducing organisms chelate the iron, resulting in a clear media with green precipitate.

A 1% salinity was used for all medias. Culturing temperature was set at 30ºC.
Final readings were taken after full 28 days of incubation.

DNA Isolation for qPCR and Amplicon Metagenomics

DNA isolated from the samples were used for both the qPCR and 16S amplicon metagenomics assays. Scale samples such as those from Rager Mountain are atypical samples for DNA isolation, as they consist mostly of non-biological material including possible inhibitors of the DNA isolation and downstream analysis steps. DNA isolations had to be performed multiple times to identify the approach that worked best for that individual sample. The most challenging part is separation of a bacterial fraction away from non-biological materials in the sample. For solid samples, a combination of extraction in sterile PBS buffer and centrifugation was used to isolate a bacterial fraction away from other material in the sample. For liquid samples, a combination of filtration (using sterile 0.2 micron polyethersulfone (PES) membrane filter units) and / or centrifugation. Centrifugation was performed either in 50 ml centrifuge tubes, centrifuged at 2000 g for 50 minutes, or in 2 ml sample tubes, centrifuged for 10,000 g for 15 minutes, depending on volume. Pellets, containing bacteria and additional sample solids, were resuspended in the DNA isolation buffer and processed. For samples with bacteria concentrated by filtration, after filtration the bacteria are trapped on the filter surface while sterile liquids flow through the filtrate reservoir. Bacteria on the surface of the membrane are eluted with sterile PBS buffer, and pelleted by centrifugation. Once a bacterial pellet fraction was prepared, total DNA was isolated using the Qiagen DNeasy UltraClean Microbial Kit (12224-250). Additionally, a "direct isolation" approach was used, in which sample was placed directly into the DNA isolation reagents without the initial bacterial concentration steps. This approach utilized the Qiagen DNeasy Soil DNA Isolation Kit (47014) and / or the Qiagen DNeasy PowerMax Soil DNA Isolation Kit (12988-10) methods, although DNA yields using these approaches were generally not sufficient for downstream analysis.

Primers for 16S qPCR microbial quantification:

515F-GTGCCAGCMGCCGCGGTAA
806R-GGACTACHVGGGTWTCTAAT.
16S probe TACAAGGCCCGGGAACGTATTCACCG
For qPCR, 2.5uL of Sample DNA was loaded into 10uL Quanta Perfecta Tough Mix (QuantaBio) and run on a Roche 480 LightCyler ® with the following cycling conditions: one cycle at 50ºC for 2 minutes, one cycle at 95ºC for 10 minutes, 35 cycles at 95ºC for 15 seconds and 60ºC for 1 minute, and finally, one cycle at 40ºC for 30 seconds. Results of qPCR were scored based on CT score (a positive result was recorded if the CT was ≤30 cycles, negative if CT>30 cycles)..

Amplicon Metagenomics

Illumina 2-step MiSeq
Samples were amplified for sequencing in a two-step process. The forward primer was constructed with (5'-3') the Illumina i5 sequencing primer (TCGTCGGCAGCGTCAGATGTGTATAAGAGACAG) and the indicated forward primer. The reverse primer was constructed with (5'-3') the Illumina i7 sequencing primer (GTCTCGTGGGCTCGGAGATGTGTATAAGAGACAG) and the indicated reverse primer. Amplifications were performed in 25 ul reactions with Qiagen HotStar Taq master mix (Qiagen Inc, Valencia, California), 1ul of each 5uM primer, and 1ul of template. Reactions were performed on ABI Veriti thermocyclers (Applied Biosystems, Carlsbad, California) under the following thermal profile: 95○C for 5 min, then 35 cycles of 94○C for 30 sec, 54○C for 40 sec, 72○C for 1 min, followed by one cycle of 72○C for 10 min and 4○C hold.
Products from the first stage amplification were added to a second PCR based on qualitatively determine concentrations. Primers for the second PCR were designed based on the Illumina Nextera PCR primers as follows: Forward - AATGATACGGCGACCACCGAGATCTACAC[i5index]TCGTCGGCAGCGTC and Reverse - CAAGCAGAAGACGGCATACGAGAT[i7index]GTCTCGTGGGCTCGG. The second stage amplification was run the same as the first stage except for 10 cycles.
Amplification products were visualized with eGels (Life Technologies, Grand Island, New York). Products were then pooled equimolar and each pool was size selected in two rounds using SPRIselect (BeckmanCoulter, Indianapolis, Indiana) in a 0.7 ratio for both rounds. Size selected pools were then run on a Fragment Analyzer (Advanced Analytical, Ankeny, Iowa) to assess the size distribution, quantified using the Qubit 3.0 fluorometer (Life Technologies), and loaded on an Illumina MiSeq (Illumina, Inc. San Diego, California) 2x300 flow cell at 10pM and sequenced.

Notes on Taxonomic and Metabolic Assignment
Organisms are referred to by the identity of the most closely matched organism in the database. However, this does not indicate 100% identity. In most cases, the most closely matched organisms are referred to as "uncultured organism" and as such there is no physiological or metabolic information for them. Organisms that fall below the cutoff for taxonomic assignment are listed as unclassified. Due to the unusual source of samples, a large number of organisms in the samples may unclassified. This indicates that they are novel organisms that have not been described in the scientific literature.
Metabolic assignments are inferred by the metabolic characteristics of the most closely related organism for which experimental data has been provided. Some metabolic groupings are overlapping and non-exclusive, e.g. many fermentative organisms generate organic acids or are capable of sulfidogenesis under some conditions. An overview of select metabolisms is provided in Appendix B.

Overview of Select Metabolic Processes

APB: Acid-Producing Bacteria
Acid-producing bacteria are of specific interest to the oilfield community as acid production directly and aggressively promotes corrosion. Several metabolic pathways result in the production of acids, including fermentation pathways that generate organic acids such as lactic acid and acetic acid, as well as those that generate inorganic acids such as sulfuric acid as a byproduct of the oxidation of inorganic sulfur compound. Not all fermentative pathways result in acidification of the surrounding environment. The identification of bacteria as acid producing does not necessarily indicate acidification of bulk fluids.

Biodeg: Biodegradation
Some bacterial genera and species have the capacity to utilize "atypical" or "unusual" substrates as carbon sources. These bacteria are loosely referred to as Biodeg, for "Biodegradation". The definition used here for "atypical or unusual substrates" with reference to bacterial metabolism includes compounds that most bacteria cannot utilize as a food source. Unusual compounds Biodeg organisms utilize include disinfectants, antibiotics, xenobiotics and detergents. Some degrade long chain polymers of sugars and carbohydrates, such as those found in cell wall materials. Others are able to degrade hydrocarbons. Hydrocarbons, including alkanes, alkenes, aromatic hydrocarbons, and waxes, are found naturally in great variety in crude oil and other petroleum compounds. Due to their structural diversity, most bacteria lack the capacity to utilize petroleum hydrocarbons as food sources. Each type of hydrocarbon-degrading microorganism is likely to be capable of metabolizing a few specific types of hydrocarbons.

IRB: Iron-Reducing Bacteria, Fe(III)RB
Some microbes can use Fe(III) as an electron acceptor, reducing it to Fe(II). Iron reduction has been observed under both acidophilic and neutrophilic conditions. Two common iron-reducing genera are Shewanella and Geobacter. In addition to IRB activity, Shewanella species produce chelators that solubilize Fe(III) oxides (Lovley et al, 2004). Shewanella are capable of growing in corrosive biofilms where they have been shown to remove the protective H2 film layer that normally protects iron surfaces from corrosion under anoxic conditions. should not be confused with iron oxidizing bacteria, which are aerobes responsible for a rust brown staining and slimy growth in surface waters.

NRB: Nitrate Reducing Bacteria
NRB reduce nitrates to nitrites, nitrous oxide, or nitrogen under anaerobic conditions in a process termed denitrification. Most are heterotrophic facultative anaerobic bacteria including such common bacteria as *Paracoccus, Pseudomonas, Alcaligenes,* and *Bradyrhizobioium*. A few bacteria use such reduction processes as hydrogen acceptor reactions and hence as a source of energy; in this case the end product is ammonia. Denitrification is a normal part of nitrogen cycling and not all NRB are of concern to O&G infrastructure.

A subcategory of NRB is the **NRSOB**: Nitrate-Reducing Sulfur-Oxidizing Bacteria are a specific subgroup of NRB whose levels are increased in reservoirs following nitrate injections (Gittel et al 2009; Grigoryan et al, 2008; Hubert and Voordouw, 2007). Growth of NRSOB suppresses the activity of SRB, and thus reducing sulfidogenisis. Some Epsilonproteobacteria can also oxidize petroleum sulfur compounds and utilize nitrate as an electron acceptor for growth, and thus may be considered hydrocarbon degrading. Massive dominance of related Epsilonproteobacteria has been observed in other petroleum samples, for example in formation waters from a Canadian oil sands reservoir containing severely biodegraded oil. (Kodama, Y and Kazuya Watanabe, 2003; Hubert et al, 2011). Sulfurospirillum are nitrate-reducing, sulfur oxidizing bacteria (NRSOB) members of the class Epsilonproteobacteria and are sometimes referred to as “Campylobacter” in older publications. The way in which nitrate addition can affect the SRB population involves several pathways. First, nitrate is a thermodynamically more favorable electron acceptor than sulfate, thus NRB have a competitive advantage. To emphasize the complexity of the metabolism in oilfield samples, it should be noted that under some conditions, these bacteria are also sulfidogens capable of reducing sulfur and thus producing H_2S (Finster K et al, 1997).

Sulfidogenesis: (e.g. SRB, TRB, SuRB)
The metabolic pathways of most interest to the oilfield community are those that generate significant levels of hydrogen sulfide (H_2S). In addition to inorganic processes, biogenic processes can generate significant levels of hydrogen sulfide, primarily through the action of sulfidogenic bacteria. Bacteria that evolve hydrogen sulfide are commonly referred to as “sulfidogens”. Sulfate-reducing bacteria (SRB) are particularly aggressive at sulfide production and are the group of bacteria most commonly implicated oil filed biogenic sulfide production (Barton et al, 2009). Hydrogen sulfide formation by sulfate-reducing bacteria (SRB) under strict anaerobic circumstances is a common problem in sediments, sewer systems, oil reservoirs and anaerobic effluents (Holmer & Storkholm, 2001; McComas et al., 2001). The emission of H_2S into the atmosphere of sewer systems does not only imply odor nuisances and possible health risks. It also induces the biological production of sulfuric acid in the aerobic zones, causing severe corrosion of the inner surface of concrete sewer structures (Sand, 1987; Vincke et al., 2002). Hence, preventive or curative actions are needed.

While SRB are traditionally associated with O&G system sulfide generation, sulfur- and thiosulfate-reducing bacteria (SuRB and TRB, respectively) can also generate significant levels of H_2S and contribute to corrosion and souring (Hulecki JC et al, 2009, Magot et al 1997, Agrawal et al, 2010). Compared to SRB, the TRB are harder to classify taxonomically, as they are members of bacterial genera that can include non-tSRB members. Examples of sulfidogenic TRB commonly found in oilfield samples include *Halanaerobium congolense*, as well as some *Thermoanaerobacter*, and *Spirochaeta*. Additionally, many common enteric bacteria are sulfidogenic, including *Citrobacter* and *Salmonella*.

Thermophiles:
A thermophile is an organism that can survive and often thrives in environments having relatively high temperatures ranging between 45 and 122 °C.

Methanogens:

Methanogens are Archaea that produce methane as a metabolic byproduct in anoxic conditions. Methanogens are found in different environments including wetlands (marsh gas), animal digestive tracts (methane production of cattle and in farts), and anaerobic digestor sludges of wastewater treatment systems. Some methanogens are extremophiles and can be found in hot springs, submarine hydrothermal vents as well as in the "solid" rock of the Earth's crust, kilometers below the surface. Methanogens are associated with microbial influenced corrosion. Hydrogenotrophic methanogens are believed to cause metal corrosion through cathodic depolarization, whereas the acetotrophic methanogens grow syntrophically with corrosion-causing SRB.

Appendix D References

1. Angelez-Chavez, C., Mora-Mendoza, J.L., Garcia-Esquivel, R., Padilla-Viveros, A.A., Perez, R., Flores, O. and Martinez, L. (2002) Microbiologically influenced corrosion by Citrobacter in sour gas pipelines. Mater Perform 41, 50-55.
2. Balch, W. E.; Schoberth, S.; Tanner, R. S.; Wolfe, R. S. (1977). Acetobacterium, a New Genus of Hydrogen-Oxidizing, Carbon Dioxide-Reducing, Anaerobic Bacteria. International Journal of Systematic Bacteriology 27 (4): 355.
3. Barton LL, Fauque GD. (2009) Biochemistry, physiology and biotechnology of sulfate-reducing bacteria. Adv Appl Microbiol. 68:41-98.
4. Bermont-Bouis D, Janvier M, Grimont PA, Dupont I, Vallaeys T. (2007) Both sulfate-reducing bacteria and Enterobacteriaceae take part in marine biocorrosion of carbon steel. J Appl Microbiol. 102:161-168.
5. Bermont-Bouis D, Janvier M, Grimont PA, Dupont I, Vallaeys T. (2007) Both sulfate-reducing bacteria and Enterobacteriaceae take part in marine biocorrosion of carbon steel. J Appl Microbiol. 102:161-168.
6. Boone DR, Whitman WB, Rouviere P (1994). "Diversity and taxonomy of methanogens". In JG Ferry, ed. Methanogenesis: Ecology, Physiology, Biochemistry & Genetics. Pp 35-80.
7. D'Ippolito S, de Castro RE, Herrera Seitz K. (2011) Chemotactic responses to gas oil of Halomonas spp. strains isolated from saline environments in Argentina. Rev Argent Microbiol. 43(2):107-10.
8. Dice, L.R., "Measures of the Amount of Ecologic Association Between Species," *Ecology* 26, 3, (1945): pp.297-302
9. Hubert CR Oldenburg TB, Fustic M, Gray ND, Larter SR, Penn K, Rowan AK, Seshadri R, Sherry A, Swainsbury R, Voordouw G, Voordouw JK, Head IM. (2012) Massive dominance of Epsilonproteobacteria in formation waters from a Canadian oil sands reservoir containing severely biodegraded oil. Environ Microbiol. 14(2):387-404.
10. Kryachko Y, Dong X, Sensen CW, Voordouw G. (2012) Compositions of microbial communities associated with oil and water in a mesothermic oil field. Antonie Van Leeuwenhoek. 101: 3, pp 493-506
11. Kwon S, Moon E, Kim TS, Hong S, Park HD. (2011) Pyrosequencing demonstrated complex microbial communities in a membrane filtration system for a drinking water treatment plant. Microbes Environ. 26(2):149-55.
12. Li XX, Yang T, Mbadinga SM, Liu JF, Yang SZ, Gu JD, Mu BZ. Responses of Microbial Community Composition to Temperature Gradient and Carbon Steel Corrosion in Production Water of Petroleum Reservoir. Front Microbiol. 2017 Dec 5;8:2379.
13. Lonergan DJ, Jenter HL, Coates JD, Phillips EJ, Schmidt TM, Lovley DR (1996) Phylogenetic analysis of dissimilatory Fe(III)-reducing bacteria. J Bacteriol. 178(8):2402-8.
14. Montoya D, Ar_valo C, Gonzales S, Aristizabal F, Schwarz WH. (2001) New solvent-producing Clostridium sp. strains, hydrolyzing a wide range of polysaccharides, are closely related to Clostridium butyricum. J Ind Microbiol Biotechnol. 27(5):329-35.
15. Pham,V.D., Hnatow,L.L., Zhang,S., Fallon,R.D., Jackson,S.C., Tomb,J.F., DeLong,E.F. and Keeler,S.J. (2009) Characterizing microbial diversity in production water from an Alaskan mesothermic petroleum reservoir with two independent molecular methods Environ. Microbiol. 11 (1), 176-187.
16. Rajasekar A, Anandkumar B, Maruthamuthu S, Ting YP, Rahman PK. (2010) Characterization of corrosive bacterial consortia isolated from petroleum-product-transporting pipelines. Appl Microbiol Biotechnol. 85(4):1175-88.
17. Ravot G, Ollivier B, Magot M, Patel B, Crolet J, Fardeau M, Garcia J. (1995) Thiosulfate reduction, an important physiological feature shared by members of the order thermotogales. Appl Environ Microbiol. 61(5):2053-5.
18. Vigneron A, Alsop EB, Chambers B, Lomans BP, Head IM, Tsesmetzis N. Complementary Microorganisms in Highly Corrosive Biofilms from an Offshore Oil Production Facility. Appl Environ Microbiol. 2016 Apr 4;82(8):2545-2554.
19. Vigneron A, Head IM, Tsesmetzis N. Damage to offshore production facilities by corrosive microbial biofilms. Appl Microbiol Biotechnol. 2018 Mar;102(6):2525-2533.
20. *Yan, Z., Zheng, X.-W., Chen, J.-Y., Han, J.-S. and Han, B.-Z. (2013), Effect of different Bacillus strains on the profile of organic acids in a liquid culture of Daqu. J. Inst. Brew., 119: 78-83.* https://doi.org/10.1002/jib.58 https://onlinelibrary.wiley.com/doi/epdf/10.1002/jib.58
21. Zhang T, Ye L, Tong AH, Shao MF, Lok S. (2011) Ammonia-oxidizing archaea and ammonia-oxidizing bacteria in six full-scale wastewater treatment bioreactors. Appl Microbiol Biotechnol. 91(4):1215-25.

Project Report

Microbial Population Analysis of Organisms Associated with the Rager Mountain Gas Storage Failure

Well 2251 & Compressor Station Fluids

Prepared for
Ravi M. Krishnamurthy
Blade Energy Partners

Prepared by:
Elizabeth Summer, PhD
Ecolyse, Inc
11142 Hopes Creek Road
College Station, Texas 77845

Final Report

June 20, 2023

Well 2251 Microbiological Analysis: Statement of Findings

Microbiological analysis was conducted on well pad soil and 7" casing OD scale collected from well 2251 in Feb - March 2023. These results represent the microbial population at the time of sampling. At the time of sampling, even though the soil profile was similar to that of soils from other locations within the facility, the microbial levels in the C001 scale samples were extremely low, less than 300 cells per g for GHB, with IRB and SRB were not detected. qPCR results supported the MPN data, indicating microbial load was below the limit of detection of the assay. Because microbial load in these samples was so low, MIC seems unlikely.

Compressor Station Fluids Microbiological Analysis: Statement of Findings

Microbiological analysis was conducted on fluids collected from the Compressor Station pond and separator in March 2023. These results represent the microbial population at the time of sampling.

Compressor Station Pond Samples
At the time of sample, MPN and genetic data both supported a model in which the two compressor station pond samples were dominated by GHB, levels of between 10^5 and 10^7 cells per ml, while APB, SRB, and IRB levels, although present, were extremely minor components of the population. The predominant organisms in the pond samples were the GHB Pseudomonas and Sphingomonas. This is not a population of bacteria associated with MIC.

Compressor Station Separator Samples
Clear fluid sample: Of the two compressor station separator samples, one (the clear sample) contained negligible bacteria as determined by both MPN and qPCR.
Black fluid sample: The black compressor station sample, in contrast, showed little evidence of microbial activity by MPN culture-based assay. However, DNA was isolated from the sample, and qPCR indicated around 6.2E+04 microbial cells per ml liquid. Population profile analysis of this sample identified a single species, Thermoanaerobacterium saccharolyticum as constituting over 91% of the sample
Thermoanaerobacterium saccharolyticum is a strict anaerobe, spore forming clostridia.
Thermoanaerobacterium species include sulfidogens and acid producing members.
It is likely this organism failed to grow in the MPN cultures, and so additional work is required to determine if the strain present in the compressor station separator black fluids is indeed a sulfidogen and or acid producing organism.

M 979-694-6500 ● F 979-694-6511 ● 11142 Hopes Creek Road ● College Station, Texas 77845 ● www.ecolyse.com

Well 2251 and Compressor Station Fluids Population Analysis: Detailed Methods and Results

Sample Information

Well 2251

- For well 2251, 4 samples were collected and analyzed.
- These samples included:
  - Well 2251 pad area soil pre-samples were collected on Feb 16 2023 Soil" refers to rock, dirt, and mud collected around wellsite% 1 sample
  - Well 2251 7" casing joint C001 OD scale% 3 samples
- "Scale" refers to all solids scraped from surfaces. These were primarily metal flakes

Compressor Station Fluids

- For compressor station fluids, 4 samples were collected and analyzed
- These samples included:
  - Black fluids from the separator
  - Clear fluids from the separator
  - Clear pond fluids
  - Emulsion pond fluids
- Table 1 provides an overview of well 2251 and Compressor Station Fluid samples
- Appendix A provides more details on each sample

Table 1. Well 2251, and Compressor Station Sample Overview

#	Sample Date	Well	Sample Description	Type	Quantity
1.A Well 2251 Well site soil, 7" casing OD					
3	2/16/23	2251	Well 2251 Soils	Soil	162.0
62	4/01/23	2251	Well 2251, 7" casing OD, C001 top of joint	S	23.2 g
63	4/03/23	2251	Well 2251, 7" casing OD, C001 top of joint	S	508.5 g
64	4/03/23	2251	Well 2251, 7" casing OD, C001 10'6" from top	S	9.2 g
1.B Compressor Station Fluid Samples					
57	3/28/23	CS	Compressor station separator fluid, Black.	L	~200 ml
58	3/28/23	CS	Compressor station separator fluid, Clear.	L	~200 ml
60	4/01/23	CS	Compressor Station pond sample, Clear	L	500 ml
61	4/01/23	CS	Compressor Station pond sample, Emulsion	L	500 ml

Details of Samples used for MPN and DNA based microbial population analysis. Exact samples included in each pool are found in Appendix A. Collection date and well pad. Description of each sample includes well, OD or ID, casing joint, detail of sample type. Sample types are Soil, L liquid, S scale. Soil refers to dirt and rocks collected from the well pads. Scale refers to any solids originating on the surface of a casing joint or tree. S is Scale typically contains a large amount of metal flakes. Amount of material collected is provided in ml or g.

Methods Used for Microbial Population Profiles Evaluation

- Testing microbial populations for corrosion potential is based on recommendations and guidelines established by NACE (National Association of Corrosion Engineers),.
- NACE Standard Test Methods include those described in the following documents:

NACE ID	Item	Standard Test Method
TM0194	21224	Field Monitoring of Bacterial Growth in Oil and Gas Systems
TM0212	21260	Detection, Testing, and Evaluation of Microbiologically Influenced Corrosion on Internal Surfaces of Pipeline
TM0106	21248	Detection, Testing, and Evaluation of Microbiologically Influenced Corrosion (MIC) on External Surfaces of Buried Pipeline

- NACE recognizes that the subsurface and infrastructure systems being sampled vary greatly with respect to accessibility, as well as physical, chemical, and biological traits, and thus it is impossible to give an exact list of methods or protocols that must be followed absolutely.
- Guidelines must be adapted to any given situation and system.
- In recognition of these guidelines, a conservative, combined approach was adopted for the Rager Mountain project.
- The approach used included the most traditional and well-established method (triplicate MPN set up in standard medias for APB, SRB, IRB and GHB) method, along with two more advanced approaches (qPCR and amplicon metagenomics)
- **Interpretation of results:** Microbiological data does not provide simple “action level” “cut-off concentrations” data. MIC is a highly complex problem, impacted not only by the numbers and extreme diversity of organisms, but their metabolic activity levels, and fluctuations in environmental physio-chemical conditions (for example, nutrients, temperature, water levels, water circulation, chemical treatments).

NACE TM0194-94 statement of interpretation of MPN data:
1.1.8 The simple presence of bacteria in a system does not necessarily indicate that they are causing a problem. In addition, bacterial populations causing problems in one situation, or system, may be harmless in another. Therefore, “action” concentrations for bacterial contamination cannot be given. Rather, bacterial population determination are one more diagnostic tool useful in assessing oilfield problems**.**

Project Results: MPN Culture-Based Bacterial Diversity Analysis

1. Triplicate, Culture -Based MPN Method

MPN stands for “Most Probably Number” and is a culture-based method for the quantification of specific types of bacteria in a sample. The data generated is in terms of “bacteria per ml” or “bacteria per g” of sample, where “bacterial types” are members of a phenotypic group rather than a taxonomic group. The identity of the organisms quantified is based on the use of the selective indicator artificial growth media used to set up the assay. Indicator medias contain a substrate that undergoes a visible chemical change when certain types of bacteria grow in them, for example, addition of a pH indicator will provide strong visual evidence for the growth of acid producing bacteria that have dropped the media pH. Selective medias contain substrates and conditions that promote the growth of certain types of bacteria, for example, anaerobic conditions and addition of sulfate promotes the growth of sulfate reducing bacteria.

Figure 1 shows what the indicator, selective medias used in this study look like:

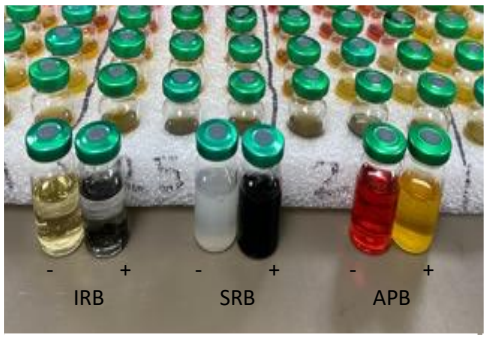

A. How + plus and - minus bacterial growth appears in 3 selective indicator medias used for this project: IRB (iron reducing bacteria), MPB (SRB: sulfate reducing bacteria), PRD (APB: acid producing bacteria)

B. Triplicate MPN set-up for 4 samples (samples 24, 25, 26, 27). There are 3 dilution series columns set up in parallel for each sample, so 24 media bottles are inoculated per sample.

Figure 1. MPN microbial culture vials.

MPN Method Advantages

- Minimal sample manipulation is required to set up assay.
- Easy to interpret results
- Low-tech and easy to set up in the field.
- Determines the number of live, culturable bacteria in the sample.
- Provides experimental phenotypic data.
- Traditional method, recommended by NACE as a standard method.
- Historical approach that is widely used in throughout the industry.
- Can be used for the analysis of anaerobic organisms.

MPN Method Disadvantages

- There are well-known limitations inherent in culture-based analysis,
- **NACE TM0194 describes some of these limitations (direct quote):**
  - *3.1.1 Bacterial culturing in artificial growth media is accepted as the standard technique for the estimation of bacteria numbers. However, users should be aware of the limitations of the culture technique:*
  - *3.1.1.1 Any culture medium grows only those bacteria able to use the nutrients provided.*
  - *3.1.1.2 Culture medium conditions (pH, osmotic balance, redox potential, etc.) prevent the growth of some bacteria and enhance the growth of others.*
  - *3.1.1.3 Conditions induced by sampling and culturing procedures, such as exposure to oxygen, may hamper the growth of strict anaerobes.*
  - *3.1.1.4 Only a small percentage of the viable bacteria in a sample can be recovered by any single medium; i.e., culture media methods may underestimate the number of bacteria in a sample.*
  - *3.1.1.5 Some bacteria cannot be grown on culture media at all.*

Well 2251 and Compressor Station Fluids – Culture-Based MPN Enumeration of APB, GHB, SRB, and IRB

- MPN analysis was set up with 4 well 2251 and 4 compressor station fluid samples, in 3 medias each (PRD, MPB, IRB)
- These 3 medias provide quantitative data for 4 metabolic categories: APB, GHB, SRB, IRB
  - **PRD** (phenol red dextrose) culture media is used for enumeration of **APB** (acid producing bacteria) and **GHB** (general heterotrophic bacteria).
    - APB convert the bright red media to bright yellow.
    - GHB appear as turbid growth in the red media.

        - All cultures positive for APB are considered positive for GHB.
    - **MPB** (modified Postgate's B) culture media is used for enumeration of **SRB** (sulfate reducing bacteria). Although MPB is somewhat selected for SRB, other H2S producing sulfidogenic bacteria such as peptide fermenting organisms and thiosulfate reducing bacteria will sometime grow in MPB, and also generate a positive response.
        - **SRB and Sulfidogens** generate H2S, forming a black FeS precipitate.
    - **IRB** (iron reducing bacteria) culture media is clear and slightly yellow-green, with no precipitate.
        - **IRB** Iron reducing organisms chelate the iron, resulting in a clear media with green precipitate.
- As per NACE standards, readings were taken weekly for 4 weeks.
- Resulting values were converted to microbial cells per g or ml of starting material, after accounting for the initial dilution of the sample used to inoculate the first bottle in each dilution series.
- Resulting values were converted to microbial cells per g or ml of starting material, after accounting for the initial dilution of the sample used to inoculate the first bottle in each dilution series.
- Table 2 shows the results of after 4 weeks of growth, for all 8 well 2251 and CS samples.

Table 2. Well 2251 and Compressor Station; Results of MPN Analysis

#	Well	Sample Description	Type	APB	GHB	IRB	SRB
2.A Well 2251 Well site soil, 7" casing OD							
3	2251	Well 2251 Soils	Soil	2.9E+07	1.6E+09	5.3E+03	1.8E+04
62	2251	Well 2251, 7" casing OD, C001 top of joint	S	2.5E+01	9.5E+01	<LOD	<LOD
63	2251	Well 2251, 7" casing OD, C001 top of joint	S	9.0E+00	2.5E+01	<LOD	<LOD
64	2251	Well 2251, 7" casing OD, C001 10'6" from top	S	9.5E+01	2.5E+02	<LOD	<LOD
2.B Compressor Station Fluid Samples							
57	CS	Compressor station separator fluid, Black.	L	6.0E+00	1.2E+02	2.5E+01	<LOD
58	CS	Compressor station separator fluid, Clear.	L	6.0E+00	7.5E+01	2.5E+01	<LOD
60	CS	Compressor Station pond sample, Clear	L	1.1E+01	2.0E+05	<LOD	<LOD
61	CS	Compressor Station pond sample, Emulsion	L	9.5E+02	4.5E+07	4.0E+01	1.5E+01

MPN Results Table Legend. Results of population analysis by triplicate MPN method. Values are the culturable bacteria per g of each sample, set up in triplicate, after 28 days of growth. SRB: Sulfate-Reducing Bacteria. APB: Acid Producing Bacteria, GHB: General Heterotrophic Bacteria, IRB: Iron Reducing Bacteria, Yellow are >10^6, Red are between 10^4 - 10^6, Green are between 10^3 - 10^4, White are <10^3, Grey <LOD indicates "below limit of detection", e.g. no growth

Well 2251 MPN Analysis Overall Results

- Out of 4 samples collected from well 2251:
    - Soil sample tested positive for APB, GHB, IRB, and SRB
    - The 3 C001 scale samples contained neglidgable APB and GHB, and no IRB or SRB
    - The average cell density for C001 scale samples was less than 100 cells per g sample
    - **This is an insignificant concentration of bacteria**.

Compressor Station Fluids MPN Analysis Overall Results Fig 2, Table 3

- Out of 4 samples collected from well 2251:
    - The two separator fluid samples tested positive for APB, GHB, IRB, but at very low levels
        - Cell densities all less than 120 cells per g, a negligible level
        - No SRB were detected in the separator fluids
    - The compressor station pond samples contained significant levels of GHB,
        - GHB in the clear and emulsion sample at 2.0E+05 and 4.5E+07, respectively
        - Almost no APB, IRB, and SRB grew in the culture bottles from the pond samples

Profiles of organisms from well 2251 C001 scale and compressor station fluids is quite different from that of fluids and scale from wells 2244 and 2248,

In contrast, the well 2251 soil sample was quite similar to the soil sample from wells 2244 and 2248.

Figure 2 and Table 3. Well 2251 and Compressor Station Fluid MPN Data Summarized by Sample Type

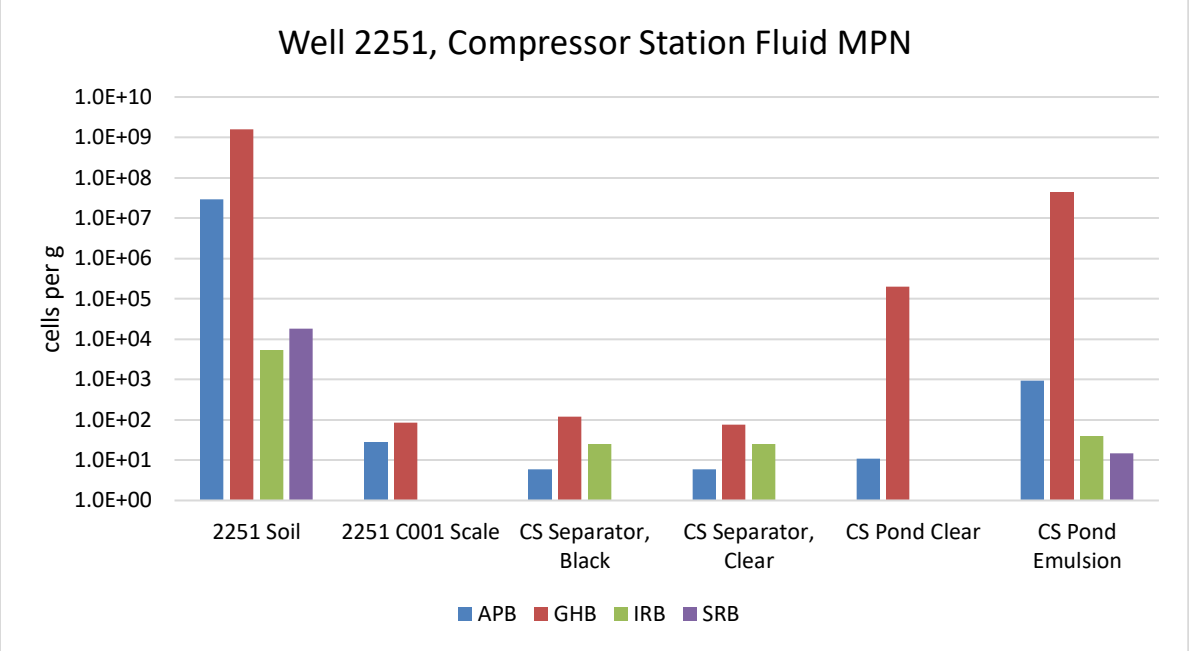

Figure 2. Graphical representation of data in Table 3.

Table 3. Summary MPN Culture Based Microbial Density Wells 2251, Compressor Station.

Sample Group	Sample Description	Type	APB	GHB	IRB	SRB
3	2251 Soil	Soil	2.9E+07	1.6E+09	5.3E+03	1.8E+04
62, 63, 54	2251 C001 Scale	S	2.8E+01	8.4E+01	<LOD	<LOD
57	CS Separator, Black	L	6.0E+00	1.2E+02	2.5E+01	<LOD
58	CS Separator, Clear	L	6.0E+00	7.5E+01	2.5E+01	<LOD
60	CS Pond Clear	L	1.1E+01	2.0E+05	<LOD	<LOD
61	CS Pond Emulsion	L	9.5E+02	4.5E+07	4.0E+01	1.5E+01

Averages were calculated from Ln for each sample group. Results of population analysis by triplicate MPN method. Values are the culturable bacteria per g of each sample, set up in triplicate, after 28 days of growth. SRB: Sulfate-Reducing Bacteria. APB: Acid Producing Bacteria, GHB: General Heterotrophic Bacteria, IRB: Iron Reducing Bacteria, Yellow are >10^6, Red are 10^4 - 10^6, Green are 10^3 - 10^4, White are <10^3, Grey <LOD are "below limit of detection", e.g. no growth. CS is compressor station.

Project Results: Bacterial Diversity Analysis by Genetic Approaches

- qPCR and Amplicon Metagenomics are two approaches that rely on DNA isolation from a sample
- Isolated DNA is used for two types of analysis: qPCR and Amplicon Metagenomics
- qPCR provides quantitative data on total microbial load per g or ml sample
- Amplicon metagenomics provides identification of the types of microbes in a sample
- Information gathered includes the types of bacteria and the % in the population
- Amplicon metagenomics and qPCR do not differentiate between live and dead cells
- The identity of the species in the sample is used to predict the physiological or metabolic role that organism might have in the environment
- The prediction is done by comparing the organisms identified to the research on that type of organism, available in the scientific literature
- Not every organism has been studied enough to understand its metabolism
- Following traits assigned to identified bacteria and archaea where possible:
    - **Sulfidogen**-includes all bacteria that can produce sulfide or H_2S as a metabolic byproduct. This includes "true" SRB as well as TRB (thiosulfate-reducing bacteria) SuRB(sulfur-reducing bacteria) and peptide-fermenting bacteria (such as some Clostridia)
    - **SRB**-(sulfate-reducing bacteria) "true" SRB, utilize sulfate as respiratory electron acceptor and produce sulfide as a metabolic byproduct
    - **APB**-(acid-producing bacteria) these make organic and/or inorganic acids. Not all APB result in a lowering of ambient pH. Organisms that produce inorganic acids are often acidophilic, and grow at very low corrosive pH.
    - **IRB**-(iron-reducing bacteria) many are strongly corrosive
    - **NRB**-(nitrate-reducing bacteria) many bacteria are nitrate reducers. Of particular relevance to the O&G industry are the NRSOB (nitrate-reducing sulfur-oxidizing bacteria) promoted by nitrate injections.
    - **Biodeg**-biodegrading bacteria. These bacteria are capable of breaking down unusual substrates such as O&G hydrocarbons **(HC),** petrochemicals, cellulose, toxic chemicals etc.
    - **Methanogen** – Archaea that produce methane as a metabolic byproduct under anaerobic growth
    - **Methylotroph**- Utilize reduced one-carbon compounds, such as methanol or methane, as the carbon source for their growth; and multi-carbon compounds that contain no carbon-carbon bonds, such as dimethyl ether and dimethylamine.
    - **Phototroph**- photosynthetic organisms, these include both aerobes and anaerobes.
- Percent of population, and number of unique microbial types (species) are provided as results

Well 2251 and Compressor Station Fluids Genetic Based Diversity Analysis

DNA Isolation and qPCR from Well 2251 and Compressor Station Fluid Samples (Table 4)

Well 2251 qPCR Results

- DNA was isolated from 4 of the 4 well 2251 samples
- qPCR was conducted using “universal” primers that detect both bacteria and archaea.
- qPCR results
  - Soils: qPCR corroborated MPN results, indicating soils contained high microbial load of 9.6E+09 cells per g
  - C001 OD scale: qPCR corroborated MPN results, indicating all three casing scale samples contained negligible microbial cells
  - DNA population data was generated for the soil sample, but not the casing scale

Compressor Station qPCR Results

- DNA was isolated from 4 of the 4 Compressor Station fluid samples
- qPCR was conducted using “universal” primers that detect both bacteria and archaea.
- qPCR results
  - CS separator fluid, Black.
    - qPCR indicated microbial load more than 2 log orders higher then determined by MPN
  - CS separator fluid, Clear.
    - qPCR corroborated MPN results, indicating CS separator clear sample contained negligible microbial cells
  - CS pond sample, clear
    - qPCR indicated close agreement between microbial levels by qPCR and MPN
  - CS pond sample, emulsion
    - qPCR detected an almost 2 log order lower microbial load by qPCR then did MPN
    - This is a somewhat atypical result that happens when organisms in the sample are resistant to efficient DNA isolation, but grow well in culture
- Sequence data was generated for 3 of the 4 compressor station fluid samples

TABLE 4. RM Well 2251, and Compressor Station qPCR Results

#	DNA ID	Sample Description	Type	Seq Data?	qPCR Cells /g	MPN Max Cells /g
5.B Well 2251 Well site soil, 7” casing OD						
3	OG230207-003	Well 2251 Soils	Soil	Yes	9.6E+09	1.6E+09
62	OG230406-006	Well 2251, 7" casing OD, C001 top of joint	S	no	<LOD	9.5E+01
63	OG230406-007	Well 2251, 7" casing OD, C001 top of joint	S	no	<LOD	2.5E+01
64	OG230406-008	Well 2251, 7" casing OD, C001 10'6" from top	S	no	<LOD	2.5E+02
5.C Compressor Station Fluid Samples						
57	OG230409-004	Compressor station separator fluid, Black.	L	Yes	6.2E+04	1.2E+02
58	OG230409-005	Compressor station separator fluid, Clear.	L	no	<LOD	7.5E+01
60	OG230409-001	Compressor Station pond sample, clear	L	Yes	6.4E+04	2.0E+05
61	OG230409-002	Compressor Station pond sample, emulsion	L	Yes	3.1E+05	4.5E+07

Results of qPCR quantification of total microbes in samples from well 2248, well 2251, and the compressor station liquids. qPCR results, in microbial cells per g or ml sample, are provided. <LOD indicates “below the limit of detection”. These same DNA were subject to 16S amplicon metagenomics, and “Sequence Data” indicates of population profiles was obtained from the sample. Highlighted gray are samples that yielded population data. The data from MPN analysis is also provided, using values from Table 2. *nd is “not determined” due to insufficient amount of sample for both MPN and DNA isolation.

Well 2251 Microbial Diversity Analysis by Amplicon Metagenomics

- The scale samples from well 2251 contained close to 0 microbes per g, as determined by MPN and qPCR analysis
- Because there were no bacteria, no population profile could be elucidated for the scale samples
- Data was obtained for the soil sample, however as this sample is not particularly relevant on its one, the data is only briefly summarized.

Well 2251 Soil Sample Population Profile Summary

- 62993 sequences were analyzed, corresponding to 374 species
- 48% of the organisms were "Unclassified"
- 10% of the organisms were "unclassified Class Acidobacteriia"
- Sulfidogens were present at less than 1% of the population.
- GHB and biodegrading organisms dominated the sample
- IRB were identified, at 1.08% of the population
- APB were identified, predominantly an Acidobacterium, at 3% of the population
- Most organisms were present at less than 0.1% of the sample
- Predominant organisms, 15 out of 374, are provided in Table 5

Table 5. Well 2251 Soil Sample Microbial Diversity, The most abundant organisms

Species	OG230207-003 Well 2251 Soils	Traits of Interest: Metabolic, Taxonomic, Physiological
Unclassified	46.534	Polyphyletic; Unknown; Varies
Unclassified Class Acidobacteriia	*10.35%*	*Unknown, includes acid tolerant bacteria and APB*
Methylocystis sp	4.397	Alphaproteobacteria; Methylotroph
Mycobacterium sp	2.869	Actinobacteria; Environmental; Widespread
Hyphomicrobium sp	2.683	Aerobe; Alphaproteobacteria; BioDeg; Methylotroph; Soil
Acidobacterium sp	2.629	Acidobacteria; Acidophile; Aerobe; APB
Bradyrhizobium sp	2.018	Alphaproteobacteria; NiF
Bacillus sp	1.413	Bacilli; BioDeg; Diverse; Firmicutes; GHB; Spore
Steroidobacter sp	1.346	BioDeg; Gammaproteobacteria
Sphingomonas sp	1.326	Aerobe; Alphaproteobacteria; BioDeg; BioDeg PAH; GHB
Gemmata sp	1.187	Planctomycetes; Unknown
Herbaspirillum sp	0.949	Aerobe; Betaproteobacteria; NiF
Holophaga sp	0.937	Acidobacteria; BioDeg; BioDeg HC
Planctomyces sp	0.927	Planctomycetes
Pseudomonas sp	0.864	Aerobe; BioDeg; Gammaproteobacteria; GHB; Varies; Common

The value is the % of the total population. BioDeg are biodegrading organisms. PAH is polyaromatic hydrocarbons, HC are hydrocarbons, NiF are nitrogen fixing.
"Unclassified Class Acidobacteriia" is a subset of Unclassified

Compressor Station Fluids Microbial Diversity Analysis

- Population profile data was obtained for 3 samples containing the highest microbial levels as determined by MPN and qPCR
- Between 71976 and 88795 sequences were analyzed from each sample
- These corresponded to 417 different microbes
- The CS Separator black liquid sample was noticeable reduced in types of microbes, with only 31 species identified as compared to 392 and 161 for the other two samples

Table 6.A provides an overall summary of population profile data from compressor station fluid samples.

Table 6. Compressor Station Microbial Population Profile Analysis: Overview of all DNA sequence data sets				
Seq ID	OG230409-001	OG230409-002	OG230409-004	Total
Sample Details	s60. CS Pond Clear	s61. CS Pond Emulsion	s57 CS Separator Black Liquid	3 Samples
# Sequences	75956	71976	88795	236727
# Unique Species	392	161	31	417
6.B Selected Traits Relative Abundance and Number Species				
Aerobe	72.27% 60	85.96% 34	0.07% 10	49.35% 64
Anaerobe	0.64% 28	0.09% 8	99.74% 7	37.65% 32
APB	0.77% 19	0.19% 10	99.73% 5	37.71% 22
BioDeg	69.02% 69	75.16% 39	0.03% 8	45.01% 74
GHB	60.69% 53	74.39% 23	0.04% 7	42.11% 57
IRB	0.50% 6	0.026% 4	0% 0	0.18% 8
Sulfidogen	0.19% 10	0.075% 5	92.38% 5	34.74% 15
Varies	46.91% 2	60.19% 2	0.13% 2	33.4% 2
6.C Selected Classes: Relative Abundance and Number Species				
Gammaproteobacteria	41.53% 45	69.63% 22	0.03% 4	34.51% 49
Alphaproteobacteria	22.21% 64	16.27% 29	0.01% 4	12.08% 67
Betaproteobacteria	16.12% 32	9.35% 15	0.02% 4	8.02% 34
Unclassified	8.91% 24	1.15% 6	0.11% 1	3.25% 24
Clostridia	0.31% 15	0.08% 6	99.777% 8	37.55% 20

Compressor Station Population Breakdown: Number of sequences analyzed and the number of species identified in each sample. 6.B.Selected physiological traits relative abundance and number of species. In each cell, the first number is % of total population, yellow are >10%. The second Number is number of species. Selected Traits: Aerobe (growth in oxygen), APB (acid producing bacteria), BioDeg (biodegrading organism) GHB (General Heterotrophic Bacteria), IRB (Iron Reducing Bacteria), Sulfidogen (Hydrogen Sulfide Producing), Note that for Selected Traits of Interest, the % add up to more than 100 because organisms have more than one trait (e.g. Some sulfidogens, APB, GHB, and IRB are spore-forming). 6.C Selected taxonomic classes with the highest number of associated species, relative abundance in the sample and number of species belonging to that class. In each cell, the first number is % of total population, yellow are >10%. Note that for taxonomic classification, the % will add up to 100 at most, because organisms belong to only one class. Unclassified organisms did not closely match an organism with a full taxonomic annotation and category includes multiple different types of organisms.

Compressor Station microbial population: Functional Trait and Classes Profiles Table 6.B, 6.C

- Each of the species identified in the samples was assigned a "Functional Trait Profile" that includes select metabolic, physiological, ecological, and taxonomic tags. Note that the functional trait % of population adds up to over 100% because organisms can have more than 1 functional trait assigned (eg, some GHB are also APB and Biodegrading organisms).
- The trait profile tags are generated by analysis of the published scientific literature for that species, or closely related species (when relevant). The trait assignment database in inherently incomplete, because not every organism has been subject to the same degree of experimental investigation, and so the information is not known. Despite nuances and limitations, "Trait Profile" analysis is the best way to correlate the identity of the organisms in a sample to insight as to what the organisms identified in a sample are actually doing.
- Table 6.B provides the functional trait overview for each of the samples sequenced from compressor station fluid samples. Only the traits with the highest % of the population of each sample are included.
- Table 7 provides the most abundant organisms from these samples.
- Table 8 provides the list of all sulfidogens and IRB in the samples
- Two very distinct populations emerged from the analysis.
- The two pond samples were nearly identical to each other, while the black fluid from the separator was quite different.

Compressor Station Pond Clear and Emulsion Samples

- Pond Clear and Emulsion samples were dominated by aerobic, biodegrading organisms
- IRB and sulfidogens were both <1% of the population
- Most organisms were classified as either Gammaproteobacteria, Alphaproteobacteria, or Betaproteobacteria
- Dominant genera included Pseudomonas and Sphingomonas, both GHB.
- Sulfidogens and IRB were present, but at less than 1% of the sample
- Genetic data supported MPN results that these samples are dominated by GHB and contain only minor levels of APB, IRB, or SRB.

Compressor Station Separator Black Liquid Sample

- Over 91% of the sequences from the compressor station black liquid sample originated from a single species: Thermoanaerobacterium saccharolyticum
- Thermoanaerobacterium saccharolyticum is a clostridial, spore forming anaerobe known to produce alcohols
- Many, but not all, Thermoanaerobacterium species are APB and / or sulfidogens, which is why this organism is annotated as such
- MPN data for this sample did not test positive for acid production or sulfidogenisis, however MPN results were almost 3 log orders lower then what was detected by qPCR, suggesting that the predominant organism (Thermoanaerobacterium) was not growing in culture
    - Sequence analysis of DNA isolated from the culture would clarify this point.
- This requires more research to determine if the Thermoanaerobacterium present in fluids from the compressor station is actually a sulfidogen or not
- If fluids from the separator contain elevated sulfides, this would be good evidence that this organism is a sulfidogen.

Table 7. Compressor Station Fluids Most Abundant Organisms				
Sequence ID	OG230409 -001	OG230409 -002	OG230409 -004	Select Traits of Interest:
Species	s60. CS Pond Clear Fluid	s61. CS Pond Emulsion Fluid	s57 CS Separator Black Fluid	Metabolic, Physiological, Ecological, Taxonomic
Arcobacter venerupis	0.10	1.85	0.01	Epsilonproteobacteria; Injections; Nitrate; NRB; NRSOB; SOB
Clostridium luticellarii	0.01	0.02	7.35	Anaerobe; APB; Clostridia; Ferm; Firmicutes; Spore
Flavobacterium sp	1.12	0.07	0.00	Aerobe; Bacteroidetes; BioDeg; BioDeg HC; Water
Herbaspirillum sp	1.00	0.10	0.02	Aerobe; Betaproteobacteria; NiF
Herminiimonas sp	0.21	1.32	0.00	Betaproteobacteria; Heavy Metal
Janthinobacterium sp	7.35	6.89	0.00	Aerobe; Antimicrobial; Natural Dye Betaproteobacteria; Biofilm; Violet;
Legionella sp	0.52	4.07	0.00	Aerobe; Gammaproteobacteria
Massilia sp	3.78	0.47	0.00	Betaproteobacteria; BioDeg; Filamentous; Soil
Methylophilus sp	1.40	0.04	0.00	Betaproteobacteria; Methylotroph
Pseudomonas sp	38.75	59.06	0.01	Aerobe; BioDeg; Gammaproteobacteria; GHB; Varies; Versatile; Widespread
Serratia sp	0.16	6.41	0.002	Biofilm; Gammaproteobacteria; MIC
Sphingomonas sp	18.67	14.76	0.00	Aerobe; Alphaproteobacteria; BioDeg; BioDeg PAH; GHB; Marine
Thermoanaerobacterium saccharolyticum	0.09	0.05	91.86	Anaerobe; APB; Clostridia; Firmicutes; NRB; Spore; Sulfidogen; Thermophile; TRB
Unclassified	8.16	1.12	0.12	Polyphyletic; Unknown; Varies

Top 20 organism identified in compressor station fluid samples. The value is the % of the total population. Yellow are >10% of the population, Blue are 1 – 10% of the population, White are <1% Gray are 0% not identified in sample. Trait Details: Polyphyletic (is not a homogenous grouping and includes multiple species) Unknown (traits are not known), Varies (likely to have multiple different traits), BioDeg are biodegrading organisms. PAH is polyaromatic hydrocarbons, HC are hydrocarbons, NiF are nitrogen fixing, GHB (general heterotrophic bacteria), Activated Sludge (present in activated sludge), Spore (spore-forming organism), APB (acid producing bacteria), Anaerobe / Aerobe (growth in absence or presence of oxygen, respectively), NRB (nitrate reducing bacteria), SOB (Sulfur oxidizing bacteria), NRSOB (nitrate reducing, sulfur oxidizing bacteria)

Table 8. Compressor Station Fluids Sulfidogens and IRB				
Sequence ID	OG230 409-001	OG230 409-002	OG230 409-004	Select Traits of Interest:
Species	s60. CS Pond Clear Fluid	s61. CS Pond Emulsion Fluid	s57 CS Separator Black Fluid	Metabolic, Physiological, Ecological, Taxonomic
Desulfocurvus sp	0.009	0	0	Anaerobe; Deltaproteobacteria; Gas storage well; SRB; Sulfidogen
Desulfomonile sp	0.004	0	0	Anaerobe; BioDeg; BioDeg Benzene; Deltaproteobacteria; SRB; Sulfidogen
Desulforegula sp	0.009	0	0	Anaerobe; Deltaproteobacteria; SRB; Sulfidogen
Desulfosporosinus sp	0.003	0.006	0	Anaerobe; Clostridia; Firmicutes; Spore; SRB; Sulfidogen
Garciella sp	0.005	0	0	Clostridia; Firmicutes; NRB; Oilfield; Sulfidogen; TRB
Haematobacter sp	0.007	0	0	Aerobe; Alphaproteobacteria; Sulfidogen
Moorella thermoacetica	0	0	0.328	Acetogen; Anaerobe; APB; Clostridia; Ferm; Firmicutes; NRB; Spore; Sulfidogen; Thermophile; TRB
Thermoanaerobacter mathranii	0	0	0.012	Anaerobe; Clostridia; Ethanologenic; Ferm; Firmicutes; Sulfidogen; Thermophile; TRB
Thermoanaerobacter sp	0	0	0.003	Anaerobe; Clostridia; Ethanologenic; Ferm; Firmicutes; Sulfidogen; Thermophile; TRB
Thermoanaerobacterium saccharolyticum	0.093	0.053	91.863	Anaerobe; APB; Clostridia; Firmicutes; NRB; Spore; Sulfidogen; Thermophile; TRB
Thermoanaerobacterium thermosaccharolyticum	0	0	0.175	Anaerobe; APB; Clostridia; Firmicutes; NRB; Spore; Sulfidogen; Thermophile; TRB
Anaeromyxobacter sp	0.043	0.004	0	Anaerobe; Deltaproteobacteria; IRB; XRB
Bacillus thermoamylovorans	0.009	0	0	Bacilli; Firmicutes; IRB; Spore; Thermophile
Desulfitobacterium sp	0.047	0.006	0	Anaerobe; BioDeg; BioDeg halogenated organic compounds; Clostridia; Ferm; Firmicutes; Metal Reduction; NiF; SIRB; Spore; Sulfidogen; SuRB; TRB
Desulfuromonas sp	0.003	0	0	Anaerobe; Deltaproteobacteria; IRB; Sulfidogen; SuRB
Geobacter sp	0.065	0.003	0	Anaerobe; BioDeg; BioDeg HC; Biofilm; Deltaproteobacteria; IRB; Metal Reduction; Microbial Fuel Cell
Pelobacter sp	0.078	0	0	Anaerobe; Deltaproteobacteria; IRB
Rhodoferax sp	0.305	0.011	0	Betaproteobacteria; IRB
Shewanella sp	0	0.008	0	Facultative Anaerobe; Gammaproteobacteria; IRB; Sulfidogen; TRB

Sulfidogens and IRB identified in compressor station fluid samples. The value is the % of the total population. Yellow are >10% of the population, Blue are 1 – 10% of the population, White are <1% Gray are 0% not identified in sample. Trait Details: Sulfidogens include SRB, TRB, SuRB, peptide fermenting organisms. Polyphyletic (is not a homogenous grouping and includes multiple species) Unknown (traits are not known), Varies (likely to have multiple different traits), BioDeg (biodegrading organism capable of utilization of specialized substrates) GHB (general heterotrophic bacteria), Activated Sludge (present in activated sludge), Spore (spore-forming organism), APB (acid producing bacteria), Anaerobe / Aerobe (growth in absence or presence of oxygen, respectively)

Pool	BLRM Sample ID	Corresponding Blade Sample ID	Sample Description: Source Well, Casing Joint, Sample Type	Sample Date	Quantity g or ml
49	BLRM230317-001	no sample ID	Well 2248 Scale Annulus valve Solids	3/17/23	0.8
50	BLRM230317-002	no sample ID	Well 2248 Scale Annulus valve Solids	3/17/23	0.8
51	BLRM230326-001	no sample ID	Well 2248 Fluids Annulus Liquid Sample	3/26/23	500
52	BLRM230326-002	RM-2248-C001-S1	Well 2248, C001 Scale Sample OD	3/26/23	190
53	BLRM230326-003	RM-2248-C001-S2	Well 2248, C001 Scale Sample Couplings	3/26/23	28.2
54	BLRM230326-004	no sample ID	Well 2248, C001 OD Scale, 4 - 5 lbs	3/26/23	2360
55	BLRM230326-005	no sample ID	Well 2248 Scale OD Scale, Conductor	3/26/23	91.5
56	BLRM230328-001	2248-C001-S4	Well 2248 Scale C001 Scale OD sample	3/28/23	7.5
57	BLRM230328-002	no sample ID	Compressor Station Seperator Fluid, Black. Chemical smell	3/28/23	200
58	BLRM230328-003	no sample ID	Compressor Station Seperator Fluid, Clear. Chemical smell	3/28/23	200
59	BLRM230329-001	RM-2248-958-S1	Well 2248 Scale Uppermost 9 5/8" casing ID scrape	3/29/23	70.8
60	BLRM230401-001	RM-Pond-L1	Compressor Station Fluid pond sample, clear	4/1/23	500
61	BLRM230401-002	RM-Pond-L2	Compressor Station Fluid pond sample, emulsion	4/1/23	500
62	BLRM230403-001	RM-2251-C001-S01	Well 2251 Scale 7" OD, C001 top of joint	4/3/23	23.2
63	BLRM230403-002	RM-2251-C001-S02	Well 2251 Scale 7" OD, C001 top of joint	4/3/23	508.5
64	BLRM230403-003	RM-2251-C001-S03	Well 2251 Scale 7" OD, C001 10'6" top of cement	4/3/23	9.2

Appendix A. Well 2248, 2251 and Compressor Station Samples. BLRM numbers are "Blade Rager Mountain" sample identification numbers indicating year, month, day of collection.

Sequence ID	OG230409-001	OG230409-002	OG230409-004	Select Traits of Interest:
Species	s60. CS Pond Clear Fluid	s61. CS Pond Emulsion Fluid	s57 CS Separator Black Fluid	Metabolic, Physiological, Ecological, Taxonomic
Acetobacterium sp	0.008	0	0	Acetic Acid; Acetogen; Anaerobe; APB; Clostridia; Firmicutes
Acidiferrobacter sp	0.022	0	0	Acidophile; APB; Faculatative Anaerobe; FeOX; GammaP; NiF; SOX
Acidiferrobacter thiooxydans	0.003	0	0	Acidophile; APB; Faculatative Anaerobe; FeOX; GammaP; NiF; SOX
Acidimicrobium sp	0.011	0.001	0	Acidophile; Actinobacteria; APB; FeOX; SOB
Acidisoma sp	0.007	0	0	Acidophile; AlphaP; APB; Psychrophile
Acidisphaera sp	0.003	0.053	0	Acidophile; Aerobe; AlphaP; APB; Psychrophile
Aciditerrimonas sp	0.013	0	0	Acidophile; Actinobacteria; APB; FeOX; SOB
Acidobacterium sp	0.212	0.008	0	Acidobacteria; Acidophile; Aerobe; APB
Acidocella sp	0.008	0	0	Acidophile; AlphaP; APB
Acidothermus sp	0.013	0.001	0	Acidophile; Actinobacteria; APB; BioDeg Cellulose; Thermophile
Acinetobacter sp	0.325	0.007	0	Aerobe; BioDeg HC; GammaP; Soil
Actinoallomurus sp	0	0.004	0	
Actinomadura alba	0.008	0	0	Actinomycete; Soil; Spore
Actinomyces sp	0.021	0	0	Actinobacteria; Ferm
Actinoplanes friuliensis	0.037	0.003	0	
Actinoplanes toevensis	0.012	0	0	Actinobacteria
Actinotalea fermentans	0.012	0.001	0	Actinobacteria; BioDeg Cellulose
Adhaeribacter sp	0.005	0	0	Bacteroidetes; Biofilm; GHB
Adhaeribacter terreus	0.026	0	0	Bacteroidetes
Aeromicrobium fastidiosum	0.096	0.007	0	
Aeromonas sp	0.018	0	0	Facultative Anaerobe; GammaP; GHB; Water
Afipia sp	0.018	0.001	0	AlphaP; Biofilm; MIC
Agreia sp	0.301	0.061	0	Actinobacteria
Alcaligenes faecalis	0.005	0	0.001	Aerobe; Alkaliphile; BetaP; NRB
Aliihoeflea sp	0.003	0	0	
Alkalilimnicola sp	0.004	0	0	Alkaliphile; GammaP
Alkalispirillum sp	0.013	0	0	Alkaliphile; GammaP
Alkanindiges hongkongensis	0	0.004	0	Alkaliphile; BioDeg HC; GammaP
Alkanindiges illinoisensis	0.587	0.017	0	Alkaliphile; BioDeg HC; GammaP; Oilfield

Sequence ID	OG230409-001	OG230409-002	OG230409-004	Select Traits of Interest:
Species	s60. CS Pond Clear Fluid	s61. CS Pond Emulsion Fluid	s57 CS Separator Black Fluid	Metabolic, Physiological, Ecological, Taxonomic
Altererythrobacter sp	0.182	0.018	0	AlphaP; CT
Amaricoccus sp	0.057	0	0	AlphaP; GHB
Amaricoccus tamworthensis	0.009	0	0	AlphaP
Aminobacter sp	0.005	0	0	AlphaP
Anaerolinea sp	0.02	0	0	Anaerobe; BioDeg; Chloroflexi; Filamentous; Thermophile
Anaeromyxobacter sp	0.043	0.004	0	Anaerobe; DeltaP; IRB; XRB
Anderseniella sp	0.025	0	0	Aerobe; AlphaP; GHB; Pigmented
Aquabacterium sp	0.291	0.01	0	Aerobe; BioDeg; MIC
Aquicella sp	0.068	0.007	0	GammaP; Pathogen; Protazoan Pathogen
Aquihabitans daechungensis	0.016	0.003	0	Acidobacteria; Actinobacteria
Aquimonas sp	0.009	0	0	GammaP; GHB
Arcicella sp	0.025	0	0	Bacteroidetes; GHB
Arcobacter nitrofigilis	0.029	0.01	0.002	EpsilonP; Nitrate Injections; NRB; NRSOB; SOB
Arcobacter sp	0	0.003	0	EpsilonP; Nitrate Injections; NRB; NRSOB; SOB
Arcobacter venerupis	0.099	1.845	0.006	EpsilonP; Injections; Nitrate; NRB; NRSOB; SOB
Arenimonas aquatica	0.013	0.004	0	GammaP; GHB
Arenimonas sp	0.086	0	0	GammaP; GHB
Arthrobacter sp	0.313	0.004	0	Actinobacteria; Aerobe; GHB; Soil
Asticcacaulis solisilvae	0.005	0.003	0	
Asticcacaulis sp	0.012	0.011	0	AlphaP; Unknown
Atopostipes sp	0	0.001	0	APB; Ferm; Firmicutes; LAB; Lactobacillales
Aurantimonas sp	0.138	0	0	AlphaP; MnOX
Aureimonas ferruginea	0.053	0	0	
Azohydromonas lata	0.078	0.008	0	BetaP; BioDeg; NiF
Azospirillum sp	0.003	0	0	AlphaP; NiF
Bacillus sp	0.187	0.011	0	Bacilli; BioDeg; Diverse; Firmicutes; GHB; Spore
Bacillus thermoamylovorans	0.009	0	0	Bacilli; Firmicutes; IRB; Spore; Thermophile
Bacteriovorax stolpii	0.028	0.007	0	Bacterial Predator; DeltaP
Bacteroides coprocola	0.008	0	0	Anaerobe; Bacteroidetes; BioDeg; Ferm

Sequence ID	OG230409-001	OG230409-002	OG230409-004	Select Traits of Interest:
Species	s60. CS Pond Clear Fluid	s61. CS Pond Emulsion Fluid	s57 CS Separator Black Fluid	Metabolic, Physiological, Ecological, Taxonomic
Bacteroides plebeius	0.016	0	0	Anaerobe; Bacteroidetes; BioDeg; Ferm
Bacteroides sp	0.025	0	0	Anaerobe; Bacteroidetes; BioDeg; Ferm
Balneimonas sp	0.003	0	0	AlphaP
Bdellovibrio exovorus	0.062	0.01	0	Bacterial Predator; DeltaP
Bdellovibrio sp	0.236	0.013	0	Bacterial Predator; DeltaP
Beggiatoa sp	0.018	0.001	0	Biofilm; GammaP; OX; SOB; White mats hydrocarbon seeps
Beijerinckia sp	0.078	0.088	0	AlphaP
Bellilinea sp	0.007	0	0	Chloroflexi; Oilfield; Tilling pond
Blastococcus sp	0.078	0	0	Actinobacteria; Aerobe; Sediment; Stone; Unknown; Water
Bordetella sp	0.009	0	0	BetaP; Environmental; GHB
Bosea sp	0.053	0.003	0	AlphaP; GHB
Brachybacterium sp	0	0.001	0	Actinobacteria; BioDeg HC
Bradyrhizobium sp	0.134	0.006	0	AlphaP; NiF
Brevibacterium sp	0	0	0.002	Actinobacteria; BioDeg HC
Brevundimonas sp	0.548	0.044	0	Aerobe; AlphaP; BioDeg HC; GHB
Brucella sp	0.004	0	0	AlphaP
Burkholderia sp	0.033	0.101	0	Aerobe; BetaP; BioDeg; Soil
Burkholderia tropica	0.007	0	0	Aerobe; BetaP; BioDeg; Soil
Byssovorax sp	0.041	0	0	BioDeg Cellulose; DeltaP
Caenimonas sp	0.032	0.003	0	BetaP
Caldanaerobius sp	0	0	0.041	
Caldilinea sp	0.029	0	0	Chloroflexi; Facultative; Filamentous; Thermophile
Candidatus Brocadia caroliniensis	0.012	0	0	
Candidatus Desulforudis sp	0.008	0	0	Clostridia; Firmicutes
Candidatus Lumbricincola sp	0.021	0	0	
Candidatus Metachlamydia lacustris	0.003	0	0	Amoeba Symbiont; Chlamydiae; Symbiont
Candidatus Microthrix sp	0.047	0	0	Filamentous

Sequence ID	OG230409-001	OG230409-002	OG230409-004	Select Traits of Interest:
Species	s60. CS Pond Clear Fluid	s61. CS Pond Emulsion Fluid	s57 CS Separator Black Fluid	Metabolic, Physiological, Ecological, Taxonomic
Candidatus Odyssella sp	0.011	0	0	
Candidatus Protochlamydia amoebophila	0.008	0	0	Chlamydiae
Candidatus Protochlamydia sp	0.012	0.001	0	Chlamydiae
Candidatus Soleaferrea massiliensis	0.005	0	0	Clostridia; Firmicutes
Carnobacterium maltaromaticum	0.018	0.001	0	Firmicutes; Lactobacillales
Carnobacterium sp	0.007	0	0.001	Firmicutes; Lactobacillales
Caulobacter sp	0.074	0.107	0	Aerobe; AlphaP; GHB; Oligotroph
Cellulomonas sp	0.011	0.003	0	Actinobacteria; Aerobe; BioDeg Cellulose; Facultative Anaerobe
Cellvibrio gandavensis	0.059	0.003	0	Aerobe; BioDeg Agar; BioDeg Cellulose; GammaP
Cellvibrio sp	0.137	0.006	0	Aerobe; BioDeg Agar; BioDeg Cellulose; GammaP
Chitinophaga sp	0.093	0	0	Aerobe; Bacteroidetes; BioDeg
Chlamydia sp	0.005	0	0	Chlamydiae; Endosymbiont; Parasite; Pathogen
Chloroflexus sp	0.134	0.004	0	Anoxygenic Phototroph; Chloroflexi; FAP; Filamentous; Phototroph
Chloronema giganteum	0.013	0	0	Chloroflexi
Chondromyces sp	0.011	0.004	0	DeltaP
Chroococcidiopsis sp	0.036	0	0	Phototroph
Chroococcus sp	0.008	0	0	Phototroph
Chryseobacterium jeonii	0.007	0	0	
Chryseobacterium luteum	0.011	0	0	
Chryseobacterium sp	0.037	0	0	Aerobe; Bacteroidetes; BioDeg; Food; Pigmented; Soil; Wastewater
Citreicella sp	0.005	0.003	0	AlphaP
Citrobacter sp	0.013	0.003	0	Aerobe; Biofilm; GammaP; MIC; NRB; Sulfidogen
Clostridium botulinum	0.004	0	0.001	Anaerobe; Clostridia; Ferm; Firmicutes; GHB; Pathogen; Saprophyte; Spore
Clostridium cavendishii	0.007	0	0	
Clostridium hydrogeniformans	0.009	0	0	
Clostridium luticellarii	0.013	0.018	7.354	Anaerobe; APB; Clostridia; Ferm; Firmicutes; Spore
Clostridium sp	0.076	0.003	0	Anaerobe; Clostridia; Diverse; Ferm; Firmicutes; GHB; Saprophyte; Spore

Sequence ID	OG230409-001	OG230409-002	OG230409-004	Select Traits of Interest:
Species	s60. CS Pond Clear Fluid	s61. CS Pond Emulsion Fluid	s57 CS Separator Black Fluid	Metabolic, Physiological, Ecological, Taxonomic
Cohnella sp	0.005	0	0	Aerobe; Bacilli; BioDeg Cellulose; Firmicutes; Spore
Conexibacter sp	0.137	0.01	0	Actinobacteria; NRB
Conexibacter woesei	0.028	0.004	0	Actinobacteria
Coxiella cheraxi	0.012	0	0	GammaP
Coxiella endosymbiont	0.012	0	0	Endosymbiont
Coxiella sp	0.005	0	0	GammaP
Crocinitomix sp	0.005	0	0	Bacteroidetes; GHB
Cyanobacterium sp	0.062	0	0	Phototroph
Cystobacter sp	0.008	0	0	DeltaP
Cytophaga sp	0.008	0	0	Aerobe; Bacteroidetes; BioDeg Cellulose; Soil
Defluvibacter sp	0	0	0.002	Aerobe; AlphaP; Aquamicrobium; BioDeg chlorophenol; WWTP
Defluviicoccus sp	0.011	0	0	AlphaP
Deinococcus hopiensis	0.016	0	0	Deinococcus-Thermus; polyextremophile; Radiation Resistant
Deinococcus navajonensis	0.007	0	0	
Deinococcus radiomollis	0.017	0	0	Deinococcus-Thermus; polyextremophile; Radiation Resistant
Deinococcus sp	0.083	0.006	0	Deinococcus-Thermus; polyextremophile; Radiation Resistant
Derxia sp	0.042	0	0	BetaP; NiF
Desulfitobacterium sp	0.047	0.006	0	Anaerobe; BioDeg halogenated organic compounds; Clostridia; Ferm; Firmicutes; Metal Reduction; Ni
Desulfocurvus sp	0.009	0	0	Anaerobe; DeltaP; Gas storage well; SRB; Sulfidogen
Desulfomonile sp	0.004	0	0	Anaerobe; BioDeg Benzene; DeltaP; SRB; Sulfidogen
Desulforegula sp	0.009	0	0	Anaerobe; DeltaP; SRB; Sulfidogen
Desulfosporosinus sp	0.003	0.006	0	Anaerobe; Clostridia; Firmicutes; Spore; SRB; Sulfidogen
Desulfuromonas sp	0.003	0	0	Anaerobe; DeltaP; IRB; Sulfidogen; SuRB
Devosia sp	0.141	0.014	0	AlphaP; GHB; NiF
Dietzia sp	0.111	0.001	0	Actinobacteria; Aerobe; BioDeg; GHB
Duganella sp	0.566	0.299	0	Aerobe; BetaP; GHB; Soil
Dyadobacter beijingensis	0	0.003	0	
Dyadobacter koreensis	0.083	0.238	0	Aerobe; Bacteroidetes; BioDeg
Dyadobacter sp	0.038	0	0	Aerobe; Bacteroidetes; BioDeg

Sequence ID	OG230409-001	OG230409-002	OG230409-004	Select Traits of Interest:
Species	s60. CS Pond Clear Fluid	s61. CS Pond Emulsion Fluid	s57 CS Separator Black Fluid	Metabolic, Physiological, Ecological, Taxonomic
Ectothiorhodospira sp	0.026	0	0	Anaerobe; GammaP; Halophile; Phototroph; Purple Sulfur Bacteria; Sulfide-Oxidizing
Elusimicrobium sp	0.007	0	0	Elusimicrobia; Ultrabacterium
Emticicia sp	0.008	0	0	Bacteroidetes; GHB
Ensifer sp	0.046	0.492	0	AlphaP
Enteractinococcus fodinae	0	0.001	0	APB; Coal mine; Generalist; GHB; Soil
Epilithonimonas sp	0.057	0	0	Bacteroidetes
Eubacterium sp	0.022	0	0	Acetic Acid; Acetogen; Anaerobe; APB; Butyrate; Clostridia; Ethanol; Firmicutes; SynGas
Falsochrobactrum ovis	0	0	0.002	Aerobe; AlphaP; Generalist; GHB
Ferribacterium sp	0.018	0.001	0	BetaP
Ferrimicrobium sp	0.021	0	0	Acidophile; Actinobacteria; APB; FeOX; SOB
Ferruginibacter sp	0.025	0	0	Bacteroidetes; BioDeg
Fimbriimonas ginsengisoli	0.003	0	0	
Flavisolibacter sp	0.028	0	0	Bacteroidetes; Industrial Wastewater
Flavitalea sp	0.011	0	0	Bacteroidetes
Flavobacterium aquatile	0.049	0	0	Aerobe; Bacteroidetes; Water
Flavobacterium caeni	0.043	0	0	Aerobe; Bacteroidetes; BioDeg; Sludge
Flavobacterium cauense	0.011	0	0	Aerobe; Bacteroidetes; Water
Flavobacterium rivuli	0.059	0.028	0	Aerobe; Bacteroidetes; GHB
Flavobacterium sp	1.118	0.065	0	Aerobe; Bacteroidetes; BioDeg HC; Water
Flexibacter sp	0.042	0	0	Bacteroidetes; BioDeg HC; Oilfield
Fluviicola sp	0.022	0	0	Bacterioplankton; Bacteroidetes; GHB
Fluviicola taffensis	0.021	0	0	Bacterioplankton; Bacteroidetes; GHB
Frankia sp	0.016	0	0	Actinobacteria; NiF
Fusobacterium sp	0.009	0	0	Anaerobe; Fusobacteria; Pathogen
Gaiella sp	0.068	0.001	0	
Gallionella sp	0.004	0	0	BetaP; Biofilm
Garciella sp	0.005	0	0	Clostridia; Firmicutes; NRB; Oilfield; Sulfidogen; TRB
Geminicoccus roseus	0.008	0	0	GHB
Gemmata sp	0.067	0.003	0	Planctomycetes; Unknown

Sequence ID	OG230409-001	OG230409-002	OG230409-004	Select Traits of Interest:
Species	s60. CS Pond Clear Fluid	s61. CS Pond Emulsion Fluid	s57 CS Separator Black Fluid	Metabolic, Physiological, Ecological, Taxonomic
Gemmatimonas phototrophica	0.012	0	0	Gemmatimonadetes; Phototroph
Gemmatimonas sp	0.008	0	0	Gemmatimonadetes; GHB; Oligotroph
Geobacter sp	0.065	0.003	0	Anaerobe; BioDeg HC; Biofilm; DeltaP; IRB; Metal Reduction; Microbial Fuel Cell
Georgenia sp	0.001	0	0.001	Actinobacteria; BioDeg
Gracilibacter sp	0.008	0	0	Clostridia; Ferm; Firmicutes; GHB
Granulicella paludicola	0.011	0	0	
Haematobacter sp	0.007	0	0	Aerobe; AlphaP; Sulfidogen
Haliangium sp	0.036	0	0	DeltaP
Haloactinobacterium album	0.001	0	0	
Halochromatium sp	0	0.001	0	GammaP; Halophile; Phototroph; Purple Sulfur Bacteria
Halospirulina sp	0.058	0.018	0	Halophile; Phototroph
Hansschlegelia plantiphila	0.017	0	0	AlphaP
Herbaspirillum sp	1.001	0.099	0.017	Aerobe; BetaP; NiF
Herminiimonas sp	0.208	1.321	0	BetaP; Heavy Metal
Hirschia sp	0.007	0	0	AlphaP
Holophaga sp	0.009	0	0	Acidobacteria; BioDeg HC
Homoserinibacter gongjuensis	0.074	0.004	0	
Hongiella sp	0.197	0.003	0	Bacteroidetes; GHB
Hydrogenophaga sp	0.179	0	0	Aerobe; BetaP; BioDeg HC
Hylemonella gracilis	0.013	0	0	BetaP; Wastewater
Hymenobacter algoricola	0.011	0	0	
Hymenobacter elongatus	0.041	0	0	
Hymenobacter gelipurpurascens	0.025	0	0	Bacteroidetes; BioDeg; GHB
Hymenobacter ginsengisoli	0.043	0	0	Bacteroidetes; BioDeg; GHB
Hymenobacter kanuolensis	0.009	0	0	Bacteroidetes; BioDeg; GHB
Hymenobacter metalli	0.018	0	0	
Hymenobacter soli	0.038	0	0	Bacteroidetes; BioDeg; GHB
Hymenobacter sp	0.054	0	0	Bacteroidetes; BioDeg; GHB
Hyphomicrobium sp	0.115	0.01	0	Aerobe; AlphaP; BioDeg; Methylotroph; Soil

Sequence ID	OG230409-001	OG230409-002	OG230409-004	Select Traits of Interest:
Species	s60. CS Pond Clear Fluid	s61. CS Pond Emulsion Fluid	s57 CS Separator Black Fluid	Metabolic, Physiological, Ecological, Taxonomic
Iamia sp	0.034	0	0	Actinobacteria
Ignavibacterium sp	0.012	0	0	Ignavibacteriae
Ilumatobacter sp	0.007	0	0	Actinobacteria
Iodobacter sp	0.003	0	0	BetaP; NRB
Isosphaera sp	0.003	0	0	Planctomycetes
Janthinobacterium sp	7.354	6.888	0	Aerobe; Antimicrobial; BetaP; Biofilm; Dark Violet; Natural Dye
Jatrophihabitans sp	0.004	0.004	0	
Jeotgalicoccus coquinae	0	0	0.001	Faculatative Anaerobe; Fish sauce; Generalist; GHB; Halophile
Kaistia granuli	0.005	0	0	AlphaP
Kineosporia rhamnosa	0.116	0	0	
Larkinella insperata	0.005	0.001	0	Aerobe; Sediments; Soil
Leadbetterella sp	0.011	0	0	Bacteroidetes
Legionella beliardensis	0.005	0	0	Aerobe; GammaP
Legionella sp	0.521	4.065	0	Aerobe; GammaP
Leptolyngbya sp	0.012	0	0	Cyanobacteria; dry biofilms; Phototroph
Leucobacter aridicollis	0	0	0.002	Actinobacteria; Aerobe; BioDeg chromium compounds; Biosurfactant Producing; Chromium tolorant
Leucobacter sp	0.037	0.003	0	Actinobacteria; BioDeg
Levilinea sp	0.007	0	0	Alaska; Chloroflexi; Oilfield; Produced Water
Lewinella sp	0.004	0	0	Bacteroidetes; Filamentous; GHB
Limnohabitans sp	0.009	0	0	BetaP; GHB
Lishizhenia sp	0.182	0.006	0	
Litorilinea aerophila	0.005	0	0	Aerobe; Chloroflexi; Thermophile
Litorilinea sp	0.004	0	0	
Longilinea sp	0.011	0	0	Anaerobe; Chloroflexi; Consortium Member; Filamentous; Methanogenic Community Member
Luedemannella sp	0.007	0	0	
Luteibacter rhizovicinus	0.003	0	0	Aerobe; GammaP; GHB
Luteolibacter sp	0.021	0.003	0	Verrucomicrobia
Lysinibacillus massiliensis	0.038	0.003	0	Bacilli; Environmental; Firmicute; GHB; Spore
Lysobacter sp	0.303	0.011	0	BioDeg HC; GammaP

Sequence ID	OG230409-001	OG230409-002	OG230409-004	Select Traits of Interest:
Species	s60. CS Pond Clear Fluid	s61. CS Pond Emulsion Fluid	s57 CS Separator Black Fluid	Metabolic, Physiological, Ecological, Taxonomic
Lysobacter spongiicola	0.012	0.001	0	
Marinobacter sp	0.033	0.001	0.002	Aerobe; BioDeg HC; GammaP; NRB
Marinobacterium sp	0.007	0.011	0.015	Aerobe; BioDeg; GammaP; GHB
Marmoricola sp	0.026	0.003	0	Actinobacteria; GHB
Massilia sp	3.78	0.472	0	BetaP; BioDeg; Filamentous; Soil
Mesorhizobium sp	0.021	0	0	AlphaP; NiF; Soil
Methanosarcina sp	0.003	0	0	Anaerobe; Archaea; Methanogen
Methylobacillus sp	0.074	0.004	0	BetaP; Methylotroph
Methylobacter sp	0.032	0.003	0	GammaP; Methylotroph
Methylobacterium sp	0.456	0.028	0	Aerobe; AlphaP; Methylotroph
Methylocaldum sp	0.138	0.008	0	GammaP; Methylotroph
Methylocystis sp	0.016	0.001	0	AlphaP; Methylotroph
Methylomicrobium alcaliphilum	0.012	0	0	GammaP; Methylotroph
Methylomonas sp	0	0.003	0	GammaP; Methylotroph
Methylophilus sp	1.402	0.038	0	BetaP; Methylotroph
Methylotenera sp	0.047	0	0	BetaP; Methylotroph
Methylovorus sp	0	0.024	0	BetaP; Methylotroph
Micavibrio sp	0.018	0	0	Bacterial Predator
Microcoleus steenstrupii	0.009	0	0	Phototroph
Microcoleus vaginatus	0.009	0	0	Phototroph
Microvirga zambiensis	0.028	0.003	0	AlphaP
Modestobacter lapidis	0.071	0.001	0	
Modestobacter sp	0.004	0	0	Aerobe; AlphaP; Soil; Soil Crust
Moorella thermoacetica	0	0	0.328	Acetogen; Anaerobe; APB; Clostridia; Ferm; Firmicutes; NRB; Spore; Sulfidogen; Thermophile; TRB
Mucilaginibacter gynuensis	0.005	0.044	0	
Mucilaginibacter sp	0.219	0.054	0	Acidophile; APB; Bacteroidetes; BioDeg Cellulose; Facultative Anaerobe
Mycobacterium sp	0.199	0.008	0	Actinobacteria; Environmental; Widespread
Myxococcus sp	0.008	0	0	DeltaP
Nakamurella sp	0.022	0.001	0	Actinobacteria

Sequence ID	OG230409-001	OG230409-002	OG230409-004	Select Traits of Interest:
Species	s60. CS Pond Clear Fluid	s61. CS Pond Emulsion Fluid	s57 CS Separator Black Fluid	Metabolic, Physiological, Ecological, Taxonomic
Nannocystis sp	0.021	0	0	DeltaP
Neochlamydia sp	0.009	0	0	Chlamydiae
Niastella sp	0.122	0	0	Bacteroidetes
Nibrella saemangeumensis	0.009	0	0	
Nitratireductor sp	0.013	0	0	AlphaP; Facultative Anaerobe; NRB
Nitrosococcus sp	0.007	0	0	GammaP; Halophile; NOB
Nitrosospira sp	0.009	0	0	Aerobe; AOB; AOX; BetaP
Nitrosovibrio sp	0.009	0	0	Aerobe; AOB; AOX; BetaP
Nitrospira sp	0.03	0	0	Nitrospinae; NOB
Nocardia sp	0.091	0.003	0	Actinobacteria; Aerobe; Filamentous
Nocardioides dilutus	0.018	0	0	
Nocardioides halotolerans	0.025	0	0	
Nocardioides iriomotensis	0.062	0	0	Actinobacteria; Filamentous
Nocardioides sp	0.403	0.028	0	Actinobacteria; Filamentous
Nocardiopsis sp	0	0.003	0	Actinobacteria; Filamentous
Nodosilinea sp	0.012	0	0	Cyanobacteria; Phototroph
Nordella sp	0.045	0.003	0	
Nostoc sp	0.018	0	0	Phototroph
Novosphingobium sp	0.088	0.051	0	AlphaP; BioDeg
Oceanobacillus chironomi	0.004	0	0	
Oceanobacillus massiliensis	0.025	0.001	0	
Oceanobacillus sp	0.003	0	0	Bacilli; Ferm; Firmicutes; Halophile; Spore
Ochrobactrum sp	0	0	0.001	AlphaP; NiF
Oerskovia sp	0.003	0	0	
Ohtaekwangia koreensis	0.011	0	0	
Ohtaekwangia sp	0.025	0	0	Bacteroidetes
Oligoflexus tunisiensis	0.004	0.003	0	Oligoflexia
Opitutus sp	0.047	0	0	Ferm; Verrucomicrobia
Ornithinimicrobium sp	0.009	0	0	Actinobacteria

Sequence ID	OG230409-001	OG230409-002	OG230409-004	Select Traits of Interest:
Species	s60. CS Pond Clear Fluid	s61. CS Pond Emulsion Fluid	s57 CS Separator Black Fluid	Metabolic, Physiological, Ecological, Taxonomic
Paenalcaligenes hominis	0	0	0.006	Aerobe; Bacteroidetes; BetaP; Bioreactor; Generalist; GHB
Paenibacillus macquariensis	0.021	0	0	
Paenibacillus sp	0.036	0.008	0	Bacilli; BioDeg EPS; BioDeg PAH; Dendritiformis colonies; Facultative Anaerobe; Firmicute; Firmicutes;
Paludibacter sp	0.009	0	0	Bacteroidetes; Ferm
Parachlamydia sp	0.018	0	0	Chlamydiae; Unknown
Paracoccus sp	0.017	0	0	AlphaP; APB; BioDeg; Facultative Anaerobe; Mitochondrial Ancestor; NRB
Paracraurococcus sp	0.033	0	0	AlphaP; APB
Parasegetibacter luojiensis	0.005	0.001	0	Bacteroidetes
Pasteuria sp	0.003	0	0	Bacilli; Firmicutes
Patulibacter minatonensis	0.037	0.007	0	Actinobacteria
Pedobacter aquatilis	0.013	0.004	0	Bacteroidetes; BioDeg; Soil
Pedobacter luteus	0.253	0.014	0	Aerobe; Bacteroidetes; Soil
Pedobacter sp	0.889	0.042	0	Bacteroidetes; BioDeg; Soil
Pedomicrobium sp	0.013	0	0	AlphaP
Pelagibacterium sp	0.061	0.004	0	
Pelobacter sp	0.078	0	0	Anaerobe; DeltaP; IRB
Peredibacter sp	0.066	0.007	0	Bacterial Predator; DeltaP
Peredibacter starrii	0.067	0.004	0	DeltaP; Ferm
Perlucidibaca sp	0.011	0	0	GammaP; GHB
Petrobacter sp	0.016	0	0	Aerobe; BetaP; NRB; Oilfied; Oilfield; Thermophile
Phaselicystis sp	0.005	0	0	
Phenylobacterium sp	0.115	0.003	0	Aerobe; AlphaP; GHB
Phormidium sp	0.003	0	0	Cyanobacteria; Oilfield; Phototroph
Phytohabitans flavus	0.003	0	0	
Phytoplasma sp	0.049	0.006	0	Tenericutes
Pirellula sp	0.008	0	0	Planctomycetes
Planctomyces sp	0.036	0	0	Planctomycetes
Polaromonas sp	0.005	0	0	BetaP; BioDeg HC
Polymorphobacter multimanifer	0.017	0	0	Aerobe; GHB; Sphingomonad

Sequence ID	OG230409-001	OG230409-002	OG230409-004	Select Traits of Interest:
Species	s60. CS Pond Clear Fluid	s61. CS Pond Emulsion Fluid	s57 CS Separator Black Fluid	Metabolic, Physiological, Ecological, Taxonomic
Pontibacter indicus	0.011	0	0	
Porphyrobacter sp	0.004	0	0	AlphaP; BioDeg; Phototroph
Prochlorococcus sp	0.022	0	0	Phototroph
Prosthecobacter sp	0.011	0	0	Verrucomicrobia
Protochlamydia naegleriophila	0.003	0	0	Chlamydiae; Unknown
Pseudochrobactrum sp	0.005	0.018	0.01	Aerobe; AlphaP; GHB
Pseudolabrys sp	0.004	0	0	AlphaP
Pseudomonas sp	38.749	59.063	0.012	Aerobe; BioDeg; GammaP; GHB; Varies; Versatile; Widespread
Pseudonocardia sp	0.08	0.067	0	Actinobacteria
Pseudonocardia tetrahydrofuranoxydans	0.007	0	0	
Pseudorhodobacter sp	0.083	0.001	0	AlphaP
Pseudoxanthomonas sp	0.026	0.001	0	BioDeg HC; GammaP
Pseudoxanthomonas spadix	0.007	0	0	GammaP
Psychrobacter sp	0.029	0	0	BioDeg HC; GammaP; Oilfield
Ralstonia sp	0.014	0	0	BetaP; BioDeg HC
Rhabdobacter roseus	0.003	0	0	
Rhizobium sp	0.201	0.532	0	AlphaP; NiF
Rhodocista sp	0.012	0	0	AlphaP; Phototroph
Rhodococcus sp	0.296	0.029	0	Actinobacteria; BioDeg
Rhodoferax sp	0.305	0.011	0	BetaP; IRB
Rhodomicrobium sp	0.011	0	0	AlphaP
Rhodopirellula sp	0.004	0	0	Planctomycetes
Rhodoplanes sp	0.108	0.003	0	AlphaP; Phototroph
Rhodopseudomonas sp	0.011	0	0	AlphaP; Phototroph
Rhodothermus sp	0.005	0	0	Bacteroidetes
Rhodovulum kholense	0.025	0	0	
Rickettsiella endosymbiont	0.005	0	0	
Roseobacter sp	0.004	0	0	AlphaP; Phototroph

Sequence ID	OG230409-001	OG230409-002	OG230409-004	Select Traits of Interest:
Species	s60. CS Pond Clear Fluid	s61. CS Pond Emulsion Fluid	s57 CS Separator Black Fluid	Metabolic, Physiological, Ecological, Taxonomic
Roseomonas sp	0.076	0.001	0	AlphaP; GHB
Ruania albidiflava	0.026	0	0	Actinomycete; Aerobe; Generalist; GHB
Rubellimicrobium sp	0.039	0.001	0	AlphaP; GHB
Rubrobacter sp	0.053	0.003	0	Actinobacteria; BioDeg
Rudaea sp	0.005	0	0	
Rudanella lutea	0.034	0	0	
Salinibacter sp	0.004	0	0	Bacteroidetes; Ferm; Halophile
Sandaracinus sp	0.007	0.003	0	DeltaP
Serratia sp	0.159	6.405	0.002	Biofilm; GammaP; MIC
Shewanella sp	0	0.008	0	Facultative Anaerobe; GammaP; IRB; Sulfidogen; TRB
Singulisphaera sp	0.003	0	0	Planctomycetes
Sinorhizobium sp	0.061	0	0	AlphaP; NiF
Skermanella sp	0.033	0	0	AlphaP
Skermanella stibiiresistens	0.005	0	0	AlphaP
Smaragdicoccus niigatensis	0.03	0	0	
Solirubrobacter sp	0.005	0	0	Actinobacteria
Solitalea koreensis	0.014	0.003	0	
Sphaerobacter sp	0.033	0.004	0	Chloroflexi; Wastewater
Sphaerotilus sp	0.036	0.003	0	Filamentous
Sphingobacterium sp	0.016	0	0	Aerobe; Bacteroidetes; BioDeg; GHB
Sphingobium sp	0.075	0.004	0	Aerobe; AlphaP; BioDeg Herbacides; Soil
Sphingomonas japonica	0.003	0	0	Aerobe; AlphaP; GHB; Marine
Sphingomonas sp	18.67	14.76	0	Aerobe; AlphaP; BioDeg PAH; GHB; Marine
Sphingopyxis sp	0.124	0.011	0	Aerobe; AlphaP; BioDeg HC
Spirobacillus sp	0.009	0.001	0	
Spirosoma linguale	0.042	0	0	Bacteroidetes
Spirosoma oryzae	0.007	0	0	
Spirosoma rigui	0.045	0	0	Bacteroidetes
Spirosoma sp	0.18	0.004	0	Bacteroidetes; Wastewater

Sequence ID	OG230409-001	OG230409-002	OG230409-004	Select Traits of Interest:
Species	s60. CS Pond Clear Fluid	s61. CS Pond Emulsion Fluid	s57 CS Separator Black Fluid	Metabolic, Physiological, Ecological, Taxonomic
Spirosoma spitsbergense	0.037	0	0	
Sporacetigenium sp	0.004	0.003	0	Alkaliphile; Anaerobe; Anaerobic Digester; Ferm; WWTP
Sporichthya sp	0.003	0	0	Actinobacteria; BioDeg
Sporocytophaga sp	0.042	0.007	0	Bacteroidetes; BioDeg Cellulose
Sporomusa malonica	0.003	0	0	Anaerobe; APB; Firmicutes; Homoacetogen; Negativicutes; Spore
Sporosarcina sp	0.016	0.001	0	Bacilli; Firmicutes
Staphylococcus lentus	0	0.004	0.002	
Steroidobacter sp	0.007	0	0	BioDeg; GammaP
Streptomyces sp	0.065	0.006	0	Actinobacteria; Antibiotic Producing; BioDeg; Filamentous; Soil; Spore
Streptosporangium sp	0.007	0	0	Actinobacteria; Alaska; Oilfield; Produced Water
Sulfurospirillum sp	0.07	0.668	0.007	EpsilonP; Facultative Anaerobe; NRB; NRSOB; Oilfield; SOB
Syntrophus sp	0.013	0	0	Anaerobe; BioDeg HC; DeltaP; Methanogen Syntroph; Sludge; Syntroph; Thermophile
Tahibacter aquaticus	0.003	0	0	
Terriglobus roseus	0.008	0.01	0	Acidobacteria
Terriglobus sp	0.007	0	0	Acidobacteria; GHB
Terrimonas sp	0.045	0.003	0	Aerobe; Bacteroidetes; GHB
Tetrasphaera sp	0.224	0.011	0	Actinobacteria
Thermoactinomyces daqus	0.003	0	0	
Thermoanaerobacter mathranii	0	0	0.012	Anaerobe; Clostridia; Ethanologenic; Ferm; Firmicutes; Sulfidogen; Thermophile; TRB
Thermoanaerobacter sp	0	0	0.003	Anaerobe; Clostridia; Ethanologenic; Ferm; Firmicutes; Sulfidogen; Thermophile; TRB
Thermoanaerobacterium saccharolyticum	0.093	0.053	91.863	Anaerobe; APB; Clostridia; Firmicutes; NRB; Spore; Sulfidogen; Thermophile; TRB
Thermoanaerobacterium thermosaccharolyticum	0	0	0.175	Anaerobe; APB; Clostridia; Firmicutes; NRB; Spore; Sulfidogen; Thermophile; TRB
Thermobaculum sp	0.007	0	0	EpsilonP; Thermophile
Thermoleophilum sp	0.007	0	0	Actinobacteria; Thermophile
Thermomonas sp	0.003	0	0	Aerobe; GammaP; GHB
Thiobacillus sp	0.011	0	0	BetaP; NRB; NRSOB; SOB
Thiobacter sp	0.018	0	0	SOB; Thermophile

Sequence ID	OG230409-001	OG230409-002	OG230409-004	Select Traits of Interest:
Species	s60. CS Pond Clear Fluid	s61. CS Pond Emulsion Fluid	s57 CS Separator Black Fluid	Metabolic, Physiological, Ecological, Taxonomic
Thiocystis violacea	0.004	0	0	GammaP
Thioprofundum sp	0.004	0	0	Facultative Anaerobe; Filamentous; GammaP; NRB; NRSOB; SOB; Sulfide-Oxidizing
Thiorhodospira sp	0.016	0	0	Anaerobe; GammaP; Phototroph; Purple Sulfur Bacteria
Thiothrix sp	0.004	0	0	Activated Sludge; Bulking; Filamentous; GammaP; Microaerophile; NRB; NRSOB; SOB; Wastewater
Trichococcus sp	0.054	0.004	0.007	Activated Sludge; APB; Facultative Anaerobe; Ferm; Filamentous; Firmicutes; Lactobacillales; WWTP
Tumebacillus sp	0.007	0	0	
Turicibacter sp	0.012	0	0	Anaerobe; Erysipelotrichia; Firmicutes; Unknown
Unclassified	8.157	1.123	0.119	Polyphyletic; Unknown; Varies
Uncultured bacterium	0.086	0.013	0	Unknown
Undibacterium sp	0.009	0.006	0	BetaP; Unknown
Vampirovibrio sp	0.007	0	0	
Variovorax sp	0.861	0.079	0.001	BetaP; BioDeg HC; BioDeg Phenol
Verminephrobacter aporrectodeae	0.009	0	0	
Verrucomicrobium sp	0.126	0	0	Ferm; Verrucomicrobia
Williamsia sp	0.232	0.007	0	Actinobacteria; Filamentous; Foam
Zavarzinella formosa	0.003	0	0	
Zavarzinella sp	0.017	0	0	
Zoogloea oleivorans	0.011	0	0	

Sequence ID	OG230409-001	OG230409-002	OG230409-004	Select Traits of Interest:
Species	s60. CS Pond Clear Fluid	s61. CS Pond Emulsion Fluid	s57 CS Separator Black Fluid	Metabolic, Physiological, Ecological, Taxonomic
Appendix B. Complete list of all organisms identified in Compressor Station Fluid samples				
Values are % of population. Yellow are > 10%, Green are 1 - 10%, Gray are 0%.				
Trait Abbreviations: Acetogen (Acetate producing, via fermentation or CO2 fixation), Acidophile (Growth at low pH), Aerobe (Oxygen requiring), Alkaliphile (Growth at high pH), Anaerobe (Grows only under anoxic conditions), AOB (Ammonia Oxidizing Bacteria), AOX (Ammonia Oxidizing Bacteria), APB (Acid-Producing Bacteria), BioDeg (Biodegrading unusual substrates, catabolically versatile, with the ability to utilize a wide range of unusual substrates, such as pyridine, herbicides, chlorinated biphenyls, and oil), BioDeg HC (Petroleum Hydrocarbon-Degrading Bacteria), BioDeg PAH (Polyaromatic Hydrocarbon-Degrading Bacteria), Biofilm (Biofilm Member), Diverse (Exhibit metabolic diversity), Ethanologenic (Ethanol producing), Facultative (Grows under both aerobic and anaerobic conditions), FAP (Filamentous Anoxygenic Phototroph), Ferm (Fermentative), Filamentous (Forms long filaments), GHB (General Heterotrophic Bacteria), Halophile (Salt tolerant), IRB (Iron-Reducing Bacterial), LAB (Lactic Acid Bacteria), Methanogen (Archaea that produce methane), Methylotroph (Utilize methane, methanol, and other simple carbons), MIC (Microbial-Influenced Corrosion), NiF (Nitrogen Fixing), NOB (Nitrite Oxidizing Bacteria), NRB (Nitrate-Reducing Bacteria), NRSOB (Nitrate-Reducing Sulfur-Oxidizing Bacteria), Oilfield (Found in oilfield samples), Oligotroph (Growth under low nutrient conditions), OX (Oxidizing Bacteria), Pathogen (Disease-causing), Phototroph (Phototrophic, Photosynthetic), Sludge (Component of WWTP Sludges), SOB (Sulfur-Oxidizing Bacteria), Soil (Found in soil), SOX (Sulfur-Oxidizing Bacteria), Spore (Spore-forming bacteria), SRB (SRB, Sulfate-Reducing Bacteria), Sulfidogen (Hydrogen Sulfide Producing (includes SRB, TRB, SuRB and some peptide fermentation bacteria),), SuRB (Sulfur Reducing Bacteria), Syntroph (Mutualistic sharing of metabolic byproducts), Thermophile (Growth above 50oC), TRB (Thiosulfate Reducing Bacteria), Wastewater (Wastewater Associated), WWTP (Wastewater Treatment Plant),				
Under "Select Traits of Interest" sulfidogens are highlighted in red, archaea in yellow, IRB in green.				
GammaP, BetaP, AlphaP and DeltaP are Gammaproteobacteria, Betaproteobacteria, Alphaproteobacteria, and Deltaproteobacteria				

Appendix C: Methods

Sample Collection

In all, 11 sets of samples, encompassing 109 individual samples, were collected between Feb 16, 2023 and April 3 2023. Sampling locations were sites within the Rager Mountain gas storage facility, Equitrans Midstream Corp, 555 Dishong Mountain Road, Johnstown PA 15906 USA. Sites within the facility included wells 2244, 2248, and 2251. Most samples were collected from well 2244 as it was the well involved in the failure event. Samples were predominantly of two types: solid scale material scraped from the outer diameter surface (OD) of the 7" casing joints and liquid annular fluids pumped from the annulus of the 7" and 9 5/8" casing. Additional samples included ID materials from 9 5/8 casing, soil from the surrounding area, grease on casing surface, material from the ID of the well head master valve and tree, as well as liquids collected in the compressor station and a pond. For scale samples, 2" disposable plastic putty knives were used to debride surface scale and solids, care was taken to use a new putty knife for each sample. Solids were stored in sterile Whirl-Pak bags (18 oz, 4.5" X 9"). Liquid samples were collected and stored in 500 ml HDPE Nalgene bottles. After collection, all samples were stored in a refrigerator prior to overnight shipping from Pennsylvania to Texas for analysis.

MPN Analysis

For MPN analysis, each sample is initially diluted in 20 ml of sterile PBS. The quantity of starting material added to the initial dilution varied from sample to sample, depending on sample type and amount of available sample, and the variation in initial sample used is corrected for when determining the dilution factor to adjust the final values. From these 20 ml initial dilutions, 1 ml is used to inoculate each of the primary dilution series bottles, 3 per media type. Each primary dilution was subject to eightfold serial dilution. Selective media used for this project were Modified Postgate's B Broth (MPB) for the growth of Sulfate-Reducing Bacteria, Phenol Dextrose Red Broth (PRD) for the enumeration of acid-producing bacteria (APB) and general heterotrophic bacteria (GHB), and Iron-Reducing Broth (IRB) for the enumeration of iron-reducing bacteria. Dilutions were carried out in triplicate. All medias were at 1% salinity. Incubations were conducted at 30^{o}C. Growth was assayed every 7 days, for a total of 28 days. Growth was compared to the FDA Bacterial Analytical Manual appendix 2 to determine the most probable number. It should be noted that the MPN is an estimate of growth units or colony-forming units and not individual bacterial cells.

For the samples from Rager Mountain, in order set up MPN analysis, a measured amount (g or ml) of each sample was first suspended in 20 ml of sterile PBS buffer and vortexed vigorously for 1 minute. Heavy solids were allowed to gravity settle. 1 ml of this initial dilution was used to inoculate each of the first bottles in the dilution series, creating the initial inoculations, with each bottle containing 10 ml such that each dilution is 10X. The initial inoculations were then subject to 7 additional serial 10-fold dilutions as such: 1 ml was transferred to the next media bottle in the series, shaken to mix, then a new syringe was used to transfer 1 ml into the next media bottle in the series, etc, until 8 media bottles were inoculated in the dilution series. Each dilution series was set up in triplicate (3 times) and cultures are incubated for 28 days at 30 ^{o}C to allow for microbial growth). The presence of growth is recorded every week for 4 weeks at which time the number of positive bottles in a dilution series are used to calculate the starting concentration of bacteria in the initial inoculum, and this number adjusted based on the amount of starting material added to the initial 20 ml dilution used to inoculate the first bottles in the dilution series.

The following media types were chosen for this project, each provides information on a different phenotypic population:

Media	Full Name	Type of Organisms Detected
MPB	Modified Postgate's Medium B	Sulfidogen, SRB (sulfate reducing bacteria).
PRD	Phenol Red Dextrose	APB (acid producing bacteria) and GHB (general heterotrophic bacteria).
IRB	Iron Reducing Bacteria Media	IRB (iron reducing bacteria).

- **PRD** (phenol red dextrose) culture media is used for enumeration of **APB** (acid producing bacteria) and **GHB** (general heterotrophic bacteria).
  - APB convert the bright red media to bright yellow.
  - GHB appear as turbid growth in the red media.
  - All cultures positive for APB are considered positive for GHB.
- **MPB** (modified Postgate's B) culture media is used for enumeration of **SRB** (sulfate reducing bacteria). Although MPB is somewhat selected for SRB, other H2S producing sulfidogenic bacteria such as peptide fermenting organisms and thiosulfate reducing bacteria will sometime grow in MPB, and also generate a positive response.
  - **SRB and Sulfidogens** generate H2S, forming a black FeS precipitate.
- **IRB** (iron reducing bacteria) culture media is clear and slightly yellow-green, with no precipitate.
  - **IRB** Iron reducing organisms chelate the iron, resulting in a clear media with green precipitate.

A 1% salinity was used for all medias. Culturing temperature was set at 30ºC.
Final readings were taken after full 28 days of incubation.

DNA Isolation for qPCR and Amplicon Metagenomics

DNA isolated from the samples were used for both the qPCR and 16S amplicon metagenomics assays. Scale samples such as those from Rager Mountain are atypical samples for DNA isolation, as they consist mostly of non-biological material including possible inhibitors of the DNA isolation and downstream analysis steps. DNA isolations had to be performed multiple times to identify the approach that worked best for that individual sample. The most challenging part is separation of a bacterial fraction away from non-biological materials in the sample. For solid samples, a combination of extraction in sterile PBS buffer and centrifugation was used to isolate a bacterial fraction away from other material in the sample. For liquid samples, a combination of filtration (using sterile 0.2 micron polyethersulfone (PES) membrane filter units) and / or centrifugation. Centrifugation was performed either in 50 ml centrifuge tubes, centrifuged at 2000 g for 50 minutes, or in 2 ml sample tubes, centrifuged for 10,000 g for 15 minutes, depending on volume. Pellets, containing bacteria and additional sample solids, were resuspended in the DNA isolation buffer and processed. For samples with bacteria concentrated by filtration, after filtration the bacteria are trapped on the filter surface while sterile liquids flow through the filtrate reservoir. Bacteria on the surface of the membrane are eluted with sterile PBS buffer, and pelleted by centrifugation. Once a bacterial pellet fraction was prepared, total DNA was isolated using the Qiagen DNeasy UltraClean Microbial Kit (12224-250). Additionally, a "direct isolation" approach was used, in which sample was placed directly into the DNA isolation reagents without the initial bacterial concentration steps. This approach utilized the Qiagen DNeasy Soil DNA Isolation Kit (47014) and / or the Qiagen DNeasy PowerMax Soil DNA Isolation Kit (12988-10) methods, although DNA yields using these approaches were generally not sufficient for downstream analysis.

Primers for 16S qPCR microbial quantification:

515F-GTGCCAGCMGCCGCGGTAA
806R-GGACTACHVGGGTWTCTAAT.
16S probe TACAAGGCCCGGGAACGTATTCACCG
For qPCR, 2.5uL of Sample DNA was loaded into 10uL Quanta Perfecta Tough Mix (QuantaBio) and run on a Roche 480 LightCyler ® with the following cycling conditions: one cycle at 50ºC for 2 minutes, one cycle at 95ºC for 10 minutes, 35 cycles at 95ºC for 15 seconds and 60ºC for 1 minute, and finally, one cycle at 40ºC for 30 seconds. Results of qPCR were scored based on CT score (a positive result was recorded if the CT was ≤30 cycles, negative if CT>30 cycles)..

Amplicon Metagenomics

Illumina 2-step MiSeq
Samples were amplified for sequencing in a two-step process. The forward primer was constructed with (5'-3') the Illumina i5 sequencing primer (TCGTCGGCAGCGTCAGATGTGTATAAGAGACAG) and the indicated forward primer. The reverse primer was constructed with (5'-3') the Illumina i7 sequencing primer (GTCTCGTGGGCTCGGAGATGTGTATAAGAGACAG) and the indicated reverse primer. Amplifications were performed in 25 ul reactions with Qiagen HotStar Taq master mix (Qiagen Inc, Valencia, California), 1ul of each 5uM primer, and 1ul of template. Reactions were performed on ABI Veriti thermocyclers (Applied Biosystems, Carlsbad, California) under the following thermal profile: 95○C for 5 min, then 35 cycles of 94○C for 30 sec, 54○C for 40 sec, 72○C for 1 min, followed by one cycle of 72○C for 10 min and 4○C hold.
Products from the first stage amplification were added to a second PCR based on qualitatively determine concentrations. Primers for the second PCR were designed based on the Illumina Nextera PCR primers as follows: Forward - AATGATACGGCGACCACCGAGATCTACAC[i5index]TCGTCGGCAGCGTC and Reverse - CAAGCAGAAGACGGCATACGAGAT[i7index]GTCTCGTGGGCTCGG. The second stage amplification was run the same as the first stage except for 10 cycles.
Amplification products were visualized with eGels (Life Technologies, Grand Island, New York). Products were then pooled equimolar and each pool was size selected in two rounds using SPRIselect (BeckmanCoulter, Indianapolis, Indiana) in a 0.7 ratio for both rounds. Size selected pools were then run on a Fragment Analyzer (Advanced Analytical, Ankeny, Iowa) to assess the size distribution, quantified using the Qubit 3.0 fluorometer (Life Technologies), and loaded on an Illumina MiSeq (Illumina, Inc. San Diego, California) 2x300 flow cell at 10pM and sequenced.

Notes on Taxonomic and Metabolic Assignment
Organisms are referred to by the identity of the most closely matched organism in the database. However, this does not indicate 100% identity. In most cases, the most closely matched organisms are referred to as "uncultured organism" and as such there is no physiological or metabolic information for them. Organisms that fall below the cutoff for taxonomic assignment are listed as unclassified. Due to the unusual source of samples, a large number of organisms in the samples may unclassified. This indicates that they are novel organisms that have not been described in the scientific literature.
Metabolic assignments are inferred by the metabolic characteristics of the most closely related organism for which experimental data has been provided. Some metabolic groupings are overlapping and non-exclusive, e.g. many fermentative organisms generate organic acids or are capable of sulfidogenesis under some conditions. An overview of select metabolisms is provided in Appendix B.

Overview of Select Metabolic Processes

APB: Acid-Producing Bacteria
Acid-producing bacteria are of specific interest to the oilfield community as acid production directly and aggressively promotes corrosion. Several metabolic pathways result in the production of acids, including fermentation pathways that generate organic acids such as lactic acid and acetic acid, as well as those that generate inorganic acids such as sulfuric acid as a byproduct of the oxidation of inorganic sulfur compound. Not all fermentative pathways result in acidification of the surrounding environment. The identification of bacteria as acid producing does not necessarily indicate acidification of bulk fluids.

Biodeg: Biodegradation
Some bacterial genera and species have the capacity to utilize "atypical" or "unusual" substrates as carbon sources. These bacteria are loosely referred to as Biodeg, for "Biodegradation". The definition used here for "atypical or unusual substrates" with reference to bacterial metabolism includes compounds that most bacteria cannot utilize as a food source. Unusual compounds Biodeg organisms utilize include disinfectants, antibiotics, xenobiotics and detergents. Some degrade long chain polymers of sugars and carbohydrates, such as those found in cell wall materials. Others are able to degrade hydrocarbons. Hydrocarbons, including alkanes, alkenes, aromatic hydrocarbons, and waxes, are found naturally in great variety in crude oil and other petroleum compounds. Due to their structural diversity, most bacteria lack the capacity to utilize petroleum hydrocarbons as food sources. Each type of hydrocarbon-degrading microorganism is likely to be capable of metabolizing a few specific types of hydrocarbons.

IRB: Iron-Reducing Bacteria, Fe(III)RB
Some microbes can use Fe(III) as an electron acceptor, reducing it to Fe(II). Iron reduction has been observed under both acidophilic and neutrophilic conditions. Two common iron-reducing genera are Shewanella and Geobacter. In addition to IRB activity, Shewanella species produce chelators that solubilize Fe(III) oxides (Lovley et al, 2004). Shewanella are capable of growing in corrosive biofilms where they have been shown to remove the protective H2 film layer that normally protects iron surfaces from corrosion under anoxic conditions. should not be confused with iron oxidizing bacteria, which are aerobes responsible for a rust brown staining and slimy growth in surface waters.

NRB: Nitrate Reducing Bacteria
NRB reduce nitrates to nitrites, nitrous oxide, or nitrogen under anaerobic conditions in a process termed denitrification. Most are heterotrophic facultative anaerobic bacteria including such common bacteria as *Paracoccus, Pseudomonas, Alcaligenes,* and *Bradyrhizobioium*. A few bacteria use such reduction processes as hydrogen acceptor reactions and hence as a source of energy; in this case the end product is ammonia. Denitrification is a normal part of nitrogen cycling and not all NRB are of concern to O&G infrastructure.

A subcategory of NRB is the **NRSOB**: Nitrate-Reducing Sulfur-Oxidizing Bacteria are a specific subgroup of NRB whose levels are increased in reservoirs following nitrate injections (Gittel et al 2009; Grigoryan et al, 2008; Hubert and Voordouw, 2007). Growth of NRSOB suppresses the activity of SRB, and thus reducing sulfidogenisis. Some Epsilonproteobacteria can also oxidize petroleum sulfur compounds and utilize nitrate as an electron acceptor for growth, and thus may be considered hydrocarbon degrading. Massive dominance of related Epsilonproteobacteria has been observed in other petroleum samples, for example in formation waters from a Canadian oil sands reservoir containing severely biodegraded oil. (Kodama, Y and Kazuya Watanabe, 2003; Hubert et al, 2011). Sulfurospirillum are nitrate-reducing, sulfur oxidizing bacteria (NRSOB) members of the class Epsilonproteobacteria and are sometimes referred to as “Campylobacter” in older publications. The way in which nitrate addition can affect the SRB population involves several pathways. First, nitrate is a thermodynamically more favorable electron acceptor than sulfate, thus NRB have a competitive advantage. To emphasize the complexity of the metabolism in oilfield samples, it should be noted that under some conditions, these bacteria are also sulfidogens capable of reducing sulfur and thus producing H_2S (Finster K et al, 1997).

Sulfidogenesis: (e.g. SRB, TRB, SuRB)
The metabolic pathways of most interest to the oilfield community are those that generate significant levels of hydrogen sulfide (H_2S). In addition to inorganic processes, biogenic processes can generate significant levels of hydrogen sulfide, primarily through the action of sulfidogenic bacteria. Bacteria that evolve hydrogen sulfide are commonly referred to as “sulfidogens”. Sulfate-reducing bacteria (SRB) are particularly aggressive at sulfide production and are the group of bacteria most commonly implicated oil filed biogenic sulfide production (Barton et al, 2009). Hydrogen sulfide formation by sulfate-reducing bacteria (SRB) under strict anaerobic circumstances is a common problem in sediments, sewer systems, oil reservoirs and anaerobic effluents (Holmer & Storkholm, 2001; McComas et al., 2001). The emission of H_2S into the atmosphere of sewer systems does not only imply odor nuisances and possible health risks. It also induces the biological production of sulfuric acid in the aerobic zones, causing severe corrosion of the inner surface of concrete sewer structures (Sand, 1987; Vincke et al., 2002). Hence, preventive or curative actions are needed.

While SRB are traditionally associated with O&G system sulfide generation, sulfur- and thiosulfate-reducing bacteria (SuRB and TRB, respectively) can also generate significant levels of H_2S and contribute to corrosion and souring (Hulecki JC et al, 2009, Magot et al 1997, Agrawal et al, 2010). Compared to SRB, the TRB are harder to classify taxonomically, as they are members of bacterial genera that can include non-tSRB members. Examples of sulfidogenic TRB commonly found in oilfield samples include *Halanaerobium congolense*, as well as some *Thermoanaerobacter*, and *Spirochaeta*. Additionally, many common enteric bacteria are sulfidogenic, including *Citrobacter* and *Salmonella*.

Thermophiles:
A thermophile is an organism that can survive and often thrives in environments having relatively high temperatures ranging between 45 and 122 °C.

Methanogens:

Methanogens are Archaea that produce methane as a metabolic byproduct in anoxic conditions. Methanogens are found in different environments including wetlands (marsh gas), animal digestive tracts (methane production of cattle and in farts), and anaerobic digestor sludges of wastewater treatment systems. Some methanogens are extremophiles and can be found in hot springs, submarine hydrothermal vents as well as in the "solid" rock of the Earth's crust, kilometers below the surface. Methanogens are associated with microbial influenced corrosion. Hydrogenotrophic methanogens are believed to cause metal corrosion through cathodic depolarization, whereas the acetotrophic methanogens grow syntrophically with corrosion-causing SRB.

Appendix D References

1. Angelez-Chavez, C., Mora-Mendoza, J.L., Garcia-Esquivel, R., Padilla-Viveros, A.A., Perez, R., Flores, O. and Martinez, L. (2002) Microbiologically influenced corrosion by Citrobacter in sour gas pipelines. Mater Perform 41, 50-55.
2. Balch, W. E.; Schoberth, S.; Tanner, R. S.; Wolfe, R. S. (1977). Acetobacterium, a New Genus of Hydrogen-Oxidizing, Carbon Dioxide-Reducing, Anaerobic Bacteria. International Journal of Systematic Bacteriology 27 (4): 355.
3. Barton LL, Fauque GD. (2009) Biochemistry, physiology and biotechnology of sulfate-reducing bacteria. Adv Appl Microbiol. 68:41-98.
4. Bermont-Bouis D, Janvier M, Grimont PA, Dupont I, Vallaeys T. (2007) Both sulfate-reducing bacteria and Enterobacteriaceae take part in marine biocorrosion of carbon steel. J Appl Microbiol. 102:161-168.
5. Bermont-Bouis D, Janvier M, Grimont PA, Dupont I, Vallaeys T. (2007) Both sulfate-reducing bacteria and Enterobacteriaceae take part in marine biocorrosion of carbon steel. J Appl Microbiol. 102:161-168.
6. Boone DR, Whitman WB, Rouviere P (1994). "Diversity and taxonomy of methanogens". In JG Ferry, ed. Methanogenesis: Ecology, Physiology, Biochemistry & Genetics. Pp 35-80.
7. D'Ippolito S, de Castro RE, Herrera Seitz K. (2011) Chemotactic responses to gas oil of Halomonas spp. strains isolated from saline environments in Argentina. Rev Argent Microbiol. 43(2):107-10.
8. Dice, L.R., "Measures of the Amount of Ecologic Association Between Species," *Ecology* 26, 3, (1945): pp.297-302
9. Hubert CR Oldenburg TB, Fustic M, Gray ND, Larter SR, Penn K, Rowan AK, Seshadri R, Sherry A, Swainsbury R, Voordouw G, Voordouw JK, Head IM. (2012) Massive dominance of Epsilonproteobacteria in formation waters from a Canadian oil sands reservoir containing severely biodegraded oil. Environ Microbiol. 14(2):387-404.
10. Kryachko Y, Dong X, Sensen CW, Voordouw G. (2012) Compositions of microbial communities associated with oil and water in a mesothermic oil field. Antonie Van Leeuwenhoek. 101: 3, pp 493-506
11. Kwon S, Moon E, Kim TS, Hong S, Park HD. (2011) Pyrosequencing demonstrated complex microbial communities in a membrane filtration system for a drinking water treatment plant. Microbes Environ. 26(2):149-55.
12. Li XX, Yang T, Mbadinga SM, Liu JF, Yang SZ, Gu JD, Mu BZ. Responses of Microbial Community Composition to Temperature Gradient and Carbon Steel Corrosion in Production Water of Petroleum Reservoir. Front Microbiol. 2017 Dec 5;8:2379.
13. Lonergan DJ, Jenter HL, Coates JD, Phillips EJ, Schmidt TM, Lovley DR (1996) Phylogenetic analysis of dissimilatory Fe(III)-reducing bacteria. J Bacteriol. 178(8):2402-8.
14. Montoya D, Ar_valo C, Gonzales S, Aristizabal F, Schwarz WH. (2001) New solvent-producing Clostridium sp. strains, hydrolyzing a wide range of polysaccharides, are closely related to Clostridium butyricum. J Ind Microbiol Biotechnol. 27(5):329-35.
15. Pham,V.D., Hnatow,L.L., Zhang,S., Fallon,R.D., Jackson,S.C., Tomb,J.F., DeLong,E.F. and Keeler,S.J. (2009) Characterizing microbial diversity in production water from an Alaskan mesothermic petroleum reservoir with two independent molecular methods Environ. Microbiol. 11 (1), 176-187.
16. Rajasekar A, Anandkumar B, Maruthamuthu S, Ting YP, Rahman PK. (2010) Characterization of corrosive bacterial consortia isolated from petroleum-product-transporting pipelines. Appl Microbiol Biotechnol. 85(4):1175-88.
17. Ravot G, Ollivier B, Magot M, Patel B, Crolet J, Fardeau M, Garcia J. (1995) Thiosulfate reduction, an important physiological feature shared by members of the order thermotogales. Appl Environ Microbiol. 61(5):2053-5.
18. Vigneron A, Alsop EB, Chambers B, Lomans BP, Head IM, Tsesmetzis N. Complementary Microorganisms in Highly Corrosive Biofilms from an Offshore Oil Production Facility. Appl Environ Microbiol. 2016 Apr 4;82(8):2545-2554.
19. Vigneron A, Head IM, Tsesmetzis N. Damage to offshore production facilities by corrosive microbial biofilms. Appl Microbiol Biotechnol. 2018 Mar;102(6):2525-2533.
20. *Yan, Z., Zheng, X.-W., Chen, J.-Y., Han, J.-S. and Han, B.-Z. (2013), Effect of different Bacillus strains on the profile of organic acids in a liquid culture of Daqu. J. Inst. Brew., 119: 78-83.* https://doi.org/10.1002/jib.58 https://onlinelibrary.wiley.com/doi/epdf/10.1002/jib.58
21. Zhang T, Ye L, Tong AH, Shao MF, Lok S. (2011) Ammonia-oxidizing archaea and ammonia-oxidizing bacteria in six full-scale wastewater treatment bioreactors. Appl Microbiol Biotechnol. 91(4):1215-25.

A.13 Large Format Appendix

A.13.1 Large Format Root Cause Analysis Chart

Refer to file: Appendix A.13.1 RCA Chart 2023-08-20.pdf

The file can be printed on large paper or a plotter. The default paper size is A0.

A.13.2 Gamma Ray Neutron Temperature Composite Log

Refer to file: Appendix A.13.2 GRNT_2016_2022_Composite.png